SPECIES TAXONOMY, PHYLOGENY, AND BIOGEOGRAPHY OF THE BRONTOTHERIIDAE (MAMMALIA: PERISSODACTYLA)

MATTHEW C. MIHLBACHLER

Division of Paleontology
American Museum of Natural History

Present address:
Anatomy Department
New York College of Osteopathic Medicine
Northern Boulevard
Old Westbury, NY 11568 8000
e-mail: mmihlbac@nyit.edu

BULLETIN OF THE AMERICAN MUSEUM OF NATURAL HISTORY
CENTRAL PARK WEST AT 79TH STREET, NEW YORK, NY 10024
Number 311, 475 pp., 202 figures, 15 tables
Issued June 3, 2008

Copyright © American Museum of Natural History 2008 ISSN 0003-0090

CONTENTS

Abstract 5
Introduction 6
Brontothere Research in the Osbornian and Post-Osbornian Eras 9
Methods of Taxonomic Revision 13
Species Concept and Species Delimitation 14
Measurements 17
Institutional Abbreviations 19
Systematic Paleontology 19
Bunobrontops savagei 19
Mesatirhinus junius 22
Desmatotitan tukhumensis 33
Acrotitan ulanshirehensis 36
Dolichorhinus hyognathus 38
Sphenocoelus uintensis 49
Microtitan mongoliensis 59
Fossendorhinus diploconus 63
Metarhinus fluviatilis 69
Metarhinus abbotti 74
Metarhinus sp. 79
Sthenodectes incisivum 85
Telmatherium validus 93
Qufutitan zhoui 106
Wickia brevirhinus 114
Metatelmatherium ultimum 122
Epimanteoceras formosus 133
Protitan grangeri 141
Protitan minor 152
Protitanotherium emarginatum 157
Rhinotitan kaiseni 167
Rhinotitan andrewsi 174
Rhinotitan sp. 182
Nanotitanops shanghuangensis 184
Pollyosbornia altidens 186
Pygmaetitan panxianensis 189
Gnathotitan berkeyi 196
Aktautitan hippopotamopus 202
Brachydiastematherium transylvanicum 203
Metatitan primus 206
Metatitan relictus 212
Metatitan khaitshinus 220
Nasamplus progressus 231
Protembolotherium efremovi 233
Embolotherium andrewsi 243
Embolotherium grangeri 251
Pachytitan ajax 265
Diplacodon elatus 267
Parabrontops gobiensis 280
cf. *Parabrontops gobiensis* (?) mandibles 287
Eubrontotherium clarnoensis 290
Protitanops curryi 298
Notiotitanops mississippiensis 303

Dianotitan lunanensis 308
Duchesneodus uintensis 316
Miscellaneous Dubious, Problematic, and Unnamed Potential Taxa 328
Dolichorhinus vallidens 329
Duchesneodus primitivus 330
Sivatitanops birmanicum 331
"*Metatelmatherium* (?)" *lahirii* 334
"*Sivatitanops* (?)" *rugosidens* 335
Tanyorhinus harundivorax 336
Manteoceras foris 337
Manteoceras pratensis 337
Duchesneodus californicus 337
"*Metatelmatherium* (?)" *browni* 339
Protitanotherium koreanicum 341
Metatelmatherium parvum 345
Hyotitan thomsoni 345
"*Protitan*?" *cingulatus* 347
Epimanteoceras praecursor 351
Rhinotitan orientalis 351
"Eotitanops?" dayi 352
Rhinotitan quadridens 353
Duchesneodus thyboi 354
Epimanteoceras amplus 355
Arctotitan honghoensis 359
Pakotitanops latidentatus 361
Mulkrajanops moghliensis 362
"*Microtitan*?" *elongatus* 363
Protitan major 364
cf. *Palaeosyops* sp. (Palaeosyops sp. sensu Gabounia, 1977) 364
cf. *Metarhinus* sp. (*Microtitan* sp. sensu Qi and Beard, 1996) 365
cf. *Palaeosyops* sp. (*Bunobrontops* sp. sensu Holroyd and Ciochon, 2000) 365
Camp Margetts "mandible taxon A" 366
Camp Margetts "mandible taxon B" 369
Camp Margetts "mandible taxon C" 371
Phylogenetic Characters 372
Cranial Characters 374
Upper Dental Characters 381
Mandible and Lower Dental Characters 388
Phylogenetic Analysis of Brontotheriidae 390
Ingroup taxa 390
Outgroup taxa 392
Data 393
Methods of Phylogenetic Analysis 393
Results of PAUP Searches 393
Consensus Trees and Wildcards 396
Brontothere Phylogeny and Classification 398
History 398
Brontothere higher taxa 407
Brontotheriidae 408
Eotitanopinae 408
Palaeosyopinae 408
Brontotheriinae 409
Dolichorhinini 409

Brontotheriini 409
Rhadinorhinina 410
Telmatheriina 410
Brontotheriina 410
Brontotheriita 411
Embolotheriita 411
Metarhinus 412
Protitan 412
Rhinotitan 412
Metatitan 412
Embolotherium 412
Megacerops 413
A Revised Classification of the Brontotheriidae 413
Brontothere Origins and Cladistic Biogeography 414
Brontothere Origins 415
Cladistically Implied Intercontinental Dispersals 418
Conclusion 419
Acknowledgements 419
References 420
Appendix 1: Craniodental Measurements 430

ABSTRACT

The Brontotheriidae is an extinct family of Eocene perissodactyls known from North America, Asia, and, rarely, Eastern Europe. Brontotheres are widely recognized as having evolved very large body size and conspicuous frontonasal horns, although these traits do not characterize every species. Characters shared by all brontotheriids include an anteroposteriorly abbreviated face and an elongate postorbital cranium. Dentally, brontotheriids share bunoselenodont upper molars with a W-shaped ectoloph, isolated lingual cusps, and with paraconules, metaconules, and transverse molar crests that are either vestigial or absent. Early North American paleontologists such as Leidy, Cope, Marsh, and Osborn placed considerable emphasis on brontothere research, however, since Osborn's massive 1929 monograph on North American brontotheres, serious research on this diverse Eocene family has waned. Nonetheless, a great need for a revision of the Brontotheriidae has long been recognized because earlier works on brontothere taxonomy and systematics, particularly those of Osborn, are universally considered problematic due to their reliance on the discredited theory of orthogenesis.

The present study reevaluates the species taxonomy of brontotheres based on craniodental materials. All known taxa were considered for revision except North American representatives of *Eotitanops*, *Palaeosyops*, and *Megacerops*. A phylogenetic species concept, where species are defined as the smallest diagnosable clusters of specimens, was adopted for this study. Monospecific quarry samples (mass death assemblages) consistently suggest that certain characters, including canine size, horn size, and many premolar characters show intraspecific polymorphic tendencies; such characters were not generally used to delimit species. All characters found to be monomorphic within mass death assemblages were considered when delimiting taxa.

A total of 116 potential species were considered for revision. Among these species, 41 were found to be valid, 34 species were found to be invalid junior synonyms of valid species, 31 species were found to be nonima dubia, and three others were found to be problematic due to extremely fragmentary fossils, but not necessarily invalid. One new species, *Wickia brevirhinus*, is named and six other potential species are recognized but remain unnamed due to very poor fossil material.

Phylogenetic analysis of 47 brontotheriid taxa was undertaken with 227 states distributed among 87 characters. The outgroup method was employed using *Hyracotherium*, *Pachynolophus*, *Danjiangia*, and *Lambdotherium*. Two analyses were performed, one with ordered multistate characters and another with unordered multistate characters. Both analyses yielded large numbers of most parsimonious trees. A strict reduced consensus was used to identify and prune fragmentary wildcard taxa a posteriori. Not surprisingly, the results of the phylogenetic analysis differ substantially from prior orthogenetic hypotheses of brontothere phylogeny and a radical revision in the higher classification of brontotheres is presented. *Eotitanops* and *Palaeosyops* are the most basal members of the Brontotheriidae. All other brontotheres form a clade, Brontotheriinae, which is supported by numerous molar apomorphies suggesting increased functional emphasis on shearing on the outer wall of enamel of the upper molars. Many of the previously named brontothere subfamilies are clearly paraphyletic while others correspond to subclades of the Brontotheriinae and have been assigned new ranks, resulting in a revised classification consisting of internested monophyletic taxa.

Nine to twelve intercontinental dispersals, mostly in the middle Eocene (Uintan and Irdinmanhan land mammal "ages") between North America and Asia are implied by the cladistic results. The timing of these dispersals agrees with prior conclusions regarding the timing of large influxes of mammal taxa into North America from Asia. However, the frequency of interchanges is far greater than previously surmised. Following basic MacArthur-Wilson island biogeography theory, North America, the smaller continent, is viewed as a cul-de-sac, receiving repeated waves of immigrants from Asia, the larger continent. However, the phylogenetic results of the Brontotheriidae suggest the possibility that the predominant direction of dispersal could have been in the opposite direction; this result questions the validity of applying island biogeography theory to continent-scale dispersal dynamics.

INTRODUCTION

In addition to their historical importance as domestic animals (horses), or more recently as icons of endangered wildlife (rhinos), perissodactyls, the order of mammals containing modern tapirs, rhinos, and horses, are noteworthy for their high levels of past diversity, which contrasts with their diminished modern diversity. With the possible exception of horses (Simpson, 1951), interest in perissodactyl evolution waned in the mid–20th century and despite renewed interest in perissodactyl systematics (MacFadden, 1992; Hooker, 1994; Cerdeño, 1995; Holbrook, 1999; Froehlich, 1999, 2002; Antoine, 2002; Lucas and Holbrook, 2004; Prothero, 2005), various groups remain in a state of neglect. Among the most neglected perissodactyls are the Brontotheriidae, an extinct family that is confined to the Eocene of North America, Asia, and Europe. Brontotheres are notable for having evolved bony frontonasal protuberances (or "horns") and body sizes approximating those of extant rhinos and elephants. Brontotheres are one of the more diverse groups of ungulates and during the Eocene they exceeded other perissodactyl families in terms of overall diversity. Brontotheres are among the most abundantly represented ungulates in Eocene fossil-bearing terrestrial deposits. The bulk of the known brontothere fossil record is from central Asia and western North America (Osborn, 1929a, 1929b; Granger and Gregory, 1943; Yanovskaya, 1980; Wang, 1982). Brontothere records are fewer and more fragmentary in other regions, but it is evident that this family had an essentially Holarctic distribution with the exception of Western Europe. Brontothere fossils have also been recovered from eastern Europe (Nikolov and Heissig, 1985; Lucas and Schoch, 1989a), eastern Russia (Yanovskaya, 1957), Kazakstan (Yanovskaya, 1953; Emry et al., 1998; Mihlbachler et al., 2004a), Pakistan (Dehm and Oettingen-Spielberg, 1958; West, 1980; Kumar and Sahni, 1985), southeast Asia (Pilgrim, 1925; Colbert, 1938; Holroyd and Ciochon, 2000; Tsubamoto et al., 2000; Qi and Beard, 1996), Korea (Takai, 1939), Japan (Miyata and Tomida, 2003), the southeastern United States (Gazin and Sullivan, 1942), and in northern regions of Canada (Eberle and Storer, 1999; Eberle, 2006).

Brontotheres have humble beginnings as relatively rare, small, unspecialized animals in the early Eocene (e.g., *Eotitanops*), but quickly radiated into an assortment of species that developed unique and bizarre skulls. Some achieved enormous body sizes in comparison to other contemporary perissodactyls such as horses, tapirs, and rhinos, which, by comparison, were relatively small throughout the Eocene (fig. 1). With massive bodies and robust graviportal limbs, the largest brontotheres superficially resemble rhinos. However, brontothere horns were made of bone, not keratin; they retained four front digits, whereas modern rhinos have only three. Additionally, brontotheres show subtle differences in their overall limb proportions in comparison to modern rhinos (Mihlbachler et al., 2004a).

The exact phylogenetic position of brontotheres within the Perissodactyla is unresolved. Brontotheres are traditionally grouped within the suborder Hippomorpha along with horses, palaeotheres, and sometimes chalicotheres (Wood, 1937; Simpson, 1945; Scott, 1941; Radinsky, 1969). Froehlich (1999) suggested that brontotheres are actually a subclade of the Palaeotheriidae. Others have included them with tapirs and rhinos in the Ceratomorpha (McKenna and Bell, 1997), while others still have excluded them from other major perissodactyl clades (Prothero and Schoch, 1989) and considered them the sister taxon of all other perissodactyls (Hooker, 1984), or placed them at an unresolved polytomy with other major radiations of perissodactyls (Janis et al., 1998).

Characters that typify brontotheres include an elongated postorbital cranium and an abbreviated face (Osborn, 1929a; Mader, 1989, 1998). In some species (e.g., *Duchesneodus uintensis*) this condition is extreme, with the orbits positioned near the very front of the elongate skull. Some brontotheres evolved extremely dolichocephalic (elongated) skulls (e.g., *Dolichorhinus*), while others evolved massive laterally paired sexually dimorphic bony horns composed of the

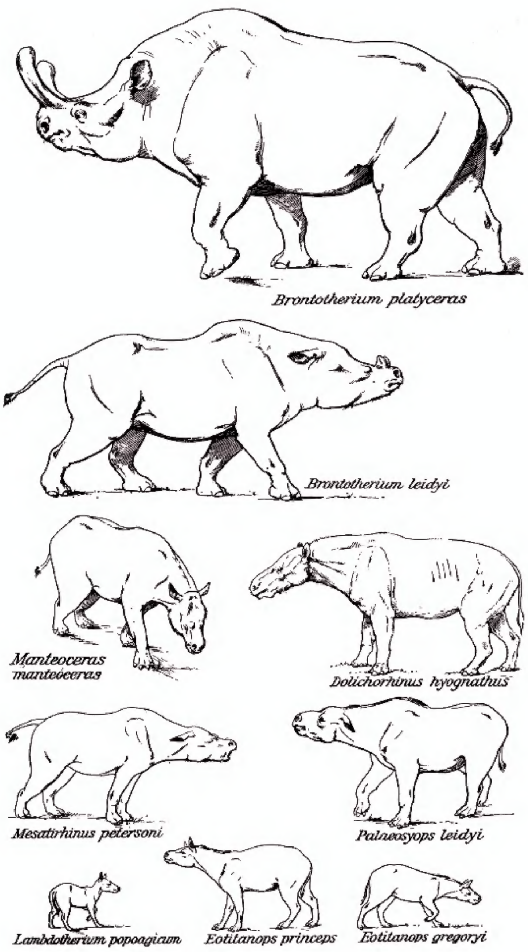

Fig. 1. Reconstructions of assorted North American brontotheriids and the brontotheriioid *Lambdotherium popoagicum* from Osborn (1929a). Synonyms used in this paper are as follows: *Brontotherium platyceras* and *Brontotherium leidyi* (= *Megacerops coloradensis* sensu Mihlbachler et al., 2004b), *Manteoceras manteoceras* (= *Telmatherium validus*), *Dolichorhinus hyognathus* (= *Dolichorhinus hyognathus*), *Mesatirhinus petersoni* (= *Mesatirhinus junius*), *Palaeosyops leidyi* (= *Palaeosyops robustus* sensu Gunnell and Yarbrough, 2000), *Eotitanops princeps* (= *Eotitanops borealis* sensu Gunnell and Yarbrough, 2000), and *Eotitanops gregoryi* (= *Eotitanops minimus* sensu Gunnell and Yarbrough, 2000).

frontal and nasal bone, and deeply concave saddle-shaped skulls with grossly expanded zygomatic arches (e.g., *Megacerops*). (While recognizing that the various cranial appendages seen in ungulates, such as giraffe ossicones, cervid antlers, bovid horns, rhino horns, and brontothere frontonasal protuberances are non-homologous, as a matter of convenience I adopt a generalized usage of the term "horn" for cranial appendages of brontotheres and other ungulates.) Brontothere horns resemble the secondary sex characters (e.g., horns, tusks) commonly seen in many sexually dimorphic extant ungulates and seem to suggest a polygynous and possibly gregarious form of sociality (Jarman, 1983; Loison et al., 1999). Other brontotheres, such as *Embolotherium*, had acquired a single, massive battering ram–like process extending upward from the face, suggesting expanded and highly modified narial morphologies (Mihlbachler and Solounias, 2004) (fig. 2). Though superficially similar to rhinos, brontothere horns are composed of bone, not keratin, and therefore preserve as fossils, unlike rhino horns. Brontothere horns are most similar to the ossicones of modern giraffes; they lack grooves for nutrient blood vessels, tend to show evidence of secondary bone grown (probably due to head clashes), and were likely to have been covered by skin (Mihlbachler et al., 2004b).

Despite the variety of bizarre head shapes seen among brontotheres, this group is most easily characterized by its distinctive upper molar pattern, which consists of a W-shaped ectoloph that is at least half the labiolingual width of the entire upper molar crown, with a strong parastyle and mesostyle, and isolated lingual cusps (protocone and hypocone). Transversely (labiolingually) oriented upper molar lophs (protoloph, metaloph) and other cusps (paraconules and metaconules) are either vestigial or absent (Osborn, 1929a; Radinsky, 1969; Mader, 1989, 1998). The distinctive brontothere molar represents a crown-type that is completely nonexistent today, although a similar kind of bunolophodont dental morphology evolved in another extinct perissodactyl family, the Chalicotheriidae (Radinsky, 1969; Coombs, 1998). Brontothere teeth have been previously characterized as weak or mechanically inferior (Osborn, 1929a; Mader 1998) largely because they did not evolve extreme hypsodonty unlike many other lineages of ungulates (e.g., horses). Functionally, brontothere dentitions have been described as having a

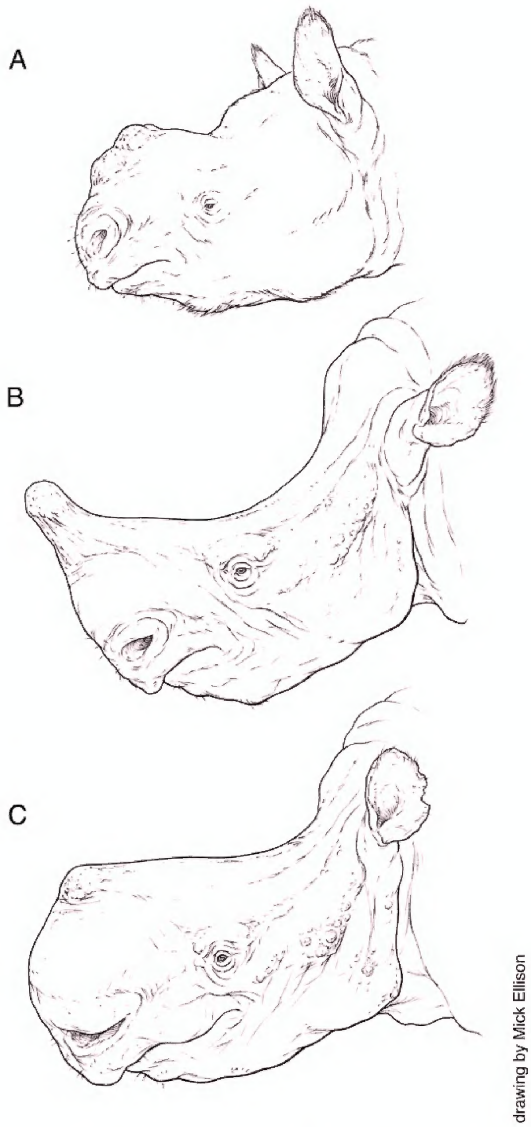

Fig. 2. Reconstructions of the heads of central Asian brontothere species. **(A)** *Metatitan primus*, **(B)** *Embolotherium andrewsi*, **(C)** and *Embolotherium grangeri*.

dual function of shearing (ectoloph) and crushing (lingual cusps) (Osborn, 1929a; Radinsky, 1969; Mader, 1998). This bunolophodont dental morphology has been interpreted to indicate a diet of selective folivory/frugivory (Janis, 2000). However, the immense size of many species suggests that at least some species must have been nonselective feeders, despite their dental morphology. Indeed, microwear patterns of brontothere

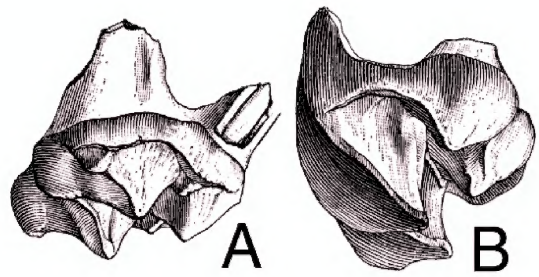

Fig. 3. Anterior views from Osborn (1929a) of **(A)** the relatively plesiomorphic upper molar of *Palaeosyops*, and **(B)** the relatively apomorphic upper molar of the Brontotheriine, *Megacerops coloradensis* (sensu Mihlbachler et al., 2004b).

molars suggest a strictly folivorous diet that is similar to that of the black rhinoceros (*Diceros bicornis*) or moose (*Alces alces*), both very large herbivores with diets consisting mostly of leaves and other fibrous woody material (Mihlbachler and Solounias, 2002).

The brontothere dental battery is not evolutionarily static despite notions to the contrary (Radinsky, 1969); early species had short crowns and thick enamel, however a transformation from this thick-enameled brachydont type of tooth to a more hypsodont and thin enameled type of molar did occur among brontotheres (fig. 3). Functionally, this transition seems related to more emphasis being placed on the vertical shearing action of the labial wall of enamel of the ectoloph. Surprisingly, microwear patterns do not suggest a significant change in diet associated with this morphological transformation (Mihlbachler and Solounias, 2002). Other conspicuous dental transformations in brontotheres include the reduction of the anterior dentition to a vestigial state and the semimolarization of the premolars (Osborn, 1929a; Radinsky, 1969).

The majority of brontotheres (all except *Eotitanops* and *Palaeosyops*) have the more advanced molar condition. One species, *Bunobrontops savagei*, is clearly an intermediate form; it retains the very brachydont crown, but shows some derived molar characters. In an earlier analysis of brontothere phylogeny, those brontotheres, including *B. savagei*, showing derived molar characters related to this functional transformation form a robust and well-supported

clade (Mihlbachler 2003a). In this paper, I apply the subfamily name, Brontotheriinae, for this clade of brontotheres showing advanced dental characters. More formal definitions of Brontotheriidae, Brontotheriinae, and other higher brontothere taxa, are described near the end of this paper, following the phylogenetic analysis.

For the most part, brontotheres have been neglected by systematists and other paleontologists, despite their apparent taxic diversity, their large size, wide variety of appealing cranial morphologies, their conspicuous presence among the exhibits of most major natural history museums, and the overwhelming number of storage units in many museum collections that are filled with brontothere fossils. In contrast to the intense interest in brontotheres showed by early paleontologists such as J. Leidy, E.D. Cope, O.C. Marsh, and particularly, H.F. Osborn, (see review in Osborn, 1929a and in Prothero and Schoch, 2002) there is a dearth of recent literature on the systematics, phylogeny, or overall paleobiology of the Brontotheriidae. Nonetheless, Osborn's (1929a) exhaustive monograph on brontotheres, which remains the primary reference for this family, is almost universally recognized as deeply flawed, with severely oversplit alpha-level taxonomy, paraphyletic higher taxa, and discredited theories regarding evolution (Scott, 1941; Radinsky, 1969; Prothero, 1994; Prothero and Schoch, 2002; Alroy, 2003). Nevertheless, despite the prevalence of brontotheres in Holarctic Eocene mammal faunas, little effort has been focused on rectifying the seriously flawed state of brontothere systematics. Unfortunately, subsequent brontothere taxonomists such as Granger and Gregory (1943) and Yanovskaya (1980) used methods similar to Osborn's and only compounded the problem by erecting more problematic taxa and generating questionable phylogenetic hypotheses. In the recent literature, only a few short papers on the genus-level taxonomy of North American brontotheres (Mader, 1989, 1998) and on the species level phylogeny of Asian horned brontotheres (Mihlbachler et al., 2004a) have made serious attempts to rectify the chaotic state of brontothere phylogenetic systematics. However, the main task of overhauling the species taxonomy of brontotheres and developing a cladistically derived hypothesis that includes both Asian and North American species has not been accomplished until now.

Brontothere Research in the Osbornian and Post-Osbornian Eras

The early history of brontothere research in North America is recounted by Osborn (1929a) with additional information in Prothero and Schoch (2002), Mihlbachler et al. (2004b), and Lucas (2004), and is only briefly recounted here. Brontothere fossils were among the first fossil vertebrates from the western United States to be described. Joseph Leidy was the first to provide scientific descriptions of brontothere fossils, although the material he examined was mostly fragmentary and did not allow him to develop of good understanding of what a brontothere was or looked like. However, Cope and Marsh were the first to examine entire skulls, and, in the case of Marsh, entire skeletons (Marsh, 1889). Marsh (1873) first recognized brontotheres as perissodactyls, coined the term Brontotheridae (later amended to Brontotheriidae) and wrote papers outlining the principle characteristics of this group (Marsh, 1874, 1876). Marsh's concept of the Brontotheriidae was originally confined to horned varieties of the White River Formation of North America; the earlier hornless varieties known to him were referred to as the "Limnohyidae" Marsh (1875), although he did observe a phylogenetic connection between the earlier hornless species and the later horned species via the discovery of *Diplacodon elatus*, an essentially intermediate form between the horned and hornless varieties that were known at the time (Marsh, 1875). In addition to Brontotheriidae Marsh (1873) and Limnohyidae Marsh (1875), several alternative familial names were coined, including Titanotheriidae Flower (1876), Menodontidae Cope (1881), and with Osborn unknowingly coining a term twice, Titanotheriidae Osborn (1889). Cope (1887) and Earle (1892) presented early ideas about brontothere phylogeny, although the diversity of brontotheres was not well understood at the time.

As a New York social elite, founder of the Department of Mammal Paleontology (later to be expanded to include all vertebrates), and, thereafter, president of the American Museum of Natural History, Henry Fairfield Osborn devoted the extensive resources that he had at his disposal to amassing one of the world's most scientifically valuable collections of fossil vertebrates, including the world's largest and most comprehensive collection of brontotheres from North America and Asia. Osborn spent a large portion of his scientific career studying brontotheres (Osborn et al., 1878; Scott and Osborn, 1887; Osborn and Wortman, 1895; Osborn, 1895, 1896, 1897, 1902a, 1908a, 1913, 1914, 1916, 1919, 1923, 1925, 1929b) and formulating theories on evolution and extinction derived from these studies (Osborn, 1902b, 1902c, 1908b, 1911, 1931, 1934). Many early paleontologists, particularly those who worked on large vertebrates, are regarded today as poor taxonomists with the tendency to oversplit taxa (Alroy, 2003). Osborn is no exception, but he stands out because he wrote extensively on his own evolutionary theories. It is therefore possible to understand how his evolutionary views influenced his taxonomic decisions, which reveals how fundamentally incompatible his work, and that of those who followed him, is with current phylogenetic theory and practice.

Osborn's ultimate work on brontotheres (or "titanotheres" as Osborn and many others have called them) culminated in his massive two-volume monograph, "Titanotheres of Ancient Wyoming and Nebraska" (Osborn, 1929a). The monograph largely represents collaboration between William King Gregory and Osborn himself. The titanothere monograph is exhaustive in scope, and includes a meticulous recounting of the history of early research, the original descriptions and figures of all previously named species (as of about 1920, when the monograph was mostly completed), complete descriptions of skulls, dentition, and postcrania of every brontothere known at the time, biostratigraphic summaries of the major fossil bearing strata of the North American Tertiary, and a preliminary summary of Asian brontotheres that were being recovered by the then ongoing central Asiatic expeditions of the American Museum of Natural History. Moreover, hundreds of pages are devoted to general methodological principles, biomechanics, soft tissue reconstruction, functional morphology, adaptation, paleoecology, evolutionary theory, and extinction theory.

Initially, Osborn (1896) had adopted a straightforward "monophyletic" interpretation of brontothere phylogeny that is roughly compatible with more recent evolutionary theory in the sense that organisms with similar characters are initially hypothesized as closely related. However, Osborn's evolutionary theories, which, he claimed, were largely developed through pure induction (Osborn, 1930), evolved though the years (Osborn, 1902c, 1908, 1911). In 1914, Osborn proposed his "polyphyletic" hypothesis of brontothere phylogeny, by which he recognized eleven subfamilies. In Osborn's polyphyletic interpretation, which was retained in the 1929 monograph, evolution was thought to be driven by an internal driving force (a hereditary germ) that caused lineages to evolve in parallel, thus resulting in groups with phylogenetically disparate origins giving rise to nearly identical, but distantly related taxa. Osborn drew analogies between the evolution of lineages (which he called "aristogenesis") with ontogenesis and related extinction to ideas of overadaptation or racial senescence. Osborn thought that a variety of processes caused evolution, including saltation, Darwinian natural selection, and germ-motivated orthogenesis. However, he dismissed most of these factors, including natural selection, as insignificant evolutionary driving forces and instead considered the germ the dominant evolutionary force, driving change in a predetermined direction.

To Osborn, evolution consisted of two types of "biocharacters", rectigradations (new characters) and allometrons (changes in proportions). In practice, Osborn (1929a) was preoccupied with locating "rudimentary" characters, particularly horns and tooth cusps and documenting changes within perceived lineages in the proportions of dentition, skulls, and limb segments via a series of indices, such as the cranial index (skull length/skull width). By his admission, the rudimentary characters that were deemed

important rectigradations were often imperceptible on actual specimens. Osborn (1929a) described and labeled rudimentary horns and cusps on many of the specimens figured in his monograph, diagnosed taxa, and identified perceived lineages with these structures, although in many cases direct examination of the fossils reveals no such clear structures. Perceived lineages were identified not only by their characters, but also by rates of "phylogenetic progress" as judged by changes in proportions. Sister lineages would continue to evolve in parallel because of their shared evolutionary destiny, but at different rates. Perceived lineages could be identified by their rates of evolutionary progress. In Osborn's species concept, species were arbitrary divisions along a path of germinally motivated evolutionary progress, so that nearly every minor variant would be labeled a new species. Osborn (1929a) paid lip service to recognizing sexual dimorphism, ontogenetic change, and the effects of taphonomic distortion, and he attempted to determine the sex of nearly all the specimens that he described. However, minor variations in characters that were to be deemed by him to be phylogenetically important, particularly horn, dental, and cranial index characters, were considered to indicate separate species or even separate lineages. For instance, based on Osborn's methods, minor variations in characters that were perceived as phylogenetically significant among specimens from the same stratigraphic level would indicate multiple lineages evolving in parallel at separate rates. The possibility that such differences were due to intraspecific variation was not generally considered.

Like most other paleontologists whose work preceded the "Modern Synthesis" of evolutionary theory that took place in the 1930s and 1940s, Osborn's taxonomy and phylogenetic hypotheses, which are wedded to discredited evolutionary theories, can be rejected outright. However, the problem generated by Osborn's work is compounded by the fact that the methods and results presented in his 1929 monograph have been used, often uncritically, by post–"Modern Synthesis" paleontologists as the primary reference work for nearly all subsequent research on brontotheres, leading to equally dubious results by others who have dabbled in brontothere taxonomy and other aspects of paleobiology in the post-Osbornian era. Unfortunately, Osborn's (1929a) practice of figuring, describing, and placing emphasis on "rudimentary" structures that are not always clearly present on the specimens has misled several researchers (Lane, 1932; Wilson, 1977; McCarroll et al., 1996a). For example, Wilson (1977) named a new species of horned brontothere, *Sthenodectes australis*. The referral of this new species to the genus *Sthenodectes* is clearly erroneous and was based on Osborn's (1929a) inaccurate description of the holotype skull of *S. incisivum* (CMNH 2398), which he claimed had a horn (and even labeled a horn on his figure of that specimen), even when there is plainly no such structure on the actual specimen. No specimen of *Sthenodectes incisivum* has a horn, and Wilson's (1977) horned species is actually more comparable to *Protitanotherium*, an early horned brontothere (see remarks under *Protitanotherium emarginatum*).

William Berryman Scott (1941), a colleague and lifelong friend of Osborn's, rejected Osborn's hypersplit taxonomy outright, but did not provide a definitive solution to the brontothere problem. However, in 1945 Scott described a large sample of associated *Duchesneodus uintensis* material from a single fossil quarry. Peterson (1931) preliminarily reported this quarry. Scott readily accepted the differences in the specimens as intraspecific variation, ontogeny, and taphonomic distortion. The discovery of the presumably monospecific quarry sample of *Duchesneodus uintensis* and Scott's description of it is significant because it was among the first of several apparently monospecific brontothere death assemblages now known that appear to document intraspecific variability, including variability in the very characters that Osborn and others had used to split nearly every specimen into separate species (also see Lucas and Schoch, 1989b).

Few followed Scott's (1941, 1945) lead in recognizing the hypersplit nature of brontothere taxonomy. New species of North American brontotheres and minor taxonomic revisions have trickled into the literature over the years following Osborn's (1929a) monograph, which was essentially completed in

1920 (Cook, 1926; Peterson, 1931, 1934; Stock, 1935, 1936; Russell, 1940; Stovall, 1948; West and Dawson, 1975; Wilson, 1977; Lucas and Schoch, 1982, 1989b; Mader and Alexander, 1995; Gunnell and Yarborough, 2000; Mader, 2000). Nonetheless, little attempt has been made to extensively revise Osborn's deeply flawed taxonomy, except for Mader's (1989, 1998) work on the higher-level taxonomy of North American brontotheres. However, Mader's revision of higher taxa (genera) was not substantiated by a published reworking of brontothere species taxonomy.

Although North American brontothere diversity had been well documented by the beginning of the 20th century, it was not until 1912 that the first brontotheres were reported from Asia, from the Pondaung Formation of Myanmar (Burma) (Pilgrim and Cotter, 1916; Pilgrim, 1925). In the 1920s and early 1930s, field crews from the American Museum of Natural History revealed a diversity of brontotheres in the Eocene deposits of central and southeast Asia (Osborn, 1923, 1925, 1929a, 1929b; Colbert, 1938; Granger and Gregory, 1938, 1943) that rivaled the known diversity of brontotheres in North America. Osborn (1923, 1925, 1929a, 1929b) published a series of papers with short and hurried descriptions of some of this material, in some cases actually describing and figuring the specimens while still in their plaster encasings. Despite his tendency to oversplit North American brontotheres, Osborn adopted the peculiar practice of lumping most of the newly discovered Asian brontotheres into various North American genera (*Telmatherium*, *Manteoceras*, *Dolichorhinus*, *Protitanotherium*), despite that fact that many of the Asian specimens obviously represent very different taxa. Following Osborn's death, Granger and Gregory (1943) extensively revised the taxonomy of central Asian brontotheres. Recognizing problems with Osborn's genus-level assignments of Asian brontotheres, Granger and Gregory (1943) erected many new genus names and assigned Asian taxa to new subfamilies. However, they adopted the general methodology of Osborn (1929a) and oversplit species based on barely perceptible differences in size, proportions, often when the differences are clearly attributable to taphonomic distortion or ontogeny. They perceived such differences as evolutionary stages, and, like Osborn, they did not consider the possibility that such minor differences simply represented random intraspecific variation, as Scott (1945) demonstrated shortly thereafter.

Although it has remained the primary reference for Asian brontotheres, the revision of central Asian brontotheres (Granger and Gregory, 1943) was clearly done in a hurried fashion and it has numerous problems. Some specimens were mistakenly referred to multiple species. Specimens that are obviously juveniles were apparently confused as adults, thus resulting in extremely erroneous taxon diagnoses. Species diagnoses tended to describe single specimens, while the lists of referred specimens provided by Granger and Gregory (1943) were carelessly assembled without consideration of whether they possessed the diagnostic features of the particular species to which they were assigned. In some instances, specimens that Osborn had correctly identified were actually misidentified by Granger and Gregory (1943). Granger and Gregory (1943) admitted that many of the species included in their revision were not even valid.

Subsequently, many paleontologists, primarily Chinese and Russian workers, have continued to name Asian brontothere taxa and a few have reevaluated Asian brontothere taxonomy on a limited scale (Dehm and Oettingen-Spielberg, 1958; Chow and Hu, 1959; Xu and Chiu, 1962; Chow et al., 1974; Yanovskaya, 1953, 1957, 1976; Dashzeveg, 1975; Wang, 1978, 1982; Miao, 1982; Ye, 1983; Qi, 1987; Qi and Beard, 1996; Wang, 1997; Holroyd and Ciochon, 2000; Mihlbachler et al., 2004a). However, the AMNH collection from the Central Asiatic Expeditions of the 1920s and 1930s is still the largest collection of Asian brontotheres in the world and contains the majority of holotypes, but for the most part this large but poorly documented collection has remained unutilized until recently (Mihlbachler et al., 2004a). The problematic work of Granger and Gregory (1943), which represents all that subsequent Chinese, Mongolian, and Russian workers had to go on, has only compounded the problem of Asian bron-

tothere systematics. For instance, Yanovskaya (1980) contributed a major monograph on Mongolian brontotheres and described several new species. However, much of Yanovskaya's work is unreliable because she did not have direct access to the AMNH collection of Asian brontotheres. As a result the majority of the material reported in her monograph was misidentified (Mihlbachler et al., 2004a). Recently, Wang et al. (1999) provided a review of Chinese brontotheres, although no attempt was made to revise the taxonomy or evaluate phylogeny.

Granger and Gregory (1943) were the first to propose an explicit phylogenetic hypothesis of Asian brontotheres. They largely viewed the radiation of Asian brontotheres as separate from those of North America, but noted some similarities between North American and Asian brontotheres during what is now considered the middle Eocene. Yanovskaya (1980) and Wang (1982) proposed similar phylogenies for Asian brontotheres but used outdated methods similar to those of the 1940's. Mihlbachler et al. (2004a) recently developed a phylogenetic hypothesis of Asian horned brontotheres, but noted that Asian brontotheres, although commonly viewed as being a separate radiation, probably do not constitute a truly monophyletic assemblage. However, the interrelationships of North American and Asian brontotheres have not been rigorously examined, due to the lack of published phylogenetic analyses that incorporate taxa from both continents.

METHODS OF TAXONOMIC REVISION

The aim of this work is to provide a cladistically generated phylogenetic hypothesis of the Brontotheriidae that includes all the known valid species. Because of the presently dubious nature of many brontothere species and lack of reliable published descriptions and figures, it was necessary to first evaluate the taxonomic validity of most species and provide adequate descriptions that (1) allow for the unambiguous diagnosis of terminal taxa (species), (2) examine patterns of intraspecific variability, and (3) facilitate the development of phylogenetic character data. Teeth, skulls, and mandibles are incorporated into this study. Postcrania were not used, largely due to a lack of associated cranial and postcranial material for most species. For the most part actual specimens or casts were examined with some exceptions. In several instances references were made to published figures and archived photographs of specimens that were lost or were otherwise inaccessible.

I was able to examine and describe the craniodental morphology of nearly every taxon that had ever been named. Two recently named species, *Aktautitan hippopotamopus* Mihlbachler et al. (2004a) and *Eubrontotherium clarnoensis* (Mihlbachler, 2007), were named and described using the methods consistent with those adopted here and are a part of this study, but they were published separately. As far as I am aware, all known Asian taxa are addressed here with the exception of a yet undescribed brontothere from Japan (Miyata and Tomida, 2003). All North American brontotheres were included in the phylogenic analysis, but some of them were not considered for taxonomic revision; these include: *Eotitanops* Osborn (1907), an unnamed species referred to as cf. *Eotitanops* by Eberle (2006), *Palaeosyops* Leidy (1870a), and *Megacerops* (sensu Mihlbachler et al. 2004b). Gunnell and Yarborough (2000) recently examined *Eotitanops* and *Palaeosyops*. *Eotitanops* and *Palaeosyops*, which are presumably the most basal brontotheres, have already been incorporated into general analyses of perissodactyl phylogeny (Froehlich, 1999; Lucas and Holbrook, 2004) and are not as problematic as most other brontothere taxa.

Late Eocene brontotheres (*Megacerops* sensu Mihlbachler et al., 2004b) primarily from the Chadron Formation have previously been assigned to a number of genera, including *Menodus* Pomel (1849), *Titanotherium* Leidy (1852), *Megacerops* Leidy (1870b), *Brontotherium* Marsh (1873), *Symborodon* Cope (1873b), *Brontops* Marsh (1887), *Menops* Marsh (1887), *Titanops* Marsh (1887), *Allops* Marsh (1887), *Diploclonus* Marsh (1890), *Ateleodon* Schlaikjer (1935), and other genera were not revised here. These brontotheres consist of hundreds of complete skulls that, according to Osborn (1929a), represent at least 37 species. Others consider them to represent far fewer than 37 species

(Scott, 1941; Clark et al., 1967; Mader, 1989, 1998; Mihlbachler et al., 2004b). A revision of these particular brontotheres is beyond the scope of this paper but is preliminarily addressed in Mihlbachler et al. (2004b) and will be addressed more extensively in a future publication. Many of the invalid taxa, including nomina dubia are discussed with other taxa when appropriate, although there is a separate section on miscellaneous dubious species and other problematic taxa. Dubious taxa not considered in this paper are those that were already established as dubious by Osborn (1929a).

In the following revision, I provide only diagnoses and descriptions of species taxa. Higher taxa are discussed following the results of the cladistic analysis. Within the descriptions, intraspecific variation is meticulously documented using all of the specimens assigned to a particular species. Terminology for the upper and lower premolars and molars used in the descriptions is shown in figure 4.

It is traditional to provide a diagnosis for each species. While it is agreed that a species diagnosis should contain information that validates a taxon, there is not complete agreement on how this should be done (e.g., differential diagnosis versus apomorphy-based or autapomorphy-based diagnoses). It is obvious that the main function of the diagnosis, taxon validation, is also served by the coded character data (table 13). If the character data demonstrate a unique combination of states, then the species is validated. The traditional diagnoses given in this paper consist of two parts: (1) an abbreviated description pointing out some of the more obvious characters used in identification and (2) one or a few sentences that explicitly validates the species by using the minimal amount of information necessary to differentiate it from the most similar taxa.

Species Concept and Species Delimitation

Despite the large body of literature on theoretical species concepts, paleontologists do not usually explicitly state or explain their species concepts when diagnosing new taxa or revising previously named taxa or performing phylogenetic analyses with species. Because of the many deterministic and stochastic processes associated with speciation, species boundaries are often fuzzy and different methods are widely known to yield discordant results (Sites et al., 2004). Species-level taxonomy in paleontology is often viewed as a subjective process and species are often based on minor size differences between specimens or other minor differences found between specimens, despite the fact that size and shape should be expected to vary to some degree in all species. For instance, body-size fluctuations among modern species are clearly documented by the Pleistocene and Holocene record (e.g., Mihlbachler et al., 2002). Species boundaries are also sometimes placed between specimens or groups of specimens that are from different localities or different stratigraphic levels, even when there may be substantial size overlap between these samples and/or when other clear diagnostic characters are not present. The taxonomic relevance of such distinctions is ambiguous and taxa delineated in such terms are not necessarily suited to cladistic analysis if differing combinations of character states and/or other autapomorphies cannot characterize them.

Given the amount of taxonomic revision presented in this work, it seems appropriate to devote some discussion to species delimitation, how it was accomplished, and suggestions for future approaches. Because of the sometimes fuzzy nature of species boundaries and/or limitations in the available data, complete objectivity is not always possible when delimitating species; those represented by fossils tend to be more problematic due to the inevitably highly fragmented nature of at least some of the material. However, I was able to apply a reasonably objective set of operational criteria for delimiting species that is theoretically consistent with the phylogenetic species concept, which defines species operationally as the smallest diagnosable clusters of specimens (Cracraft, 1989; Nixon and Wheeler, 1990; Wheeler and Platnick, 2000). No two fossils are exactly alike, and those practicing taxonomy and/or working with species as terminals in phylogenetic analyses must ultimately draw a distinction between tokogenic character variation (sexual dimorphism, ontogeny, or other popula-

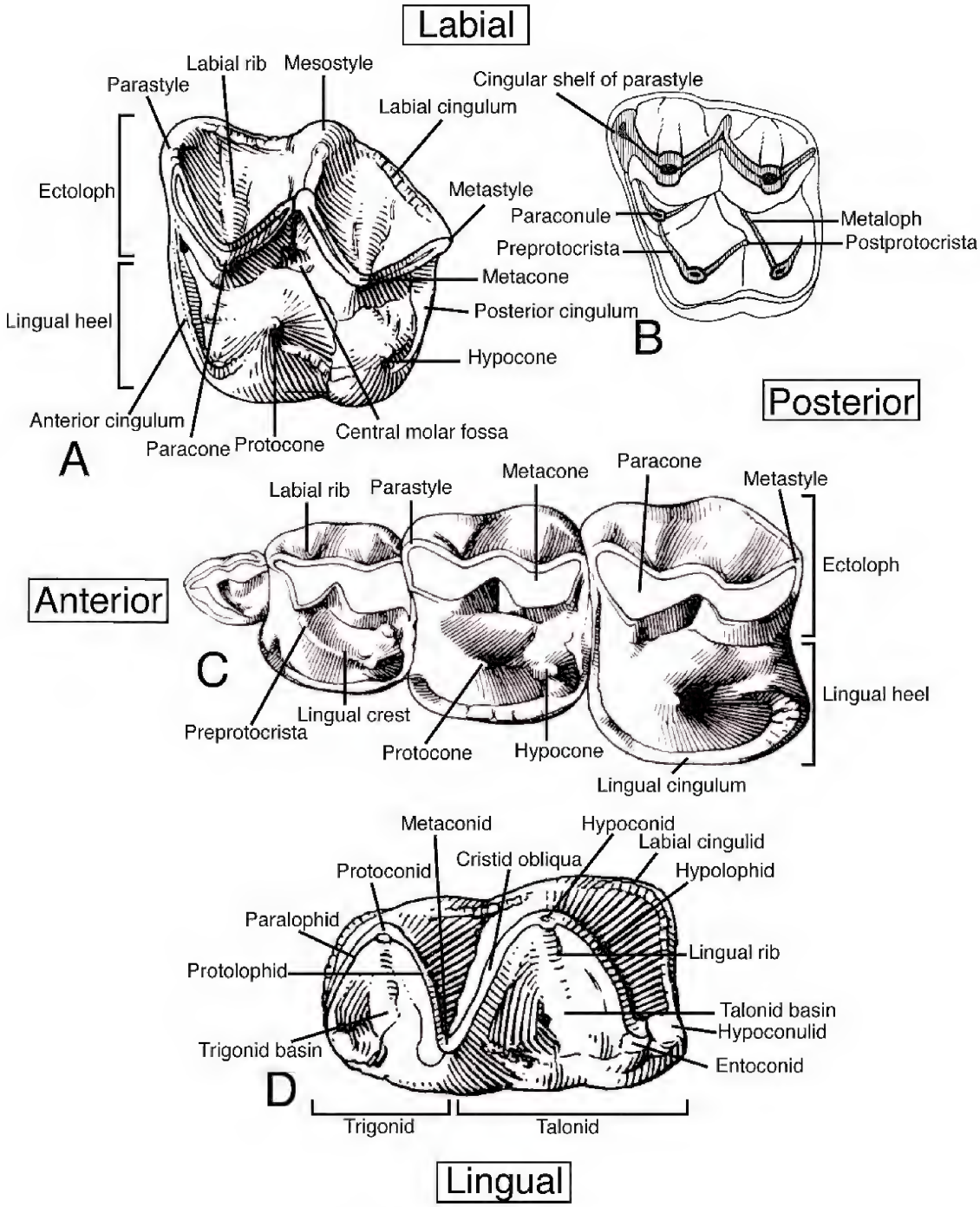

Fig. 4. Dental terminology for upper and lower cheek teeth. **(A)** Generalized brontothere upper molar, **(B)** *Lambdotherium* upper molar, showing characters that are either vestigial or absent in some or all brontotheriids, **(C)** generalized brontothere upper premolars (P1–P4), **(D)** brontothere lower molar. Figures of teeth are taken from Osborn (1929a).

tion variation) and phylogenetic character variation (species differences). Making this distinction is particularly problematic for fossil species because information on populations is severely limited. Nevertheless, considerable specimen-to-specimen variability was encountered among brontothere fossils. Treating all of these differences as taxonomically significant would have resulted in hundreds of obviously invalid species, with most represented by only a single specimen. This is essentially the same pitfall that misled earlier taxonomists into erecting unrealistic numbers of species.

To develop a set of taxon delimitation criteria, characters with tokogenic tendencies were identified and differentiated from species-level characters using a method comparable to population aggregation analysis (Davis and Nixon, 1992; Sites et al., 2004), but modified in ways to deal with the more restricted information about fossil populations. In population-aggregation analysis, (1) all individuals sampled from a population are assumed to be conspecific and (2) two or more populations are considered conspecific when the individuals drawn from these populations show identical character attributes, while populations that show one or more different character attributes are delimited. In true population-aggregation analysis, population boundaries are drawn around clusters of specimens (e.g., specimens collected from one locality), which are then assumed to be conspecific. In comparison to extant species whose individuals are sampled over a single geological interval, it is more difficult to draw population boundaries around clusters of fossils, even if they occur in a single geographic locality because the specimens are often separated by geological time. Moreover, many of the important fossil specimens are in older museum collections and lack adequate locality and stratigraphic data. In these instances, the degree to which such specimens are separated by time is very poorly constrained. Nonetheless, it is important to consider all specimens that show different combinations of character attributes. However, the addition of the time dimension increases the difficulty of determining whether differences between individual fossil specimens represent intraspecific polymorphism (taxonomically insignificant tokogenic variation), whereby specimens would be grouped into one species, or whether the differences are a consequence of evolution (taxonomically significant phylogenetic differences), in which case the specimens would be subdivided among multiple species.

One way of testing for the taxonomic significance of character differences between two or more temporally asynchronous fossil specimens would be by examining the populations of closely related species for which population information is available. For instance, suppose that two fossil specimens that are temporally asynchronous and/or from different localities show two different states for a single character, but that character is found to have polymorphic tendencies (i.e., exhibits both states) within one or more of the populations of the species comprising the extant phylogenetic bracket of the two fossil specimens. In this case, the conspecificity of these specimens cannot be falsified. One the other hand, if the same character shows monomorphic tendencies (exhibits one state) within all of the populations of the species comprising the extant phylogenetic bracket, the two specimens in question can be considered separate species. An extant phylogenetic bracket approach is perhaps an ideal way to approach the problem of species delimitation and would work best when dealing with taxa (actually, specimens) with a more refined phylogenetic background. However, this approach was not completely feasible with brontotheres; they are all, of course, extinct, with no close living relatives. Moreover, prior to this study, the interrelationships of brontotheres were poorly understood, and their position in relation to other perissodactyls remains ambiguous.

Fortunately, however, population information is available for a few brontothere species that are known from quarry samples containing assemblages of associated individuals who died instantaneously or during a very brief interval of time. Such mass death assemblages offer rare glimpses into the populations of extinct species (Voorhies, 1969; Turnbull and Martill, 1988; Lucas and Schoch, 1989b; Berger, 1983; Berger et al. 2001; Mihlbachler, 2003b, 2005; Prothero,

2005). The existing brontothere mass death assemblages (all assumed to be monospecific) were used as guidelines to preliminarily screen for characters with intraspecific polymorphic (tokogenic) tendencies that were potentially uninformative of species boundaries. Mass death assemblages of *Metarhinus* sp., *Duchesneodus uintensis*, and *Megacerops coloradensis* (Turnbull and Martill, 1988; Scott, 1945; Gregory and Cook, 1928) were examined. A few other species, such as *Eubrontotherium clarnoensis*, are known from more limited numbers of associated individuals but were also valuable in identifying characters with polymorphic tendencies. It was found that all of these samples contained common patterns of polymorphism. All samples revealed conspicuous intraspecific variability in premolar morphology, canine size, the size and presence of the M3 hypocone, horn size and shape, and overall skull robusticity. (These characters and their polymorphic tendencies are discussed in more detail in the individual species descriptions.) The consistency of this pattern from assemblage to assemblage suggests a widespread pattern of intraspecific polymorphism throughout the Brontotheriidae. The apparent tokogenic variation in horns, canine size, and overall skull robusticity most likely relates to sexual dimorphism (Mihlbachler et al., 2004b). Notably, other tokogenic variation, particularly the rampant variability of premolar morphology is also apparent in other perissodactyls, most notably ceratomorphs including both rhinocerotoids and tapiroids (Matthew, 1931; Radinsky, 1963, 1967a, 1967b; Prothero, 2005). Before paleontologists like Matthew and Simpson began thinking in terms of population variability, rampant premolar variation led to similar taxonomic oversplitting in these groups. Apparently, this pattern of tokogenic variability is widespread throughout the Perissodactyla.

In the next level of analysis, individual brontothere specimens were examined considering only those characters that did not show polymorphic tendencies in the mass death assemblages. Groups of specimens showing identical attributes were considered conspecific, while specimens showing one or more different character attributes among characters showing monomorphic tendencies were considered different species. Finally, once the specimens had been aggregated into species-specific groups, the rules of zoological nomenclature were used to determine the proper species name.

Utilization of this modified population-aggregation analysis method led to the synonomization of many species and the discovery a few new ones, while many other species were rendered dubious or otherwise problematic. The dubious status of many species relates largely to that fact that many specimens were not directly comparable because they were not known from anatomically overlapping parts (e.g., a jaw and a skull). In instances where two or more specimens representing non-overlapping parts were of similar size and from similar time periods and geographically similar regions, conspecificity could not be falsified. In such instances, if two or more noncomparable specimens were a type, I considered no more than one of these to be valid, while the remaining were considered nomina dubia.

Measurements

Morphometric data were compiled during this study. Unfortunately, quantitative methods (e.g., principal-components analysis) did not prove to be very useful in delimiting species; the distorted condition of most brontothere specimens would have severely complicated any interpretation made from such analyses. Likewise, variable dental wear limited morphometric analysis of dentitions. Nor was overall size an important factor in delimiting species. Many brontothere species overlap in body size. There were a few exceptions where two morphologically similar species were found to be vastly different in body size; in these cases, the difference is obvious without examining quantitative data. More kinds of measurements were taken than are actually reported, but many of the cranial and mandibular measurements are easily influenced by distortion. Therefore, I have limited the included measurements to basic dental measurements and a few basic cranial measurements. All dental measurements and cranial measurements of small skulls were made with digital calipers; cranial

measurements of larger specimens were taken with a combination of large wooden calipers or a metric tape measure. Measuring methods differ due to the unmanageable size of many specimens, some of which could not easily be removed from their storage units. For those species known from adequate samples, basic summary statistics (mean, standard deviation, coefficient of variation) of a few variables have been provided in tables to document general size variability within species. The remaining morphometric data on specimens used in this study is provided in appendix 1 in the hope that it will be useful in the identification and/or comparison of future specimens. Although most of these data were not directly utilized in the study, it is nevertheless important to document size. Moreover, the morphometric data were mostly gathered by a single observer (myself) using consistent landmarks and are more reliable than the vast pool of morphometric data on brontotheres from other published sources, which were collected by many different observers, often on heavily distorted specimens, and without well-defined landmarks. The measurements are described below. For the dental abbreviations, upper case letters refer to upper teeth and lower case letters refer to lower teeth.

1. I1l and i1L (first incisor length)—greatest length of medial incisor, measured mesiodistally.
2. I1W and i1W (first incisor width)—greatest labiolingual width of medial incisor crown.
3. I2L and i2L (second incisor length)—greatest length of intermediate incisor, measured mesiodistally.
4. I2W and i2W (second incisor width)—greatest labiolingual width of intermediate incisor crown.
5. I3L and i3L (third incisor length)—greatest length of lateral incisor, measured mesiodistally.
6. I3W and i3W (third incisor width)—greatest labiolingual width of lateral incisor crown.
7. CL and cL (canine length)—maximum diameter of canine crown, measured at the proximal base of the canine crown.
8. P1L and p1L (first premolar length)—maximum anteroposterior length of first premolar.
9. P1W and p1W (first premolar width)—maximum labiolingual width of first premolar.
10. P2L and p2L (second premolar length)—maximum anteroposterior length of second premolar. In upper premolars, this was measured on the labial side; in lower premolars, it was measured from the lingual side, or in heavily worn teeth, through the middle of the tooth.
11. P2W and p2W (second premolar width)—labiolingual width of second premolar. In upper teeth, this was measured from the labial side of the paracone to the lingual side of the protocone. In lower teeth, the maximum width of the talonid was measured.
12. P3L and p3L (third premolar length)—maximum anteroposterior length of third premolar, as described under measurement 10.
13. P3W and p3W (third premolar width)—labiolingual width of third premolar, as described under measurement 11.
14. P4L and p4L (fourth premolar length)—maximum anteroposterior length of fourth premolar, as described under measurement 10.
15. P4W and p4W (fourth premolar width)—labiolingual width of fourth premolar, as described under measurement 11.
16. M1L and m1L (first molar length)—maximum anteroposterior length of first molar. In upper teeth, this is measured on the labial side. In lower teeth, this was measured on the lingual side or, in heavily worn teeth, along the midline of the tooth.
17. M1W and m1W (first molar width)—labiolingual width of first molar. In upper teeth, this was measured from the labial margin of the mesostyle to the lingual margin of the protocone. In lower teeth, the width of the talonid was measured.
18. M2L and m2L (second molar length)—maximum anteroposterior length of second molar, as described under measurement 16.
19. M2W and m2w (second molar width)—labiolingual width of second molar, as described under measurement 17.
20. M3L and m3L (third molar length)—maximum anteroposterior length of third molar, as described under measurement 16.
21. M3W and m3W (third molar width)—labiolingual width of third molar, as described under measurement 17.
22. P2–P4 and p2–p4 (premolar row length)—maximum length of premolar tooth row, excluding P1 or p1.
23. M1–M3 and m1–m3 (molar row length)—maximum length of molar row.
24. P2–M3 and p2–m3 (cheektooth row length)—maximum length of cheektooth row, excluding P1 or p1.

25. VL (ventral skull length)—length of skull measured on the ventral surface from the incision to the occipital condyles.
26. MVL (modified ventral skull length)—length of skull measured from the anterior margin of the P2 (either right or left) to the occipital condyle of the same side.
27. SW (skull width)—maximal skull width measured across the maximum span of the zygomatic arches. Note that among all of the listed metric variables, this particular variable (along with other possible variables related to skull width) is the most likely to have been effected by subtle distortion, and these data should be examined with caution.

INSTITUTIONAL ABBREVIATIONS

AMNH	Division of Vertebrate Paleontology, American Museum of Natural History, New York
ANSP	Academy of Natural Sciences of Philadelphia, Philadelphia
BMNH	British Museum of Natural History, London
CMNH	Carnegie Museum of Natural History, Pittsburgh
DMNH	Denver Museum of Nature and Science, Denver
F:AM	Frick Collection, Division of Paleontology, American Museum of Natural History, New York
FMNH	Field Museum of Natural History, Chicago
GSI	Geological Survey of India, Calcutta
GSP	Geological Survey of Pakistan, Islamabad
IVPP	Institute of Vertebrate Palaeontology and Palaeoanthropology, Beijing
KAN	Institute of Zoology, Kazak Academy of Sciences, Almaty, Kazakstan
LACM	Natural History Museum of Los Angeles County, Los Angeles
LACM/CIT	California Institute of Technology collection now housed in the Los Angeles County Museum, Los Angeles
NMC	National Museum of Canada, Ottawa
NMMP	Paleontology Department of the National Museum, Myanmar
PIN	Paleontological Institute of the Russian Academy of Sciences, Moscow
SDSM	Museum of Geology, South Dakota School of Mines and Technology, Rapid City, South Dakota
SMNH	Saskatchewan Museum of Natural History, Regina
TMM	Texas Memorial Museum, University of Texas, Austin
UCM	Museum of Natural History, University of Colorado, Boulder
UCMP	Museum of Paleontology, University of California at Berkeley, Berkeley
UMUT CV	Cenozoic vertebrate in the University Museum of the University of Tokyo, Japan
USNM	United States National Museum of Natural History, Smithsonian Institution, Washington
VM	Geological Museum of China, Beijing, China
VPL/K	Punjab University, Chandigarh, India
YPM	Yale Peabody Museum of Natural History, Yale University, New Haven Connecticut
YPM PU	Princeton University Natural History Museum (now in the collection of the Yale Peabody Museum of Natural History)

SYSTEMATIC PALEONTOLOGY

CLASS MAMMALIA LINNEAUS, 1785
ORDER PERISSODACTYLA OWEN, 1848
FAMILY BRONTOTHERIIDAE MARSH, 1873
SUBFAMILY BRONTOTHERIINAE MARSH, 1873

Bunobrontops savagei Holroyd and Ciochon, 2000

HOLOTYPE: UCMP 128416, a right M2.

TYPE LOCALITY: Pondaung Formation, approximately 3 miles (4.8 km) north of Bahin village, Pale Township, Myanmar.

AGE: Middle Eocene (Sharamurunian land mammal "age").

REFERRED SPECIMENS: **(all from the Pondaung Formation of Myanmar)** UCMP 128391, a left M2; UCMP 128414, a right m3; UCMP 147045, a right M3; UCMP 147046, a right molar protocone; UCMP 147047, a left m1 or m2 talonid; UCMP 147048, a left m1 or m2 trigonid; NMMP-KU 0312, a left M3; NMMP-KU 0313, a partial right upper molar (M3?); NMMP-KU 0319, a right molar fragment with a protocone and paracone; NMMP-KU 0333, a left m1 or m2 talonid.

DIAGNOSIS: *Bunobrontops savagei* exhibits a unique and highly distinctive combination of molar characteristics that differentiate it from primitive brontotheres such as *Palaeosyops* as well as all more derived species of Brontotheriinae. Molar plesiomorphies retained by *B. savagei* include a brachydont ectoloph, strong upper and lower molar ribs (most clearly visible in specimens with minimal dental wear), rounded lingual sides of the paracone and metacone, retention of small paraconules and a metalophlike ridge of enamel on the (M2) hypocone, and a rather short and broad m3. *Bunobrontops savagei* lacks both a central molar fossa and an anterolingual cingular cusp on the upper molars. Brontotheriine molar apomorphies exhibited by *B. savagei* include the lack of a cingular shelf on the parastyle, and a lingually directed ectoloph. The lingual enamel of the upper molar ectoloph is similar in thickness to the labial ectoloph enamel, a condition intermediate between the thickened enamel of *Palaeosyops* and the thinned enamel of most other brontotheriines. Finally, the upper and lower molars of *Bunobrontops savagei* tend to have deep, conspicuous crenulations, an autapomorphic condition.

DESCRIPTION

UPPER DENTITION: *Bunobrontops savagei* is known only from isolated upper and lower molars, but because of the distinctive molar morphology of this species, even partial molars retain diagnostic features (fig. 5). The upper molars of *Bunobrontops savagei* exhibit the strongly W-shaped molar wear facet that is characteristic of brontotheriines, but the molar morphology of this species is intermediate between more primitive brontotheres such as *Palaeosyops* and *Eotitanops* and more highly derived brontotheriines. The upper molar parastyle lacks a strong anterior cingulum that in more primitive brontotheres such as *Palaeosyops* forms a small anterolabial occlusal shelf. However, like *Palaeosyops*, the upper molar ectoloph is very brachydont and not much taller than the lingual cusps. The ectoloph is shorter than any other brontotheriine. However, the labial wall of the ectoloph is nearly flat and is angled in a lingual direction. This resembles other brontotheriines and contrasts with *Palaeosyops* in which the labial walls of the paracone and metacone are strongly concave, leading to more erect cusps. Holroyd and Ciochon (2000) described the labial ribs of the upper molars as slightly developed; however, this seems to be an artifact of wear in the holotype (UCMP 128416, fig. 5a), because a nearly unworn molar, NMMP-KU 0313 (fig. 5c), has wide and prominent labial ribs that are similar to those of *Palaeosyops* but are broader and more distinct than those seen in more advanced brontotheriines.

The lingual sides of the paracone and metacone of *Bunobrontops savagei* are rounded as seen in *Palaeosyops*. This contrasts with more derived brontotheriines in which the inner sides of the paracone and paracone are acutely wedged, particularly toward the distal apex of the cusps. The enamel on the lingual margins of the paracone and metacone is about as thick as that of the labial enamel; however, the enamel between these cusps is slightly thinner on the lingual side of the ectoloph. Overall, the lingual ectoloph enamel in *Bunobrontops savagei* seems intermediate in thickness. The lingual ectoloph enamel is thinner in comparison to *Palaeosyops*. However, the lingual ectoloph enamel of other brontotheriines is much thinner than that of *Bunobrontops savagei*.

The upper molars of *Bunobrontops savagei* lack some apomorphies that are distinctive of more advanced brontotheriines, such as a central molar fossa and an anterolingual cingular cusp. Several plesiomorphic traits are retained. For instance, there is a small anteriorly positioned paraconule. The upper

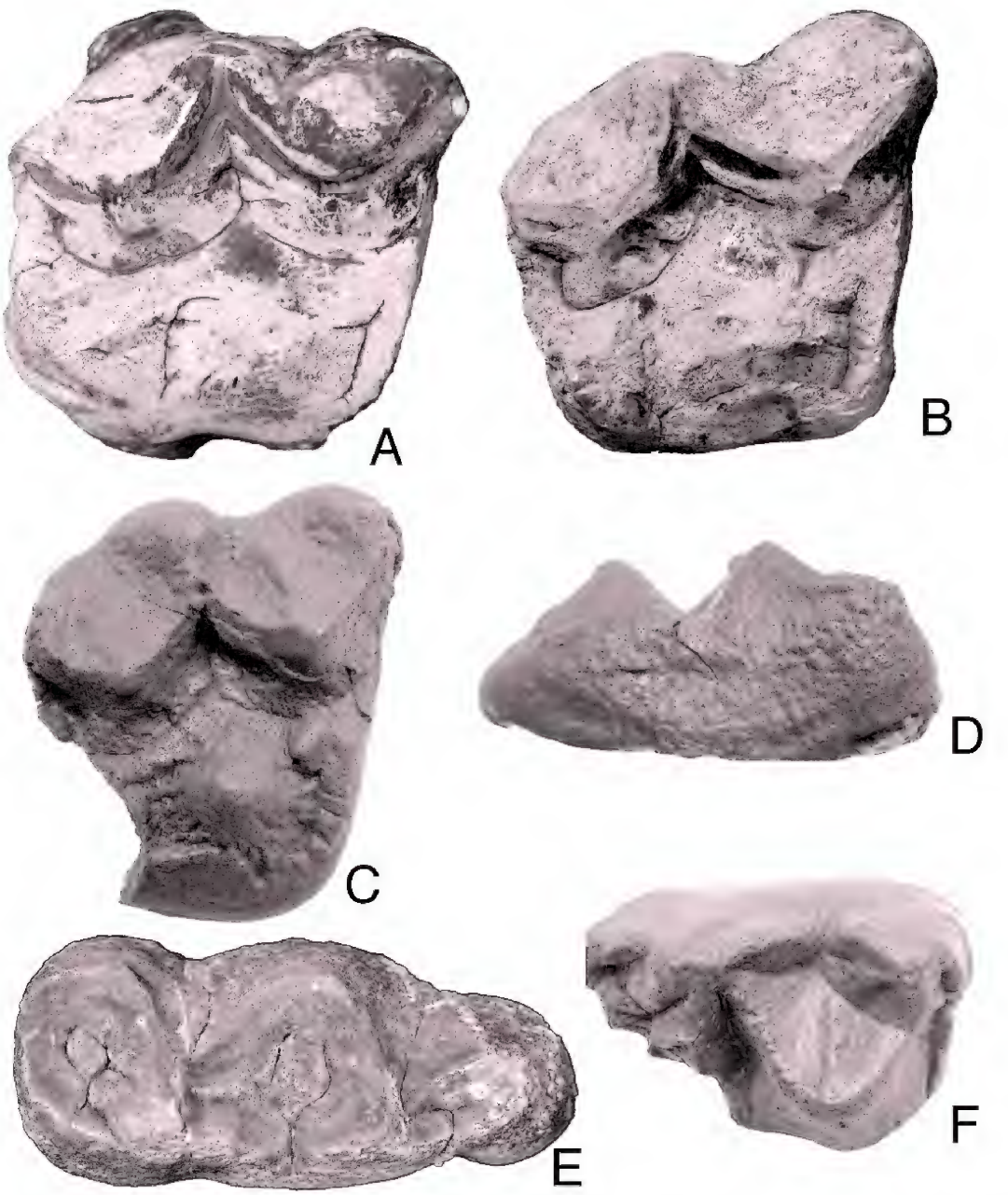

Fig. 5. Selected molars of *Bunobrontops savagei*. **(A)** A right M2 (UCMP 128416, holotype), **(B)** a right M3 (UCMP 147045), **(C)** occlusal and **(D)** anterior views of a right upper molar (M3?) (cast of NMMP-KU 0313), **(E)** a right m3 (UCMP 128414), and **(F)** a left partial molar (cast of NMMP-KU 0333).

molars also retain a prominent metalophlike ridge that runs down the labial slope of the hypocone in an anterolabial direction. One M3, UCMP 147045 (fig. 5b) lacks a hypocone, although the posterolingual corner of the tooth bears a thick, crenulated, raised cingulum. Another M3, NMMP-KU 0312 (not shown), has a similar raised posterolingual cingulum and a metalophlike ridge of enamel situated just lingual to the metacone. The labial cingulum of the molars is weak. There is no lingual cingulum, although

the posterior cingulum wraps around the lingual side of the hypocone in M2.

The dentition of *Bunobrontops savagei* is peculiar in that the enamel is crenulated, with narrow grooves running along the lingual bases of the ectolophs in the valleys between the protocones and hypocones, and on the anterior and distal sides of the molar crowns. The enamel of heavily worn specimens tends to be much smoother than the roughened and heavily crenulated enamel of unworn or lightly worn specimens.

LOWER DENTITION: The single complete lower molar, UCMP 128414 (fig. 5e), a right m3, is identifiable as *B. savagei* largely because of the peculiar enamel crenulations in the trigonid and talonid occlusal valleys; these crenulations characteristically resemble those of the upper molars. The basins of the trigonid and talonid are very shallow. The m3 is only slightly longer than those of *Palaeosyops* with a length/width ratio of 2.0, but it is clearly shorter and broader than most brontotheriines whose length/width ratios are always above 2.0. The deep crenulations in the occlusal basins tend to obscure the lingual lower molar ribs of the protoconid and hypoconid. However, a lingual lower molar rib is prominent in NMMP-KU 0333 (fig. 5f), an unworn lower molar fragment. In UCMP 128414, the cristid obliqua intersects the protolophid in the middle of the tooth, rather than meeting the metaconid. This character is unusual, and seems to be limited to this specimen. Another specimen, NMMP-KU 0333, an m1 or m2 fragment, has a cristid obliqua that joins the metaconid on the lingual side of the tooth. A slight cingulid surrounds the base of the hypoconulid of the m3 (Holroyd and Ciochon, 2000), but cingulids are generally very weak or absent in the lower molars of *Bunobrontops savagei.*

REMARKS

Holroyd and Ciochon (2000) based *Bunobrontops savagei* on isolated teeth from the Pondaung Formation, Myanmar. In the same year, Tsubamoto et al. (2000) reported several additional specimens, all isolated teeth, from the Pondaung Formation that clearly represent the same species. Despite the extremely fragmentary nature of brontothere material from the Pondaung Formation, *Bunobrontops savagei* can clearly be distinguished from other Pondaung brontotheres, and, indeed, all other brontotheres due to a unique combination of molar characters. These include plesiomorphic characters shared with basal brontotheres like *Palaeosyops*, such as a brachydont ectoloph, prominent labial ribs, and rounded lingual sides of the paracone and metacone. Derived characters shared with other brontotheriines such as *Mesatirhinus junius* include a lingually angled ectoloph, unthickened enamel on the lingual sides of the paracone and metacone, and the lack of a cingular parastyle shelf. Holroyd and Ciochon (2000) recognized that *Bunobrontops savagei* represents a clear morphological link for what is otherwise an abrupt morphological transition from the more bunodont molar condition seen in *Palaeosyops* and *Eotitanops*, to the more derived molars of advanced brontotheres.

Mesatirhinus junius (Leidy, 1872)

HOLOTYPE: ANSP 10349, a right p4; ANSP 10348, a partial left m3, apparently from the same individual.

TYPE LOCALITY: Bridger Basin, Wyoming.

SYNONYMS: *Mesatirhinus megarhinus* (Earle, 1891); *Mesatirhinus petersoni* Osborn, 1908a.

AGE: Middle Eocene (Bridgerian and possibly early Uintan land mammal "ages")

REFERRED SPECIMENS: **(From the Bridger Basin, Wyoming)** AMNH 1509, a skull with right and left P1–M3; AMNH 1523, a palate with right P1–M3, left P1, and P3–M3; AMNH 1520, a left mandibular ramus with c–m3; AMNH 1551, a partial left mandibular ramus with c and p2–m2; AMNH 1567, a mandible with right c, p2–m3 and left c–m3; AMNH 1627, a mandible fragment with right m3; AMNH 12184 (holotype of *Mesatirhinus petersoni*), a skull missing the occiput and right zygomatic arch with right P2, P3, P4–M3 (partial), left P2–P4, M1–M2 (partial), and M3; AMNH 12191, a right maxilla fragment with M2–M3 and a left mandibular fragment with p2–m3; AMNH 12199, a mandible with right and left p3–m3; AMNH

12202, a skull missing the premaxillae with right C–M3 and left P2–M3; AMNH 12206, a skull fragment with right C–P4, M1–M2 (partial), left P1–P4, and M1–M3 (partial); AMNH 12211, a mandible with right i3(?), p2, p3, p4 (partial) and left p2–m1; AMNH 12686, maxillary fragments with right M2 and M3; BMNH.M10471 (formerly AMNH 1556), a skull with right P1–M3 and left C–M3; UCM 72430, a crushed skull fragment; USNM 26111, a mandible with right p2–p4, m3, left p3–p4, m1 (partial), and m2–m3; USNM 26116, a skull with right P2–M3 and left P4–M3; USNM 26123, a fragmented skull; USNM 26136, a skull with right C, P3–M3 and left C–M3; USNM 26148, a left mandibular ramus with p2–m3; USNM 26151, a mandible with right, left p3–m3, and fragmentary canines and incisors; USNM 363884, a left mandibular ramus with p2–m2, isolated incisors and p1; YPM PU 10242, a left maxilla fragment and associated upper teeth, including right P2–M1, left M2, and M3; YPM 11070, a partial skull with right P2–M3; YPM 11148, a skull with right P1–M3, left P3, M1–M3; YPM 11149, a skull with right and left M3; YPM 16420, a partial skull with left P2–P3, M1–M3; YPM 16423, a right maxilla with P2–M3; YPM 16421, a partial mandible with p4–m3, YPM 16722, a right maxilla fragment with P4–M2, M3 (partial), and left maxilla fragment with M1–M3; YPM 16725, a left mandibular ramus with p3–m3; YPM 16732, a left mandibular ramus with c, p2–m3; YPM 16743, a mandible fragment with left m2–m3; YPM PU10118, a mandible with right and left p3–m3; YPM PU10184, a partial mandible with right p3–m3 and left m1–m3; **(from the Washakie Basin of Wyoming)** AMNH 1512, a mandible with right and left p2–m3; AMNH 1513, an anterior half of skull with right P2, P3, P4, M3 (partial), and left C–M2, M3 (partial); AMNH 1514, a premaxilla-maxilla with I1–M3; AMNH 1571, a palate with right I1–M3, left I2, C, P1–P3, and P4 (partial); AMNH 1575, a partial mandible with right i2–c, left i2–c, and p2–m3; AMNH 1577, a mandible with right and left p2–m3; AMNH 1651a, a left maxilla fragment with M1–M3; AMNH 13178, a partial mandible with right c, p2–p3 (partial), left i2 (?), c, p2, p4–m3; FMNH PM1676, a crushed skull with right P2, P4–M1 and left P4–M1; FMNH PM27939, a skull with C–M3; FMNH PM36045, a skull with right P2–M3, left C–P4, and M1–M3 (all partial); FMNH PM39945, a partially prepared palate with crushed cheek teeth; FMNH PM54864, a crushed skull fragment with left P2–M3; YPM PU10008 (holotype of *Mesatirhinus megarhinus*), a partial skull with very poorly preserved molars; YPM PU10041, a posterior part of a cranium; **(from the Sand Wash Basin of Moffat County, Colorado)** DMNH 8103, a right maxilla with C–M3; DMNH 9687, a left mandibular ramus with p3–m3; DMNH 29950, a partial skull (in two pieces) missing nasals and frontals with right P4–M1 (partial), and M2–M3; (no locality data) YPM PU25021, a crushed skull with right P2–M3, left C, P2–P4, M1–M3 (all partial), and a mandible with right and left p3–m3.

DIAGNOSIS: *Mesatirhinus junius* is a small hornless brontothere in which the frontal bone does not overlap or intrude into the nasal bone. The nasal incision extends posteriorly to between the anterior margin of P4 and the posterolateral root of M1. The nasal process is horizontal, unelevated, of relatively constant transverse width, narrow, with thin and deep lateral walls, and without a well-defined or strongly rounded distal margin. The orbits do not protrude laterally and are positioned over the M2 with the anterior lateral root of M2 and posterior lateral root of M1 below the anterior orbital rim. There is a prominent infraorbital process on the jugal. The premaxillomaxillary rostrum deepens posteriorly and it is not enclosed dorsally by bone. Other cranial characteristics include a flat or convex dorsal cranial surface, a sagittal crest, thin and weakly curved zygomatic arches, a ventrally open external auditory pseudomeatus, and wide occipital condyles.

Dentally, *Mesatirhinus junius* is characterized by large subcaniniform upper incisors, a postcanine diastema, a simple P1, a distinct P2 metacone, weak premolar preprotocristae and/or paraconules, and short crests extending posteriorly from the protocones of the premolars. Premolar hypocones are absent. The molars of *M. junius* have tall, lingually angled ectolophs with weak labial ribs, and

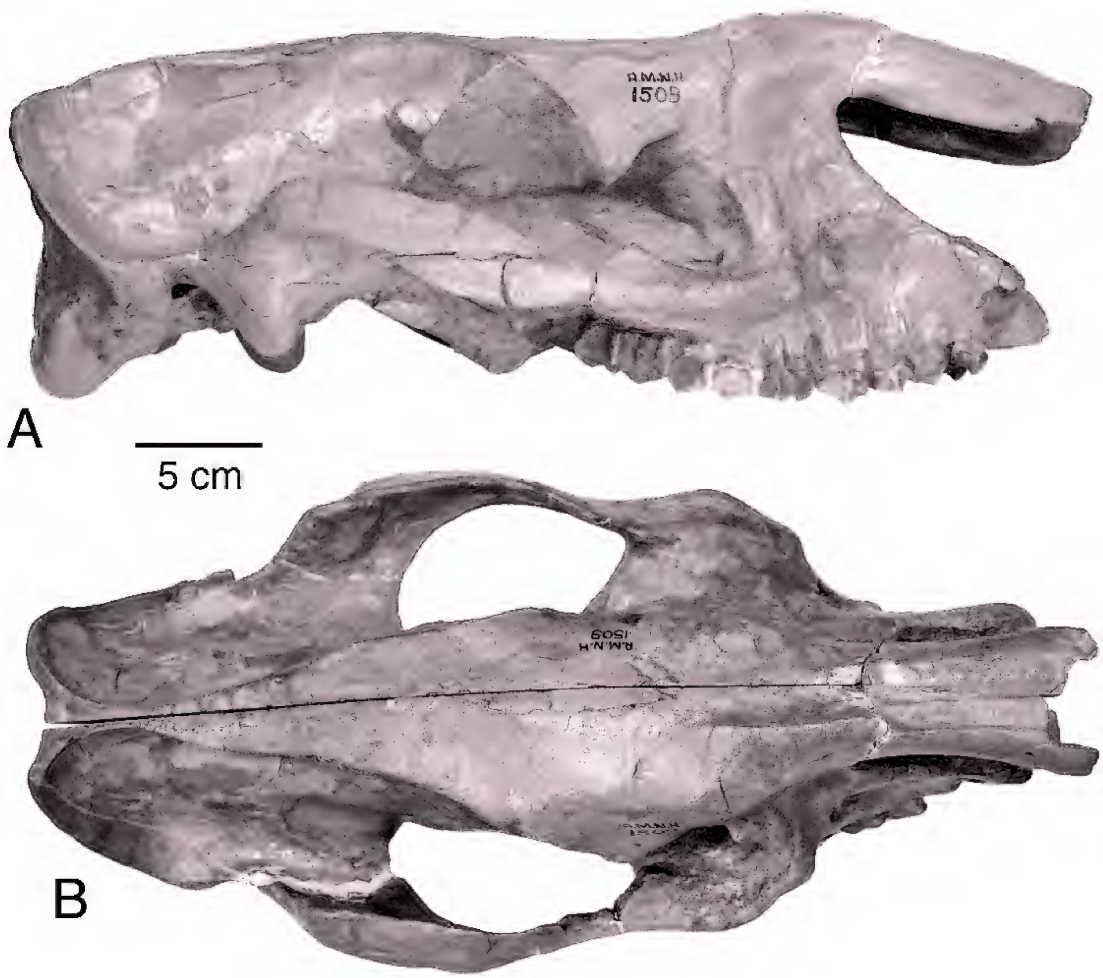

Fig. 6. A skull referred to *Mesatirhinus junius* (AMNH 1509). **(A)** Right view, **(B)** dorsal view.

somewhat thinned lingual ectoloph enamel with wedge-shaped paracones and metacones. A cingular parastyle shelf is absent. *Mesatirhinus junius* molars retain vestigial paraconules and metalophs, and they lack central fossae and anterolingual cingular cusps. The lower dentition of *M. junius* is characterized by large semispatulate incisors that are all of a similar size, a short p1–p2 diastema, an elongate p2 trigonid, a metaconid on p4 but not on p2 and p3, shallow molar basins, and a slender m3.

Mesatirhinus junius is very similar to *Sphenocoelus uintensis* but is clearly distinct from that species due to its smaller size, more brachycephalic proportions, and lack of paired ventral sphenoidal fossae. *M. junius* is similar in size to *Metarhinus*, but can be differentiated from it by its unspecialized rostrum.

Description

Skull: Many skulls of *Mesatirhinus junius* are known, but because each one is damaged or distorted in some way it is necessary to refer to several specimens for a full description. The following description is primarily based on AMNH 1509 (fig. 6), AMNH 12202 (fig. 7a, fig. 8a), USNM 26116 (fig. 7b), and AMNH 12184 (fig. 7c). *M. junius* is a small (table 1) hornless brontothere similar in size to *Metarhinus*, but it is smaller than other late Bridgerian taxa, e.g., *Telmatherium* and *Palaeosyops*, that are contemporaneous with it. The

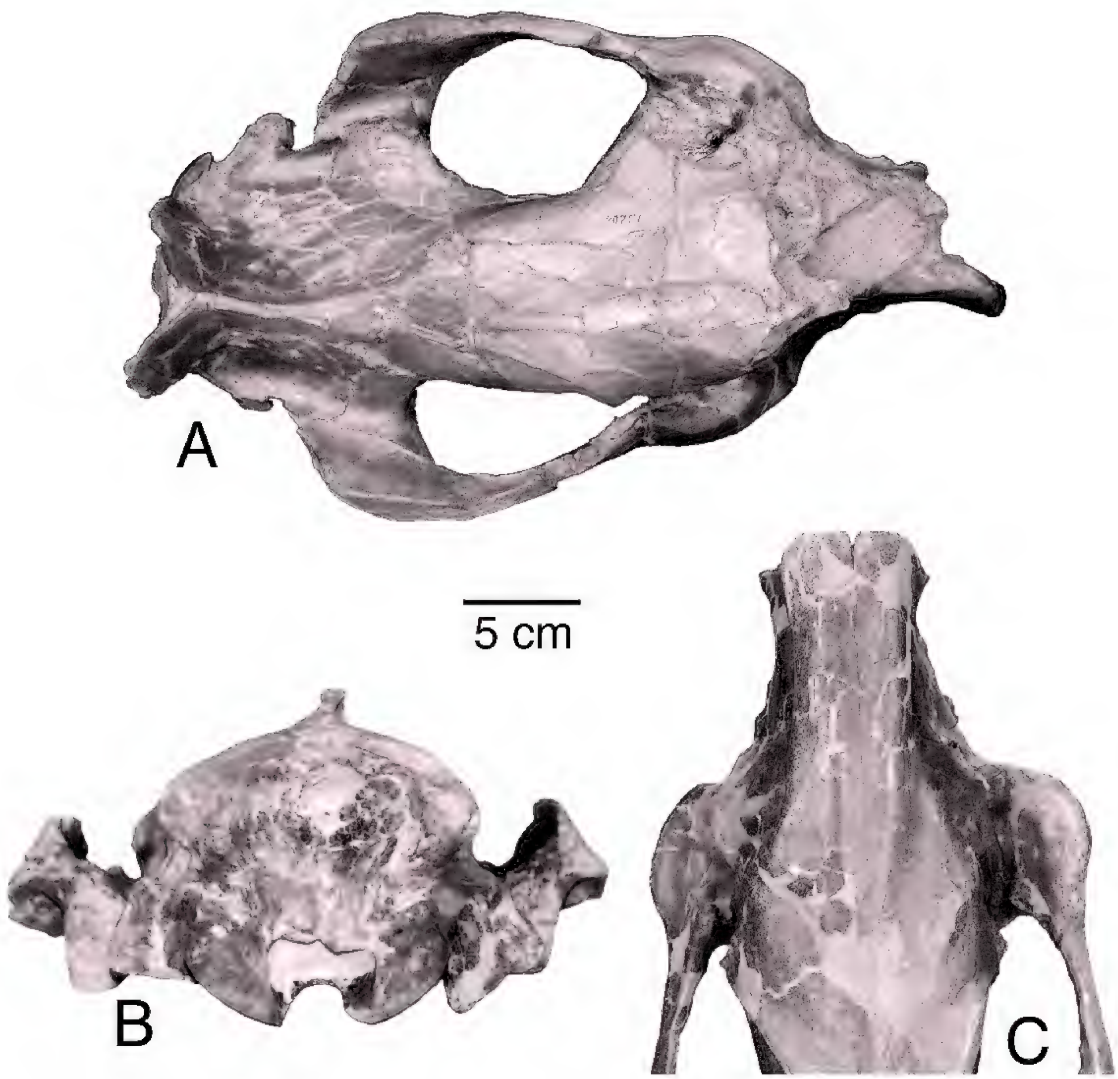

Fig. 7. Selected skulls referred to *Mesatirhinus junius*. **(A)** Dorsal view of AMNH 12202 showing thinner sagittal crest than AMNH 1509, **(B)** posterior view of USNM 26116 showing undistorted occiput, **(C)** dorsal view of anterior part of AMNH 12184 showing complete nasal process.

general morphology of the skull most closely resembles *Sphenocoelus uintensis*, though it is smaller and more brachycephalic.

The frontonasal suture is not clear in most of the specimens. Osborn's (1929a: fig. 328) illustration of AMNH 1556 (now in the British Museum with number BMNH. M10471) seems to portray a suture that looks more like a crack on the actual specimen. The frontonasal suture on the left side of the skull of AMNH 12184, also figured by Osborn (1929a: fig. 327), appears as a deeply convoluted line. This represents a true frontonasal suture and indicates the absence of a frontal process overlapping the nasal bone like that seen in *Telmatherium validus*.

The nasal bones tend to be poorly fused together. The nasal process is shorter than the premaxillomaxillary rostrum and is transversely narrower. The nasal process is slightly angled downward as it projects from the skull. The sides of the nasal process form relatively thin and deep vertical walls. From a dorsal view, the nasal process appears to be slightly constricted proximally in AMNH 1509, but in other specimens, such as AMNH

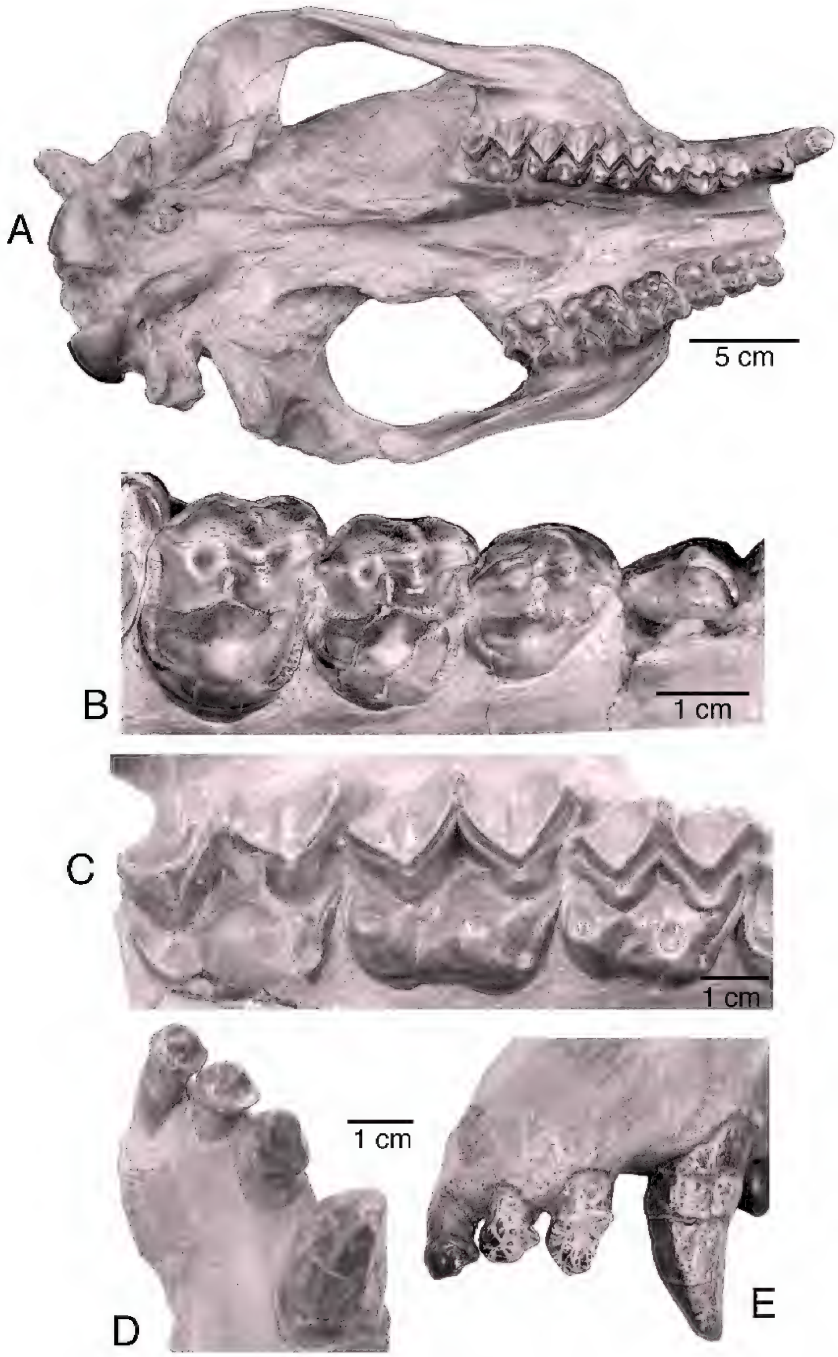

Fig. 8. Ventral surface of the skull and upper teeth of *Mesatirhinus junius*. **(A)** Ventral view of AMNH 12202, **(B)** right premolars of AMNH 12202, **(C)** right molars of AMNH 12202, **(D)** lingual view of left incisors of AMNH 1514, **(E)** labial incisor view of left incisors of AMNH 1514.

TABLE 1
Summary statistics for selected morphometric variables of *Mesatirhinus junius*
See Methods for measurement definitions

	N	Mean	SD	Min.	Max.	CV
C L	8	17.6	1.6	15.5	20.5	9.3
P3 L	20	17.6	1.7	14.7	19.8	9.7
P3 W	20	20.2	1.5	18.0	23.2	7.6
M2 L	20	35.1	3.1	30.1	40.1	8.9
M2 W	17	33.0	2.2	29.0	37.1	6.8
P2–P4	18	51.5	4.0	45.2	58.4	7.7
M1–M3	22	92.0	6.2	82.1	104.7	6.7
V L	4	401.8	24.5	372	430	6.1
C L	8	15.5	2.4	10.9	18.25	15.4
p3 L	17	17.3	1.0	15.7	19.24	5.7
p3 W	15	10.9	0.8	10.0	12.39	7.2
m2 L	22	29.3	1.9	24.8	32.5	6.3
m2 W	21	18.7	1.5	14.9	21.4	8.3
p2–p4	14	54.0	3.2	50.1	59.9	5.9
m1–m3	19	98.3	4.6	85.1	104.8	4.7

12184, the nasal process is more nearly constant in width. The anterior margin of the nasal process is flat from a dorsal view, except for a median notch. The anterior edge of the nasal process is thin, roughened, and angled downward only slightly.

The nasal incision of *Mesatirhinus junius* is long and shallow. The position of the posterior margin of the nasal incision fluctuates slightly from the anterior margin of M1 (e.g., AMNH 1509, AMNH 12184) to the posterolateral root of M1 (YPM 11070). The orbits tend to be positioned more or less over the M2 although its position with respect to the molars varies slightly. For instance, in YPM 10008, the alveolus for the anterior lateral root of M1 is directly below the anterior edge of the orbital rim; this is somewhat more anteriorly positioned than the majority of *M. junius* specimens where the anterior lateral root of M2 and posterior lateral root of M1 are situated below the anterior orbital rim.

A shallow facial concavity exists between the nasal incision and orbit. The facial concavity is bordered superiorly by a prominent rim of bone that abruptly meets the nearly flat dorsal surface of the skull. The rim gives this part of the skull a somewhat thickened appearance. Osborn (1929a) described this species as having incipient horns, although Mader (1989) could not corroborate the presence of incipient horns. Later, McCarroll et al. (1996a) reported an incipient horn on FMNH PM27939, although it seemed to occur only on one side (right) of the specimen. Although, the prominent rim of bone above the facial concavity tends to gives this area of the face a thickened appearance, I agree with Mader's (1989) judgment that there is no distinct hornlike structure on any specimen of *M. junius*.

From a lateral view, the dorsal margin of the premaxillomaxillary rostrum is steeply sloped, so that the posterior notch of the nasal incision is level with the top of the orbit. The premaxillae most often are not fused at the symphysis; however, they are occasionally fully co-ossified (e.g., AMNH 1571). The premaxillomaxillary suture is not always clear, but it is clearly visible on USNM 26136 (not figured). In this specimen, the ascending nasal process of the premaxilla does not reach the posterior notch of the nasal incision, and, therefore, does not contact the nasal bone. The premaxillomaxillary rostral cavity and the nasal cavity form a single continuous osteological cavity; this condition is normal, but differs substantially from *Dolichorhinus* and *Metarhinus*, in which the premaxillomaxillary rostral cavity is completely enclosed in bone.

Among the least distorted skulls of *Mesatirhinus junius*, the dorsal surface of the skull above the orbits is flat or slightly convex from a lateral view. The lateral profile of the dorsal surface of the posterior half of the skull varies from flat to slightly convex. The parasagittal ridges tend to be thin but distinct, and join medially to form a sagittal crest.

The zygomatic arches of *Mesatirhinus junius* are thin and weakly curved, like those of *Sphenocoelus* and *Dolichorhinus*. From a lateral view, the jugal zygomatic process is horizontal while the zygomatic process of the squamosal is slightly angled posterodorsally, giving the zygomatics a weak curvature. From a dorsal view, the zygomatic arches are slightly bowed laterally. *M. junius* possesses a large laterally projecting infraorbital process on the jugal. The size of this process varies (compare AMNH 1509 to AMNH 12184), although they tend to be large and conspicuous like those of *Sphenocoelus*, and they are more distinct than those of *Metarhinus*.

From dorsal views of the skulls, the nuchal crest is anteromedially angled. From lateral views, the occiput is slightly tilted backward. The occiput of *Mesatirhinus junius* is best preserved in USNM 26116. From the posterior view, the nuchal crest is arched dorsally. The dorsal portion of the occiput is nearly as wide as the posterior portion and the occiput is constricted in the middle. Occipital pillars are evident, but they are weak, and the central depression in the occiput is shallow. The occipital condyles are very wide, a condition shared with *Sphenocoelus uintensis* and *Dolichorhinus hyognathus*.

Unlike many other brontotheres, there is no horseshoe-shaped emargination around the opening of the posterior nares of *Mesatirhinus junius*. A small medial process typically projects posteriorly from the anterior rim of the posterior nares (although it is not preserved on AMNH 12202). The anterior margin of the posterior nares varies in position from between the M2 protocones (AMNH 12202) to between the M3 hypocones (AMNH 36045). Most frequently, the position of the posterior nares is anterior to the posterior margin of the M2. The elongate posterior narial canal formed by the posterior nares does not extend into the body of the sphenoid as in *Sphenocoelus uintensis*. The mastoid process does not contact the postglenoid process, thus the opening of the external auditory pseudomeatus is unconstricted ventrally. Other aspects of the basicranium of *M. junius* are typical of other brontotheres, such as a widely separated foramen ovale and foramen lacerum.

Upper Dentition: Few specimens of *Mesatirhinus junius* have preserved upper incisors; a partial skull, AMNH 1514, includes a complete row of three left incisors (fig. 8d, e). The incisors are large and arch anterior to the canines. The tips of I1 and I2 are worn off, but these incisors appear to have had conular crowns. The I3 crown is somewhat larger than those of I1 and I2 and is more nearly caniniform in shape. Each of the canines has a distinct lingual cingulum. The canines of *Mesatirhinus junius* are generally of moderate size, like those of *Dolichorhinus hyognathus*. The incisors of AMNH 1514 are separated by very short gaps, although this may have not been the case in other specimens. Finally, there are both short precanine and postcanine diastemata. The postcanine diastema is shorter than P2.

Complete cheektooth rows are preserved in many specimens of *Mesatirhinus junius*. The following description of the premolars and molars of *M. junius* is primarily of AMNH 12202 (fig. 8a–c) but information from other specimens is provided. P1 is slightly shorter than P2, although it is much narrower and with a simpler crown. The P1 crown has a single cusp and an elongate posterior heel. There is no P1–P2 diastema.

The anterior side of P2 is more steeply angled posterolingually than P3 and P4, thus giving the P2 crown a more oblique shape and a relatively narrower lingual side. P3 and P4 are progressively less oblique in outline; their anterior and posterior sides are nearly parallel. The parastyle and metastyle of P2 are angled slightly lingually. The P3 parastyle and metastyle are nearly straight, while those of P4 are slightly angled labially. The labial paracone rib of P2 is broad while those of P3 and P4 are progressively narrower and less distinct. The metacone of P2 is positioned somewhat more lingually in comparison to P3 and P4. Because of these differences the

labial side of P2 is rounder than the labial sides of P3 and P4.

In AMNH 12202 a short lingual crest extends posteriorly from the protocone on P2–P4, but in some specimens this lingual crest is absent (e.g., AMNH 1514). Each premolar exhibits a small but distinct preprotocrista that extends from the anterior slope of the protocone and meets the ectoloph at a point anterior to the lingual base of the paracone. In AMNH 12202, the preprotocrista of P2 tends to be wider, while those of more posterior premolars (P3 and P4) are thinner and sometimes have a small but distinct paraconule. The preprotocrista of P2 is discontinuous with the small anterior cingulum. However, this morphology is highly variable. For instance, in AMNH 1523, the lingual side of the P2 crown is severely shifted posteriorly; the protocone is posterior to the metacone, and the preprotocrista attaches to the lingual base of the metacone. AMNH 1514 shows an entirely different morphology whereby the preprotocrista contacts the lingual base of the ectoloph at a point anterior to the protocone.

No hypocone is found on any of the premolars of *Mesatirhinus junius*. The anterior and posterior cingula of P2–P4 stretch around the anterolingual and posterolingual corners of the crown but they do not join on the lingual side. The labial premolar cingula of the P2 and P3 connect to the posterior slope of the paracone ribs, thus forming a ridge that runs from the posterolabial base of the crown to the occlusal peak of the paracone. The P4 labial cingulum stretches across the proximal base of the crown and does not join the paracone rib. However, in some specimens (e.g., AMNH 1513) the labial cingulum of P4 is incomplete and does not stretch across the base of the paracone.

The molars of *Mesatirhinus junius* exhibit numerous apomorphies shared with other brontotheriines. For instance, the anterior cingulum is very thin labially and does not form a thick shelf at the peak of the parastyle. The ectoloph is taller than the lingual cusps. The labial paracone and metacone ribs are thin and indistinct. Overall, the labial side of the ectoloph is strongly angled lingually. The lingual wall of the ectoloph enamel thickens slightly around the lingual sides of the paracone and metacone, but not to the degree seen in *Palaeosyops* or *Eotitanops*. The lingual ectoloph enamel that stretches between the cusps is about as thick as the labial sheet of enamel. In unworn teeth, such as the M3 of AMNH 12202, the lingual sides of the paracone and metacone are wedge-shaped, but in more worn molars such as the M2 and M1 of the same specimen the lingual sides of these cusps become progressively rounded near the proximal base of the cusp.

The molars of *Mesatirhinus junius* retain small and essentially vestigial paraconules. The presence of paraconules appears to be a fixed condition. There is a very small but distinct crest of enamel that runs along the anterolabial slope of the hypocone of M1 and M2 that connects to the inner base of the metacone. Sometimes this structure is long and crestlike as on the M2 of AMNH 12202, and other times it is shorter and cusp-like as on the M1 of the same specimen. This crest seems to be a vestigial remnant of a metaloph. It should be noted that evidence of the paraconules and the metaloph fades with wear, and in heavily worn molars the evidence for these structures is erased.

The molars of *Mesatirhinus junius* lack central molar fossae and anterolingual cingular cusps. A hypocone is not present on the M3, although a thick cingulum wraps around the posterolingual corner of the crown. Rarely (e.g., USNM 26136), a very small cusp is seen near the posterolingual corner of the M3 that could be interpreted as a rudimentary hypocone. Lingual cingula are absent on the molars, while the labial molar cingula are faint and discontinuous around the mesostyles.

Mandible and Lower Dentition: Four skulls of *Mesatirhinus junius* are associated with mandibles (AMNH 12191, FMNH PM36045, USNM 26116, and YPM PU25021). Unfortunately, these mandibles lack incisors and have incomplete, heavily worn sets of cheek teeth. However, several mandibles recovered from the Upper Bridger (Bridger C–D) and the lower parts of the Washakie Basin (Washakie A of Granger 1909 and TWKK–TWKA1 of McCarroll et al., 1996b) are consistent in size and morphology with the few mandibles that are

directly associated with *M. junius* skulls. Among these jaws, the cheek teeth, particularly M3, are far too slender and thin-enameled for any species of *Palaeosyops*. *Telmatherium validus* co-occurs with *M. junius* in the upper Bridger and lower Washakie formations and has similar lower dentition. Other than their smaller size, *M. junius* mandibles and lower dentition lack any obvious characters that clearly distinguish them from *Telmatherium validus*. However, those referred to *M. junius* are well below the lower size range of *T. validus*. There are no other small brontotheres from upper Bridger and/or lower Washakie sediments to whom these mandibles could belong.

Pictured is a complete mandible, AMNH 1567 (fig. 9a, b). The mandible is similar in proportion to most other Bridgerian and Uintan hornless brontotheres except *Dolichorhinus*, whose mandible is more slender. In *Mesatirhinus junius* the position of the posterior margin of the symphysis fluctuates slightly but it is generally positioned between the talonid of p2 and the trigonid of p3. The inferior angle of the mandible tends to be quite steep ($\geq 45°$).

Complete sets of relatively unworn lower incisors of *Mesatirhinus junius* are rare, although the alveolar surface suggests that the incisor row was arched and extended anterior to the canines. One partial jaw, USNM 363884, includes a complete set of nearly unworn but isolated left incisors (fig. 9d, e). The crowns are large, of similar size, and bilaterally asymmetrical. The i1 and i2 have rounded apices and are semispatulate. The i3 is more mesiodistally elongate than i1 or i2 is more lingually curved. Each incisor has a thin but distinct lingual cingulid. Another specimen, AMNH 1575 (fig. 9f), has a partial incisor row with more damaged incisors, but with essentially the same morphology. The i3 of this specimen is more subcaniniform in shape than the i2, with a short, lingually curved crown. There are no diastemata between the incisors or canines.

The following description of the lower premolars is based primarily on AMNH 1520 (fig. 9c), a specimen with nearly unworn premolars, but other specimens provide additional information on variation. The p1 is isolated by a postcanine diastema and a p1–p2 diastema. The postcanine diastema tends to be shorter than the p2. The p1–p2 diastema is even shorter. The p1 has a small simple crown with a single cusp and a very short talonid heel.

The trigonid of p2 is nearly twice as long as the talonid; the p3 trigonid is also distinctly longer than the talonid. However, the p4 trigonid is slightly shorter than the talonid. The talonid and trigonid are of nearly equal width in p2 and p3, although in most specimens (e.g., YPM 16725 and YPM PU10184) the p3 talonid is slightly wider than the trigonid. The p4 talonid is always wider than the trigonid. The paralophids of the p2 and p3 are angled in a slightly lingual direction, creating a small lingual trigonid notch, while the paralophid of p4 curves fully lingually, creating a much larger lingual trigonid notch. The protolophids of p2 and p3 are straight but are angled slightly lingually; in p4 the paralophid arches 90° lingually and is fully molariform. Metaconids are absent on p2 and p3; however, there is a large lingually positioned molariform metaconid on p4. The talonid of p2 tends to have a short and/or poorly developed cristid obliqua and hypolophid, and the lingual side of the p2 talonid is a slightly concave sloped surface. However, p3 and p4 have more or less basin-shaped talonids with longer cristids obliqua and hypolophids. Lingual premolar cingulids are absent and labial premolar cingulids are generally weak.

The molars of *Mesatirhinus junius* are typical with relatively thin enamel, shallow trigonid and talonid basins, and with an elongate m3. Labial molar cingulids are generally weak and lingual molar cingulids are absent. A thin beaded cingulid wraps around to the distal end of the hypoconulid of the m3 of some specimens.

Remarks

Leidy (1872) originally assigned *Mesatirhinus junius* to the genus *Palaeosyops* Leidy (1870a). This species was named from portions of a lower jaw from an unspecified stratigraphic level from Fort Bridger, Wyoming. The material was later described as "several small fragments of the right side of a lower jaw, together with a sketch of a larger

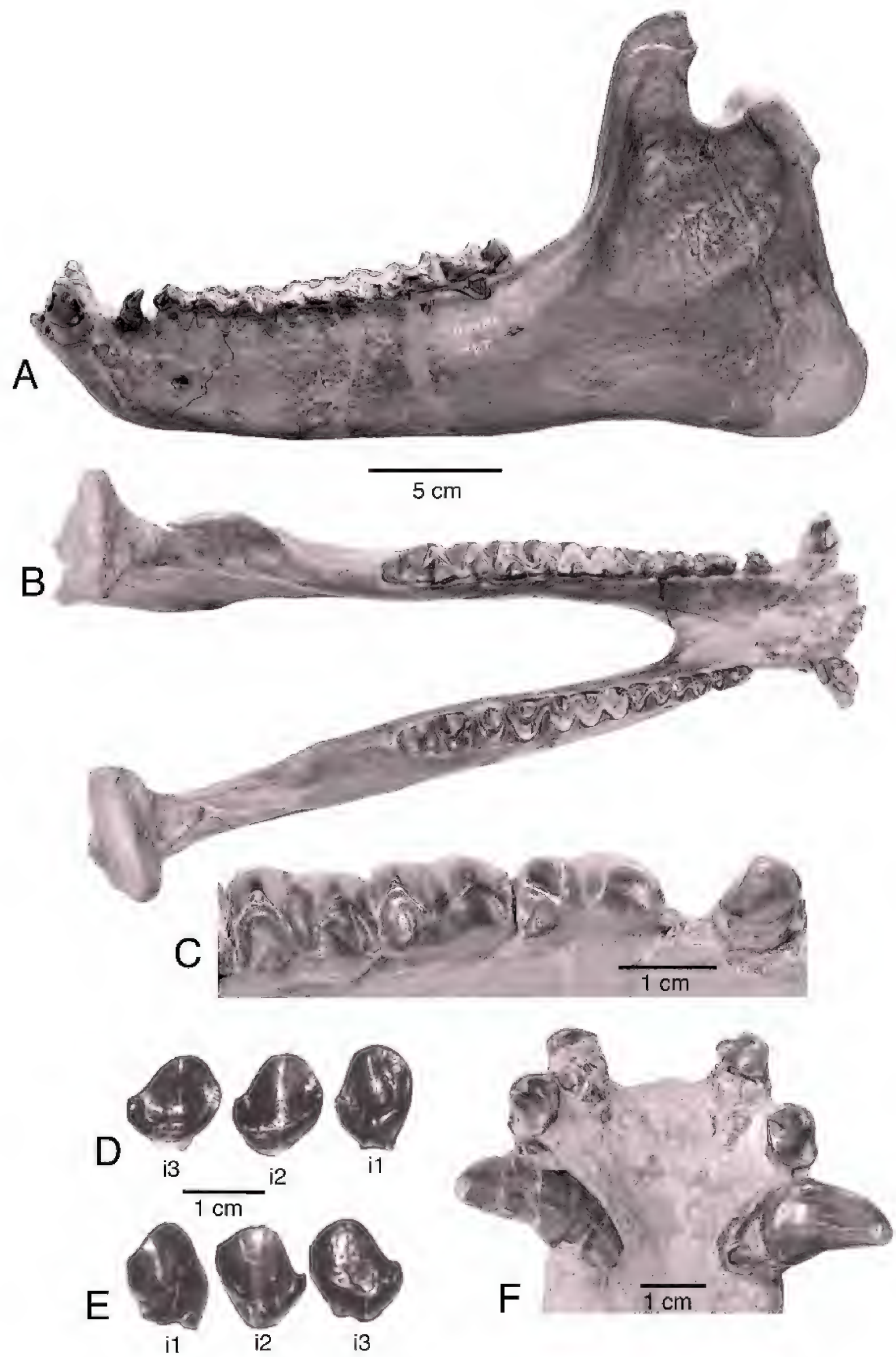

Fig. 9. Selected mandibles and lower teeth of *Mesatirhinus junius*. **(A)** Left view of AMNH 1567, **(B)** dorsal view of AMNH 1567, **(C)** left premolars of AMNH 1520, **(D–E)** left lower incisors of USNM 363884, **(F)** anterior dentition of AMNH 1575.

Fig. 10. Holotype of *Mesatirhinus junius*. **(A)** Right p4 (ANSP 10349), **(B)** partial right m3 (ANSP 10348). Illustrations from Osborn (1929a).

fragment of the left side, containing the last premolar and the succeeding molars" (Leidy, 1873: p. 57). Leidy (1872; 1873) did not figure any of these specimens or provide specimen numbers, but he did provide measurements for the specimen he had described as *Palaeosyops junius*. Later, Osborn noted, "Of this type material only p4 (right) and the posterior half of m3 (right) were located in the collection of the Academy of Natural Sciences of Philadelphia" (Osborn, 1929a: 159); he considered these specimens (fig. 10) cotypes. However, if they are from a single individual, as Leidy's (1873) description seems to imply, they are not cotypes, but a single holotype. The original measurements provided by Leidy (1873) for the p4 and m3 are consistent with ANSP 10349 (p4) and ANSP 10348 (m3 fragment): breadth (anteroposterior length) of last premolar = 8 lines (16.9 mm), thickness (width) of last premolar = 5.5 lines (11.6 mm), thickness of third molar at middle = 7 lines (14.8 mm). Spamer et al. (1995) list these specimens as the syntypes of *Mesatirhinus junius* (fig. 10).

Earle (1891) erected another species, *Mesatirhinus megarhinus*, which he also assigned to the genus *Palaeosyops*. *Palaeosyops megarhinus* was based on a nearly complete skull, YPM PU10008, with poorly preserved teeth from an unspecified stratigraphic level of the Washakie Basin, Wyoming. It is worth noting that Earle's (1891, 1892) figures of the holotype (YPM PU10008) show a complete left zygomatic arch, a complete nasal process, and a complete occiput. Currently, the distal end of the nasal process is not preserved, the zygomatic arches are incomplete, and the occiput is missing in the holotype.

Osborn (1908a) recognized that Earle's *Palaeosyops megarhinus* differed from other *Palaeosyops* species and erected the genus name *Mesatirhinus* for it. *Mesatirhinus megarhinus* was diagnosed by its infraorbital process, sagittal crest, and upper molars with flattened outer cusps and reduced conules. In that same paper Osborn (1908a) erected a new species, *M. petersoni*, based on a partial skull (AMNH 12184) from Bridger D. Osborn (1908a) did not state how *M. petersoni* was distinct from *M. megarhinus* in clear morphological terms. He noted that the preorbital facial region was more elongate, and that the grinding teeth occupy more space. However, considering the fact that specimens are damaged and distorted to varying degrees, the subtle distinctions between these two species is clearly suspect.

Ultimately, Osborn (1929a) accepted three species of *Mesatirhinus*: *M. junius* (Leidy), *M. megarhinus* (Earle), and *M. petersoni* Osborn. Osborn (1929a) considered *Mesatirhinus junius* the earliest form of *Mesatirhinus* and suggested that the holotype was probably from Bridger B. Osborn states, "The type lower molar of *M. junius*, according to Leidy's description, was found near Fort Bridger, Wyo., at a geological level that Granger places in Bridger B" (1929a: 388). However, Leidy's description states that the fossils were "received from Dr. J. Van A. Carter, of Fort Bridger, Wyoming" (Leidy, 1892: 277). Leidy (1872, 1873) did not state that the fossil was "found near Fort Bridger" (contra Osborn, 1929a). Therefore, the stratigraphic provenience of the holotype of *M. junius* is unknown. There is no direct evidence of the occurrence of *Mesatirhinus* in Bridger B, although it is relatively common in Bridger C–D.

Mader (1998) recognized only a single species, *Mesatirhinus megarhinus*. He considered *M. junius* to be a nomen dubium but suggested that *M. junius* is a potential senior synonym of *M. megarhinus*. In contrast, Gunnell and Yarborough (2000) considered *M. junius* to be a synonym of *Palaeosyops paludosus*. Nonetheless, it can be shown that *M. junius* is a valid name, that it is distinct from *Palaeosyops*, and that it is the senior synonym of both *M. megarhinus* and *M. petersoni*. Among brontotheres that occur in the Bridgerian, the m3 of the holotype of *M. junius* (ANSP 10348) is smaller than *Palaeo-*

syops from Bridger B, or from Bridger C–D, and, more importantly, it is far too slender and thin enameled for a m3 of *Palaeosyops*. It is also much too large for *Eotitanops*. Strictly speaking, the morphology and proportions of the holotype of *Mesatirhinus junius* are not different from *Telmatherium validus*; however, it is considerably smaller than all known specimens of *T. validus*. Moreover, the holotype of *M. junius* falls within the size range of other materials that have been referred to as *Mesatirhinus* (table 1). Therefore, *M. junius* is the earliest name that pertains to *Mesatirhinus*. *M. megarhinus* (Earle) and *M. petersoni* Osborn appear to represent the same species and are considered junior synonyms of *M. junius* (Leidy).

The material referred to *Mesatirhinus junius* consists mostly of specimens from late Bridgerian deposits of the Bridger Basin (Bridger C–D) and Washakie Basin (Washakie A of Granger [1909] and TKWW–TWKA1 of McCarroll et al. [1996b]). There is evidence, however, that *Mesatirhinus junius* ranges into the early Uintan. A crushed anterior cranial fragment (FMNH PM54864) is from early Uintan deposits (Washakie Basin, TWKA2). Another specimen, FMNH PM1676, a crushed skull, is recorded from the "upper Washakie". Generally, "upper Washakie" refers to the Uintan portion of the Washakie deposits (see Granger, 1909), but the exact stratigraphic position of this specimen is uncertain. There are two probable specimens of *M. junius* from the Sand Wash Basin: DMNH 8103, a left maxilla; and DMNH 29950, a left partial skull. These specimens possess a prominent infraorbital process, a deep nasal incision, and they lack central fossae on the upper molars. This combination of characters is consistent with *M. junius* and rules out all other Uintan brontotheres except *Sphenocoelus uintensis* Osborn (1895). These specimens are considerably smaller than *S. uintensis*. They are slightly larger than Bridgerian specimens of *Mesatirhinus junius*, but only by millimeters. It is therefore probable that (1) these specimens are a new species slightly larger than the *M. junius* from the Bridgerian land mammal "age", or (2) *M. junius* survived into the early Uintan but was slightly larger at that particular time and place. Because the material at hand does not clearly indicate a morphologically distinct species, the latter possibility is preferable; therefore, these specimens are referred to *M. junius*.

Desmatotitan tukhumensis Granger and Gregory, 1943

HOLOTYPE: AMNH 21606, a partial mandible with right i1–c, p2–m3, left i1, i3, and c.

TYPE LOCALITY: Ulan Shireh Formation, four miles north of Tukhum Lamasery, Inner Mongolia, China.

AGE: Middle Eocene (Irdinmanhan land mammal "age").

DIAGNOSIS: *Desmatotitan tukhumensis* is an intermediate-sized brontothere with three pairs of large incisors that strongly arch anterior to the canines. The i1 and i2 are semispatulate while the i3 is subcaniniform. The posterior margin of the symphysis extends to the p3 metaconid. There is both a postcanine diastema and a short p1–p2 diastema. The p1 is anchored obliquely in the jaw. Metaconids are absent on p2–p3 but present on p4. The molar ribs are weak, the lingual enamel is thinner than the labial enamel, and m3 is more elongate than those of *Palaeosyops* and *Bunobrontops*.

Desmatotitan tukhumensis is one of a few brontotheres with a p1–p2 diastema. Among these, *D. tukhumensis* is most similar in size and morphology to *Mesatirhinus junius*. It shares with *M. junius* a semispatulate i1 and i2. However, the premolars of *D. tukhumensis* are broader than those of *M. junius*, the crescents of the lower molars are more strongly rounded, and the p1 is anchored obliquely in the jaw.

DESCRIPTION

MANDIBLE AND LOWER DENTITION: The holotype jaw of *Desmatotitan tukhumensis* (AMNH 21606) includes a symphysis and right ramus with a complete set of teeth that are not heavily worn (fig. 11). The ramus is very thin and the roots of the cheek teeth are exposed, possibly reflecting poor health near the time of death. The left side of the symphysis is not preserved but it has been

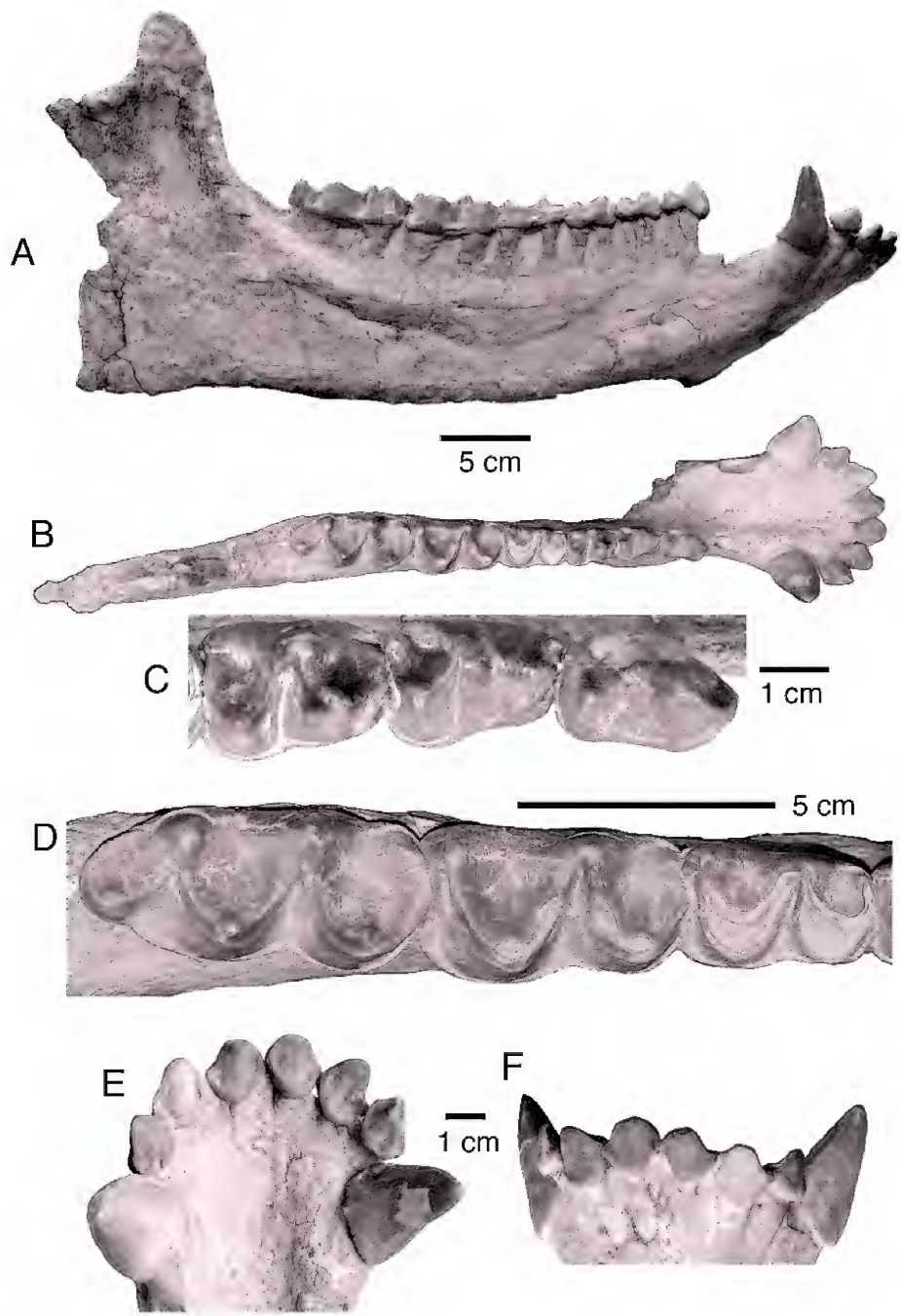

Fig. 11. The holotype of *Desmatotitan tukhumensis* (AMNH 21606). **(A)** Right view, **(B)** dorsal view, **(C)** right premolars (p2–p4), **(D)** right molars, **(E)** lingual view of anterior dentition, **(F)** labial view of anterior dentition.

reconstructed with plaster. Judging by the intact right side, the proportions of the symphysis as it is reconstructed is accurate. The angle of the inferior margin of the symphysis is somewhat less then 45°. The symphysis extended about to the middle of the p3.

The lower dental formula (3-1-4-3) is unreduced. The incisor row forms a strong arch anterior to the canines. Overall, the incisors are large and are all roughly of similar size. The crowns of the i1 and i2 are semispatulate and i3 is more subcaniniform and mesiodistally elongate but with a slightly shorter crown. The apices of both i1s are worn off. The distal apex of i2 forms a dull rounded tip. A distinct lingual cingulid is present on each incisor. The lingual cingulid of the i3 is less distinct than those of i1 and i2. The canine is both large in diameter and in height.

There are no diastemata between any of the incisors or canines. However, there is a relatively long postcanine diastema. On the alveolar surface, between the canine and p2, an elongate p1 alveolus extends into the mandible in a posteroventral direction, indicating that the root of p1 was anchored obliquely in the mandible. The position of the p1 alveolus indicates a short p1–p2 diastema.

The p2 trigonid is nearly twice as long as the talonid. Moreover, the trigonids of p3 and p4 are somewhat longer than their talonids. The lingual side of the p2 is incomplete although the trigonid and talonid of that tooth appear to have been similar in width. However, the talonids of p3 and p4 are distinctly wider than the trigonids. The paralophid of p2 curves slightly lingually, creating a small lingual trigonid basin. The protolophid is not curved although it is slightly lingually angled. The paralophid and protolophid of p3 have orientations similar to those of p2, but the protolophid is more curved and longer in p3, resulting in a shallow but broad lingual trigonid notch. The paralophid and protolophid of the p4 each arch fully lingually, creating a nearly molariform trigonid notch. The p2 and p3 lack metaconids, while p4 has a large lingually positioned metaconid. The p2 talonid has a short but distinct cristid obliqua and hypolophid; the lingual side of the p2 talonid is a slightly convex sloped surface. The cristids obliqua and hypolophids of p3 and p4 are longer, creating broader and more nearly molariform talonid basins. The labial premolar cingulids are strong, but they are discontinuous around the proximal bases of the protoconids.

The basins of the molars are shallow, the labial ribs are very weak, and the lingual enamel is thinner than the labial enamel. The m3 is proportionately longer than those of *Palaeosyops* or *Bunobrontops*, and is similar in proportions to *Sthenodectes incisivum*, but it is relatively short in comparison to most other brontotheres. The double crescent-shaped lophids of the lower molars, particularly that of m3, are very rounded in shape. The labial molar cingulids are distinct and continuous around the proximal bases of the cusps. There is an additional strong beaded cingulid on the lingual side of the m3 hypoconulid, although lingual cingulids are otherwise absent in the holotype of *D. tukhumensis*. The m2 shows the tendency for the protoconid and hypoconid to form rounded exposures of dentin in early stages of wear, a plesiomorphic wear pattern seen in basal brontotheres such as *Palaeosyops* and *Eotitanops*. In more progressive states of wear, characterized by the m1, this plesiomorphic wear pattern is not notable.

Remarks

Granger and Gregory (1943) recognized AMNH 21606 as a distinct species and concluded that it was a close ally of *Metatelmatherium* Granger and Gregory (1938). With only a single mandible, it is difficult to confirm Granger and Gregory's conclusion. Characteristics of the molars, such as the weak labial ribs, and the thinner lingual enamel are different from *Palaeosyops* and *Bunobrontops* and suggest a close relationship with more advanced brontotheres. Among more advanced brontotheres, a p1–p2 diastema is seen in *Dolichorhinus*, *Mesatirhinus*, *Telmatherium*, and *Metatelmatherium*. Among these, only *Metatelmatherium* occurs in Asia. However, the incisors of *Desmatotitan tukhumensis* are decidedly less subcaniniform than those of *Metatelmatherium*. In this respect, *D. tukhumensis* more

closely resembles *Mesatirhinus*. However, the relatively broad premolars and very rounded lower molar crescents are out of character with North American specimens of *Mesatirhinus junius*. In this respect *D. tukhumensis* seems to resemble *Microtitan mongoliensis*, although that species differs from *D. tukhumensis* in having a much more elongate m3, narrower premolars, much smaller body size, and absence of a p1–p2 diastema. For this reason *Desmatotitan tukhumensis* is accepted, although more material is clearly needed to generate a more thorough diagnosis of this species.

Acrotitan ulanshirehensis Ye, 1983

HOLOTYPE: IVPP V6686, a partial mandible with left p3 and p4.

TYPE LOCALITY: Ulan Shireh Formation, Inner Mongolia, China.

AGE: Middle Eocene (Irdinmanhan land mammal "age")

DIAGNOSIS: *Acrotitan ulanshirehensis* is a small brontothere with two pairs of large incisors that arch anterior to the canines. The posterior margin of the symphysis extends to the anterior margin of the p3. There is a short postcanine diastema and a long p1–p2 diastema. The molar ribs are weak and the lingual enamel is thinner than the labial enamel.

Acrotitan ulanshirehensis is one of two brontotheres known to have a reduced number of lower incisors. The other, *Megacerops coloradensis*, is substantially larger and lacks mandibular diastemata. Additionally, *Acrotitan ulanshirehensis* has an elongate p1–p2 diastema and an obliquely oriented p1.

DESCRIPTION

MANDIBLE AND LOWER DENTITION: The holotype of *Acrotitan ulanshirehensis* (IVPP V6686) is a partial mandible of a small brontothere. The mandibular symphysis is elongate and narrow. The inferior margin of the mandibular symphysis is shallow and forms an angle less than 45°. The posterior margin of the symphysis extends to the anterior margin of the p3. The crowns of the anterior dentition are not preserved; however, the alveoli indicate a reduced number of incisors (two pairs). Justification for the dental formula as interpreted here (2-1-4-?) is labeled in fig. 12. From the anterior view of the specimen, two pairs of small alveoli are seen between a pair of very large alveoli. The right pair of small alveoli are empty, although the roots remain in the left pair. The large pair of alveoli also contain roots. The two pairs of small alveoli at the front of the jaw are clearly incisor alveoli. The pair of much larger alveoli that are lateral to the smaller incisor alveoli could either represent a third pair of very enlarged incisors, or, more likely, the canines. Immediately behind the canines is a smaller anteriorly angled dental alveolus that undoubtedly held the p1, which, in brontotheres, is a small, single rooted tooth. Moving posteriorly, the additional alveoli held the anterior and posterior roots of the p2.

The orientation and size of the incisor alveoli indicate relatively small and procumbent incisors that are ovoid in cross section and were probably arranged in a small arch. The central incisors are separated by a short median diastema. The canines were relatively large with rounded cross sections. The postcanine diastema was rather short. The p1 alveolus indicates a simple, single-rooted tooth with a somewhat anteriorly directed orientation. There is a diastema between the p1and p2 that is substantially longer than the postcanine diastema.

The trigonids of p3 and p4 are slightly shorter and narrower than their respective talonids. The paralophid of p3 is short and angled anterolingually. The protolophid is straight and angled about equally lingually and posteriorly. The paralophid and protolophid of p4 are each angled more strongly lingually, creating a large molariform trigonid notch. The lingual enamel of the premolars is thinner than the labial enamel. A portion of the lingual enamel of the p3 is broken off and it is difficult to discern whether this tooth had a metaconid. Typically, brontothere premolars that have strongly lingually angled protolophids, such as this p3, also have metaconids, but it is difficult to confirm that in this specimen. Likewise, the lingual enamel of p4 is broken away. However, from the lateral view of the

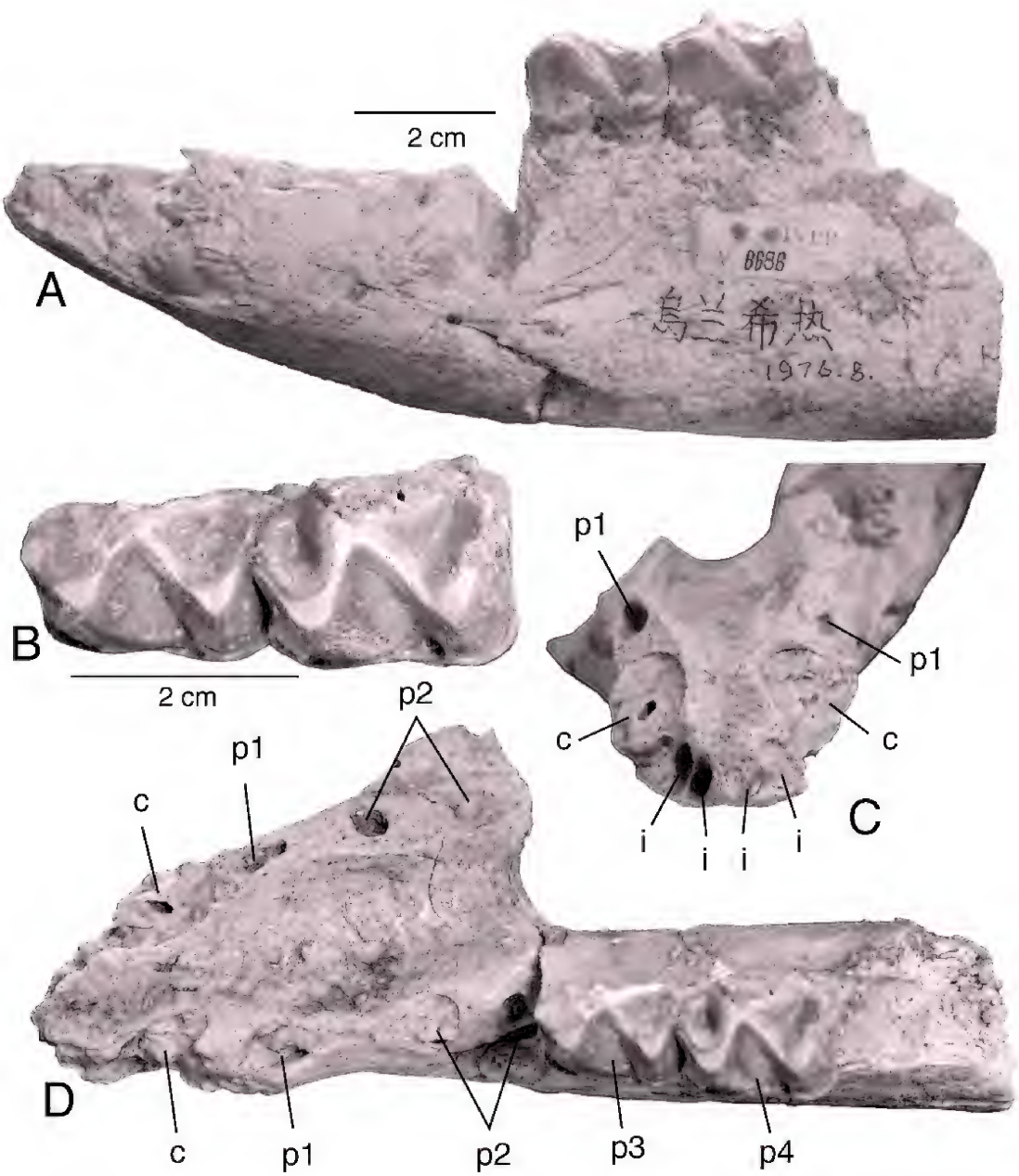

Fig. 12. The holotype mandible of *Acrotitan ulanshirehensis* (IVPP V6686) with revised interpretation of dentition. **(A)** Left view, **(B)** dorsal view of left p3 and p4, **(C)** anterior view showing dental fragments and alveoli of anterior dentition, **(D)** dorsal view.

tooth, the protolophid rises lingually as it stretches from the protoconid toward the junction with the cristid obliqua. This strongly suggests that a p4 metaconid was present. The cristids obliqua and hypolophids of p3 and p4 are long and obliquely angled, thus creating broad and nearly molariform talonid basins. The labial premolar cingulids are distinct although lingual cingulids appear to be absent.

REMARKS

Acrotitan ulanshirehensis is based on a small and rather peculiar brontothere mandible (IVPP V6686). No other specimens have ever been assigned to this species. The brief description provided by Ye (1983) of *A. ulanshirehensis* is puzzling. Ye (1983) described the posterior margin of the symphysis as terminating anterior to the p2, although the symphysis clearly extends to the anterior margin of the p3. More puzzlingly, the dental formula was described as 3-1-4-3, although there only appear to be two pairs of lower incisors. Moreover, no molars are preserved with the specimen. Thus, the dental formula is 2-1-4-?. Among those brontotheres for which lower incisors (or mandibles with alveoli) are known, only one other brontothere, the large North American Chadronian (late Eocene) species *Megacerops coloradensis*, is characterized by a similar mandibular dental formula.

In addition to *Acrotitan*, the following taxa retain a p1–p2 diastema: *Eotitanops*, *Palaeosyops*, *Mesatirhinus junius*, *Dolichorhinus hyognathus*, and *Desmatotitan tukhumensis*. Additionally a p1–p2 diastema is occasionally present in *Metatelmatherium ultimum* and *Telmatherium validus*. The postcanine diastema of IVPP V6686 is rather long (16 mm), while the postcanine diastemata of these other taxa are typically shorter (usually less than 10 mm), despite the much larger size of most of these species. The p1–p2 diastema of *Dolichorhinus*, however, ranges up to 19 mm. However, diastema length is quite variable within brontothere species. For example p1–p2 diastema length ranges from 7 mm to 18 mm within *D. hyognathus*. Therefore, the unusual length of the postcanine diastema of IVPP V6686 might be a characteristic of this particular individual rather than a character of the species, *Acrotitan ulanshirehensis*. Brontotheres that are similar in size to *Acrotitan ulanshirehensis*, such as *Microtitan*, *Metatitan*, and *Pygmaetitan*, all lack p1–p2 diastemata.

In addition to its small size and reduced number of incisors, a potentially diagnostically important characteristic of *Acrotitan ulanshirehensis* is the oblique orientation of p1. In nearly all brontotheres, p1 is typically rooted vertically in the jaw. However in IVPP V6686, the alveolus of p1 is slanted, indicating a posteroventrally rooted p1. The holotype specimen of *Desmatotitan tukhumensis* (AMNH 21606), a larger brontothere with three incisors, has a similarly angled p1, suggesting these taxa may have a sister relationship.

Dolichorhinus hyognathus (Osborn, 1889)

HOLOTYPE: YPM PU10273, a mandible with right i1–c, left i3, c, p2, m2 (partial), and m3.

TYPE LOCALITY: Adobe Town Member (Washakie B of Granger, 1909) of the Washakie Formation, Sweetwater County, Wyoming.

SYNONYMS: *Dolichorhinus cornutum* (Osborn, 1895); *D. intermedius* Osborn, 1908a; *D. heterodon* Douglass, 1909; *D. longiceps* Douglass, 1909; *D. superior* (Riggs, 1912); *D. fluminalis* Riggs, 1912.

AGE: Middle Eocene (early Uintan land mammal "age").

REFERRED SPECIMENS: **(From the Wagonhound Member of the Uinta Basin, Utah)** AMNH 1832, skull fragments; AMNH 1836, a right mandibular ramus with p2–m3; AMNH 1837 (holotype of *Dolichorhinus intermedius*), a skull with left C–M3; AMNH 1840, a partial left mandibular ramus with p2–m3; AMNH 1843, an anterior portion of skull with partial cheek teeth; AMNH 1845, a partial skull missing the nasal and premaxillae with right P4–M3 and left M2–M3; AMNH 1847, a dorsal surface of a skull; AMNH 1849, a skull fragment; AMNH 1850, a skull with right and left C–M3; AMNH 1851 (holotype of *D. cornutum*), a skull with complete right and left dentition; AMNH 1852, a skull with right P1–M3 and left P2–M3; AMNH 1854, a partial mandible with right i2–c, p2–m1, left c, and p2–m1; AMNH 1856, a complete mandible with complete dentition; AMNH 1857, a mandible with heavily worn teeth including right i1–i2, p2–m3, left i1–i2, c, and p1–p4; AMNH 1858, a juvenile mandible with right c (erupting), p1, p4 (?), left p1, p4 (erupting), m1–m2, and m3 (erupting); CMNH 2340 (holotype of *D. heterodon*), a skull with right P3–M3 and left partial cheek teeth; CMNH

2347, a skull with left and right P2–M3; CMNH 2865, a skull with left P4–M3, partial right ramus with m2–m3; CMNH 2964, a skull fragment; CMNH 3095, a partial skull with no dentition; CMNH 3096, a skull with right M1–M3 (heavily worn); CMNH 3117, a posterior half of a skull with right and left M2–M3; CMNH 3119, a skull fragment; CMNH 11071, a complete skeleton; CMNH 11080, partial skull with right C–M3; CMNH 11081 (holotype of *D. longiceps*), a skull with right C, P2–M3 and left P2–M3; CMNH 11083, a skull (partially prepared); CMNH 11091, a skull, broken into two large fragments with right M1–M3, and a partial right mandibular ramus with m2–m3; CMNH 11092, a mandible with left p1, p2 (partial), and p3–m3; FMNH P12167, a skull with right C–M3, left I1–I2, C, P2–M3, and a mandible with right and left p2–m3; FMNH P12175, a skull with right and left C–M3; FMNH P12176, a skull with a left M3; FMNH P12182, a skull with right P2–P3 (partial), P4–M3, and left P3–M2; FMNH P12168 (holotype of *D. superior*), a skull with right C–P4, M3, and left C, P2–M3; FMNH P12193, a skull with right and left P1–M3; FMNH P12200, a skull with right and left P3–M3; FMNH P12205 (holotype of *D. fluminalis*), a skull with right I1–M3 and left I1–P2, M1 (partial), M2–M3; FMNH P12215, a skull with complete dentition; LACM 128402, a skull with right P3–M3 (partial) and left P1–M3; UCMP 31845, a partial skull with left P1–M3; UCMP 31846, a partial skull with partial dentition; USNM 6702, a partial mandible with right p4–m2 and left c–m2; USNM 6703, a skull with right P2–P4 and left P1–2, P4–M3; USNM (uncatalogued), premaxillomaxillary rostrum; YPM PU11241, a skull with right P1–M3 and left C (partial), P1–M3; **(from the Adobe Town Member [Washakie B of Granger, 1909] of the Washakie Basin, Wyoming)** AMNH 13164, a complete skull with complete right dentition, left C–M3, and a mandible with right i1–p4, m2–m3 (partial), and left i1–m2, m3 (partial); CMNH 9413, a skull with right P1–M3 and left I2–M3; FMNH PM3870, a skull with right and left I3–M3; FMNH PM3873, a skull with right and left P2–M3; FMNH PM26100, a mandible with damaged teeth.

DIAGNOSIS: *Dolichorhinus hyognathus* is an intermediate-sized brontothere. The frontal bone does not overlap or protrude into the nasal bone. A small superorbital protuberance, primarily on the nasal bone, is seen in some specimens. The cranium of *Dolichorhinus hyognathus* is highly dolichocephalic. The nasal incision extends to the posterior margin of the P4. The nasal process is horizontal, unelevated, of relatively constant transverse width, narrow, with thin and relatively deep lateral walls, and without a strongly rounded distal margin. The orbits do not project laterally and are positioned directly over the posterior half of M2 and the anterior half of M3, with the anterolateral root of M2 and the posterolateral root of M1 directly below the anterior orbital rim. The prominent infraorbital process of the jugal also extends onto the maxillary, often to form a double flange. The premaxilla is robust and does not contact the nasal bone. The premaxillomaxillary rostrum does not deepen proximally and it is enclosed dorsally by bone. *Dolichorhinus hyognathus* lacks a sagittal crest, but the parasagittal ridges strongly constrict the dorsal surface of the skull posteriorly. Other cranial characteristics include a strongly dorsally arched cranium, thin and weakly curved zygomatic arches, a ventrally open and posteromedially angled external auditory pseudomeatus, and disproportionately wide occipital condyles. The functional posterior nares are shifted posteriorly by a bony palatal extension and posteriorly extended maxilloturbinates.

Dentally, *Dolichorhinus hyognathus* has large subcaniniform upper incisors, a postcanine diastema, a simple P1, a distinct P2 metacone, weak premolar preprotocristae, and short crests extending posteriorly from the premolar protocones. Premolar hypocones are exceedingly rare and inconspicuous when present. The molars have tall, lingually angled ectolophs with weak labial ribs, and thinned lingual ectoloph enamel with wedge-shaped paracones and metacones. A cingular parastyle shelf and an anterolingual cingular cusp are absent. Central molar fossae are present. *D. hyognathus* molars occasionally retain vestigial paraconules. All traces of a metaloph are lost. The lower dentition of *D. hyognathus* includes large subcaniniform in-

cisors all of similar size, a postcanine diastema, a p1–p2 diastema of variable length, an elongate p2 trigonid, a metaconid on p4 but not on p2 and p3, shallow molar basins, and a slender m3.

Dolichorhinus hyognathus is most similar to *Sphenocoelus uintensis* in its hyperdolichocephalic skull, but it can be differentiated by the absence of both large fossae in the sphenoid and a sagittal crest, and by the presence of a highly specialized premaxillomaxillary rostrum and a more dorsally arched cranium.

Description

Skull: The following description of the skull of *Dolichorhinus hyognathus* is primarily based on AMNH 1845, AMNH 1851, AMNH 13164, and FMNH P12175, although other specimens provide additional information on variation. FMNH P12175 (fig. 13a, c,) and AMNH 1851 (fig. 13b, d) are complete and undistorted skulls. AMNH 1845 is another skull that has an intact occiput (fig. 13e). Finally, the skull of AMNH 13164 (figs. 13f, 14a) is slightly crushed dorsoventrally, obscuring some aspects of the shape of the cranium, but otherwise the preservation of this specimen is exquisite and reveals details of the rostrum and ventral surface that are not well-preserved in other skulls.

Dolichorhinus hyognathus is an intermediate-sized (table 2) brontothere that is most notable for its extremely dolichocephalic skull and dorsally arching cranium. Only *Sphenocoelus uintensis* has a similarly elongate cranium. *D. hyognathus* lacks conspicuous horns, although many specimens, such as AMNH 1851 possess small but distinct nasal protuberances. Others, such as FMNH P12175, have much weaker nasal protuberances. The nasal protuberance of AMNH 1851 is small, elliptical, projects laterally, and is positioned directly above the orbit. The frontonasal suture runs behind the nasal protuberance and recedes posteromedially, but it is acutely redirected anteriorly near the midline. *D. hyognathus* does not possess a forward projection of the frontal bone like that seen in *Telmatherium validus*. The hornlike protuberance rests entirely on the nasal bone. Thus, *D. hyognathus* is the only brontothere known to have a hornlike protuberance that is predominantly on the nasal bone rather than on both the frontal and nasal bone.

The nasal incision of *Dolichorhinus hyognathus* is shallow and long. It extends as far back as the posterior margin of the P4. From a lateral view the orbits are elliptical. The bottom of the orbit is positioned directly over the posterior half of M2 and anterior half of M3. The anterolateral root of M2 and the posterolateral root of M1 are positioned directly below the anterior orbital rim. The orbits do not protrude laterally as in *Metarhinus*.

The nasal bones tend to be poorly fused together. In FMNH P12175, the nasal process is slightly longer than the premaxillomaxillary rostrum, although in other specimens (e.g., AMNH 1851) the nasal process and the rostrum are about the same length. The nasal process is horizontal. The lateral margins of the nasal process form dorsoventrally deep and thin vertical walls. Typically, the depth of the lateral walls is nearly constant, but they become shallower near the distal end. The anterior margin of the nasal process is thin, roughened, and strongly deflected downward. From the dorsal view the nasal process is narrow and of nearly constant width throughout its length, although it is sometimes slightly constricted at its proximal end.

The premaxillomaxillary rostrum of *Dolichorhinus hyognathus* is long and slightly upturned. From a lateral view, the dorsal margin of the rostrum is horizontal. Normally, the rostral cavity, which houses the vomeronasal organ, is bordered laterally and ventrally by the maxillaries and is open dorsally, thus forming a continuous osteological space with the nasal cavity. However, in *D. hyognathus*, the rostral cavity is completely covered by bone dorsally and is separated from the nasal chamber. This condition is shared with *Metarhinus*. In most specimens, the elements of the rostrum are completely fused into a solid dorsal cover and a distinct dorsal ridge of bone (the apparent osteological marker for the cartilaginous nasal septum) runs the length of the rostrum and extends into the nasal cavity of the skull.

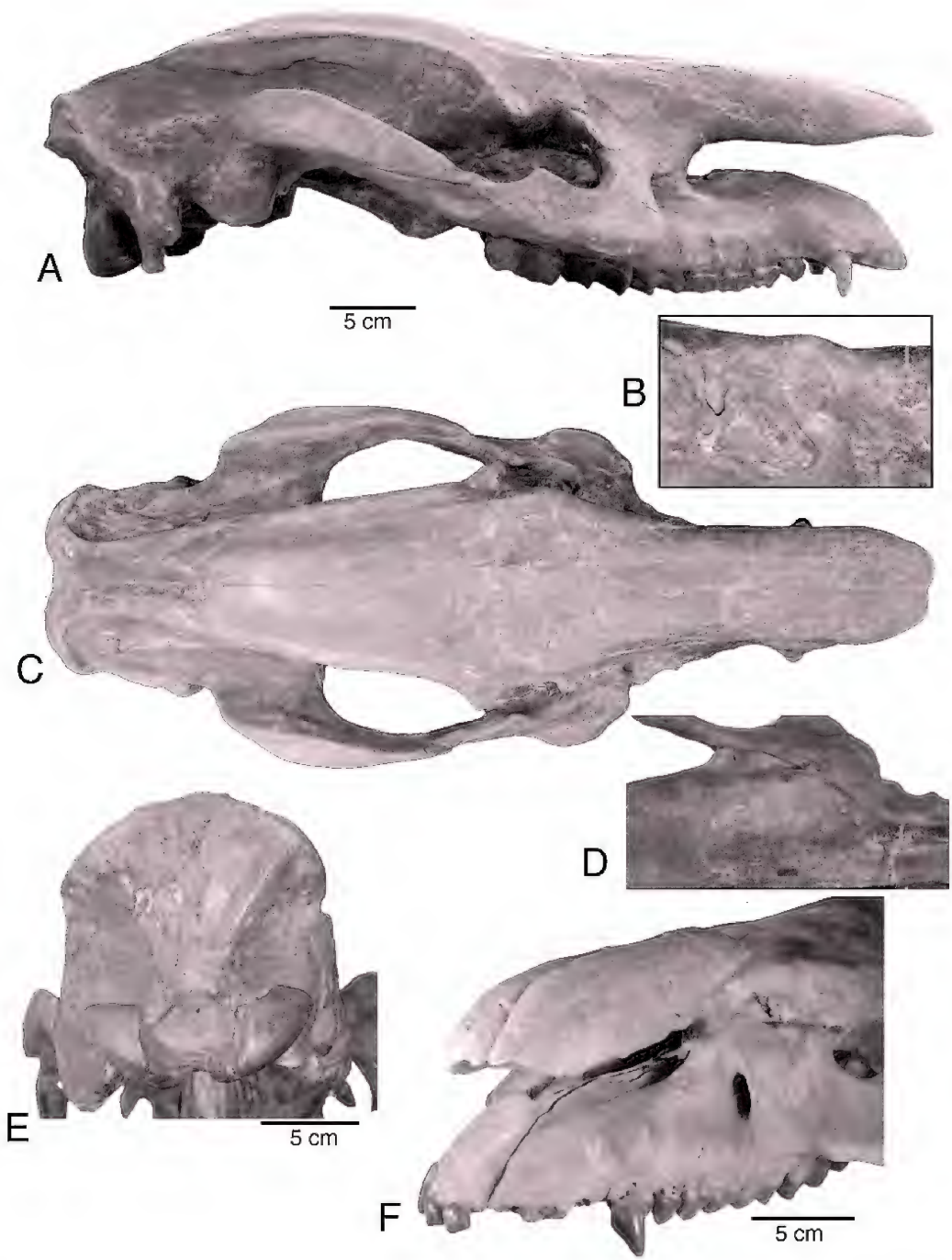

Fig. 13. Selected skulls referred to *Dolichorhinus hyognathus*. **(A)** Right lateral view of FMNH P12175, **(B)** right lateral view of orbit and nasal horn of AMNH 1851, **(C)** dorsal view of FMNH P12175, **(D)** dorsal view of superorbital region of AMNH 1851, **(E)** posterior view of AMNH 1845, **(F)** oblique view of AMNH 13164 showing details of premaxillomaxillary rostrum.

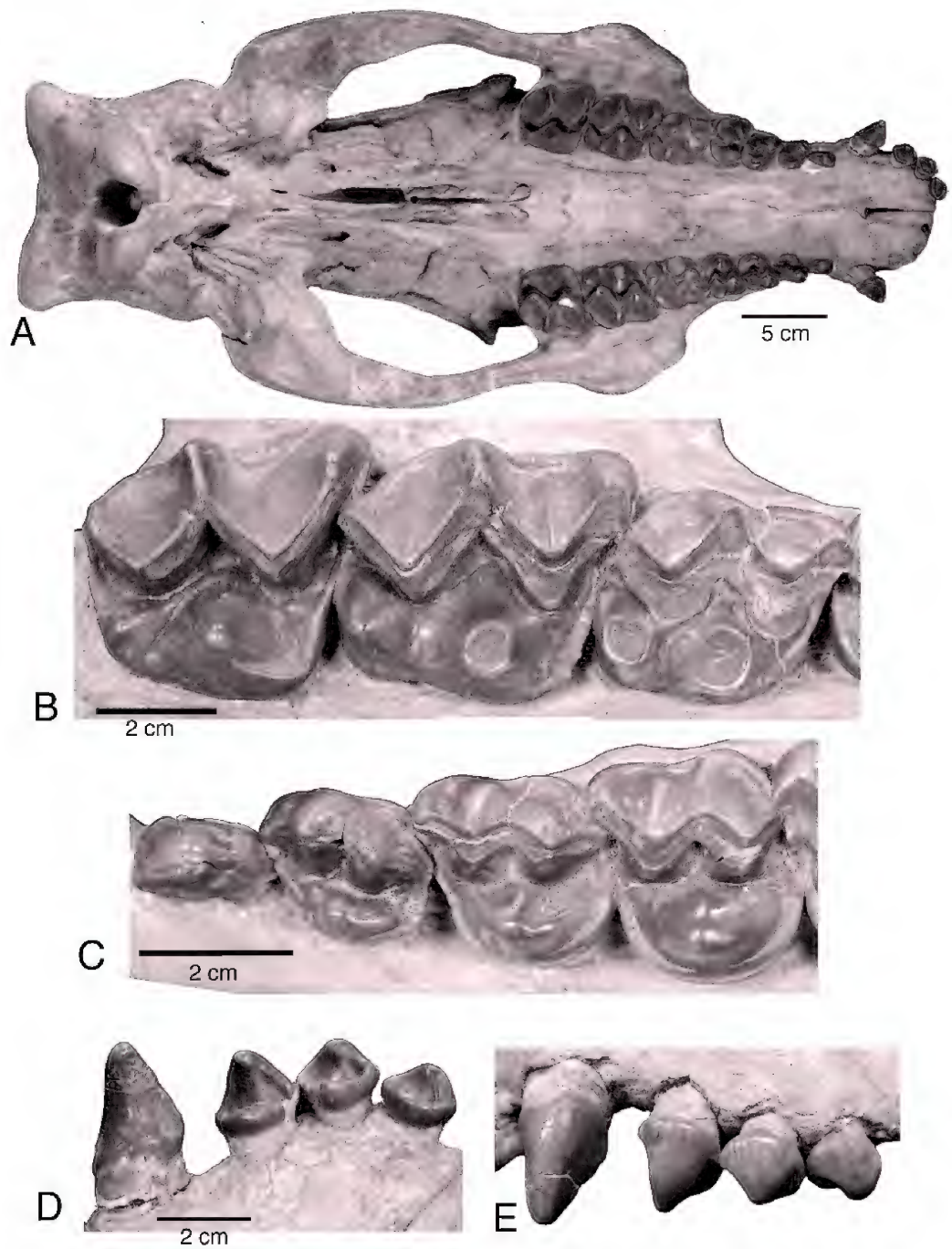

Fig. 14. The ventral surface and upper dentition of *Dolichorhinus hyognathus*, AMNH 13164. **(A)** Ventral view of skull, **(B)** right molars, **(C)** left premolars, **(D)** lingual view of right incisors, **(E)** labial view of right incisors.

TABLE 2
Summary statistics for selected morphometric variables of *Dolichorhinus hyognathus*
See Methods for measurement definitions

	Number	Mean	SD	Min.	Max.	CV
C L	15	19.2	3.1	15.9	25.3	16.0
P3 L	24	22.2	2.6	17.4	26.9	11.5
P3 W	24	22.8	1.8	19.6	26.0	7.9
M2 L	24	43.8	5.2	34.2	52.1	11.9
M2 W	23	41.2	3.5	35.4	47.0	8.5
P2–P4	21	62.1	5.3	53.0	71.6	8.6
M1–M3	27	120.1	10.9	94.8	140.0	9.0
VL	18	530.9	43.0	440	585	8.1
c L	8	20.1	2.0	17.3	22.8	10.0
p3 L	10	22.4	1.8	20.3	24.9	8.0
p3 W	9	14.4	0.9	12.9	15.6	6.5
m2 L	12	40.5	3.2	36.0	46.2	8.0
m2 W	10	25.4	2.1	21.8	28.3	8.1
p2–p4	12	69.1	4.2	63.3	77.3	6.1
m1–m3	10	133.0	7.0	123.1	141.3	5.3

The skull of AMNH 13164 allows for a more precise description of the specialized rostrum. The premaxillae are joined at the midline for almost their entire length and they form a domelike roof above the incisors. The posterior tips of the premaxillae diverge posterolaterally forming a posterior notch between the premaxillae. A thin pair of bones emerges horizontally from the nasal cavity and covers the dorsal surface of the rostrum, inserting into the notch formed by the premaxillae. Laterally, these small bones are sutured to the maxillaries. The origin of this unusual bony cover is uncertain. It continues posteriorly into the skull, but most specimens are filled with sediment or they are too heavily damaged to trace this structure internally. It seems most likely that these bones represent extensions of the maxilloturbinates, which, in the cross-sectional view of AMNH 1851 appear to extend into the rostral cavity below the surface of the bony covering (see Osborn, 1929a: fig 254c).

The dorsal surface of the skull above the orbits is slightly concave. Behind the orbits, the dorsal surface is strongly convex because the posterior half of the skull is strongly arched dorsally. The parasagittal ridges do not join to form a sagittal crest; instead, the parasagittal ridges remain separate throughout their length, although they strongly constrict the dorsal surface of the skull posteriorly.

The zygomatic arches are thin, shallow, and slightly bowed laterally. The jugal portion of the zygomatic arch is horizontal, while the squamosal portion is angled posterodorsally, thus giving the zygomatic arch a weak curvature. A conspicuous rounded infraorbital process extends ventrolaterally from the jugal. This process is similar to those of *Mesatirhinus* and *Sphenocoelus*, though it is generally larger and more laterally projected. In most specimens of *D. hyognathus* the flange created by the infraorbital process extends onto the maxillary forming a distinct secondary process. The degree to which the jugal and maxillary infraorbital processes are separated varies; sometimes it appears as a single flange (e.g., CMNH 3117).

From a dorsal view of the skull the nuchal crest has a shallow but wide median notch. From the posterior view, the nuchal crest is strongly arched dorsally. The width of the upper portion of the occiput is similar to the width of the ventral portion in AMNH 1845, although in other specimens the dorsal portion of the occiput is narrower. The width of the occiput is not strongly constricted in the middle as in *Mesatirhinus*. Small occipital pillars are visible on the posterior surface of

the occiput, although the middle of the occiput is not deeply recessed between these structures. The occipital condyles of *Dolichorhinus hyognathus* seem disproportionately large and are almost as wide as the entire occiput.

Peterson (1924) first noted many of the peculiar aspects of the posterior nares of *Dolichorhinus hyognathus*. A distinct rim of bone, seemingly the original position of the posterior nares, is positioned between the anterior margins of the M3s. The position of this rim fluctuates between the hypocones of the M2 (e.g., CMNH 3117) to between the M3 protocones (e.g., FMNH P12167). A raised palatal extension is seen behind the original margin of the posterior nares. In AMNH 13164, this palatal extension is about three cm long and shifts the position of the posterior nares to a point between the posterior margins of the M3s. However, this palatal extension is commonly longer and shifts the posterior nares to well behind the M3s (e.g., AMNH 1845). A short median process extends posteriorly from both the original border of the posterior nares and from the palatal extension. Behind the palatal extension, an elongate posterior narial canal is bisected lengthwise by a thin vomerine septum. Two elongate pouches of bone (choanal pouches) project beyond the palatal extension and fill roughly the anterior two thirds of the posterior narial canal. The bony choanal pouches that extend beyond the palatal extension are similar to those seen in *Telmatherium validus* and *Metarhinus abbotti*, although they are more elongate and positioned much farther posteriorly in *D. hyognathus*. The thin pouches appear to be extensions of the maxilloturbinates, as seen in a cross section of AMNH 1851 (see Osborn 1929a: fig 254c). Finally, the functional posterior nares are situated near the end of the posterior narial canal. In AMNH 13164, the posteriorly shifted right functional posterior naris can be clearly seen behind the bony choanal pouch. The left posterior naris of this specimen is still filled with sediment.

Dolichorhinus hyognathus lacks large paired ventral sphenoidal fossae as seen in *Sphenocoelus uintensis*, however in AMNH 13164 a pair of very small ovoid pits can be seen on the ventral surface of the basisphenoid. The pits are separated by a rod-shaped structure that joins the thin vomerine septum. However, most other specimens of *D. hyognathus* lack these small pits entirely and have a relatively normal basisphenoid.

The external auditory pseudomeatus enters the skull at a posteromedial angle, a condition shared with *Sphenocoelus*. Other aspects of the basicranium of *Dolichorhinus hyognathus* are more typical. For instance, the external auditory pseudomeatus is wide and unconstricted ventrally. The main basicranial foramina such as the foramen lacerum and the foramen ovale are widely spaced.

Upper Dentition: The following description of the upper dentition of *Dolichorhinus hyognathus* is based primarily on AMNH 13164 (fig. 14), although additional information from other specimens is provided. The three upper incisors are large and form an arched row that extends anterior to the canines. The incisors increase in size laterally. The crowns are subcaniniform: they are short, pointed, and lingually curved. Each crown is only slightly bilaterally asymmetrical from the lingual view. Each incisor has a thick lingual cingulum. No specimen of *D. hyognathus* exhibits labial incisor cingula. The precanine and postcanine diastemata are shorter than the P2. The canine of AMNH 13164 is small, as is typical of many specimens of this species.

The P1 crown is relatively simple with a single cusp and a narrow posterior heel. Other specimens (e.g., AMNH 1852) have slightly less elongate P1s. There is no P1–P2 diastema, although a p1–p2 diastema is found in the mandible (see below). The remaining premolars (P2–P4) become progressively larger and less oblique posteriorly. The anterior margin of the P2 crown is strongly posterolingually angled, although in other specimens the P2 is more nearly square (e.g., AMNH 1851). The parastyle and metastyle of P2 arch slightly lingually. The parastyle and metastyle of P3 are nearly straight, while those of P4 are angled labially. The labial paracone ribs of the P2–P4 become shorter and narrower in more posterior premolars. The metacone of P2 is shifted lingually in comparison to those of P3 and P4. Because of these differences, the labial wall of the P2 is rounder than those of

P3 and P4. A small bulge of enamel can be found at the labial base of the metacone of P4. This small bulge is not present in every specimen, and in some others it is enlarged and forms a short mesostyle (CMNH 11081, FMNH P12182).

The lingual side of the P2 crown exhibits a large protocone, a distinct lingual crest extending posteriorly from the protocone, and a small preprotocrista. In P3, these crests are faint. P4 lacks these crests altogether, but there is a tiny beadlike paraconule. The lingual sides of the premolars of *Dolichorhinus hyognathus* are morphologically unstable. For instance, in FMNH PM3870 there are no lingual crests extending posteriorly from the protocones and each premolar (P2–P4) has a small but distinct preprotocrista. Other specimens have large lingual crests extending posteriorly from the protocones, or even distinct hypocones, but this last condition is very rare. For instance, CMNH 11081, a specimen with heavily worn dentition, has a small hypocone on P2. The shape of the wear facets on P3 and P4 of that specimen suggests that hypocones were present on those premolars as well, but were worn off.

The labial cingula of the premolars are thin but distinct. They tend to be discontinuous around the proximal base of the paracone in P2 and P3, but continuous around the base of the paracone of P4. The anterior and posterior premolar cingula are thick and stretch around the lingual sides of the crowns. They are not connected lingually in AMNH 13164, but in other specimens (e.g., AMNH 1850) they form continuous lingual cingula.

The molars of *Dolichorhinus hyognathus* exhibit numerous brontotheriine apomorphies such as tall, lingually angled ectolophs, weak labial ribs, thin lingual ectoloph enamel, and wedge-shaped lingual borders of the paracone and metacone visible in molars that are not heavily worn. The anterior cingulum is thin and passes proximally to the distal peak of the parastyle. *D. hyognathus* molars lack anterolingual cingular cusps. Shallow central molar fossae are invariably present. Each of the molars of AMNH 13164 retains a vestigial paraconule, however the size and presence of paraconules in the molars of *D. hyognathus* is variable (e.g., smaller in FMNH P12182, absent in FMNH P12175). All traces of a metaloph on M1 and M2 are lost. The M3 of AMNH 13164 has a small hypocone and small metalophlike ridge. However, the presence and size of these structures varies. For instance, in FMNH P12175 and FMNH P12188 the M3 hypocone is as large as that of the M2. On the other hand, FMNH PM3873 lacks a M3 hypocone altogether.

Mandible and Lower Dentition: The description of the mandible and lower dentition of *Dolichorhinus hyognathus* is based on two nearly perfectly preserved and essentially identical mandibles (AMNH 13164 and AMNH 1856) with complete and lightly worn teeth (fig. 15). The holotype mandible (YPM PU10273) is also pictured (fig. 16). The mandible of *D. hyognathus* is distinctive in the slenderness of the horizontal ramus. The ascending ramus is short. The coronoid process is long, curves posteriorly, and is taller than the mandibular condyle. The symphysis is long and relatively slender in comparison to most other brontotheriids. The inferior margin of the symphysis has a very shallow angle (much less than 45°), although the symphyses of AMNH 13164 and AMNH 1856 are somewhat steeper than that of the holotype. The symphysis extends posteriorly to the trigonid of the p3, although in some specimens it extends only to the p2 talonid (e.g., AMNH 1587).

The three lower incisors are rather large and form a broad semicircular arch. The incisors are mesiodistally elongate and roughly of the same size. The crowns are short, lingually curved, slightly bilaterally asymmetrical, and with blunt distal points. From the lingual view, the incisors each have a prominent lingual rib and distinct lingual cingulid. It is apparent from specimens with more heavily worn incisors that these characters tend to fade with wear. No labial cingulids are seen on the lower incisors. There are no gaps between any of the incisors, although there is occasionally a very short precanine diastema. The lower postcanine diastema is typically longer than the upper postcanine diastema. In AMNH 1856 and AMNH 13164, the postcanine diastema is about the length of the p2. The lower canine is typically small.

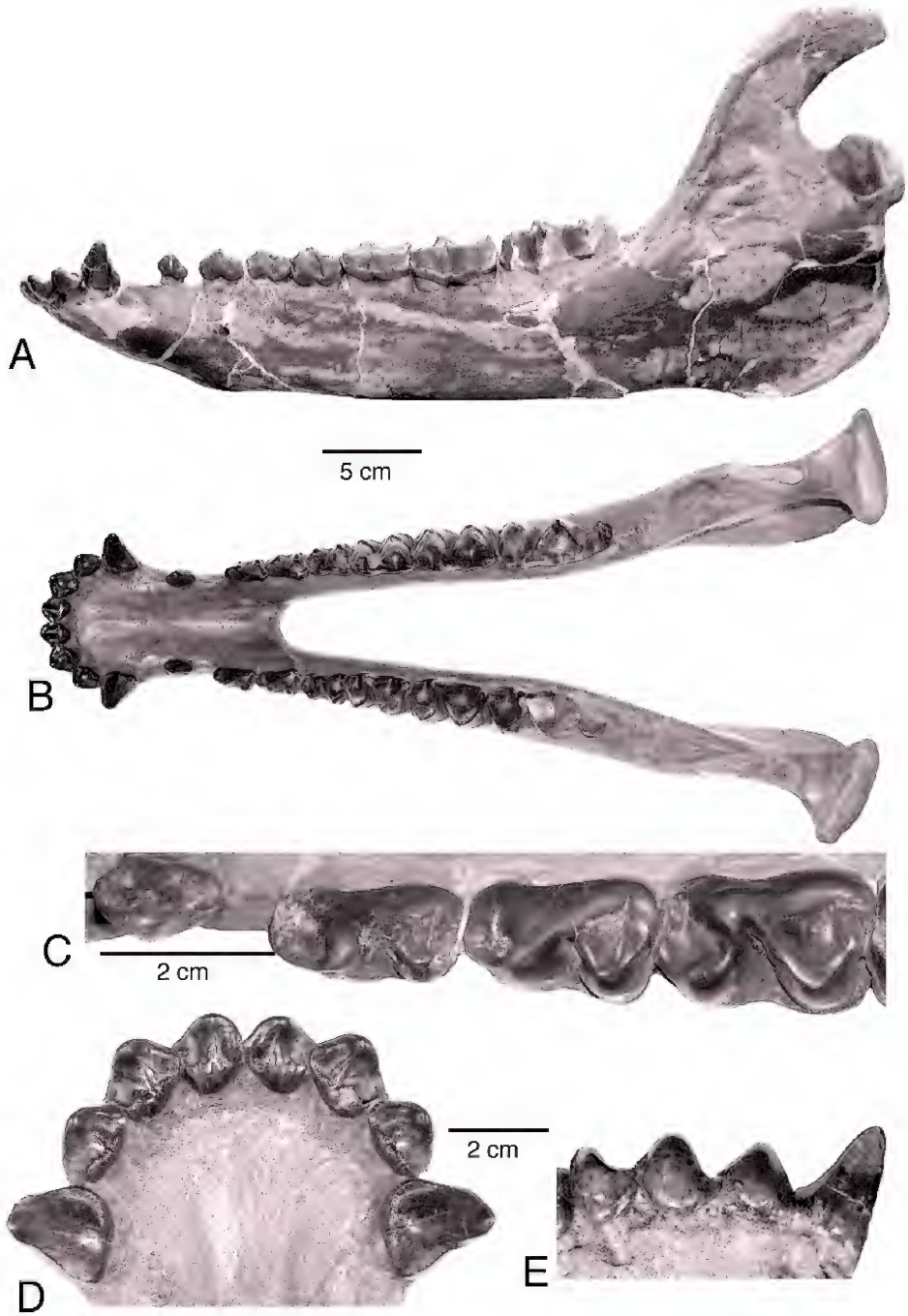

Fig. 15. Selected views of mandibles and lower dentitions of *Dolichorhinus hyognathus*. **(A)** Left view of AMNH 13164, **(B)** dorsal view of AMNH 1856, **(C)** left premolars of AMNH 1856, **(D)** lingual view of incisors and canines of AMNH 1856, **(E)** labial view of left incisors and canine of AMNH 1856.

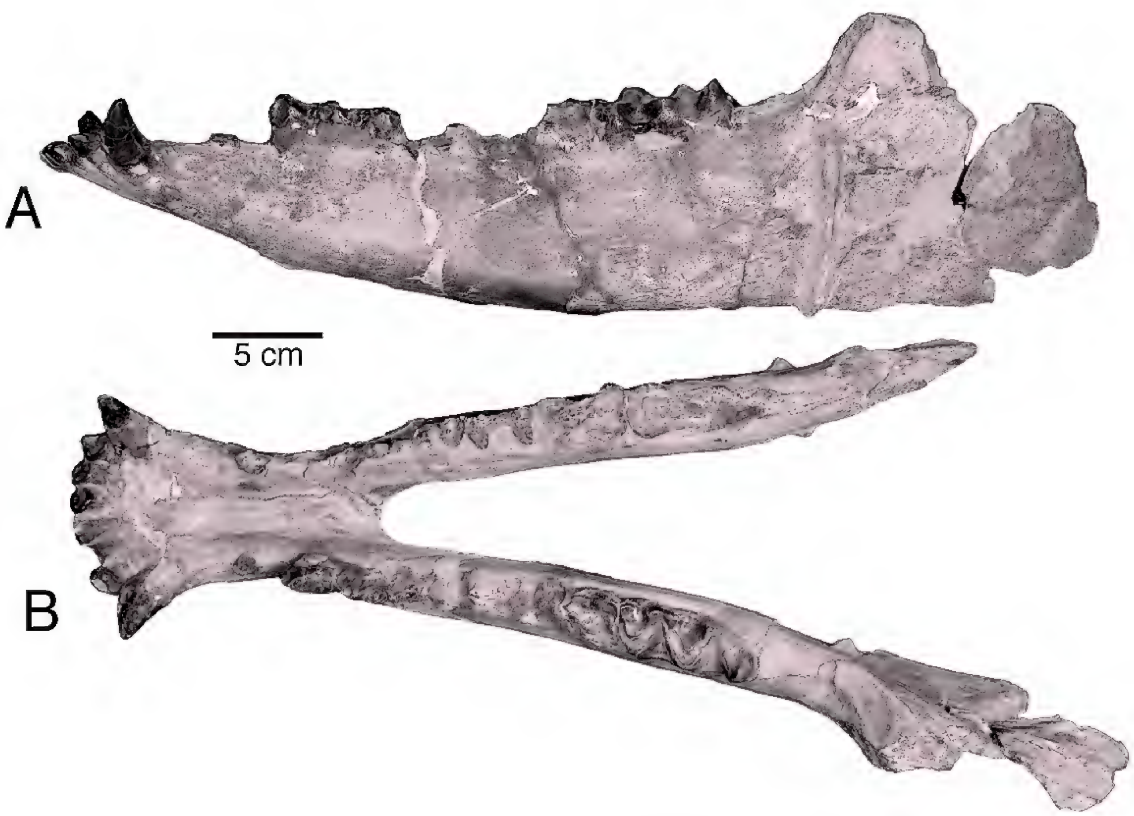

Fig. 16. Holotype of *Dolichorhinus hyognathus* (courtesy of Division of Vertebrate Paleontology, YPM PU10273. © 2005 Peabody Museum of Natural History, Yale University, New Haven, Connecticut, USA. All rights reserved.). **(A)** Left view, **(B)** dorsal view.

The p1 is a small elongate tooth with a single cusp and a narrow bladelike talonid heel. A p1–p2 diastema is always present, although its length is variable. In AMNH 13164, for instance, it is visibly shorter than that of the holotype jaw, YPM PU10273. The trigonid of the p2 is much longer than the talonid, although the trigonid and talonid are of similar width. The paralophid of p2 is essentially straight, although in some specimens it can curve slightly lingually, creating a small lingual notch in the trigonid. The p2 protolophid is short, straight, and extends in a posterior direction from the protoconid. The p3 trigonid is slightly longer and narrower than the talonid. The paralophid of the p3 curves in a slightly lingual direction, creating a distinct lingual notch in the trigonid. The p3 protolophid extends about equally lingually and posteriorly from the protoconid. The p4 trigonid is clearly shorter and narrower than the talonid. The paralophid of p4 strongly arches lingually creating a very broad lingual notch in the trigonid. The p4 is the only premolar with a large lingually positioned metaconid. The p2 talonid has a short cristid obliqua and hypolophid with a shallow sloping notch on the lingual side of the crown. The talonids of p3 and p4 have longer and more well-developed cristids obliqua and hypolophids with broader and more nearly molariform talonid basins.

The lower molars of *Dolichorhinus hyognathus* have relatively thin lingual enamel, shallow talonid and trigonid basins, and an elongate m3. The cheek teeth of AMNH 13164 lack lingual cingulids and the labial cingulids are thin and discontinuous around the bases of the cusps. The distinctness of the labial cingulids is variable; this is at least partly related to the degree of dental wear.

Remarks

Dolichorhinus hyognathus (Osborn, 1889) was based on a mandible, YPM PU10273 (fig. 18). The holotype can be distinguished from *Sphenocoelus*, *Mesatirhinus*, *Telmatherium*, *Sthenodectes*, and *Metarhinus* by the combination of its more slender proportions, shallow angle of the ventral margin of the symphysis, and retention of a p1–p2 diastema. Osborn (1889) originally assigned this species to the genus *Palaeosyops*. Shortly thereafter, Earle (1892), who described YPM PU10273 in more detail, reassigned this species to the genus *Telmatotherium* (a variation on the spelling of *Telmatherium*).

In 1895, Osborn described a complete skull (AMNH 1851) that he referred to *Telmatotherium cornutum*; he also referred several skulls to the same species, including AMNH 1850, AMNH 1847, AMNH 1848, AMNH 1852, and AMNH 1837. These specimens represent a species that was "remarkable for its very long flat-topped cranium and its incipient knoblike osseous horns borne chiefly upon the nasals, but partly upon the frontals" (Osborn, 1895: 92). None of these skulls was associated with a jaw that would allow direct comparison with the type jaw of *T. hyognathus*. Nonetheless, Osborn conjecturally referred several mandibles (AMNH 1857, AMNH 1858, AMNH 1854, and AMNH 1855) to *T. cornutum*. Based on these jaws, he distinguished *T. cornutum* from *T. hyognathus* "by the presence of two incisors" (p. 92). However, this was clearly a mistake, because one of these mandibles (AMNH 1854) shows three unmistakable incisor alveoli. The other specimens are too damaged or the teeth are too worn to determine the number of incisors.

Shortly thereafter, Hatcher (1895) reassigned the species *Telmatotherium cornutum* to a new genus, *Dolichorhinus*, but made no mention of *T. hyognathus*. Subsequently, Osborn (1908a) named another species, *D. intermedius*. This species was based on a skull (AMNH 1837) that was essentially the same as those he had referred to *D. cornutum*. Douglass (1909) and Riggs (1912) continued the trend of erecting new species based on skulls similar to those that Osborn had referred to *D. cornutum*. Douglass (1909) erected *D. heterodon* (CMNH 2340) and *D. longiceps* (CMNH 2347), while Riggs (1912) erected *D. fluminalis* (FMNH P12205) and *D. superior* (FMNH P12168). (The holotype of *D. superior* was mistakenly reported by Riggs (1912) to be FMNH P12188. However, records at the FMNH indicate that the holotype specimen has always been catalogued as FMNH P12168 [William Simpson, personal commun., 2004]). When all of these supposed species were distinguished from others, differentiaion was based on (1) minor size differences or (2) taphonomic distortion and/or damage. However, all of these holotype skulls strongly resemble the holotype skull of *Dolichorhinus cornutum*, and I have not been able to find any compelling morphological differences between them. Peterson (1924) expressed doubt over the validity of the large number of *Dolichorhinus* species, although he did little to rectify this problem and continued to "provisionally" accept all of the species that had been named by Osborn, Douglass, and Riggs.

Osborn (1908a, 1929a) ultimately concluded that the neglected holotype jaw of *Telmatotherium hyognathus* (Osborn) (YPM PU10273) represented the same species as the holotype skull of *Dolichorhinus cornutum* (AMNH 1851). Osborn (1929a) reassigned *T. hyognathus* to the genus *Dolichorhinus* and considered *D. cornutum* to be a junior synonym of *D. hyognathus*. At that point, *D. hyognathus* became the type species of *Dolichorhinus*. Despite this one revision, Osborn (1929a) continued to recognize all of the other species of *Dolichorhinus* as valid, despite the similarities of the holotype skulls of each of these supposed species.

Mader (1989) expressed doubt about Osborn's (1908a) decision to synonomize *D. cornutum* with *D. hyognathus*; he considered *D. cornutum* to be the type species and considered *D. hyognathus* to be a nomen dubium. Subsequently, Mader (1998) accepted only two species of *Dolichorhinus*, *D. hyognathus* and *D. intermedius*, but he mistakenly reassigned these species to the genus *Sphenocoelus*. However, it can be shown that *Dolichorhinus* (sensu Hatcher and sensu Osborn) is clearly distinct from *Sphenocoelus* (sensu Osborn). There are at least six conspicuous differences between

Sphenocoelus and *Dolichorhinus*: (1) *Sphenocoelus* lacks the specialized morphology of the premaxillomaxillary rostrum seen in *Dolichorhinus*. (2) *Sphenocoelus* has large ventral sphenoidal fossae, while *Dolichorhinus* does not. (3) *Sphenocoelus* has a sagittal crest, while *Dolichorhinus* does not. (4) The posterior half of the cranium of *Dolichorhinus* is more strongly arched than that of *Sphenocoelus*. (5) *Dolichorhinus* molars have distinct central fossae, whereas central molar fossae are apparently variable in *Sphenocoelus*. (6) Finally, there is a p1–p2 diastema in the mandibles of *Dolichorhinus*, whereas *Sphenocoelus* lacks a p1–p2 diastema.

Fortunately, there are at least two associated skulls and mandibles (e.g., AMNH 13164 and CMNH 11017) that allow one to confirm that the holotype mandible of *Dolichorhinus hyognathus* does belong to the same species as the highly elongate, distinctive skulls that represent other supposed species of *Dolichorhinus* (*D. cornutum*, *D. intermedius*, *D. heterodon*, *D. longiceps*, *D. superior*, and *D. fluminalis*). The characteristics found to be variable among these specimens is consistent with intraspecific variation found in most species of brontotheres and does not suggest multiple species. These variable characters include the presence or absence of M3 hypocones, the presence or absence of molar paraconules, the presence or absence of a minor P4 mesostyle, the variable lingual morphology of the premolars, and the size and distinctness of hornlike protuberances. Therefore, all other species of *Dolichorhinus* are considered junior synonyms of *D. hyognathus* (Osborn, 1889).

Sphenocoelus uintensis Osborn, 1895

HOLOTYPE: AMNH 1501, the posterior part of a skull.

TYPE LOCALITY: Northeastern Utah, Wagonhound Member (Uinta B1) of the Uinta Formation, Wyoming.

SYNONYMS: *Tanyorhinus blairi* Cook, 1926 and *Tanyorhinus bridgeri* Cook, 1926.

AGE: Middle Eocene (early Uintan land mammal "age").

REFERRED SPECIMENS: **(From the Wagonhound Member of the Uinta Formation of Utah)** CMNH 2963, a posterior part of a cranium (partially prepared); **(from the Sand Wash Basin of Moffat County, Colorado)** DMNH 479 (holotype of *Tanyorhinus bridgeri*), a skull with left P3–P4, M2–M3; DMNH 484, a right maxilla with C, P2–M2; DMNH 507, an anterior portion of a skull with left P1–M3; DMNH 509, an anterior portion of a skull with right P3–P4 (all partial) and left P2–P3; DMNH 517, a right premaxillomaxillary fragment with isolated incisors and isolated P2–M1; DMNH 541 (holotype of *Tanyorhinus blairi*, in part), a skull with P1–P4, M3, and left P1–M3; DMNH 542 (holotype of *Tanyorhinus blairi*, in part), a mandible with right i1–m3, left i1–p4, and m2–m3; DMNH 2830, a skull with right I2–I3, P1–M3, left P2–M3, and a complete mandible with complete dentition; DMNH 14219, a mandible with complete dentition; DMNH 29411, a skull with right P1–M3 and left C–M3; **(from the Adobe Town Member [Washakie B of Granger, 1909] of the Washakie Formation, Wyoming)** UCMP 81281, a partial mandible with right p3–p4 and left p2–m1; UCMP 81301, a skull that is missing the premaxilla and zygomatic arches with right P3–M3 and left M1–M3; UCMP 81443, a partial mandible with right i1–c, p2–p4, and left i1–p3.

SPECIMENS REFERRED TO CF. *SPHENOCOELUS*: The following specimens are consistent with *Sphenocoelus uintensis* and probably belong to that species, but they lack sufficiently diagnostic characters to definitively refer them to *S. uintensis*: **(from the Sand Wash Basin of Moffat County, Colorado)** DMNH 504, a mandible with right and left p1–m3; DMNH 505, a partial mandible with right m1–m2, left m2–m3, isolated canine, and right p4; DMNH 506, left M1–M3 (very worn); DMNH 506a, right M3; DMNH 556, a mandible fragment with right p4–m2 and m3 (partial); DMNH 2584, a partial mandible with right p2–m3; **(from the Adobe Town Member [Washakie B of Granger, 1909] of the Washakie Formation, Wyoming)** UCMP 81294, a partial mandible with right p3–m3; UCMP 81299, a partial mandible with right p3–m3; UCMP 81366, a mandible fragment with left p4–m2; UCMP 81369, a left M1 or M2; UCMP 81370, a mandible fragment with left p3–m1; UCMP

81402, a right maxilla fragment with P1–P4; UCMP 81412, a left P2; UCMP 81413, left p2; UCMP 81414, a left P3 or P4; UCMP 81416, a right P4; UCMP 81422, a right M2 (partial), and M3; UCMP 81438, a right maxilla fragment with P1 (roots) and P2–P3; UCMP 81440, a partial mandible with broken incisors, right p2–p4, left m2 (partial) and m3; UCMP 81448, a partial mandible with left p3–m3; UCMP 81451, a partial mandible with right p2 (partial), p3–m2, and m3 (partial); UCMP 81462, an isolated incisor.

DIAGNOSIS: *Sphenocoelus uintensis* is an intermediate-sized hornless brontothere in which the frontal bone does not overlap or intrude into the nasal bone. The cranium of *S. uintensis* is highly dolichocephalic. The nasal incision extends as far back as the anterior margin of the M1. The nasal process is horizontal, unelevated, of relatively constant transverse width, narrow, with thin and relatively shallow lateral walls, and without a well-defined or strongly rounded distal margin. The orbits do not protrude laterally; they are positioned above the posterior part of M2 and the anterior part of M3 with the anterolateral root of M2 and the posterolateral root of M1 below the anterior orbital rim. There is a prominent infraorbital process on the jugal. The premaxillomaxillary rostrum deepens posteriorly and is not covered by bone dorsally. Other cranial characteristics include a short sagittal crest, thin and weakly curved zygomatic arches, a ventrally open and steeply posteriorly angled external auditory pseudomeatus, disproportionately wide occipital condyles, and large paired ventral sphenoidal fossae. The cranium is dorsally arched but more weakly so than *Dolichorhinus*.

Dentally, *Sphenocoelus uintensis* is characterized by large subcaniniform upper incisors, a postcanine diastema, a simple P1, a distinct P2 metacone, weak premolar preprotocristae, and with short crests extending posteriorly from the premolar protocones. Premolar hypocones are absent. The molars of *S. uintensis* have tall, lingually angled ectolophs with weak labial ribs, and thinned lingual ectoloph enamel with wedge-shaped paracones and metacones. A cingular parastyle shelf and an anterolingual cingular cusp are absent. Central molar fossae are present in some specimens but absent in others. *S. uintensis* molars occasionally retain vestigial paraconules, but all traces of a metaloph are lost. The lower dentition of *S. uintensis* includes large semispatulate incisors that are all of a similar size, a postcanine diastema, no p1–p2 diastema, an elongate p2 trigonid, a metaconid on p4 but not on p2 and p3, shallow molar basins, and a slender m3.

Sphenocoelus uintensis is most similar to *Mesatirhinus junius*, but it is clearly distinct from that species due to its larger size, more dolichocephalic proportions, and paired ventral sphenoidal fossae. Likewise, paired sphenoidal fossae, an unspecialized premaxillomaxillary rostrum, and a sagittal crest distinctly set it apart from *Dolichorhinus hyognathus*.

DESCRIPTION

SKULL: The holotype of *Sphenocoelus uintensis* (AMNH 1501) is the posterior part of a skull from the Uinta Basin that has suffered minor shearing distortion but is otherwise in good condition (fig. 17). Other specimens referable to *S. uintensis* have been recovered from the Sand Wash Basin of Colorado (e.g., Cook, 1926) and from a collection of the Washakie Basin of Wyoming made by McKenna and Kent in 1954. Among these are several complete (or nearly complete) skulls and a variety of cranial fragments and mandibles. The following description of the skull and upper dentition is based upon the holotype and five other skulls, UCMP 81301 (fig. 18b) DMNH 479 (fig. 18a), DMNH 541 (not shown), DMNH 2830 (figs. 18c–d, 19a), and DMNH 29411 (not shown). Other specimens provide additional information on variation.

Sphenocoelus uintensis is an intermediate-sized brontothere (table 3) whose skull is generally similar to *Mesatirhinus junius* but notably more dolichocephalic. Hornlike nasal or frontonasal protuberances are not seen in *S. uintensis*. The frontonasal suture, most clearly visible in UCMP 81310 (not shown), recedes posteromedially, but near the midline the direction of the suture is acutely redirected anteriorly. The frontal does not overlap the nasal or protrude into the nasal as in *Telmatherium validus*.

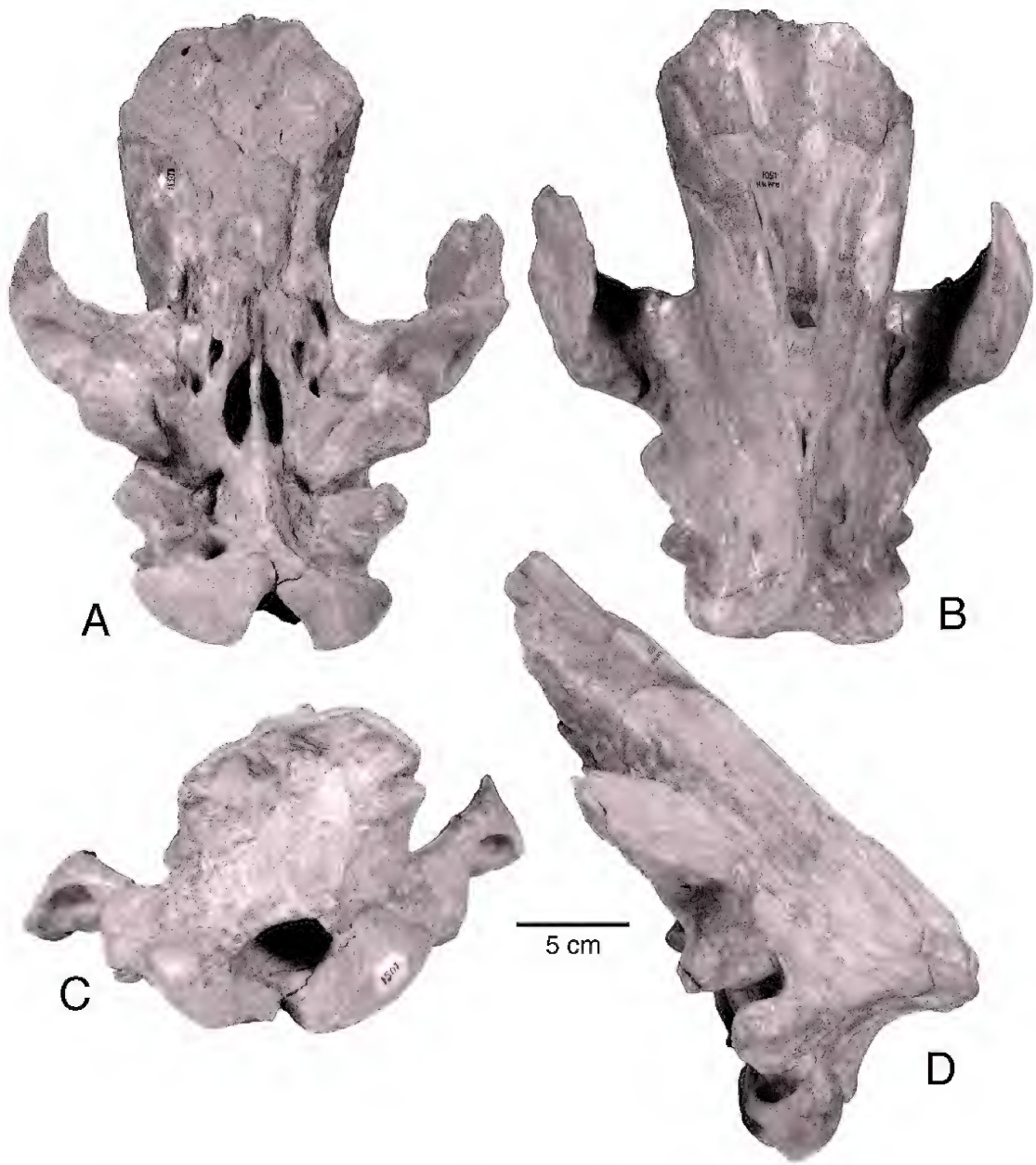

Fig. 17. Holotype partial cranium of *Sphenocoelus uintensis* (AMNH 1501). **(A)** Ventral view, **(B)** dorsal view, **(C)** posterior view, **(D)** left view.

The nasal incision is shallow and long and extends as far back as the anterior edge of M1, while the orbit is positioned above the posterior part of M2 and the anterior part of M3. The anterolateral root of the M2 and the posterolateral root of the M1 are situated directly below the anterior orbital rim.

The premaxillomaxillary rostrum lacks the specializations seen in *Dolichorhinus*. From a lateral view of the skull the dorsal edge of the premaxillomaxillary rostrum ascends posterodorsally. The posteriormost notch of the nasal incision is level with the top of the orbit. The nasal processes of the premaxillae

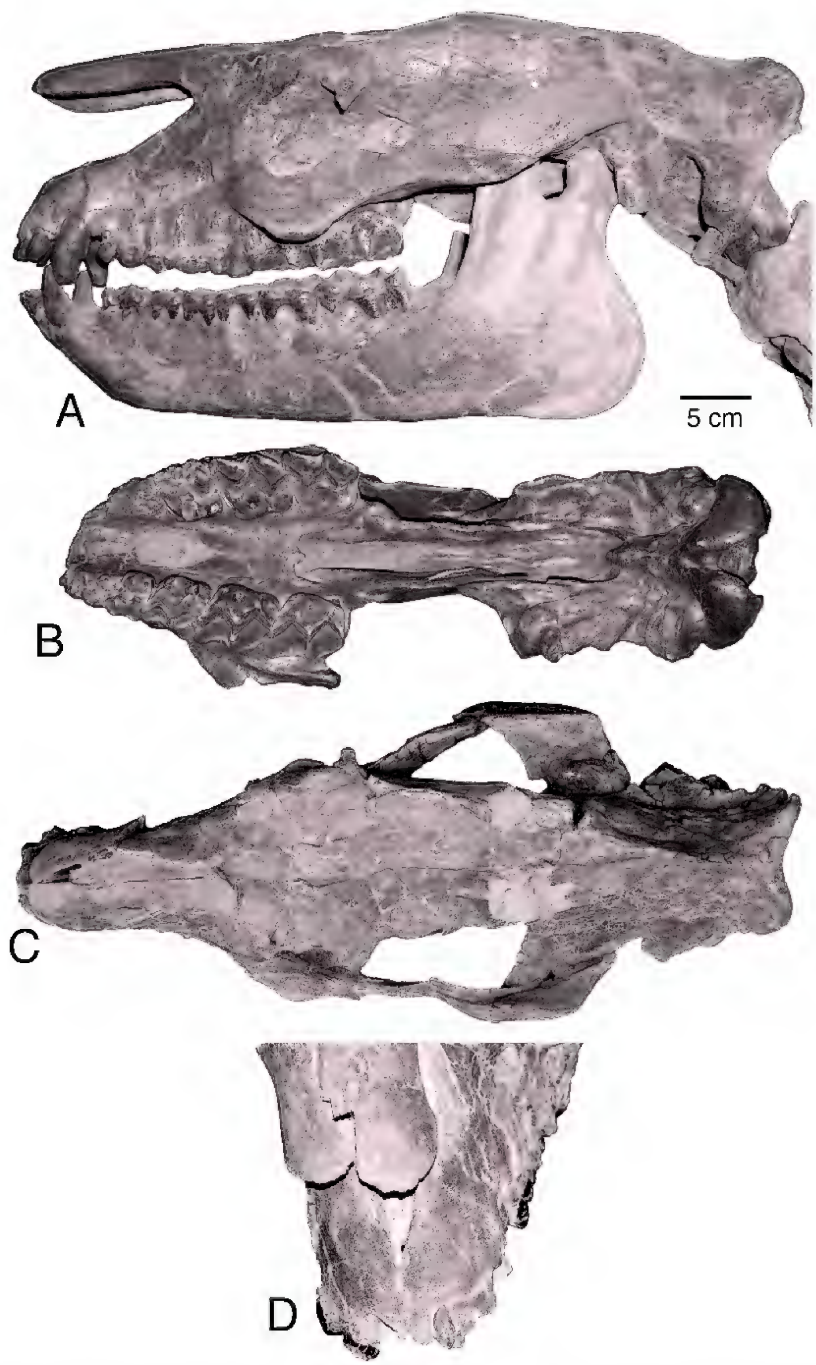

Fig. 18. Selected skulls referred to *Sphenocoelus uintensis*. **(A)** Left view of DMNH 479, the holotype of *Tanyorhinus bridgeri*, **(B)** ventral view of UCMP 81310, **(C)** dorsal view of DMNH 2830, **(D)** anterodorsal view of the nasal and rostrum of DMNH 2830.

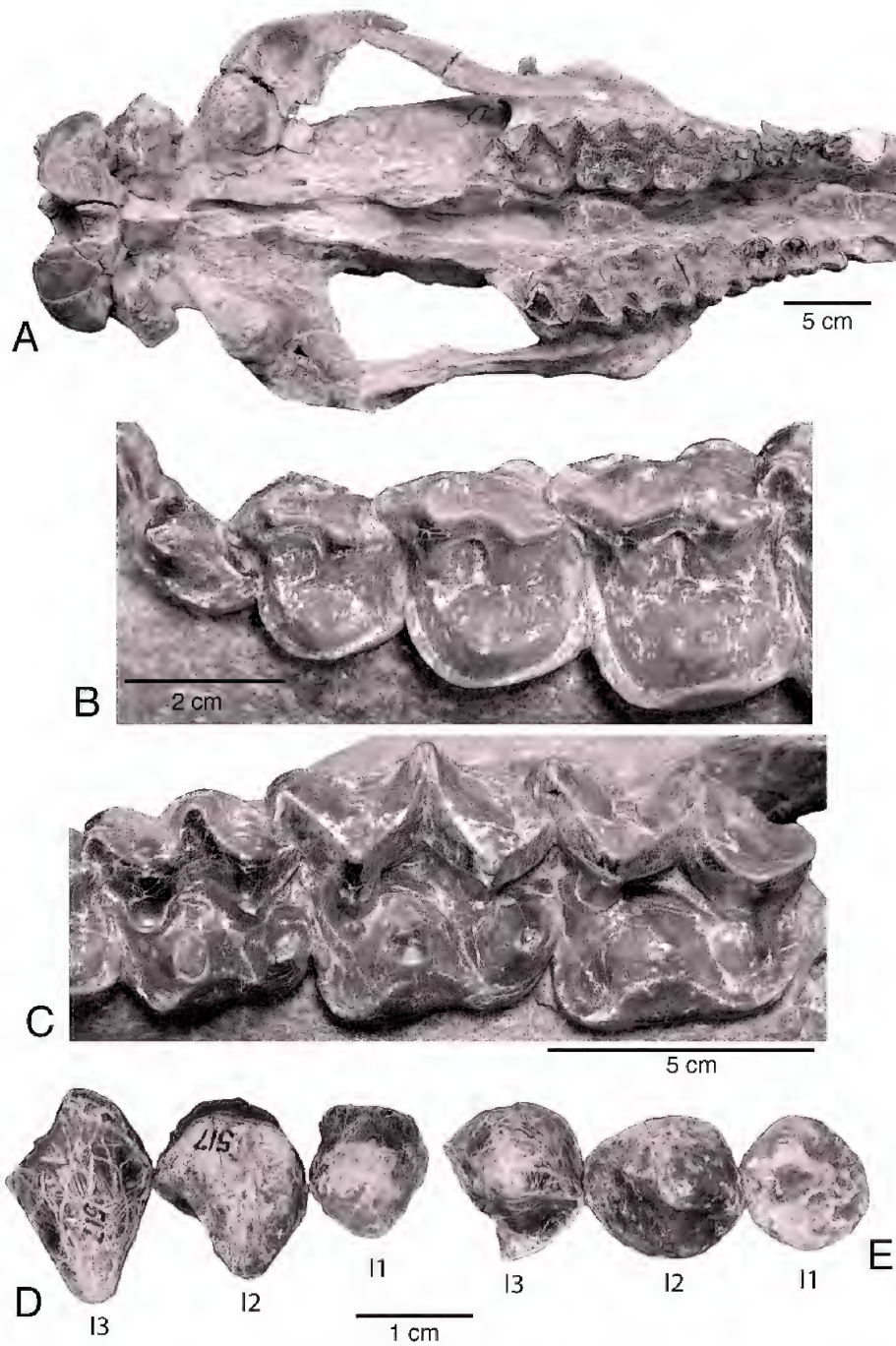

Fig. 19. Views of the ventral skull surface and upper teeth of *Sphenocoelus uintensis*. **(A)** Ventral view of DMNH 2830, **(B)** left premolars of DMNH 29411, **(C)** left molars of DMNH 29411, **(D)** labial view and **(E)** occlusal view of isolated right incisors of DMNH 517.

TABLE 3
Summary statistics for selected morphometric variables of *Sphenocoelus uintensis*
See Methods for measurement definitions

	N	mean	SD	Min.	Max.	CV
C L	4	22.2	2.0	20.4	25.0	8.8
P3 L	11	21.3	2.0	17.7	24.0	9.2
P3 W	10	25.1	1.7	2.6	28.9	6.6
M2 L	8	45.7	2.8	42	49.2	6.2
M2 W	8	43.2	2.6	40.1	46.5	6.0
P2–P4	7	66.4	4.2	63.4	75.3	6.3
M1–M3	6	125.0	7.1	116	135.3	5.7
VL	3	538.7	22.9	524	565	4.2
c L	4	20.3	1.4	18.8	22.0	7.0
p3 L	14	22.7	1.0	20.5	23.7	4.2
p3 W	12	15.3	1.2	13.9	17.7	8.1
m2 L	12	41.3	2.2	37	44.1	5.4
m2 W	10	26.7	2.2	24.3	30.9	8.3
p2–p4	7	69.4	2.0	66.5	72.5	2.9
m1–m3	7	135.0	6.5	126	142.0	4.8

diverge laterally and the premaxillomaxillary cavity is open dorsally. A distinct remnant of the right premaxillomaxillary suture in UCMP 81310 indicates that the premaxilla does not contact the nasal bone.

The bones of the nasal process are not strongly fused together. The nasal processes are slightly shorter and somewhat narrower than the premaxillomaxillary rostrum. The transverse width of the nasal process is nearly constant throughout its length. In the least distorted skulls, such as DMNH 479, the nasal process extends horizontally from the skull, or it bends just slightly downward so that the dorsal surface of the nasal process is slightly convex. The lateral walls of the nasal process are relatively thin and dorsoventrally shallow, but they are of constant depth throughout the length of the nasal process. The anterior border of the nasal process is thin, roughened, and angled downward moderately.

The dorsal surface of holotype skull fragment (AMNH 1501) is essentially flat, although complete skulls indicate a more dorsally arched cranium. In the least distorted skulls (DMNH 29411, DMNH 479, and UCMP 81301), the dorsal surface of the skull above the orbits is flat or slightly concave. However, the dorsal surface of the posterior half of the skull is strongly convex. The highly elongated posterior half of the cranium tends to be slightly dorsally arched from a lateral view, but not as strongly as the skull of *Dolichorhinus hyognathus*. In the holotype and in other specimens, the parasagittal ridges merge to form a short sagittal crest.

The zygomatic arches are relatively thin, slender, and slightly bowed laterally. The jugal portion of the zygomatic is essentially horizontal, while the squamosal portion rises posteriorly at a moderate angle, thus giving the zygomatic arch a weakly curved shape. The jugal of *Sphenocoelus uintensis* has a large rounded infraorbital process. The infraorbital process resembles those of *Mesatirhinus* and *Dolichorhinus*, but it is larger and more distinct than that of *Metarhinus*.

The occipital can be adequately described from the holotype skull (AMNH 1501). The occiput is moderately tilted backward. From a dorsal view of the skull the nuchal crest is thin and concave. From the posterior view the nuchal crest is arched. The center of the occiput is not deeply recessed between the small occipital pillars. The occiput is narrower dorsally than it is ventrally. The occipital condyles of *Sphenocoelus uintensis* are disproportionately very large and almost as wide as the entire occiput.

Many aspects of the ventral surface of the skull of *Sphenocoelus uintensis* are most clearly revealed in UCMP 81310 (fig. 18b). The anterior rim of the posterior nares is

positioned at the anterior margin of the M3. The anterior edge of the posterior nares is abrupt; that is, there is no horseshoe-shaped emargination, nor is there a bony palatal extension like that of *Dolichorhinus*. A short median process protrudes posteriorly from the midline of the anterior edge of the posterior nares, marking the posteriormost contact point of the vomer and palatal bones. The posterior narial canal is extremely long and continues into a large cavity in the sphenoid bone. The vomer is missing in UCMP 81310, but it would have originally formed a long, thin plate of bone that bisected the elongate posterior narial canal. Remnants of the elongate vomer can be seen in the form of a thin ridge of bone running along the dorsal roof of the posterior narial canal in UCMP 81301.

The posterior narial canal continues into a large vacuity in the sphenoid bone. Deep vacuities in the sphenoid can also be seen in the holotype (AMNH 1501) and in all other skulls of *Sphenocoelus uintensis*. Osborn referred to these fossae as "pits" (Osborn, 1895) and "sphenoidal pits" (Osborn, 1929a). In some specimens, such as UCMP 81310, the cavities formed by the ventral sphenoidal fossae are large, although they seem to have been narrower in others such as AMNH 1501 and DMNH 2830. The basisphenoid is highly modified and forms a narrow septum that partitions the ventral sphenoidal fossae; this is most clearly seen in AMNH 1501 (fig. 17). The partitioning basisphenoid is so thin that it is commonly not preserved.

In most of the specimens the ventral sphenoidal fossae form a continuous channel with the posterior narial canal. The thin partitioning basisphenoid would have connected with the elongate vomer to form a continuous partition of the posterior narial canal and sphenoidal fossae. The holotype (AMNH 1501) is somewhat unusual in this respect because the ventral sphenoid fossae appear to extend deeper into the ventral surface of the cranium, thus forming distinct pits. Apparently the depth and diameter of the ventral sphenoidal fossae are intraspecifically variable.

The external auditory pseudomeatus, formed by the mastoid and postglenoid processes of the squamosal bone, enters the skull at a strongly posteromedial angle, a condition shared with *Dolichorhinus*. Other aspects of the basicranium of *Sphenocoelus uintensis* are more typical. For instance, the external auditory pseudomeatus is not enclosed ventrally and the foramen ovale is widely separated from the foramen lacerum. One final peculiar aspect of *S. uintensis* is a distinct fossa on the ventral surface of the zygomatic process of the squamosal just lateral to the glenoid fossa (this is best seen on the holotype skull fragment, AMNH 1501).

Upper Dentition: Unfortunately, none of the skulls of *Sphenocoelus uintensis* has an intact set of upper incisors. In DMNH 2830 there are six incisor alveoli that form a semicircular arch anterior to the canines and are separated from the canines by a short I3–C diastema (fig. 19a). The two preserved incisors (right I2, I3) are large and though they are worn, they appear to have been subcaniniform (conular and lingually curved). The I3 is larger than the I2. Three isolated incisors are associated with DMNH 517, a maxilla that appears to be *S. uintensis* (fig. 19d, e). Although there is no way to know which crown is which, judging by comparison with the partial set of incisors in the skull of DMNH 2830, they appear to form a right incisor row, with the smallest incisor I1 and the largest I3. The crowns are subcaniniform with lingually curved crowns and narrow lingual heels. The I1 is the shortest incisor, while I2 and I3 are progressively taller and larger in diameter.

The canines are not well preserved in any of the skulls. One specimen, DMNH 29411, retains a left canine with a tall crown and a rounded cross section. Another specimen, DMNH 2830, includes an isolated canine of similar morphology. Despite the rather dolichocephalic proportions of the skull of *S. uintensis*, the postcanine diastemata of *S. uintensis* is very short in all specimens and is usually only a few millimeters long.

The most adequately preserved sets of cheek teeth are of DMNH 2830, DMNH 29411, and UCMP 81310. Figured are the complete and relatively unworn cheek teeth of DMNH 29411 (fig. 19b, c). The P1 is simple, with a single cusp and a low posterior heel. The P2 is slightly oblique in outline due

to a posterolingually angled anterior edge. The anterior and posterior sides of P3 and P4 are more nearly parallel. The labial side of P2 is strongly rounded, while those of P3 and P4 are progressively flatter. The parastyle of P2 arches slightly lingually, while the metastyle is nearly straight. The metacone of P2 is positioned slightly lingually with respect to the protocone. The parastyle and metastyle of P3 are straight, while those of P4 are angled slightly labially. Small labial paracone ribs are present on P2–P4 and become progressively shorter on more posterior premolars.

A very small but distinct preprotocrista connects the protocone with the lingual base of the paracone in P2. In P3 and P4 this crest becomes progressively smaller, so that it is barely perceptible in P4. A low crest descends the posterior slope of the protocone on P2–P4. This lingual crest is not present on more worn sets of dentition (e.g., DMNH 2830), although it is present on the P2, P3, and P4 of DMNH 29411. Yet in others (e.g., UCMP 81301) the lingual crest is not seen on P4. There are no hypocones on the premolars. The anterior and posterior cingula of the premolars are thick and most often stretch around the lingual side forming a continuous lingual cingulum, although it is occasionally discontinuous, as is the case in UCMP 81301. The labial premolar cingula of the P2 and P3 typically connect to the posterior ridge of the paracone rib, but the labial cingulum of P4 most often stretches across the base of the crown.

The molars are *Sphenocoelus uintensis* have tall, lingually angled ectolophs, weak labial ribs, thin lingual ectoloph enamel, and wedge-shaped lingual sides of the paracone and metacone in molars that are not heavily worn (e.g., M3). The anterior cingulum is thin and passes proximally to the distal peak of the parastyle. *Sphenocoelus uintensis* molars lack an anterolingual cingular cusp. Very small paraconules are occasionally retained on the molars, although no evidence of a metaloph was found on any specimen. Among the specimens referred to *Sphenocoelus uintensis*, some (DMNH 507, DMNH 484, and DMNH 29411) have shallow but distinct central fossae in the molars. However, in other specimens (UCMP 81301, DMNH 2830, DMNH 541, and DMNH 517) they appear to be absent or very shallow. A M3 hypocone is generally absent, although a thick cingulum traces around the distolingual corner of the M3 crown. Cook (1926) reported a small "postero-internal" cusp on the M3 of DMNH 479, but I was unable to examine the ventral surface of that skull because it is part of a composite skeleton encased in glass on exhibit at the DMNH. The lingual molar cingula are typically discontinuous around the protocone and hypocone. Likewise, the labial molar cingula are thin and tend to be discontinuous around the mesostyles.

MANDIBLE AND LOWER DENTITION: One skull of *Sphenocoelus uintensis* is associated with a mandible (DMNH 2830) that retains a complete set of well-worn lower teeth (fig. 20a–b). Additionally, several mandibles, some with less worn dentition, are morphologically consistent with the mandible of DMNH 2830, but are not directly associated with diagnosable skulls. The following description of the mandible and lower dentition of *S. uintensis* is based primarily on DMNH 2830 and other specimens with well-preserved incisors and premolars (UCMP 81281 and UCMP 81443) (fig. 20c–e).

The horizontal ramus of *S. uintensis* is elongate and shallow, like that of *Dolichorhinus*. However, the ventral margin of the symphysis is steeper than *Dolichorhinus hyognathus*, and more similar to that of *Mesatirhinus*. The position of the posterior margin of the symphysis varies slightly but it usually extends to the posterior part of the p3. The three pairs of incisors are large and form an arched row that reaches anterior to the canines. The incisors increase in size laterally. There are small gaps between the incisors of DMNH 2830, but these gaps are probably a result of extensive wear. UCMP 81443 has a better set of incisors, though they are also heavily worn. In this specimen, there are no gaps between the incisors. Judging by the shape of the wear facets of UCMP 81443, the i1 and i2 were semispatulate, while the i3 was more subcaniniform. A distinct lingual cingulid can be seen on each incisor. Moreover, each incisor has a distinct labial cingulid.

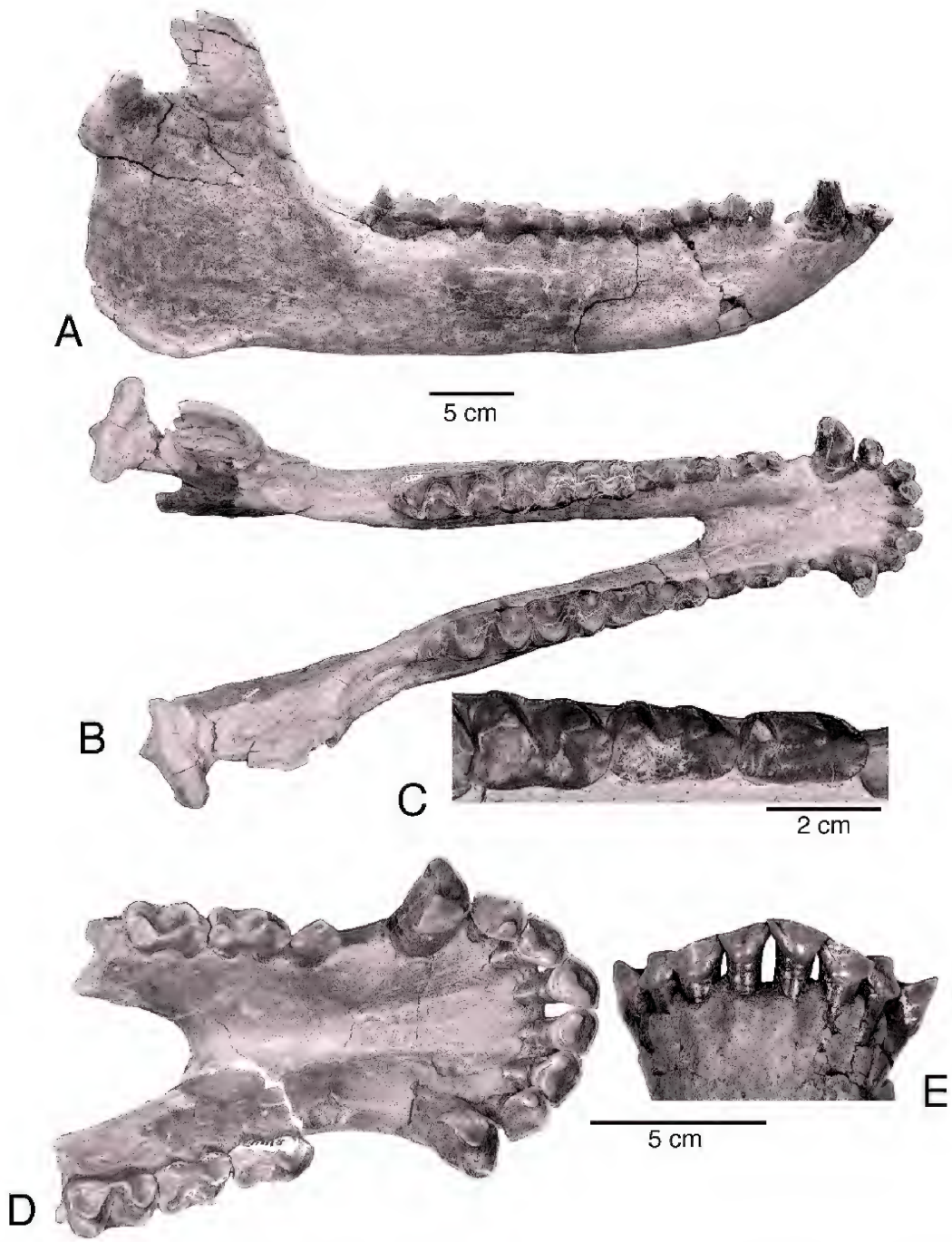

Fig. 20. Selected mandibles and lower dentitions of *Sphenocoelus uintensis*. **(A)** Right view of DMNH 2830, **(B)** dorsal view of DMNH 2830, **(C)** left p2, p3, and p4 of UCMP 81281, **(D)** dorsal view of UCMP 81443, **(E)** labial view of incisors and canines of UCMP 81443.

The lower canines of DMNH 2830 are large although the canines of other specimens (UCMP 81443) are somewhat smaller. The canine is followed by a postcanine diastema that is generally shorter than the p2. However, the lower postcanine diastema is longer than the upper postcanine diastema. The p1 is a simple tooth with a single cusp and a short and narrow talonid. There is no p1–p2 diastema in DMNH 2839 or any other mandible referred to *Sphenocoelus uintensis*. This is an important diagnostic feature that helps to differentiate the mandibles of *S. uintensis* from those of *Dolichorhinus hyognathus*, a species with a distinct p1–p2 diastema.

The p2–p4 of DMNH 2830 and UCMP 81443 are moderately worn, but much of their morphology is still discernable. UCMP 81281 has unworn premolars. The p2 trigonid is much longer than the talonid, but the trigonid and talonid are of similar width. The talonid and trigonid of p3 are of comparable length but the trigonid is slightly narrower than the talonid. The trigonid of the p4 is both shorter and narrower than the talonid. The paralophid of the p2 is either straight (e.g., UCMP 81281) or slightly arched lingually (UCMP 81443), thus creating a small lingual notch in the trigonid. The p3 paralophid arches at a slightly more lingual angle than that of the p2. The p4 paralophid is strongly directed lingually, creating a broad lingual trigonid notch; that of p3 is angled somewhat lingually, and that of p4 arches fully lingually. A metaconid is present only on p4. The talonid of p2 has only a minor lingual notch and a short cristid obliqua and hypolophid. The p3 and p4 have longer cristids obliqua and hypolophids with much broader talonid basins.

The molars of *Sphenocoelus uintensis* are typical of brontotheriines, with relatively thin lingual enamel and an elongate m3. The m3 hypoconulid heel of DMNH 2830 is unusually narrow, but this is atypical. Other specimens have a broader m3 hypoconulid. Lingual cingulids are absent, while the labial cingulids of p2–m3 vary in distinctness (this is related to wear), and tend to be discontinuous around the protoconid. Occasionally the m3 cingulid traces around the distal end of the hypoconulid (e.g., DMNH 14219).

Remarks

Osborn (1895) recognized that AMNH 1501 (fig. 17) represented a new species, *Sphenocoelus uintensis*, due primarily to the peculiar pair of ventral sphenoidal fossae. Because the specimen lacked teeth, Osborn (1895) was initially unsure what family of perissodactyls *S. uintensis* belonged to, but he ultimately (Osborn, 1929a) concluded that *S. uintensis* was a brontothere largely because of the relative positions of the basicranial foramina, and the similarity of the glenoid facets to that of *Dolichorhinus*. Osborn (1929a) also noted similarities between AMNH 1501 and YPM PU10041, a braincase of a brontothere that is probably *Mesatirhinus junius*.

In retrospect, by the time Osborn's (1929a) argument for *Sphenocoelus uintensis* as brontothere was published, Cook (1926) had described several complete brontothere skulls from the Sand Wash Basin of Moffat County, Colorado. However, Cook (1926) made no comparison of this material with Osborn's holotype of *S. uintensis*, nor did he mention the conspicuous ventral sphenoidal fossae of these specimens. He erected a new genus and two new species, *Tanyorhinus blairi* (DMNH 541) and *T. bridgeri* (DMNH 479). These species were differentiated from each other by minor differences in size (6%), and a variety of other characters that can be attributed to taphonomic distortion (e.g., more curved zygomatic arches) and other aspects of variation that do not warrant species distinctions (e.g., variable presence of M3 hypocone). The apparent difference in head orientation between these two supposed species suggested by Cook (1926) is artificial and can mostly be attributed to deformation in the more poorly preserved specimen (DMNH 541).

Mader (1998) considered *Tanyorhinus blairi* and *T. bridgeri* to be junior synonyms of *Sphenocoelus uintensis*, a revision that is upheld here. Mader (1989) also considered the genera *Dolichorhinus* Hatcher (1895) and *Dolichorhinoides* Granger and Gregory (1943) to be junior synonyms of the genus *Sphenocoelus*. However, *Dolichorhinoides* is actually a synonym of *Epimanteoceras* Granger and Gregory (1943), a taxon that

clearly differs from *Sphenocoelus* in numerous ways, including the absence of ventral sphenoidal fossae, the absence of a sagittal crest, the presence of small frontonasal protuberances, and significantly, more molarized premolars. Additionally, *Dolichorhinus* differs from *Sphenocoelus* in many significant ways, including the specialized rostrum, the bony palatal extension, the more strongly arched cranium, and the p1–p2 diastemata. Additionally, *Sphenocoelus* differs from *Dolichorhinus* in having large ventral sphenoidal fossa, a sagittal crest, and a steeper mandibular symphysis.

In overall appearance, the skulls of *Sphenocoelus uintensis* resemble those of *Mesatirhinus junius*, although *M. junius* lacks ventral sphenoidal fossae and is smaller than *S. uintensis*. Several brontotheres share large ventral sphenoidal fossae with *Sphenocoelus* including *Protitan*, *Diplacodon*, *and Metatitan*.

Microtitan mongoliensis (Osborn, 1925)

NEOTYPE: AMNH 22099, a partial mandible with right p1 alveolus and p2–m3.

TYPE LOCALITY: Ulan Shireh Formation, eight miles north of Tukhum Lamasery, Inner Mongolia, China.

AGE: Middle Eocene (Irdinmanhan land mammal "age").

REFERRED SPECIMEN: **(From the same locality as the neotype)** AMNH 21611, a left maxilla with C–M3.

DIAGNOSIS: *Microtitan mongoliensis* is one of several relatively small Asian brontotheres. The dorsal surface of the maxilla rises steeply posteriorly indicating that the rostrum lacks the specializations seen in *Metarhinus* or *Dolichorhinus*. Dentally, *Microtitan mongoliensis* is characterized by a simple P1, a distinct P2 metacone, exceedingly weak labial paracone ribs, and weak premolar preprotocristae. *M. mongoliensis* premolars lack lingual crests (although this trait could be intraspecifically variable). Premolar hypocones are absent. The molars of *M. mongoliensis* have tall, lingually angled ectolophs with weak labial ribs, and thinned lingual ectoloph enamel with wedge-shaped paracones and metacones. A cingular parastyle shelf is absent. *M. mongoliensis* molars lack paraconules or metalophs. Central molar fossae and anterolingual cingular cusps are absent. Lower dental characters of *M. mongoliensis* include the absence of a p1–p2 diastema, an elongate p2 trigonid, a large metaconid on p4 but not on p2 and p3, shallow molar basins, rounded molar crescents, and a very elongate m3.

Microtitan mongoliensis can be readily differentiated from the vast majority of brontotheres on the basis of size, although it is within the size range of *Metarhinus*. *Microtitan* can be readily differentiated from *Metarhinus* by the ascending dorsal surface of the rostrum and lack of central molar fossae.

DESCRIPTION

SKULL: *Microtitan mongoliensis* is much smaller than the majority of brontotheres, yet it is distinctly larger than the three smallest species, *Pygmaetitan panxianensis*, *Acrotitan ulanshirehensis*, and *Nanotitanops shanghuangensis*. However, *Microtitan mongoliensis* is within the size range of *Metarhinus*. The best cranial fragment referred to *M. mongoliensis* is AMNH 21611, a left maxilla with a canine and a complete cheektooth series (fig. 21). Although the premaxilla of that specimen is not preserved, the remaining contact surface for the premaxilla can be seen on the inner side of the maxilla above the root of the canine. This surface ends above the P2. A small intact portion of the ventral edge of the nasal incision is visible on the maxilla above the P2. Although the nasal incision extended at least to this point, the specimen does not reveal the position of the posterior margin of the nasal incision. The anterodorsal surface of the preorbital portion of the maxilla rises posteriorly at a steep angle. This indicates that the premaxillomaxillary rostrum lacked the specializations seen in *Metarhinus*, in which the rostrum does not deepen posteriorly. The exact position of the orbit is indeterminate, although the surface of the orbital floor (formed by the maxilla) is intact and positioned above the M2 and M3. The orbit would have been positioned directly above the M2 or slightly behind it.

UPPER DENTITION: The canine of AMNH 21611 is of moderate size, is slightly

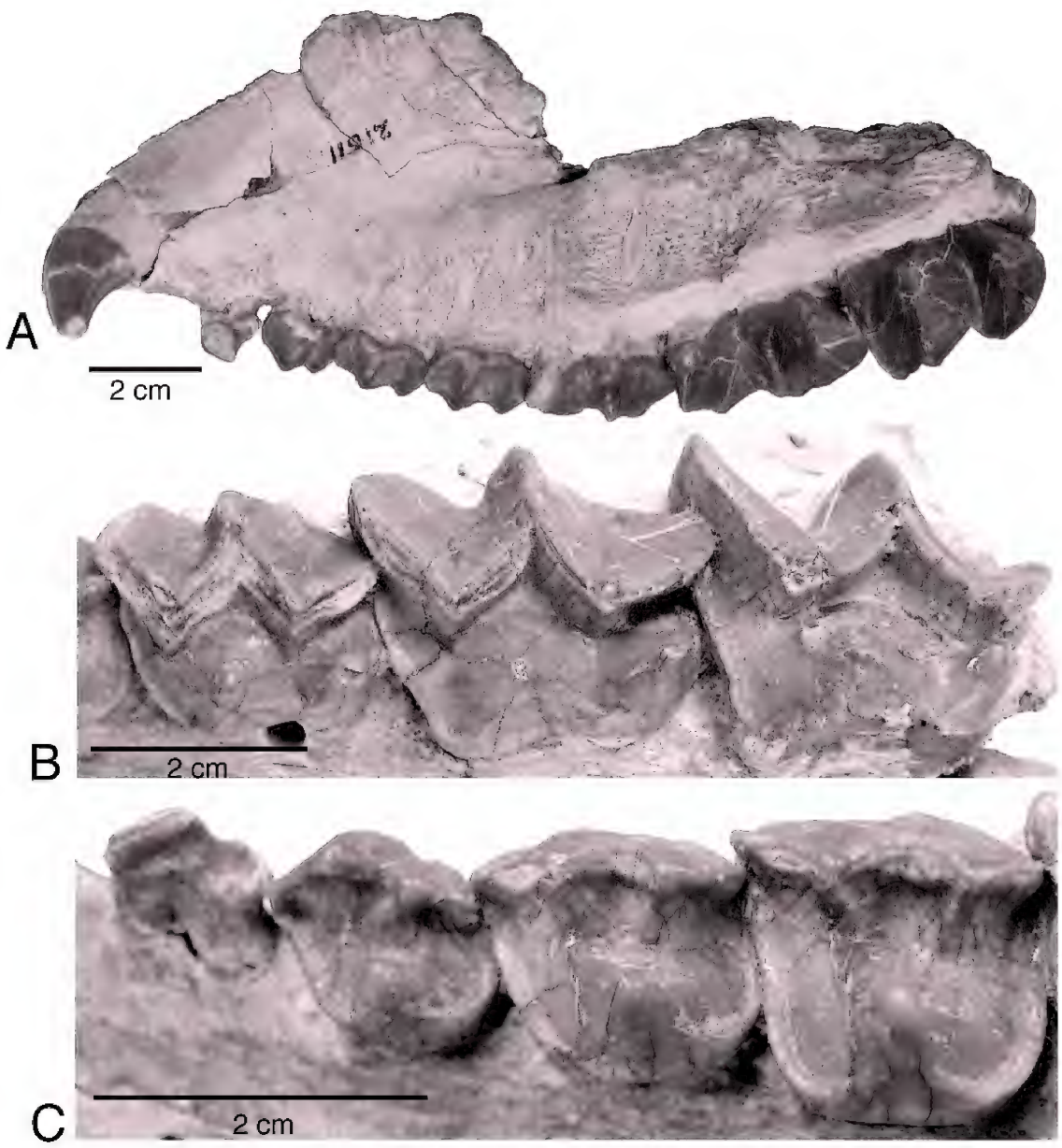

Fig. 21. A cranial fragment referred to *Microtitan mongoliensis* (AMNH 21611). **(A)** Left view, **(B)** left molars, **(C)** left premolars.

elliptical in cross section, and has no distinct cingulum. The length of the postcanine diastema is similar to the length of the P2. The P1 is a simple tooth with a single cusp and an elongate posterior heel (fig. 21c). Most of the enamel of P1 on the labial side of the cusp and on the posterior and lingual sides of the posterior heel is missing. Despite this damage, it is clear that P1 was a very narrow tooth. The P2 and P3 are obliquely shaped due to their posterolingually angled anterior margins, while P4 is more rectangular. The parastyle of P2 is arched lingually, while the parastyle of P3 is nearly straight, and the P4 parastyle is slightly angled labially. The P2 metastyle is angled slightly lingually while those of P3 and P4 are straight. Labial paracone ribs can be seen

on the P3 and P4 but they are weak. The metacone of P2 is strongly shifted lingually while those of P3 and P4 are positioned directly behind the protocone. Because of these differences the ectoloph of P2 is more rounded than the ectolophs of P3 and P4. The lingual heels of P2–P3 have large protocones. Premolar hypocones are absent. A small preprotocrista can be seen on the P2. In P3, there is a faint preprotocrista, while P4 lacks this feature completely. None of the premolars exhibits a lingual crest. The labial premolar cingula are extremely weak. The anterior and posterior premolar cingula arch around the lingual sides of the crowns, but they do not join lingually to form continuous lingual cingula.

The upper molars of *Microtitan mongoliensis* exhibit typical brontotheriine apomorphies, including tall, lingually angled ectolophs, weak labial ribs, thin lingual ectoloph enamel, and wedge-shaped lingual sides of the paracone and metacone. The anterior cingulum is thin and passes proximally to the distal peak of the parastyle. Paraconules and metalophs are completely absent. *M. mongoliensis* molars lack both anterolingual cingular cusps and central molar fossae. The M3 of AMNH 21611 has a well-developed hypocone that is somewhat smaller than the hypocones of M1 and M2. Lingual and labial molar cingula are essentially absent. One peculiar aspect of the molars of this specimen is the deep notch formed at the labial side of the paracone of each molar.

Mandible and Lower Dentition: The neotype, AMNH 22099, is a partial right ramus with a p1 alveolus (p1 missing) and complete p2–m3 (fig. 22). The partial ramus is reconstructed from fragments with plaster filling a significant gap on the ventral border of the ramus. The dorsal view of the partial ramus suggests that the symphysis extended to the talonid of p2. There is no diastema between the p1 alveolus and the p2. The premolars are slender, particularly p2. The trigonid of p2 is elongate and at least twice as long as the talonid. The p3 trigonid is much longer than the talonid as well. Finally, the p4 trigonid and talonid are of similar length. The trigonids of all the premolars are somewhat narrower than their talonids. The paralophid of p2 curves slightly lingually, although there is almost no lingual trigonid notch. The p2 protolophid is lingually positioned but directed posteriorly. The p3 paralophid is strongly angled lingually, creating a more distinct lingual trigonid notch. The p3 protolophid is straight, but it is angled slightly lingually. The paralophid and protolophid of the p4 are more nearly molariform and arch fully lingually. Among the premolars, only the p4 exhibits a large, lingually positioned metaconid. However, a small metaconid-like feature can be seen at the junction of the protolophid and cristid obliqua on the p3. Give the rudimentary nature of this structure, it is possible that a p3 metaconid was variably present. The talonid of p2 has a short but well-developed cristid obliqua and a very short hypolophid. The lingual surface of the talonid is a sloped, slightly convex surface. On the other hand, the talonids of p3 and p4 are more nearly molariform with longer cristids obliqua, longer hypolophids, and much broader basins. Labial and lingual premolar cingulids are absent.

The lower molars of AMNH 22099 have relatively thin enamel, shallow talonid and trigonid basins, and very weak lingual ribs. The m3 is one of the most elongate among brontotheres. The molars of AMNH 22099 have unusually rounded crescents, as noted by Granger and Gregory (1943). The hypoconulids of m1 and m2, though small in all brontotheres, are quite pronounced in AMNH 22099. Labial molar cingulids are exceedingly faint, and lingual molar cingulids are absent. The m3 of AMNH 22099 has a groove near the labial base of its crown that is probably a hypoplasia.

Remarks

Osborn (1925, 1929) described a new species, "*Metarhinus*?" *mongoliensis*, from a mandible fragment with a p4 and m1 (AMNH 20167) from the Irdin Manha Formation of Inner Mongolia (fig. 23). Despite the fragmentary nature of this specimen, it is clearly much smaller than any species of Asian brontothere that was known at the time. However, the size of AMNH 20167 is within the reach of the

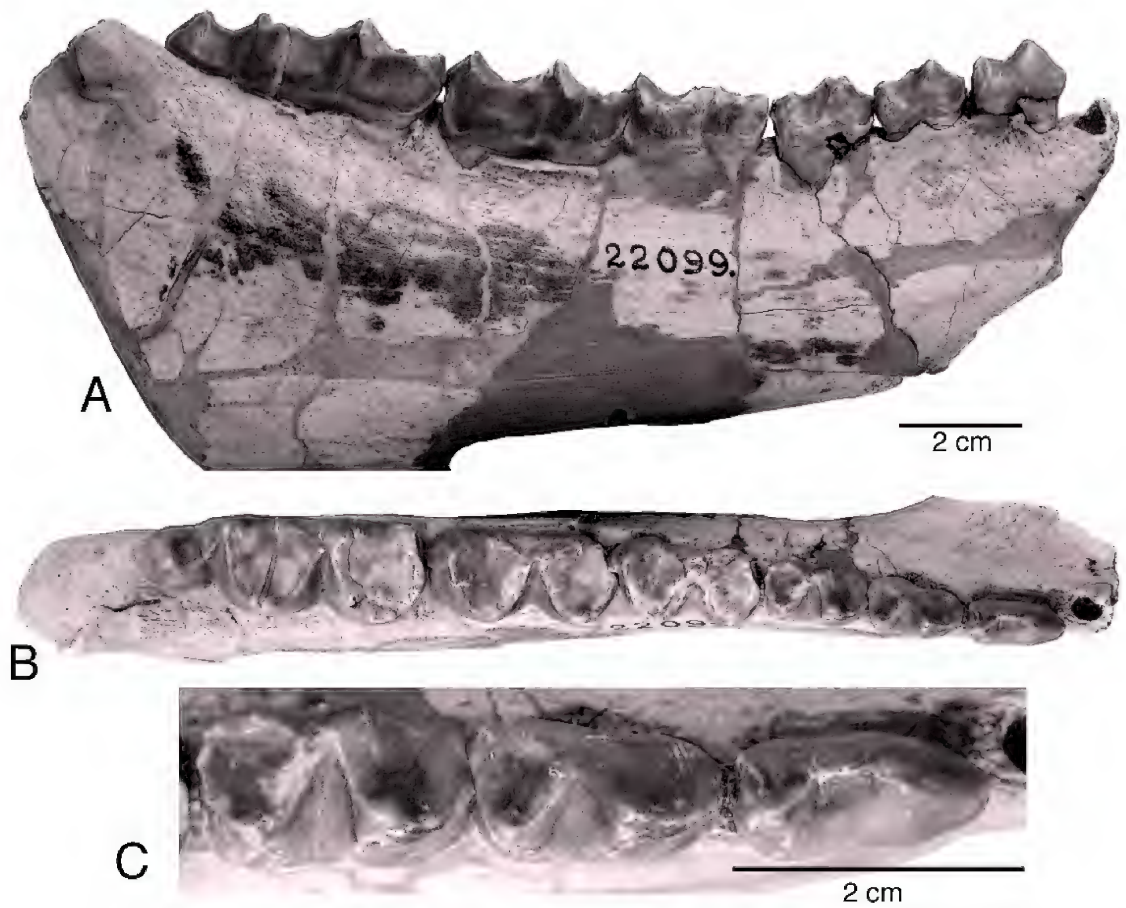

Fig. 22. The proposed neotype jaw of *Microtitan mongoliensis* (AMNH 22099). **(A)** Right view, **(B)** dorsal view, **(C)** right p2, p3, and p4.

North American species *Metarhinus fluviatilis*. Therefore, Osborn (1925) questionably referred this new species to *Metarhinus*. Better material was available to Granger and Gregory (1943) and they erected a new genus, *Microtitan*, for this species.

Because the original holotype of *Microtitan mongoliensis* lacked any diagnostic feature other than size, Granger and Gregory (1943) designated a neotype, AMNH 22099, a partial right jaw with p2–m3. Due to the fragmentary nature of the holotype of *Microtitan mongoliensis*, a reconsideration of these specimens is warranted to determine which, if any, can be realistically referred to *M. mongoliensis*, or whether that species should even be considered valid. The holotype of *M. mongoliensis* (AMNH 20167) is a small fragment of mandible with right p4 and m1 (fig. 23a, b). Overall, it is a rather unremarkable fossil, but several peculiarities about AMNH 20167 suggest that it is actually made up of multiple individuals. For instance, AMNH 20167 includes a barely worn DP4 that is obviously from a very young individual (fig. 23c). On the other hand, the mandible fragment of AMNH 20167 contains an erupted p4 and m1. The m1 shows a significant amount of wear. The lower dentition obviously represents an older individual than the nearly unworn deciduous premolar. More evidence suggests that the mandible fragment itself is a composite specimen. The lower teeth are disproportionately small in comparison to the actual mandible fragment. Closer inspection reveals that the dorsal surface of the mandible fragment is actually a weathered surface.

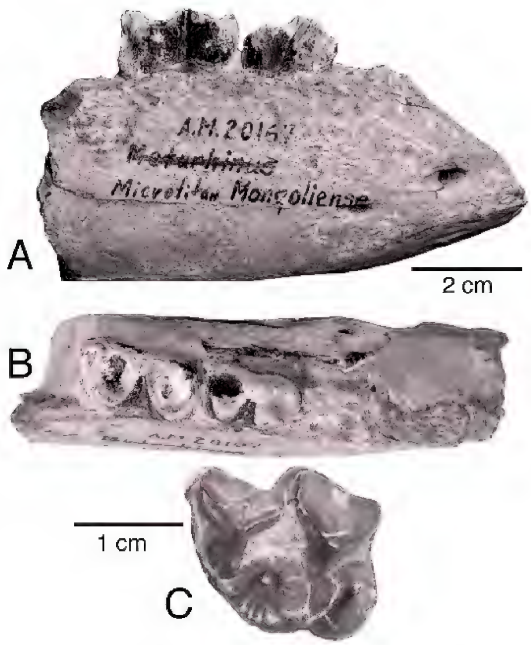

Fig. 23. The composite holotype specimen of *Microtitan mongoliensis* (AMNH 20167). **(A)** Right view of mandible fragment, **(B)** dorsal view of mandible fragment, **(C)** isolated left DP4.

The true alveolar surface has been weathered or broken away. Because the teeth are resting directly upon the weathered surface of bone, the conclusion that the teeth are not in situ is inescapable. Various adhesive materials and plaster can be traced around the borders of the p4 and m1. Therefore, the mandible fragment is probably from a larger individual than those represented by the actual teeth. The two lower teeth are more consistent with a single individual in size and in their degree of wear. Therefore, the m1 and p4 are possibly from the same individual, but this is not certain. In terms of size, the teeth of AMNH 20167 are similar to the North American brontothere *Metarhinus fluviatilis*, but because the specimen is too fragmentary to readily distinguish it from this taxon, *Microtitan mongoliensis* could be considered a nomen dubium.

Granger's and Gregory's (1943) neotype (AMNH 22099) is a more sufficiently diagnostic specimen, particularly due to the relatively slender p2 and p3 with elongate trigonids, the rather rounded molar crescents, and the hyperelongate m3. I recommend that AMNH 22099 continue to be recognized as the neotype specimen for *Microtitan*. The alternative to designating a neotype, rejecting *Microtitan* outright, is not recommended. At present, it is well understood that *Microtitan* represents a small Irdinmanhan aged brontothere that, until this paper, was most adequately diagnosed and described by Granger and Gregory (1943).

The maxilla and upper cheektooth series (AMNH 21611) is not directly referable to *Microtitan mongoliensis* (due to a lack of associated skulls and jaws) but there is little doubt that it represents that same species because of its occurrence in the same locality, its nearly identical size, and relatively elongate M3. Therefore, I continue to include AMNH 21611 in *M. mongoliensis*.

No other specimens reported since Granger and Gregory (1943) can be assigned to *Microtitan*. The mandible (PIN 3107-25) assigned to *Microtitan* by Yanovskaya (1980) from the Khaichin Formation does not actually belong to a brontothere. *"Microtitan?" elongatus* Qi (1987) is presently a nomen dubium, although it is possibly a synonym of *M. mongoliensis*. Dental fragments from the southern Jiangsu Province of China referred to *Microtitan* sp. by Qi and Beard (1996) (herein referred to cf. *Metarhinus* sp.) belong to an unnamed new species of *Microtitan*-sized brontothere.

Fossendorhinus diploconus (Osborn, 1895) new genus

HOLOTYPE: AMNH 1863, a partial skull with right C–P1 (roots only), P2 (partial), P3–M3, left P1–P2 (roots only), and P3–M3.

TYPE LOCALITY: Wagonhound Member (Uinta B) of the Uinta Formation, Uinta Basin, Utah.

AGE: Middle Eocene (early Uintan land mammal "age").

ETYMOLOGY: *Fossendorhinus* combines the Latin term *fossa* ("ditch") with Greek terms, *endo* ("inside") and *rhinus* ("nose"). This combination refers to the internal fossae seen within the nasal cavity of this species.

DIAGNOSIS: *Fossendorhinus diploconus* is an intermediate-sized hornless brontothere. The nasal incision extends posteriorly as far back as the anterior margin of the M1. The

orbits are positioned above the M2 and protrude laterally, though not to the degree seen in *Metarhinus*. The premaxilla is robust and does not contact the nasal bone. The premaxillomaxillary rostral cavity is open dorsally and there are two large fossae inside the nasal chamber. The premaxillomaxillary rostrum is strongly upturned and is relatively constant in thickness throughout its length. Other cranial features include a well-developed sagittal crest, a strongly concave mid-cranial dorsal surface, a strongly convex posterior dorsal surface, thin and strongly curved zygomatic arches, and a ventrally open and mediolaterally directed external auditory pseudomeatus.

Dentally, *Fossendorhinus diploconus* has three large upper incisors, a distinct P2 metacone, weak premolar preprotocristae, short lingual crests extending posteriorly from the premolar protocones, and small hypocones on P2 and P3. The molars have tall, lingually angled ectolophs with weak labial ribs, and thinned lingual ectoloph enamel with wedge-shaped paracones and metacones. A cingular parastyle shelf and an anterolingual cingular cusp are absent. Central molar fossae are present. All traces of molar paraconules and metalophs are lost.

Fossendorhinus diploconus is most similar to *Metarhinus*, but can be clearly differentiated from *Metarhinus* by the autapomorphic fossae inside the nasal chamber, the less laterally protruding orbits, and the more strongly upturned rostrum.

Description

Skull: The holotype of *Fossendorhinus diploconus* (AMNH 1863) is a skull lacking the nasal process (fig. 24). The skull has been subjected to a minor amount of sheering distortion. Prior figures of the specimen in Osborn (1895: fig. 6) and in Osborn (1929a: figs. 362 and 363) misleadingly portray the skull as undistorted, and less damaged than it actually is. The shape of the right side of the skull is well preserved, except for a significant portion of the squamosal, which has been reconstructed with plaster. The left side of the skull is mostly complete, but it has been more severely crushed and the zygomatic arch has been forced inward.

There is no hornlike protuberance on this specimen. Osborn's (1929a: fig. 363) figure of this specimen includes an unlabeled line that seems to portray the frontonasal suture. However, the line drawn in Osborn's figure actually corresponds to a large crack in the specimen, not a suture. There is no discernable frontonasal suture in this specimen.

The nasal incision of *Fossendorhinus diploconus* strongly constricts the face, but not to the degree seen in *Metarhinus*. The nasal incision extends as far back as the anterior margin of the M1. The orbit is positioned directly over the M2. The posterolateral root of M1 is positioned below the anterior rim of the orbit. The right orbit protrudes somewhat laterally from the skull, but not to the degree seen in *Metarhinus*. The proximal base of the nasal process is preserved on the right side. This remnant suggests a rather thin nasal process that was nearly flat or had very shallow lateral walls, similar to those of *Metarhinus*.

The most distinctive characteristics of *Fossendorhinus diploconus* are in the premaxillomaxillary rostrum and the nasal chamber. From the lateral view of the skull it can be seen that the premaxillomaxillary rostrum is a consistent depth from the proximal end to the distal end. The dorsal margin of the rostrum does not rise above the midlevel of the orbit. In comparison to *Metarhinus*, the premaxillomaxillary rostrum is more strongly curved upward. The pronounced upward curvature of the rostrum does not appear to be a result of taphonomic distortion. On the right side there are a few large cracks in the face, but the proportions appear to be essentially intact.

The premaxillae have become detached at the symphysis and the left premaxilla has been displaced laterally, ventrally, and anteriorly. A roughened groove of bone on the right side, probably representing the premaxillomaxillary suture suggests that the premaxilla did not extend to the posterior base of the nasal incision. The median symphyseal contact surface of the right premaxilla is flat and long (~7.1 centimeters), although Osborn (1895) described it as short. The dorsal surface of the rostrum is not covered by bone as seen in *Metarhinus* or *Dolichorhinus*. However, the rostrum of *F. diploconus* shows

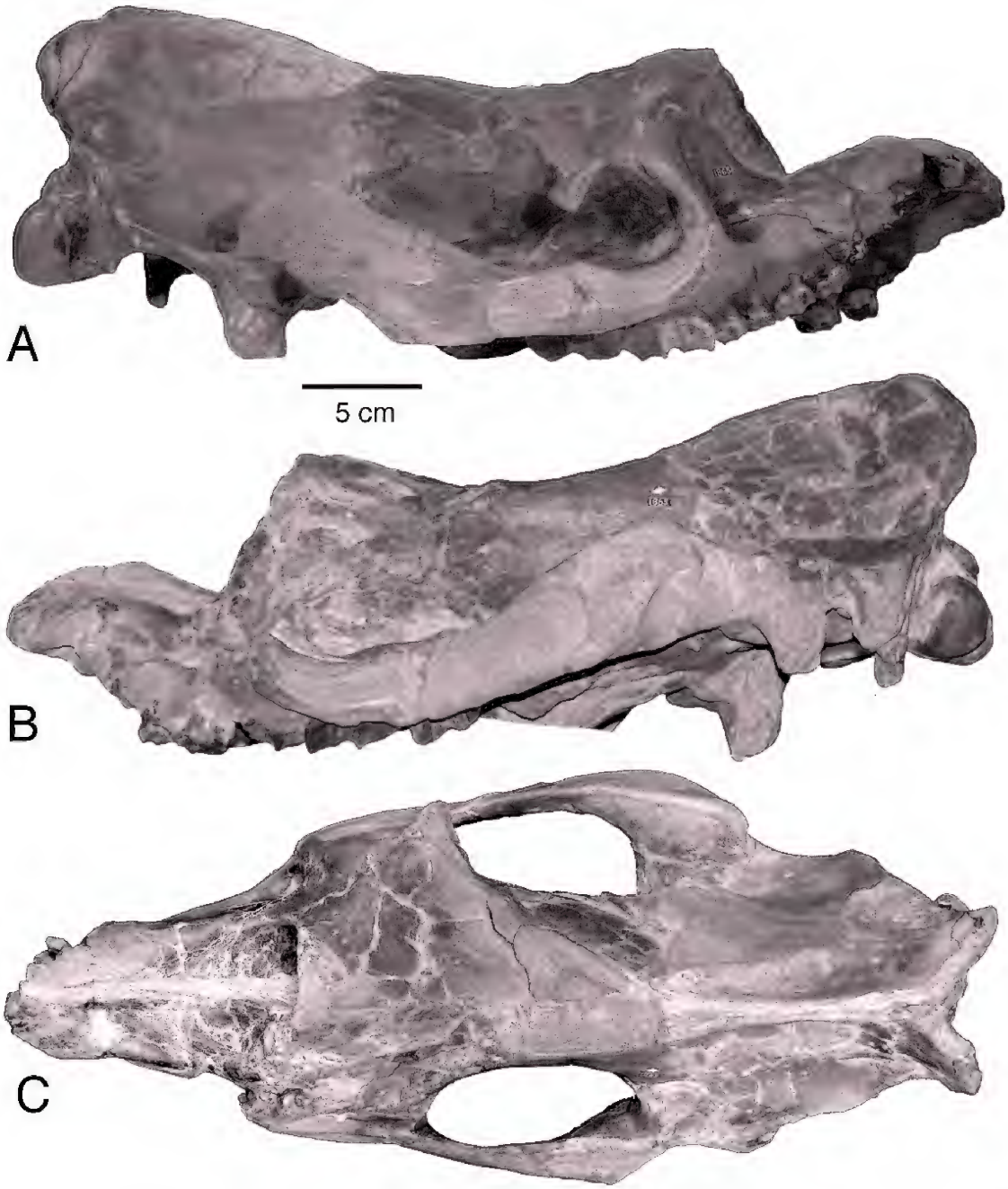

Fig. 24. The holotype of *Fossendorhinus diploconus* (AMNH 1863). **(A)** Right view, **(B)** left view, **(C)** dorsal view.

a number of autapomorphic specializations (fig. 25a, b). The premaxillary symphysis arches dorsally. Behind the symphysis are two large internal ovoid fossae. The internal fossae are recessed below the dorsal surface of the rostrum and extend well behind the nasal incision. An additional smaller fossa appears in the upper corner, just beneath what was the proximal base of the nasal process. This small fossa is intact on the right

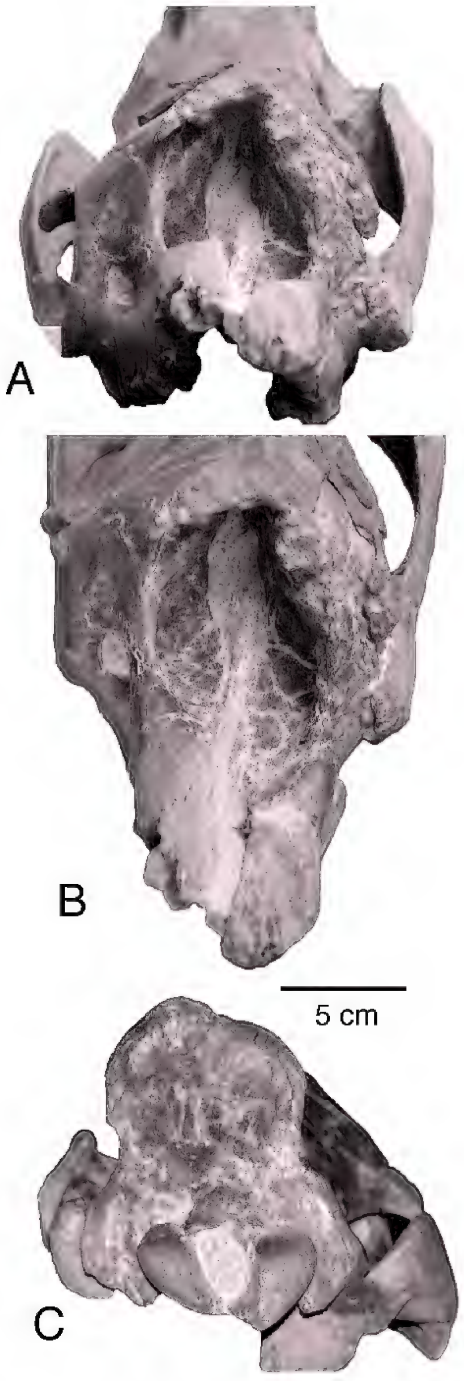

Fig. 25. The holotype of *Fossendorhinus diploconus* (AMNH 1863). **(A)** Anterior view, **(B)** anterodorsal view of rostrum, **(C)** posterior view.

side, but only the very bottom of the fossa is preserved on the left side. The bone that forms these internal fossae fills a large portion of the volume of the nasal chamber. Consequently, the internal nasal cavity is very narrow.

From a lateral view the midsection of the dorsal surface of the skull is strongly concave. Although two large cracks that run through the right side of the frontal area may exaggerate the concave superorbital profile, the individual bone fragments on this surface are concave as well. The dorsal surface of the posterior portion of the cranium is convex in lateral profile. The parasagittal ridges converge medially into a long sagittal crest.

The zygomatic arch is thin and bladelike in cross section. The right zygomatic is less damaged. It is only slightly bowed laterally. The jugal section of the zygomatic is dorsoventrally shallow and is more or less horizontal while the squamosal portion is deeper and angled posterodorsally, giving the zygomatic arch a moderately curved shape. Although Osborn (1908a) described this specimen as lacking an infraorbital jugal process, as seen in *Metarhinus*, the surface of the jugal is flaked off on the ventral surface of the inferior rim of the orbit. This damage seems superficial and it is doubtful that this specimen possessed a large infraorbital process, though it is possible that a small infraorbital process was present.

From the dorsal view, the nuchal crest is very narrow and swept backward, although this appears to be exaggerated by lateral crushing. From the posterior view (fig. 25c), the nuchal crest is strongly arched dorsally. The overall proportions of the occiput are distorted, although the occiput is narrower dorsally than it is ventrally, and it is slightly waisted. There are small but distinct occipital pillars, and a median depression in the occiput between the occipital pillars.

The ventral surface of the skull is poorly preserved, but several features are discernable (fig. 26a). Although the palate has been crushed laterally, the right side of the posterior nares is preserved and is positioned slightly anterior to the M3. The posterior narial canal appears to have been elongate, but it is severely damaged. Finally, the

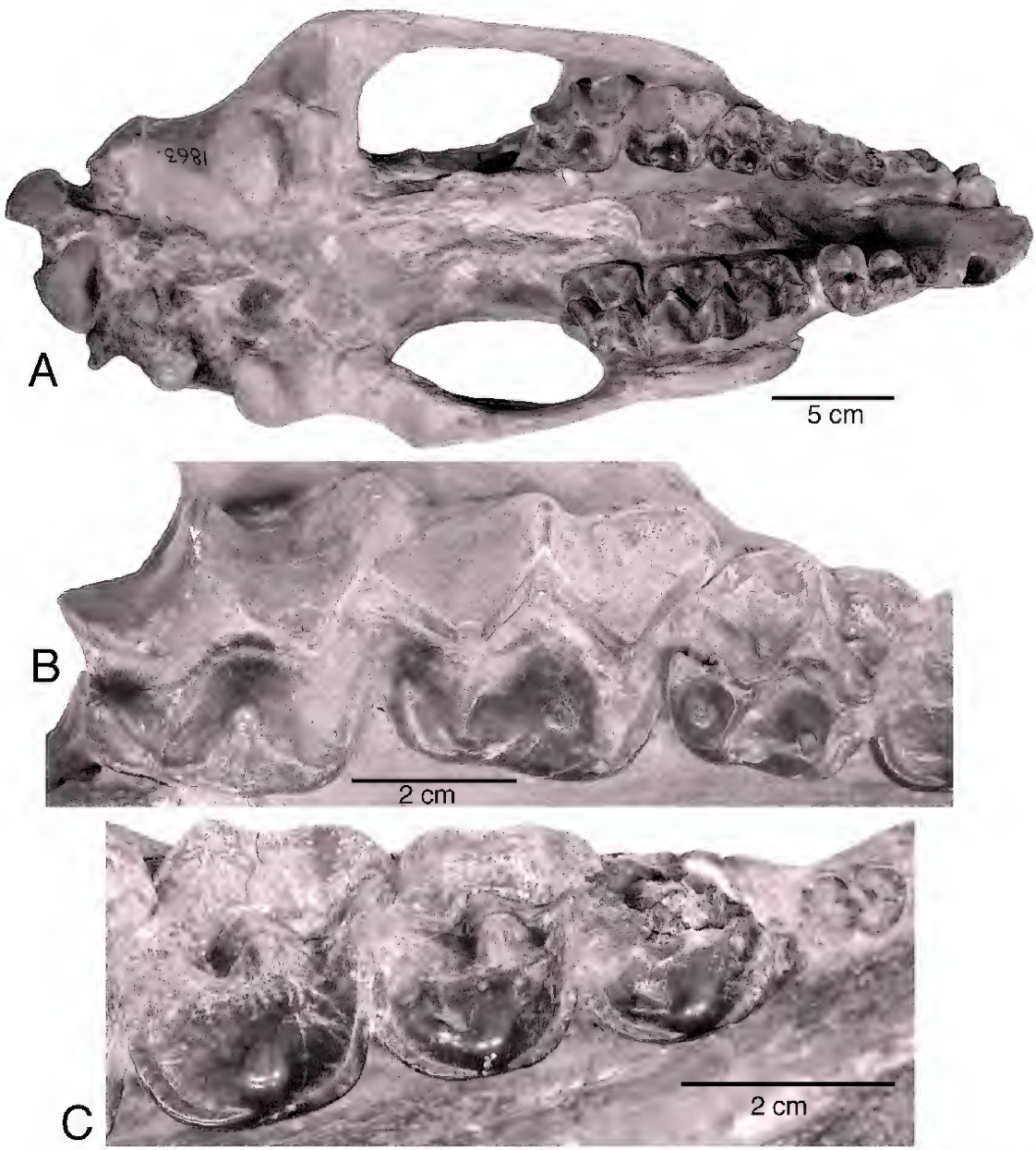

Fig. 26. The holotype of *Fossendorhinus diploconus* (AMNH 1863). **(A)** Ventral view, **(B)** right molars, **(C)** right premolars.

basicranium, though badly damaged, is typical with a foramen ovale well separated from the foramen lacerum. The opening for the external auditory pseudomeatus, preserved on the left side, is wide and unconstricted ventrally.

Upper Dentition: No incisors or canines are preserved with AMNH 1863, however there are clearly three pairs of incisor alveoli. The size of the alveoli and shape of the premaxillae suggest relatively large incisors and an arched incisor row. The canine alveoli suggest relatively small canines that are comparable in size to those of *Dolichorhinus* and *Metarhinus*. There is both a short precanine diastema and postcanine diastemata.

The P1 is not preserved but the remnants of the roots indicate a small, double-rooted premolar (fig. 26c). The ectoloph of P2 is not preserved although the shape of the P2 appears to have been similar to those of P3 and P4. The parastyle and metastyle of P3 are relatively straight. The parastyle of P4 is labially angled, although the P4 metastyle is relatively straight. Prominent labial paracone ribs can be seen on P3 and P4; the P4 labial paracone rib is smaller. There is a large bulge at the proximal base of the P4 ectoloph near the metacone. This bulge is similar in position to the mesostyles to one that is occasionally seen on the P4s of some brontothere species. Each premolar (P2–P4) has a large centrally positioned protocone. Additional lingual features in the P2 include a rudimentary preprotocrista with a distinct paraconule and a distinct crest extending posteriorly from the protocone that is connected to a very small hypocone-like swelling. The lingual side of P3 is morphologically similar to that of P2. However, the preprotocrista, the lingual crest extending posteriorly from the protocone, and the hypocone are less distinct. Finally, the lingual side of the P4 crown is devoid of any features except for the large protocone. The labial premolar cingula of P3–P4 are very thin. The anterior and posterior premolar cingula wrap around the lingual side of the crown but do not join lingually.

The molars of *Fossendorhinus diploconus* exhibit numerous brontotheriine apomorphies including tall lingually angled ectolophs, weak labial ribs, thin lingual ectoloph enamel, and wedge-shaped lingual sides of the paracone and metacone in molars that are not heavily worn (M2 and M3) (fig. 26b). The anterior cingulum is thin and passes proximally to the distal peak of the parastyle. *F. diploconus* molars lack anterolingual cingular cusps but possess distinct central molar fossae. All traces of paraconules and metalophs are absent. The trivial name (*diploconus*) alludes to the two lingual cusps of the M3, a protocone, and a large hypocone that is similar in size to the hypocones of the more anterior molars. However, the size and/or presence of a M3 hypocone could vary in this species as it does in many other brontothere species. The labial molar cingula are distinct but weak and they are discontinuous around the mesostyles. The lingual molar cingula are distinct between the protocone and hypocone, but they are discontinuous around the protocone and hypocone.

Remarks

Fossendorhinus diploconus (Osborn, 1895) is based upon a single skull (AMNH 1863) from the Uinta Basin (Uinta B). Osborn (1895) originally referred this species to the genus "*Telmatotherium*" (a variant on the spelling of *Telmatherium*), but he subsequently reassigned it to the genus *Metarhinus* (Osborn, 1908a). Osborn (1908a) differentiated this species from other species of *Metarhinus* based on the lack of an infraorbital process. However, AMNH 1863 is damaged in the area where the infraorbital process would occur if it were present. It is unclear whether a small infraorbital process was present on the holotype skull.

Riggs (1912) and Osborn (1929a) reassigned *"Metarhinus" diploconus* to another genus, *Rhadinorhinus* (now considered a synonym of *Metarhinus*). More recently, Mader (1998) reassigned this species to the genus *Metarhinus* and synonomized it with *Metarhinus abbotti* (Riggs, 1912). The repeated revisions and associations of this species with *Metarhinus* are, nonetheless, all contradicted by the distinct characteristics of AMNH 1863, which seem to clearly differentiate it from other species of *Metarhinus* (*M. fluviatilis* and *M. abbotti*). These distinctions include the less prominently protruding orbits, the more strongly upturned rostrum, the more deeply concave dorsal midcranial surface, and the small premolar hypocones. More compellingly, the autapomorphic features found in the rostrum of AMNH 1863 are distinctly different from *Metarhinus*. Recent removal of the hard sandstone matrix from the nasal chamber of the holotype (AMNH 1863) revealed a pair of large fossae in the floor of the rostrum and inside the nasal chamber. These peculiar nasal fossae, not known to prior authors, warrant the designation to the new genus.

Currently, AMNH 1863 is the only specimen that clearly represents *Fossendorhinus diploconus*. However, AMNH 2055, a poorly

preserved and incompletely prepared skull probably represents this species, but the diagnostic morphology of the rostrum is obscured by sandstone matrix.

Metarhinus fluviatilis Osborn, 1908a

NEOTYPE: FMNH P12187, a complete skull missing only the incisors.

TYPE LOCALITY: Wagonhound Member (Uinta B) of the Uinta Formation, Uinta Basin, Utah.

AGE: Middle Eocene (early Uintan land mammal "age").

SYNONYMS: *Metarhinus riparius* Riggs, 1912.

REFERRED SPECIMENS: **(From the Wagonhound Member of the Uinta Formation of Utah)** FMNH P12186 (holotype of *Metarhinus riparius*), a skull with heavily worn dentition including right C–P1, P2–P3 (partial), M3, left C–P4, and M2–M3; FMNH P12201, a subadult skull with right I3–C (erupting), P1, P2–P3 (erupting), DP4, M1–M2, M3 (erupting), left P1, P2–P3 (erupting), DP4, M1–M2, and M3 (erupting); YPM 13125, a skull with heavily worn dentition including right C, P2, P3–M3, left C–M3, and a partial mandible with right i2 (?), and left p2–m3; FMNH P12173, a skull with right C, P3–P4, M2–M3 (all partial), left P2–P4, M2–M3; **(from the Adobe Town Member of the Washakie Formation of Wyoming)** FMNH PM1733, a palate with a partial nasal bone, right C–M3, and left P1–M3; FMNH PM3935, an anterior half of a skull with right P2–M3 and left P1–M3; FMNH PM44655, a fragmented skull with right M2–M3, left P2–P4, M1–M2 (partial), and M3; UCM 44939, a complete skull with right P2–M3 and left M3 (partial); UCMP 81278, a skull missing the posterior end with right and left C, and P2–M3.

DIAGNOSIS: *Metarhinus fluviatilis* is a small hornless brontothere in which the frontal bone intrudes slightly into the surface of the nasal bone splitting off a small lateral nasal splint from the main body of the nasal. The posterior margin of the nasal incision is above the anterior margin of the M2. The nasal process broadens distally, is thin, horizontal, unelevated, with very shallow lateral walls, and without a strongly rounded distal margin. The orbits are positioned above the M2 and strongly protrude laterally. The premaxillomaxillary rostral cavity is enclosed by bone dorsally and its dorsal surface is nearly horizontal. Other cranial characteristics include a small infraorbital process, a sagittal crest, a dorsal cranial surface that is flat or slightly convex postorbitally, strongly curved and unbowed or weakly bowed zygomatic arches, and a ventrally open and mediolaterally angled external auditory pseudomeatus. Ventral sphenoidal fossae are absent.

Dentally, *Metarhinus fluviatilis* can be characterized as having large subcaniniform upper incisors, a simple P1, a distinct P2 metacone, weak premolar preprotocristae on P2 and P3, and with short lingual crests occasionally extending posteriorly from the premolar protocones. Premolar hypocones are absent. The molars of *M. fluviatilis* have tall, lingually angled ectolophs with weak labial ribs, and thinned lingual ectoloph enamel with wedge-shaped paracones and metacones. Central molar fossae and anterolingual cingular cusps are present. Cingular parastyle shelves, paraconules, and metalophs are absent. The mandibular symphysis extends to the p3. The p3 has a distinct metaconid (although this character may be variable). The lower molars of *M. fluviatilis* can be characterized as having shallow molar basins and a slender m3.

Metarhinus fluviatilis shares with *Dolichorhinus hyognathus* and *Metarhinus abbotti* a rostrum that is sealed dorsally by bone. The skull of *M. fluviatilis* most clearly differs from *Dolichorhinus* in its shorter proportions, prominent sagittal crest, and laterally protruding orbits. The skull of *M. fluviatilis* is undifferentiated from *M. abbotti* except for the distally broadening nasal process.

DESCRIPTION

SKULL: The proposed neotype of *Metarhinus fluviatilis* (FMNH P12187) is an exceptionally complete and undistorted skull with lightly worn teeth (figs. 27, 28a). It is missing only the incisors. Riggs's original figure of FMNH P12187 (Riggs, 1912: pl. VIII) depicts a left I2 (?) although it is presently lost, or not with the specimen. In addition,

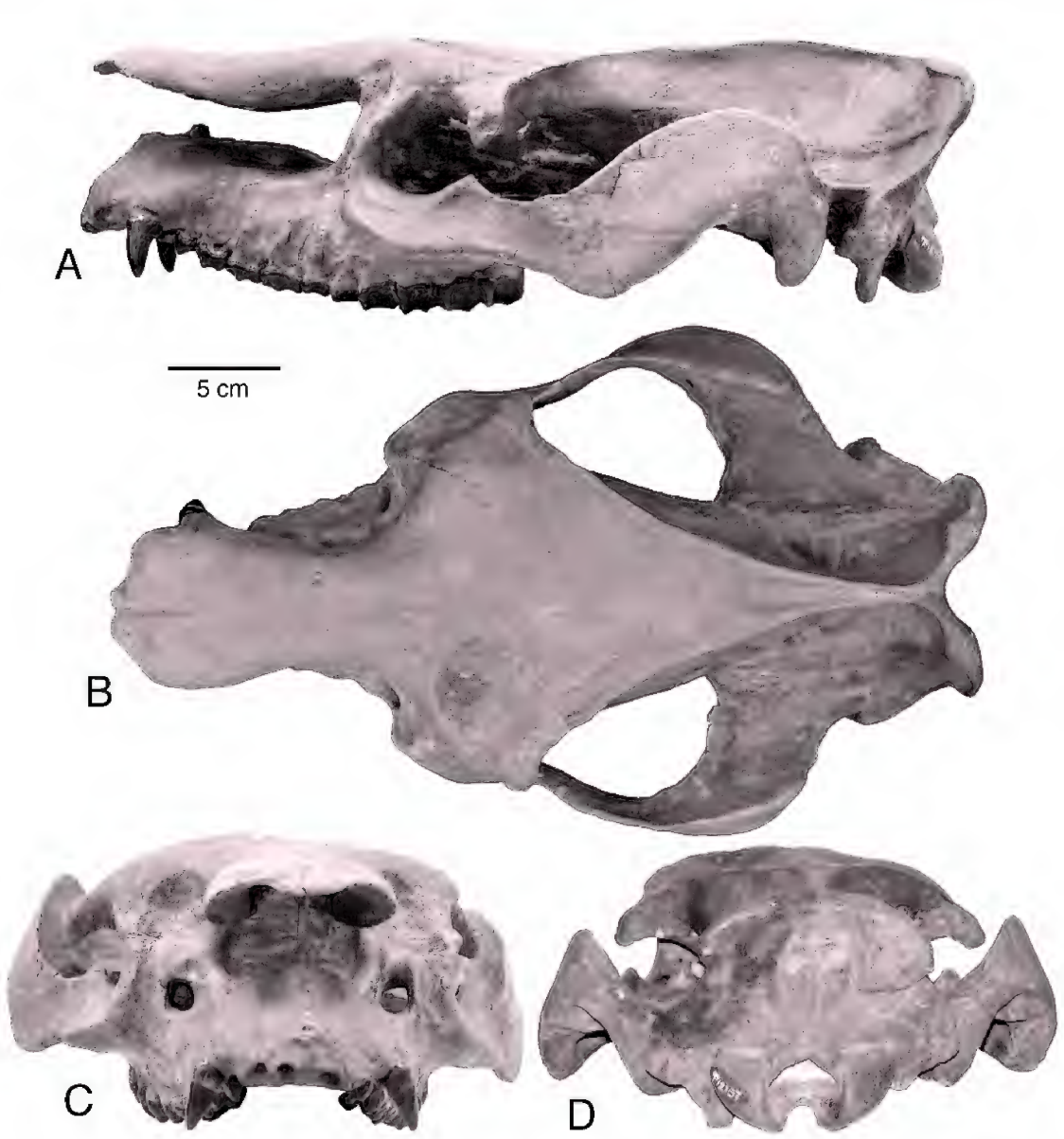

Fig. 27. The neotype of *Metarhinus fluviatilis* (FMNH P12187). **(A)** Left view, **(B)** dorsal view, **(C)** anterior view, **(D)** posterior view.

several views of another well-preserved specimen, UCM 44939, are shown (fig. 29).

Metarhinus fluviatilis is a rather small (table 4), hornless brontothere that is most similar in size to the contemporaneous early Uintan brontotheres *M. abbotti* and *Fossendorhinus diploconus*. In most specimens the sutures of the facial bones are not discernable, although they can be seen in UCM 44939. The posterolateral portion of the nasal bone is split by a short triangular process of frontal bone. The lateral portion of the frontal bone forms a short but distinct lateral nasal splint that extends in a posteroventral direction between the frontal and maxilla and makes a narrow contact with the lacrimal bone. This configuration is also seen in several other hornless brontotheres (e.g., *Telmatherium*), but in *M. fluviatilis*, the triangular process and lateral nasal splint

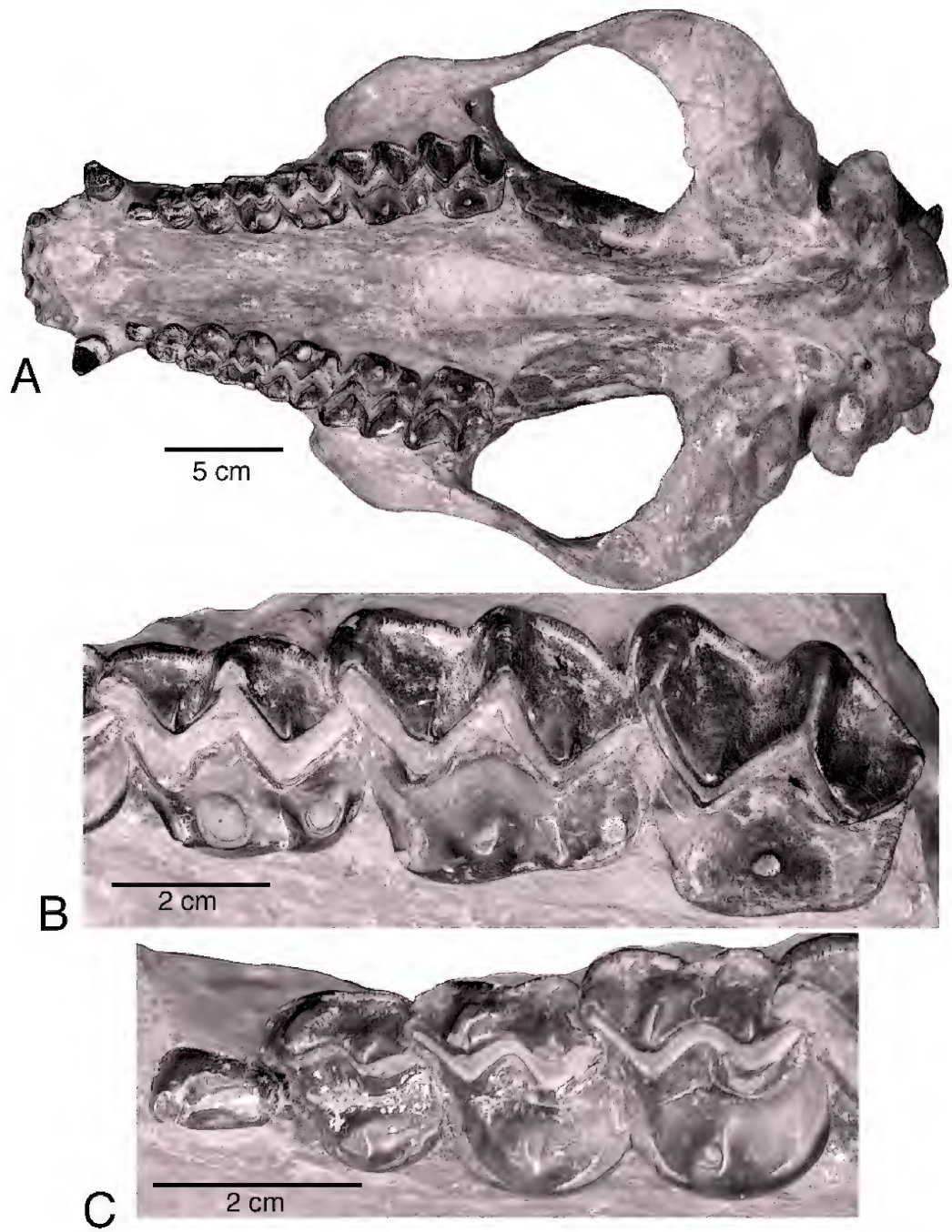

Fig. 28. The neotype of *Metarhinus fluviatilis* (FMNH P12187). **(A)** Ventral view, **(B)** left molars, **(C)** left premolars.

are relatively short. Riggs (1912) and Osborn (1929a) described rudimentary horns in specimens of *M. fluviatilis* (FMNH P12186, FMNH P12187, FMNH P12194), but no such structures can be discerned on the actual specimens. The lateral views of some skulls, such as FMNH P12187, are deceptive because the nasal process is angled slightly

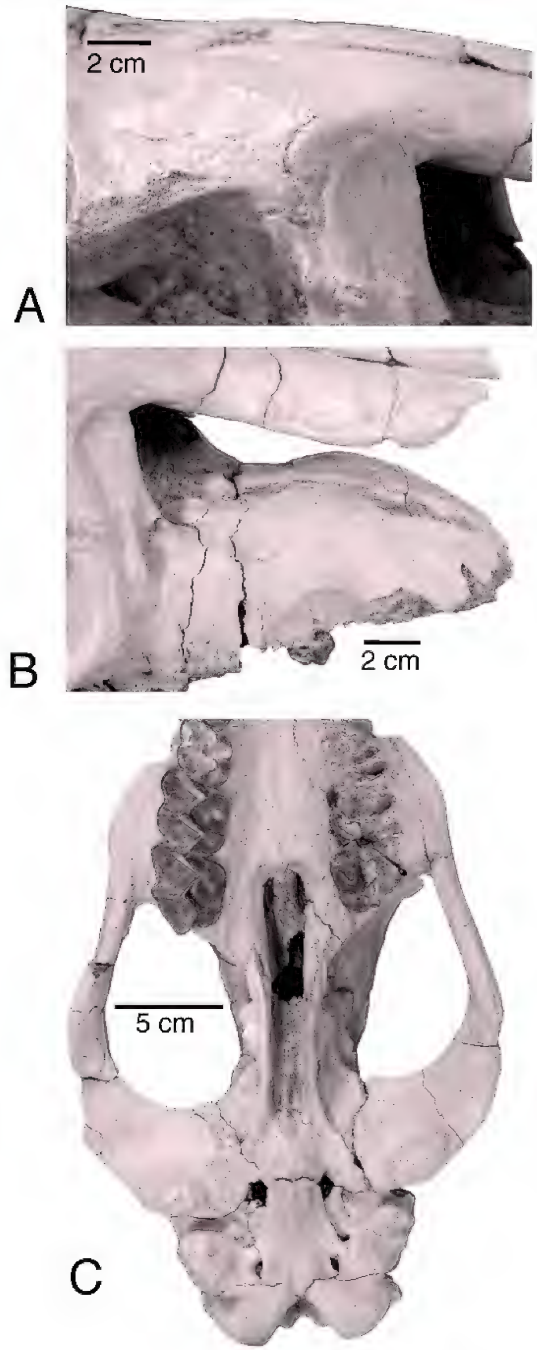

Fig. 29. A skull (UCM 44939) of *Metarhinus fluviatilis*. **(A)** Right view of face showing frontonasal suture, nasomaxillary suture, and nasallacrimal contact, **(B)** right view of premaxillomaxillary rostrum, **(C)** ventral view.

downward; this gives the appearance of a raised area between the orbits and the nasal incision. Often, the nasal bone is forced further downward taphonomically, exaggerating the effect. However, there are no distinct hornlike protuberances on any specimen of *M. fluviatilis*.

The face of *Metarhinus fluviatilis* is highly constricted by the long nasal incision. The nasal incision extends to the anterior rim of the orbit and to the anterior margin of the M2. The orbit is situated over the M2, with the posterolateral root of M1 and anterolateral root of M2 situated below the anterior orbital rim. The orbits of this species have been described as prominent, or laterally protruding (Osborn, 1908a, 1929a). The appearance of prominent orbits is manifested by a broad and relatively flattened frontal between the orbits, a transverse constriction of the dorsal surface of the skull anterior to the orbits, and a recessed surface of bone between the deep nasal incision and the anterior rim of the orbit that forms a narrow wall of bone facing anteriorly just in front of the orbit.

The nasal process of *Metarhinus fluviatilis* is long. In FMNH P12187 it is as long as the premaxillomaxillary rostrum. The nasal process is angled slightly downward and it is somewhat bowed downward in the center so that the dorsal surface is concave. The lateral walls of the nasal process are thin, shallow, and nearly constant in dorsoventral depth from the proximal end to about the midpoint of the nasal process. On the distal half of the nasal process the lateral walls become shallower distally. The anterior edge of the nasal process is thin, roughened, and deflected downward. From the dorsal view the width of the nasal process is constricted proximally, broadens distally, and has an imperfectly rounded anterior edge. Other specimens with complete (or nearly complete) nasal processes are consistent with this description except that the nasal process is slightly shorter than the premaxillomaxillary rostrum most of the time (e.g., FMNH P12173, FMNH PM3935, UCM 44939, UCMP 81278, YPM 13145).

From the lateral view, the premaxillomaxillary rostrum is long, slightly upturned, and of relatively constant thickness throughout its length. The dorsal margin of the rostrum

TABLE 4
Summary statistics for selected morphometric variables of *Metarhinus fluviatilis*
See Methods for measurement definitions

	N	Mean	SD	Min.	Max.	CV
C L	6	17.0	1.6	15.1	18.9	9.2
P3 L	8	18.3	1.2	16.8	19.9	6.5
P3 W	8	21.5	1.0	19.9	22.8	4.6
M2 L	8	37.9	1.9	36.4	41.4	4.9
M2 W	8	35.2	1.6	32.8	37.1	4.5
P2–P4	9	52.5	1.6	49.9	54.6	3.1
M1–M3	8	96.4	4.5	88.8	102.8	4.6
VL	6	391.2	19.4	360	408	5.0

is not raised above the lower half of the orbit. However, the posterior margin of the nasal incision extends to the level of the upper rim of the orbit. The rostrum of *Metarhinus fluviatilis* is highly specialized in the same manner as *Dolichorhinus* and *M. abbotti* where the rostral cavity is entirely enclosed by bone. In the available specimens of *M. fluviatilis* the dorsal covering is solid and no distinct sutures can be seen. The premaxillary symphysis is elongate and extends the entire length of the rostrum. This can be best seen in UCM 44939, where the symphysis is unossified. From an anterior view of FMNH P12187 the premaxillae form a solid dome of bone with a thick median ridge of bone (the osteological marker for the nasal septum) running anteroposteriorly along the superior margin of the premaxillomaxillary process. This ridge continues along the dorsal surface of the rostrum into the skull.

From a lateral profile of FMNH P12187, the dorsal surface of the skull is essentially flat over the orbits, and convex over the posterior half of the skull. From the dorsal view of the skull, the parasagittal ridges converge into a short sagittal crest. The zygomatic arches are thin and not strongly bowed. The jugal portion of the zygomatic arch is dorsoventrally shallow and horizontal, while the squamosal portion is deeper and rises posteriorly, giving the zygomatic arch a strong curvature. Some of the specimens are more gracile than the holotype with longer and thinner sagittal crests and thinner zygomatic arches (e.g., FMNH P12186, UCM 44939). Despite this variation, there are no discrete broad-skulled and narrow-skulled groups as hypothesized by Riggs (1912). There is a small infraorbital process on the jugal. The infraorbital process is much smaller than those of *Dolichorhinus*, *Sphenocoelus*, *or Mesatirhinus*, but is similar to that of *Metarhinus abbotti*. In the center of the zygomatic arch the ventral margin of the jugal is extended ventrally forming a small flange, although this structure is less pronounced in other specimens of *Metarhinus fluviatilis* and is always much less conspicuous than the large ventral zygomatic flange seen in *Metatelmatherium ultimum*.

From a dorsal view the nuchal crest is strongly notched medially. From a lateral view the occiput is moderately tilted backward. From a posterior view the dorsal border of the occiput is arched. The dorsal half of the occiput is narrower than the ventral portion and it is somewhat constricted in the middle. The center of the occiput is deeply recessed between two prominent occipital pillars.

The ventral surface of the skull of *Metarhinus fluviatilis* is well preserved in both FMNH P12187 and UCM 44939. The anterior rim of the posterior nares varies in its position from between the M2 hypocones (FMNH P12187) to between the anterior edges of the M3s (UCM 44939). A narrow horseshoe-shaped rim emarginates the anterior and lateral margins of the posterior nares. The anterior rim of bone and the emargination each have a small posteriorly projecting median process. Remnants of posteriorly shifted turbinates can be seen in the posterior narial canal of UCM 44939, where the matrix inside the skull has been

removed. Though the matrix has not been removed from inside the skulls of other specimens, thin slivers of bone suspended in the matrix filling the posterior narial choanae can be seen in some skulls (e.g., FMNH P12201) that also appear to represent posteriorly extended turbinates. The posterior narial canal is elongate and tends to extend onto the anterior part of the sphenoid, but large ventral sphenoidal fossae are absent. In other ways the basicrania of these specimens are otherwise typical with a widely separated foramen ovale and foramen lacerum. The mastoid process does not contact the postglenoid process ventrally; therefore, the external auditory pseudomeatus is open ventrally.

Upper Dentition: No known skull of *Metarhinus fluviatilis* contains upper incisors. Earlier figures of the neotype (Riggs, 1912: pl. VIII) depict a large, subcaniniform I2(?), but that incisor is no longer attached to the skull and it is apparently lost. The incisor alveoli and/or partial roots indicate an unreduced number of incisors (three pairs) that form an arched row anterior to the canines. The canines are generally small, but tend to vary in size more than the other teeth. Short precanine and postcanine diastemata are consistently present.

The description of the cheek teeth of *Metarhinus fluviatilis* is primarily based on FMNH P12187 (fig. 28b, c), but is supplemented by information from other specimens. The P1 crown is a small and simple tooth with a single cusp and an elongate posterior heel. In FMNH P12201 (not shown), the P1 is unworn; the cusp of that tooth curves lingually and a thin lingual cingulum is present. The P2 of FMNH P12187 is slightly more oblique in outline than P3 and P4 due to a more posterolingually angled anterior margin. In other specimens the P2 can be less oblique (e.g., FMNH PM3935). The parastyle of P2 is straight, while those of P3 and P4 are somewhat labially directed. The metastyles of P2 and P3 are essentially straight, while the P4 metastyle is angled slightly labially. The labial walls of P2–P4 have distinct labial paracone ribs that become shorter and narrower in more posterior premolars. The lingual heel of the P2 is as developed as those of P3 and P4. There is only a single large lingual cusp (protocone) on the P2–P4; premolar hypocones are absent. On P2 and P3 there is both a small but distinct preprotocrista and a short lingual crest. In P4, the preprotocrista is extremely faint, and there is no lingual crest. The labial cingula are discontinuous around the paracone of P2 and P3, but there tends to be continuous cingulum around the labial base of the crown of P4. The anterior and posterior premolar cingula extend around the lingual sides of the crowns but do not join in FMNH P12187. Occasionally (e.g., FMNH P12173), there are continuous lingual premolar cingula.

Molar apomorphies seen in *Metarhinus fluviatilis* include tall, lingually angled ectolophs, weak labial ribs, thin lingual ectoloph enamel, and wedge-shaped lingual sides of the paracone and metacone in molars that are not heavily worn. The anterior cingulum is thin and passes proximally to the distal peak of the parastyle. The molars invariably have shallow central molar fossae. Very small anterolingual cingular peaks can be seen on FMNH P12187, although in other specimens (e.g., UCM 44939 and UCMP 81287), small anterolingual cingular cusps are usually more distinct. There are no traces of paraconules or metalophs. The M3 of FMNH P12187 lacks a hypocone, but the posterolingual cingulum is thick and rough. However, an M3 hypocone is occasionally present (e.g., FMNH P12186), though it is never as large as that of the M1 or M2 hypocone. The labial molar cingula are thin but distinct and discontinuous around the labial bases of the mesostyles; lingual molar cingula are essentially absent.

Mandible and Lower Dentition: Only one identifiable skull of *Metarhinus fluviatilis* (YPM 13125) is associated with a partial mandible. The p3 of this mandible has a large metaconid, a character that is variable among the *Metarhinus* sp. mandibles that are further described below.

Metarhinus abbotti (Riggs, 1912)

Holotype: FMNH P12179, a complete skull, somewhat crushed dorsoventrally, with complete dentition.

TYPE LOCALITY: Wagonhound Member (Uinta B) of the Uinta Formation, Uinta Basin, Northeast Utah.

AGE: Middle Eocene (Early Uintan land mammal "age").

REFERRED SPECIMENS: (From the Wagonhound Member of the Uinta Basin, Utah) CMNH 2866, a complete skull with heavily worn teeth including right P2–M3 and left P1–M3; CMNH 3510, an anterior portion of a skull (partially prepared) with heavily worn teeth including right I2?–I3?, P1 (partial), P2–M1, left I3?, P1–M3.

DIAGNOSIS: *Metarhinus abbotti* is a small hornless brontothere. The nasal incision extends to the anterior margin of M2. The nasal process tapers distally. It is thin, horizontal, unelevated, and with very shallow lateral walls. The orbits are positioned above the M2 and strongly protrude laterally as in *Metarhinus fluviatilis*. The premaxillomaxillary rostral cavity is enclosed by bone dorsally and its dorsal surface is nearly horizontal. Other cranial characteristics include a small infraorbital process, a sagittal crest, a dorsal cranial surface that is flat or slightly convex postorbitally, strongly curved and unbowed or weakly bowed zygomatic arches, and a ventrally open and mediolaterally angled external auditory pseudomeatus. Ventral sphenoidal fossae are absent among the known specimens.

Dentally, *Metarhinus abbotti* has large subcaniniform upper incisors, a simple P1, a distinct P2 metacone, occasional weak premolar preprotocristae, and occasional short lingual crests. Premolar hypocones are absent. The molars of *M. abbotti* have tall, lingually angled ectolophs with weak labial ribs, and thinned lingual ectoloph enamel with wedge-shaped paracones and metacones. Central molar fossae and anterolingual cingular cusps are present. Cingular parastyle shelves, paraconules, and metalophs are absent.

Metarhinus abbotti shares with *Dolichorhinus hyognathus* and *M. fluviatilis* a rostrum that is sealed dorsally by bone. The skull of *M. abbotti* most clearly differs from *D. hyognathus* in its shorter proportions, prominent sagittal crest, and laterally protruding orbits. The skull of *M. abbotti* is undifferentiated from *M. fluviatilis* except for the distally tapered nasal process.

DESCRIPTION

SKULL: The holotype of *Metarhinus abbotti* (FMNH P12179) is a complete skull although it is somewhat crushed dorsoventrally (fig. 30). Small portions of the right premaxilla and right zygomatic arch are reconstructed with plaster. The dentition of FMNH P12179 is complete; however, substantial portions of the canine crowns are plaster so that measurements of the canine crowns are probably not reliable. There are no visible sutures on FMNH P12179. Two additional skulls, CMNH 2866 and CMNH 3510, are identified as *Metarhinus abbotti*. Although it is more poorly preserved than the holotype, CMNH 2866 (fig. 31) is undistorted and more faithfully reveals the general shape of the cranium from a lateral view.

Metarhinus abbotti is a small (table 5) hornless brontothere most similar in size to *M. fluviatilis* and *Fossendorhinus diploconus*. The nasal incision extends as far back as the posterolateral root of M1. The orbit is positioned directly above M2, while the posterolateral root of M1 is positioned below the anterior rim of the orbit. The face is greatly constricted in FMNH P12179 but somewhat less than that seen in some specimens of *M. fluviatilis*. However, CMNH 2866 shows greater facial constriction. The orbits of *M. abbotti* protrude laterally to a degree similar to that of *M. fluviatilis* (see description of *M. fluviatilis* for further explanation).

The nasal process of the holotype is very thin, narrow, shorter than the premaxillomaxillary rostrum, and it projects in a slightly upward direction. The upward orientation of the nasal process of the holotype appears to be a taphonomic artifact related to the dorsoventral crushing above and behind the orbits. The nasal process of CMNH 2866 is horizontal. The side of the nasal bone forms a very shallow lateral wall. The lateral wall is truncated at the midpoint of the nasal process and the distal half of the nasal process is nearly flat. In FMNH P12179 the nasal process tapers continuously from the proximal end to the distal end and the distal margin is rounded. However, the shape of the nasal bone appears to be variable. In CMNH 2866 and CMNH 3510 the proximal two

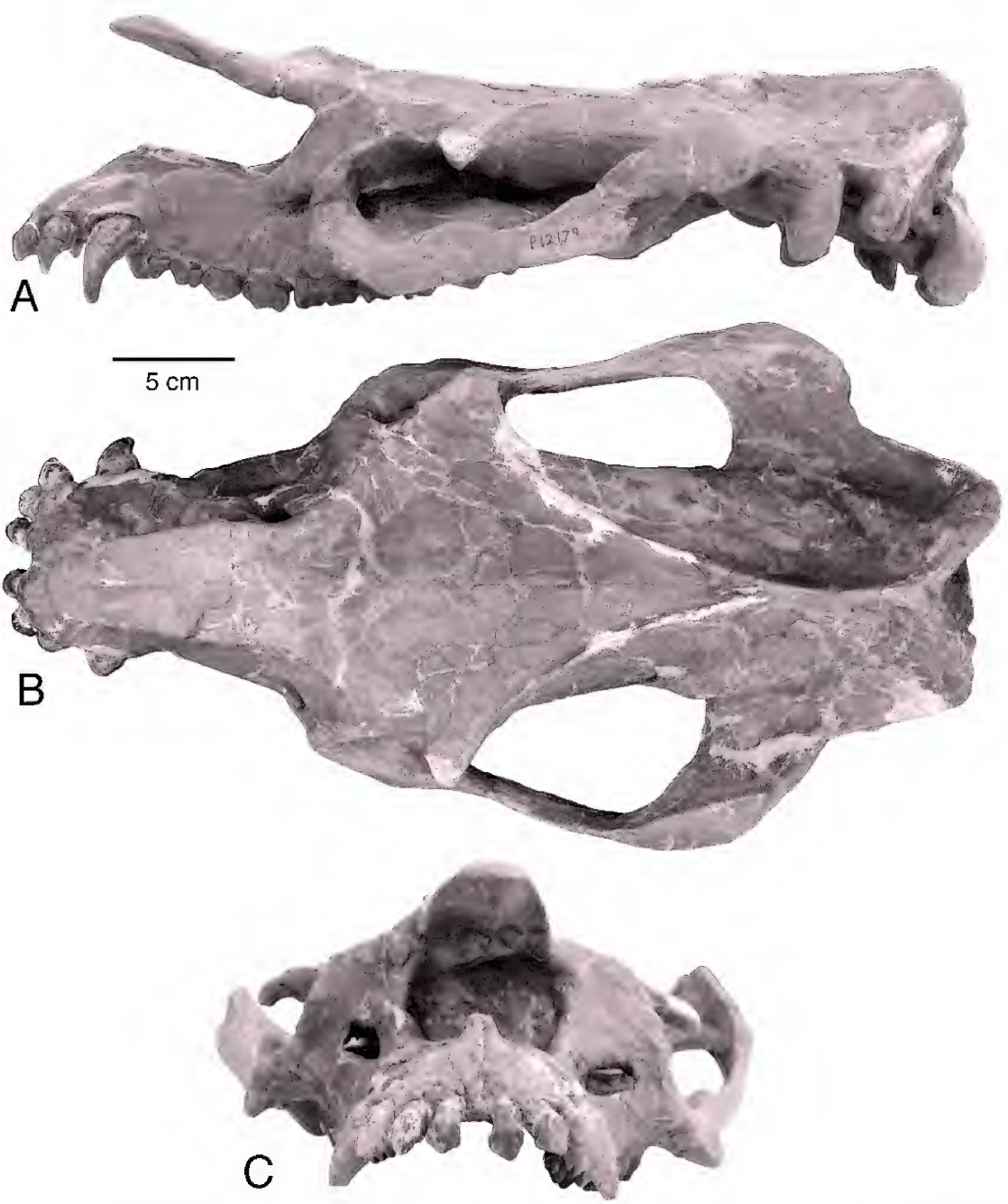

Fig. 30. The holotype of *Metarhinus abbotti* (FMNH P12179). **(A)** Left view, **(B)** dorsal view, **(C)** anterior view.

thirds of the nasal process has a constant width while the distal third tapers.

The premaxillomaxillary rostrum is undifferentiated from that of *Metarhinus fluviatilis*. From a lateral view, the premaxillomaxillary rostrum is long, of relatively constant dorsoventral depth, and slightly curved upward. The dorsal surface of the rostrum is horizontal and the rostrum does not deepen proximally. The premaxillary sym-

Fig. 31. Left view of a skull referred to *Metarhinus abbotti* (CMNH 2866).

physis is very long and it extends the entire length of the rostrum. Consequently, the dorsal surface of the rostrum is completely covered by a solid layer of bone. From the anterior view the premaxillae form a dome with a tall ridge of bone running mesially along the full length of the rostrum.

From a lateral view the dorsal surface of FMNH P12179 is flat above and behind the orbits. However, in the uncrushed specimen, CMNH 2866, the postorbital dorsal surface is more convex. The sagittal crest is very thin. Likewise, the zygomatic arches are very thin, dorsoventrally shallow, and are not laterally bowed. From a lateral view, the zygomatic arches are strongly curved. The infraorbital jugal process of *Metarhinus abbotti* can be seen most clearly from the anterior view (fig. 30c). It is small like that of *M. fluviatilis*.

From a lateral view the occiput is moderately tiled backward. From a dorsal view the nuchal crest is deeply notched medially. From a posterior view (not shown) the dorsal margin of the occiput is arched and the center of the occiput is deeply recessed between two prominent occipital pillars.

In comparison to specimens of *Metarhinus fluviatilis* (particularly FMNH P12187, seen in fig. 28), the holotype of *M. abbotti* is gracile. However, other specimens such as CMNH 2866 are more robust with somewhat deeper zygomatic arches and less slender proportions. In particular, CMNH 2866 resembles some of the more gracile specimens of *Metarhinus fluviatilis*. Therefore, it is difficult to separate these two species based on the depth of the zygomatic arches or general robusticity of the skull.

The ventral view of FMNH P12179 (fig. 32a) does not notably differ from *Metarhinus fluviatilis*. The anterior rim of the posterior nares is positioned between the M2s, the emargination of the posterior nares is narrow, and there are no ventral sphenoidal fossae, although the posterior narial canal extends onto the anterior part of the sphenoid. The foramen oval is widely separated from the foramen lacerum and the external

TABLE 5
Summary statistics for selected morphometric variables of *Metarhinus abbotti*
See Methods for measurement definitions

	N	Mean	SD	Min.	Max.	CV
P3 L	3	20.1	1.0	19.3	21.3	5.0
P3 W	3	23.3	0.8	22.6	24.3	3.6
M2 L	3	36.3	1.7	34.7	38.1	4.7
M2 W	2	41.0	3.1	38.9	43.2	7.5
P2–P4	3	56.1	0.3	55.9	56.5	0.6
M1–M3	3	102.4	1.1	101.4	103.6	1.1
VL	2	418	11.3	410	426	2.7

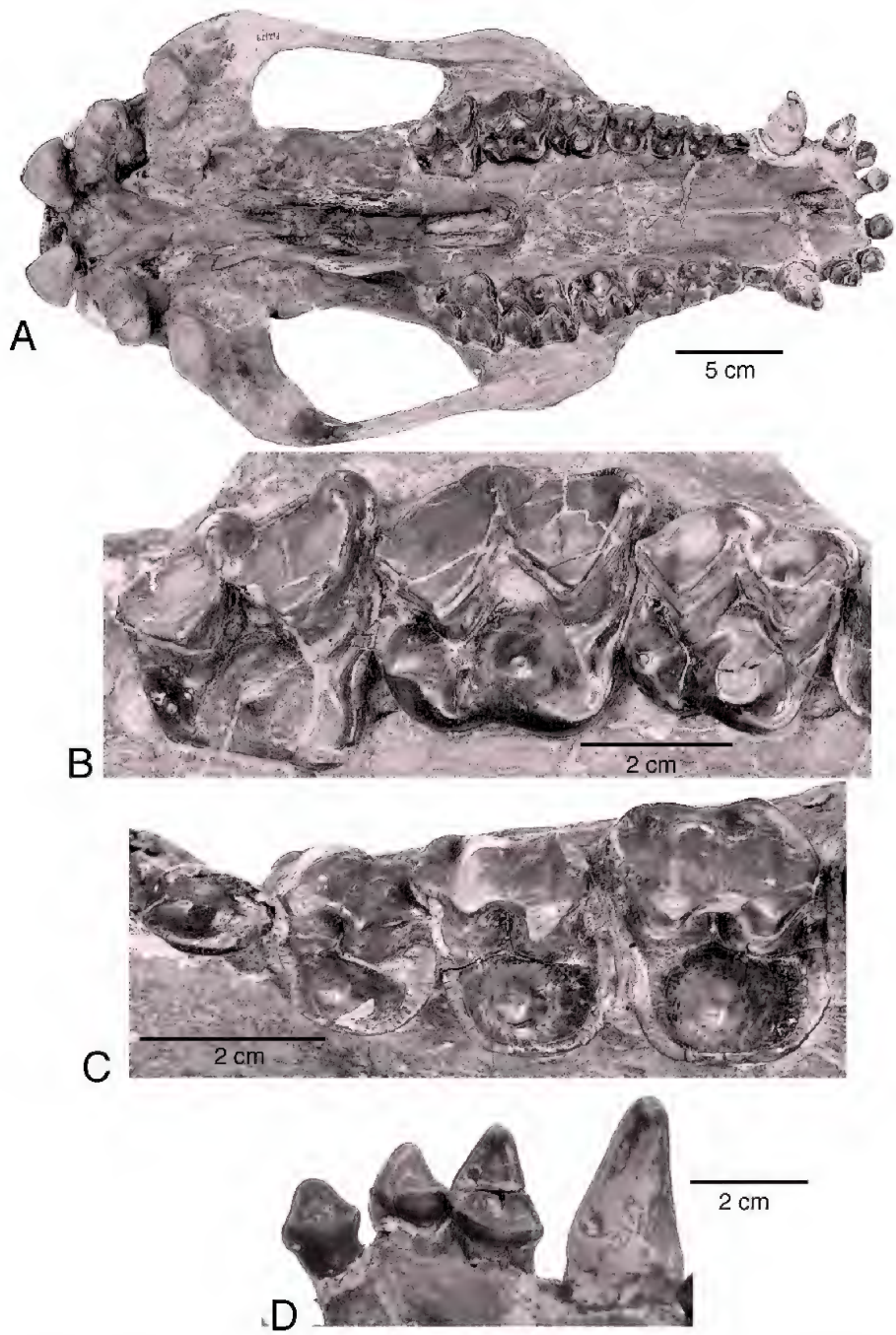

Fig. 32. The holotype of *Metarhinus abbotti* (FMNH P12179). **(A)** Ventral view, **(B)** right molars, **(C)** left premolars, **(D)** lingual view of left incisors and canine.

auditory pseudomeatus is open ventrally. A pair of thin bony choanal pouches can clearly be seen in the anterior portion of the posterior narial canal of FMNH P12179.

UPPER DENTITION: The holotype of *Metarhinus abbotti* (FMNH P12179) is the only specimen with well-preserved teeth (fig. 32), although some information on variation in

the premolars can be gleaned from other specimens. *M. abbotti* has an unreduced upper dental formula (3-1-4-3). The incisors are large and form an arched row that extends anterior to the canines. The incisors are subcaniniform with short, lingually curved crowns, and distinct lingual cingula. The incisors increase in size laterally, with i3 being the largest and most caniniform incisor. There is both a short precanine diastema and a postcanine diastema. The crowns of the canines are fragmented and reconstructed with plaster. The remnants of real enamel embedded in the plaster reconstruction suggest that the canines were rather small.

The P1 is a small and simple tooth with a single cusp and an elongate posterior heel. There is a distinct lingual cingulum on the P1. The P2 is more oblique in outline than the P3 and P4 because of a slightly more posterolingually angled anterior margin and a slightly more lingually shifted metacone. The P2 parastyle is straight, while those of P3 and P4 are angled slightly labially. The metastyles of P2–P4 are nearly straight. The labial paracone ribs of P2–P4 are distinct and become smaller in more posterior premolars. The protocones of P2–P4 are relatively tall. In P2, the protocone is slightly ovoid, but those of P3 and P4 are progressively more cone-shaped. There are no additional lingual cusps or crests on the premolars of FMNH P12179; however, the premolars of CMNH 3510 exhibit vestigial yet distinct preprotocrista on P2 and P3. The anterior and posterior premolar cingula typically join lingually, forming continuous lingual cingula, but this is not always the case, as in the P2 of FMNH P12179, where the lingual cingula are discontinuous.

The molars of *Metarhinus abbotti* show typical brontotheriine apomorphies including tall, lingually angled ectolophs, weak labial ribs, thin lingual ectoloph enamel, and wedge-shaped lingual sides of the paracone and metacone in molars that are not heavily worn (M2 and M3). The anterior cingulum is thin and passes proximally to the distal peak of the parastyle. Each molar has a shallow central molar fossa. There are no traces of paraconules or metalophs. There are strong anterolingual cingular peaks on the M2 and M3. It is weaker on M1, but this is because it is more heavily worn. A M3 hypocone is present, but it is not bilaterally symmetrical; on the right side it is a small but distinct cusp and the distal cingulum ascends to the apex of the right M3 hypocone; on the left side the hypocone is smaller and the cingulum appears to wrap around the mesiodistal corner of the M3. The labial molar cingula are thin and discontinuous around the labial bases of the mesostyles. The lingual molar cingula are discontinuous around the protocone and hypocone.

Metarhinus sp.

Includes nomina dubia: *Metarhinus fluviatilis* Osborn, 1908a; *Metarhinus earlei* Osborn, 1908a; *Metarhinus cristatus* Riggs, 1912; *Heterotitanops parvus* Peterson, 1914a; *Telmatherium accola* Cook, 1926; *Telmatherium advocata* Cook, 1926; *Metarhinus pater* Stock, 1937

REFERRED SPECIMENS: **(From the Wagonhound Member of the Uinta Formation, Uinta Basin, Utah)** AMNH 1500 (holotype of *Metarhinus fluviatilis*), a skull with right I1–M3 and left I2–M3; AMNH 1859, a mandible with right c–m3 and left i3–m3; AMNH 1864, a left maxilla fragment with P3–M1, M2 (partial); AMNH 1865, a partial mandible with left p3–m3; AMNH 1877, a crushed skull; AMNH 1946, right P3–M3, left P2–M3, and a partial mandible with right c–m3; AMNH 2059, a partial mandible with right i1, c, p2, and left i1–m3; CMNH 2909, a juvenile skull and skeleton (holotype of *Heterotitanops parvus*); CMNH 3098, a skull right P2–M3, left C–M3, and isolated incisors and canine fragment; CMNH 3125, a partial mandible with right p3–m3; CMNH 3133, a mandible with right c–m1, left i2, and c–m3; CMNH 3142, a maxilla fragment with partial molars and a partial mandible with right i1–c, p2–m3, and left i1–c; CMNH 3371, a partial mandible with left p1–m3; CMNH 3842, a partial mandible with right i1–m2, m3 (partial), left i1–m3; CMNH 11924, a mandible with right i1–i2, p3–m3, and left i1–m3; CMNH 16736, a palate with right P4–M3 and left P1–M3; FMNH P12169, a skull with right P1–M3 and left I3–M3; FMNH P12174, a crushed skull with right and left

M1–M3; FMNH P12178, a mandible with right p3–p4 and left p2–m3; FMNH P12178, a mandible with right p2–m3, left i1, and p1–m3; FMNH P12183, a partially prepared skull and mandible with exposed left upper and lower cheektooth rows; FMNH P12190, a mandible with right and left m1–m3; FMNH P12194 (holotype of *M. cristatus*), the posterior portion of a skull with right and left M2–M3; FMNH P12195, a mandible with right c, p2–m3, left c, and p2–m3; YPM 11284, a partial mandible with right p4 and m1–m3 (partial); **(from the Adobe Town Member of the Washakie Formation of Wyoming)** AMNH 13166 (holotype of *Metarhinus earlei*), a skull with right P4, M3, left P2–P4, and M2–M3; AMNH 13179, a mandible with right p1–m3 and left c–m3; CMNH 9409, a crushed skull with right P2–M3 and left P4–M3; FMNH PM1456, a partial mandible with left p3–m3 (all partial); FMNH PM1511, a partial mandible with right i2–c, p2–p4, and left i3–m3; FMNH PM1517 (in part), a right maxilla fragment with P2–P4; FMNH PM1519, a palate with right P2–P4, and left P3–M3; FMNH PM1675, a partial mandible with right and left dp2–dp4, m1, and m2 (unerupted); FMNH PM1680, a rostrum with right P1–P2 (partial), and P3–M1; FMNH PM1715, a mandible with right i1 (?), p2–p4, m3, left i1 (?) p1–p4, and m3; FMNH PM1730, a rostrum with right P2–M1; FMNH PM1731, the posterior portion of a skull with right and left M1–M2, and isolated right P3–P4; FMNH PM1732, a left maxilla and jugal with P2–M3; FMNH PM1734, a partial mandible with right p2–m3; FMNH PM39947, a mandible with right p2–m3; UCMP 81273, a mandible with right c–m3 and left p1–m3; UCMP 81285, a right maxilla with P4–M2; YPM 16834, a partial mandible with right i1–i2, c, left i1–c, and p2–p4; **(from the "Metarhinus Quarry" of the Adobe Town Member of the Washakie Basin, Washakie Formation, Wyoming)** FMNH PM28001, a mandible with right i2, c, p2–m3, and left i1–m3; FMNH PM28002, a partial mandible with left i2–m3; FMNH PM28003, a partial mandible with right p1–m3; FMNH PM28004, a partial mandible with right i2–m3; FMNH PM28006, a mandible with right c, p2–m3, left c, and p2–m3; FMNH PM28014, a partial mandible with right and left p1, dp2–dp4, and m1 (unerupted); FMNH PM28342, a partial mandible with right p2–m3, left p1–p3, and m2–m3; FMNH PM28343, a partial mandible with right p2–m3 and left p2–m2; FMNH PM28344, a partial mandible with right p2–m2, left c, p2, p3–p4 (partial), m2–m3 (partial); FMNH P28345, a skull fragment with right P2–M3 and left P2–M3; FMNH PM28348, a palate with right I2 (?), C, P1–M3, left C, P1, and P3–M3; FMNH PM28359, a right p2–p4; FMNH PM30388, a right maxilla with P2–M3; FMNH PM30422, a mandible with right i2 (?), p1–m3, left i3, and p1–m3; FMNH PM30432, a crushed skull with right and left P2–P4; FMNH PM30434, a partial mandible with right and left p1, dp2–dp4, m1 (unerupted); FMNH PM30435, a mandible with right i2–i3, p1–m3, left i3, and p1–m3; FMNH PM35932, a skull with right and left P1–M3; FMNH PM35933, a mandible with right p3–m3 and left p2–m3; FMNH PM35970, a mandible with right p2–m3, left canine, and p2–m3; FMNH PM35996, a mandible with right i2–i3, p2–m3, left i2 (?), and p2–m3; FMNH PM36053, a skull fragment with left P3–M1 (partial); FMNH PM36054, a skull fragment with right P3–M3 (partial), left P1–M1, and M2 (partial); **(from the Sand Wash Basin of Moffat County, Colorado)** DMNH 543, a partial mandible with left p2–m3; DMNH 544 (holotype of *Telmatherium accola*), a mandible with right p2–m3 and left c–m3; DMNH 550 (holotype of *T. advocata*), a mandible with right i3, left i1, c, p2–m2, and m3 (erupting); DMNH 2611, a right maxilla with M1–M3; **(from the Friars Formation of San Diego County, California)** LACM/CIT 2037 (holotype of *Metarhinus pater*), a right maxilla with C–M3; UCMP 95774, a right maxilla with M1–M3; UCMP 95808, a right maxilla with DP4 and M1; UCMP 95809, a left maxilla fragment with P3–P4; UCMP 95831, a left M1 or M2; UCMP 95780, a partial mandible with left m1–m3; UCMP 95813, a partial mandible with right m2 (partial), and m3; UCMP 95841, a mandible fragment with right p2–p3; UCMP 106011, right p3, p4, and m1; UCMP 113182, fragments of a skull, jaw and some isolated lower teeth; UCMP 113189, a right

p2; UCMP 113194, a mandible fragment with right m2; UCMP 113201, a partial mandible with right dp3–dp4, and m1; UCMP 113203, a mandible fragment with left m3.

Description

Because the only clear distinction between *Metarhinus fluviatilis* and *M. abbotti* is the shape of the nasal bone, the vast majority of *Metarhinus* specimens cannot be assigned to either species. These specimens include jaws as well as skulls that lack preserved nasal bones. Among the fossil collections studied for this revision, specimens that could belong to either species of *Metarhinus* are known from the early Uintan Wagonhound Member of the Uinta Formation of Utah, the middle Adobe Town Member of the Washakie Formation of Wyoming, the Sand Wash Basin of Colorado, and from the Poway and Murray Canyon local faunas of the Friars Formation of San Diego County, California. These include 30 skulls and skull fragments. Four of these have associated mandibles and/or lower dental elements. Also included are an additional 50 complete and partial mandibles.

Among these specimens are the holotype skulls of *Metarhinus fluviatilis* Osborn (1908a) (AMNH 1500), as well as the holotypes of *M. earlei* Osborn (1908a) (AMNH 13166), *M. cristatus* Riggs (1912) (FMNH P12194), and *M. pater* Stock (1937) (CIT 2037). This large group of specimens provides further information on the morphology of *Metarhinus*. Therefore, they are described below, particularly as they pertain to intraspecific variation and missing phylogenetic data for *M. fluviatilis* and *M. abbotti*.

Skull and Upper Dentition: None of the *Metarhinus* sp. skulls have well-preserved upper incisors, however many specimens have preserved alveoli or partial sets of well-worn incisors. These all suggest large incisors, consistent in morphology with those of the holotype of *Metarhinus abbotti*. The incisor morphology of *M. fluviatilis* was probably not different from that of *M. abbotti*. A significant number of the skulls show variable premolar morphologies. Numerous specimens (e.g., AMNH 1864, FMNH PM1517, FMNH PM1730, FMNH PM1732, and FMNH P12169) have a small crest extending posteriorly from the protocone of P2 and P3. Occasionally a very small lingual crest can be seen on the P4 protocone. A premolar hypocone is never present. One atypical specimen (FMNH PM36054) has a P1 with an unusual lingual heel with a large protocone. The M3s of these specimens consistently have hypocones that are variable in size but they are always smaller than the hypocones of the M1 and M2.

Mandible and Lower Dentition: The following description of the mandible of *Metarhinus* sp. is primarily based on AMNH 2059 (fig. 33), although additional information from other specimens is given. The inferior margin of the symphysis is angled about 45° or somewhat less than that. The posterior margin of the symphysis is between the talonids of the p3 in AMNH 2059. However, its position fluctuates between the anterior margin of p3 and the posterior margin of p3. The dental formula is unreduced (3-1-4-3). The incisors are large, form a semicircular arch anterior to the canines, and are positioned closely together. The incisors are subcaniniform with short lingually curved crowns and blunt points. Each incisor has a strong lingual cingulid. The canines are somewhat variable in size, but generally, they are small and slender with lingual cingulids that are much weaker than those of the incisors. There is no precanine diastema in AMNH 2059 although a short precanine diastema is occasionally present in other specimens. The postcanine diastema of AMNH 2059 is shorter than the p2 although some specimens have a slightly longer postcanine diastema. AMNH 2059 lacks a p1–p2 diastema while other specimens (e.g., UCMP 81273) have a minor p1–p2 diastema.

The p1 is a simple tooth with a single cusp and a short talonid heel. The p2 and p3 trigonids are longer than the talonid, while the p4 trigonid is shorter than the talonid. The trigonids of p2–p4 are narrower than their respective talonids. The paralophid of p2 arches slightly lingually, creating a small lingual trigonid notch. The p2 protolophid is lingually positioned and posteriorly directed. The p2 lacks a metaconid. The p3 and p4 trigonids are more molariform with strongly

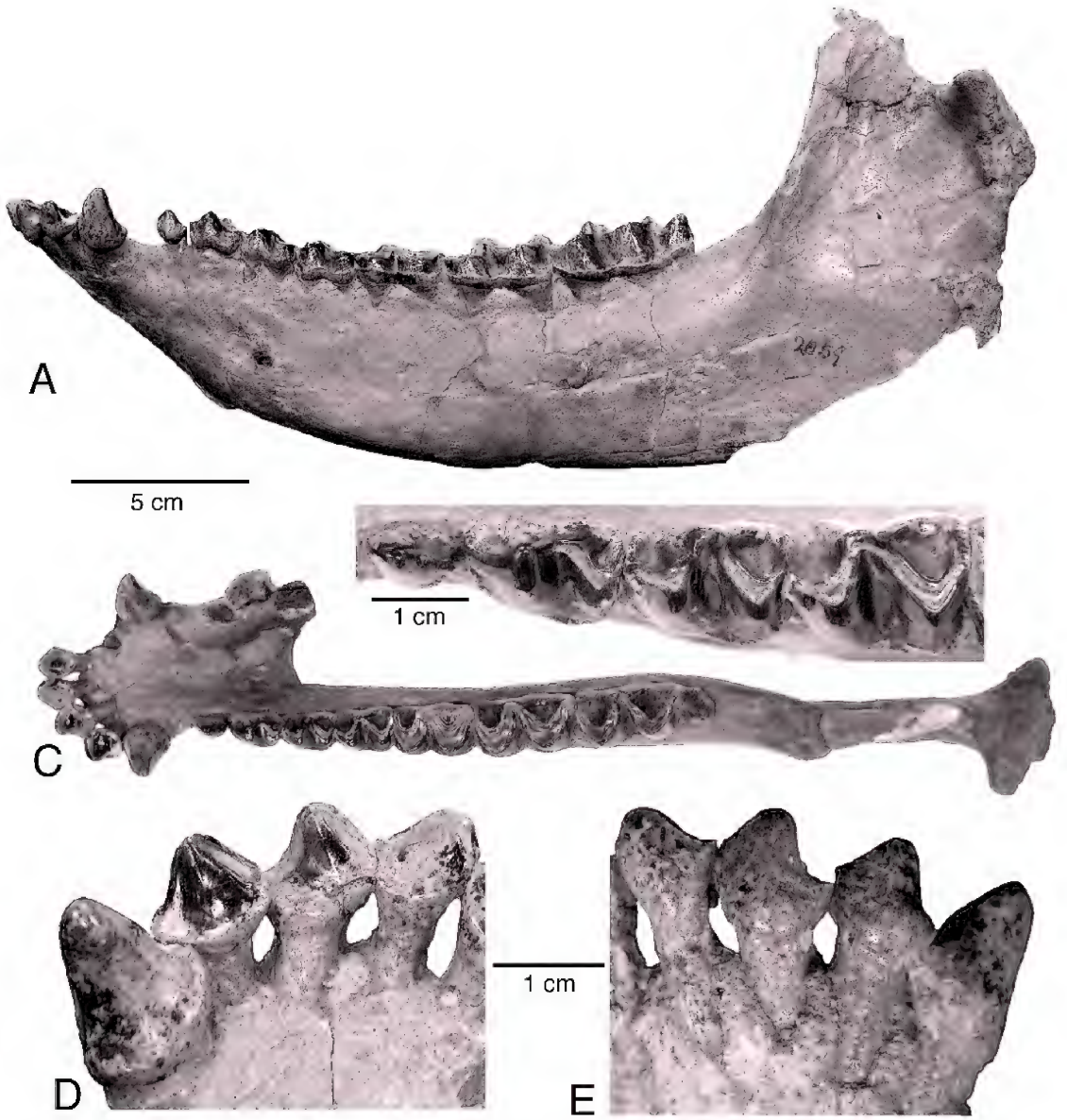

Fig. 33. A mandible (AMNH 2059) referred to *Metarhinus* sp. **(A)** Left view, **(B)** left premolars, **(C)** dorsal view, **(D)** left incisors and canine, lingual view, **(E)** left incisors and canine, labial view.

lingually arched paralophids and protolophids, a broad lingual notch, and a large lingually positioned metaconid. The talonid of the p2 has a well-developed cristid obliqua, a small lingual notch, and a short hypolophid. The talonids of p3 and p4 are more developed with more basinlike depressions and longer hypolophids. The lower molars are typical with thin enamel, shallow trigonid and talonid basins, and an elongate m3.

Although the majority of the unidentified mandibles have a large metaconid on p3, it is occasionally absent (e.g., AMNH 1859, CMNH 3125, FMNH P12178) or very small (e.g., CMNH 3371). The presence or absence of a p3 metaconid is known to be variable in *Lambdotherium* (Bonillas, 1936) and among some brontotheriids (e.g., *Rhinotitan*). In this instance, it is possible that either this character is intraspecifically variable in *Me-*

tarhinus fluviatilis and *M. abbotti*, or the m3 metaconid is present in *M. fluviatilis* but absent in *M. abbotti*. The former scenario is more likely based on the monospecific death assemblage of *Metarhinus* sp. from the Washakie Formation where the p3 metaconid is both absent and present. If this assemblage is truly monospecific, as it has been presumed to be (Turnbull and Martill, 1988; see below), one must conclude that the p3 metaconid is intraspecifically variable. It is reasonably safe to infer that the jaws and lower dentition of *M. fluviatilis* and *M. abbotti* were not significantly differentiated. Therefore, these mandibles were used in coding the mandible and lower dental characters of *M. fluviatilis* and *M. abbotti* for the phylogenetic analysis.

Remarks

In 1908, Osborn (1908a) named a new genus and species, *Metarhinus fluviatilis*, from a skull (AMNH 1500) from the Uinta Basin with worn dentition and missing the nasal process. The specimen shows a unique combination of characters that clearly sets it apart from other species that were known at the time. These characters include prominent orbits, a long nasal incision, and a small infraorbital process. In the same paper, Osborn (1908a) named another species, *Metarhinus earlei*, based on AMNH 13166, a skull also missing the nasal bones that is slightly larger than AMNH 1500 but similar to it in other respects. In 1912, Riggs (1912) erected two more species of *Metarhinus*. These include *M. riparius*, based on a complete skull (FMNH P12186) with nasal bones, and *M. cristatus*, based on the posterior portion of a skull (FMNH P12194). Riggs (1912) thought that he saw two lineages of *Metarhinus* evolving (presumably) from a small primitive *M. fluviatilis*. *M. earlei* and *M. cristatus* represented a broad-headed form, and *M. riparius* represented a narrow-headed form. Osborn (1929a) generally agreed with this interpretation. However, most of the differences in these "lineages" can be attributed to taphonomic distortion. For instance, the sagittal crest is exaggerated in skulls with crushed braincases. Other reported differences are simply unsubstantiated. For instance, the expansion of the nasal bones was one of the distinctions of these lineages, however, only one of the four holotypes has preserved nasals. Curiously, Osborn (1929a) recognized the influence of taphonomic distortion on the differences in the proportions of the various holotypes but he did not reject any of the supposed *Metarhinus* species. Finally, Stock (1937) named a fifth species, *Metarhinus pater*, based on CIT 2037, a right premaxilla and maxilla from the sandstones of the Poway Conglomerate of San Diego County, California. Although Stock (1937) questionably referred this species to *Metarhinus*, the holotype is consistent with other species that had been referred to *Metarhinus*.

Riggs (1912) based a new genus and species, *Rhadinorhinus abbotti*, on a complete skull (FMNH P12179). Riggs' (1912) decision to erect a new genus for FMNH P12179 is curious because it closely resembles the other supposed species of *Metarhinus*. However, the nasal process of FMNH P12179 tapers distally, whereas some of the skulls that have been attributed to *Metarhinus* have a distally widening nasal process. However, Riggs' (1912) and Osborn's (1929a) referrals of species with the distally widening nasals to the genus *Metarhinus* and referrals of species with distally tapering nasals to the genus *Rhadinorhinus* is arbitrary because the morphology of the nasal processes of the type species of *Metarhinus*, *M. fluviatilis*, is unknown.

Despite the numerous species named by Osborn and Riggs, there appear to only be two diagnosable species, one with distally tapering nasals and one with distally broadening nasals. These species appear to be undifferentiated in every other respect. Unfortunately, the holotype of the type species of *Metarhinus* (*M. fluviatilis*) lacks a nasal bone and its specific identity is uncertain. Therefore the validity of the genus *Metarhinus* is questionable. On the other hand, the genus *Rhadinorhinus* is less problematic because the holotype of *R. abbotti* includes a complete (distally tapering) nasal bone. Nonetheless, in more recent revisions, Mader (1989) continued the dubious practice of using *Metarhinus fluviatilis* for the species with distally widening nasals, and *Rhadino-*

rhinus abbotti for the species with distally tapering nasals. In a later revision (Mader, 1998), *Rhadinorhinus abbotti* was mistakenly considered a junior synonym of *Metarhinus diploconus* (now *Fossendorhinus diploconus*). However, *Fossendorhinus diploconus* is clearly different from both *M. fluviatilis* and *M. abbotti* and can no longer be considered a potential synonym of either species.

Despite the fact that *Metarhinus* is problematic due to unknown nasal morphology of the type species, *M. fluviatilis*, *Metarhinus* is a well-known taxon with biostratigraphic importance (e.g., Prothero 1996; McCarroll et al. 1996b; Robinson et al. 2004). To reject *Metarhinus* outright would generate serious inconsistencies in the literature on North American mammal biostratigraphy. It has been long assumed that *M. fluviatilis* represents the particular species with the distally widening nasals (Osborn 1929a; Mader 1989, 1998). Therefore, to continue the use of *Metarhinus*, I suggest that FMNH P12187, a complete skull with distally broadening nasals, be designated as the neotype for *Metarhinus fluviatilis*. Secondly, *Rhadinorhinus abbotti* is valid and represents the species with the distally tapering nasal bone. However, it is convenient to consider *Rhadinorhinus* a junior synonym of *Metarhinus* because the large number of museum specimens that pertain to either *fluviatilis* or *abbotti* but cannot be identified to either due to nonpreservation of the nasal bone are identified on specimen labels and museum catalogs as *Metarhinus* sp. Grouping *fluviatilis* and *abbotti* into one genus, *Metarhinus*, maintains accuracy in the identification of these specimens and published biostratigraphic data that are based on these specimens. The remaining species of *Metarhinus* are invalid. *M. riparius* is the only other *Metarhinus* species represented by a holotype with a preserved nasal bone. The nasal bone of that specimen indicates that *M. riparius* is a junior synonym of *M. fluviatilis*. Other species attributed to *Metarhinus* whose holotypes lack nasal bones, *M. earlei*, *M. cristatus*, *M. pater*, are nomina dubia.

In addition to the above nomina dubia, Peterson (1914a) described a skull and skeleton of a very young, possibly fetal brontothere from the early Uintan (Uinta B1) that he gave a new name, *Heterotitanops parvus* (CMNH 2909). Given the very young ontogenetic age of the animal, this species is not valid and it probably represents a known species of similar age although this specimen cannot be clearly assigned to any particular species. Osborn (1929a) noted that it resembled *Dolichorhinus* in the absence of a sagittal crest but this similarity was dismissed as an artifact of ontogeny. Ultimately Osborn (1929a) considered it most likely to be *Metarhinus fluviatilis*, primarily based on comparisons of the deciduous dentition with the adult dentition of that species. However, the assignment to *M. fluviatilis* is uncertain since the neonate specimen lacks a nasal process. At any rate, the specimen is simply too young to clearly refer to any particular species of brontothere; juvenile brontothere materials are uncommon and too poorly documented to make an appropriate comparison of CMNH 2909 with other species. *Heterotitanops parvus* is a nomen dubium, but it could be a synonym of *Metarhinus* sp.

The summary statistics of those few specimens that are directly identifiable as *Metarhinus abbotti* and *M. fluviatilis* can be found in tables 4 and 5. *M. abbotti* appears to be larger than *M. fluviatilis* in premolar length and ventral skull length. These species slightly overlap in total cheektooth row length and completely overlap in molar row length. Although the few specimens identifiable as *M. abbotti* appear to be larger in some respects than those specimens identifiable as *M. fluviatilis*, plots of any of these variables (not shown) for the entire *Metarhinus* sp. group do no reveal any clear bimodal distributions that might suggest two size groups.

A catastrophic death assemblage found in overbank deposits associated with sandstone channels from the Adobe Town Member of the Washakie Formation provides a rare glimpse at the population variability of a brontothere species. This sample was initially identified as *Mesatirhinus* sp. (Turnbull and Martill, 1988), but was demonstrated by McCarroll et al. (1996a) to be *Metarhinus* sp. No specimen with intact nasal bones is known from the quarry. Therefore, the quarry sample could represent either *Metarhinus fluviatilis* or *M. abbotti*. It is often

TABLE 6
Summary statistics for selected morphometric variables of *Metarhinus* sp. from the "Metarhinus quarry"
See Methods for measurement definitions

	N	Mean	SD	Min.	Max.	CV
C L	1	16.6		16.6	16.6	
P3 L	6	19.0	1.5	17.3	21.8	8.1
P3 W	5	21.6	0.9	20.4	22.8	4.0
M2 L	5	38.2	1.7	36.6	40.5	4.6
M2 W	5	36.4	1.8	34.0	38.9	4.9
P2–P4	6	53.0	2.7	49.97	57.6	5.0
M1–M3	5	103.4	3.1	100.2	108.1	3.0
VL	2	395	35.4	370	420	9.0
c L	3	19.4	0.2	19.2	19.5	1.0
p3 L	14	18.0	1.1	16.6	19.5	5.9
p3 W	13	14.5	0.9	13.3	16.6	6.2
m2 L	11	34.4	1.5	31.8	36.5	4.4
m2 W	11	22.4	1.3	20.3	24.3	6.0
p2–p4	13	55.5	2.9	51.2	61.1	5.2
m1–m3	12	110.0	5.3	105.0	122.5	4.8

presumed that large quarry samples, particularly catastrophic death assemblages, are monospecific. Turnbull and Martill (1988) assumed this sample to represent a monospecific herd. Modern ungulate catastrophic death assemblages are monospecific (Berger et al., 2001), although they do not necessarily indicate herds (Mihlbachler, 2003b). It is probable that this sample, though not necessarily representing a herd, is a monospecific death assemblage. (Indeed, I have assumed this as outlined in the explanation of the methodology used in this study). The summary statistics for the *Metarhinus* sp. quarry sample are given in table 6. The coefficients of variation are compatible with a monospecific population, although they do no falsify the possibility that two similarly sized taxa are present. The average values of the quarry sample seem slightly closer to the average values of *M. fluviatilis*. However, the size ranges of two of the variables (P3 length, P2–P4 length) virtually span the size range of both species. Additionally, M1–M3 length and P2–M3 length span the entire size range of *M. abbotti*. Clearly, size is not a realistic means for assigning specimens to either species of *Metarhinus*.

Sthenodectes incisivum (Douglass, 1909)

HOLOTYPE: CMNH 2398, a skull lacking the nasal process with right I1, I2–C (crowns broken off), P1–P4 (partial), M1–M3, left I1–C, and P2–M3.

TYPE LOCALITY: Wagonhound Member (Uinta B) of the Uinta Formation, Northeast of Well #2 Uinta County, Utah.

SYNONYMS: *Sthenodectes priscus* Peterson, 1934.

AGE: Middle Eocene (early Uintan land mammal "age").

REFERRED SPECIMENS: **(From the Wagonhound Member of the Uinta Formation of Utah)** CMNH 9928, right and left maxillary fragments with right P2–P3 (partial) and left P3–P4 (partial); CMNH 11437 (holotype of *Sthenodectes priscus*), a partial skull with right C–M3, left P3–M3 (all partial), and an associated mandible with right i1–i2, c–m3, and left i1–m3; FMNH P12166, a mandible with complete dentition; FMNH P12165 (mistakenly referred to P12168 by Osborn [1929a]), a partial skull with complete dentition; **(from the Washakie Formation of Wyoming)** YPM 16883, a partial mandible with right i2–p2, p3 (partial), p4, m1(partial), left i1–i2, and c–m3.

DIAGNOSIS: *Sthenodectes incisivum* is an intermediate-sized hornless brontothere in which the frontal bone intrudes into the nasal bone, thus splitting off a small lateral splint of nasal bone from the main body of the nasal. The nasal splint and overlapping frontal process are small and the suture is not

often discernable. The nasal incision extends as far back as the P1. The nasal process is very short, horizontal, unelevated, of relatively constant transverse width, narrow, and with thin and moderately deep lateral walls. The orbits are positioned above M2 and protrude laterally, but as strongly as in *Metarhinus*. The lateral margin of the premaxillomaxillary rostrum deepens posteriorly and the rostral cavity is not sealed dorsally. Other cranial characteristics include a strongly concave midcranial dorsal surface, a flatter posterior cranial surface, a sagittal crest, strongly curved zygomatic arches, and a ventrally open and mediolaterally angled external auditory pseudomeatus. Ventral sphenoidal fossae, infraorbital processes, and a ventral zygomatic flange are all absent.

Dentally, *Sthenodectes incisivum* has oversized subcaniniform incisors, simple P1 that is surrounded on all sides by cingula, and a distinct P2 metacone. The lingual features of the P2–P4 are tall, and the lingual premolar cingula are thick and continuous. Other dental characteristics include weak premolar preprotocristae, and short lingual crests extending posteriorly from the premolar protocones. Premolar hypocones are absent. The upper molars of *S. incisivum* have tall, lingually angled ectolophs with weak labial ribs and thinned lingual ectoloph enamel with wedge-shaped paracones and metacones. A cingular parastyle shelf is absent. Central molar fossae and anterolingual cingular cusps are present, while paraconules and metalophs are absent. The lower dentition of *S. incisivum* is characterized by oversized subcaniniform incisors of uniform size, no p1–p2 diastema, a metaconid on p4 but not on p2 or p3, shallow molar basins, and a slender m3.

Only two brontotheres have greatly enlarged incisors, *Sthenodectes incisivum* and *Pygmaetitan panxianensis*. *P. panxianensis* is significantly smaller than *Sthenodectes incisivum* and it has a more complex p1.

Description

Skull: The holotype of *Sthenodectes incisivum* (CMNH 2398) is a nearly complete skull (fig. 34). The only significant missing portion is the nasal process. The skull has been dorsoventrally flattened, thus distorting the shape of the skull from a lateral view. Earlier figures in Douglass (1909) misleadingly depict a seemingly undistorted skull. The shape of the skull is less distorted from a dorsal view (fig. 34b) although the braincase has collapsed inwardly, exaggerating the height of the sagittal crest. Two other skulls of *S. incisivum* are known. These include CMNH 11437 (holotype of *S. priscus*) (fig. 35) and FMNH P12165 (fig. 36a). The skull of CMNH 11437, though less complete, is not dorsoventrally crushed and it offers a more faithful representation of the shape of the skull from a lateral view. The dorsal surface of FMNH P12165 is not preserved, but that skull is uncrushed as well, and its ventral surface is the best of the three skulls.

Sthenodectes incisivum is a medium-sized hornless brontothere. Osborn (1929a: fig. 301) labeled a "horn" and Peterson (1934) discussed "horn swellings", however, there are no hornlike protuberances in the holotype or any other specimen of *S. incisivum*. In CMNH 2398 there appears to be a thickened ridge of bone in front of the orbit that arches over the maxilla. This feature is not seen in the undistorted specimen, CMNH 11437. Portions of the facial sutures can be seen on CMNH 2398 and, although they are indistinct, they reveal the specialized facial configuration where the frontal bone intrudes into the nasal bone. Part of the right frontonasal suture can be seen on the dorsal surface. The frontal bone projects anteriorly and splits off the posterolateral portion of the nasal bone from the main body of the nasal. From the lateral view of the right side of the skull (not shown) a short lateral nasal splint can be seen dividing the frontal bone and maxilla, although it is indistinct and difficult to see without carefully examining the actual specimen. Note that Douglass' (1909: fig. 1) original figure of the holotype does not accurately portray the shape of the frontonasal contact.

The nasal incision is very short and most similar to those of *Metatelmatherium ultimum* and *Wickia brevirhinus*. This can most easily be seen on CMNH 11437, in which the nasal process is complete. In that specimen the nasal incision extends as far back as the P1. The orbit is situated directly above the M2

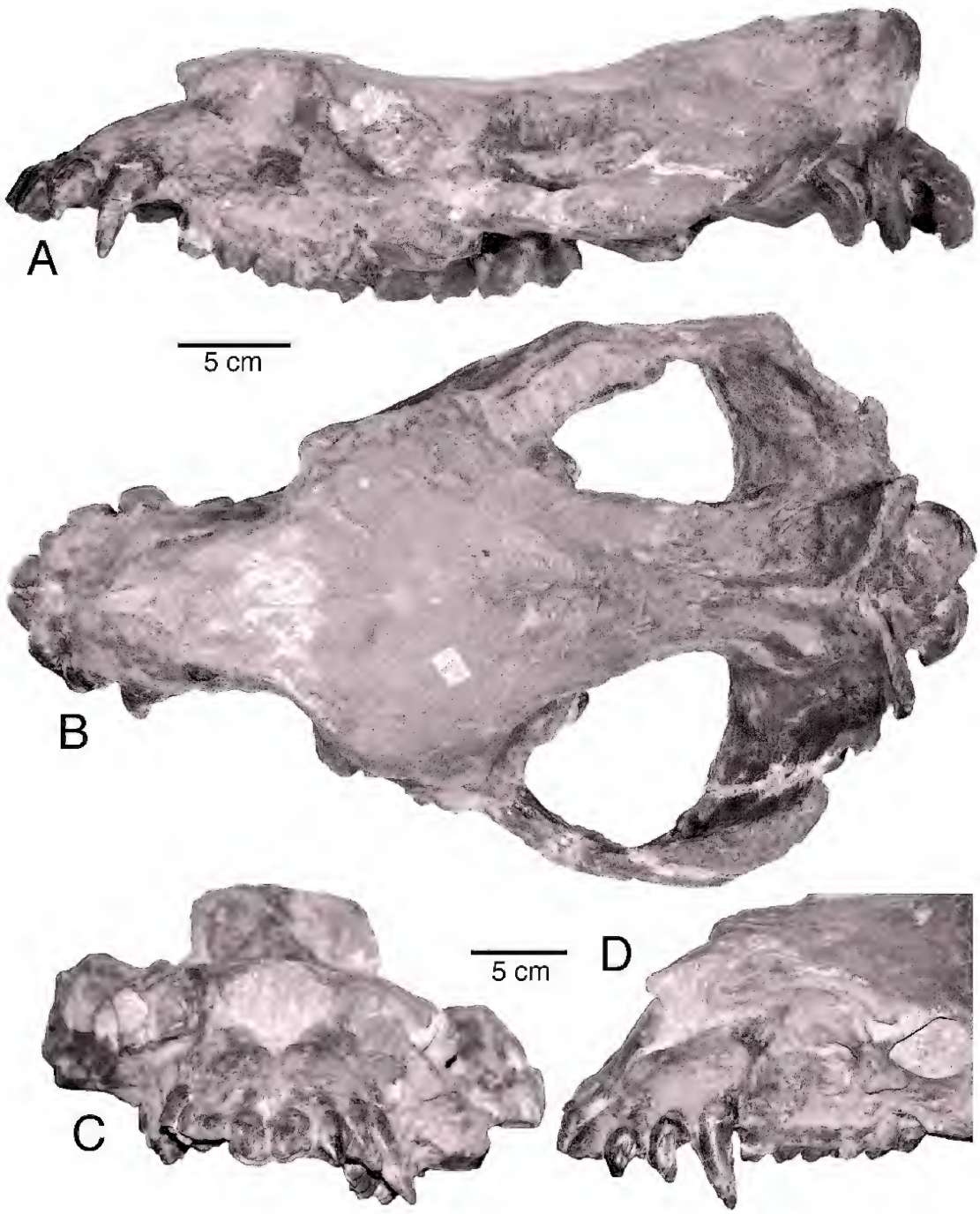

Fig. 34. The holotype of *Sthenodectes incisivum* (CMNH 2398). **(A)** Left view, **(B)** dorsal view, **(C)** anterior view, **(D)** anterolateral view.

Fig. 35. Right view of a skull referred to *Sthenodectes incisivum* (CM 11437).

and the posterior portion of the M1. The anterolateral root of M1 is positioned below the anterior rim of the orbit. The region of maxillary bone between the orbits and nasal incision forms a shallow concavity.

In the holotype (CMNH 2398), there is a triangular vacuity on either side of the skull just in front of the orbit. Douglass (1909) described these as a feature of *Sthenodectes incisivum*. However, Gregory (1912) and Osborn (1929a) concluded they were an artifactual result of damage, a conclusion that is borne out by other specimens that are undistorted and lack these vacuities.

CMNH 11437 has a complete nasal process. The nasal process is horizontal, relatively narrow, and it is slightly shorter than the premaxillomaxillary rostrum. The sides form shallow lateral walls. The anterior edge of the nasal process is not preserved.

The premaxillomaxillary rostrum of *Sthenodectes incisivum* is large and thick. The robust condition of the rostrum relates to the enlarged anterior dentition of this species. The premaxillae are completely fused at the midline. There are no discernable premaxillomaxillary sutures in the holotype. In FMNH P12165 an indistinct premaxillomaxillary suture indicates that the premaxilla terminates about at the posterior notch of the nasal incision. The premaxilla does not contact the nasal. From the lateral view the dorsal margin of the rostrum slopes posterodorsally. From the anterior view it can be seen that the sides of the rostrum diverge posterolaterally and the rostral cavity is dorsally open.

From a lateral view the dorsal surface of the skull is concave midcranially, but it becomes flattened or even slightly convex posteriorly. From a dorsal view the skull is broad between the orbits. The orbits protrude laterally to a degree similar to *Fossendorhinus*, but not to the extreme degree seen in *Metarhinus*. The parasagittal ridges converge and form a true sagittal crest, although the height of the sagittal crest of the holotype is exaggerated by the crushed braincase. The zygomatic arches are broad and bowed from the dorsal view. From a lateral view the jugal portion of the zygomatic arch is shallow and horizontal. The squamosal portion is deeper and angled posterodorsally, giving the zygomatic arch a strong curvature. *Sthenodectes incisivum* lacks an infraorbital process like that seen in *Metarhinus*. It also lacks an enlarged ventral zygomatic flange as seen in *Metatelmatherium*.

The nuchal crest is thin and from a dorsal view it is angled anteromedially. The occiput is only slightly tilted backward. From a posterior view, the occiput is not well preserved. However, it seems that the dorsal portion of the occiput is somewhat narrower than the ventral portion. The dorsal margin of the occiput is arched moderately. There are distinct occipital pillars on the posterior surface of the occiput; however, the deeply recessed pit in the center of the occiput

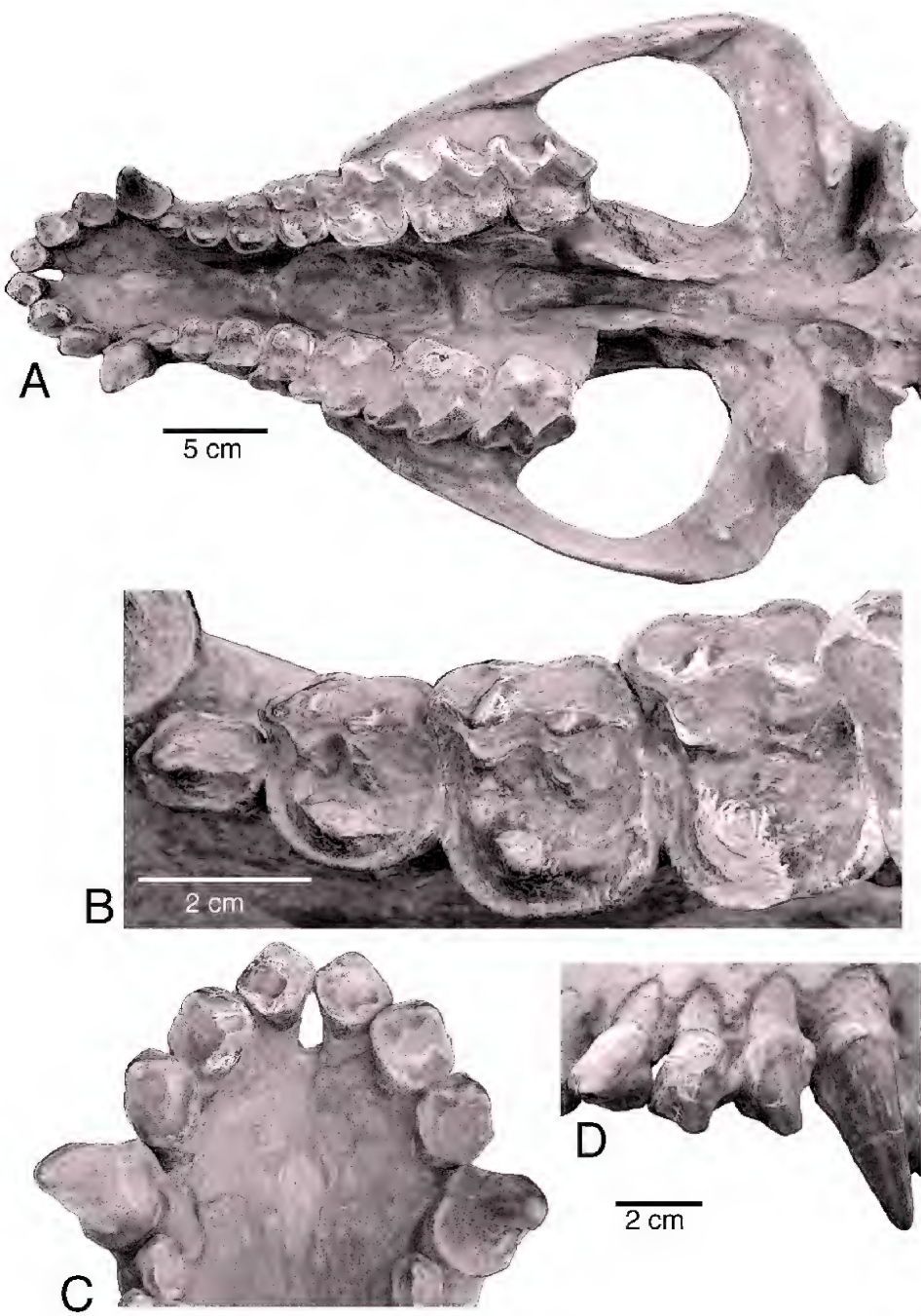

Fig. 36. A skull referred to *Sthenodectes incisivum* (FMNH P12165). **(A)** Ventral view, **(B)** left premolars, **(C)** lingual view of incisors and canine, **(D)** labial view of left incisors and canine.

between the occipital pillars is exaggerated by distortion.

The ventral surface of the skull of *Sthenodectes incisivum* is best preserved in FMNH P12165 (fig. 36a). The anterior rim of the posterior nares is positioned anterior to the M3. There is a narrow emargination around the anterior and lateral sides of the posterior

nares. The posterior narial canal is elongate and extends posterior to the pterygoid processes, but it does not continue into the sphenoid. A remnant of the thin vomerine septum is preserved at the posterior end of the posterior narial canal of the holotype, but it is not preserved in FMNH P12165. The posterior narial canal of FMNH P12165 is partially filled with sediment. In the holotype (CMNH 2398), the posterior narial canal is mostly cleaned of matrix. In that specimen, the anterior half of the posterior narial canal is lined with a surface of wavy bone with anteroposteriorly directed grooves. It is possible that this wavy layer of bone represents maxilloturbinates continuing into the posterior narial canal, similar to that seen in *Dolichorhinus*; however, the dorsoventral crushing of the holotype limits interpretation.

In the basicranium of the holotype skull (CMNH 2398) the mastoid process contacts the posterior wall of the postglenoid process, thus forming a tubelike external auditory pseudomeatus. Gregory (1912) and Osborn (1929a) noted this characteristic; however, the ventrally closed external auditory pseudomeatus of the holotype appears to be an artifact of distortion. In the less distorted specimen, FMNH P12165 (fig. 36a), the postglenoid and mastoid processes do not contact each other, thus leaving a ventrally open external auditory pseudomeatus. In other respects, the basicranium of *Sthenodectes incisivum* is typical of brontotheres with a widely separated foramen ovale and foramen lacerum.

Upper Dentition: The upper dentition of the holotype (CMNH 2398) and that of FMNH P12165 are essentially the same although those of the later are more complete and less worn (fig. 36). Dentally, *Sthenodectes incisivum* is most easily distinguished by its large teeth, particularly the oversized incisors and canine that rival the premolars in size. The incisor row forms a semicircular arch that is positioned anterior to the canines. The anterior teeth are positioned closely together and there are no diastemata in the entire dental battery. The crowns of the I1s converge medially and make contact at the midline. The incisors progressively increase in size laterally. The apices of I1 and I2 are worn slightly, but all three incisors appear to have been tall and essentially subcaniniform in shape. All three upper incisors display a broad lingual cingulum. The lingual heel of I1 is thick and tall, forming a large fossa in the center of the crown between the main cusp and the lingual heel. In more distal incisors the central incisor fossa is less prominent. The canine is extremely tall and pointed and it has a distinct posterolingual cingulum. The canine of CMNH 11437 is smaller than the canines of FMNH P12165 or CMNH 2398.

There is no postcanine diastema in FMNH P12165 or in CMNH 2398 although the P1s are placed somewhat medially to the canines. The lateral view of CMNH 11437 suggests a short postcanine diastema. This is partially related to the medial placement of the P1. Additionally, the canine appears to be displaced slightly in this specimen.

The P1 is poorly preserved in the holotype, but that of FMNH P12165 is intact. The P1 is a small tooth with a single cusp and a posterior heel. However, the P1 is unusual in that the crown is completely encircled by a cingulum. The same characteristic morphology is seen in CMNH 11437. The P2–P4 are essentially rectangular in outline although the lingual margin of P2 is rounded. The parastyle of P2 is directed anteriorly while the parastyles of P3 and P4 are directed slightly labially. The metacone of P2 is positioned directly posteriorly from the paracone. The metastyle of P2 arches somewhat lingually while those of P3 and P4 are nearly straight. There are distinct labial paracone ribs on the P2–P4 that become progressively smaller in more posterior premolars.

The lingual features of the P2–P4 are unusually tall, although photos of the occlusal surfaces do not clearly reveal this character. On each premolar there is a tall protocone, but hypocones are not present. On the P2 there is both a small preprotocrista as well as a short lingual crest extending posteriorly from the protocone. On the P3 these crests are less distinct and in P4 they are essentially absent. This lingual premolar morphology of the holotype differs slightly. In that specimen the lingual side of the P2 has a single ovoid loph that arches around the lingual side of the crown. On the P3 there is a similar structure, but it could best be

described as an ovoid protocone. The maxillary fragments of CMNH 9928 offer a glimpse at the unworn lingual morphology of the P3 and P4. The lingual morphology is similar to that of the other specimens, but a very short thin lingual crest can be seen extending posteriorly from the P4 protocone. This crest would be quickly obliterated by wear and could have originally been present in premolars of specimens with more dental wear. The labial cingula of P2–P4 tend to be continuous or slightly discontinuous. The lingual cingula, on the other hand, are always thick and continuous.

The molars of *Sthenodectes incisivum* exhibit numerous brontotheriine apomorphies, including tall, lingually angled ectolophs, weak labial ribs, thin lingual ectoloph enamel, and wedge-shaped lingual sides of the paracone and metacone in molars that are not heavily worn. The anterior cingulum is thin and passes proximally to the distal peak of the parastyle. *S. incisivum* molars exhibit both small anterolingual cingular peaks and shallow central fossae. There are no traces of paraconules of metalophs, nor is there a hypocone on the M3, although the posterolingual cingulum of the M3 can be very thick. The labial cingulum is distinct, but it is discontinuous around the mesostyles. Unlike the lingual premolar cingula, the lingual molar cingula are weak.

Mandible and Lower Dentition: Fortunately, one skull of *Sthenodectes incisivum* (CMNH 11437) is associated with a mandible (fig. 37a, b). That specimen reveals that the lower incisors, like the uppers incisors, are greatly enlarged. Other mandibles are referable to *S. incisivum* due to their large incisors, including YPM 16883, a partial mandible with very lightly worn lower dentition (fig. 37c–f).

The inferior margin of the symphysis is steep ($\geq 45°$). The position of the posterior margin of the symphysis fluctuates between the midpoint of the p3 and the posterior margin of p3. The lower incisors form a semicircular arch anterior to the canines. The crowns are distinctly tall and pointed with very thick lingual cingulids. The incisors are all of similar size although the i3 is shorter and more mesiodistally elongate than the other incisors. The canine is very tall with a thick lingual cingulid.

There are no diastemata throughout the entire lower dentition of YPM 16883. However, in other specimens, FMNH P12166 and CMNH 11437l, there are short postcanine diastemata. This is perhaps related to the fact that the canines of these specimens are smaller that those of YPM 16883.

The p1 is a small single-cusped tooth with a slightly elongate talonid heel. The trigonid of p2 is nearly twice as long as the talonid. The p3 trigonid is somewhat longer than the talonid, while the p4 trigonid is similar in length to the talonid. The talonid and trigonid are of similar width in p2, while in p3 and p4 the talonid is broader than the trigonid. The paralophid of p2 is incomplete, but other specimens indicate that it arches slightly lingually, resulting in a small lingual trigonid notch. The protolophid is straight but positioned lingually. The trigonid of p3 is similar to that of the p2, but the lingual notch is somewhat larger and the protolophid is more lingually directed. The paralophid and protolophid of p4 arch 90° lingually. The protolophid of p4 ends in a large metaconid, while metaconids are absent on p2 and p3. The talonid of p2 has a well-developed cristid obliqua, a short hypolophid, and a weakly developed lingual notch. The talonids of p3 and p4 are more strongly developed with longer hypolophids, longer cristids obliqua, and more molariform basins. The p1 and p2 have distinct lingual and labial cingulids. The p3 and p4 lack lingual cingulids but retain labial cingulids.

The molars are typical advanced brontothere molars with thin lingual enamel, weak lingual ribs, an elongate m3, and a widened m3 hypoconulid. The labial molar cingulid is thick but variably continuous and discontinuous around the paracone and hypocone.

Remarks

When Douglass (1909) named *Sthenodectes incisivum* he questionably referred it to the genus *Telmatherium*, although he commented that it probably was a different genus. Douglass' (1909) description of "*Telmatherium*?" *incisivum* was brief and insuffi-

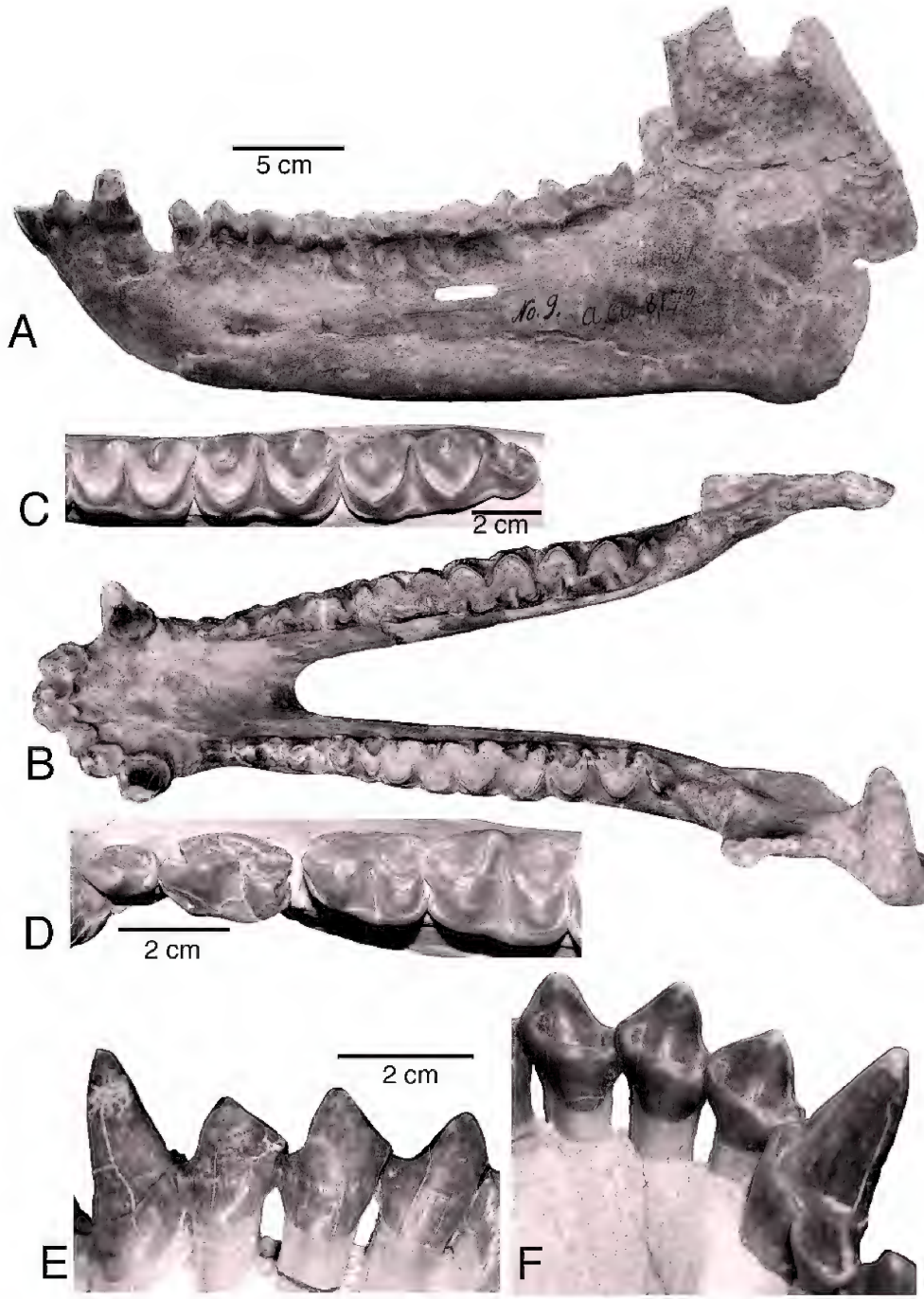

Fig. 37. Selected views of mandibles referred to *Sthenodectes incisivum*. **(A)** Left view and **(B)** dorsal view of CMNH 11437. **(C)** Left molars, **(D)** left premolars, **(E)** labial view of right incisors and canine, and **(F)** lingual view of right incisors and canine of YPM 16883. (© 2005 Peabody Museum of Natural History, Yale University, New Haven, Connecticut, USA. All rights reserved.)

cient. Gregory (1912) made a more thorough comparison of the holotype with other brontotheres and concluded that it represented a new genus, and, thus, revised the name to *S. incisivum*. Gregory (1912) distinguished *S. incisivum* from *Metatelmatherium ultimum* by (1) the enlarged incisors, (2) the absence of a postcanine diastema, (3) thickened premolar cingula, (4) the ventrally enclosed external auditory pseudomeatus, (5) tapering nasals, and a few other less significant details. Gregory's (1912) observations generally distinguished *S. incisivum* from all known brontotheres, except for character four, an error related to taphonomic distortion of the holotype skull. In the same year, Riggs (1912) referred two additional specimens to *S. incisivum*, a skull (FMNH P12165, mistakenly referred to as P 12168 by Osborn [1929a]) and a mandible (FMNH P12166).

Peterson (1934) named another species, *Sthenodectes priscus*, based on CMNH 11437. Peterson distinguished this species from *S. incisivum* based on the rounder shape and thinner cingulum of the canine, less hypsodont dentition, less developed cingula, and a short diastema. Each of these characteristics is refutable. The rounder shape of the canine and its thinner cingulum are related to the smaller size of the canine. Canine size is variable within many brontothere species and, thus, does not warrant a distinct species. Although the premolar cingula of *S. incisivum* tend to be thick in comparison to other species, the minor differences in the thickness of the lingual premolar cingulum between CMNH 11437 and CMNH 2389 are consistent with a pattern of intraspecific variability in cingula thickness seen in most brontothere species. Finally, the apparently less hypsodont dentition has to do with the fact that the teeth of CMNH 11437 are more worn than are those of CMNH 2398. Therefore, *S. priscus* is considered a junior synonym of *S. incisivum*.

Telmatherium validus Marsh 1872

LECTOTYPE: YPM 11120, a partial skull with right I3, C, P1, P3–M2 and left I1, I2, C, P1–M3.

TYPE LOCALITY: Near Henry's Fork of the Green River, Wyoming, Twin Buttes Member of the Bridger Formation (Bridger C or D).

SYNONYMS: *Telmatherium cultridens* Osborn, Scott, and Speir, 1878; *Manteoceras manteoceras* Hay, 1901; *Manteoceras washakiensis* Osborn, 1908a.

AGE: Middle Eocene (late Bridgerian land mammal "age").

REFERRED SPECIMENS: **(From the Twin Buttes Member [Bridger C–D] of the Bridger Basin, Wyoming)** AMNH 1511, a skull with right I3–M3, and left P2–M3; AMNH 1532, a palate with right P2–M3, left C (partial), and P2–M3; AMNH 1545 (associated with USNM 6700), a mandible with right p4–m3, left p4–m1, m2 (partial), and m3; AMNH 1560, a mandible with right i3–c, p3, p4, m2, m3 (partial), left i2, c, and p2–m3; AMNH 1563, a mandible with right p2–m3 and left p3–m3; AMNH 1566, a mandible with right i1–m3 and left i3–m3; AMNH 1569 (holotype of *Manteoceras manteoceras*), a skull with no complete teeth; AMNH 1587, a crushed skull with right M1–M3 and left P1–M3, and a right mandibular ramus with p4 (partial) and m1–m3; AMNH 12193, a mandible with right m2, left c, and p4–m3; AMNH 12194, a left maxilla with P4–M3; AMNH 12204, a crushed skull with right P4–M3, left P3–M3, and a crushed mandible with right c, p3, p4, left c, p4, and m1–m3; AMNH 12210, a mandible with p4–m3; AMNH 12214, a right M3; AMNH 12678, a skull with right I1–P4, M2, M3, left I2–C (partial), P1–M1 (severely damaged), M2, and M3; AMNH 12687, a right mandibular ramus with p2–m3; AMNH 12681, a mandible with left p3 (partial), and p4–m3; AMNH 12683, an anterior portion of a skull (in two pieces) with right C–M1, M2–M3 (all partial), and left I1–M3; UCM 69355, a mandible with right and left i1–13, c (erupting), and p1–m2; UCM 73736, a crushed skull fragment with left P1–P3; UCMP 31344, a right mandibular ramus with p3–m3; USNM 6700 (associated with AMNH 1545), a crushed skull with right P1–M3, left C, P2–M3; USNM 12836, a mandible with right p3–m3, left p4–m3, and an isolated canine; USNM 13455, a partial mandible with right p3–m3, left p2, and p4–m3; USNM 13456, a partial skull with right and left maxillae with C–M3; USNM 26113, a

right maxilla with P4–M3; USNM 26114, a left maxilla fragment with M1–M3; USNM 26119, a crushed skull with right P2–M3, left C, and P2–M3; USNM 26121, a right mandibular ramus with i2–m3; USNM 26140, a skull with right P3 (partial), P4–M1, and left P3–M1; USNM 26162, a partial skull with right and left P2–M3, and a mandible with right p2–m3; USNM 26302, a mandible with right p4–m3 and left i2–m3; YPM 16415, a left maxilla fragment with M1, M2, and M3 (partial); YPM 16729, a partial skull (in two pieces) with left C, and P2–M3; YPM PU10027 (holotype of *Telmatherium cultridens*), a right maxilla with I1–M3 and a left mandible fragment with p2–m3; YPM PU10361, a mandible with m1–m3; **(from the lower Adobe Town Member [Washakie A of Granger, 1909] of the Washakie Formation of Wyoming)** AMNH 1570, an anterior portion of a skull with right and left P1–M3; AMNH 2353, a skull with right P2, M1–M3, and left P1–M3; AMNH 2354, a skull fragment with right P1, M2–M3, and left P2–M3; AMNH 2356, a right mandibular ramus with dp3, dp4, m1, and m2; AMNH 13165 (holotype of *Manteoceras washakiensis*), a partial skull with right M2, M3, and left C–M3; AMNH 13176, a crushed mandible with left p1–m3; FMNH PM2328, a mandible with right i3–m3 and left p1–m3; FMNH PM55576, a partial mandible with right i1–m2, and left i1–p4; YPM PU16103, a mandible with right p1–m3 and left c–m3; **(from the Aycross Formation, Absaroka Range, Wyoming)** AMNH 105429, associated upper dentition including right P2–M3 and left P2–M2; (no locality data) YPM 47288, associated dentition with right and left P2–M3; YPM PU25022, a palate with right P2–M3 and left P1, P2, P4–M3.

DIAGNOSIS: *Telmatherium validus* is an intermediate-sized hornless brontothere. The frontal bone intrudes into the surface of the nasal bone splitting off a small lateral nasal splint from the main body of the nasal. The nasal splint is larger, more strongly arched, and more distinct than those of *Wickia brevirhinus* or *Metatelmatherium ultimum*. The nasal incision extends to the P2. The nasal process is horizontal, unelevated, of relatively constant transverse width, narrow, with thin and relatively deep lateral walls, and without a well-defined or strongly rounded distal margin. The orbits are positioned above the M2 and do not project laterally. The premaxillomaxillary rostral cavity is not enclosed by bone dorsally. Other cranial characteristics include a dorsal cranial surface that is either flat or strongly elevated and convex posteriorly, strongly convergent parasagittal ridges that are separated posteriorly by a narrow pit, strongly curved and moderately bowed zygomatic arches, and a ventrally open and mediolaterally angled external auditory pseudomeatus. Ventral sphenoidal fossae are absent.

Telmatherium validus has large subcaniniform upper incisors, a postcanine diastema, a simple P1, a distinct P2 metacone, weak premolar preprotocristae, and short lingual crests occasionally extending posteriorly from the premolar protocones. Premolar hypocones are absent. The molars of *T. validus* have tall, lingually angled ectolophs with weak labial ribs, and thinned lingual ectoloph enamel with wedge-shaped paracones and metacones. Central molar fossae, a cingular parastyle shelf, and well-developed anterolingual cingular cusps are absent. Metalophs are absent, but vestigial paraconules are occasionally present. The lower dentition of *T. validus* includes large subcaniniform incisors that are all of similar size, a p1–p2 diastema (variably present), a postcanine diastema, an elongate p2 trigonid, a metaconid on p4 but not on p2 or p3, shallow molar basins, and a slender m3.

Telmatherium validus is most similar to *Metatelmatherium ultimum* and *Wickia brevirhinus*. It differs from *Metatelmatherium ultimum* in the more posteriorly extended nasal incision, thicker parasagittal ridges, broader forehead, and by lacking a ventral zygomatic flange. *Telmatherium validus* is distinct from *Wickia brevirhinus* in the more posteriorly extended nasal incision and the less robust premaxillae.

DESCRIPTION

SKULL: Although numerous skulls of *Telmatherium validus* are known, no single specimen allows for a complete description of the entire skull. The following description of the skull of the *T. validus* is based primarily

on the lectotype YPM 11120 (fig. 38), AMNH 12678 (fig. 39), AMNH 1511 (fig. 40), USNM 26140 (fig. 41), AMNH 13165 (fig. 42), and AMNH 1570 (fig. 43), but additional information from other specimens is provided. *T. validus* is an intermediate-sized (table 7) hornless brontothere whose skull is most similar to *Wickia brevirhinus* and, to a lesser extent, *Metatelmatherium ultimum*. The frontonasal suture is plainly visible on AMNH 12678, USNM 26140, and most other skulls. The frontal bone forms a pair of short triangular processes just above and anterior to the orbits. On the surface this frontal process appears to protrude into the posterolateral portion of the nasal bone. However, in specimens where the frontal and nasal bones have become detached (e.g., YPM PU10027) it can be seen that the frontal process actually onlaps the nasal bone and sits within a grooved triangular depression in the nasal bone. On the surface, the frontal splits the posterolateral corner of the nasal bone, forming a lateral nasal splint that separates off from the main body of the nasal bone. The nasal splint is strongly arched and broadly contacts the maxillary. The nasomaxillary suture forms a tall arch. The overlapping triangular frontal process and lateral nasal splint of *T. validus* is shared with many other brontotheres including *Metarhinus*, *Sthenodectes*, *Qufutitan*, *Wickia*, *Metatelmatherium*, as well as those brontotheres with frontonasal protuberances (horns). Among hornless brontotheres that are characterized by this particular frontonasal configuration, with the possible exception of *Qufutitan*, the lateral nasal splint appears to be longer, wider, and more distinctly curved in *T. validus*, and its contact with the frontal and maxilla is more distinct on the surface of the skull.

Telmatherium validus has been described as having a rudimentary horn or frontonasal swelling (Osborn 1895, 1929a; Mader, 1989, 1998). Figures of *T. validus*, particularly those published by Osborn (e.g., fig. 7 in Osborn, 1895) greatly exaggerate the relief of the overlapping portions of the frontal and nasal bone. I can find no distinct frontonasal protuberances on any of the specimens. The overlapping triangular frontal process is flush with the surface of the nasal bone. However, some specimens present an illusion of small frontonasal protuberances from a lateral viewpoint. For instance, in AMNH 12678 the region above the preorbital concavity appears to be raised. This effect in AMNH 12678 is partly an illusion related to a large crack running transversely across the dorsal surface of the skull. The skull roof above the orbits has been forced downward. Additionally, the shallow preorbital fossa in the maxilla gives the region above it a prominent appearance. However, the triangular frontal process is flush with the dorsal surface of the skull. An actual frontonasal protuberance is not present in USNM 26140, where the facial area is undistorted.

The overlapping frontal and nasal bones of *Telmatherium validus* have long been thought of as the morphological precursor of the frontonasal horns seen in other brontotheres, thus suggesting that *Telmatherium* is the ancestor or sister taxon of horned brontotheres (Osborn, 1929a; Mader, 1989, 1998). It is, no doubt, very likely that the configuration of facial bones of *T. validus* does represent the ancestral state of brontothere horns, but that does not suggest any particularly close relationship of *T. validus* with horned brontotheres because the same facial configuration exists among numerous hornless brontotheres.

The nasal incision of *Telmatherium validus* is longer than those of *Wickia brevirhinus* and *Metatelmatherium ultimum*. In AMNH 12678, the nasal incision extends approximately to the protocone of the P2. In all specimens of *T. validus* the nasal incision extends posteriorly past the anterior margin of the P2. The longest nasal incision seen in a skull of *T. validus* is found in AMNH 1511, where the nasal incision extends to the posterior margin of P2. The orbits do not protrude laterally as in *Metarhinus*. The orbit of AMNH 12678 is positioned directly over the M2 and over the alveolus of the M1. The anterior rim of the orbit is positioned directly above the alveolus of the anterior lateral root of the M1. However, the position of the orbit varies slightly from individual to individual, and in specimens with less extremely worn dentition (e.g., AMNH 1511), the posterior lateral root of the M1 is positioned below the orbit.

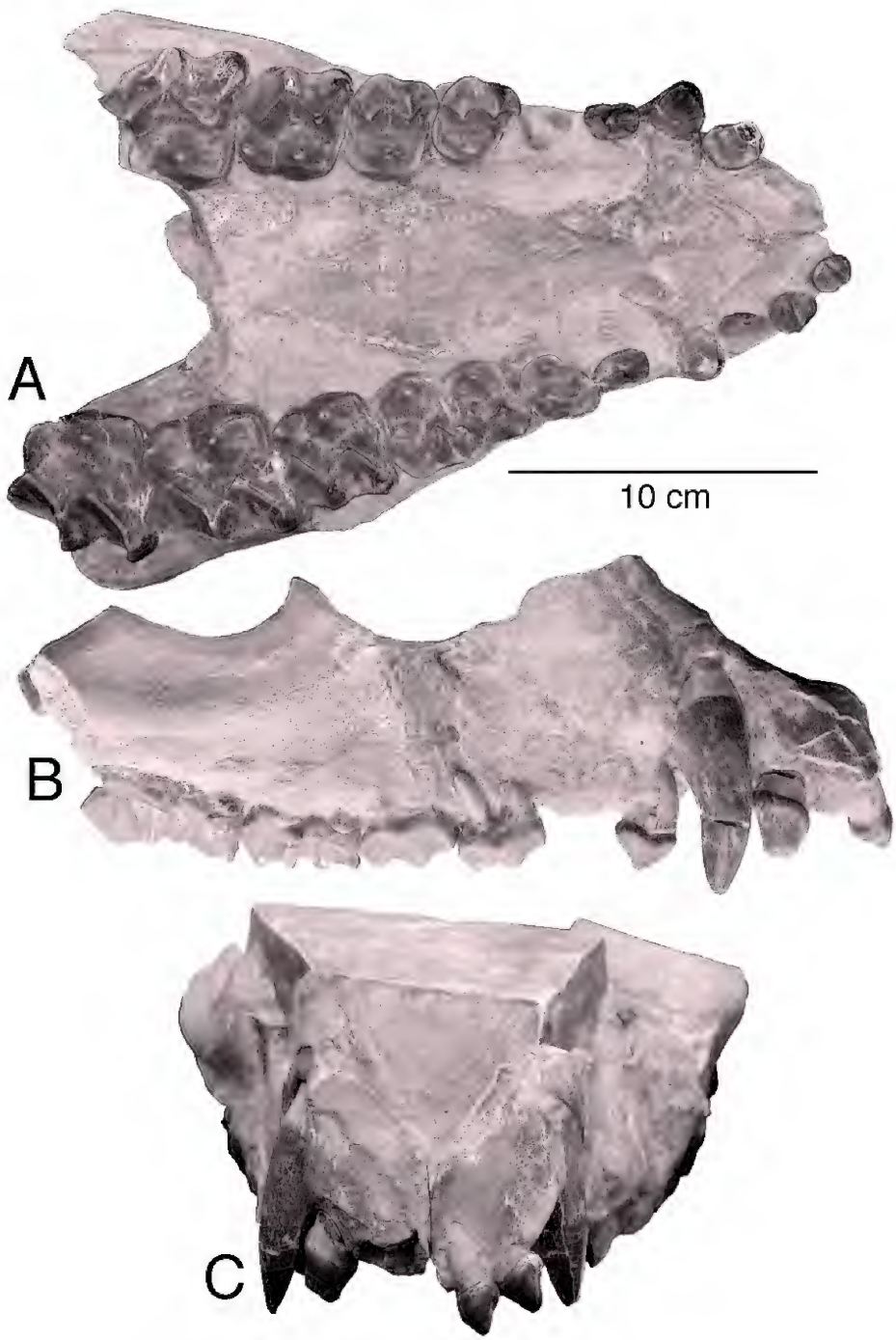

Fig. 38. Lectotype of *Telmatherium validus* (YPM 11120). **(A)** Ventral view, **(B)** right view, **(C)** anterior view. (© 2005 Peabody Museum of Natural History, Yale University, New Haven, Connecticut, USA. All rights reserved.)

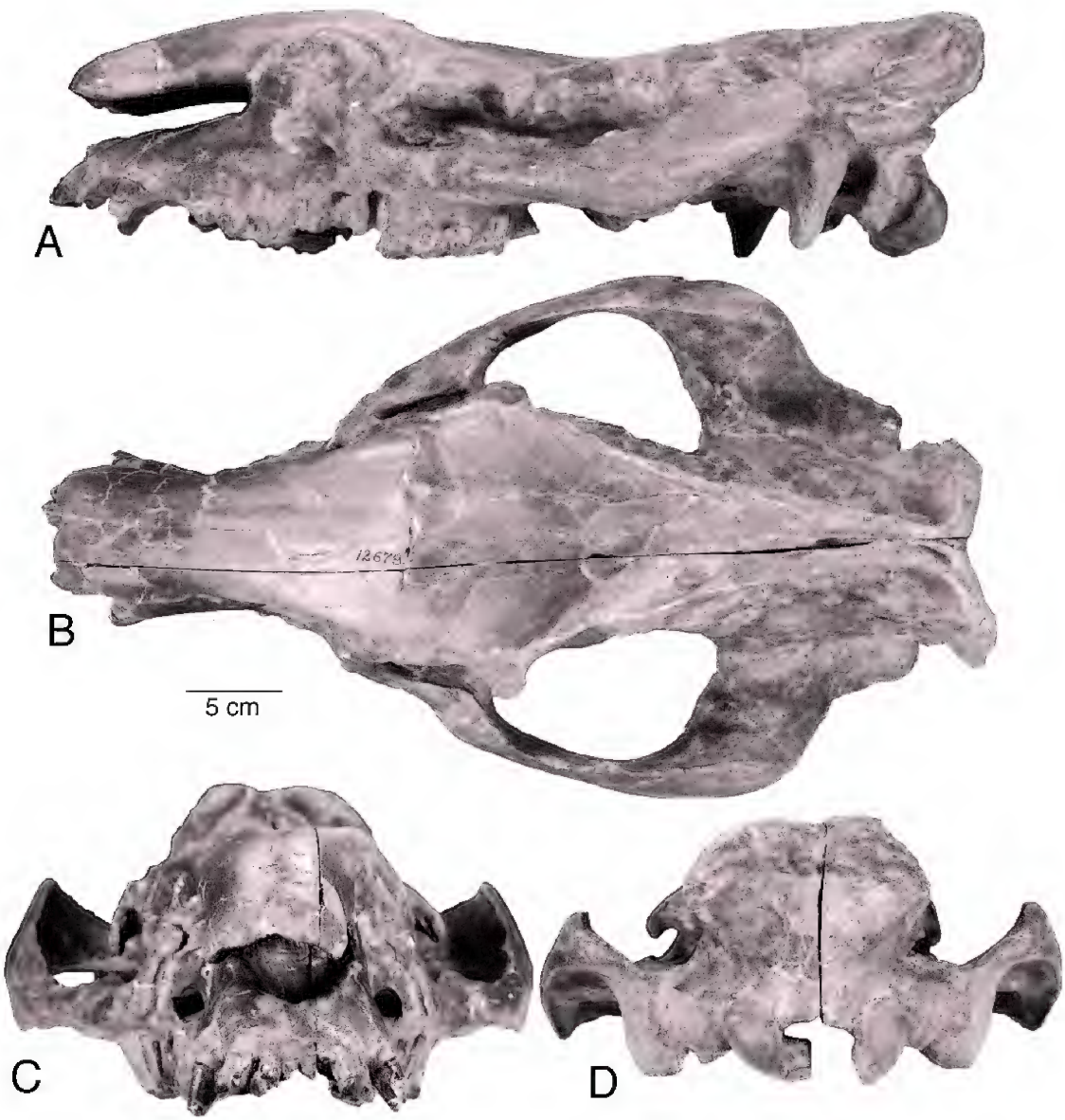

Fig. 39. A skull (AMNH 12678) of *Telmatherium validus*. **(A)** Left view, **(B)** dorsal view, **(C)** anterior view, **(D)** posterior view.

The nasal bones tend to be poorly fused together. The nasal process is shorter than the premaxillomaxillary rostrum. In AMNH 12678, the nasal process is angled slightly downward, although the downward angle is somewhat exaggerated. In specimens with less dorsoventral crushing, such as USNM 26140, the nasal process is more horizontal, but its dorsal surface is slightly convex from its lateral profile. The lateral walls of the nasal process are vertical and dorsoventrally deep. The sides of the nasal process form deep and essentially vertical lateral walls that are of relatively constant depth throughout the length of the nasal process. The distal edge of the nasal process is thin, rough, and deflected downward (fig. 39c). From the dorsal view, the nasal process is narrower than the premaxillomaxillary rostrum, and is more or less constant in width throughout its

Fig. 40. Right view of a skull (AMNH 1511) of *Telmatherium validus*.

length, although it is sometimes slightly constricted proximally (e.g., USNM 26140).

From a lateral view the posterodorsal slope of the dorsal margin of the premaxillomaxillary rostrum is relatively shallow. The premaxillomaxillary sutures of the lectotype YPM 11120 and many other specimens (e.g., AMNH 12678, AMNH 1569, AMNH 1570, USNM 26140) are plainly visible. The premaxilla truncates before reaching the posterior notch of the nasal incision. Thus, the premaxilla does not contact the nasal bone. The premaxillae are generally thick and well developed although they tend not to be as robust as those of *Wickia brevirhinus*. In AMNH 12678 the premaxillae are strongly fused at the symphysis. However, in other specimens, including the lectotype (YPM 11120), the premaxillae are not strongly fused. The degree of ossification of the symphysis seems to covary inversely with the size of the canines and the corresponding robustness of the maxillae. In AMNH 12678, the canines are relatively small, the maxillaries are comparatively slender and narrow, and the premaxillae are fully coossified. In contrast, the canines of YPM 11120 and AMNH 1570 are much larger in diameter, the maxillaries are more robust, and the premaxillary symphysis is not strongly coossified. Posterior to the premaxillary symphysis, the nasal processes of the premaxillae diverge laterally. The premaxillomaxillary rostral cavity is not dorsally enclosed by bone.

Fig. 41. Anterolateral view of the left side of the face of *Telmatherium validus* (USNM 26140).

In comparison to *Wickia brevirhinus* and *Metatelmatherium ultimum*, the dorsal roof of the skull of *Telmatherium validus* is wider and less transversely arched. From a lateral profile, the dorsal surface of the skull above the orbits is slightly concave or it can be flat. Behind the orbits the dorsal surface is flat in AMNH 12678. In some specimens (e.g., AMNH 1511), the postorbital portion of the dorsal cranial surface is strongly convex with an elevated posterior end. The dorsal cranial profile of AMNH 1511 bears a strong resemblance to *Palaeosyops*, with a steep slope between the elevated posterior portion and the lowered midcranial frontal area.

The parasagittal ridges of *Telmatherium validus* tend to be prominent, although there is variation in the thickness of the parasag-

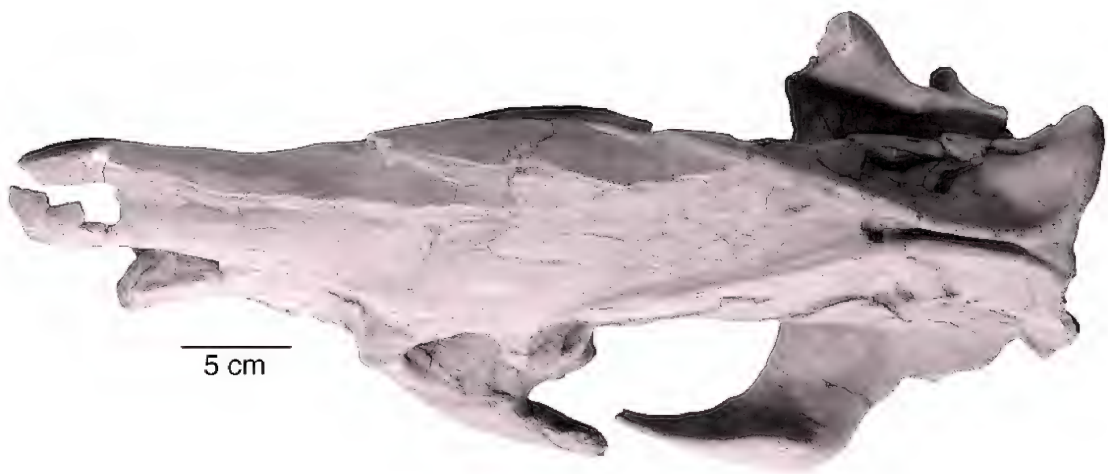

Fig. 42. The dorsal view of a skull of *Telmatherium validus* (AMNH 13165) showing intact parasagittal ridges.

ittal ridges. For instance, AMNH 12678 and AMNH 13165 are among the more gracile specimens. One of the most robust specimens is AMNH 1569 (not shown) with extremely thickened parasagittal ridges. The parasagittal ridges of all *T. validus* specimens strongly constrict the dorsal surface posteriorly, but they never completely join to form a sagittal crest. Instead, they remain separated by several millimeters and a deep narrow pit is formed in the midline of the dorsal surface between the medially constricted parasagittal ridges.

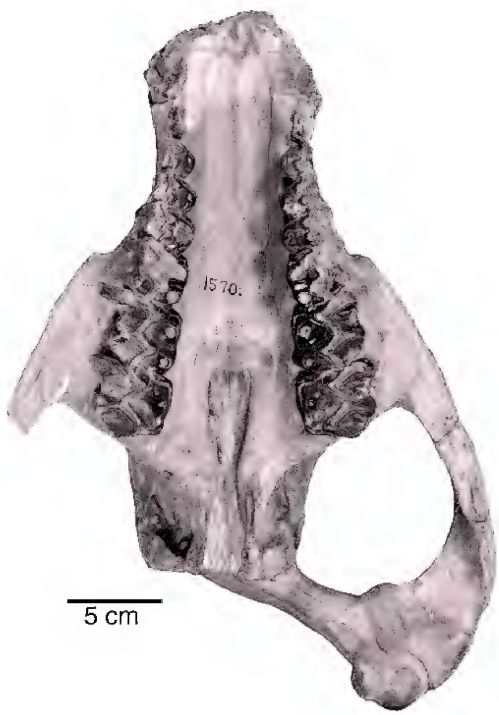

Fig. 43. Ventral view of a skull of *Telmatherium validus* (AMNH 1570).

The depth and thickness of the zygomatic arches of *Telmatherium validus* are variable. Those of AMNH 12678 are among the more gracile. From a lateral view, the jugal portion of the zygomatic arch is essentially horizontal, while the squamosal portion rises posteriorly, giving the zygomatic arch a distinct curvature. The zygomatic arches are moderately bowed laterally. *Telmatherium validus* lacks a prominent ventral flange on the jugal below the contact with the squamosal as seen in *Metatelmatherium*. Likewise, there is no infraorbital jugal process as seen in *Sphenocoelus*.

The nuchal crest is of moderate thickness, and from the dorsal view of the skull of AMNH 12678 it is concave. From a lateral view the occiput of *T. validus* is moderately tilted backward. From the posterior view, the nuchal crest is dorsally arched; the upper portion of the occiput is narrower than the posterior portion and the occiput is constricted in the middle. The occipital pillars are distinct but not massive and the central depression of the occiput is shallow.

TABLE 7
Summary statistics for selected morphometric variables of *Telmatherium validus*
See Methods for measurement definitions

	N	Mean	SD	Min.	Max.	CV
C L	9	26.8	3.2	22.5	31.3	12.1
P3 L	20	21.7	1.5	19.4	24.1	6.7
P3 W	18	24.3	2.4	17.3	27.4	9.8
M2 L	23	43.8	3.0	38.3	50.8	6.8
M2 W	16	42.4	2.9	38.6	47.5	6.8
P2–P4	18	65.2	6.2	56.4	83.4	9.5
M1–M3	19	114.1	7.7	103.8	127.5	6.7
VL	5	484	21.6	460	515	4.5
c L	10	23.4	2.5	18.3	26.6	10.5
p3 L	19	21.4	1.4	19.0	23.91	6.8
p3 W	19	14.0	1.2	10.6	16.1	8.7
m2 L	25	38.2	2.6	32.0	44.4	6.8
m2 W	23	23.8	2.2	20.4	29.1	9.5
p2–p4	9	67.2	4.7	59.0	73.8	6.9
m1–m3	15	121.9	5.7	110.0	132.4	4.7

The palate and posterior nares of *Telmatherium validus* are best preserved in AMNH 1570. The posterior nares are rimmed anteriorly and laterally by a horseshoe-shaped emargination. The anterior edge of the posterior nares is positioned about at the posterior margin of the M2, although in other specimens the position of the posterior nares fluctuates from between the M2 hypocones to slightly behind the anterior margin of M3. In AMNH 1570 two thin unbroken choanal pouches (maxilloturbinates) protrude beyond the anterior rim of the posterior nares. These choanal pouches are similar in position to those of *Metarhinus abbotti*, and they are not as posteriorly shifted as those of *Dolichorhinus*. There are clear remnants of bony choanal pouches in others specimens of *T. validus* as well (e.g., AMNH, 12678, AMNH 1569; UCMP 6700).

The posterior narial canal is elongate, but it does not extend significantly into the basisphenoid. As in other brontotheres, a thin vomerine septum bisects the posterior narial canal, although it is usually obscured by sediment filling the posterior narial canal, or it was destroyed when the sediment filling the posterior narial canal was removed. Although there are no large ventral sphenoidal fossae in *Telmatherium validus*, in at least one specimen (USNM 6700), the posterior narial canal extends slightly into the sphenoid, and the anterior end of the sphenoid body narrows anteriorly and forms part of the part of the partitioning septum, along with the vomer. The basicranial foramina of *T. validus* are typical of brontotheres, with a widely separated foramen ovale and foramen lacerum. The mastoid process does not contact the postglenoid process and the external auditory pseudomeatus is, therefore, unconstricted ventrally.

Upper Dentition: The description of the upper dentition of *Telmatherium validus* is primarily based on the lectotype (YPM 11120) (figs. 38, 44), but other specimens are noted to document variation. The lectotype includes a complete set of lightly worn upper teeth indicating an unreduced dental formula (3-1-4-3). The incisors are large and increase in size laterally. The crowns of I1 and I2 are short, round in outline, pointed at the apex, and slightly lingually curved. Each incisor is bordered lingually by a distinct cingulum. The I3 crown is taller but otherwise similar to I1 and I2. The incisor row strongly arches anterior to the canines and it is separated from the canines by a short precanine diastema.

The lectotype canine is large and tall with two distinct ridges that extend down the sides of the crown. The canines of *Telmatherium validus* are variable in size, but they could never be characterized as being very small.

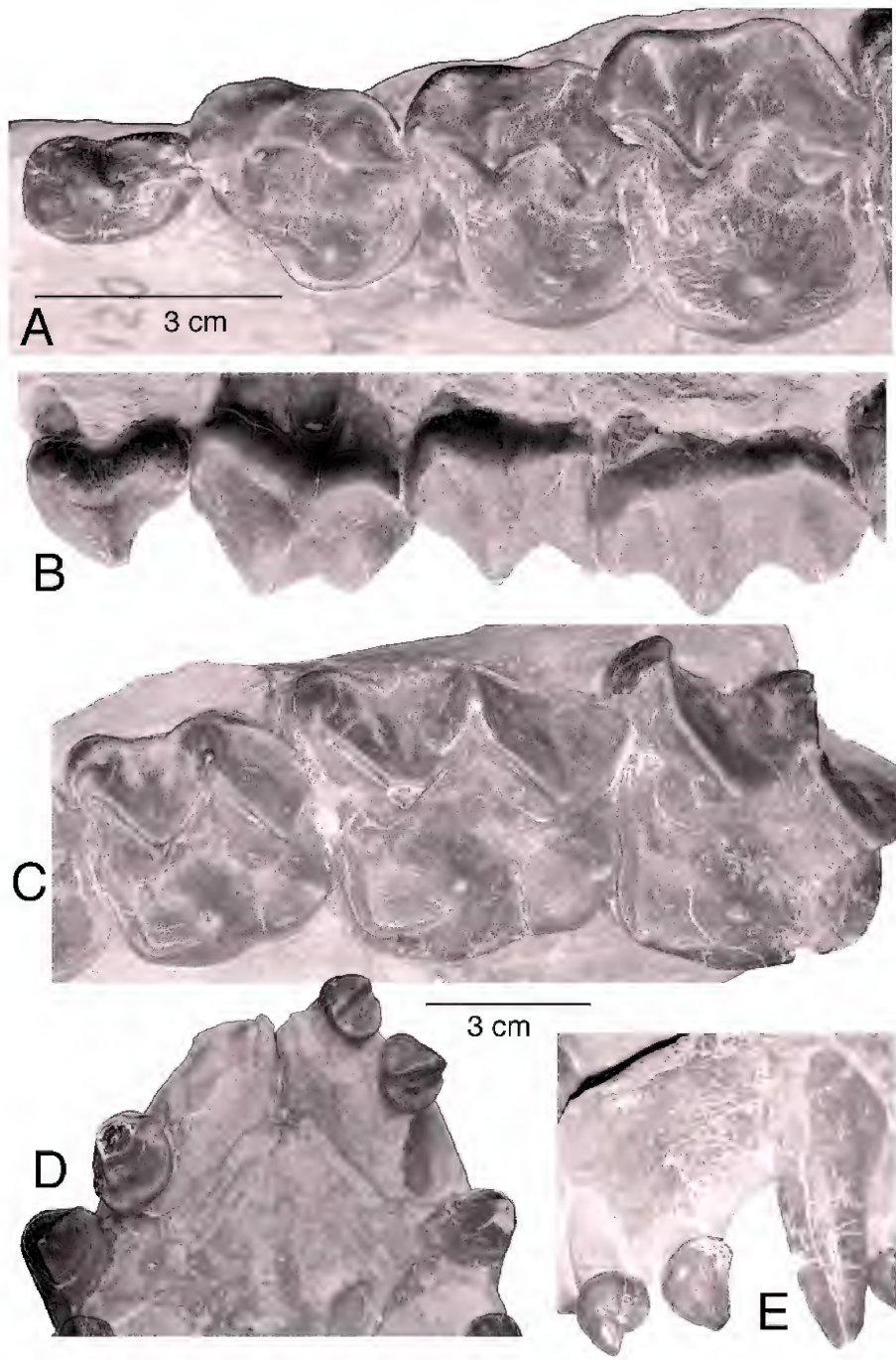

Fig. 44. The lectotype of *Telmatherium validus* (YPM 11120) **(A)** Occlusal view of left premolars, **(B)** lateral view of left premolars, **(C)** occlusal view of left molars, **(D)** occlusal view of incisors and canine, **(E)**, labial view of left I2, I3, C. (© 2005 Peabody Museum of Natural History, Yale University, New Haven, Connecticut, USA. All rights reserved.)

The length of the postcanine diastema is very short in YMP 11120, but in other specimens it can be slightly longer than the P2.

The P1 is small and simple with a single cusp, a posterior heel, and a thin but distinct lingual cingulum. A very short P1–P2 diastema is not seen in the lectotype. In the remaining skulls a P1–P2 diastema is most often absent, but it is occasionally present (e.g., AMNH 1569). The anterior margin of the P2 of YPM 11120 is steeply angled posterolingually. There is a marked discontinuity in shape from the rather oblique P2 crown to the more rectangular crowns of P3 and P4.

The parastyle of P2 arches slightly lingually, while the parastyle of P3 is nearly straight, and the P4 parastyle is angled labially. The P2 metastyle is slightly angled lingually, while those of P3 and P4 are more or less straight. The labial ribs of the paracones are prominent, although they follow the typical pattern of becoming narrower in progressively posterior premolars.

The lingual heel of the P2 is small and posteriorly shifted. A small protocone is seen on the lingual shelf. In the lectotype the small preprotocrista is angled anteriorly and forms part of the anterior cingulum. The lingual heels of P3 and P4 are much wider so that the anterior and posterior sides of the crowns are nearly parallel and the protocones are more centrally positioned between the paracone and metacone. Tiny paraconules can be seen on the P3 and P4 of the lectotype, although they are most often absent in other specimens. More typically, a very low preprotocrista connects the protocone to the lingual side of the ectoloph of P3 and P4 (e.g., YPM PU10027, AMNH 13165).

The premolars (P2–P4) of the lectotype lack distinct lingual crests; however, on other specimens, such as YPM PU10027, there is a minor lingual crest on P3 and a barely discernable lingual crest on P4. Occasionally, P2 lacks a distinct protocone; instead, a tall crest of enamel arches around the lingual side of the crown (e.g., YPM 47288). In one specimen (YPM PU10027) P2 has a small hypocone; however, a hypocone does not occur on the premolars of any other specimen of *Telmatherium validus*.

The labial cingula of the P2–P4 are thin and incomplete. In the lectotype the lingual cingulum of P2 is continuous around the base of the protocone. The anterior and posterior cingula of the P3 and P4 arch around the lingual side of the crown, but they are not connected lingually. However, in other specimens continuous cingula wrap around the anterior, lingual, and posterior sides of the crowns of P3 and P4.

The molars of *Telmatherium validus* exhibit the derived characteristics typical of brontotheriines including tall, lingually angled ectolophs, thin labial ribs, thin lingual ectoloph enamel, and wedge-shaped lingual sides of the paracone and metacone. The anterior cingulum is thin and passes proximally to the distal peak of the parastyle. *T. validus* molars lack an anterolingual cingula cusp or central molar fossae. All traces of a metaloph are lost, although each of the molars of the lectotype retains a tiny paraconule. In other specimens tiny paraconules are variably present. In YPM PU10027, for instance, a paraconule is present on the M1, but this feature is not detectible in the M2. Other specimens lack distinct paraconules, but they have a very low preprotocrista-like crest at the lingual base of the paracone (e.g., AMNH 2353). Yet others show no evidence of paraconules or preprotocristae (e.g., AMNH 12194), but this is the least frequent condition. None of the specimens of *T. validus* has an M3 hypocone, although the posterolingual cingulum of the M3 is rather thick and raised in the lectotype. The labial cingula of the molars tend to be thin and discontinuous around the mesostyles. The anterior cingulum of each molar terminates at the lingual base of the protocone and does not continue around the lingual side of the crown.

Mandible and Lower Dentition: A number of *Telmatherium validus* skulls are associated with mandibles: AMNH 1587, AMNH 2353, AMNH 12204, and YPM PU10027. There are additional mandibles without associated skulls from the upper Bridger C–D and the lower Washakie formations whose molars are far too slender for *Palaeosyops*, fall well above the upper size range of *Mesatirhinus junius*, and are within the size range of *T. validus*. The most complete mandibles that are referred to *T. validus* are AMNH 1560, AMNH 1566

(fig. 45b, d), FMNH PM2328 (fig. 45a), FMNH PM55576 (fig. 45c), and USNM 26121. The general shape of these mandibles does not differ notably from the contemporaneous taxon, *M. junius*. The inferior margin of the symphysis is typically steep ($\geq 45°$). The symphysis extends to a point between the talonid of the p2 (e.g., AMNH 1560) and the trigonid of the p3 (e.g., AMNH 1566).

The lower dentition of *T. validus* is not differentiated from the contemporaneous species, *M. junius* in any way other than size. FMNH PM55576 includes a complete set of lower incisors. The incisors are large, positioned closely together, and form a row that arches anterior to the canines. The apex of i1 is worn off. The apex of i2 is lightly worn but the crown is still rather pointed. Finally, the i3 is essentially unworn and has a pointed apex. All of the incisors are roughly of the same size; however the i3 is more mesiodistally elongate than the other incisors. Each incisor has a thin but distinct lingual cingulid. A precanine diastema is generally absent. The postcanine diastema is generally about the same length as p2 or slightly shorter. The p1–p2 diastema is typically very short (e.g., AMNH 1566) or absent (e.g., FMNH PM2328); however one mandible (AMNH 1563) has a p1–p2 diastema that exceeds the anteroposterior length of the p2.

The p1 is a small and simple tooth with a single cusp and a short talonid heel. (Note that the posterior end of the p1 is broken in AMNH 1566 [fig. 45d]). The p2 trigonid is nearly twice the length of the talonid. The p3 trigonid is also longer than the talonid, while the p4 trigonid is slightly shorter than the talonid. The p2 trigonid and talonid are of similar width. The p3 trigonid is about the same width as the talonid or slightly narrower. The p4 talonid is slightly wider than the trigonid. The paralophids of p2 and p3 are slightly angled lingually, creating a very small lingual notch in the trigonids. The protolophids of the p2 and p3 are essentially straight. However, in comparison to that of p2, the p3 protolophid is positioned more lingually with respect to the protoconid. Both p2 and p3 lack metaconids. The trigonid of p4 is significantly more molariform. The paralophid arches fully lingually. The p4 protolophid arches 90° lingually and is connected to a large, lingually positioned metaconid. The lingual orientation of the p4 paralophid and protolophid results in a very broad lingual trigonid notch. The talonid of the p2 is narrow with a weakly developed cristid obliqua and a very short hypolophid. The lingual side of the p2 trigonid forms a slightly concave sloped surface. The p3 and p4 have more developed cristids obliqua and longer hypolophids. The lingual-talonid notches of p3 and p4 are broader than that of p2, although they do not quite form molariform basins. Lingual premolar cingulids are absent, while the labial premolar cingulids tend to be either weak or absent.

The lower molars of *Telmatherium validus* are typical with relatively thin enamel, shallow talonid and trigonid basins, and an elongate m3. Labial molar cingulids are generally weak while lingual molar cingulids are absent.

Remarks

The taxonomic history of *Telmatherium validus* and its various synonyms is remarkably convoluted. Marsh (1872) named *T. validus* from "the greater portion of a skull with teeth, and portions of several other skeletons" that were collected by the Yale expedition of 1871 to the Green River Basin. Later, Marsh (1880) amended the genus name to *Telmatotherium* and this spelling was adopted by numerous authors (e.g., Earle, 1892; Hatcher, 1895; Osborn, 1895), although Osborn (1929a) eventually reverted to the original spelling, *Telmatherium*.

Marsh (1872) did not specify which of the specimens was to be the holotype of *Telmatherium validus*, although his description depended heavily on a partial skull. Osborn (1929a) considered the holotype to be YPM 11120. No other specimen in the Yale Peabody Museum matches the description and measurements provided by Marsh (1872). Therefore, Osborn's assignment of YPM 11120 as the holotype specimen is undoubtedly accurate. However, the specimen is a lectotype because "portions of several other skeletons" were initially reported along with YPM 11120.

Osborn et al. (1878) named *Leurocephalus cultridens* from a partial skull and mandible

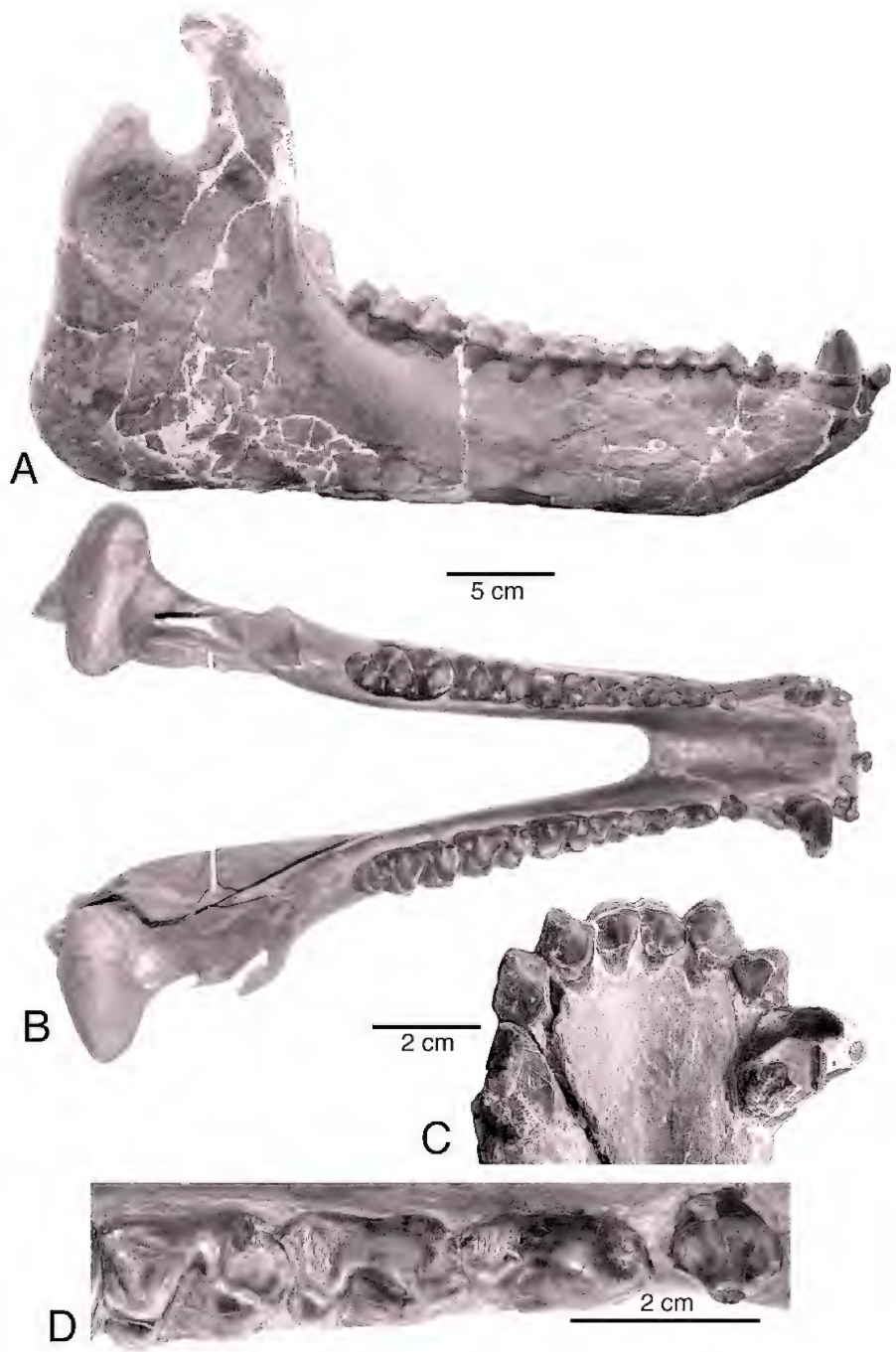

Fig. 45. Selected views of mandibles referred to *Telmatherium validus*. **(A)** Right view of FMNH PM2328, **(B)** dorsal view of AMNH 1566, **(C)** lingual view of incisors and canine of FMNH PM55576, **(D)** right premolars of AMNH 1566.

from the Bridger Basin. No number was given to the specimen, but their figure of *L. cultridens* clearly matches YPM PU10027. Earle (1891, 1892) subsequently reassigned this species to the genus *Telmatherium*, but he continued to recognize it is as distinct from the type species, *T. validus*.

Eventually, Earle (1892) and Osborn (1895) began to use the genus *Telmatherium* as a dumping ground for middle Eocene brontotheres. Several species that eventually were assigned to other genera (e.g., *Metatelmatherium*, *Dolichorhinus*, *Mesatirhinus*) were grouped into *Telmatherium* at one time or another. Among these was *Palaeosyops vallidens* Cope (1872), a taxon that was reassigned to *Telmatherium* by Osborn (1895). *Telmatherium vallidens* (Cope) (not to be confused with *Telmatherium validus* Marsh) is represented by a partial mandible (AMNH 5098, a lectotype assigned by Osborn [1929a]). This species is presently considered a nomen dubium. However, in 1895, Osborn considered *Telmatherium vallidens* (Cope) to be valid and went so far as to conjecturally refer two additional skulls to this species (AMNH 1569 and AMNH 1570).

Osborn's (1895) referral of these two skulls to *Telmatherium vallidens* (Cope) was a grave mistake because it initiated a string of taxonomic blunders that was continued by Hatcher, Osborn, Matthew, and Hay, thus generating a confusing series of invalid taxonomic revisions related to these two skulls. Going on a recommendation made by J. L. Wortman, Hatcher (1895) reassigned *T. vallidens* (Cope) to a new genus, *Manteoceras*; however, Hatcher's diagnosis of *Manteoceras vallidens* (Cope) does not actually refer to the lectotype jaw (AMNH 5098). Instead, Hatcher's (1895) diagnosis is exclusively made up of cranial characters, and his description and figure (Hatcher, 1895: pl. 39: fig. 2) of *Manteoceras vallidens* were clearly based on the skulls (AMNH 1569 and AMNH 1570) that Osborn had conjecturally referred to that species.

Another species was reported by Matthew (1899), *Palaeosyops manteoceras* Osborn ex ms., although no holotype was reported. Hay (1901) designated a holotype for this species, AMNH 1569, one of the skulls that had been conjecturally referred to *Manteoceras vallidens* by Osborn (1895). Hay (1901) also reassigned *Palaeosyops manteoceras* to Hatcher's genus *Manteoceras*. A third species, *Manteoceras washakiensis*, was eventually named by Osborn (Osborn, 1908a) with yet another skull (AMNH 13165).

Ultimately, in contrast to his opinion of 1895, Osborn (1929a) concluded that the skulls he had referred to *Manteoceras vallidens* (Cope) (AMNH 1569 and AMNH 1570) did not really belong to that species. He removed those specimens from *M. vallidens* (Cope), reassigned it to the genus *Dolichorhinus*, and redefined *Dolichorhinus vallidens* (Cope) based only on the lectotype jaw (AMNH 5098).

At that point, it would have been more reasonable of Osborn to consider *Manteoceras* the senior synonym of *Dolichorhinus*. However, because Hatcher's (1895) earlier diagnosis of *Manteoceras* was based entirely on skulls (AMNH 1569 and AMNH 1570) rather than the lectotype jaw (AMNH 5098) of *Manteoceras vallidens* (Cope), Osborn (1929a) rationalized that *Manteoceras* should continue to be applied to the species to which these skulls were now thought to have belonged, that is, *Manteoceras manteoceras* Hay.

Regardless of how *Manteoceras* was ultimately used by Osborn (1929a), that genus name is invalid because Hatcher's (1895) original diagnosis of *Manteoceras* is based on an invalid species concept, *Manteoceras vallidens* sensu Osborn (1895) (i.e., it was based on two skulls that were incorrectly referred to the type species of *Manteoceras*). Despite the confusing series of taxonomic errors associated with these skulls, it was never recognized by any of the involved authors that AMNH 1569 and AMNH 1570 actually belong to *Telmatherium validus* Marsh (1872).

Three previously named species can be considered junior synonyms of *Telmatherium validus* Marsh. These include *Telmatherium (Leurocephalus) cultridens* (Osborn et al., 1878), *Manteoceras manteoceras* Hay, and *M. washakiensis* Osborn. Osborn (1929a) believed *Manteoceras* and *Telmatherium* to be two distinct "lineages". However, most of the differences noted by Osborn (1929a) between the *Telmatherium* and *Manteoceras*

"lineages" were are actually based on comparisons of specimens belonging to *Telmatherium validus* (but assigned by Osborn to *M. manteoceras* and *M. washakiensis*) with another species altogether, *T. ultimum* Osborn (1908a), a species that Osborn had believed was the terminal member of the *Telmatherium* "lineage". *Telmatherium ultimum* (described below) is clearly distinct from *T. validus* or any of its synonyms, including *T. cultridens*, *M. manteoceras*, and *M. washakiensis*; it was finally removed from *Telmatherium* by Granger and Gregory (1943) and assigned to *Metatelmatherium*. Excluding observations involving *Metatelmatherium ultimum*, the actual differences noted by Osborn (1929a) between *Manteoceras* and *Telmatherium* are minor and can easily be attributed to dental wear, damage, and/or intraspecific variation. The similarities between *Manteoceras* and *Telmatherium* (sans *Metatelmatherium ultimum*) were attributed by Osborn (1929a) to parallel evolution, although without justification. Mader (1989) concluded that *Manteoceras* was synonymous with *Telmatherium*. In a later revision, Mader (1998) considered *T. cultridens*, *M. manteoceras*, and *M. washakiensis* to be junior synonyms of *T. validus* Marsh; these revisions are all upheld here, although justification of these revisions (none were provided by Mader, 1998) are needed.

Telmatherium cultridens was thought by Osborn (1929a) to represent a less "progressive" stage of *Telmatherium*, although the minor differences in size and in the premolar morphology of its holotype (YPM PU10027) could just as easily represent individual variation. The holotype of *Manteoceras manteoceras* (AMNH 1569) is a skull that lacks teeth. It is therefore not possible to directly compare it to the lectotype of *T. validus* (YPM 11120), which mostly consists of upper teeth. However, numerous skulls similar to that of AMNH 1569 have teeth that are consistent in size and morphology with those of the lectotype of *T. validus*. The holotype of *M. washakiensis* (AMNH 13165) is one of the more gracile skulls among this group, but nonetheless one that is consistent cranially and dentally with other specimens of *T. validus*.

Finally, *Telmatherium validus* Marsh can be considered valid for the following reasons. (1) The dentition of the lectotype of *T. validus* (YPM 11120) is similar to that of *Mesatirhinus junius* (a contemporaneous Bridgerian species), but it is larger than the upper size limit of *M. junius*. (2) Additionally, its P2 is somewhat different from that of *Mesatirhinus junius*, with a less lingually positioned metacone. (3) The lectotype is morphologically consistent with and falls within the size range of a group of more complete specimens (including the holotype skulls of *Manteoceras manteoceras* and *Manteoceras washakiensis*) from the upper Bridger (C–D) and lower part of the Washakie Basin (Lower Adobe Town Member of McCarroll et al., 1996b) that represents a species of hornless brontothere. (3) *Telmatherium validus* is most similar to *Wickia brevirhinus* and *Metatelmatherium ultimum*, although it can be distinguished from both by a deeper nasal incision; additionally, the splint of nasal bone that separates the triangular frontal process from the maxilla on the surface of the skull is larger and more prominent in *T. validus*.

Qufutitan zhoui Wang and Wang, 1997

HOLOTYPE: IVPP V8067, the anterior portion of a skull with right I2, C, P2–M2, M3 (partial), and left I3–M1, M2 (partial).

TYPE LOCALITY: Dong Huangzhuang, Qufu City, Shandong Province; Huangzhuang Formation, China.

AGE: Late middle Eocene (Sharamurunian land mammal "age" (Wang and Wang, 1997).

DIAGNOSIS: *Qufutitan zhoui* is the largest known brontothere that lacks conspicuous frontonasal protuberances. The frontal bone forms an anteriorly projecting triangular process that overlaps the nasal bone, thus splitting off a lateral nasal splint from the main body of the nasal. The lateral nasal incision does not extend posterior to the anterior margin of the P1. The nasal process slightly broadens distally; it is nearly horizontal, unelevated, narrow, with thin lateral walls, and without a well-defined or strongly rounded distal edge. The orbits are positioned directly above the posterior portion of M1 and the M2. The orbits do not project

laterally. The premaxillomaxillary rostrum deepens posteriorly and it is not enclosed by bone dorsally. The premaxillary symphysis is vertical with a prominent dorsal ridge and a convex anterior margin. The dorsal surface of the skull is broad and nearly flat above the orbits, and the skull was probably not saddle-shaped.

Dentally, *Qufutitan zhoui* has small, globular upper incisors that form an arched incisor row. Premolar characteristics include a distinct metacone and hypocone on the P1, a distinct P2 metaconid, and weak premolar preprotocristae. Weak premolar hypocones are present on P2, P3, and P4. The lingual margins of the premolar metacones are strongly angled anterolingually. The molars of *Qufutitan zhoui* have tall, lingually angled ectolophs with weak labial ribs, and thinned lingual ectoloph enamel with wedge-shaped paracones and metacones. A cingular parastyle shelf is absent. Central molar fossae, anterolingual cingular cusps, paraconules, and metalophs are absent.

Qufutitan zhoui closely resembles *Telmatherium validus*, *Metatelmatherium ultimum*, *Wickia brevirhinus*, and *Epimanteoceras formosus*, but it retains the following unique combination of characters: a long face with a relatively short nasal incision, a broad and flat forehead, a complex P1, small premolar hypocones, and the lack of central fossae and anterolingual cingular cusps on the upper molars. Moreover, *Q. zhoui* is the only brontothere that lacks conspicuous frontonasal protuberance but at the same time possesses small globular upper incisors and a vertical premaxillary symphysis.

Description

Skull: The holotype of *Qufutitan zhoui* (IVPP V8067) consists of the anterior portion of a very large skull (figs. 46–48). The antorbital region is essentially complete and in good condition, although it suffers from numerous cracks and a minor amount of distortion. The portion of the skull above the orbits is crushed downward, a large transverse crack runs across the proximal portion of the nasal process, and the nasal process appears to be artificially deflected downward. Additionally, the left nasal bone is pressed downward.

Judging by the holotype, *Qufutitan zhoui* is the largest brontothere to lack conspicuous frontonasal swellings. In terms of the overall shape of the skull, *Q. zhoui* closely resembles *Telmatherium validus*, *Metatelmatherium ultimum*, *Wickia brevirhinus*, and *Epimanteoceras formosus*. *Q. zhoui* is significantly larger than *Telmatherium validus*, *Metatelmatherium ultimum*, and *Wickia brevirhinus*, but *Epimanteoceras formosus* is of a similar size.

A portion of the large anteriorly projecting triangular protrusion of bone on the left dorsal surface of IVPP V8067 is partly an artifact of damage to the fossil. However, the right margin of the triangular protrusion on IVPP V8067 is a crack. The actual frontonasal sutures of IVPP V8067 can be distinguished from cracks upon close inspection (fig. 46). From the dorsal view of the skull, a triangular process of the frontal bone overrides the nasal bone. From the left lateral view, an arched splint of the nasal bone can be seen running between the maxilla and the overriding frontal process, thus maintaining contact with the lacrimal.

The lateral antorbital surface of the maxilla of IVPP V8067 forms a shallow facial concavity. The relative distance between the orbit and lateral nasal incision is greater than that of comparable brontotheres, and that distance contibutes to a longer face in *Qufutitan zhoui*. The nasal incision of *Qufutitan* is similar in length to *Telmatherium validus* and *Epimanteoceras formosus*. However, the faces of these taxa are relatively shorter and the nasal incisions of *Telmatherium* and *Epimanteoceras* extend to a point above the P2. However, the lateral nasal incision of *Qufutitan zhoui* does not extend posteriorly beyond the anterior margin of P1.

The orbit of *Qufutitan zhoui* is positioned directly above the posterior portion of M1 and M2, while the anterior orbital rim is situated above the anterior root of M1. This orbital position is slightly more anterior than that of *Epimanteoceras formosus*, *Metatelmatherium ultimum*, and *Wickia brevirhinus*, but similar to *Telmatherium validus*.

The moderate downward angle of the nasal bone of IVPP V8067 is probably a

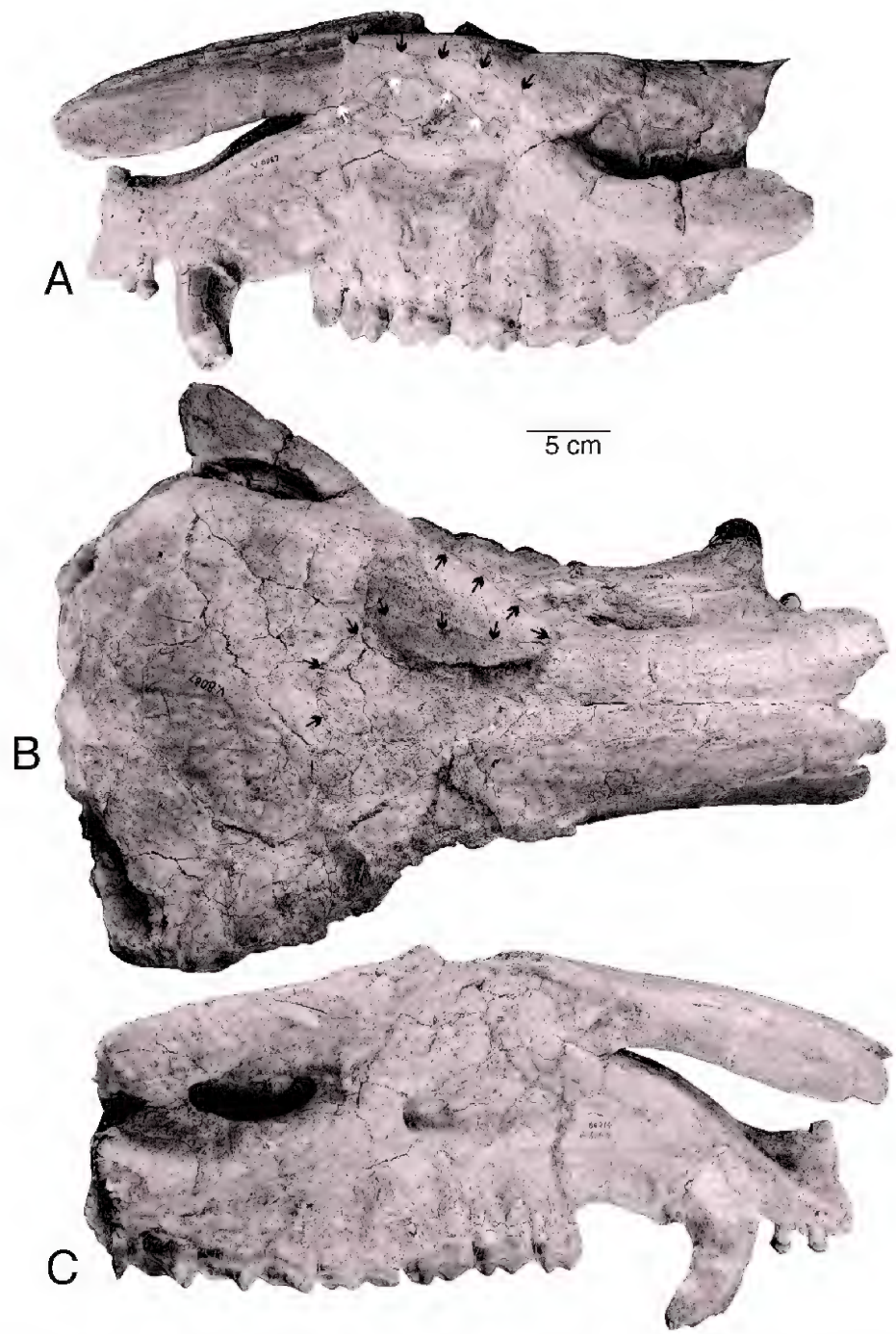

Fig. 46. The holotype of *Qufutitan zhoui* (IVPP V8067). **(A)** Left view, **(B)** dorsal view, **(C)** right view. In A and B, the black arrows are resting on the frontal bone. In A, the white arrows are resting on the maxilla. All arrows point to the frontonasal and nasomaxillary sutures.

Fig. 47. Anterior view of the holotype skull of *Qufutitan zhoui* (IVPP V8067).

taphonomic artifact and, originally, it would have extended more horizontally from the skull. The nasal process is slightly longer than the premaxillomaxillary rostrum. The sides of the nasal process form deep and thin lateral walls that extend to the distal end of the nasal process. The nasal bones are incompletely co-ossified. The left and right nasal bones have become detached at the midline and the left side has been artificially depressed. From the dorsal view it can be seen that the nasal process is narrower than the premaxillomaxillary rostrum. The nasal process is of nearly constant width throughout its length, although it broadens slightly near the distal end. The anterior margin of the nasal process is mostly broken away although intact remnants of the distal edge remain on the anterolateral corners, indicating a thin and roughened distal nasal margin. The slight distal flaring of the nasal process resembles that in *Epimanteoceras formosus* in particular. However, the overall the morphology of the nasal process of *Qufutitan zhoui* does not differ significantly from that of *Telmatherium*, *Metatelmatherium*, or *Wickia*.

Some aspects of the rostrum of *Qufutitan zhoui* are unspecialized and typical. For instance, from the lateral view of IVPP V8067, the rostrum deepens posteriorly; the dorsolateral margin slopes posterodorsally and rises to about the midlevel of the orbit. The rostrum lacks the highly specialized dorsal bony cover seen in *Dolichorhinus* and *Metarhinus*. Despite these regularities, the rostrum of *Q. zhoui* has several peculiar features that distinctly differ from most other brontotheres. The elongate premaxillomaxillary rostrum of *Q. zhoui* contributes to the appearance of the relatively long face. Although there is a slightly upward curvature to the rostra of most brontotheres, the rostrum of IVPP V8067 seems to curve slightly downward. The premaxillomaxillary suture can be seen on the left side of the specimen, running along the dorsolateral border of the rostrum. The premaxilla does not contact the nasal bone; however, the nasal process of the premaxilla is long, slender, and extends nearly to the posterior notch of the lateral nasal incision. The premaxillary symphysis of *Q. zhoui* is nearly vertical, thus giving the incisors a nearly vertical orientation. In lateral profile the anterior margin of the symphysis is concave. Finally, there is a prominent U-shaped ridge of bone surrounding the notch on the dorsal surface of the premaxillary symphysis that is formed by the posterolaterally divergent premaxillary nasal processes. In contrast to *Qufutitan zhoui*, the premaxillae of nearly all other brontotheres have a more posterodorsally reclined premaxillary symphysis with more anteriorly angled incisors, a more convex or flat anterodorsal surface, and a less prominent (or absent) dorsal ridge.

Little can be said about the postorbital portion of the skull of *Qufutitan zhoui*; however, the skull does not appear to have been saddle-shaped. The forehead is realtively broad and flat. In this respect *Q. zhoui* resembles both *Telmatherium* and *Epimanteoceras*. The foreheads of *Metatelmatherium* and *Wickia* are narrower and more transversely arched.

From the ventral view of IVPP V8067 the anterior rim of the posterior nares is positioned just anterior to the M3. There is a relatively wide emargination along the anterior margin that is marked by a thin ridge of bone. The lateral margins of the posterior nares are not preserved; however, the emargination probably continued around the lateral margins of the posterior nares, thus forming a horseshoe-shaped emargination similar to that seen in most other brontotheres.

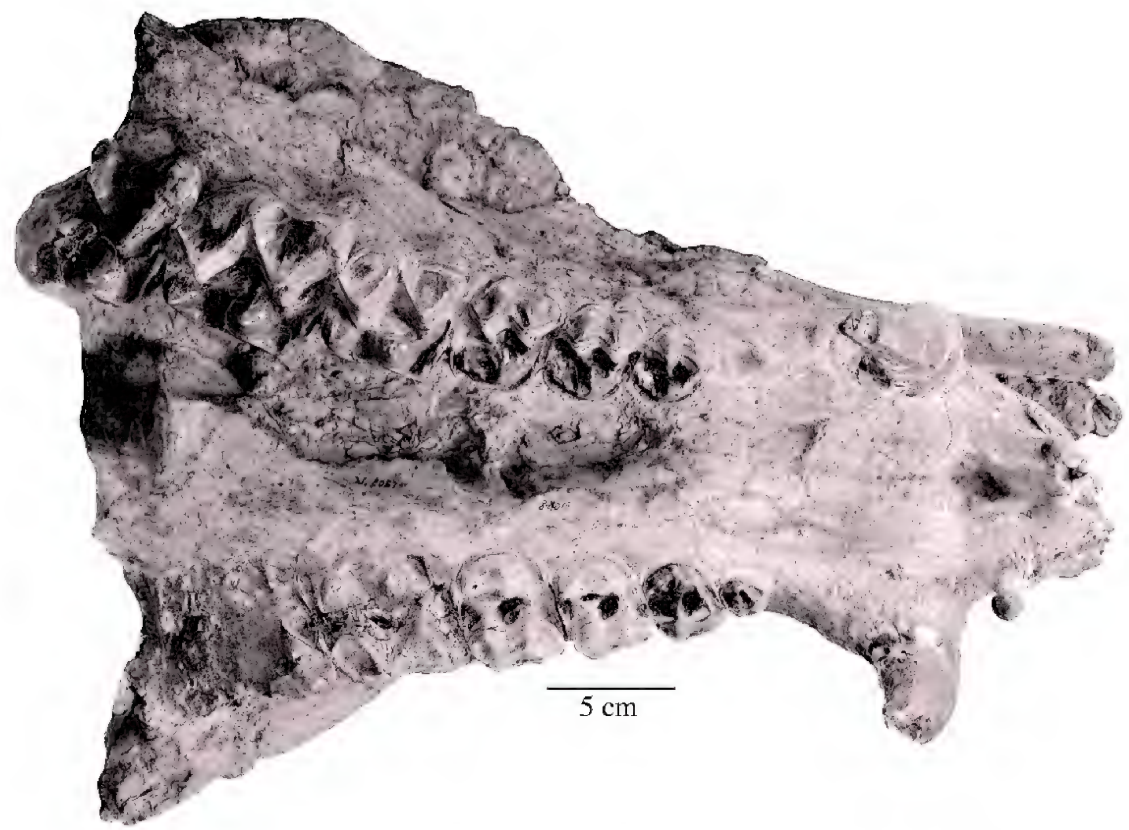

Fig. 48. Ventral view of the holotype skull of *Qufutitan zhoui* (IVPP V8067).

UPPER DENTITION: The holotype of *Qufutitan zhoui* (IVPP V8067) retains a nearly complete set of upper dentition (figs. 48, 49, 50). Only two incisors are preserved, although the alveoli are reasonably well preserved and indicate a dental formula of 3-1-4-3. The incisors form an arched row anterior to the canines. A small median notch on the alveolar surface of the premaxilla suggests a minor diastema between the central incisors. The right I2 and left I3 are in a minimal state of wear. Both incisors are similar in size and are relatively small and globular in shape. There are no incisor cingula. The remaining unworn surfaces of the enamel crowns are crenulated. Each incisor bears one or more irregularly shaped and irregularly positioned enamel protuberances. The relatively small globular incisors, a condition similar to the incisors of more advanced horned brontotheres (e.g., *Duchesneodus*, *Dianotitan*), are unusual for a hornless brontothere. There is a short diastema between the I3–C and a longer postcanine diastema. The canines of IVPP V8067 are very large and posteriorly curved.

The left premolar row (P1–P4) of IVPP V8067 is complete with a particularly well-preserved and minimally worn P1 and P2. However, the surfaces of the left P3 and P4 are somewhat weathered. The right P1 is missing although the remaining premolars are complete, minimally worn, and unweathered. The P1 of IVPP V8067 is substantially smaller than the other premolars, although it exhibits relatively advanced crown morphology. The P1 crown has both a well-developed ectoloph and lingual heel. The crown is nearly rectangular, although the anterior edge is strongly angled posterolingually, thus giving the tooth an oblique appearance. There is both a distinct paracone and metacone on the P1. The labial swelling of the paracone is much larger than the metacone. The parastyle is long and slightly lingually arched, while the metastyle is

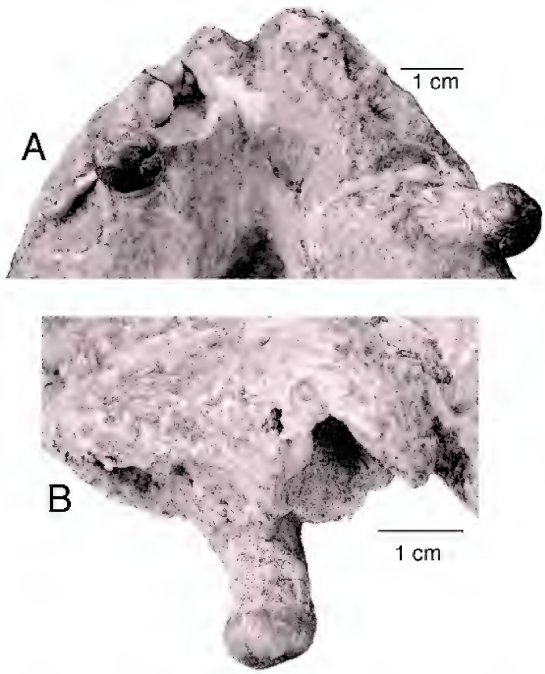

Fig. 49. Incisors and incisor alveoli of the holotype skull of *Qufutitan zhoui* (IVPP V8067). **(A)** Ventral view, **(B)** labial view.

shorter and uncurved. The lingual side of the crown bears a well-developed and somewhat posteriorly shifted protocone, as well as a strongly developed preprotocrista that connects the protocone to the lingual base of the paracone. A much less distinct and shorter lingual crest projects straight posteriorly from the protocone. A continuous cingulum stretches from the lingual edge of the parastyle, wraps around the lingual margin of the crown, and meets the lingual edge of the metastyle.

The P2, P3, and P4 are more nearly rectangular in outline than the P1, with parallel anterior and posterior sides. Distinctly pinched paracone ribs can be seen on the labial surfaces of P2–P4. The labial swellings of the metacone are broader and rounder that the labial paracone ribs. The metacone of P2 is only slightly more lingually positioned than those of P3 and P4. The P2 parastyle projects straight anteriorly, while the P3 and P4 parastyles are strongly angled labially. The metastyles of P2 and P3 project straight posteriorly, while the P4 metastyle is angled somewhat labially. The lingual band of enamel on the ectolophs of P2, P3, and P4 is thinner than the labial band of enamel. A small but distinct preprotocrista connects the paracone and metacone on P2. P3 and P4 have progressively smaller and less distinct preprotocrista. No paraconules or metaconules can be seen on any of the premolars. The lingual margins of the metacone of P2, P3, and P4 form distinct vertical wedges that are strongly angled anterolingually.

A lingual crest of relatively low relief extends posteriorly from the protocone of the P2 and connects it to a very small hypocone that can now be identified only by a small exposure of dentine on the posterolingual corner of the crown. The lingual morphologies of the P3 and P4 are similar, although the hypocones are more distinct than that of the P2. Each of these premolars (P2–P4) has a strong continuous cingulum that wraps around the anterior, lingual, and posterior margins of the tooth. Likewise, each of these premolars has a distinct and continuous labial cingulum.

The premolars of *Qufutitan zhoui* distinctly differ from those of *Telmatherium*, *Metatelmatherium*, and *Wickia*. These taxa have simpler single-cusped P1s, and hypocones are not seen on any of the premolars. Moreover, *Telmatherium* occasionally has premolar paraconules and a diastema between P1 and P2. The premolars of *Epimanteoceras formosus* compare well with *Q. zhoui* in most respects. In particular, both taxa tend to have poorly developed hypocones. However, the strongly wedged and anterolingually angled margin of the premolar metacones of *Q. zhoui* is an autapomorphic condition.

The right molar row of IVPP V8067 is moderately worn and the posterior portion of M3 is not preserved. Typical brontotheriine molar apomorphies seen in *Qufutitan zhoui* include a narrow anterolabial cingulum that passes below the apex of the parastyle, a relatively tall and lingually angled ectoloph, weak labial paracone and metacone ribs, thin lingual ectoloph enamel, and wedge-shaped lingual margins of the paracone and metacone. Anterolingual cingular cusps and central molar fossae do not occur on any of the molars. *Q. zhoui* molars lack vestigial paraconules. Although the posterolingual corner

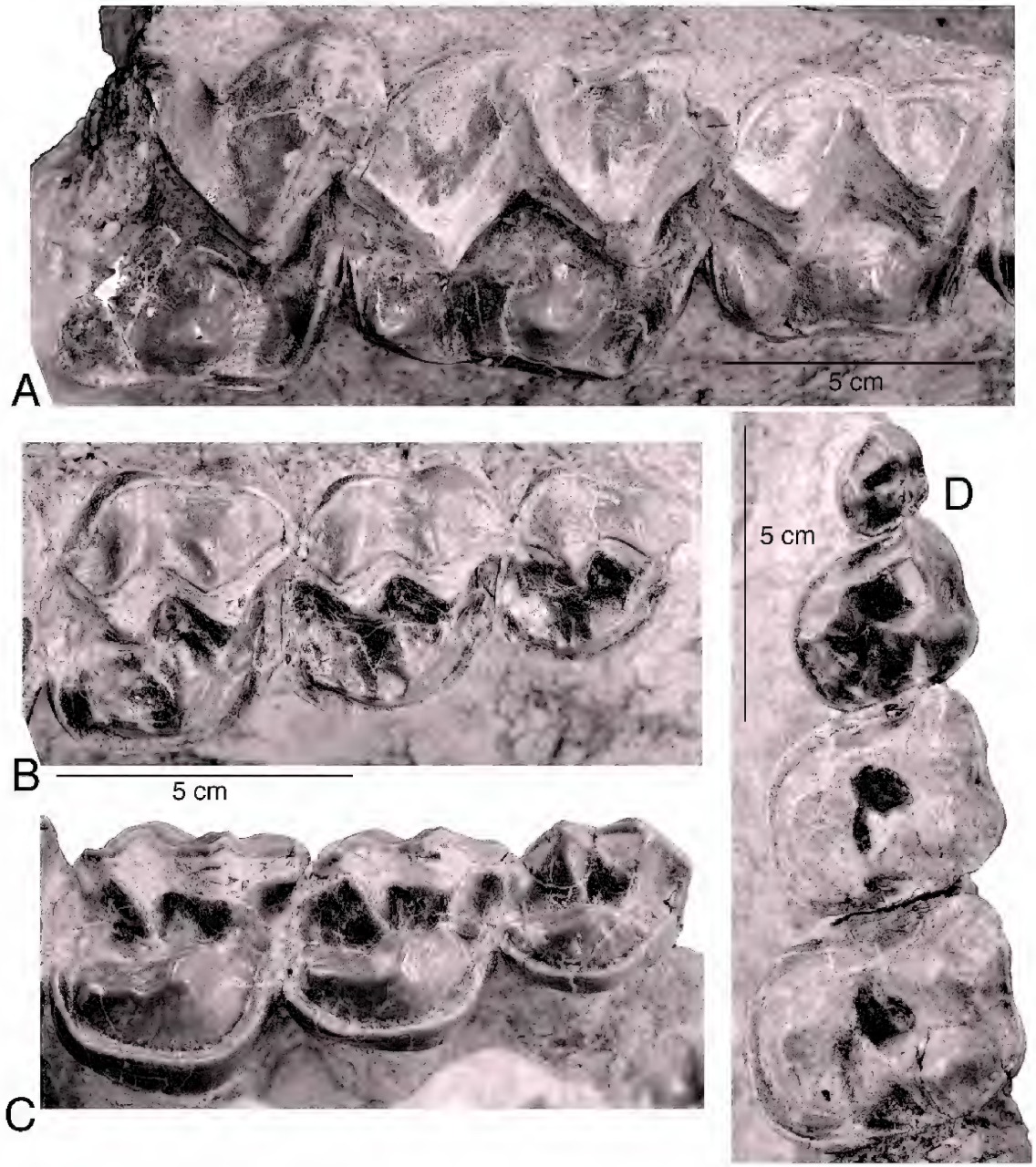

Fig. 50. Cheek teeth of the holotype skull of *Qufutitan zhoui* (IVPP V8067). **(A)** Right molars, **(B)** right premolars (P2–P4), **(C)** right premolars rotated slightly (P2–P4), **(D)** left premolars (P1–P4).

of the M3 is lost, enough of the specimen is preserved to suggest that a hypocone either was not present or was poorly developed. Lingual molar cingula in IVPP V8067 are thin and discontinuous around the margins of the protocone.

Remarks

Wang and Wang (1997) named a new genus and species of very large hornless brontothere, *Qufutitan zhoui*, based on the anterior portion of a skull (IVPP V8067).

Wang and Wang (1997) diagnosed *Q. zhoui* by its large size, straight nasals, shallow nasal incision, weak hornlike swelling, well-developed premaxillary suture projection, upper incisors reduced with "global-shaped" crowns, large upper canine, developed C1–P1 diastema, nonmolariform premolars, weak hypocone on P2–P4, wide upper molars with no preconule (= paraconule as used in this paper) or metaconule. Not all of these characters are particularly diagnostic. For instance, the molars of *Qufutitan*, described as wide by Wang and Wang (1997), are not different in overall proportions than other brontotheres. Moreover, the premolars of all brontotheres can roughly be described as "nonmolariform".

I was not able to confirm that IVPP V8067 has a "weak horn-like swelling" (contra Wang and Wang, 1997). As noted in the above description, there is a large triangular projection of bone on the left dorsal surface of the skull that overlaps the nasal bone, although in *Qufutitan zhoui* the surface of the overlapping frontal process is flush or nearly flush with the dorsal surface of the skull. A number of other middle Eocene brontothere taxa are known to exhibit the same frontonasal configuration, but like *Qufutitan* they lack conspicuous frontonasal protuberances. These taxa include *Telmatherium validus*, *Metarhinus fluviatilis*, *Sthenodectes incisivum*, *Wickia brevirhinus*, *Metatelmatherium ultimum*, and *Epimanteoceras formosus*. Among these taxa, only *Epimanteoceras formosus* has a minor frontonasal swelling, and even in that species the swelling occurs in only one of the two known specimens.

Wang and Wang (1997) briefly compared *Qufutitan zhoui* to *Metatelmatherium*; a more extensive comparison of *Qufutitan zhoui* to other brontotheres is warranted. As noted above, *Qufutitan zhoui* closely resembles *Telmatherium validus*, *Wickia brevirhinus*, *Metatelmatherium ultimum*, and *Epimanteoceras formosus*. All express the same derived frontonasal configuration, but they otherwise have relatively unspecialized skulls. Closer examination reveals that in addition to its unusually large size *Qufutitan zhoui* expresses a unique combination of characters that strongly differentiates it from *Telmatherium*, *Wickia*, *Metatelmatherium*, and *Epimanteoceras*; these characters include a long face with a relatively short nasal incision, a broad and flat forehead, a complex P1, small premolar hypocones, and the lack of a central fossa and anterolingual cingular cusps on the upper molars. Additionally, the strongly posterolingually angled premolar metacones is an autapomorphic condition that is not seen in other brontotheres. However, it is the unusual morphology of the premaxilla and the small globular incisors that most conspicuously distinguishes *Qufutitan zhoui* from other hornless brontotheres. With the exception of *Qufutitan zhoui*, small globular incisors are only seen among the most advanced horned brontotheres. All hornless brontotheres other than *Qufutitan zhoui* have larger and more subcaniniform incisors.

Strangely, several aspects of the incisor and rostral morphology of *Qufutitan zhoui* resemble the giant late Eocene Asian brontothere, *Embolotherium*. For instance, *E. andrewsi*, *E. grangeri*, and *Q. zhoui* are the only brontotheres to have globular upper incisors but retain a plesiomorphically arched incisor row. Other brontotheres with globular incisors exhibit a straight incisor row. Secondly, the vertical orientation of the premaxillary symphysis of *Q. zhoui*, with its concave anterior margin and pronounced dorsal ridge, are conditions that are otherwise only seen in the premaxillae of *E. andrewsi* and *E. grangeri*. Aside from these similarities *Q. zhoui* is obviously very different from *Embolotherium*.

Qufutitan zhoui is known only from a partial skull. However, there are a variety of brontothere species, known only from mandibles, to which *Qufutitan* cannot be directly compared. Nonetheless, it is worth considering the possibility that one of these "mandible taxa" is synonymous with *Q. zhoui*. Based on the long rostrum and long postcanine diastema of *Q. zhoui*, the mandible probably had a relatively elongate symphysis with a rather long lower postcanine diastema and small globular or semispatulate incisors. *Pollyosbornia altidens* and *Hyotitan thomsoni* closely resemble the anticipated mandible of *Q. zhoui*. Both are relatively large brontotheres exhibiting an arched incisor row, a long symphysis, and a long postcanine

diastema. *Hyotitan thomsoni*, in particular, seems a likely synonym of *Q. zhoui*. The lower incisors of *Hyotitan* are rather smallish and form a slightly arched row. Further congruence between the skull of *Q. zhoui* with the mandible of *H. thomsoni* is represented by the relatively advanced upper and lower premolar morphologies, the very large canines, and the unusually pronounced labial premolar cingula/cingulids. *H. thomsoni* is more or less compatible with the anticipated mandible and lower dentition of *Q. zhoui* and it is possible that these species are synonyms. Therefore one of these species must be considered dubious. *H. thomsoni* Granger and Gregory, 1943, is the senior name. However, as a matter of convenience, I presently consider *Q. zhoui* to be the valid species; the character information derived from its holotype skull is superior to the more limited character data retrievable from the holotype jaw (AMNH 26401) of *H. thomsoni*. If further discoveries indicate that these species are indeed synonymous, *Q. zhoui* should be considered a junior synonym of *H. thomsoni*.

Wickia brevirhinus, new genus and species

HOLOTYPE: CMNH 11380, a skull with right I3, C, P2–M3, left C, P2 (partial), and P3–M3.

TYPE LOCALITY: Sand Wash Basin, Moffat County Colorado.

AGE: Middle Eocene (early Uintan land mammal "age").

ETYMOLOGY: "Wick", nickname of paleontologist William Berryman Scott (Scott, 1939). The trivial name, *brevirhinus*, refers to the short nasal incision and short nasal process of this species.

REFERRED SPECIMEN: **(From the Sand Wash Basin, Moffat County Colorado)** CMNH 11382, an anterior portion of a cranium with right I3–M3, left I1–M3, and a mandible with right p1–m3, left i2, and p1–m3; **(from the Adobe Town Member of the Washakie Formation, Sweetwater County, Wyoming)** UCMP 81300, a skull missing the right zygomatic arch, with right I3, C (partial), P1–M3, and left I3–M3.

DIAGNOSIS: *Wickia brevirhinus* is a relatively large hornless brontothere, one of several in which the frontal bone intrudes into the nasal bone, thus splitting off a small lateral splint of nasal bone from the main body of the nasal. The size and shape of the nasal splint is similar to that of *Metatelmatherium ultimum* and less pronounced than that of *Telmatherium validus*. The nasal incision is short and extends posteriorly to the P1. The nasal process is very short, horizontal, unelevated, of relatively constant transverse width, narrow, with thin and relatively deep lateral walls, and without a well-defined or strongly rounded distal margin. The orbits do not project laterally and they are positioned above M2 with the roots of M1 below the anterior orbital rim. Neither an infraorbital process nor a ventral zygomatic flange is present on the jugal. The premaxilla is extremely robust and does not contact the nasal bone. The premaxillomaxillary rostral cavity is not enclosed by bone dorsally. Other cranial characteristics include a relatively flat dorsal cranial surface, an elevated occiput, deep, strongly curved, and laterally bowed zygomatic arches, and a ventrally open and mediolaterally angled external auditory pseudomeatus. Large ventral sphenoidal fossae are absent. A sagittal crest is absent, but the dorsal surface of the cranium is very narrow and the parasagittal ridges strongly constrict the dorsal surface of the cranium.

Dentally, *Wickia brevirhinus* has large subcaniniform upper incisors, a simple P1, a distinct P2 metacone, weak premolar preprotocristae, and short lingual crests extending posteriorly from the premolar protocones. Premolar hypocones are absent. The upper molars of *W. brevirhinus* have tall, lingually angled ectolophs with weak labial ribs, and thinned lingual ectoloph enamel with wedge-shaped paracones and metacones. Small anterolingual cingular cusps are present, but central molar fossae and cingular parastyle shelves are absent in the molars. *W. brevirhinus* molars appear to retain vestigial paraconules. Anterolingual cingular cusps are present. The upper molars lack paraconules or metalophs. The lower dentition of *W. brevirhinus* includes a postcanine diastema, a p1–p2 diastema (variably present), an elongate p2 trigonid, a poorly developed p2 talonid, a metaconid on p4 but

not on p2 or p3, shallow molar basins, and a slender m3.

Wickia brevirhinus is most similar to *Telmatherium validus* and *Metatelmatherium ultimum*, but it is distinct from these species primarily by the combination of a very short nasal incision, a short nasal process, lack of a sagittal crest, lack of a ventral zygomatic flange, and possibly a poorly developed p2 talonid.

Description

Skull: The following description of *Wickia brevirhinus* is based upon the holotype skull (CMNH 11380) (figs. 51, 54a) as well as the referred specimens (UCMP 81300) (figs. 52 and 54c) and CMNH 11382 (figs. 53, 54b). *W. brevirhinus* is a large hornless brontothere that is most similar in size to *Metatelmatherium ultimum*. All skulls reveal a frontonasal configuration that resembles those of *Metatelmatherium* and *Telmatherium*, but the sutures can most clearly be seen on CMNH 11382. A thin, arched splint of the nasal bone can be seen branching in a posteroventral direction from the main body of the nasal. A triangular process of the frontal bone enters the notch between the main body of the nasal bone and the posteroventrally directed nasal splint. From the dorsal views of all skulls, parts of the frontonasal suture can be seen receding in a posteromedial direction. The shape of the nasal splint and the intruding frontal bone is more like that of *Metatelmatherium* where the nasal splint is relatively short, narrow, and only slightly arched. Likewise, the triangular process that intrudes into the nasal bone is relatively short and inconspicuous. In *Telmatherium validus* the nasal splint and frontal process are larger and more pronounced.

The face of *Wickia brevirhinus* is tall. The maxilla extends upward to the level of the upper rim of the orbit, where it meets the ventral edge of the nasal splint and forms an arched nasomaxillary suture. The maxilla forms a very shallow preorbital fossa. The nasal incision of *W. brevirhinus* is shorter than that of *Telmatherium* but similar to *Metatelmatherium*; the posterior notch of the nasal incision is positioned between the canine and the P2 in CMNH 11380. The nasal incision extends as far back as the P1 in CMNH 1382 and UCMP 11380. The orbit of *W. brevirhinus* is positioned directly above M2. The posterolateral root of M1 is rooted below the anteriormost edge of the orbital floor. The anterolateral root of M1 is situated directly below the anterior orbital rim.

The nasal process of the holotype is not preserved, but it is complete in the referred specimens. The nasal bones are poorly fused together. The nasal process is shorter than the premaxillomaxillary rostrum in UCMP 81300, but it is of similar length to the rostrum in CMNH 11382. The nasal process is slightly curved downward, resulting in a convex dorsal surface. The lateral margins of the nasal process form dorsoventrally deep and thin vertical walls that are of relatively constant depth throughout most of their length, but become shallower near the distal end. From a dorsal view the nasal process is narrower than the premaxillomaxillary rostrum and it tapirs slightly distally with a somewhat convex distal edge. The anterior edge of the nasal process is thin, roughened, and deflected downward.

From the lateral view the dorsal margin of the premaxillomaxillary rostrum rises steeply posterodorsally so that the posterior notch of the nasal incision is at the level of the upper half of the orbit. The rostral cavity is open dorsally and continuous with the nasal cavity. The premaxillomaxillary sutures are clearly visible in CMNH 11380. The nasal processes of the premaxillae diverge laterally in a posterior direction and they are truncated before reaching the posterior notch of the nasal incision. The premaxillae of CMNH 11380 are massive and they do not contact each other medially, thus the premaxillary symphysis is not ossified. The premaxillae of UCMP 81300 and CMNH 11382 are somewhat less massive than those of the holotype and they contact each other mesially, although they are not strongly co-ossified. Overall, the premaxillae of *Wickia brevirhinus* seem more massive than those of *Metatelmatherium* or *Telmatherium*. The degree of premaxillary robusticity is somewhat variable in these species and relates to variation in canine size.

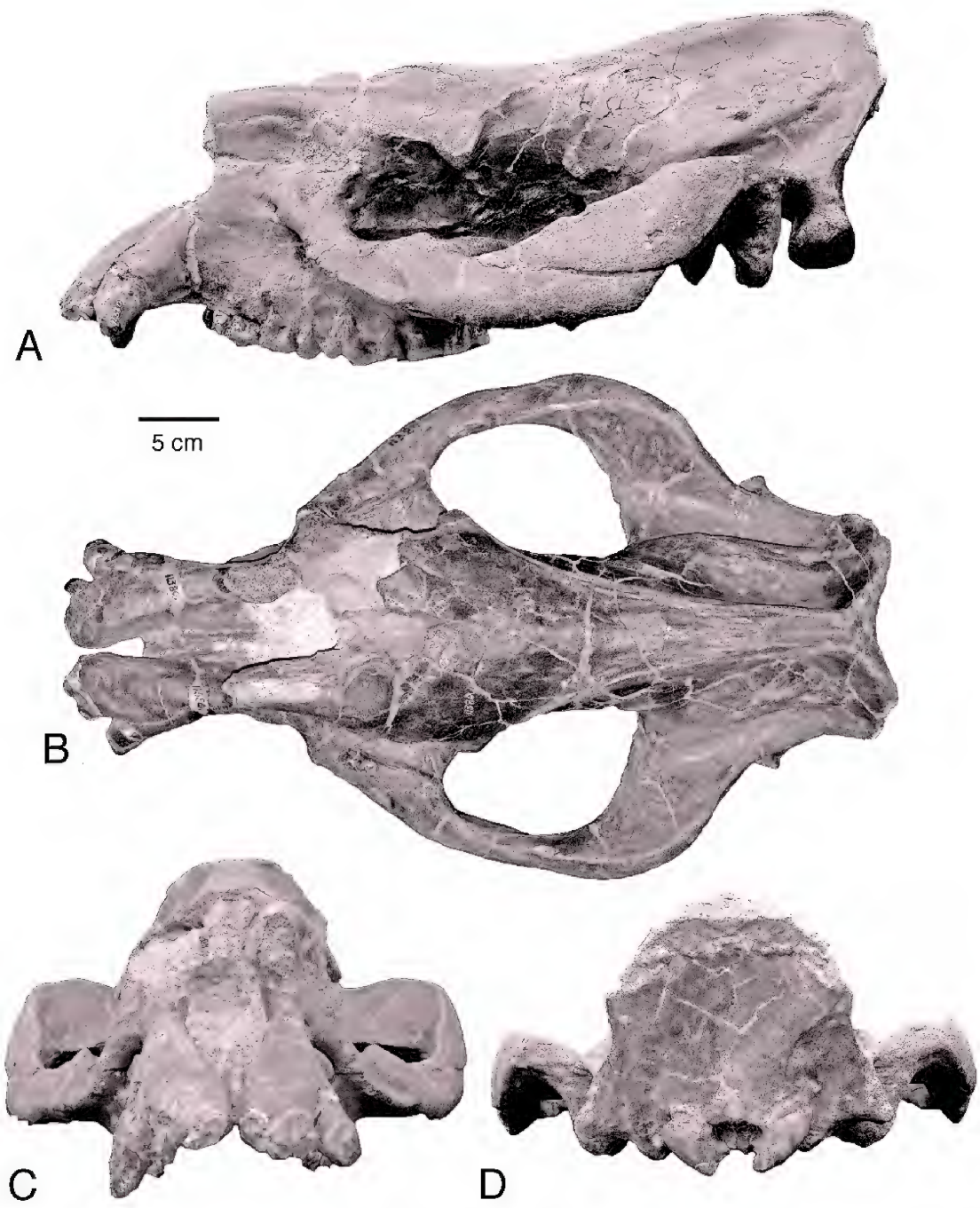

Fig. 51. Holotype skull of *Wickia brevirhinus* (CMNH 11380). **(A)** Left view, **(B)** dorsal view, **(C)** anterior view, **(D)** posterior view.

The skull of *Wickia brevirhinus* is rather tall and the posterior portion of the cranium is elevated. From a lateral view the dorsal surface of the skull above the orbits is flat. Behind the orbits the dorsal surface of the skull is slightly convex in lateral profile. From a dorsal view the dorsal surface of the skull is postorbitally very narrow, although

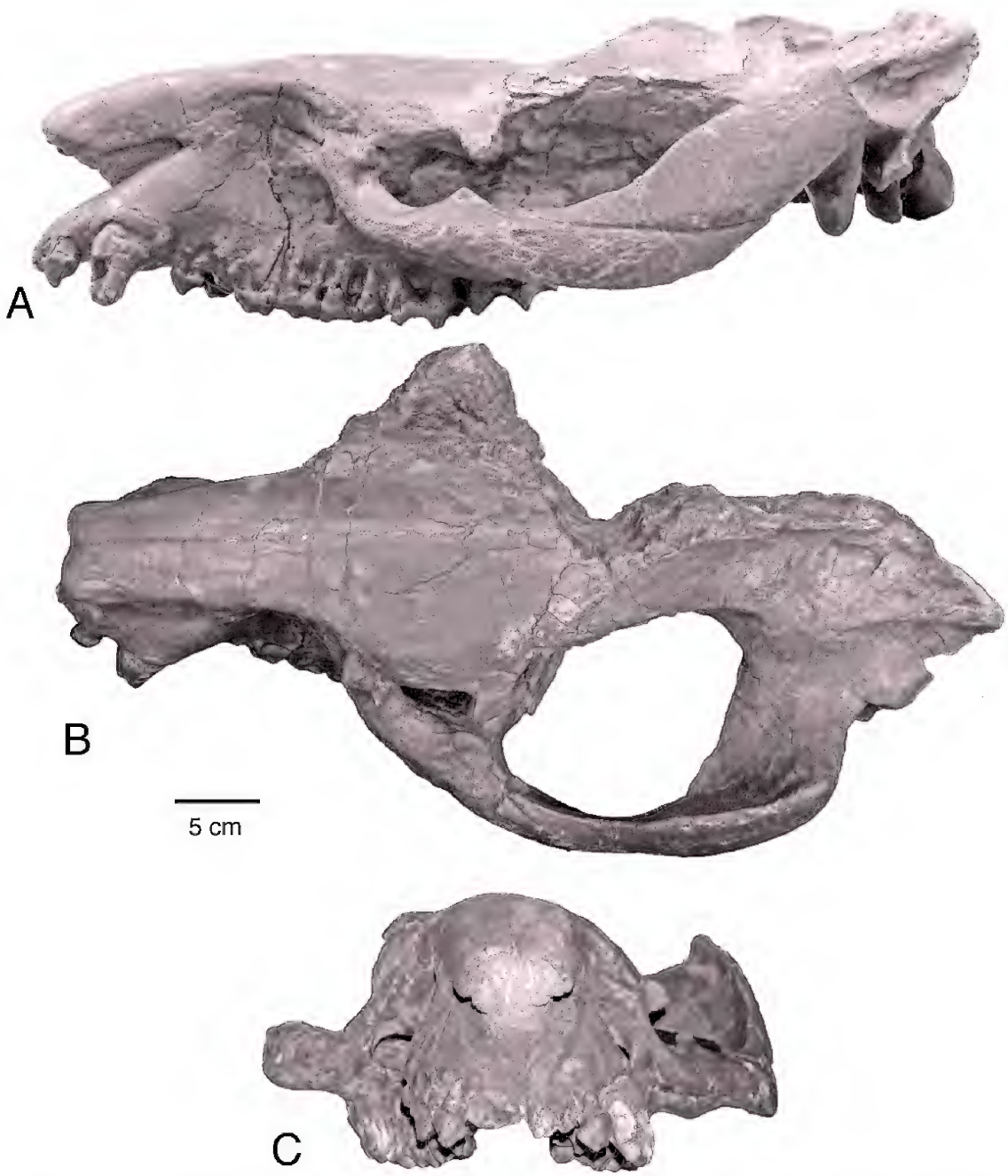

Fig. 52. A skull referred to *Wickia brevirhinus* (UCMP 81300). **(A)** Left view, **(B)** dorsal view, **(C)** anterior view.

the parasagittal ridges do not meet to form a true sagittal crest. An elongate shallow pit resides in the constriction of the parasagittal ridges at the posterior end of the skull.

The zygomatic arches of *Wickia brevirhinus* are deep and very strongly bowed laterally. The jugal portion of the zygomatic is essentially horizontal while the zygomatic

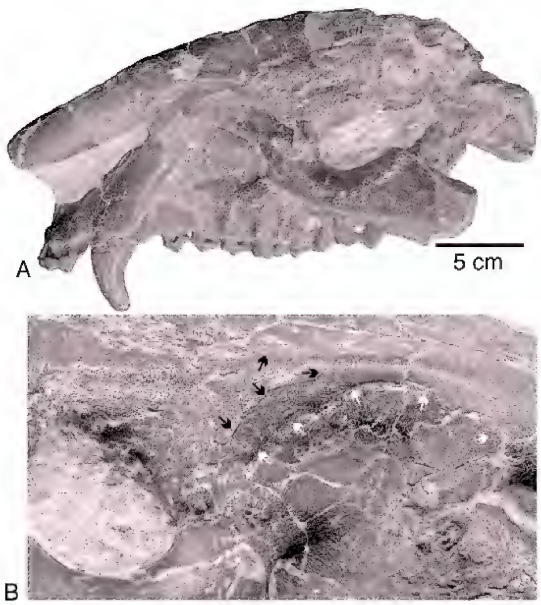

Fig. 53. A partial skull referred to *Wickia brevirhinus* (CMNH 11382). **(A)** Left view, **(B)** close up of right face showing frontonasal and nasomaxillary sutures. White arrows on the maxilla point to the nasomaxillary suture. Black arrows on the frontal point to the frontonasal suture.

process of the squamosal is steeply angled posterodorsally, giving the zygomatic arch a strongly curved appearance. The large ventral flange that extends from the inferior margin of the zygomatic process of the jugal in *Metatelmatherium* is not seen among the skulls of *W. brevirhinus*. *W. brevirhinus* also lacks an infraorbital jugal process like that seen in *Sphenocoelus uintensis*.

The nuchal crest of CMNH 11380 is concave from the dorsal view. From the lateral view the occiput is moderately tilted backward. From the posterior view the nuchal crest is dorsally arched, the upper half of the occiput is narrower than the lower portion and the middle is slightly constricted. The occipital pillars are prominent like in *Telmatherium validus* and the central occipital pit between them is shallow. The nuchal crest of CMNH 11380 is very rugose on its posterior surface, while the remainder of the occipital surface is much smoother. *Wickia brevirhinus* lacks a distinctive notch with facetlike margins above the foramen magnum that is seen in *Metatelmatherium ultimum*.

From the ventral views of CMNH 11380 and UCMP 81300 the posterior nares are rimmed by a distinct horseshoe-shaped emargination. The anterior rim of the posterior nares is positioned between the hypocones of the M3. A distinct anteroposteriorly oriented ridge emerges from the midline of the palate and extends posteriorly beyond the anterior rim of the posterior nares. Neither specimen bears evidence of posteriorly extended maxilloturbinates, although they could have been present but were not preserved.

The vomer forms a thin septum that bisects the elongate posterior narial canal. The posterior narial canal of CMNH 11380 extends into the sphenoid bone, but it does not extend past the foramen ovale. The morphology of the posterior narial canal of the referred specimen, UCMP 81300, is presently obscured by a large mass of wax, although the posterior narial canal does not appear to extend quite as far posteriorly in this specimen. Other aspects of the basicranium of *Wickia brevirhinus* are typical. For instance, the foramen ovale is widely separate from the foramen lacerum. The external auditory pseudomeatus enters the skull in a strictly mediolateral direction and is not constricted ventrally by the mastoid process.

Upper Dentition: All three specimens of *Wickia brevirhinus* have partial sets of upper incisors (fig. 54). The incisor row forms a short arch anterior to the canines. Though the incisor rows are incompletely preserved, the premaxilla shows room for three large incisors. Little else is noteworthy about the incisors of CMNH 11380. In UCMP 81300, only the left and right I3s are preserved. The nearly intact I3s are large with pointed and lingually curved subcaniniform crowns. A thin cingulum can be seen tracing around the lingual base of the right I3. The I3s are separated from the canines by a distinct diastema on both specimens. The canines themselves are relatively large. The left I1 and I2 of CMNH 11382 are preserved, but they are heavily worn. These incisors are large, yet they are smaller than the large caniniform I3.

The P1s of CMNH 11380 are lost and their alveoli are mostly reabsorbed, nearly erasing all evidence of P1. Due to the absence of P1 the length of the postcanine diastema cannot

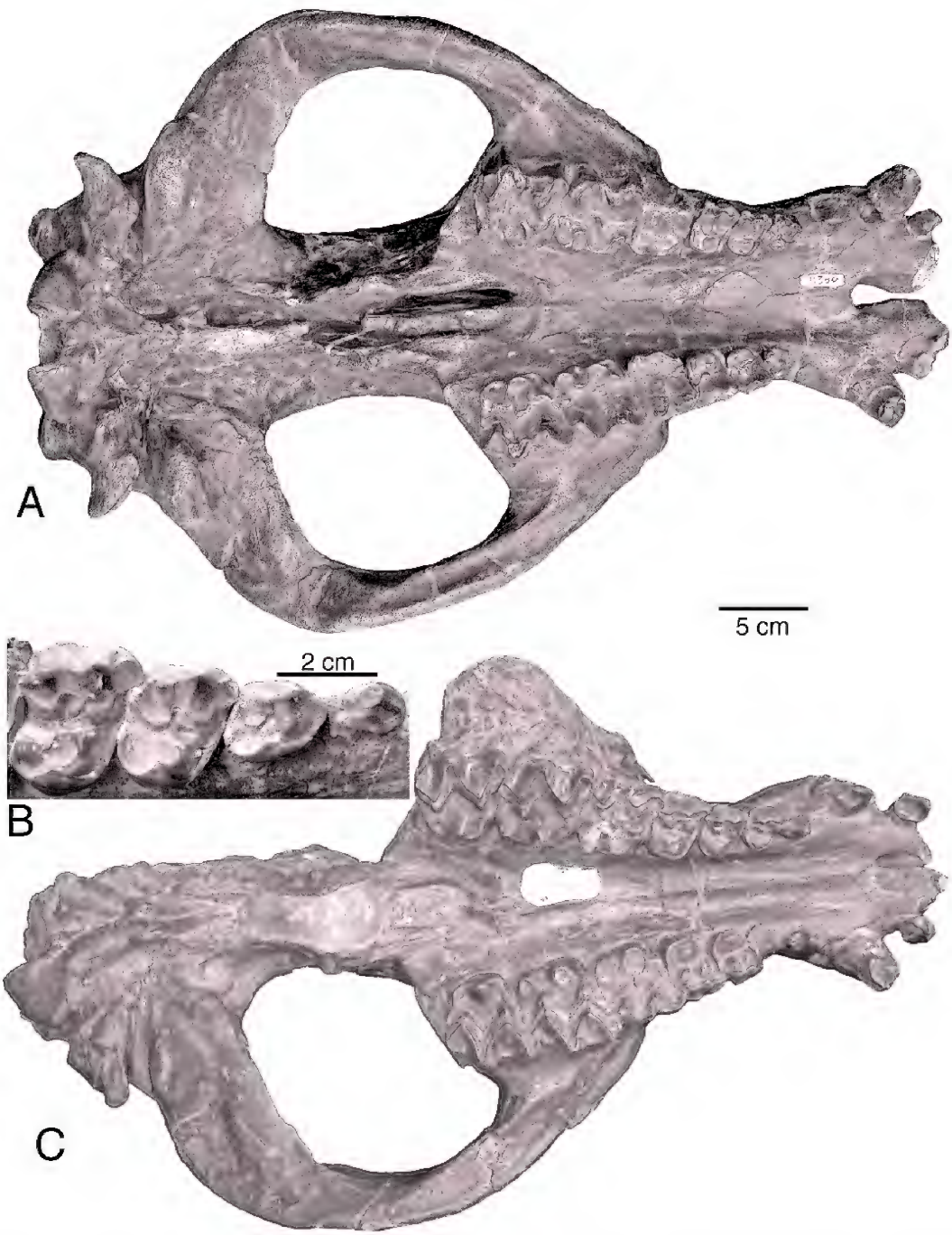

Fig. 54. Views of the ventral surface of skull and upper dentition of *Wickia brevirhinus*. **(A)** Ventral view of CMNH 11380, **(B)** right premolars of CMNH 11382, **(C)** ventral view of UCMP 81300.

easily be judged from this specimen, although the gap between the canine and P2 is quite long. The P1s are still present in CMNH 11382 (fig. 54b) and UCMP 81300 (fig. 54c). In these specimens the postcanine diastema is relatively short. P1 is small with a simple crown with a single cusp, a posterior heel, and a thin lingual cingulum. There is no P1–P2 diastema.

The crowns of the P2–P4 of UCMP 11380 are heavily worn and reveal only basic details, while those of UCMP 81300 and CMNH 11382 are substantially less worn. The anterior margin of P2 is angled posterolingually, giving the crown of that tooth a somewhat more oblique outline. P3 is less oblique in outline while the anterior and posterior sides of P4 are essentially parallel. The parastyle and metastyle of the P2 arch slightly lingually, while those of P3 are approximately straight. The parastyle of P4 is strongly angled anterolabially, while the metastyle of P4 is straight. The labial sides of the paracones of P3 and P4 are more strongly convex than those of the metacones.

In CMNH 11380 and CMNH 11382, the lingual side of the P2 is heavily worn. However, on the P2 of UCMP 81300 a short crest extends anterolingually from the protocone and continues along the anterior side of the crown. The lingual side of P2 exhibits a short preprotocrista as well as a short lingual crest extending posteriorly from the protocone. In P3 there is a small but distinct preprotocrista and a short lingual crest. Finally P4 has a very indistinct preprotocrista and there is no lingual crest. However, a lingual crest is present on the P4 of CMNH 11382. None of the premolars has a hypocone.

The molars of CMNH 11380 are extremely worn, and their proportions have been significantly altered by interstitial wear. The molars of UCMP 81300 and CMNH 11832 serve as better sources for the molar morphology of this species. The molars of *Wickia brevirhinus* exhibit typical brontotheriine traits including tall, lingually angled ectolophs, weak labial ribs, thin lingual ectoloph enamel, and wedge-shaped lingual sides of the paracone and metacone in molars that are not heavily worn (e.g., M3). The anterior cingulum is thin and passes proximally to the distal peak of the parastyle. *W. brevirhinus* molars exhibit small anterolingual cingular peaks, but they lack central molar fossae. The molars retain vestigial paraconules. The M3 lacks a hypocone.

Mandible and Lower Dentition: The holotype of *Wickia brevirhinus* lacks an associated mandible, however, a referred specimen, CMNH 11382, includes a complete mandible with partially preserved incisors and complete cheektooth rows (fig. 55). The ramus of CMNH 11382 is similar in proportion to those of *Telmatherium validus* and *Metatelmatherium ultimum*, including a tall coronoid process and relatively steeply angled (~45°) ventral margin of the symphysis. The symphysis extends posteriorly to the p3 metaconid.

The remnants of the three incisors of CMNH 11382 are relatively large and form a short arch anterior to the canines, although they are too damaged to describe other details of their morphology. There is no precanine diastema, but the postcanine diastema is somewhat longer than the p2.

The p1 of CMNH 11382 is small and simple with a single cusp and a short talonid heel. There is no p1–p2 diastema. The p2 of CMNH 11382 is slender and ovoid in outline. The trigonid of the p2 is nearly twice the length of the talonid, the p3 trigonid is somewhat longer than the talonid, and the p4 trigonid is slightly shorter than the talonid. The p2 trigonid and talonid are of similar width, while the trigonids are narrower than the talonids in p3 and p4. The p2 paralophid projects anteriorly from the protoconid and there is only a slight lingual notch in the p2 trigonid. The p2 protolophid is short and posteriorly directed. The paralophid of p3 is angled about 45° lingually, creating a distinct lingual notch in the trigonid. The p3 protolophid is straight but positioned lingually. Finally, the p4 trigonid is essentially molariform with a lingually arching paralophid and protolophid. A distinct metaconid is seen only on the p4. The p2 talonid of CMNH 11382 is very simple; the cristid obliqua is not well developed and there is essentially no talonid basin or hypolophid. The p3 and p4 of CMNH 11382 have more well-developed cristids obliqua, elongate hypolophids, and broader basins.

Fig. 55. Mandible of *Wickia brevirhinus* (CMNH 11382). **(A)** Right view, **(B)** left premolars, **(C)** dorsal view.

The molars of *Wickia brevirhinus* are typical, with thinner lingual enamel, shallow talonid and trigonid basins, and an elongated m3. The labial cingulid is discontinuous around the bases of the cusps, but it is continuous between them. The m3 cingulum does not wrap around the distal end of the m3.

REMARKS

Wickia brevirhinus is based on a skull (CMNH 11380) from the Sand Wash Basin of Colorado. In addition, a partial skull and mandible (CMNH 11380) from the Sand Wash Basin and a partial skull (UCMP 81300) from the middle Adobe Town Member of the Washakie Formation of Wyoming are referable to *W. brevirhinus*. West and Dawson (1975) originally assigned two of these specimens, CMNH 11380 and CMNH 11382, to *Manteoceras pratensis* Cook (1926). However, *M. pratensis* is based upon a poorly preserved partial mandible with deciduous teeth and is considered a nomen dubium in this paper.

Nonetheless, West and Dawson (1975) noted that CMNH 11380 and CMNH 11382 share attributes with *Manteoceras manteoceras* (= *Telmatherium validus*) and *Metatelmatherium ultimum*. However, *Wickia brevirhinus* distinctly differs from both of these species due to a unique combination of characters. The skulls of *W. brevirhinus* differ most conspicuously from *Telmatherium validus* in the shorter nasal incision although there are other minor differences such as the narrower and shorter lateral nasal splint, less prominent parasagittal ridges, and minor anterolingual cingular cusps on the molars. *W. brevirhinus* differs from *Metatelmatherium ultimum* most conspicuously in the lack of a true sagittal crest, the lack of a large ventral flange on the zygomatic arch, and in having more prominent occipital pillars. Moreover, *W. brevirhinus* lacks the notch on the anterior rim of the foramen magnum that is seen in the type skull of *Metatelmatherium ultimum*. Finally, the p2 talonid of *W. brevirhinus* is poorly developed in comparison to *Telmatherium validus* or *Metatelmatherium ultimum*.

In many ways *Wickia brevirhinus* is morphologically intermediate between *Telmatherium validus* and *Metatelmatherium ultimum*. Temporally, it also bridges the gap between the late Bridgerian *T. validus* and the late Uintan *M. ultimum*. *W. brevirhinus* specimens from the Sand Wash Basin of Colorado are either latest Bridgerian or Early Uintan in age. The Washakie Basin skull, UCMP 81300, from above level 17 of Granger (1909), which occurs within the middle Adobe Town Member of the Washakie Formation (TWKA2), suggests an earliest Uintan age for *W. brevirhinus* (McCarroll et al., 1996b).

Metatelmatherium ultimum (Osborn, 1908a)

HOLOTYPE: AMNH 2060, a complete skull with right I2, C (partial), P1–M3, left I2–I3, C (partial), P1–M3, and a partial mandible with symphysis and right ramus with c (partial), p3 (partial), p4–m3.

TYPE LOCALITY: Myton Member (lower part of Uinta C) of the Uinta Formation of Utah.

SYNONYMS: *Manteoceras uintensis* Douglass, 1909; *Metatelmatherium cristatum* Granger and Gregory, 1938.

AGE: Middle Eocene (Uintan and Irdinmanhan land mammal "ages").

REFERRED SPECIMENS: **(From the Myton Member of the Uinta Basin of Utah)** AMNH 2004, an anterior portion of a skull with right I2 (partial), I3–M3, left I2 (partial), I3, and P3–M3; AMNH 2029, a crushed ventral surface of a skull with right P1, P2, P4, M1–M3 (partial), left P1–P4, and M1–M3 (all partial); AMNH 2033, a mandible with partial symphysis and right ramus with p2–m3; CMNH 2339, a partial skull with no teeth; CMNH 2388 (holotype of *Manteoceras uintensis*), a crushed anterior portion of a skull with right I1–M3, left I1, I3, C (partial), P1–P3, P4–M3 (all partial); CMNH 2354, a skull fragment with right P2–M1 and left P2–P4 (partial); **(from the Adobe Town Member of the Washakie Formation of Wyoming)** UCMP 81447, a skull with right I1–M3 (all broken) and left I3–M3; **(from the Wind River Basin, Hot Springs County, Wyoming)** YPM 14158, a skull with no complete teeth; **(from the "Irdin Manha" Formation [sensu Radinsky, 1964] Camp Margetts area, Inner Mongolia, China)** AMNH 26411 (holotype of *Metatelmatherium cristatum*), a complete skull with right and left I2–M3, and a mandible with right i1, i3–p1, p2 (partial), p3–m3, and left i1–m3.

DIAGNOSIS: *Metatelmatherium ultimum* is a large hornless brontothere. The frontal bone intrudes into the nasal bone and splits off a small lateral splint of nasal bone from

the main body of the nasal. The size and shape of the nasal splint is similar to that of *Wickia brevirhinus* and less pronounced than that of *Telmatherium validus*. The nasal incision is short and does not extend posteriorly beyond the P1. The nasal process is very short, horizontal, unelevated, of relatively constant transverse width, narrow, with thin and relatively deep lateral walls, and without a well-defined or strongly rounded distal margin. The orbits do not protrude laterally. The orbits are positioned directly above the M2 with the posterolateral root of M1 directly below the anterior rim of the orbit. The premaxillomaxillary rostrum deepens proximally and the rostral cavity is dorsally sealed by bone. Other cranial characteristics include a relatively flat dorsal cranial surface (from a lateral view), a short sagittal crest, an elevated occiput, deep and strongly curved zygomatic arches that are very strongly bowed laterally, a large ventral zygomatic flange on the jugal, and a ventrally open and mediolaterally angled external auditory pseudomeatus. Ventral sphenoidal fossae are absent.

Dentally, *Metatelmatherium ultimum* has large subcaniniform upper incisors, a simple P1, a distinct P2 metacone, a postcanine diastema, weak premolar preprotocristae, and short lingual crests extending posteriorly from the premolar protocones. Premolar hypocones are absent. The molars of *M. ultimum* have tall, lingually angled ectolophs with weak labial ribs, and thinned lingual ectoloph enamel with wedge-shaped paracones and metacones. Central molar fossae and cingular parastyle shelves are absent, but small anterolingual cingular cusps are present. The upper molars lack paraconules and metalophs. The lower dentition of *M. ultimum* includes large subcaniniform incisors that are all of similar size, a postcanine diastema, a p1–p2 diastema (variably present), an elongate p2 trigonid, a metaconid on p4 but not on p2 or p3, shallow molar basins, and a slender m3.

Metatelmatherium ultimum is most similar to *Telmatherium validus* and *Wickia brevirhinus*, but it is clearly distinct from these species primarily due to the unique combination of a very short nasal incision, a true sagittal crest, absence of strong occipital pillars, a deep notch in the dorsal rim of the foramen magnum, and a large ventral zygomatic flange.

Description

Skull: The holotype skull of *Metatelmatherium ultimum* (AMNH 2060) is nearly whole and undistorted (fig. 56). Only the nasal process is fragmentary, but it is nearly complete and has been reassembled and reattached to the skull. Seven other skulls from North America are referable to *M. ultimum*, as well as an associated skull and mandible from Asia (AMNH 26411) (fig. 57). The following description of the skull of *M. ultimum* is based primarily on the holotype but is supplemented by other specimens where noted.

Metatelmatherium ultimum is a relatively large (table 8) hornless brontothere whose skull most closely resembles those of *Telmatherium validus* and *Wickia brevirhinus*. Upon close inspection the sutures in the facial area are discernable in AMNH 2060 although they are indistinct. The sutures of the facial bones are more distinct in a referred specimen (YPM 14158) (fig. 58). The frontonasal suture recedes posteriorly toward the midline, but near the midline it is acutely redirected anteriorly. The nasal bone is split by a small triangular process of the frontal just above and anterior to the orbits. The small splint of nasal bone that branches off the main body of the nasal arches posteroventrally between the frontal and the maxilla. Below this splint, the nasomaxillary suture is strongly dorsally arched. The face of *M. ultimum* is tall and the maxilla forms a shallow preorbital fossa. The shape and configuration of the facial bones of *M. ultimum* most closely resembles that of *Wickia brevirhinus*. The frontonasal suture in *Telmatherium validus* is more pronounced, the triangular frontal process is longer, and the nasal splint is broader, longer, and more arched. Previous figures of AMNH 2060 incorrectly depicted the configuration of the facial sutures of *M. ultimum* (Osborn, 1908a: fig. 17; 1929a: figs. 126, 294–296, pl. 51a). In these earlier figures, the frontal bone is depicted as having a broad contact with the maxilla rather than being separated by the lateral nasal splint.

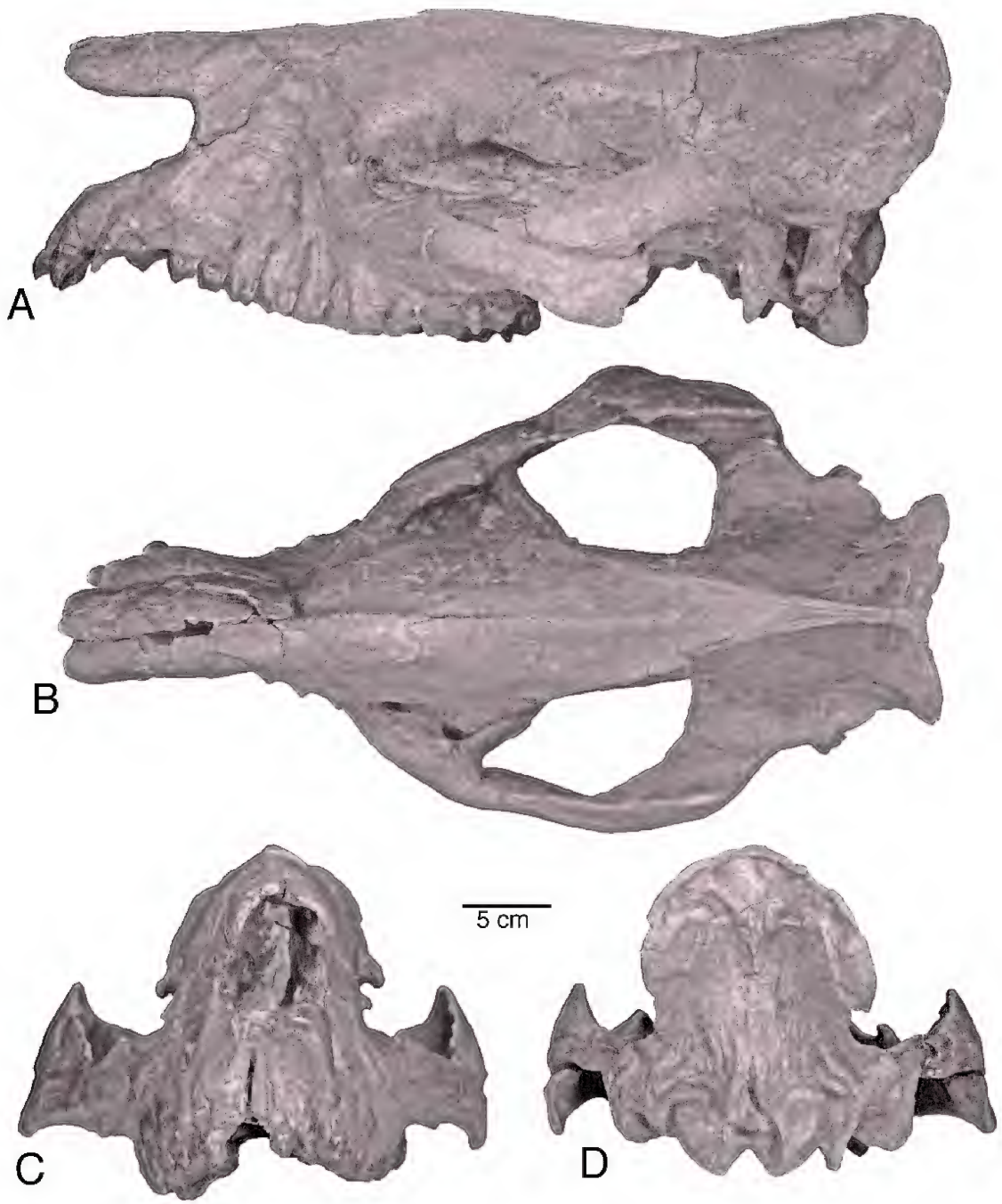

Fig. 56. Holotype skull of *Metatelmatherium ultimum* (AMNH 2060). **(A)** Left view, **(B)** dorsal view, **(C)** anterior view, **(D)** posterior view.

Earlier descriptions of *Metatelmatherium ultimum* are misleading in other respects. For instance, Osborn (1929a: 346) described "horn rudiments" in male skulls. He considered the holotype (AMNH 2060) to be a female skull but regarded AMNH 2004 as male. In reexamining AMNH 2004, the triangular frontal process does not form a

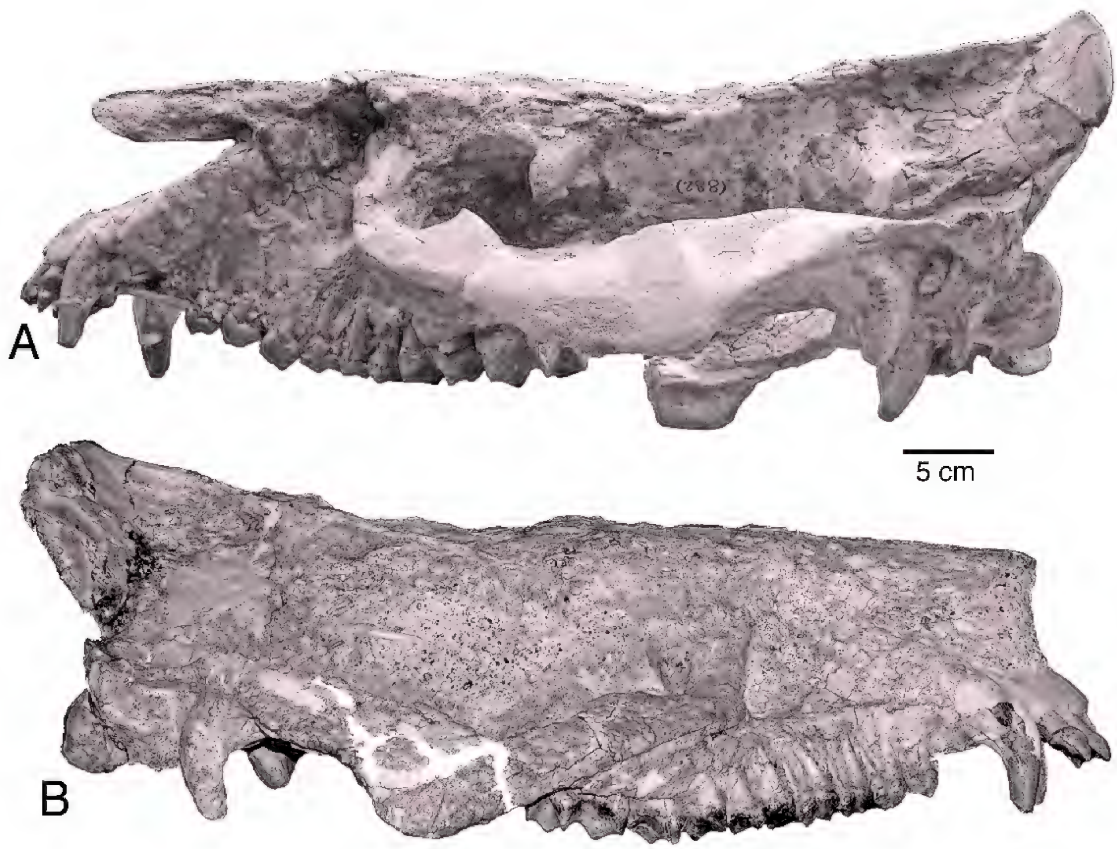

Fig. 57. Skull of *Metatelmatherium ultimum* (AMNH 26411) from Asia. **(A)** Left view, **(B)** right view.

thickened protuberance; nor can I find a structure that could be interpreted as a "horn rudiment" in any other specimen of *M. ultimum*.

The nasal incision of *Metatelmatherium ultimum* is very short; in AMNH 2060 it extends only to the anterior margin of the P1. The position of the posterior margin of the nasal incision is similar to that of *Wickia*, but much shorter than *Telmatherium*. Because of the short nasal incision the preorbital region of the face appears to be quite long. The orbits are positioned directly above M2 while the posterior lateral root of M1 is positioned directly below the anterior rim of the orbit.

The nasal bones are poorly fused. The nasal process is thin, projects horizontally from the skull, and is shorter than the premaxillomaxillary rostrum. In the holotype the nasal process is straight with a flat dorsal margin. The sides of the nasal process form deep, thin, and vertical lateral walls. The depth of the lateral walls is relatively constant throughout the length of the nasal process, but they become shallower at the very distal end. From a dorsal view the nasal process is narrower than the rostrum. Other specimens with more intact nasal processes (e.g., AMNH 2004, CMNH 2339) are morphologically consistent with that of the holotype. These specimens also more clearly reveal that the anterior edge of the nasal process is thin, roughened, and very slightly downwardly deflected.

From the lateral view the dorsal border of the premaxillomaxillary process is steeply sloped posterodorsally so that the posterior margin of the nasal incision is elevated to the level of the upper rim of the orbit. The rostral cavity is open dorsally. The premaxillomaxillary suture is clearly visible on the right side of AMNH 2060 and the premaxilla termi-

TABLE 8
Summary statistics for selected morphometric variables of *Metatelmatherium ultimum*
See Methods for measurement definitions

	N	Mean	SD	Min.	Max.	CV
C L	5	25.6	5.6	17.6	32.4	21.8
P3 L	7	24.1	3.4	20.0	28.3	13.9
P3 W	7	27.9	3.6	22.1	31.3	12.8
M2 L	4	53.9	3.2	51.1	58.1	6.0
M2 W	4	53.1	3.2	48.7	56.5	6.1
P2–P4	6	70.5	8.7	56.3	82.4	12.3
M1–M3	5	131.3	12.8	110.6	144.7	9.8
VL	5	535.4	44.7	475	570	8.4
c L	1	26.4		26.4	26.4	
p3 L	2	24.2	0.74	23.7	24.8	3.1
p3 W	2	17.3	1.6	16.2	18.5	9.2
m2 L	3	48.1	1.2	46.8	49.1	2.5
m2 W	3	29.9	1.5	28.4	31.3	4.9
p2–p4	2	75.7	2.5	74.0	77.5	3.3
m1–m3	3	153.1	4.4	148.4	157	2.9

nates near the posterior notch of the nasal incision. There is no contact of the nasal and premaxillary bones. The premaxillae are not co-ossified at the symphysis. The premaxillae are not nearly as massive as those of *Wickia*.

Like *Wickia*, the skull of *Metatelmatherium ultimum* is tall and the occiput is elevated. This condition is most extreme in CMNH 2339 (fig. 59). From a lateral view, the dorsal surface of the skull is flat or slightly convex over the orbits. Postorbitally, the dorsal surface is flat, although it is angled posterodorsally. From the dorsal view of AMNH 2060 the skull is very narrow between the orbits. From the anterior view the dorsal cranial roof is vaulted. The appearance of a narrow arched skull roof seems to be slightly exaggerated by some lateral crushing in the holotype. In specimens that are less laterally crushed (e.g., CMNH 2399, YPM 14158, UCMP 81477), the dorsal roof of the cranium is wider and less vaulted than that of the holotype. Nonetheless, the superorbital dorsal skull roof is narrow in *M. ultimum*. The parasagittal ridges merge posteriorly to form a short but thin sagittal crest. Each parasagittal ridge forms a prominent ridge on the sagittal crest, although there is no distinct median pit between the parasagittal ridges as seen in *Telmatherium*.

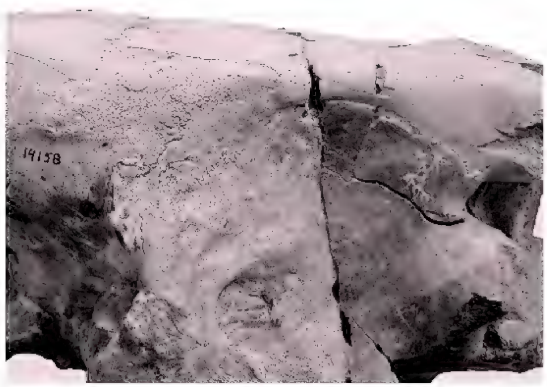

Fig. 58. Close-up view of the right face of a skull of *Metatelmatherium ultimum* showing the configuration of the maxilla, nasal, and frontal bones. (Courtesy of Division of Vertebrate Paleontology, YPM 14158. © 2005 Peabody Museum of Natural History, Yale University, New Haven, Connecticut, USA. All rights reserved.)

From a dorsal view of AMNH 2060 the nuchal crest is very thin and concave. From a lateral view the occiput is slightly tilted backward. From a posterior view, the nuchal crest is strongly arched dorsally. The dorsal portion of the occiput is somewhat narrower than the ventral portion and the middle of the occiput is constricted. The occiput of AMNH 2060 is unusual in a number of respects. The entire surface of the occiput is roughened, particularly above the occipital condyles and below the nuchal crest. Two

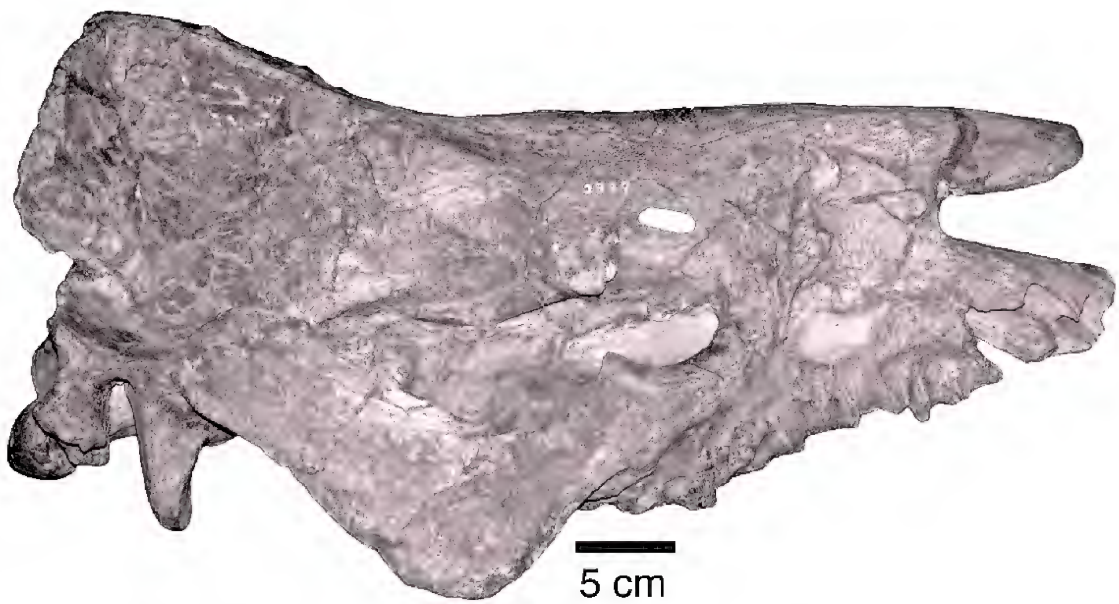

Fig. 59. Lateral right view of a skull (CMNH 2339) of *Metatelmatherium ultimum*.

short crests originate near the top of the nuchal crest and converge ventromedially into a small process in the central depression of the occiput. The thick occipital pillars seen in most other brontothere skulls are not discernable in AMNH 2060. Finally, there is a tall and narrow median notch on the upper margin of the foramen magnum. On the lateral edges of this notch are two elongate, smooth, facetlike surfaces.

The zygomatics of *Metatelmatherium ultimum* are deep, relatively thin, and very strongly bowed laterally. The jugal portion of the zygomatic process is angled downward at a shallow angle, while the squamosal portion of the zygomatic is steeply angled posterodorsally, giving the zygomatic arch a strong curvature. The curvature of the zygomatic is exaggerated by a large flange on the ventral margin of the zygomatic process of the jugal just below the junction with the squamosal. A similar flange is occasionally seen on the skulls of other brontotheres (e.g., *Epimanteoceras formosus*), but it is always less conspicuous in comparison to *M. ultimum*, where the ventral zygomatic flange is pronounced and greatly influences the overall appearance of the zygomatic arch. The ventral flange is always conspicuous but its size varies; in CMNH 2339 the prominence of the ventral zygomatic flange is extreme (fig. 59). An infraorbital process of the jugal, such as that of *Sphenocoelus*, is not seen in *M. ultimum*.

In AMNH 2060, the posterior nares are rimmed by a narrow horseshoe-shaped emargination (fig. 60a). The anterior rim of the posterior nares is situated between the anterior edges of the M3s. In other specimens, the anterior rim of the posterior nares fluctuates in its position from between the anterior edge of M3 to between the protocones of M2. A thin ridge of bone runs along the midline of the palate and extends past the anterior margin of the posterior nares. The posterior narial canal does not extend into the basisphenoid bone. The thin vomerine septum that bisected the posterior narial canal is not preserved in AMNH 2060, although remnants of it can be seen in the roof of the posterior narial canal. The basicranium of AMNH 2060 is quite short. The configuration of the basicranial foramina is typical, with the foramina of the alar canal, the foramen ovale, and the foramen lacerum being widely separated. The external auditory pseudomeatus is narrow; however, the mastoid process does not make contact with the postglenoid process and the external auditory pseudomeatus is unconstricted ventrally.

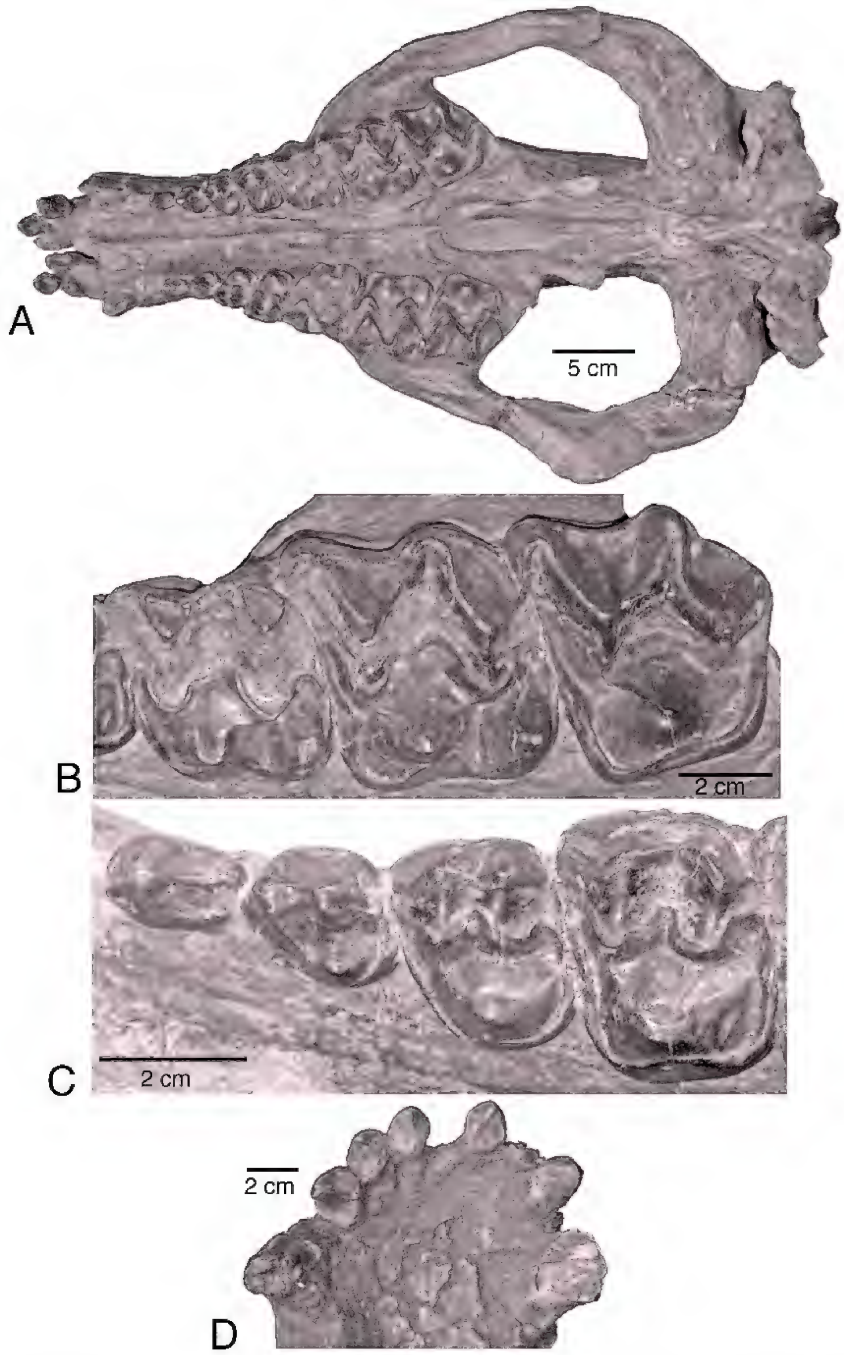

Fig. 60. Ventral view of the skull and upper dentition of *Metatelmatherium ultimum*. **(A)** Ventral view, **(B)** left molars, and **(C)** left premolars of AMNH 2060, **(D)** upper incisors and canines of CMNH 2388.

Upper Dentition: The following description of the upper dentition is primarily based on the holotype (AMNH 2060) (fig. 60a–c), although this specimen has an incomplete incisor row. The incisors of AMNH 2060 are large and arch anterior to the canines. Alveoli indicate three pairs of incisors. The I1 crowns of AMNH 2060 are

not preserved, although the root of the left I1 is preserved. Judging by the root of I1 it was the smallest incisor. The complete I1s of CMNH 2388 (fig. 60d) confirm that the I1 is the smallest incisor. The I1 is subcaniniform and similar in shape to the I2 and I3. I2 and I3 are large and subcaniniform with a single lingually curved cusp and a very thin lingual cingulum. No labial cingula are seen on the upper incisors. The I3 is larger in diameter and taller than the I2. The canine is bordered by a short precanine diastema and a longer postcanine diastema. The crowns of both canines are fragmentary in AMNH 2060, but in other specimens the canines vary in size from moderate to relatively large, except in the Asian skull (AMNH 26411), which has very large canines.

P1 is relatively large. It is about the same length as P2, but it is narrower and with a simpler morphology, including a single cusp and a posterior heel. A thin cingulum can be seen in the lingual side of the posterior heel. The posterior heel of the P1 of the Asian specimen (AMNH 26411) is somewhat wider than those of the North American specimens. There is no P1–P2 diastema in any specimen. The P2 of AMNH 2060 is oblique in shape due to the steeply posterolingually angled anterior margin. P2 is less oblique in AMNH 2004, although the P2s of other specimens are more similar to the holotype in this respect. In AMNH 2060 and other specimens P3 is much less oblique and P4 is not oblique.

The P2 parastyle and metastyle arch slightly lingually, while the P3 parastyle and metastyle are nearly straight. The P4 parastyle is strongly angled lingually, while the metastyle is straight. Because of these shape differences the outer wall of the ectoloph of P2 is more curved than those of P3 and P4. In AMNH 2060 each premolar (P2–P4) has a small distinct labial paracone rib though the ectolophs are too worn to compare their relative sizes. The premolars of AMNH 2004 are less worn and reveal that the labial paracone ribs are distinct and become narrower and shorter in more posterior premolars.

On the P2 of AMNH 2060 there is a small protocone with a small but distinct preprotocrista and a short lingual crest extending posteriorly from the protocone. The lingual morphology of P2 varies in other skulls. For instance, on the P2 of AMNH 2004 there is no distinct protocone; instead, a large crest arches around the lingual side of the crown. The lingual heels of P3 and P4, though larger and wider than that of P2, have less distinct preprotocristae and less distinct lingual crests. There are no hypocones on any premolars of *Metatelmatherium ultimum*. The labial cingula of the premolars tend to be discontinuous around the paracones except on the P4. The lingual cingula of the P2–P4 vary from being completely continuous to slightly discontinuous around the protocone.

The molars of AMNH 2060 are heavily worn and M1 and M2 have been shortened by interstitial wear. The M3 is minimally worn and preserves a number of brontotherine traits including tall, lingually angled ectolophs, weak labial ribs, thin lingual ectoloph enamel, and wedge-shaped lingual sides of the paracone and metacone. The anterior cingulum is thin and passes proximally to the distal peak of the parastyle. There is a small anterolingual cingular peak on each molar. Central molar fossae are absent. The molars have no visible remnants of paraconules or metalophs. There is no hypocone on the M3, but a thick cingulum traces around the distolingual corner of the M3 crown. The labial molar cingula tend to be thick at the bases of the cusps, but they are discontinuous around the mesostyles. The lingual cingulum of the molars is thick, but it is only continuous around the base of the protocone of the M3.

Mandible and Lower Dentition:
The holotype of *Metatelmatherium ultimum* (AMNH 2060) includes an associated partial mandible with p4–m3. Another partial mandible, AMNH 2033, is consistent with the holotype mandible, and has a nearly complete symphysis with complete p2–m3 (fig. 61). The mandible associated with the Asian skull, AMNH 26411, is fully complete with a nearly complete set of lower dentition (fig. 62).

In comparison to AMNH 26411, the partial mandible of AMNH 2033 has a slightly more slender coronoid process and a somewhat narrower symphysis with a steeper inferior margin. However, these

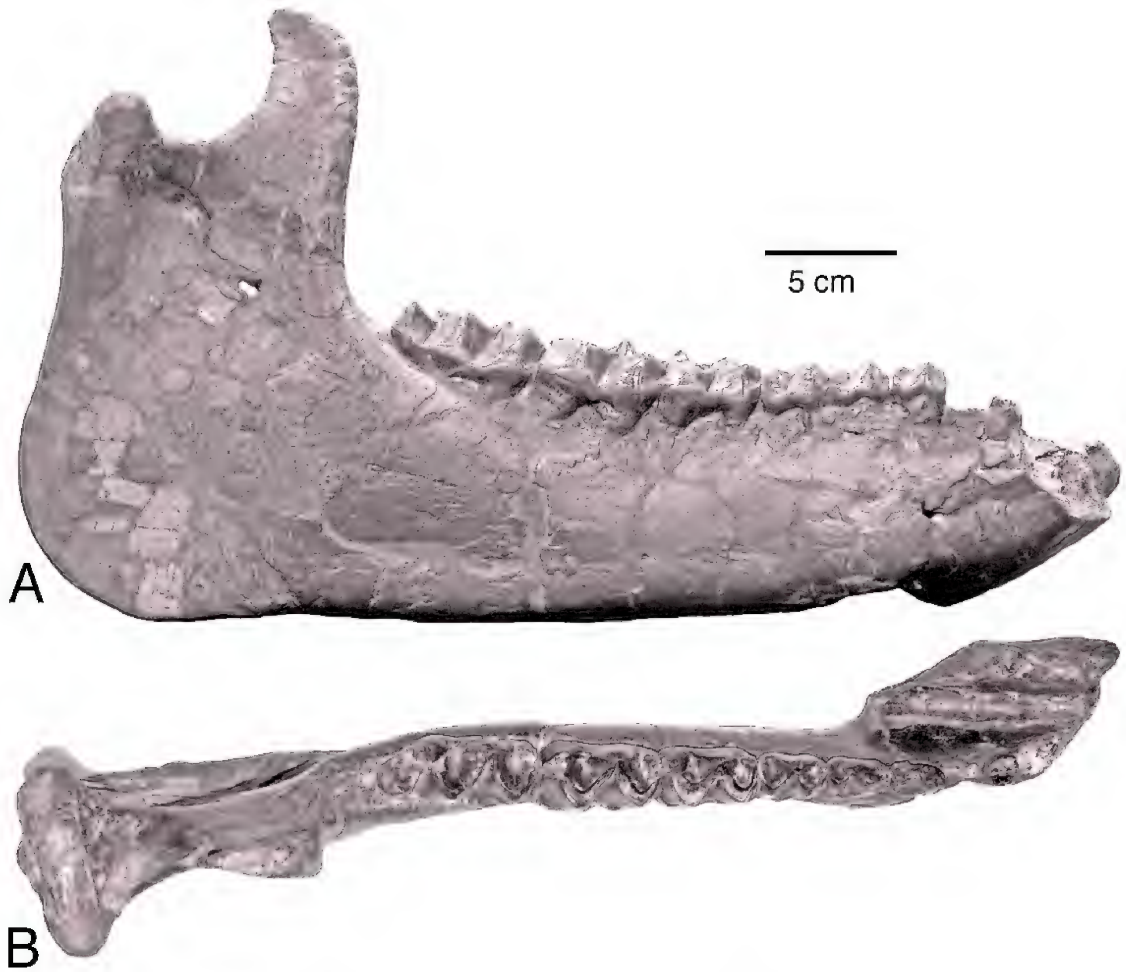

Fig. 61. Mandible of *Metatelmatherium ultimum* (AMNH 2033). **(A)** Right view **(B)** dorsal view.

differences could be attributed to distortion and damage in AMNH 26411. The coronoid process of AMNH 26411 is crushed and partially reconstructed with plaster. In addition, the symphysis has gaps that are filled with plaster and the seemingly wider symphysis and shallower inferior margin could relate to the way in which this specimen has been distorted and subsequently reconstructed. Additionally, the larger canines of the Asian specimen, with their rather bulbous roots, influence the size and shape of the symphysis. The posterior margin of the mandibular symphysis fluctuates in position from between the talonid of the p2 (AMNH 26411) to between the anterior margins of the p3 (AMNH 2033).

The lower incisors of AMNH 26411 are somewhat smaller than the upper incisors of the same specimen. The incisor row forms a short arch anterior to the canines. The apex of i1 is rounded although this seems due to wear. The i2 is larger and the apex is much more pointed. The i3 is about the same size as i2, although it is stouter and more subcaniniform. Lingual cingulids can still be discerned on these incisors, but labial cingulids are absent. The extremely procumbent condition of the incisors of AMNH 26411 is an artifact of distortion. In life the lower incisors would have been more nearly vertical. The canines of the Asian specimen are relatively large. There is no precanine diastema, but the postcanine

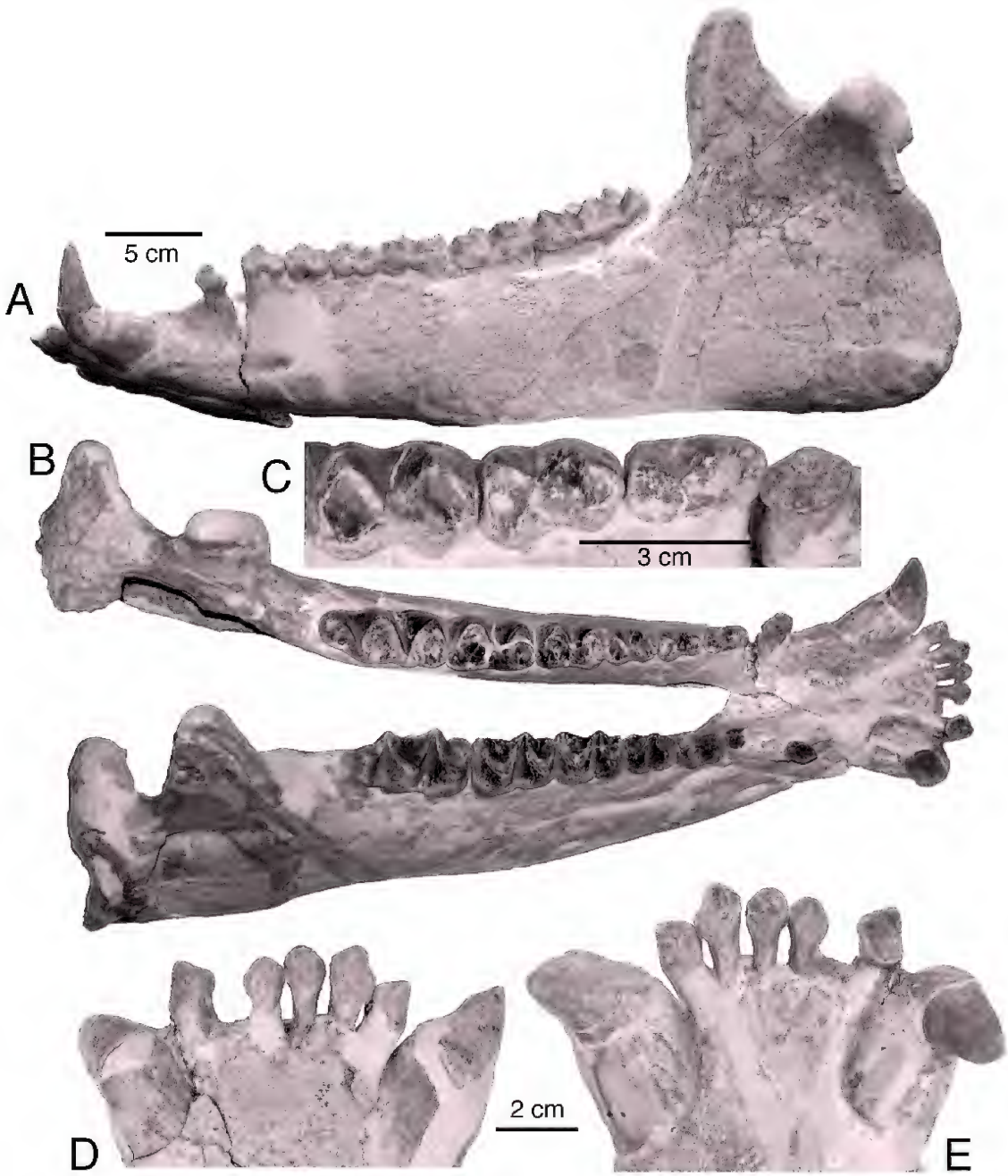

Fig. 62. Mandible of *Metatelmatherium ultimum* (AMNH 26411) from Asia. **(A)** Left view, **(B)** dorsal view, **(C)** left premolars, **(D)** labial view of incisors and canines, **(E)** lingual view of incisors and canines.

diastema in these specimens is relatively longer.

The p1 of AMNH 26411 is small and simple with a single cusp and a short talonid heel. AMNH 2033 has a short p1–p2 diastema. However, AMNH 26411 lacks a p1–p2 diastema. The p2 trigonid is nearly twice as long at the talonid. The p3 trigonid is somewhat longer than the talonid. The talonid and trigonid of the p4 are of similar

length. The trigonids of p2, p3, and p4 are narrower than the talonids. The p2 paralophid curves slightly lingually as it projects from the protoconid, creating a slight lingual notch in the trigonid. The p2 protolophid is straight but slightly angled lingually. The paralophid of p3 is angled about 45° lingually, creating a distinct lingual notch in the trigonid. The p3 protolophid is straight but weakly angled in the lingual direction. Finally, the p4 trigonid is essentially molariform with a lingually arching paralophid and protolophid. A distinct metaconid is seen only on the p4. The talonids of the p2–p4 are well developed with distinct cristids obliqua and hypolophids. The lingual surface of the p2 talonid forms a steeply sloped surface, although the p3 and p4 have nearly molariform talonid basins.

The molars of *Metatelmatherium ultimum* are typical with thinner lingual enamel, shallow talonid and trigonid basins, and an elongated m3. The labial cingulid is discontinuous around the bases of the cusps. The m3 cingulid does not wrap around the distal end of the m3.

Remarks

Osborn (1908a) originally referred *Metatelmatherium ultimum* to the genus *Telmatherium*. Although this species was based on a very well-preserved skull and a partial right mandible (AMNH 2060), Osborn's (1908a) initial description amounted to no more than four brief sentences. Douglass (1909) named another species, *Manteoceras uintensis*, on an anterior portion of a cranium with a complete set of upper dentition (CMNH 2388). Douglass' only stated reason for differentiating this species from *Telmatherium ultimum* is, at best, a dubious distinction, "The zygomatic arch is not very heavy.... It is not nearly so heavy as in *Telmatherium ultimum*" (Douglass, 1909: 307). The figure of CMNH 2388 in Douglass (1909: figs. 4, 5) shows this specimen to be more complete and better preserved than it actually is. Although the specimen is figured as having zygomatic arches, only the anteriormost portion of the right arch is actually preserved.

Osborn (1929a) continued to accept *Telmatherium ultimum* and *Manteoceras uintensis* as separate species, and he believed them to belong to different lineages. He distinguished *M. uintensis* from *T. ultimum* based on "the obliquely flattened form of the infraorbital portion of the malars" (Osborn, 1929a: 374). However, when one considers that the specimens are subtly distorted in different dimensions, one cannot realistically consider this difference as significant. Mader (1989) considered these two species to be synonymous and that revision is upheld here.

Granger and Gregory (1938) named a new genus and species, *Metatelmatherium cristatum* from a complete skull and mandible (AMNH 26411) from the Camp Margetts area of Inner Mongolia. Granger and Gregory (1943) noted that North American specimens referred to *Telmatherium ultimum* are nearly identical to *M. cristatum*. Therefore, they referred the North American species, *T. ultimum*, to their new genus, *Metatelmatherium*. They noted that the type skull of the North American species "so closely resembles the type of our *Metatelmatherium cristatum* that one can barely discover specific differences between them, while their congeneric relationship becomes more evident the longer they are studied" (Granger and Gregory, 1943: 356).

Granger and Gregory (1943) distinguished *Metatelmatherium cristatum* from *M. ultimum* by its apparently larger size, the shorter and broader coronoid process, and the relatively longer and more sloping mandibular symphysis. However, all of these distinctions are dubious. The Asian skull is larger than the holotype but not significantly. In fact, many of its dimensions fall well within the range of North American *M. ultimum*. Though the skull is uncrushed, it has experienced severe expanding matrix distortion (sensu White, 2003). The skull looks larger than it probably was when it was intact, and some aspects of its shape could be subtly distorted. In the jaw of the Asian specimen the coronoid process is fragmented, its distal tip is missing, and there are copious amounts of plaster filling gaps between the bone fragments. The symphysis seems wider that that of the North American specimen, AMNH 2033. However, there are large amounts of plaster in the mandibular symphysis of the Asian jaw, and the degree to

which the shape of the symphysis has been influenced by distortion and reconstruction is uncertain. Given the variability in canine size of other brontotheres species, the influence that the unusually large canine of the Asian specimen had on the overall shape of the anterior portion of the mandible is probably not taxonomically significant. Another difference, the wider posterior heel of the P1, is not much more compelling particularly when one considers the high level of intraspecific variation in brontothere premolars. For instance, wide and narrow P1 posterior heels can be found in a single individual of *Protitanotherium emarginatum* (YPM PU11242).

In more recent revisions Mader (1989; 1998) continued to recognize *Metatelmatherium cristatum* and *M. ultimum* as distinct species. However, *M. cristatum* Granger and Gregory (1938) is here considered to be a junior synonym of *Metatelmatherium ultimum* (Osborn, 1908a). Thus, *M. ultimum* becomes the type species of *Metatelmatherium*.

Metatelmatherium ultimum as defined here primarily occurs in the late Uintan deposits of the Uinta Basin, but it is also known from the Adobe town member of the Washakie Formation (UCMP 81447), the Wind River Basin (YPM 14158), and the "Irdin Manha" (put in quotes to denote uncertain relationship with the type Irdin Manha beds [Radinsky, 1964]) of the Camp Margetts area of Inner Mongolia (AMNH 26411). These specimens are morphologically consistent with the *M. ultimum* material from the Uinta Formation, although the Washakie Basin specimen is notably smaller and could represent an earlier (early Uintan) species of *Metatelmatherium*, although, based on the present material, the only differentiating factor would be size. Presently, I include this specimen with *M. ultimum*.

Some authors have not accepted the generic distinction of *Metatelmatherium* from *Telmatherium* (Qi, 1987), while most others have accepted it (Russell and Zhai, 1987; Prothero, 1996; Mader, 1989, 1998). *Metatelmatherium ultimum* is similar to *Telmatherium validus*, but can be differentiated from it on the following features: the very large ventral flange on the zygomatic arch, the extremely shallow nasal incision, short nasal processes, thinner sagittal crest, the narrow vaulted cranial roof, and small anterolingual cingular peaks on the molars. *M. ultimum* is more similar to *Wickia brevirhinus*, but it can be distinguished from that species primarily by the large autapomorphic ventral zygomatic flange, thin sagittal crest and, possibly, the more developed p2 talonid. Several other species have been assigned to *Metatelmatherium*, although they are all now considered to be nomina dubia and are further discussed in the section dealing with miscellaneous dubious taxa.

Epimanteoceras formosus Granger and Gregory (1943)

HOLOTYPE: AMNH 21613, a complete skull with complete dentition.

TYPE LOCALITY: Ulan Shireh Formation, four miles north of Tukhum Lamasery, Inner Mongolia, China.

AGE: Middle Eocene (Irdinmanhan land mammal "age").

SYNONYMS: *Dolichorhinoides angustidens* Granger and Gregory, 1943.

REFERRED SPECIMEN: **(From the Ulan Shireh Formation, eight miles north of Tukhum-in-Sumu, Inner Mongolia)** AMNH 21607 (holotype of *Dolichorhinoides angustidens*), a partial skull with right P1–M3, left P4 (partial), and M1–M3.

DIAGNOSIS: *Epimanteoceras formosus* is a large brontothere with poorly developed frontonasal horns. The frontal bone intrudes into the surface of the nasal bone, thus splitting off a lateral nasal splint from the main body of the nasal bone. Some specimens of *Epimanteoceras formosus* exhibit a distinct but weakly developed frontonasal protuberance. The nasal incision extends as far back as the P2. The nasal process broadens distally; it is nearly horizontal, unelevated, narrow, with thin lateral walls, and without a well-defined or strongly rounded distal margin. The orbits are positioned above the posterior portion of M2 and the anterior portion of M3. The orbits do not protrude laterally. The premaxillomaxillary rostrum deepens posteriorly and it is not enclosed by bone dorsally. Other cranial characteristics include a dorsal cranial surface that is convex but incompletely saddle-

shaped, separated parasagittal ridges, distinctly curved zygomatic arches, and a ventrally open and mediolaterally angled external auditory pseudomeatus. Additionally, *E. formosus* is unique in having a very robust superorbital process and a distinct lateral temporal ridge.

Epimanteoceras formosus has subcaniniform upper incisors, a metacone on the P1, a distinct P2 metacone, and weak premolar preprotocristae. Premolar hypocones are present and connected to the protocones, but they are small and occasionally absent in some of the premolars. The molars of *E. formosus* have tall, lingually angled ectolophs with weak labial ribs, and thinned lingual ectoloph enamel with wedge-shaped paracones and metacones. A cingular parastyle shelf is absent. Central molar fossae are present, however, anterolingual cingular cusps are absent. Paraconules and metalophs are absent.

The skull of *Epimanteoceras formosus* is morphologically intermediate between *Telmatherium* and *Protitan*. It can be most easily distinguished from the former by its greater size, more widely separated parasagittal ridges, and distinct central molar fossae. It can be distinguished from the later by its more weakly developed frontonasal protuberance, incompletely saddled-shaped cranium, and lack of a postzygomatic process. The upper premolars are significantly more molarized than either *Protitan* or *Telmatherium*.

Description

Skull: *Epimanteoceras formosus* is a large brontothere that is most similar in size to *Protitan grangeri* and *Protitanotherium emarginatum*. This species is known from a nearly complete and undistorted holotype skull (AMNH 21613) (fig. 63). The only significantly reconstructed portion of the skull is the left posterior region. An additional partial skull, AMNH 21607, is referable to *E. formosus* (fig. 64). This skull is less complete, laterally compressed, and the dorsal surface is distinctly warped; however, this skull is superior to the holotype in some ways; it is ontogenetically younger than the holotype with less worn cheek teeth and more distinct cranial sutures. Additionally, this specimen was less extensively prepared and some aspects of the ventral surface of the skull are less damaged and not covered with plaster.

It can be seen on AMNH 21613 and even more clearly on AMNH 21607 that the distinctive configuration of facial bones seen in some hornless brontotheres, such as *Telmatherium*, is shared by *Epimanteoceras formosus*. A large triangular process of the frontal bone splits the posterolateral portion of the nasal bone. Dorsally, the frontonasal suture recedes posteromedially, but at the midline it is acutely reoriented anteriorly. Laterally, the frontonasal suture is directed sharply backward toward the orbit. The lateral nasal splint arcs posteroventrally and contacts the lacrimal bone, thus preventing contact of the maxilla and frontal bone. The nasomaxillary suture is less distinct than the frontonasal suture (and cannot clearly be seen in the photo), but it forms a dorsally arched contact between the lateral nasal splint and the maxilla.

In AMNH 21613 the overlapping frontal process forms a small but distinct protuberance above and directly anterior to the orbit. This frontonasal protuberance is not as well developed as those of *Protitan* species, but it is more distinctly more developed than that of *Telmatherium* in which the triangular frontal process is flush with the dorsal surface of the skull. In addition to the frontal nasal protuberance, AMNH 21613 has a very thick and prominent superorbital process that overhangs the orbits. This superorbital process is thickened with a roughened surface that is semicontinuous with that of the frontonasal protuberance. In AMNH 21607, the triangular process does not form a distinct frontonasal protuberance and it is smooth and nearly flush with the surface of the skull. Likewise, the superorbital processes seem less laterally prominent but this could be attributed to the fact that the skull is laterally compressed, and/or that the specimens is ontogenetically younger than the holotype skull.

The maxilla forms a shallow preorbital concavity. The face is only moderately constricted by the nasal incision, which extends to a point above the anterior margin of P2. The orbit is positioned over the

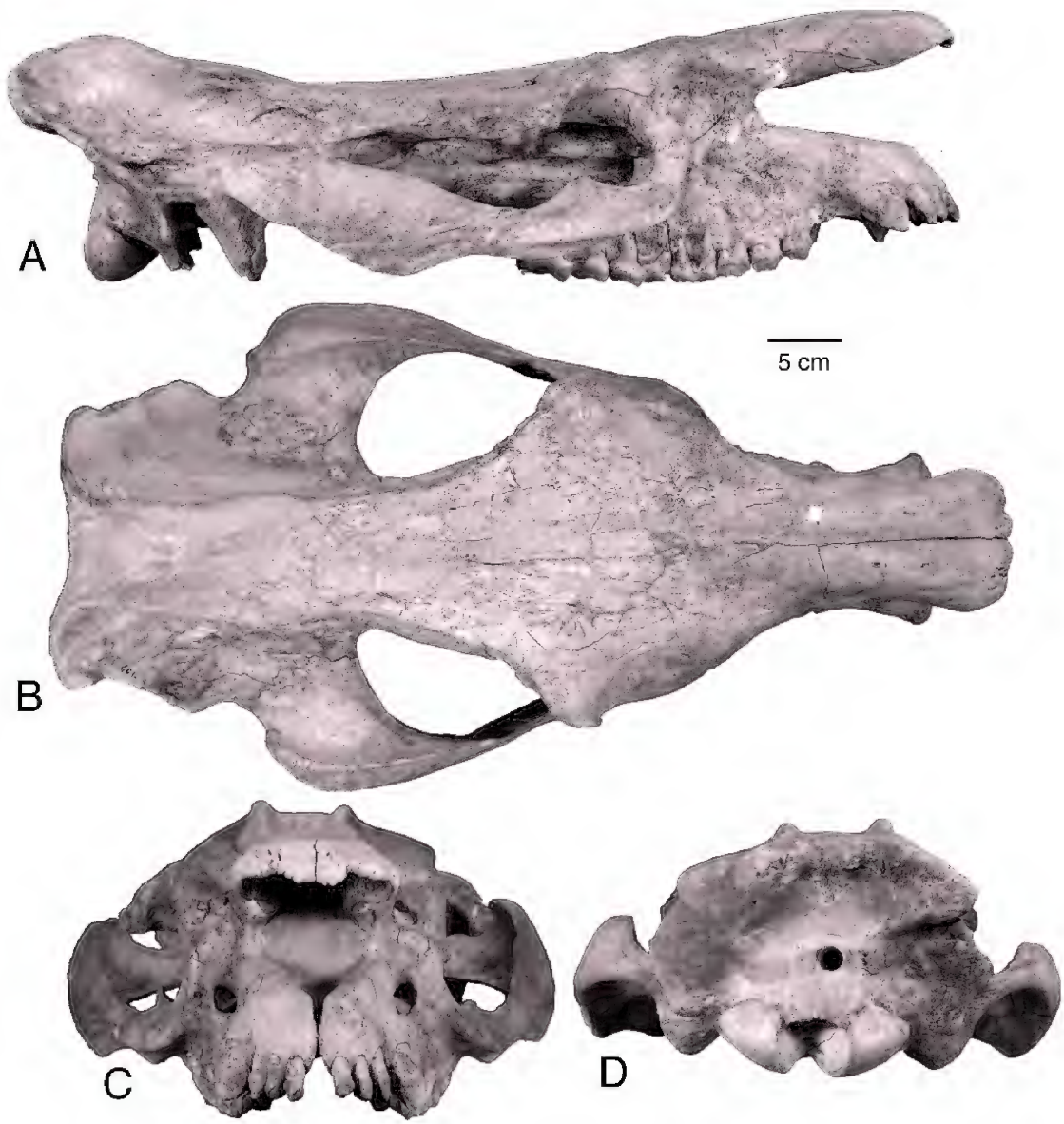

Fig. 63. The holotype skull of *Epimanteoceras formosus* (AMNH 21613). **(A)** Right view, **(B)** dorsal view, **(C)** anterior view, **(D)** posterior view.

anterior portion of M3 and the posterior portion of M2. The anterolateral root of M2 and posterolateral root of M1 rest directly below the anterior rim of the orbit.

The nasal process is the same length as the premaxillomaxillary rostrum. The nasal process of AMNH 21613 is nearly straight and the dorsal surface of the nasal process is slightly convex from the lateral view. The nasal process projects anteriorly from the skull in a slightly upward direction. In contrast, the nasal process of AMNH 21607 has a slight downward curvature. This subtle difference in nasal orientation may relate to taphonomic distortion in the latter specimen. The sides of the nasal process form deep and thin vertical walls that extend to the distal end of the nasal process. From the dorsal view it can be seen that the nasal bones are poorly ossified. The nasal process is narrower

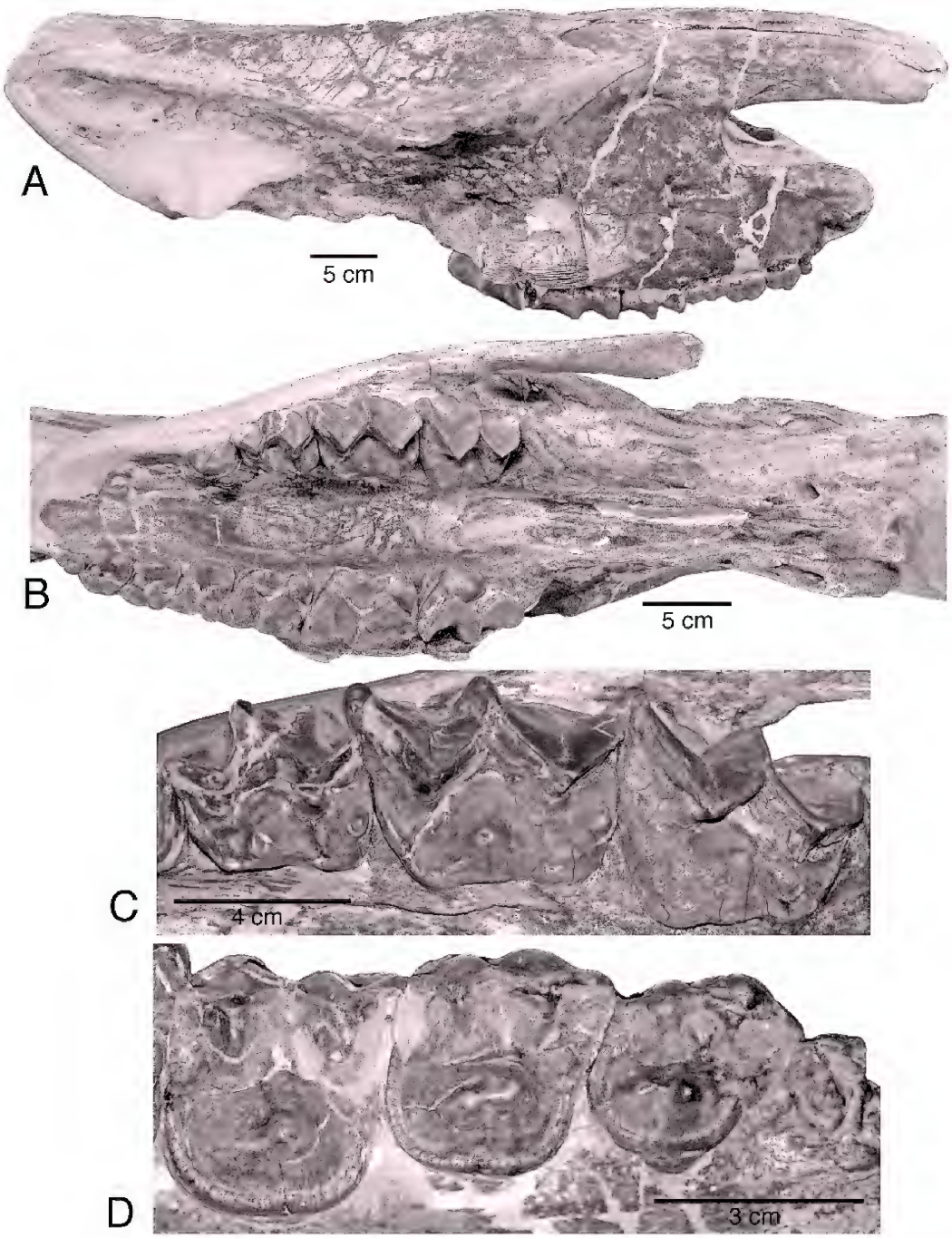

Fig. 64. A skull (AMNH 21607) referred to *Epimanteoceras formosus*. **(A)** Right view with skull rotated slightly to see to dorsal surface, **(B)** ventral view, **(C)** left molars, **(D)** right premolars.

than the premaxillomaxillary rostrum, although the nasal process significantly broadens distally. The distal edge of the nasal process is thin, roughened, and nearly flat from a dorsal view. However, the anterior view reveals that the anterior edge is turned downward. The mesiodistal corners of each nasal bone form a single downturned distal tip.

The premaxillomaxillary rostrum is robust and from a lateral view it appears to deepen in a posterior direction. The dorsolateral surface of the rostrum rises posteriorly at a shallow angle so that the posterior notch of the nasal incision is level with the upper rim of the orbit. The premaxillomaxillary suture is distinct in AMNH 21613. The nasal processes of the premaxillae are truncated anterior to the posterior notch of the nasal incision and do not contact the nasal bone. The premaxillary symphysis of AMNH 21613 is not ossified. From the anterior view the lateral margins of the rostrum are posterolaterally divergent and the rostral cavity is open dorsally and continuous with the nasal cavity.

The dorsal surface of the skull of *Epimanteoceras formosus* forms a shallow concavity. However, the skull is incompletely saddle-shaped; the dorsal surface is flat or slightly convex posteriorly. From a dorsal view the parasagittal ridges remain separate throughout their length and only moderately constrict the dorsal surface posteriorly. The parasagittal ridges are prominent and they can be seen standing out in relief from the posterior view of AMNH 21613.

The zygomatic arches are rather thin. From a dorsal view the jugal portion of the zygomatic is straight and strongly angled posterolaterally. From a lateral view the jugal portion is shallow and horizontal, while the squamosal portion of the zygomatic arch is deeper and rises posteriorly at a shallow angle, thus giving the zygomatic arch a distinct curvature. A small ventral flange can be seen below the jugal-squamosal contact, but this flange is not nearly as conspicuous as that of *Metatelmatherium*. A postzygomatic process, as seen in *Protitan*, is not present. One peculiar aspect of the skull of *Epimanteoceras formosus* is the presence of a prominent temporal ridge that extends anteroposteriorly on the lateral surface of the skull behind the zygomatic arch.

The occipital region is the least well-preserved portion of the holotype specimen. From the right side it can be seen that the occiput is strongly tilted backward. From a dorsal view the nuchal crest is mildly concave. From the posterior view the dorsal margin is weakly dorsally arched. The upper half of the occiput is somewhat narrower than the lower half and it appears to be somewhat constricted in the middle. One can discern a weak occipital pillar on the right posterior surface of the occiput although few other details of the occiput are preserved.

The posterior nares of both specimens of *Epimanteoceras formosus* are rimmed by a U-shaped emargination (figs. 64b, 65a). The posterior narial canal is elongate, but it does not extend into the basisphenoid. The anterior margin of the posterior nares is positioned between the M3 protocones in AMNH 21613, although the exact edge is obscured by plaster that fills the posterior narial canal. In AMNH 21607 the anterior edge of the posterior nares is slightly anterior to the M3 protocones. Many details of the holotype specimen are obscured by plaster filling the posterior narial canal. However, in AMNH 21607 many of the thinner more fragile elements of the posterior narial canal can be seen (fig. 64b). A thin, raised, horizontal plate of bone extends posteriorly from the palatal margin of the posterior nares and covers the choanae to a point behind M3. A large crack can be seen running through this bony palatal extension and the posterior portion is crushed. Behind the palatal extension, the posterior narial canal is filled with sediment. The thin elongate vomer can be seen bisecting the posterior narial canal. Two thin and broken choanal pouches of bone suspended in the remaining sediment are exposed directly behind the secondary bony palate. These bony pouches most likely represent posteriorly shifted maxilloturbinates, as seen, for instance, in *Dolichorhinus*. Behind these choanal pouches, the sediment filling the posterior half of the right posterior naris is free of any bone fragments. The left posterior naris has been filled with white plaster and is clearly visible. This plaster filled gap fills the

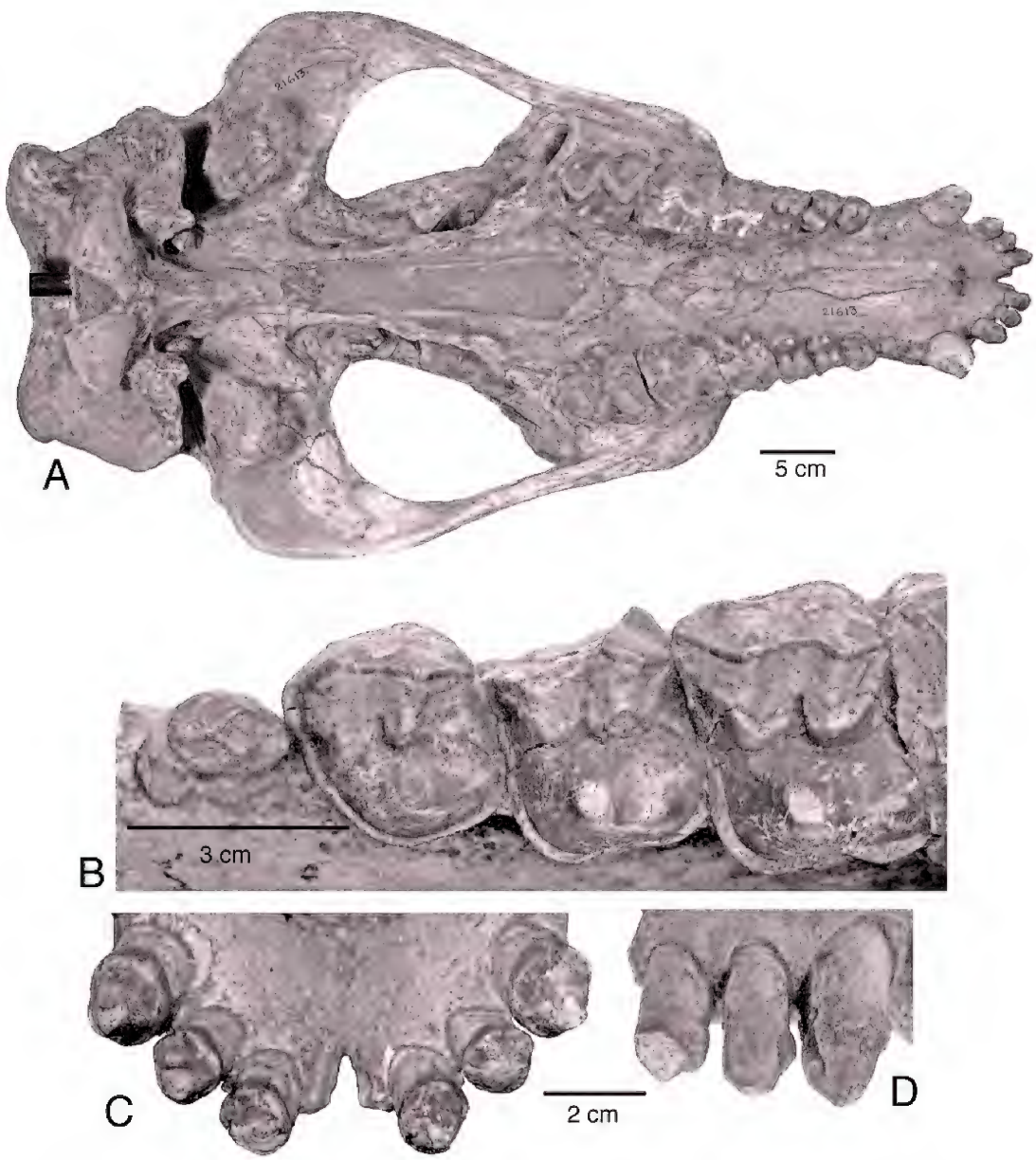

Fig. 65. The holotype skull and upper dentition of *Epimanteoceras formosus* (AMNH 21613). **(A)** Ventral view of skull, **(B)** left premolars, **(C)** lingual view of incisors and canines, **(D)** labial view of left incisors.

posteriorly shifted functional posterior nares. Thus, the functional posterior nares are posteriorly shifted in *Epimanteoceras formosus*, a condition closely resembling that of *Dolichorhinus*.

The configuration of the basicranial foramina is typical; the foramina of the alar canal, the foramen ovale, and the foramen lacerum are widely separate. The external auditory pseudomeatus is wide, ventrally unconstricted, and enters the skull in a mediolateral direction.

Upper Dentition: The holotype (AMNH 21613) retains a complete set of upper dentition (fig. 65) indicating an unreduced dental formula (3-1-4-3) while the referred specimen,

AMNH 21607, retains a set of less worn cheek teeth (fig. 64b, c, d). The incisors of AMNH 21613 are similar in size to those of *Protitan*. There are small diastemata between each incisor. The incisor apices are worn, but these teeth are essentially subcaniniform, with short, pointed, and slightly lingually curved crowns, and with distinct lingual cingula. The incisors become progressively larger from I1 to I3. The incisor row forms a broad arch anterior to the canines. The canines of AMNH 21613 are heavily worn and broken though they appear to have been quite large.

The premolars of the two skulls differ in several ways and there are notable bilateral asymmetries in right and left dentitions, suggesting that the premolars may have been morphologically unstable in *Epimanteoceras formosus*. The P1 of AMNH 21613 is heavily worn, although it appears that a paracone and a smaller metacone were present. The P1 of AMNH 21607 is incomplete, but it is less worn. That specimen suggests a more complex P1 with a lingual heel and possibly a small protocone. The P2 of both specimens is more oblique than P3 or P4. The parastyle of AMNH 21613 is straight, although the less worn P2 of AMNH 21607 suggests that the parastyle arches slightly lingually. The parastyle of P3 on AMNH 21613 is broken, but it is straight on AMNH 21607. The p4 parastyles of both specimens are angled slightly labially. The metastyles of P2 and P3 are straight while that of P4 is angled slightly labially. Distinct labial paracone ribs can be seen in AMNH 21607; these become smaller in more posterior premolars. Finally, the metacone of the P2 in both specimens is slightly lingually shifted.

The lingual features of the premolars (P2–P4) are higher in relief than those of *Protitan* and the lingual heels are relatively broader. Very faint preprotocristae can be seen on the P2–P4 of AMNH 21613, but only on the P2 of AMNH 21607. The P2s of AMNH 21613 each retain a prominent lingual crest extending posteriorly from the protocone, although there are no P2 hypocones. In contrast, hypocones on the P2s of AMNH 21607 are present and positioned very closely to the protocone. On AMNH 21613, the hypocones of the P3s are bilaterally asymmetrical; it is absent on the right P3 but on the left P3 there is a hypocone positioned close to the protocone and connected to it by a short lingual crest. The P3s of AMNH 21607 have distinct hypocones that are poorly separated from the protocones. The P4s of AMNH 21613 have distinct hypocones that are connected to the protocones by short lingual crests. Hypocones are absent on the P4s of AMNH 21607; nonetheless, the P4 crowns retain prominent lingual crests extending posteriorly from the protocones. The labial premolar cingula of both specimens are weak. On AMNH 21613 the lingual cingulum of P2 is continuous, while cingula of P3 and P4 are slightly discontinuous. On AMNH 21607 the lingual cingula of the P2–P3 are thicker and more continuous, but this final difference may relate to the fact that the premolars of this specimen are less worn.

The molars of *Epimanteoceras formosus* exhibit numerous brontotheriine apomorphies, including tall, lingually angled ectolophs, weak labial ribs, thin lingual ectoloph enamel, and wedge-shaped lingual sides of the paracone and metacone in those molars that are not heavily worn. The anterior cingulum is thin and passes proximally to the distal peak of the parastyle. Shallow central molar fossae are present, but anterolingual cingular cusps are absent. *E. formosus* molars lack vestigial paraconules, and all evidence of metalophs in M1 and M2 is lost. The M3 of AMNH 21613 has a small metalophlike ridge, while AMNH 21607 has a very tiny hypocone. Labial molar cingula in AMNH 21613 are thin and beaded, while lingual molar cingula are absent.

Remarks

Epimanteoceras formosus was first described from a single specimen (AMNH 21613), an essentially complete and remarkably undistorted skull with heavily worn teeth. Granger and Gregory (1943) remarked that *E. formosus* was "distinctly advanced beyond the stage of *Manteoceras* (= *Telmatherium*) and in the direction of *Rhinotitan*" (Granger and Gregory, 1943: 358). Seemingly, this remark stems from the fact that the holotype cranium of *E. formosus* is intermediate in size and morphology between

Telmatherium validus and those of brontotheres with conspicuous frontonasal protuberances such as *Rhinotitan*. Although other brontothere species with the characteristic overlapping triangular frontal process, such as *Telmatherium validus*, have been misleadingly described as having rudimentary horns (e.g., Osborn, 1929a), *E. formosus* is the only brontothere known to have weakly developed frontonasal protuberances. Other brontotheres either lack a distinct frontonasal protuberance or have a more conspicuous one.

Granger and Gregory (1943) noted that another specimen, AMNH 21607, is remarkably similar to *Epimanteoceras formosus*, but they erected a new taxon, *Dolichorhinoides angustidens*, for it. It is curious that Granger and Gregory (1943) chose the name *Dolichorhinoides* because they state "this skull differs conspicuously from those of the American *Dolichorhinus*" (Granger and Gregory, 1943: 363). Mader (1998) considered both *Dolichorhinoides* and *Dolichorhinus* to be junior synonyms of *Sphenocoelus*. It was demonstrated earlier in this paper that *Dolichorhinus* is actually very distinct from *Sphenocoelus* (see remarks under *Dolichorhinus hyognathus*), and it is argued below that the holotype of *Dolichorhinoides angustidens* is likewise different from both *Sphenocoelus* and *Dolichorhinus*.

The bony palatal extension, the extremely posteriorly situated maxilloturbinates, and posteriorly shifted functional posterior nares seen in AMNH 21607 resemble *Dolichorhinus hyognathus*. However, because these elements are extremely fragile, they cannot be investigated in the majority of brontothere specimens, and hence these characters are unknown for many species. Additionally, AMNH 21607 is inconsistent with the following aspects of Mader's (1998) diagnosis of *Sphenocoelus* (which, in his concept, included *Dolichorhinus*). (1) *Sphenocoelus* (sensu Mader, 1998) lacks hypocones on the premolars (unmolarized premolars, sensu Mader, 1998) whereas the P2–P3 of AMNH 21607 have hypocones. (2) Small, vestigial paraconules or metaconules are variably present on molars of *Sphenocoelus* (sensu Mader, 1998), but they are absent on AMNH 21607. (3) The skulls of *Sphenocoelus* (sensu Mader, 1998) are highly elongate; however, the apparently elongate skull of AMNH 21607 is largely a product of moderate lateral crushing. (4) *Sphenocoelus* (sensu Mader, 1998) possesses a large infraorbital process, but AMNH 21607 lacks this character. Additionally, the triangular process of the frontal bone overlapping the nasal bone that is clearly discernable on AMNH 21607 is not seen in *Sphenocoelus uintensis* or *Dolichorhinus hyognathus*. Finally, the postorbital portions of the crania of *Dolichorhinus* and *Sphenocoelus* are arched dorsally while that of AMNH 21607 is not.

After further examination of the holotypes of *Epimanteoceras formosus* (AMNH 21613) and *Dolichorhinoides angustidens* (AMNH 21607), these specimens do not appear to vary in any way that is seemingly taxonomically significant, and these specimens almost certainly represent the same species. Variability in the size and distinctness of the frontonasal protuberance is found among nearly all species of horned brontotheres. Likewise, extensive variation in the lingual morphology of the premolars is the rule rather than an exception within brontothere species.

Granger and Gregory (1943) concluded that the only clear distinction between *Epimanteoceras formosus* (AMNH 21613) and *Dolichorhinoides angustidens* (AMNH 21607) was the more elongate molars of the later. However, the difference can be attributed to dental wear in AMNH 21613, and, less significantly, to taphonomic deformation of AMNH 21607. Wood (1938) documented extreme ontogenetic shortening of the molars of rhinoceroses. A similar phenomenon occurs among brontotheres. Brontothere upper molars are longer on the labial side of the tooth. In AMNH 21607, where the molars are less worn, they are longer on the labial side than on the lingual side. Consequently, adjacent molars contact each other on the labial side but do not contact each other on the lingual side (fig. 64c). In comparison, the dentition of AMNH 21613 is more extensively worn (fig. 65a). In the later specimen, the labial and lingual sides of M1 and M2 are nearly the same length and the adjacent molars contact each other both labially and lingually. However, the anterior

and posterior enamel of the M1 and the anterior enamel of M2 are completely worn off. Clearly, the ectolophs of these teeth have been significantly shortened by interstitial wear, yet the sides of the molars are still in close contact. Apparently, the maxilla remodeled as the teeth shortened so that molars maintained contact despite having become significantly shorter on the labial side. Wear patterns in other brontothere molars exhibit the same pattern of ontogenetic tooth-row shortening. It is therefore evident that maximum lengths of the molars and even tooth-row lengths are influenced by dental wear.

In addition to differences in molar proportions due to interstitial wear, the molar proportions of AMNH 21607 have been taphonomically distorted. That specimen is laterally compressed and although the teeth appear to be minimally damaged, closer inspection reveals that the molars have been labiolingually compressed, thus exaggerating their relative length. A structural weakness exists in brontothere molars between the ectoloph and the lingual cusps. Those features contributing to the weak point include (1) increased ectoloph height without associated increase in height of the lingual side of the tooth, and (2) the appearance of the central molar fossa at the base of the ectoloph. Brontothere molars with these features are often cracked at this weak point and are susceptible to significant distortion from lateral crushing but without obvious damage to the tooth. Essentially, the tall ectoloph can be forced up over the lower lingual side of the tooth. This sort of damage is most evident in the right M3 of AMNH 21607 (fig. 64b) where the tooth has been considerably narrowed because the ectoloph has been forced over the lingual side of the tooth. The distortion is subtler on the left M3 where the shape of the tooth along the anterior margin is intact, but the posterior half of the ectoloph has been lingually displaced (fig. 64c). The damage to the M1 and M2 is less obvious, but tiny thrust faults in the enamel suggest a small amount of lingual displacement of the ectolophs.

A reliable comparison of the relative dimensions of the molars of AMNH 21613 and AMNH 21607 is clearly hampered by the extensive wear in the former and subtle distortion in the latter. However, measurements of a limited number of seemingly intact dimensions are possible. For instance, the left M3 of AMNH 21613 is less extensively worn. It is thus possible to compare M3 anteroposterior length in AMNH 21613 and 21607 if measured at the proximal base of the crown. At this location, the lengths are similar (AMNH 21613 = 70 mm; AMNH 21607 = 68 mm). Likewise, the left M3 of AMNH 21607 seems to be nearly intact along its anterior edge, thus allowing for a single comparison of the undistorted labiolingual widths of the M3s (AMNH 21613 = 58 mm; AMNH 21607 = 57 mm). Ratios calculated from the length of M3 divided by the width of the anterior margin yield nearly identical values (1.2 for AMNH 21613 and 1.19 for AMNH 21607). Therefore, it is relatively safe to conclude that whatever apparent differences exist in the dental dimensions of AMNH 21613 and 21607 that were observed by Granger and Gregory (1943) they can largely be attributed to wear and distortion. With little else to distinguish *Dolichorhinoides angustidens* as a valid taxon, it is here considered a junior synonym of *Epimanteoceras formosus*.

The only valid species of *Epimanteoceras* is *E. formosus*. Other species assigned to *Epimanteoceras*, including *E. praecursor* Yanovskaya (1953) from the upper Eocene of Kazakstan, and *E. amplus* Yanovskaya (1976) from the late Eocene Ergilin Dzo of Mongolia, are dubious species and are further discussed in the section dealing with nomina dubia and other problematic taxa. Another dubious taxon, "*Protitan*?" *cingulatus*, known only from a set of mandibles, is possibly a junior synonym of *E. formosus*.

Protitan grangeri (Osborn, 1925)

HOLOTYPE: AMNH 20103, a complete skull and mandible.

TYPE LOCALITY: Irdin Manha Formation, one half mile south of the Kalgan Urga telegraph line, Inner Mongolia, China.

AGE: Middle Eocene (Irdinmanhan land mammal "age").

SYNONYMS: *Dolichorhinus olseni* Osborn, 1925; "*Manteoceras*?" *irdinensis* Os-

born, 1925; *Protitan robustus* Granger and Gregory, 1943; *Protitan bellus* Granger and Gregory, 1943; *Protitan obliquidens* Granger and Gregory, 1943.

REFERRED SPECIMENS: **(From the Irdin Manha Formation, Inner Mongolia)** AMNH 19179, a mandible fragment with left p2 (partial), p3–m2, and m3 (partial); AMNH 20104 (holotype of *Protitan robustus*), a partial mandible with right i1–c, p2–p3, and left i1–m3; AMNH 20108, a right maxilla with P1–M3; AMNH 20109 (holotype of *Dolichorhinus olseni*), a mandible with right i3, p1–m3, and left c–m3; AMNH 20111 (holotype of "*Manteoceras*?" *irdinensis*), a mandible fragment with right m1–m3; AMNH 20112, a partial mandible with i2–c and p2–m3; AMNH 20113, an anterior portion of a cranium with right C, P2–P4, and M1 (partial); AMNH 20114, an anterior portion of a cranium with right I2–M1, left C, and P2–M3; AMNH 20119, a mandible fragment with right p4–m2; AMNH 20120, a right maxilla fragment with M1–M3; AMNH 20123, a left maxilla fragment with P4–M2; AMNH 20125 (holotype of *Protitan obliquidens*), a left maxilla fragment with P1–P3; AMNH 20126, a mandible fragment with left p3–m2; **(from the Ulan Shireh Formation of Inner Mongolia)** AMNH 26104 (holotype of *Protitan bellus*), a ventral surface of a cranium with right and left I2–M3; **(from the ?"Houldjin" beds at Camp Margetts)** AMNH 26421, a mandible with some intact incisors, right p2–m3, and left p1–m3.

DIAGNOSIS: *Protitan grangeri* is a large brontothere with small but distinct elliptical frontonasal horns positioned low on the skull and far in front of the orbit. The nasal incision is dorsoventrally shallow and extends posteriorly to the P3. The nasal process is slightly angled downward, unelevated, long and broad, with thickened sides, and with a thin and strongly rounded distal edge with a downturned distal tip. The orbits are positioned above the posterior portion of M2 and the anterior portion of M3. The premaxillomaxillary rostrum deepens posteriorly and it is not enclosed by bone dorsally. Other cranial characteristics include a saddle-shaped cranium, separate parasagittal ridges that strongly constrict the dorsal width of the cranium posteriorly, postzygomatic processes, large ventral sphenoidal fossae, nearly straight zygomatic arches, and a ventrally unconstricted and mediolaterally angled external auditory pseudomeatus.

Dentally, *Protitan grangeri* has three large to intermediate-sized subcaniniform upper incisors, a simple P1, and a distinct P2 metacone. Premolar hypocones are absent, although a short crest usually extends from the protocones. The molars of *P. grangeri* have tall, lingually angled ectolophs with weak labial ribs, and thinned lingual ectoloph enamel with wedge-shaped paracones and metacones. A cingular parastyle shelf is absent. Very shallow central molar fossae are present. Anterolingual cingular cusps are absent. Paraconules and metalophs are absent. The lower dentition of *P. grangeri* includes three large incisors, a semispatulate i1 and i2, and a more subcaniniform i3. Additional lower dental characters include, a distinct postcanine diastema, a metaconid on p4 but not on p2 or p3, shallow molar basins, and a slender m3.

Protitan grangeri closely resembles *Protitanotherium emarginatum* and *Protitan minor*. It can be most easily distinguished from *Protitanotherium* by the larger more subcaniniform incisors, a ventrally unconstricted external auditory pseudomeatus, and postzygomatic processes. *Protitan grangeri* can be distinguished from *Protitan minor* by its anteroposteriorly shorter nasal incision, thicker nasal, more anteriorly positioned horns, and mediolaterally angled auditory pseudomeatus.

DESCRIPTION

SKULL: The holotype of *Protitan grangeri* (AMNH 20103) is a complete and relatively undistorted skull (figs. 66, 67) and jaw (fig. 68) with a complete set of dentition, but with rather poorly preserved cheek teeth. No other complete skulls of *P. grangeri* are known, although there are several additional partial crania, including AMNH 26104, a complete ventral surface, and several anterior portions of skulls including AMNH 20108, AMNH 20114, and AMNH 20113. The following description of *P. grangeri* is based primarily on AMNH 20103, but additional

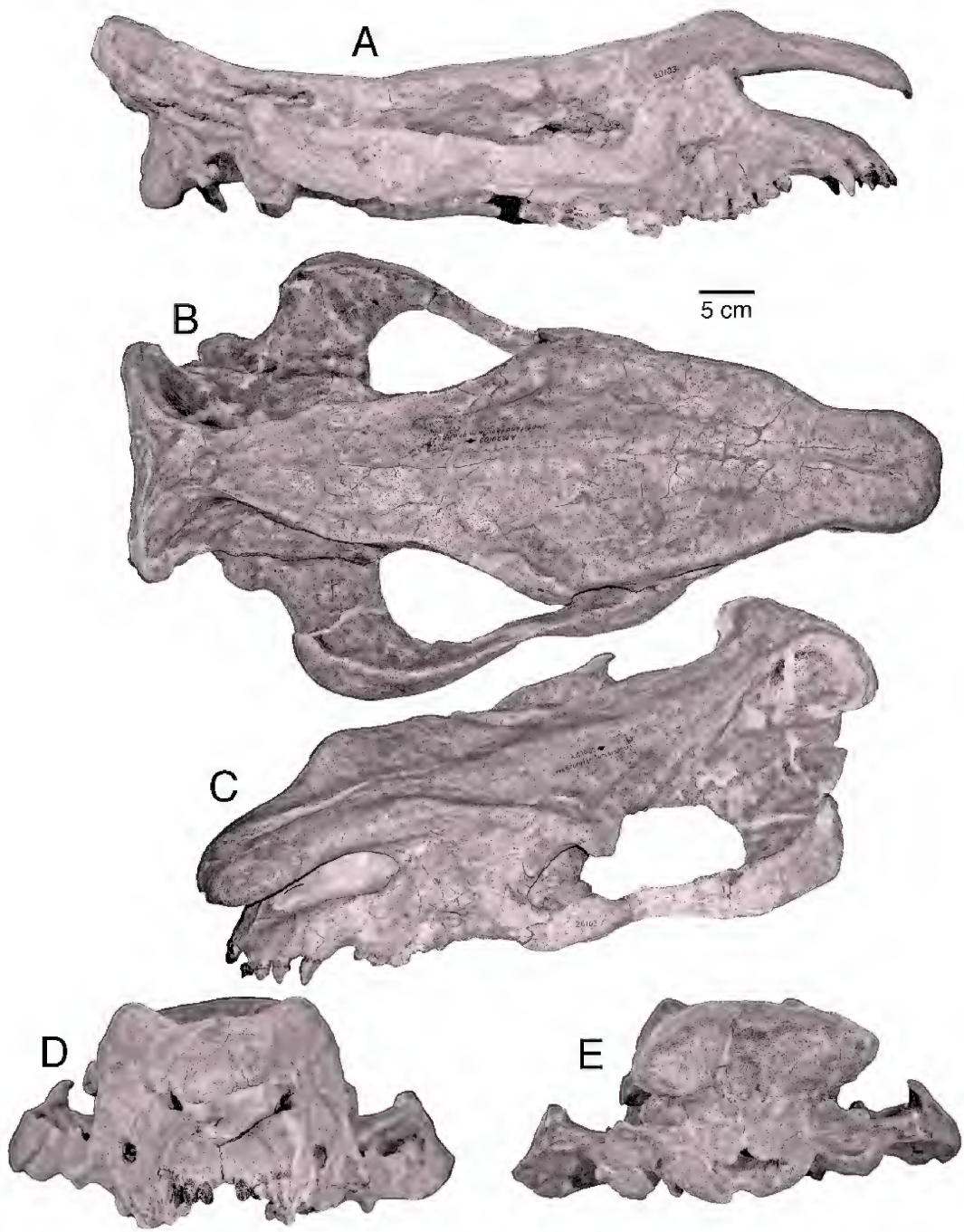

Fig. 66. The holotype skull of *Protitan grangeri* (AMNH 20103). **(A)** Right view, **(B)** dorsal view, **(C)** oblique view, **(D)** anterior view, **(E)** posterior view.

information is taken from these other specimens where noted.

Protitan grangeri is a large (table 9) brontothere with an elongate cranium and small but conspicuous frontonasal protuberances that are similar in size to those of *Protitan minor* and *Protitanotherium emarginatum*. From the right side of the skull the

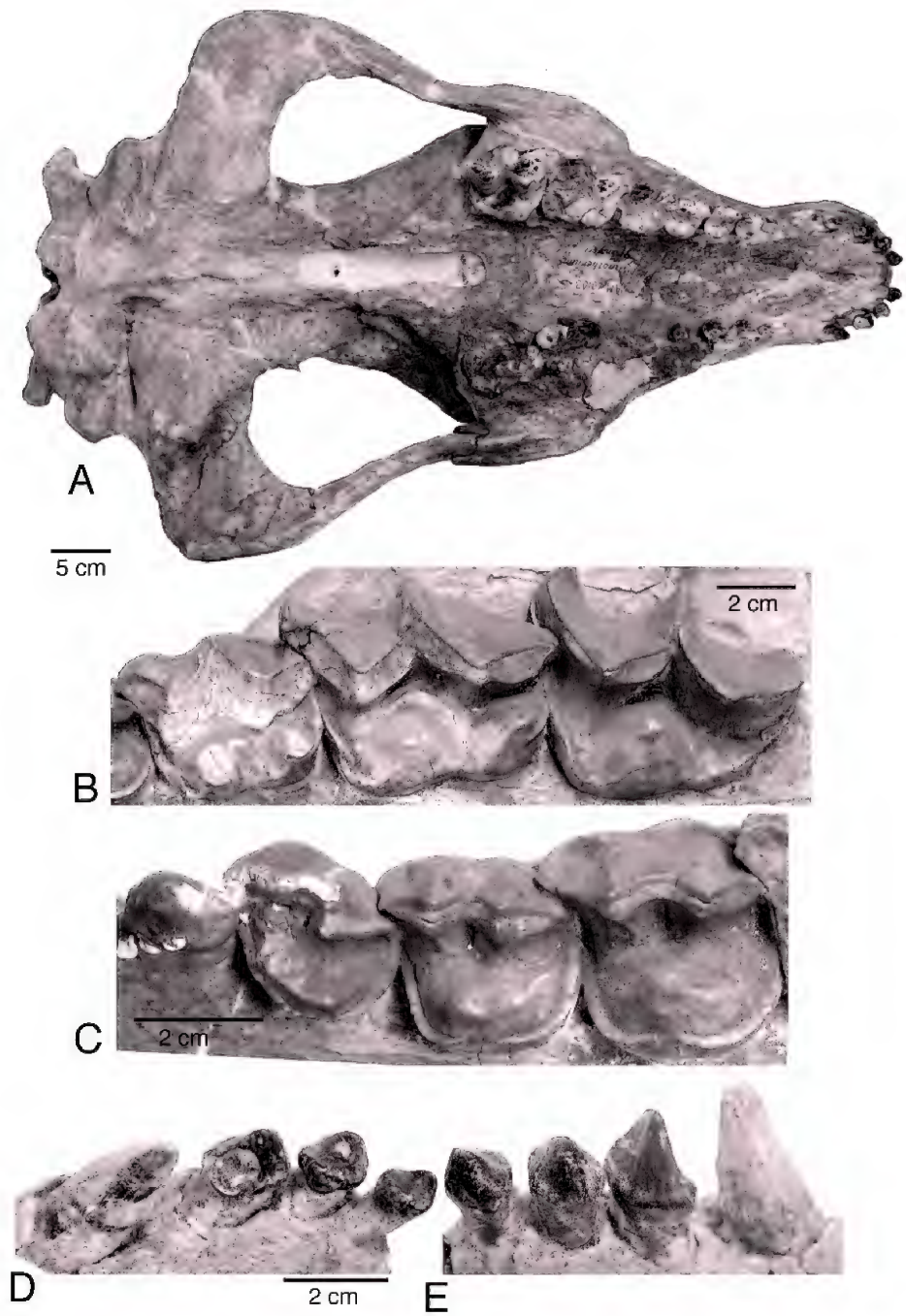

Fig. 67. The ventral surface of the skull of *Protitan grangeri* and upper dentition. **(A)** Ventral view of AMNH 20103 (holotype), **(B)** left molars of AMNH 26104, **(C)** left premolars of AMNH 26104, **(D)** lingual view of right incisors and canine of AMNH 20103 (holotype), **(E)** labial view of the right incisors and canine of AMNH 20103 (holotype).

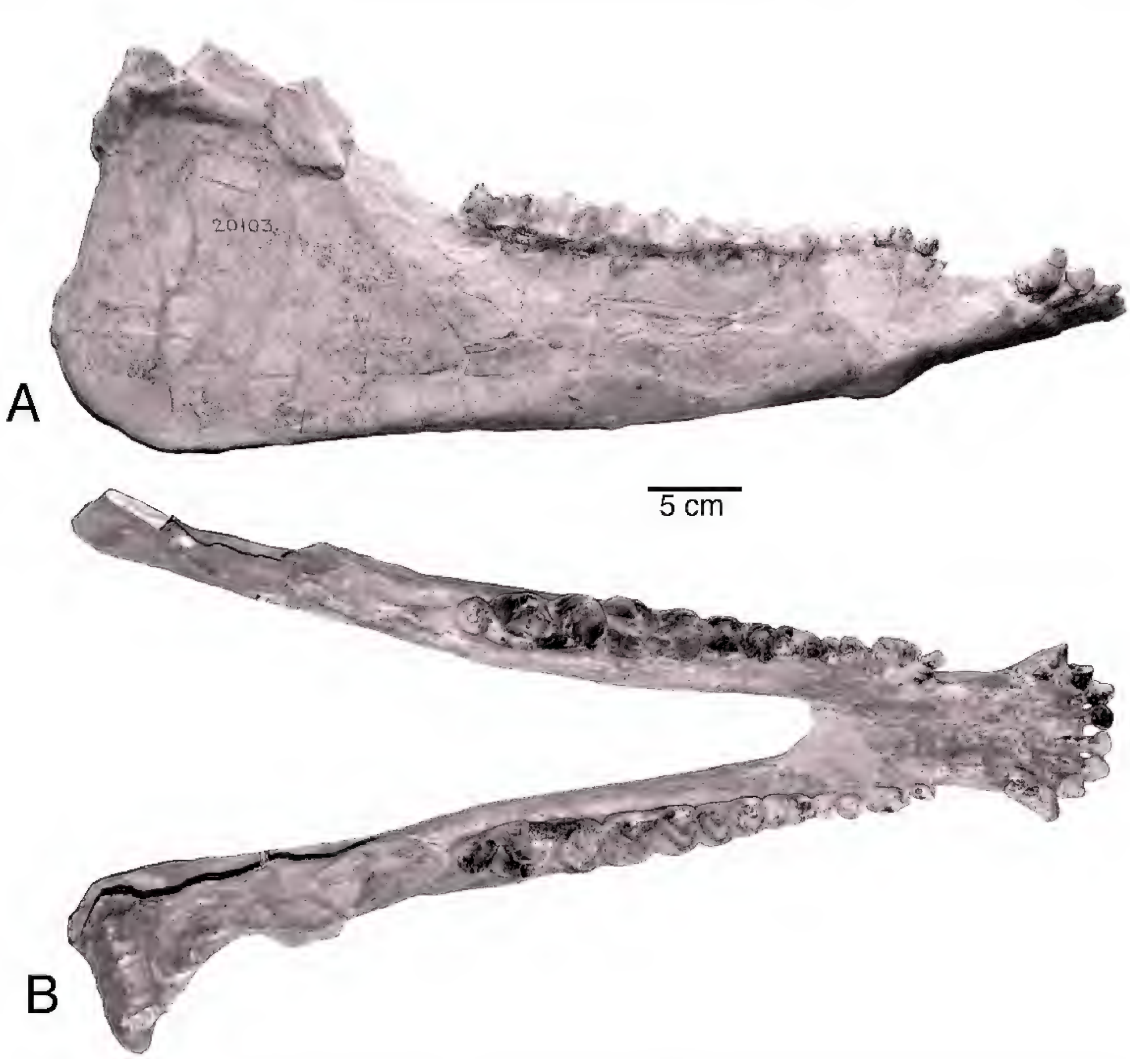

Fig. 68. The holotype mandible of *Protitan grangeri* (AMNH 20103). **(A)** Right view, **(B)** dorsal view.

frontal bone can clearly be seen overlapping the nasal bone and extending to the peak of the horn. The horns of AMNH 20103 are short and elliptical in shape with a longer anteroposterior axis. The peaks of the horns lack distinct rugosities, and the surfaces of the horns are no rougher than the remaining surface of the skull. The horns project dorsolaterally from the sides of the skull and they are widely separated by a broad and flat forehead. The horns are positioned low on the skull although they are much further anterior to the orbits in comparison to those of *Protitan minor* and *Protitanotherium emarginatum*.

Like *Protitan minor* and *Protitanotherium emarginatum*, the nasal incision is dorsoventrally shallow. However, it is anteroposteriorly shorter than in other taxa. The nasal incision extends posteriorly to the P3 and the orbit is positioned over the anterior portion of M3 and the posterior portion of M2. The anterolateral root of M2 rests below the anterior rim of the orbit.

From the lateral view of the skull the nasal process of the holotype curves downward anteriorly and is the same length as the premaxillomaxillary rostrum. The sides of the nasal process are thickened, rounded, and angled downward. The sides are not up-

TABLE 9
Summary statistics for selected morphometric variables of *Protitan grangeri*
See Methods for measurement definitions

	N	Mean	SD	Min.	Max.	CV
C L	4	23.0	5.0	19.8	30.4	21.6
P3 L	7	27.1	3.0	22.3	31.6	11.2
P3 W	7	31.0	2.6	27.7	35.9	8.3
M2 L	6	66.6	5.7	59.3	74.7	8.5
M2 W	5	54.4	.7	48.3	57.7	6.8
P2–P4	4	80.9	1.5	79.9	83.2	1.9
M1–M3	4	171.8	11.3	162	188	6.6
V L	2	711	0	711	711	0
c L	4	22.0	4.5	17.9	28.3	20.5
p3 L	7	27.8	2.5	24.0	31.8	8.8
p3 W	7	17.4	2.7	14.3	20.9	15.2
m2 L	8	57.6	3.9	52.8	62	6.7
m2 W	8	32.3	2.3	28.1	34.7	7.2
p2–p4	5	84.6	7.4	75.9	94.7	8.7
m1–m3	6	184.8	14.4	168	204	7.8

turned as are the nasals of *Diplacodon elatus*. Thin, vertical lateral walls, such as those seen in *Epimanteoceras formosus* and other hornless brontotheres, are not seen in *Protitan grangeri*. From a dorsal view of the skull it can be seen that the nasal bones are strongly fused together. The nasal process is wide, about the same width as the premaxillomaxillary rostrum. Throughout its length the nasal process is nearly constant in width. The distal edge of the nasal process is strongly rounded although there is a slight anterior notch at the midline. From the lateral and anterior views of the skull it can be seen that the anterior end of the nasal process is thinned and strongly curved downward. The anterior edge of the nasal process is thin and irregular.

From the lateral view of the holotype skull, the dorsolateral margin of the premaxillomaxillary rostrum rises posteriorly at a shallow angle so that the posterior notch of the nasal incision is at the level of the upper rim of the orbit. The premaxillae contact each other medially at the premaxillomaxillary symphysis although the symphysis is not completely fused. The premaxillomaxillary suture can be seen in AMNH 20103 most clearly from the oblique view of the skull. The premaxilla is truncated before reaching the posterior notch of the nasal incision, thus, the premaxilla does not contact the nasal bone. The dorsolateral margins of the premaxillae diverge posterolaterally and the rostral cavity is dorsally open.

From the lateral view the dorsal surface of the skull is fully concave from the orbits to the nuchal crest, forming a completely saddle-shaped cranium. The parasagittal ridges remain separate and do not form a sagittal crest although they strongly constrict the dorsal surface of the cranium posteriorly. The zygomatic arches are rather shallow dorsoventrally and have a narrow rectangular cross section. The zygomatic arches of AMNH 26104 are somewhat thicker and more robust than those of AMNH 20103, but they are otherwise similar. The zygomatic arch is essentially uncurved from a lateral view. From a dorsal view the zygomatic arches are bowed slightly inward. However, the zygomatic arches of AMNH 20103 are composed of several fragments that have been bonded together with plaster and it is probable that the inwardly bowed shape is an artifact of distortion and subsequent reconstruction of the fossil. Unlike the holotype, the zygomatic arches of AMNH 26104 are not inwardly bowed. Discounting the slight inward bowing of the zygomatics of the holotype, the zygomatic arches appear to have been straight and strongly angled posterolaterally. The posterodorsal end of each of the zygomatic arches exhibits a small

dorsally projecting process that was referred to by Granger and Gregory (1943) as a "postzygomatic horn" (Granger and Gregory, 1943: 359). One of these postzygomatic processes can most easily be seen on the right side of the skull (fig. 66).

From the lateral view of the skull the occiput is moderately angled backward. From the dorsal view the nuchal crest is nearly flat. From the posterior view the dorsal rim of the occiput is dorsally arched. The dorsal portion of the occiput is slightly narrower than the ventral portion of the occiput and the occiput is strongly constricted in the middle. Weak occipital pillars are evident on the posterior surface of the occiput, although the central depression of the occiput is rather shallow.

From the ventral view of AMNH 20103 (fig. 67a) the anterior rim of the posterior nares is situated slightly behind the M3 protocones. The narial canal is rimmed by a rather wide U-shaped emargination. In both the holotype specimen and the other complete ventral skull surface (AMNH 26104), the elongate posterior canal is filled with plaster. In AMNH 20103 roughly the posterior half of the elongate posterior narial canal is free of plaster. In that specimen the canal extends significantly into the basisphenoid. The ventral sphenoidal fossae are rather large, but they are shallow. These were called presphenoid pits by Osborn (1925, 1929a) and were called basisphenoid pits by Granger and Gregory (1943). A remnant of the thin bony septum formed by the main body of the sphenoid that partitions the ventral sphenoidal fossae is still preserved in position.

Other aspects of the basicranium of AMNH 20103 and AMNH 26104 are rather typical, such as the widely separated foramen ovale and foramen lacerum. The occiput and basicranium are not disproportionately widened as those of *Rhinotitan andrewsi* or *Metatitan*. The external auditory pseudomeatus is directed mediolaterally. From the lateral view the external auditory pseudomeatus is wide and open ventrally.

Upper Dentition: The holotype of *Protitan grangeri* (AMNH 26103) retains a complete dentition (fig. 67a). Although the incisors of the holotype are in good condition (fig. 67d–e), the cheek teeth are poorly preserved. However, AMNH 26104 has a nearly complete set of upper dentition whose cheek teeth are significantly less worn and less damaged than those of AMNH 26103. Therefore, the cheek teeth of AMNH 26104 are shown in close-up (fig. 67b, c).

Protitan grangeri retains an unreduced dental formula (3-1-4-3). The incisors and canines of the holotype are relatively small, though by no means are they as reduced as those of *Protitanotherium emarginatum*. The anterior dentitions of other specimens referred to *Protitan grangeri* are larger. For instance, the incisors and canines of AMNH 26104 are distinctly larger than those of AMNH 20103. However, the premaxillae of both specimens are of similar size; in AMNH 20103 there are small diastemata between the incisors, whereas in AMNH 26104 there are no diastemata between the incisors (except for a median diastema). Osborn (1929a) attributed the smaller size of the incisors of AMNH 20103 to sexual dimorphism. Variation in incisor and canine size seen here and in other brontotheres such as *Aktautitan hippopotamopus* and *Gnathotitan berkeyi* probably represents sexual dimorphism.

The incisors of *Protitan grangeri* form an arched row anterior to the canines. They increase in size laterally and retain plesiomorphic subcaniniform morphology with short but conical and lingually curved crowns with distinct lingual cingula. Labial incisor cingula are absent. The canine of AMNH 20103 is small while that of AMNH 26104 is larger, even though it is otherwise morphologically similar. There is both a short precanine diastema and a longer postcanine diastema. The postcanine diastema of AMNH 26104 seems proportionally shorter but this difference can largely be attributed to the larger canine.

The P1 is a single-cusped tooth with an elongate posterior heel. The anterior margin of P2 is angled posterolingually, giving the tooth a somewhat oblique shape. The anterior and posterior margins of P3 and P4 are more nearly parallel. The parastyle and metastyle of P2 arch somewhat lingually. The parastyle and metastyle of P3 are nearly straight. The parastyle of P4 is slightly angled lingually while the metastyle is more nearly straight. The labial margin of the P2 proto-

cone is very convex, while the paracones of P3 and P4 have distinct labial ribs. Finally, the metacone of P2 is lingually shifted, while those of P3 and P4 are more labially positioned. As a consequence, the ectoloph of P2 is rounder than those of P3 and P4.

The lingual features of the premolars have a relatively low level of topographic relief and they exhibit considerable intraspecific variation. On the P2 of the holotype specimen (AMNH 20103) there is a distinct protocone followed by a short lingual crest. However, in AMNH 26104 a single loph of enamel stretches around the anterolingual side of the P2 crown and although there are no distinct lingual cusps. The P2s of AMNH 20103 and AMNH 26104 have small preprotocristae. A less distinct preprotocrista is seen on the P3 of the holotype and it is absent on the P3 of AMNH 26104. The P3 protocones are followed by short lingual crests on both specimens. A preprotocrista is not seen on the P4 of either specimen. A lingual crest is not seen on the P4 of the holotype, but a short lingual crest is present on the P4 of AMNH 26104. A few specimens have small paraconules on the P2–P4 but these are most often absent. Premolar hypocones are nearly always absent in *P. grangeri*, though one specimen, AMNH 20123, has a very small hypocone positioned close to the protocone of the P4. Labial premolar cingula are weak. The anterior and posterior premolar cingula wrap around the lingual sides of the crowns and join to form continuous lingual cingula. Among all of the available specimens, the lingual premolar cingula range from continuous around the protocone to slightly discontinuous.

The upper molars of *Protitan grangeri* show numerous brontotheriine apomorphies, including tall, lingually angled ectolophs, very weak labial ribs, thin lingual ectoloph enamel, and wedge-shaped lingual sides of the paracone and metacone in molars that are not heavily worn. The anterior cingulum is thin and passes proximally to the distal peak of the parastyle. Shallow central molar fossae are present but anterolingual cingular cusps are absent. All evidence of paraconules and metalophs is lost. There is no trace of a hypocone on any M3 of *P. grangeri*. Labial molar cingula are weak and lingual molar cingula are absent.

Mandible and Lower Dentition: The holotype mandible (AMNH 20103) is missing only the condyles and coronoid processes (fig. 68). The lower dentition of the holotype is complete, but cheek teeth are poorly preserved. However, the lower dentition of a referred specimen (AMNH 20104) is complete, similar to that of the holotype, and in more pristine condition. Therefore, the lower teeth of this specimen are figured in close-up (fig. 69).

The coronoid process of AMNH 20104 is tall, slender, and moderately curved. The mandibular symphysis is long and narrow in AMNH 20103, although it is somewhat more robust in AMNH 20104. The angle of the ventral margin of the symphysis of AMNH 20103 is shallow ($< 45°$). However, as noted by Granger and Gregory (1943), the shallow orientation of the symphysis seems to have been influenced by taphonomic distortion. A segment of the right ramus below the p3 is reconstructed with plaster, suggesting that the anterior portion of the mandible has been forced or rotated downward. The anterior portion of AMNH 20104 is more intact and suggests a steeper mandibular symphysis. The exact posterior edge of the symphysis is obscured by plaster in AMNH 20103, but in AMNH 20104, the symphysis extends posteriorly to the talonid of the p3.

The lower incisors are relatively large and they form an arched row anterior to the canines. In the holotype the crowns of i1 and i2 are significantly worn, but those of AMNH 20104 are nearly unworn. The crowns of i1 and i2 are generally semispatulate with rounded apices, while i3 has a more sharply defined apex. There are distinct lingual cingulids on i1–i3. Labial cingulids are not seen. The i3 is mesiodistally elongate in comparison to i1 or i2. Each incisor is roughly of similar size. The lower canines of AMNH 20103 are notably smaller than those of AMNH 20104. The length of the lower postcanine diastema, the only diastema of the lower dentition, covaries with canine size. In AMNH 20103 the postcanine diastema is about double the length of the p2 whereas in AMNH 20104 the postcanine diastema is

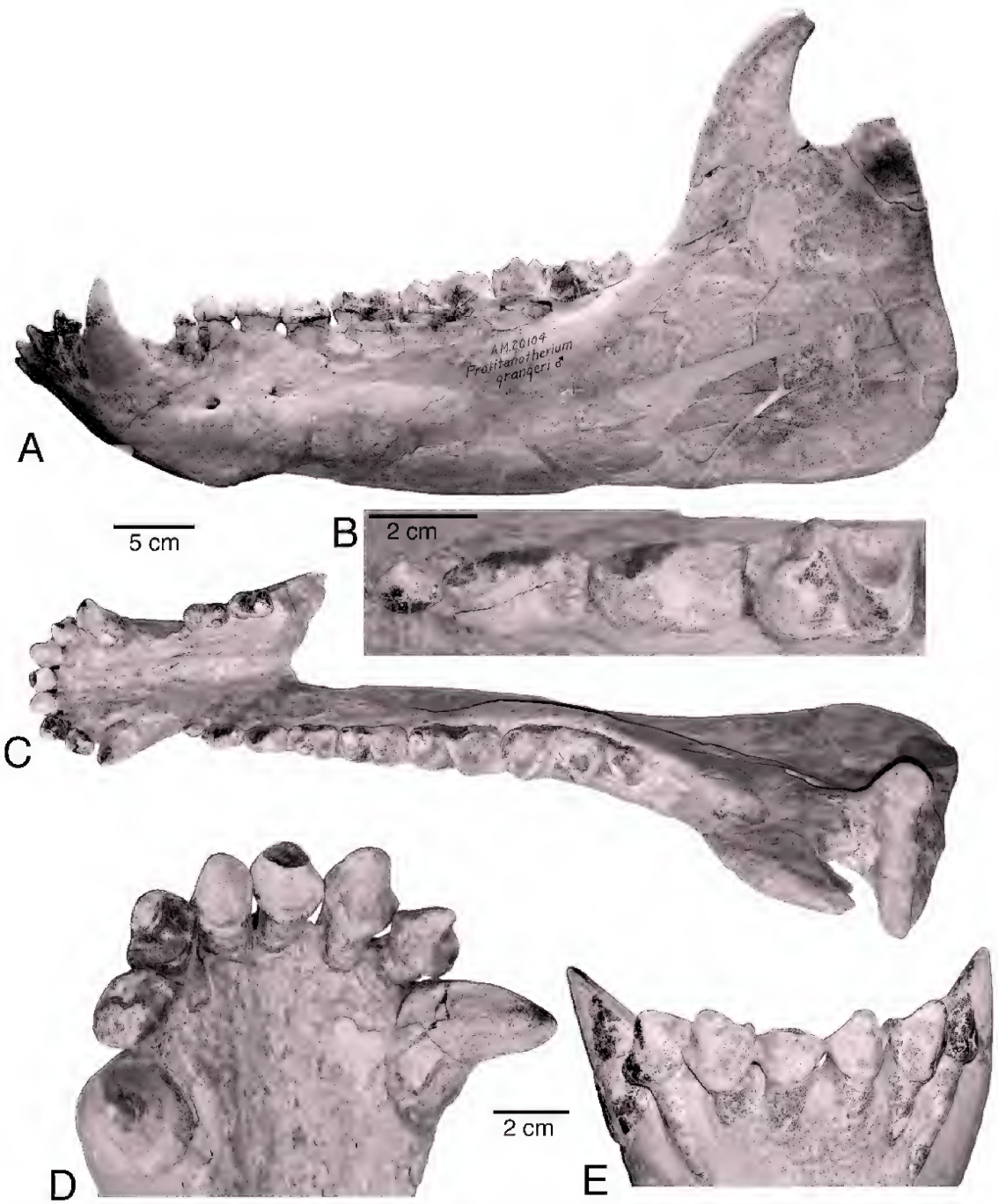

Fig. 69. A mandible referred to *Protitan grangeri* (AMNH 20104). **(A)** Left view, **(B)** left premolars, **(C)** dorsal view, **(D)** lingual view of incisors and canines, **(E)** labial view of incisors and canines.

shorter, corresponding to the larger size of the canines.

The lower premolars are low crowned and relatively slender. The p1 is a very small tooth with a single cusp and a short talonid heel. The trigonid of p2 is much longer than the talonid. The p3 trigonid is somewhat longer than the talonid, while the p4 trigonid

is similar in length to the talonid. The trigonid and talonid of p2 are of similar width, while the p3 and p4 trigonids are slightly narrower than their talonids. The p2 paralophid barely arches lingually and there is only a minor lingual trigonid notch. The p2 protolophid extends in a posterior direction, but it is positioned lingually. The p3 paralophid arches slightly lingually, creating a more distinct lingual trigonid notch. The p3 protolophid is moderately angled lingually. Metaconids are absent on p2 and p3. The trigonid of p4 is more molariform with a strongly lingually arching paralophid and protolophid and a large lingually positioned metaconid. The talonid of p2 is very small, with a very short cristid obliqua and hypolophid. The lingual face of the p2 talonid is a flat and sloped surface. The cristids obliqua and hypolophids of p3 and p4 are progressively longer although the lingual face of p3 forms only a broad concave surface. However, the talonid of p4 has a nearly molariform talonid basin. Labial and lingual premolar cingulids are essentially absent although a very faint labial cingulid can be seen on p4.

The lower molars of *Protitan grangeri* are typical with relatively thin lingual enamel, shallow trigonid and talonid basins, and an elongate m3. There are no lingual cingulids. Labial molar cingulids are distinct although they tend to be discontinuous around the paraconids and metaconids.

Remarks

Protitan grangeri (Osborn, 1925) is based on a complete skull and jaw (AMNH 20103). Osborn (1925) originally referred this species to the genus *Protitanotherium*, based on the "elongate horns", the "broad shovel-shaped nasals", the "saddle-shaped cranial top", and several other minor details. Several other species have been referred to *Protitan*, although most of these turn out to be invalid synonyms and nomina dubia. Osborn named two other Asian brontothere species, *Dolichorhinus olseni* Osborn (1925) and "*Manteoceras*?" *irdinensis* Osborn (1925). In their revision of Mongolian brontotheres, Granger and Gregory (1943) erected a new genus, *Protitan*, with *P. grangeri* serving as the type species. In addition to *Protitan grangeri*, Granger and Gregory (1943) named five other species of *Protitan*, including *P. minor*, *P. robustus*, *P. bellus*, *P. obliquidens*, and "*Protitan*?" *cingulatus*. They considered *Dolichorhinus olseni* Osborn (1925) and "*Manteoceras*?" *irdinensis* Osborn (1925) to be synonyms of *Protitan grangeri*.

Among these species, *Protitan minor* is the only other species previously referred to *Protitan* that may actually belong to this genus, although even its membership is questionable (see remarks under *Protitan minor*). "*Protitan*?" *cingulatus* is a dubious species that may actually be synonymous with *Epimanteoceras formosus*. The remaining species, *Dolichorhinus olseni*, "*Manteoceras*?" *irdinensis*, *P. robustus*, *P. bellus*, and *P. obliquidens* are junior synonyms of *P. grangeri*.

Dolichorhinus olseni was based on a complete mandible (AMNH 20109) lacking most of its anterior dentition. It is not clear why Osborn (1925, 1929a) assigned this species to *Dolichorhinus*. Osborn did not attempt to differentiate *Dolichorhinus olseni* from *Protitan grangeri*, despite that fact that these taxa are based on very similar fossil material. Granger and Gregory (1943) considered *D. olseni* to be a junior synonym of *P. grangeri*, but they noted that the m3 was slightly shorter than on the holotype of *P. grangeri* (AMNH 20103).

"*Manteoceras*?" *irdinensis* is based on a partial ramus with m1–m3 that is reconstructed in such a way that suggests a very short space for a premolar row and a very short and flattened symphysis. All these features are relevant to Osborn's (1925) diagnosis, which includes an apparently reduced number of premolars (judging by the premolar alveoli), unusually procumbent incisors (judged by the angle of the symphysis), and a short symphysis. The short symphysis is artificial and related to the fact that the anterior end is missing. Additionally, the ramus has been incorrectly reconstructed; the symphysis is plastered directly to the horizontal ramus, although a segment of the horizontal ramus appears to be missing, thus giving the artificial appearance of a shortened jaw. Likewise, the shallow angle of the symphysis and, hence, the procumbent nature of the incisor alveoli are simply a result

of how the specimen has been reconstructed. The molar measurements of this specimen are similar to *Protitan grangeri*. Thus, "*Manteoceras*?" *irdinensis* is considered a junior synonym of *P. grangeri*.

Granger and Gregory (1943) based *Protitan robustus* on a partial mandible with complete and lightly worn dentition (AMNH 20104). This species was diagnosed on the following criteria: (1) size large (presumably in comparison to *P. grangeri*), (2) incisors large, wide spreading, (3) canines very massive with recurved crowns, and (4) "postcanine diastema short". However, none of these observations clearly differentiates *P. robustus* from *Protitan grangeri*. AMNH 20104 is larger than the holotype of *P. grangeri* (AMNH 20103), but the difference is not extreme and this specimen easily fits into an acceptable size range for *P. grangeri* (table 9). Granger and Gregory (1943) actually noted that the dentition of AMNH 20104 nearly fit onto AMNH 26104 (holotype of *P. bellus*, a synonym of *P. grangeri*; see next paragraph), but they even rejected the possibility that these two specimens are the same species because the match was not perfect! (Intraspecific variation and taphonomic distortion were largely ignored by Granger and Gregory [1943].) In comparing AMNH 20104 with the holotype mandible (AMNH 20103) of *P. grangeri*, the larger size of the incisors and canines of the former is consistent with sexual dimorphism. Likewise, the shorter postcanine diastema can be explained by the fact that the canine root of AMNH 20104 is much larger and takes up more space. Nothing else appears to differentiate this specimen from *P. grangeri*.

Protitan bellus was based on a ventral surface of a skull with a nearly complete set of upper dentition (AMNH 26104). Granger and Gregory (1943) distinguished *P. bellus* from *P. grangeri* with the following diagnosis: (1) upper molars anteroposteriorly longer than in *P. grangeri*, especially M1. (2) P3 with incipient tetartocone (= hypocone) swelling, (3) P4 more elongate, (4) incisors much larger than in the type of *P. grangeri*, and (5) width across opposite M3 distinctly larger. Observations 1, 3, and 5 were based on ratios in which AMNH 26104 differs slightly from AMNH 20103 (See table 5 of Granger and Gregory, 1943). However, either these differences can be attributed to the more damaged and more heavily worn state of the dentition of AMNH 20103 compared with that of AMNH 26104 (observations 1 and 3), or the differences are so small (4%) that they do not warrant a taxonomic distinction (observation 5). While I could not confirm the presence of an "incipient hypocone" on the P3 of AMNH 26104 (observation 2), there are small lingual crests on the P3 and P4. These are not present in the holotype of *Protitan grangeri*; however, this character is strongly variable in most brontothere species. Moreover, other specimens that Granger and Gregory (1943) referred to *P. grangeri* show similar variations in premolar morphology. Therefore, AMNH 26104 does not really stand out in this respect. Clear differences between AMNH 20103 and AMNH 26104 include the large incisors and canines (observation 4 of Granger and Gregory [1943]), larger size, and thicker zygomatic processes. These character differences are most consistent with sexual dimorphism. AMNH 26104 is marginally larger than the holotype of *P. grangeri*.

The obliqueness of the premolars (P2–P3) of a maxillary fragment (AMNH 20125) led Granger and Gregory (1943) to assign it to yet another a new species, *Protitan obliquidens*. Granger and Gregory (1943) remark in their diagnosis: crown pattern of P2, P3 very oblique both on the anterointernal and posteroexternal. However, this specimen does not really stand out in comparison to other specimens of *Protitan*. In particular, the P2 of all *Protitan* specimens is oblique in appearance, although the extent of obliqueness is somewhat variable. As Granger and Gregory (1943) note, the shape of the premolars closely resembles those of AMNH 26104 except in the much greater maximum oblique width of P2. However, the difference in the shape of the P2 of AMNH 20125 is subtle and the P2 and P3 are cracked in numerous places with bits of matrix and plaster between the spaces; the teeth of this specimen are clearly distorted to a minor degree. The minor differences in the apparent degrees of obliqueness of these teeth can largely be attributed to this distortion. Realistically, the molar dimensions of AMNH 20109 are

similar to those of *Protitan grangeri* and this specimen is likely to represent the same species.

Subsequent to Granger and Gregory's (1943) publication, paleontologists working with Asian brontothere material have shown a mistaken tendency to assign large middle Eocene brontothere fossils to the genus *Protitan*, although their use of *Protitan* has been far too broad; none of the material outside of the original AMNH central Asiatic expedition collection resembles the species referred to *Protitan* by Granger and Gregory (1943). Two species named by Yanovskaya (1980), *P. khaitshinus* and *P. reshetovi*, are actually *Metatitan*. Yanovskaya (1980) incorrectly reassigned *Protitan robustus* to the genus *Epimanteoceras* and wrongly synonomized it with *Epimanteoceras amplus* (a dubious species that is, nonetheless, very different from *Protitan* and might be a synonym of *Nasamplus progressus*). None of the material described in Yanovskaya's (1980) monograph on Mongolian brontotheres appears to belong to any species of *Protitan*. Qi et al. (1992) referred another specimen (IVPP–V10104, presumed to represent a single individual) from the Tukhum beds of Erden Obo (Urtyn Obo) to *Protitan* sp. The material includes an elongate m3 and an assortment of postcranial elements. Although the size of the m3 is consistent with *P. grangeri*, it lacks diagnostic characters and could belong to one of a number of brontotheres including *Epimanteoceras*, *Metatitan*, or others. Preliminary reports of a brontothere from the Ily Basin of Kazakstan were referred to *Protitan* (Emry et al., 1997; Emry and Lucas, 2002, 2003; Lucas and Emry, 2001), although this brontothere turned out to be a new genus and species, *Aktautitan hippopotamopus* (Mihlbachler et al., 2004a). Most recently, Huang and Zheng (2004) named a new species, *Protitan major*, from the Lumeiyi Formation of China, although the material assigned to this species represents a brontothere with much more advanced dentition and it possibly belongs to *Metatitan*. Other material from the Lumeiyi formation assigned to *Protitan* cf. *P. robustus* by Zheng et al. (1978) and Huang and Zheng (2004) lack sufficient diagnostic characters for species or genus identification.

Protitan minor Granger and Gregory, 1943

HOLOTYPE: AMNH 26416, a skull missing the distal end of the nasal process. (Presently the canines are missing although they were originally recovered and can be seen in older photographs of the specimen).

TYPE LOCALITY: "Probably top of Irdin Manha beds", Camp Margetts, Inner Mongolia, China.

AGE: Middle Eocene (Irdinmanhan land mammal "age").

REFERRED SPECIMEN: **(From 1 mile west of Camp Margetts, ?Irdin Manha beds, Inner Mongolia)** AMNH 26417, a left anterior quarter of a skull with I3 and P2–M3.

DIAGNOSIS: *Protitan minor* is an intermediate-sized brontothere with small but distinct elliptical frontonasal horns that are positioned low on the skull and slightly in front of the orbits. The nasal incision extends posteriorly to the M1 and is dorsoventrally shallow. The nasal process is slightly angled downward, unelevated, long, broad, and with thin and shallow sidewalls. The orbits are positioned above the posterior portion of M2 and the anterior portion of M3. The premaxillomaxillary rostrum thickens posteriorly and it is not enclosed by bone dorsally. Other cranial characteristics include a saddle-shaped cranium, separate parasagittal ridges that strongly constrict the dorsal surface of the cranium posteriorly, postzygomatic processes, nearly straight zygomatic arches, and a ventrally unconstricted and posteromedially angled external auditory pseudomeatus.

Dentally, *Protitan minor* has three large subcaniniform upper incisors, a simple P1, and a distinct P2 metacone. Premolar hypocones are absent but short lingual crests are present in some premolars. The molars have tall lingually angled ectolophs with weak labial ribs, and thinned lingual ectoloph enamel with wedge-shaped paracones and metacones. A cingular parastyle shelf is absent. Very shallow central molar fossae are present. Anterolingual cingular cusps are absent. Paraconules and metalophs are absent.

Protitan minor most closely resembles *Protitanotherium emarginatum* and *Protitan grangeri*. It can be most easily distinguished

from *Protitanotherium* by the larger and more subcaniniform incisors, postzygomatic processes, and the ventrally unconstricted external auditory pseudomeatus. *Protitan minor* can be distinguished from *Protitan grangeri* by a posteriorly deeper nasal incision, thinner nasal process, more posteriorly positioned horns, and a posteromedially angled auditory pseudomeatus.

Description

Skull: AMNH 26416 is a nearly complete skull with significant amounts of plaster filling in a large portion of the occiput and parts of the frontoparietal (fig. 70). The nasal process is mostly missing (although it is has been reconstructed as if very short), and the skull has suffered a minor amount of lateral sheering distortion. Otherwise the proportions of the skull appear to be relatively undistorted. A second specimen, AMNH 26417, a left anterior quarter of a cranium, has a more complete nasal process (fig. 71).

Protitan minor is most similar to that of *Protitan grangeri* and *Protitanotherium emarginatum* although it is smaller than these species. The frontonasal protuberances are similar to those of *Protitan grangeri* and *Protitanotherium emarginatum*; they are short and elliptical with a longer anteroposterior axis. The frontonasal protuberances are positioned low on the skull and slightly in front of the orbits. This differs from *Protitan grangeri* whose horns are positioned far anterior to the orbits. The frontal bone can be seen overlapping the nasal bone and extending to the peak of the frontonasal protuberance.

The nasal incision is dorsoventrally shallow, but it is longer than that of *Protitan grangeri* and extends to a point above the M1 mesostyle. The anterior rim of the orbit rests over the posterior lateral root of the M1 and the anterolateral root of the M2. The orbit is positioned directly over the posterior half of the M2 and the anterior portion of the M3. In AMNH 26417 the nasal process is nearly horizontal, but it is angled downward slightly and is about as long at the premaxillomaxillary rostrum. The nasal process is much thinner than that of *Protitan grangeri*. In this respect it is similar to the nasal bones of *Telmatherium validus* and *Epimanteoceras formosus*. However, the lateral wall of the nasal process is much shallower than *Telmatherium* and most other hornless brontotheres.

The premaxillomaxillary rostrum of *Protitan minor* is typical in most respects. From the lateral view it deepens posteriorly and the dorsolateral margin rises posterodorsally so that the posterior notch of the nasal incision is at the level of the upper rim of the orbit. From the dorsal view of the skull the dorsolateral margins of the rostrum diverge posterolaterally and the rostral cavity (which is presently filled with plaster) is not dorsally sealed by bone. The premaxillae fully contact each other at the symphysis. The premaxillomaxillary suture is visible from the left side of the skull; the premaxilla truncates anterior to the posterior notch of the nasal incision and, therefore, does not contact the nasals.

The postorbital cranium is much longer than the facial region of the skull. The dorsal surface of the cranium of *Protitan minor* is essentially saddle-shaped. The posterior half of the frontoparietal is clearly concave. The anterior half is more flat, although this portion of the dorsal surface is somewhat warped, and from the dorsal view it can be seen that large portions of skull between the orbits are missing. Otherwise the general shape of the postorbital cranium of AMNH 26416 is similar to *Protitan grangeri*. The parasagittal ridges converge medially and constrict the dorsal surface of the skull posteriorly, but they do not form a sagittal crest. The zygomatic arches are relatively thin, shallow, and laterally unbowed. From a lateral view, the jugal portion of the zygomatic is horizontal. The squamosal portion of the zygomatic is angled upward posteriorly but at a very shallow angle, and there is essentially no curvature of the zygomatic arch. The posterodorsal end of each of the zygomatic arches exhibits a dorsally projecting postzygomatic process that is similar to that of *Protitan grangeri*.

Although poorly preserved, the overall shape of the occiput seems to resemble that of *Protitan grangeri*. The occiput appears to be tilted backward. From a dorsal view of the skull, the nuchal crest is concave. From the

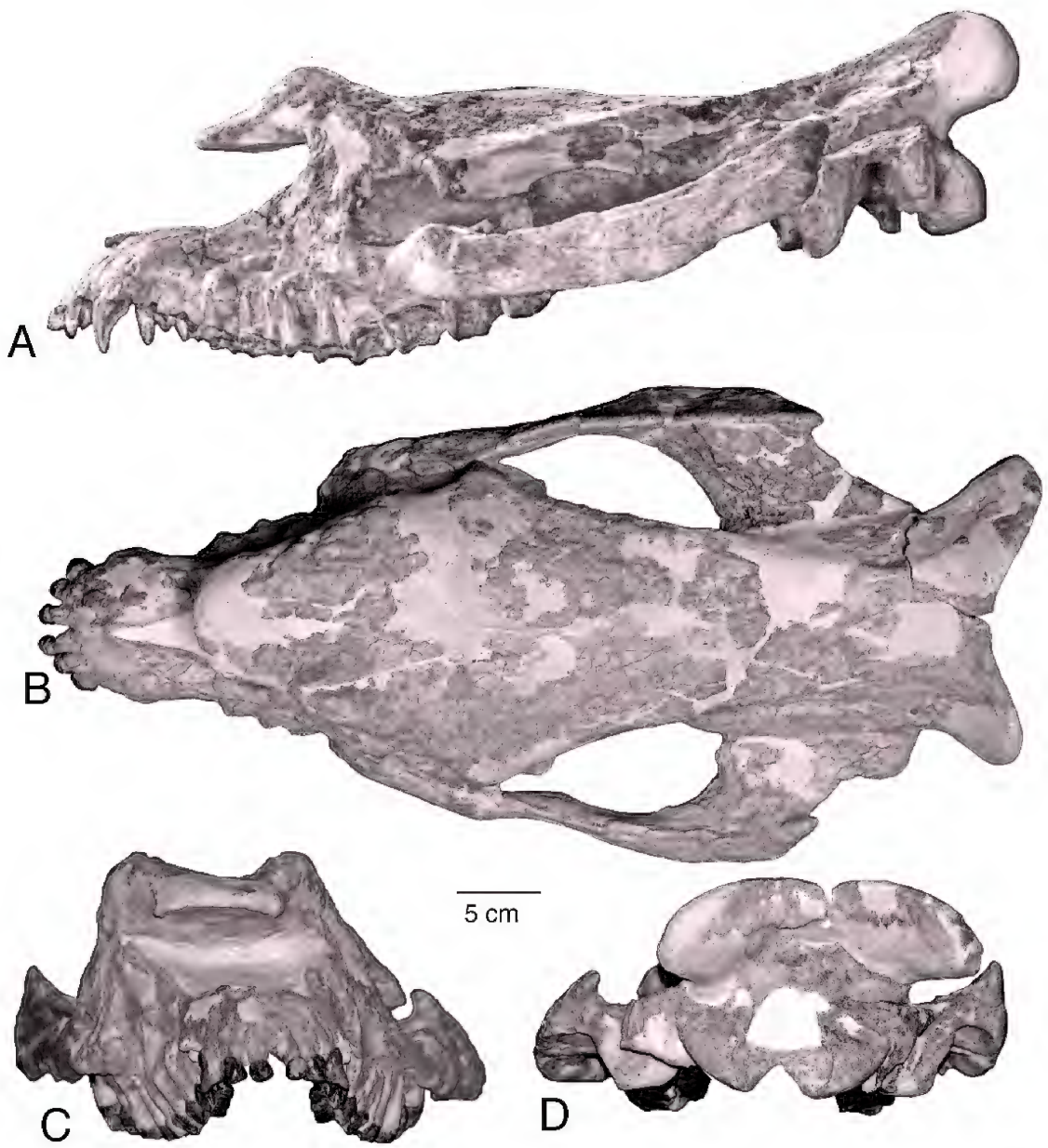

Fig. 70. The holotype skull of *"Protitan" minor* (AMNH 26416). **(A)** Left view originally published by Granger and Gregory (1943: pl. 8a; photo from the American Museum of Natural History vertebrate paleontology archive) showing the left canine (now lost), **(B)** dorsal view, **(C)** anterior view, **(D)** posterior view.

posterior view the dorsal half of the occiput is heavily reconstructed, but it appears to have been about as wide as the posterior portion. The occiput appears to have been constricted in the middle.

The posterior nares of AMNH 26416 are slightly more anteriorly positioned in comparison to *Protitan grangeri* (fig. 72a). The anterior rim of the posterior nares seems to be positioned slightly anterior to the M3.

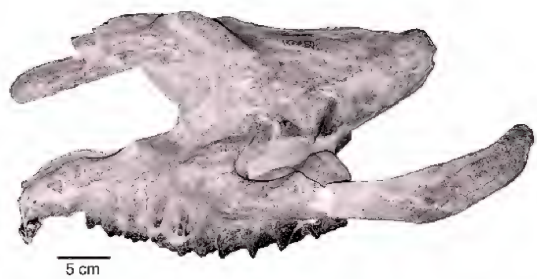

Fig. 71. Left lateral view of a partial skull (AMNH 26417) of *"Protitan" minor*.

However, the elongate posterior narial canal is completely filled with plaster, thus obscuring other details of the posterior nares. Two large ventral sphenoidal fossae are present and are distinctly partitioned by a thin bony septum formed by the basisphenoid. Like *Protitan grangeri*, the external auditory pseudomeatus forms a broad ventrally unconstricted opening; however, it enters the skull in a posteromedial direction.

Upper Dentition: The teeth of the holotype skull (AMNH 26416) are complete (except for the lost canines), undamaged, and for the most part, they are only lightly worn (fig. 72). The incisors of *Protitan minor* are relatively large but with small diastemata between them. They form a distinct arch anterior to the canines. The tips of the incisors are worn, but each incisor appears to have been subcaniniform with a short, lingually curved crown and a distinct lingual cingulum. The I3 is distinctly larger and taller than the I1 or I2 and it is more caniniform. Relatively large canines were once present and can be seen in older photographs of AMNH 26416 (fig. 70a). However, the canines are now missing (fig. 72a). There are both short precanine and postcanine diastemata.

The cheek teeth are not differentiated from those of *Protitan grangeri*. The P1 is a single-cusped tooth with an elongate posterior heel. A small lingual cingulum is also visible on the P1. The anterior margin of P2 is angled distolingually, giving the tooth a strongly oblique shape. The anterior and posterior margins of P3 and P4 are closer to parallel. The parastyle of P2 is straight, although the ectoloph and the metastyle are directed in a posterolingual direction. The parastyle and metastyle of P3 are nearly straight, while the parastyle and metastyle of P4 are distinctly angled labially. The labial margin of the P2 paracone is very convex, while the paracones of P3 and P4 have distinct labial ribs. The metacone of P2 is lingually shifted, while those of P3 and P4 are more labially positioned. Because of these differences the outer surface of P2 is rounder than those of P3 and P4.

Like *Protitan grangeri* the lingual features of the premolars have low topographic relief. Only a single lingual cusp (protocone) is present on P2–P4. A small preprotocrista is seen on the P2. A faint preprotocrista can be discerned on the P3. Additionally, the protocones of P2 and P3 are each followed by a short lingual crest. The lingual heel of P4 is devoid of any crests. The anterior and posterior premolar cingula wrap around the lingual side of the crowns and nearly join together, but they do not form completely continuous lingual cingula.

The molars show typical brontotheriine apomorphies, including tall, lingually angled ectolophs, very weak labial ribs, thin lingual ectoloph enamel, and wedge-shaped lingual sides of the paracone and metacone in molars that are not heavily worn. The anterior cingulum is thin and passes proximally to the distal peak of the parastyle. Central molar fossae are present, but they are very shallow and almost indistinct. Anterolingual cingular cusps are absent. All traces of paraconules and metalophs are lost. M3 lacks a hypocone. Labial molar cingula are weak, and lingual molar cingula are absent.

Remarks

Protitan minor Granger and Gregory (1943) is based on a nearly complete skull (AMNH 26416) from the Camp Margetts area of Inner Mongolia. Along with *P. grangeri*, *P. minor* is one of only two brontotheres with conspicuous frontonasal horns that retains a ventrally unconstricted external auditory pseudomeatus. Granger and Gregory (1943) did not explicitly state how *P. minor* differed from *P. grangeri* although there are several differences. In addition to being distinctly smaller, *P. minor* can clearly be differentiated by its shorter

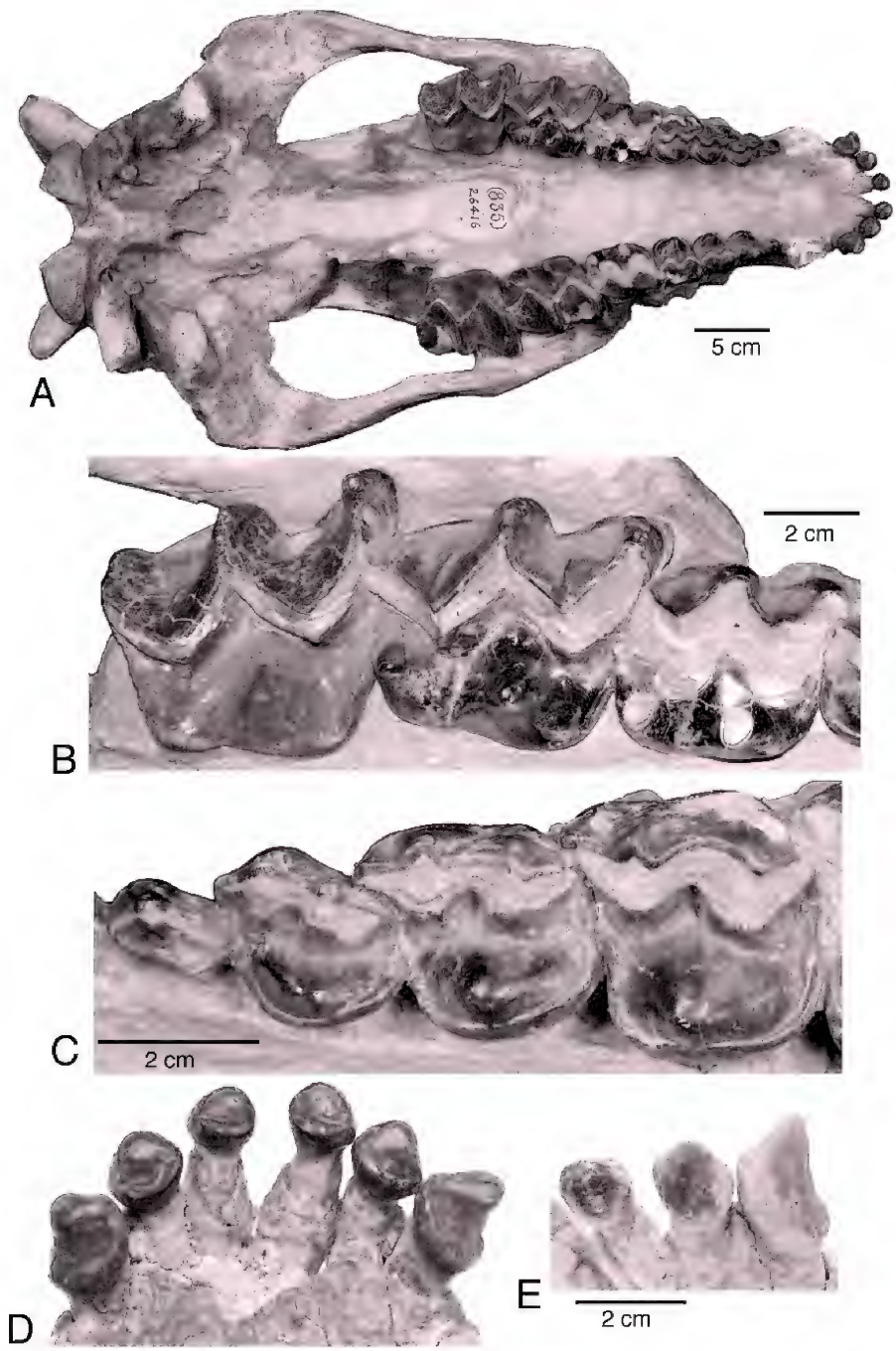

Fig. 72. The holotype skull of *"Protitan" minor* (AMNH 26416). **(A)** Ventral view (note that the canines have been lost since Granger and Gregory [1943]), **(B)** right molars, **(C)** left premolars, **(D)** lingual view of incisors, **(E)** labial view of right incisors.

more constricted face, more posteriorly positioned horns, and thinner nasal bone.

No mandibles or lower teeth can presently be referred to *Protitan minor*. However, considering that the upper dentitions of *P. grangeri* and *P. minor* are undifferentiated, it seems likely the lower dental morphologies of these species were similar. Granger and Gregory (1943) referred several mandibles from the Camp Margetts area of Inner Mongolia to *P. minor*; however, the large metaconid seen on the p3 of these specimens is inconsistent with what one would expect of the lower dentition of *P. minor*. Therefore, I have removed these specimens from *P. minor* and reassigned them to an unnamed taxon, informally referred to as Camp Margetts "taxon A" (see section on dubious and problematic taxa).

Yet another mandible (AMNH 26419) from the "Houldjin" beds of Camp Margetts, with extremely worn incisors, a complete and moderate-sized left canine, and right and left premolars, closely resembles what one would predict for *Protitan minor* in terms of size and overall morphology. Unlike the mandibles assigned to Camp Margetts "taxon A", the p3 of this specimen lacks a metaconid. This specimen could represent *P. minor*. Additionally, Dong and Ai (2001) referred a left p1–p4 and right m1 from the lower part of the Tunggur Formation of Inner Mongolia to *P. minor*. These referrals were based primarily on size and there is no conclusive evidence that they actually belong to P. *minor*.

Protitanotherium emarginatum Hatcher, 1895

HOLOTYPE: YPM-PU 11242, the anterior portion of a cranium with incisors and canines, and a partial mandible with right i1–p2, left i1–m2, and m3 (partial).

TYPE LOCALITY: Kennedy's Hole, Myton Member (Uinta C) of the Uinta Formation, Uinta Basin, Utah, eight miles north of White River and 25 miles east of Ouray Agency.

AGE: Middle Eocene (late Uintan land mammal "age").

SYNONYMS: *Protitanotherium superbum* Osborn, 1908a; *Sthenodectes australis* Wilson, 1977.

REFERRED SPECIMENS: **(From the Myton member of the Uinta Formation of Utah)** AMNH 2501 (holotype of *Protitanotherium superbum*), a left maxilla fragment with M2–M3, and a partial mandible with right p1–m3 and left c–m3; YPM PU11213, a distal fragment of a nasal process; CMNH 2855, a dorsal surface of the anterior portion of a cranium; YPM 11146, an anterior portion of a mandible with right i1, i2 (partial), i3–c, p2–p3, p4 (partial), left i1, i2 (broken), and i3–p4; **(from the Pruett Formation of the Agua Fria Area in Trans-Pecos Texas)** TMM 41723-3 (holotype of *Sthenodectes australis*), a skull with right C–M3 and left P1–M3; TMM 41723-6, a skull with right and left P1–M3, TMM 41747-106, a partial skull with right C–M3, left P1–M3, and isolated right I3.

DIAGNOSIS: *Protitanotherium emarginatum* is a large brontothere with small, elliptical frontonasal horns positioned low on the skull. The nasal incision is dorsoventrally shallow and extends as far back as the P4. The nasal process is nearly horizontal, unelevated, short and broad, with thickened sides, and with a thickened and imperfectly rounded distal edge with a distinct median notch. The lateral margins of the nasal process are not upturned. The orbits are positioned above M2. The premaxillomaxillary rostrum thickens posteriorly and it is not sealed by bone dorsally. Other cranial characteristics include a saddle-shaped cranium, separate parasagittal ridges that strongly constrict the dorsal surface of the cranium posteriorly, nearly straight zygomatic arches, and tube-shaped and mediolaterally angled external auditory pseudomeati. The posterior narial canal does not extend past the foramen ovale and large ventral sphenoidal fossae are absent.

Dentally, *Protitanotherium emarginatum* has three intermediate-sized subglobular upper incisors, and metacones on P1 and P2. Premolar hypocones are absent, although a short lingual crest can occasionally be seen extending from the protocones. The molars have tall lingually angled ectolophs with weak labial ribs, and thinned lingual ectoloph enamel with wedge-shaped paracones and metacones. A cingular parastyle shelf is absent. Central molar fossae are present,

but anterolingual cingular cusps are absent. Paraconules and metalophs are absent. The lower dentition includes three intermediate-sized semispatulate incisors with an enlarged i2, a distinct postcanine diastema, a metaconid on p4 but not on p2 or p3, shallow molar basins, and a slender m3.

Protitanotherium emarginatum most closely resembles *Protitan grangeri* and *Protitan minor*, but it can be most easily distinguished from these species by the smaller, less subcaniniform incisors and tube-shaped external auditory pseudomeatus. Additionally, *Protitanotherium emarginatum* is distinct from *Diplacodon elatus* in its relatively smaller horns, dorsoventrally shallow nasal incision, less deeply saddle-shaped cranium, differently shaped nasal process, and less molarized premolars.

Description

Skull: The holotype of *Protitanotherium emarginatum* consists of the preorbital portion of a skull (fig. 73) and a partial mandible (fig. 77). The skull has been slightly sheared. None of the previously published figures of this specimen (Hatcher, 1895; Osborn, 1929a) clearly differentiates real bone from those parts that are reconstructed with plaster. A large fragment of maxilla and nasal bone is missing from the left face between the orbits and nasal incision. In the mandible the crowns of the left canine and left i3 are almost entirely reconstructed. The lingual half of the left m2 is plaster, as is the majority of the left m3.

In addition to the holotype, two nearly complete skulls from the Pruett Formation of Texas allow for a more thorough description of the skull of *Protitanotherium emarginatum*. TMM 41723-3 (fig. 74) is most significantly damaged in the region above the orbits; essentially the frontonasal horns appear to have been forced back and down over the orbits, significantly distorting this region of the skull including the frontonasal protuberances. Neither the original figures of this specimen nor the initial description of Wilson (1977) reveals that the specimen is damaged in this way. Additionally, the left zygomatic arch is incomplete although a large central segment of it is reconstructed. The second skull, TMM 41723-6 (fig. 75), is less distorted, although the nasal bone is split and the left zygomatic arch is incomplete.

The horns of the holotype (fig. 73) are oval, widely separated on the skull, and they project in a dorsolateral direction. They are larger and more prominent than those of *Protitan grangeri* or *P. minor*, but they are smaller than those seen on most specimens of *Diplacodon elatus*. The horns of TMM 41723-3 (fig. 74) are similar in size and shape although they seem to be directed somewhat more laterally. TMM 41723-6 almost completely lacks hornlike protuberances (fig. 75). The considerable size variation in the horns of *P. emarginatum* is not unlike other horned brontotheres (e.g., *Diplacodon elatus*).

From a lateral view of the holotype skull it can be seen that the short horns are formed by both the frontal and nasal bones. This configuration of facial bones resembles that of *Telmatherium validus*, which has an anteriorly projecting process of the frontal bone overlapping the nasal bone. The nasal bone forms the proximal base of the frontonasal protuberance. Two thin sheets of roughened bone appear to overlap the upper surface of the nasal swelling. The upper layer extends to the peak of the protuberance and represents the frontal bone. The lower layer extends over the entire protuberance. It is not clear whether the lower layer is part of the frontal bone or it represents secondary growth of the nasal bone. Below the frontonasal protuberance, the nasal contacts the maxillary in a distinct arch.

The horns of the holotype skull are positioned above the preorbital portion of the face and they are not highly elevated above the skull as in *Diplacodon elatus*. In TMM 41723-3 the horns are positioned directly above the orbits, although this portion of the cranium is clearly distorted in that area and the horns have been displaced posteriorly. An earlier reconstruction of this specimen (Wilson, 1977: fig. 2) places the horns anterior to the orbits.

Due to the fragmentary nature of the holotype specimen it is difficult to define the position of the posterior margin of the nasal or the position of the orbit with respect to the dentition. The length of the nasal incision is similar to *Protitan minor*. In TMM skulls, the

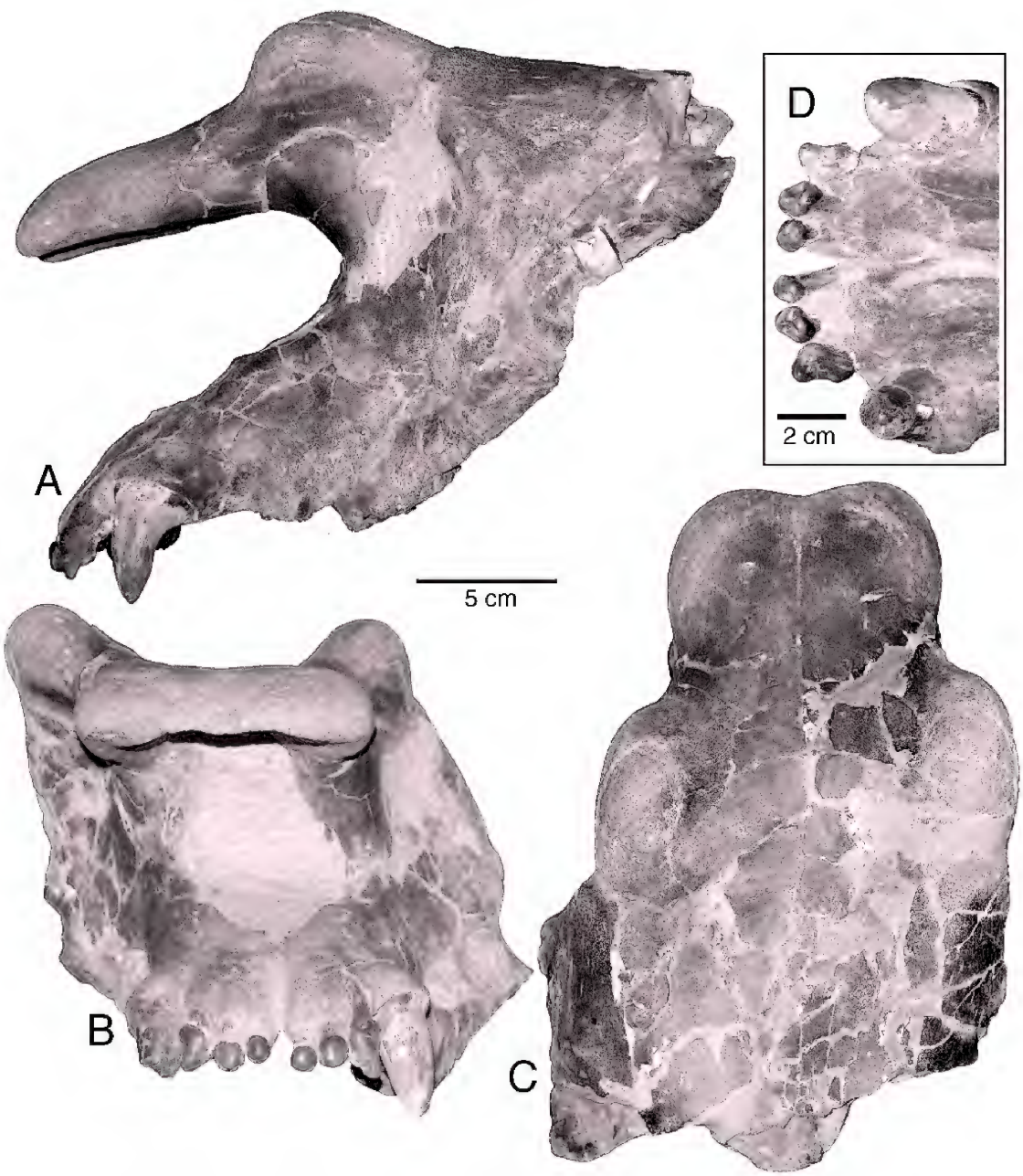

Fig. 73. The holotype skull of *Protitanotherium emarginatum*. (Division of Vertebrate Paleontology, YPM PU11242. © 2005 Peabody Museum of Natural History, Yale University, New Haven, Connecticut, USA. All rights reserved.) **(A)** Left view, **(B)** anterior view, **(C)** dorsal view, **(D)** lingual view of incisors and canines.

nasal incision extends to the P4 and the orbits are positioned more or less above the M2.

Unlike *Diplacodon elatus*, the nasal incision of *Protitanotherium emarginatum* is dorsoventrally shallow. The nasal process of the holotype is unelevated, straight, angled slightly downward, and it is shorter than the premaxillomaxillary rostrum. The sides of the nasal process are thickened. The thickened lateral edges extend downward, but they

Fig. 74. A skull referred to *Protitanotherium emarginatum* (TMM 41723-3). **(A)** Dorsal view, **(B)** left view.

do not form deep vertical walls. The sides of the nasal process are not upturned as in *D. elatus*. From a dorsal view the nasal bones are strongly fused but the nasal suture is still visible. The nasal process is as wide as the premaxillomaxillary rostrum although its width is slightly constricted proximally. The distal margin nasal process is nearly flat, although it is somewhat concave medially. The anterior edge of the nasal process of TMM 41723-3 is more rounded and more strongly notched at the midline in comparison to the holotype. From the anterior view of the holotype, the anterior edge of the nasal process is relatively flat, thick, and mildly roughened. The anterior margin is not strongly deflected downward at the midline as in *Protitan grangeri* or *D. elatus*.

The premaxillomaxillary rostrum is best preserved in the holotype (fig. 73). From the lateral view the dorsolateral margin of the rostrum rises posterodorsally at a very shallow angle. The premaxillae are strongly fused at the symphysis. A premaxillomaxillary suture can be seen although it is indistinct. The premaxillae end before reaching the posterior notch of the nasal incision and they do not contact the nasal bone. From the anterior view the dorsolateral margins of the rostrum are laterally divergent and the rostral cavity is not sealed dorsally by bone.

Although the holotype is merely an anterior cranial fragment, Hatcher (1895) described the skull of *Protitanotherium emarginatum* as "slightly concave anteroposteriorly? and further characterized by the ab-

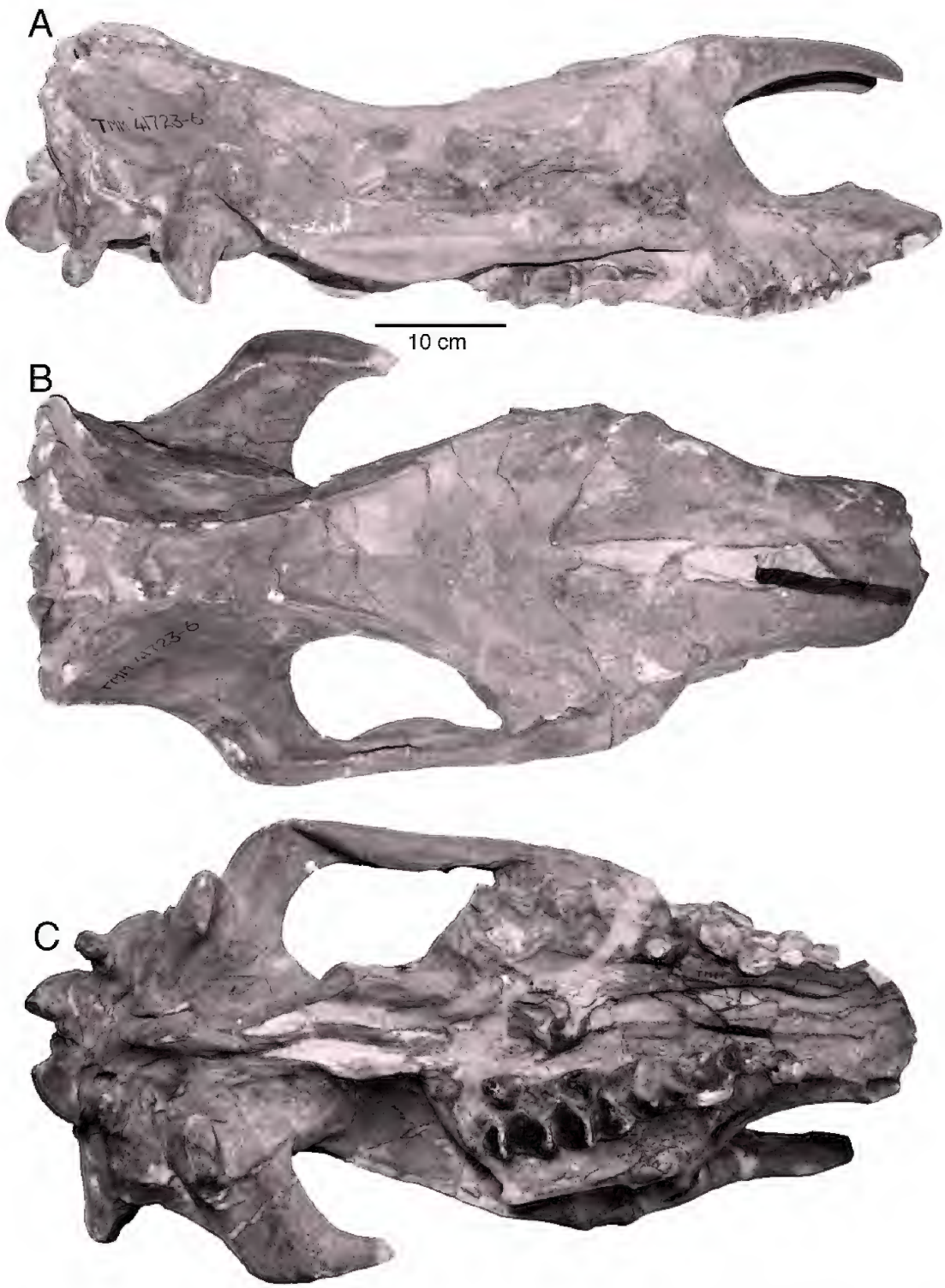

Fig. 75. A skull referred to *Protitanotherium emarginatum* (TMM 41723-6). **(A)** Right view, **(B)** dorsal view, **(C)** ventral view.

sence of a sagittal crest" (Hatcher, 1895: 1085). Hatcher must have made these observations on parts of the holotype that have been lost. Hatcher (1895) indicates, "the posterior region had already weathered out and was badly injured, but many of the pieces have been fitted together and show some of the more important characters of this region of the skull" (Hatcher, 1895: 1084–1085). The TMM specimens are consistent with Hatcher's observations on these missing pieces. The dorsal surfaces of these skulls are concave from the orbits to the nuchal crest. The parasagittal ridges do not join to form a sagittal crest, although they strongly constrict the posterior portion of the dorsal surface.

The zygomatic arches of TMM 41723-3 are thick whereas those of TMM 41723-6 are thinner; this variation corresponds with the differing degrees of horn development and canine size in these specimens. In both specimens, the jugal portion of the zygomatic is straight from a dorsal view and from a lateral view it is horizontal. The squamosal portion of the zygomatic is very weakly angled posterodorsally and the zygomatic arch is almost completely straight from a lateral view. A posterior zygomatic processes is not seen in *Protitanotherium emarginatum*.

There is no discernable infraorbital process on the TMM specimens. Nonetheless, Wilson (1977) described the TMM specimens as "give[ing] the appearance of having an infraorbital protuberance, but if the effect of the crushing were removed, such a protuberance would probably not have been more prominent than in CMNH 2398" (Wilson, 1977: 5). (CMNH 2398 is the holotype of *Sthenodectes incisivum*.) It is not clear what Wilson (1977) meant by this statement, since the lower portion of the orbit and suborbital region do not appear to be significantly distorted.

The occiputs of the TMM specimens are wide and strongly tilted backward. The dorsal portion is essentially the same width as the ventral portion and the occiput is not constricted in its middle. The nuchal crest is thin and is somewhat concave at the midline.

The anterior rim of the posterior nares is positioned between the protocones of the M3s in TMM 41723-3 and at the anterior margin of M3 in TMM 41723-6. The posterior nares of both specimens are rimmed by a distinct U-shaped emargination. In TMM 41723-6 the posterior nares have been more fully cleared of sediment, revealing that the full width of the bony emargination that surrounds the posterior nares. In TMM 41723-6 the thin vomer can be seen bisecting the elongate posterior canal and joining with the sphenoid. The posterior narial canal, which is filled with sediment, extends somewhat into the sphenoid but not posterior to the foramen ovale. Large ventral sphenoidal fossae are not seen on this specimen. Other aspects of the basicranium, such as the widely separated foramen ovale and foramen lacerum, are typical for brontotheres. The mastoid process is short and curves anteroventrally, contacting the postglenoid process, thus, the external auditory pseudomeatus is closed ventrally and tube-shaped. This configuration differs from *Protitan*, but resembles all other horned brontotheres.

Upper Dentition: The upper incisors of the holotype are in good condition and lightly worn (fig. 73d). No other upper teeth are preserved on the holotype except for the poorly preserved canines. On the other hand, the TMM specimens lack incisors but have more complete cheek teeth, particularly TMM 41723-3 (fig. 76b, d).

Overall, the incisors of YPM-PU 11242 are significantly smaller than those of *Protitan*. The incisors increase in size laterally. The crowns of I1 and I2 are very short and blunt, although distinct lingual cingula can be seen on these teeth. The I3, on the other hand, is much larger and more subcaniniform than I1 or I2. The incisor row forms a very shallow arch that is positioned anterior to the canines. The I3 and canine are separated by a large diastema. Though the crowns of both canines are incomplete, it is apparent from the roots and the base of the right canine crown that the canines of this specimen were very large. The canines of TMM 41723-3 are of a similar size, although the left canine alveolus of TMM 41723-6 (fig. 75c) indicates a somewhat smaller canine. A distinct postcanine diastema is consistently present in these specimens, although its length is variable.

No cheek teeth are attached to the holotype skull, however, Hatcher (1895: pl.

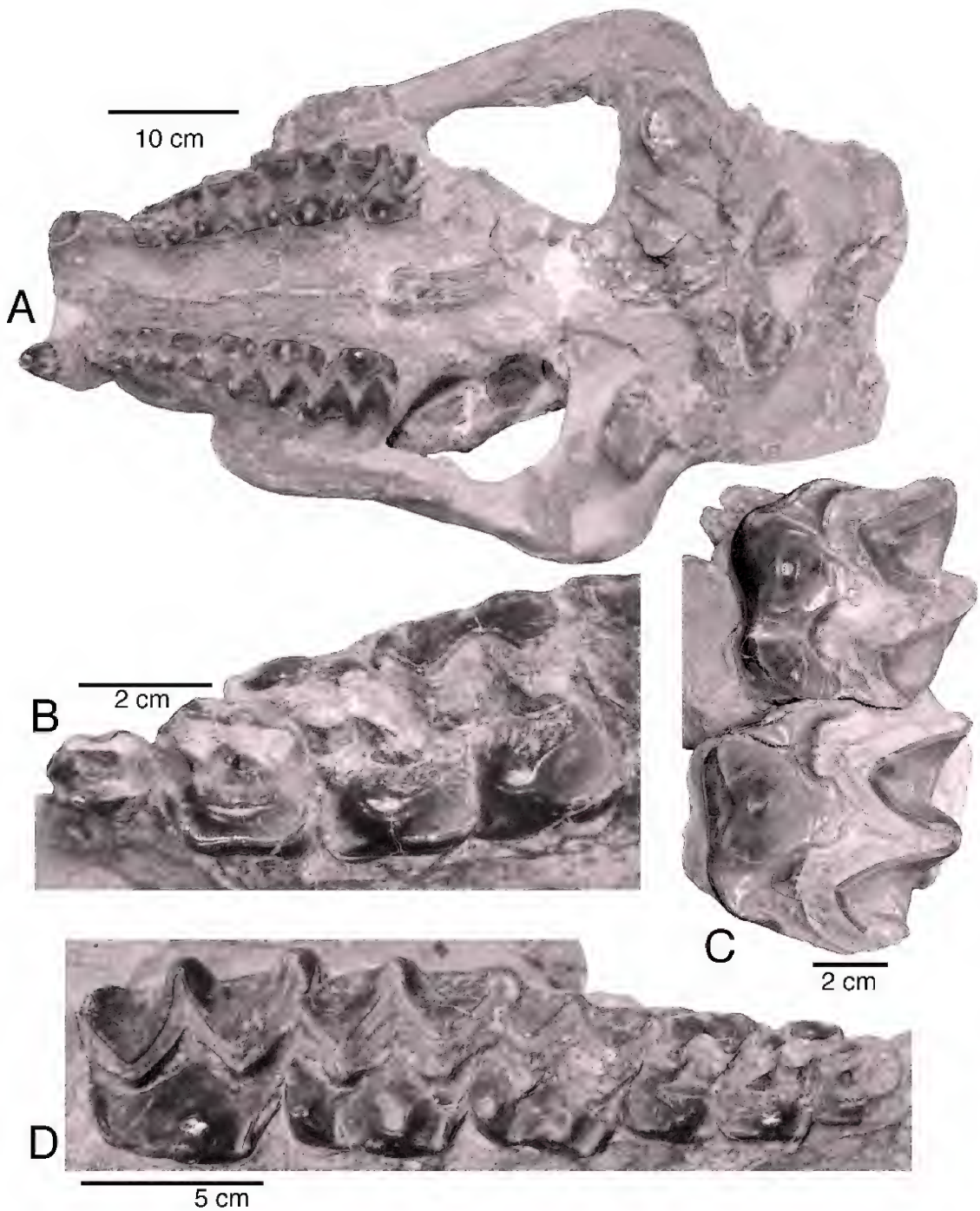

Fig. 76. Ventral views of skulls and upper dentition referred to *Protitanotherium emarginatum*. **(A)** ventral view of TMM 41723-3, **(B)** left premolars of TMM 41723-3, **(C)** M2 and M3 of AMNH 2501, **(D)** right P2–M3 of TMM 41723-3.

38) and Osborn (1929a: fig. 317) each figured and described a left P1. The tooth was lost sometime after the fossil was molded, because the tooth is present on plaster casts found in numerous North American museums. Hatcher (1895) described it as "a very simple tooth fixed in the jaw by two roots, and consisting of a single cone with a posterior heel" (Hatcher, 1895: 1086). Osborn described the P1 somewhat differently as a "bifanged tooth...with a simple protocone, a sessile or rudimentary posterior heel, and a posterointernal cingulum and concavity" (Osborn, 1929a: 378). Inspection of a cast (AMNH 10385) reveals that Osborn's (1929a) description is more accurate. There is both a paracone and a smaller metacone, although wear has virtually obliterated the metacone. However, Osborn's identification of a protocone on the P1 is misleading. There is a small, posteriorly positioned lingual heel with a minor undulation of enamel on it, but it does not bear a distinct protocone. The P1 of TMM 41723-3 is smaller than the P2, but it is morphologically very similar, with two labial cusps of similar size, a relatively straight ectoloph, and a well-developed lingual heel. The lingual heel appears to have a small protocone and a small anteroposteriorly oriented lingual crest.

The P2–P4 of TMM 41723-3 are in good condition (fig. 76b). These teeth are closely pressed together. The P2 crown is slightly oblique, while the P3 and P4 crowns are progressively more rectangular. The anterior margins of P3 and P4 are worn away because of interstitial wear resulting in the formation of concave anterior margins. It is interesting that the posterior margins of P2 and P3 fit perfectly into the concave worn anterior margins of P3 and P4, but curiously, the posterior margins of P2 and P3 seem not to have been experienced significant interstitial wear. The ectoloph of P2 is straight, although in P3 and P4, the parastyles are somewhat labially directed. Distinct labial paracone ribs can be seen on P2–P4, though they become progressively smaller in more posterior premolars. The lingual heels of the P2–P4 are broad with nearly flat lingual edges. There are no distinct lingual cusps on the P2. Rather, a short lingual crest extends anteroposteriorly along the lingual side of the crown and is joined anteriorly by a small preprotocrista. Both P3 and P4 have a distinct protocone. The preprotocrista of P3 is faint, while the P4 has no preprotocrista. The protocones of P3 and P4 are followed posteriorly by very weak lingual crests. There are no hypocones on any of the premolars, thus the premolars of *Protitanotherium emarginatum* are significantly less molarized than are those of the contemporary species, *Diplacodon elatus*. The labial premolar cingula are weak. The lingual P2 cingulum is strong and continuous. The lingual cingulum of P2 is slightly discontinuous and it is more discontinuous on P4.

In addition to the molars of TMM 41723-3 (fig. 76d), a close up view of the M2 and M3 of AMNH 2501 is provided (fig. 76c). The molars of *Protitanotherium emarginatum* exhibit typical brontotheriine apomorphies including tall, lingually angled ectolophs, weak labial ribs, thin lingual ectoloph enamel, and wedge-shaped lingual sides of the paracone and metacone in relatively unworn molars. The anterior cingulum is thin and passes proximally to the distal peak of the parastyle. The following traits can be more distinctly seen in AMNH 2501. Shallow but distinct central molar fossae are present. The lingual portion of the anterior cingulum is thickened, but it does not form a distinct anterolingual cingular peak. All remnants of paraconules or metalophs are lost. There is no hypocone on the M3, but a portion of the posterior cingulum is thickened. The labial molar cingulum tends to be weak and discontinuous around the mesostyles.

Mandible and Lower Dentition: In the mandible of the holotype (fig. 77) the inferior margin of the symphysis is angled slightly less than 45° and it extends to the anterior margin of p4. The ascending ramus is not preserved, although in another specimen, AMNH 2501 (fig. 78), the coronoid process is long, slender, moderately curved, stands higher than the condyle, and is not generally different from other brontotheres.

The lower incisors are significantly smaller than those of *Protitan grangeri*. They are more similar in size to those of *Diplacodon elatus*, but they are not reduced to the essentially vestigial condition seen in more advanced horned brontotheres such as *Duch-*

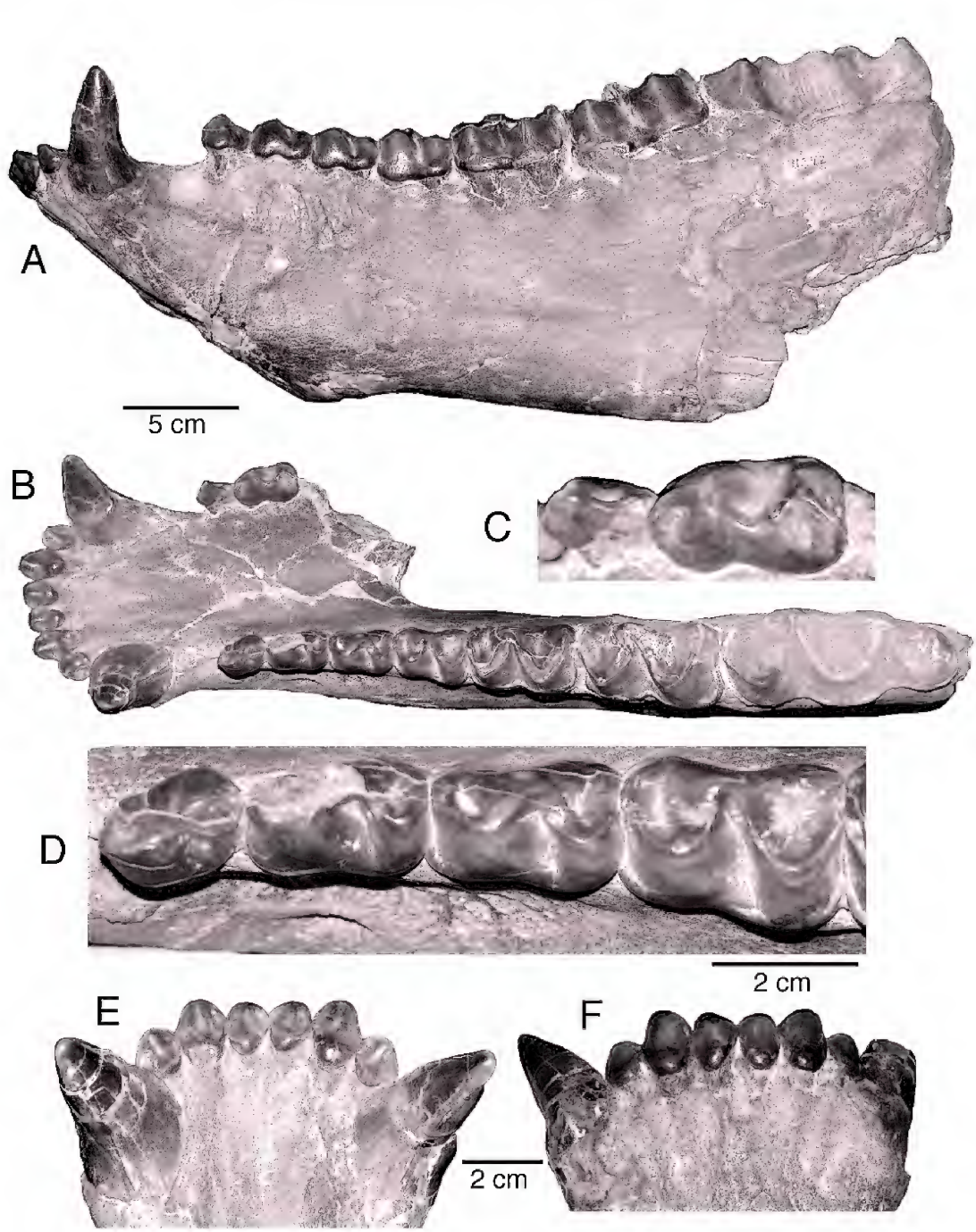

Fig. 77. The holotype mandible of *Protitanotherium emarginatum*. (Division of Vertebrate Paleontology, YPM PU11242. © 2005 Peabody Museum of Natural History, Yale University, New Haven, Connecticut, USA. All rights reserved.). **(A)** Left view, **(B)** dorsal view, **(C)** right p1 and p2, **(D)** left premolars, **(E)** lingual view of incisors and canines, **(F)** labial view of incisors and canines.

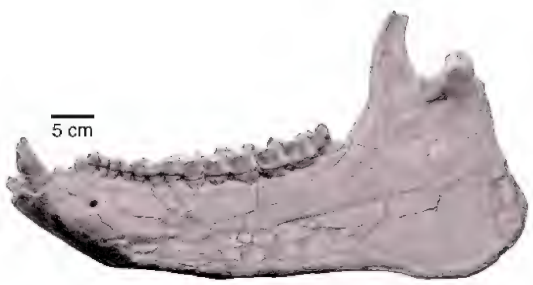

Fig. 78. Left view of a mandible referred to *Protitanotherium emarginatum* (AMNH 2501).

esneodus uintensis. The lower incisors are only lightly worn. They are semispatulate in shape. The i2 is significantly larger than either the i1 or the i3 in height and in labiolingual width. There are no labial cingulids and the lingual cingulids are faint. The incisors form only a slight arch anterior to the canines. The lower canines of both YPM-PU 11242 and AMNH 2501 are rather large. There is no precanine diastema. The postcanine diastema is asymmetrical in YPM PU11242. On the right side it is slightly longer than the p2, but on the left side it is a little shorter.

The right and left p1s of YPM-PU 11242 are bilaterally asymmetrical. The right p1 is a narrow single cusped tooth with an elongate posterior talonid heel. The left p1 is notably wider, particularly the posterior portion of the crown. The p2–p4 have relatively low slender crowns. The trigonids of p2 and p3 are less than twice as long as the talonids. The trigonid and talonid of p4 are of similar length. The talonids of p2–p4 are slightly wider than the trigonids. On p2 and p3 the paralophids and protolophids extend from the protoconid in a slightly lingual direction. There is only a small lingual trigonid notch on the p2, although the lingual trigonid notch of the p3 is large. The paralophid and protolophid of p4 arch 90° lingually, forming a nearly molariform trigonid basin. Metaconids are absent on p2 and p3 but they are present on p4. The cristids obliqua and hypolophids of p2 and p3 are well developed, but they are short and the lingual-talonid notch does not form a molariform basin. However, the cristid obliqua and hypolophid of p4 are much longer and create a more molariform talonid basin. Lingual premolar cingulids are absent, while labial premolar cingulids are absent (p2, p3) or very weak (p4).

The molars are typical, with thin lingual enamel, weak lingual ribs, and shallow talonid basins. The m3 of the holotype is incomplete but that of AMNH 2501 is elongate. The labial cingulids of the molars are much stronger in comparison to the premolars.

Remarks

Hatcher (1895) named *Protitanotherium emarginatum* from a specimen (YPM-PU 11242) consisting of the anterior portion of a skull with short frontonasal horns and a partial mandible. Previously, Marsh (1875) had named another species of horned brontothere, *Diplacodon elatus*. When Hatcher (1895) described *P. emarginatum* the existence of a horn in *D. elatus* was in question. For this reason Hatcher (1895) cautiously referred his new species to the genus *Diplacodon* but suggested, "should future discoveries show that there are hornless forms with the same dental characters as *Diplacodon*, it will be necessary to establish for the present specimen (YPM-PU 11242) a new genus, which may be called *Protitanotherium*" (Hatcher, 1895: 1084). Although it turns out that *Diplacodon elatus* does have horns, Osborn (1929a) demonstrated several distinctions between Hatcher's (1895) *D. emarginatum* and Marsh's *D. elatus*. Therefore, he adopted Hatcher's recommended genus name, *Protitanotherium*. Lucas and Schoch (1989a) felt that *Protitanotherium* was a junior synonym of *Diplacodon*, however Mader (1989; 1998) concluded that *Protitanotherium* was sufficiently different to warrant its distinct genus name. Mader's conclusion is accepted here.

Several additional specimens from the Uinta Formation are referred to *Protitanotherium emarginatum*, including the holotype mandible (AMNH 2501) of *P. superbum* Osborn (1908a). Osborn's specific characters for *P. superbum* do not clearly diagnose a new species. These include: "Canines in males very robust; p1 double fanged (an erroneous description); post canine diastema abbreviated; premolar series relatively abbreviated; p2

with very large talonid and crescentic protoconid; p3, p4 with talonid heavy and prominent, *i.e.*, submolariform, but no entoconid; m3 with hypoconulid sharply constricted off at base" (Osborn, 1908a). The mandible and cheek teeth of AMNH 2501 sufficiently resemble the holotype of *P. emarginatum* to refer it to that species. It distinctly differs from the contemporaneous horned species, *Diplacodon elatus*, particularly in the absence of a p3 metaconid. AMNH 2501 is somewhat larger than the holotype of *P. emarginatum*, but it falls within an acceptable body size range for that species. Other specimens, such as the nasal bone YPM PU11213 are larger than the holotype as well, suggesting that the type specimen is a rather small individual of the species. A pair of upper molars (left M2, M3) is also assigned to AMNH 2501 although Osborn (1908a) made no mention of these upper molars in the original description of *P. superbum*. Later, Osborn (1929a) assumed that these upper molars were part of the same specimen. Whether or not these upper molars are associated with the mandible (AMNH 2501) is questionable, but both, nonetheless, seem to belong to *P. emarginatum*.

A brontothere consistent with *Protitanotherium emarginatum* also occurs in the Whistler Squat local fauna of the Pruett Formation of the Big Bend–Trans-Pecos area, Texas, although until now that material has not formally been recognized as *P. emarginatum*. Wilson (1977) described this material as a new species, *Sthenodectes australis*. This species was based primarily on two nearly complete skulls. Wilson (1977) mistakenly referred this species to the genus *Sthenodectes*. According to Wilson (1977: 7) "the length of the tooth row and the approximate size of the teeth show that the partial skull is close to *Sthenodectes*." And secondly "the very large molars in proportion to the skull length, the advanced condition of the premolars, and the very rudimentary horns...seems to best fit *Sthenodectes*" (Wilson, 1977: 8). Despite Wilson's conclusion, it is clear that these skulls are far closer to *Protitanotherium* than *Sthenodectes*. It seems that Wilson (1977) failed to compare the material to *P. emarginatum*, largely because his comparisons were based on upper tooth measurements, elements lacking largely lacking in the holotype of *P. emarginatum*. Moreover, as with most work done on brontotheres after 1929, Wilson (1977) drew heavily from Osborn (1929a). Osborn (1929a: fig. 301) erroneously figured *Sthenodectes incisivum* as having a small horn. Actually, none of the *S. incisivum* specimens has a horn. Mader (1998) suggested that the skulls described by Wilson (1977) might be referable to *Protitanotherium*, but he made no formal revision. Indeed, the skulls of TMM 41723-3 and TMM 41723-6 are consistent with *P. emarginatum*. Differences between these skulls and the holotype of *P. emarginatum*, such as the morphology of P1 and variation in horn and canine size, are characters that are intraspecifically variable in other brontotheres. *S. australis* appears to be a junior synonym of *P. emarginatum*. Wilson (1977) referred several other specimens to *S. australis*, including some partial mandibles. These specimens could belong to *P. emarginatum*, but they lack sufficiently diagnostic morphology to make conclusive identifications.

Rhinotitan kaiseni (Osborn, 1925)

HOLOTYPE: AMNH 20252, a skull and mandible with extremely worn teeth.

TYPE LOCALITY: Shara Murun Formation, Ula Usu, Baron Sog Mesa, Inner Mongolia.

AGE: Middle Eocene (Sharamurunian land mammal "age").

REFERRED SPECIMENS: **(From the Shara Murun Formation, Ula Usu, Baron Sog Mesa, Inner Mongolia)** AMNH 20257, a ventral surface of a skull with a complete set of upper dentition; FMNH P14048 (formerly AMNH 20260), a skull and mandible with complete sets of upper and lower dentition.

DIAGNOSIS: *Rhinotitan kaiseni* is a large brontothere with small, elliptical frontonasal horns. The horns are positioned far in front of and high above the orbits. The nasal incision is dorsoventrally deep and extends posteriorly to P3. The orbit is positioned above M2 with posterolateral and anterolateral roots of M1 below the anterior orbital rim. The nasal process is unelevated, slightly angled upward, relatively narrow, not strong-

ly rounded anteriorly, and with deep lateral walls that arch around the anterior end of the nasal process. Proximally, the lateral walls of the nasal process deepen and angle ventromedially. The premaxillomaxillary rostrum thickens posteriorly and it is not enclosed by bone dorsally. Other cranial characteristics include an incompletely saddle-shaped cranium, a dorsal cranial surface that is not constricted posteriorly by parasagittal ridges, a narrow emargination surrounding the posterior nares, nearly straight zygomatic arches, and a ventrally constricted and posteromedially angled external auditory pseudomeatus. Ventral sphenoidal fossae and postzygomatic processes are absent.

Dentally, *Rhinotitan kaiseni* has three large but short subcaniniform upper incisors. The P1 crown is complex and there is a distinct P2 metacone. Premolar hypocones are present although the protocones and hypocones of P2 and P3 are sometimes fused into a single lingual crest. The molars of *R. kaiseni* have tall, lingually angled ectolophs with weak labial ribs, and thinned lingual ectoloph enamel with wedge-shaped paracones and metacones. A cingular parastyle shelf is absent. Distinct central molar fossae are present but anterolingual cingular cusps are absent. Paraconules and metalophs are absent. The lower dentition of *R. kaiseni* includes three large incisors. The i1 and i2 are semispatulate, while the i3 is more subcaniniform. There is a distinct postcanine diastema and an occasional small p3 metaconid. The p2 trigonid is nearly twice the length of the talonid. The lower molars have shallow basins and the m3 is slender.

Rhinotitan kaiseni can be distinguished from most other horned brontotheres by the combination of large incisors and an incompletely saddle-shaped cranium. *R. andrewsi* shares these traits, but *R. kaiseni* can be further distinguished from *R. andrewsi* by the narrower basicranium, more anterior position of the frontonasal horns, downfolded anterior margin of the nasal process, and subcaniniform upper incisors.

Description

Skull: The holotype of *Rhinotitan kaiseni* (AMNH 20252) includes a complete skull (fig. 79) and an associated mandible. The skull is complete, but it has experienced some shearing distortion and the dorsal surface of the skull is warped. Additionally, there is another complete skull (fig. 80) and associated mandible (fig. 82) (FMNH P14048: originally AMNH 20260). The skull consists of hundreds of small bone fragments held together with plaster, yet the specimen retains its general shape although its overall size appears to be swollen due to expanding matrix distortion (sensu White, 2003). A third specimen (AMNH 20257) consists of an undistorted ventral surface of a skull (fig. 81a).

Rhinotitan kaiseni is a large horned brontothere similar in size to *Protitan grangeri* and *Protitanotherium emarginatum*. There are no discernable sutures on the holotype skull (AMNH 20252), but judging by the extreme dental wear this animal died at a very old age. FMNH P14048 is an ontogenetically younger individual with minimally worn adult dentition. On that specimen the posterodorsal surfaces of the right and left horns are less damaged than the surrounding bone. Portions of the frontonasal suture are visible on both the lateral and dorsal views, indicating that the horn is composed of both frontal and nasal elements.

The horns of AMNH 20252 are small but prominent and project almost horizontally from the skull. They are proximally elliptical, but the distal peaks of the horns form round roughened knobs. In FMNH P14048 the horns do not project laterally. In both skulls, the horns are positioned far anterior to the orbits. This differs from *Rhinotitan andrewsi* where the horns are more posteriorly positioned. The horns of *R. kaiseni* are positioned well out onto the nasal process and are high above the orbits.

The nasal incision extends posteriorly to a point above the anterior margin of the P3. The nasal incision is dorsoventrally deep. The posterior notch of the nasal incision is positioned slightly higher than the orbit. The orbit is above M2 while the posterolateral and anterolateral roots of M1 rest below the anterior orbital rim.

From the lateral view the nasal process is slightly longer than the premaxillomaxillary rostrum. The nasal process of AMNH 20252

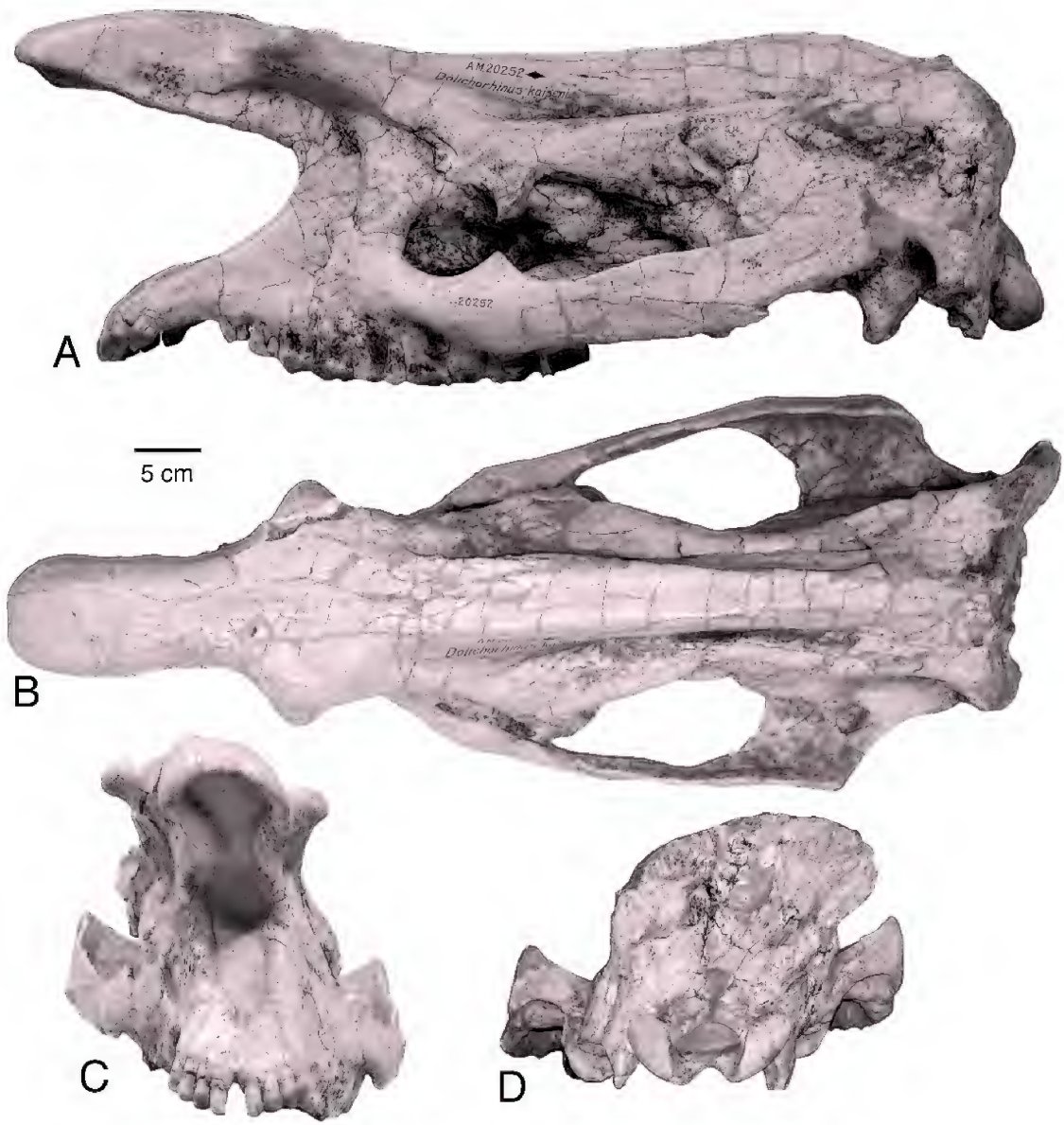

Fig. 79. The holotype skull of *Rhinotitan kaiseni* (AMNH 20252). **(A)** Left view, **(B)** dorsal view, **(C)** anterior view, **(D)** posterior view.

appears to be angled slightly upward. The sides of the nasal process form deep lateral walls; these are deeper and thinner than those of *R. andrewsi*. The lateral walls are shallower toward the distal end of the nasal process. From the dorsal view, the width of the nasal process is relatively constant throughout its length and the anterior margin is nearly flat. From the anterior view the distal end of the nasal process is downfolded. Toward the proximal end of the nasal process the lateral walls are weakly angled ventromedially and they constrict the space between them, but this condition is not as severe in *R. kaiseni* as it is in *R. andrewsi*.

From a lateral view the premaxillomaxillary rostrum is thin distally, but it deepens proximally. The dorsal margin of the rostrum is steeply sloped posterodorsally. From the anterior view the premaxillary symphysis is

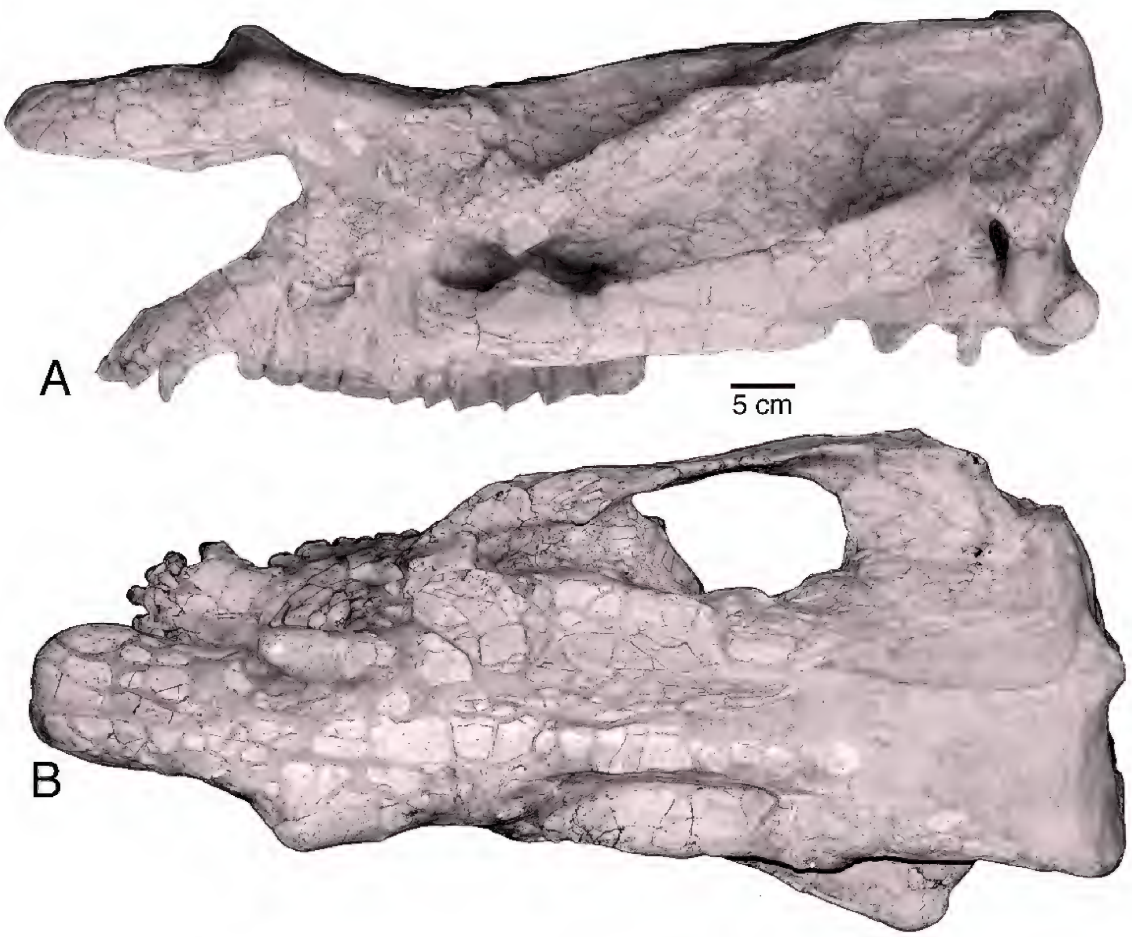

Fig. 80. A skull referred to *Rhinotitan kaiseni* (FMNH P14048). **(A)** Left view, **(B)** dorsal view.

completely fused. The dorsolateral margins of the rostrum diverge laterally behind the symphysis and the rostral cavity is not sealed over by bone. From the anterior view the nasal opening of the skull is very tall and narrow.

The dorsal surface of the skull is artificially warped. However, unlike many horned brontotheres, the skull does not appear to have been saddle-shaped. Rather, the shape of the skull in lateral profile more closely resembles *Rhinotitan andrewsi* and more primitive hornless brontotheres (e.g., *Telmatherium*) in which the dorsal surface is concave over the middle of the skull, but the dorsal surface of the skull is more convex over the posterior end of the skull.

The parasagittal ridges are not prominent on AMNH 20252 and the dorsal surface of the skull is not laterally constricted posteriorly. From a lateral view, the zygomatic arches are relatively shallow. The jugal portion of the zygomatic is horizontal, while the squamosal portion rises posteriorly at a very shallow angle and the zygomatic arch is nearly straight. From the dorsal view, the zygomatic arches are thin, straight, and not strongly angled laterally. A postzygomatic process, as seen in *Protitan grangeri* and *Metatitan relictus*, is absent in *Rhinotitan kaiseni*.

From a lateral view the occiput is nearly vertical. The nuchal crest is damaged, but from a dorsal view, it appears to have been concave. From the posterior view, the nuchal crest is dorsally arched. The dorsal and ventral halves of the occiput are the same width, although the occiput seems to have

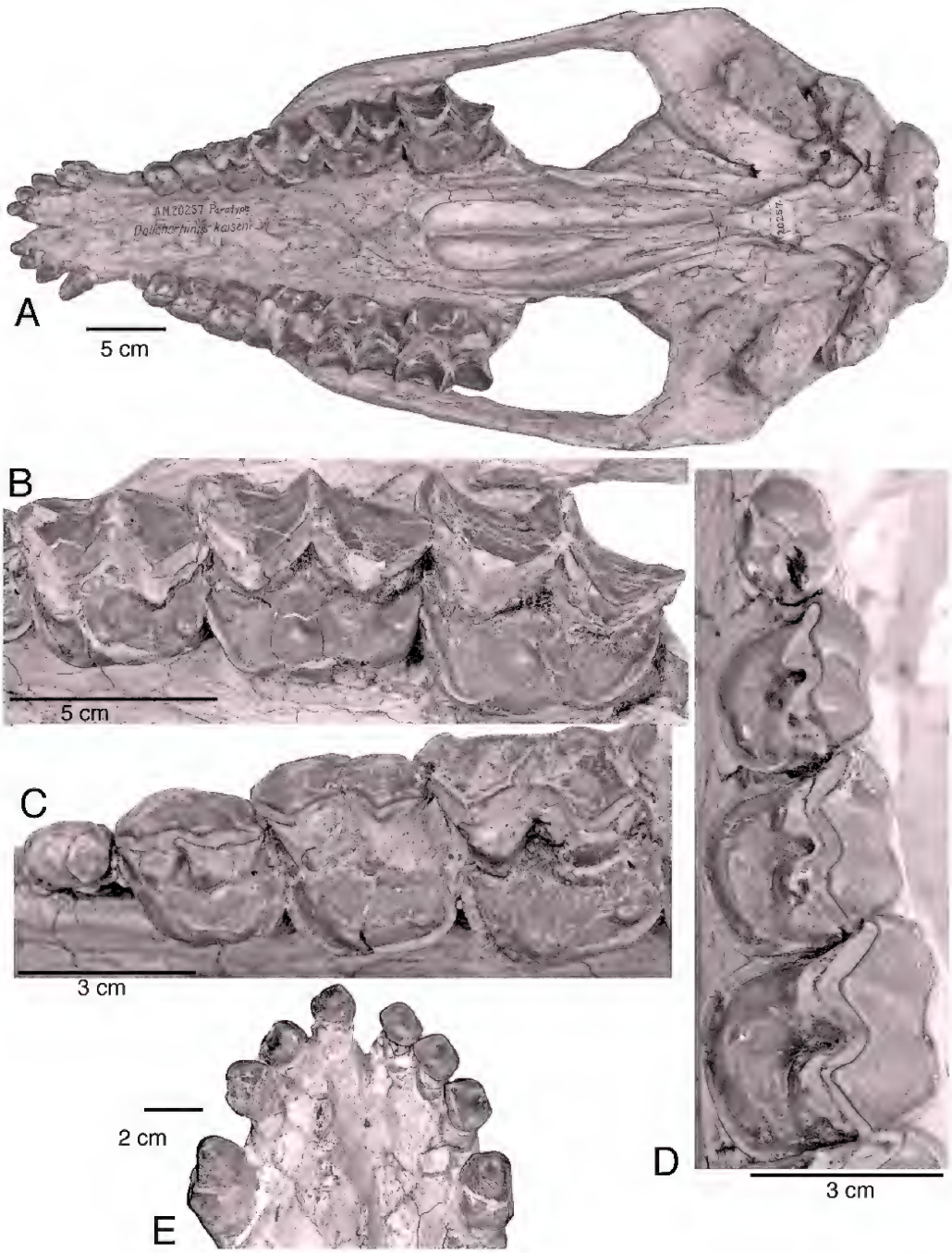

Fig. 81. Ventral surface and upper dentitions of skulls referred to *Rhinotitan kaiseni*. **(A)** Ventral view of AMNH 20257, **(B)** left molars of AMNH 20257, **(C)** left premolars of AMNH 20257, **(D)** left premolars of FMNH P14048, **(E)** lingual view of incisors and canines of FMNH P14048.

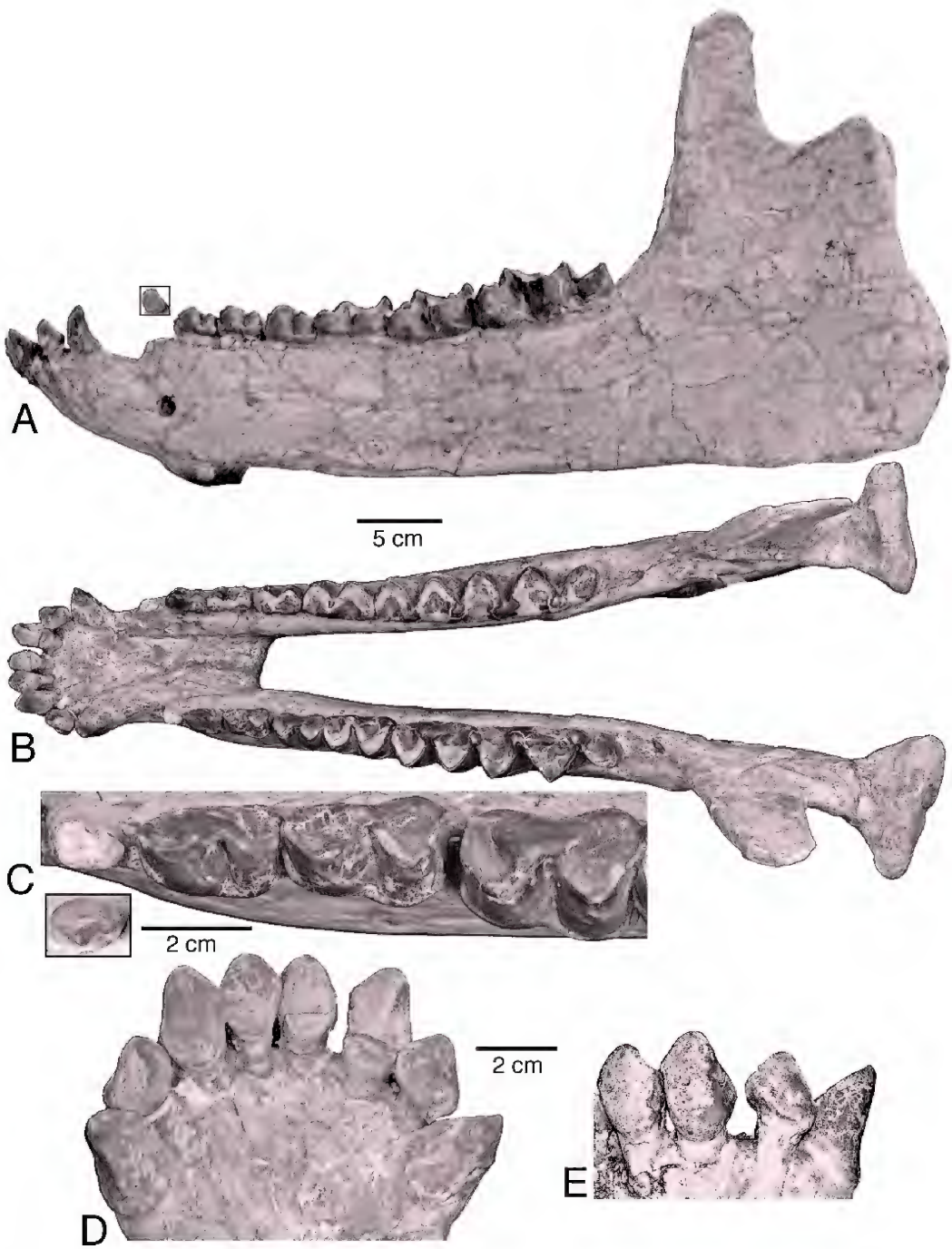

Fig. 82. Mandible (FMNH P14048) of *Rhinotitan kaiseni*, associated with the skull in Fig. 80. **(A)** Left view shown with a cast of the p1 (original p1 has been lost), **(B)** dorsal view, **(C)** left premolars shown with a cast of the p1 (now lost), **(D)** lingual view of incisors and canines, **(E)** labial view of left incisors and canines.

been moderately constricted in the middle. The surface of the occiput has weak occipital pillars with a shallow pit in the center.

In the holotype specimen (AMNH 20252) the anterior rim of the posterior nares is positioned somewhere behind M2, although its exact position is obscured by plaster. In AMNH 20257 the anterior edge of the posterior nares is slightly anterior to the M3 protocones. The posterior nares are rimmed by a narrow emargination. The vomerine septum seen in AMNH 20257 bisecting the posterior narial canal is mostly made of plaster except at its posteriormost end. There are no sphenoidal fossae in any of the specimens of *R. kaiseni*. The external auditory pseudomeatus is tube-shaped and enters the skull at a strongly posteromedial angle. The configuration of the basicranial foramina is typical, with widely separated foramen ovale and foramen lacerum. The width of the basicranium, measured at the mastoid processes, is slightly narrower than the width across the M3s; this distinctly differs from skulls of *Rhinotitan andrewsi* whose basicranium is wider that the total width across the M3s.

Upper Dentition: The teeth of the holotype skull are too worn to describe, but the upper dentitions of AMNH 20257 and FMNH P14048 are complete and not heavily worn (fig. 81). The incisor rows of AMNH 20257 and FMNH P14048 are complete, although those of the latter are the least worn. The incisors number three per side, are large, and form an arched row that extends anterior to the canines. The incisors increase in size laterally. The incisors of *Rhinotitan kaiseni* are less globular than those of *R. andrewsi*. When the I1 and I2 are nearly unworn, as in FMNH P14048, the crowns retain a relatively subcaniniform shape, although they are very short and have smooth lingual cingula. The I3 has a similar shape, but it is taller and more subcaniniform. The canines of all *R. kaiseni* specimens tend to be relatively small. There is a short precanine diastema and a longer postcanine diastema.

The P1 crown of AMNH 20257 is not preserved. The P1 of FMNH P14048 is much smaller than more posterior molars, but its morphology is relatively advanced and the crown has a nearly round outline. A metacone is distinctly present and is similar in size to the paracone. There is a small lingual heel with a small protocone. In both specimens the crown of P2 seems more obliquely shaped than the crowns of P3 or P4 due to its more posterolingually angled anterior margin. The P3 and P4 are less oblique in shape and the anterior and posterior margins of these teeth are nearly parallel. The P2 metacone is not shifted lingually. The parastyle and metastyle of P2 are straight. The parastyles of P3 and P4 are directed somewhat labially, although the metastyles of these teeth are essentially straight. The labial margin of the P2 paracone is rounded, while the paracones of P3 and P4 have small but distinct labial ribs.

The lingual features of the crowns of P2–P4 have low relief and invariably include a protocone and a lingual crest that extends posteriorly from the protocone. Vestigial preprotocrista are seen on P2 and P3, but this trait is not evident on P4. In other respects the lingual premolar morphology is variable. For instance, there is notable bilateral asymmetry in the presence and distinctness of premolar hypocones in AMNH 20257. The left P2 has a hypocone that is incompletely separated from the protocone, while the P3 and P4 each have small, well-separated hypocones. The right P2 is similar to the left side, but unlike their left counterparts, the right P3 and P4 lack distinct hypocones. The premolars of FMNH P14048 are more bilaterally symmetrical; P2 has a distinct hypocone that is connected to the protocone, but P3 and P4 lack hypocones. The lingual premolar cingula are also variable. The lingual premolar cingula of AMNH 20257 are discontinuous, while the lingual premolar cingula of FMNH P14048 are continuous on the P2 and P3 but discontinuous on the P4. Likewise, the labial premolar cingula of FMNH P14048 tend to be weaker than those of AMNH 20257.

The upper molars of *Rhinotitan kaiseni* show typical brontotheriine apomorphies, including tall, lingually angled ectolophs, very weak labial ribs, thin lingual ectoloph enamel, and wedge-shaped lingual sides of the paracone and metacone in molars that are not heavily worn. The anterior cingulum is thin and passes proximally to the distal

peak of the parastyle. Distinct shallow central molar fossae are present, but anterolingual cingular cusps are absent. All evidence of paraconules and metalophs is lost. There is no trace of a hypocone on any M3 of *R. kaiseni*, although the distolingual cingulum of the M3 is thickened. Labial molar cingula are weak and lingual molar cingula are absent.

MANDIBLE AND LOWER DENTITION: Although the holotype (AMNH 20252) includes an associated mandible, the lower teeth are extremely worn. However, a second skull, FMNH P14048, is associated with a complete and essentially undistorted mandible with a complete set of lightly worn dentition (fig. 82). The inferior margin of the symphysis has a shallow angle ($< 45°$). The symphysis extends to the talonid of the p3. The incisors number three per side and form an arch anterior to the canines. The lower incisors are large, while i2 is clearly the largest incisor. The crowns of i1 and i2 are tall and semispatulate with rounded apices. The i3 crown is shorter and mesiodistally more elongate. There are slight lingual incisor cingulids and no labial incisor cingulids. There are no diastemata between the incisors or the canines. The canines are rather small. The postcanine diastema of FMNH P14148 is similar in length to p2, although that of the holotype is slightly longer.

A left p1 was originally associated with FMNH P14048, but it has been lost. Fortunately, the left p1 is still present on a cast of the jaw (AMNH 20260). The p1 cast is shown in proportion to the original specimen in fig. 82a and 82c. The p1 is a small narrow tooth with a single cusp and a short talonid heel. The p2 trigonid is less than twice the length of the talonid, while the trigonid and talonid have similar widths. The talonid and trigonid of p3 and p4 are about equal in length, but the talonid is distinctly wider than the trigonid. The paralophid of p2 arches slightly lingually, creating a small lingual trigonid notch. The p2 protolophid is straight but lingually positioned. The p2 lacks a metaconid. The trigonid of the p3 is more molariform with a strongly lingually paralophid and metalophid that create a much broader lingual-trigonid notch. In addition, p3 has a small but distinct metaconid. The trigonid of p4 is essentially molariform with a fully lingually arched paralophid and protolophid, and a large lingually positioned metaconid. The talonid of p2 has a relatively short cristid obliqua and hypolophid; these features create a small lingual-talonid notch. The cristids obliqua and hypolophids of p3 and p4 are longer and the talonid basins are more molariform. There are no lingual cingulids on the premolars and the labial cingulids are weak.

The lower molars of *Rhinotitan kaiseni* are typical. They have relatively thin lingual enamel, shallow trigonid and talonid basins, and the m3 is elongate. There are no lingual cingulids. Labial molar cingulids are weak and they tend to be discontinuous around the labial cusps. A cingulid is not seen around the hypoconulid of the m3.

Rhinotitan andrewsi (Osborn, 1925)

HOLOTYPE: AMNH 20271, a skull missing the nasal, with right I2–M3, left I2–C, and P2–M3.

TYPE LOCALITY: Shara Murun Formation, Ula Usu, Baron Sog Formation, Shara Murun Region, Inner Mongolia, China.

AGE: Middle Eocene (Sharamurunian land mammal "age").

REFERRED SPECIMENS: **(From the Shara Murun Formation, Ula Usu, Baron Sog Mesa, Shara Murun Region, Inner Mongolia)** AMNH 20254, a skull with right I1–I2 (damaged), I3, C (damaged), P1–M3, left I2 (damaged), I3, C (damaged), and P1–M3; AMNH 20261, a laterally crushed skull with right C–M3 and left I3–M3; AMNH 20263, a palate with right and left I2–M3; IVPP V3254-1, a partial skull with right I1–C, P2–M3, left I1–I3, P2–M3, a mandible with right i1–c, p2–m3, left i1–c and p2–m3, and a skeleton; IVPP V3254-2, a complete skull with complete dentition except left I1, and a mandible with right p1–m3, left p2, and p4–m3; PIN 2198-3, a partial skull with right P2–M2, M3 (partial and unerupted) and left P1–M2; PIN 2198-5, a skull with right P2–M3 and left I2–C, P1–M3: PIN 7130-3 with right and left P2–M3.

DIAGNOSIS: *Rhinotitan andrewsi* is a large horned brontothere with small, ellipti-

cal, and widely separated frontonasal horns. The horns are positioned slightly in front of the orbits and high above the orbits. The nasal incision is dorsoventrally deep and extends to the P4. The orbit is above the M2 with the posterolateral and anterolateral roots of M1 below the anterior orbital rim. The nasal process is either horizontal or slightly angled upward, relatively broad, not strongly rounded anteriorly, and with thick lateral walls that do not arch around the anterior margin. Proximally, the lateral walls of the nasal process deepen and angle ventromedially, greatly constricting the dorsal portion of the nasal cavity. The premaxillomaxillary rostrum thickens posteriorly and it is not enclosed by bone dorsally. Other cranial characteristics include a marginally saddle-shaped or incompletely saddle-shaped cranium, a dorsal cranial surface that is not constricted posteriorly by parasagittal ridges, a narrow emargination surrounding the posterior nares, nearly straight zygomatic arches, and a ventrally constricted and posteromedially angled external auditory pseudomeatus. Ventral sphenoidal fossae and postzygomatic processes are absent.

Dentally, *Rhinotitan andrewsi* has three large incisors. The I1 and I2 are subglobular, while I3 is more subcaniniform. P1 is complex, there is a distinct P2 metacone, and premolar hypocones are occasionally present, although in P2 and P3 the protocone and hypocone sometimes take the form of a single lingual crest. The molars have tall, lingually angled ectolophs with weak labial ribs, and thinned lingual ectoloph enamel with wedge-shaped paracones and metacones. A cingular parastyle shelf is absent. Distinct central molar fossae are present, but anterolingual cingular cusps are absent. Paraconules and metalophs are absent. The lower dentition of *R. andrewsi* includes three large incisors; the i1 and i2 are semispatulate, while the i3 is more subcaniniform. There is a distinct postcanine diastema and the p2 trigonid is nearly twice the length of the talonid. The lower molars have shallow basins and the m3 is slender.

Rhinotitan andrewsi can be distinguished from most other horned brontotheres by the combination of large incisors and an incompletely saddle-shaped cranium. *R. andrewsi* is most easily distinguished from *R. kaiseni* by the wider basicranium, the more posterior position of the frontonasal horns, the less downturned anterior margin of the nasal process, and the more subglobular I1 and I2.

Description

Skull: The holotype of *Rhinotitan andrewsi* (AMNH 20271) is a large skull missing the nasal bones (fig. 83). The ventral surface of the skull and the zygomatic arches are well preserved, although large portions of the cranium are incomplete and reconstructed with copious amounts of plaster. There are several additional skulls of *R. andrewsi*, all from the Shara Murun Formation, including material in the AMNH collection, the IVPP collection previously described by Wang (1982), and undescribed material in the PIN collection. Each skull is crushed, heavily reconstructed with plaster, and/or damaged in some way, rendering it difficult to precisely interpret the shape of the skull without considering several specimens. In addition to the holotype, I have figured lateral views of AMNH 20254, IVPP V3254-1, IVPPV 3254-2 (fig. 84), and a more extensive set angles of PIN 7130-3 (fig. 85).

Rhinotitan andrewsi is larger than *R. kaiseni*, but the size difference is probably not so extreme that there was no overlap in body size among members of these species. The horns of all *R. andrewsi* specimens are highly elliptical with the longer axis in the anteroposterior direction, and they tend to project strongly laterally. There is a moderate amount of size variation in the horns and some are rather smooth while others have more rugose surfaces. The horns are widely separated laterally and they are elevated above the orbits to a degree similar to *Diplacodon elatus*. From a lateral view the horns rest upon a superorbital pillar that rises from the orbit at about a 45° angle. The horns are more posteriorly positioned than those of *R. kaiseni*. They are positioned in front of the orbits and rest directly above the posterior margin of the nasal incision (IVPP V3254-2) or in front of it (PIN 7130-3). Such minor differences in the position and height of the horns may relate to taphonomic distortion.

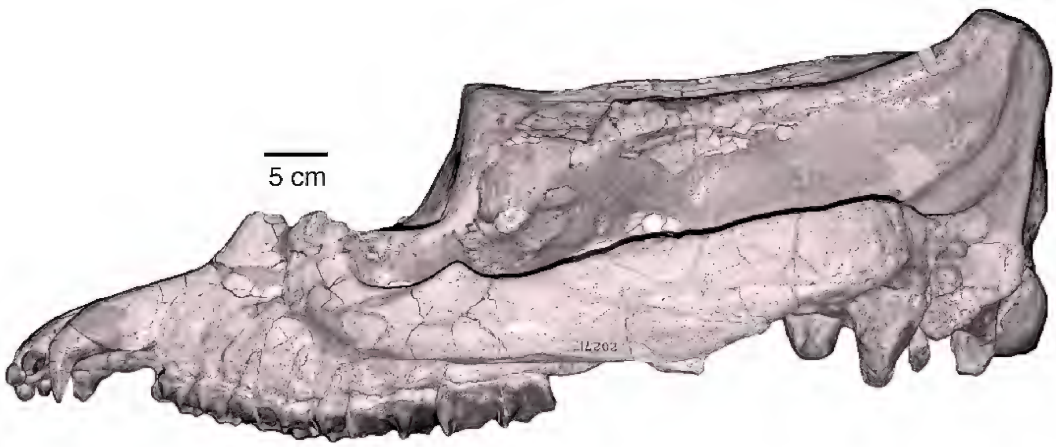

Fig. 83. Left view of the holotype specimen of *Rhinotitan andrewsi* (AMNH 20271).

The nasal incision is so dorsoventrally deep that its posterior margin is significantly higher than the orbit. The nasal incision of *Rhinotitan andrewsi* is longer than that of *R. kaiseni*. In the holotype (AMNH 20271), the incomplete posterior margin of the nasal incision appears to extend to the anterior edge of P4. The posterior margin of the nasal incision of PIN 7130-3 is also positioned about at the anterior margin of P4. There is some fluctuation in the exact position of the posterior margin of the posterior nares; in AMNH 20254 it is slightly more anterior than the P4, while those of IVPP V3254-1 and IVPP V3254-2 are slightly posterior to the anterior margin of P4.

The position of the orbit of *Rhinotitan andrewsi* is not significantly different from that of *R. kaiseni*. For instance in the holotype (AMNH 20271), the M2 is directly below the orbit and the lateral roots of M1 are below the anterior rim of the orbit. Among other specimens, the exact position of the orbit fluctuates slightly. For instance, in AMNH 20254, the posterolateral root of the M1 is clearly behind the anterior orbital rim.

In some of the skulls (e.g., IVPP V3245-1, AMNH 20254) the nasal process slants upward; this character has been used as evidence for drawing phylogenetic lines between *Rhinotitan* and embolotheres (*Protembolotherium* and *Embolotherium*) (Yanovskaya, 1980; Wang, 1982). However, for the most part, the upward slant of the nasal processes of these specimens seems related to taphonomic distortion. In IVPP V3254-1, the horns and the entire nasal process are strongly angled upward at about a 45° angle. However, there is an abrupt kink in the dorsal surface of the skull just behind the orbits, suggesting that the entire frontonasal region has been artificially rotated upward. Other specimens of *R. andrewsi* with upwardly angled nasals (e.g., AMNH 20245) also clearly suffer from heavy distortion in the anterior portion of the skull. IVPP 3254-2 is minimally distorted and suggests that the nasal process may have been slightly angled upward, similar to that seen in *R. kaiseni*. However, another skull, PIN 7130-3 has a more normal horizontal nasal process with a slightly downward bend to it. In conclusion, the nasal process was either horizontal or it was only slightly angled upward.

The nasal process is similar in length to that of the premaxillomaxillary rostrum in some specimens (e.g., IVPP V3254-1, and IVPP V3254-2), but in others (PIN 7130-3 and AMNH 20254) the nasal process clearly extends anterior to the rostrum. The most complete nasal processes (IVPP V3254-2 and PIN 7130-3) have distally tapering widths. The distal margin of the nasal process is flat or slightly rounded with a small median notch. From a strictly lateral view, the lateral wall of the nasal process appears to be relatively shallow. However, the view of the ventral side of the nasal process of PIN 7130-3 reveals that the lateral walls are strongly directed medially (fig. 85C). Proximally, the

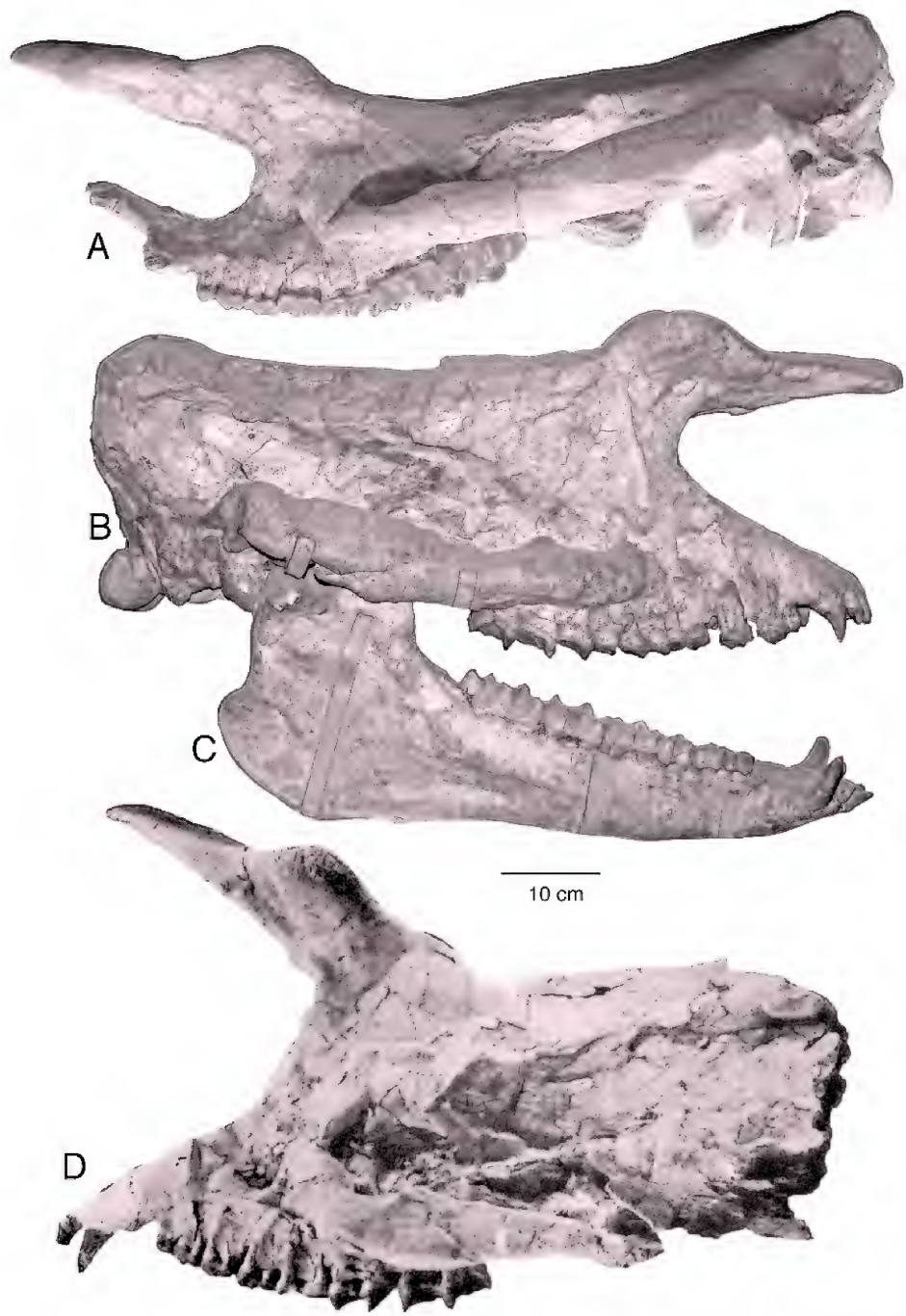

Fig. 84. Specimens referred to *Rhinotitan andrewsi*. **(A)** Left view of AMNH 20254, **(B)** right view of the skull of IVPP V3254-2, **(C)** right view of the mandible of IVPP V3254-1, **(D)** left view of the skull of IVPP V3245-1. D is from Wang (1982).

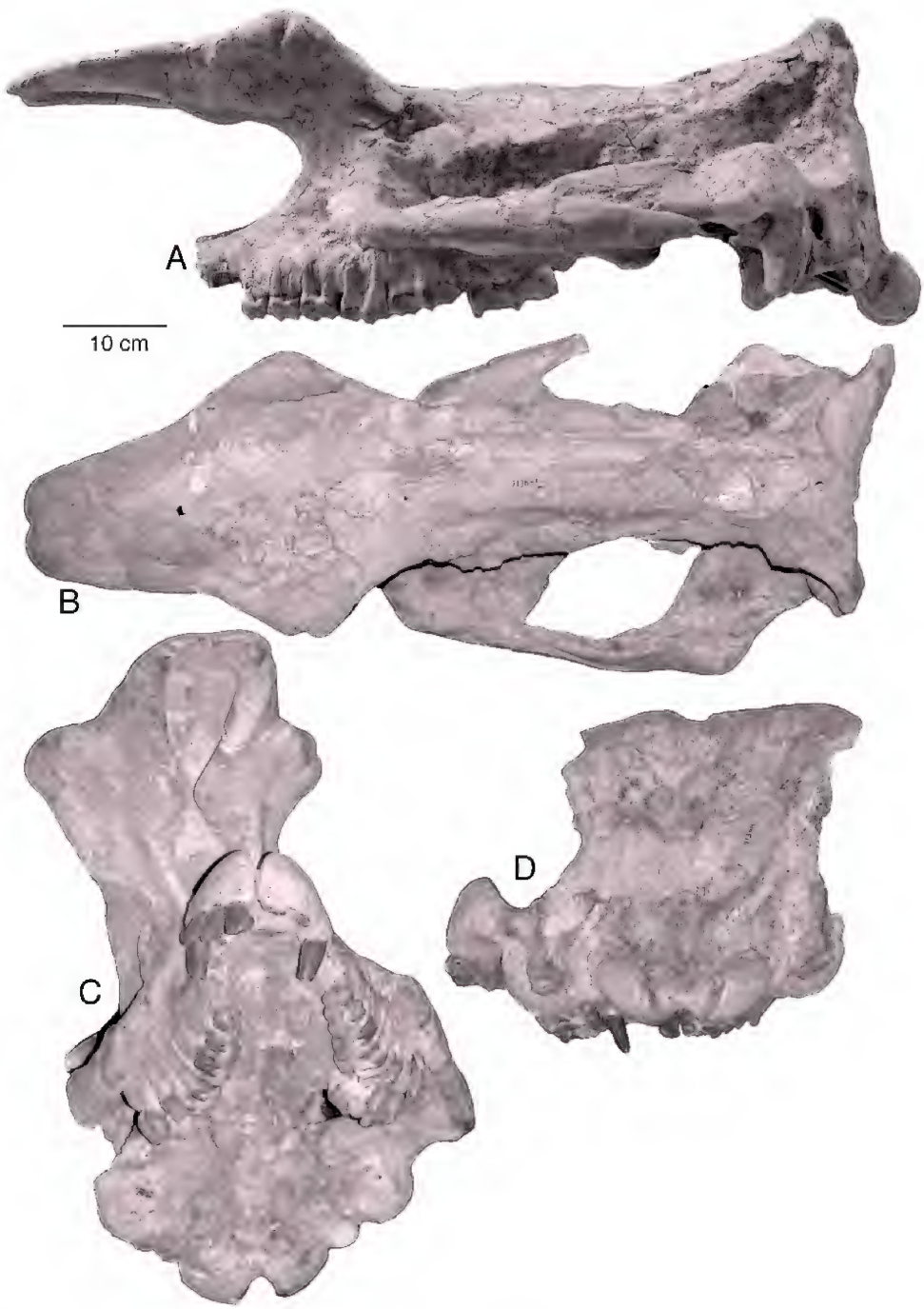

Fig. 85. A skull referred to *Rhinotitan andrewsi* (PIN 7130-3). **(A)** Left view, **(B)** dorsal view, **(C)** anteroventral view, **(D)** posterior view. Note that the premaxilla and incisors seen in C are a plaster reconstruction. The reconstructed premaxilla has been cropped off in A.

lateral walls become thicker, deeper, and they are strongly angled ventromedially, severely constricting the upper portion of the nasal cavity. The lateral walls of the nasal process are very shallow toward the distal end of the nasal and they do not continue around the anterior margin of the nasal as they do in *Rhinotitan kaiseni*.

The premaxillomaxillary rostrum is not clearly differentiated from *Rhinotitan kaiseni*. From the lateral view of the holotype (AMNH 20271), the rostrum is relatively shallow. At a point above the P3 the dorsal margin of the rostrum curves sharply upward, giving the dorsal surface of the rostrum a concave appearance. PIN 7131-3 has a similar appearance. On the other hand, the dorsal margins of the rostra of IVPP V3254-1 and IVPP V3254-2 are flatter and angled sharply posterodorsally. The premaxillary symphysis is completely ossified. Behind the symphysis, the dorsolateral margins of the rostrum diverge laterally and the rostral cavity is not sealed over by bone. Like in *R. kaiseni*, the nasal opening of the skull is very tall and narrow.

Interpretation of the shape of the dorsal surface of the skull of *R. andrewsi* is difficult. The dorsal surfaces of the holotype (AMNH 20271) and AMNH 20254 are nearly flat, but these specimens are unreliable due to the degree of plaster reconstruction. The dorsal surface of IVPP V3254-2 is barely concave, while that of PIN 7130-3 is somewhat more deeply concave. However, IVPP V3254-1 suggests a more bulbous cranium, with a somewhat convex postorbital dorsal surface similar to that of *Metatitan*. Like *R. kaiseni*, the dorsal surface of the skull broadens posteriorly and the parasagittal ridges do not greatly constrict the posterodorsal surface of the skull. (Note that the dorsal surface of PIN 7130-3 is artificially narrowed due to transverse buckling.) The zygomatic arches of *R. andrewsi* tend to be thicker and somewhat deeper than those of *R. kaiseni*, although in at least one specimen (AMNH 20261), the zygomatics are thin. From lateral views the entire zygomatic arch is straight and nearly horizontal. From a dorsal view the zygomatic arches are nearly straight are not strongly bowed laterally.

The occiput is nearly vertical like that of *Rhinotitan kaiseni*. The nuchal crest is slightly concave from a dorsal view. From the posterior view the nuchal crest is barely arched dorsally. Overall, the occiput is large, tall, and broad. The dorsal and ventral halves of the occiput are the about the same width, and the width of the occiput does not appear to have been constricted in the middle. The surface of the occiput has weak occipital pillars with a shallow pit in the center of the occiput.

The ventral surface of the holotype skull (AMNH 20271) is seen in fig. 86a. The anterior rim of the posterior nares is positioned slightly anterior to the M3 protocones. The posterior nares are rimmed by a very narrow emargination. In AMNH 20271 this emargination is partially covered by plaster, but it is completely exposed on AMNH 20254 (not shown) and slightly narrower that that of *Rhinotitan kaiseni* and more squarish (rather than horseshoe-shaped). The posterior narial canal does not extend into the sphenoid as it does, for instance, in *Diplacodon elatus*. The arrangement of the basicranial foramina is typical, with a widely separated foramen lacerum and foramen ovale. The mastoid process curves anteroventrally and contacts the postglenoid process forming a tube-shaped external auditory pseudomeatus. Like *R. kaiseni*, the external auditory pseudomeatus enters the skull in a strongly posteromedial direction.

One peculiar aspect of the basicranium of *Rhinotitan andrewsi* is its width. In specimens where the basicranium is complete and undistorted (AMNH 20271, AMNH 20254, IVPP V3254-2) the width of the basicranium (measured as the distance between the lateral sides of the mastoid processes) is consistently wider than the width measured between the lateral sides of the M3s. For instance, in the holotype (AMNH 20271), the distance across the mastoid processes (315 mm) exceeds the outside width of the M3s (260 mm). The condition seen in *R. andrewsi* is intermediate between most brontotheres, where the basicranium is narrower than the distance across the M3s, and *Metatitan*, where the basicranium is even more extremely widened. Nonetheless, *R. andrewsi* consistently differs in this regard from skulls of *R. kaiseni* where

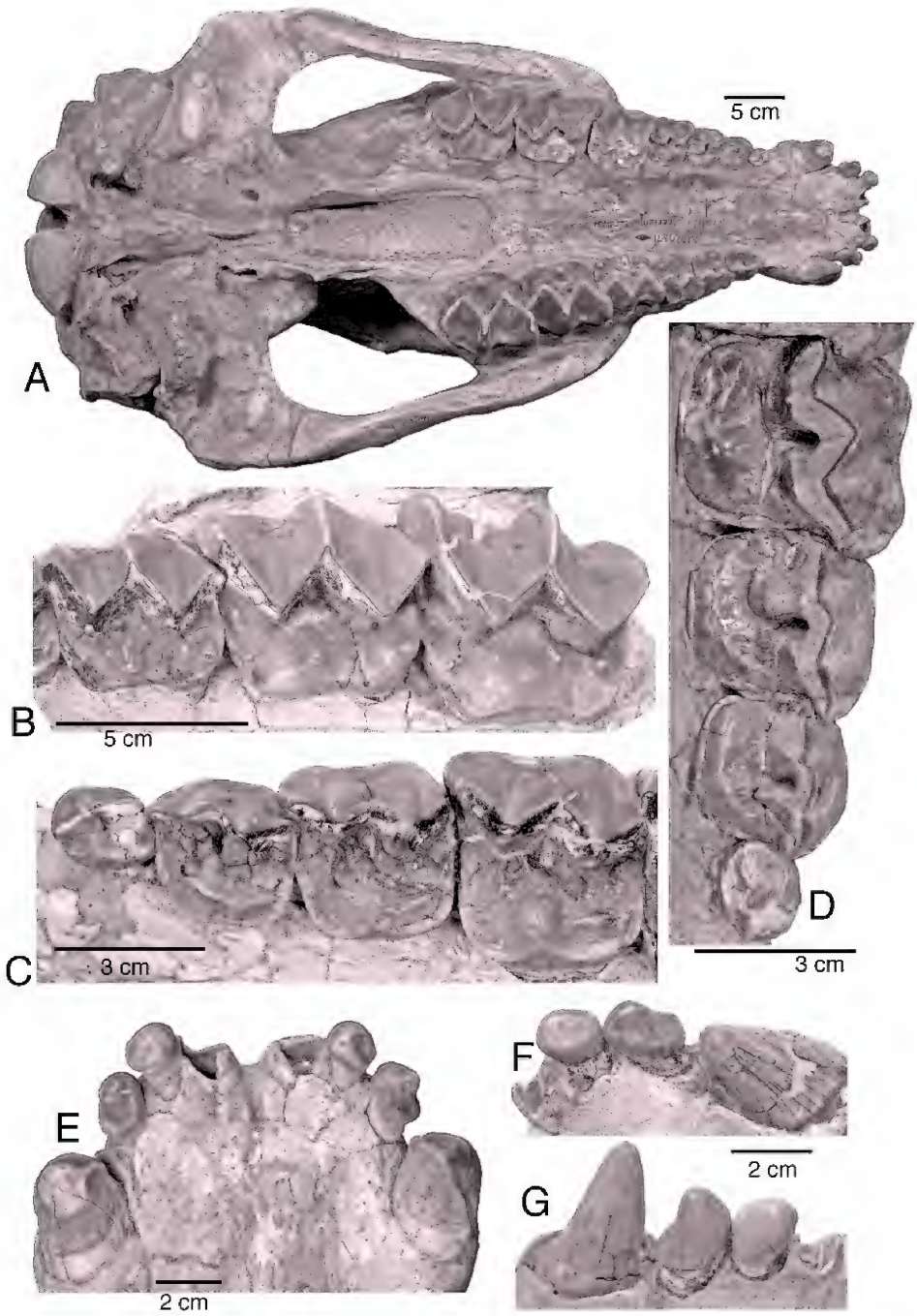

Fig. 86. Ventral view and upper dentition of *Rhinotitan andrewsi*. **(A)** Ventral view of the holotype skull (AMNH 20271), **(B)** left molars of AMNH 20254, **(C)** left premolars of AMNH 20254, **(D)** right premolars of the AMNH 20271 (holotype), **(E)** incisors and canines of the AMNH 20271 (holotype), **(F)** lingual view of left I2–C of AMNH 20263, **(G)** labial view of left I2–C of AMNH 20263.

the outside width of the M3s is greater than the width of the basicranium.

Upper Dentition: Most of the specimens of *Rhinotitan andrewsi* have well-preserved and lightly worn teeth. In addition to the ventral surface of the holotype (AMNH 20271) (fig. 86a), pictured in close-up are the upper premolars and molars of AMNH 20254 (fig. 86b–c), the upper premolars, canines, and incisors of AMNH 20271 (fig. 86d–e), and the unworn incisors and canine of AMNH 20263 (fig. 86f–g).

The incisors are large and form a slightly arched row anterior to canines. Complete I1s are only seen with IVPP V2354-1 and IVPP V3254-2. The I1s of these specimens are worn, but they appear to be similar to the I2 although somewhat smaller. The I2 and I3 are intact in a number of specimens, including AMNH 20271. Another specimen, AMNH 20263, has incisors that are very similar to those of AMNH 20271, but they are essentially unworn. In these specimens, I2 is nearly a featureless crown, although in the least worn specimen the crown is subglobular in appearance with a very short cusplike apex. The I3 is slightly larger than the I2 and it is taller and with a more conical crown and a more distinct lingual cingulum. However, the incisors of AMNH 20271 and AMNH 20263 are more globular than those of *Rhinotitan kaiseni*. The size of the canines among specimens of *R. andrewsi* varies; they are relatively large in all specimens except AMNH 20261 (not shown). There are distinct precanine and postcanine diastemata in *R. andrewsi*. The postcanine diastema tends to be shorter than the P2.

The crown of P1 is nearly round in outline. There are two lingual cusps, a large paracone, and a smaller metacone that is positioned at the very posterior end of the P1 ectoloph. The lingual heel of P1 is well developed with a small protocone that is partially absorbed by a crest that runs along the lingual side of crown. P2–P4 are more rectangular; the anterior and posterior sides of these teeth are nearly parallel and the lingual sides are only slightly rounded. The parastyle and metastyle of P2 are straight and the metacone is not strongly shifted lingually, thus the ectoloph is nearly straight. On P3 and P4 the parastyles are strongly angled labially, while the metastyles are weakly angled labially. The outer swelling of the P2 paracone is minor, but there are small but distinct labial paracone ribs on P3 and P4. A mesostyle is not seen on any of the premolars of *Rhinotitan andrewsi*.

The lingual features of the premolar crowns have low relief. In the holotype, AMNH 20271, the lingual sides of the P2–P4 have two cusps, a protocone and hypocone that are connected by a lingual crest. A vestigial preprotocrista can also be seen on P2 and P3, but it is not detectable on P4. In P2, the protocone and hypocone are spaced apart, but these cusps are almost fully absorbed by the connecting crest. In P3, the cusps are also indistinct, but they are positioned more closely together. Finally, on the P4, the protocone and much smaller hypocone are widely separate and less strongly connected. Other specimens of *Rhinotitan andrewsi* show variable lingual premolar morphology. For instance, in AMNH 20261 (not show) there are distinct hypocones on P2–P4. On this specimen, the hypocones are only weakly connected to the protocone and the P3 hypocone is positioned more distantly behind the protocone. Yet in AMNH 20254 there are no distinct lingual cusps on P2 and P3; instead, there is a single lingual crest that arches along the lingual side of the crown. The P4 of AMNH 20254 has a protocone and a smaller hypocone that are distinctly separated. In AMNH 20263, the P2 and P3 are similar to those of AMNH 20254, but the P4 of that specimen has only a centrally positioned protocone with no hypocone or connecting crest. Labial premolar cingula are very weak; the lingual premolar cingula vary from continuous (e.g., AMNH 20271) to slightly discontinuous (e.g., AMNH 20254).

The upper molars of *Rhinotitan andrewsi* show numerous brontotheriine features, including tall, lingually angled ectolophs, very weak labial ribs, thin lingual ectoloph enamel, and wedge-shaped lingual sides of the paracone and metacone in molars that are not heavily worn. The anterior cingulum is thin and passes proximally to the distal peak of the parastyle. Distinct central molar fossae are present. However, anterolingual cingular cusps are not seen. No traces of paraconules

or metalophs remain. One specimen, AMNH 20254, has a small hypocone on the M3, although other specimens show no trace of an M3 hypocone. Labial molar cingula are generally weak, and lingual molar cingula are very weak between the protocone and hypocone.

MANDIBLE AND LOWER DENTITION: The skulls, IVPP V3254-1 and IVPP V3254-2, are associated with mandibles. The mandible of IVPP V3245-1 is presently articulated with the skull of IVPP V3254-2 and is seen in fig. 84c. I was not able to find the mandible belonging to the skull of IVPP V3254-2, but a photo of it can be seen in Wang (1982: pl. 4). The horizontal ramus of IVPP V3254-1 is slender and deepens posteriorly, while that of IVPP V3254-2 is deeper overall. Additionally, the angle of the inferior margin of IVPP V3254-1 is very shallow (much less than 45°), while that of IVPP V3254-2 is angled about 45°. The symphyses of these mandibles extend to the trigonid of p4. The lower incisor row of IVPP V3254-1 is nearly intact and is not differentiated from *Rhinotitan kaiseni*. The incisors are large, tall, semispatulate, and form a slightly arched row anterior to the canines. The i2 is distinctly the largest incisor. Each of the incisors has a small lingual cingulid. The canines of that particular specimen are relatively large. The lower cheek teeth of *R. andrewsi* are not clearly differentiated from *R. kaiseni*. Both specimens lack evidence of a p3 metaconid. They fall within the morphological range of the specimens described below as *Rhinotitan* sp.

Rhinotitan sp.
Includes the nomen dubium, *Rhinotitan mongoliensis* (Osborn, 1923)

REFERRED SPECIMENS: **(From the Shara Murun Formation Ula Usu, Baron Sog Mesa, Shara Murun Region, Inner Mongolia)** AMNH 18653 (holotype of *Rhinotitan mongoliensis*), a mandible fragment with right p2–m3; AMNH 20251, a left mandibular ramus with p2–m3; AMNH 20256, a palate with right C–M2, left P1–M2, M3 (unerupted), a mandible with right i1–i2, c (erupting), p1, p3–m2, m3 (erupting), left i1–i2, p1–m2, and m3 (erupting); AMNH 20262, a left mandibular ramus with p1–m2, m3 (erupting), four isolated incisors and a canine; AMNH 20269, a partial mandibular symphysis with right and left i1–i2, isolated canine and right p1; AMNH 20270, a right maxilla with P1–M2; AMNH 20272, mandible fragment with right i2?, c, p3–m3, and a left ramus with i2?, c, and p2–m3; AMNH 20273, right and left mandibular rami with p2–m3; AMNH 20280, a fragmented skull with right P2–P3, dp4, P4 (unerupted), M1, M2 unerupted, left P1–P3, dp4, P4 (unerupted), and M1; AMNH 21598, a palate with right and left P1–P3, dp4, P4 (unerupted), and M1–M2; **(from the Shara Murun Formation, four miles north of Baron Sog Lamasery, Baron Sog Mesa, Shara Murun Region, Inner Mongolia)** AMNH 21603, a partial mandible with right i2–p4 and left i1–m3; AMNH 21605, a partial mandible with poorly preserved incisors and right c, p2 (partial), and p3–m3; PIN 2198-2, a mandible with right and left p2–m3.

DESCRIPTION

UPPER DENTITION: Many specimens from the Shara Murun Formation with well-preserved upper and/or lower sets of cheek teeth clearly belong to a species of *Rhinotitan*, but because the two known species, *R. kaiseni* and *R. andrewsi*, do not have clearly differentiated cheek teeth, the majority of these specimens can be assigned only to the genus level (i.e., *Rhinotitan* sp.) Four palates with essentially unworn upper cheek teeth (AMNH 20256, AMNH 20270, AMNH 20280, AMNH 21598) demonstrate a degree of variability in the lingual features of the premolars (P2–P4) similar to both *R. kaiseni* and *R. andrewsi*. The lingual side of the P2 varies from having a single crest with no distinct cusps to having a slightly discernable protocone within the lingual crest. P3 varies in similar way, but occasionally there is a very small hypocone present. Finally, P4 has a large protocone, a very low crest is occasionally present, and a tiny hypocone is sometimes present.

MANDIBLE AND LOWER DENTITION: The mandibles referable to *Rhinotitan* sp. demonstrate variability in the presence of the p3 metaconid. In the majority of these

specimens the p3 metaconid is absent. However, AMNH 18653 (holotype of *Rhinotitan mongoliensis*), AMNH 20251, and PIN 2198-2 exhibit small metaconids on the p3. The metaconid is smaller and not as lingually positioned as that of p4 or those of the molars. The canines of these mandibles are highly variable in size as well, with some specimens having large curved crowns and bulbous roots (AMNH 20269, 20272) and others with smaller less curved crowns and less bulbous roots (AMNH 21605).

Remarks

The first brontothere described from the Central Asiatic Expeditions of the American Museum of Natural History is *Protitanotherium mongoliensis* Osborn, 1923. Osborn (1923, 1925, 1929a) based this species on a partial lower cheektooth row (AMNH 18653). In 1925 Osborn named two more species. One of these, *P. andrewsi*, was based on a large skull (AMNH 20271) lacking the horns and nasal region. No mandible or lower teeth were associated with this skull but Osborn conjecturally assigned another mandible, AMNH 20251, as the paratype of *P. andrewsi*. Osborn then distinguished *P. mongoliensis* from *P. andrewsi* based on "progressive mutations and rectigradations warranting a specific separation" (Osborn, 1925: 6), but he did not indicate specifically what the distinguishing characters were.

The third species, *Dolichorhinus kaiseni* Osborn (1925), was based on an associated skull and mandible (AMNH 20252). Osborn assigned this species to *Dolichorhinus* because its elongate cranium and long nasal bones seemed similar to that of the North American genus *Dolichorhinus*. However, Osborn (1925) noted that it differed from North American *Dolichorhinus* primarily in its larger size and more distinct horns. Osborn (1925) did not compare *D. kaiseni* with *Protitanotherium mongoliensis* or *P. andrewsi*. The teeth of the holotype of *D. kaiseni* are so worn that any comparison to the dentition of other brontotheres is not possible. However, another specimen (FMNH P14048; formerly AMNH 20260) assigned to *Dolichorhinus kaiseni* by Osborn (1925) includes a nearly complete and minimally worn set of upper and lower teeth that Osborn could have compared to *P. mongoliensis* and *P. andrewsi*.

Granger and Gregory (1943) were the first to recognize the similarities among the numerous specimens that were referred *Protitanotherium mongoliensis*, *R. andrewsi*, and *Dolichorhinus kaiseni*. These were assigned to a new genus, *Rhinotitan*, to which *R. kaiseni* was considered the type species. *Rhinotitan* was characterized by Granger and Gregory (1943) as having long upturned nasals, small oval horns, a wide occiput, premolars with "tetartocone ridges", and a metaconid variably present on p3. Granger and Gregory (1943) continued to accept all three species, but unfortunately they provided dubious species diagnoses. *Rhinotitan kaiseni* was diagnosed by its smaller dimensions and relatively wider P4. Even more dubious is their distinction of *R. mongoliensis* and *R. andrewsi*. The specific character of *R. mongoliensis*, "P2–P4 in neotype with tetartocones [hypocones] less distinct from the deuterocone [protocone] crest than in the type of *R. andrewsi*" (Granger and Gregory, 1943: 365) is based on a set of upper dentition (AMNH 20263) that they conjecturally referred to *R. mongoliensis* and considered to be the neotype.

Ironically, Granger and Gregory (1943) recognized that their specific distinctions of the three supposed species of *Rhinotitan* did not hold up when all the specimens in the AMNH collection were considered, and that the dentition of other specimens bridged the gaps between these species. Granger and Gregory (1943) considered the various holotypes, paratypes, and neotypes of the three species of *Rhinotitan* to represent arbitrary divisions between evolutionary stages for a continuous series represented by *R. kaiseni–R. mongoliensis–R. andrewsi*. Granger and Gregory (1943) did not consider the alternative possibility that the seemingly continuous variation, particularly that of the premolars, might represent intraspecific variation rather than progressive evolutionary stages. This alternative hypothesis is supported by the fact that nearly all of the *Rhinotitan* material is from the same locality and formation. Moreover, most other brontothere species exhibit similar levels of seemingly random intraspecific variation in the lingual morphology of the premolars.

Other attempts to revise the species-level taxonomy of *Rhinotitan* are problematic as well. Prior to Granger and Gregory's (1943) work, Takai (1939) recognized problems with Osborn's taxonomy and considered *R. mongoliensis* and *R. andrewsi* to represent opposite sexes of the same species. More recently Wang (1982) described two associated skulls and jaws (IVPP V3254-1 and IVPP V3254-2) and drew similar conclusions to those of Takai (1939). Wang (1982) considered *R. andrewsi* to be a junior synonym of *R. mongoliensis*, and considered the minor variations in the cheek teeth to represent individual variation. However, neither Takai (1939) nor Wang (1982) considered *Rhinotitan kaiseni*, although the cheek teeth of that species are indistinguishable from the other supposed *Rhinotitan* species.

My observations on the *Rhinotitan* material suggest two distinct species, *R. kaiseni* and *R. andrewsi*, that can be differentiated by the following characteristics: relative width of the basicranium, position of the frontonasal horns, shape of the nasal process, and the morphology of the upper incisors. Because the cheektooth morphologies of these species are not differentiated, much of the *Rhinotitan* material, consisting of partial jaws and palates, must be referred to *Rhinotitan* sp. For this reason, *Rhinotitan mongoliensis* (Osborn, 1923), whose holotype consists of a lower cheektooth row, must be considered a nomen dubium.

Nanotitanops shanghuangensis (Qi and Beard, 1996)

HOLOTYPE: IVPP V11032, a right premolar, most probably a P2 or P3.

TYPE LOCALITY: IVPP locality 93006D, a fissure-filling located in the Shanghuang Limestone Quarry, near the village of Shanghuang, Liyang County, southern Jiangsu Province, China.

AGE: Middle Eocene (Irdinmanhan or early Sharamurunian land mammal "age").

SYNONYMS: *Nanotitan* Qi and Beard, 1996, not *Nanotitan* Sharov, 1968

REFERRED SPECIMENS: **(From the same locality as the holotype)** IVPP V11002, a right P2 or P3; IVPP V11003, a left P2 or P3; IVPP V11004, a left P2 or P3; IVPP V11005, a left P1 or P2; IVPP V11006, a right P1; IVPP V11007, a left M1 or M2; IVPP V11008, a left M1 or M2; IVPP V11010, a left m1 or m2; IVPP V11011, a right m1 or m2; IVPP V11013, a right m1 or deciduous premolar; IVPP V11014: a right m1 or deciduous premolar.

DIAGNOSIS: *Nanotitanops shanghuangensis* is the smallest known brontotheriid. It can be characterized as having a P1 with a weak metacone and small lingual heel, a distinct P2 metacone, weak premolar preprotocristae, and with short lingual crests extending posteriorly from the premolar protocones with an occasional premolar hypocone. The molars of *N. shanghuangensis* have tall, lingually angled ectolophs with weak labial ribs, and thinned lingual ectoloph enamel with wedge-shaped paracones and metacones. A cingular parastyle shelf is absent. Central molar fossae are present but anterolingual cingular cusps are absent. *N. shanghuangensis* molars retain vestigial paraconules, but all traces of metalophs are lost. The lower molars of *N. shanghuangensis* have shallow molar basins and weak lingual ribs.

Nanotitanops shanghuangensis can most easily be distinguished by its very small size. In addition to minuscule size, this species is the only brontothere to have a relatively complex P1 (with two labial cusps and a small lingual heel) but to retain vestigial paraconules in the upper molars.

DESCRIPTION

UPPER AND LOWER DENTITION: *Nanotitanops shanghuangensis* is known only from isolated teeth (fig. 87). In the original description, Qi and Beard (1996) identified all the specimens to specific dental homologues, but they did not explicitly state how or why these exact identifications were made. Upon reexamining the material, I am unconvinced that all of these isolated dental elements can be identified to their specific dental homologues. There are problems, in particular, with several of the original premolar identifications.

The original assignment of IVPP V11006 (fig. 87f) as a P1 seems accurate. It is significantly smaller than the premolars, IVPP V11004, IVPP V11032, IVPP V11003,

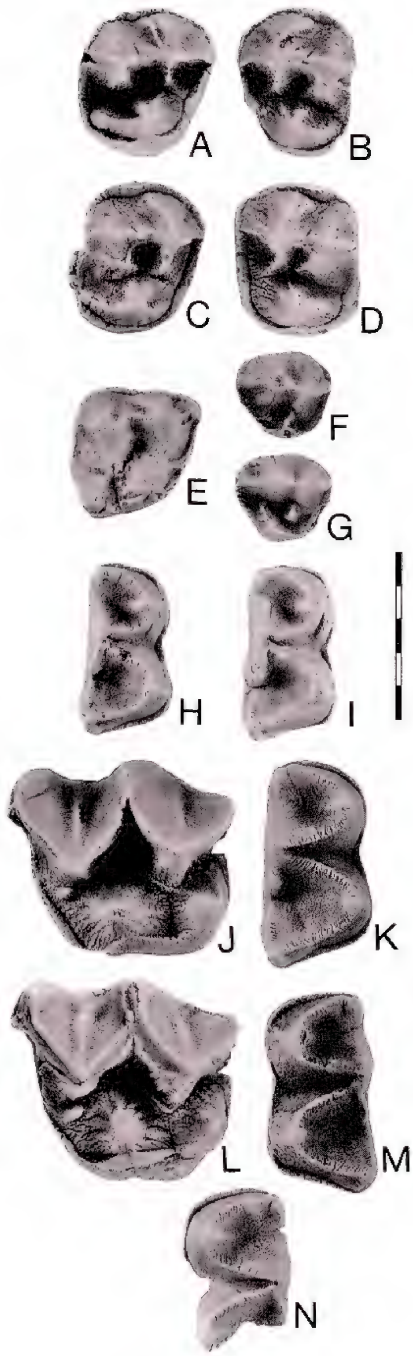

Fig. 87. Specimens referred to *Nanotitanops shanghuangensis* by Qi and Beard, 1996. **(A)** IVPP V11032 (holotype), **(B)** IVPP V11003, **(C)** IVPP V11002, **(D)** IVPP V11004, **(E)** IVPP V11009 (does not belong to *Nanotitanops shanghuangensis*) **(F)** IVPP V11006, **(G)** IVPP V11005, **(H)** IVPP V11014, **(I)** IVPP V11013, **(J)** IVPP V11008, **(K)** IVPP V11011, **(L)** IVPP V11007, **(M)** IVPP V11010, **(N)** IVPP V11012. All photos from Qi and Beard (1996).

and IVPP V11002, and it is semirounded in outline. There are two poorly differentiated labial cusps, there is no discernable labial rib on the paracone, the cingulum is thin, and the lingual shelf is very small with small protoconelike cusp and a short loph connecting the lingual cusp to the lingual base of the metacone.

IVPP V11005 (fig. 87g) was originally identified as a P2, although it might be a P1. The specimen is nearly the same size as IVPP V11006. Among brontotheres, P2s are usually much larger than P1s. IVPP V11005 differs from IVPP V11006 in some ways. The paracone and metacone are more distinct, and the small lingual shelf has a loph that arches around the anterolingual corner of the crown that connects to the lingual base of the paracone. This loph is absent in IVPP V11006. There is a short loph at the lingual base of the metacone. In IVPP V11006 this loph is continuous with the protocone, but in IVPP V11005 it is discontinuous from the protocone. The exact morphology of the lingual features of the premolars tend to vary in most brontothere species and it is therefore possible that morphological differences between IVPP V11005 and IVPP V11006 represent intraspecific variation of the P1.

Based on their larger size, labial paracone ribs, large lingual shelves with large protocone lingual crests, occasional small hypocones (IVPP V11032), rhomboidal or rectangular outlines, and thick cingula, IVPP V11032, V V11002, V11003, and V11004 most certainly represent premolar elements other than P1.

IVPP V11004 (fig. 87d) was originally identified as a P3 although this is questionable. A P4 can probably be ruled out because the parastyle arches lingually; in brontotheres, the P4 parastyle usually projects labially while the parastyles of P3 can be straight or slightly lingually angled. Therefore, this tooth could be either a P2 or P3. The size of the labial rib of the paracone suggests that a P2 is more likely, although the rectangular shape of the tooth is more

consistent with a P3. The specific position of this tooth is basically indeterminate.

IVPP V11032, the holotype, was originally identified as a P4 (fig. 87a). This specimen has a very small hypocone that is placed distantly from the protocone, but is connected to it by the lingual crest. In species where a premolar hypocone is variably present (e.g., *Epimanteoceras formosus*), the occurrence of a hypocone on P2, P3, and P4 does not follow a clear pattern that might facilitate identification of the exact position of this tooth. However, the parastyle of IVPP V11032 arches slightly lingually and the labial paracone rib is wide, probably ruling out the P4. In comparison to IVPP V11004, this tooth is much more oblique, suggesting, rather, a P2.

IVPP V11002 (fig. 87c) was originally identified as a P4, but the lingually arched parastyle, oblique shape and wide labial paracone rib suggest a more anterior premolar. Finally, IVPP V11003 (fig. 87b), originally identified as a P3, could just as well be identified as a P2. To summarize, all of these premolars seem to represent P2s, P3s, or P4s, but none of them can be identified with any certainty.

IVPP 11007 and IVPP 11008 were originally identified as M1s, although they could just as easily represent M2s (fig. 87j, l); there are no obvious differences between the M1s and M2s of brontotheres other than relative size and overall degree of wear, but these differences are not helpful for identifying isolated teeth. The molars of *Nanotitanops shanghuangensis* exhibit increased ectoloph height, lingually arched labial walls, weak labial ribs, thin lingual ectoloph enamel, and wedge-shaped lingual sides of the paracone and metacone. The anterior cingulum is thin and passes proximally to the distal peak of the parastyle. *N. shanghuangensis* molars lack an anterolingual cingular cusp, although shallow central molar fossae are present. Each of these molars retains a vestigial paraconule, although there is no trace of a metaloph. Labial molar cingula are absent, although weak lingual molar cingula are present.

IVPP V11010 and IVPP V11011 were identified as m1s, although they could be m2s (fig. 87k, m). These lower molars exhibit morphology typical of advanced brontotheres with relatively shallow talonid and trigonid basins and very weak lingual ribs.

IVPP V11013 and IVPP V11014 were identified as a dp3 and dp4, respectively. These teeth are essentially molariform although IVPP V11014 is relatively narrower than the adult molars (fig. 87h). IVPP V11013, on the other hand, is more similar in proportions (fig. 87i). It is probable that these teeth are deciduous premolars, although there is no compelling reason to conclude that these teeth could not actually be adult molars of one or more smaller individuals.

Finally, IVPP V11009 was identified as a DP4, although this specimen is not from a brontotheriid (fig. 87e). There is no mesostyle, a feature seen in all brontothere upper molars and deciduous upper premolars (dp2–dp4) (Osborn, 1929a; Butler, 1952). The parastyle is much lower than the valley between the paracone and metacone, whereas in brontothere molars and deciduous premolars these two areas are the same height.

Remarks

Qi and Beard (1996) described *Nanotitan shanghuangensis* from numerous teeth from a single fissure quarry of what clearly represents the smallest known brontothere. Moreover, it is somewhat smaller than *Lambdotherium*, and with far more advanced dental morphology. The genus was later renamed *Nanotitanops*, because *Nanotitan* is preoccupied (Qi and Beard, 1998). Although the materials consist of isolated and unassociated teeth, their uniquely small size suggests that they can presently be referred to a single species. One of the specimens originally referred to this species (IVPP V11009) turns out not to represent a brontothere, but possibly some other perissodactyl.

Pollyosbornia altidens (Osborn 1908a) new genus

Holotype: AMNH 2025, a partial mandible with right p1–m3 and left c–m1.

Type Locality: Uinta Formation (Uinta C) of the Uinta Basin, Utah.

Age: Middle Eocene (Uintan land mammal "age").

ETYMOLOGY: "Polly" was the undergraduate nickname of paleontologist Henry Fairfield Osborn at Princeton, given to him because of his apparent "girlish appearance" (Scott, 1939).

DIAGNOSIS: *Pollyosbornia altidens* is a large brontothere with an unreduced dental formula (3-1-4-3). The incisors are of moderate or large size and form an arched incisor row. The symphysis is relatively elongate and extends posteriorly to the p3 talonid. Other features include a relatively long postcanine diastema, a metaconid on p3 and p4 but not on p2, a very poorly developed p2 talonid, a p2 trigonid that is at least twice the length of the talonid, an elongate m3, and shallow trigonid and talonid molar basins.

From what can be discerned of the poorly preserved holotype mandible, *Pollyosbornia altidens* is more or less consistent with *Diplacodon elatus* except for its larger size, and more poorly developed p2 talonid.

DESCRIPTION

MANDIBLE AND LOWER DENTITION: The holotype and only known specimen of *Pollyosbornia altidens* (AMNH 2025) is nearly complete although it is poorly preserved (fig. 88). In particular, the symphysis appears to have been crushed transversely and a significant portion of the left ramus has been reconstructed. Therefore, some aspects of the shape of the jaw are unreliable. The incisors are missing, but the preserved alveoli indicate 3 pairs of incisors. Judging by the size of the alveoli, the incisors were large to moderate in size, but they were not reduced to a vestigial state. The alveolar surface of the incisor row arches anterior to the canines.

The mandibular symphysis is relatively long and the postcanine diastema is substantially longer than the p2, although the elongate nature of the symphysis could be exaggerated by lateral crushing. The symphysis extends to the talonid of the p3. The p1 has a simple single-rooted cusp with a short talonid heel. In comparison to those of p3 and p4, the trigonid of p2 is proportionately large, while the talonid is very small. The trigonid of p2 is more than twice as long as the talonid. On the p3, the trigonid is moderately longer than the talonid, while the p4 trigonid and p4 talonid are of similar length. The trigonid of p2 is slightly wider than the talonid, but on the p3 and p4, the trigonids are slightly narrower than the talonids. The paralophid of p2 is not angled lingually and there is no lingual trigonid notch on that tooth. The p2 protolophid is only barely angled lingually. The paralophids and protolophids of p3 and p4 strongly arch lingually. The lingual trigonid notch of p3 is long and narrow, while the trigonid of p4 is essentially molariform. The p2 lacks a distinct metaconid but large, lingually positioned metaconids are present on p3 and p4. The talonid of p2 is small and narrow with a poorly developed cristid obliqua and hypolophid and a very small lingual-talonid notch. However, the talonids of p3 and p4 are large with long cristids obliqua and hypolophids with molariform basins. The premolars lack lingual cingulids. Labial cingulids occur only in the notch between the protoconid and hypoconid of the p3 and p4. The molars of AMNH 2025 are indistinctive; the occlusal basins are shallow, and the m3 is elongate, lingual molar cingulids are absent, and labial cingulids are present, but they are discontinuous around the protoconid and hypoconid.

REMARKS

Osborn's (1908a) original description of the only known specimen of "*Telmatherium*?" *altidens* (AMNH 2025) consists of three brief sentences that do not clearly justify a new species, nor do they justify his questionable assignment of this species to the genus *Telmatherium*. Later, Osborn (1929a) provided a more extensive description and included justifications for considering this species a member of *Telmatherium* (which, in Osborn's concept also included *Metatelmatherium ultimum*). These justifications include the large canine, the large lower incisors, the long postcanine diastema, the state of molarization of p2, and the size of the molars. However, all these arguments are refutable. For instance, the size of the canine tends to vary intraspecifically. Canine size is certainly not a diagnostic character of *Telmatherium* or *Metatelmatherium*. Moreover, the size of the only preserved canine of AMNH 2025 (left) is highly exaggerated by

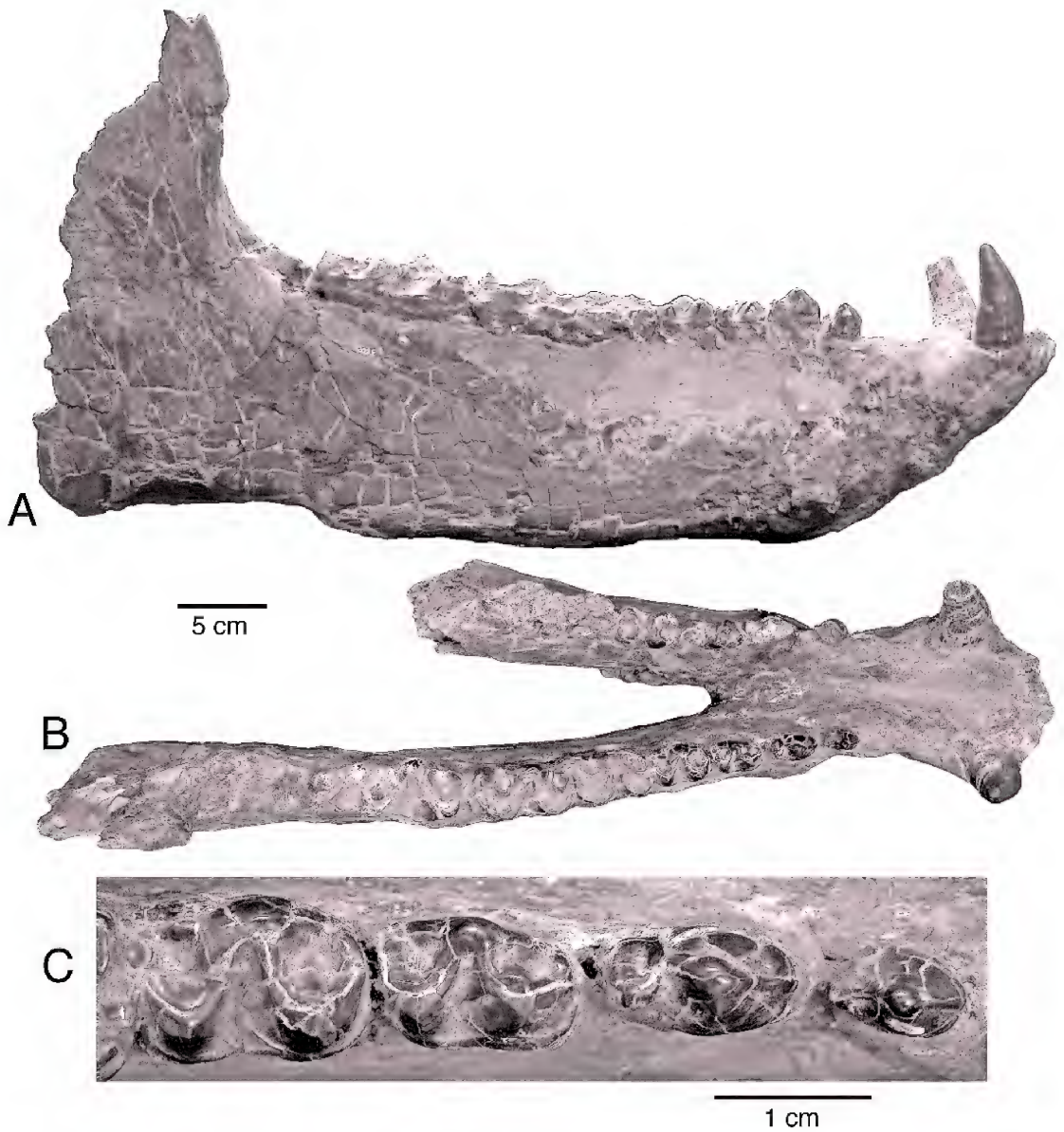

Fig. 88. Holotype of *Pollyosbornia altidens* (AMNH 2025). **(A)** Right view, **(B)** dorsal view, **(C)** right premolars.

severe expanding-matrix distortion (sensu White, 2003). None of the incisors were recovered. The incisor alveoli are distorted to varying degrees, prohibiting a precise interpretation of the size of the incisors. The postcanine diastema of AMNH 2025 is actually longer than that of *Telmatherium* or *Metatelmatherium*. The p2 of AMNH 2025 does not appear to resemble *Telmatherium* or *Metatelmatherium* any more closely than it resembles a number of other brontotheres (e.g., *Mesatirhinus junius*). Finally, the molars of AMNH 2025 are much larger than *Telmatherium* and *Metatelmatherium* molars.

Judging by its size, long postcanine diastema, and large p3 metaconid, this specimen does not belong to *Telmatherium* or *Metatelmatherium*. Rather, AMNH 2025 is closer to horned brontotheres such as *Protitanotherium emarginatum* or *Diplacodon elatus*,

although this mandible does not seem referable to these species either.

The premolars of AMNH 2025 exhibit a peculiar set of traits not shared by *Protitanotherium* or *Diplacodon*. *P. emarginatum* is most easily ruled out by its lack of a large p3 metaconid. On the other hand, *D. elatus* possesses a large p3 metaconid, as does AMNH 2025. The degree of molarization of the p3 and p4 of AMNH 2025 is similar to *D. elatus*, but the p2 is much less molariform. For instance, the paralophid is short and straight, the talonid is very small, and the cristid obliqua and hypolophid are poorly developed. Additionally, AMNH 2025 is larger than known specimens of *D. elatus*. The large size, relatively molariform p3 and p4, in combination with the relatively primitive p2, suggest that this mandible represents a unique species and undoubtedly belongs to a genus other than *Telmatherium*. Despite the poor nature of the holotype, and the lack of other referable specimens, there appears to be enough evidence to conclude that the species is valid, although I have removed it from *Telmatherium* and placed it in a new genus, *Pollyosbornia*. The long postcanine diastema, long symphysis, and relatively deep symphysis resemble *Gnathotitan berkeyi* to a degree, but it is not clear to what extent these traits are real or products of distortion.

Pygmaetitan panxianensis Miao, 1982

HOLOTYPE: IVPP V6521, a left upper tooth row with I3–M3.

TYPE LOCALITY: Shinao Formation, Shinao Basin, Panxian County, Guizhou Province, China.

AGE: Late Eocene? (= early Oligocene sensu Russell and Zhai [1987]).

REFERRED SPECIMENS: **(All from the same locality as the holotype)** IVPP V6522, a left maxillary fragment with P4–M3; IVPP V6523, left P2 and a mandible fragment with right i3, m1 (partial), m2, m3 (unerupted), left i1–i3, and other incisor or canine fragments; IVPP V6524, a left mandible fragment with m2 (partial) and m3; IVPP V6525, a partial juvenile mandible with right dc?, dp2–dp4, m1 (unerupted), left di2?, di3?, dp2, dp3, and dp4 (partial); IVPP V6526-1, a fragment of a left juvenile maxilla with DC?, P1 (unerupted), DP2, DP3, and DP4 (partial); IVPP V6526-2, a left mandible fragment with dc (root only), p1 (unerupted), and dp3–dp4; IVPP V6527, a left maxillary and jugal fragment with DP3 and DP4; IVPP V6528, a right maxilla fragment with dp2–dp4 (all damaged); IVPP V6529, a left mandible fragment with dp2 and dp3 (partial).

DIAGNOSIS: *Pygmaetitan panxianensis* is intermediate in size between *Nanotitanops shanghuangensis* and *Microtitan mongoliensis*. Dentally, *Pygmaetitan panxianensis* has an enlarged and subcaniniform incisor, a diminished postcanine diastema, a distinct P1 metacone, a distinct P2 metacone, and weak premolar preprotocristae. Hypocones are not seen on P2, P3, or P4. The molars of *Pygmaetitan panxianensis* have tall, lingually angled ectolophs with weak labial ribs, and thinned lingual ectoloph enamel with wedge-shaped paracones and metacones. A cingular parastyle shelf is absent. Central molar fossae and anterolingual cingular cusps are present, while paraconules and metalophs are absent. The upper molar mesostyles are labially expanded. The lower molars have deep valleylike basins and the m3 is elongate.

Pygmaetitan panxianensis shares with *Sthenodectes incisivum* the unique combination of an enlarged I3, diminished postcanine diastema, and no molar paraconules. However, *P. panxianensis* is clearly much smaller than *S. incisivum* and has a more complex P1 and taller lower molar crowns.

DESCRIPTION

UPPER DENTITION: The following description of the adult upper dentition of *Pygmaetitan panxianensis* is based on the holotype specimen, IVPP V6521 (fig. 89a), with additional observations made on IVPP V6522 (now shown), IVPP V6523 (fig. 89b), IVPP V6526-1 (fig. 92 a, b), and IVPP V6527 (fig. 92c). The holotype, consisting of a left maxillary fragment with a complete cheek-tooth row, represents a small but remarkably advanced brontothere. The maxillary fragment itself is too poorly preserved to describe any characteristics of the skull. The teeth are only moderately worn, thus facilitating a reasonably complete description of the upper dentition; however, most of the dental

surface is corroded and pitted, thus obscuring some of the finer details.

The only preserved incisor on the holotype, presumably an I3, is greatly enlarged. This incisor is attached to a small fragment of bone that has been glued onto the main maxilla fragment, although these two fragments do not appear to occlude precisely. It is therefore not possible to definitively determine whether the disproportionately large incisor actually belongs to the same individual. However, this large upper incisor is consistent in size with the large lower incisors that characterize this species (see below). *Pygmaetitan panxianensis* is one of two brontotheres with greatly enlarged incisors. The other example is *Sthenodectes incisivum*. This upper incisor is plesiomorphic in other respects; the crown is subcaniniform with a strong lingual cingulum. It has developed a broad lingual wear facet the spans the entire height of the crown.

The upper canine is very large as well, with a diameter that exceeds that of the incisor by about a millimeter. The crown of the canine is either worn away or broken off. The specimen lacks a diastema between the incisor and canine, although this could be an artifact of the loss of the bony fragments that would have been positioned between the larger maxillary fragment and the smaller fragment holding the incisor. A minor gap of a few millimeters separates the canine from the P1.

The P1 of IVPP V6521 is severely worn. Discernable topographical features include a paracone, a straight parastyle, a part of a small lingual heel with a small protoconelike cusp (worn flat), and a small ridge situated anterolingually from the paracone. The posterior portion of the crown is broken off. An intact and unerupted P1 is preserved with IVPP V6526-1 (fig. 92a, b). The P1 of that specimen exhibits two distinct labial cusps, a large paracone and a somewhat smaller metacone. The parastyle is bent slightly lingually while the metastyle is essentially straight. The P1 does not show a well-developed lingual heel, although a thick cingulum extends along the entire lingual margin of the crown. A sharp ridge ascends the lingual side of the metacone and joins the lingual cingulum, forming a small triangular

Fig. 89. Upper adult dentition of *Pygmaetitan panxianensis*. **(A)** The holotype (IVPP V6521), and **(B)** an additional left P2 (IVPP V6523).

peak. A similar ridge climbs the lingual side of the paracone, although it is less distinct and forms a smaller peak at its junction with the cingulum.

The P2, P3, and P4 are successively larger. These premolars are strongly rectangular in outline with parallel anterior and posterior margins. The P2 of the holotype is incomplete; the labial sheet of enamel has been lost. However, IVPP V6523 includes a complete and unworn P2 (fig. 89b). This specimen exhibits a prominent labial paracone rib, and a much smaller labial metacone rib. The parastyle is straight. The metacone is fully developed, but it is positioned close to the paracone and is strongly shifted lingually. Finally, the metastyle is straight, but strongly angled lingually. These features give the ectoloph a rather arched or rounded appearance. The labial sheet of enamel has been lost on the P3 of the holotype. The P4 of the holotype has suffered breakage at the midline of the tooth and its width is probably exaggerated; it may have had a small labial rib, but damage to the surface of the enamel and a minor amount of extraneously concreted material obscures it. The ectolophs of the P3 and P4 are flexed slightly labially in the middle, giving them a sort of rudimentary mesostyle. This mesostyle is more apparent in the P4. The ectoloph of P3 is straight, while that of P4 is incipiently W-shaped due to an anterolabially angled parastyle in addition to the more distinct mesostyle. The lingual heels of P2, P3, and P4 are broad, although only a single lingual cusp (protocone) can be found on each premolar. The protocones of P2 and P3 are tall, slightly anteriorly positioned, and are followed by short lingual crests that arch posterolabially. On P2 this crest ends at the posterior cingulum. Additionally a faint preprotocrista can be seen on the P2, connecting the anterolabial base of the protocone to the lingual base of the paracone. The P2 of IVPP V6523 lacks a strong lingual crest, although there is a very small pinpoint of enamel in the hypocone position. The P3 of the holotype has a small but distinct lingual crest that ends at the junction of the metacone and posterior cingulum where there is a distinct swelling that could be interpreted either as a metaconule, or a labially positioned hypocone. The preprotocrista of P3 is exceedingly faint. A lingual crest can be seen on P4, although it is indistinct. The P4 lingual crest is more distinct on IVPP V6522, although it is much less developed than the lingual crest of the P3 of IVPP V6521. Given the rudimentary nature of the lingual crest, and the hypoconelike and metaconule-like structures on the lingual sides of the premolars, it is probable that these characters were intraspecifically variable, like many other brontotheres.

The labial cingula of P3 and P4 are absent or they were excessively weak. A strong and continuous cingulum stretches around the anterior, lingual, and posterior margins of P2, P3, and P4. On P3 and P4 the anterior cingulum has been partially worn away by interstitial wear.

The left M1 of IVPP V6521 is heavily worn and incomplete; fragments of the posterior side are missing and the tooth has experienced severe interstitial wear, thus distorting its length/width proportion. The M2 is heavily worn as well, although the specimen is complete and has suffered a lesser amount of interstitial wear. The M3 is complete, only lightly worn and most clearly exhibits a full suite of molar characters. Advanced molar characters, best seen in the moderately worn M3, include a narrow anterolabial cingulum that passes below the apex of the parastyle, a relatively tall and lingually angled ectoloph, thin lingual ectoloph enamel, and wedge-shaped lingual margins of the paracone and metacone. There are no discernable labial paracone or metacone ribs, although weak ribs might have been present. Other advanced features include well-developed anterolingual cingular cusps and a round central molar fossa. The molars lack any trace of vestigial paraconules. The mesostyle of M3 is labially expanded. M1 and M2 probably had similarly labially expanded mesostyles, although this structure has been more dramatically worn in these teeth. A small metalophlike ridge can be seen along the anterolabial slope of the hypocones of M1 and M2. The M3 hypocone is well developed but smaller than that of the M2, and it lacks the metalophlike ridge. Labial and lingual molar cingula are thin and discontinuous around the margins of the main cusps.

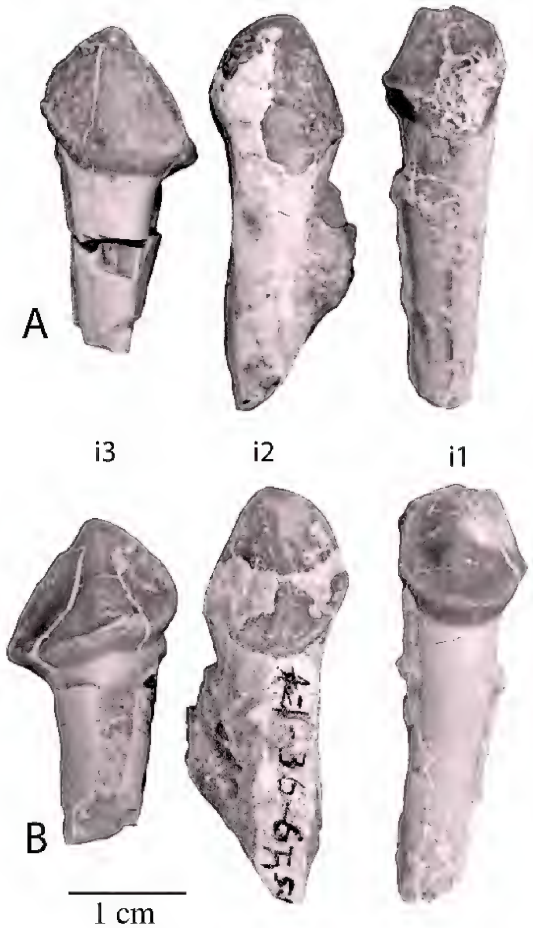

Fig. 90. Lower left incisors of *Pygmaetitan panxianensis* (IVPP 6523). **(A)** Labial view, **(B)** lingual view.

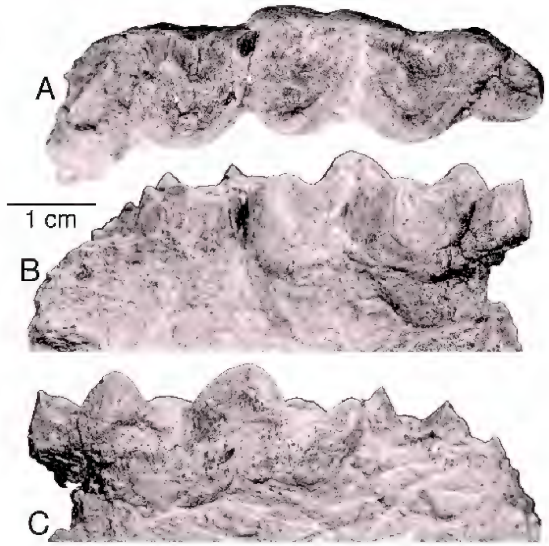

Fig. 91. A mandible fragment with a partial m2 and complete m3 referred to *Pygmaetitan panxianensis* (IVPP V6524). **(A)** Dorsal view, **(B)**, left (labial) view, **(C)** medial (lingual) view.

LOWER DENTITION: IVPP V6523 includes a number of isolated lower incisors, including a complete left incisor row (i1–i3) (fig. 90). The lower incisor crowns are rather large. They are all about the same size, although they differ in shape. The i1 and i2 have a semispatulate shape with rounded apices. The i3, on the other hand, is more subcaniniform with a pointed apex. From a lingual view, the i1 and i2 crowns are slightly asymmetrical, while the i3 is mesiodistally more elongate and more severely asymmetrical. Thin lingual cingulids are present in all three lower incisors. Labial cingulids are absent.

IVPP V6524 includes a partial m2 and a complete m3 (fig. 91). IVPP V6525 contains an exposed but unerupted m1 (fig. 93). The lower molars of *Pygmaetitan panxianensis* have relatively thin enamel. The talonid and trigonid basins are relatively deep and valley-, or V-, shaped. Weak lingual protoconid and hypoconid ribs are often seen in the lower molars of brontotheres, but they are not evident in these specimens. The m3 is elongate. Labial molar cingulids are exceedingly faint, but this cingulid can be seen wrapping around the posterior margin of the hypoconulid. Lingual cingulids are absent.

DECIDUOUS UPPER DENTITION: Most of the known specimens of *Pygmaetitan panxianensis* are juveniles. The best juvenile specimen with upper deciduous dentition is IVPP V6526-1 (fig. 92a, b). The anteriormost tooth of IVPP V6525-1 is probably a deciduous canine. The unerupted tooth just behind it is a P1 and is described above with the adult dentition. The remaining teeth are DP2, DP3, and a portion of DP4. An additional specimen, IVPP V6527 (fig. 92c), has a complete DP4. The deciduous premolars are more molarized than the adult premolars. The deciduous premolars show a trend of being progressively "derived" posteriorly. In other words, the anterior deciduous premolars are the least molariform and retain a

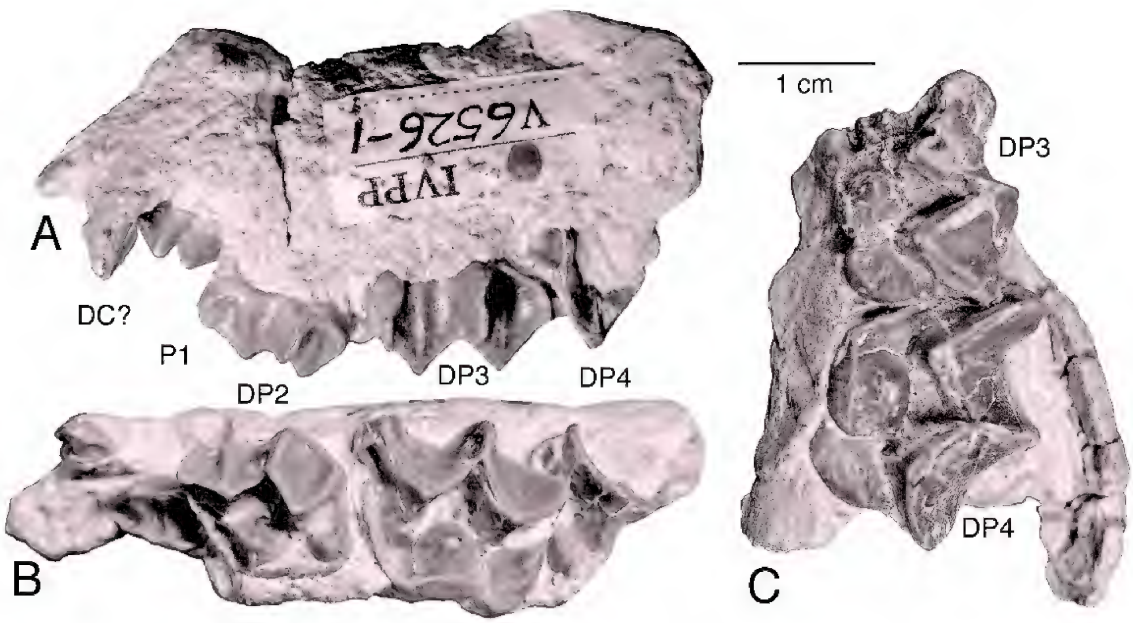

Fig. 92. Deciduous upper dentitions of *Pygmaetitan panxianensis*. **(A)** Left view of IVPP V6526-1, **(B)** ventral view of IVPP V6526-1, **(C)** ventral view of IVPP V6527.

number of plesiomorphic states. Moving posteriorly, the deciduous premolars increasingly show a number of apomorphic conditions that resemble the adult molars.

All of the deciduous premolars share with the molars the following conditions: relatively tall ectolophs, thin enamel on the lingual band of the ectoloph, angled lingual margins of the paracone and metacone, and relatively weak labial ribs. The DP2 is more asymmetrical than typical adult molars. The anterior portion of the ectoloph is more elongate than the posterior portion. The DP3 and DP4, on the other hand, are fully molariform in terms of their overall shape. The mesostyle of the DP2 is small and angled posterolabially. The parastyle is less strongly deflected lingually. Because of the smaller mesostyle and less labially directed parastyle, the labial margins of the cusps are not as deeply concave as those of the adult molars. The DP3 and DP4 mesostyles are well developed; however, the DP3 and DP4 mesostyles are less labially expanded that those of the adult molars. A small but distinct preprotocrista is present on the DP2, although a distinct paraconule is not embedded in this crest. DP3 lacks a preprotocrista, although it retains a small paraconule. DP4, like the adult molars, entirely lacks a preprotocrista and paraconule. A deep central molar fossa is not seen on DP2, although, like the molars, DP3 and DP4 express this condition. The lingual cingulum of DP2 climbs to the peak of the parastyle; this character resembles the most basal brontotheres such as *Eotitanops* and *Palaeosyops*, although the cingulum does not form a thickened parastylar shelf as seen in these taxa. In adult molars of more derived brontotheres, the anterior cingulum wraps around the anterolabial margin of the tooth in a position proximal to the peak of the parastyle; the DP3 and DP4 of *Pygmaetitan panxianensis* show this condition. DP4 shares with the adult molars a strong anterolingual cingular cusp, although this structure is absent on DP2 as well as DP3. Finally, the lingual cingulum of DP2 is thick and continuous with the anterior and posterior cingula; the lingual cingula of DP3 and DP4 are very weak and more closely match the adult condition.

JUVENILE MANDIBLE AND DECIDUOUS LOWER DENTITION: IVPP V6525 is a nearly complete juvenile mandible with deciduous dentition (fig. 93a, b). IVPP V6526-2 contains an additional set of deciduous premolars that are somewhat better preserved

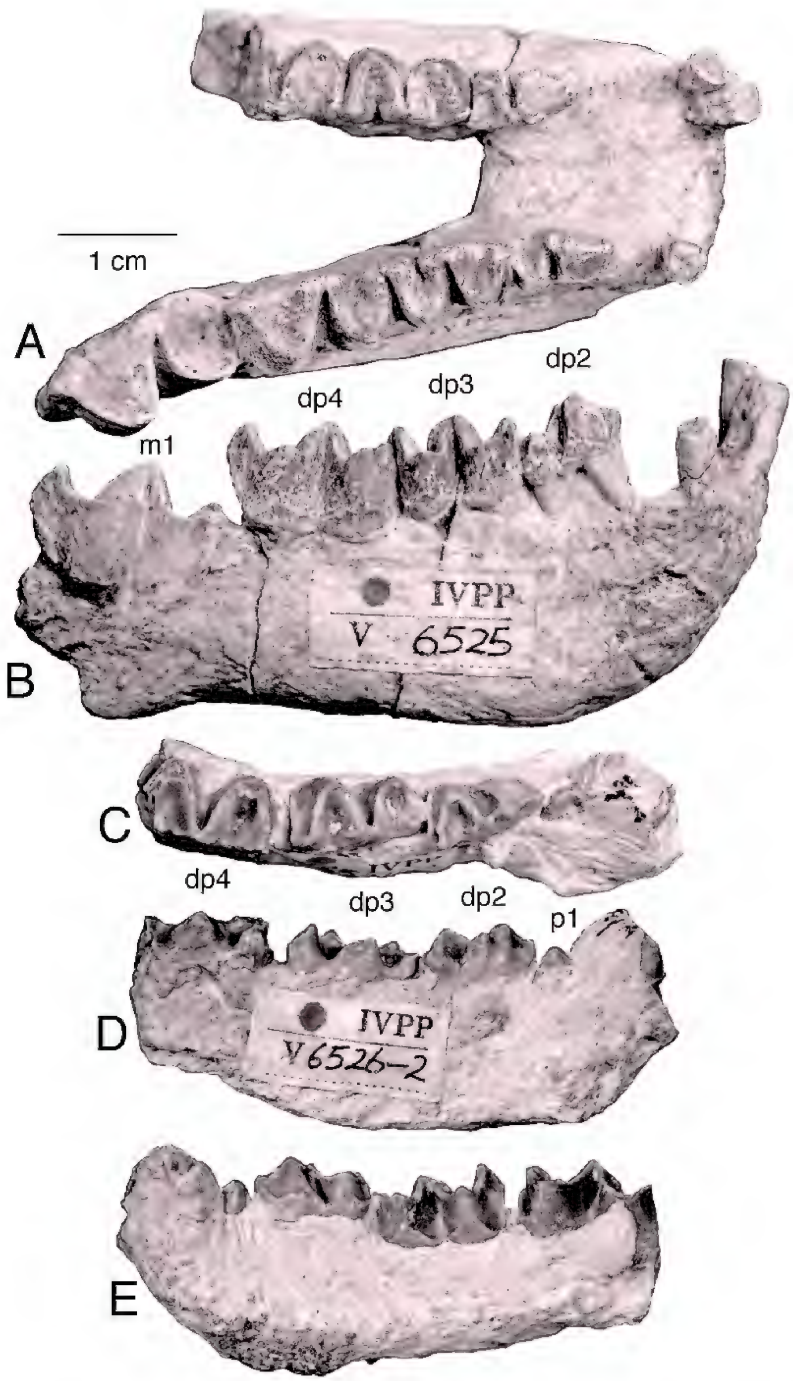

Fig. 93. Juvenile mandibles and deciduous lower dentition referred to *Pygmaetitan panxianensis*. **(A)** Dorsal view of IVPP V6525, **(B)** right view of IVPP V6525, **(C)** occlusal view of deciduous dentition of IVPP V6526-2, **(D)** medial (lingual) view of IVPP V6526-2, **(E)** right (labial) view of IVPP V6526-2.

(fig. 92c, d, e). The mandibular symphysis of IVPP V6525 is short and very broad and the inferior angle of the symphysis is nearly vertical. Although there were undoubtedly ontogenetic changes in the overall shape of the mandible, it is likely that the adult mandible possessed similar peculiarities, even if not as extreme. Unfortunately, the crowns of the right di2, di3, and left dc are not preserved. A dp1 or p1 is not present in IVPP V6525, and there is a short gap between the dc and dp2. This gap is filled by an erupting P1 in IVPP V6526-2, thus indicating the absence of a postcanine diastema, at least at this ontogenetic stage. The morphology of the dp2 generally resembles a typical adult brontothere p2, although a large metaconid is present; metaconids are not typically found in the adult p2s of brontotheres. The dp2 metaconid is situated very close to the protoconid and is positioned posteriorly and slightly lingually from it. The dp2 contrasts with the molariform condition in the following ways: the trigonid is relatively longer, the paralophid and protolophid are straight rather than lingually arched, the protoconid is positioned medially rather than labially, and the talonid of dp2 is essentially molariform, with lingually arching cristid obliqua and hypolophid forming a U-shaped crest that is remarkably deep in comparison to typical brontothere adult premolars or molars. The dp3 and dp4 contrast with typical adult premolars in their possession of a pronounced entoconid, and they are essentially molariform, although they have somewhat more elongate proportions than typical adult molars, and also have remarkably deep U-shaped crests. As noted above, the lower adult molars are remarkably tall in comparison to typical brontotheres, with deep valley-shaped trigonid and talonid basins. The lateral views of IVPP V6525 and IVPP V6526-2 reveal that the deciduous premolars increase in crown height posteriorly. In IVPP V6525, the dp4 approaches the remarkable crown height of the unerupted m1.

Remarks

Pygmaetitan panxianensis Miao, 1982, is based on a maxillary fragment with a nearly complete set of adult upper dentition. Miao (1982) noted that *P. panxianensis* is easily differentiated from small North American brontotheres, and except for its enlarged incisors and canine, is similar in many ways to derived brontotheres from the late Eocene. Miao (1982) briefly compared *P. panxianensis* with *Eotitanops* and *Microtitan* and more detailed comparisons with small Asian and North American brontotheres are made here.

Pygmaetitan panxianensis is substantially larger than the minuscule *Nanotitanops shanghuangensis*, with cheek-tooth dimensions that are more than double. Additionally, *N. shanghuangensis* molars retain small paraconules, whereas *P. panxianensis* molars do not. The cheek teeth dimensions of the holotype specimen of *P. panxianensis* just slightly exceed the largest specimens of *Eotitanops*, and are similar in size to the smallest *Palaeosyops* specimens. Nonetheless, the molars of *Pygmaetitan panxianensis* are clearly more advanced than *Eotitanops* and *Palaeosyops*, and clearly establish it as a member of the Brontotheriinae. Other small brontotheres, *Microtitan mongoliensis*, *Mesatirhinus junius*, *Metarhinus fluviatilis*, *Metarhinus abbotti*, and *Fossendorhinus diploconus* exceed *Pygmaetitan* in size by a substantial margin. Moreover, none of these species has extremely enlarged incisors or a P1 metacone, nor do they lack a postcanine diastema. Size comparison with *Acrotitan ulanshirehensis* is complicated by the lack of comparable dental material, although *Acrotitan* seems somewhat larger. However, the narrow mandibular symphysis, small incisor alveoli, and long p1–p2 diastema of *Acrotitan ulanshirehensis* are obviously out of character with the enlarged upper incisor and reduced upper postcanine diastema of *Pygmaetitan panxianensis*.

The extremely enlarged incisor of *Pygmaetitan panxianensis* is a characteristic shared with *Sthenodectes incisivum*, a much larger North American hornless Uintan brontothere. The deep, valley-shaped trigonid and talonid basins seen in the adult lower molars closely resemble the gigantic late Eocene Asian brontothere, *Embolotherium*. The very labially expanded mesostyle that is best seen in the M3 of IVPP V6521 is perhaps an autapomorphic condition, although it is difficult to compare mesostyle proportions to

species that are only known from specimens with heavily worn teeth.

Many juvenile specimens were found with adult specimens of *Pygmaetitan panxianensis*, and were assigned to this species by Miao (1982). As Butler (1952) noted, the upper deciduous premolars of brontotheres tend to be molariform, although the more anterior deciduous premolars tend to lag behind in the accumulation of typical molar apomorphies. This appears to be the case in *Pygmaetitan*. In terms of adult molar characters, the DP2 retains the greatest number of plesiomorphic character states; the DP3 has an intermediate number of plesiomorphic states, and the DP4 has the least. Despite the more "primitive" condition of the deciduous dentition in comparison to the adult molars, the deciduous premolars of *Pygmaetitan* are quite molariform in comparison to other brontothere species where the DP2 is substantially more elongated (Butler, 1952). However, because of the lack of comparable material for most other brontothere species, the phylogenetic or taxonomic value of the deciduous teeth of *Pygmaetitan panxianensis* is uncertain. Since Butler's (1952) analysis of the deciduous dentition of perissodactyls, deciduous dental material has been collected for several more brontothere species, although at present there are no descriptions of this material.

Gnathotitan berkeyi (Osborn, 1925)

LECTOTYPE: AMNH 20106, a mandible with right c–m3, left c, and p2–m3.

TYPE LOCALITY: Telegraph Line Camp, Irdin Manha Formation, Inner Mongolia, China.

AGE: Middle Eocene (Irdinmanhan land mammal "age").

REFERRED SPECIMENS: **(From the Irdin Manha Formation, Inner Mongolia)** AMNH 20107, a partial right mandible with i1–m1, m2 (partial); AMNH 20115, a partial juvenile mandible with unerupted incisor, p1, dp2–dp4 (all damaged), and m1; AMNH 20121, a left maxilla fragment with canine alveolus and P1–M3; AMNH 141231 (formerly part of AMNH 20106), a right maxillary fragment with C–M3.

Two other specimens, AMNH 20124 (a mandible) and AMNH 20127 (a palate with premolars and molars), were referred to *Gnathotitan berkeyi* by Osborn (1925). Both of these specimens were sent to the Chinese Geological Survey in 1928 and are apparently lost.

DIAGNOSIS: *Gnathotitan berkeyi* is a large brontothere with a semicomplex P1 (indistinct metacone and small lingual heel) and a distinct P2 metacone. Lingual crests extending from the protocones of the P2–P4 are always present. A premolar hypocone is occasionally present although it is never well separated from the protocone. The molars of *G. berkeyi* are elongate and have tall, lingually angled ectolophs with weak labial ribs and thinned lingual ectoloph enamel with wedge-shaped paracones and metacones. A cingular parastyle shelf is absent. Distinct central molar fossae and weakly developed anterolingual cingular cusps are present. Paraconules and metalophs are absent. The lower dentition of *G. berkeyi* includes three large subcaniniform incisors. There is a distinct postcanine diastema, a p2 trigonid that is more than twice as long as the talonid, a small metaconid on p3, and a large metaconid on p4. The lower molars have shallow basins and the m3 is slender and very elongate.

Gnathotitan berkeyi can be distinguished from all other brontotheres by its disproportionately large and deep mandible, which exceeds the mandibles of all other brontotheres in depth and size.

DESCRIPTION

SKULL: The skull of *Gnathotitan berkeyi* is known only from two maxillary fragments, AMNH 20121 (fig. 94) and AMNH 141231 (fig. 95). The lower portion of the orbit is seen in AMNH 20121 and suggests that the anterior rim of the orbit was positioned over the posterior portion of M2. The dorsal margin of the maxilla is intact to a point between the P1 and P2 and indicates that the nasal incision extended at least to this point, but the true anteroposterior length of the nasal incision is unclear.

UPPER DENTITION: The upper incisors of *Gnathotitan berkeyi* are unknown, but the cheek-tooth rows are complete in both maxillae (figs. 94, 95). The canine of AMNH

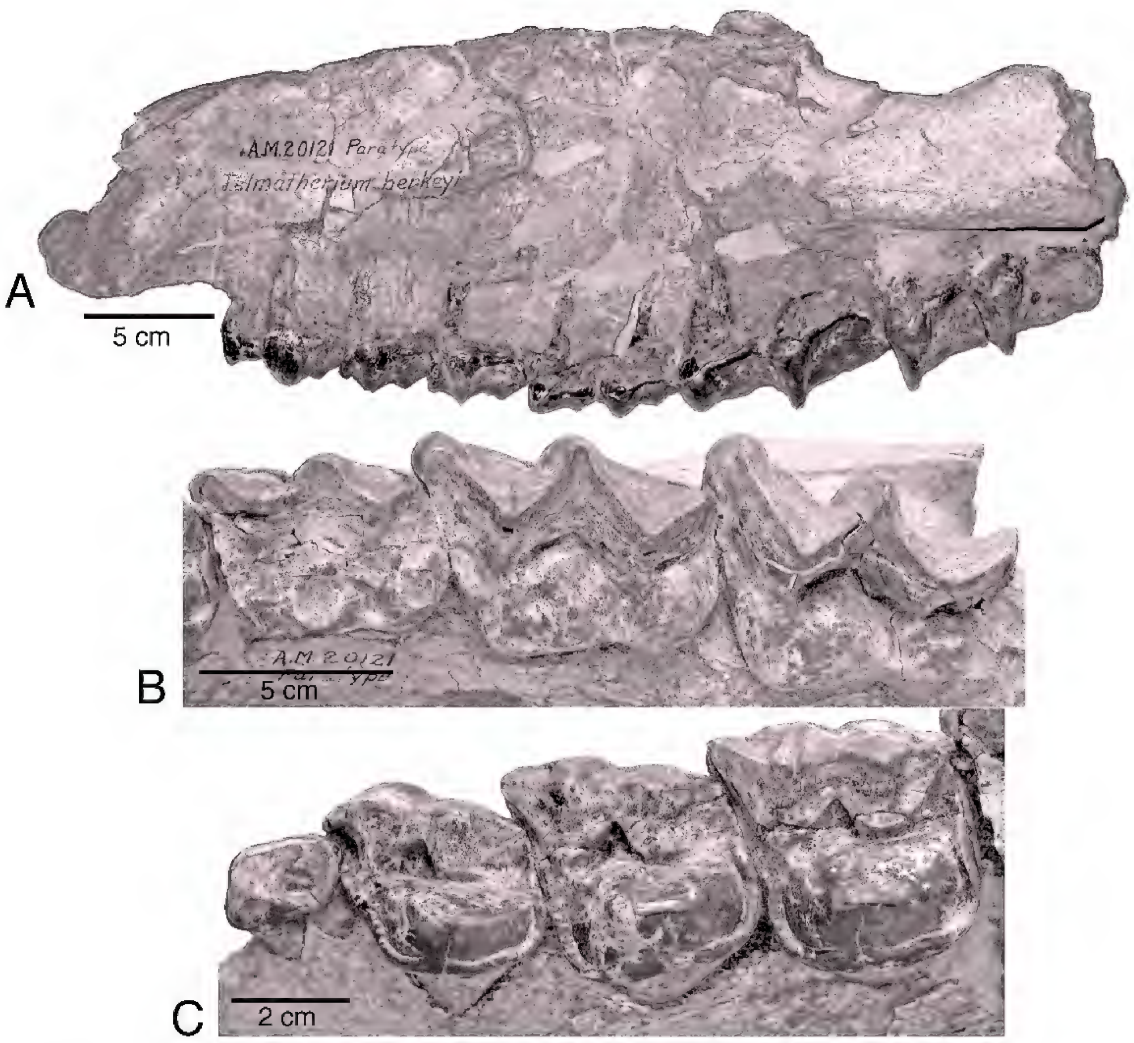

Fig. 94. A maxilla referred to *Gnathotitan berkeyi* (AMNH 20121). **(A)** Left (labial) view, **(B)** left molars, **(C)** left premolars.

20121 is not preserved, but the alveolus indicates a canine of very small diameter. In contrast, the canine of AMNH 141231 is large with a bulbous root. A postcanine diastema follows the canines of both specimens.

The P1 is a small ovoid tooth that consists of a large paracone, a much shorter and indistinct metacone, and a very small lingual heel with a small protocone. A short preprotocrista connects the protocone to the paracone. The size of the lingual heel is variable. On AMNH 20121 the P2 is more oblique than P3 or P4 due to the posterolingually angled anterior margin and the lingually shifted metacone. The parastyle of P2 is nearly straight, while the metastyle is angled lingually. The P3 and P4 are more rectangular because of nearly parallel anterior and posterior sides and a nearly flat lingual side. Likewise, the metacones are not as strongly shifted lingually in comparison to P2. The parastyles of P3 and P4 are directed somewhat labially, while the metastyles are nearly straight. The paracone of P2 is swelled buccally, while P3 and P4 have small but well-defined labial paracone ribs.

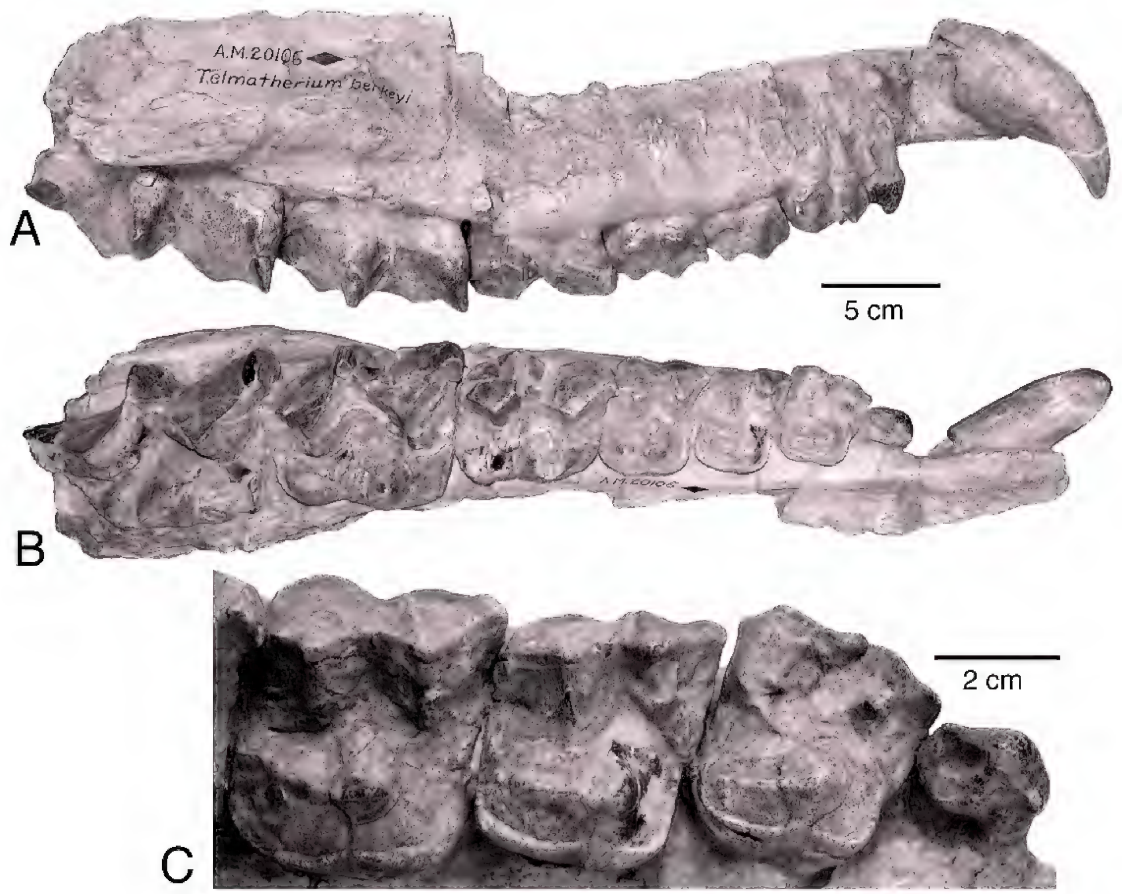

Fig. 95. A maxilla referred to *Gnathotitan berkeyi* (AMNH 141231, formerly part of AMNH 20106). **(A)** Right (labial) view, **(B)** ventral view, **(C)** right premolars.

The lingual features of the P2–P4 have relatively high relief. On each of the molars, a very low and short preprotocrista can be seen; it is strongest on the P2 and smallest on the P4. A long lingual crest extends posteriorly from the protocone of P2. On the P3 of AMNH 20121 a tall but short lingual crest connects the protocone to a large hypocone-like swelling. The P3 is similar to P4 except that the protocone and hypocone are even more closely positioned, so that they form a single large ovoid cusp with a short lingual crest at its apex. The lingual premolar morphology of AMNH 141231 differs from that of AMNH 20121. In that specimen, the lingual sides of the P2, P3, and P4 have a single lingual cusp (protocone) and a long lingual crest extending posteriorly from the protocone. The labial premolar cingula are very weak. In AMNH 20121 the anterior and posterior premolar cingula do not join lingually. In AMNH 141231 there is a continuous lingual cingulum on P3 and P4 but not on P2.

The upper molars of *Gnathotitan berkeyi* are notably elongate. This is most evident in M2 and M3. M1 appears to have been shortened somewhat by interstitial wear. The molars show typical brontotheriine traits including tall, lingually angled ectolophs, very weak labial ribs, thin lingual ectoloph enamel, and wedge-shaped lingual sides of the paracone and metacone in molars that are not heavily worn. The anterior cingulum is thin and passes proximally to the distal peak of the parastyle. Shallow central molar fossae are seen on each of the molars. On the M1, there is a wear facet on the anterolingual cingulum; on M2 and M3 small but distinct anterolingual cingular peaks are evident. All

evidence of paraconules and metalophs is lost. The M3 hypocone varies. In AMNH 20121, the M3 hypocone is nearly as large as those of the more anterior molars and is separated from the protocone by a deep valley. However, in AMNH 141231, there are two very small hypoconelike points of enamel. Labial molar cingula are weak, and lingual molar cingula are absent.

MANDIBLE AND LOWER DENTITION: The mandible and lower dentition of *Gnathotitan berkeyi* are known from the lectotype (AMNH 20106), which consists of a nearly complete mandible that is missing its incisors (fig. 96). (The left p1 is mistakenly glued onto the mandible as an incisor.) The lectotype is laterally crushed, thus its proportions are distorted, but from a lateral view the shape of the mandible seems reasonably intact. Additionally, a partial right ramus with well-preserved incisors, premolars, and a symphysis offer more details (fig. 97).

At 805 mm in length, AMNH 20106 is the largest known brontothere mandible. (The second largest brontothere mandible I have ever encountered (724 mm in length) is AMNH 1051, a specimen of *Megacerops* sp. (sensu Mihlbachler et al., 2004b). Despite the profoundly large mandible, *Gnathotitan berkeyi* was probably not the largest brontothere in terms of body mass. For instance, the length of the cheek-tooth row is exceeded by other large brontotheres (e.g., *Aktautitan*). In addition to its excessive size, the mandible is unique in the great depth of the horizontal ramus. Another peculiar aspect of its shape is the distinct bulge on the inferior margin of the horizontal ramus. The bulge is present on both sides, but it is somewhat asymmetrical. On the right side it is below m2 and m3, while on the left side it is below m3 and somewhat posterior to m3. The peculiar shape of the inferior margin was considered by Osborn (1925, 1929a) to be a species-level character. However, the bulge could be a neoplasia or tumor paleopathology (Bruce Rothschild, personal commun., 2003), although a thorough paleopathological analysis has not been undertaken. In addition to the large bulge in the center of the ramus, the mandible bulges directly below the symphysis. This second characteristic is repeated in AMNH 20107, suggesting that it is probably not related to a paleopathology.

Osborn (1925) described the coronoid process of AMNH 20106 as wide, though there is so much plaster involved in the reconstruction of that part of the mandible that this observation is doubtful. The symphysis of AMNH 20106 is long and its inferior margin is steeply angled slightly more than 45°. This great length and steep orientation of the symphysis is clearly related to the extreme depth of the ramus. However, lateral crushing has clearly exaggerated the narrow-elongate shape of the symphysis of the lectotype. The cross-sectional shape of the symphysis can be seen from the medial view of AMNH 20107. The symphysis extends to the talonid of the p3.

Although no incisors are preserved with AMNH 20106, there are clearly six alveoli that form an arched row anterior to the canines. A complete right lower incisor row is preserved in AMNH 20107. The incisors are large and positioned closely together with no diastemata. Each crown is composed of a dulled point with narrow mesial and distal margins. The i2 is the largest incisor, though barely so. It exceeds the other incisors in size primarily in crown height. The i3 is slightly more mesiodistally elongate than the other incisors, but otherwise it is similar to i1 and i2. Each incisor has a distinct lingual cingulid. There are no labial incisor cingulids in *Gnathotitan berkeyi*.

The canine of AMNH 20106 is very small, while the canine of AMNH 20107 is much larger. Likewise, the postcanine diastema of AMNH 20107 appears to be shorter than that of the lectotype.

The left p1 is a small narrow tooth with a single cusp and a small talonid heel. The talonid of p2 is more than twice the length of the talonid but about the same width. The p3 and p4 trigonids are about the same length as their talonids, but the talonids are somewhat wider. The paralophid of p2 arches slightly lingually, thus creating a small lingual-trigonid notch. The protolophid of p2 is straight and slightly deflected lingually. There is no metaconid on the p2. The p3 paralophid and protolophid are more strongly angled lingually, creating broader lingual-trigonid notches. The p3 has a small meta-

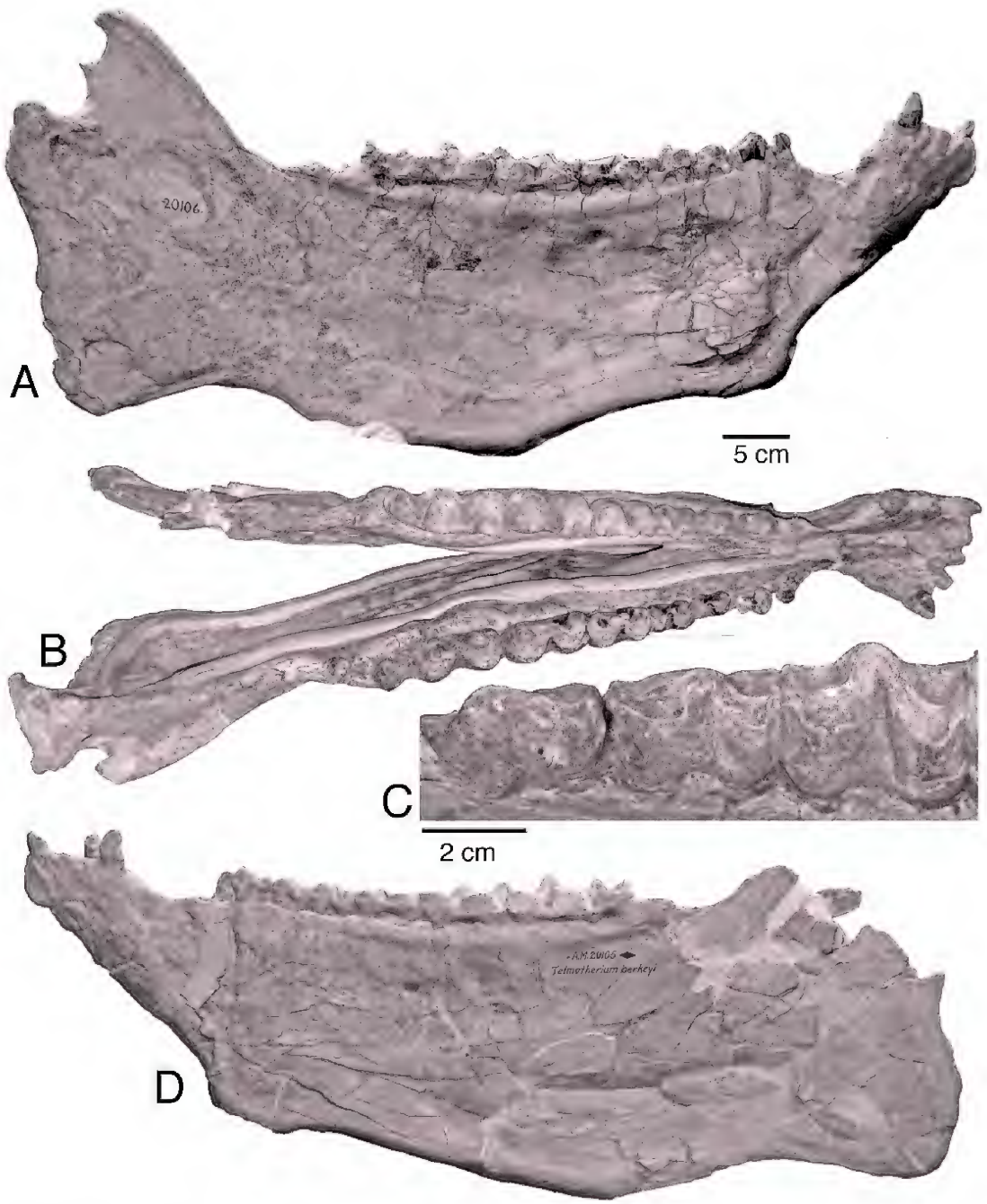

Fig. 96. The lectotype mandible of *Gnathotitan berkeyi* (AMNH 20106). **(A)** Right view, **(B)** dorsal view, **(C)** left p2–p4, **(D)** left view.

conid that is positioned about equally lingually and posteriorly from the protoconid. The p4 trigonid is essentially molariform with a fully lingually arched paralophid and protolophid, a molariform trigonid basin, and a large lingually positioned metaconid. The cristids obliqua and hypolophids of p2–p4 are well developed, although on the p2 the

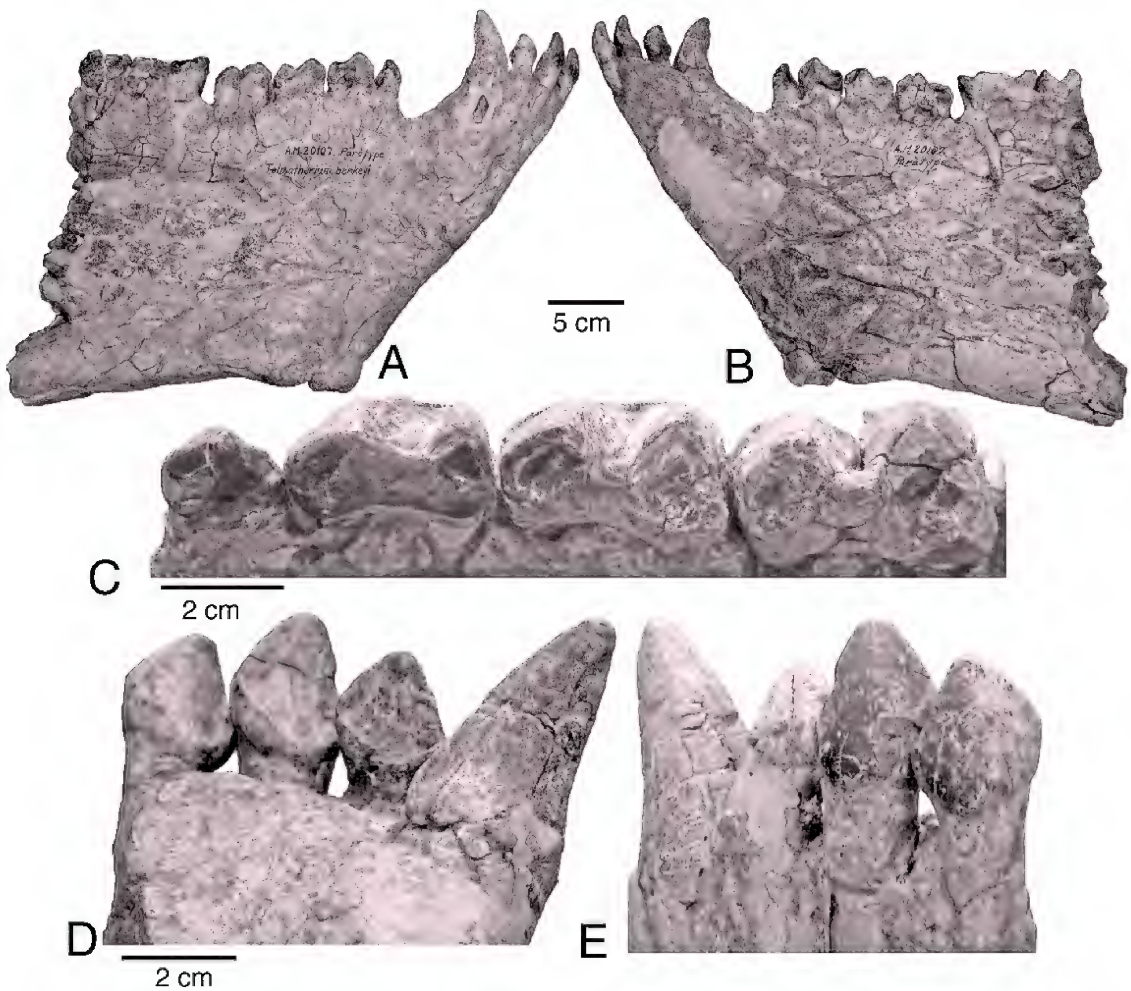

Fig. 97. A partial mandible referred to *Gnathotitan berkeyi* (AMNH 20107). **(A)** Right view, **(B)** medial view of right side, **(C)** right premolars, **(D)** lingual view of right incisors, **(E)** labial view of right incisors.

talonid basin is small. The talonid basins of p3 and p4 are broader and nearly molariform. Labial premolar cingulids of *Gnathotitan berkeyi* tend to be weak, while lingual premolar cingulids are absent.

The molars of *Gnathotitan berkeyi* are typical, with shallow basins, thin lingual enamel, and an elongate m3. However, the m3 is among the most elongate among brontotheres with an m3 length/width ratio (2.94) that rivals *Aktautitan* (Mihlbachler et al., 2004a). Labial molar cingulids are thin and lingual molar cingulids are absent. The m3 hypoconulid has a faint cingulid tracing around it.

Remarks

The Central Asiatic Expedition of the American Museum of Natural History recovered seven specimens (two are now lost) that represent a species of very large brontothere with elongate molars and a very deep mandible. Osborn (1925) assigned holotype status to a mandible and maxilla that had originally been given the same catalog number (AMNH 20106), although these specimens do not actually belong to a single individual (see below for clarification). Osborn (1925, 1929a) originally assigned *Gnathotitan berkeyi* to the genus *Telmather-*

ium. However, *G. berkeyi* is clearly different from any other material that Osborn (1929a) had referred to *Telmatherium*. Osborn's (1925) only indication as to why he though *G. berkeyi* belonged to *Telmatherium* was that "the canines resemble those of *Telmatherium* and *Menodus*" (Osborn, 1925: 9). However, no special similarities in the canines of these taxa were actually pointed out, nor could I find any. Granger and Gregory (1943) correctly recognized this species as distinct from all other brontotheres and assigned it to its own genus.

The holotype of *Gnathotitan berkeyi* (AMNH 20106), as previously described by Osborn (1925; 1929a) and Granger and Gregory (1943), includes a mandible and right maxilla that were both originally assigned to AMNH 20106. However, Walter Granger's field notes for the 1923 Central Asiatic Expedition in the AMNH vertebrate paleontology archives indicate for field number 163 (= AMNH 20106), "association between maxilla and lower jaw questionable". This detail was either ignored or unnoticed by Osborn (1925, 1929a) and Granger and Gregory (1943), who considered the maxilla and mandible to be parts of a single holotype. Because the jaw and maxilla are not certainly associated (and evidence presented below further suggests they represent separate individuals), the jaw and mandible should be considered syntypes rather than a single holotype. The AMNH catalog has been modified to reflect this by assigning a new number to the maxilla (AMNH 141231), while the mandible retains the original number (AMNH 20106). Among the syntypes, the mandible (AMNH 20106) is designated as the lectotype.

Other evidence suggests that the lectotype mandible (AMNH 20106) and the maxilla (AMNH 141231) represent separate individuals of the same species. Most notably, the canine of the maxilla is much larger than the canine of the mandible. The diameter of the maxillary canine (36.4 mm) at the base of the crown is 71% greater than that of the mandibular canine (21.2 mm). Canine size is commonly variable in brontothere species. However, the upper and lower canines of a single individual are usually of a similar size. For comparison, the upper canine of KAN N2/875 (the holotype of *Aktautitan hippopotamopus*) is only 5% larger in diameter than the lower canine (Mihlbachler et al., 2004a). The disparity in canine size between the maxilla (AMNH 141231) and mandible (AMNH 20106) of the *G. berkeyi* syntypes strongly suggests that these specimens represent two individuals, possibly of different sexes. The other specimens referred to *G. berkeyi* also indicate canine size dimorphism. The additional mandible, AMNH 20107, has canines that are much larger (diameter = 29 mm) than those of the lectotype mandible. Likewise, the additional maxilla, AMNH 20121, has a canine alveolus that is much smaller in diameter than that bulbous canine root of the syntype maxilla.

Aktautitan hippopotamopus Mihlbachler, Lucas, and Emry, 2004a

HOLOTYPE: KAN N2/875, a complete skull, mandible, and skeleton lacking only parts of the right tarsus and pes.

TYPE LOCALITY: Kyzylbulak Formation, Kyzyl Murun near Aktau Mountain, Ily Basin, Kazakstan.

AGE: Middle Eocene (Irdinmanhan land mammal "age").

REFERRED SPECIMENS: **(From the same locality as the holotype)** KAN N2/873, a complete skull and articulated mandible, complete dentition, and fully articulated right forelimb with radius, ulna, and manus, and a partial left manus; KAN N/2 639, anterior portion of a cranium.

DIAGNOSIS: *Aktautitan hippopotamopus* is a large brontothere with small frontonasal horns that are elevated high above the orbits. The nasal process and horns are elevated to the peak of a tall frontonasal process that rises anterodorsally from above the orbit at an angle of about 45°. The nasal incision is dorsoventrally deep and it extends posteriorly to the P4. The orbit is positioned over the M2. The elevated nasal process is angled downward, not strongly rounded anteriorly, and with lateral walls that are deep proximally and shallow distally. The premaxillomaxillary rostrum deepens posteriorly and is not enclosed by bone dorsally. Other cranial characteristics include a saddle-shaped cranium, separate parasagittal ridges, nearly

straight zygomatic arches, and a ventrally unconstricted and mediolaterally angled external auditory pseudomeatus. Postzygomatic processes, as seen in *Metatitan*, are absent.

Dentally, *Aktautitan hippopotamopus* has three large upper incisors including a subglobular I1, and more subcaniniform I2 and I3, a distinct postcanine diastema, a complex P1, a distinct P2 metacone, and weak preprotocristae on the P2 and P3. Premolar hypocones are absent. The upper molars have tall, lingually angled ectolophs with weak labial ribs, and thinned lingual ectoloph enamel with wedge-shaped paracones and metacones. A cingular parastyle shelf is absent. Distinct central molar fossae and anterolingual cingular cusps are present. Paraconules and metalophs are absent. The three lower incisors are large and subcaniniform. The i2 is the largest incisor. There is a distinct postcanine diastema and a small p3 metaconid. The p2 trigonid is nearly twice the length of the talonid. The lower molars have shallow basins and m3 is long and slender.

Aktautitan hippopotamopus shares with *Metatitan* the unique combination of having closely positioned horns and a nasal process that are elevated to the peak of a superorbital frontonasal process. However, it differs from *Metatitan* in its more anteriorly positioned orbits, more poorly developed p3 metaconid, postcanine diastemata, and larger and more subcaniniform incisors.

Remarks

Aktautitan hippopotamopus is a large brontothere from the middle Eocene Kyzylbulak Formation of Kazakstan that resembles *Metatitan* in its elevated horns and nasal process, but differs from *Metatitan* in a number of respects. Preliminary reports of this new species mistakenly attributed it to the genus *Protitan* (Emry et al., 1997; Emry and Lucas, 2002, 2003; Lucas and Emry, 2001). The formal description of *A. hippopotamopus* represents a part of this study and follows methods and a format similar to that used here but was published elsewhere (Mihlbachler et al., 2004a).

Brachydiastematherium transylvanicum Böckh and Maty, 1876

Holotype: Anterior part of a lower jaw with several incisors, right c, p2–p3 and left c–m1.

Type Locality: Andrásháza (Seibenbürgen), Hungary (Transylvania), eastern Hungary, about 150 miles northeast of Belgrade.

Age: Middle Eocene (?).

Diagnosis: *Brachydiastematherium transylvanicum* is a large brontothere with a mandible very similar to *Metatitan*. Features of the holotype jaw are a robust mandibular symphysis that extends behind the p4, intermediately sized incisors that are semispatulate and subcaniniform that form an arched row anterior to the canines. A postcanine diastema is absent. A metaconid is absent on p2, but present on p3 and p4. The p2 trigonid and talonid have similar lengths. The labial notch in the crown of p2 is broad.

Brachydiastematherium transylvanicum can be distinguished from *Metatitan relictus* and *M. primus* by its larger more spatulate incisors with distinct lingual cingulids and a much broader labial p2 notch. *B.* resembles *M. khaitshinus* in these respects; however, the p4 of *B. transylvanicum* has an autapomorphic crest extending posteriorly from the middle of the cristid obliqua.

Description

Mandible and Lower Dentition: The holotype of *Brachydiastematherium transylvanicum* consists of the anterior portion of a mandible with an incomplete set of lower teeth. The following description is based primarily on cast material in the AMNH (108188) and the figure provided by Osborn (1929a), reprinted here as fig. 98. The angle of the inferior margin of the symphysis was relatively shallow. The posterior margin of the symphysis is incomplete; however, what is left indicates that it originally extended behind the talonid of p4. The alveolar incisor surface is incomplete and all but one of the incisors (left i3) is completely detached. However, the preserved portion of the symphysis seems to indicate

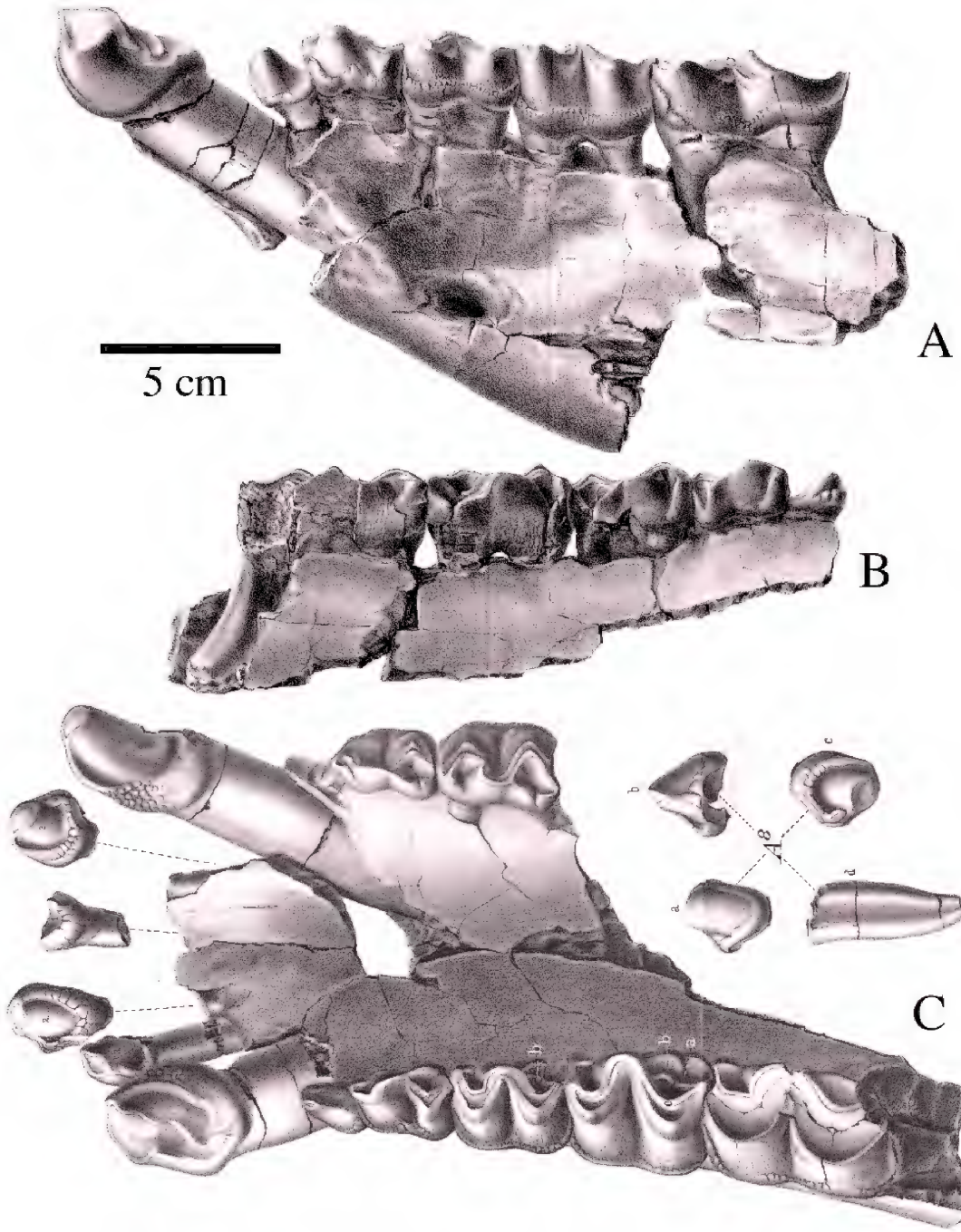

Fig. 98. The holotype of *Brachydiastematherium transylvanicum*. **(A)** Left view, **(B)** medial (lingual) view of left cheek teeth, **(C)** dorsal view. Illustrations from Osborn (1929a).

that the incisor row arched slightly anterior to the canines. The incisors are of moderate size. One of these incisors is semispatulate, while the other is slightly more conical. Each of the incisors has a distinct beaded lingual cingulid. The canines are somewhat large and have prominent lingual cingulids.

Brachydiastematherium transylvanicum lacks a postcanine diastema. The p1 has a single cusp and a broad talonid heel. The trigonid of the p2 is only slightly longer than the talonid; the p3 trigonid is about the same length as the talonid, and the p4 trigonid is shorter than the talonid. The paralophid of p2 is slightly angled lingually, creating a small but distinct lingual notch. The p2 protolophid is straight but deflected slightly lingually. The trigonids of the p3 and p4 are more molariform with paralophids and protolophids that arch fully lingually, creating nearly molariform basins. The talonids of p2, p3, and p4 are well developed with long cristids obliqua, long hypolophids, and broad, valleylike talonid basins. Lingual premolar cingulids are absent. The labial cingulid of the p2 is relatively faint and discontinuous around the base of the protoconid and hypoconid. However, the labial cingulids of p3 and p4 are thin, but they are distinct and continuous. Finally, the p4 has an unusual crest of enamel extending posteriorly from the middle of the cristid obliqua. This crest is also present on p3, but it is shorter and less distinct. The left m1 is the only preserved lower molar. It is heavily worn and lacks any features worthy of mention.

Remarks

Böckh (1876) described the first undoubted brontothere from eastern Europe, *Brachydiastematherium transylvanicum*. Presently, no other material is directly referable to this species. This fossil is considered to be middle Eocene (Uintan equivalent) by Lucas and Schoch (1989a), although this assessment is based on the opinion, expressed by Lucas (1983a) and Lucas and Schoch (1989a), that *B. transylvanicum* is a senior synonym of North American Uintan (Uinta C) genus, *Diplacodon*. However, *B. transylvanicum* differs from *Diplacodon elatus* in significant ways. For instance, there is no postcanine diastema; the p3 metaconid is essentially molariform, and the talonids of the premolars are generally much broader. *Brachydiastematherium* is similar to *Metatitan* in these respects.

In an analysis of Asian brontothere relationships, Mihlbachler et al. (2004a) found *Brachydiastematherium* to share close phylogenetic affinity with *Metatitan* and considered the possibility that *Metatitan* is actually a junior synonym of *Brachydiastematherium*. In particular, *B. transylvanicum* is very similar to *M. khaitshinus*. Both species share moderately sized semispatulate incisors and a broad labial notch on the p2. *M. relictus* and *M. primus* have smaller more globular incisors and a much narrower labial notch on the p2. However, the unusual enamel crest extending posteriorly from the cristid obliqua of the p4 of *B. transylvanicum* is not seen in *M. khaitshinus*. The taxonomic significance of this unusual crest is uncertain. It could be an autapomorphic character of *B. transylvanicum*, although it is also possible that it is an anomalous characteristic of the individual represented by the only known specimen. Presently I consider it to be an autapomorphy of *B. transylvanicum*. If my interpretation of this character is correct, it validates *B. transylvanicum*, although better material is clearly needed.

When considering the taxonomic identity of *Brachydiastematherium transylvanicum*, one must also consider other brontothere fossils found in Europe. Nikolov and Heissig (1985) described several brontothere teeth from the Black Sea Coast of Bulgaria, representing the second find of European brontotheres. The incomplete nature of European brontothere fossils limits comparison of the material described by Nikolov and Heissig (1985) with the holotype of *B. transylvanicum*. It is nonetheless possible that they represent more material of the same species. However, the upper premolars of these specimens are most consistent with *Sivatitanops birmanicum*, a species otherwise known only from Pondaung sandstones of Myanmar, southeast Asia. A partial skull from Pondaung deposits that is possibly *Sivatitanops birmanicum* is also similar to the jaw holotype of *B. transylvanicum* in lacking a postcanine diastema, but having incisors that are somewhat larger and less globular than other brontotheres (e.g., *Metatitan*) that lack postcanine diastemata. It is therefore possible that *S. birmanicum* is a junior synonym of *B. transylvanicum* or that these species are closely allied (along with *Metatitan*?). (For more discussion of the

possible synonymy of these taxa see remarks under *S. birmanicum*.)

Metatitan primus Granger and Gregory, 1943

HOLOTYPE: AMNH 26101, a partial skull with intact left side, left C–M3, partial mandible with complete incisor row, canines, and left p2–m3.

TYPE LOCALITY: ?Ulan Gochu Formation, Chimney Butte, North Mesa, Shara Murun Region, Inner Mongolia, China.

AGE: ?Late Eocene (?Ulangochuian land mammal "age").

REFERRED SPECIMEN: **(From the same locality as the holotype)** AMNH 26102, a partial mandible with left c and m1–m3.

DIAGNOSIS: *Metatitan primus* is a large brontothere with small closely spaced frontonasal horns that are positioned high above the orbits. The nasal process and horns are elevated to the peak of a tall frontonasal process that rises anterodorsally from above the orbits at an angle greater than 45°. The nasal incision is deep and extends to the anterior margin of the M1. The orbit is positioned over the posterior portion of M2 and the anterior portion of M3. The elevated nasal process is horizontal, relatively broad, not strongly rounded anteriorly, and with lateral walls that are deep proximally and shallow distally. The premaxillomaxillary rostrum deepens posteriorly and it is not enclosed by bone dorsally. Other cranial characteristics include a bulbous and incompletely saddle-shaped cranium. The posterior end of the cranium is extremely widened. The parasagittal ridges are not prominent and they do not constrict the dorsal surface posteriorly. There is a small dome on the dorsal surface of the skull. The zygomatic blades are nearly straight and they extend nearly to the posteriormost end of the skull where they form a 90° angle with the lateral zygomatic wing of the squamosal. The external auditory pseudomeatus enters the skull in a mediolateral direction and is ventrally constricted. Finally, a broad postzygomatic process is present.

Dentally, *Metatitan primus* is characterized by a complex P1, a distinct P2 metacone, and hypocones on P2–P4 that are positioned close to the protocones and not well separated from them. Upper and lower postcanine diastemata are absent. The molars of *M. primus* have tall lingually angled ectolophs with weak labial ribs, and thinned lingual ectoloph enamel with wedge-shaped paracones and metacones. A cingular parastyle shelf is absent. Distinct central molar fossae and small anterolingual cingular cusps are present. Paraconules and metalophs are absent. The lower dentition of *Metatitan* includes three very small incisors that form a nearly straight row. The i1 and i2 are short and wedge-shaped, while the i3 is somewhat more conical. A metaconid is present on the p3 and p4. The p2 trigonid is not much longer than the talonid. The lower molars have shallow basins and the m3 is elongate.

Metatitan relictus shares with *M. primus* and *M. khaitshinus* the unique combination of the following traits: horns and a nasal process elevated to the peak of a superorbital frontonasal process, posteriorly positioned orbits, an extremely widened skull, anteroposteriorly shortened basicranium, and lack of postcanine diastemata. *M. primus* differs from these species most obviously by its remarkably bulbous cranium.

DESCRIPTION

SKULL: The holotype of *Metatitan primus* (AMNH 26101) is complete on its left side and does not appear to be significantly distorted. The right side of the skull is severely weathered and essentially featureless (fig. 99). The facial area of *M. primus* is similar to that of *Aktautitan hippopotamopus* Mihlbachler et al. (2004a) and other species of *Metatitan*. The small horns are positioned closely together and are highly elevated above the orbits. The protuberances rest on a tall superorbital pillar that rises from above the orbits at an angle steeper than 45°. The nasal process is elevated to the peak of this structure. Consequently, the nasal cavity is dorsoventrally deep, and the posterior margin of the nasal incision rises much higher than the orbits. The nasal and frontal bones are completely co-ossified, so it is not possible to determine the exact position of the frontonasal suture. However, the morphology of the face of *M. primus* is so similar

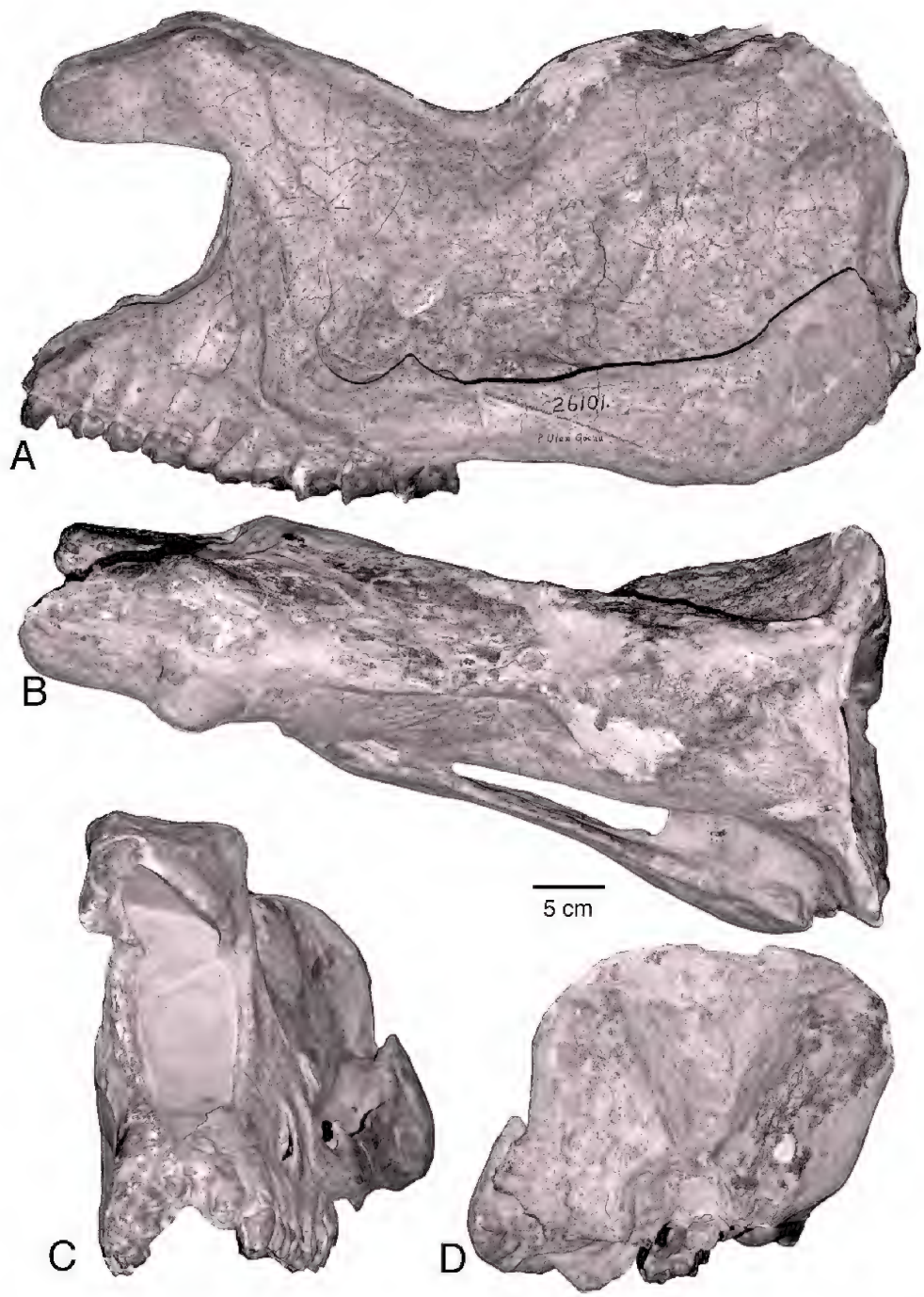

Fig. 99. The holotype skull of *Metatitan primus* (AMNH 26101). **(A)** Left view, **(B)** dorsal view, **(C)** anterior view, **(D)** posterior view.

to *A. hippopotamopus*, *M. relictus*, and *M. khaitshinus* (where the frontonasal contact is visible) there is little doubt that this large process is composed of the nasal bone anteroventrally and the frontal bone posterodorsally. The frontonasal protuberances are small, rounded, and slightly rugose at the surface and are perched at the lateral edges

of the peak of the singular frontonasal process.

The nasal incision extends posteriorly to the anterior margin of the M1. The orbit is positioned over the posterior portion of M2 and the anterior portion of M3. The anterolateral root of M2 and the posterolateral root of M1 are positioned below the anterior rim of the orbit. The nasal process of AMNH 26101 extends nearly horizontally from the peak of the frontonasal process, although the flat dorsal surface is angled slightly downward. The nasal process is broad and slightly shorter than the premaxillomaxillary rostrum. The lateral walls of the nasal process are dorsoventrally deep and thin. The lateral walls are deepest proximally. The lateral walls extend to the end of the nasal process, but they shallow distally. The anterior edge of the nasal process is slightly turned downward. From the dorsal view the anterior edge of the nasal looks rounded and the nasal process appears to taper distally, but these are artifacts of how the specimen has been distorted. Direct inspection of the specimen reveals that the nasal process was not tapered distally, and the anterior margin was nearly flat with a distinct median notch.

From a lateral view it can be seen that the premaxillomaxillary rostrum is mildly curved upward. The rostrum deepens proximally. From an anterior view, the rostrum is broad, although the right side has been smashed inward. The dorsolateral margin of the rostrum (intact on the left side) angles posterolaterally and the rostral cavity is not sealed over dorsally. The maxilla and premaxilla appear to be completely fused; thus, a premaxillomaxillary suture is not discernable in this specimen. The opening of the nasal cavity is large and taller than it is broad.

The overall shape of the cranium of *Metatitan primus* is distinctive and somewhat bizarre. In addition to the elevated horns and nasals, the postorbital cranium is remarkably bulbous. Nonetheless, the general proportions of the facial and cranial regions are similar to those of other brontotheres, with a short face and an elongate cranium. The dorsal surface in the midsection of the skull is strongly concave and forms a deep transverse channellike depression. The dorsal surface of the posterior half of the skull is convex, thus resulting in an incompletely saddle-shaped skull. Directly behind the midcranial concavity is a centrally positioned convex dome. Curiously, this dome is similar in size and position to the dorsal dome seen in *Duchesneodus uintensis*. Between the dome and the occiput is a distinct pit. The dorsal surface of the skull continues to broaden posteriorly and the parasagittal ridges do not constrict the skull posteriorly. The parasagittal ridges are essentially absorbed into the swollen cranium and exist only as faint ridges running from the postorbital processes of the frontal to the occiput.

Overall, the zygomatic arch is relatively deep and thin. From a lateral view the zygomatic arch is peculiar in that it extends almost to the very end of the skull. The entire zygomatic arch is straight except for the posterior end where is it deflected upward. From the dorsal view the zygomatic arch is thin and very straight and angled posterolaterally. If the right side of the skull were intact, the zygomatic arches would have given the skull a wedge-shaped appearance. A peculiar feature of the zygomatics of *Metatitan primus*, shared with *M. relictus*, is the fact that the winged-shaped extension of the squamosal that connects the cranium to the zygomatic arch is very short and extends almost straight laterally from the side of the skull and forms an abrupt 90° angle with the actual zygomatic blade. *M. primus* also has a posterior zygomatic process similar to that of *Protitan grangeri*, although from a lateral view, the posterior zygomatic process is much broader than that of *P. grangeri*.

From a dorsal view the nuchal crest is slightly concave. From a posterior view, the dorsal margin of the occiput is slightly arched dorsally. The occiput itself is vertical and extremely broad. The dorsal half is similar in width to the ventral half and the occiput is not constricted in the middle. The surface of the occiput has distinct occipital pillars with a shallow triangular depression between them.

The ventral surface of the skull of *Metatitan primus* is incomplete (fig. 100a), although the following details can be discerned. The posterior nares are not preserved, however a remnant of a wide lateral emargination of the posterior nares can be seen posteromedial to the left M3. This wide

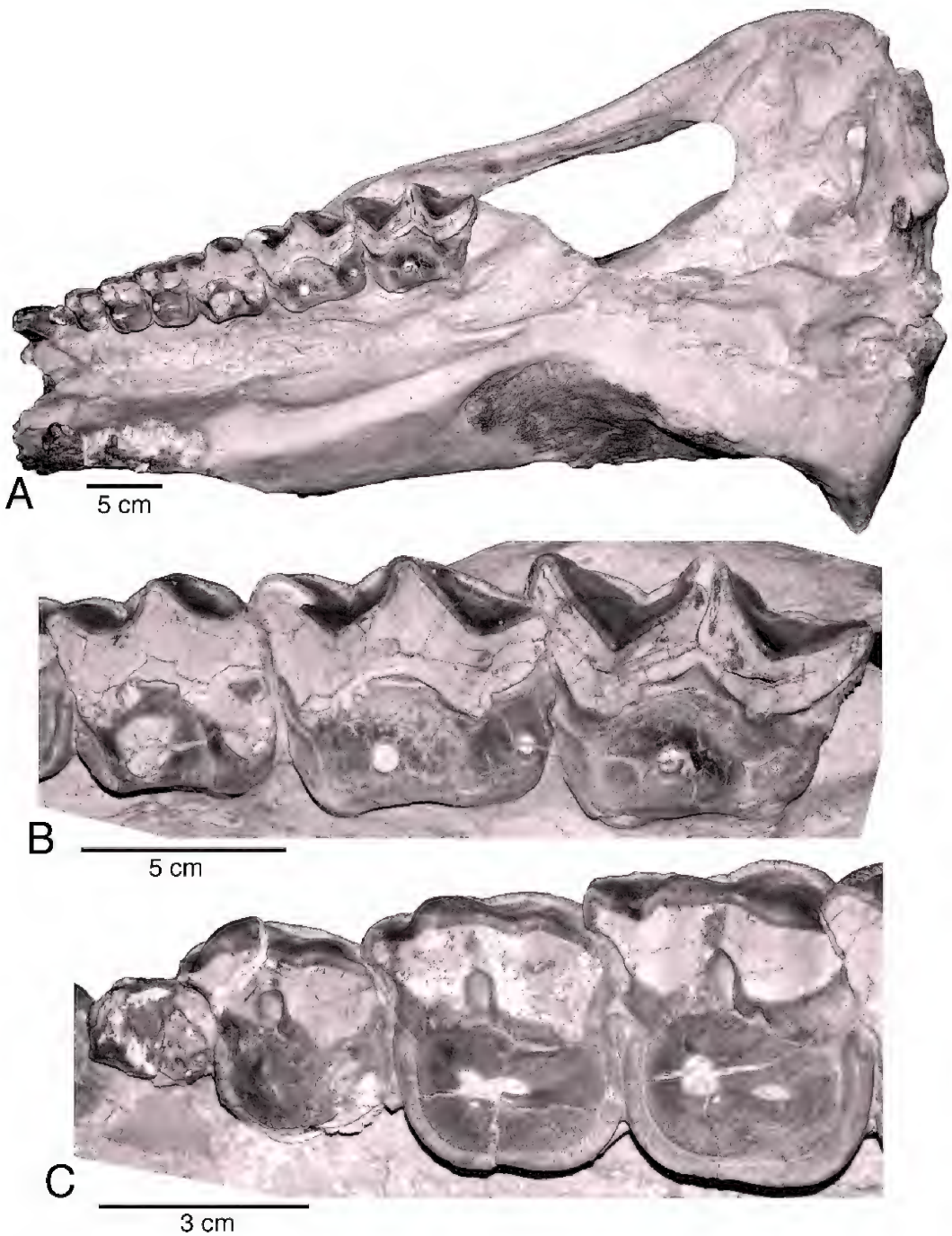

Fig. 100. The holotype skull of *Metatitan primus* (AMNH 26101). **(A)** Ventral view, **(B)** left molars, **(C)** left premolars.

emargination resembles those seen in more complete specimens of *M. relictus* and *M. khaitshinus*. The basicranium of *Metatitan primus* is very short. The external auditory pseudomeatus is positioned at the very end of the skull and can be seen just behind the zygomatic arch from the lateral view, forming a tube-shaped opening. Although it is not

possible to measure the width of the basicranium due to the damaged right side, the posterior end of the skull of *Metatitan primus* is very broad and the basicranium would have been much wider the outside distance across the M3s.

Upper Dentition: The upper incisors of *Metatitan primus* are unknown, but the left canine and cheek teeth are well preserved in the holotype specimen (fig. 100). The canine is of moderate size. The P1 crown is rounded in outline, but its exact morphology is obscured by damage and wear. However, its overall shape suggests a relatively advanced P1 with a distinct paracone, metacone, and well-developed lingual heel.

The crowns of P2–P4 are nearly rectangular in outline due to the nearly parallel anterior and posterior margins and the nearly flat lingual margins. The parastyle and metastyle of P2 are nearly straight. The parastyle of P3 is barely directed labially, while the P4 parastyle is more strongly angled labially. The metastyle of P3 is straight. The P4 metastyle could have been straight or slightly labially directed, but it has been worn away by the adjacent M1. There are distinct labial ribs on the paracones of P2–P4; it is broadest on P2 and is progressively narrower on more posterior premolars. There are no mesostyles on any of the premolars.

Small preprotocristae are seen on P2 and P3 but not on P4. The lingual sides of P2–P4 have distinct protocones and hypocones that are separated to varying degrees. On P2 the hypocone is smaller than the protocone, although the enamel of the hypocone is worn or broken off, thus giving it a slightly smaller apparent size. On P3 the hypocone is smaller and lower than the protocone and these cusps are positioned very closely together and are almost completely conjoined into a single ovoid cusp. Finally, the P4 hypocone is smaller and shorter than that of the protocone and sits on the shallow posterior slope of the protocone. Labial premolar cingula are distinct but thin. The lingual cingulum of P2 is broken off, but the lingual cingula of P3 and P4 are thick and continuous.

The upper molars of *Metatitan primus* are elongate, although the M1 has been significantly shortened by interstitial wear. The upper molars show typical brontotheriine traits, including tall, lingually angled ectolophs, very weak labial ribs, thin lingual ectoloph enamel, and wedge-shaped lingual sides of the paracone and metacone in molars that are not heavily worn (e.g., M3). The anterior cingulum is thin and passes proximally to the distal peak of the parastyle. Distinct shallow central molar fossae and small anterolingual cingular cusps are present. All evidence of paraconules and metalophs is lost. There is no hypocone on M3, although there is a distinct peak of enamel on the cingulum of the distolingual corner of M3. Labial molar cingula are thin but distinct, while lingual molar cingula are absent.

Mandible and Lower Dentition: The holotype mandible consists of a symphysis and a left ramus that is missing the coronoid process and mandibular condyle (fig. 101). The inferior margin of the symphysis is angled about 45°. From a dorsal view the symphysis is broad and extends to the anterior margin of the p4. The three incisors are very small and form a nearly straight row that is positioned only slightly anterior to the canines. The crown of i2 (most complete on the right side) is the largest incisor especially in crown height and labiolingual width. The apices of the i1 and i2 are worn off, but these incisors appear to have had very short, wedge-shaped crowns. The i3 is more rounded in outline, with a short conular crown. The i1 and i2 have a distinct but thin lingual cingulid. The lingual cingulid is faint on i3. There are no diastemata between the incisors or canines. The p1 is missing, but the p1 alveolus fills the gap between the canine and p2, indicating the absence of a postcanine diastema.

Overall, the p2–p4 are rather broad. The p2 trigonid is only marginally longer and is distinctly narrower than the talonid. The trigonids of p3 and p4 are both shorter and narrower that the talonids. The very anterior end of the of p2 is not preserved and the morphology of this area is obscure, but it seems that the paralophid is strongly curved lingually, thus creating a relatively broad lingual-trigonid notch. The p2 protolophid arches lingually nearly 90°. The p2 protoconid is positioned labially, and the protolophid and cristid obliqua intersect at a point

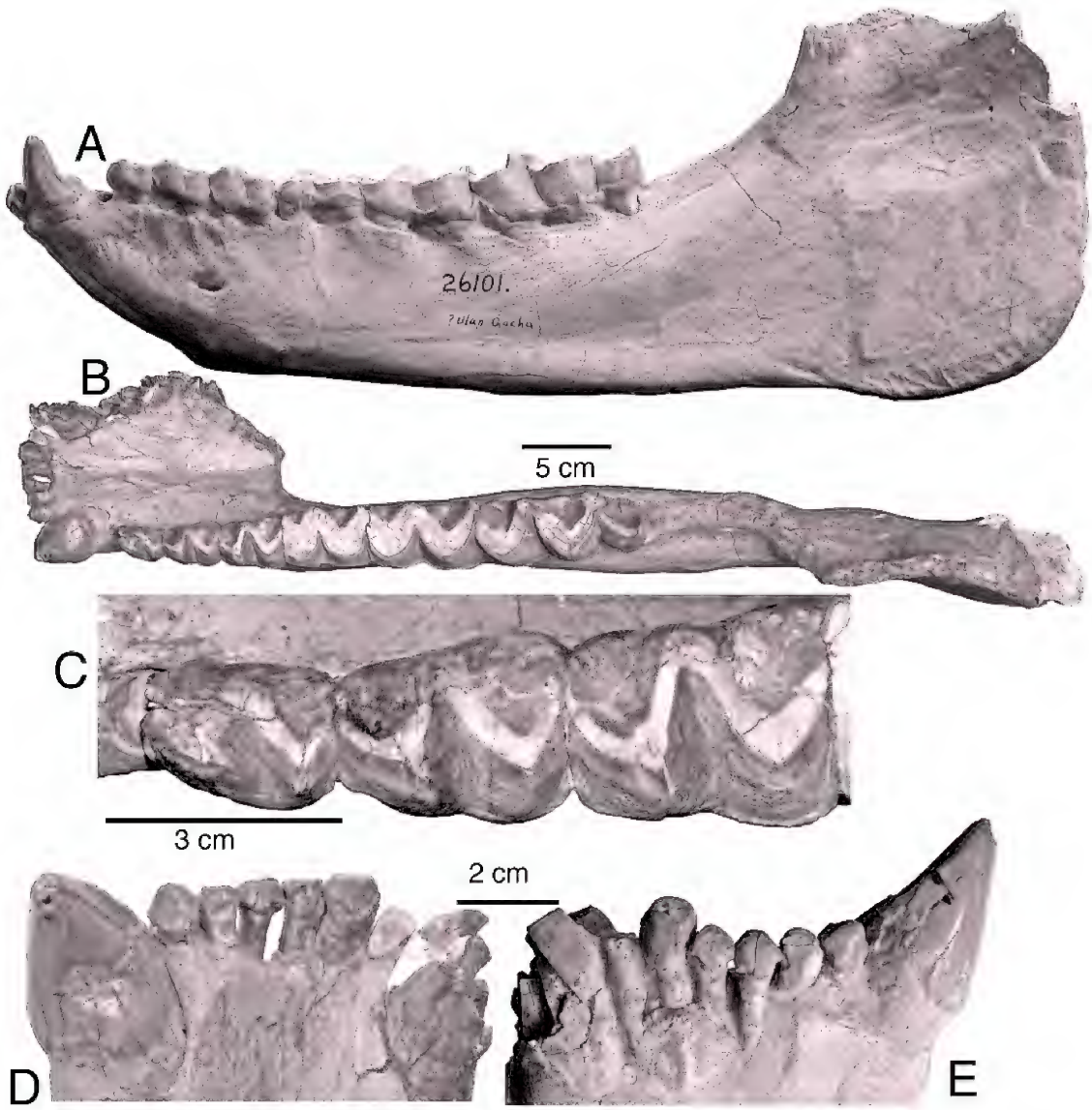

Fig. 101. The holotype mandible of *Metatitan primus* (AMNH 26101). **(A)** Left view, **(B)** dorsal view, **(C)** left p2–p4, **(D)** lingual view of incisors and canines, **(E)** labial view of incisors and canines.

lingual from the protoconid. This configuration is essentially molariform. Finally, there is a deep labial notch on the p2 between the trigonid and talonid that is directed anterolingually. In more posterior cheek teeth this labial notch is directed more lingually.

The paralophids and metalophids of p3 and p4 arch fully lingually, thus creating nearly molariform trigonid basins. Both of these premolars have a large lingually positioned metaconid. The morphology of the p2 is also consistent with a metaconid, although the crown is too damaged to determine if a metaconid was present on that tooth. The talonids of p2–p4 have well-developed cristids obliqua and hypolophids with molariform talonid basins. These structures are significantly broader in p3 and p4. Labial premolar cingulids are weak and lingual premolar cingulids are absent.

The lower molars of *Metatitan primus* have relatively thin lingual enamel and shallow trig-

onid and talonid basins. The m3 is elongate. There are no lingual cingulids. Labial molar cingulids are thin, but they are distinct and continuous around the paraconids and metaconids. A thin beaded cingulid can be seen tracing around the hypoconulid of the m3.

Metatitan relictus Granger and Gregory, 1943

HOLOTYPE: AMNH 26391, a skull heavily reconstructed with plaster, with right I2–M3, left I2–C, P2–M3, and a mandible with right i2–c, p3–m3, left i1–i3, and p4–m3.

TYPE LOCALITY: "Houldjin" beds, one mile west of Camp Margetts, Inner Mongolia, China.

AGE: Middle Eocene (Irdinmanhan land mammal "age").

REFERRED SPECIMENS: **(From the "Houldjin" beds near Camp Margetts, Inner Mongolia)** AMNH 26395, a skull missing the right horn, nasal, and occiput, with right I1, I3, C, M1–M3, left I1–I3, and canine (fragmentary); AMNH 26396, fragments of a facial portion of a cranium, palate, and basicranium with right P2–M (damaged); AMNH 26397, a partial skull with right I1–C, P4–M3, left I3, P4 (fragmentary), and M2–M3; AMNH 26398, a complete ventral surface of a skull with nasal, horn fragment, parietal fragment, right I1–M3, left I2–M1 (partial), and M2–M3; AMNH 26399, a complete left side of a skull with right C, P1–P4, left C (partial), and P4–M3; AMNH 26406, a left premaxilla and maxilla fragment with I3–M2; AMNH 26402, a mandibular symphysis and right ramus with right i1–m3 and left i2–c; AMNH 26404, a mandibular symphysis with complete incisor row, canines, right p2, and left p2–p3; AMNH 26405, a fragmentary mandibular symphysis and left partial ramus with right left canine, and a right partial ramus with p4–m1, and m2 (partial); AMNH 26407, a right mandibular ramus with c, and p2–m3; AMNH 26420, a left partial ramus with p3–m2, and m3 (partial); AMNH 26427, a partial mandible with right i3–c, p4–m3, and left c–p4; AMNH 26429, a right partial ramus with p4 (partial) and m1–m3.

DIAGNOSIS: *Metatitan relictus* is a large brontothere with small frontonasal horns that are positioned high above the orbits. The nasal process and horns are elevated to the peak of a tall frontonasal process that rises from the orbits at about 45°. The nasal incision is dorsoventrally deep and extends to the anterior margin of the M2. The orbit is positioned over the posterior portion of M2 and the anterior portion of M3. The elevated nasal process is horizontal, relatively broad, not strongly rounded distally, and with lateral walls that are deep proximally and shallow distally. The premaxillomaxillary rostrum deepens posteriorly and it is not enclosed by bone dorsally. Other cranial characteristics include an incompletely saddle-shaped cranium. The posterior end of the cranium is extremely widened. The parasagittal ridges are prominent, but they do not constrict the dorsal surface posteriorly. The zygomatic blades are nearly straight and they extend nearly to the posteriormost end of the skull where they form a 90° angle with the lateral zygomatic wing of the squamosal. The external auditory pseudomeatus enters the skull in a mediolateral direction and it is ventrally constricted. A broad postzygomatic process is present. The emargination of the posterior nares is wide, and the posterior nares are completely behind the M3. Large ventral sphenoidal fossae are present.

Dentally, *Metatitan relictus* is characterized by three small incisors that form a nearly straight row, a globular I1 and I2, and a subcaniniform I3. The P1 is complex and the P2 has a distinct metacone. Premolar hypocones are uncommon, but there is usually a lingual crest extending posteriorly from the premolar protocones. Upper and lower postcanine diastemata are absent. The molars of *M. relictus* have tall, lingually angled ectolophs with weak labial ribs, and thinned lingual ectoloph enamel with wedge-shaped paracones and metacones. A cingular parastyle shelf is absent. Distinct central molar fossae and small anterolingual cingular cusps are present. Paraconules and metalophs are absent. The lower dentition of *Metatitan relictus* includes three very small incisors that form nearly a straight row. The i1 and i2 are short and wedge-shaped, while the i3 is somewhat more conical. Metaconids are present on p3, p4, and occasionally on p2. The p2 trigonid is not much longer than the

talonid. The lower molars have shallow basins and the m3 is elongate.

Metatitan relictus shares with *M. primus* and *M. khaitshinus* the unique combination of the following traits: horns and a nasal process elevated to the peak of a superorbital frontonasal process, posteriorly positioned orbits, an extremely widened skull, anteroposteriorly shortened basicranium, and lack of postcanine diastemata. *M. relictus* differs from *M. khaitshinus* in having more posteriorly positioned posterior nares, small lower incisors forming a straight row, and a narrow labial notch on p2. *M. relictus* is most easily differentiated from *M. primus* by the extremely swollen appearance of the cranium of the latter.

Description

Skull: The badly damaged but nearly complete holotype skull of *Metatitan relictus* (AMNH 26391) is missing large portions, although the ventral half is essentially complete and undistorted (fig. 102). None of the numerous additional skulls of *M. relictus* is complete (fig. 103). Those figured are AMNH 26399 (fig. 103a), AMNH 26395 (fig. 103b, c), AMNH 26397 (fig. 103d) and a part of AMNH 26398 (fig. 103e).

The horns and nasal process of the holotype are not preserved, but this area can be described from other specimens. The facial area of *Metatitan relictus* is similar to that of *M. primus* and *M. khaitshinus*. The small horns are highly elevated above the orbits and rest on a tall frontonasal process that rises from above the orbits at approximately an angle of 45°. The horizontal nasal process is elevated to the peak of this tall process. A distinct line representing the frontonasal contact can be seen from the lateral views of AMNH 26399 and AMNH 26395. The frontonasal process is composed of the nasal bone anteroventrally and the frontal bone posterodorsally; the peak of the horn is formed by the frontal bone. The frontonasal process of *M. relictus* is somewhat shorter and less steeply angled than those of *M. primus and M. khaitshinus*; consequently, the nasal chamber is not as deep. Nonetheless, the posterior margin of the nasal incision is dorsoventrally relatively deep in comparison to brontotheres whose nasal processes are not elevated (e.g., *Protitan*). In specimens where the face is complete (AMNH 26399), the posterior margin of the nasal incision rises higher than the orbits.

The horns are variable in size, although they are always small. For instance, in AMNH 26399 they do not rise higher than the dorsal surface of the nasal process. In AMNH 26395 the horns are larger with more significant relief. Those with relief form small, rounded knobs that typically have rugose surfaces. The horns vary in their orientation; the majority of specimens have horns that do not project laterally, however, one specimen, AMNH 26396, has horns that project almost completely laterally.

The nasal incision of the holotype (AMNH 26391) extended at least to P4, but the nasal incision is incomplete. Other specimens with complete faces indicate that the nasal incision extended behind P4. In AMNH 26399 the nasal incision extends to the anterior margin of M2. The position of the orbit is the same as that of *Metatitan primus* where the posterior part of M2 and the anterior part of M3 are directly beneath the orbit with the anterior lateral root of M2 positioned below the anterior rim of the orbit.

The nasal process, most complete in AMNH 26395 and AMNH 26399, does not differ substantially from that of *Metatitan primus*. The nasal process tends to be shorter than the premaxillomaxillary rostrum. It projects horizontally from the skull from its elevated position, although the flat dorsal surface tends to be angled downward. The lateral margins of the nasal process are unthickened and they are deep proximally and shallow anteriorly. From the dorsal views the nasal processes of these specimens are not tapered or flared distally. The anterior edge of the nasal process is turned downward slightly and from the dorsal view it is nearly flat, although some, such as AMNH 26395, show a deep medial notch at the distal end.

The premaxillomaxillary rostrum deepens posteriorly and its dorsal margin is steeply sloped posterodorsally. A premaxillomaxillary suture is not visible in any specimen of *Metatitan relictus*. The rostrum is relatively

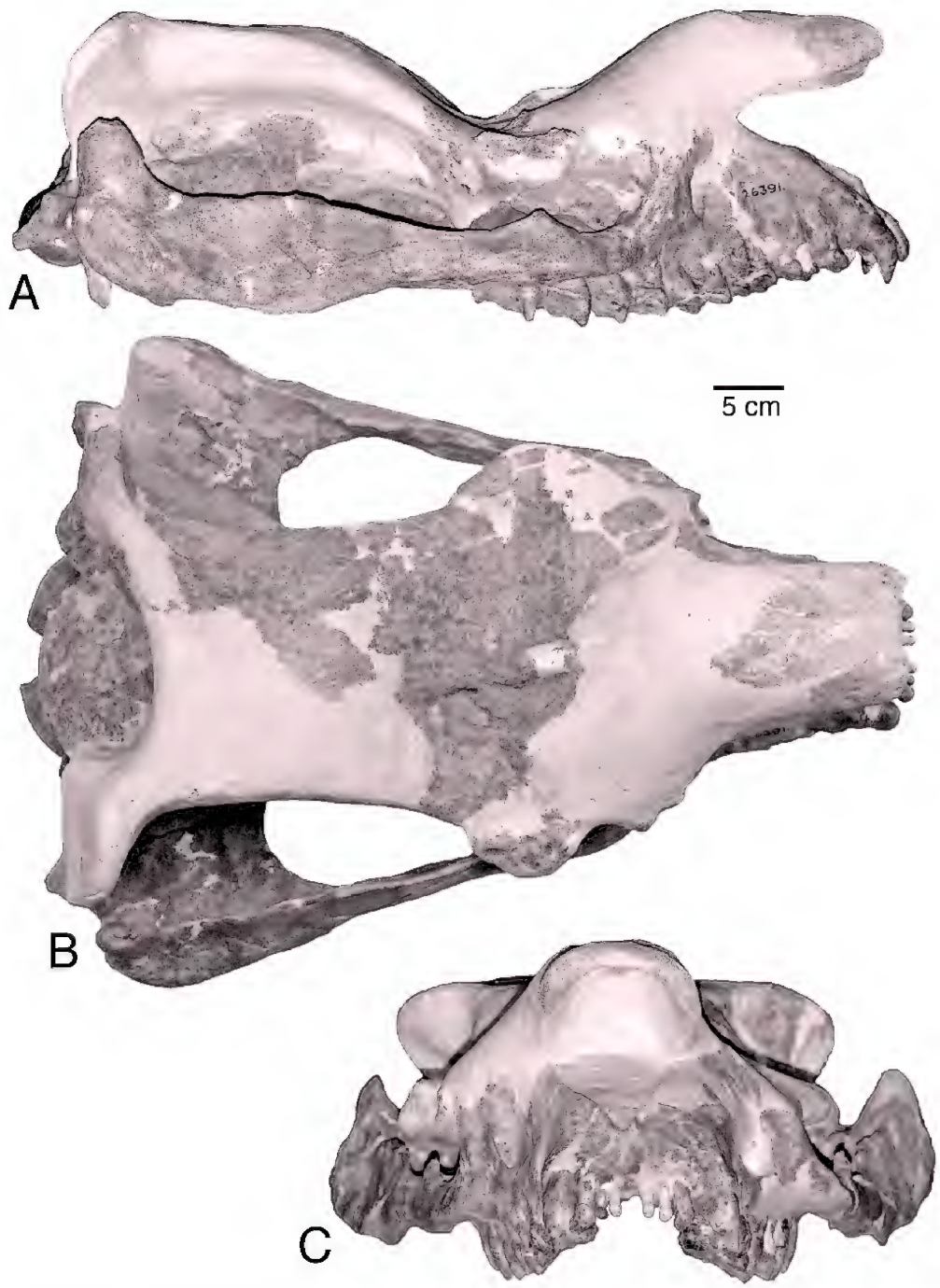

Fig. 102. The holotype skull of *Metatitan relictus* (AMNH 26391). **(A)** Right view, **(B)** dorsal view, **(C)** anterior view.

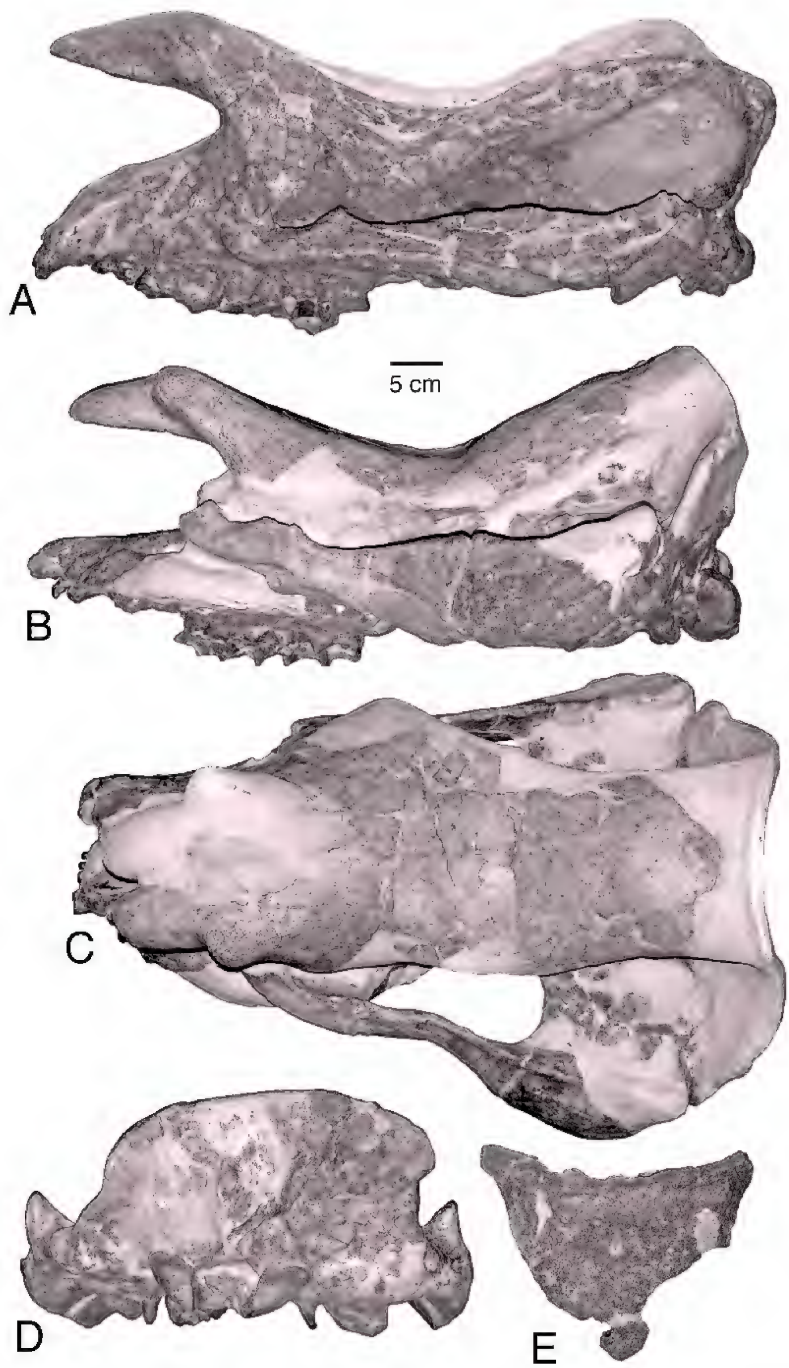

Fig. 103. Specimens referred to *Metatitan relictus*. **(A)** Left view of AMNH 26399, **(B)** left view of AMNH 26395, **(C)** dorsal view of AMNH 26395, **(D)** posterior view of AMNH 26397, **(E)** dorsal view of occipital-parietal fragment of AMNH 26398.

wide. The dorsolateral margins of the rostrum are laterally divergent behind the premaxillary symphysis and the rostral cavity is not enclosed by bone dorsally.

The cranium of *Metatitan relictus* is not extremely swollen like that of *M. primus*. The dorsal surface of the holotype (AMNH 26391) is incomplete, but a deep concavity runs transversely just behind the orbits. Other skulls of *M. relictus* are also deeply concave midcranially just behind the orbits. The dorsal surface of the posterior part of the cranium is slightly convex, thus the skull of *M. relictus* is incompletely saddle-shaped. *M. relictus* lacks the central parietal dome seen in *M. primus*. The parasagittal ridges of *M. relictus* are prominent in contrast to *M. primus* and overhang the sides of the cranium somewhat. The dorsal view of AMNH 26395 best illustrates the very broad dorsal surface of the cranium.

The jugal portion of the zygomatic arch is shallow in comparison to the much deeper squamosal portion. From a lateral view the zygomatic blade is straight, although it is deflected upward at the posteriormost end, where there is a tall posterior zygomatic process. From the dorsal view of AMNH 26391 the zygomatic blades are thin and straight, and they diverge posterolaterally, creating a wedge-shaped skull. The zygomatic blade of AMNH 26395 is strongly bowed inward, but this seems to be an artifact of distortion. The wedge-shape of the zygomatic arch resembles *Metatitan primus* and *M. khaitshinus* where the lateral wings of the squamosals are positioned at the posteriormost end of the skull and they project laterally to form an abrupt 90° angle with the zygomatic blades.

The occiputs of most skulls of *Metatitan relictus* are poorly preserved, but all suggest a very broad occiput that is mildly tilted backward, unlike the more vertical occiputs of *M. primus* and *M. khaitshinus*. The skull of AMNH 26398 includes an unbroken fragment with the greater part of an intact nuchal crest (fig. 103e). This piece is consistent with a very wide occiput with a nuchal crest that is slightly concave from the dorsal view and dorsally arched from the posterior view. The occiput of AMNH 26397 is reasonably complete on the right side. That specimen suggests that the dorsal and ventral halves of the occiput are of a similar width and that it was not constricted in the middle. The surface does not suggest distinct occipital pillars, but this could relate to the poor condition of the surface of the occiput.

It can be seen from the ventral view of AMNH 26391 that the posterior nares are constricted by a wide horseshoe-shaped emargination (fig. 104a). The anterior rim of the posterior nares is shifted behind the M3s, so that the posterior nares are more posteriorly positioned than those of *M. khaitshinus*. The posterior narial canal appears to extend well into the sphenoid bone, although other aspects of the posterior narial canal are difficult to discern due to poor preservation and plaster. The basicranium is very wide and anteroposteriorly compressed. The width of the skull across the mastoid processes is much greater than the width across the M3s. A ratio calculated from the width of the basicranium of AMNH 26391 divided by the width across the M3s (ratio = 1.63) is greater than that of any other brontothere for which this ratio can be calculated except for *M. khaitshinus*. The external auditory pseudomeatus, which is positioned at the posteriormost end of the cranium, is tube-shaped and it enters the skull in a mediolateral direction.

Upper Dentition: In the holotype (AMNH 26391) half of the incisors (right I1, left I1, I2) are missing and have been sculpted with plaster (fig. 104a). However, the skull of AMNH 26398 includes a complete set of right upper incisors (fig. 104e, f). The incisors are positioned slightly anterior to the canines and form a nearly straight row. The number of incisors (three pairs) is unreduced, although they are very small and vestigial in appearance. The I1 and I2 have an amorphous globular appearance. The I3 is larger and has a taller, more conical crown. The apex is blunt, but this could relate to wear. There is a distinct lingual cingulum on the I3, but cingula are absent on I1 and I2. The canines of *Metatitan relictus* tend to be rather small. There seems to be a short precanine diastema in most specimens, but postcanine diastemata are absent. In AMNH 26406, a young individual, the erupting canine is crowded by I3 and P1 (fig. 104d).

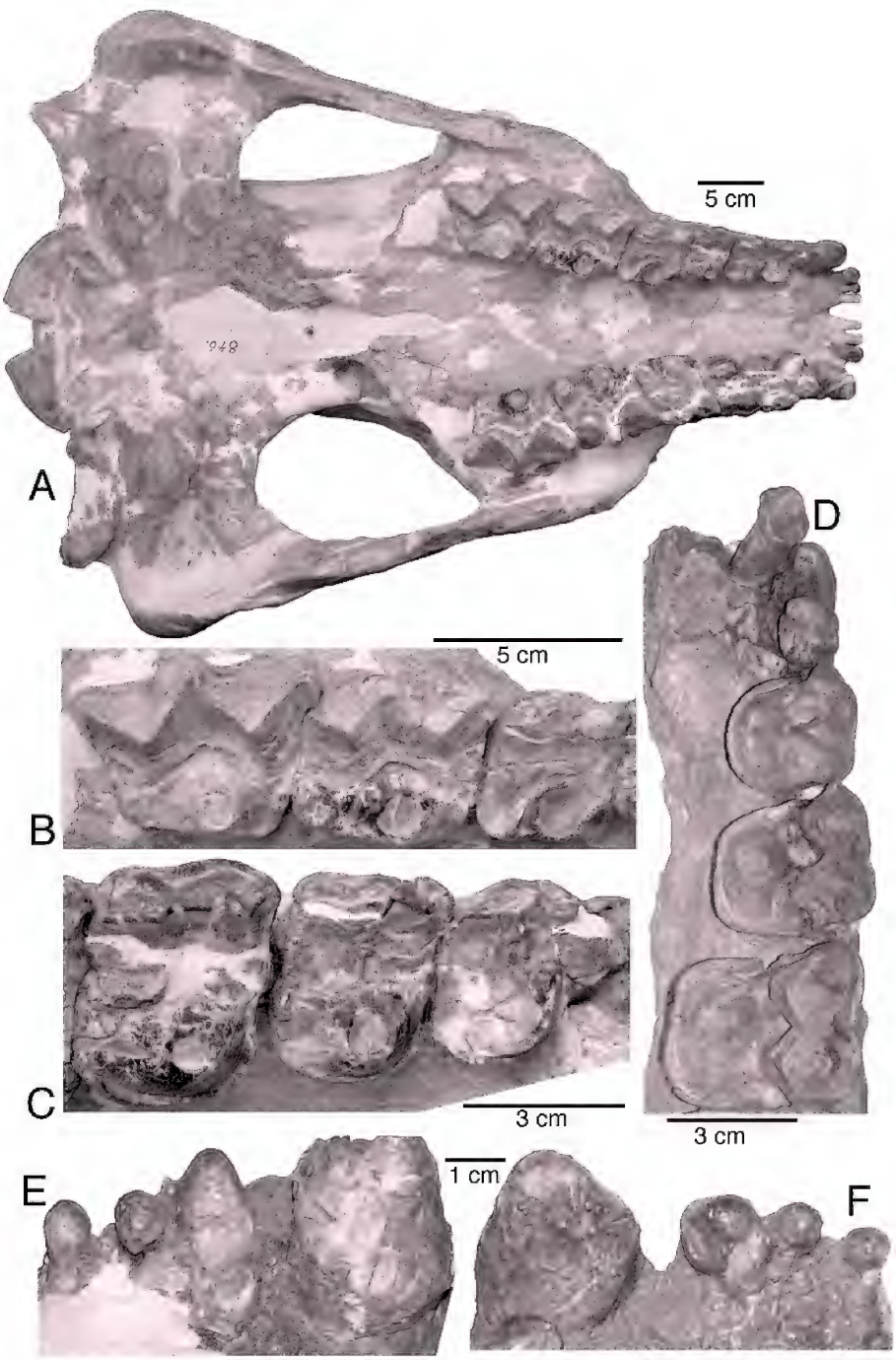

Fig. 104. Ventral view of the skull and upper dentitions of *Metatitan relictus*. **(A)** Ventral view of AMNH 26391, **(B)** right molars of AMNH 26391, **(C)** right premolars of AMNH 26391, **(D)** left I3–P4 of AMNH 26406, **(E)** labial view of right canine and incisors of AMNH 26398, **(F)** lingual view of right canine and incisors of AMNH 26398.

There is no postcanine diastema, not even when P1 and P2 are missing. For instance, on the left side of AMNH 26391, P1 and its alveolus are missing and P2 is closely pressed to the canine root, indicating that some remodeling of the left maxillary must have occurred in this individual subsequent to the loss of the left P1.

In addition to the relatively worn premolars of the holotype (AMNH 26391) (fig. 104c), the nearly unworn premolars of AMNH 26406 are shown in close-up (fig. 104d). The crown morphology of P1 is obliterated in AMNH 26391. In AMNH 26406 the P1 is nearly round in outline. It has a large paracone, a distinct but smaller metacone, and a small posteriorly shifted lingual heel. The P2 and P3 of *M. relictus* are slightly oblique due to a weakly distolingually angled anterior margin. P4, on the other hand, is more nearly rectangular, with parallel anterior and posterior margins. The parastyle of P2 is straight, but those of P3 and P4 are deflected anterolabially. The metastyle of P2 is straight, while those of P3 and P4 are slightly deflected posterolabially. The P2 ectoloph is essentially straight. Small labial paracone ribs can be seen on P2–P4; these become smaller in more posterior premolars. Mesostyles are absent on all premolars, although there is a distinct labial bulge at the base of the crown near the P4 metacone of AMNH 26391.

The lingual features of P2 are obliterated in AMNH 26391. Though heavily worn, the lingual features of P3 and P4 are still discernable. On both P3 and P4, there is an oval area of dentine exposed behind the protocone, suggesting that a small hypocone was present and well separated from the protocone. The lingual premolar morphologies of other specimens differ notably from that of AMNH 26391. In AMNH 26406 there is a large P2 protocone and a slightly smaller hypocone that is positioned closely to the protocone. The hypocone is connected to the protocone by a short lingual crest that is almost as tall as the cusp apices. On the P2 of AMNH 26399, a large ovoid cusp rests on the lingual side of the crown that could represent two conjoined cusps, but the hypocone is not distinct from the protocone. The P3 of AMNH 26406 has a large protocone and a distinct lingual crest, but there is no hypocone. The P4 of that specimen retains a single, large protocone with no crest or hypocone. The protocones of AMNH 26406 and AMNH 26391 are anteriorly positioned, but the protocones of P3 and P4 are sometimes more centrally positioned by comparison. Moreover, a lingual crest is variably present (e.g., AMNH 26397) and absent (e.g., AMNH 26396) on P3 and P4. Apparently, P3 and P4 hypocones were infrequently present; no other AMNH specimen of *Metatitan relictus* other than the holotype (AMNH 26391) has distinct P3–P4 hypocones. A small preprotocrista is usually visible on P2, but it is exceedingly faint on P3 and absent on P4. Labial premolar cingula are distinct but thin. The lingual premolar cingula are most often continuous around the lingual sides of the crowns.

The upper molars of *Metatitan relictus* are elongate, although the lengths of M1 and M2 on the holotype (AMNH 26391) have been significantly shorted by interstitial wear (fig. 104b). The molars of this specimen are well worn, but along with molars of other specimens, they indicate typical brontotherine apomorphies, including tall, lingually angled ectolophs, very weak labial ribs, thin lingual ectoloph enamel, and wedge-shaped lingual sides of the paracone and metacone in molars that are not heavily worn. The anterior cingulum is thin and passes proximally to the distal peak of the parastyle. Distinct shallow central molar fossae and small anterolingual cingular cusps are present. All evidence of paraconules and metalophs is lost. There is no trace of a hypocone on M3, although the distolingual cingulum of the M3 is thickened and raised. Labial molar cingula are weak and lingual molar cingula are absent.

Mandible and Lower Dentition: The holotype mandible (AMNH 26391) is complete except for the left condyle and a large portion of the symphysis, which has been reconstructed with plaster (fig. 105a, c) The right coronoid process is tall, narrow, and slightly curved. The ventral margin of the symphysis is slightly steeper than 45°. (Other specimens with less plaster in the symphysis confirm that the reconstruction of AMNH 26391 is accurate). The symphysis is broad and extends posterior to the m1 metaconid.

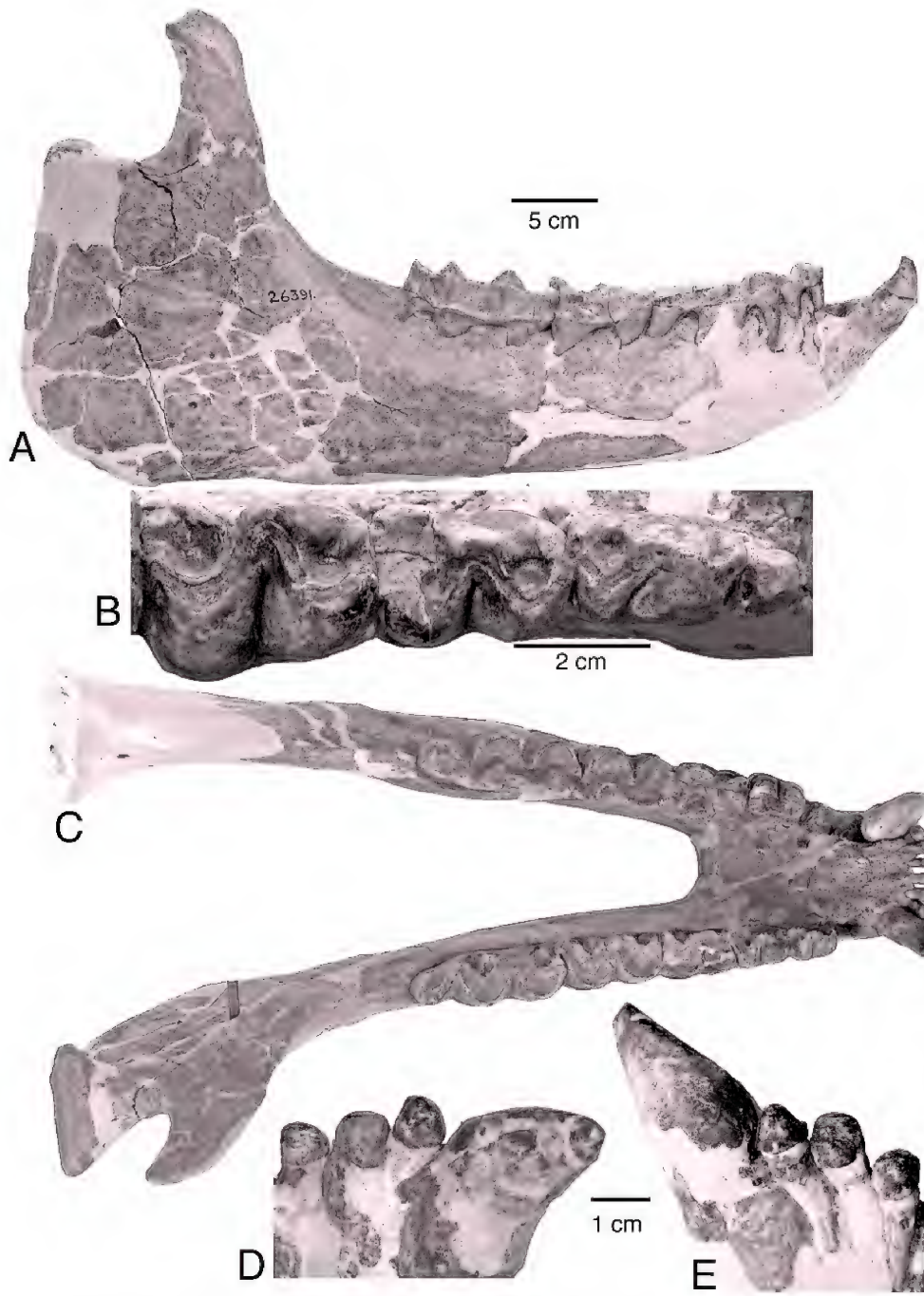

Fig. 105. Mandible and lower dentition of *Metatitan relictus*. **(A)** Right view of AMNH 26391, **(B)** right premolars of AMNH 26402, **(C)** dorsal view of AMNH 26391, **(D)** lingual and **(E)** labial views of the right incisors and canine of AMNH 26402.

The incisors are very small and form a nearly straight row between the canines. The i2 is somewhat larger than the other incisors. The incisor crowns of AMNH 26391 are heavily worn, but they are clearly short and have small lingual cingulids. The incisors of AMNH 26402 are less worn (fig. 105d, e). The crown of i1 is essentially featureless. The crown of i2 is somewhat larger and more wedge-shaped with a small lingual cingulid. The i3 is smaller than the i2, and it is more rounded in outline with a blunt apex. The lower canines of *Metatitan relictus* are variable in size, but they are generally small. There are no precanine or postcanine diastemata. In the holotype (AMNH 26391) p1 and p2 have fallen out. On the right side there is small space between the canine and the p2 alveolus, but on left side the p2 diastema is right next to alveolus of the canine. Other specimens with more complete sets of premolars lack postcanine diastema altogether, even when p1 is absent.

The more complete and less worn premolar row of AMNH 26402 is shown in close-up (fig. 105b). The p1 crown consists of a small cusp with a broad talonid heel. The trigonids of p2–p4 are similar in length to the talonids. The trigonid and talonid of p2 are of similar width, but on p3 and p4 the talonid is wider than the trigonid. The paralophid of p2 arches strongly lingually, although the lingual trigonid notch is small. The lingually positioned protolophid extends from the protoconid in a posterior direction. There is no p2 metaconid on AMNH 26402. Another specimen, AMNH 26427, exhibits a small p2 metaconid and a more lingually oriented protolophid. Like *Metatitan primus*, a deep and narrow labial groove extends between the p2 trigonid and talonid. This groove is directed anterolingually, while those of p3 and p4 are more lingually directed. In p3 and p4 of AMNH 26402 the paralophids and protolophids arch fully lingually, creating nearly molariform trigonid basins. The p3 and p4 also have large lingually positioned metaconids. The talonids are well developed in p2–p4 with long hypolophids, long cristids obliqua, and broad talonid basins. Labial premolar cingulids are weak and lingual premolar cingulids are absent.

The molars of *Metatitan relictus* are typical with shallow trigonid and talonid basins and thin lingual enamel. The m3 is very elongate. Labial molar cingulids are distinct, but they vary in thickness and are strongest on the talonid and usually discontinuous on the trigonid. Lingual molar cingulids are absent. The m3 cingulid of all specimens of *M. relictus* ends on the labial side and does not wrap around the hypoconulid as it does in *M. primus*.

Metatitan khaitshinus (Yanovskaya, 1954)

HOLOTYPE: PIN 3745-1, a skull with a large block of plaster obscuring its dorsal surface, with right and left P1–M3.

TYPE LOCALITY: Khaichin Formation, Khaichin-Ula V, Southwestern Mongolia.

AGE: Middle Eocene (Irdinmanhan land mammal "age").

SYNONYMS: *Metatitan reshetovi* (Yanovskaya, 1980).

REFERRED SPECIMENS: **(From the Khaichin Formation, Khaichin-Ula V, Southwestern Mongolia)** PIN 3745-2, a mandible with right i2 (?), c–m3 and left i2–m3; PIN 3745-3, a skull with right P2–M3 and left C–M3; PIN 3754-4, a skull with right P1–P3, P4 (partial), M2–M3 (partial) and left P1–M2; PIN 3745-8, a partial edentulous skull; PIN 3745-9, a partial edentulous skull; PIN 3745-11 (holotype of *Metatitan reshetovi*), a skull missing the nasal process with right C, P2–M3 and left C, P2–M3; PIN 3745-12, the ventral surface of a skull with right and left P2–M3; PIN 3745-28, a mandible with right i2–m3, left i3–c, and p2–m3; PIN 3745-31, a mandible with right p2–m3, left c, and p2–m3.

The specimens listed above are those that I was able to relocate in the PIN collection. Other specimens including two more partial skulls (PIN 3745-5, 6), and many mandibles (PIN 3745 14–17, 19, 22, 23, 26, 27, 30) were referred to *M. khaitshinus* by Yanovskaya (1980) but could not be located in the PIN collection.

DIAGNOSIS: *Metatitan khaitshinus* is a large brontothere with small frontonasal horns that are elevated high above the orbits. The nasal process and horns are elevated to the peak of a tall frontonasal process that

rises anterodorsally from above the orbit at an angle greater than 45°. The nasal incision is dorsoventrally deep and its posterior margin extends posteriorly to the anterior margin of M2. The orbit is positioned over the posterior portion of M2 and the anterior portion of M3. The elevated nasal process is horizontal, relatively broad, not strongly rounded distally, and with lateral walls that are deeper proximally and shallower distally. The premaxillomaxillary rostrum deepens posteriorly and it is not enclosed by bone dorsally. The cranium is incompletely saddle-shaped. The posterior end of the cranium is extremely widened. The parasagittal ridges are prominent, but they do not constrict the dorsal surface posteriorly. The zygomatic blades are nearly straight and they extend nearly to the posteriormost end of the skull where they form a 90° angle with the lateral zygomatic wing of the squamosal. The external auditory pseudomeatus enters the skull in a mediolateral direction and it is ventrally constricted. A broad postzygomatic process is present. The emargination of the posterior nares is wide and the anterior margin of the posterior nares is positioned between the M3s. Large ventral sphenoidal fossae are present.

Metatitan khaitshinus has a complex P1 and a distinct P2 metacone. Premolar hypocones range from poorly developed to well developed and completely separated from the protocone. Upper and lower postcanine diastemata are absent. The molars have tall, lingually angled ectolophs with weak labial ribs, and thinned lingual ectoloph enamel with wedge-shaped paracones and metacones. A cingular parastyle shelf is absent. Distinct central molar fossae and small anterolingual cingular cusps are present. Paraconules and metalophs are absent. The mandible has a robust symphysis that extends to p4. The lower dentition of *M. khaitshinus* includes three moderately sized incisors that form a slightly arched incisor row. The i1 and i2 are semispatulate, while the i3 is somewhat more conical. Metaconids are present on p3 and p4, but not on p2. The p2 trigonid is not much longer than the talonid. The lower molars have shallow basins and m3 is elongate.

Metatitan khaitshinus shares with *M. relictus* and *M. primus* the combination of the following traits: horns and a nasal process elevated to the peak of a superorbital frontonasal process, posteriorly positioned orbits, an extremely widened skull, anteroposteriorly shortened basicranium, and lack of postcanine diastemata. However, *M. khaitshinus* differs from *M. relictus* and *M. primus* in having more anteriorly positioned posterior nares, larger lower incisors forming an arched row, and a broad labial notch on p2. *M. khaitshinus* has a more vertical occiput than *M. relictus*. It has a less constricted face than *M. primus* and its lacks the conspicuously bulbous cranium of that species.

Description

Skull: The following description of the skull of *Metatitan khaitshinus* refers primarily to the holotype (PIN 3745-1) but additional observations on other specimens are noted. The holotype of *M. khaitshinus* (PIN 3745-1) is a nearly complete skull (figs. 106 and 107). A large block of plaster is presently fixed to the dorsal surface of the skull, suggesting that it is incomplete or damaged. However, the specimen is not significantly distorted or damaged in any other way. This species is also known from several other reasonably complete specimens; two of them are figured here. PIN 3745-3 is a complete skull that is slightly crushed dorsoventrally (fig. 108). The anterior rim of the orbit is broken and the dorsal portion is displaced medially and ventrally with respect to the ventral portion of the anterior margin; consequently the orbit has become ovalized in contrast to the very rounded orbit of the holotype. Another skull, PIN 3745-11 (fig. 109), is dentally immature with an unerupted M3 crown. This skull is undistorted, but its nasal process and horns are unpreserved. This skull differs from the others in several ways although the differences are probably related to its subadult age.

The frontonasal region of *Metatitan khaitshinus* resembles *M. primus* and *M. relictus* in having closely positioned horns that are elevated above the orbits along with the nasal process. The horns and nasal process are elevated to a degree similar to that seen in *M. primus*, but to a degree that is greater than

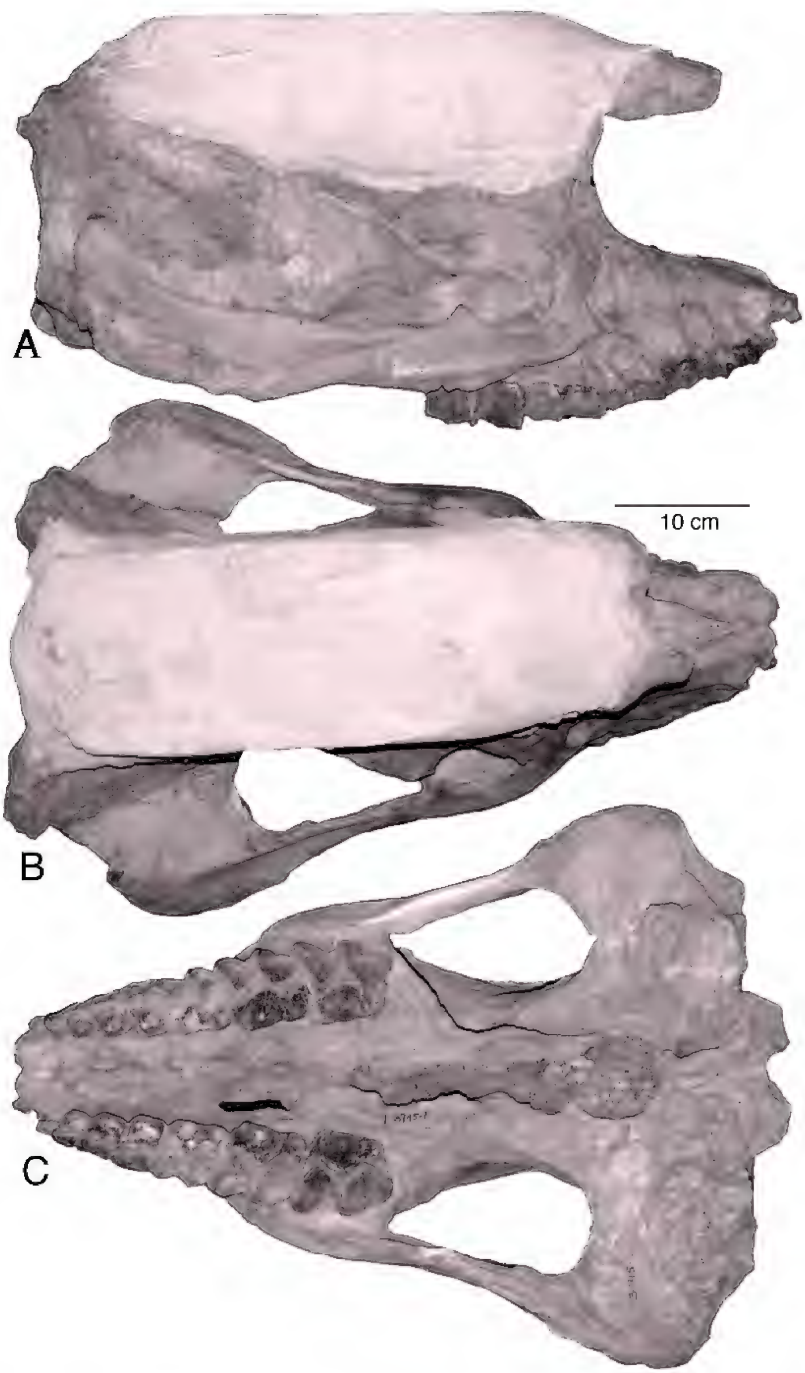

Fig. 106. The holotype skull of *Metatitan khaitshinus* (PIN 3745-1). **(A)** Right view, **(B)** dorsal view, **(C)** ventral view.

that of *M. relictus*. The horns of the holotype just barely protrude out from under the front edge of the plaster covering and are positioned over the nasal incision. In PIN 3745-3 the horns and nasal process are not as highly elevated, but the difference is related to the dorsoventrally crushed condition of that specimen. The horns of that specimen form

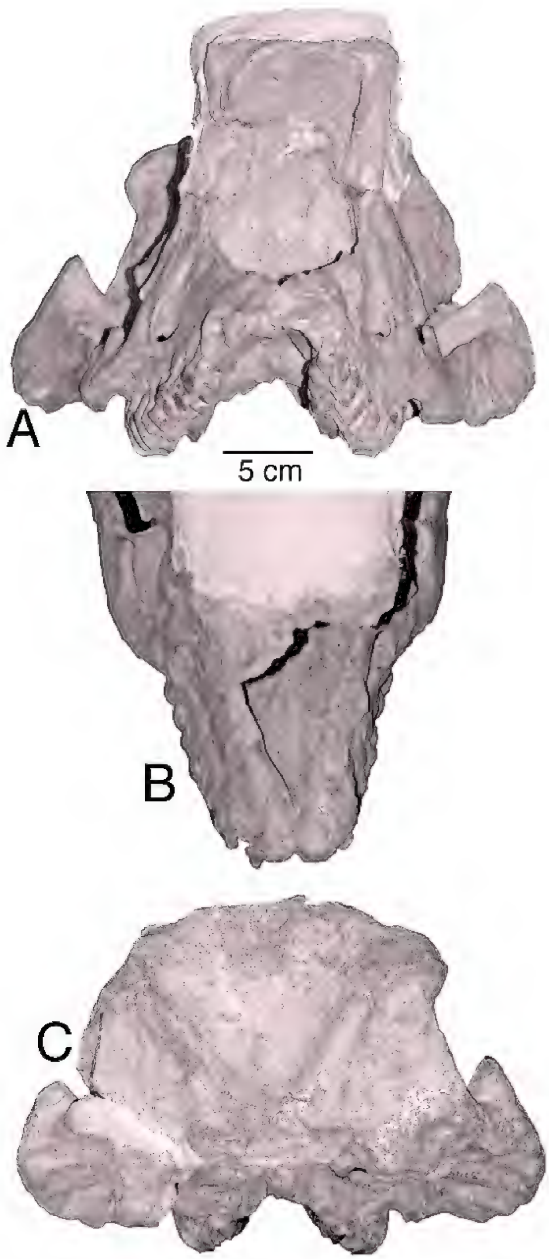

Fig. 107. The holotype skull of *Metatitan khaitshinus* (PIN 3745-1). **(A)** Anterior view, **(B)** dorsal view of rostrum, **(C)** posterior view.

small, rounded dorsolaterally projecting knobs. The contact of the frontal and nasal bone can be clearly discerned on the left horn of PIN 3745-3. The frontal bone forms the posterodorsal surface of the frontonasal process and extends to the peak of the horn. The nasals bone forms the anteroventral portion of the frontonasal process and makes up the base and anterior portion of the horn.

The nasal cavity of *Metatitan khaitshinus* is voluminous due to the elevated nasal process. In the uncrushed holotype the posterior margin of the nasal incision rises much higher than the orbits. The posterior margin of the nasal incision extends to a point above the M1. Like other species of *Metatitan* the orbit is positioned rather posteriorly. The posterior part of M2 and the anterior part of M3 are directly beneath the orbit with the anterolateral root of M2 positioned beneath the anterior rim of the orbit. The nasal process is much shorter than the premaxillo-maxillary rostrum and it projects from the skull in a horizontal direction. The lateral walls of the nasal process are unthickened and relatively shallow although they slightly deepen proximally. The width of the nasal process tapers slightly distally. The anterior margin of the nasal process is not strongly rounded because of a deep median notch.

The premaxillomaxillary rostrum is wide; it deepens posteriorly and its dorsal margin is sloped posterodorsally. A premaxillomaxillary suture is not visible on any of the specimens. The dorsolateral margins of the rostrum diverge laterally behind the premaxillary symphysis. The rostral cavity is open to the nasal cavity and not dorsally enclosed by bone.

The skull of *Metatitan khaitshinus* is similar to other species of *Metatitan* in its exceptional width. The postorbital portion of the cranium most closely resembles *M. relictus* and does not take on the extremely swollen appearance seen in the cranium of *M. primus*. While most horned brontotheres have saddle-shaped skulls, the crania of *M. relictus* and *M. primus* are incompletely saddle-shaped. However, this character is difficult to determine for *M. khaitshinus*. The dorsal surface of the holotype is obscured. The dorsal surface of PIN 3745-3 is concave from the horns to the occiput although this may be an artifact of crushing. However, several other specimens with less distorted crania, such as PIN 3745-4, PIN 3745-8, PIN 3745-9, and PIN 3745-11, indicate an incompletely saddle-shaped skull with a deep convexity in the center of the skull, but with a flat or more concave surface

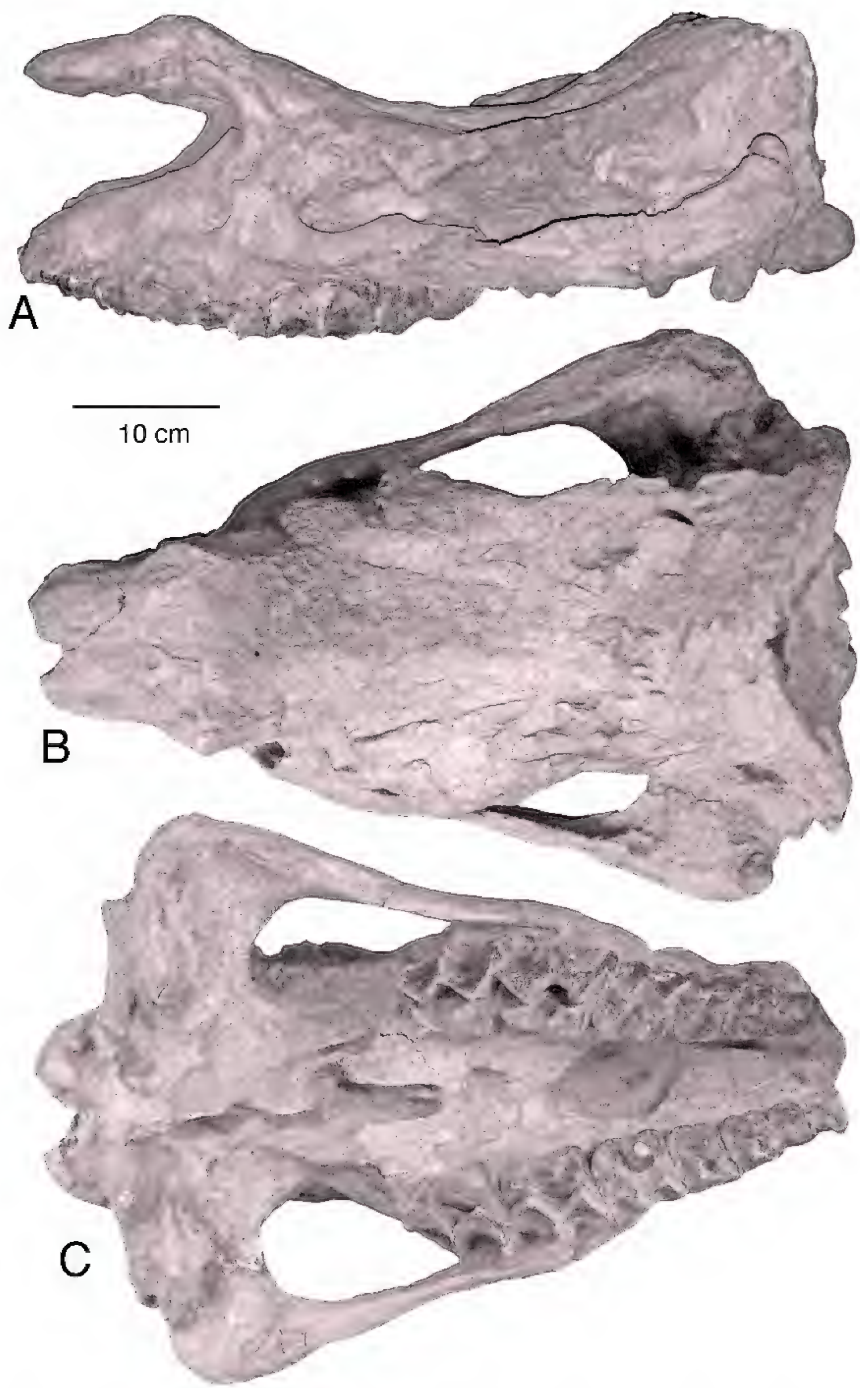

Fig. 108. A skull referred to *Metatitan khaitshinus* (PIN 3745-3). **(A)** Left view, **(B)** dorsal view, **(C)** ventral view.

Fig. 109. Left view of the holotype skull of *Metatitan reshetovi*, now referred to *Metatitan khaitshinus* (PIN 3745-11).

over the posterior portion of the cranium. The central parietal dome seen in *M. primus* is distinctly absent in skulls of *M. khaitshinus*.

The parasagittal ridges of *M. khaitshinus* are prominent. In the holotype (PIN 3745-1) they can be seen originating from the postorbital process of the frontal and sloping in a posterodorsal direction toward the occiput. From the dorsal view of PIN 3745-3 the parasagittal ridges appear to strongly overhang the sides of the skull. The parasagittal ridges are widely separated and they do not constrict the posterodorsal surface of the skull.

From lateral views of the skulls of *Metatitan khaitshinus* the zygomatic blade is straight, although it is deflected strongly upward at the posterior end where there is a tall posterior zygomatic process similar to that of *M. relictus*. From dorsal views of the skulls the zygomatic blades are thin, straight, and they diverge strongly posterolaterally, thus creating a strongly wedge-shaped skull. Like other species of *Metatitan*, the zygomatics extend nearly to the posterior end of the cranium, and the lateral wings of the squamosals are positioned at the posteriormost end of the skull and form an abrupt, nearly 90° angle with the zygomatic blades.

The nuchal crest of the holotype is obscured by plaster. From a dorsal view of PIN 3745-3 the nuchal crest is strongly concave. From a posterior view the dorsal margin of the occiput is arched dorsally. The occiput itself is extremely broad and like *M. primus* it is vertical. The dorsal half of the occiput is similar in width to the ventral half and the occiput is not strongly constricted in the middle. The surface of the occiput has narrow occipital pillars with a shallow triangular depression between them.

The posterior nares of the holotype are partially damaged while those of PIN 3745-3 are intact. However, in both specimens the posterior nares are constricted by a wide horseshoe-shaped emargination similar to that of *Metatitan relictus*. However, the posterior nares are more anteriorly situated than those of *M. relictus*; the anterior margin of the posterior nares of *M. khaitshinus* is consistently positioned roughly between the protocones of M3 while the posterior nares of *M. relictus* are entirely behind M3. This is one of the major features distinguishing these two species. Other aspects of the ventral surface of *M. khaitshinus* closely resemble *M. relictus*. The posterior narial canal is elongate and extends well into the sphenoid bone where it broadens notably, forming a rounded depression. The elongate vomer is not preserved in the holotype, but remnants of it are seen in PIN 3745-3 bisecting the elongate posterior narial canal and ventral sphenoidal fossae. In PIN 3745-3 the left sphenoidal fossa is clear of sediment while the right sphenoidal fossa is still filled with matrix. The basicranium is very wide and anteroposteriorly compressed. The width of the skull,

measured from the left and right mastoid processes, is much greater than the width across the M3s. Ratios calculated from the width of the basicrania of PIN 3745-1 and PIN 3745-3 divided by the width across the M3s yield values (1.73 and 1.47, respectively) that are similar to those calculated for *M. relictus*. The external auditory pseudomeatus is tube-shaped, enters the skull in a mediolateral direction, and it is positioned at the posteriormost end of the cranium.

Upper Dentition: The upper incisors of *Metatitan khaitshinus* are unknown. The incisor alveolar border of PIN 3745-1 suggests a broad and somewhat arched incisor row (fig. 106) This interpretation agrees with the lower incisors (see below). The juvenile skull, PIN 3745-11, has a pair of small canines (fig. 109). Another specimen, PIN 3745-12 (not shown), has a pair of similarly sized canines that are very heavily worn. A postcanine diastema is not present in any specimen. The short postcanine gap in PIN 3745-11 is the result of P1 having fallen out.

The premolars of *Protitan khaitshinus* show a remarkable amount of intraspecific variability that is, nonetheless, a pattern typical of brontothere species. The labial aspects of the premolars are morphologically fairly stable, while the lingual sides are morphologically variable. To demonstrate this pattern of intraspecific variability close-ups of the premolars of the holotype (PIN 3745-1) (fig. 110a) and three other specimens (PIN 3745-3, PIN 3745-11, PIN 3745-12) (fig. 110b–d) are shown.

The P1 of the holotype is heavily worn. PIN 3745-3 has a less worn P1 and has a morphology that is typical of many advanced brontotheres. The crown is rounded in outline with a distinct paracone, a metacone of roughly similar size, and a small lingual heel with a small lingual crest. P2–P4 have parallel anterior and posterior sides. P2 is slightly oblique in outline, while P3–P4 are more nearly rectangular. The parastyle of P2 is straight, but those of P3 and P4 are deflected anterolabially. The metastyles of P2–P4 are nearly straight. A broad labial paracone rib can be seen on the P2. The labial paracone ribs of P3 and P4 are much narrower and progressively smaller. Mesostyles are absent on all premolars.

As noted above, the lingual heels of the P2–P4 are variable. The holotype specimen is the least molariform, while the premolars of the remaining specimens are more molariform. The P2 of PIN 3745-1 has only one distinct lingual cusp, consisting of a large central ovoid cusp with a very short lingual crest at its peak. A small preprotocrista arches anterolabially from the peak of the lingual cusp, but it does not reach the paracone. The P2 of PIN 3745-3 is similar, but it appears to have two lingual cusps that are strongly fused together. PIN 3745-11 has two well-separated lingual cusps that are connected by a small lingual crest. The lingual crest continues posterior to the apex of the hypocone and ends at the posterior cingulum. Finally, the P2 of PIN 3745-12 has two equally sized and fully separated lingual cusps.

The P3 shows a similar degree of variability in relative molarization. The least molarized P3s have partially separated protocones and hypocones (PIN 3745-1, PIN 3745-3). Other specimens have two fully separated lingual cusps of similar size. One of these, PIN 3745-11 has a small lingual crest, while the other, PIN 3745-12, does not. The lingual heel of the P4 shows a lesser amount of variation and a lesser degree of overall molarization. Three of the figured upper premolar rows have a single lingual cusp without a preprotocrista or lingual crest on the P4. Only one of these specimens (PIN 3745-11) has a small lingual crest. The posterior portion of this crest thickens into an elongate hypoconelike structure. Labial premolar cingula are distinct but thin. The lingual premolar cingula are thick and continuous around the lingual sides of the crowns.

PIN 3745-11 (fig. 110e) has the least worn and best-preserved molars available for *Metatitan khaitshinus*. Other than the fact that they are less worn, they do not differ in any notable way from those of the holotype or other specimens belonging to this species. The upper molars are elongate. The molars of other specimens tend to be shorter, but this is primarily related to wear. Typical brontotheriine apomorphies are present, including tall, lingually angled ectolophs, very weak labial ribs, thin lingual ectoloph enam-

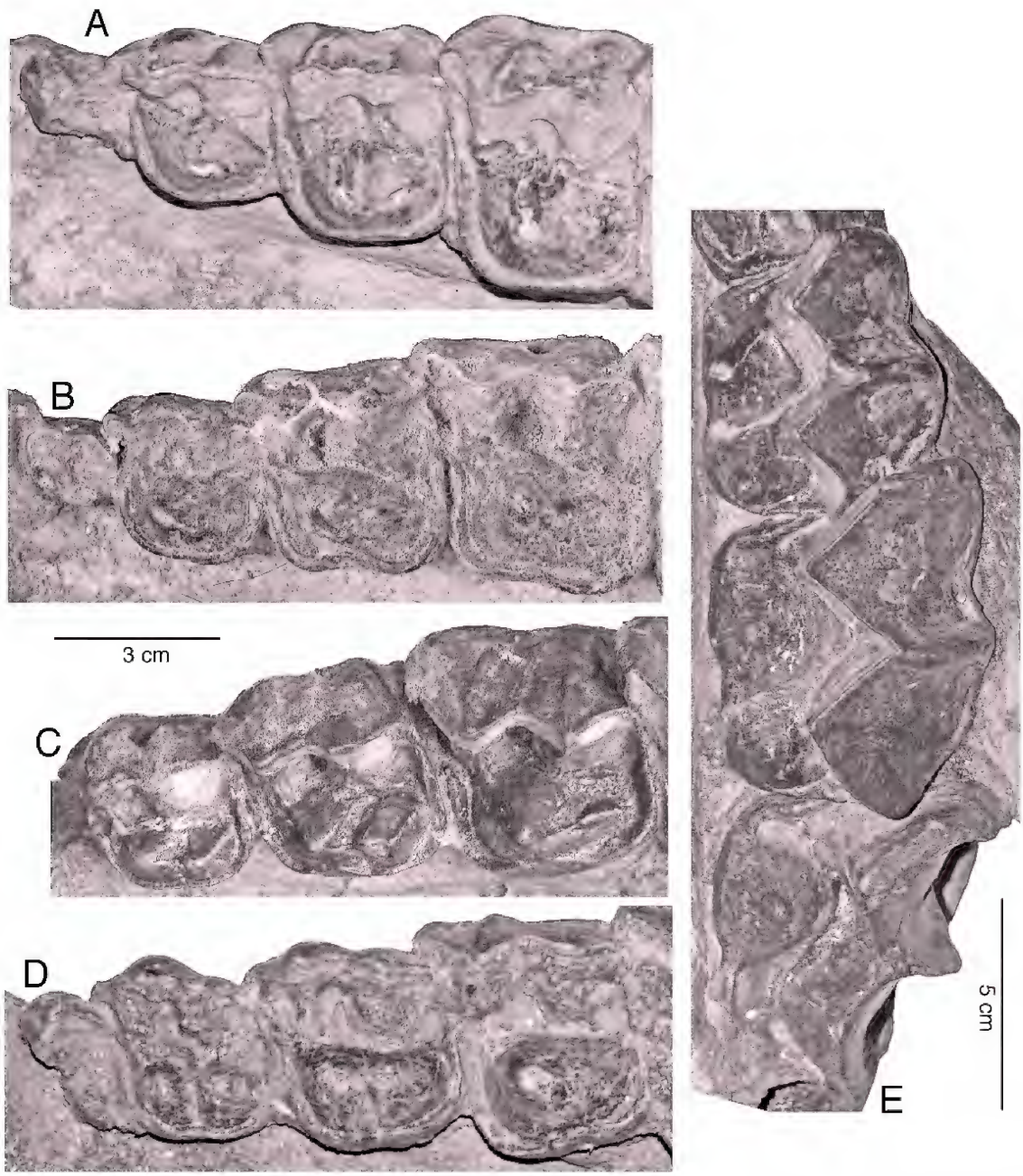

Fig. 110. Close-ups of the upper dentition of *Metatitan khaitshinus*. **(A)** Left premolars of PIN 3745-1 (holotype), **(B)** left premolars of PIN 3745-3, **(C)** reflection of right P2–P4 of PIN 3745-11, **(D)** left premolars of PIN 3745-12, **(E)** left upper molars of PIN 3745-11.

el, and wedge-shaped lingual sides of the paracone and metacone in molars that are not heavily worn. The anterior cingulum is thin and passes proximally to the distal peak of the parastyle. Distinct, shallow central molar fossae and small anterolingual cingular cusps are present. There is no evidence of paraconules or metalophs. There is no hypocone on the M3 although the distolingual cingulum of the M3 is thickened and

raised. Labial molar cingula are weak and lingual molar cingula are absent or extremely weak.

MANDIBLE AND LOWER DENTITION: Yanovskaya (1980) referred numerous mandibles to *Metatitan khaitshinus* although I was able to locate only one of these, PIN 3745-31 (fig. 111). This specimen is nearly complete but it lacks the condyles. The angle of the ventral margin of the symphysis is near 45°. The symphysis is broad and extends to the P4. The dental formula is unreduced (3-1-4-3).

The incisors are of moderate size and they form a slight arch anterior to the canines. This differs from other species of *Metatitan* in which the incisors form a straighter row and are reduced to a very small and essentially vestigial condition. The lower incisors of *M. khaitshinus* more closely resemble those of *Brachydiastematherium transylvanicum*. In general the lower incisors have a semispatulate morphology. The apex of the i1 is worn flat. The i2 and i3 have arched apices. The i2 is the largest incisor. Each lower incisor has a distinct lingual cingulid. Labial cingulids are absent. There are no diastemata between the incisors or canines. The postcanine gap seen in PIN 3745-31 is the space for the missing p1, for which signs of the alveolus are still present. A genuine postcanine diastema (gap between canine and p1) is not present.

The remaining premolars (p2–p4) show a degree of molarization similar to other species of *Metatitan* and *Brachydiastematherium transylvanicum*, although some distinctions can be found and are noted below. The trigonids of p2–p4 are similar in length and width to their talonids. The paralophid of p2 arches strongly lingually generating a small lingual trigonid notch. The protolophid is straight, but it is angled in a posterolingual direction. There is no p2 metaconid although it might have been variably present as in *M. relictus*. The labial notch formed by the p2 protolophid and cristid obliqua is broad, shallow, and points lingually. This trait resembles *B. transylvanicum* but differs from both *M. relictus* and *M. primus* in which the labial p2 notch forms a deep narrow posterolingually angled groove. The right p3 that is shown in close up (fig. 111c) is damaged. However, the left p3 (fig. 111b) has a fully lingually arched paralophid and protolophid, creating a nearly molariform trigonid basin. The trigonid of the p4 is equally molariform. Both p3 and p4 have large lingually positioned metaconids. The talonids of p2–p4 are well developed with long hypolophids, long cristids obliqua, and broad talonid basins. The p4 of *M. khaitshinus* lacks the unusual crest of enamel extending posteriorly from the middle of the cristid oblique that is seen in *B. transylvanicum*. Labial premolar cingulids are weak and lingual premolar cingulids are absent.

The molars of *Metatitan khaitshinus* are typical with shallow trigonid and talonid basins and thin lingual enamel. The m3 is very elongate. Labial molar cingulids are distinct. Lingual molar cingulids are absent. The m3 cingulid does not wrap completely around the hypoconulid.

REMARKS

Three diagnosable brontothere species can be assigned to *Metatitan*: *M. primus* Granger and Gregory (1943) (the type species), *M. relictus* Granger and Gregory (1943), and *M. khaitshinus* (Yanovskaya, 1980). Granger and Gregory (1943) erected *Metatitan* for a group of brontotheres characterized by extremely widened skulls, a short basioccipital, small frontonasal horns, small incisors, no postcanine diastema, and relatively advanced premolars. Granger and Gregory (1943) considered these species to be derived from *Rhinotitan* and to have bridged the morphological gap between the bizarre battering ram of *Embolotherium* and the more typical paired frontonasal horns of most other horned brontotheres. The type species, *Metatitan primus*, "points the way to *Embolotherium*, since its horns are displaced forward in front of the orbit and joined by a transverse connecting crest" (Granger and Gregory, 1943: 367). Granger and Gregory (1943) seem to have been referring to the fact that the frontal and nasal bone forms a single large process that rises above the orbits at a steep angle. This was thought to be the precursor of the ram of *Embolotherium*, a hypothesis that is further supported by the phylogenetic analysis of Asian horned brontotheres in Mihlbachler et al. (2004a). How-

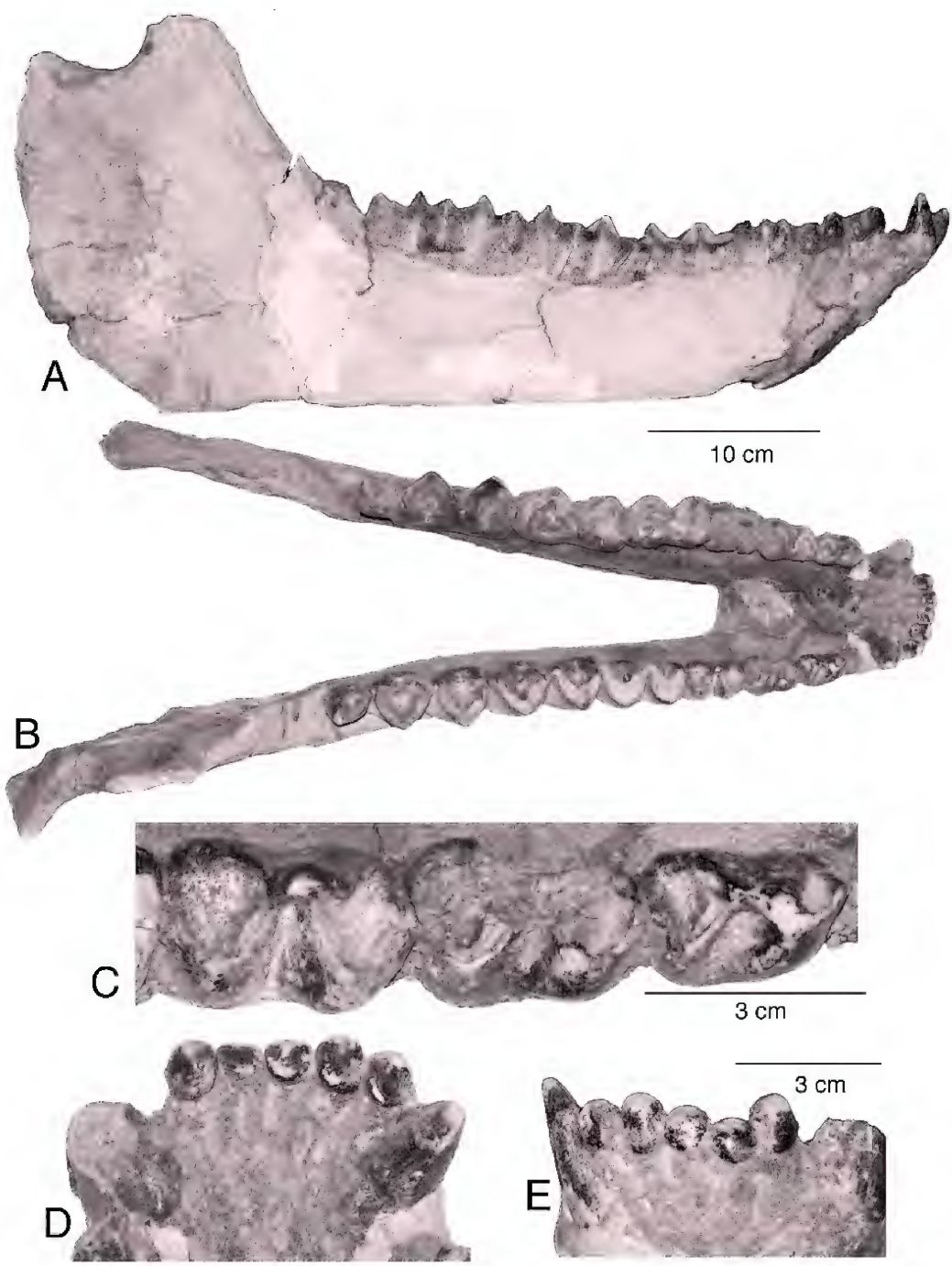

Fig. 111. Mandible referred to *Metatitan khaitshinus* (PIN 3745-31). **(A)** Right view, **(B)** dorsal view, **(C)** right p2–p4, **(D)** lingual view of incisors and canines, **(E)** labial view of incisors and canines.

ever, unlike *Embolotherium*, the nasal processes are retained in *Metatitan* and they are elevated to the peak of the frontonasal pillar, whereas in *Embolotherium* they are lost. *Aktautitan hippopotamopus*, a taxon not known to Granger and Gregory (1943), shares the *Metatitan*-like frontonasal morphology, but differs from *Metatitan* primarily in having large incisors, a postcanine diastema, less molarized premolars, and a more saddle-shaped cranium.

In addition to the type species, *Metatitan primus*, Granger and Gregory (1943) assigned two other species to *Metatitan*, *M. relictus* and *M. progressus*. Both of these species are valid, although the latter species is now placed in a new genus, *Nasamplus*. Most of the brontothere material collected in the Camp Margetts area during the 1930 Central Asiatic Expedition of the American Museum of Natural History represents *M. relictus*. *M. relictus* can be distinguished from *M. primus* by its less swollen cranium, more prominent parasagittal ridges, and deeper nasal incision. It is possible that that premolar hypocones occur less frequently in *M. relictus*, but this cannot be confirmed without additional specimens of *M. primus*.

Additional *Metatitan* fossils from Mongolia were described by Yanovskaya (1980) although she misidentified much of the material. Yanovskaya (1980) erroneously referred a skull, mandible, and numerous postcranial elements from the Ergilin Dzo of Inner Mongolia to *M. relictus*. Mihlbachler et al. (2004a) recognized that this material was not *Metatitan* and found it to be more similar to *Parabrontops gobiensis*. In this revision, that material is assigned to *Eubrontotherium clarnoensis*.

In the same monograph, Yanovskaya (1980) described numerous *Metatitan* fossils but misidentified them as *Protitan*. Yanovskaya (1980) erected two species based on a large collection of brontothere material from the Khaichin Formation of southwestern Mongolia; *P. khaitshinus* (Yanovskaya, 1980) was based on a complete skull (PIN 3745-1) (fig. 106) while *P. reshetovi* was based on a subadult skull (PIN 3745-11) (fig. 109). Mihlbachler et al. (2004a) first demonstrated the close similarity of these species with *Metatitan*, and they considered Yanovskya's *Protitan* synonymous with *Metatitan*. Working from descriptions and figures published by Yanovskaya (1980), Mihlbachler et al. (2004a) preliminarily suggested that (1) *P. khaitshinus* is a junior synonym of *M. relictus*, (2) that *P. reshetovi* is possibly a valid species, and that (3) *Brachydiastematherium transylvanicum* (the only brontothere species named from Europe) might actually be synonymous with a species of *Metatitan*.

After directly examining the material in the PIN collection these conclusions must be modified. Based on more substantial observations taken directly from the specimens, *M. khaitshinus* can be differentiated from both *M. relictus* and *M. primus* and thus constitutes a valid species. Although similar to *M. relictus* and *M. primus*, *M. khaitshinus* differs in substantial ways. *M. khaitshinus* has more anteriorly positioned posterior nares, a more arched lower incisor row, larger lower incisors, and it lacks the long narrow groove-like labial notch in the p2 that characterizes *M. primus* and *M. relictus*. *M. khaitshinus* appears to have a more vertical occiput than *M. relictus*. It has a less constricted face than *M. primus* and its lacks the autapomorphic dorsal dome of that species.

Secondly, *Metatitan reshetovi* cannot be differentiated from *M. khaitshinus* and is therefore a junior synonym of the later. Yanovskaya (1980) diagnosed *M. reshetovi* as having a narrower skull, narrower nasal, and more molarized premolars. However, the differences in relative skull width and nasal width between *M. khaitshinus* and the type of *M. reshetovi* (PIN 3745-11) are barely noticeable. For instance, Yanovskaya (1980) found only a 5% difference in skull width (calculated as a ratio with skull length). Considering the possible effects of subtle distortion and the subadult age of PIN 3745-11, these differences are of dubious taxonomic significance. Among the specimens attributed to *M. khaitshinus* and *M. reshetovi* there is conspicuous variation in the relative degree of premolar molarization. Specimens without premolar hypocones or poorly developed premolar hypocones were assigned to *M. khaitshinus* by Yanovskaya (1980), while others with more developed premolar

hypocones were assigned to *M. reshetovi*. However, the variation in premolar molarization in these specimens is arguably continuous. Moreover, conspicuous intraspecific variation in lingual premolar morphology is a common pattern of intraspecific variation that is seen within many other brontothere species.

Thirdly, to the extent that they can be compared, *M. khaitshinus* is very similar to *Brachydiastematherium transylvanicum* from Europe. Currently *B. transylvanicum* is known only from its type specimen, a partial mandible that is almost identical to the mandible of *M. khaitshinus*. They are of similar size, both lack postcanine diastemata, and both differ from *M. relictus* and *M. primus* in the same ways: namely, each has larger, less globular incisors with lingual cingulids and each has a broader and more lingually pointed labial notch on the p2. *B. transylvanicum* and *M. khaitshinus* differ in only one detectable way: *B. transylvanicum* has an unusual crest extending posteriorly from the cristid oblique that is absent in *M. khaitshinus*. For this reason I consider these species to be distinct, but further discoveries may indicate that these species are synonymous.

Nasamplus progressus (Granger and Gregory 1943), new genus

HOLOTYPE: AMNH 26014, a skull fragment including portions of the right orbit, frontal, nasal, maxilla, and P4–M1.

TYPE LOCALITY: Ulan Gochu, Jhama Obo, East Mesa, Shara Murun Region, Inner Mongolia, China. (Ulan Gochu [used in quotes] denotes uncertain correlation with the type Ulan Gochu beds at Baron Sog and refers to a faunal zone rather than a formation; see Radinsky, 1964.)

AGE: Late Eocene (Ulangochuian land mammal "age").

ETYMOLOGY: The genus name, *Nasamplus*, is a combination of the Latin terms *nasus* ("nose") and *amplus* ("large"). This name refers to the elevated nasal process of this species, which results in a large nasal cavity.

DIAGNOSIS: *Nasamplus progressus* is a large brontothere in which the frontonasal horns are fused into a single transverse crest. The frontonasal crest and nasal process are elevated high above the orbits on a frontonasal process (ram). The nasal incision is very deep and extends posteriorly about to the anterior margin of M1. The orbit is positioned above the posterior portion of M1. The elevated nasal process is horizontal and with lateral walls that are deep proximally. The P4 of *Metatitan primus* has a distinct hypocone that is well separated from the paracone. A central fossa is present on M1.

The skull fragment representing *Nasamplus progressus* is morphologically intermediate between *Aktautitan* and *Metatitan* on the one hand and *Protembolotherium* and *Embolotherium* on the other. *Nasamplus progresses* resembles *Aktautitan* and *Metatitan* in having an elevated horizontal nasal process, but like *Protembolotherium* and *Embolotherium* the horns are fused into a transverse frontonasal crest at the peak of the frontonasal ram.

DESCRIPTION

SKULL AND UPPER DENTITION: The single fragmentary specimen of *Nasamplus progressus* (AMNH 26014) (fig. 112) indicates a large brontothere with a frontonasal morphology that is intermediate between the condition seen in *Aktautitan* and *Metatitan*, and the more derived condition of *Protembolotherium* and *Embolotherium*. As in *Metatitan* and *Aktautitan* the frontonasal protuberance is elevated high above the orbit, although it is more highly elevated in *N. progressus*. The angle of the superorbital frontonasal process upon which the frontonasal protuberance rests is steeper than 45°. The frontonasal contact is visible from the lateral view on the upper half of the frontonasal process. The frontal bone forms the posterodorsal surface of the frontonasal process while the nasal bone forms the anteroventral surface. The frontonasal contact is even more distinct from the dorsal view of the cranial fragment. At the peak of the frontonasal process the posterolateral border of the nasal bone is bordered by a thick section of frontal bone. The line of frontonasal contact recedes posteromedially and at the midline the frontal bone is thinnest. The frontal bone does not form a

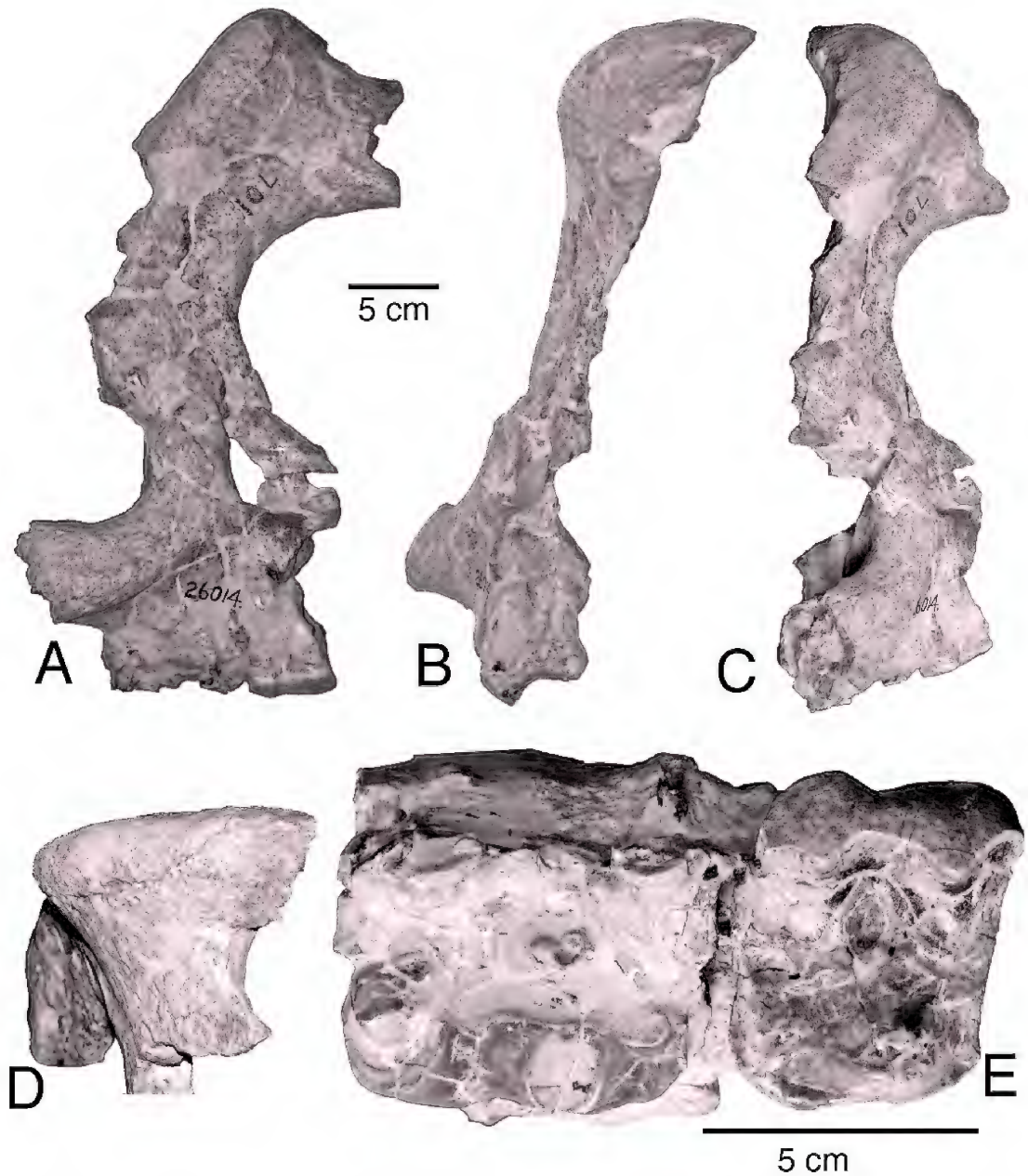

Fig. 112. The holotype cranial fragment of *Nasamplus progressus* (AMNH 26014). **(A)** Right view, **(B)** anterior view, **(C)** posterior view, slightly rotated laterally, **(D)** dorsal view, **(E)** right P4–M1.

pair of distinct protuberances. Instead, there is a single transverse crest formed at the peak of the frontonasal process that is formed by both the frontal and nasal bones. The surface of this crest is roughened and from the anterior view it is dorsally arched. The configuration of the frontal and nasal bones and the transverse frontonasal crest at the peak of the frontonasal process of *Nasamplus progressus* closely resembles the rams of *Protembolotherium* and *Embolotherium*.

However, unlike *Protembolotherium* and *Embolotherium*, *Nasamplus progressus* retains a large horizontal nasal process that, like

Metatitan and *Aktautitan*, is elevated to the peak of the frontonasal process. Only the proximal end of the nasal process is preserved. The lateral walls of the proximal end of the nasal process are very deep.

The orbit is positioned above the posterior portion of M1 with the anterolateral root of M1 below the anterior orbital rim. Due to the elevated nasal process the nasal incision is very deep and it extends posteriorly about to the anterior margin of M1.

Only two teeth, P4 and M1, are preserved in the fragmentary holotype and these are heavily worn. P4 is essentially rectangular with a labially oriented parastyle and a straight metastyle. A labial paracone rib is not discernable. On the lingual side of the tooth, there is both a protocone and a smaller but well-developed hypocone. The hypocone is positioned on the very distal side of the crown and connected to the protocone by a minor lingual crest. The labial cingulum of P4 is very weak, and the lingual P4 cingulum is thick but slightly discontinuous. M1 is extremely worn and the ectoloph is not preserved. A small remnant of the central fossa is visible in the center of M1.

Remarks

Granger and Gregory (1943) originally assigned *Nasamplus progressus* to *Metatitan*. Mihlbachler et al. (2004a) found that *Metatitan progressus* did not group into a monophyletic clade with other species of *Metatitan*, but that it grouped closer to *Embolotherium*. Unfortunately, no specimen other than the fragmentary holotype has ever been reported and although the holotype is only a very small cranial fragment, the right combination of features are preserved to determine that this specimen represents a distinct taxon that is essentially intermediate between *Metatitan* and *Embolotherium*. Therefore, this species is assigned a new genus name, *Nasamplus*.

This specimen led Granger and Gregory (1943) to conclude that the distinctive "battering ram" of *Embolotherium* was derived from a *Metatitan*-like morphology, involving the increasing height of the frontonasal process and the eventual loss of the nasal process. *Nasamplus progressus* seems to represent an intermediate stage in which the frontonasal process is increased in height and forms a battering ram–like crest at the peak but the horizontal nasal process has not yet been reduced or lost.

Protembolotherium efremovi Yanovskaya, 1954

Holotype: PIN 473-311, a skull lacking the nasal elements with right P2–M3 and left P3–M3.

Type Locality: Ergilin Dzo (lower part), Dornogobi Province, Outer Mongolia

Age: Late Eocene (Ulangochuian [Ergilian] land mammal "age").

Referred Specimens: **(From Ergilin Dzo [lower part, Outer Mongolia)** PIN 473-310, a partial skull missing its left and ventral surfaces; PIN 3109-40, a partial skull missing its left and ventral surfaces.

Diagnosis: *Protembolotherium efremovi* is a large brontothere that is very similar to *Embolotherium*. Its most distinctive features are a pair of small secondary horns positioned above the orbits, and a tall, nearly vertical process of bone (a "ram"), probably composed of the frontal and nasal bones. The ram rises from above the orbits and arches backward. The ram tends to be shorter than those of *Embolotherium andrewsi* and *E. grangeri*. The peak of the ram is a transverse crest that forms the distal margin of the anteroventral nasal channel, sometimes with rugose swellings at the distolateral corners. The nasal incision extends posteriorly to the anterior margin of P4 and the orbits are positioned above the M2 and the posterior portion of M1. A horizontal nasal process can be absent or it persists in a diminished form as a flat triangular process that is elevated to the peak of the ram. The dorsal margin of the rostrum is strongly sloped so that the premaxillomaxillary rostrum deepens posteriorly. The rostrum is not enclosed by bone dorsally. Other cranial characteristics include a saddle-shaped cranium, a robust occiput, and weakly curved zygomatic arches with prominent lateral swellings. The external auditory pseudomeatus enters the skull in a posteromedial direction and is ventrally constricted.

Dentally, *Protembolotherium efremovi* is characterized by a distinct P2 metacone, and hypocones on P2–P4 that are connected to the protocone (to varying degrees) by lingual crests. The molars of *P. efremovi* have tall, lingually angled ectolophs with weak labial ribs, and thinned lingual ectoloph enamel with wedge-shaped paracones and metacones. A cingular parastyle shelf is absent. Deep central molar fossae and large anterolingual cingular cusps are present. Paraconules and metalophs are absent.

Protembolotherium efremovi is one of three species with an enlarged frontonasal battering ram. It can be differentiated from *Embolotherium* in the following ways: there is a pair of small secondary horns positioned above the orbits, the dorsal margin of the rostrum is steeply sloped upward, the skull is less deeply saddle-shaped, the occiput is shorter and more erect, the ram is somewhat shorter, and occasionally a reduced remnant of the nasal process is seen in an elevated position at the peak of the ram. It can be further differentiated from *E. andrewsi* by its less robust occiput, less prominent parasagittal ridge, and more laterally bowed zygomatic arches. It can be further differentiated from E. *grangeri* by its shorter nasal incision, more anterior position of the ram, and the backward curvature of the ram.

Description

Skull: The holotype skull of *Protembolotherium efremovi* (PIN 473-311) is missing the frontonasal region and a small portion of the right basicranium and occiput (fig. 113). In other respects the skull is essentially complete and not greatly distorted. Additional skulls referred to *P. efremovi* are PIN 473-310 (fig. 114) and PIN 3109-40 (fig. 115). These three skulls indicate a species that is large, but perhaps smaller on average than *Embolotherium andrewsi* and *Embolotherium grangeri*. The two referred skulls (PIN 473-310 and PIN 3109-40) have relatively complete and undistorted right and dorsal sides but they are lacking complete left and ventral surfaces. Both of these specimens exhibit two conspicuous features in the frontonasal region that are not preserved on the holotype specimen but that are, nonetheless, critical to the identification and characterization of this species. These features are (1) a large battering ram–like structure similar to that of *Embolotherium* and (2) an autapomorphic pair of short and widely spaced secondary hornlike bony protuberances positioned directly above the orbits. The hornlike protuberances of both of these specimens are rather narrow and they project dorsally, posteriorly, and laterally. In *Protembolotherium efremovi* the ram is massive and well developed although it is shorter than those of *Embolotherium andrewsi* and *Embolotherium grangeri*. Several aspects of the ram specifically resemble *Embolotherium andrewsi*. For instance, the ram originates from a position above and slightly anterior to the orbits, it protrudes from the skull in an anterodorsal direction at an angle greater than 45°, and curves slightly backward, thus resulting in a concave posterodorsal surface and a convex anteroventral surface. However, because of its shorter length the backward curvature of the ram is somewhat less pronounced and the distal end does not achieve the vertical angle that is seen in some specimens of *Embolotherium andrewsi* (such as AMNH 26001, see fig. 117). The ram of *Protembolotherium efremovi* broadens distally and a deep nasal channel runs along the anteroventral surface and continues into the nasal cavity of the skull. Like *E. andrewsi*, the nasal cavity extended to the distal end of the ram and was extraordinarily tall, although nostril position (elevated to the peak of the ram, or positioned more normally in a low position) remains unknown (Mihlbachler and Solounias, 2004). This nasal channel is bordered laterally by thick but rather shallow walls. The lateral walls moderately constrict the nasal channel at the proximal end of the ram, but not to the degree seen in *Embolotherium andrewsi*, nor is the nasal channel extremely deepened at the proximal end of the ram.

Protembolotherium efremovi has a pair of small secondary horns positioned above the orbits that are completely separated from the ram. On first impression the horns of *P. efremovi* appear to be homologous to the paired frontonasal horns typical of many brontotheres while the ram has the superficial appearance of an enlarged and upturned

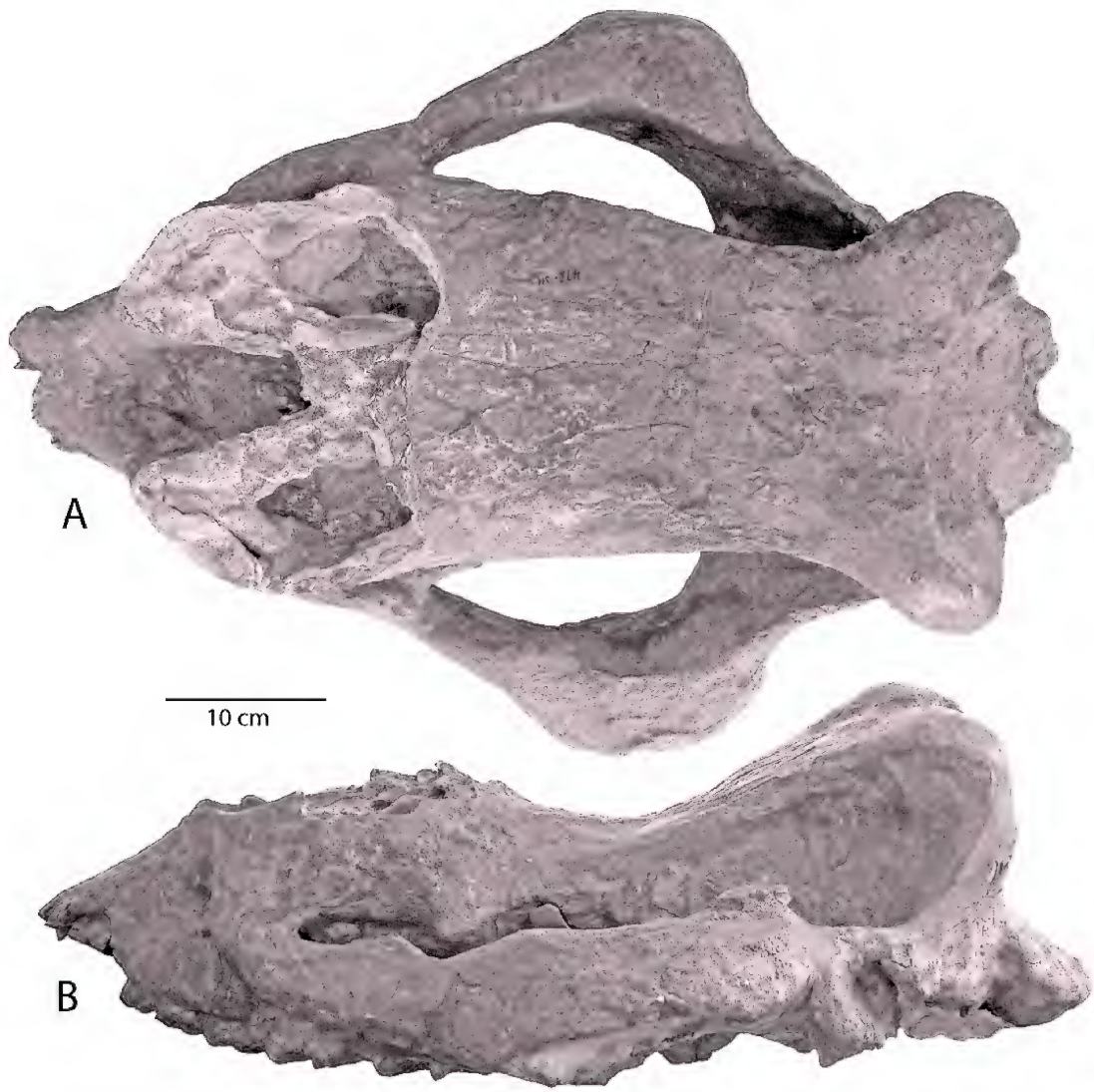

Fig. 113. The holotype skull of *Protembolotherium efremovi* (PIN 473-311). **(A)** Dorsal view, **(B)** left view.

nasal process, the portion of nasal bone that in less derived brontotheres typically forms the dorsal margin of the nasal incision. Evidence of the sutural configuration of the facial bones would be valuable in determining the best hypothesis of homology of these structures, but unfortunately none of the relevant sutures are discernable on any of these specimens. However, there seems little doubt that the ram itself is homologous to that of *Embolotherium andrewsi*, in which there is clear evidence that the distal surface of the ram is homologous to the tips of the frontonasal horns of other horned brontotheres. Therefore, the small secondary horns of *P. efremovi* do not appear to be homologous with the paired frontonasal horns of other horned brontotheres.

The distal end of the ram of PIN 3109-40, in particular, is unique and takes on an intermediate condition between *Embolotherium andrewsi* and less derived species, such as *Nasamplus*, *Metatitan*, and *Aktautitan*. From the anterior view, the distal surface of the ram is concave. At each distal corner is a large pachyostotic swelling. From the lateral

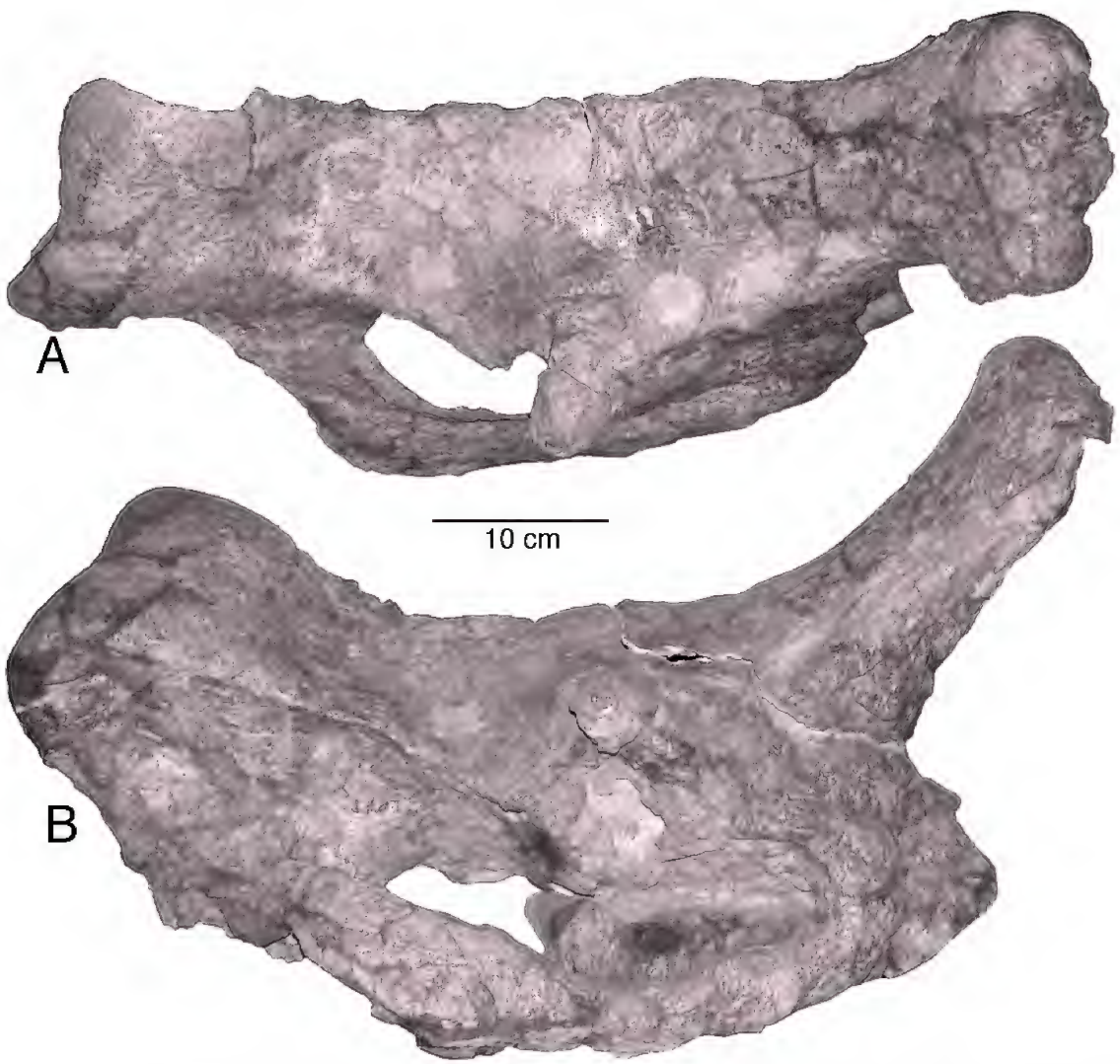

Fig. 114. A skull referred to *Protembolotherium efremovi* (PIN 473-310). **(A)** Dorsal view, **(B)** right view.

view the pachyostotic swelling is continuous with the lateral emargination of the ram. A more peculiar feature present in PIN 3109-40 but not seen in PIN 473-310 is the relatively flat process that projects anteriorly and slightly ventrally from between the two distolateral swellings. This process appears to be the free end of a reduced nasal process that in less derived species (e.g., *Protitan*, *Metatitan*) extends anterior to the frontonasal horn and forms the dorsal margin of the nasal incision. In *Embolotherium andrewsi* this structure is entirely lost. In the other specimen, PIN 473-310, the lateral swellings at the distal end of the ram are less pronounced; however, the free end of the nasal bone is essentially absent (or absorbed by the ram) as in *E. andrewsi*. If Yanovskaya (1954, 1980) and I are correct in assigning these skulls to a single species, the reduced nasal process was variable within *P. efremovi*, sometimes appearing in diminished state as in PIN 3109-40, and sometimes completely diminished as in PIN 473-310. Unfortunately both of these specimens are edentulous, so it is difficult to gauge their ontogenetic ages,

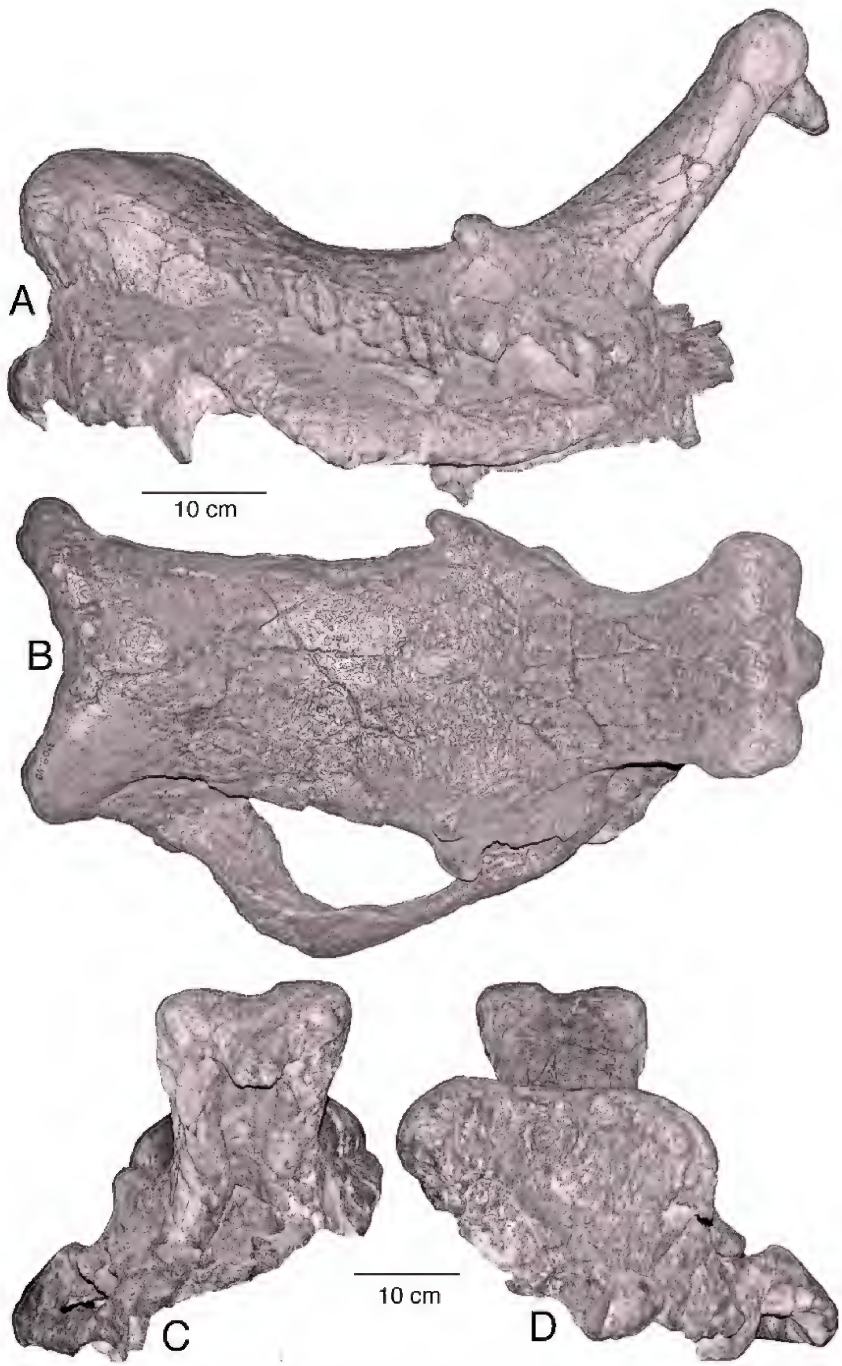

Fig. 115. A skull referred to *Protembolotherium efremovi* (PIN 3109-40). **(A)** Right view, **(B)** dorsal view, **(C)** anterior view, **(D)** posterior view.

although variation at the distal end of the ram might have been related to the ontogenetic process.

In the holotype (PIN 473-311) the posterior border of the nasal incision extends as far back as the posterior margin of P3. This is similar to *Embolotherium andrewsi*. Likewise, the position of the orbit is similar; it is positioned directly above M2 with the anterior rim of the orbit positioned approximately over the anterolateral root of M1. The nasal incisions of PIN 3109-40 and PIN 473-310 are complete and their posterior margins are entirely anterior to the orbits; however, the position of the nasal incision and the orbits cannot be determined with respect to the dentition due to the edentulous condition of these specimens.

None of the three skulls of *Protembolotherium efremovi* has a complete premaxillomaxillary rostrum although most of it is preserved with the type skull (PIN 473-311). Unfortunately premaxillomaxillary sutures are not clearly discernable. From a lateral view the rostrum is rather short. The ventral surface of the rostrum is curved slightly upward. The dorsal margin of the rostrum is flat and steeply angled posterodorsally so that it rises to a level just slightly higher than the orbits. From anterior and dorsal views the rostrum is broad and the lateral margins diverge posterolaterally to create a broad cavity on the dorsal side of the rostrum that is continuous with the nasal cavity. In these respects the rostrum is unspecialized and different from the rather shallow and abbreviated rostrum of *Embolotherium andrewsi* or the elongate *Tapirus*-like rostrum of *Embolotherium grangeri*. PIN 3109-40 has a less completely preserved rostrum; its dorsal surface appears to have been flatter than that of PIN 473-311, although it is so incomplete that I am not confident that the shape of this specimen can be accurately interpreted.

The entire dorsal surface of the skull of *Protembolotherium efremovi* is concave (saddle-shaped) though not as deeply as that of *Embolotherium andrewsi*. The parasagittal ridges extend along the sides of the skull from the postorbital process of the frontal bone to the upper corner of the occiput. These ridges are not as prominent as those of *E. andrewsi*. From a dorsal view the parasagittal ridges are widely separated and they barely constrict the dorsal surface posteriorly.

In the holotype (PIN 473-311), the zygomatic arches are massive and laterally expanded, with a large swelling at the junction of the jugal and squamosal bones. From the dorsal view the zygomatic process of the jugal is relatively straight anterior to the swelling and it projects posterolaterally. The degree to which the zygomatic arches bow out laterally is intermediate between *Embolotherium andrewsi* on the one hand, in which the jugal processes project in a predominantly posterior direction, and *Embolotherium grangeri* on the other, whose zygomatic arches are more strongly bowed. The remaining skulls of *Protembolotherium efremovi* demonstrate conspicuous intraspecific variation in the size of the zygomatic swellings. In both PIN 473-310 and PIN 3109-40 the zygomatic arches are thinner with lesser amounts of swelling in the center of the arch. Similar intraspecific variation in the thickness of the zygomatic swellings is documented in other species that possess such swellings and probably represents sexual dimorphism (Mihlbachler et al., 2004b). From lateral views of the skulls the jugal portion of the zygomatic arch anterior to the swelling is shallower than the squamosal portion of the zygomatic arch. There is a small ventral flange on the jugal below the massive swelling. The jugal portion of the zygomatic is essentially horizontal while the squamosal portion is angled slightly upward, thus giving the zygomatic arch a weak curvature.

From a dorsal view the nuchal crest is thickened with posterolaterally angled wing-like expansions. The posterior margin of the occiput is concave, although it lacks the deep median notch seen in *Embolotherium andrewsi*. The overall degree of robustness of the occiput is more or less typical of large horned brontotheres, although it is not nearly as massive as the occiput of *E. andrewsi*. From a lateral view the occiput is rather short and it is not as strongly tilted backward as the occiputs of *E. andrewsi* and *E. grangeri*. The best-preserved occiput is that of PIN 3109-40. The dorsal margin of the occiput is slightly concave, the width of the

occiput is slightly constricted in the middle, and the dorsal and ventral portions of the occiput are of similar width. The posterior surface of the occiput has two distinct but relatively weak occipital pillars with a shallow central depression between them. It these respects the occiput most closely resembles *E. grangeri*.

The ventral surface of the skull of *Protembolotherium efremovi* can only be described from the holotype (PIN 473-311) (fig. 116). The anterior margin of the posterior nares is positioned near the posterior margin of M3; this position is slightly more anterior to the posterior nares than those in *Embolotherium andrewsi* and *E. grangeri* in which the anterior margin is typically a short distance behind M3. Other characteristics of the ventral surface of PIN 473-311 are essentially indistinguishable from *E. andrewsi* and *E. grangeri*. The anterior and lateral sides of the posterior narial opening are rimmed by a wide U-shaped emargination. The ridge demarcating this emargination is faint, but it can be seen upon examination of the specimen. This emargination is widest on the anterior margin and tapers along the lateral margins. The vomer, which would have bisected the posterior narial canal, is not preserved although a remnant in the form of a small ridge of bone can still be seen running along the upper (dorsal) surface of the posterior narial canal. The posterior narial canal seems to intrude slightly into the sphenoid bone (a typical condition of brontotheres), but large sphenoidal pits like those of *Metatitan* or *Protitan*, for instance, are not present in *P. efremovi*. The basicranium seems rather narrow, although this effect is exaggerated because part of the right side is broken away. The total width of the basicranium at the position of the mastoid processes does not exceed the distance across the right and left M3s and the basicranium is not nearly as widened as in *Metatitan*. The configuration of the basicranial foramina is typical as well with a widely separated foramen ovale and foramen lacerum. The mastoid process is shorter than the postglenoid process and it curves anteroventrally forming a tube-shaped external auditory pseudomeatus. (This character can also be seen in PIN 3109-40.) The external auditory pseudomeatus extends into the basicranium in a posteromedial direction, a condition shared with *E. andrewsi* and *E. grangeri*.

Upper Dentition: Of the three known skulls of *Protembolotherium efremovi* only the holotype (PIN 473-311) includes upper dentition, consisting of an incomplete set of moderate to heavily worn and rather poorly preserved upper teeth, which includes the right P2–M3 and the left P3–M3 (fig. 116). Neither the upper incisors nor their alveoli are preserved. The crowns of the canines are not preserved, although bits of the roots of both right and left canines remain inside their alveoli. The canines appear to have been small though well developed. Apparently the canines have not reached the tiny essentially vestigial state seen in *Embolotherium andrewsi*. The transverse distance across the roots of the canines is about the same as the distance across the P1s, further indicating that the rostrum is not as reduced as that of *E. andrewsi*. (In *E. andrewsi* the transverse distance across the canines is notably less than that of the P1s.) Like *E. grangeri* there is a short postcanine diastema, although unlike *E. grangeri* the width of the rostrum is not constricted at this point.

The P1s are missing although well-preserved alveoli indicate that single-rooted P1s were present in life. The remaining premolars are nearly rectangular in outline with nearly parallel anterior and posterior margins. The parastyle of P2 is missing. The parastyles of P3 and P4 are directed anterolabially. The metastyles of the P2, P3, and P4 are essentially straight. Minor labial paracone ribs can be found on P3 and P4 (P2 is too damaged to discern this character). The labial paracone rib of P3 is broader than that of P4. None of the premolars has a distinct mesostyle. Labial cingula are discernable on the premolars, but they are very thin and poorly developed.

The lingual features of P2 consist of a protocone and nearly equally sized hypocone. Each of these cusps is embedded in a strongly developed lingual connecting crest. The connecting crest arches around the anterolingual corner of the crown forming a small preprotocrista. The protocone of P3 is a well-developed tall cusp, while the hypocone is significantly smaller. The lingual

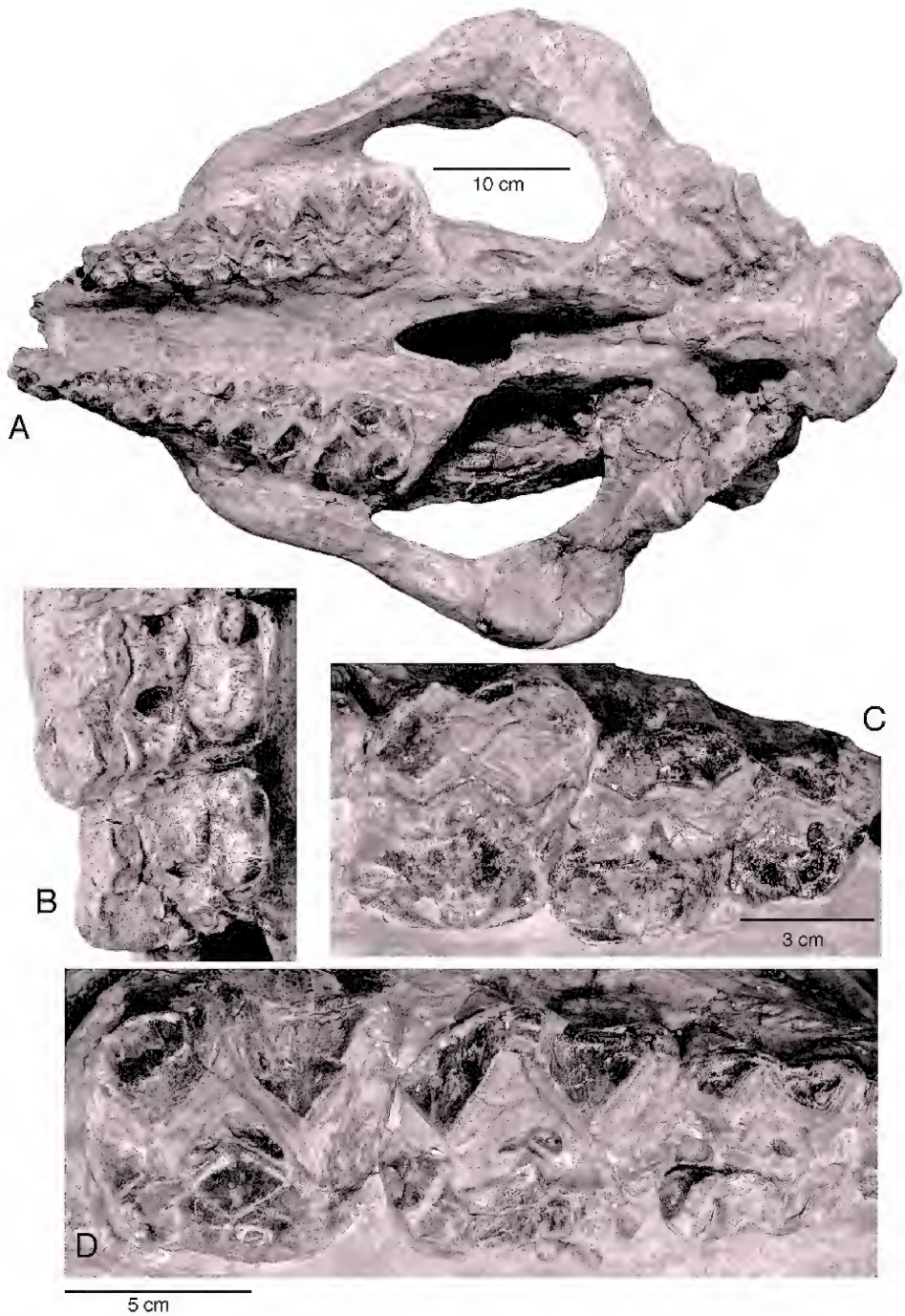

Fig. 116. The holotype skull of *Protembolotherium efremovi* (PIN 473-311). **(A)** Ventral view, **(B)** left P3–P4, **(C)** right P2–P4, **(D)** right molars.

morphology of P4 is similar to that of P3, although the hypocone is more completely disconnected from the protocone. The protocone and hypocone of P3 are barely connected by a poorly developed lingual crest. Preprotocristae are not discernable on either P3 or P4, indicating that they were either absent or so poorly developed that

they have been worn off. The lingual premolar cingula tend to be discontinuous or barely continuous around the lingual margins of the protocones and they tend to be particularly thick next to the hypocones, most notably on P4.

The upper molars are heavily worn and fragmented although many typical brontotheriine traits can be discerned on them, including tall (though now very worn) and lingually angled ectolophs, very weak (and on some teeth absent) labial ribs, thin lingual ectoloph enamel, and wedge-shaped lingual sides of the paracone and metacone in the least worn molars. The anterior cingulum (though impossible to see on the photographs) is thin and passes proximally to the apex of the parastyle. Deep central molar fossae and tall anterolingual cingular cusps are present. Parts of the central molar fossae can still be seen on all three molars. The anterolingual cingular cusp, however, is completely worn away on the M1s, but it is still discernable on M2 and M3. There are no traces of paraconules or metalophs on any of the molars. Both right and left M3 appear to have had a rather small hypocone. Labial molar cingula are very weak and lingual molar cingula are mostly absent or have been worn off. A very thin cingulum appears to wrap around the anterolingual corner of M3.

Remarks

Yanovskaya (1954) initially described *Protembolotherium efremovi* from two skulls and a variety of other specimens from the late Eocene Ergilin Dzo Formation of Outer Mongolia. *P. efremovi* is a large Asian brontothere that is most easily recognized by its *Embolotherium*-like "battering ram" that protrudes upward from the anterior end of the skull, as well as an autapomorphic pair of short secondary horns that are positioned above the orbits. It is a curious fact that Yanovskaya (1954) assigned holotype status to a skull, PIN 473-311, in which the frontonasal portion, and consequently all evidence for these diagnostically useful characters, is not preserved. Another skull (PIN 473-310) that preserves the battering ram and secondary horn was referred to *P. efremovi* by Yanovskaya (1954). Decades later, Yanovskaya (1980) referred a third skull (PIN 3109-40) from Ergilin Dzo to *P. efremovi*. This specimen is unique in retaining an anteriorly projecting nasal process at the peak of the ram.

In addition to these three skulls several additional fragmentary specimens were initially referred to *Protembolotherium efremovi* (PIN 473-139, 473-141, 473-216, 473-217, 473-397, 473-654, 473-656, PIN 473-708) by Yanovskaya (1954). I was unable to find these additional specimens in the PIN collection, however, I am reasonably certain that it would be difficult or impossible to narrow down the specific identity of most of them due to their fragmentary condition. One of these, PIN 473-139, is a partial mandible with left p2–m2 that Yanovskaya (1954: fig. 7 and pl. 3) figured; however, based on these figures I am unable to differentiate that specimen from mandibles of *Embolotherium andrewsi* or *E. grangeri*. Presently, there are no mandibles or lower dentitions associated with diagnostic *P. efremovi* fossils.

To summarize, the specimens that are relevant to the diagnosis and characterization of *Protembolotherium efremovi* are three skulls: the holotype (PIN 473-311) is missing the entire frontonasal region; a second specimen (PIN 473-310) has an *Embolotherium*-like ram and an additional horn above the orbit. Finally, the third specimen (PIN 3109-40), in addition to having a ram and additional horns, retains a short nasal process projecting from the peak of the ram. It is necessary to assess the cranial morphology of the type (PIN 473-311) in more detail to determine what features (if any) distinguish it from other brontothere species, and if there is truly enough evidence to conclude that the remaining skulls (with the more diagnostic elements that are not preserved in the type) are indeed the same species as the type.

Despite the lack of preservation of the ram in the type (PIN 473-311), certain characteristics of this specimen show a combination of states very similar to *Embolotherium andrewsi* and *E. grangeri*; this includes the very widened dorsal cranial surface, the fully saddle-shaped skull, prominent swellings in the zygomatic arches, the high relief of the lingual premolar cusps, the relatively deep

central molar fossa, and the well-developed anterolingual cingular cusps on the molars and the sharp posteromedial angle of the external auditory pseudomeatus. No other brontotheres share this last condition except two small North American brontotheres (*Dolichorhinus*, *Sphenocoelus*) that are otherwise clearly very different from PIN 473-311. Therefore, it is evident that the type of *P. efremovi* belongs to an *Embolotherium*-like species.

On the other hand, the type of *P. efremovi* exhibits a number of features that are structurally very different from both *Embolotherium andrewsi* and *E. grangeri*. For instance, the skull is not as deeply saddle-shaped. The occiput is shorter and not tilted backward to the degree seen in *E. andrewsi* or *E. grangeri*. In other respects the occiput is similar to *E. grangeri*, but it is not nearly as massive as that of *E. andrewsi*. The nuchal crest is not as thick and rugose, the occipital pillars are not nearly as prominent, and the dorsal portion of the occiput is not broader than the ventral portion. Further differences with *E. andrewsi* include the much less prominent parasagittal ridges and more laterally bowed zygomatic arches. The rostrum differs substantially from both species of *Embolotherium*. The dorsal margin of the rostrum is steeply sloped posterodorsally, so that the rostrum deepens proximally while those of *E. andrewsi* and *E. grangeri* do not. Furthermore, the rostrum of *P. efremovi* is much broader than that of *E. andrewsi*. At the same time, the rostrum of PIN 473-311 is not nearly as elongate as that of *E. grangeri* and there is no constriction at the postcanine diastema. Moreover, the nasal cavity of *E. grangeri* is much longer with the nasal incision extending above the orbits, whereas in PIN 473-311 the nasal incision appears to be entirely anterior to the orbit. Finally, though they are not completely preserved, the canines of PIN 473-311 seem larger and more developed than the globular incisiform or cuplike vestigial canines of *E. andrewsi* and *E. grangeri*.

The additional skulls referred to *Protembolotherium efremovi* (PIN 473-310 and 3109-40), to the extent that they are preserved, share the same combination of similarities and differences with *Embolotherium andrewsi* and *E. grangeri* that are seen in the type specimen of *P. efremovi* (PIN 473-311). Based on the morphological congruence of these three skulls it is probable that they represent the same species. Unfortunately, it is not feasible to compare the type of *P. efremovi* with *Nasamplus progressus* from the "Ulan Gochu" faunal zone (sensu Radinsky, 1964) of Inner Mongolia, a species known only from a single cranial fragment. However, the two skulls referred to *P. efremovi*, PIN 473-310 and PIN 3109-40, are quite distinct from *Nasamplus*, primarily (to the extent that they can be compared) because of their well-developed rams with diminished (or absent) nasal processes.

Protembolotherium efremovi is the third valid species found to possess the "battering ram" that was first discovered in the genus *Embolotherium*. The extremely derived and bizarre ram structure was initially interpreted by Osborn (1929b) as having a separate origin from the paired frontonasal horns of other brontotheres. Later Granger and Gregory (1943) interpreted the ram as homologous with the frontonasal horns of other brontotheres. More recently reported evidence suggests that Granger's and Gregory's (1943) idea is the better hypothesis (Mihlbachler et al., 2004a; Mihlbachler and Solounias, 2004). The evolution of the ram of *Embolotherium* and *Protembolotherium* is best explained by a morphological transformation series starting from a condition similar to that of *Metatitan* where the paired frontonasal horns and the free end of the nasal process are elevated on a frontonasal pillar. The ram itself is a grossly amplified frontonasal process that initially formed the base of the horns and the frontonasal pillar, the portion of the skull upon which the horns rested. The original free end of the nasal process is lost or, in the words of Granger and Gregory (1943), "absorbed" by the ram. The distal surface of the ram is homologous to the peaks of the frontonasal horns, fused into a transverse crest. Some evidence for this is seen in the apparent remnants of a sutural pattern of facial bones in *Embolotherium andrewsi* and *Nasamplus progressus*. *Nasamplus* represents an intermediate condition one step derived from *Metatitan* and *Aktautitan*, in which the frontonasal horns have been

fused into a single transverse crest at the top of an enlarged frontonasal process, but the free end of the nasal process is still present and unreduced. *Protembolotherium efremovi* represents a further derived condition in which the ram is more fully developed, although it is still shorter than that of *E. andrewsi* and has shallower lateral margins that do not constrict the nasal cavity as strongly. Perhaps more significantly, the process that protrudes from the peak of the ram of PIN 3109-40 seems to be the reduced remnant of the free end of the nasal bone. If this interpretation is correct the small horn-like protuberances above the orbits of PIN 3109-40 and PIN 473-310 are secondary horns and they are not homologous with the paired frontonasal horns of other horned brontotheres.

If Yanovskaya (1954, 1980) and I are correct in referring PIN 3109-40 and PIN 473-310 to the same species, this implies that the nasal process, which is still present in *Nasamplus* but lost or absorbed in *Embolotherium*, was occasionally present in a diminished state (PIN 3109-40) but also was occasionally absent (PIN 473-310) in *Protembolotherium efremovi*. It seems obvious that, as with *Embolotherium*, the ram of this species would have undergone considerable ontogenetic change throughout life. After all, it seems very unlikely that embolotheres could have given birth to calves with fully developed rams. It is entirely possible that the loss of an already diminished nasal process was part of the ontogenetic process. Unfortunately, both PIN 473-310 and PIN 3109-40 are edentulous, rendering it impossible to determine the relative ontogenetic ages of these skulls even though the lack of unfused sutures in these skulls suggests that all of the skulls were well into their adult years. The North American species *Megacerops coloradensis* (sensu Mihlbachler et al., 2004b) is known from hundreds of specimens and exhibits considerable variation in the size and shape of the nasal process. In that species the variation is clearly related to the size of the frontonasal horns (Mihlbachler, 2004). In smaller specimens of *M. coloradensis* with more gracile horns the nasal process is well developed and takes on more typical proportions; however, in many of the larger specimens with huge swollen frontonasal horns the nasal process is reduced to a small triangular remnant and most of it seems to have been absorbed by the bony growth related to the massive horns. In *Megacerops*, this variation seems related to sexual dimorphism. Given these possible explanations (ontogeny, sexual dimorphism) for variation in the nasal process, it is difficult to justify the differences between PIN 473-310 and PIN 3109-40 as taxonomically significant (i.e., indicating two species). Therefore I presently accept Yanovskaya's (1954, 1980) conclusions that these specimens are conspecific and that both belong to *Protembolotherium efremovi*.

Embolotherium andrewsi Osborn, 1929b

HOLOTYPE: AMNH 26001, a skull missing the premaxillomaxillary rostrum and right zygomatic arch, with fragmentary right M2–M3 and left M3.

TYPE LOCALITY: "Ulan Gochu", Urtyn Obo, "middle white" or "gray" beds, 125 feet below Baron Sog unconformity, Shara Murun Region, Inner Mongolia, China. (Ulan Gochu [used in quotes] denotes uncertain correlation with the type Ulan Gochu beds at Baron Sog and refers to a faunal zone rather than a formation. [Radinsky, 1964])

AGE: Late Eocene (Ulangochuian land mammal "age").

SYNONYMS: *Embolotherium ultimum* Granger and Gregory, 1943; *Embolotherium ergilense* Dashzeveg, 1975.

REFERRED SPECIMENS: **(From the "Ulan Gochu" fanual zone [sensu Radinsky, 1964] of the Shara Murun Region, Urtyn Obo and East Mesa, Inner Mongolia)** AMNH 20352, an occipital fragment; AMNH 26011, a left mandibular ramus and symphysis with right p3 and p4 (partial), left p3–p4 (partial), and m1–m3; AMNH 26000 (specimen lost, but photos exist in vertebrate paleontology archives at the AMNH), a skull with right P1–M3 and left P2–M3; AMNH 26003, a skull with right P2–M3 and left C–M3; AMNH 26006, a left ramus with p2–m3; AMNH 26007, a partial mandible with partial right ramus and complete left ramus with right p2–p4, left p2 (partial), and p3–m3; AMNH 26008, a right ramus with p2–m3; AMNH

26009, a skull with right I1–M3, left I2 (?), P1–M3, and a mandible with right i1, i2–i3 (roots), c–m3, left i2, i2–c (roots), and p2–m3; AMNH 26010, a crushed skull missing the frontonasal process with right I3–M3 and left C–M3; IVPP V11959, a skull with right P2–P4, M2–M3, left M2–M3, and a mandible with right i1?, p2–m3 and left i1–i3, and p2–m3; PIN 2200-1, an edentulous skull; PIN 2200-2, a mandible with right and left m3; **(from the Baron Sog Formation at Baron Sog Mesa, Inner Mongolia)** AMNH 21604 (holotype of *Embolotherium ultimum*), a crushed basicranium with right M2 (partial) and M3; AMNH 22114: left maxillary fragment with P3–P4, M1 (partial); **(from the Ergilin Dzo Formation, Outer Mongolia)** National Museum in Ulan-Bator, item 10 (holotype of *Embolotherium ergilense*), a skull missing the premaxillae and most of the maxillary dentition.

DIAGNOSIS: *Embolotherium andrewsi* is a very large brontothere with a tall and nearly vertical process of bone ("ram") that originates above the orbits and appears to be composed of the frontal and nasal bones. At the peak of the ram is a rugose transverse crest that forms the distal margin of nasal channel that runs along the anteroventral surface of the ram. The nasal incision extends posteriorly to the anterior margin of P4. The orbits are positioned above the M2 and the posterior portion of M1. A horizontal nasal process is absent. The premaxillomaxillary rostrum is small and short, it slightly thickens posteriorly, and is not enclosed by bone dorsally. A pair of tall, thin bony ridges is seen on the dorsal surface of the rostrum. Other cranial characteristics include a deeply saddle-shaped cranium, an extremely robust occiput, very prominent parasagittal ridges that overhang the sides of the cranium and do not constrict the dorsal surface of the skull posteriorly, and weakly curved zygomatic arches with massive swellings. The external auditory pseudomeatus enters the skull in a posterolateral direction and is ventrally constricted. The posterior nares are shifted behind M3. Large ventral sphenoidal fossae are absent.

Dentally, *Embolotherium andrewsi* has three very small incisors that form a semicircular row. The canines are irregular and they are not always fully erupted. There is a distinct P2 metacone. Hypocones are present on P2–P4 and strongly connected to the protocone by lingual crests. The molars of *E. andrewsi* have tall, lingually angled ectolophs with weak labial ribs, and thinned lingual ectoloph enamel with wedge-shaped paracones and metacones. A cingular parastyle shelf is absent. Deep central molar fossae and large anterolingual cingular cusps are present. Paraconules and metalophs are absent. The lower dentition of *E. andrewsi* includes three small incisors that form an arch anterior to the canines. Metaconids are present on p3, p4, and occasionally on p2. The p2 trigonid is only marginally longer than the talonid. The lower molars have deep valleylike basins and m3 is elongate.

Embolotherium andrewsi can be distinguished from *E. grangeri* in the following ways: ram more vertical, positioned above orbits; nasal channel of ram distally emarginated; rostrum and incisors much smaller; dorsal premaxillary ridge smaller; occiput more massive; zygomatic arches not strongly bowed laterally; parasagittal ridges more prominent; premolar hypocones less strongly separated from protocones; M3 hypocone is smaller; and cingulum of M3 continuous around the distolingual corner of the crown.

DESCRIPTION

SKULL: The holotype of *Embolotherium andrewsi* (AMNH 26001) is a very large skull that is missing the left zygomatic arch, the rostrum, and most of the dentition (fig. 117). Except for the missing portions, the skull is well preserved and undistorted. A few areas are filled in with plaster where the skull surface is not preserved. In particular, the dorsal surface of the skull is made up of numerous fragments with small plaster-filled gaps between them, although more intact specimens show a similar morphology. More complete skulls of *E. andrewsi* include AMNH 26003 (fig. 118b, c, and fig. 119a), AMNH 26009 (fig. 118a, and see Mihlbachler et al., 2004a: fig. 19k, l), and IVPP V11959 (see Wang [2000] for figure). (Note that the published photo of AMNH 26003 in Osborn [1929b: fig. 5] is unreliable because the

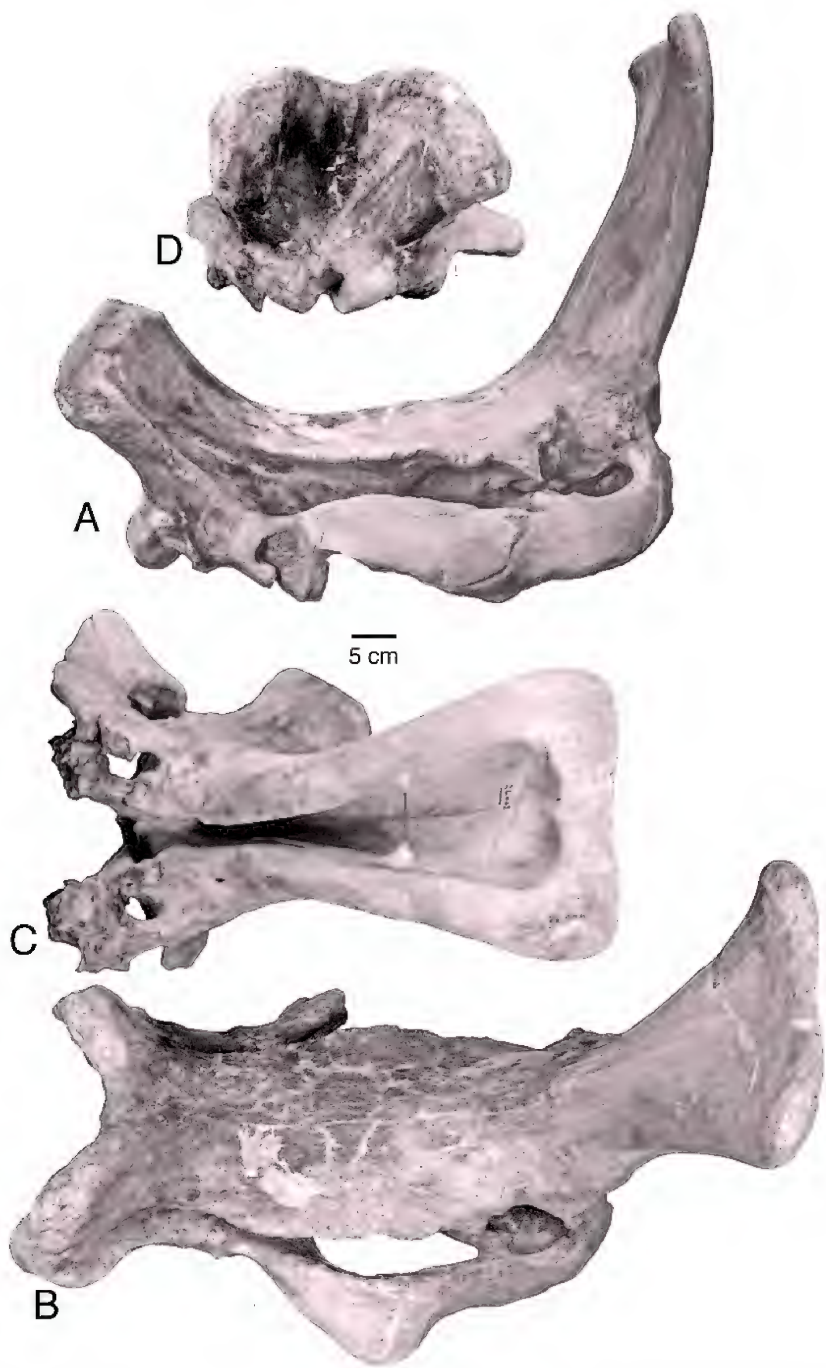

Fig. 117. The holotype specimen of *Embolotherium andrewsi* (AMNH 26001). **(A)** Right view, **(B)** dorsal view, **(C)** anterior view, **(D)** posterior view.

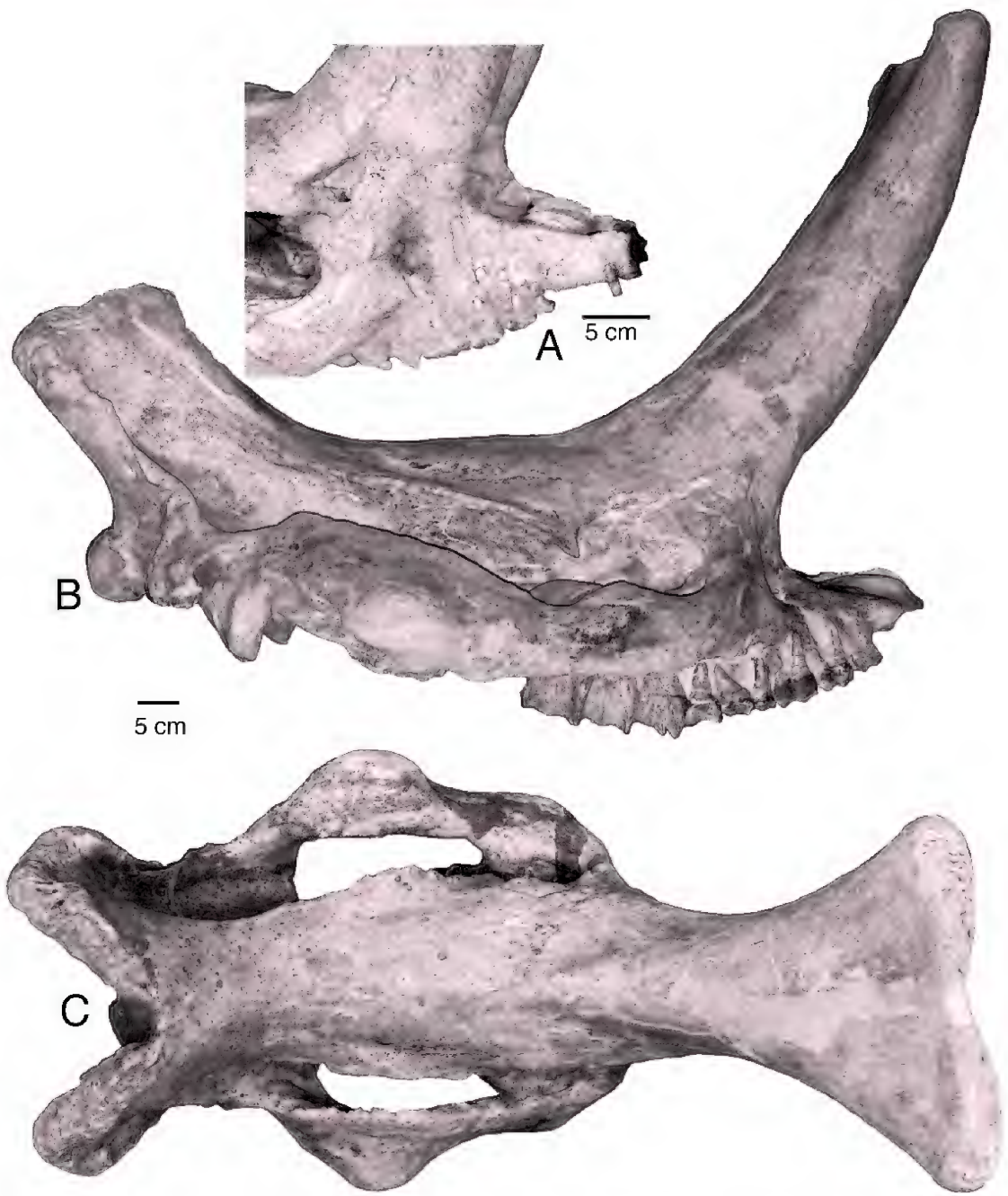

Fig. 118. Skulls of *Embolotherium andrewsi*. **(A)** right face of AMNH 26009, **(B)** Right view of AMNH 26003, **(C)** dorsal view of AMNH 26003.

specimen was actually photographed while it was wrapped with plaster).

Embolotherium andrewsi is one of the largest brontotheres, rivaled in size only by *E. grangeri*, *Megacerops coloradensis* (sensu Mihlbachler et al., 2004b), and possibly *Gnathotitan berkeyi*. The most conspicuous feature of *E. andrewsi* is the large battering ram– like structure (henceforth referred to as the "ram") that has the superficial appear-

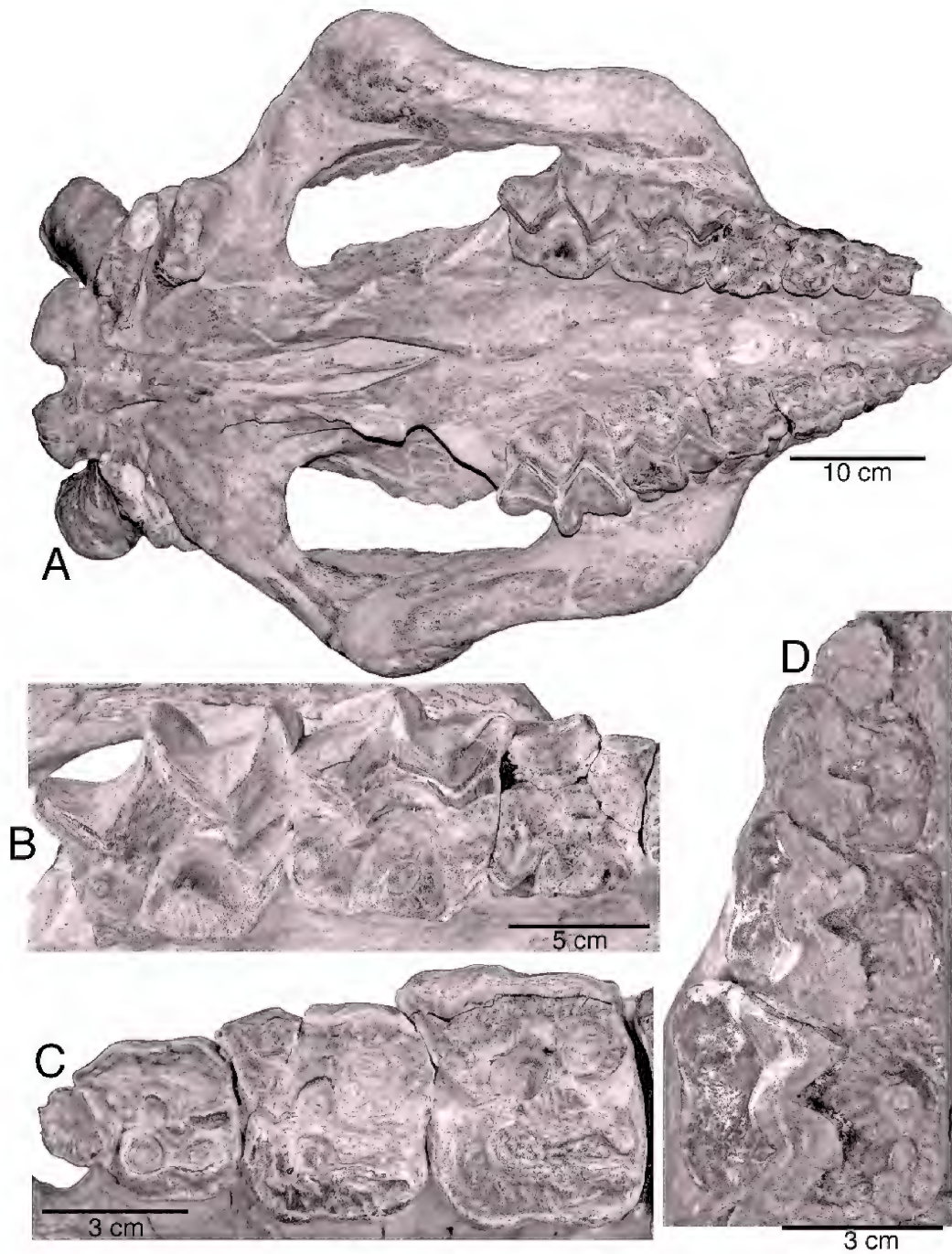

Fig. 119. Ventral view of skull and upper dentition of *Embolotherium andrewsi*. **(A)** Ventral view of AMNH 26003, **(B)** right molars of AMNH 26003, **(C)** left premolars of AMNH 26003, **(D)** right premolars of AMNH 26010.

ance of an enlarged and upturned nasal process. From the lateral view the ram originates just above the orbits. It curves posteriorly as it rises from the skull so that at its peak it is nearly vertical. The rams of the referred skulls tend to be less vertical than the holotype. The anteroventral surface of the ram is convex while the posterodorsal surface is concave. The ram broadens distally. A deep nasal channel runs along the anteroventral surface of the ram. The nasal channel is bordered laterally by deep and thick walls that line the side of the ram. Toward the proximal end of the ram the lateral sides are deep and constrict the nasal channel. At the distal end of the ram a thick rim of bone forms a distinct distal border for the nasal channel. The nasal channel broadens distally and is bifurcated slightly at the distal end by a short wedge of bone below the distal margin. The inner surface of the nasal channel is bisected its entire length by a thin ridge of bone that runs along the midline; this appears to represent the osteological marker for the cartilaginous nasal septum that extended to the distal peak of the ram (Mihlbachler and Solounias, 2004).

Reconstructions of *Embolotherium andrewsi* in Osborn (1929a, 1929b) depict the ram as a hornlike process, with the nostrils positioned very low in a normal rhinolike position just above the premaxilla. However, the deep channel on the anteroventral surface of the ram and the ossified marker for the nasal septum indicate that the nasal cavity extended to the peak of the ram. Wang (2000) depicted the nostrils as elevated to the peak of this structure although the true position of the nostrils is uncertain.

The distal margin of the ram forms a broad transverse crest that is marked by a coarse rugosity on the anterior and dorsal surfaces of the distal margin. The upper surface of the distal margin of the ram is slightly convex from the anterior view. From the dorsal view the distal margin is thinner medially and thicker laterally. Closer inspection of the peak of the ram reveals that in most specimens a weak but distinct groove on the posterolateral side of the distal rim continues down the side of the ram for several centimeters. The groove cannot be traced farther down the ram beyond a few centimeters from its peak; however, this groove resembles the frontonasal contact seen on the frontonasal crest of *Nasamplus progressus*. If this groove does represent a sutural remnant, then it indicates that the frontal bone rises to the peak of the ram and that the ram is actually a frontonasal process, with the posterodorsal surface formed from the frontal bone and the anteroventral surface from the nasal bone. This frontonasal process is structurally similar to those of *Aktautitan*, *Metatitan*, and *Nasamplus*, although it is much taller and more massive, as are those of *Protembolotherium efremovi* and *E. grangeri*. The actual nasal process (which normally extends horizontally from the peak of the frontonasal process) appears to have been lost in *Embolotherium andrewsi*.

Due to the large frontonasal ram the nasal incision of *Embolotherium andrewsi* is dorsoventrally very deep. In specimens such as AMNH 26003 and AMNH 26009, which have the premaxillomaxillary rostrum complete, the nasal incision extends posteriorly to the anterior margin of P4. The posterior margin of the nasal incision is anterior to the orbit, and unlike *E. grangeri* the nasal incision does not extend over the orbit. The orbits of *E. andrewsi* are positioned directly above the M2 and the posterior portion of M1. The anterolateral root of M1 is positioned directly below the anterior rim of the orbit.

The premaxillomaxillary rostrum is complete in AMNH 26003 and AMNH 26009, although more details can be seen in the latter. From a lateral view the rostrum of AMNH 26003 is strongly curved upward, but in AMNH 26009 the rostrum is straighter. Premaxillomaxillary sutures are not discernable on any specimen. As a whole, the premaxillomaxillary process is short, shallow, and narrow. It is small in comparison to those of *Protembolotherium efremovi* and *Embolotherium grangeri*. The rostrum deepens slightly posteriorly. The premaxillary symphysis is not ossified and the premaxillae are separated by a small median gap. On the dorsal surface of the rostrum of AMNH 26009 are two pairs of thin, roughened ridges of bone. The smaller pair is at the distal end of the rostrum and the larger pair is positioned at about the midpoint of the

rostrum. The medial surfaces of these ridges are flat. These ridges of bone probably served as osteological supports for the tall, cartilaginous nasal septum that would have extended to the peak of the ram, although they are not as thickened and rugose as the equivalent dorsal rostral ridges seen on *E. grangeri*.

The entire dorsal surface of the skull of *Embolotherium andrewsi* is deeply saddle-shaped. The parasagittal ridges are very prominent and greatly overhang the sides of the cranium. The extent to which the parasagittal ridges overhang the skull is most pronounced in the holotype (AMNH 26001) and not quite as pronounced in other specimens. From a dorsal view the parasagittal ridges are widely separated throughout their length, although they barely constrict the dorsal surface posteriorly.

The zygomatic arches are massive. From the dorsal view the zygomatic arches are essentially straight and parallel except for a large swelling at the junction of the jugal and squamosal bones. Among specimens of *E. andrewsi* the size of the swelling is variable. They are largest in AMNH 26001 and somewhat smaller in AMNH 26009 and AMNH 26010.

From the lateral view the jugal and squamosal portions of the zygomatic arch have similar depths. There is a small ventral flange below the massive swelling. The jugal portion of the zygomatic is essentially horizontal, although the squamosal portion is angled slightly upward, thus giving the zygomatics a weak curvature.

The occiput of *Embolotherium andrewsi* is far more massive than that of *E. grangeri* and *Protembolotherium efremovi* and rivals the occiputs seen in the largest specimens of *Megacerops* (sensu Mihlbachler et al., 2004b). From a dorsal view the nuchal crest is thick and rugose. It is also concave and very deeply notched medially. From a lateral view the occiput is strongly titled backward. From a posterior view the dorsal margin of the occiput is notched medially. The dorsal portion of the occiput is wider than the ventral portion. The lateral wings of the massive nuchal crest are supported by massive bony pillars and the center of the occiput is deeply recessed in the middle.

The ventral surface of AMNH 26003 is the most complete and best preserved among the available specimens (fig. 119a). The posterior nares of *Embolotherium andrewsi* are positioned completely behind the M3s in all specimens. Direct inspection of the specimens reveals a faint ridge of bone arching around the anterior and lateral margins of the posterior nares. This ridge indicates a horseshoe-shaped emargination similar to that seen, for instance, in *Metatitan relictus*, although in *E. andrewsi* this emargination is wider. The posterior narial canal itself is rather short in comparison to most other brontotheres. The vomer, which bisects the posterior narial canal, can be seen in AMNH 26003. The posterior narial canal seems to extend slightly into the sphenoid, but large ventral sphenoidal pits like those of *Protitan* or *Metatitan* are distinctly absent. The basicranium is not greatly widened or anteroposteriorly abbreviated like that of *Metatitan*. The configuration of the basicranial foramina is typical with a widely separated foramen ovale and foramen lacerum. The mastoid process is shorter than the postglenoid process and it curves anteroventrally, thus contacting the postglenoid process and forming a tube-shaped external auditory pseudomeatus. The external auditory pseudomeatus also extends into the basicranium in a posteromedial direction, a condition shared with *E. grangeri* and *Protembolotherium*, and a few other more primitive taxa such as *Rhinotitan kaiseni*, *Dolichorhinus*, and *Sphenocoelus*.

Upper Dentition: The teeth of the holotype (AMNH 26001) were not recovered except for some of the molars, but even these are fragmented. Therefore, the description of the dentition is based primarily on referred specimens, AMNH 26003 (fig. 119a–c), AMNH 26010 (fig. 119d), and AMNH 26009 (fig. 120).

The number of incisors is unreduced (three pairs). There are six intact small incisor alveoli (not shown) in AMNH 26010. The complete left incisor row is preserved in AMNH 26009. The incisors of *Embolotherium andrewsi* are very small, are separated by large gaps, project straight down, and form a semicircular row anterior to the canines. Because of the narrow premaxillomaxillary

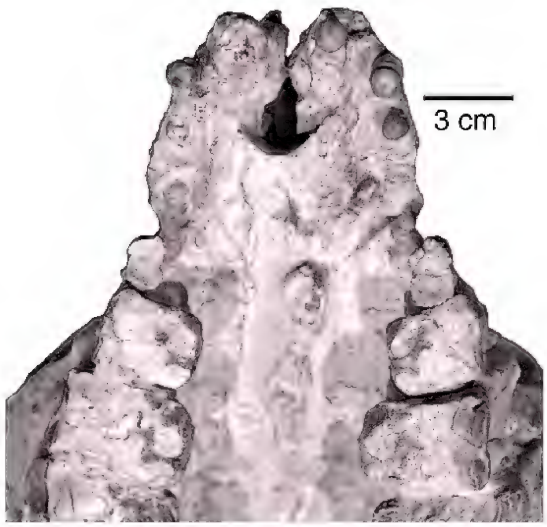

Fig. 120. Anterior upper dentition of *Embolotherium andrewsi* (AMNH 26009).

rostrum the diameter of the anterior tooth row is less than the width across the P1s. In AMNH 26009 a fragment of enamel is impacted into the left side of the palate medial to the diastema between I3 and P1. This is presumably a vestige of the canine. In AMNH 26003 and 26010 the canines are present, but they are only slightly larger than the incisors, and they appear to be only partially erupted, even though these specimens are clearly adults. The canine crowns have a peculiar cup-shape. The tendency for the canines to be small, highly irregular, and incompletely unerupted suggests that these teeth are truly vestigial.

In AMNH 26010 and AMNH 26003 there are very short diastemata between the I3 and canine, and between the canine and P1. Most of the available specimens of *Embolotherium andrewsi* exhibit heavy cheek-tooth wear. AMNH 26003 and AMNH 26010 have the least worn cheek teeth. The P1 is much smaller than the other premolars. The P1 crown is nearly as wide as it is long, but further details of its morphology are obliterated by wear. The remaining premolars are nearly rectangular in outline, although the anterior margins of the premolars are concave. The parastyle of the P2 is directed anteriorly, although the parastyles of P3–P4 are oriented anterolabially. The P2–P4 metastyles are heavily worn, but they appear to have been directed slightly lingually or they were straight. Very small labial paracone ribs are present on P2–P4. These ribs become progressively narrower in consecutively posterior premolars. None of the premolars has a mesostyle. Labial premolar cingula are generally very faint or absent.

The lingual features of P2 always include a protocone and a slightly smaller hypocone. Preprotocristae are absent or so weak that they are not readily discernable. In AMNH 26010 the hypocone of P2 is slightly smaller than the protocone and completely disconnected from it and there is no trace of a lingual crest. However, on AMNH 26003 the protocone and hypocone are connected by a lingual crest. In AMNH 26010, the P3 protocone and hypocone of P2 are more closely positioned and are fully connected by a wide, tall lingual crest. The crest absorbs the cusps to such a great degree that they are barely discernable as distinct cusps. In other specimens, such as AMNH 26003, the paracone and hypocone of the P3 are more widely separated and more distinct, but a tall lingual crest always connects them. In the P4 of AMNH 26010 the protocone and hypocone are distinct cusps, they are positioned closely together, the hypocone is slightly smaller than the protocone, and it is not connected to it by a lingual crest. In other specimens, such as AMNH 26003, a distinct P4 connecting crest is always present. The texture of the surface of the enamel on the lingual side of the premolars crowns varies from highly crenulated to smooth. The lingual premolar cingulum varies from continuous around the lingual side of the protocone to slightly discontinuous.

One specimen, AMNH 22114, a maxillary fragment with an unworn P3–P4, has a small crest of enamel that stretches from the posterior slope of the hypocone to the posterior cingulum. This crest is anomalous and does not appear on any other *Embolotherium andrewsi* specimen.

The upper molars of *Embolotherium andrewsi* show typical brontotheriine traits, including tall, lingually angled ectolophs (the ectolophs of *E. andrewsi* are among the tallest among brontotheres), very weak labial ribs, thin lingual ectoloph enamel, and

wedge-shaped lingual sides of the paracone and metacone in molars that are not heavily worn. The anterior cingulum is thin and passes proximally to the distal peak of the parastyle. Deep central molar fossae and large anterolingual cingular cusps are present. All evidence of paraconules and metalophs is lost. There is always a hypocone on the M3 of *E. andrewsi* although it varies in morphology from a functional cusp, though smaller and shorter than the paracone (e.g., AMNH 26003), to a series of two or three tiny cusps (e.g., AMNH 26010). Labial molar cingula are weak while lingual molar cingula are absent. The cingulum of the M3 continuously wraps around the distolingual corner of the crown in all specimens of *E. andrewsi*.

Mandible and Lower Dentition: Two *Embolotherium andrewsi* skulls are associated with mandibles, AMNH 26009 (fig. 121e, f) and IVPP V11959 (see Wang, 2000). Based on comparison with these mandibles several other mandibles are referable to *E. andrewsi*, including AMNH 26008, a specimen with lightly worn cheek teeth (fig. 121a–d). The horizontal ramus of AMNH 26008 is shallow but it deepens posteriorly. The inferior margin of the symphysis is angled slightly less than 45°. Overall, the ascending ramus is very short and the coronoid process is short and moderately curved backward. The symphysis, most nearly intact in AMNH 26009, is broad and extends to the m1 trigonid, but in other specimens it extends only to the p4 metaconid (e.g., AMNH 26008).

The incisors of AMNH 26009 are small and form a semicircular arch anterior to the canines. Only the crowns of the i1s are preserved, but they are so worn that they cannot readily be described although they appear to have been somewhat semispatulate. The less worn incisors of IVPP V11959 also suggest a semispatulate shape. The lower canines are fully erupted (unlike the upper canines which sometimes do not fully erupt) and they are not much larger than the lower incisors. The canine crown is blunt. All of the incisors, the canine, and the p1 are separated by very short diastemata. The anterior tooth row forms a broad semicircular arch. In other words, the canines are anterior to p1 and they are not shifted lingually as are the upper canines.

AMNH 26009 includes a small p1 although it is too worn to describe. No other specimen of *E. andrewsi* has a p1 preserved with it. The description of the remaining cheek teeth (p2–m3) is based on the more nearly pristine lower dentitions of AMNH 26006, AMNH 26007, and AMNH 26008. The trigonid of the p2 is only slightly longer than the talonid, but the talonids of p3 and p4 are somewhat longer than the trigonids. The talonids of p2–p4 are all wider than the trigonids. The paralophid and protolophid of the p2 are angled somewhat lingually, thus creating a narrow but long lingual trigonid notch. The trigonids of p3 and p4 are essentially molariform with fully lingually arched paralophids and protolophids and a deep and broad lingual notch. A small lingual bulge in the p2 at the junction of the protolophid and cristid obliqua of AMNH 26008 can be interpreted as a metaconid, although other specimens lack a distinct p2 metaconid. Large, lingually positioned metaconids can be found on the p3 and p4. The p2–p4 talonids of *E. andrewsi* have well-developed cristids obliqua and hypolophids. The talonid basins of the p2–p4 progressively broaden posteriorly and have deep talonid valleys similar to those of the molars. Labial premolar cingulids are weak while lingual premolar cingulids are absent.

The thin lingual enamel of the lower molars and the elongate m3 are typical brontotheriine characters. However, in *Embolotherium andrewsi* the trigonids and talonids of the lower molars form deep valleys rather than the broad shallow basins that characterize most other brontotheres. Lingual molar cingulids are absent and the labial cingulids tend to be discontinuous around the labial bases of the trigonids, talonids, and hypoconulid heel, but the cingulids can be relatively thick between them.

Embolotherium grangeri Osborn, 1929b

Holotype: AMNH 26002, a skull with right and left P1–M3, and three isolated upper incisors.

Type Locality: "Ulan Gochu", East Mesa, "middle red" beds, Shara Murun Region, Inner Mongolia, China. (Ulan Go-

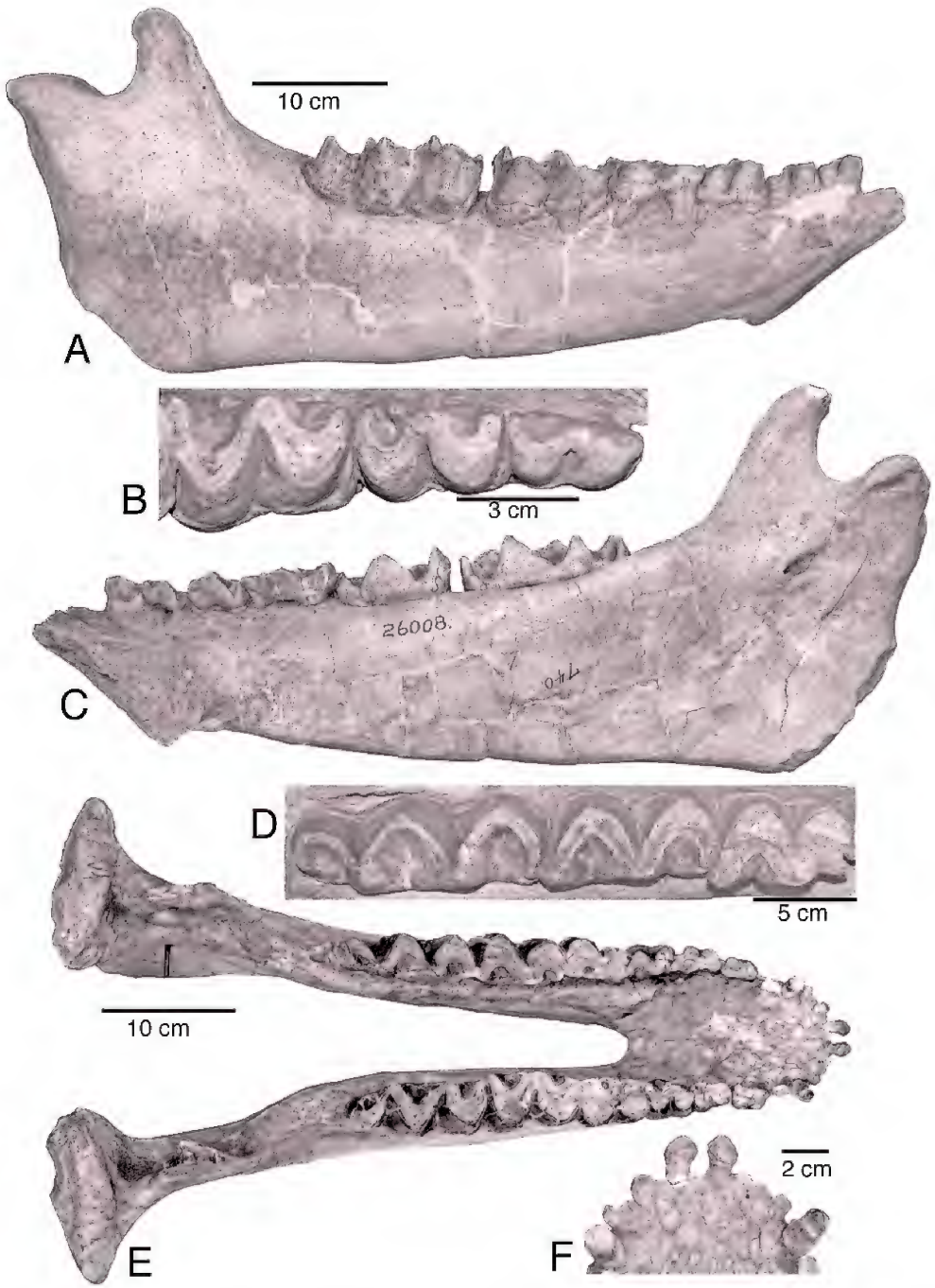

Fig. 121. Mandibles and lower dentition of *Embolotherium andrewsi*. **(A)** Right view of AMNH 26008, **(B)** right p2–p4 of AMNH 26008, **(C)** medial (lingual) view of right ramus of AMNH 26008, **(D)** left molars of AMNH 26008, **(E)** dorsal view of AMNH 26009, **(F)** lingual view of incisors and canine of AMNH 26009.

chu [used in quotes] refers to a faunal zone rather than a formation. [Radinsky, 1964])

AGE: Late Eocene (Ulangochuian land mammal "age").

SYNONYMS: *Embolotherium louksii* Osborn, 1929b; *Titanodectes ingens* Granger and Gregory, 1943; *Titanodectes minor* Granger and Gregory, 1943; *Embolotherium insigne* Yanovskaya, 1980.

REFERRED SPECIMENS: **(From the "Ulan Gochu" faunal zone [sensu Radinsky, 1964] of the Shara Murun Region, East Mesa, Inner Mongolia)** AMNH 26004, the complete ventral surface of a skull with left and right P2–M3 and the distal portion of the ram; AMNH 26040, the anterior portion of a juvenile skull with right DP2–DP4, M1, left P1, DP2–DP4, M1, an associated pair of premaxillae with unerupted incisors, numerous isolated deciduous incisors, and a mandible with canines and incisors (unerupted), right and left p1, dp2–dp4, and m1; **(from the "Shara Murun" Formation [sensu Radinsky, 1964] of the Shara Murun Region, East Mesa, Inner Mongolia)** AMNH 26005 (holotype of *Titanodectes ingens*), a mandible in three pieces, right ramus, left ramus, and a symphysis with right i1–m3, left i1–c, and p3–m3; AMNH 26132 (holotype of *Titanodectes minor*), a partial mandible with right p3–m1, left p2–m1, and a separate symphysis fragment with right i1–c and left i2–i3; (From the Ulan Gochu Formation of the Shara Murun Region, Baron Sog Mesa, Inner Mongolia) AMNH 21610 (holotype of *Embolotherium louksii*), a partial skull with erupting ?M3; **(from the "Baron Sog" Formation [sensu Radinsky, 1964] of the Shara Murun Region, East Mesa, Inner Mongolia)** AMNH 26018, a mandible fragment with right p4–m3 and isolated (?)left incisors and canine; **(from the Shara Murun Formation of the Shara Murun Region, Baron Sog Mesa, Inner Mongolia)** AMNH 21600, a mandible with right i1–i2, p2–m3, left i2–c, and p2–m3 **(from the Ergilin-Dzo Svita at Khoer Dzan, Outer Mongolia)** PIN 3110-52 (holotype of *Embolotherium insigne*), a partial skull with left molars. The PIN also holds a large but uncatalogued collection of *Embolotherium grangeri* from Khoer Dzan (to be described in a later publication), including skulls from individuals of numerous ontogenetic stages.

DIAGNOSIS: *Embolotherium grangeri* is a very large brontothere with a tall process of bone (ram) that rises from behind the orbits at approximately a 45° angle. The rugose transverse crest at the peak of the ram does not form a distal emargination for the nasal channel. The nasal incision extends above the orbits to the anterior margin of the M3. The orbits are positioned above M2. The premaxillomaxillary rostrum is long, deepens slightly proximally, and is not fully enclosed by bone dorsally. A thick U-shaped ridge of bone is seen on the dorsal surface of the premaxilla. Other cranial characteristics include a saddle-shaped cranium, an unthickened occiput, prominent parasagittal ridges that do not constrict the dorsal surface of the skull posteriorly, and weakly curved and laterally bowed zygomatic arches with massive swellings. The external auditory pseudomeatus enters the skull in a posterolateral direction and is ventrally constricted. The posterior nares are shifted posteriorly behind M3. Large ventral sphenoidal fossae are absent.

Dentally, *Embolotherium grangeri* has three relatively large but globular upper incisors that form a semicircular row. The canines are very small. There is a distinct P2 metacone. Hypocones are present on P2–P4 and are either weakly connected to the protocone by a lingual crest or they are completely separated from it. The molars of *E. grangeri* have tall, lingually angled ectolophs with weak labial ribs, and thinned lingual ectoloph enamel with wedge-shaped paracones and metacones. A cingular parastyle shelf is absent. Deep central molar fossae and large anterolingual cingular cusps are present. Paraconules and metalophs are absent. The lower dentition of *E. grangeri* includes three large semispatulate incisors that form an arch anterior to the canines. The i2 is the largest incisor. A metaconid is present on p3, p4, and occasionally on p2. The p2 trigonid is only marginally longer than the talonid. The lower molars have deep valleylike basins and the m3 is elongate.

Embolotherium grangeri can be distinguished from *E. andrewsi* in the following ways: ram less vertical, positioned behind orbits; nasal channel of ram not distally emarginated; rostrum and incisors much

larger; dorsal rostral ridge larger; occiput less massive; zygomatic arches strongly bowed laterally; parasagittal ridges less prominent; premolar hypocones more strongly separated from the protocones; M3 hypocone larger; and cingulum of M3 discontinuous around the distolingual corner of the crown.

Description

Skull: The holotype of *Embolotherium grangeri* (AMNH 26002) is a complete and nearly undistorted cranium with only minor fragments of missing bone that have been replaced with plaster (fig. 122). The most significant damage to the holotype specimen is a large crack on the dorsal and lateral surfaces of the skull just behind the base of the ram. The bone anterior to this crack is depressed about a centimeter, suggesting that the ram has been forced downward. However, comparison of this skull with other specimens seems to confirm that the angle of the ram is essentially intact. *Embolotherium grangeri* has never been described or figured from the fully prepared type specimen. Unfortunately, the only previously published photos and drawings of AMNH 26002 (Osborn, 1929a: fig. 797; 1929b: figs. 3b, 7) were made while the specimen was still in its plaster wrappings and some aspects of its shape in these older figures are misleading (relating to pieces of sediment that had been wrapped with the specimen). In addition to the holotype there is an additional adult specimen of a larger individual that consists of a ventral surface of the skull and the distal segment of the ram (AMNH 26004) (fig. 123), and three partial subadult skulls (AMNH 21610, AMNH 26040, and PIN 3110-52). *E. grangeri* is similar in size to *E. andrewsi* and shares with it a massive upturned ram. The ram of *E. grangeri* originates from behind the orbits, rather than from above as in *E. andrewsi*. The ram projects from the skull at approximately 45°. From a lateral view the ram is nearly straight, but it is slightly curved downward. The posterodorsal surface is convex and the anteroventral margin is slightly concave. Like *E. andrewsi* the lateral walls of the ram are deep and thick, forming a ventral nasal channel that runs to the distal end of the ram. The lateral walls are about the same depth throughout the length of the ram although they become slightly shallower distally. Proximally, the lateral walls are shallower than those of *E. andrewsi* and they do not constrict the nasal channel. A thin ossified ridge (osteological marker for the cartilaginous nasal septum) runs along the anteroventral surface of the ram and extends to the distal end. As in *E. andrewsi*, the nasal channel and ossified marker for the nasal septum indicate that the nasal cavity would have extended to the distal end of the ram, although the actual position of the nostrils is uncertain. However, because of the more posterior position of the ram and its shallower angle, the space between the ram and the rostrum is tremendous, suggesting an enormous nasal cavity (Mihlbachler and Solounias, 2004). The nasal channel is bifurcated distally by a wedge-shaped process that extends from the anteroventral surface at the distal end of the ram. The wedge-shaped process and distal bifurcation of the nasal channel is best seen in the ram of AMNH 26004 (fig. 123b). This structure appears as a median bulge from the dorsal view of AMNH 26002 (fig. 122b). The strong rim of bone that emarginates the distal end of the nasal channel in the ram of *E. andrewsi* is absent in adult specimens of *E. grangeri*. Instead, the nasal channel is open distally. However, like *E. andrewsi*, the distal surface of the ram is very rugose, particularly in AMNH 26004.

The ram of *Embolotherium grangeri* superficially resembles the nasal processes of other brontotheres. In particular, the lateral walls, deep ventral nasal channel, and distally widening shape resemble the nasal processes of brontotheres such as *Epimanteoceras formosus*, although the ram is obviously longer, more massive, and more steeply angled upward. There are no discernable sutures on any of the previously described specimens of *Embolotherium grangeri*, and this has led to some ambiguity in interpreting the structural makeup of the ram of *E. grangeri* (Mihlbachler et al., 2004a). However, the uncatalogued collection of *E. grangeri* from Khoer Dzan at PIN contains specimens that clearly reveal the ram of *E. grangeri* to be structurally homologous to the rams of *E.*

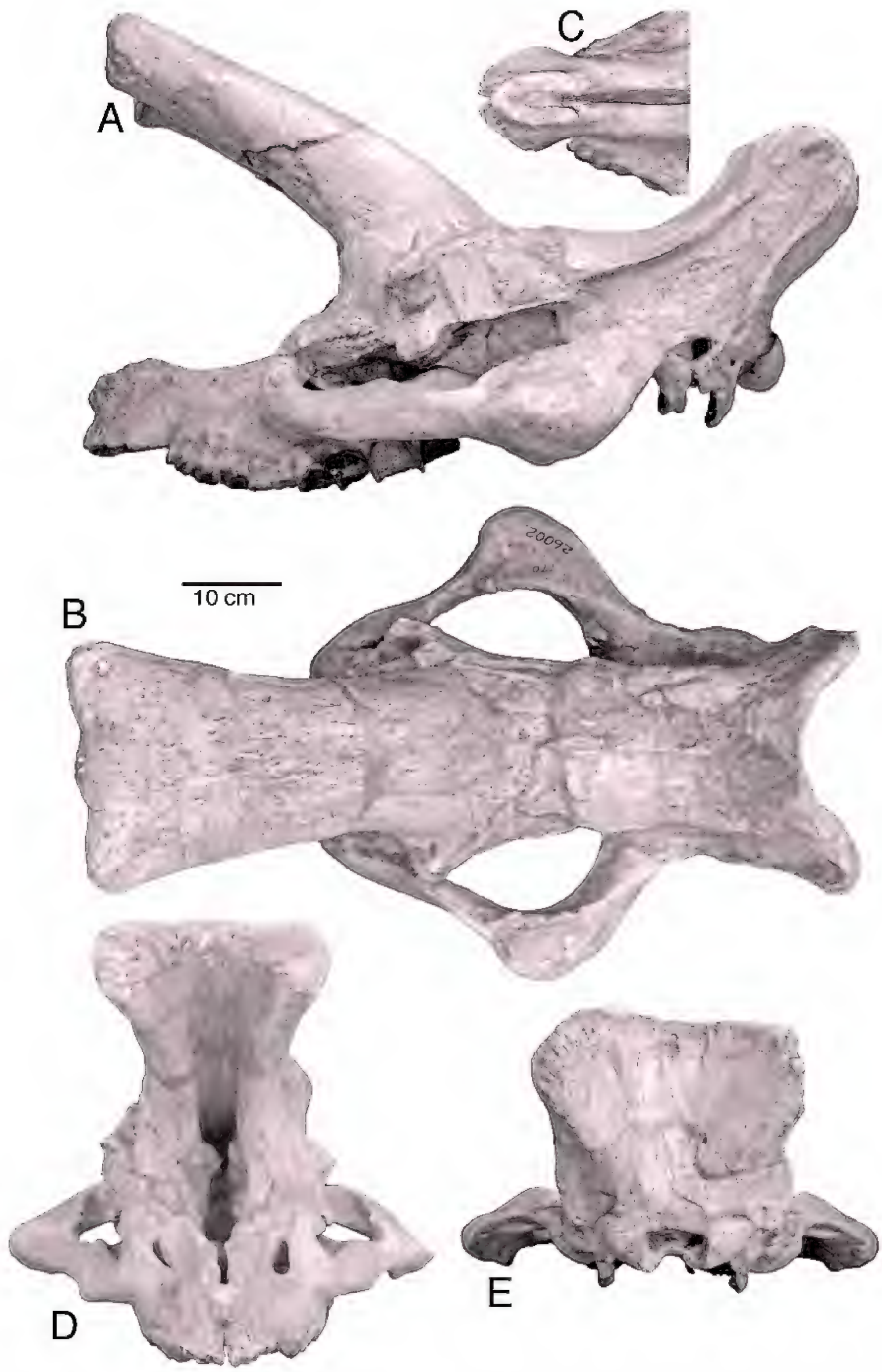

Fig. 122. The holotype of *Embolotherium grangeri* (AMNH 26002). **(A)** Left view, **(B)** dorsal view, **(C)** dorsal view of rostrum, **(D)** anterior view, **(E)** posterior view.

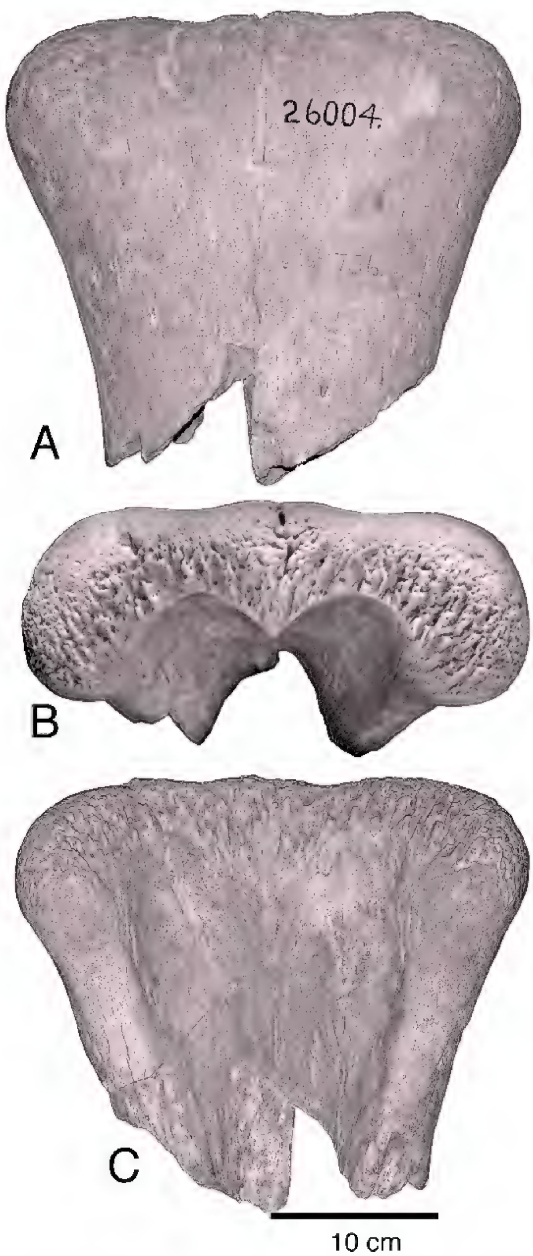

Fig. 123. Distal ram fragment of *Embolotherium grangeri* (AMNH 26004). **(A)** Posterodorsal surface, **(B)** distal surface, **(C)** anteroventral surface.

andrewsi and *Protembolotherium efremovi*, and with the paired frontonasal horns of other brontotheres.

The nasal incision of *Embolotherium grangeri* is very deep. The posterior margin of the nasal incision extends above the orbit and is directly above the anterior margin of M3. The orbit is positioned above M2, with the anterolateral root of M2 and posterolateral root of M1 situated below the anterior rim of the orbit.

The dorsal margin of the rostrum is long and deepens slightly posteriorly. The dorsal margin is nearly horizontal and does not rise above the midpoint of the orbit. The premaxillae are completely fused at the symphysis and the premaxillomaxillary sutures are not discernable. The premaxillary symphysis is nearly vertical. Above the symphysis is a tall and thick U-shaped ridge of bone. This ridge is thicker and more rugose than the anterodorsal rostral ridge seen in *Embolotherium andrewsi*. The sidewalls of the rostrum are parallel and constrict the dorsal opening of the premaxillomaxillary chamber to form an elongate narrow channel along the dorsal rostral surface.

The dorsal surface of the cranium is deeply saddle-shaped. The parasagittal ridges are widely separated throughout their length and do not significantly constrict the dorsal surface posteriorly. The parasagittal ridges are less prominent than those of *Embolotherium andrewsi* and only slightly overhang the sides of the cranium. The zygomatic arches of *E. grangeri* resemble those of *E. andrewsi* in having massive swellings at the junction of the jugal and squamosal. From a lateral view, the jugal portion of the zygomatic is horizontal and it is not as deep as that of *E. andrewsi*. The squamosal portion of the zygomatic is deeper and slightly sloped upward, giving the zygomatic arch a weak curvature. There is a small ventral flange below the large zygomatic swelling. From the dorsal view the zygomatic arch is thinner than that of *E. andrewsi* except for the large central swelling. Additionally, the zygomatics are more strongly bowed laterally.

From a lateral view the posterior end of the cranium is similar to that of *Embolotherium andrewsi*. The dorsal surface is strongly curved upward and the occiput is strongly tilted backward. However, the occiput and nuchal crest of *E. grangeri* are neither as massive nor as rugose as those of *E. andrewsi*. From the dorsal view of the skull the nuchal crest is concave, but it is not as deeply notched as that of *E. andrewsi*, and the

nuchal crest is comparatively thin. From the posterior view the occiput is nearly square. The dorsal margin of the occiput is essentially flat. The dorsal portion of the occiput is as wide as the posterior portion and the occiput is not constricted in the middle. The bony pillars on the surface of the occiput are not as massive as those of *E. andrewsi* and the central depression of the occiput is not as deep.

Like *Embolotherium andrewsi* the posterior nares of *E. grangeri* are positioned completely behind M3 (fig. 124a). Paired ventral sphenoidal fossae are absent. The proportions of the basicranium are essentially normal. The transverse width across the mastoid processes is less than the transverse distance across the M3s. The configuration of the basicranial foramina are typical, with a widely spaced foramen ovale and foramen lacerum. Like in *E. andrewsi* the external auditory pseudomeatus enters the skull at a posteromedial angle. The mastoid process is shorter than the postglenoid process; it curves anteroventrally, contacts the postglenoid process, and forms a tube-shaped external auditory pseudomeatus.

Upper Dentition: The description of the upper dentition of *E. grangeri* is based primarily on the holotype, AMNH 26002 (fig. 124), although important taxonomic information on the dental formula and morphology of the upper teeth of *E. grangeri* is provided by a juvenile specimen (AMNH 26040) that is discussed further below.

Although no incisors or canines are preserved within the holotype skull (AMNH 26002), the intact alveoli indicate an unreduced dental formula (3-1-4-3). The incisor and canine alveoli form a semicircular arch. The diameter of the anterior tooth row arch (measured transversely across the canines) is similar to the width across the P1s, so that the canines are positioned anteriorly to the P1s rather than anterolingually as in *E. andrewsi*. A small diastema is present between the I3 alveolus and canine. The sizes of the incisor alveoli indicate that the incisors were significantly larger than those of *Embolotherium andrewsi*.

Three complete isolated incisors that are consistent in size with the incisor alveoli of the holotype skull were assigned the same field number (770) and catalog number (AMNH 26002) (fig. 124d, e). The association of these incisors with the holotype is uncertain because the canine alveoli of the skull are filled with sediment, indicating that the incisors of the holotype must have fallen out of the skull before burial. The isolated incisors were probably found somewhere in close proximity to the skull, but they do not necessarily belong with the holotype. Nonetheless, similar incisors found in the juvenile skull (AMNH 26040; see below) confirm that these isolated incisors belong to the species *E. grangeri*. The ovoid-globular crowns are angled lingually. One of them has a small irregular lingual cingulum. Another incisor crown has a shallow pit on the lingual side of the crown apex and the third has a completely smooth surface. Otherwise, the crowns are essentially featureless and globular, although they are abnormally large in comparison to other brontotheres with similar globular incisors. Nonetheless, the absence of regular wear facets on these teeth suggests they may have been vestigial.

The canine alveoli of AMNH 26002 suggest that the canines were not much larger than the incisors, and the juvenile specimen described below (AMNH 26040) confirms this. The postcanine diastema is similar in length to the P2. The P1s are heavily worn, but the left P1 reveals a paracone, a metacone, and a small posteriorly shifted lingual heel with a small lophlike cusp. The remaining premolars (P2–P4) are nearly as rectangular (not oblique), although the anterior margins of these premolars are concave. The parastyle of P2 is angled slightly lingually. The parastyles of P3 and P4 are directed somewhat labially. The metastyles of these teeth are worn, but appear to have been straight or slightly curved labially. There are distinct but weak labial paracone ribs on each of these premolars, although they are relatively smaller on progressively posterior premolars. A mesostyle is not present on any premolar. Preprotocristae are not seen on the premolars of AMNH 26002. There are two distinct lingual cusps on P2–P4. The P2 hypocone is about the same size as the protocone and it is barely connected to it. The hypocones of P3 and P4 are slightly smaller then the protocones. These cusps are

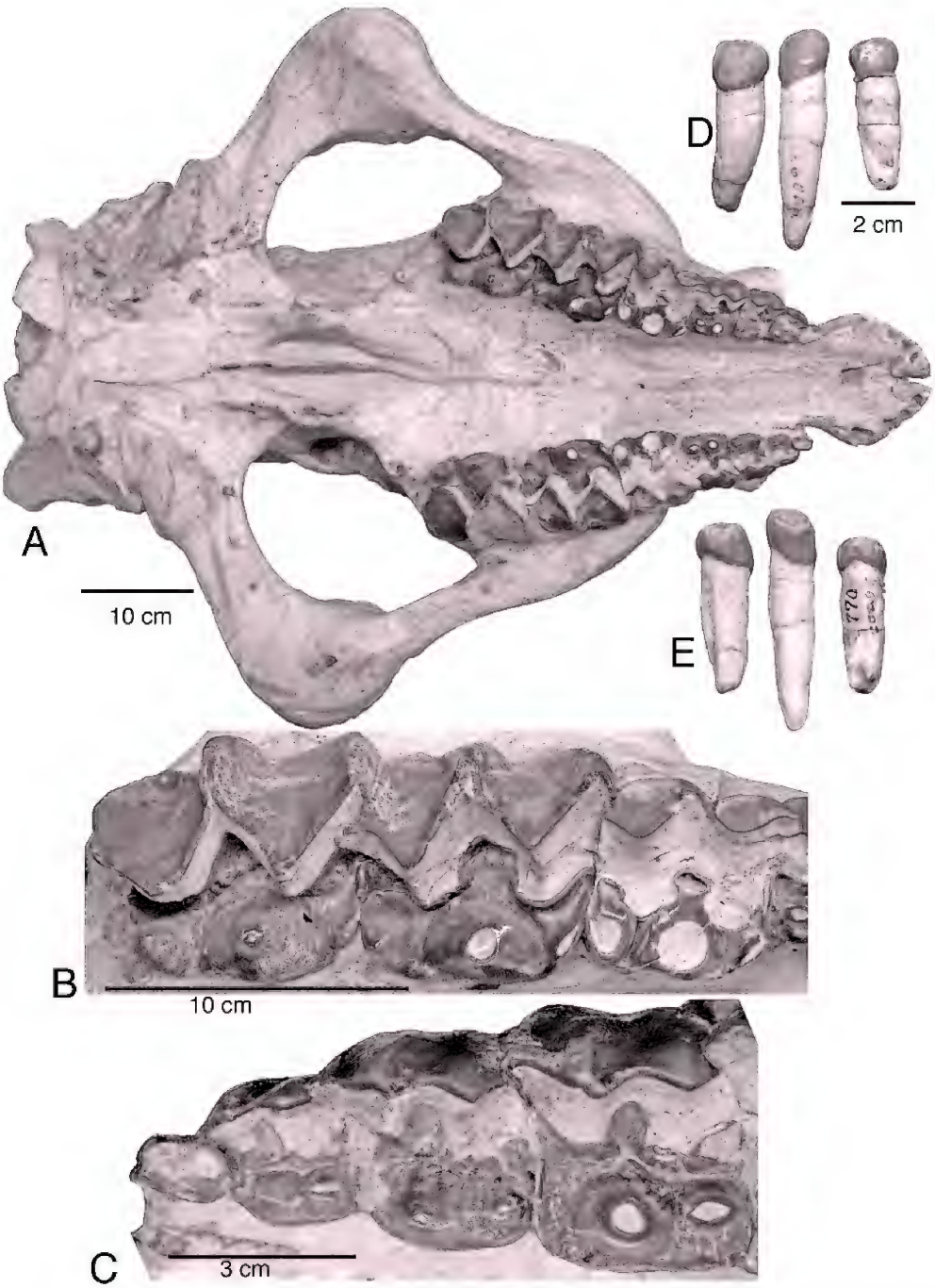

Fig. 124. Ventral view of skull and upper dentition of *Embolotherium grangeri* (AMNH 26002). **(A)** Ventral surface of skull, **(B)** right molars, **(C)** left premolars, **(D)** labial view of isolated incisors, **(E)** lingual view of isolated incisors.

completely separated because there are no lingual connecting crests on the premolars. The labial premolar cingula are weak while the lingual cingula of P2–P4 are weak and discontinuous around the lingual base of the paracone.

The premolars of another adult specimen, AMNH 26004, differ from those of AMNH 26002 in the following ways: the hypocone and protocone of P2 are connected by a stronger, taller lingual crest; in P3 and P4 the hypocones are smaller and connected to the protocone by a thin connecting crest; the lingual cingulum is thicker and continuous.

The upper molars of *Embolotherium grangeri* show typical brontotheriine characteristics, including tall and lingually angled ectolophs, very weak labial ribs, thin lingual ectoloph enamel, and wedge-shaped lingual sides of the paracone and metacone in molars that are not heavily worn. The anterior cingulum is thin and passes proximally to the distal peak of the parastyle. Deep central molar fossae and large anterolingual cingular cusps are present. All evidence of paraconules and metalophs is lost. The M3 hypocones of *E. grangeri* are nearly the same in size and shape as those of the M1 and M2. Labial molar cingula are weak while lingual molar cingula are absent. The cingulum of M3 is discontinuous and does not wrap around the distolingual base of the crown of M3 as it does in *Embolotherium andrewsi*.

Mandible and Lower Dentition: None of the adult skulls of *Embolotherium grangeri* is associated with a mandible, although a juvenile skull, AMNH 26040, is associated with a mandible that includes a complete set of unerupted adult anterior dentition. That specimen, described further below, is an important link for identifying other mandibles of *E. grangeri*. Among these are AMNH 26005, AMNH 26132, and AMNH 21600 (fig. 125). The largest of these specimens, AMNH 26005, consists of three pieces, two separate mandibular rami (not shown), and a crushed fragment of the symphysis (fig. 125e). The most complete specimen is AMNH 21600, a nearly complete and uncrushed mandible that is missing some incisors and cheek teeth (fig. 125a–c). Finally, AMNH 26132 consists of the anterior portion of the mandible with a separately preserved anterior fragment of the symphysis with lightly worn incisors and canine (fig. 125f–h).

The horizontal ramus of AMNH 21600 is shallow and deepens slightly posteriorly. The ventral margin of the symphysis has a shallow angle ($< 45°$). The symphysis extends to the talonid of the p4.

The incisors of these specimens form semicircular arches in front of the canines. The i2 is the largest incisor. The crowns of i1 and i2 are semispatulate with convex labial sides and flat or slightly concave lingual sides. The i3 crown is more conular. Lingual cingulids are very weak or absent. Labial cingulids are not seen, although faint labial cingulids can be seen in the unworn incisors of AMNH 26040 (fig. 128). The canines of AMNH 26005 and AMNH 21600 are about the same size as the incisors, no greater in diameter or height than i3. However, the canines of AMNH 26132 are taller than the incisors and they are more lingually curved. Nonetheless, the canines of all specimens can generally be described as very small. There are no diastemata between the anterior dentitions of these specimens. However, a postcanine diastema is present.

The p1 is not preserved in AMNH 21600, nor is there a p1 alveolus, although the p1 could have fallen out in life with the alveolus being lost due to bone remodeling. In AMNH 26005 the p1 is tiny in comparison to the posterior cheek teeth and it is heavily worn. The p1 of the juvenile specimen (AMNH 26040, fig. 125d) is unworn. Its crown consists of a single cusp and a talonid heel. In AMNH 21600, the p2 trigonid and talonid are similar in length, although the trigonid is slightly narrower. The trigonids of p3 and p4 are slightly shorter and narrower than their talonids. The p2 paralophid of AMNH 21600 is broken. The p2 paralophid of AMNH 26132 is strongly curved lingually. The p2 protolophid of AMNH 26100 is straight and not angled lingually, although the entire lophid is positioned lingually. The p2 protolophid of AMNH 26132 is angled lingually and the trigonid has a broad lingual notch. Additionally, AMNH 26132 has a small p2 metaconid while AMNH 26100 does not. Similar intraspecific variability in the presence and absence of a p2 metaconid is

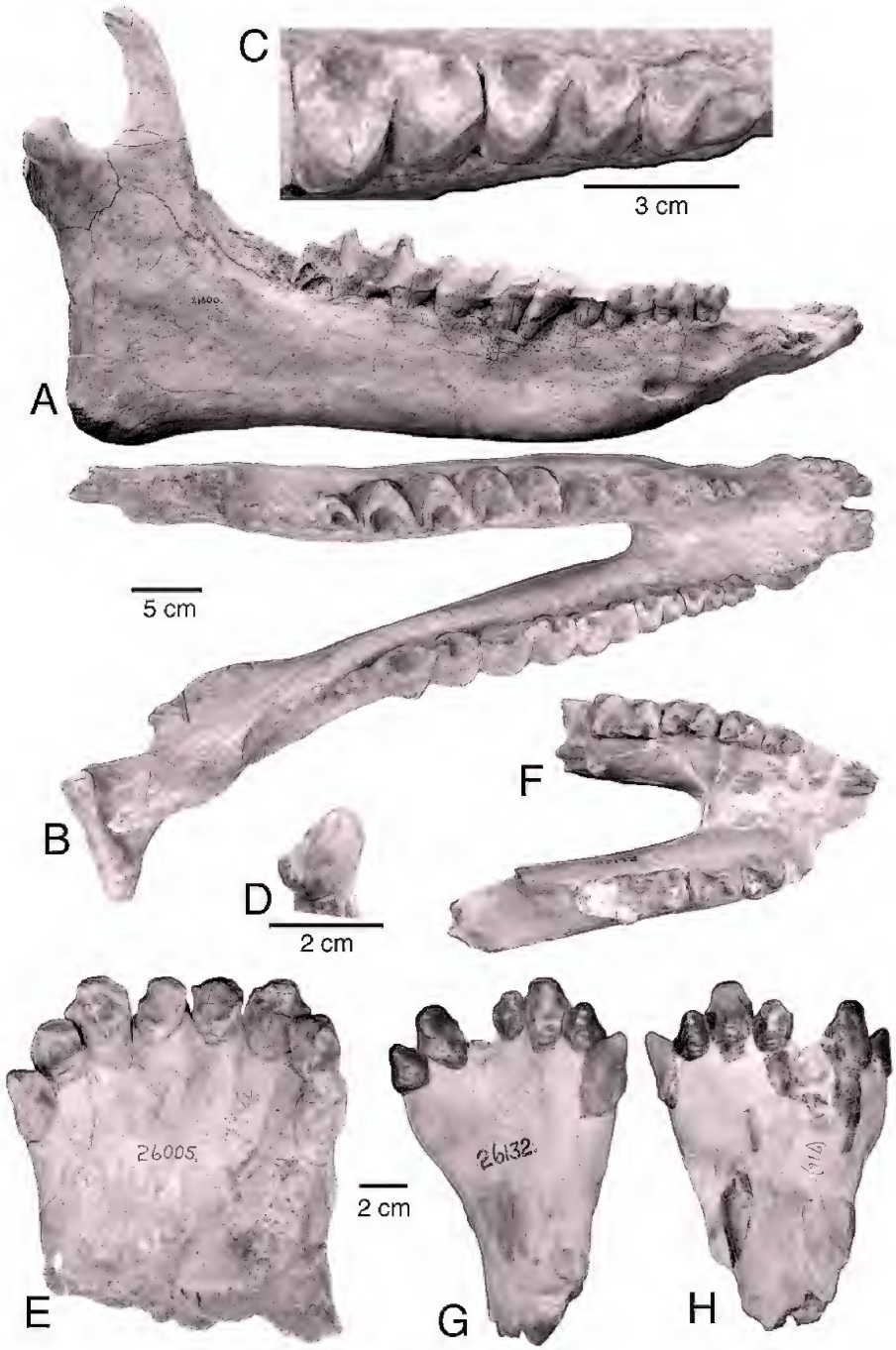

Fig. 125. Mandibles and lower incisors of *Embolotherium grangeri*. **(A)** Right view of AMNH 21600, **(B)** dorsal view of AMNH 21600, **(C)** right p2–p4 of AMNH 21600, **(D)** reflection of left p1 of AMNH 26040, **(E)** lingual view of incisors and canines of AMNH 26005, **(F)** dorsal view of AMNH 26132, **(G)** lingual view of incisors and canines of AMNH 26132, **(H)** labial view of incisors and canines of AMNH 26132.

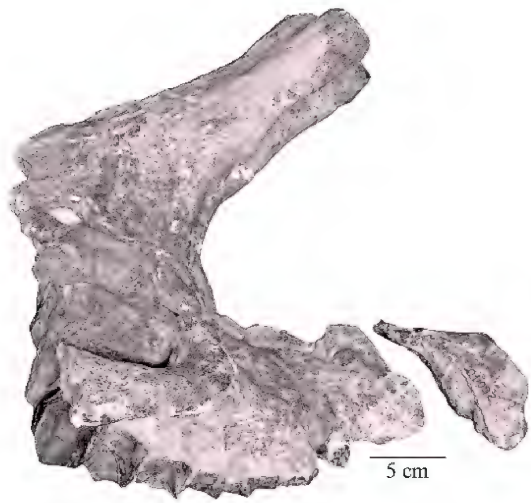

Fig. 126. Juvenile skull of *Embolotherium grangeri* (AMNH 26040) with detached premaxilla.

seen in *Embolotherium andrewsi*. The paralophids and protolophids of p3 and p4 arch lingually 90°, forming nearly molariform trigonid valleys. The talonids of p2–p4 have well-developed cristids obliqua and hypolophids with deep valleylike talonid basins similar to those of the molars. Labial premolar cingulids are weak while lingual premolar cingulids are absent.

The thin lingual enamel of the lower molars and the elongate m3 of *Embolotherium grangeri* are typical brontotheriine traits. However, like *E. andrewsi*, the trigonids and talonids form deep valleys rather than broad shallow basins. Lingual molar cingulids are absent and the labial cingulids tend to be discontinuous around the labial bases of the trigonids, talonids, and hypoconulid heel, but the cingulids can be somewhat thick between them.

Juvenile Skull and Mandible: AMNH 26040, a juvenile specimen, is the only skull of *Embolotherium grangeri* associated with a mandible (figs. 126–128). It is a critical specimen for linking the adult skulls and mandibles described above because it includes numerous isolated deciduous anterior teeth and complete sets of unerupted adult incisors embedded within the premaxilla and mandible. Parts of the specimen are described in detail by Granger and Gregory (1943), although their interpretation of the anterior dentition is erroneous. Gregory (Granger and Gregory, 1943: figs. 10, 11) worked out an arrangement of the isolated deciduous dentition of AMNH 26040; however, there are clearly errors in that arrangement. For instance, the root of the specimen referred to as a left deciduous I3 (diameter = 8.5 mm) is too wide to fit within the left dI3 alveolus (diameter = 7.1 mm). Any attempt to correctly arrange the deciduous incisors of AMNH 26040 at this point would be guesswork.

Other errors in Granger and Gregory's (1943) interpretation of the unerupted adult anterior dentition of AMNH 26040 led them to mistakenly assign adult mandibles (described above) to a completely different genus, *Titanodectes*. The original and corrected interpretations of the dentition of the premaxillary fragment of AMNH 26040 can be seen in fig. 127. Granger and Gregory (1943) identified a ridge running along the side of the premaxillary fragment as the premaxillomaxillary suture, leading them to conclude that there were only two pairs of adult incisors. The large unerupted crowns preserved in the premaxillary fragment were interpreted as I2, I3, and the canine. The first incisor (I1) was presumed to be lost. However, all six of the unerupted adult teeth in this fragment are incisors. The canine itself can be seen in an unerupted state on the left maxillary of the main skull piece and not on the detached premaxillary fragment. The portion that was labeled as a maxillary in the original figure of Granger and Gregory (1943; seen here in fig. 127a) is actually the contact surface on the premaxilla for the maxilla. No part of the maxilla is actually attached to this fragment. Therefore, the three unerupted teeth visible in the fragment are actually I1, I2, and I3. The unerupted incisors of AMNH 26040 resemble the isolated incisors that are associated with the holotype (AMNH 26002) with large globular crowns and short lingual cingula on I2 and I3, but not on I1.

Granger and Gregory (1943) also mistakenly interpreted the mandible of AMNH 26040 as having two pairs of incisors when there are actually three. Removal of bone fragments from this specimen reveals additional unexposed teeth that were not known

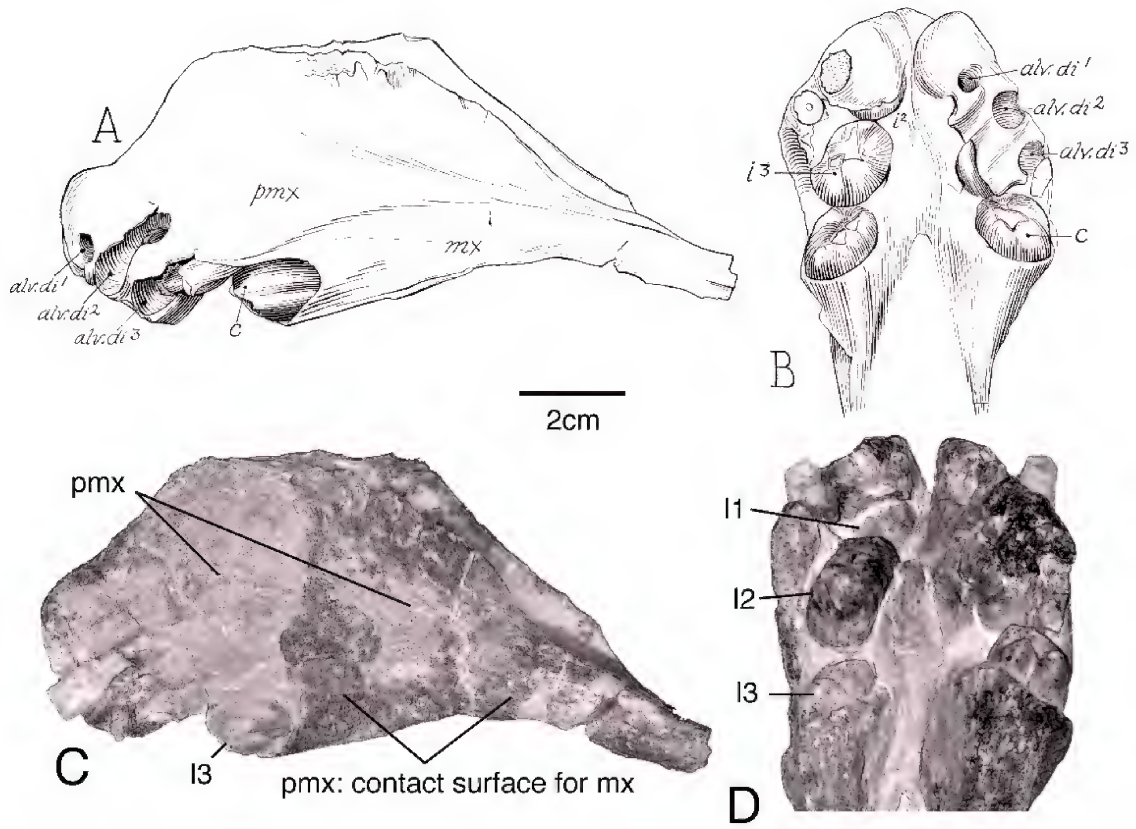

Fig. 127. Premaxillary fragment associated with the juvenile skull of *Embolotherium grangeri* (AMNH 26040) seen in Fig. 126. **(A)** Interpretation of the dentition by Granger and Gregory (1943) from left view, and **(B)** ventral view. The revised interpretation is shown **(C)** from the left view and **(D)** the ventral view.

to Granger and Gregory (1943) (fig. 128). The unaltered specimen contains two pairs of unerupted but exposed crowns of large adult incisors (fig. 128b). Removal of the left i1 reveals an additional unexposed incisor directly behind the i1 and i3 (fig. 128c). Although not shown, the right i2 is also buried in bone behind the right i1 and i3. Finally, the anterior portion of the jaw containing all of the incisors was removed. The piece that was removed is that portion anterior to the large crack just in front of the p1 that can be seen from the lateral view of the specimen in figure 128a. Removal of this piece revealed two unerupted canine crowns (fig. 128d). The lower adult incisors of AMNH 26040 are very large, tall, and semispatulate with rounded occlusal edges and faint traces of labial cingulids. The canines are small and are not nearly caniniform due to their very blunt rounded tips. These incisors are distinctly different from the very small lower incisors of *Embolotherium andrewsi*, but the incisors and canines closely resemble those of adult mandibles of *E. grangeri*.

Remarks

Osborn (1929b) described the genus, *Embolotherium*, and three species, *E. andrewsi*, *E. grangeri*, and *E. louksii*, from material collected in the Shara Murun Region of Inner Mongolia. He erected a new subfamily for this genus, Embolotheriinae. The most conspicuously diagnostic feature of *Embolotherium* is the massive, upturned, and elongated "battering-ram nose" for which this beast is named and which Osborn believed functioned in "battering, assaulting, attacking, and tossing" (Osborn, 1929b: 19). The three species recognized by Osborn

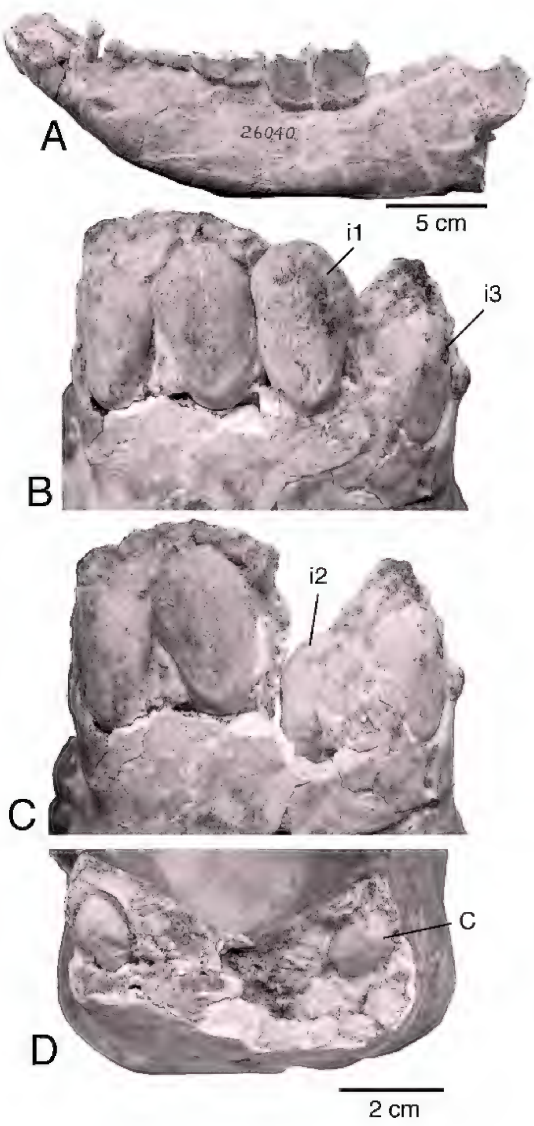

Fig. 128. Mandible associated with juvenile skull of *"Embolotherium" grangeri* (AMNH 26040). **(A)** Left view, **(B)** anterior (labial) view before fragments were removed, **(C)** anterior (labial) view with left i1 removed, revealing unexposed left i2, **(D)** anterior view after fragments containing the incisors were removed showing unexposed canines.

(1929a, 1929b) were distinguished primarily on characteristics of the ram and the rostrum. Granger and Gregory (1943) recognized the same three species, and added an additional species, *Embolotherium ultimum*, based on a particularly large partial cranium (AMNH 21604). Granger and Gregory (1943) mistakenly erected a new genus, *Titanodectes*, and two species, *T. ingens* and *T. minor*, for mandibles that turn out to belong to *E. grangeri*. Additional species of *Embolotherium* were added by Dashzeveg (1975) (*E. ergilense*) and Yanovskaya (1980) (*E. insigne*) based on skulls from the Ergilin Dzo of Mongolia. Most recently, Wang (2000) described an additional skull (IVPP V11959) of *E. andrewsi*.

Reanalysis of the known specimens reveals, however, that among these six species, only the first two, *Embolotherium andrewsi* and *E. grangeri* are valid. *E. andrewsi* was designated as the type species by Osborn (1929b). *E. grangeri* differs from *E. andrewsi* in several respects. The ram of *E. andrewsi* is curved upward while that of *E. grangeri* is straight or slightly curved downward. The ram of *E. grangeri* originates from the skull at a point posterior to the orbits, while that of *E. andrewsi* rises from above the orbits. Consequently, the nasal incision of *E. grangeri* is posteriorly much deeper. The large rim of bone that emarginates the distal border of the ventral nasal channel of the ram in *E. andrewsi* is not seen in adult specimens of *E. grangeri*. The rostrum of *E. grangeri* is longer and more robust than that of *E. andrewsi* with a much thicker dorsal premaxillary ridge. However, the nuchal crest and occiput of *E. grangeri* are far less robust. The zygomatic arches are shallower and more strongly bowed laterally. The upper and lower incisors of *E. grangeri* are much larger than those of *E. andrewsi*, and the anterior tooth row has a greater diameter. The hypocone of the upper premolars is more separated from the protocone. The M3 hypocone is taller and larger, and finally, the cingulum of the M3 is not continuous around the distolingual corner of the crown as it is in *E. andrewsi*.

Embolotherium ultimum (AMNH 21604) is a junior synonym of *E. andrewsi*. It was diagnosed primarily by its larger size. In particular, Granger and Gregory (1943) noted, "M3 of great size and relative width". However, the size of M3 is exaggerated by numerous wide cracks in the tooth. Moreover, AMNH 21604 shares numerous characteristics with *E. andrewsi*. These include massive occipital pillars, a small M3 hypo-

cone, and a continuous cingulum wrapping around the distolingual corner of M3. The holotype of *Embolotherium ergilense* (National Museum in Ulan-Bator, item 10) is also morphologically congruent with *E. andrewsi*, although appears to be larger and more robust than other specimens.

The remaining four species are synonyms of *Embolotherium grangeri*. These include *Embolotherium louksii*, *Titanodectes ingens*, *Titanodectes minor*, and *Embolotherium insigne*. *E. louksii* (AMNH 21610) and *E. insigne* (PIN 3110-52) are based on partial crania. Although the teeth of AMNH 21610 are mostly unpreserved, part of an unerupted right molar (M3?) is present, indicating that this individual is a subadult. Likewise, PIN 3110-52 appears to be a young individual with a newly erupted M3. Both specimens are consistent with *E. grangeri* in the posteriorly positioned ram behind the orbit, its ~45° angle of orientation, and the posteriorly deep nasal incision. Originally, *E. louksii* and *E. insigne* were distinguished from *E. grangeri* by the fact that the rams of their holotypes are shorter and appear straight rather than slightly curved downward. When one considers the fact that the proximal portion of the ram of AMNH 21610 consists of small bone fragments and significant amounts of plaster, this difference is not significant. Furthermore, it is hard to imagine that there were not radical ontogenetic changes in the size and the shape of the ram. Therefore, minor variation in the size and shape of the ram among subadults or young adults is undoubtedly ontogenetic and probably not taxonomically relevant. New data from the undescribed *Embolotherium grangeri* collection from Khoer Dzan currently housed at PIN will help resolve this problem.

Granger and Gregory (1943) erected a new genus, *Titanodectes*, for adult mandibles of *E. grangeri* because of their erroneous interpretation of the anterior dentition of *Embolotherium*. They described *Embolotherium* adults as retaining the deciduous incisors. It was thought that not only were the adult incisors reduced to two pairs, but also they remained unerupted throughout adulthood. The origin of this puzzling interpretation originates primarily from a juvenile skull and mandible (AMNH 26040) of *E. grangeri* (though referred to *E. louksii* by Granger and Gregory [1943]). This juvenile specimen (described more fully above) includes a set of deciduous incisors and a full set of six unerupted adult incisors. Granger and Gregory (1943) recognized the juvenile age of this specimen but for unknown reasons inferred that its condition characterizes adults, despite the fact that numerous adult specimens completely contradict their interpretation. All adult skulls of *Embolotherium* indicate three, not two, incisors. In adult skulls of *E. grangeri* the large incisors are fully erupted and the small deciduous incisors are not retained.

In recognizing Granger and Gregory's (1943) error it is apparent that the mandibles previously referred to *Titanodectes* actually belong to *Embolotherium grangeri*. Although Granger and Gregory (1943) named two species of *Titanodectes*, *T. ingens* and *T. minor*, the holotypes of these species were distinguished only by their size differences. *Embolotherium grangeri* skulls (particularly those from the undescribed Khoer Dzan collection at PIN) seem to demonstrate about as much size variability as the "*Titanodectes*" jaws. Therefore, both *Titanodectes* species can be regarded as synonyms of *Embolotherium grangeri*.

A final note is made on the stratigraphic occurrences of *Embolotherium*. Most of the *Embolotherium* material from the AMNH expeditions was collected from the "Ulan Gochu" and "Shara Murun" faunal zones (sensu Radinsky, 1964) of the East Mesa and Urtyn Obo of the Shara Murun region. In reviewing field records of these expeditions, Radinsky (1964) found that the stratigraphic data associated with specimens from those areas was questionable due to difficulties correlating the strata with the type Ulan Gochu and Shara Murun sections at Baron Sog Mesa. However, *Embolotherium* materials are more definitively known from the Shara Murun Beds at Baron Sog Mesa (AMNH 21600, *E. grangeri*), the Ulan Gochu of Baron Sog Mesa (AMNH 21601, *E. grangeri*), as well as from the Baron Sog Formation at Baron Sog Mesa (AMNH 21604, *E. andrewsi*). The occurrence of *Embolotherium* in all three of these formations at Baron Sog Mesa as well as their occurrence in the Ergilin Dzo of Outer

Mongolia suggests a Sharamurunian-Ulangochuian age for *Embolotherium*.

Pachytitan ajax Granger and Gregory, 1943

HOLOTYPE: AMNH 21612, a poorly preserved anterior fragment of a skull with left I3, C, and P2–M3.

TYPE LOCALITY: Shara Murun Formation, four miles north of Baron Sog Lamasery, Baron Sog Mesa, Shara Murun region, Inner Mongolia, China.

AGE: Middle Eocene (Sharamurunian land mammal "age").

DIAGNOSIS: *Pachytitan ajax* is a very large brontothere with short robust horns. The nasal incision is dorsoventrally deep and extends to the anterior edge of M1. The nasal process is unelevated, relatively broad, strongly rounded, thick, downturned anteriorly, and with very thick lateral walls that deepen proximally and are angled ventromedially. The premaxillomaxillary rostrum deepens posteriorly.

Dentally, *Pachytitan ajax* is characterized by three large or intermediate-sized upper incisors. There is a distinct P2 metacone. Premolar hypocones are well developed and only weakly connected to the protocone. The molars of *Pachytitan ajax* have tall, lingually angled ectolophs with weak labial ribs, and thinned lingual ectoloph enamel with wedge-shaped paracones and metacones. A cingular parastyle shelf is absent. Central molar fossae are present, but anterolingual cingular cusps are absent. Paraconules and metalophs are absent.

Pachytitan ajax is most similar to *Rhinotitan andrewsi* and *Diplacodon elatus*. It differs from the former primarily in the more massive nasal process with a more strongly rounded and downturned anterior margin, and by its more molariform premolars. *Pachytitan ajax* differs from *Diplacodon elatus* most clearly in the deep proximal lateral walls of the nasal process and the flat rather than upturned distal lateral margins of the nasal process.

DESCRIPTION

SKULL: *Pachytitan ajax* is a large horned brontothere that is known only from the holotype specimen (AMNH 21612), which consists of a poorly preserved anterior portion of a skull (fig. 129). The right view shows a complete horn and nasal process; the left side includes a partial premaxillomaxillary rostrum, a poorly preserved I3 and canine, and a complete but heavily damaged cheek-tooth row. The two primary pieces, (1) the right horn and nasal and (2) the left maxilla are plastered together, but these two pieces do not actually appear to contact each other. Therefore, some aspects of the shape of the skull, such as the orientation of the nasal process are not necessarily reliable.

No sutures are discernable on this specimen, although it is probable that the horn is composed of both frontal and nasal components. The surface of the horn is rugose. The horn is large, projects in a dorsal direction, and is elliptical in cross section with its longest axis in an anteroposterior direction. However, the shape of the horn and its orientation seem to be affected by lateral crushing. The lateral side of the horn appears to have been smashed and dislocated medially, so that shape and orientation of the horn has been altered. The position of the horn with respect to the orbit is not clear, but it appears to have been located above and behind the posterior margin of the nasal incision. Judging from the left side, the nasal incision extended nearly to the anterior edge of M1. The nasal incision appears to have been rather deep, like that of *Rhinotitan*. The nasal process is reconstructed as if it had been angled slightly upward; Granger and Gregory (1943) described the nasal process of this specimen as being "sharply upturned" (p. 366). However, considering the copious amount of plaster in the specimen, the original orientation of the nasal process is uncertain. It is clear, however, that the dorsal surface of the nasal process is not turned upward with respect to the dorsal surface of the skull that is posterior to the horn. This suggests, rather, that the nasal process was not sharply upturned (contra Granger and Gregory, 1943).

The external surface of the nasal process is nearly intact on the right side. The nasal process is massive. The dorsal surface of the nasal process is flat, and the distal end is curved downward. The lateral walls are very

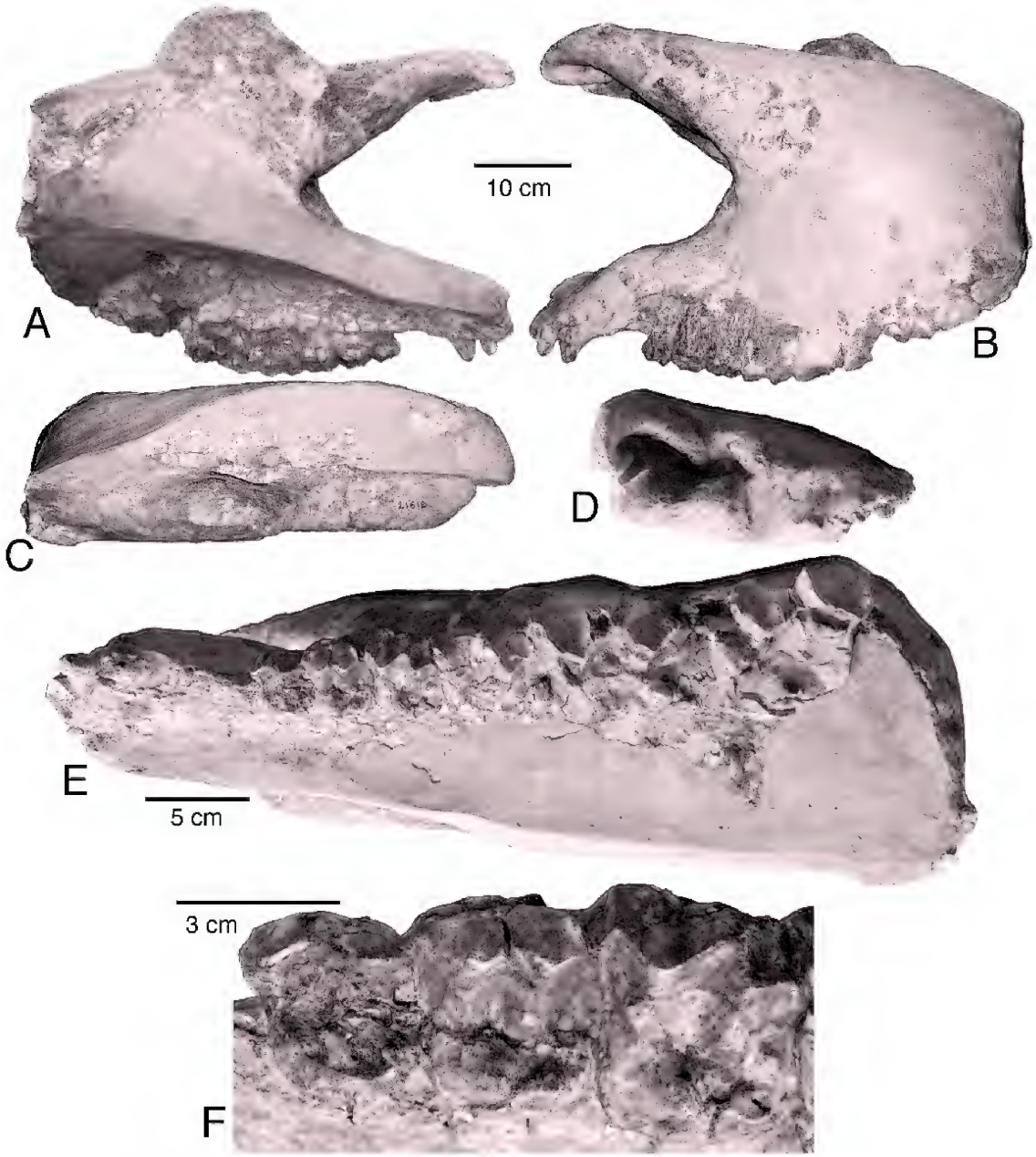

Fig. 129. The holotype of *Pachytitan ajax* (AMNH 21612). **(A)** Right view, **(B)** left view, **(C)** dorsal view, **(D)** anterior view, **(E)** ventral view, **(F)** left premolars.

thick and are very deep at the proximal end of the nasal process. However, the lateral walls shallow distally so that the anterior end of the nasal process lacks lateral walls. From the anterior view (fig. 129d) it can be seen that the thick lateral walls curve ventromedially and nearly partition the nasal chamber of the skull into two openings. In this respect the nasal processes of *Pachytitan ajax* resemble *Rhinotitan andrewsi*, although the lateral walls of the nasal process of *P. ajax* are much deeper and do not curve medially as sharply

as in *R. andrewsi*. The distal end of the nasal process is strongly rounded and the anterior margin is thick and quite rugose.

The premaxillomaxillary rostrum is similar in length to the nasal process. From a lateral view the rostrum deepens posteriorly and its lateral dorsal surface is sloped dorsoventrally. Little else of the cranial morphology of *Pachytitan ajax* can be described from the fragmentary holotype.

Upper Dentition: The crowns of I1 and I2 are not preserved and the crown of I3 is too poorly preserved to precisely judge its morphology. However, the incisors appear to have been either large or intermediate in size, but they do not appear to have reached a small vestigial state. Additionally, the incisors are positioned completely anterior to the canine rather than between the canines. The canine itself is of moderate size. There is a short precanine diastema. The postcanine diastema is longer than the P2.

P1 is not preserved. P2–P4 are complete but badly damaged. In outline, P2–P4 are nearly rectangular although the anterior margin of P2 is slightly angled more posterolingually. The parastyle and metastyle of P2 are straight. The parastyles of P3 and P4 are more strongly angled labially. The P3 metastyle is straight while the P4 metastyle is deflected labially. The labial side of the P2 paracone is rounded while P3 and P4 have slight labial paracone ribs. P4 has a well-developed mesostyle that is situated closer to the metacone than the paracone. The other premolars lack mesostyles. Although it is possible that a P4 mesostyle is a characteristic of this species, this seems unlikely considering that specimens of other brontothere species occasionally show a P4 mesostyle, but it never seems to occur in any brontothere species as a fixed state.

The lingual margins of the P2–P4 are nearly flat. The lingual morphology of P2 is uncertain, but there appears to have been two lingual cusps or a single lingual crest. P3 and P4 have two distinct lingual cusps that are weakly connected. The hypocones of P3 and P4 are positioned well behind the protocones and are similar in size to the protocones. Labial premolar cingula are weak. P4 has a continuous lingual cingulum, but the lingual cingulum of P3 is slightly discontinuous.

The molars are too damaged for precise description and measurement. However, the shape of the wear facet is consistent with those of other brontotheriines. The ectoloph is substantially taller than the lingual cusps, the inner band of enamel is thinner than the outer band, and the lingual sides of the paracone and metacone are wedge-shaped. Central molar fossae are present, but anterolingual cingula cusps appear to have been absent. There is no evidence of paraconules on the molars, nor does the M3 have a hypocone.

Remarks

Granger and Gregory (1943) based *Pachytitan ajax* on a single specimen (AMNH 21612) and differentiated it from *Rhinotitan* by its larger size, more massive upturned nasals, large horns, and more advanced premolars. Due to the poor condition of the specimen, the interpretation of the nasal bone as upturned is conjectural. Likewise, when one considers the apparent variability of horn size in other brontothere species the larger horns of AMNH 21612 are not strong evidence for a distinct species. However, the premolars of *Pachytitan ajax* are distinctly more molarized than those of *Rhinotitan* due to the well-developed hypocones that are only weakly connected to the protocones. In this respect the premolars of *P. ajax* more closely resemble those of *Diplacodon elatus* and more advanced brontotheres such as *Embolotherium* or *Parabrontops*.

Cranially, *Pachytitan ajax* seems most similar to *Rhinotitan andrewsi* and *Diplacodon elatus*. *Pachytitan ajax* shares with *Rhinotitan andrewsi* (and differs from *Diplacodon elatus*) in its deep lateral nasal walls that are strongly angled ventromedially. However, the nasal bone of *P. ajax* is more massive than *R. andrewsi* and it has a thick, strongly rounded, and downwardly curved distal end; in these respects the nasal process of *P. ajax* more closely resembles *Diplacodon elatus*.

Diplacodon elatus Marsh, 1875

Holotype: YPM 11180, a flattened skull with right P2 (partial), P3–M3, left C

(partial), P2 (partial), P3–P4, M1 (partial), and M2–M3.

TYPE LOCALITY: Myton Member (Uinta C) of the Uinta Formation, Uinta Basin, Utah.

AGE: Middle Eocene (late Uintan land mammal "age").

SYNONYMS: *Eotitanotherium osborni* (Peterson, 1914b); *Diplacodon* (*Pseudodiplacodon*) *progressus* Peterson, 1934.

REFERRED SPECIMENS: **(From the Myton Member of the Uinta Formation of Utah)** AMNH 21887, a skull with right and left P1–M3; CMNH 2858, an anterior portion of a skull with right P2 (partial), P3, left I1-canine, and P2; CMNH 2859 (holotype of *Eotitanotherium osborni*), an anterior portion of a skull with right I1–C, left I1–M3, a partial mandible with right i3–m3, and numerous postcranial elements; CMNH 10200, a skull with right and left P1–M3; CMNH 11819, a fragment of a palate with right M1–M3; CMNH 11876, a mandible with right c–m3 and left i3–m3; CMNH 11877, a complete mandible with right c, p2–m3, and left p1–m3; CMNH 11879 (holotype of *Diplacodon progressum*), a skull with right I2–I3, P1, P4, M2–M3, left P2–M3, a partial mandible with left p2 (partial), p3–m3, and numerous postcranial elements; CMNH 11895, an anterior portion of a skull with right I3, P2, P4, M1–M3, and left P2–M3; CMNH 11828, an anterior portion of a skull with right P2–M3, and left C–M3; CMNH 11881 skull (partially prepared) with right C, P2–M3, and left C–M3; CMNH 11967, a partial mandible with right i2–i3, c, p1–m3, and left i2; FMNH P14632 skull with right C–M3 and left I3–M3; FMNH P14633, a skull with right C–M3, left C–M3 and isolated right incisors; FMNH P14634, a complete mandible with complete lower dentition; FMNH P14638, a left mandibular ramus with p2–m3 and a vertebral atlas; FMNH P14640 (in part), a partial mandible with right i3, c, p1, m2 (partial), m3, and left p2–m3; FMNH P14799 dorsoventrally crushed skull with right P1–M3 and left P4–M3; FMNH P15446, a laterally crushed skull with right I1–I2, C–M3, left I1–C, and P2–M3.

DIAGNOSIS: *Diplacodon elatus* is somewhat larger than *Protitan minor* but smaller than *Protitanotherium emarginatum* with horns of variable size that are positioned high above the orbits. The nasal incision is dorsoventrally deep and it extends posteriorly to the P4. The nasal process is slightly angled downward; it is broad, with thickened and upturned sides, and with a strongly rounded distal edge with a downturned distal tip. The nasal process is not elevated to the peaks of the horns. The orbits are positioned above the M2 and the posterior part of M1. The premaxillomaxillary rostrum hangs down posteriorly and it is not enclosed by bone dorsally. Other cranial characteristics include a saddle-shaped cranium, separate parasagittal ridges that moderately constrict the dorsal width of the cranium posteriorly, lack of a bony emargination surrounding the posterior nares, large ventral sphenoidal fossae, nearly straight zygomatic arches, and a ventrally constricted and mediolaterally angled external auditory pseudomeatus.

Dentally, *Diplacodon elatus* has three intermediate-sized upper incisors, globular I1 and I2, a more subcaniniform I3, a complex P1, and a distinct P2 metacone. Premolar hypocones are present although the protocone and hypocone of P2 and P3 sometimes take the form of a single lingual crest. The molars of *Diplacodon elatus* have tall, lingually angled ectolophs with weak labial ribs and thinned lingual ectoloph enamel with wedge-shaped paracones and metacones. A cingular parastyle shelf is absent. Distinct central molar fossae are present. Anterolingual cingular cusps tend to be weakly developed. Paraconules and metalophs are absent. The lower dentition includes three intermediate-sized incisors. The i1 and i2 are semispatulate while the i3 is more subcaniniform. There is a distinct postcanine diastema. There is a distinct metaconid on p3 and p4 but not on p2. The p2 trigonid and talonid are of similar length. The lower molars have shallow basins and the m3 is slender.

Diplacodon elatus can be distinguished from *Protitanotherium*, *Rhinotitan*, and more plesiomorphic brontotheres such as *Protitan* by its elevated horns, deep nasal incision, significantly more molarized premolars, and by its autapomorphic nasal morphology with upturned sides. Other brontotheres with

premolars that are undifferentiated from those of *Diplacodon elatus* have smaller incisors, taller lower premolars, and/or a radically different skull shape.

Description

Skull: The holotype of *Diplacodon elatus* (YPM 11180) consists of a skull that is preserved in two pieces, an anterior portion (fig. 130), and a posterior portion (not shown). The specimen is extremely flattened and the only parts of the skull that are readily describable are the cheek teeth. However, *D. elatus* is also known from many complete and undistorted skulls and jaws. Two of the best skulls are FMNH P14632 and FMNH P14633 (figs. 131 and 133) from which the following description is primarily based. However, other specimens offer numerous important details on variation in this species.

Diplacodon elatus is rather small (table 10) for a horned brontothere. It is larger than *Protitan minor* but is smaller than *Protitanotherium emarginatum* or *Protitan grangeri*. There is no discernable frontonasal suture on any specimen. However, it is probable that like other horned brontotheres, the horns are composed of frontal and nasal elements, but these elements are completely fused together. Juvenile specimens may provide a more definitive answer, but none are currently known.

In cross section the horns vary from being round to somewhat elliptical. The surfaces of the horns are rugose, although some specimens have smooth horn surfaces. The horns range in size from being very small to quite massive, although they are never extremely tall as in some specimens of *Megacerops* (sensu Mihlbachler et al., 2004b). Many of the specimens have horns that are about the same size as either those of CMNH 2859 (fig. 132a), a gracile specimen, or CMNH 11879A (fig. 132b), a more robust specimen. However, numerous specimens (e.g., AMNH 21887, CMNH 2858, CMNH 11881, FMNH P14632, FMNH P14632, FMNH P14633) have horns that are intermediate in size. A single specimen, CMNH 11828, has horns that are very small and exist only as small rugose ridges.

Despite conspicuous variation in horn size and horn surface texture, the position and orientation on the horns is much less variable. The horns tend to project anterodorsally and laterally to varying degrees. They are positioned high above the orbits and are elevated upon tall superorbital pillars that project from above the orbits in an anterodorsal direction at about a 45° angle. This differs from *Protitanotherium* and *Protitan* whose horns are lower on the skull, a placement that more closely resembles more derived taxa such as *Aktautitan* and *Metatitan*. However, unlike these taxa, the nasal process of *Diplacodon elatus* is not elevated to the very peak of the frontonasal protuberances.

The nasal incision extends posteriorly to a point that fluctuates between the anterior and posterior margins of the P4. Although the nasal process is not elevated to the apex of the horns as in *Metatitan* and *Aktautitan*, it is nonetheless higher than those of *Protitanotherium* and *Protitan*, resulting in a dorsoventrally deep nasal incision where the posterior notch of the nasal incision rises higher than the orbit. The orbits of *Diplacodon elatus* are shifted anteriorly; all the roots of M2 and the posterolateral root of M1 are positioned directly below the orbit. The anterolateral root of M1 is positioned directly below the anterior orbital rim.

The nasal bones of *Diplacodon elatus* are completely fused. The length of the nasal process varies; it is typically a little shorter than the premaxillomaxillary rostrum, but occasionally, such as in CMNH 2859 (fig. 132a), it is nearly as long as the rostrum. The nasal process is as broad as the rostrum and it has thickened sides. From a dorsal view the nasal process of CMNH 14632 is distally tapered and the anterior end is strongly rounded, although in some specimens (e.g., AMNH 21887) the sides are more nearly parallel and somewhat constricted proximally. The distal tip of the nasal process is roughened and strongly curved downward. The sides of the nasal process are autapomorphically upturned rather than turned downward. The upturned sides of the nasal process are most easily seen from the anterior view where the dorsal surface of the nasal process is concave in a transverse direction

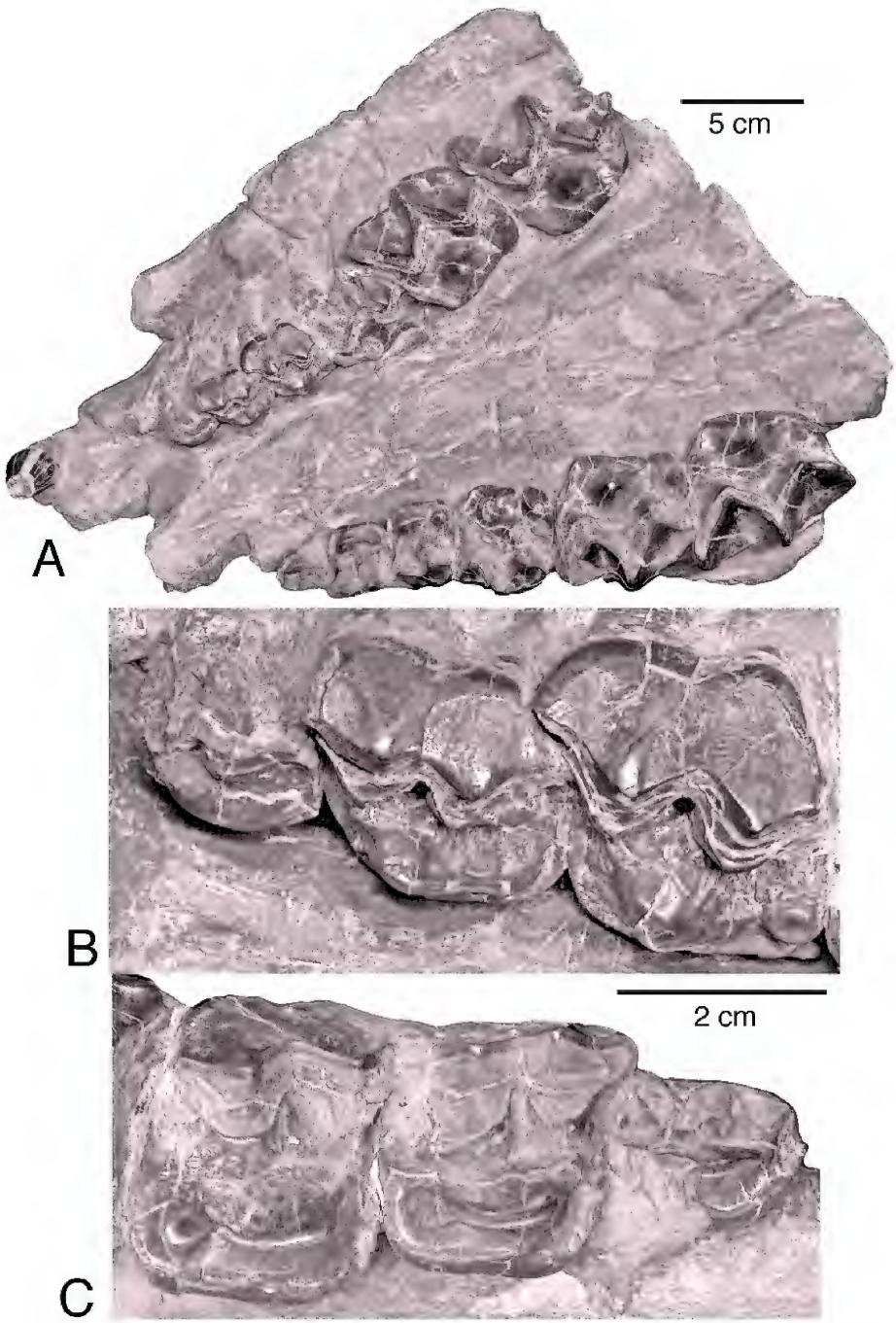

Fig. 130. The holotype of *Diplacodon elatus*. (Division of Vertebrate Paleontology, YPM 11180. © 2005 Peabody Museum of Natural History, Yale University, New Haven, Connecticut, USA. All rights reserved.) **(A)** Ventral view of palate, **(B)** left P2–P4, **(C)** right P2–P4.

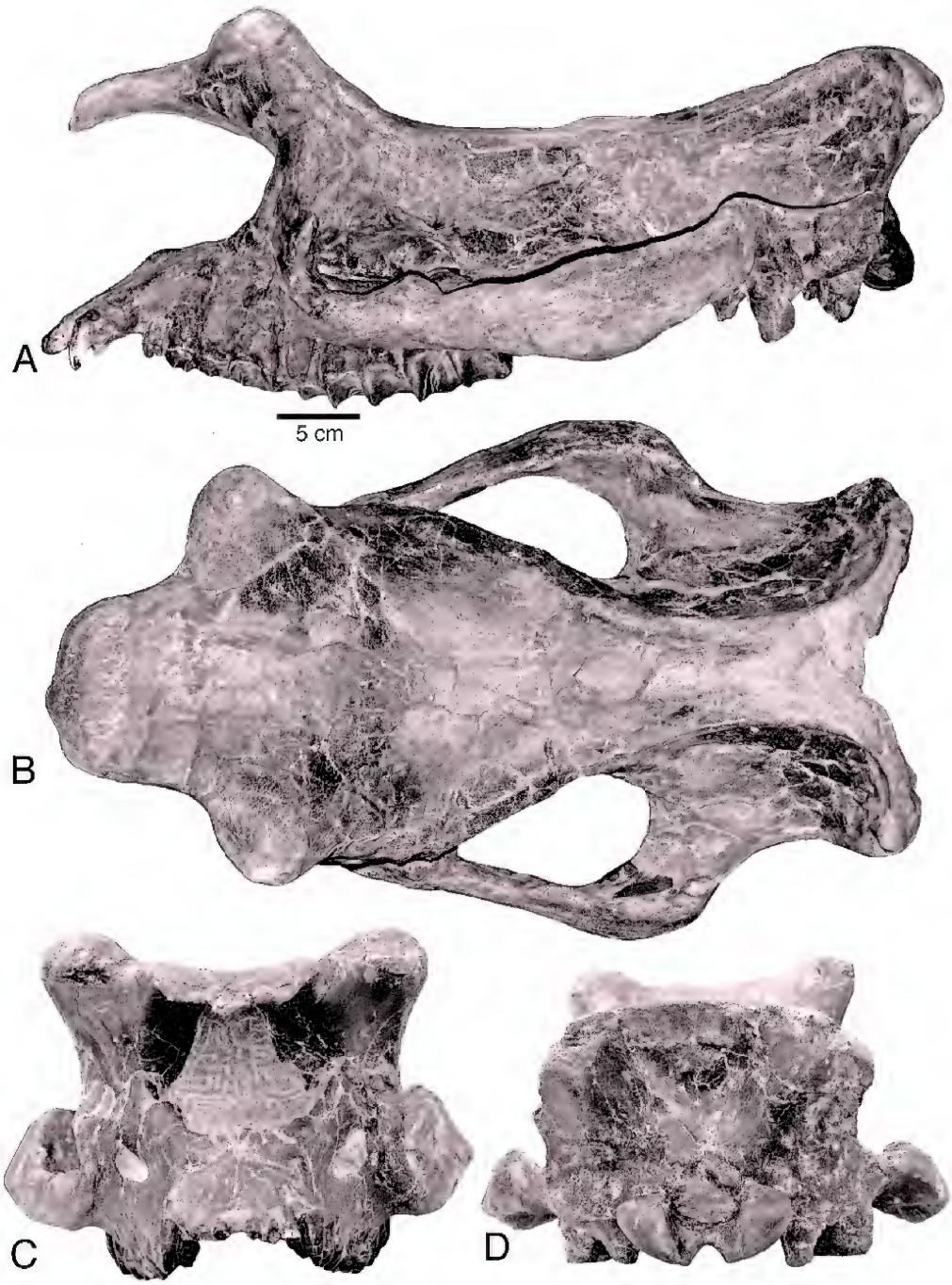

Fig. 131. Skulls referred to *Diplacodon elatus*. **(A)** Left view of FMNH P14632, **(B)** dorsal view of FMNH P14632, **(C)** anterior view of FMNH P14633, **(D)** posterior view of FMNH P144633.

(fig. 131c). In more gracile specimens, such as CMNH 2859 (fig. 132a), the nasal process is thinner and more nearly flat in cross section, although the dorsal surface is still convex in a mediolateral direction. (Note that previously published figures of another specimen, CMNH 2856 [Peterson, 1914b: pl. 8, and reprinted in Osborn, 1929a: fig. 365] give the

TABLE 10
Summary statistics for selected morphometric variables of *Diplacodon elatus*
See Methods for measurement definitions

	N	Mean	SD	Min.	Max.	CV
C L	7	20.2	3.1	14.4	22.6	15.4
P3 L	12	27.0	2.3	23.6	31.4	8.7
P3 W	11	30.4	1.8	27.8	34.7	6.1
M2 L	13	56.6	6.7	42.2	64.3	11.8
M2 W	11	54.2	2.8	49.6	58.9	5.3
P2–P4	11	78.5	3.4	73.7	83.7	4.3
M1–M3	12	158.9	10.1	140	172	6.4
V L	7	573.1	20.1	550	607	3.5
c L	6	20.1	3.6	15.8	25.0	17.7
p3 L	8	24.3	1.9	21.2	27.7	8.0
p3 W	7	17.1	1.2	14.5	17.9	7.2
m2 L	8	50.6	2.6	47.4	54.3	5.1
m2 W	6	29.1	1.6	27.9	32.5	5.3
p2–p4	8	75.5	5.6	66.3	81.6	7.4
m1–m3	8	158.9	15.9	122.2	172	10.0

misleading impression that the lateral margins are not upturned.) In the most robust specimens, such as CMNH 11879A (fig. 132b), a distinct rugosity traces around the edges of the nasal process, the dorsal surface is more strongly concave in cross section, and the distal end is more strongly curved downward. The variation in shape and thickness of the nasal process is generally related to the size and robusticity of the horns although the correlation is not perfect. For instance, CMNH 11828 (not shown) has a relatively thick nasal bone, though the horns are small.

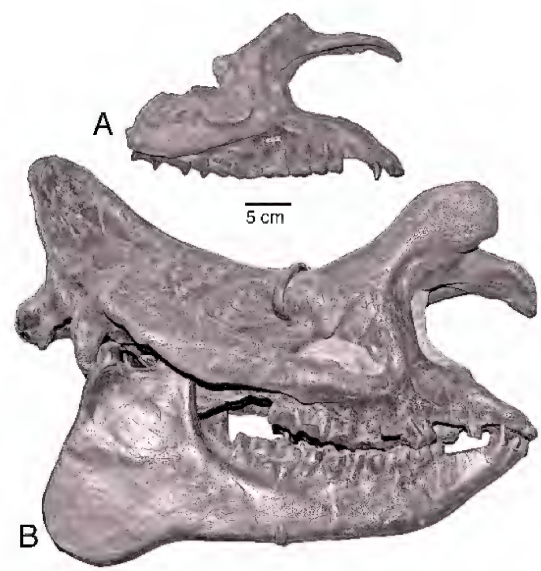

Fig. 132. Skulls referred to *Diplacodon elatus* illustrating opposite extremes in horn and nasal development and robustness. **(A)** Reflection of left view of CMNH 2859, **(B)** right view of CMNH 11879A.

From a lateral view (fig. 131a), the dorsal surface of the premaxilla is flat and steeply angled posterodorsally. Behind the symphysis the dorsal surface of the premaxilla is nearly horizontal. From the anterior view it can be seen that the premaxillary symphysis is rather long. Behind the symphysis the dorsolateral margins of the rostrum diverge laterally and the rostral cavity is not enclosed by bone dorsally. A distinct premaxillomaxillary suture has not been observed in any available specimen of *Diplacodon elatus*.

The dorsal surfaces of the skulls of *Diplacodon elatus* are strongly convex or saddle-shaped. The parasagittal ridges remain separate throughout their length and moderately constrict the dorsal surface of the cranium posteriorly but to a lesser degree than seen in *Protitanotherium emarginatum*. From the lateral view of the skull the zygomatic arch is not very deep. The jugal portion of the zygomatic arch is horizontal, while the squamosal portion is slightly sloped upward posteriorly, but as a whole, the zygomatic arch is nearly straight. From a

Fig. 133. Ventral view of a skull (FMNH P14633) of *Diplacodon elatus*.

dorsal view the zygomatic arch is relatively thin, straight, and strongly angled posterolaterally.

The occiput is moderately tilted backward. From a dorsal view the nuchal crest is slightly convex. From the posterior view the dorsal margin of the occiput is barely arched dorsally. The widths of the dorsal and ventral portions of the occiput are nearly the same and the occiput is very slightly constricted in the middle. There are strong occipital pillars of the surface of the occiput and there is a shallow central depression.

The position of the anterior margin of the posterior nares is somewhat variable. It is most often positioned slightly anterior to the M3 protocones as in CMNH 14633 (fig. 133). In a few specimens, such as FMNH P14632, it is slightly anterior to the M3. The bony horseshoe-shaped rim that typically emarginates the posterior nares of many brontotheres is not seen in *Diplacodon elatus*.

The posterior narial canal is elongate and continues far into the sphenoid via a pair of ventral sphenoidal fossae. In CMNH 14633 the elongate posterior narial canal has been fully cleared of sediment on the left side, thus exposing the deep ventral sphenoidal fossa and the elongate vomer that joins the septumlike basisphenoid to form a continuous partitioning septum. Every specimen of *Diplacodon elatus* in which the basicranium is preserved has distinct ventral sphenoidal fossae.

The short mastoid process arches anteroventrally and contacts the longer postglenoid process, thus creating a tubelike external auditory pseudomeatus that enters the skull in a mediolateral direction. The configuration of the basicranial foramina is consistent with those of other brontotheres with widely separate foramina of the alar canal, foramen ovale, and foramen lacerum.

Upper Dentition: In all of the known skulls the upper incisors are either not preserved or they are heavily worn and/or damaged. One specimen (CMNH 2859) has a set of worn but nearly complete incisors (fig. 134a). Additionally, isolated incisors are associated with FMNH P14633 (fig. 134b, c). Two nearly intact sets of cheek teeth are present in FMNH P14632 and FMNH P14633 (fig. 135). These specimens, along with others including the holotype (YPM 11180, fig. 130), indicate conspicuous intra-

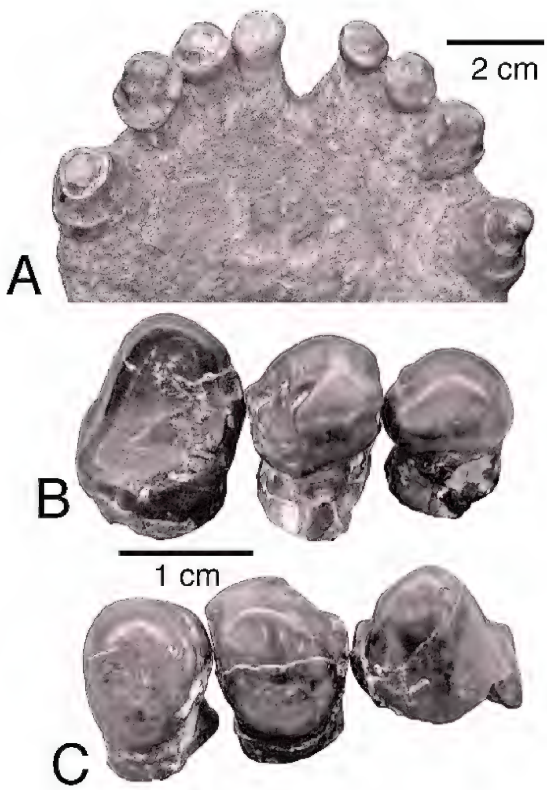

Fig. 134. Incisors and canines of *Diplacodon elatus*. **(A)** Lingual view of CMNH 2859, **(B)** lingual, and **(C)** labial views of isolated incisors associated with FMNH P14633.

specific variation in cheek-tooth morphology that is further described below.

The dental formula of *Diplacodon elatus* is unreduced (3-1-4-3). The incisors are small in comparison to *Protitan* and other more plesiomorphic brontotheres, but they have not reached the vestigial state as seen, for example, in *Duchesneodus*. The incisors are not clearly differentiated from those of *Protitanotherium emarginatum* although they arch slightly more anterior to the canines. The I1 and I2 appear to have been subglobular, particularly those of FMNH P14633. The I1 and I2 of CMNH 2859 retain small lingual cingula. The substantial amount of wear on this specimen obscures other details. The I3 is larger than I1 or I2 and though worn in both specimens, it is clearly taller and more caniniform. The left incisors of CMNH 2859 are separated by very short diastemata. There is always a distinct diastema between the I3 and canine. The canines tend to be small with a weak distal cingulum. The postcanine diastema varies in length from slightly longer than the P2 to slightly shorter. The canines tend to be smaller than those of *Protitanotherium*, the postcanine diastema tends to be longer, and the distal end of the rostrum is somewhat narrower.

The P1 of FMNH P14632 is well worn, but two labial bulges in the crown indicate that both a paracone and metacone were present. The P1 crown is rounded. A lingual heel was clearly present, but further details are obliterated by wear. The P1 of FMNH P16633 is less worn. In that specimen there is single large protocone on the lingual heel. This protocone is connected to the paracone by short preprotocrista. Additionally, there is a short lingual crest that arches around the posterolingual border of the crown.

The P2–P4 of FMNH P14632 are subrectangular with nearly flat lingual margins. The anterior and posterior sides are nearly rectangular, but the lingual sides of P2 and P3 are slightly narrower than the labial sides. In other specimens, such as FMNH P14633, the P2 can be slightly more oblique in shape due to a more strongly distolingually angled anterior margin. The parastyle and metastyle of the P2 are straight. The parastyle of P3 is slightly angled labially while the metaconid is straight. The parastyle and metastyle of P4 are strongly labially directed. The labial sides of the P2 paracone and metacone form small swellings. In P3 and P4 there are more distinct labial paracone ribs. Although a P4 mesostyle is occasionally seen among specimens of brontotheres such as in *Pachytitan* or *Protitanops*, none of the P4s of *Diplacodon elatus* has a mesostyle.

The lingual features of the P2–P4 tend to be higher in relief in comparison to *Protitan*, *Protitanotherium*, or *Rhinotitan*. A distinct preprotocrista can be seen on P2–P4, although this structure tends to be larger on more anterior premolars. The P2–P4 of *Diplacodon elatus* tend to have two lingual cusps, a protocone and a hypocone. The exact morphology of the lingual side of the crown is variable. In AMNH 14632 the P2–P4 have distinct protocones and smaller hypocones. The P2 hypocone is not connected to the protocone by a lingual crest.

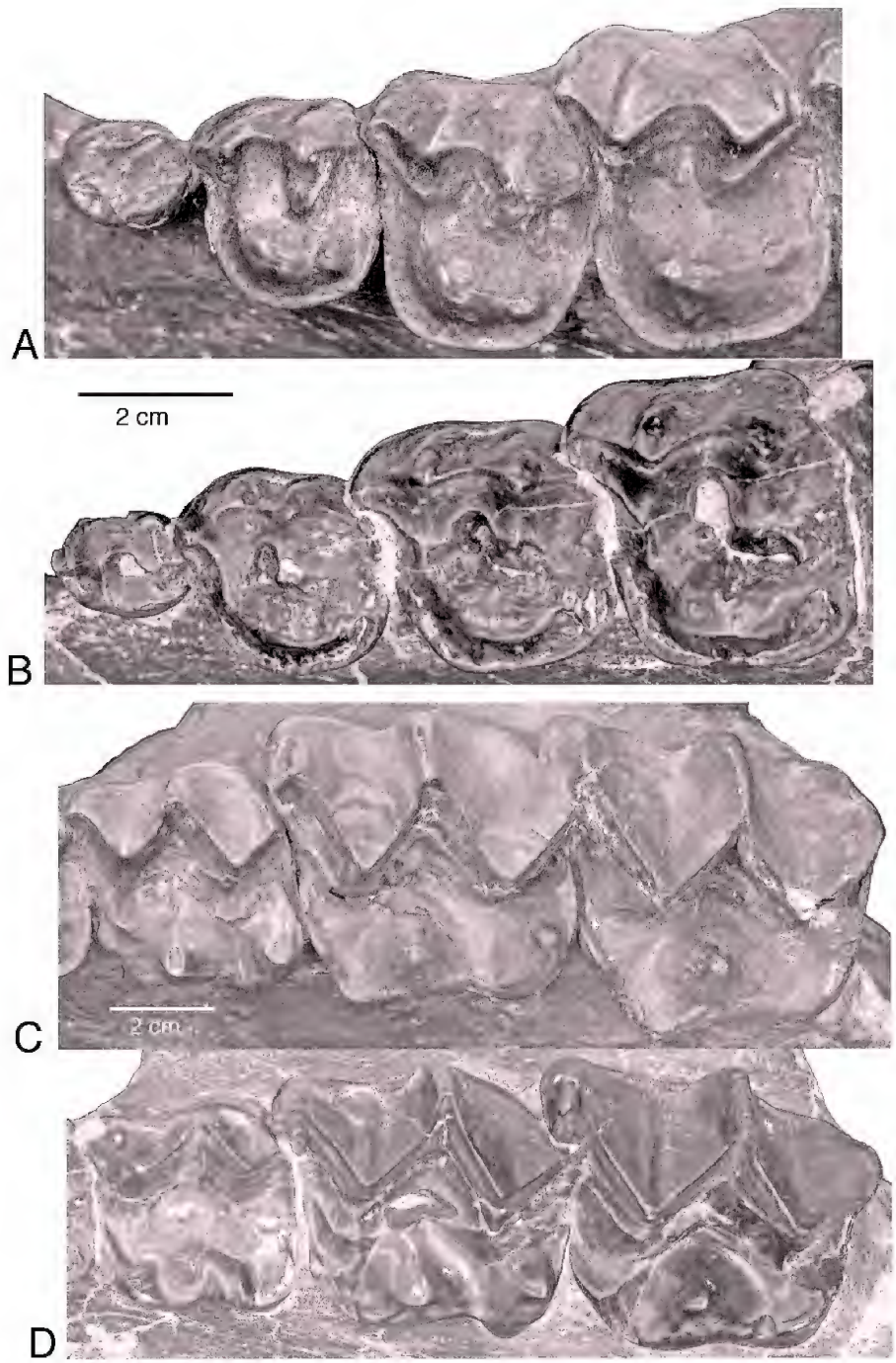

Fig. 135. Cheek teeth of *Diplacodon elatus*. **(A)** Left premolars of FMNH P14632, **(B)** reflection of right premolars of FMNH P14633, **(C)** left molars of FMNH P14632, **(D)** reflection of right molars of FMNH P14633.

However, the P3 and P4 hypocones are connected to the protocones by a thin lingual crest. In each of these premolars the hypocone is positioned distantly from the protocone. FMNH P14633 exhibits a different morphology. In that specimen, there are no distinct lingual cusps on the P2, although a rounded crest arches around the lingual margin of the crown. In P3, the lingual crest is much thicker than that of P2 and it completely absorbs the protocone and hypocone. There is a distinct protocone and hypocone on P4, although, in this instance, the cusps are positioned very closely together and are of approximately the same size.

The upper premolars of the holotype specimen (fig. 130) demonstrate bilateral asymmetry. In that specimen there is a lingual crest on the right P2, but there are no distinct lingual cusps. On the left P2 there are two widely spaced cusps connected by a lingual crest. On the right P4 the small hypocone is connected to the protocone by a crest, while on the left P4 there is no connecting crest.

Variation in the size and distinctness of the lingual cusps, and their degree of separation is seemingly random in each individual tooth. However, when one examines all the specimens the lingual side of P2 ranges from having a single tall lingual crest with no distinct cusps to having two distinct lingual cusps that are weakly connected by a thin crest. P3 most often has a distinct protocone and a smaller hypocone. The connecting crest itself is sometimes nearly as tall as the lingual cusps, but it can also be much shorter. P4 is more variable in this respect. There are always two distinct cusps that are usually connected to varying degrees by a connecting crest of variable height, but occasionally, as in FMNH P14632, the hypocone is much smaller and it is positioned on the base of the posterior slope of the protocone. Despite the overall variability, a general pattern does emerge; P2 shows a tendency to have large lingual crests that often absorb the lingual cusps, while P4 tends to have more distinct labial cusps with the connecting crest reduced or absent. P3 is usually intermediate.

Labial premolar cingula are always weak or absent in *Diplacodon elatus*. The lingual cingula of the P2–P4 are always thicker. It is consistently thickest on P2 and it is never discontinuous. Occasionally the lingual cingulum of P3 and P4 is slightly discontinuous around the lingual margin of the crown.

The upper molars of *Diplacodon elatus* show numerous advanced features, including tall, lingually angled ectolophs, very weak labial ribs, thin lingual ectoloph enamel, and wedge-shaped lingual sides of the paracone and metacone in molars that are not heavily worn. The anterior cingulum is thin and passes proximally to the distal peak of the parastyle. Distinct central molar fossae are present. In the holotype specimen (fig. 130) the anterolingual cingulum of the molars thickens and rises slightly but does not form a strong anterolingual cingular cusp. Other specimens, such as FMNH P14632 (fig. 135c), reflect the condition seen in the holotype. However, other specimens, such as FMNH P14633 (fig. 135d) show strong anterolingual cingular peaks on the molars.

Mader (1989, 1998) noted that paraconules or metaconules are occasionally present on the molars of *Diplacodon* (= *Pseudodiplacodon*). However, I found no evidence of paraconules or metaconules in any of the specimens. Nor is there any evidence of a vestigial metaloph. Mader (1989, 1998) also noted the occasional presence of a hypocone (or "pseudhypocone") on M3, but none of the specimens has a distinct hypocone. Although no hypocone is present, the lingual side of the M3 is broad and squarish with a large space posterior to the protocone and a thick cingulum that wraps around the distolingual corner of the crown. Labial molar cingula are generally weak and lingual molar cingula are very weak between the protocone and hypocone, or they are absent altogether.

MANDIBLE AND LOWER DENTITION: The only skulls of *Diplacodon elatus* that are associated with mandibles are CMNH 2859 and CMNH 11879. However, each of these mandibles is incomplete. The mandible of CMNH 2859 is missing its incisors, but that specimen has the most unworn and complete set of lower premolars available for *Diplacodon elatus*, and is therefore figured in close up (fig. 136c). There are also several mandibles and partial mandibles from the Myton Member of the Uinta Formation that

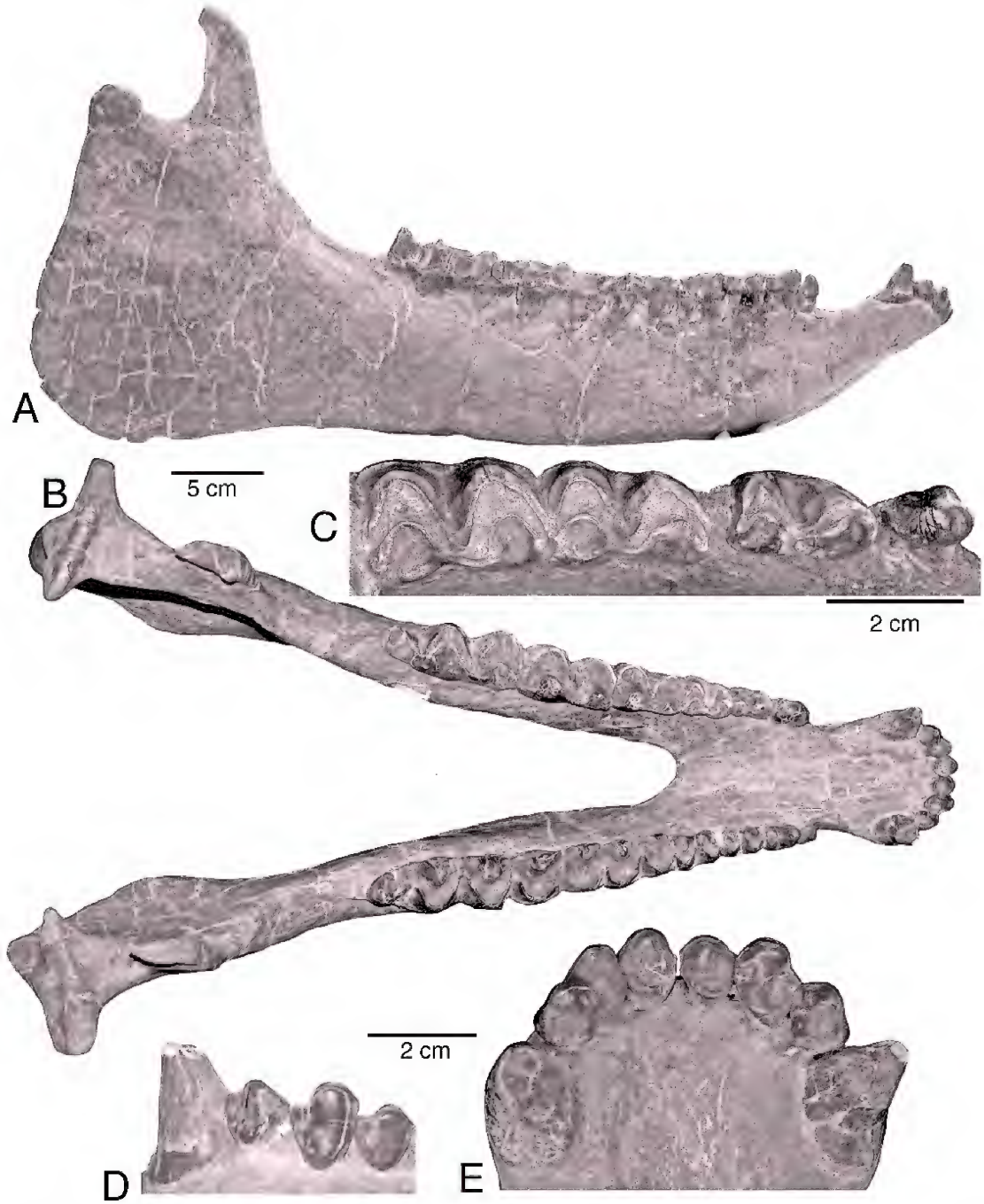

Fig. 136. Mandible and lower dentition of *Diplacodon elatus*. **(A)** Right view of FMNH P14634, **(B)** dorsal view of FMNH P14634, **(C)** right lower premolars of CMNH 2859, **(D)** labial view of right incisors and canine of FMNH P14634, **(E)** lingual view of incisors and canines of FMNH P14634.

are not associated with skulls but that are consistent with CMNH 2859 and CMNH 11879 and are referable to *D. elatus*. Among these, FMNH P14634 is the most complete *D. elatus* mandible (fig. 136a, b, d, e).

The mandible of FMNH P14634 has a thin coronoid process that rises above the mandibular condyle. The inferior margin of the symphysis is angled slightly less than 45°. From the dorsal view of the mandible the mandibular symphysis is longer and more slender than that of *Protitanotherium emarginatum* and with a longer postcanine diastema. The posterior portion of the symphysis extends to the talonid of p4 in FMNH P 14634, but the symphysis more typically ends at the posterior edge of the p3 (CMNH 11876, 11877, 11967).

Like the upper incisors, the lowers are smaller than those of *Protitan grangeri*, but they have not reached a vestigial stage. The lower incisors of *Diplacodon elatus* are not clearly differentiated from those of *Protitanotherium*, although the incisor row is more arched. The i2 is the largest incisor; this is most obvious from the labial view (fig 136d). The crowns of the i1 and i2 are semispatulate with rounded apices and narrow lingual cingulids. The i3 is shorter and more mesiodistally elongate in comparison to i1 or i2. A single left i3 is also preserved with CMNH 2859 (not shown). The i3 of that specimen seems taller and somewhat more subcaniniform than the i3 of FMNH P14634. There are no diastemata between any of the lower incisors or canines. The lower canines are of small to moderate size and the postcanine diastemata of FMNH P14634 and other specimens of *D. elatus* are consistently longer than those of *Protitanotherium emarginatum*.

The lower premolars of *Diplacodon elatus* are relatively slender and low-crowned. In general, their proportions do not differ notably from *Protitanotherium emarginatum*. The p1 is a simple, single-cusped tooth with a talonid heel and a weak lingual cingulid. The trigonid of p2 is slightly longer than the talonid. This differs from *Protitanotherium*, whose p2 trigonid is nearly twice the length of the talonid. The p3 trigonid of *D. elatus* is slightly longer than the talonid, while the trigonid and talonid of p4 are of similar length. The trigonids of p2–p4 are all barely narrower than their talonids. The paralophid of p2 arches lingually but at an angle less than 45°, thus creating a small lingual trigonid notch. The protolophid of p2 is nearly straight, but it is lingually positioned. The paralophid of p3 is relatively long and arches lingually about 45°, while the p4 paralophid is molariform and arches 90° lingually. The protolophids of p3 and p4 are molariform and arch almost completely lingually. The trigonid of p3 has a very broad lingual notch, while the trigonid of p4 has an essentially molariform basin. The p2 lacks a metaconid, but p3 and p4 possess a large lingually positioned metaconid. The talonids of p2–p4 have well developed cristids obliqua and hypolophids. These elements are more elongate in more posterior premolars, creating increasingly molariform talonid basins. The labial premolar cingulids are weak to absent and lingual premolar cingulids are absent.

The lower molars of *Diplacodon elatus* are typical. They have relatively thin lingual enamel, shallow trigonid and talonid basins, and the m3 is elongate. There are no lingual cingulids, but labial molar cingulids are distinct although they tend to be discontinuous around the paraconids and metaconids.

Remarks

Marsh (1875) based *Diplacodon elatus* on a dorsoventrally crushed skull (YPM 11180) with comparatively undistorted cheek teeth (fig. 130). Marsh (1875) asserted that *D. elatus* was hornless. The dorsal surface of the holotype does appear to lack horns as Marsh (1875) had observed, but the specimen is severely flattened and it was apparent to others that the specimen was far too damaged to realistically determine the presence or absence of horns in *D. elatus* from its holotype (Hatcher, 1895; Osborn, 1929a). The only readily describable parts of the holotype are the cheek teeth, which indicate a brontothere that is somewhat smaller than *Protitanotherium emarginatum*, also from the Myton Member of the Uinta Formation, and with significantly more molarized premolars.

Several complete and less distorted specimens of *Diplacodon elatus* from the Myton

member of the Uinta Formation have since been discovered, although many of them have been assigned to a variety of other names. Peterson (1914b) named a new species, *Diploceras osborni*, from the anterior portion of a skull and mandible (CMNH 2859) (figs. 132a, 134a, 136b). Peterson (1914b) relegated another partial skull (CMNH 2858) as the cotype. The later specimen differs distinctly from the former with its larger and more rugose horns, which Peterson (1914b) attributed to sexual dimorphism. Peterson (1914c) later renamed the genus to *Eotitanotherium* after discovering that *Diploceras* was preoccupied by a mollusk. Peterson (1914b) did not clearly differentiate *Eotitanotherium osborni* from *Diplacodon elatus*, although he mentioned that *Eotitanotherium osborni* had shorter, blunter canines, a less ridgelike deuterocone (protocone) on the P2, and more distinct lingual cusps on the P3. None of these observations warrant a clear taxonomic distinction considering (1) the poor state of preservation of the canine in the holotype of *D. elatus*, (2) and the large degree of essentially continuous morphological variation seen in the upper premolars of brontotheres.

Peterson (1934) named yet another species, *Diplacodon progressum*, based on a skull (CMNH 11879A) (fig. 132b) and nearly complete skeleton (CMNH 11879). The horns of that specimen are robust and similar to those of Peterson's paratype of *Eotitanotherium osborni*. Peterson (1934) differentiated *D. progressum* from *D. elatus* with the following observations, (1) "Facial region is shorter in *D. progressum*", (2) "the premolar series in the new species is farther advanced in molarization than in *D. elatus*, the individual teeth being more perfectly quadrate in *D. progressum*, P2 being especially advanced" (Peterson, 1934: 353). The first observation was based only on the slightly shorter premolar length and might simply relate to the fact that the specimens are of slightly different sizes. Moreover, the extremely crushed and incomplete condition of the holotype of *D. elatus* (YPM 11180) complicates any comparison. The second observation is questionable as well; the slight difference in the squareness of the premolars is consistent with a pattern of intraspecific premolar variation generally found in brontotheres and does not represent a taxonomically significant difference.

Peterson (1934) distinguished *Diplacodon progressum* from *Eotitanotherium osborni* on the observations that the (1) nasals "are shorter and heavier", and (2) "the alveolar border of the premaxillary border is noticeably shorter" (Peterson, 1934: 353). Upon reexamining the specimens, the second observation cannot be confirmed. The first observation relates to the fact that the holotype of *D. progressum* is more robust in comparison to the holotype of *E. osborni*. This distinction contradicts Peterson's (1914a) earlier concept of *E. osborni* whereby differing degrees of robustness were attributed to sexual dimorphism. Specimens that have since been referred to either *E. osborni* or *D. progressum* vary only in the general robustness of the skull (including horn size and nasal thickness) and in the degree to which the lingual cusps of the premolars are separated or connected by a lingual crest.

Based on these aspects of variation Mader (1989, 1998) continued to accept *Eotitanotherium osborni* and *Diplacodon progressum*. Mader (1989) suggested that *E. osborni* was probably a junior synonym of *D. elatus* but he preferred to view the later as a nomen dubium because of the crushed nature of the holotype of that species. Because *Diplacodon* was not considered valid, Mader (2000) erected a new genus, *Pseudodiplacodon*, for the *progressum* species. Mader (2000) continued to distinguish *E. osborni* and *P. progressum* based on horn size, nasal thickness, and the degree of separation of the lingual cusps on the P4.

In considering all of the specimens, Mader's (2000) distinctions of *Eotitanotherium* and *Pseudodiplacodon* seem to represent continuous intraspecific variation. For instance, many of the specimens assigned to *Pseudodiplacodon progressum* by Mader (2000) have horns that are intermediate in size between the holotypes of *E. osborni* and *P. progressum* (e.g., AMNH 21887, CMNH 2858, CMNH 11881, CMNH 14632, FMNH P14632, and FMNH P14633) (for example, compare specimens in fig. 131 to fig. 132). In addition, specimens assigned to *P. progressum* by Mader (2000) distinctly vary in the

degree to which the lingual premolar cusps are separated. For example, in FMNH P14632 the hypocones and premolars are well separated, although in FMNH P14633 the lingual cusps are very poorly separated (fig. 135). Finally, the nasal bones of one of the three specimens that was earlier referred to *E. osborni* by Mader (1989) has a nasal bone that is as thick as those specimens referred to *P. progressum* by Mader (2000).

The variation in horn size, nasal thickness, and lingual premolar morphology among these specimens is seemingly continuous and is generally consistent with a pattern of intraspecific cranial variation found in other brontotheres. Additionally, the lingual premolar morphology is found to be variable in most brontothere species. Given the continuous nature of this variation, the specimens in question cannot be easily partitioned into discretely diagnosable units. Therefore, if specimens previously referred to *Eotitanotherium osborni* or *Pseudodiplacodon progressum* represent a single taxon, as is concluded here, *Diplacodon elatus* Marsh is a valid species. *E. osborni* (Peterson) and *P. progressum* (Peterson) are junior synonyms of *D. elatus*.

Specimens referred to *Diplacodon elatus* are confined to the Myton Member of the Uinta Formation. However, a large undescribed *Diplacodon*-like skull (AMNH 117163) with very heavily worn dentition was collected by Malcolm McKenna from Mudstone Peak in the Wiggins Formation of Wyoming. Previously, Mader (1998) suggested this skull belongs to *Protitanotherium*, but this is almost certainly not correct. The skull very closely resembles *Diplacodon*, particularly in its dual lingual premolar cusps, deep nasal incision, and distinctively upturned lateral margins of the nasal process. The skull, AMNH 117163, differs from typical *Diplacodon elatus* from the Uinta Formation in only a few ways. It is considerably larger, has more elliptical horns (with the longest axis anteroposterior), and the parasagittal ridges constrict the dorsal surface of the skull more severely than typical *D. elatus* skulls. This specimen could represent a new species of *Diplacodon*, but it has not yet been thoroughly studied. Some or all of these differences may relate to sexual dimorphism or intraspecific variation. For the time being its taxonomic identity is uncertain.

Parabrontops gobiensis (Osborn, 1925)

HOLOTYPE: AMNH 20354, a severely distorted skull with right P1–P4 (broken but complete), M1–M3 (severely damaged), left P3–M1 (partial), and M2–M3.

TYPE LOCALITY: Urtyn Obo Formation, Urtyn Obo, Shara Murun Region, Inner Mongolia, China.

AGE: Late Eocene (Ulangochuian land mammal "age").

REFERRED SPECIMENS: **(From the "Ulan Gochu" faunal zone [sensu Radinsky, 1964], Urtyn Obo, Shara Murun Region, Inner Mongolia)**; AMNH 26020, a partial skull lacking the occiput, basicranium and left zygomatic arch, with right C–M3. (Ulan Gochu [used in quotes] refers to a faunal zone rather than a formation; see Radinsky, 1964.)

The following mandibles could belong to *Parabrontops gobiensis*: **(from the Urtyn Obo Formation, Urtyn Obo, Shara Murun Region, Inner Mongolia)** AMNH 26019, a mandible with right and left incisors and canines (roots only), and p1–m3; AMNH 26021, a partial mandible with left p1–m3; **(from the "Shara Murun" Formation [sensu Radinsky, 1964], East Mesa, Shara Murun Region, Inner Mongolia)** AMNH 26131, a mandible with right and left i1–m3.

DIAGNOSIS: *Parabrontops gobiensis* is a large horned brontothere with short massive elliptical frontonasal horns. The horns are positioned low on the skull and directly above the orbits. The nasal incision extends to the anterior margin of the P4. The anterior rim of the orbit is above the anterolateral root of M1 and the posterolateral root of P4. The nasal process is very thick, unelevated, horizontal, strongly rounded anteriorly, with thickened lateral walls, and with a downturned distal tip. The premaxillomaxillary rostrum thickens posteriorly and it is not enclosed by bone dorsally. Other cranial characteristics include a saddle-shaped cranium, a dorsal cranial surface that is moderately constricted posteriorly by parasagittal ridges, a narrow emargination surrounding the posterior nares, nearly straight zygomatic

arches, and a ventrally constricted and mediolaterally angled external auditory pseudomeatus. Ventral sphenoidal fossae and postzygomatic processes are absent. Large zygomatic swellings are absent.

Dentally, *Parabrontops gobiensis* is characterized by three small upper incisors that form a straight row, a postcanine diastema, a complex P1, a distinct P2 metacone, and distinct premolar hypocones on P3 and P4. The molars of *Parabrontops gobiensis* have tall, lingually angled ectolophs with weak labial ribs, and thinned lingual ectoloph enamel with wedge-shaped paracones and metacones. A cingular parastyle shelf is absent. Distinct central molar fossae and anterolingual cingular cusps are present. Paraconules and metalophs are absent.

Parabrontops gobiensis shares with *Eubrontotherium clarnoensis* the combination of very small upper incisors, paired horns that are widely spaced and unelevated, and relatively straight zygomatic arches that lack conspicuous swellings. *Parabrontops gobiensis* differs from *Eubrontotherium* most clearly in the retention of three upper incisors.

Description

Skull: The holotype skull of *Parabrontops gobiensis* (AMNH 20354) is a nearly complete skull, although it is severely distorted. In addition to being crushed, it is laterally sheared and twisted so that the dorsal surface has been displaced far to the left of the ventral surface (figs. 137, 139). Many of the bone fragments, particularly in the facial area, are separated by plaster-filled gaps. AMNH 20260 is a partial skull missing the occiput, basicranium, and the left zygomatic arch (figs. 138, 140a). This skull, though less complete than the holotype, is not severely distorted.

There is conspicuous variation in the size and shape of the horns. The horns of the holotype (AMNH 20354) are large but short and slightly elliptical in cross section with the longest axis in an anteroposterior direction. The horns of AMNH 26020 are more massive and more strongly elliptical. On the side of the right horn of the holotype (AMNH 20354) the contact of the frontal and nasal bones can be seen revealing a configuration like most other horned brontotheres whose horn is composed of both the frontal and nasal bones. The frontonasal suture rises from the base of the horn and curves anteriorly along the side of the frontonasal horn. The peak and posterior surface of the horn is formed by the frontal. The proximal base and anterior side of the horn is formed by the nasal bone. The frontonasal contact is not readily discernable on AMNH 26020 where these elements appear to be more fully fused. The horns are essentially vertical in orientation, positioned low on the skull, and almost directly above the orbits. On AMNH 20354 the distal ends of the horns are roughened and each has a large pit at the apex. These unusual pits are unique to this specimen and appear to be an artifact of some form of damage. On AMNH 26020 the entire horn surface is roughened.

The holotype skull (AMNH 20354) is so distorted that the proportions of the face cannot be precisely described from that specimen although this area is more nearly intact in AMNH 26020. The nasal incision is very shallow and the posterior margin is not higher than the orbit. The nasal incision extends posteriorly to the anterior margin of P4. The orbit is situated directly above the anterior part of M2 and the posterolateral root of M1. The anterior rim of the orbit is above the anterolateral root of M1 and the posterolateral root of P4.

Despite the severe distortion, the nasal process of the holotype (AMNH 20354) is in good condition. From a dorsal view the nasal process is rather broad, of relatively constant width throughout its length, and the distal margin appears to be weakly rounded. From a lateral view the nasal process projects more or less horizontally from the skull. The sides of the nasal process form thickened and downturned lateral walls. The anterior margin is not as thickened as the lateral walls. The more complete nasal process of AMNH 26020 is similar to the holotype, although it is much thicker and the more nearly intact anterior edge is strongly rounded with a downturned distal tip. The lateral walls are very thick proximally and shallow distally. Additionally, from a dorsal view the nasal process tapers distally. The nasal bones are completely fused together, although at the

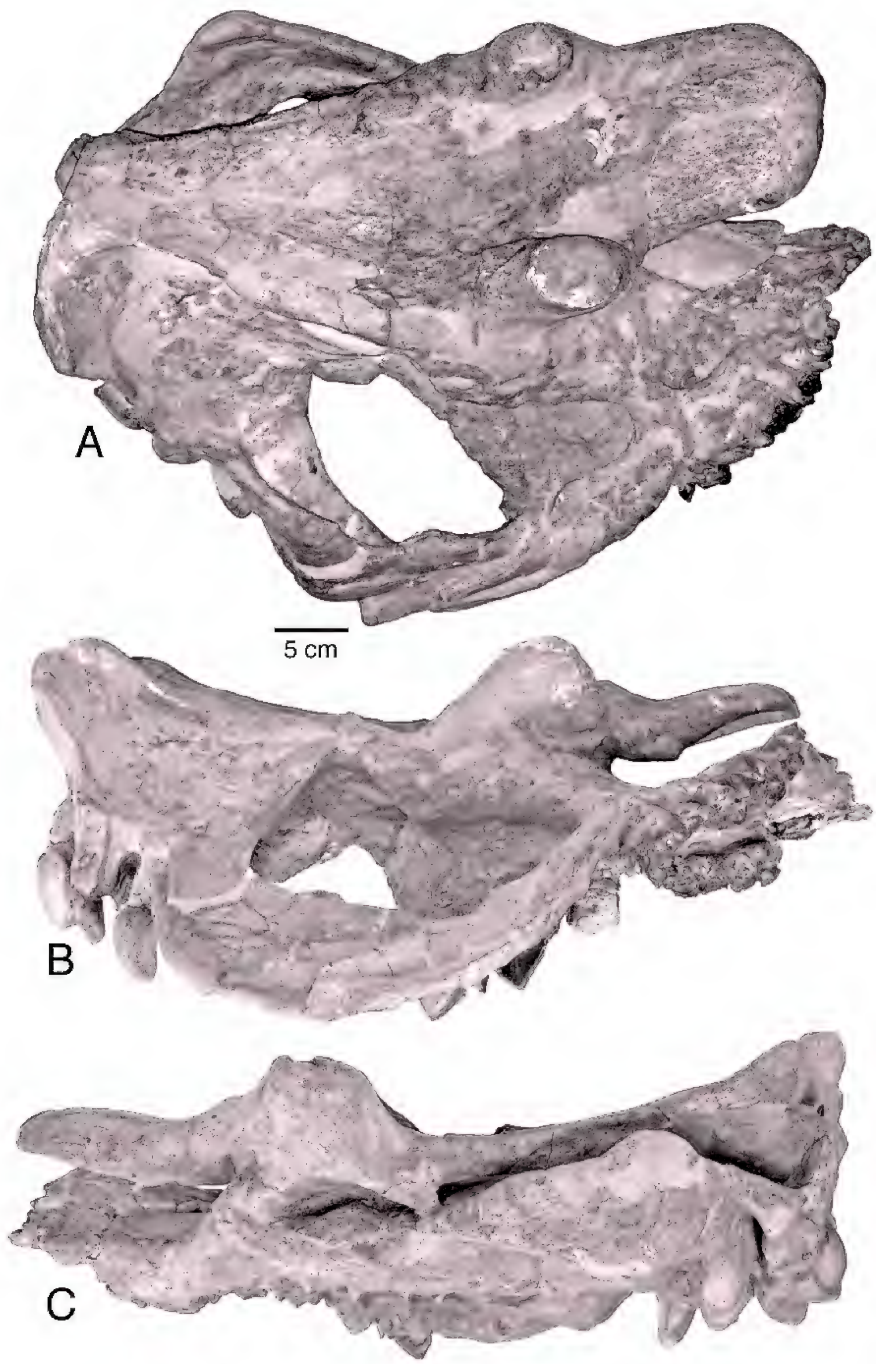

Fig. 137. The holotype skull of *Parabrontops gobiensis* (AMNH 20354). **(A)** Dorsal view, **(B)** right view, **(C)** left view.

distal tip they separate, creating a small median notch.

The nasal process and premaxillomaxillary rostrum are similar in length. The rostrum of the holotype (AMNH 20354) is severely twisted, but it is undistorted in AMNH 26020. From a lateral view the rostrum curves upward distally and deepens proxi-

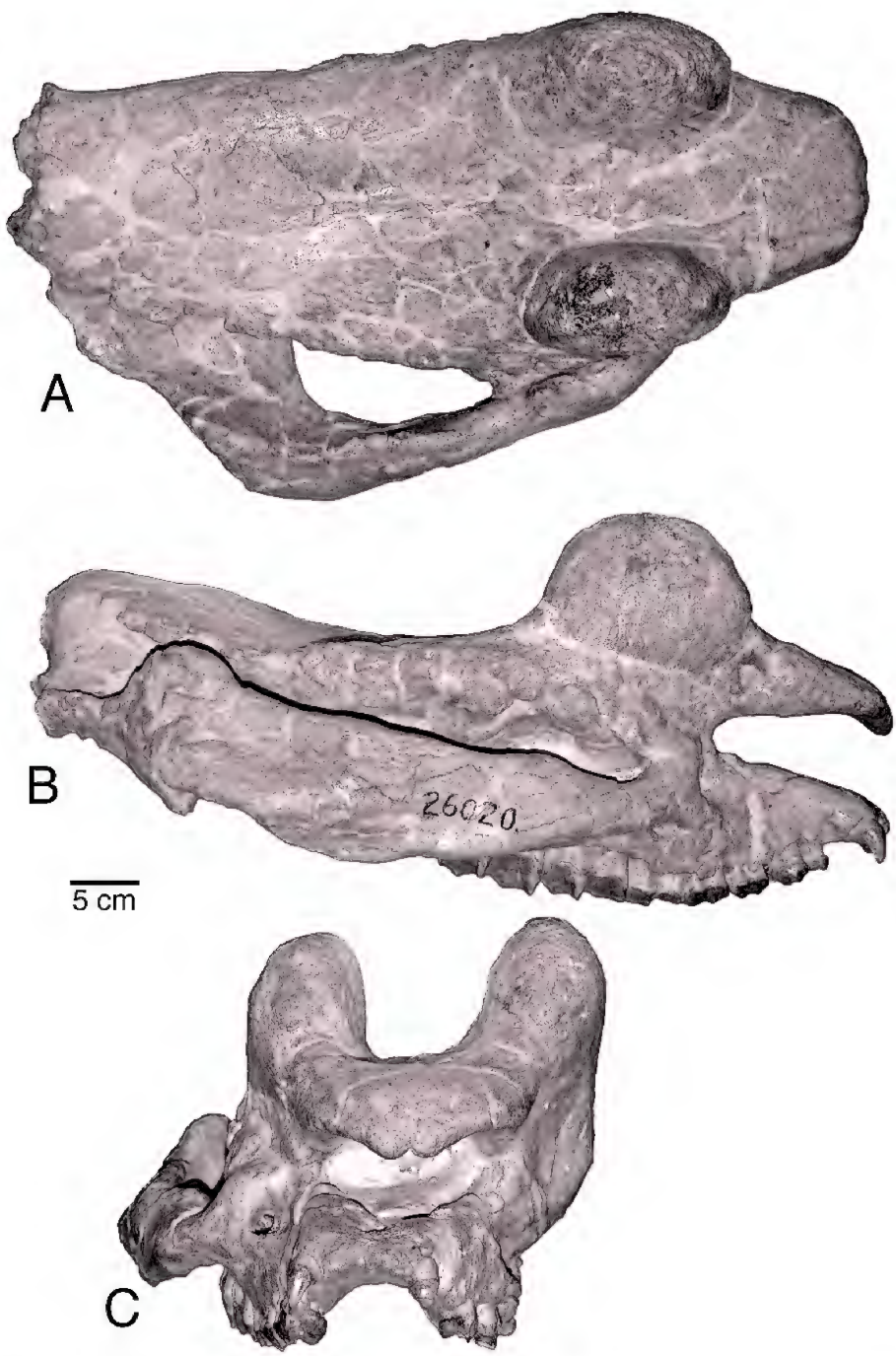

Fig. 138. A skull referred to *Parabrontops gobiensis* (AMNH 26020). **(A)** Dorsal view, **(B)** right view, **(C)** anterior view.

Fig. 139. Ventral view of the holotype of *Parabrontops gobiensis* (AMNH 20354).

mally. The dorsal margin of the rostrum rises posteriorly to the level of the midpoint of the orbit. The anterior margin of the premaxilla is flat and does not extend far beyond the canines. The premaxillomaxillary suture is not visible. Behind the premaxillary symphysis the dorsolateral margins of the rostrum diverge posterolaterally and the dorsal surface of the rostrum is not sealed by bone.

Though crushed, the holotype skull (AMNH 20354) indicates a shallow saddle-shaped cranium. The dorsal surface of AMNH 26020 is incomplete. In the holotype the left parasagittal ridge is complete and appears to moderately constrict the posterodorsal surface. In AMNH 26020 the parasagittal ridges appear to be more distantly separated posteriorly; however, there are significant plaster-filled gaps between the bone fragments in this part of the skull. Therefore, the width of the posterodorsal roof appears to be exaggerated in that specimen.

The left zygomatic arch of the holotype (AMNH 20354) is in relatively good condition and resembles the zygomatic arch of AMNH 26020. The zygomatic arch is thick and rectangular in cross section. From a dorsal view the zygomatic arch is straight and angled posterolaterally. Large central zygomatic swellings as seen in *Protitanops*, *Duchesneodus*, and *Megacerops* (sensu Mihlbachler et al., 2004b) are not present on any specimen of *Parabrontops gobiensis*. From a lateral view the jugal zygomatic process is horizontal. It is shallow anteriorly and deepens posteriorly. The squamosal zygomatic process is deep and straight, thus the zygomatic arch has essentially no curvature.

Granger and Gregory (1943) described the occiput (preserved only partially in AMNH 20354) as wide, although realistically the

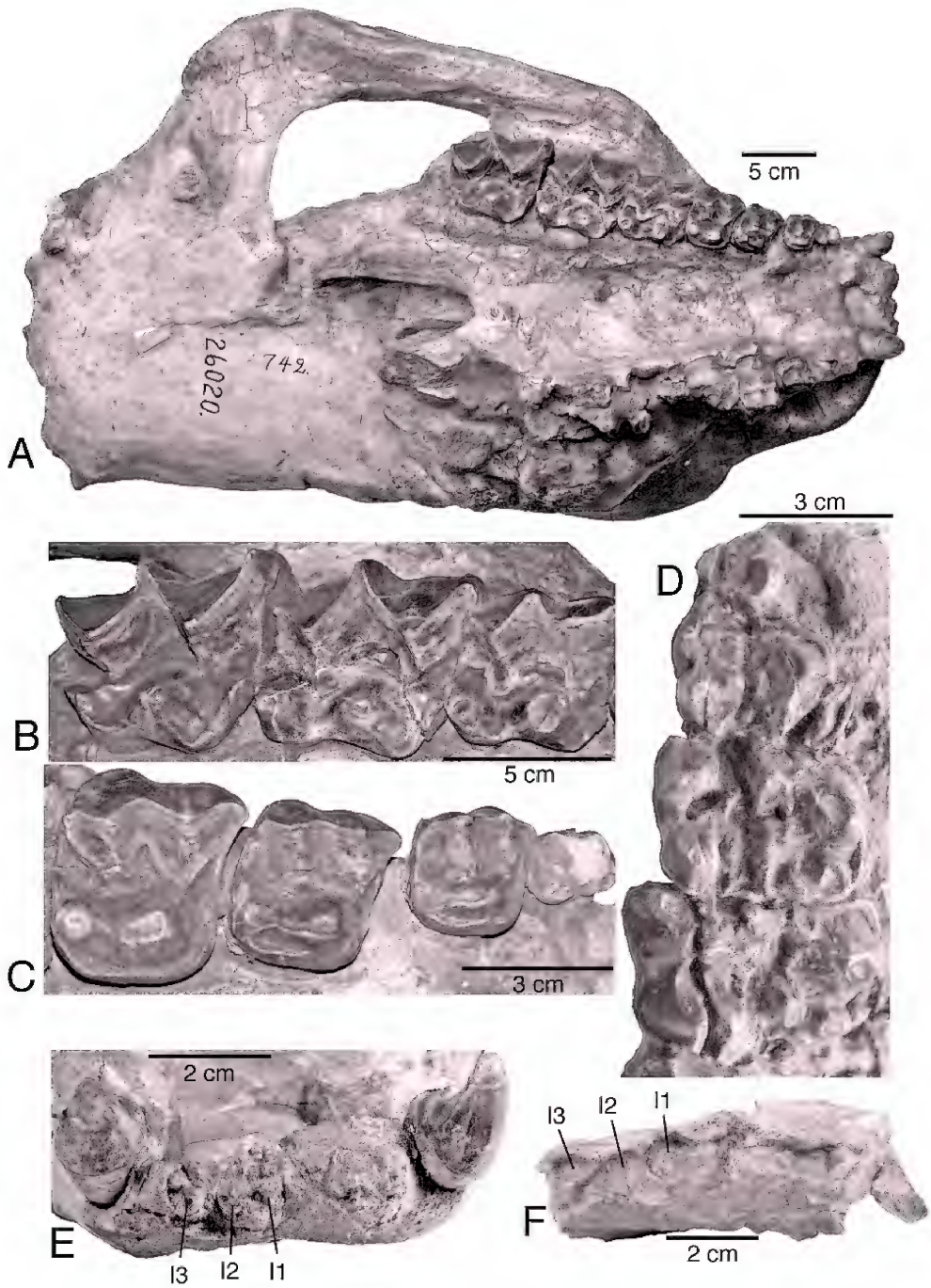

Fig. 140. Ventral view of skull and upper dentition of *Parabrontops gobiensis*. **(A)** Ventral view of AMNH 26020, **(B)** right molars of AMNH 26020, **(C)** right premolars of AMNH 26020, **(D)** right premolars of AMNH 20354, **(E)** canines and incisor roots of AMNH 26020, **(F)** incisor alveoli of premaxilla fragment associated with AMNH 20354 (in fig. 137 this fragment has been reattached to the skull).

shape and proportions of the occiput cannot be readily described with any certainty. However, from the ventral view of AMNH 20354 the posterior end of the skull does not appear to have been greatly widened as seen in *Metatitan* or *Rhinotitan andrewsi.*

The anterior rim of the posterior nares is positioned between the protocones of M3 in AMNH 20354, and slightly more posteriorly in AMNH 26020. A horseshoe-shaped rim emarginates the posterior nares. The elongate posterior narial canal does not appear to extend into the body of the sphenoid in AMNH 20354, although this area is poorly preserved. The entire basicranium of AMNH 20354 is poorly preserved, although one can discern that the foramen ovale and foramen lacerum are widely separated. The mastoid process is much shorter than the postglenoid process and it constricts the opening of the external auditory pseudomeatus, but it does not arch anteriorly to contact the postglenoid process. Thus, the external auditory pseudomeatus does not appear to be tube-shaped in AMNH 20354, although it is uncertain whether this reflects the actual condition of *Parabrontops gobiensis* or whether it is an artifact of distortion.

Upper Dentition: Close-ups of the upper dentition of *Parabrontops gobiensis* can be seen in figure 140. The holotype (AMNH 20354) lacks incisors and canines, although the remaining alveoli indicate an unreduced dental formula (3-1-4-3). Three small right incisor alveoli can be seen on the premaxilla of the holotype (fig. 140f). AMNH 26020 also lacks incisors, although portions of the roots of left I1, I2, and I3 are labeled in fig. 140e. The roots of the I2 and I3 are clearly preserved in AMNH 26020. Granger and Gregory (1943) state, "the alveoli of the medial pair of incisors (I1), if formerly present, are not evident" (Granger and Gregory, 1943: 367). However, Granger and Gregory (1943) were mistaken; a remnant of the root of the left I1 is present. The right I1, on the other hand, appears to be absent. Probably, it was lost during life due to bone remodeling. There are two very small globular incisor crowns associated with AMNH 26020 although neither of these articulates with the fragments that are still rooted in the skull and they certainly do not belong to the same individual. The incisor row of AMNH 26020 is narrow, nearly straight, and positioned only slightly anterior to the space between the canines. The complete canines of AMNH 26020 are very small. There is no precanine diastema, but a distinct short postcanine diastema is present.

The cheek teeth of AMNH 20354 are smashed, although the morphology of the right premolars and left posterior molars is partially discernable (figs. 139 and 140d). Additionally, the right cheek-tooth row of AMNH 26020 is intact (fig. 140b, c). The P1 is heavily worn. It is smaller than those premolars that are posterior to it, but it is nearly as broad (transversely) as it is long (anteroposteriorly). The morphology of P1 is relatively advanced with two distinct labial cusps that are joined by an ectoloph, and a small lingual heel with a small protocone.

The P2–P4 of AMNH 20354 are bisected by a large crack that separates the ectolophs from the lingual heels; therefore the widths of these teeth are exaggerated. The dimensions of the P2–P4 are nearly intact in AMNH 26020, although the P2 and P3 of that specimen are separated by an artificial gap. The premolars are nearly rectangular, although the anterior margins of P2 and P3 are slightly angled more posterolingually than the posterior margins. The labial paracone ribs are small but well defined and become progressively narrower in consecutively posterior premolars. The parastyle of P2 is straight or arched somewhat lingually. The P3 parastyle is angled slightly labially, while the P4 parastyle is strongly arched labially. The metastyles of P2 and P3 are straight while that of P4 is angled slightly labially. The lingual side of the P2 of AMNH 20354 is damaged, but a large protocone and lingual crest extending posteriorly from it can be discerned. The hypocone is either absent or so small that the lingual crest has absorbed it. Two distinct lingual cusps can be found on P3–P4. The hypocones of P3 and P4 are smaller than the protocones and are not connected by a crest. The P2–P4 of AMNH 26020 vary from the holotype in that the hypocones of the P3 and P4 are strongly connected to the protocone by a lingual crest. In both specimens a low but distinct preprotocrista is seen on P2. The preprotocrista

is less distinct on P3 and is not discernable on P4. There is no evidence of anterolingual cingular cusps on any of the premolars. The premolar cingula are continuous around the lingual side of the crowns of AMNH 20354, but in AMNH 26020 the lingual cingula are slightly discontinuous on P2 and P3.

The upper molars of *Parabrontops gobiensis* show typical brontotheriine characteristics, including increased ectoloph height, convex and lingually angled labial walls, very weak labial ribs, thin lingual ectoloph enamel, and wedge-shaped lingual sides of the paracone and metacone in molars that are not heavily worn. The anterior cingulum is thin and passes proximally to the distal peak of the parastyle. Distinct central molar fossae are seen in M1–M3. All evidence of paraconules and metalophs is absent. The M3 exhibits a large anterolingual cingular cusp. This feature is less obvious on M1 and M2, but this appears to be due to the greater extent of wear of those teeth. The M3 has a very small pointed hypocone. The labial and lingual molar cingula are very weak and discontinuous.

cf. *Parabrontops gobiensis* mandibles

REFERRED SPECIMENS: **(From the Urtyn Obo Formation, Urtyn Obo, Shara Murun Region, Inner Mongolia)** AMNH 26019, a mandible with right and left incisors and canines (roots only), and p1–m3; AMNH 26021, a partial mandible with left p1–m3; **(from the "Shara Murun" Formation [sensu Radinsky, 1964], East Mesa, Shara Murun Region, Inner Mongolia)** AMNH 26131, a mandible with right and left i1–m3.

DESCRIPTION

MANDIBLE AND LOWER DENTITION: None of the AMNH skulls of *Parabrontops gobiensis* is directly associated with a mandible, although several mandibles in the collection might represent this species. Granger and Gregory (1943) referred two mandibles to *P. gobiensis*, AMNH 26019 and AMNH 26131. There are minor differences between these two specimens and the others that are described below.

Generally, these mandibles are consistent with what one would predict for the mandible of *Parabrontops gobiensis* with three small lower incisors that form a nearly straight row between the incisors and a short postcanine diastema. The combination of these characters rule out most other species of other large Asian brontotheres (e.g., *Protitan*, *Rhinotitan*, or *Metatitan*). The most complete of these mandibles (AMNH 26131) is the larger of the two (fig. 141). The ventral margin of the symphysis is convex and steeper than 45°. The symphysis extends to the talonid of the p4; however, this position of the posterior margin of the symphysis appears to have been effected by a paleopathology, possibly a dento-alveolar abscess near or on the lingual side of P4 and M1, that has resulted in a swollen right ramus.

Six small incisors form nearly a straight row between the anterior margins of the canines. The incisors appear to be wedge-shaped, although the apices of the crowns are worn. The incisors lack distinct lingual cingulids although this could be related to wear. The i2 is the largest incisor. The canines are of moderate size. There are no precanine diastema or gaps between the incisors. The postcanine diastema is about as long as p2.

The p1 is small with a small talonid heel. The p2 trigonid is much longer and slightly narrower than the talonid. The p3 and p4 trigonids and talonids are of similar width, although the trigonids are narrower. The paralophid of p2 is weakly angled lingually, creating a small lingual trigonid notch. The p2 protolophid is straight, but it is positioned lingually. The paralophids and metalophids of p3 and p4 are strongly arched lingually, creating nearly molariform trigonid basins. A large, lingually positioned metaconid is found on p3 and p4 but not on p2. The talonids of p2–p4 all have well-developed cristids obliqua and hypolophids with broad basins. Labial and lingual premolar cingulids are essentially absent. The molars are typical with thin lingual enamel, shallow talonid and trigonid basins, and m3 is elongate. There are very thin labial molar cingulids but no lingual molar cingulids.

The other mandible referred to *Parabrontops gobiensis* (AMNH 26019) by Granger and Gregory (1943) differs from AMNH

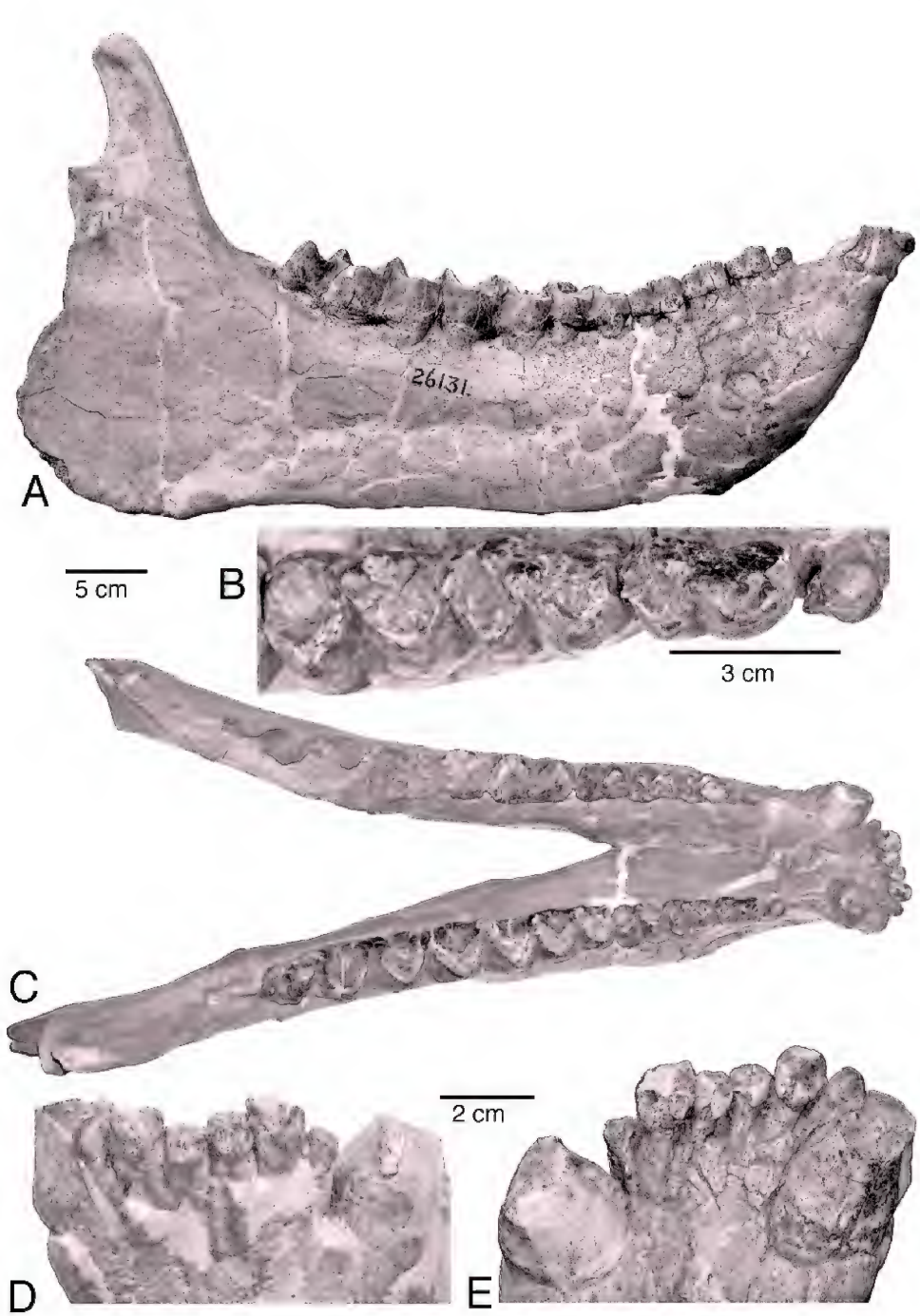

Fig. 141. A possible mandible of *Parabrontops gobiensis* (AMNH 26131). **(A)** Right view, **(B)** right premolars, **(C)** dorsal view, **(D)** labial view of incisors and canines, **(E)** lingual view of incisors and canines.

26131 in several ways (fig. 142). The inferior margin of the symphysis is angled slightly less than 45°, although the extent to which distortion has affected this variable in either AMNH 26131 or AMNH 26019 is uncertain. The posterior margin of the symphysis is slightly more anterior, although comparison of this character is complicated by the

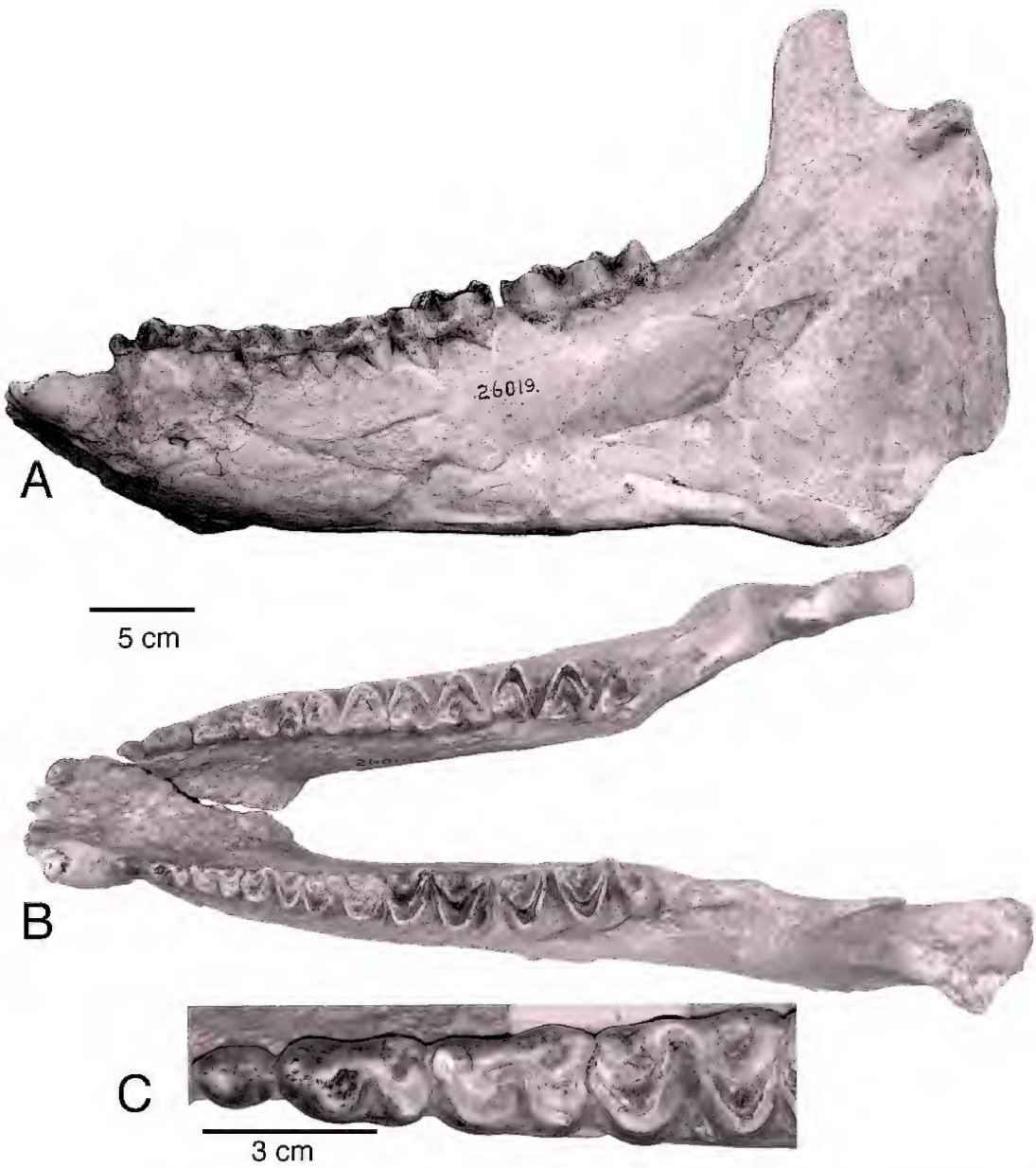

Fig. 142. A possible mandible of *Parabrontops gobiensis* (AMNH 26019). **(A)** Left view, **(B)** dorsal view, **(C)** left premolars.

seemingly pathological condition of the ramus in AMNH 26131. The most obvious difference between these two specimens is the premolars. The premolars of AMNH 26019 seem less molariform. The p2 talonid has a broad lingual notch, but lacks a basinlike depression. The p3 paralophid is only weakly lingually angled, the p3 protolophid is straight, and there is no sign of a p3 metaconid. Additionally, the m3 of AMNH 26019 is proportionately shorter.

Remarks

Osborn (1925) named *Parabrontops gobiensis* from a nearly complete but extremely

crushed and distorted skull. Osborn (1925) originally assigned this species to the North American genus *Brontops* (= *Megacerops* sensu Mihlbachler et al., 2004b). Osborn's initial description of the holotype was very brief and was based on the "cranium reconstructed after comparison with that of *Brontops brachycephalus*" (Osborn, 1925: 5). Subsequently, Osborn (1929a) described and figured an interpretation of the skull had it been undistorted.

Because Osborn's (1929a) reconstruction was based on North American *Brontops*, the reconstruction of the holotype skull figured by Osborn (1929a), and the cranial measurements that were provided are not necessarily reliable. Granger and Gregory (1943) were the first to actually figure and describe the specimen in its extremely distorted condition. They assigned this species to its own genus, *Parabrontops*.

The material from the AMNH collection that was originally described by Granger and Gregory (1943) is the only material assignable to *P. gobiensis*. Yanovskaya (1980) referred another skull of *P. gobiensis* from the Ergilin Dzo, but this specimen is more consistent with *Eubrontotherium clarnoensis*. Likewise, Mihlbachler et al. (2004a) wrongly suggested that other materials from the PIN collection (the material misidentified as *Metatitan relictus* by Yanovskaya [1980]) could belong to *P. gobiensis*; all of these materials are now referred to *Eubrontotherium clarnoensis*. Hu (1961) referred a set of upper molars (IVPP V2490) from an unknown formation in the Hami Basin of China to *Parabrontops* (see Russell and Zhai, 1987), although this specimen lacks characters that are diagnostic of *P. gobiensis*.

Granger and Gregory (1943) considered *Parabrontops* to be very closely related to *Metatitan*; they suggested that the only differences between these taxa are the larger horns and lesser width of the incisive border of the premaxillary. However, *Parabrontops gobiensis* differs from *Metatitan* in several other ways, such as the lack of paired ventral sphenoidal fossae, the more completely saddle-shaped skull, the presence of a postcanine diastema, and substantially more molarized premolars. Moreover, the horns and nasal process are not elevated, and the basicranium and occiput are not widened as in *Metatitan*. *Parabrontops* more closely resembles *Dianotitan*, *Eubrontotherium*, *Protitanops*, *Duchesneodus*, and *Megacerops*. *Parabrontops* shares with these species relatively large, widely separated frontonasal horns and reduced globular incisors. Recognizing these similarities, Wang (1982) considered *Parabrontops* to have closer phylogenetic affinities with North American "Brontopinae" than with other Asian brontotheres. *Parabrontops gobiensis* closely resembles *Eubrontotherium*, particularly in its small incisors and in lacking conspicuous zygomatic swellings. However, *Parabrontops gobiensis* differs from *Eubrontotherium* in its retention of three upper incisors.

Eubrontotherium clarnoensis Mihlbachler, 2007

HOLOTYPE: UCMP 126100, a skull missing the occiput with right and left I3–M3.

TYPE LOCALITY: UCMP locality I-V75203, Clarno Formation, Hancock Quarry, Wheeler, Oregon.

AGE: Late or Middle Eocene of North America (latest Uintan, Duchesnean, or Chadronian land mammal "age"?), Late Eocene of Asia (Ulangochuian land mammal "age").

REFERRED SPECIMENS: (See Mihlbachler [2007] for a list of referred specimens from the Hancock Quarry locality); **(from Ergilin Dzo (lower part), Dornogobi Province, Outer Mongolia)** an associated partial skeleton all assigned to PIN 3109 with the following numbers: 90, a partial skull missing the left zygomatic and left side of cranium with right I1–M3, and left I1–M2, M3 (partial); 91, a mandible with right and left i1–m3; a partial postcranial skeleton with the following numbers 92–102, 103, 104, 106, 111–116, 142–231, 232; PIN 3109-39, a flattened skull with right and left I2–M3.

DIAGNOSIS: *Eubrontotherium clarnoensis* is a large horned brontothere with small rounded frontonasal horns. The horns are positioned anterior to the orbits and high on the skull, but the horns and nasal process are not elevated to the degree seen in *Diplacodon elatus*. The nasal incision extends as far back as the anterior margin of the P4. The anterior

rim of the orbit is between the anterior and posterior lateral roots of the M1. The nasal process is broad, horizontal, slightly downturned, of nearly constant width throughout its length, strongly rounded anteriorly, and with shallow and thickened lateral walls. The premaxillomaxillary rostrum thickens posteriorly and it is not enclosed by bone dorsally. Other cranial characteristics include a saddle-shaped cranium, a dorsal cranial surface that is moderately constricted posteriorly by parasagittal ridges, a narrow emargination surrounding the posterior nares, moderately curved zygomatic arches, and a ventrally constricted and mediolaterally angled external auditory pseudomeatus. Ventral sphenoidal fossae, postzygomatic processes, and lateral zygomatic swellings are absent.

Dentally, *Eubrontotherium clarnoensis* is characterized by two small, globular upper incisors that form a straight row, a long postcanine diastema, a complex P1, a distinct P2 metacone, and premolar hypocones on P2–P4. The molars have tall, lingually angled ectolophs with weak labial ribs and thinned lingual ectoloph enamel with wedge-shaped paracones and metacones. A cingular parastyle shelf is absent. Central molar fossae and anterolingual cingular cusps are present. Paraconules and metalophs are absent. The lower dentition of *Eubrontotherium clarnoensis* includes three very small wedge-shaped lower incisors, a distinct postcanine diastema, a metaconid on p4 but not on p2 and p3, and a p2 trigonid that is less than twice the length of the talonid. The lower molars have shallow basins and the m3 is slender.

Eubrontotherium clarnoensis is the only brontothere species that simultaneously lacks large zygomatic swellings and has a a reduced number of upper incisors.

Description

The type specimen of *Eubrontotherium clarnoensis* and other material representing this species from the type Hancock Quarry locality of Oregon was described by Mihlbachler (2007) and is not repeated here. The material described below is additional material from Asia that is consistent with *Eubrontotherium clarnoensis*, and appears to document the occurrence of the same species in Asia.

Skull: PIN 3109-90 is a partial skull that is missing the left zygomatic arch and much of the left side of the cranium (fig. 143). Although the surface of the skull is extensively fractured, it does not appear to be significantly crushed or distorted, although the right zygomatic arch seems to have been displaced slightly medially. From a lateral view this specimen provides a more faithful representation of the shape of the skull of *Eubrontotherium clarnoensis* in comparison to the type skull from Oregon (UCMP 126100) which is dorsoventrally flattened. A significantly more damaged skull, PIN 3109-39 (fig. 144), is also referable *E. clarnoensis*. This specimen is dorsoventrally crushed and is missing its frontonasal region and the dorsal portion of the occiput.

The horns of PIN 3109-90 are relatively smooth, short, and with slightly elliptical bases but with more rounded peaks. The horns project in an anterodorsolateral direction and are positioned between the orbits and the nasal incision. The contact of the frontal and nasal bones can clearly be seen on the lateral surface of the right horn in PIN 3109-90. The frontal forms the apex and posterodorsal surface of the horn, while the nasal forms the base and anterodorsal surface. The horns and nasal process are elevated well above the orbits in this specimen, although not to the degree seen in *Diplacodon elatus*. The right and left nasal bones are completely co-ossified. The nasal process is broad and slightly shorter than the premaxillomaxillary rostrum. From a lateral view the nasal process curves downward and its dorsal surface is somewhat convex. The lateral margins of the nasal process are very thick, curved downward, and become somewhat deeper proximally. The distal margin of the nasal is strongly rounded but it is not strongly downturned. The distal margin of the nasal process is thick but not as thick as the lateral margins. The nasal incision extends posteriorly to a point above the anterior margin of P4. The orbit is directly above the posterior part of M2 and the anterior part of M1, with the anterolateral root of M1 positioned directly below the anterior orbital rim.

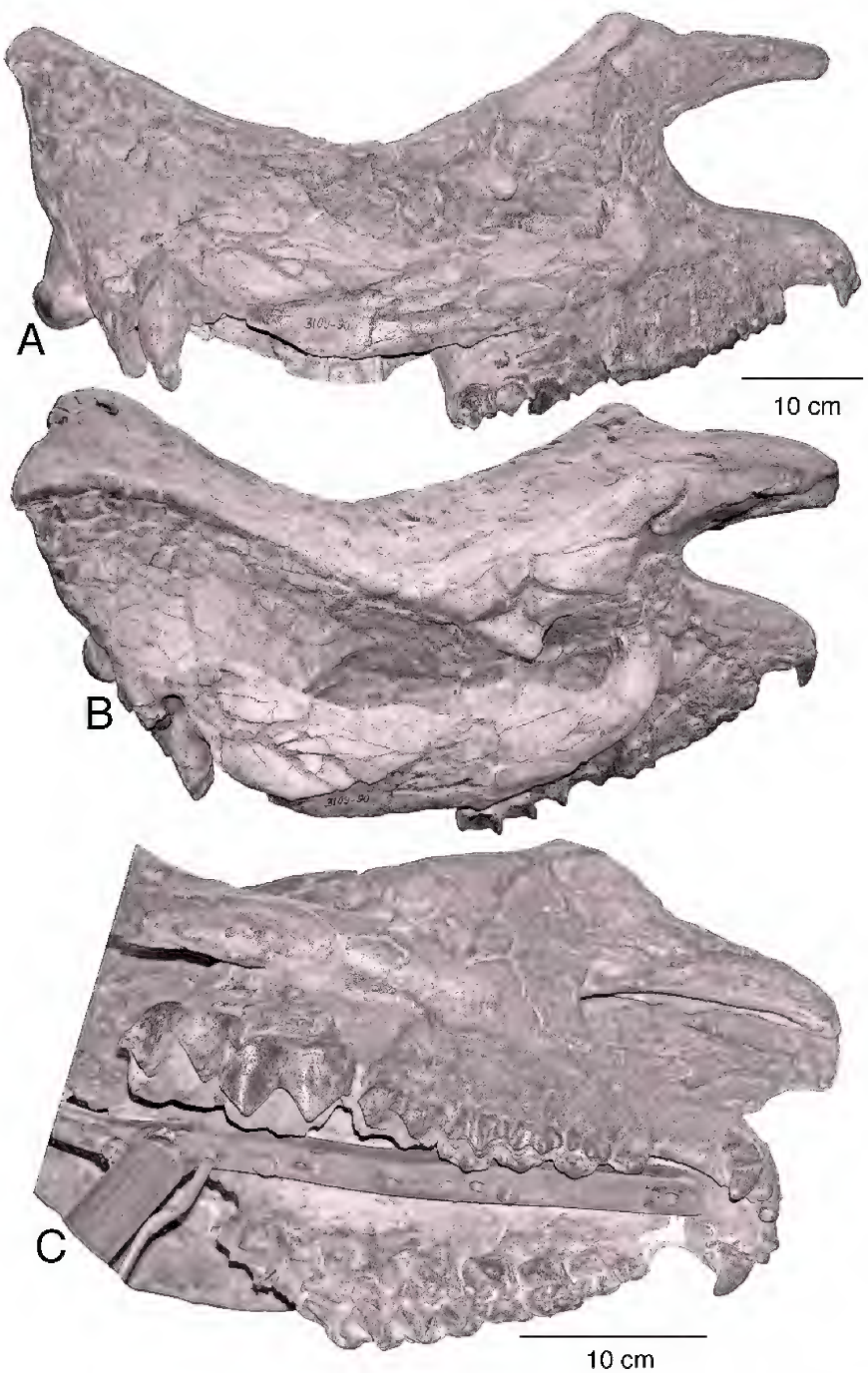

Fig. 143. Asian skull of *Eubrontotherium clarnoensis* (PIN 3109-90). **(A)** Right view, **(B)** right view rotated to see the dorsal surface, **(C)** right view rotated to see the ventral surface.

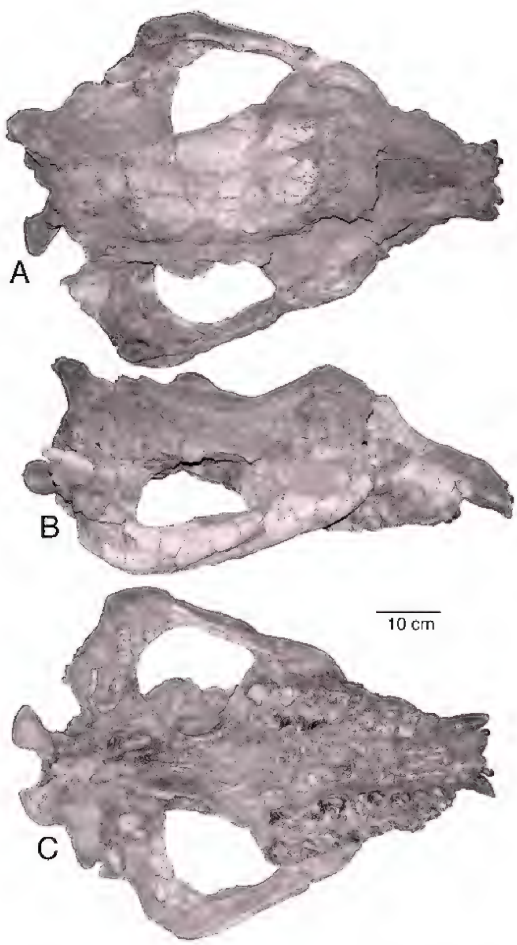

Fig. 144. Asian skull referred to *Eubrontotherium clarnoensis* (PIN 3109-39). **(A)** Dorsal view, **(B)** right view, **(C)** ventral view.

From the lateral view, the premaxillomaxillary rostrum is slightly longer than the nasal process. The rostrum curves upward distally although the anteriormost portion is angled slightly downward. The rostrum deepens proximally while its lateral dorsal margin slopes upward and rises to about the midlevel of the orbit. The premaxilla is short and does not extend anterior to the canines.

The dorsal surface of the skull is fully concave. The parasagittal ridges are prominent and remain widely separated throughout their length, although they moderately constrict the transverse width of the posterodorsal cranial surface. From a lateral view the zygomatic process of the jugal is horizontal while the zygomatic process of the squamosal is sloped posterodorsally, thus giving the zygomatic arch a moderate curvature that is more pronounced than that of *Parabrontops*. From a dorsal view the zygomatic arch is straight, thin, and angled posterolaterally. Neither PIN 3109-90 nor PIN 3109-39 has strongly laterally bowed zygomatic arches or thick laterally projecting zygomatic swellings at the junction of the jugal and squamosals.

The occiput of PIN 3109-90 is poorly preserved, limiting its description. It is moderately tilted backward with a relatively flat nuchal crest. The dorsal portion of the occiput is similar in width to the ventral portion. The nuchal crest appears to have a small median notch. The nuchal crest of PIN 3109-90 is thinner than that of UCMP 126101, the only North American specimen of *Eubrontotherium clarnoensis* with a preserved nuchal crest. However, that particular skull (UCMP 126101) is rather robust in comparison to other North American specimens; nuchal crest thickness appears to covary with overall cranial robustness and could be related to sexual dimorphism.

The ventral surface of the skull of PIN 3109-90 is incomplete and is presently obscured by a steel mounting frame. However, a few details can be discerned from Yanovkaya's (1980) original figure of it, reprinted in fig. 145a. The basicranium of PIN 3109-39 (fig. 144) is also complete although it is crushed. The anterior rim of the posterior nares is positioned anterior to M3. The elongate posterior narial canal does not appear to extend significantly into the sphenoid as it shallows off posteriorly, and large ventral sphenoidal fossae are not seen in either specimen. Like most other horned brontotheres, the external auditory pseudomeatus is tube-shaped and enters the skull in a mediolateral direction.

Upper Dentition: The dentition of PIN 3109-90 is less worn than that of PIN 3109-39 and thus provides the bulk of the following description (fig. 145). Both skulls indicate two pairs of upper incisors that form a nearly straight row directly anterior to the canines. In PIN 3109-90 both incisor pairs are present with a large median diastema between the central pair. The other skull, PIN 3109-39, retains the outer pair, although

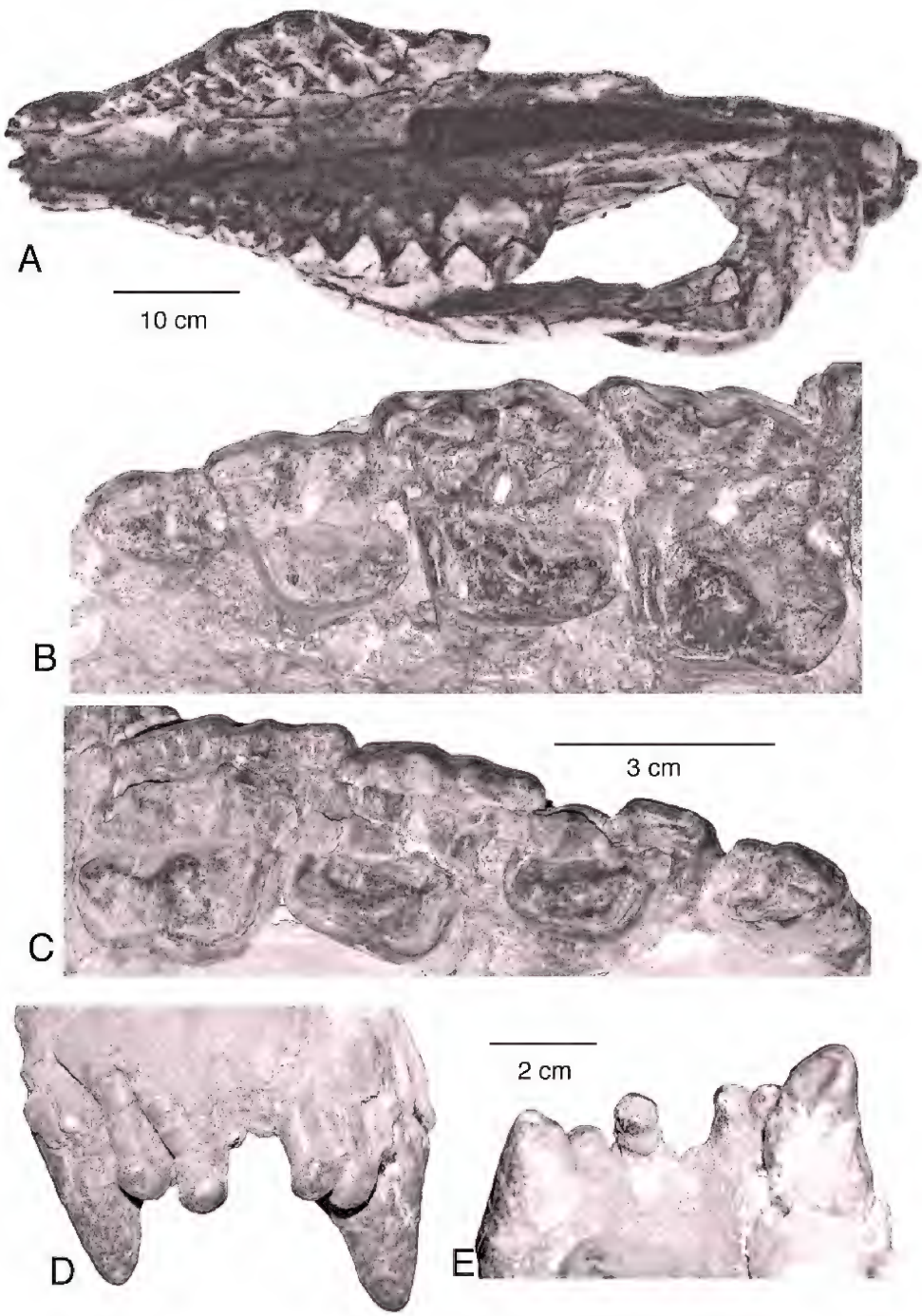

Fig. 145. Ventral view of skull and dentition of Asian *Eubrontotherium clarnoensis* (PIN 3109-90). **(A)** Ventral view (from Yanovskaya [1980]), **(B)** left P1–P4, **(C)** right P1–P4, **(D)** labial view of incisors and canines, **(E)** lingual view of incisors and canines.

the alveoli for the central pair are still present. Both the medial and lateral incisors are very small (essentially vestigial) with small globular crowns. Neither specimen has any evidence of a third pair of incisors.

The canines of PIN 3109-90 are a little smaller than those of PIN 3109-39. There is a short diastema between the lateral incisor and canine in PIN 3109-39, but this diastema is absent in PIN 3109-90. However, both specimens retain a distinct postcanine diastema of variable length ranging from 1.2 cm (PIN 3109-39) to 3.5 cm (PIN 3109-90).

The P1 is small and ovoid in outline with the widest point near the posterior side of the crown. There are two distinct labial cusps, a paracone and a much smaller metacone. The lingual heel is small and posteriorly positioned. The lingual heel of the P1 has a small cusp with a small but distinct preprotocrista that attaches to the lingual side of the paracone; these features are more obvious on the right P1.

The ectolophs of the right P2–P4 are damaged. The left P2–P4 are nearly rectangular in shape with nearly parallel anterior and posterior sides; although P2 and, to a lesser extent, P3 are oblique. The P2 parastyle is angled anteriorly, while the parastyles of P3 and P4 have a more anterolabial orientation. The metastyles of P2–P4 are more or less straight and not distinctly angled labially. From an occlusal view the labial surfaces of the P2 paracone and metacone are broad convexities. The labial sides of the paracones and metacones of P3 and P4 are flatter with distinct labial ribs. Distinct labial ribs are not seen in the metacones of P3 and P4. The P4 of PIN 3109-90 has a small mesostyle. P4 mesostyles are occasionally found within numerous brontothere species, but usually only rarely. However, the P4 mesostyle appears to have been rather frequent in *Eubrontotherium clarnoensis* (Mihlbachler, 2007).

The P2–P4 of PIN 3109-90 tend to have dual lingual cusps. The P2 hypocone is poorly developed and connected to the protocone by a weak lingual crest. The hypocones of P3 and P4 are more developed, although they remain smaller than the protocone and are weakly connected to it by a small lingual crest. The P2 has a distinct preprotocrista. The P3 and P4 have discernable preprotocristae, but they are not as developed. The anterior premolar cingula thicken near their midpoints directly between the protocone and the lingual edge of the paracone. However, these cingular thickenings do not form distinct cingular cusps as occasionally seen in *Duchesneodus uintensis* and *Megacerops coloradennsis*. Labial premolar cingula tend to be weak while lingual premolar cingula are thicker and tend to be continuous or only slightly discontinuous around the lingual base of the protocone.

The upper molars of PIN 3109-90 are not well preserved, but they show a morphology that is essentially undifferentiated from closely related taxa. The ectoloph is rather tall and its labial wall is strongly angled lingually. The vertical labial ribs of the paracone and metacone are very weak. The lingual band of ectoloph enamel is much thinner than the labial band and the lingual margins of the paracone and metacone are wedge-shaped rather than rounded. The anterior cingulum of the molars is thin and passes proximally to the distal peak of the parastyle. Small anterolingual cingular cusps are present. Due to poor preservation central molar fossae are not visible on the holotype specimen; however, remnants of small central molar fossae can be seen on the extremely worn molars of the referred skull, PIN 3109-39 (fig. 144). The M3 of PIN 3109-90 has a large hypocone, while PIN 3109-39 appears to have had only a small hypocone. Labial and lingual molar cingula are exceedingly weak or absent.

Mandible and Lower Dentition:
The mandible (PIN 3109-91) is missing only the left ascending ramus (fig. 146). In comparison to the North American mandible of *Eubrontotherium clarnoensis* (UCMP 126102), the horizontal ramus of PIN 3109-91 seems deeper and the symphysis seems more narrow; however, these differences seem to relate to minor lateral crushing in PIN 3109-91. From a lateral view of PIN 3109-91, the inferior margin of the mandibular symphysis is slightly convex and seems to be angled a little less than 45°. From a dorsal view the symphysis seems rather narrow and extends posteriorly to the p4 talonid.

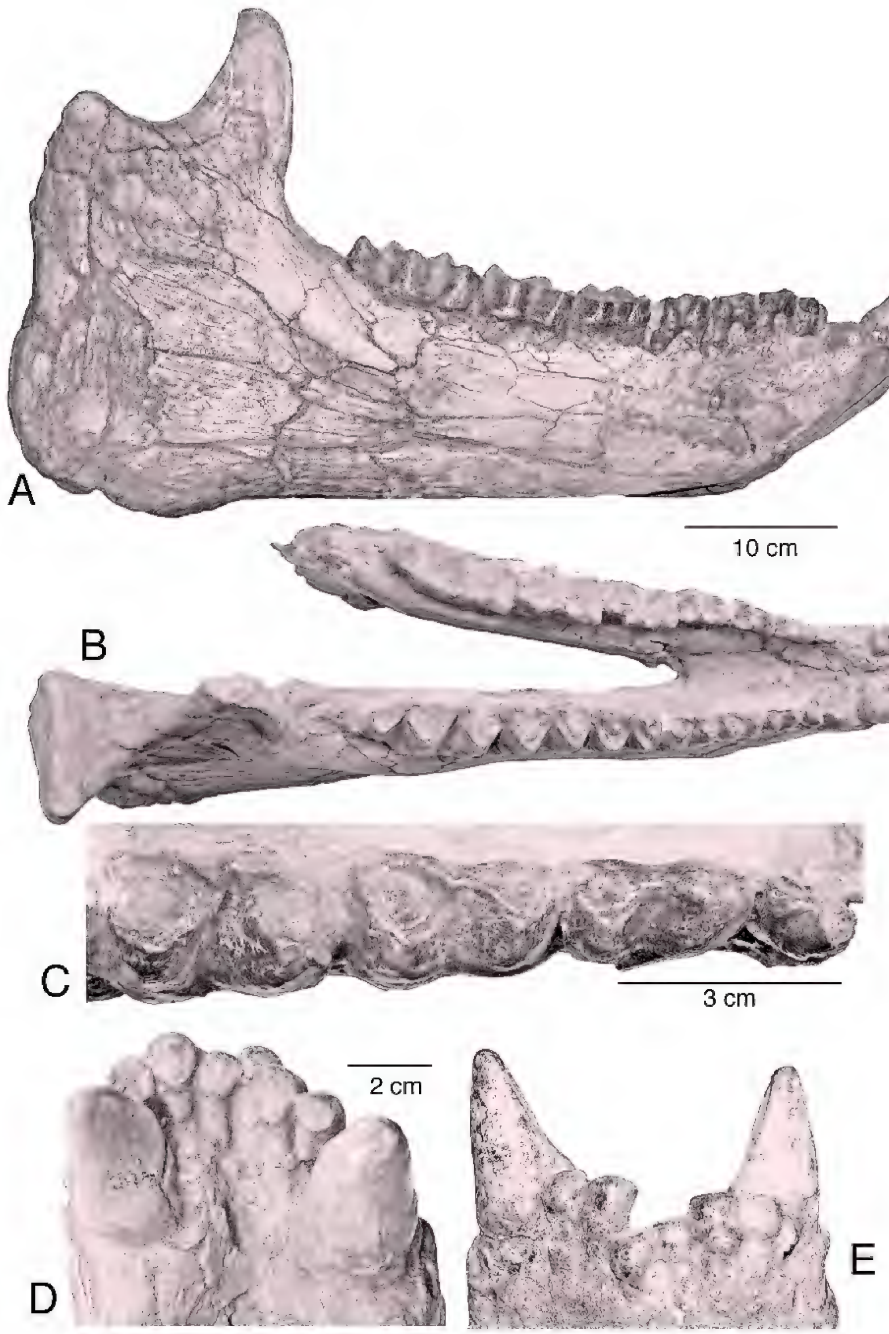

Fig. 146. Asian mandible of *Eubrontotherium clarnoensis* (PIN 3109-91). **(A)** Right view, **(B)** dorsal view, **(C)** right p1–p4, **(D)** lingual view of incisors and canines, **(E)** labial view of incisors and canines.

Although the upper incisors of *Eubrontotherium clarnoensis* are reduced to two pairs, three pairs of small lower incisors are retained. The lower incisors form a nearly straight row between the anterior margins of the canines. Each of the incisors is tiny and slightly wedge-shaped. A thin vertical rib can be seen on the lingual surface of i1 and i2. The i2 is distinctly larger than i1 or i3. Labial incisor cingulids are absent and lingual

incisor cingulids are exceptionally weak. In contrast to the North American mandible of *Eubrontotherium* in which the incisors have small gaps between them, the incisors of PIN 3109-91 appear to be unusually crowded between the canines, although this difference may also relate to transverse crushing.

The lower canines of PIN 3109-91 are relatively large. A postcanine diastema of about 3 cm is present. The p1 is small and narrow, with a single cusp and a small, simple talonid heel. The p2 trigonid is slighly narrower and longer than the p2 talonid. The p3 and p4 trigonids are narrower than the talonids, but the trigonids are more similar in length to the talonids. The paralophid of p2 arches slightly lingually, creating a small lingual trigonid notch. The p2 protolophid is angled slightly lingually. The paralophid and protolophid of p3 are more strongly angled lingually, creating a broader lingual notch. The paralophid and protolophid of p4 are longer and arch fully lingually. Metaconids are absent on p2 and p3, but a large, molariform, lingually positioned metaconid can be found on p4. The talonid of the p2 has a short cristid obliqua and hypolophid with a shallow lingual-talonid notch. The talonids of p3 and p4 have longer cristids obliqua and hypolophids with more nearly molariform talonid basins. Labial and lingual premolar cingulids are essentially absent. The lower molars of PIN 3109-91 have shallow occlusal basins, thin lingual enamel, and an elongate m3, and they are not different from other advanced brontotheres. Lingual cingulids are absent while labial cingulids tend to be weak and discontinuous around each labial cusp.

Remarks

The specimens from the Ergilin Dzo Formation of Mongolia described above were initially identified by Yanovskaya (1980) as belonging to other species. PIN 3109-90 and 3109-91 were referred to *Metatitan relictus* and PIN 3109-39 was referred to *Parabrontops gobiensis*. These identifications appear to be erroneous. The skull, PIN 3109-90, is clearly different from *M. relictus*. The horns and nasal process are not as highly elevated, the orbits are more anteriorly positioned, they have a reduced number of upper incisors, there is a distinct postcanine diastema, basisphenoidal fossae are absent, the squamosal wing forms a much shallower angle with the zygomatic arch, the occiput is not extremely widened, and the basicranium is not anteroposteriorly shortened. Likewise, the jaw of PIN 3109-91 differs from *Metatitan* most notably by a distinct postcanine diastema. Additionally, the lower premolars are more slender, less molariform, and the p3 lacks a metaconid.

As noted above, the skull of PIN 3109-39 was assigned to *Parabrontops gobiensis* by Yanovskaya (1980). Indeed, all of the PIN material in question (3109-90, 3109-91, 3109-39) is similar to *Parabrontops*. The tiny globular upper incisors and correspondingly small wedge-shaped lower incisors strongly suggest that both skulls (PIN 3109-90, PIN 3109-39) and mandible (PIN 3109-91) belong to a species similar to *P. gobiensis*. However, none of these specimens are directly referable to that species. *Parabrontops* retains three upper incisors, while the skulls PIN 3109-90 and PIN 3109-39 have only two. Further differences from *P. gobiensis* include the higher more anteriorly positioned horns, slighly more curved zygoamatic arch and slightly more distinctive preprotocrista.

The PIN specimens in question (3109-90, 91, 39) are consistent with *Eubrontotherium clarnoensis* (Mihlbachler, 2007), a recently described species that was previously known only from the Hancock Quarry, a prolific bone deposit in the Clarno Formation of Wheeler County, Oregon (Hanson, 1989, 1996). *E. clarnoensis* is the only brontothere that simultaneously has a reduced number of upper incisors and lacks conspicuous zygomatic swellings. The PIN specimens share this combination of character states and are consistent with the North American *E. clarnoensis* in other respects. The few differences between the North American and Asian specimens that can be found are attributable to taphonomic deformation. For instance, the somewhat lower horns of the type skull from the Hancock Quarry (UCMP 126100) are related to the fact that that skull has been dorsoventrally crushed. Likwise, the apparently narrower symphysis of PIN 3109-91 in comparison to the North

American material, is related to the transverse crushing of that specimen.

"Eubrontotheres" (sensu Schoch and Lucas, 1985) (infratribe Brontotheriita based on the classification presented in this paper) have been thought of primarily as a North American group notably because of their abundance in North America (i.e., *Megacerops* and *Duchesneodus*) (Schoch and Lucas, 1992). However, there are multiple Asian eubrontotheres including *Parabrontops gobiensis* and *Dianotitan lunanensis*. Additionally, *Eubrontotherium clarnoensis* apparently occurs on both continents. Finally, it is notable that while the North American Hancock Quarry *Eubrontotherium* has been attributed to middle and late Eocene land mammal ages (latest Uintan [Lucas et al., 2004], Duchesnean or Chadronian [Hanson, 1989; Lucas, 1992; Robinson et al., 2004]), the occurrence of *E. clarnoensis* in the Ergilin Dzo of Mongolia argues for a late Eocene occurrence of this species in Asia, although with so few occurrences, little can be said about the actual temporal duration of this species on either continent.

Protitanops curryi Stock, 1936

HOLOTYPE: LACM/CIT 1854, a skull with complete dentition and a partial mandible with right m3, left m1 (partial), and m2–m3.

TYPE LOCALITY: Lower red beds of the Titus Canyon Formation in Canyon East of Thimble Peak, Grapevine Mountains, California.

AGE: Late Eocene (early Chadronian land mammal "age").

DIAGNOSIS: *Protitanops curryi* is a large brontothere with large bulbous frontonasal horns. The horns are positioned slightly in front of the orbits and are not elevated high above the orbits. The nasal incision is shallow and extends to the anterior margin of the P3. The anterolateral root of M1 is situated directly below the anterior rim of the orbit. The nasal process is broad, unelevated, slightly angled downward, of nearly constant width throughout its length, strongly rounded anteriorly, and with shallow and thickened lateral walls. The premaxillomaxillary rostrum deepens posteriorly and it is not enclosed by bone dorsally. Other cranial characteristics include a deeply saddle-shaped cranium, a dorsal cranial surface that is moderately constricted posteriorly by parasagittal ridges, a narrow emargination surrounding the posterior nares, nearly straight zygomatic arches with large swellings, and a ventrally constricted and mediolaterally angled external auditory pseudomeatus. Ventral sphenoidal fossae and postzygomatic processes are absent.

Dentally, *Protitanops curryi* has two small upper incisors that form a straight row, a long postcanine diastema, a complex P1, a distinct P2 metacone, and distinct premolar hypocones on P3–P4. The upper molars have tall, lingually angled ectolophs with weak labial ribs, and thinned lingual ectoloph enamel with wedge-shaped paracones and metacones. A cingular parastyle shelf is absent. Distinct central molar fossae and anterolingual cingular cusps are present. Paraconules and metalophs are absent. The lower molars have shallow basins and the m3 is slender.

Protitanops curryi shares with *Eubrontotherium clarnoensis* and *Notiotitanops mississippiensis* the combination of a long upper postcanine diastema and a reduced number of upper incisors. *Protitanops curryi* differs from *E. clarnoensis* primarily in the large zygomatic swellings. *Protitanops curryi* differs from *N. mississippiensis* in having more posteriorly positioned orbits and a more posteriorly extended nasal incision.

DESCRIPTION

SKULL: The holotype of *Protitanops curryi* is a complete skull whose shape, from a lateral view, is reasonably intact, although the anterior and posterior views reveal that it has been subjected to lateral shearing distortion (fig. 147). The right horn is incomplete and has been reconstructed with plaster, while the left horn is complete and relatively undamaged. The following description of the skull of *P. curryi* is based mainly on the holotype. (Note that the holotype skull and jaw in fig. 147a is depicted in an approximately lifelike orientation, with the anterior end tilted down so that the occiput is almost vertical rather than tilted backward. Howev-

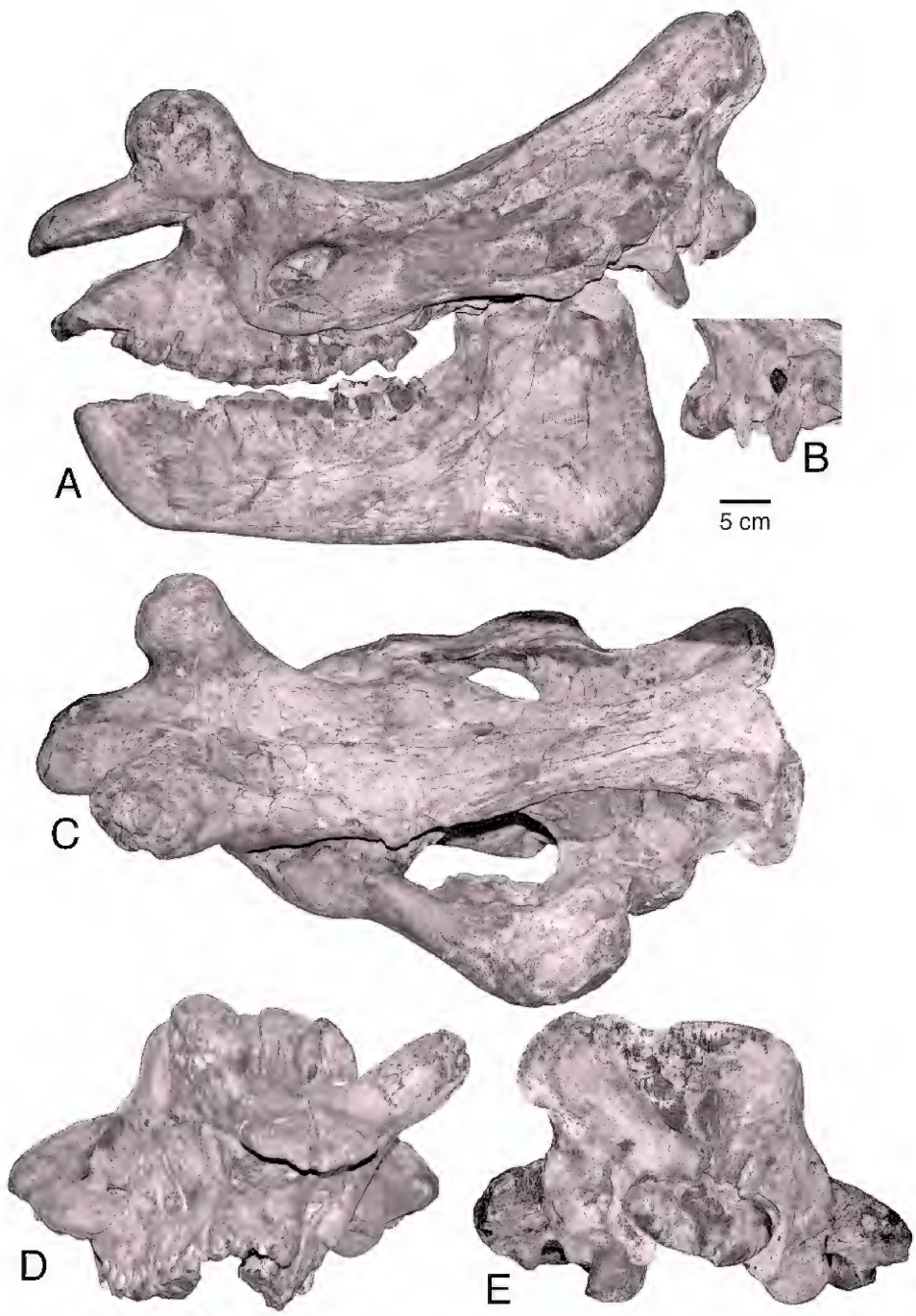

Fig. 147. The holotype skull and mandible of *Protitanops curryi* (LACM/CIT 1854). **(A)** Left view, **(B)** lateral view of right external auditory pseudomeatus, **(C)** dorsal view slightly rotated to the left, **(D)** anterior view, **(E)** posterior view.

er, other skulls in this paper are pictured in a more arbitrary horizontal position. The reader should keep this in mind when reading the following description.)

Protitanops curryi is a large horned brontothere similar in size to *Eubrontotherium*, *Notiotitanops*, and *Duchesneodus*. The left horn is large, bulbous, and somewhat ovoid in cross section; however, it is possible that the horn was originally rounder. The entire surface of the horn is roughened. The horn is positioned slightly in front of the orbit and is not highly elevated above the orbit. It is angled in an anterodorsolateral direction. The bones of the facial area (frontal, nasal, maxilla, premaxilla) are fully fused together in this individual and no sutures can be discerned.

The right half of the nasal process is reconstructed with plaster, but the left side is more or less complete. Judging by the left half, the nasal process was about as wide as the premaxillomaxillary rostrum. From a dorsal view the nasal process is nearly of constant width throughout its length and the anterior margin is rounded. From the lateral view the nasal process is about the same length as the rostrum and it is angled slightly downward. The dorsal surface of the nasal process is flat except at the very distal end where it curves downward. The sides of the nasal process are somewhat thickened and curved downward to form shallow lateral walls.

The nasal incision is shallow and extends posteriorly to the anterior margin of the P4. The orbit is positioned directly above the posterolateral root of M1 and the anterolateral root of M2. The anterolateral root of M1 is situated directly below the anterior rim of the orbit. The roots of P4 are entirely anterior to the orbital rim. With respect to the dentition, the orbits of *Protitanops curryi* are slightly more anterior than those of *Eubrontotherium clarnoensis*, more posteriorly positioned than those of *Notiotitanops mississippiensis*, but similar to some specimens of *Duchesneodus uintensis*.

The premaxillomaxillary rostrum of LACM/CIT 1854 curves upward distally. The rostrum deepens proximally and the dorsal margin slopes steeply posterodorsally, but it does not rise higher than the midpoint of the orbit. The premaxilla is short and does not extend anterior to the canines. The rostral cavity is not covered dorsally by bone behind the symphysis.

The cranium of *Protitanops curryi* is strongly saddle-shaped. There is no domelike convexity on the dorsal surface of the skull as in *Duchesneodus uintensis*. The parasagittal ridges are prominent and overhang the sides of the skull. However, the parasagittal ridges converge posteromedially and moderately constrict the posterodorsal surface. The zygomatic arches are thick with massive swellings at the junction of the jugal and squamosal, giving the zygomatic arches a strongly bowed shape. From a lateral view the zygomatic arch of the left side is essentially straight, although its midsection is reconstructed with plaster, rendering its shape dubious. The right zygomatic arch (not shown) is more intact and it is mildly curved from a lateral view.

The nuchal crest is thin and sharply notched medially. From a lateral view the occiput is strongly tilted backward. From the posterior view the dorsal portion of the occiput is similar in width to the ventral portion, and it is slightly constricted in the middle. The dorsal rim of the occiput is nearly flat, though it is notched medially. The occipital pillars are large and the central depression is rather deep, although the whole occiput is not nearly as massive as those seen in some specimens of *Megacerops* (sensu Mihlbachler et al., 2004b).

From the ventral view of the holotype skull (fig. 148a), the anterior rim of the posterior nares is situated slightly posterior to the M3 protocones. However, the exact edge of the posterior nares is covered by sediment. The posterior narial canal is elongate. The thin vomer forms a septum that divides the canal but it has not been exposed from the sediment filling the posterior narial canal. However, the vomerine septum is seen emerging posteriorly where the posterior narial canal begins to become shallow. Sediment has been left on the ventral surface of the basisphenoid where the posterior narial canal shallows, although there do not appear to be large ventral sphenoid fossae in this specimen. As with other brontotheres, the foramen ovale and foramen

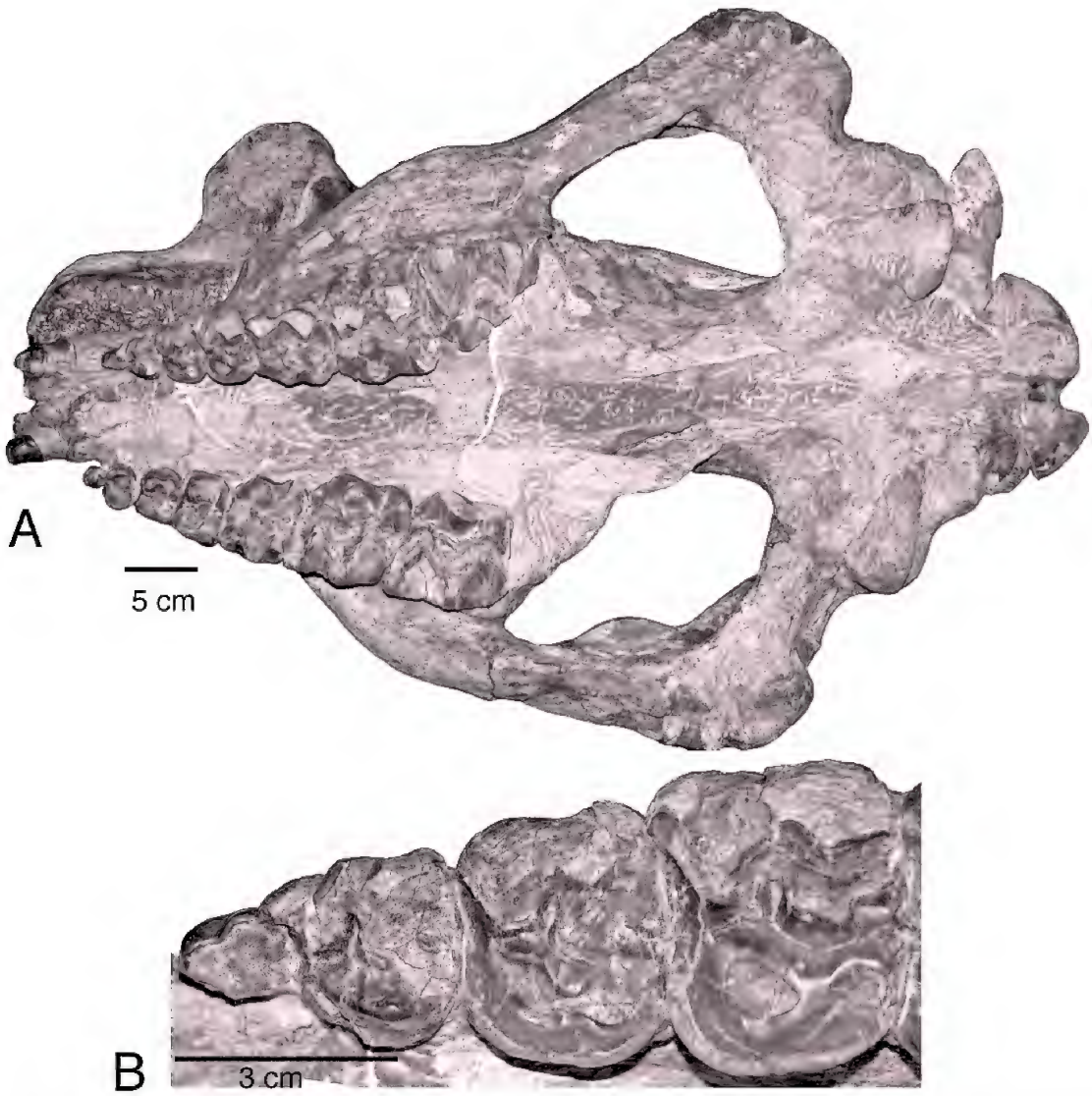

Fig. 148. The holotype skull of *Protitanops curryi* (LACM/CIT 1854). **(A)** Ventral view, **(B)** left premolars.

lacerum are widely separated. The mastoid process, best preserved on the right side (fig. 147b), curves anteriorly, contacts the postglenoid process, and forms a tube-shaped external auditory pseudomeatus.

Upper Dentition: The right incisors are complete. There are only two. The incisor crowns are very small, globular, and essentially featureless. They are positioned along the anterior edge of the canines in a straight row. There is no precanine diastema. The canines are relatively small. The postcanine diastema is similar in length to the P2.

The left premolars are shown in close-up (fig. 148b). The P1 is much smaller than the other premolars. Both right and left P1s are heavily worn, but the left side has two labial cusps (paracone and metacone) and a small lingual heel whose features are worn off. The remaining premolars (P2–P4) are heavily worn. Neither the right nor the left P2 is in good condition. The P3 and P4 are nearly

rectangular in outline with parallel anterior and posterior sides. Although damaged, the P2 parastyle appears to have extended in an anterior direction. The parastyles of P3 and P4 are deflected labially. None of the premolar metastyles are angled labially. The lingual sides of the right and left P2s exhibit a tall anteroposteriorly oriented lingual crest that almost completely absorbs the protocone and hypocone. However, both a distinct protocone and hypocone are seen on the P3 and P4. The hypocones are slightly smaller than the protocones and connected to them by a lingual crest. Small preprotocristae are discernable on P2–P4. On P3 and P4, the preprotocristae are visible as small beads of enamel that connect the protocone to the lingual base of the metacone. No anterolingual cingular cusps are seen on the premolars, although they are occasionally seen in *Duchesneodus uintensis* and *Megacerops*. The lingual cingula of the premolars are thick and continuous around the protocone.

The upper molars of *Protitanops curryi* show typical brontotheriine characteristics, including tall, lingually angled ectolophs, very weak labial ribs and thin lingual ectoloph enamel. The anterior cingulum is thin and passes proximally to the distal peak of the parastyle. All of the labial molar cusps are worn beyond their wedge-shaped lingual margins except the metacone of the right M3. Distinct central molar fossae and anterolingual cingular cusps are seen on M2–M3. The M1 is too worn to preserve these characters. There is no distinct hypocone on M3, although a crest extends from the distolingual corner of the M3 to the lingual base of the metacone. Labial and lingual molar cingula are essentially absent.

Mandible and Lower Dentition:
The holotype specimen includes a partial mandible that is missing most of the symphysis, although it was reconstructed with plaster (fig. 147a). No incisors, canines, or premolars are preserved, although the roots of the premolars allow for measurement of tooth-row length. The remainder of the mandible is of little interest, other than that it indicates that the molars are typical, with an elongate M3, thin lingual enamel, and shallow talonid and trigonid basins.

Remarks

Stock (1936) named *Protitanops curryi* from a skull and partial mandible from the early Chadronian Titus Canyon Formation of California (Emry et al., 1987). Stock (1936) recognized *Protitanops curryi* as more advanced than middle Eocene horned brontotheres such as *Diplacodon elatus* and *Protitanotherium emarginatum* due to its more greatly developed horns and smaller incisors. *Protitanops curryi* shares with *Eubrontotherium*, *Dianotitan*, *Notiotitanops*, *Duchesneodus*, and *Megacerops* (sensu Mihlbachler et al., 2004b) a reduced number of upper incisors. Only three of these taxa, *Protitanops*, *Notiotitanops*, and *Eubrontotherium*, retain postcanine diastemata. The conspicuous zygomatic swellings of *Protitanops curryi* most clearly differentiate this species from *Eubrontotherium clarnoensis*. It is more difficult to differentiate *Protitanops curryi* from *Notiotitanops mississippiensis*. *Protitanops curryi* has a longer nasal incision and a more posteriorly positioned orbit; it is possible that with more specimens these two species will be found to overlap (see remarks for *N. mississippiensis*).

Mader (1989, 1998) continued to accept *Protitanops curryi* as a valid species but only referred the holotype to that species. Other specimens could represent *Protitanops curryi*. Stock (1936) reported a partial skull, LACM/CIT 2007, from a similar stratigraphic position as the type of *P. curryi*, but he referred it to it as "Menodontine (?)". Realistically, the specimen is too incomplete to identify to a species level. A palate, LACM-CIT 2143, from the Sespe Formation of California with two small incisors, originally referred to *Duchesneodus californicus* by Stock (1938), was later referred to *Duchesneodus uintensis* by Lucas and Schoch (1989b) and Kelly (1990). This specimen retains a postcanine diastema and should be excluded from *D. uintensis* for that reason. The nasal incision of that specimen extends farther posteriorly than that of *Notiotitanops mississippiensis*, but it is consistent with *Protitanops curryi*; however, CIT 2143 cannot clearly be differentiated from *Eubrontotherium clarnoensis*. Finally, Hanson (1996) suggested that brontothere material from

the Hancock Quarry Local fauna of the Clarno Formation, Wheeler Oregon belonged to *Protitanops*. Lucas et al. (2004) also suggested that the Clarno brontothere could be *Protitanops curryi* although newer observations indicate that it is a new species, *Eubrontotherium clarnoensis* (Mihlbachler, 2007). Therefore, the holotype, LACM/CIT 1854, is the only specimen referable to *Protitanops curryi*.

Notiotitanops mississippiensis Gazin and Sullivan, 1942

HOLOTYPE: USNM 16646, the ventral half of a skull with right C–M3, left I1, C–M3, and a partial mandible with right p3–m2 and left p3–m3.

TYPE LOCALITY: Archusa Marl Member of the Cook Mountain Formation (previously considered the Lisbon Formation), about 2.5 miles south Quitman, Clarke County, Mississippi (Robinson et al., 2004).

AGE: Middle Eocene (late Uintan land mammal "age").

DIAGNOSIS: *Notiotitanops mississippiensis* is a large brontothere with a nasal incision that extends to the anterior margin of the P2. The P4 is situated directly below the anterior rim of the orbit. The premaxillomaxillary rostrum deepens posteriorly and it is not enclosed by bone dorsally. Other cranial characteristics include a narrow emargination surrounding the posterior nares, slightly curved zygomatic arches, and a ventrally constricted and mediolaterally angled external auditory pseudomeatus. Ventral sphenoidal fossae and postzygomatic processes are absent.

Dentally, *Notiotitanops mississippiensis* is characterized by two small upper incisors that form a straight row, a complex P1, a long postcanine diastema, a distinct P2 metacone, and distinct premolar hypocones on P3–P4. The upper molars of *Notiotitanops mississippiensis* have tall, lingually angled ectolophs with weak labial ribs, and thinned lingual ectoloph enamel with wedge-shaped paracones and metacones. A cingular parastyle shelf is absent. Distinct central molar fossae and anterolingual cingular cusps are present. Paraconules and metalophs are absent. The lower molars have shallow basins and the m3 is slender.

Notiotitanops mississippiensis shares with *Eubrontotherium clarnoensis* and *Protitanops curryi* the combination of a long upper postcanine diastema and a reduced number of upper incisors. *Notiotitanops mississippiensis* differs from *P. curryi* and *E. clarnoensis* in having more posteriorly positioned orbits and a nasal incision that does not extend as far posteriorly.

DESCRIPTION

SKULL: *Notiotitanops mississippiensis* is known from only a single specimen from Mississippi (USNM 16646). This specimen consists of the ventral portion of an undistorted skull (figs. 149, 150) and an associated partial mandible (fig. 151). The dorsal portion of the skull is completely weathered away, revealing a transverse cross-sectional view.

The nasal incision extended no farther posteriorly than the anterior margin of the P2. Only the ventral portion of the orbit is preserved. It is positioned more or less directly over M1 and the anterolateral root of M2. The orbit is positioned so far anteriorly, in fact, that the anterior margin of the orbital rim is positioned directly above the anterolateral root of the p4. The orbit is more anteriorly positioned than either that of *Protitanops* or *Eubrontotherium*.

The premaxillomaxillary rostrum is short. The rostrum curves upward distally and it deepens posteriorly. The dorsal margin of the rostrum slopes posterodorsally but does not rise higher than the ventral border of the orbit. The short premaxilla does not extend anterior to the canines. The premaxillary symphysis is completely fused. A premaxillomaxillary suture is not discernable. The dorsolateral margins of the rostrum diverge posterolaterally and the rostral cavity is open dorsally.

The left zygomatic arch is incomplete, but aspects of its shape can be interpreted from the remaining part. The zygomatic process of the jugal is straight, angled posterolaterally, and is roughly rectangular in cross section. The zygomatic process of the squamosal originates from the cranium at a point that is higher than the distal end of the zygomatic

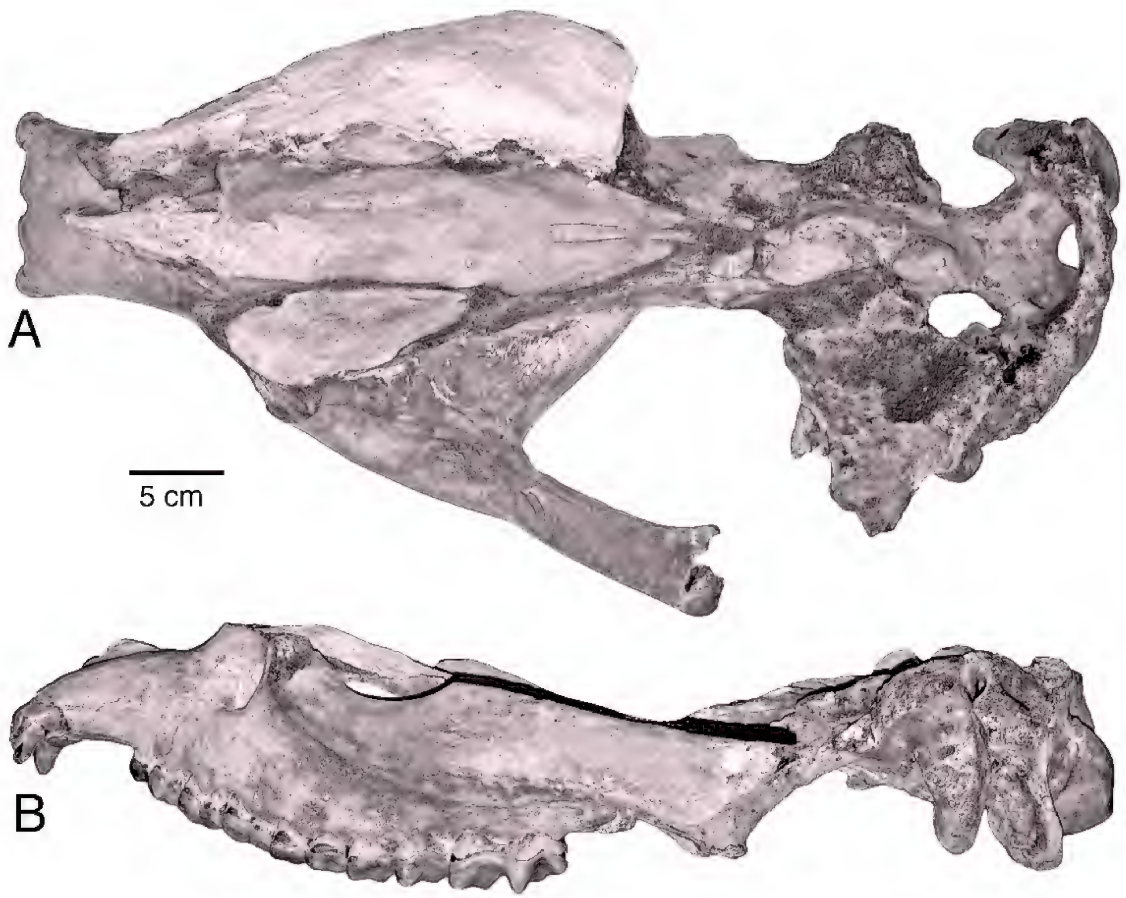

Fig. 149. The holotype skull of *Notiotitanops mississippiensis* (USNM 16646). **(A)** Dorsal view of weathered surface, **(B)** left view.

process of the jugal. Therefore, the zygomatic arch would have had a moderate curvature from a lateral view. It is not clear whether there was a large lateral zygomatic swelling as seen in *Protitanops*, *Dianotitan*, *Duchesneodus*, and *Megacerops* (sensu Mihlbachler et al., 2004b).

The weathered state of the skull provides a remarkable view of the internal structure of the skull. The various cranial sinuses and cavities are filled with lightly colored matrix and are clearly outlined by darker bone. Most notable is the teardrop-shaped, voluminous left maxillary sinus. This perspective also reveals the large maxillary tuberosity that underlies the floor of the orbits. The turbinates were apparently destroyed before burial or have been weathered away because they cannot be seen in the matrix filling the nasal chamber. However, the thin walls of the vomer can be seen from the dorsal surface directly above where the posterior nares are located.

From the ventral view of the skull (fig. 150) the anterior margin of the posterior nares is positioned slightly behind the M3 protocones. The posterior nares are rimmed by a narrow horseshoe-shaped emargination. From the ventral view the vomer is totally immersed in the remaining sediment filling the posterior narial canal, except at the posterior end where it emerges to join with the body of the sphenoid. The posterior narial canal shallows posteriorly and extends onto the sphenoid where it is bisected by the sphenoid body. However, by this point the canal is very shallow and large ventral sphenoidal fossae are not present. The

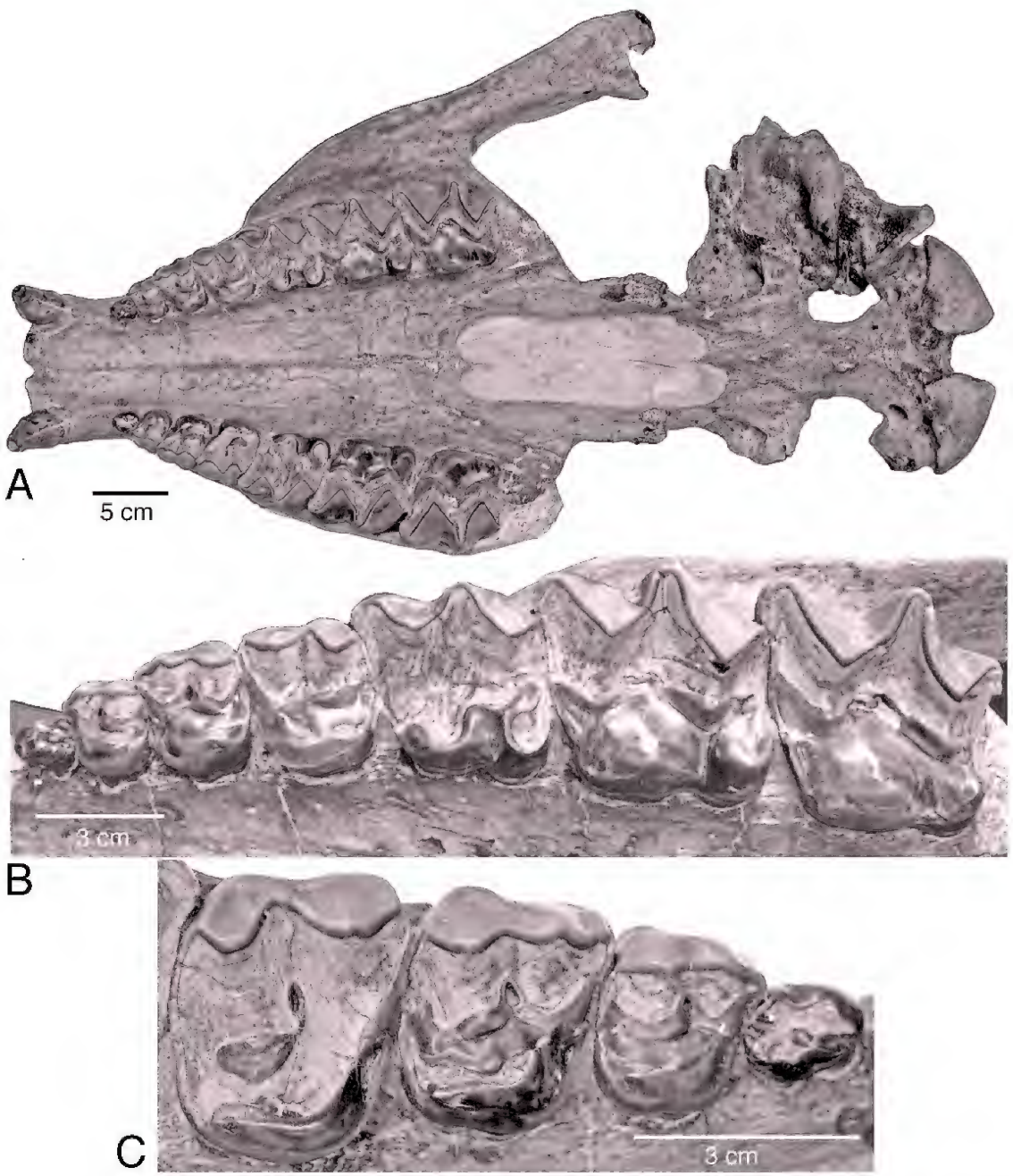

Fig. 150. The holotype skull of *Notiotitanops mississippiensis* (USNM 16646). **(A)** Ventral view, **(B)** left premolars and molars, **(C)** right premolars.

foramen ovale and foramen lacerum are well separated. The mastoid process contacts the postglenoid process and forms a small tube-shaped external auditory pseudomeatus.

The preservation of the left side of the basicranium is exquisite and includes an isolated petrosal. Further description of the basicranium of *Notiotitanops mississippiensis* was provided by Gazin and Sullivan (1942). These details are of potential interest, but they are not repeated here largely because similar details are not yet available for other species.

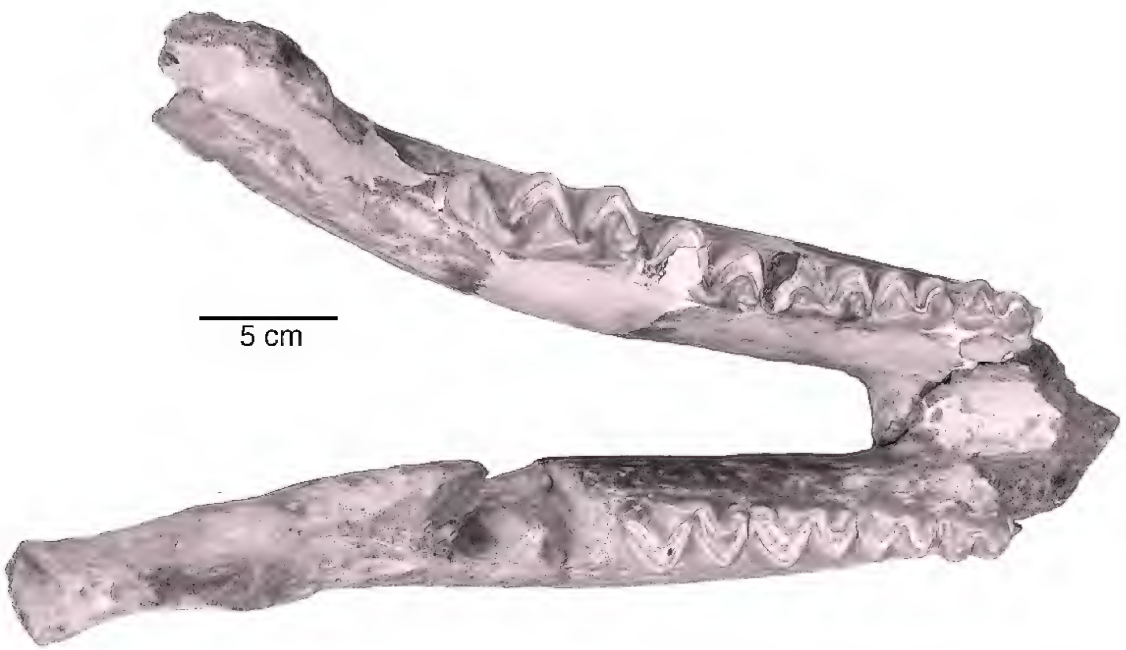

Fig. 151. Dorsal view of the holotype mandible of *Notiotitanops mississippiensis* (USNM 16646).

UPPER DENTITION: The incisors of USNM 16646 are missing except for the left lateral incisor. This tooth is now detached from the skull but can be seen in position in Gazin and Sullivan (1942). The crown of this incisor is small and globular. The incisor alveoli are intact and indicate only two pairs of incisors. The incisor alveoli form a straight row that is positioned between the anterior margins of the canines. The canines are of moderate size. The lateral incisor and canine are separated by a very brief diastema. *Notiotitanops mississippiensis* retains a post-canine diastema that is somewhat longer than P2.

The left and right cheek-tooth rows are complete, but curiously the right side is more worn (fig. 150). The P1 of *Notiotitanops mississippiensis* is small, but with a relatively complex morphology. It is nearly rounded in outline. There are two bulges on the labial wall of the ectoloph indicating two labial cusps, a paracone, and a smaller metacone. There is a small lingual shelf with a small protocone and a low preprotocrista. The anterior and posterior margins of the P2–P4 are nearly parallel. The parastyle of P2 is directed anteriorly, the parastyle of P3 is angled slightly labially, and the P4 parastyle is strongly angled labially. The metastyles of P2 and P3 are essentially straight, while the P4 metastyle is strongly angled labially. The labial side of the P2 paracone is convex, while P3 and P4 have very weak labial paracone ribs. The P4 exhibits a mesostyle that is prominent but not as well developed as those of the molars. There is also a slight bulge on the P3 ectoloph between the paracone and metacone that could be interpreted as a rudimentary mesostyle. The protocone and hypocone of P2 are positioned very closely together and are almost fully absorbed by the lingual crest. However, two distinct lingual wear facets with exposed dentin can be seen on each P2, a small. rounded protocone facet, and a small, elongate hypocone facet. The protocone and hypocone of P3 and P4 are more distinct and more distantly separated, although they are strongly connected by a lingual crest. Small but distinct preprotocristae are seen on P2–P4. The preprotocrista of P2 is the longest and tallest, while that of P4 is the lowest and shortest. The labial cingula of P2–P4 are faint. Anterolingual cingular cusps are not seen on the premolars. Lingual premolar cingula have been smoothed by

wear but they are continuous around the protocones of P3 and P4 and slightly discontinuous on the P2.

The upper molars of *Notiotitanops mississippiensis* show typical brontotheriine traits, including tall, lingually angled ectolophs, very weak labial ribs, thin lingual ectoloph enamel (though most of it is worn away), and wedge-shaped lingual margins of the paracone and metacone. The anterior cingulum is thin and passes proximally to the distal peak of the parastyle. Distinct central molar fossae are seen on M2 and M3. Anterolingual cingular cusps can be seen on M2 and M3, and they have well-developed wear facets. M1 is too worn to reveal these last two traits. The M3 exhibits a prominent hypocone that is almost as large as those of M1 and M2. Labial molar cingula are very weak and lingual molar cingula are absent.

Mandible and Lower Dentition: The holotype mandible is missing the anterior part of the symphysis and the ascending rami (fig. 151). The symphysis extends to the talonid of p4. The lower incisors, canines, p1, and p2 are not preserved. The most complete cheek-tooth row is that of the left side with p3–m3. The p3 trigonid is about as long as the trigonid, while the p4 trigonid is slightly shorter than the p4 talonid. The trigonids of p3 and p4 are narrower than the talonids. The paralophids and protolophids of p3 and p4 are strongly angled lingually. The trigonid of p3 has a comparatively narrow lingual notch, while that of p4 is broad and molariform. Each of these premolars exhibits a large lingually positioned metaconid. The talonids of p3 and p4 have well-developed cristids obliqua and hypolophids with shallow and broad basins. The molars are typical with thin lingual enamel, shallow basins, and an elongate m3. A thin, beaded cingulid can be seen tracing around the distal margin of the m3.

Remarks

Notiotitanops mississippiensis Gazin and Sullivan (1942) is known only from its holotype, which represents a rare occurrence of a brontothere fossil east of the Mississippi River. Further details of the discovery and provenience of this interesting specimen are provided by Gazin and Sullivan (1942) and are not recounted here. Gazin and Sullivan (1942) initially compared *Notiotitanops mississippiensis* to several North American horned brontotheres such as *Protitanotherium emarginatum*, *Diplacodon progressum* (= *D. elatus*), *Duchesneodus uintensis*, and others. However, they were apparently unaware that Stock (1936) had named a very similar species, *Protitanops curryi*, six years before. Gazin's and Sullivan's (1942) diagnosis of *N. mississippiensis* also fits *P. curryi*. Nonetheless, *Notiotitanops mississippiensis* has continued to be accepted as a distinct species (Mader 1989, 1998), although Krishtalka et al. (1987) suggested that it might belong to the genus *Protitanops*.

Mader's (1989, 1998) diagnoses of *Notiotitanops* and *Protitanops* differ in only two respects. *Notiotitanops* was described as having poorly separated lingual cusps on P2–P4 and a rudimentary hypocone on M3. *Protitanops* was described as having two lingual cusps and a hypocone on M3. The characterization of *Notiotitanops* as having a rudimentary hypocone is incorrect. The holotype of *N. mississippiensis* has a well-developed M3 hypocone. The point seems moot, at any rate, since the presence and size of the M3 hypocone is variable within many species. Secondly, given the intraspecific variability seen in the morphology of the lingual premolars of brontotheres, the difference between having poorly separated cusps in one specimen and two lingual cusps in another does not justify two species.

Other than minor premolar variation, the only clear way in which *Notiotitanops mississippiensis* differs from *Protitanops curryi* is in the proportions of its face. The nasal incision of *N. mississippiensis* does not extend as far posteriorly as that of *P. curryi*. Additionally, the anterior orbital rim of the holotype of *N. mississippiensis* is positioned above P4, but in the holotype of *P. curryi*, P4 is completely anterior to the orbital rim. These differences are subtle to say the least, and there tends to be some fluctuation in the exact position of the orbits and nasal incision in other brontothere species, but the differences between the holotypes of *Notiotitanops mississippiensis* and *Protitanops curryi* seems to exceed the typical degree of intraspecific

variation found in these characters. For this reason, *N. mississippiensis* is considered valid.

Dianotitan lunanensis (Chow and Hu, 1959)

HOLOTYPE: VM 547, a complete skull with right P1–M3 and left lateral incisor (I2), P2–M3

TYPE LOCALITY: Anjetsen, Lunan, Yunnan, China; Lower part of Upper Lunan beds (Chow and Hu, 1959), now considered the Lumeiyi Formation (Russell and Zhai, 1987).

AGE: Middle Eocene (Irdinmanhan or Sharamurunian land mammal "age"?).

REFERRED SPECIMEN: **(From the Lumeiyi Formation)** VM 573, a partial skull with very worn dentition including right P4–M1 and left M2–M3.

DIAGNOSIS: *Dianotitan lunanensis* is a large brontothere with small- to medium-sized ovoid frontonasal horns. The horns are positioned low on the skull, and above and slightly in front of the orbits. The lateral nasal incision extends posteriorly to a point above the anterior margin of P4. The anterior rim of the orbit is positioned directly above the anterior portion of M1. The nasal process is broad, unelevated, horizontal or slightly downturned, slightly tapered distally, strongly rounded anteriorly, and with shallow and thickened lateral walls. The premaxillomaxillary rostrum deepens posteriorly and it is not enclosed by bone dorsally. Other cranial characteristics include a saddle-shaped cranium, a dorsal cranial surface that is moderately constricted posteriorly by parasagittal ridges, laterally bowed zygomatic arches with large lateral swellings, an unnotched nuchal crest, the lack of a narrow emargination surrounding the posterior nares, weakly curved zygomatic arches, and a ventrally constricted and mediolaterally angled external auditory pseudomeatus. Ventral sphenoidal fossae and postzygomatic processes are absent.

Dentally, *Dianotitan lunanensis* has two small upper incisors that form a straight row, an insignificant postcanine diastema, a morphologically complex P1, and distinct premolar hypocones on P2–P4. The molars have tall, lingually angled ectolophs with weak labial ribs, and thinned lingual ectoloph enamel with wedge-shaped paracones and metacones. A cingular parastyle shelf is absent. Distinct central molar fossae and triangular anterolingual cingular cusps are present. Paraconules and metalophs are absent.

Dianotitan lunanensis shares only with *Duchesneodus uintensis* and *Megacerops coloradensis* the combination of a reduced number of upper incisors, conspicuous lateral zygomatic swellings, the absence of a horseshoe-shaped emargination around the posterior nares, and an insignificant postcanine diastema. *Dianotitan lunanensis* lacks the parietal dome of *Duchesneodus uintensis*. In comparison to *Megacerops coloradensis*, *Dianotitan lunanensis* has lower horns that are more posteriorly positioned and vertically oriented, the orbits are more posteriorly positioned, and the nasal incision is longer.

DESCRIPTION

SKULL: The holotype skull of *Dianotitan lunanensis* (VM 547) can be seen in figs. 152 and 153. The skull is now fixed to a steel mounting frame and it was not possible to photograph the entire ventral surface. Instead, the ventral surface of a cast from IVPP is provided (fig. 155a). The holotype skull has numerous minor cracks, particularly on its dorsal surface. However, it is nearly complete and only moderately distorted. The right frontonasal horn has been reconstructed with plaster. The skull is slightly crushed dorsoventrally. The dorsoventral flattening seems to have occurred mostly at the level of the orbit. On both sides the upper orbital rim (frontal) is lowered nearly to the level of the lower orbital rim (jugal). The holotype skull is slightly sheared as well; the dorsal surface of the skull is shifted slightly left with respect to the ventral surface.

A second skull (VM 573) is less complete (fig. 154). The right side in particular is heavily damaged. The zygomatic arches are not preserved, the distal portions of the nasal and premaxillomaxillary rostrum are not present, and most of the occiput is missing. From the ventral view of the skull it is apparent that there has been significant lateral crushing. Moreover, the basioccipital region is artificially rotated to the right.

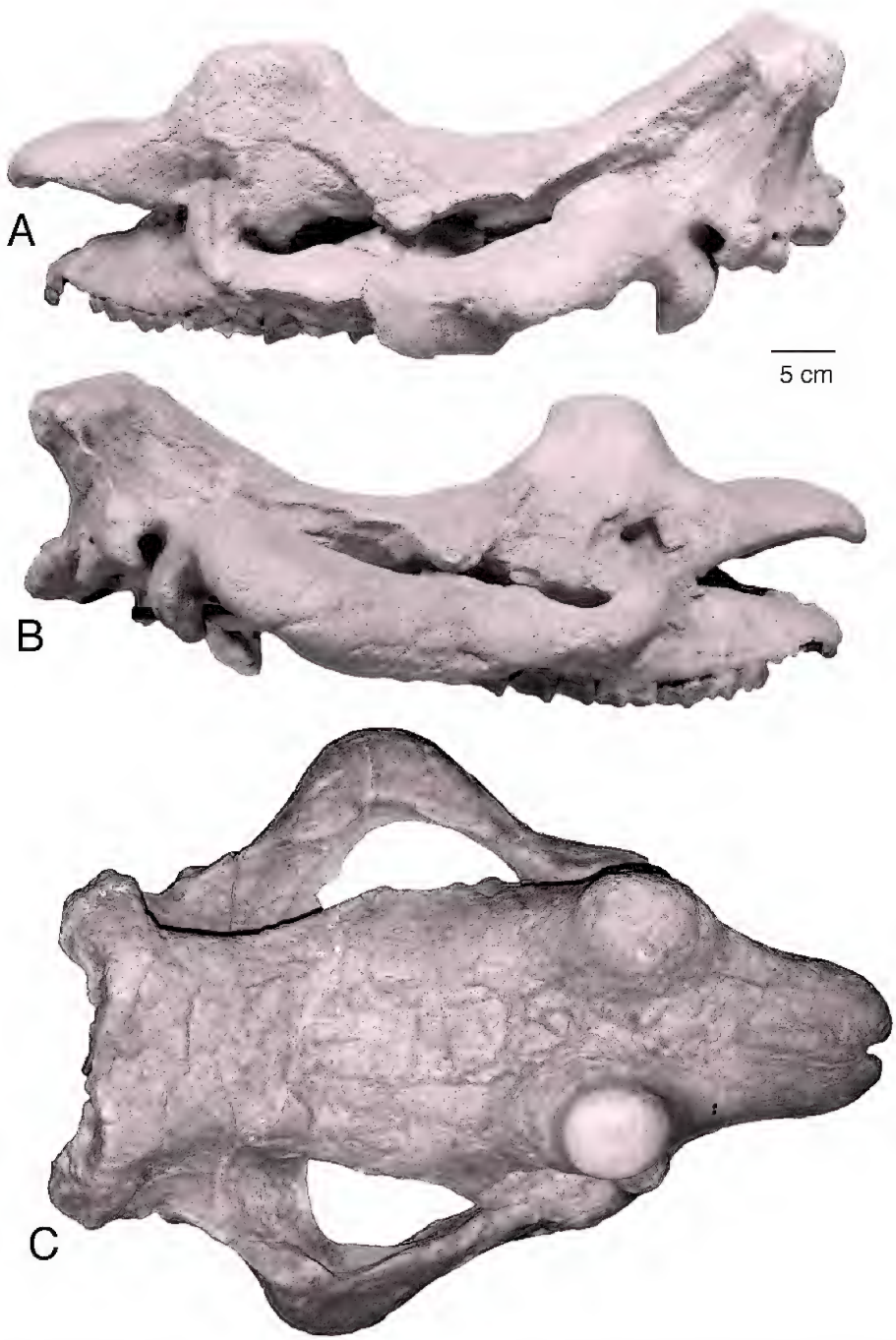

Fig. 152. The holotype skull of *Dianotitan lunanensis* (VM 547). **(A)** Left view, **(B)** right view, **(C)** dorsal view.

A definitive frontonasal suture cannot be observed on either VM 547 or VM 573, although the horns of *Dianotitan lunanensis* are presumably composed of the frontal and nasal bones like other horned brontotheres. The horn surfaces of VM 547 and VM 573 are somewhat roughened, but they lack heavy rugosities. The left frontonasal horn

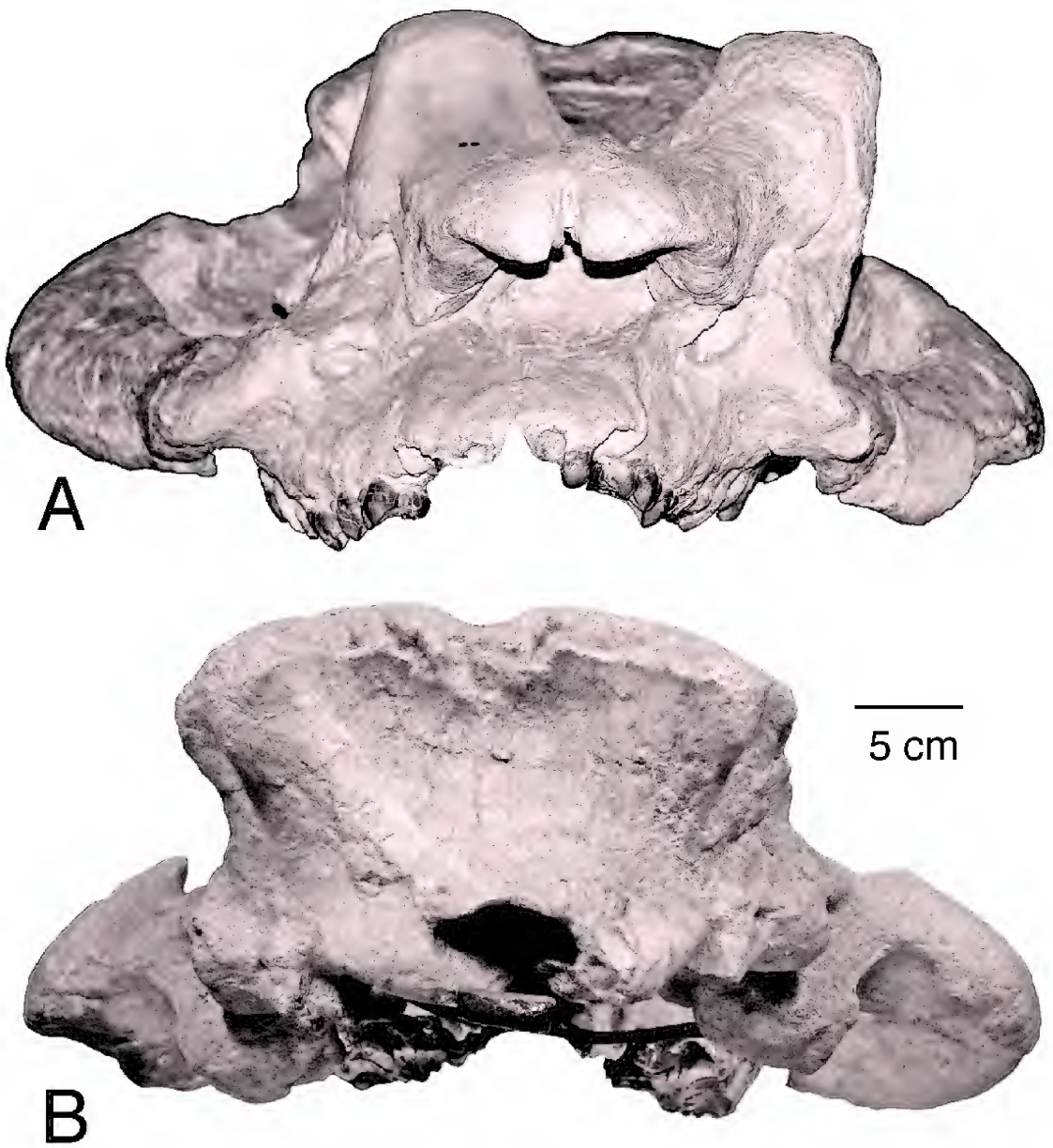

Fig. 153. The holotype skull of *Dianotitan lunanensis* (VM 547). **(A)** Anterior view, **(B)** posterior view.

of VM 547 is massive, though short, and it is rounded in cross section. The horn of VM 573 is smaller and more elliptical in cross section. However, the horn of VM 547 is more rounded in cross section than any specimen of *Protitanops* or *Parabrontops*. The horns of *Dianotitan lunanensis* are vertical, positioned low on the skull, and they rest directly above and slightly in front of the orbits.

From the dorsal view of VM 547 the nasal process is wide and completely obscures a view of the premaxillomaxillary rostrum. The nasal process is tapered and the distal end is strongly rounded. The nasal bones are strongly co-ossified, although the distal ends

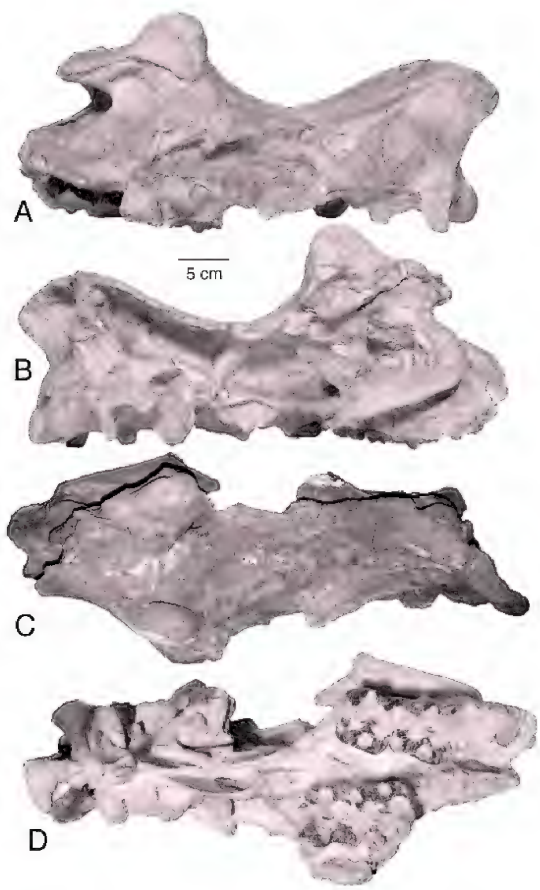

Fig. 154. A skull referred to *Dianotitan lunanensis* (VM 573). **(A)** Left view, **(B)** right view, **(C)** dorsal view, **(D)** ventral view.

of the nasal bones are unconnected, thus forming the deep median notch at the distal tip. From a lateral view of VM 547 the nasal process is slightly longer than the premaxillomaxillary rostrum. The lateral margins of the nasal process are thickened and strongly downfolded proximally. The lateral margins of the nasal process become shallower distally. The distal margin of the nasal process is distinctly curved downward. The nasal process of VM 573, though incomplete, appears to have been somewhat thinner and narrower.

The lateral nasal incision of VM 547 is very shallow; this is partly due to the dorsoventral crushing. However, the nasal bone is more or less above the orbit, indicating that the nasal bone was not highly elevated high above the orbits as in *Diplacodon elatus*. The posterior margin of the lateral nasal incision is positioned above the anterior margin of P4. The orbits are positioned directly above the posterior portion of M1 and the anterior portion of M2. The anterior orbital bony rim is positioned directly above the anterior portion of M1.

The rostrum of *Dianotitan lunanensis* is relatively unspecialized. From a lateral view of VM 547 the premaxillomaxillary rostrum curves upward and it lacks a dorsal bony covering. From a lateral view of VM 574 the rostrum deepens proximally as the dorsolateral surface of the rostrum strongly slopes posterodorsally and rises to about the midlevel of the orbit. The premaxilla is short and does not extend anterior to the canines. The premaxilla and maxilla are completely fused and a premaxillomaxillary suture cannot be seen.

The dorsal surface of the skull of *Dianotitan lunanensis* is entirely concave (saddle-shaped). The parasagittal ridges, running from the postorbital process of the frontal to the nuchal crest, are prominent in VM 547 and VM 573. The parasagittal ridges remain widely separated throughout their length and do not merge to form a sagittal crest. At their closest point the parasagittal ridges only marginally constrict the dorsal surface of the cranium. The dorsal surface of the cranium of VM 547 is notably wider than that of VM 573.

From a lateral view of VM 547 the zygomatic arches are deep, although they originate from a shallow lower orbital rim. The jugal portion of the zygomatic is relatively straight and horizontal, but the squamosal portion rises posteriorly, giving the zygomatic arch a pronounced curvature. From a dorsal view of VM 547 the zygomatic arches are strongly bowed laterally. The most conspicuous feature of the zygomatic arch is the thickened lateral swelling in the center of the arch at the junction of the jugal and squamosal bones.

From a dorsal view of VM 547 the nuchal crest is very thick, rugose, and concave. It lacks the distinct mesial notch seen in the much thinner nuchal crest of *Protitanops*. The nuchal crest of VM 573 appears to have been much thinner. From lateral views the occiputs of both specimens are mildly tilted

backward. From the posterior view of VM 537 the occiput is semirectangular. The occiput is wider than it is tall and it is mildly hourglass-shaped due to a distinctly waisted middle. A pair of thick bony occipital pillars rise from above the foramen magnum to the dorsolateral corners of the occiput. The nuchal crest is slightly arched dorsally. The occiput of *Dianotitan lunanensis* closely resembles those of *Duchesneodus uintensis* and *Megacerops coloradensis*. These species show a degree of intraspecific variability in occiput robustness that resembles the variation in nuchal crest thickness exhibited by VM 547 and VM 573.

The anterior margin of the posterior nares of VM 547 is positioned slightly behind M2. The lateral and anterior margins of the posterior nares of most brontotheres are rimmed by a depressed horseshoe-shaped emargination. This trait is diminished in *Dianotitan lunanensis* as well as *Duchesneodus uintensis* and *Megacerops coloradensis*. The posterior nares form an elongate canal that is bisected by the vomer. Ventral sphenoidal fossae are absent. The configuration of the basicranial foramina, including the widely separated foramen ovale and foramen lacerum, is typical of brontotheres. The external auditory pseudomeatus in VM 547 is tube-shaped and enclosed ventrally by an anteroventrally curving mastoid process that contacts the posterior surface of the postglenoid process. The auditory canal enters the skull at a mediolateral angle.

Upper dentition: The dentition of VM 547 is nearly complete (fig. 155) and only moderately worn. Both median incisors are missing. On the actual specimen of VM 547 only the left lateral incisor is seen, although the cast of the same specimen at IVPP has both left and right lateral incisors. The other specimen, VM 573, retains only very badly worn molars.

Though the incisor row is incomplete, the intact alveoli indicate only two pairs of upper incisors. The incisor alveoli are positioned close together except for the distinct median notch on the anterior surface of the premaxilla. The lateral incisors have tiny globular crowns. The medial incisor alveoli indicate that the medial incisors were of a similar size. The incisor row is straight and positioned slightly in front of the canine alveoli. A short diastema persists between the lateral incisor alveolus and canine alveolus. The canines are not preserved, although the diameter of the alveoli (15.2 mm) indicates rather small canines. A very short diastema, less than a centimeter in length, separates the canine and anterior premolar. This postcanine diastema is essentially insignificant in comparison to the longer postcanine diastemata of *Parabrontops*, *Eubrontotherium*, *Protitanops*, and *Notiotitanops*. On the other hand, *Duchesneodus* and *Megacerops* have either no postcanine diastema or a very short insignificant gap similar to that seen in VM 547.

The premolars of VM 547 lack species diagnostic characters. The left P1 is not present. The right P1 is heavily worn but the crown is rounded in outline. Brontotheres with similarly shaped P1s tend to have morphologically advanced P1s with two labial cusps, a large paracone and a smaller metacone, as well as a small lingual heel, often with a small protocone or a lingual crest. This morphology is detectible on the P1 of VM 547, although these advanced features are nearly obliterated by wear. The lingual bulge of the paracone can clearly be seen on the P1. On the occlusal surface of that tooth the smaller metacone is separated from the paracone by a short fossa that is not completely obliterated. The P1 metacone is partially worn away by interstitial wear. Finally, a long and narrow lingual heel is present on P1, although any cusps or crests that might have been present on this structure are worn away.

P2 is oblique with a strongly posterolingually angled anterior margin. However, P3 and P4 are nearly rectangular in outline with parallel anterior and posterior margins. The P2 parastyle curves slightly lingually, the P3 parastyle is straight, while the P4 parastyle is angled in a somewhat labial direction. The metastyles of these three premolars are short and essentially straight. The ectoloph of P2 is more rounded than those of P3 and P4. The paracone forms a prominent vertical labial rib on P2, P3, and P4. On the other hand, the metacone forms a prominent labial rib only on P2. The labial metacone rib is much smaller on P3 and it is not seen on P4.

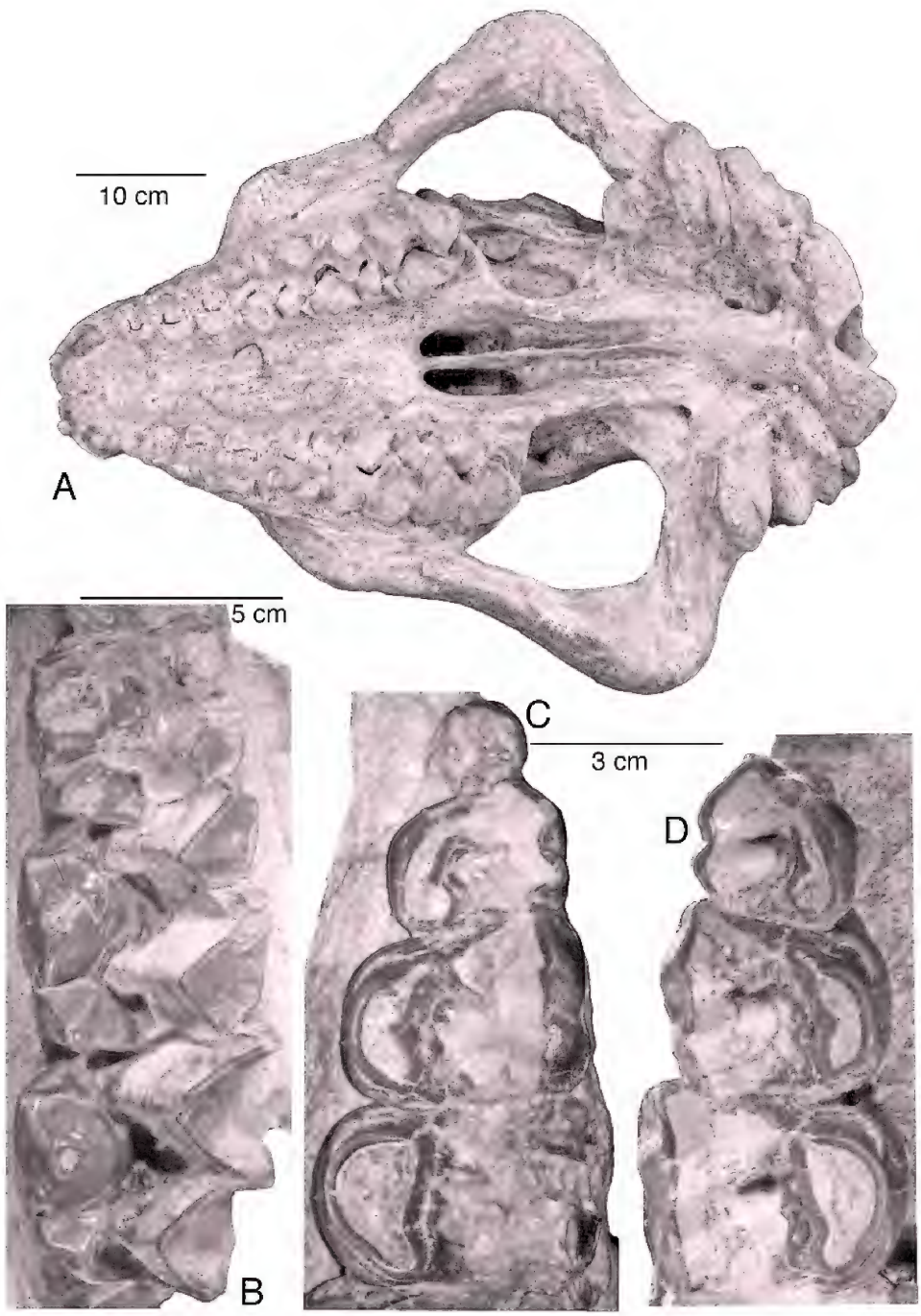

Fig. 155. The holotype skull of *Dianotitan lunanensis* (VM 547). **(A)** Ventral view, **(B)** left molars, **(C)** left premolars (P1–P4), **(D)** right premolars (P2–P4).

Mesostyles are not seen on any of the premolars.

The lingual sides of P2, P3, and P4 each possess a single oblong exposure of dentin, formed by the lingual cusps and the lingual crest that connects these cusps. The posterior bulge in the lingual exposure of dentin of P2 suggests a rather large hypocone. A heavily worn lingual crest extends anterolabially from the metacone and connects to the lingual base of the paracone. The preprotocrista, protocone, and lingual crest of P2 seem to have been fused into a single, large crest. However, P3 and P4 each possess a distinct paracone that is similar in size to the hypocone and positioned closely to it and not entirely separated from it. A distinct preprotocrista can be seen on P3. The P4 paracone swelling is significantly larger than the incompletely separated metacone swelling. The left P4 appears to retain a very short and indistinct preprotocrista, although no sign of this structure is visible on the right P4. Labial premolar cingula are weak on VM 547. The anterior and posterior cingula wrap around the lingual corners of the premolar crowns, but they do not join to form lingual cingula.

The molars of *Dianotitan lunanensis* exhibit a rather tall ectoloph. The vertical labial ribs of the paracone range in distinctness from faint to absent. The lingual band of ectoloph enamel is much thinner than the labial band and in comparison to the labial band it is almost entirely worn away. Nonetheless, the broad dentin exposure on the lingual sides of the paracone and metacone retain their original wedge shape. The M3 metacone, the least worn cusp on this specimen, retains a wedge-shaped lingual enamel margin. M1 and to a lesser extent M2 have been made significantly narrower by interstitial wear. However, interstitial wear between the contact of M2 and M3 is minor and the proportions of M3 are essentially intact. Because of interstitial wear portions of the anterior cingulum of M1 and M2 are obliterated. On M3 a very thin lingual cingulum can be seen passing around the anterolabial corner of the crown below the apex of the parastyle. A distinct central molar fossa can be seen on all three molars. In addition, each molar exhibits a well-developed triangular anterolingual cingular cusp. Paraconules are not seen on any of the molars. Each molar exhibits a distinct hypocone, although the M3 hypocone is slightly smaller than those of M1 and M2. The M1 hypocone is heavily worn. A short metalophlike ridge extends from the M2 and M3 hypocones to the lingual base of the metacone. A similar loph is visible on M3 although it passes anterior to the lingual base of the metacone. Labial cingula are very weak and lingual cingula are essentially absent on all of the molars.

Remarks

Dianotitan lunanensis (Chow and Hu, 1959) is based on a skull (VM 547) reported from "Anjetsen, Lunan, Yunnan; Lower part of Upper Lunan beds" (Chow and Hu, 1959), now considered the Lumeiyi Formation (Russell and Zhai, 1987). The age of the Lumeiyi Formation is only crudely resolved; the known fauna contains several elements of the Irdinmanhan fauna and some from the Sharamurunian fauna (Russell and Zhai, 1987), thus suggesting a middle Eocene age (McKenna and Bell, 1997). Although Chow and Hu (1959) mention only the holotype specimen of *Dianotitan lunanensis*, another less complete specimen (VM573) is referable to this species.

Chow and Hu (1959) originally assigned this species to *Parabrontops*. Later Chow et al. (1974) reassigned it to a new genus, *Dianotitan*. *Dianotitan lunanensis* was originally diagnosed by Chow and Hu (1959) as having well-developed horns, expanded zygomatic arches, reduced upper incisors, and a short postcanine diastema. Chow and Hu (1959) compared *D. lunanensis* only to *Parabrontops gobiensis* (Osborn, 1925). Chow and Hu (1959) differentiated *Dianotitan lunanensis* from *P. gobiensis* in the following ways: (1) a broader skull, (2) a reduced number of incisors, (3) smaller size, (4) a shorter nasal with a narrower anterior end, (5) smaller frontonasal horns, and (6) relatively smaller premolars. Utilizing a series of cranial indices, Chow et al (1974) also found *D. lunanensis* to have a more brachycephalic skull and different cheektooth proportions than *P. gobiensis*. However, only the first two

of Chow's and Hu's (1959) observations and the first observation of Chow et al. (1974) are valid morphological distinctions. (1) *D. lunanensis* has large laterally expanded zygomatic swellings, whereas *P. gobiensis* does not, thus giving the skull a broader or more brachycephalic appearance. (2) Secondly, *D. lunanensis* retains only two upper incisors (per side), while the incisor alveoli preserved in specimens of *P. gobiensis* indicate three upper incisors (per side).

The remaining differences noted by Chow and Hu (1959) and Chow et al. (1974) do not have any clear taxonomic significance, but rather seem related to taphonomic distortion, dental wear, and patterns of intraspecific variability that are common among brontothere species. The two specimens of *Dianotitan lunanensis* are reportedly smaller than the two known skulls of *Parabrontops gobiensis*; however, these differences are dubious. The overall sizes of the skulls differ by no more than a few centimeters (differences that could be attributed to some extent by taphonomic distortion). The dental dimensions of *P. gobiensis* and *D. lunanensis* typically differ by no more than a few millimeters, and in some dental measurements, specimens of *D. lunanensis* actually exceed those of *P. gobiensis*. In sum, these species seem to be about the same size, with slightly fluctuating proportions that may relate to distortion or dental wear.

The nasal bone of *Dianotitan lunanensis* (VM 547) is shorter and more distally tapered than that of the holotype of *Parabrontops gobiensis* (AMNH 20354). However, the *P. gobiensis* holotype skull is severely distorted and the reconstruction contains a significant amount of plaster in the nasal bone and other parts of the skull. In contrast, a less significantly distorted skull (AMNH 26020) referred to *P. gobiensis* has an undamaged nasal bone that is similar in appearance to that of *D. lunanensis*. Therefore, *D. lunanensis* and *P. gobiensis* do not appear to have differentiated nasal bones (contra Chow and Hu, 1959).

Chow and Hu (1959) stated that *Dianotitan lunanensis* has smaller horns than *Parabrontops gobiensis*, although this is misleading. Both *D. lunanensis* and *P. gobiensis* show variation in horn size. The horns of the holotype of *D. lunanensis* (VM 547) are intermediate in size between the two known specimens of *P. gobiensis*, while the smaller horns of the referred skull (VM 573) are similar in size to the holotype of *P. gobiensis* (AMNH 20354).

I could not confirm that *Dianotitan lunanensis* has relatively smaller premolars than *P. gobiensis*, as Chow and Hu (1959) and Chow et al. (1974) suggest. The calculation of a ratio of P2–P4 length/M1–M3 length yields a value of 0.50 for *D. lunanensis* (VM 547). A precise ratio cannot be calculated for the holotype of *P. gobiensis* due to severe distortion. However, the referred skull (AMNH 26020) yields a similar value of 0.53. However short taphonomic gaps are present between the premolars of AMNH 26020 that add about a centimeter to the premolar row length. Recalculation of the ratio after subtraction of these gaps yields a ratio of 0.48 for *P. gobiensis*. Thus, the premolars of *D, lunanensis* do not appear to be notably smaller than those of *P. gobiensis* (contra Chow and Hu, 1959).

The two skulls of *Dianotitan lunanensis* (VM 547 and VM 573) show variation in horn size, nasal thickness, and overall skull robustness; these characteristics are commonly variable within other brontothere species and probably represent sexual dimorphism. Both specimens possess horns that are positioned very low on the skull, above and slightly in front of the orbits, and with a nearly vertical horn orientation. This configuration most strongly resembles *Parabrontops gobiensis*. Nonetheless, *D. lunanensis* can be differentiated from *P. gobiensis* by (1) the presence of conspicuous lateral zygomatic swellings, (2) a reduced number of upper incisors, (3) an insignificant postcanine diastema, (4) and the absence of a distinct horseshoe emargination around the anterior and lateral margins of the posterior nares. Only two North American species share this combination of traits, *Duchesneodus uintensis* and *Megacerops coloradensis*. *Duchesneodus uintensis* exhibits an autapomorphic parietal dome that is clearly not present in *Dianotitan lunanensis*. Furthermore, both *Duchesneodus uintensis* and *Megacerops coloradensis* have more anteriorly situated orbits and shorter nasal incisions.

Duchesneodus uintensis (Peterson, 1931)

HOLOTYPE: CMNH 11809, a mandible with right i2–i3, c (partial), p2–m3, left c (partial), and p2–m3.

TYPE LOCALITY: LaPoint Member of the Duchesne River Formation "*Duchesneodus* quarry", 11 miles west of Vernal Utah.

AGE: Middle Eocene (Duchesnean land mammal "age").

REFERRED SPECIMENS: **(From the LaPoint Member of the Duchesne River Formation "*Duchesneodus* quarry", 11 miles west of Vernal Utah)** AMNH 32604, a skull missing its right zygomatic arch with right P3–M1 (all partial), M2, M3, and left P4–M3; CMNH 9958, an anterior fragment of a skull with right I2–P3; CMNH 9960, a right maxillary fragment with P1–M1; CMNH 11754, a skull with right I2–M3 and left I1–M3; CMNH 11757, a skull with right P1–M3 and left P1–M3; CMNH 11758, a juvenile skull with right P2, P3, DP4, M1, left C, and P2–M2; CMNH 11759, a skull with right I1–M3 and left I2–M3; CMNH 11760, a juvenile skull with right and left DP2–DP4 and M1–M2; CMNH 11761, a mandible with right i2, p2–m3, left i1–c, and p2–m3; CMNH 11766, an anterior portion of a skull with P3–M1, C, and P3–M3; CMNH 11767, a skull with right I2, P1–M3, left I1, and P1–M3; CMNH 11809, a mandible with right i1, i2, c (partial), p2–m3, left c (partial), and p2–m3; CMNH 11815, a skull with right I1–C, P2, P4–M3, left I2, C, and P4–M3; CMNH 11816, a skull missing the right zygomatic arch with right P3–M3 and left P2–M3; CMNH 11821, a partial left mandibular ramus with m2–m3; CMNH 36294, a partial juvenile skull with no teeth; FMNH PM522, a skull with right C, P3–M3, left C, P2, P3, and M2–M3; LACM 128401, a right C, P3–M3, left C, and P3–M3; **(from the LaPoint Member of the Duchesne River Formation)** FMNH PM22410, a palate with right C–M3, left I2, and P1–M3; **(from the Galisteo Formation, New Mexico)** F:AM 108521, a partial skull with right P2–M3 and left M1–M3; F:AM 108529, a nasal bone and horns; **(from the Vieja Formation, Presidio County, Texas)** FMNH PM396, a skull with right P2–M3 and left P4–M3; FMNH PM136, a skull with complete dentition; FMNH PM401, a partial mandible with right i1–i2 and left i1–i3; FMNH PM163, a partial mandible with right p3–p4, left p1 (partial), and p2–m1.

DIAGNOSIS: *Duchesneodus uintensis* is a large brontothere with small- to medium-sized, relatively rounded frontonasal horns. The horns are positioned slightly in front of the orbits and are not elevated very high above the orbits. The nasal incision extends posteriorly to the anterior margin of the P4. The anterior rim of the orbit is usually anterior to M1. The nasal process is broad, unelevated, horizontal or slightly downturned, slightly tapered distally, strongly rounded anteriorly, and with shallow and thickened lateral walls. The premaxillomaxillary rostrum deepens posteriorly and it is sealed by a dorsal bony cover. Other cranial characteristics include a saddle-shaped cranium with a conspicuous bony dome on the dorsal surface, a dorsal cranial surface that is moderately constricted posteriorly by parasagittal ridges, laterally bowed zygomatic arches with large lateral swellings, unemarginated posterior nares, curved zygomatic arches, and a ventrally constricted and mediolaterally angled external auditory pseudomeatus. Ventral sphenoidal fossae and postzygomatic processes are absent.

Dentally, *Duchesneodus uintensis* has two small upper incisors that form a straight row, no postcanine diastema, a complex P1, a distinct P2 metacone, and distinct premolar hypocones on P3–P4. The molars of *Duchesneodus uintensis* have tall, lingually angled ectolophs with weak labial ribs, and thinned lingual ectoloph enamel with wedge-shaped paracones and metacones. A cingular parastyle shelf is absent. Distinct central molar fossae and anterolingual cingular cusps are present. Paraconules and metalophs are absent. The lower dentition of *Duchesneodus uintensis* includes three very small lower incisors, a postcanine diastema, a metaconid on p3 and p4 but not on p2, and a p2 talonid that is of similar length to the trigonid. The lower molars have shallow basins and m3 is slender.

Duchesneodus uintensis shares with *Dianotitan* and *Megacerops* (sensu Mihlbachler et al., 2004b) the unique combination of a saddle-shaped cranium, lack of a postcanine diastema, and lack of a horseshoe-shaped

emargination surrounding the posterior nares. *Duchesneodus uintensis* has a conspicuous autapomorphic dome on the dorsal surface of its cranium. *Megacerops* specimens occasionally have a similar dome, but it is much less conspicuous.

Description

Skull: According to Scott (1945) the *Duchesneodus* quarry sample includes 23 skulls, and three mandibles. Lucas and Schoch (1989b) reported 11 skulls and three mandibles. I encountered 15 skulls and three mandibles. Most of these are in the CMNH collection, although some have been distributed to other museums (AMNH, FMNH, LACM). The skulls represent individuals of different ontogenetic ages and they are all distorted to varying degrees. The most complete and least distorted of the *Duchesneodus* quarry skulls is CMNH 11759 (figs. 156a, b and 157), the same specimen that was originally described by Peterson (1931). CMNH 11759 is only slightly crushed dorsoventrally. Other well-preserved skulls from the *Duchesneodus* quarry skulls are CMNH 11767 (fig. 156c, d) and CMNH 11754 (fig. 158a). In addition to the *Duchesneodus* quarry sample, a completely undistorted skull from the Vieja Formation of Texas (FMNH PM136) is seen in figures 159–161. These specimens form the basis for the following description of the skull of *Duchesneodus uintensis*, although additional information on variation from other specimens is provided.

Overall, *Duchesneodus uintensis* is a large brontothere (table 11), but it is relatively small in comparison to *Megacerops* (sensu Mihlbachler et al., 2004b). The frontonasal suture can barely be seen on the lateral side of the bony protuberance of CMNH 11759, but can be seen more clearly on other specimens (e.g., CMNH 11754, not shown). The nasal bone forms the proximal base and anterior side of the horn, while the frontal forms the superorbital pillar and the summit of the horn. The horn of CMNH 11759 is small. It is elliptical at its base, but it is more rounded distally. The summit of the horn is rugose. The horns are widely separated and are positioned immediately in front of the orbits, are not highly elevated above the orbits, and they project slightly laterally. The horns of *D. uintensis* vary in size, though they tend to be short and do not reach the extreme lengths seen in some specimens of *Megacerops* (sensu Mihlbachler et al., 2004b). The horns of CMNH 11767 are the largest and most rugose of the *Duchesneodus* quarry sample. The horns of FMNH PM136 are similar in size to those of CMNH 11767, although they are taller. In more gracile specimens, such as CMNH 11759, the horns are not elevated high above the orbits, although the horns of the more robust specimens, such as FMNH PM136 and CMNH 11767, tend to be more highly elevated above the orbits.

The nasal incision is relatively shallow in all specimens. In specimens with undistorted faces the posterior margin of the nasal incision does not rise higher than the orbit. The posterior margin of the nasal incision varies in position from the anterior margin of P4 in CMNH 11759 to above the anterior margin of M1 in CMNH 11767, although this character in the later specimen may be distorted. FMNH PM136 and other skulls are more consistent with CMNH 11759 in this regard. The orbit of CMNH 11759 is positioned above M1, with the anterior rim of the orbit above the posterolateral root of P4. The orbital position of FMNH PM136 and most other specimens is similar with the anterior orbital rim extending anterior to M1. However, the position of the orbit fluctuates slightly. For instance, in CMNH 11767 the posterolateral root of P4 is anterior to the anterior rim of the orbit, although the face of this specimen is somewhat distorted.

The nasal process is usually about the same length as the premaxillomaxillary rostrum, although in some specimens it can be slightly longer or shorter. From a lateral view the nasal process projects from the skull in a horizontal (CMNH 11759) or slightly downward (CMNH 11767, FMNH PM136) direction. The nasal process also tends to curve slightly downward so that the dorsal surface is convex. The dorsal surface is convex while the ventral surface is concave. However, the nasal process of FMNH PM136 is straighter. A downturned thickened rim of bone forms the sides of the nasal process. Overall, the

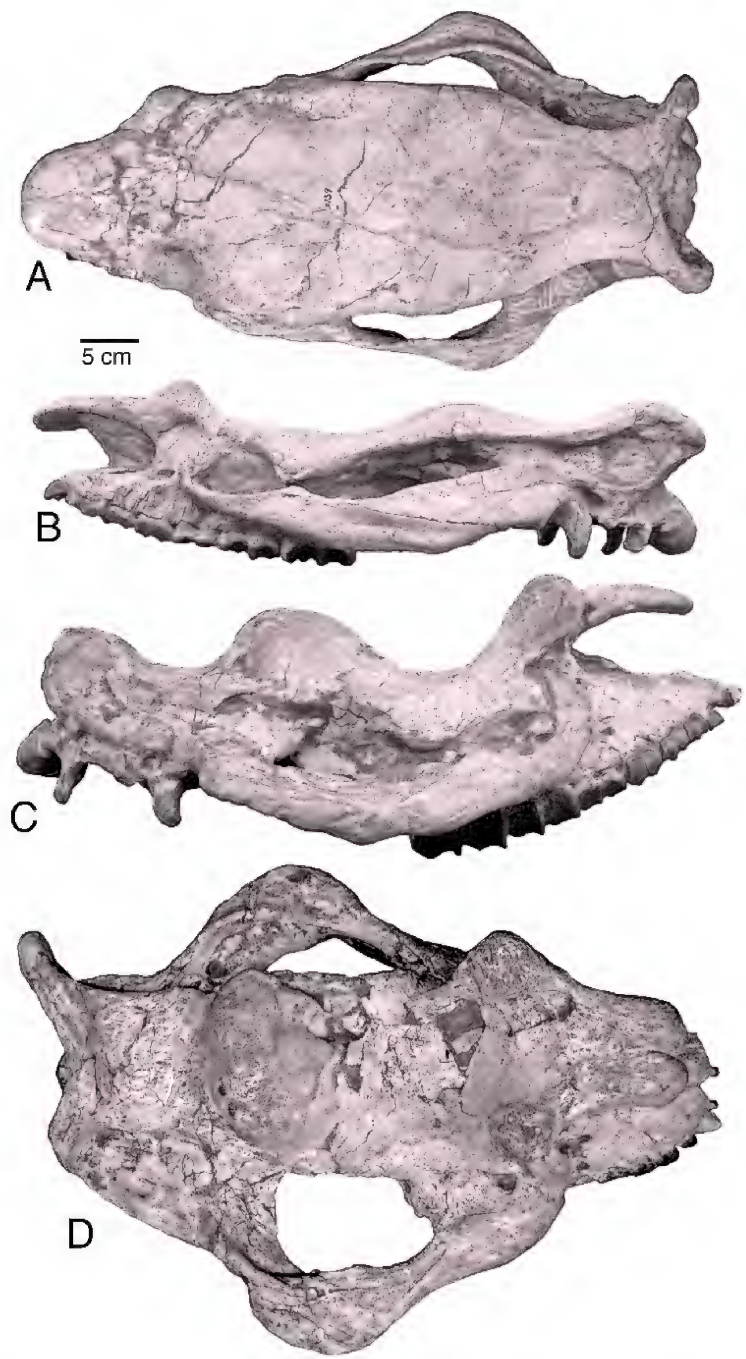

Fig. 156. *Duchesneodus uintensis* skulls from the *Duchesneodus* quarry locality. **(A)** Dorsal view of CMNH 11759, **(B)** left view of CMNH 11759, **(C)** right view of CMNH 11767, **(D)** dorsal view of CMNH 11767.

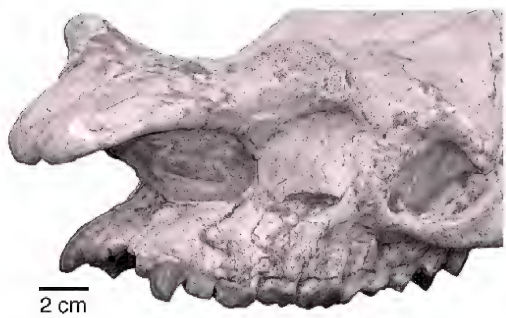

Fig. 157. Oblique view of left face of *Duchesneodus uintensis* (CMNH 11759).

lateral walls are shallow and continue to become shallower distally. From a dorsal view the nasal processes of CMNH 11759 and CMNH 11767 are relatively long and broad, although that of FMNH PM136 is shorter and narrower. The nasal process tends to taper slightly distally and the distal end is strongly rounded. The anterior edge of the nasal process is slightly downfolded and can be roughened as in FMNH PM136. The nasal bones of CMNH 11759 are fully fused, although in CMNH 11767 and FMNH PM136 the nasal bones are separated at their distal ends, forming a median notch on the anterior margin of the nasal process.

In CMNH 11759 and CMNH 11767 the premaxillomaxillary rostrum curves upward distally and the dorsal margin of the rostrum slopes posterodorsally, but it does not rise higher than the midpoint of the orbit. The rostrum deepens posteriorly. In FMNH PM136, the rostrum is thicker, shorter, and so strongly curved upward that it almost contacts the nasal process, thus greatly constricting the nasal cavity and causing the dorsal surface of the rostrum to slope posteroventrally rather than posterodorsally. The premaxilla of *Duchesneodus uintensis* is very short and does not extend anterior to the canines. The premaxillary symphysis is fully ossified in all adult specimens. From the oblique view of CMNH 11759 (fig. 157), the symphysis is long and sloped upward. Behind the symphysis the dorsolateral margins of the rostrum are laterally divergent. I have not seen a specimen of *Duchesneodus uintensis* with a visible premaxillomaxillary suture.

From lateral views the dorsal surface is completely concave except for a bizarre, domelike convexity on the dorsal surface midway between the orbit and the occiput. In CMNH 11759 this convexity is conspicuous, but it is relatively low. It is extremely large in CMNH 117167. However, among most other specimens the size of this dorsal dome is intermediate (e.g., CMNH 11754; FMNH PM136). Scott (1945) thought that this cranial convexity was unique to *D. uintensis*, but he was incorrect. As Peterson (1931) had noted earlier, a similar but subtle cranial convexity is occasionally present on skulls of *Megacerops* (sensu Mihlbachler et al., 2004b). A similar dome is also seen in *Metatitan primus*, although that species differs from *D. uintensis* in many other ways. In *D. uintensis* the size of the dorsal convexity seems to covary with the size of the horns and the thickness of the zygomatic arches (see next paragraph). The parasagittal ridges are prominent, remain widely separated, and weakly overhang the sides of the skull. The posterodorsal surface is only moderately constricted by the zygomatic arches.

The zygomatic arches of *Duchesneodus uintensis* skulls vary greatly in thickness, and the degree to which they are bowed laterally. Those of CMNH 11759 are relatively shallow and thin. From a lateral view the jugal process of the zygomatic is horizontal, while the squamosal zygomatic process slopes upward posteriorly at a shallow angle, thus giving the zygomatic a weak curvature. From the dorsal view the zygomatic arches are thin and moderately expanded laterally. The lateral swelling at the junction of the jugal and squamosal is distinct but rather small. In comparison, the zygomatic arches of CMNH 11767 and FMNH PM136 are deeper, strongly bowed laterally, have massive swellings, and are more strongly curved. The degree of variability in the size of the zygomatic swellings in *Duchesneodus* is similar to that seen in *Megacerops*. Scott (1945) and Lucas and Schoch (1989b) interpreted the notable variation in horn size, zygomatic swelling, and the dorsal dome as sexual dimorphism. This interpretation is consistent with that of Mihlbachler et al. (2004b) for *Megacerops*, in which the morphometric variation in the horns and zygomatic arches is similar in magnitude to the morphometric variability

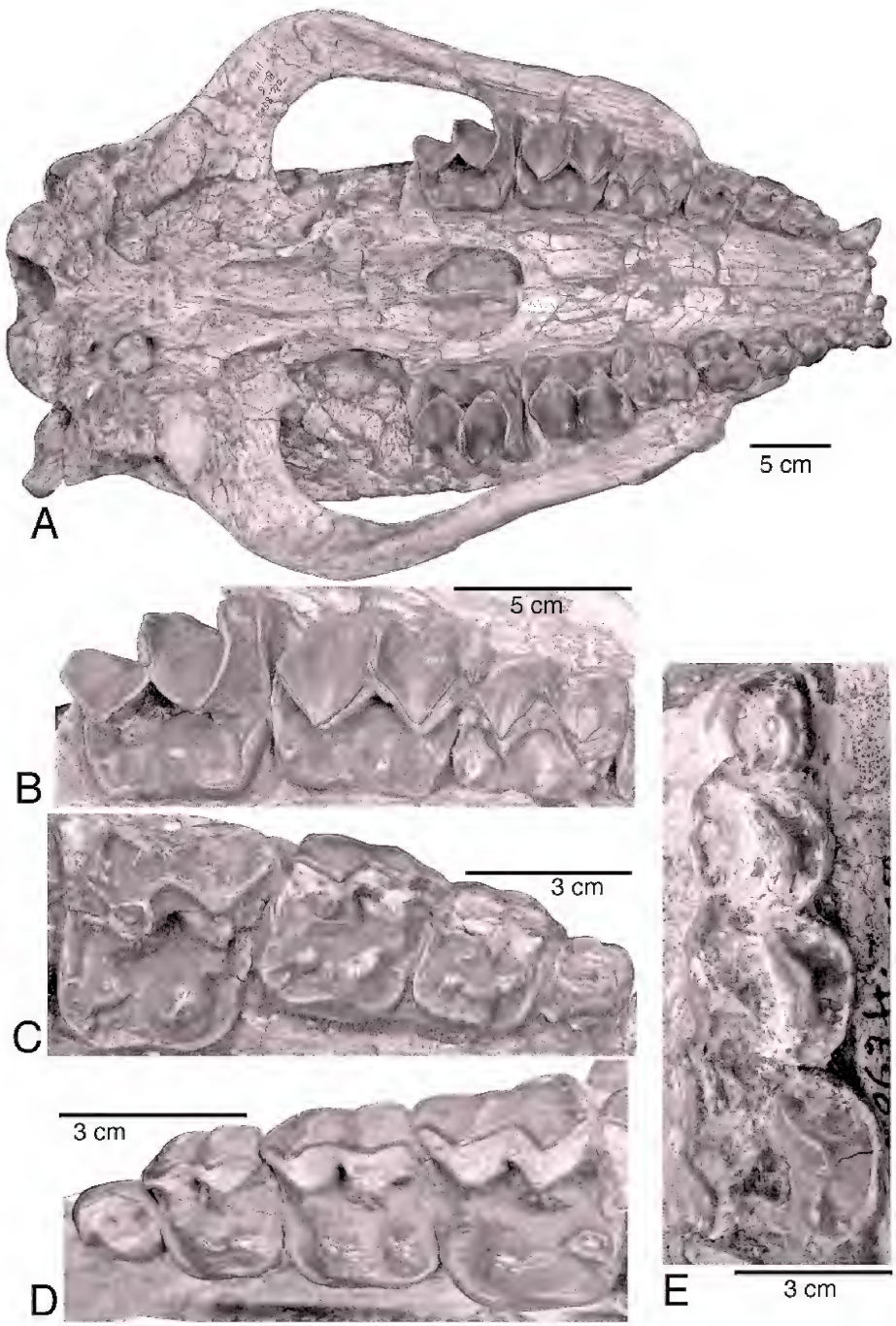

Fig. 158. Ventral views of the skull and upper dentition of *Duchesneodus uintensis*. **(A)** Ventral view of CMNH 11754, **(B)** right molars of CMNH 11754, **(C)** right premolars of CMNH 11754, **(D)** left premolars of CMNH 11767, **(E)** right premolars of CMNH 9960.

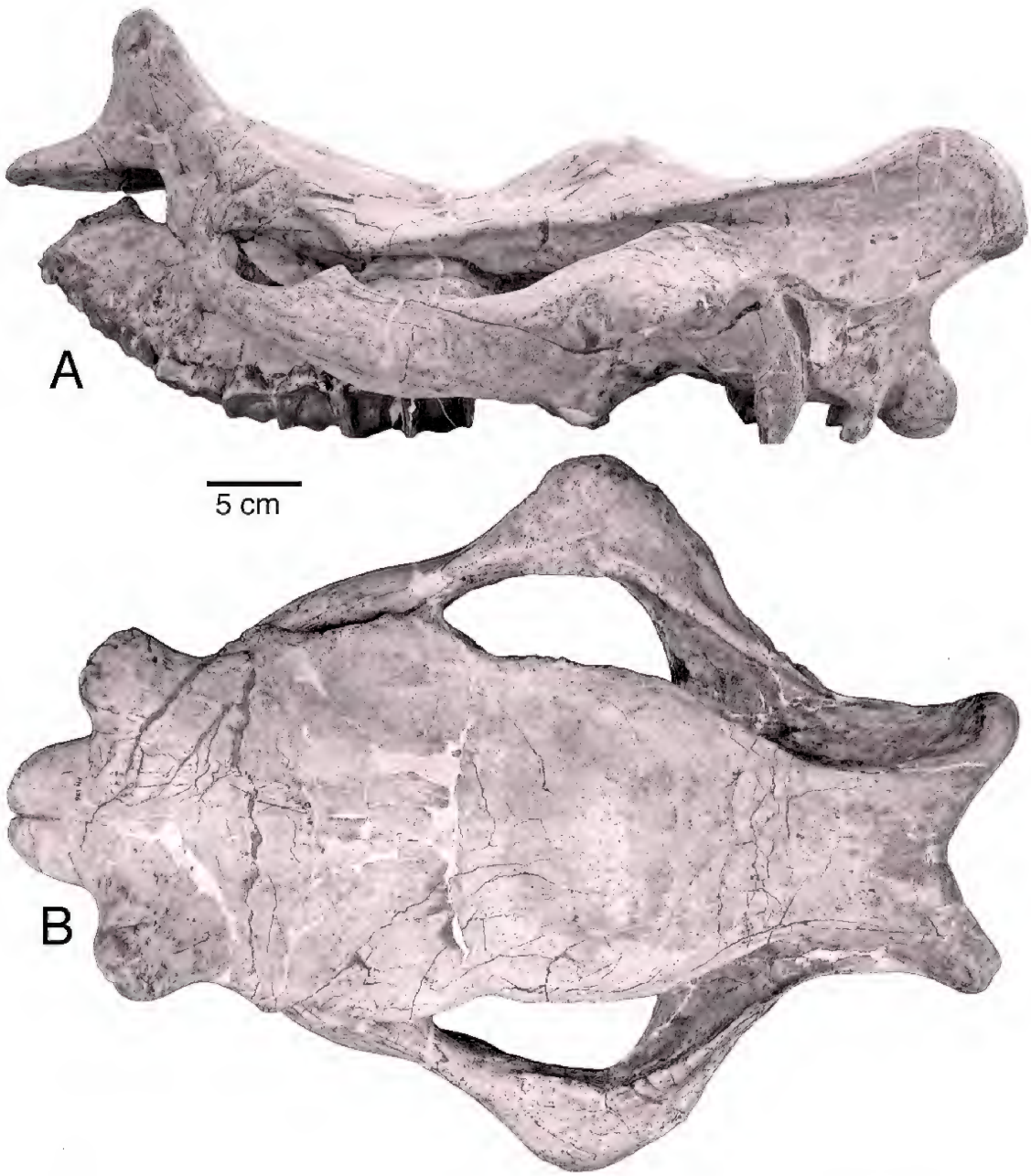

Fig. 159. A skull of *Duchesneodus uintensis* from the Vieja Formation of Texas (FMNH PM136). **(A)** Left view, **(B)** dorsal view.

documented in the sexually dimorphic structures (horns, tusks) of extant ungulates (Mihlbachler, 2004).

From a lateral view of the skull the occiput is strongly tilted backward. From a dorsal view the nuchal crest is strongly concave. From the posterior view (shown for FMNH PM136: fig. 160b), the dorsal margin of the occiput is strongly arched, although it is notched medially. The dorsal portion of the occiput is somewhat wider than the ventral portion. On the surface of the occiput there

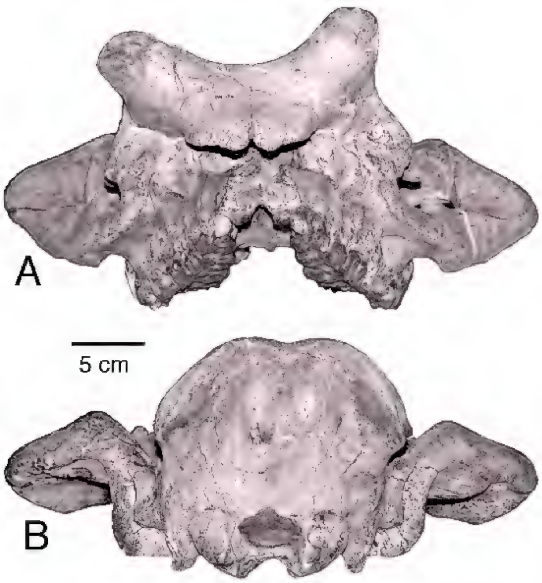

Fig. 160. A skull of *Duchesneodus uintensis* from the Vieja Formation of Texas (FMNH PM136). **(A)** Anterior view, **(B)** posterior view.

are prominent occipital pillars and a shallow central depression. Overall, the occiput of *Duchesneodus uintensis* is not as massive as that of *Megacerops*.

The anterior rim of the posterior nares is situated slightly anterior to the M3 protocones in CMNH 11759, although the position of the anterior margin of the posterior nares fluctuates among specimens from the *Duchesneodus* quarry from between the M2 hypocones to between the M3 protocones. There is no horseshoe-shaped rim of bone emarginating the anterior and lateral sides of the posterior nares.

In CMNH 11759 and FMNH PM136, the thin, elongate vomer can clearly be seen bisecting the elongate posterior narial canal. The posterior narial canal extends slightly into the region of the sphenoid, although large ventral sphenoidal fossae are not present in *D. uintensis*. The foramen ovale and foramen lacerum are widely separate. The mastoid process is short and arches forward, making contact with the posterior surface of the postglenoid process, forming a tube-shaped or ventrally constricted external auditory pseudomeatus.

Upper Dentition: Several specimens from the *Duchesneodus* quarry have well-preserved and lightly worn teeth. Pictured in close-up are the molars and premolars of CMNH 11754 (fig. 158b, c) and the premolars of CMNH 11767 (fig. 158d), CMNH 9960 (fig. 158e), and FMNH PM136 (fig. 161c). The more complete incisors and canines of FMNH PM136 are shown in close-up (fig. 161b).

There are two pairs of upper incisors. The incisors are very small, essentially featureless and globular, and of similar size. They form a straight row between the anterior margins of the canines. The canines are extremely small in FMNH PM136. They are somewhat larger in CMNH 9960, but the canines of all *D. uintensis* specimens can be characterized as small. With the exception of a median gap between the central incisors (which tends to occur in most brontotheres), there are no diastemata in the upper dentition.

The P1 is small but complex. It is nearly rounded in outline. The ectoloph has two convexities, indicating the presence of both a paracone and metacone. On the small lingual shelf, a lophlike protocone arches around the lingual side of the crown and is connected to a preprotocrista. The P2–P4 of most specimens are essentially rectangular, although the shape of P2 can be somewhat oblique as in CMNH 9960. The parastyle of P2 is straight or slightly lingually arched. The P3 parastyle is straight or somewhat labially directed. The parastyle of P4 is always strongly labially directed. The metastyles of P2 and P3 are straight, while the P4 metastyle can be directed somewhat labially. The labial paracone ribs are weak and become progressively thinner in more posterior premolars. Mesostyles are absent on the premolars of CMNH 11754, but a poorly developed mesostyle is occasionally present on the P4 (e.g., CMNH 9960, CMNH 11757, FMNH PM136).

The lingual morphology of the P2–P4 is highly variable. A protocone and hypocone are always present on these teeth, in addition to very small but distinct preprotocrista. The preprotocrista is largest on P2 and smallest on P4. However, in some specimens, such as CMNH 9960, the preprotocristae are well developed on P2, P3, and P4. On the P2 of CMNH 11754 the protocone is essentially

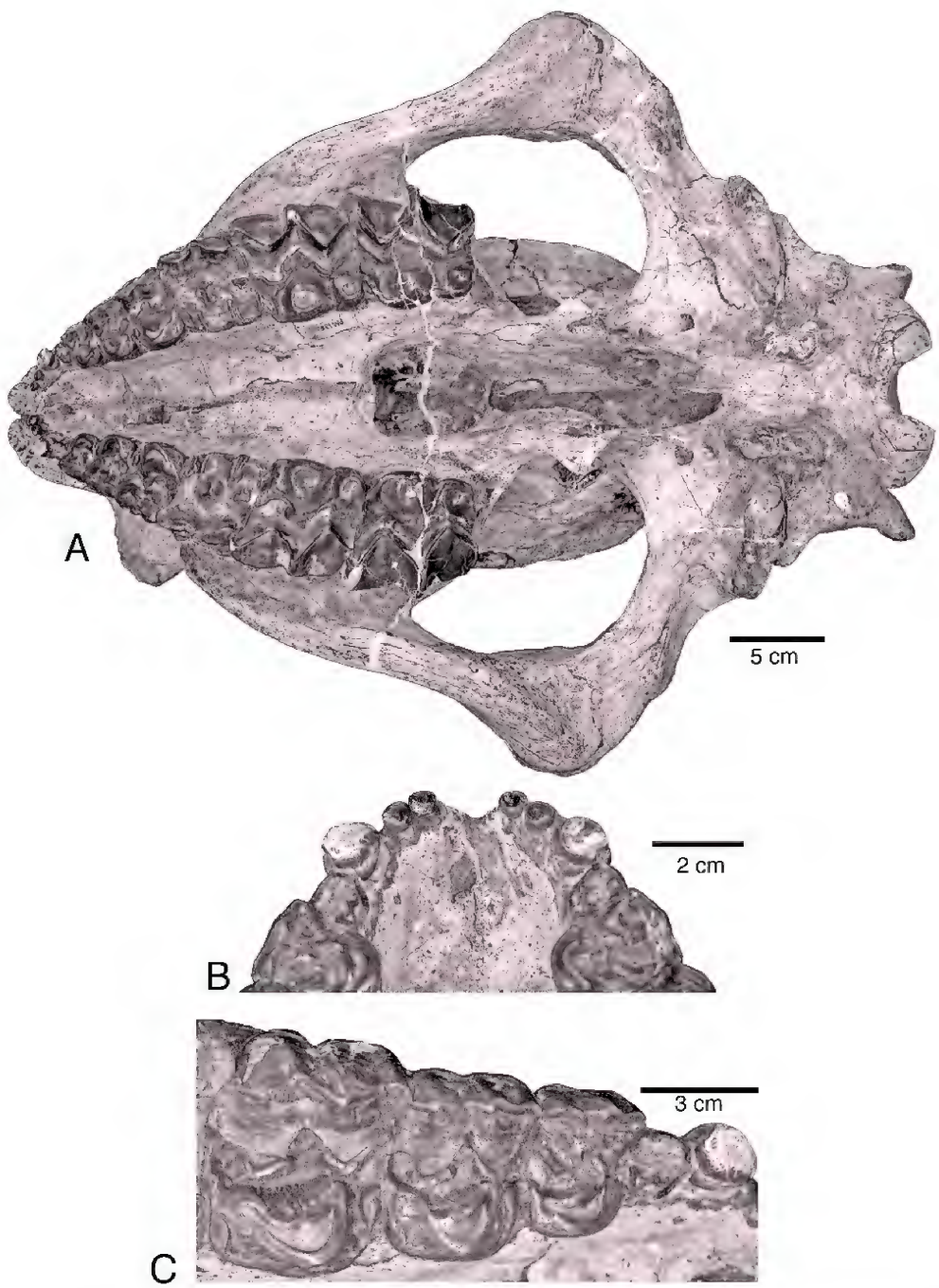

Fig. 161. A skull of *Duchesneodus uintensis* from the Vieja Formation of Texas (FMNH PM136). **(A)** Ventral view, **(B)** anterior dentition, **(C)** right canine and premolars.

absorbed by a large crest that arches around the anterolingual side of the crown. The hypocone of that tooth is distinct, but it is connected to the lingual crest. The protocones of P3 and P4 of that specimen form more discrete cusps. The hypocones of these teeth are smaller than the protocones and completely separated. The lingual premolar

TABLE 11
Summary statistics for selected morphometric variables of the "*Duchesneodus uintensis* quarry" sample
See Methods for measurement definitions

	N	Mean	SD	Min.	Max.	CV
C L	8	19.3	2.8	15.6	22.7	14.7
P3 L	11	25.3	2.1	20.6	28.8	8.3
P3 W	11	30.5	1.7	26.6	33.4	5.7
M2 L	9	59.0	5.9	51.2	66.7	10.1
M2 W	9	54.9	3.3	50.9	60.6	6.0
P2–P4	8	77.9	2.5	75.0	82.0	3.2
M1–M3	8	167.1	15.3	141.8	190	9.2
V L	8	544.1	41.1	470	610	7.6
c L	2	15.6	3.4	13.2	18	21.5
p3 L	2	22.5	1.9	21.1	23.8	8.5
p3 W	2	18.5	2.6	16.7	20.4	14.0
m2 L	2	45.8	1.5	44.8	46.8	3.2
m2 W	2	30.5	2.4	28.8	32.2	8.0
p2–p4	2	71.8	6.5	67.2	76.5	9.1
m1–m3	2	148.1	23.9	131.2	165	16.2

morphology of CMNH 11767 is similar to CMNH 11754, although the hypocones and protocones are of similar size and the P2 hypocone is more strongly connected to the protocone. Other specimens differ more dramatically. For instance, on CMNH 9960, the protocone and hypocone of P2 and P3 are completely absorbed by the prominent lingual crest. In the same specimen, the lingual cusps of P4 are strongly connected by a tall crest. The degree to which the lingual cusps are connected is intermediate between CMNH 11754 and CMNH 9960 on several specimens from the *Duchesneodus* quarry (e.g., AMNH 32604); specimens from the quarry do not exhibit distinct anterolingual cingular cusps on the premolars, although some specimens from elsewhere do. For instance, the P3 and P4 of FMNH PM136 display prominent anterolingual cingular cusps. Anterolingual cingular premolar cusps are also frequent among the *Duchesneodus californicus* (a nomen dubium) material from the Sespe Formation. Occasional anterolingual cingular premolar cusps are also seen among specimens *Megacerops* (sensu Mihlbachler et al., 2004b) and (more prominently) in *Sivatitanops birmanicum* (a nomen dubium). The labial cingula of the premolars of *D. uintensis* are absent to very weak. The lingual premolar cingula are variably continuous and discontinuous around the lingual base of the protocone.

The upper molars of *Duchesneodus uintensis* have tall, lingually angled ectolophs, very weak labial ribs, thin lingual ectoloph enamel, and wedge-shaped lingual margins of the paracone and metacone. The anterior cingulum is thin and passes proximally to the distal peak of the parastyle. Distinct central molar fossae and small anterolingual cingular cusps are present on the molars. On CMNH 11754 there is a small bead of enamel positioned distally from the anterolingual cingular cusp on all the molars, but generally *Duchesneodus uintensis* upper molars lack any structures that could be interpreted as paraconules. Metalophs are also absent on M1 and M2. The M3 hypocone morphology varies in size from a small bead of enamel (CMNH 11754) to nearly as large as those of the M1 and M2 (CMNH 11759). The labial molar cingula are always weak or absent and always discontinuous around the mesostyle. Distinct lingual cingula are lacking on the M1 and M2 of CMNH 11754, but a thin, distinct lingual cingulum can be seen on the M3 that is discontinuous around the base of the protocone.

MANDIBLE AND LOWER DENTITION: There are only three mandibles in the *Duchesneodus* quarry sample and none of

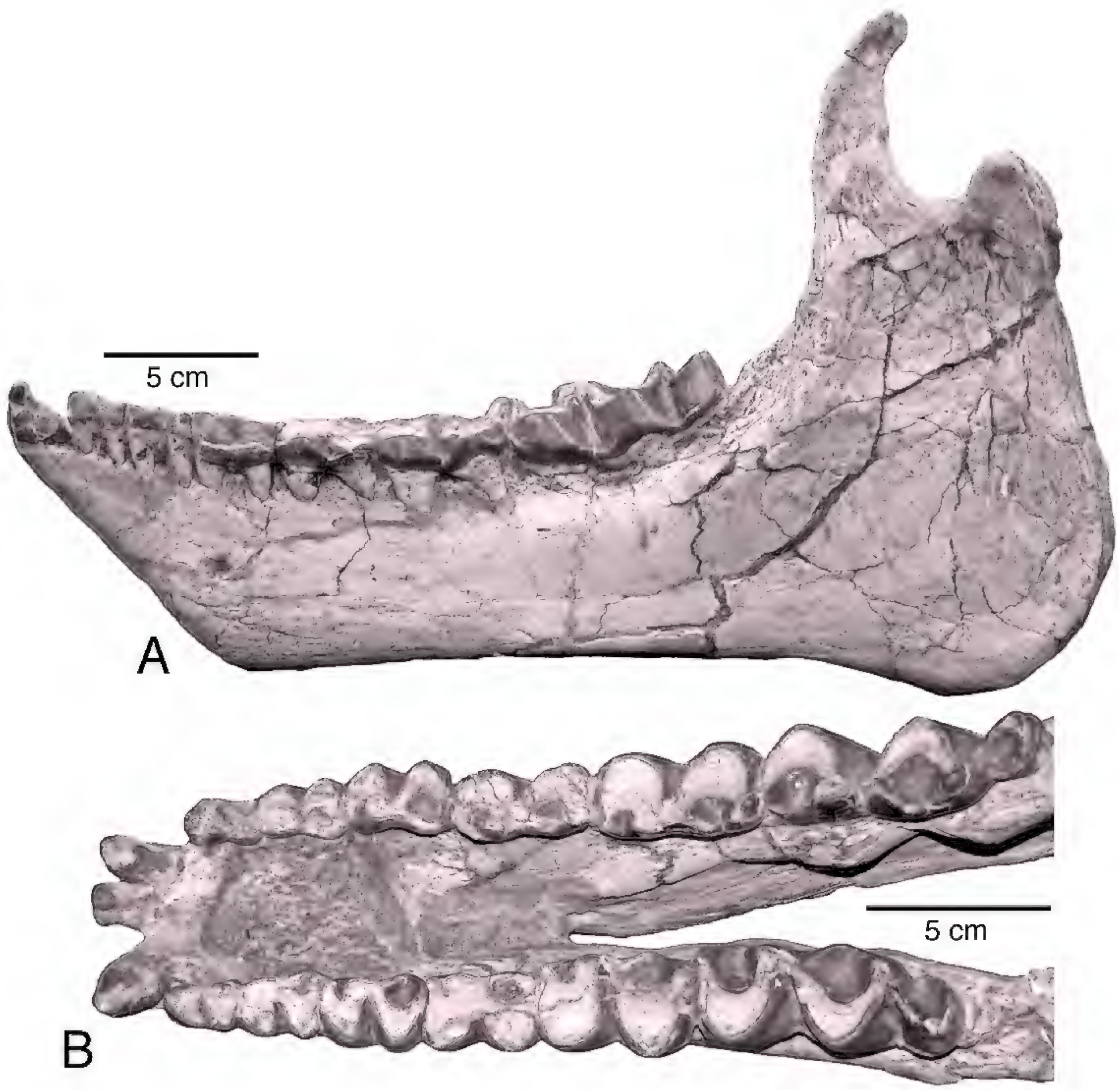

Fig. 162. The holotype mandible of *Duchesneodus uintensis* (CMNH 11809). **(A)** Left view, **(B)** dorsal view.

these is associated with a skull. One of these, CMNH 11821 (not shown), is poorly preserved and does not contribute a significant amount of morphological information. The holotype mandible (CMNH 11809) appears not to be significantly distorted from a lateral view (fig. 162). However, from a dorsal view it is clear that either the left ramus has been artificially shortened or the right ramus has been artificially elongated. Additionally, the mandible has been slightly crushed transversely. The ascending rami of the third mandible are significantly distorted, but the shape of the symphysis is essentially intact (fig. 163).

The inferior margin of the symphysis of CMNH 11809 is straight and steeply angled (>45°), while in CMNH 11761 the inferior margin is concave and with a shallower overall angle (< 45°). In these respects, both specimens contrast with the more normally convex inferior margin of *Megacerops* and more closely resemble *Eubrontotherium clarnoensis*. The symphysis of CMNH 11761 is broad and it extends to the anterior margin of m1.

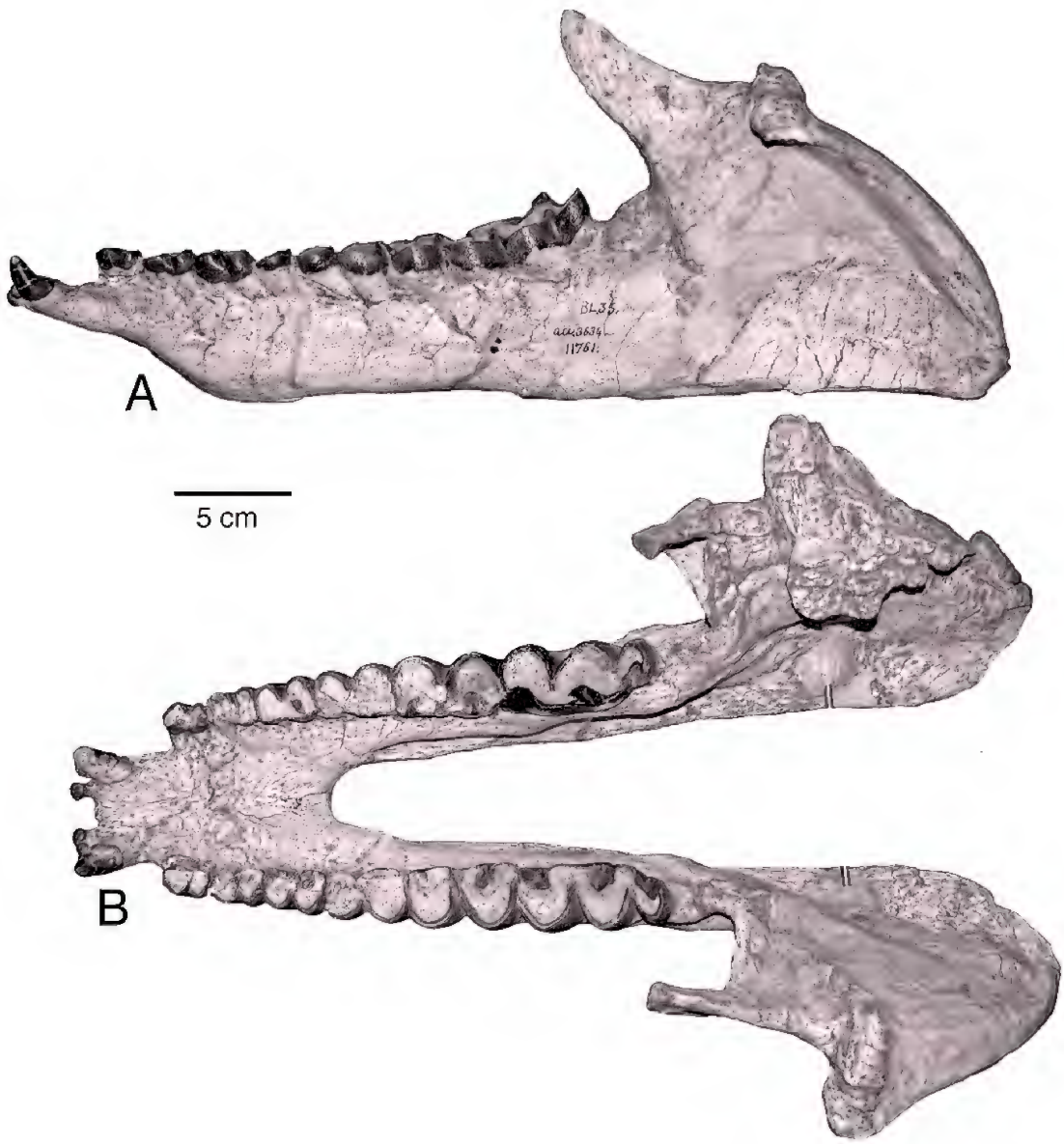

Fig. 163. A mandible referred to *Duchesneodus uintensis* (CMNH 11761). **(A)** Left view, **(B)** dorsal view.

The lower incisors are small and essentially featureless, although this is partially related to wear. The i2 is somewhat larger than i3. The incisor rows of both specimens are incomplete, but the incisor alveolar surface is most complete in CMNH 11761. The incisors form a straight row between the anterior margins of the canines. Although the number of upper incisor is reduced to two pairs, the remaining lower incisors of CMNH 11761 plus the unoccupied incisor alveoli indicate three pairs of lower incisors.

The canines of both specimens are small. The canines of CMNH 11761 are distinctly separated from the cheek teeth by a postcanine diastema that is slightly shorter than the p2. Even if a small p1 were present in that specimen there is still enough space for a short postcanine diastema. The width from canine to canine is much narrower than the

width across the p2s. A small alveolus anterior to the p2 indicates the presence of a single-rooted p1.

The heavy wear of the remaining cheek teeth prohibits a thorough description; however, the following details are revealed, particularly from the left cheek-tooth row of CMNH 11809, which seems to be the least worn available cheek-tooth row of *Duchesneodus uintensis*. The trigonid and talonid of p2 are about the same length. The trigonids of p3 and p4, on the other hand, are shorter than the talonids. The trigonids of p2–p4 are somewhat narrower than the talonids. The paralophid of p2 is arched slightly lingually, while the p2 protolophid appears to have been positioned lingually and directed posteriorly. The p2 trigonid lingual notch is small. The trigonid of p3 is very worn, but its dimensions resemble the p4 trigonid. The paralophid and protolophid of p4 arch fully lingually, creating a deep (and probably broad when unworn) lingual trigonid notch. A metaconid is not seen on p2, and although worn, the shapes of the p3 and p4 trigonids are consistent with those of other species that have a large lingually positioned metaconid. The talonids of p2 and p3 are heavily worn, but their shape suggests there were well-developed cristids obliqua and hypolophids, with nearly molariform basins, like p4. There are no distinct entoconids on the premolars of *Duchesneodus uintensis* (contra Lucas and Schoch, 1982, 1989b).

The molars are typical with shallow basins, thin lingual enamel, and an elongate m3. The labial cingulids of the premolars and molars are weak, as noted by Lucas and Schoch (1989b) in their diagnosis of *D. uintensis*, although their weakness may have resulted from heavy wear on the teeth.

Remarks

In 1929–1930 a Carnegie Museum field party led by J. L. Kay collected a large assemblage of a new species from the "Titanothere Quarry" ("*Duchesneodus* Quarry" of Lucas and Schoch [1989b]) of the Duchesne River Formation near Vernal, Utah. This new species, *Duchesneodus uintensis* (Peterson, 1931), was described from the limited material that was initially available (two jaws and a skull). It is both surprising and unfortunate that Peterson (1931) assigned holotype status to a mandible (CMNH 11809) that does not facilitate a good diagnosis of this species. A complete skull (CMNH 11759) that does facilitate a clear diagnosis of *Duchesneodus uintensis* was available to Peterson (1931) but was assigned only paratype status. The holotype jaw cannot be readily differentiated from the holotypes of *Protitanops curryi*, *Notiotitanops mississippiensis*, or from *Megacerops*. Therefore, from a strictly morphological perspective, the taxonomic identity of the holotype jaw is unclear. The skulls of the quarry, on the other hand, clearly indicate a unique species of brontothere. The validity of *Duchesneodus uintensis* relies, therefore, on the assumption that the quarry sample to which the holotype belongs is a monospecific assemblage.

Peterson's (1931) initial description of the quarry sample was intended to be preliminary and was not based on the entire assemblage. Scott (1945) subsequently provided a thorough description of the quarry assemblage and documented the morphological variation found within that sample. Rather than splitting the sample into multiple species based on minute differences (some related to taphonomic distortion) that Osborn (1929a) and other prior authors (e.g., Granger and Gregory, 1943) would have regarded as evolutionary stages, Scott (1945) recognized taphonomic variation and differentiated it from biologically relevant variation. Additionally, he readily accepted the real morphological variation in the sample as intraspecific variation. For this reason, Scott's description of *Duchesneodus uintensis* was a potentially significant advancement in brontothere taxonomy, although those who practiced brontothere taxonomy in the following decades seem not to have recognized the significance of Scott's recognition of intraspecific variation in this sample. *Duchesneodus uintensis* is similar to *Megacerops* (sensu Mihlbachler et al., 2004b), but differs most conspicuously in the retention of three lower incisors and the possession of a conspicuous dome on the dorsal surface of the skull.

Peterson (1931) originally assigned *Duchesneodus uintensis* to the genus *Teleodus*

because it possessed six globular lower incisors like the type species of *Teleodus*, *T. avus* Marsh. However, Lucas and Schoch (1982) and Lucas (2004) convincingly argued that the holotype of *T. avus* Marsh (YPM 10321) has more incisors added to it during the preparation of the specimen than actually belonged with the specimen. For this reason *Teleodus* was deemed an invalid genus by Lucas and Schoch (1982) and *Teleodus uintensis* was assigned a new genus, *Duchesneodus*.

Lucas and Schoch (1982) also transferred other species that had been previously assigned to *Teleodus* to *Duchesneodus*: *D. primitivus* (Lambe, 1908), *D. californicus* (Stock, 1935), and *D. thyboi* (Bjork, 1967). In a subsequent publication, Lucas and Schoch (1989b) further revised the genus *Duchesneodus*. *Duchesneodus californicus* and *D. thyboi* were considered junior synonyms of *D. uintensis*. However, *D. primitivus* was recognized as valid species. In addition to these taxonomic revisions, Lucas and Schoch (1989b) referred a large number of brontothere specimens to *D. uintensis*, including material from the *Duchesneodus* quarry as well as more fragmentary material that has previously been described by Bjork (1967), Nelson et al. (1980), Stock (1935; 1938), Lucas (1982, 1983b), and other material. With the exception of the *Duchesneodus* quarry material, much of the additional material is fragmentary and lacks diagnostic features. Lucas and Schoch (1989b) did not recognize that much of the very fragmentary material they considered to be *D. uintensis* is too incomplete to identify to a species level. Much of the material in their hypodigm could belong to other brontotheres such *Protitanops curryi* or *Notiotitanops mississippiensis*. Among these materials are the holotypes of *D. primitivus*, *D. californicus*, and *D. thyboi*, which are now considered nomina dubia.

Among the four species assigned to *Duchesneodus* by Lucas and Schoch (1982, 1989b) only *D. uintensis* is known from complete fossil material and is clearly valid. The list of referred specimens given here only includes specimens that can be unambiguously assigned to *D. uintensis* based on morphological characters and/or inclusion in the presumably monospecific quarry sample. Because *Duchesneodus* (sensu Lucas and Schoch, 1989b) is considered an index taxon of the Duchesnean land mammal "age", it will be important to reconsider the identification of brontothere specimens (mostly fragmentary) attributed to *Duchesneodus* by Lucas and Schoch (1989b), and the significance of this to the age assignments of various faunas considered by Lucas (1992) to be Duchesnean.

MISCELLANEOUS DUBIOUS, PROBLEMATIC, AND UNNAMED POTENTIAL TAXA

Because fossil species are often based on fragmentary material, it is inevitable that many species names will eventually be determined to be invalid. Although many species are found to be synonyms, others are dubious altogether. Many of the earliest names for brontotheres that were based on very fragmentary materials were found to be dubious by Osborn (1929a). In all of these cases, where Osborn considered a taxon to be dubious, my determinations are in agreement. Therefore those taxa considered dubious by Osborn (1929a) are not reconsidered here. In addition to the valid species and their synonyms that are discussed above, an additional 32 species (or potential species) are discussed below. These 32 taxa fall into three categories: (1) nomina dubia, (2) problematic, and (3) unnamed potential species.

The majority of these taxa (N = 23) were found to be nomina dubia. An additional eight dubious species were discussed above in prior sections dealing with *Metarhinus* and *Rhinotitan*, thus yielding a total of 31 species determined to be dubious in this study. Species considered to be nomina dubia could not be diagnosed as unique species nor could they be synonomized with other taxa. Species were considered dubious for two reasons. Most dubious species are represented by fossils that lack autapomorphies or unique combinations of character states. A smaller number of nomina dubia, including *Sivatitanops birmanicum*, *Hyotitan thomsoni*, "*Protitan*?" *cingulatus*, and *Epimanteoceras amplus*, exhibit autapomorphies or unique combinations of character states, although synonymy with other fragmentary taxa could not be

ruled out due to nonoverlapping parts (e.g., a skull from one taxon and a jaw from another), which prevents comparison.

Three other previously named species, "*Eotitanops*?" *dayi*, *Pakotitanops latidentatus*, and *Mulkrajanops moghliensis*, were considered to be problematic, but not necessarily of dubious taxonomic status. Problematic taxa are seemingly valid according to the methods of taxon delimitation used in this study, but the fossil materials (or available figures and descriptions) are so incomplete, poorly preserved, or (in cases where I could not examine original material or casts) insufficiently described in the literature that the available character data is extremely limited, thus prohibiting a thorough description or taxon diagnosis.

Finally, six potentially new species are considered below. These possibly new species are described, but for a variety of reasons, a formal name and diagnosis was not applied, pending the discovery of more appropriate material. Primarily these taxa are known from very fragmentary materials.

The dubious, problematic, and potentially new species were excluded from the phylogenetic analysis. Nonetheless, many of the specimens representing these taxa are highly significant. For instance, many of the fossils currently assigned to nomina dubia contain valuable character data if future discoveries allow them to be linked with valid species known only from highly fragmentary specimens. Additionally, many of the specimens upon which these dubious, problematic, and potential taxa are based occur in regions where brontothere fossils are rare (e.g., Europe, southeast Asia, Pakistan, Korea, etc.), and thus significantly expand our understanding of brontothere paleobiogeography, and are thus deserving of attention.

Dolichorhinus vallidens (Cope, 1872)

LECTOTYPE: AMNH 5098, a partial mandible (in two pieces) with right c (partial), p2, dp4, m1–m3, and left p4–m3.

TYPE LOCALITY: "Mammoth Buttes, Southwestern Wyoming, near headwaters of Bitter Creek"; Adobe Town Member (Washakie B of Granger, 1909) of the Washakie Formation, Wyoming

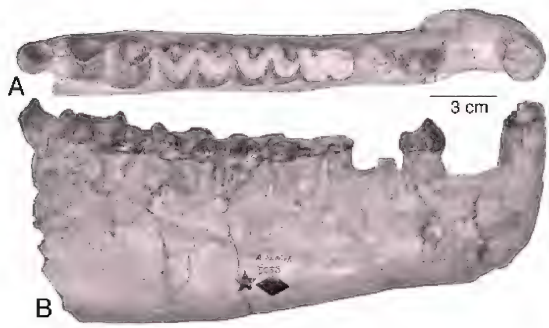

Fig. 164. The lectotype of *Dolichorhinus vallidens* (AMNH 5098). **(A)** Dorsal view, **(B)** right view.

AGE: Middle Eocene (early Uintan land mammal "age").

DETERMINATION: Nomen dubium: holotype lacks diagnostic features.

DESCRIPTION

AMNH 5098 includes a pair of right and left mandible fragments that are most similar in size to *Dolichorhinus hyognathus*, *Sphenocoelus uintensis*, and *Telmatherium validus* (fig. 164). Dental dimensions are as follows: p2L = 20.6, p2W = 12.0, p4L = 22.8, p4W = 16.2, m1L = 30.9, m1W = 19.8, m2L = 35.6, m2W = 22.2, m3L = 57.6, m3W = 23.6, p2–p4 = 64.6, m1–m3 = 122.45, p2–m3 = 188.0. The ramal fragments are dorsoventrally shallow, and the right ramus appears to be unusually short in comparison to *Dolichorhinus hyognathus* mandibles. However, the canine root has been plastered onto the specimen in an artificially posterior position. The erect orientation of the canine is artificial also. The crown of the canine is not preserved, but the diameter of the root indicates a canine of typical size. No bone anterior to the p1 alveolus is preserved. The p2 crown is held onto the ramus by plaster, however, remnants of in situ p2 roots are visible on the dorsolabial surface of the ramus.

A short diastema (~7 mm) exists between the p1 alveolus and the p2 roots, although it has been incorrectly represented in previous figures. Cope's (1884) figure of a left ramus (pl. 53, fig. 1) that was reprinted in Osborn (1929a: fig. 95: A2) is a composite drawing of

the left ramal fragment and the mirror image of the anterior part of the right ramal fragment. In this figure, a hypothetical outline of the missing p1 is drawn right next to the p2 with no diastema between them. However, this drawing is inaccurate. The right ramus of the specimen clearly has a short diastema between p1 and p2. Another figure in Cope (1885: pl. 52, fig. 3; reprinted in Osborn 1929a: fig. 95: A1) correctly illustrates the p1–p2 diastema with the root of the p1 positioned several mm anterior to the p2. Other aspects of the mandible and lower dentition of AMNH 5098 are typical of other hornless middle Eocene brontotheres.

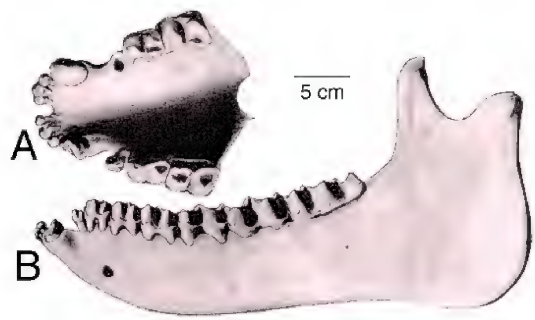

Fig. 165. The holotype mandible of *Duchesneodus primitivus* (NMC 6421). **(A)** A partial dorsal view, **(B)** left view. Figures from Osborn (1929a).

Remarks

Cope (1872) originally referred this species to the genus *Palaeosyops*. He described three specimens from three individuals, AMNH 5097 (portions of an upper dentition), AMNH 5099 (more upper dental elements), and AMNH 5098 (right and left partial mandibular rami), but did not designate a holotype. However, Cope later stated that the "lower jaws may be regarded as typical of the species" (Cope, 1884: 700). Osborn (1929a) concluded from this statement that Cope intended the mandible (AMNH 5098) to be the type, and therefore designated it as the lectotype. While the right ramus retains a dp4, the left ramus has a fully erupted and slightly worn p4. However, the degree of wear on the molars of these two jaw fragments is identical, so it remains probable that these pieces are from one individual.

The lectotype was reassigned to the genus *Telmatherium* by Osborn (1895) and then to *Manteoceras* by Hatcher (1895). Finally, Osborn (1929a) questionably referred this species to the genus *Dolichorhinus*, but he continued to recognize it as a valid species due to the artificially shortened lectotype jaw. The lectotype of *Dolichorhinus vallidens* has a distinct p1–p2 diastema, by which it can be distinguished from *Sphenocoelus uintensis*, a brontothere of similar size and dental morphology. The dimensions of the teeth that are preserved with the lectotype fall above the size ranges of *Mesatirhinus megarhinus*, *Metarhinus fluviatilis*, and *M. abbotti*. *Metatelmatherium ultimum* and *Telmatherium vallidus* are two other taxa that have short p1–p2 diastemata. The dental dimensions of the lectotype of *D. vallidens* fall below the lower size limit of *M. ultimum*. However, the fragmentary lectotype specimen (AMNH 5098) is morphologically consistent with, and falls within the dental dimensions of *Telmatherium validus* and *Dolichorhinus hyognathus*. Mader (1989) came to a similar conclusion. Therefore *Dolichorhinus vallidens* Cope is best considered a nomen dubium.

Duchesneodus primitivus (Lambe, 1908)

Holotype: NMC 6421, a partial mandible with right i1–m3, left i1–c, and p2.

Type Locality: Cypress Hills Formation, Saskatchewan, Canada.

Age: Late Eocene (Chadronian land mammal "age").

Determination: Nomen dubium, possibly a synonym of either *Protitanops curryi* or *Notiotitanops mississippiensis*.

Remarks

Lambe (1908) based *Duchesneodus primitivus* on a mandible (NMC 6421), originally referring it to the genus *Megacerops* (fig. 165). However, this specimen retains three small globular incisors and a long postcanine diastema, two characters that actually distinguish it from *Megacerops* (sensu Mihlbachler et al., 2004b). Osborn (1929a) reassigned the species to the genus *Teleodus* because it shared with *Teleodus avus* three globular lower incisor pairs. However,

Lucas and Schoch (1982) and Lucas (2004) convincingly argued that *Teleodus* was an invalid genus. They subsequently reassigned *Teleodus primitivus* to *Duchesneodus*, a genus whose type species, *D. uintensis*, retains three lower globular incisors. Lucas and Schoch (1989b) differentiated *D. primitivus* from *D. uintensis* based on the following: a relatively large postcanine diastema and vertical labial faces of the lower cheek teeth. However, this diagnosis does not justify a separate species. At least one mandible of *Duchesneodus uintensis* (CMNH 11761) has a postcanine diastema, and although it is shorter than that of NMC 6421, postcanine diastema length tends to be variable in brontothere species. Secondly, I was unable to confirm that the labial faces of the lower cheek teeth were of a different angle as suggested by Lucas and Schoch (1989b) from *Duchesneodus uintensis* or any other similar brontothere.

I can find no morphological evidence that NMC 6421 is distinct from *Duchesneodus uintensis*, except, perhaps, that the inferior margin of the symphysis is rounded in NMC 6421, while in mandibles of *D. uintensis*, the inferior margin of the symphysis tends to be straight or convex. This is weak evidence, at best, for arguing two species. Moreover, there are other large brontotheres that retain three globular incisor pairs and a postcanine diastema. Among these is *Eubrontotherium clarnoensis*; however, the anterior end of the symphysis of *E. clarnoensis* is not narrowed as in NMC 6421. Moreover, *E. clarnoensis* does not have a p3 metaconid, in contrast to NMC 6421. *E. clarnoensis* can therefore be ruled out. However, *Protitanops curryi* and *Notiotitanops mississippiensis* cannot be ruled out. The anterior portions of the mandibles of these species are not known, although each of these species has a long upper postcanine diastema similar in length to the lower postcanine diastema of NMC 6421. It is therefore possible that *D. primitivus* is either a synonym of *Protitanops curryi* or *Notiotitanops mississippiensis*. Lucas et al. (2004) suggested that *Duchesneodus primitivus* is more likely to have been synonymous with *Protitanops curryi* rather than *Notiotitanops mississippiensis*, but this assessment was based on size similarity. However, *N. mississippiensis* and *P. curryi* are each known only from holotypes and although the type of *N. mississippiensis* is somewhat smaller than that *of P. curryi*, the differences are minor and individuals of these species probably overlapped in size. Moreover, NMC 6421 is only slightly larger than the few known mandibles of *Duchesneodus uintensis*. Therefore, because *D. primitivus* could belong to (1) *Duchesneodus uintensis*, (2) *Protitanops curryi*, or (3) *Notiotitanops mississippiensis* with nearly equal probability, this species is a nomen dubium.

Sivatitanops birmanicum (Pilgrim and Cotter, 1916)

LECTOTYPE: GSI C315 (in part), lingual fragment of a premolar.

TYPE LOCALITY: Myaing Area, Myanmar (Burma).

AGE: Middle Eocene (Sharamurunian land mammal "age").

SYNONYMS: *Sivatitanops cotteri* Pilgrim, 1925.

REFERRED SPECIMENS: **(From "Myaing township of Pakokku district, 6.5 furlongs distant from hill 1258 and in a direction 9° West of South from it, Pondaung" [Pilgrim 1925])** GSI C332, a left P3 (?) (lectotype of *Sivatitanops cotteri* Pilgrim, 1925); GSI C 334, a right P4; **(from near the Black Sea coast of Bulgaria)** AMNH 108191 (cast), a right P4; AMNH 141258 (cast), a right P4. The numbers listed above for the last two specimens are numbers of casts in the AMNH; actual specimen numbers were not reported by Nikolov and Heissig (1985). Several other specimens discussed below may belong to *Sivatitanops birmanicum*, but they are not directly referable.

DETERMINATION: Nomen dubium, this species could be a synonym of *Brachydiastematherium transylvanicum*.

DESCRIPTION

Noteworthy features of the lectotype upper premolar fragment (GSI C315, in part) include a very prominent anterolingual cingular cusp and a posterolingual cingular cusp (fig. 166c). Other aspects of this fragment include a single, large protocone, and a discontinuous lingual cingulum. An antero-

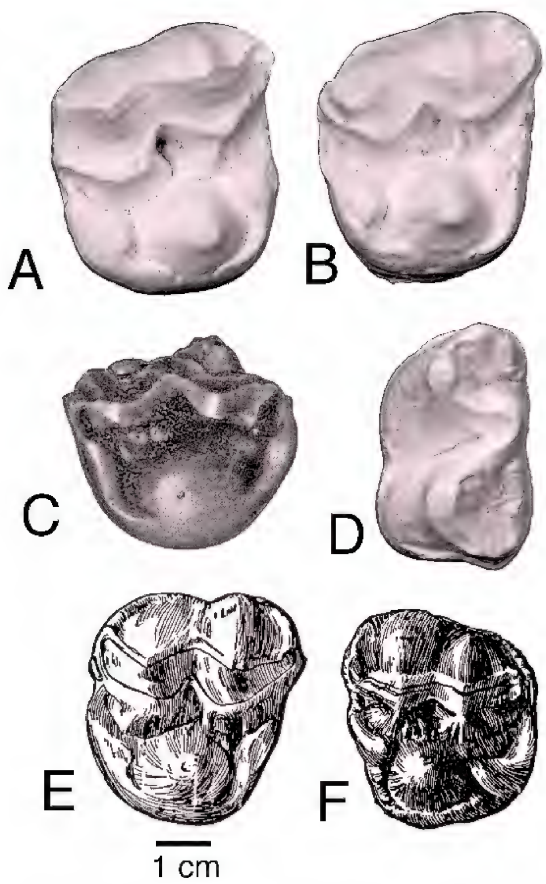

Fig. 166. Premolars of *Sivatitanops birmanicum*. **(A)** A right P4 (AMNH cast 141258), **(B)** right P4 (AMNH cast 108191); **(C)** lectotype premolar fragment (GSI C 315, in part) (from Pilgrim and Cotter, 1916), **(D)** left P4 (not certainly *S. birmanicum*) (AMNH cast 141257), **(E)** a right P4 (GSI C334) (from Pilgrim, 1925), **(F)** a left P3 (?) (GSI C332) (from Pilgrim, 1925).

lingual cingular cusp on the premolars is seen in occasional specimens of *Megacerops* and *Duchesneodus* although it is larger and more developed in premolars of *Sivatitanops birmanicum*. Other premolars described by Pilgrim (1925) such as GSI C334 (fig. 166e) and GSI C332 (fig. 166f) also have a large anterolingual cusp and posterolingual cingular cusp. In addition, two upper premolars from Bulgaria described by Nikolov and Heissig (1985) show the same distinctive characteristics (fig. 166a, b). No other specimens are directly referable to *Sivatitanops birmanicum*, although several specimens that possibly belong to this species are discussed below.

Remarks

The brontothere fossils collected from the Pondaung Formation of Myanmar seem to represent at least four species: *Sivatitanops birmanicum*, "*Metatelmatherium* (?)" *lahirii* (in part), "*Sivatitanops* (?)" *rugosidens*, and *Bunobrontops savagei*. Among these only *Bunobrontops savagei*, with its unique set of molar characters, is a clearly valid species name. The remaining three seem to represent distinct species that occur in the Pondaung, but their names are technically nomina dubia because the scrappy nature of the known materials limits comparison with species from other areas.

Pilgrim and Cotter (1916) based *Sivatitanops birmanicum* on five upper cheek-tooth fragments that were all assigned to GSI C315. Pilgrim and Cotter (1916) originally referred this species the genus "*Telmatherium* (?)". Later, Pilgrim (1925) named a new genus and species, *Sivatitanops cotteri*, from a series of isolated upper teeth. Four specimens were referred to as types: a M1 or M2 (GSI C330), a P2 (GSI C331), a P3 (GSI C332) (fig. 166f), and an upper canine (GSI C333). In addition to these four specimens, Pilgrim (1925) referred a P4 (GSI C334) (fig. 166e), an incisor (GSI C335), a P1(?) (GSI C335), and a jaw fragment with a premolar and partial canine (GSI C338) to *S. cotteri*. The P3 (?) and P4 of *S. cotteri* are similar to the lectotype premolar of "*Telmatherium* (?)" *birmanicum* (fig. 166c), particularly in the possession of prominent anterolingual and posterolingual cingular cusps. These similarities led Pilgrim (1925) to reassign *birmanicum* to *Sivatitanops*. However, *S. birmanicum* and *S. cotteri* continued to be considered separate species.

Whether the five specimens all assigned to GSI C315 originally referred to *Sivatitanops birmanicum* belong to the same individual or even the same species is open to question. I consider the lingual fragment of the premolar (fig. 166c) the lectotype because it expresses apparently diagnostic characters (anterolingual and posterolingual cingular cusps). Nor was it was never made clear which of the four

specimens of *Sivatitanops cotteri* was intended to be the holotype of that species. The P3 (?) (GSI C332) is here considered the lectotype of *S. cotteri*. That specimen also has prominent anterolingual and posterolingual cingular cusps. Therefore, *S. cotteri* is a junior synonym of *S. birmanicum*. The remaining specimens that have been referred to *S. birmanicum* and *S. cotteri* lack these diagnostic features and cannot be certainly referred to *S. birmanicum* or any other species.

In addition to the specimens discussed above, Pilgrim (1925) assigned a partial skull (GSI C329) as the cotype of *Sivatitanops birmanicum* (fig. 167). This specimen consists of an anterior portion of skull lacking the nasal processes and with poorly preserved teeth. Using this skull, Pilgrim (1925) distinguished *S. birmanicum* from *S. cotteri* with a broader molar, and a more prominent anterolingual cingular cusp. Differences in molar proportions were commonly used in the past to diagnose brontothere taxa but without recognizing that differential molar wear significantly affects the length/width proportions (see remarks under *Epimanteoceras formosus* for clarification). Pilgrim (1925) admitted that his assignment of this skull to *S. birmanicum* was arbitrary. Therefore, the identity of this skull as *S. birmanicum* is questionable.

Despite the uncertain identity of the skull (GSI C329), it is the best available brontothere specimen from the Pondaung Formation that might represent *Sivatitanops birmanicum* and an abbreviated description is given here, highlighting some of the more important characters noted by Pilgrim (1925). The dorsal surface of the cranium is broad and flat. The anterior rim of the posterior nares is located next to M3. The incisors are known only from roots, but they appear to form an arched tooth row. P1 is apparently absent and there is no diastema between C and P2. The crowns of the premolars are badly damaged. The molars have an anterolingual cingular cusp and central molar fossa. M3 has a small hypocone. The lack of a postcanine diastema is reminiscent of *Brachydiastematherium transylvanicum*, *Metatitan*, *Duchesneodus*, and *Megacerops*. However, the skulls of *Metatitan*, *Duchesneodus*, and *Megacerops* all differ from GSI C329. This leaves the possibility that *S. birmanicum* is a junior synonym of *Brachydiastematherium transylvanicum* (see below).

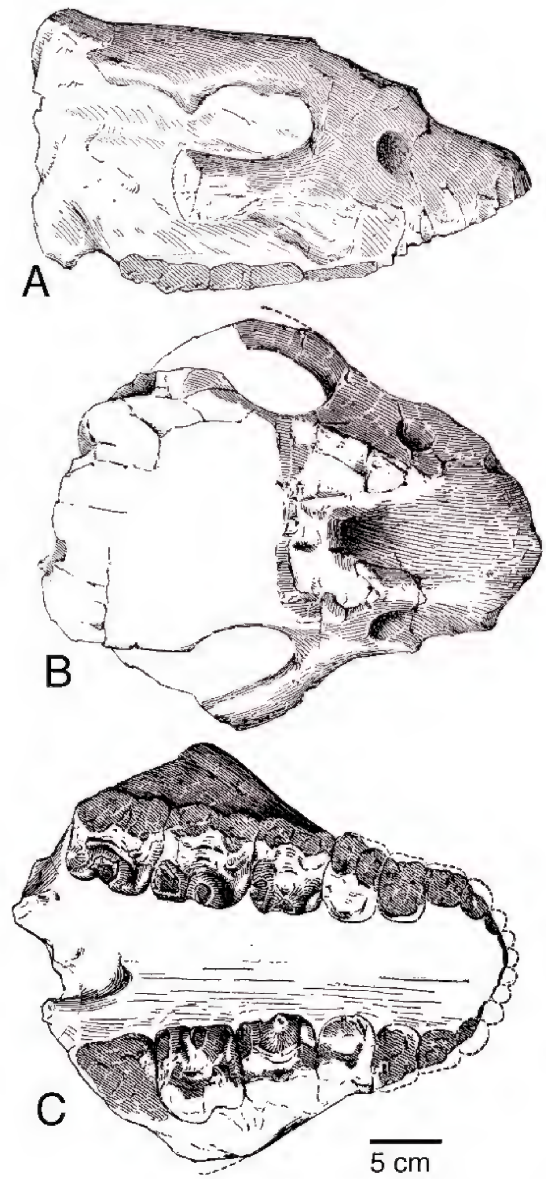

Fig. 167. A possible skull (GSI C329) of *Sivatitanops birmanicum*. **(A)** Right view, **(B)** dorsal view, **(C)** ventral view. Illustrations from Pilgrim (1925).

Colbert (1938) referred a large mandible (AMNH 20014) to *S. cotteri* (= *S. birmanicum*) although there is no evidence, other

than its general similarity in size, that this mandible is correctly identified. The mandible is massive and only the p4–m3 are completely preserved. The teeth are stereotypical in their morphology. The crown of the canine is missing, but its root is one of the largest canines of any known brontothere specimen.

Although the best brontothere material from the Pondaung Formation (skull and jaw) cannot be taxonomically identified with any certainty, several lines of evidence seem to link *Sivatitanops birmanicum* and European brontotheres. Mentioned earlier was the consistency of the skull (GSI C329) with what might be expected of the skull of *B. transylvanicum*. More compelling evidence comes from several brontothere teeth from upper Eocene strata near the Black Sea coast of Bulgaria that were described by Nikolov and Heissig (1985). This material includes two right P4s (AMNH cast 108191, AMNH cast 141258), a partial upper molar fragment, a lower left m2 (AMNH cast 141255), and a lower right p4 (AMNH cast 141257).

Nikolov and Heissig (1985) assigned these teeth to "*Menodus* (?)" *rumelicus*. The similarities of the premolars with those of *Sivatitanops* led Nikolov and Heissig (1985) to reassign "*Menodus* (?)" *rumelicus* to the genus "*Sivatitanops* (?)". Lucas and Schoch (1989a) were skeptical of the specific identification by Nikolov and Heissig (1985) due to the dubious nature of the taxon "*Menodus* (?)" *rumelicus*, whose holotype may actually be a fossil imported from North America (Osborn, 1929a; Lucas and Schoch, 1989a). The specimens described by Nikolov and Heissig (1985) are of interest not only because they are the second definite occurrence of brontotheres in Europe (second to the holotype mandible of *Brachydiastematherium transylvanicum*), but because they clearly resemble the southeast Asian species *Sivatitanops birmanicum* in the prominent anterolingual cingular cusp on the premolars and the posteriorly situated hypocones that are connected to the posterior cingulum. The p4 described by Nikolov and Heissig (1985) (fig. 166d) is similar in size to the p4 of the holotype jaw of *Brachydiastematherium transylvanicum*. However, the p4 of *Brachydiastematherium transylvanicum* has an unusual crest of enamel extending posteriorly from the middle of the cristid obliqua (fig. 98) that is not seen in the p4 pictured in fig. 176. This suggests that the *Sivatitanops*-like material from Europe described by Nikolov and Heissig may not be *Brachydiastematherium transylvanicum*, but a second European brontothere. At any rate, the available material is too incomplete to make a definitive conclusion regarding synonymy of *Brachydiastematherium* and *Sivatitanops*. Therefore, *Sivatitanops birmanicum* must be considered a nomen dubium.

"*Metatelmatherium* (?)" *lahirii* (Pilgrim, 1925)

LECTOTYPE: GSI C342, a right jugal-maxillary fragment with P4 and M1.

TYPE LOCALITY: Pondaung Formation, 1 mile east-southeast of Sinzwe village, Myanmar (Burma).

AGE: Middle Eocene (Sharamurunian land mammal "age").

DETERMINATION: Nomen dubium, possibly a synonym of *Sivatitanops birmanicum*.

REMARKS

Pilgrim (1925) named "*Eotitanotherium* (?)" *lahirii* from a few fragments including a right maxillary and jugal fragment with a heavily worn M1 and a very badly damaged P4 (GSI C 342) (fig. 168a), an ectoloph of an upper molar (GSI C341) (fig. 168c), and an upper left premolar (GSI C340) (fig. 168b). None of these was designated as the holotype, although Colbert (1938) selected GSI C342 as the lectotype and questionably reassigned this species to *Metatelmatherium*.

Pilgrim (1925) differentiated "*Metatelmatherium* (?)" *lahirii* from other Pondaung species that he had referred to *Sivatitanops* by the following features of the M1 of the lectotype specimen: the forward position of the protocone, the less pronounced anterior cingulum ridge, and the absence of a protoconule. Unfortunately, the P4 of the lectotype is too damaged to compare to other specimens. The apparent differences of the molars relate to the fact that the molar of GSI C432 is more heavily worn (including substantial interstitial wear) than molars that

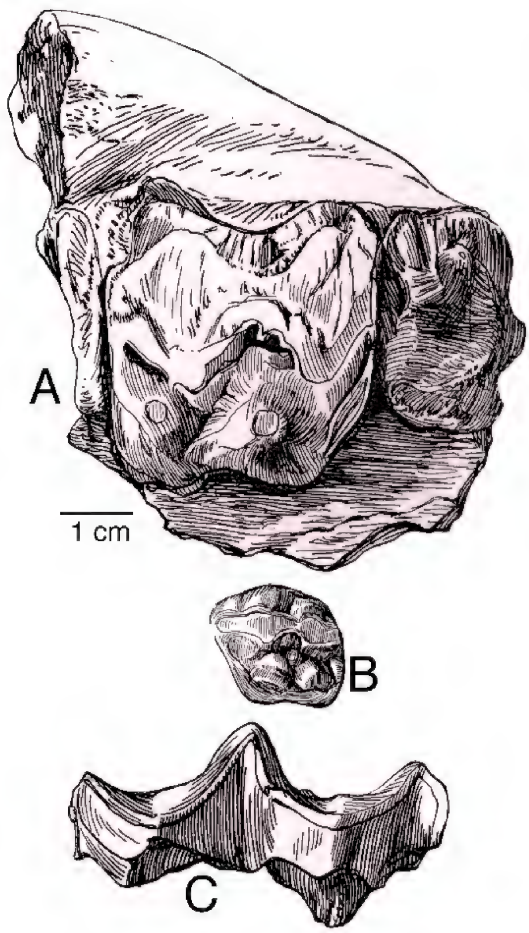

Fig. 168. Specimens previously referred to "*Metatelmatherium* (?)" *lahirii*. **(A)** GSI C 342, the lectotype, **(B)** GSI C340, and **(C)** GSI C341. All Illustrations from Pilgrim (1925).

were referred to *Sivatitanops* by Pilgrim (1925). The molar of GSI C342 is otherwise similar to those referred to *Sivatitanops* by Pilgrim (1925) with distinct central molar fossae, and a prominent anterolingual cingular cusp. These molar characters are typical of several brontothere species and the taxonomic identity of the lectotype of "*Metatelmatherium* (?)" *lahirii* (GSI C432) is uncertain, although "*Metatelmatherium* (?)" *lahirii* could be a synonym of *Sivatitanops birmanicum*.

The species name, *lahirii*, is undoubtedly invalid, due to the dubious identity of the lectotype specimen. However, an isolated premolar (GSI C340) that was originally

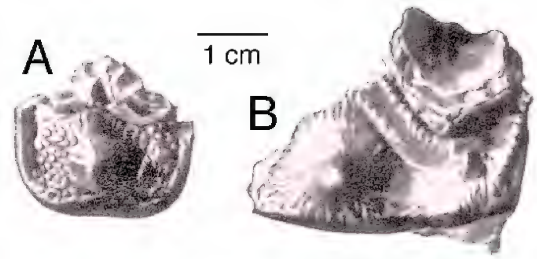

Fig. 169. The holotype of "*Sivatitanops* (?)" *rugosidens* (GSI C339). **(A)** Partial left upper premolar **(B)** partial left upper molar. All illustrations from Pilgrim (1925).

assigned to *lahirii* seems to represent a species of brontothere that is distinct from *Sivatitanops birmanicum* and "*Sivatitanops* (?)" *rugosidens*. This premolar is relatively advanced with two distinct and completely disconnected lingual cusps (protocone and hypocone). More notably, it does not exhibit the anterolingual cingular cusp that is well developed in *S. birmanicum*. This tooth is insufficient to pin down its true taxonomic identity, but the differences between this premolar and those of *S. birmanicum* and "*Sivatitanops* (?)" *rugosidens* seems to exceed the normal degree of intraspecific variation seen in the premolars of other brontothere species.

"*Sivatitanops* (?)" *rugosidens* Pilgrim, 1925

HOLOTYPE: GSI C339, a partial P4 and M1.

TYPE LOCALITY: Pondaung Formation, 1 mile east-southeast of Sinzwe village, Myanmar (Burma).

AGE: Middle Eocene (Sharamurunian land mammal "age").

DETERMINATION: Nomen dubium, holotype is best identified as cf. *Rhinotitan* sp.

REMARKS

Pilgrim (1925) based yet another species of Pondaung brontothere, "*Sivatitanops* (?)" *rugosidens*, on a lingual portion of a P4 (fig. 169a) and a lingual portion of a M1 (fig. 169b) that are reported to belong to the same individual (GSI C339). Colbert (1938) accepted this species but was of the opinion that the material was of little value. This

material is different from both *Sivatitanops birmanicum* and "*Metatelmatherium* (?)" *lahirii* and seems to represent yet another species of brontothere in the Pondaung Formation, possibly *Rhinotitan*.

The premolar is rectangular, has only a very tiny pinpoint of enamel that could be interpreted as a rudimentary hypocone, and it lacks anterolingual and posterolingual cingular cusps. Therefore, this premolar is inconsistent with *Sivatitanops birmanicum* as well as the premolar (GSI C340) that was referred by Pilgrim (1925) to "*Metatelmatherium* (?)" *lahirii* (see above). Pilgrim (1925) described the crowns of the teeth as low. Additionally, the area surrounded by the premolar protocone is rugose. Pilgrim's (1925) description and illustrations indicate specimens that compare well with *Rhinotitan*, particularly with the very low, small premolar protocone and the crenulated lingual premolar enamel. It is possible this specimen is *Rhinotitan*, although its specific identity (*R. kaiseni*, *R. andrewsi*, or another species) is uncertain. "*Sivatitanops* (?)" *rugosidens* is a nomen dubium, but its holotype is possibly a species of *Rhinotitan*.

Tanyorhinus harundivorax Cook, 1926

HOLOTYPE: DMNH 552, a partial left mandible with p3–m1.

TYPE LOCALITY: DMNH locality 225, Two bar Spring, 3/4 miles northeast, Moffat County, Colorado.

AGE: Middle Eocene (early Uintan land mammal "age").

DETERMINATION: Nomen dubium, holotype lacks diagnostic characters.

REMARKS

Cook (1926) erected a new species, *Tanyorhinus harundivorax*, from a partial mandible (DMNH 552) (fig. 170). The p3 lacks a metaconid and it has a nearly straight paralophid and metalophid. The p4 has a lingually arching paralophid and protolophid, and a large metaconid. These details are consistent with a number of Late Bridgerian and early Uintan brontotheres such as *Telmatherium validus*, *Sthenodectes incisivum*, *Wickia brevirhinus*, and *Sphenocoelus uintensis*. The teeth are somewhat more slender than those typical of *Sthenodectes incisivum* and are more similar to those of *Sphenocoelus uintensis* in their proportions. This specimen could belong to either *Sphenocoelus uintensis* or *Wickia brevirhinus*.

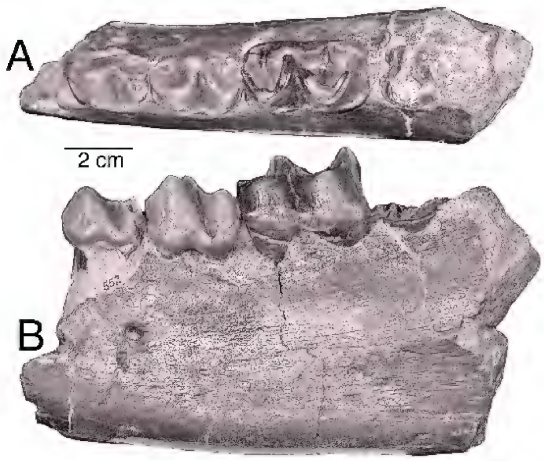

Fig. 170. Holotype of *Tanyorhinus harundivorax* (DMNH 552). **(A)** Dorsal view, **(B)** left view.

Manteoceras foris Cook, 1926

HOLOTYPE: DMNH 487, a partial mandible with right and left unerupted canines, dp2–dp4, m1, and m2 (erupting).

TYPE LOCALITY: DMNH locality 227, Two bar Spring, 1/4 mile north of Sand Wash Basin, Moffat County, Colorado.

AGE: Middle Eocene (early Uintan land mammal "age").

DETERMINATION: Nomen dubium, holotype is an unidentifiable juvenile specimen.

REMARKS

Manteoceras foris is based upon a partial juvenile mandible with deciduous premolars. However, Cook (1926) apparently did not realize that the premolars, which formed a part of his diagnosis, were deciduous teeth. Although the deciduous dentitions of a few brontotheres species have been documented, there are too few species with documented deciduous dentitions to confidently identify juvenile brontothere specimens to the species level or diagnose new species. The mandible, DMNH 487, could belong to a number of brontothere species of a similar geologic age.

Manteoceras pratensis Cook, 1926

HOLOTYPE: DMNH 489, a juvenile mandible with right and left adult incisors, c (unerupted), dp2–dp4, and right m1 (unerupted).

TYPE LOCALITY: DMNH locality 227, Two bar Spring, 1/4 mile north of Sand Wash Basin, Moffat County, Colorado.

AGE: Middle Eocene (early Uintan land mammal "age").

DETERMINATION: Nomen dubium, holotype is an unidentifiable juvenile specimen.

REMARKS

Manteoceras pratensis is based upon a partial juvenile mandible with deciduous premolars. Cook (1926) did not realize that the premolars, which formed a part of his diagnosis, were deciduous. The mandible, DMNH 489, could belong to a number of species of a similar geologic age.

Duchesneodus californicus (Stock, 1935)

HOLOTYPE: LACM/CIT 1398, a mandible fragment with left p3–m2, m3 (partial), and isolated dental elements, including a two incisors, canine, left p1, and p2.

TYPE LOCALITY: LACM/CIT locality 150 in the Brea Canyon Section of the Sespe Formation, north of Simi Valley, California.

AGE: Middle Eocene (Duchesnean land mammal "age").

REFERRED SPECIMENS: **(From LACM/CIT locality 150 in the Brea Canyon Section of the Sespe Formation, north of Simi Valley, California)** LACM/CIT 973, a left maxilla fragment with P1–P3; LACM/CIT 974–975, isolated teeth; LACM/CIT 1004, a left maxilla fragment with M2–M3; LACM/CIT 1005–1030 isolated cheek teeth; LACM/CIT 1078–1098, canines and isolated cheek teeth; LACM/CIT 1110–1118, isolated cheek teeth; LACM/CIT 1119, a mandible fragment with right p3–p4; LACM/CIT 1120, a partial mandible with right c, left c, and p2–p4; LACM/CIT 1126, a partial mandible with right c–m2 and left p3; LACM/CIT 1127–1129, isolated teeth; LACM/CIT 1132, a right P1; LACM/CIT 1135–1136, isolated teeth; LACM/CIT 1136, canine; LACM/CIT 1387–1389, partial mandibles with cheek teeth; LACM/CIT 1831–1833, isolated teeth; LACM/CIT 1834, a right maxilla fragment with C–P2; LACM/CIT 1835–1836, isolated teeth; LACM/CIT 4793–4794, partial mandibles and isolated teeth; LACM/CIT 53109–53214, isolated teeth and partial mandible fragments with teeth.

DETERMINATION: Nomen dubium, possibly a synonym of either *Protitanops curryi* or *Notiotitanops mississippiensis*.

DESCRIPTION

The holotype of *D. californicus* (LACM/CIT 1398) is an unremarkable specimen, consisting of a mandible fragment with a complete but heavily worn cheek-tooth row, several isolated small globular incisors, and a small isolated canine. The many other specimens found from the same locality are referred to this species based on the assumption of a monospecific assemblage. They are all a consistent size and do not suggest radically conflicting morphologies beyond the normal variability found in other brontothere species (e.g., variable lingual premolar morphology).

The incisors of these specimens are consistently small and globular (upper) or small and semiwedge-shaped (lowers). All of the numerous canines are small. A maxilla fragment LACM/CIT 1834 indicates a very short postcanine diastema (fig. 171a, d). The P1 is complex, with a distinct paracone, a similarly sized metacone, and a small lingual heel with a small lophlike protocone. The P2–P4 are relatively advanced with two distinct lingual cusps, a protocone and hypocone. The variation seen in the lingual premolars is similar to that seen in other species. The hypocone varies from being strongly connected from the protocone by a lingual crest (e.g., LACM/CIT 1013: fig. 171b) to being completely separated without a lingual crest (LACM/CIT 1115: fig. 171c). The P2s tend to have strong preprotocrista, while weaker preprotocrista are discernable on the P3s and P4s. Distinct anterolingual cingular cusps occur frequently on the upper premolars and can be seen on the maxilla fragment (LACM/CIT 1834), but they are occasionally absent in other specimens. Finally, the molars are like those of most other advanced

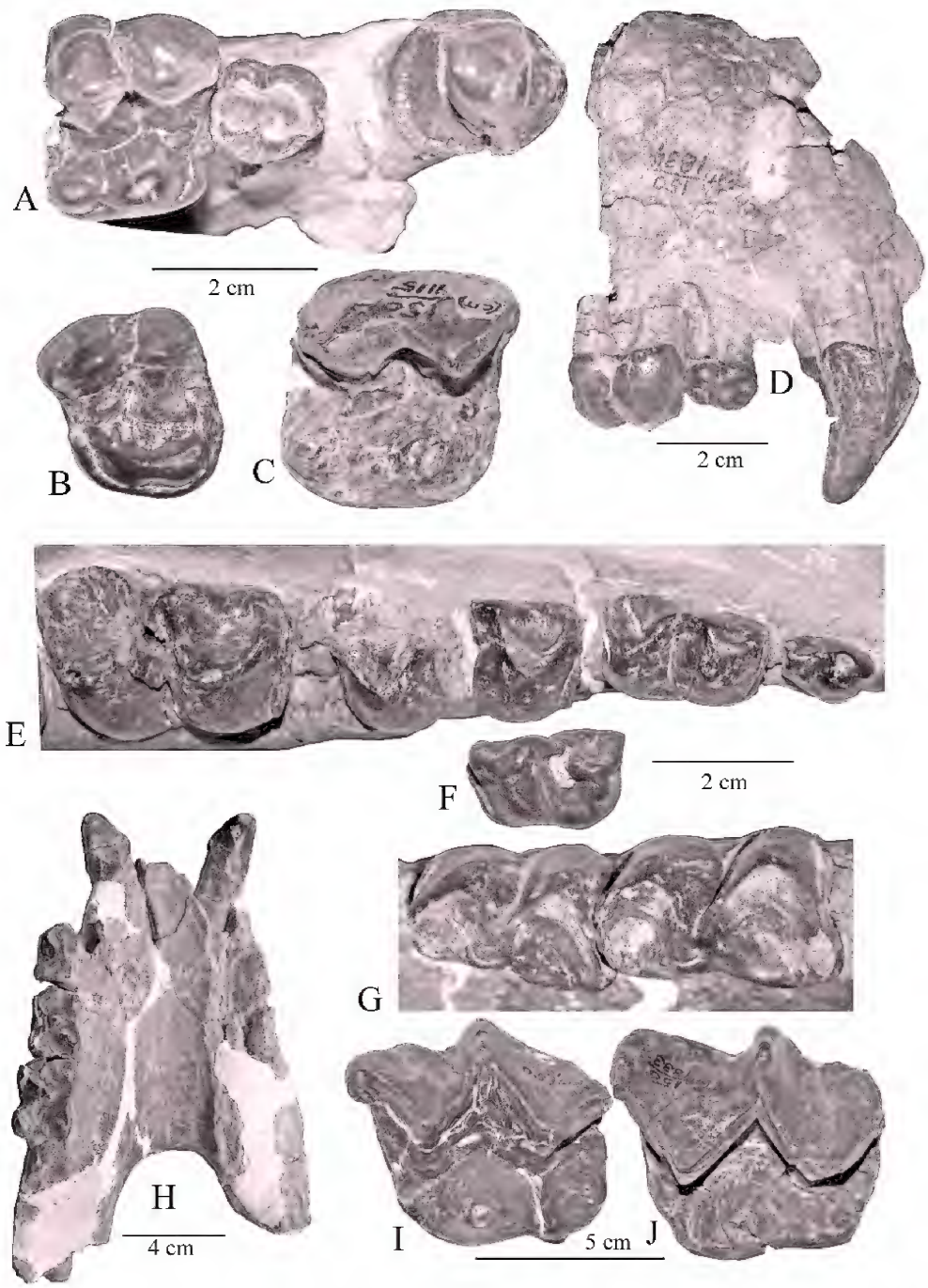

Fig. 171. Specimens referred to *Duchesneodus californicus*. **(A)** Ventral view of LACM/CIT 1834 with right C, P1, and P2, **(B)** occlusal view of left premolar (LACM/CIT 1013), **(C)** occlusal view of right premolar (LACM/CIT 1115, **(D)** right view of LACM/CIT 1834, **(E)** right p1–p4 (LACM/CIT 1126), **(F)** left p2 (LACM/CIT 1005), **(G)** right p3, p4 (LACM/CIT 1119), **(H)**, dorsal view of partial mandible (LACM/CIT 1120), **(I)** left M2 (LACM/CIT 1009), **(I)** left M3 (LACM/CIT 1832).

brontotheres with well-developed labial shearing facets, distinct anterolingual cingular cusps, and central molar fossae (fig. 171i, j). The size of the M3 hypocone varies radically, but it is always smaller than the M2 hypocone.

A partial mandible, LACM/CIT 1120, indicates a very short incisor row positioned between the anterior margins of the canines (fig. 171h). The incisors of that specimen are not preserved, although the remaining alveoli suggest only two pairs of incisors. The symphysis extends roughly to the posterior margin of p4 or slightly past it. Close-ups of the lower premolars of LACM/CIT 1126, 1005, and 1119 are shown (fig. 171e–g). The p1 is small with a relatively broad talonid heel. The trigonids of the p2s tend to be nearly twice as long as the talonids. The p2 has a slightly lingually arched paralophid, a straight protolophid, a well-developed cristid obliqua, and hypolophid, and it lacks a distinct metaconid. The p3 are p4 are more nearly molariform with lingually arching paralophids and protolophids, broader talonids, and large, lingually positioned metaconids. The lower molars are typical with thin lingual enamel, weak labial ribs, and an elongate m3.

Remarks

A large number of specimens consisting mostly of isolated teeth, and partial maxilla and mandible fragments were recovered from the Sespe Formation of southern California. Stock (1935) originally assigned this species to the genus *Teleodus*. However, upon concluding that *Teleodus* was an invalid genus, Lucas and Schoch (1982) reassigned this species to *Duchesneodus*. Subsequently, Lucas and Schoch (1989b) considered *D. californicus* a junior synonym of *Duchesneodus uintensis*. However, upon examining the fossil material, I have found it to be inconsistent with *Duchesneodus uintensis* in several ways. There is a short upper postcanine diastema, whereas in skulls of *D. uintensis*, a postcanine diastema is absent. The p2 trigonid is much longer than the talonid; in mandibles of *D. uintensis*, the p2 trigonid is only slightly longer than the talonid. Finally, there appears to have been only two lower incisors, whereas *D. uintensis* has three. It is always possible that a third incisor was present on LACM/CIT 1120 (fig. 171h), but fell out during life, and the alveolus reabsorbed. Nonetheless, the first two differences more compellingly argue against synonymy of *D. californicus* with *D. uintensis*. These characters also rule out *Megacerops* (sensu Mihlbachler et al., 2004b) and *Dianotitan lunanensis*.

Other species to which *Duchesneodus californicus* should be compared are *Eubrontotherium clarnoensis*, *Protitanops curryi*, and *Notiotitanops mississippiensis*. Like *D. californicus*, these species retain an upper postcanine diastema. *E. clarnoensis* lacks a p3 metaconid and has three lower incisors; it is not a potential synonym of *D. californicus*. The lower dentitions of *Protitanops* and *Notiotitanops* are not known. However, their upper dentitions are consistent with *D. californicus* except that the holotypes of these species lack distinct anterolingual cingular cusps on the premolars. Such cusps occur frequently on the upper premolars of *D. californicus*, but they are not present on every specimen. Considering that *Protitanops curryi* and *Notiotitanops mississippiensis* are each known only from a single specimen, this seemingly intraspecifically variable character cannot be used to validate *Duchesneodus californicus*.

To summarize, *Duchesneodus californicus* is not synonymous with *D. uintensis* (contra Lucas and Schoch, 1989b). However, the brontothere material referred to *D. californicus* is simply too fragmentary to conclusively diagnose it as a distinct species or to adequately compare it to the holotypes of *Protitanops curryi* or *Notiotitanops mississippiensis*, although it is possible that either of these species is synonymous with *D. californicus*. Therefore, *Duchesneodus californicus* is a nomen dubium.

"*Metatelmatherium* (?)" *browni* Colbert, 1938

Holotype: AMNH 20008, a left upper molar, probably a M3.

Type Locality: Pondaung Formation, two miles northeast of Gyat, Myanmar (Burma).

Age: Middle Eocene (Sharamurunian land mammal "age").

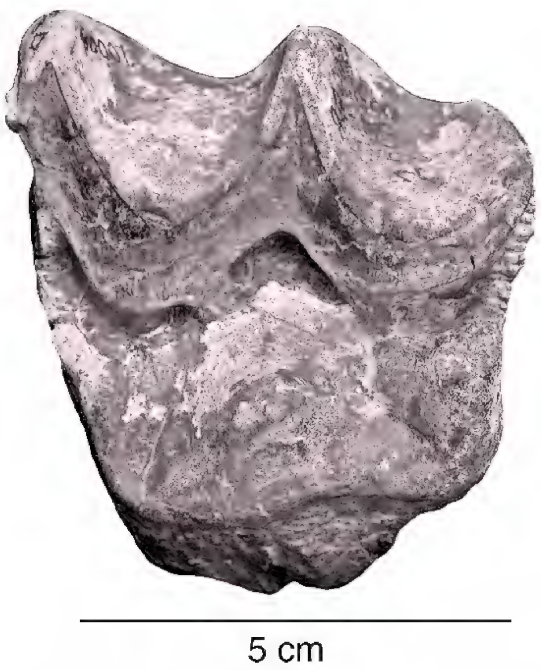

Fig. 172. The holotype upper left molar of "*Metatelmatherium* (?)" *browni* (AMNH 20008).

DETERMINATION: Nomen dubium, possibly a synonym of *Sivatitanops birmanicum*.

REMARKS

Colbert (1938) based "*Metatelmatherium* (?)" *browni* on a complete left upper molar that is probably an M3 (fig. 172). Colbert felt that this tooth was conspecific with a molar fragment (GSI C341) that had been referred to "*Metatelmatherium* (?)" *lahirii* (another nomen dubium) by Pilgrim (1925), but also felt that these specimens represented a species that was distinct from other specimens that had been referred to "*Metatelmatherium* (?)" *lahirii* by Pilgrim (1925). However, Colbert (1938) gave no reasons for these opinions.

Colbert (1938) found AMNH 20008 to be comparable to *Metatelmatherium* and listed similarities and differences of the M3s of *Metatelmatherium cristatum* (= *ultimum*) and AMNH 20008. He found AMNH 20008 comparable to *M. cristatum* (= *ultimum*) in crown height, absence of an external cingulum, and a slight ridge on the ectoloph of the paracone (probably meaning a labial paracone rib). All of the specimens used in the comparison given by Colbert (1938) are worn teeth, thus comparison of the crown height of these specimens in essentially meaningless. At any rate, crown height is not a diagnostic character of *Metatelmatherium*. The presence and thickness of external cingulum is variable among most brontothere species, and a paracone rib is common to nearly all brontothere species. Moreover, the deep central molar fossa and prominent anterolingual cingular cusp of AMNH 20008 indicate that this tooth is not *Metatelmatherium*, but that of a more derived brontothere.

Additionally, Colbert (1938) compared AMNH 20008 to another molar (GSI C330, an M1 or M2) that Pilgrim (1925) had referred to *Sivatitanops cotteri* (= *S. birmanicum*). AMNH 26008 was distinguished from that specimen by its "greater breadth index, and entirely different expression of its ectoloph, protocone and hypocone" (Colbert, 1938: 305). The meaning of "entirely different expression of ectoloph, protocone and hypocone" is unclear, but the primary differences between these molars can be attributed to the fact that AMNH 20008 is an M3 while the other is an M1 or M2. The former molar is more heavily worn, thus affecting the appearance of the ectoloph. Moreover, since the teeth are different elements their proportions are not directly comparable.

All of the upper brontothere molars from the Pondaung Formation that have been attributed to *Sivatitanops* or *Metatelmatherium* share deep central molar fossae and large anterolingual cingular cusps. Many brontotheres have similar molars; therefore, none of these isolated molars can be specifically identified. The shape of the hypocone of AMNH 20008 is peculiar; it is compressed against the distal cingulum. In this respect, it is similar the distolingual cingular cusp seen in the premolars of *Sivatitanops birmanicum*. It is possible that "*Metatelmatherium* (?)" *browni* is a junior synonym of *S. birmanicum*, but at this time "*Metatelmatherium* (?)" *browni* can considered only a nomen dubium.

Additionally, Colbert (1938) referred two partial mandibles to "*Metatelmatherium* (?)" *browni* (AMNH 20016, 20022). One of these (AMNH 20022) is a juvenile that contains a set of unerupted adult incisors, whose crowns

are large, conular, with rounded tips and thick lingual cingulids. Tsubamoto et al. (2000) referred additional mandible fragments to "*Metatelmatherium* (?)" *browni*. However, there is no conclusive evidence as to what species of Pondaung brontothere these elements belong.

Protitanotherium koreanicum Takai, 1939

HOLOTYPE: UMUT CV6034; a partial right maxilla with P2–P3 originally deposited at the Palaeontological Laboratory, Waseda University, Tokyo. Bombing during World War II destroyed the holotype, although a photograph of it can be seen in Takai (1939: pl. 1, fig. 6 and is reproduced here as fig. 173n).

AGE: Middle or late Eocene (Russell and Zhai, 1987).

TYPE LOCALITY: Hôsan Coal Field in the central part of Kôdai-dô, Northwest Tyôsen, (Korea).

REFERRED SPECIMENS: **(From the same locality as the holotype; see Takai [1939] for a complete list)** Takai (1939) referred numerous specimens to *Protitanotherium koreanicum*. Takai (1939) provided no specimen numbers, although 20 of the specimens were published as photographs by Takai (1939) have been given numbers in the UMUT collection. Table 12 matches the UMUT numbers with the figures in Takai (1939).

DETERMINATION: Nomen dubium. The holotype and referred material are too fragmentary to adequately compare to other species. The referred material might represent more than one species.

DESCRIPTION

The material referred to *Protitanotherium koreanicum* consists of a maxillary fragment and isolated teeth. The more diagnostically useful of these specimens are pictured in figure 173; additional specimens are figured in Takai (1939). UMUT CV29046 (fig. 173a, b) is an upper incisor, probably an I2. It is rather small with a subconical crown and a thick lingual cingulum, very similar to that of *Protitanotherium emarginatum* or *Diplacodon elatus*. There are two distinctly sized canines; the larger is seen in fig. 173q. Takai (1939) interpreted the canine size variation as sexual dimorphism. The P2 ectoloph of the holotype (UMUT CV6034) has a lingually angled parastyle, but with a straight metastyle (fig. 173n). The labial rib of the paracone is more prominent than the labial metacone rib. There are no distinct lingual cusps, but rather a single crest formed by a prominent preprotocrista and lingual crest. A small swelling in the position of the protocone can be seen on another P2 (UMUT CV6035) (fig. 173p). The P3 of the holotype has a straighter parastyle and a prominent labial paracone rib, but it lacks a distinct labial metacone rib; its lingual surface is damaged. The P4 included with UMUT CV6028 (fig. 173e) is heavily worn with a damaged metacone. However, UMUT CV6038 (not shown) is a complete and unworn P4 that offers additional details. The P4 parastyle is strongly angled labially. The labial paracone rib is weak and the labial metacone rib is absent. A P4 mesostyle is lacking. There are two distinct lingual cusps, a protocone and a slightly smaller hypocone that is close to the protocone but does not appear to have been connected to it by a lingual crest. The P4 of UMUT CV6028 lacks any sign of a preprotocrista, although a very rudimentary preprotocrista can be seen on other P4s (UMUT CV6037 and CV6038). All available premolar specimens have a continuous lingual cingulum, but the labial cingula of these premolars are discontinuous, especially at the base of the paracone of the P4s.

UMUT CV6028 includes a complete upper molar row (fig. 173e). The specimen has been distorted in such a way that the M2 has been rotated, with the anterior side smashed against the posterior edge of the M1. The M1 is very heavily worn, although typical brontotheriine apomorphies are evident in the more moderately worn M2 and M3, including strongly lingually angled ectolophs, a very weak labial rib on the paracone (visible on M1 only), no labial ribs on the metacones, thin lingual ectoloph enamel, and wedge-shaped lingual margins of the paracone and metacone. A shallow central molar fossa is evident on M2. A small triangulate anterolingual cingular cusp bearing a distinct wear facet can be seen on M3. There are no traces of paraconules or metalophs. The M3

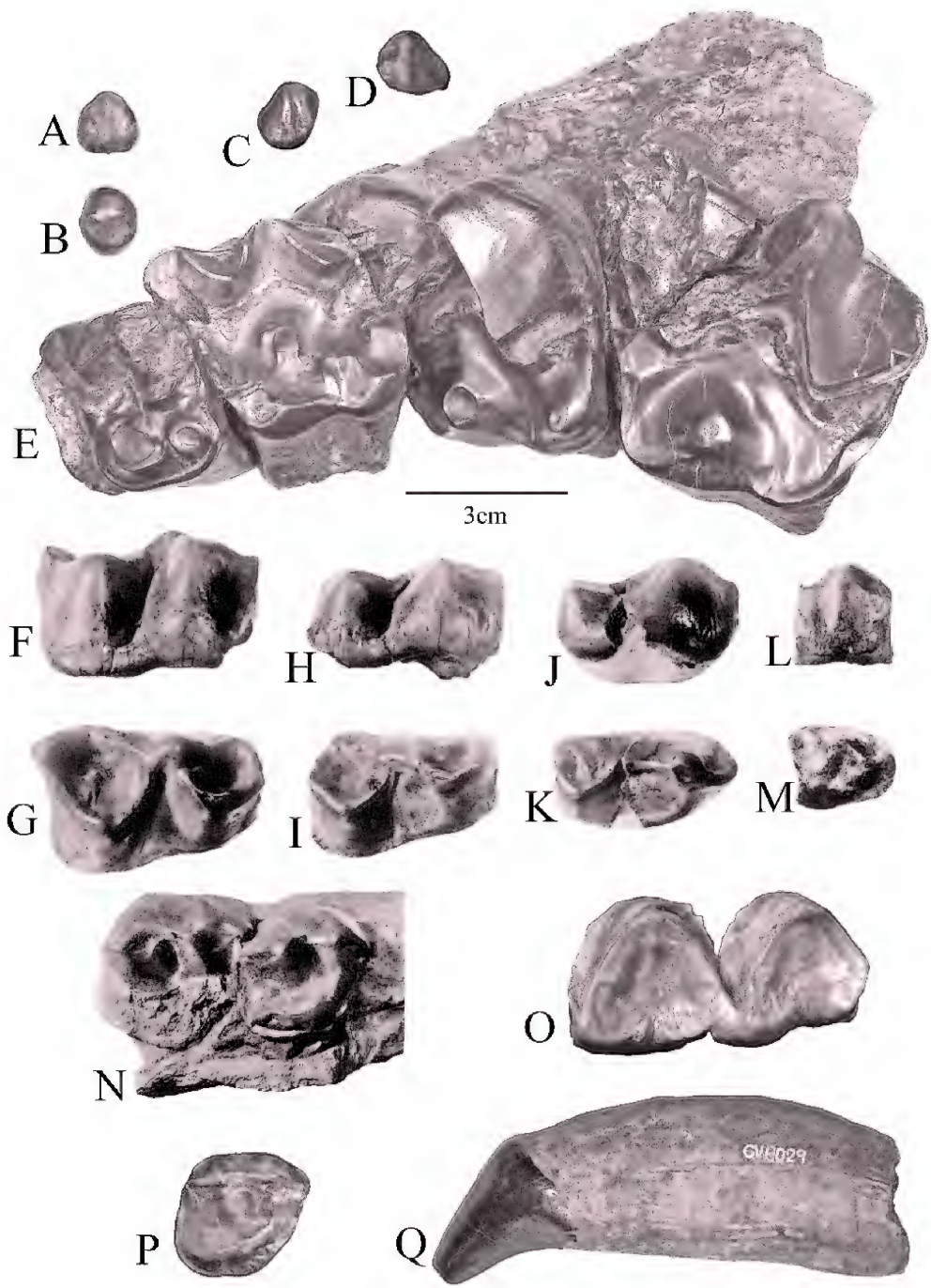

Fig. 173. Specimens previously referred to *Protitanotherium koreanicum*. **(A–B)** Labial and occlusal views of an upper incisor (UMUT CV29046), **(C–D)** labial and lingual views of right i3 (UMUT CV29047), **(E)** occlusal view of P4–M3 (UMUT CV6028), **(F–M)** labial and occlusal views of p1–p4 (UMUT CV 6040–6043), **(N)** occlusal view of right P2–P3 (UMUT CV6034), the holotype, **(O)** occlusal view of right lower molar (UMUT CV6047), **(P)** occlusal view of right P2 (UMUT CV6035), **(Q)** side view of canine (UMUT CV6029). F–N are lost specimens, with photos of them reproduced from Takai (1939).

TABLE 12
Specimens referred to *Protitanotherium koreanicum*, along with present UMUT catalog numbers and matching figure references in Takai (1939)

UMUT CV#	Takai (1939)	Element
6028	fig. 1,2; pl. 2	left maxilla fragment with P4–M3
6029	pl. 1: fig. 1	canine
6030*	pl. 1: fig. 2	canine
6031*	pl. 1: fig. 3	left DP3 (partial)
6032*	pl. 1: fig. 4	left DP4
6033	pl. 1: fig. 5	right dp4
6034* (holotype)	pl. 1: fig. 6	right maxilla fragment with P2, P3 (partial)
6035	pl. 1: fig. 7	right P2
6036*	pl. 1: fig. 8	left P2
6037*	pl. 1: fig. 9	left P3 (partial)
6038*	pl. 1: fig. 10	left P4
6039	pl. 1: fig. 11	right P4 (partial)
6040*	pl. 3: fig. 1	right p1 (partial)
6041*	pl. 3: fig. 2	right p2
6042*	pl. 3: fig. 3	right p3
6043*	pl. 3: fig. 4	right p4
6044*	pl. 3: fig. 5	left p4
6045*	pl. 3: fig. 6	left p4
6046*	pl. 3: fig. 7	left m2
6047	pl. 3: fig. 8	left m3 (partial)
29047	Not mentioned	left i3
29046	Not mentioned	upper incisor
29048	Not mentioned	left p1 (partial)

*indicates specimen is lost or destroyed.

lacks a hypocone, although the distolingual corner of the crown forms a small peak that bears a distinct wear facet. Lingual molar cingula are discontinuous and faint to absent. Labial molar cingula are thin, beaded, and discontinuous around the mesostyle and parastyle.

The lower dental elements include an i3 (fig. 173c, d), numerous premolars (fig. 173f–m), and a few isolated molars and molar fragments (fig. 173o). The i3 (UMUT CV29047) is small with a mesiodistally elongate crown; it closely resembles those of *Protitanotherium emarginatum* and *Diplacodon elatus*. Typically in brontotheres the lower premolars are progressively more molarized posteriorly, so that p1 is the least molarized and p4 most molarized. However, the p1 (UMUT CV6040) is unusual in its degree of molarization and out of step with this typical sequence. (These teeth may represent more than one species; see below). The trigonid consists of a short, somewhat lingually angled paralophid that creates a small lingual trigonid notch. The protolophid is angled about 45° posterolingually. The talonid is broad with a prominent cristid obliqua and long hypolophid, forming a broad talonid basin. The p2 (UMUT CV6041) is significantly less molarized than the p1; the trigonid is elongate and lacks a significant lingual notch, and neither the paralophid nor the protolophid are angled lingually. The talonid is the same width as the trigonid with a more poorly developed cristid obliqua and hypolophid. The lingual side of the talonid forms a slightly concave sloped surface, but a basin has not developed. The p2 lacks a metaconid. There is progressively more molarization in p3 (UMUT CV6042) and p4 (UMUT CV6041) than in p2, which represents the typical pattern. The trigonid of p3 is longer than the talonid, while the p4 trigonid is shorter than the talonid. The paralophid and protolophid of p3 are angled slightly

lingually, creating a shallow lingual notch. The paralophid and protolophid of p4 curve strongly lingually, creating a molariform trigonid basin. The p3 lacks a metaconid, while p4 has a large, lingually positioned metaconid. The talonids of p3 and p4 are broader than their trigonids. The p3 talonid has a shallow basin; that of p4 is nearly molariform. Lingual premolar cingulids are absent, while labial premolar cingulids are very weak. The molars are typical: elongate with thin lingual enamel, weak lingual ribs, and shallow talonid basins.

Remarks

Takai (1939) reported specimens of *Protitanotherium koreanicum* from four collections: (1) the Palaeontological laboratory of Waseda University, Tokyo, (2) the museum of the Geological Survey of the Government-General of Tyôsen (Korea), (3) the museum of the Geological Institute, Kyoto Imperial University, and (4) from the private collection of Tosisaburô Hodosima. Takai (1939) provided photographs of 20 specimens from the Waseda University, Kyoto University, and T. Hodosima collections. Takai (1939) gave no numbers; however, all 20 are now assigned numbers in the UMUT collection (table 12). These numbers include specimens originally from the Waseda University and Kyoto University collections that are now lost, as well as material from the T. Hodosima collection that has mostly survived. Most unfortunately, the specimens in the Waseda collection, which included the holotype specimen (UMUT CV6034) and what was described by Takai (1939) as "innumerable teeth, both complete and incomplete" were destroyed during World War II (Hiromichi Hirano of Waseda University, personal commun., 2005). Fortunately, Takai (1939) provided quality photographs of these specimens. The surviving material in the UMUT collection includes some of the best specimens, such as the maxilla fragment with P4–M3 (UMUT CV6028). Additionally, I encountered three more unidentified specimens in the UMUT collection from the same locality that were not mentioned or figured by Takai (1939).

None of the available material is sufficient to fully diagnose a distinct species; therefore, *Protitanotherium koreanicum* is a nomen dubium. And while the fossil material referred to *Protitanotherium koreanicum* may represent multiple species, the taxonomic identity of at least some of the material can be narrowed down considerably. Takai's (1939) referral of *Protitanotherium koreanicum* to the genus *Protitanotherium* follows Osborn's (1923, 1925, 1929a) practice of lumping several large Asian horned brontotheres into *Protitanotherium*. These species were eventually split into separate genera, such as *Protitan* and *Rhinotitan*, by Granger and Gregory (1943), although they did not consider *P. koreanicum* in their revision. At the species level, Takai (1939) considered *Protitanotherium koreanicum* to be most similar to *Protitan grangeri*, although examination of the material leads me to disagree. The relatively advanced upper premolars rule out all brontotheres that lack premolar hypocones or only occasionally have poorly developed premolar hypocones. Among those ruled out are *Protitanotherium emarginatum* and all species of *Protitan* and *Rhinotitan*. The upper premolars and molars are most consistent with a number of brontotheres. However, among those species with two lingual premolar cusps, only *Diplacodon elatus* has incisors that are like those associated with *Protitanotherium koreanicum*, although a comparison of incisors cannot be made with *Pachytitan ajax*, another brontothere very similar to *Diplacodon*.

The upper dentition seems to represent a species similar to *Diplacodon elatus* or *Pachytitan ajax*. The lowers of *P. koreanicum* strongly contrast with *Diplacodon*. Most notably, p3 lacks a distinct metaconid. More perplexingly, the p1 referred to *Protitanotherium koreanicum* is disproportionately molarized with respect to the other premolars. Only specimens of *Megacerops coloradensis* from the late Eocene White River deposits of North America are known to have a similarly molarized p1. Unfortunately, the lower dentition of *Pachytitan* is unknown, so a comparison cannot be made with that species.

To summarize, the upper dental material assigned to *Protitanotherium koreanicum* is

consistent with *Diplacodon elatus* and *Pachytitan ajax*. The lower dental material, excluding p1, is inconsistent with *Diplacodon elatus*, but a comparison with the lower dentition of *Pachytitan ajax* is not yet possible. Because of the possible synonymy of *Protitanotherium koreanicum* and *Pachytitan ajax*, *P. koreanicum* must be considered a nomen dubium. Nonetheless, the material is of great biogeographic significance; most of the specimens originally attributed to *P. koreanicum* seem to document a *Diplacodon*- or *Pachytitan*-like brontothere in Korea. A middle Eocene age for the Hôsan Coal Field is also supported by this conclusion. The anomalously molarized p1 (UMUT CV6040) is distinctly out of character with the other lower premolars attributed to this species, and could represent a second species, perhaps similar to *Dianotitan* or *Megacerops*.

Metatelmatherium parvum Granger and Gregory, 1943

HOLOTYPE: AMNH 20168, a left mandible fragment with p3–p4.

TYPE LOCALITY: Irdin Manha Formation, Inner Mongolia, China.

AGE: Middle Eocene (Irdinmanhan land mammal "age").

DETERMINATION: Nomen dubium, holotype lacks diagnostic characters.

REMARKS

The type of *Metatelmatherium parvum* is a mandible fragment with only two teeth (p3–p4) (AMNH 20168) that do not exhibit a diagnostic set of characters (fig. 174). In size, it is most similar to *Metatelmatherium ultimum*, but it has a more lingually oriented paralophid than the one available Asian specimen of *M. ultimum* (AMNH 26411). In this respect, the specimen more closely resembles *Protitan grangeri*, although the specimen seems somewhat smaller than fossils that belong to that species.

Hyotitan thomsoni Granger and Gregory, 1943

HOLOTYPE: AMNH 26401, a nearly complete mandible in two pieces with right i2–c, p–m3, and left i1–m3.

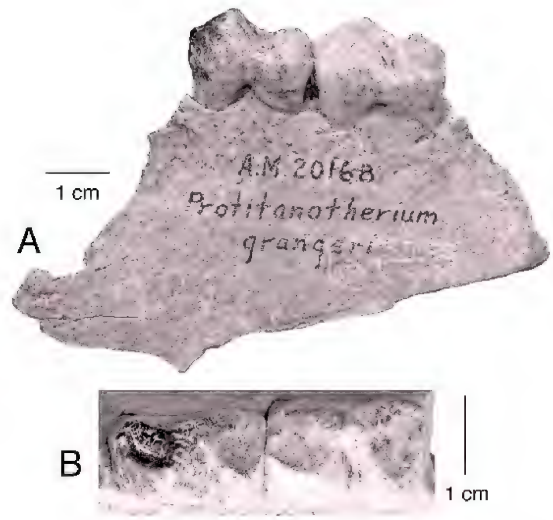

Fig. 174. The holotype of *Metatelmatherium parvum* (AMNH 20168). **(A)** Lateral view of left ramus, **(B)** p3–p4.

TYPE LOCALITY: Camp Margetts, "Houldjin" Formation, Inner Mongolia.

AGE: Middle Eocene (Irdinmanhan land mammal "age").

DETERMINATION: Nomen dubium. This species could be synonymous with *Qufutitan zhoui*.

DESCRIPTION

The holotype of *Hyotitan thomsoni* consists of a nearly complete and very large mandible (fig. 175) with only a few missing teeth. The symphysis is unusually long and narrow with a long postcanine diastema. The ventral margin of the symphysis is angled about 45°. The symphysis extends about to the midpoint of p3.

The incisor row is slightly arched anteriorly. The incisors are all similar in size. Overall, they are small and nearly featureless; however, this is partly an artifact of heavy wear.

The worn crowns show evidence of having had a semiglobular or subcaniniform shape. Traces of lingual cingulids are still apparent on the incisors, but there is no evidence of a labial incisor cingulid.

Two of the most distinctive features of *Hyotitan* are the very large canines and the relatively elongate postcanine diastema. The

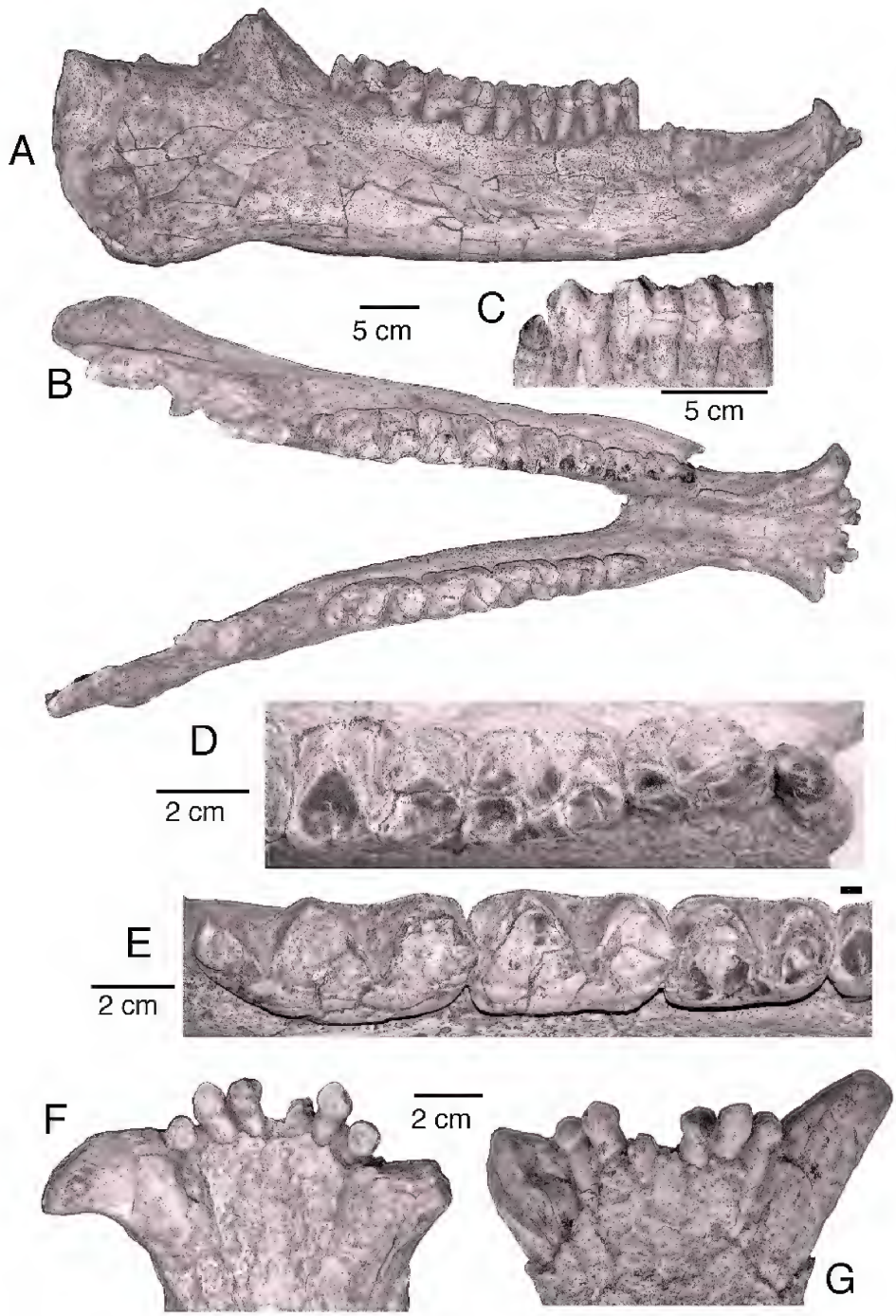

Fig. 175. Holotype of *Hyotitan thomsoni* (AMNH 26401). **(A)** Right view, **(B)** dorsal view, **(C)** lateral (labial) view of left premolars, **(D)** left premolars, **(E)** left molars, **(F)** lingual view of incisors and canines, **(G)** labial view of incisors and canines.

tusklike canines are heavily worn, but they are clearly much larger than other brontotheres of similar body size. The postcanine diastema (76 mm) is more than double the length of p2.

The premolar crowns are broad and tall and closely resemble those of "*Protitan*?" *cingulatus*. The crown of p1 sits well below the crown of p2 and consists of a single large cusp and a very short cusplike talonid heel. The trigonid of p2 is longer than the talonid, but on p3 and p4, the trigonids and talonids are of similar length. The trigonid and talonid of p2 are nearly equal in width, while the trigonids of p3 and p4 are narrower than the talonids. The paralophid of p2 arches only slightly lingually forming a minor lingual notch in the trigonid. The p2 protolophid is straight and angled slightly lingually. The p2 lacks a discernable metaconid. On the p3, the paralophid is angled somewhat more lingually and the p3 protolophid extends distolingually from the protoconid, forming a broad lingual notch in the trigonid. A distinct p3 metaconid is present at the junction of the protolophid. On p4, the paralophid and protolophid are arched strongly lingually, forming a nearly molariform trigonid basin. A large p4 metaconid is positioned mostly lingually from the protoconid. The talonid basin of p2 is small with a short cristid obliqua and hypolophid, creating a small talonid basin. The cristids obliqua and hypolophids of p3 and p4 are longer and create increasingly broader talonid basins.

The lower molars of *Hyotitan thomsoni* are relatively broad with shallow trigonid and talonid basins and very weak molar ribs. The m3 is among the shortest among brontotheres. Its length/width proportions resemble *Desmatotitan tukhumensis*. However, the hypoconulid of m3 is remarkably narrow. Finally, there is a strong labial cingulid on all cheek teeth posterior to p1.

Remarks

Granger and Gregory (1943) based *Hyotitan thomsoni* on a very large mandible, AMNH 26401. It shows a unique combination of very large canines, small but not vestigial incisors, and a very long postcanine diastema with an elongate symphysis. The canines of the holotype of *H. thomsoni* are larger than any other similarly sized brontothere except for a partial mandible (AMNH 20014) described by Colbert (1938) from the Pondaung deposits of Myanmar that is possibly *Sivatitanops birmanicum*. However, the symphysis of that specimen is much shorter than that of *Hyotitan* and the m3 is more elongate. Other large brontotheres with relatively elongate symphyses include *Pollyosbornia altidens*, *Gnathotitan berkeyi*, and *Diplacodon elatus*. The p3 metaconid and wide, well-developed p2 talonid clearly distinguishes *Hyotitan thomsoni* from *Pollyosbornia altidens*. *Gnathotitan berkeyi* has a differently shaped mandible than *H. thomsoni* and has much larger incisors and a more elongate m3. Specimens of *Diplacodon elatus* are much smaller than *Hyotitan thomsoni*, the m3 is more elongate, and the posterior margin of the symphysis is more posterior. The premolars of *Hyotitan thomsoni* most closely resemble those of "*Protitan*?" *cingulatus*, particularly in relative dimensions, strong labial cingulid, anteroposteriorly compressed p1, and p3 metaconid. However, *Hyotitan thomsoni* is much larger than "*Protitan*?" *cingulatus*, has a more elongate symphysis, and lacks the labial incisor cingulids of that species.

Hyotitan thomsoni could be a synonym of *Qufutitan zhoui*, a species known only from a partial skull. Both are of similar size and they share a remarkable number of peculiar similarities that are discussed further with remarks with *Qufutitan zhoui*. *Hyotitan thomsoni* is therefore classified here as dubious. However, it should be noted that *H. thomsoni* Granger and Gregory, 1943, has priority over *Qufutitan zhoui* Wang and Wang, 1997. In this instance, I part from the rule of priority and accept *Q. zhoui* because its holotype retains much more character data. If one adheres to ICZN rules, *H. thomsoni* is valid whereas *Q. zhoui* is dubious.

"*Protitan*?" *cingulatus* Granger and Gregory (1943)

Holotype: AMNH 26412, a right mandibular ramus with P1–M3.

Type Locality: ?"Houldjin", 10 miles west of Camp Margetts, Inner Mongolia, China.

Fig. 176. Right view of the holotype of "*Protitan*?" *cingulatus* (AMNH 26412).

REFERRED SPECIMENS: **(From the "Houldjin" beds of Camp Margetts, Inner Mongolia)** AMNH 26403, a right mandibular ramus with p1–m3; **(from the Irdin Manha Formation, Inner Mongolia)** AMNH 20110, a complete mandible missing only the left i2.

AGE: Middle Eocene (Irdinmanhan land mammal "age").

DETERMINATION: Nomen dubium; it could be a synonym of *Epimanteoceras formosus*.

DESCRIPTION

In addition to the partial holotype jaw (AMNH 26412) (fig. 176) and another partial mandible from the ?"Houldjin" of Camp Margetts (AMNH 26403), there is a virtually complete mandible (AMNH 20110) with less heavily worn teeth from the Irdin Manha Formation (fig. 177). AMNH 20110 is slightly larger than the Camp Margetts "*Protitan*?" *cingulatus* material, but it has congruent cheektooth morphology. The following description is based primarily on AMNH 20110. The cheek teeth of the holotype are more worn that that of AMNH 20110, but they match the description given below, except where noted.

The horizontal ramus of AMNH 20110 is deep and not nearly as slender as that of *Protitan grangeri*. The coronoid process is moderately curved and extends higher than the condyle. The inferior margin of the symphysis is steep and strongly curved. The symphysis extends to the p3 talonid. The incisor row is narrow and forms a semicircular arch anterior to the canines. The incisors of AMNH 20110 are similar in size to those of *Protitan grangeri* and *Epimanteoceras formosus*. The incisors are all similar in size and the i2 is not enlarged. The crowns are more or less subcaniniform. The apex of the right i1 is worn off, but it appears to have been similar in shape to the i2. The crown of the right i2 is damaged. The left i2 crown is short and conical, with a bluntly rounded apex. The i3 is somewhat more pointed. The i3 is round and not as elongate as in *Protitan grangeri*. Each incisor has a distinct lingual cingulid. Additionally, there are distinct labial cingulids on each incisor. The canines of AMNH 20110 are rather small, are almost perfectly rounded in cross section, and they are erect. A precanine diastema is absent. The postcanine diastema is slightly longer than p2.

The premolars of "*Protitan*?" *cingulatus* are much taller, broader, and more molariform than those of *Protitan grangeri* and most closely resemble those of *Hyotitan thomsoni* in their general size, proportions,

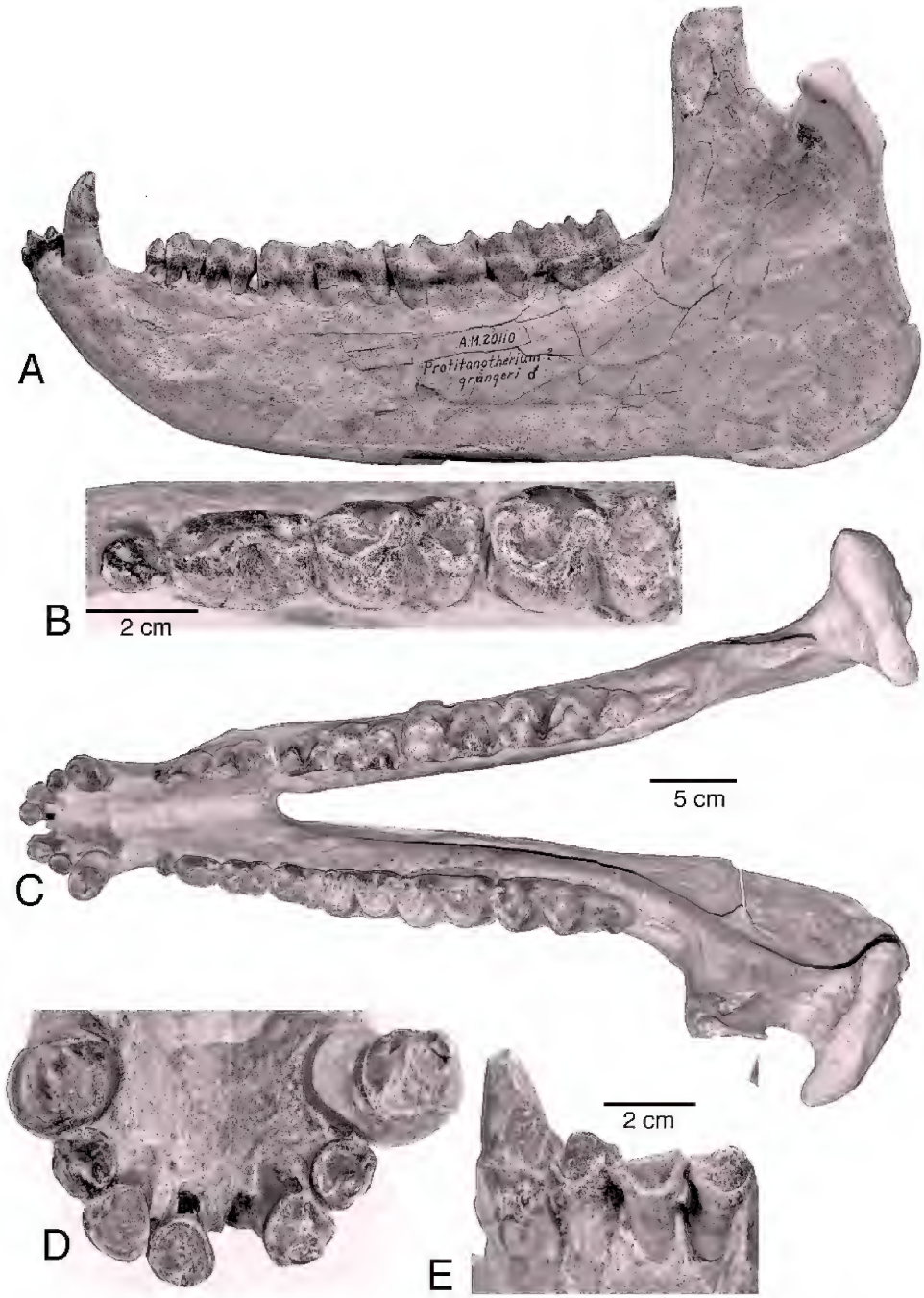

Fig. 177. A mandible referred to "*Protitan*?" *cingulatus* (AMNH 20110). **(A)** Left view, **(B)** left premolars, **(C)** dorsal view, **(D)** lingual view of incisors and canines, and **(E)** labial view of right incisors and canine.

and degree of development of labial cingulids. The p1 is very small with a single cusp and a shortened talonid heel. The trigonid of p2 is much longer than the talonid. The p3 and p4 trigonids are only slightly longer than their corresponding talonids. The trigonid and talonid of p2 are of similar width, while the p3 and p4 trigonids are slightly narrower than the talonids. The paralophid of p2 curves slightly lingually, creating a small lingual notch in the trigonid. The p2 protolophid is lingually positioned, but it is straight. The paralophid of p3 arches more strongly lingually and the protolophid arches fully lingually, creating a much broader lingual notch in the trigonid. The paralophid and protolophid of p4 arch fully lingually and form a molarlike trigonid basin. The p2 lacks a metaconid, but large, lingually positioned, and molariform metaconids are present on p3 and p4. The talonid of p2 includes a distinct but short cristid obliqua and a hypolophid that create a small lingual-talonid notch. The cristids obliqua and hypolophids of p3 and p4 are longer and form more nearly molariform basins. The angulations and lengths of the various lophids of the premolars of AMNH 26412 resemble those of AMNH 20110, but the metaconids are worn flat. Lingual premolar cingulids are absent, but the labial premolar cingulids of all *cingulatus* specimens are very strong. The labial premolar cingulids are somewhat stronger in AMNH 26412 and somewhat weaker on AMNH 20110.

The molars of "*Protitan*?" *cingulatus* are typical with relatively thin lingual enamel, shallow trigonid and talonid basins, and an elongate m3. There are no lingual cingulids, but like the premolars, the labial molar cingulids are very strong.

Remarks

Granger and Gregory (1943) erected a new species, "*Protitan*?" *cingulatus*, based on AMNH 26412. In the same paper they referred the same specimen to another species, *Protitan robustus* (considered, here, to be a junior synonym of *P. grangeri*). Presumably, AMNH 26412 was intended to serve as the holotype of "*Protitan*?" *cingulatus*, and the referral of AMNH 26412 to *P. robustus* is mostly likely an accident. Therefore I consider AMNH 26412 the holotype of "*Protitan*?" *cingulatus*. Granger and Gregory (1943) questionably referred this species to the genus *Protitan* and distinguished it from other species of *Protitan* by the heavy external cingulids on p2–m3. Although no other specimens were referred to *P. cingulatus* by Granger and Gregory (1943), one additional specimen (AMNH 26403) from Camp Margetts resembles the holotype of *cingulatus*. Additionally, a nearly complete mandible (AMNH 20110) from the Irdin Manha Formation, referred to *Protitan robustus* by Granger and Gregory (1943) is far more consistent with *cingulatus*.

The referral of this species to "*Protitan*?" is probably incorrect. The specimens referred to *cingulatus* by Granger and Gregory (1943) feature a distinctive set of morphological characters. "*Protitan*?" *cingulatus* differs from other large brontotheres, such as *Protitan grangeri*, *Rhinotitan*, *Aktautitan*, and *Protitanotherium* in having a relatively molariform p3 with a large metaconid. The premolars and quite broad and tall with very strong labial cingulids; these traits distinguish them from *Diplacodon* and *Gnathotitan*. Yet, there is a long postcanine diastema, large subcaniniform incisors, and the symphysis does not extend past p3; these traits rule out a variety of large advanced brontotheres such as *Metatitan*, *Embolotherium*, *Eubrontotherium*. The premolar morphology is essentially indistinguishable from *Hyotitan*, although "*Protitan*?" *cingulatus* is much smaller, with a shorter postcanine diastema, and a more elongate m3 with a wider hypoconulid.

In considering those brontotheres whose mandibles are unknown, a possible synonymy with *Epimanteoceras formosus*, a similarly size species from the same region and time period, seems likely. The mandibles of "*Protitan*?" *cingulatus* are consistent with what one might anticipate for the mandibles of *E. formosus*. *Epimanteoceras formosus* upper premolars are partially molarized with occasional hypocones; this degree of molarization is roughly equivalent to the degree of molarization seen in the lower premolars of *cingulatus*. *Epimanteoceras formosus* also has similar large subcaniniform upper incisors, a similar postcanine diastema, and it is virtu-

ally the same size. "*Protitan*?" *cingulatus* must be considered a nomen dubium because of the possible synonymy with *Epimanteoceras formosus*.

Epimanteoceras praecursor Yanovskaya, 1953

HOLOTYPE: Collection of the Laboratory of Paleozoology of the Zoological Institute of the Academy of Sciences Kazak SSR 3367a/51G, a right maxilla fragment with P4–M2 (the same specimen is referred to as KAN-Z-369/MP-61 by Emry et al. [1998]).

TYPE LOCALITY: 90 km to the northeast of Agadyr' in the region of the headwaters of the Sary-Su River, on a stream also called Aksoran (Russell and Zhai, 1987); Kiin Kerish, probably from locality K18 or K 20, either from Kusto or Aksyir Svita of Kazakstan (Emry et al., 1998).

AGE: Late Eocene (Ulangochuian land mammal "age").

DETERMINATION: Nomen dubium: holotype lacks diagnostic features.

REMARKS

Yanovskaya (1953) referred to the holotype of *Epimanteoceras praecursor* as SSR 3367a/51G. Later, Emry et al. (1998: fig. 6c) published a photo of an identical specimen that they identified as *Epimanteoceras* sp. with a different number KAN-Z-369/MP-61. Emry et al. (1998) did not recognize this specimen as the holotype of *E. praecursor*, although comparison with the original figure from Yanovskaya (1953) leaves little doubt that the specimen reported by Emry et al. (1998) is indeed the holotype of *E. praecursor*.

The holotype is a maxillary fragment with P4, M1, and M2 (fig. 178). The general shape, size, proportions, and characteristics of these teeth are consistent with a number of other brontotheres. The teeth are relatively advanced. P4 has a small hypocone and each of the molars has a small anterolingual cusp and a shallow central molar fossa. Yanovskaya's (1953) identification of this specimen as *Epimanteoceras* is certainly wrong. The anterolingual cingular cusps of the holotype are not consistent with *Epimanteoceras formosus*. The holotype of *E. praecursor* appears to represent a more derived brontothere. Asian brontotheres that are of similar size and have a P4 hypocone and a small anterolingual cingular cusp include *Parabrontops gobiensis*, *Dianotitan lunanensis*, *Eubrontotherium clarnoensis*, *Pachytitan ajax*, *Nasamplus progressus*. A number of North American species have the same traits. *Epimanteoceras praecursor* is a nomen dubium and its holotype could belong to one of a number of species.

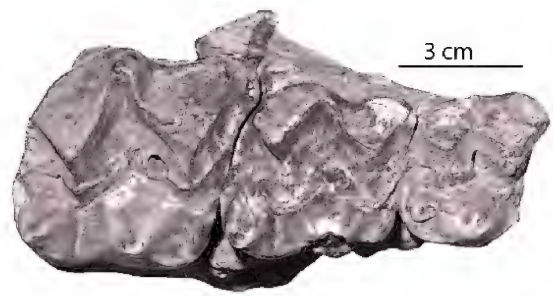

Fig. 178. Holotype of *Epimanteoceras praecursor* (KAN-Z-369/MP-61).

Rhinotitan orientalis Yanovskaya, 1957

HOLOTYPE: The holotype consists of several fragments assigned to PIN 858 that are all from a single individual according to Yanovskaya (1957): 88, part of a left M2; 35, canine fragment; 36, canine fragment; 80–81, left m3 fragment; 82, trigonid of left molar; 78, talonid of right molar; 83, trigonid of left molar; 79, talonid of right molar; 85, fragment of right P3 or P4 and trigonid of right m1; 84, right p3, 86, right p3 trigonid; 39, part of right lower canine; 24, upper incisor; 71, lower incisor; 99, right semilunar bone.

TYPE LOCALITY: Artyom mammal locality, coalmine north of Vladivostok in eastern Russia in strata termed the *Uglov Svita* ("coal formation") (Russell and Zhai, 1987).

AGE: Middle Eocene (Sharamurunian land mammal "age") (Lucas et al, 2004).

DETERMINATION: Nomen dubium, material is too fragmentary to adequately compare to other species.

REMARKS

Yanovskaya (1957) named *Rhinotitan orientalis* from isolated teeth and tooth fragments. Some of the more diagnostically useful fragments are seen in fig. 179, including a portion of an upper premolar (fig. 179a), a complete right p3 crown (fig. 179b), a lower incisor (fig. 179c) and an upper incisor (fig. 179d). Lucas et al. (2004) argued that this species is a nomen dubium. The small incisors and the well-developed premolar hypocone contrasts very strongly with true *Rhinotitan*, The tiny, semiwedge-shaped lower incisor and globular upper incisor suggest a species similar to *Parabrontops*, *Eubrontotherium*, or *Dianotitan*. The p3 lacks a metaconid, a condition consistent with *Parabrontops gobiensis* and *Eubrontotherium clarnoensis*. (The p3 is unknown for *Dianotitan*). In short, *R. orientalis* is a dubious species and the brontothere material from the Artyom locality could represent one (or more) of a number of brontotheres of middle or late Eocene age.

"*Eotitanops*?" *dayi* Dehm and Oettingen-Spielberg, 1958

HOLOTYPE: A right partial maxilla with the broken crowns of M2 and M3 in the Institute für Paläontologie und Historische Geologie, München (see plate 2, fig. 3 in Dehm and Oettingen-Spielberg [1958]).

TYPE LOCALITY: Kuldana Formation, Ganda Kas Area ("locality 25"), red-purple and greenish marls, Pakistan.

AGE: Middle Eocene.

REFERRED SPECIMENS: **(From the same locality as the holotype, all in the München collection. The following figure references refer to Dehm and Oettingen-Spielberg [1958: pl. 2: figs. 4–9])** partial M3 (fig. 4); partial left M1–M2 (fig. 5), partial right left M1–M3 (fig. 6); m3 fragment (fig. 7); mandible fragment with partial incisors and canine; (fig. 8); a mandible fragment with canine and anterior premolar roots (fig. 9); **(from H-GSP locality 68 from the Kuldana Formation, near the village of Ganda Kas)** H-GSP 573, a partial right maxilla with lingual parts of M1 and M2; H-GSP 577, a partial right M1; H-GSP 1592, a partial left M2; **(from the Chorlakki locality in the Mami Khel Formation, Kohat District, Northwest Frontier Province of Pakistan)** GSP-UM 104, a partial left M3; GSP-UM 155, left P3; GSP-UM 156 upper molar fragment; GSP-UM 1642 partial left P3?; GSP-UM 1526; partial left protocone; GSP-UM 1692, partial right paracone.

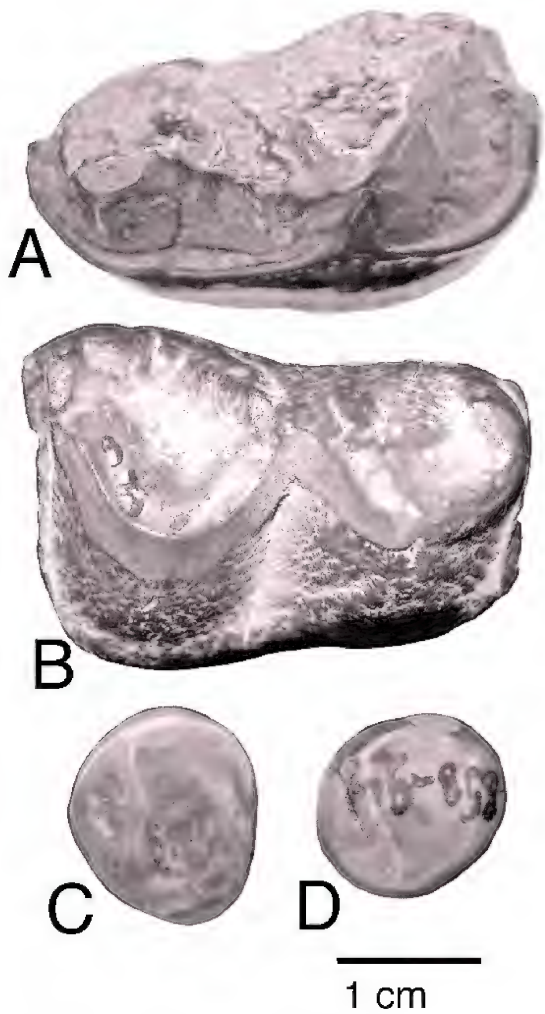

Fig. 179. Portions of the holotype of *Rhinotitan orientalis*. **(A)** PIN 858-85, **(B)** 858-84, **(C)** 858-24, **(D)** 858-71.

DETERMINATION: Problematic taxon, this species seems valid, although it probably does not belong to *Eotitanops*. The material is too fragmentary to provide a thorough description or adequate diagnosis.

REMARKS

Dehm and Oettingen-Spielberg (1958), West (1980), and Thewissen et al. (1987, 2001) described very fragmentary brontothere specimens that were referred to as "*Eotitanops*?" *dayi*, consisting mostly of partial upper molars from the Kuldana Formation in the Ganda Kas and Thatta areas and from the Mami Khel Formation near Chorlakki (fig. 180). "*Eotitanops*?" *dayi* is roughly intermediate in size between North American brontotheres, *Eotitanops* and *Palaeosyops*. The molars of the type specimen lack enamel. The other specimens referred to this species, which include partial molars with enamel, are of a consistent size, but given the poor nature of the material there is no way to determine whether they belong to a single species. The better tooth fragments show similarities with North American *Eotitanops*. For instance, M3 has a rounded lingual side. The M3s of other brontotheres have longer and flatter lingual sides, thus giving the tooth a more square appearance. Another noteworthy similarity with *Eotitanops* is a lower diastema of about 10 mm between the p1 and p2. However, *dayi* molars appear to have thinner enamel than North American *Eotitanops* with taller lingual cusps.

The available material seems to suggest a distinct species of brontothere, but the highly fragmentary material representing this *Eotitanops*-sized species is not sufficient to appropriately describe or diagnose it. Therefore, I consider this species to be problematic, but not necessarily invalid. Despite some similarities with North American *Eotitanops*, the material is simply too fragmentary to refer it *Eotitanops* or any other genus. "*Eotitanops*?" *dayi* is one of three problematic middle Eocene brontothere species of Pakistan, the others being *Pakotitanops latidentatus* and *Mulkrajanops moghliensis*.

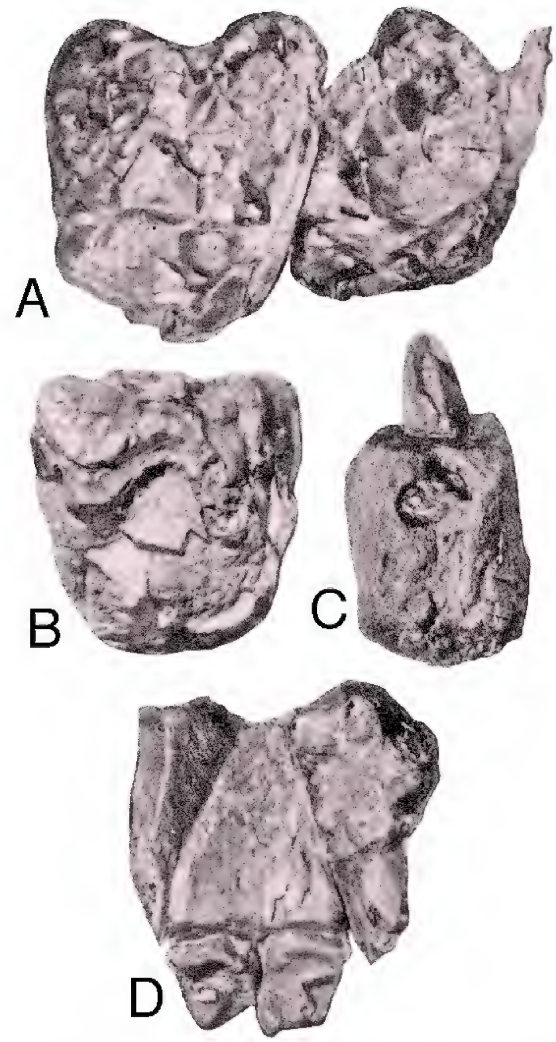

Fig. 180. Specimens referred to "*Eotitanops*?" *dayi*. **(A)** The holotype; partial crowns of right M2 and M3, **(B)** partial M3, **(C)** mandible fragment with canine and anterior premolar roots, **(D)** mandible fragment with partial incisors and canine. (All photos actual size from Dehm and Oettingen-Spielberg, 1958).

Rhinotitan quadridens Xu and Chiu, 1962

HOLOTYPE: IVPP V2651, a left P3–P4, and isolated left p2, and right p3, p4, and m1.

TYPE LOCALITY: Lumeiyi Formation, Lunan Basin, Yunnan Province, China.

AGE: Middle Eocene (Sharamurunian land mammal "age").

DETERMINATION: Nomen dubium: holotype lacks diagnostic features.

REMARKS

Rhinotitan quadridens is a nomen dubium based on a series of upper and lower cheek teeth (fig. 181). P3 and P4 are rectangular with parallel anterior and posterior sides, and flat lingual and labial margins. P3 has a well-

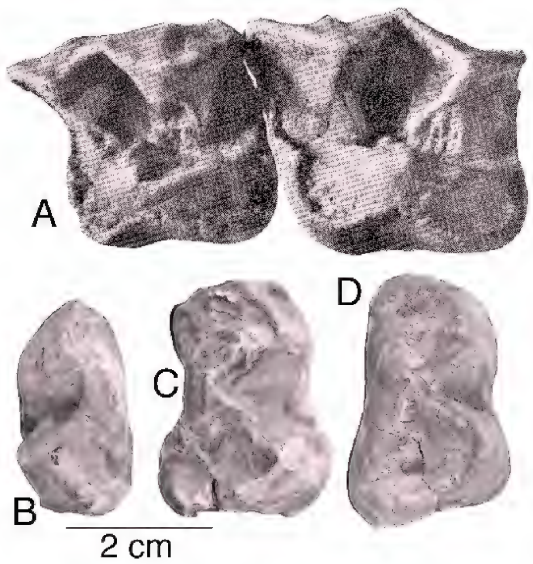

Fig. 181. Part of the holotype of *Rhinotitan quadridens* (IVPP V2651). **(A)** Left P3–P4 (from Xu and Chiu, 1962), **(B)** left p2, **(C)** right p3, and **(D)** right p4.

developed lingual crest, while P4 does not. P4 has a poorly developed mesostyle and cusp on the anterior cingulum. The p2 trigonid is only slightly longer than the talonid and it lacks a metaconid. There is an anomalous small cusp at the lingual edge of the p2 talonid basin. The teeth identified as p3 and p4 each have a well-developed metaconid. The lower premolars lack cingulids.

Xu and Chiu (1962) noted that the degree of premolar molarization resembles *Rhinotitan mongoliensis* (a nomen dubium) and *R. andrewsi*, but that it differs from other *Rhinotitan* species in its larger size, higher crowns, flatter lingual edges of P3 and P4, and well-developed secondary wrinkles (?) on P3 and P4. However, none of these specimens retains diagnostic characters that would indicate *Rhinotitan*, nor do they indicate a unique taxon. Given the considerable amount of intraspecific variation seen in the upper premolars of brontotheres, the rectangular shape of P3 and P4, prominent lingual crest on P3, lack of well-developed hypocones, and (occasional) P4 mesostyle and anterolingual cingular cusps do not sufficiently differentiate this species from several large Asian brontothere species, such as *Qufutitan zhoui*, *Epimanteoceras formosus*, *Rhinotitan kaiseni*, *Rhinotitan andrewsi*, *Gnathotitan berkeyi*, *Aktautitan hippopotamopus*, and possibly others. Moreover, size variation among these species is poorly understood because of limited sample sizes. The lower premolars are also consistent with multiple taxa, particularly *Rhinotitan*, *Gnathotitan*, and *Aktautitan*. To summarize, the specimens upon which *R. quadridens* was based do not indicate a unique taxon; nor is there enough evidence for a species-level identification. However, it is noteworthy that the material is distinct from *Dianotitan lunanensis*, a species from the same formation with well-developed premolar hypocones. Other material from the Lumeiyi Formation, assigned to another nomen dubium, *Protitan major*, consisting of an upper molar series, may also be pertinent, although comparisons are not possible due to nonoverlapping parts.

Duchesneodus thyboi (Bjork, 1967)

HOLOTYPE: SDSM 63689, a partial skull with right C, P3–M2, left I2 (?), C, P3–M2, M3 (unerupted).

TYPE LOCALITY: SDSM locality V582, Slim Buttes Formation, Harding County, South Dakota.

AGE: Middle Eocene (Duchesnean land mammal "age").

REFERRED SPECIMENS: **(See Bjork [1967] for a complete list.)** Bjork (1967) referred numerous teeth and other fragments to *Duchesneodus thyboi*. Among these specimens is SDSM 63690, a partial rostrum with a complete incisor row, right C, and P2–P4 from SDSM locality V6244.

DETERMINATION: Nomen dubium, holotype is an indeterminate juvenile specimen.

REMARKS

Bjork (1967) described *Teleodus thyboi* from a partial juvenile skull (SDSM 63689), several cranial fragments, and isolated teeth. After demonstrating *Teleodus* to be an invalid genus, Lucas and Schoch (1982) reassigned this species to *Duchesneodus*. Subsequently, they considered it a junior synonym of *D. uintensis* (Lucas and Schoch, 1989b). However, the material from which

this species was described is neither consistent with *D. uintensis*, nor does the material sufficiently indicate a distinct taxon.

The holotype specimen (SDSM 63689) (fig. 182b) indicates a brontothere with small globular upper incisors, a large canine, a distinct postcanine diastema similar in length to P2, upper premolars with small preprotocristae, and distinct premolar hypocones that are separated from the protocones by a lingual connecting crest. Another important specimen, SDSM 63690 (fig. 182a), a rostral fragment, is consistent with the holotype and further indicates a reduced number of upper incisors (two pairs). Other specimens have an occasionally strongly developed P4 mesostyle (Bjork, 1967).

The relatively long postcanine diastema differentiates *Duchesneodus thyboi* from *D. uintensis* and *Megacerops coloradensis* but several other species, such as *Eubrontotherium clarnoensis*, *Protitanops curryi*, and *Notiotitanops mississippiensis*, possess similar postcanine diastemata.

Bjork (1967) noted that the postorbital process of the jugal of SDSM 63689 was located above the metacone of the M2, thus indicating a shortened face that is characteristic of typical Chadronian brontotheres (i.e., *Megacerops*). In comparison, the orbits of *Eubrontotherium*, *Notiotitanops*, and *Protitanops* are more posteriorly positioned. However, SDSM 63689 is a subadult specimen with an unerupted M3. Although brontothere cranial ontogeny has not been carefully studied (juvenile skulls are very rare), it is fairly obvious that, as the teeth erupt, there would have been ontogenetic changes in the position of the orbit with respect to the teeth. Therefore, this character does not really differentiate *Duchesneodus thyboi* from other species. From what can be discerned from the available material *Duchesneodus thyboi* is potentially synonymous with *Eubrontotherium clarnoensis*, *Protitanops curryi*, and *Notiotitanops mississippiensis* and it is therefore a nomen dubium.

Epimanteoceras amplus Yanovskaya, 1976

HOLOTYPE: PIN 3109-41, a dorsoventrally crushed skull missing the frontonasal region with right and left P1–M3. An associated partial mandible was also described by Yanovskaya (1976), but I have been unable to examine it.

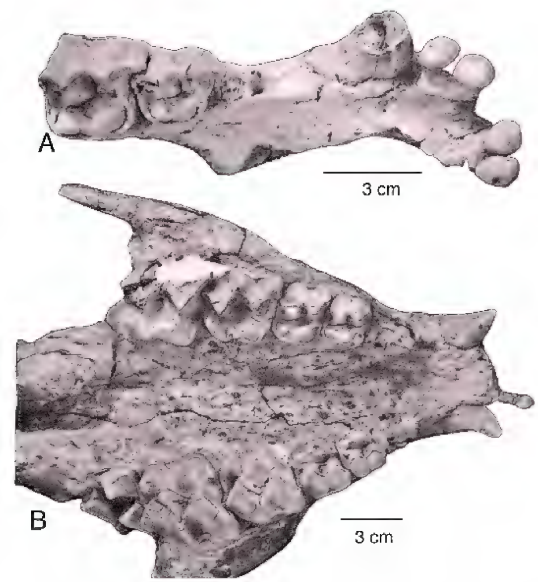

Fig. 182. Specimens referred to *Duchesneodus thyboi*. **(A)** SDSM 63690, and **(B)** SDSM 63689 (the holotype). Photos from Bjork (1967).

AGE: Late Eocene (Ulangochuian land mammal "age").

TYPE LOCALITY: Ergilin Dzo (lower part), Dornogobi Province, Outer Mongolia.

DETERMINATION: Nomen dubium. This species could be a synonym of *Nasamplus progressus*.

DESCRIPTION

SKULL: The holotype skull (PIN 3109-41) is somewhat crushed dorsoventrally and missing the frontonasal portion (fig. 183). From the ventral view, the shape of the skull is relatively intact, although the left jugal and squamosal bones have become detached on the zygomatic arch. A large crack runs through the midline of the skull. Because the frontonasal portion of the skull is missing, it cannot be determined whether this specimen possessed an enlarged ram similar to these brontotheres or whether it had a more normal frontonasal configuration. The orbit is positioned directly above M2, with the anterior rim of the orbit positioned approximately over the anterolat-

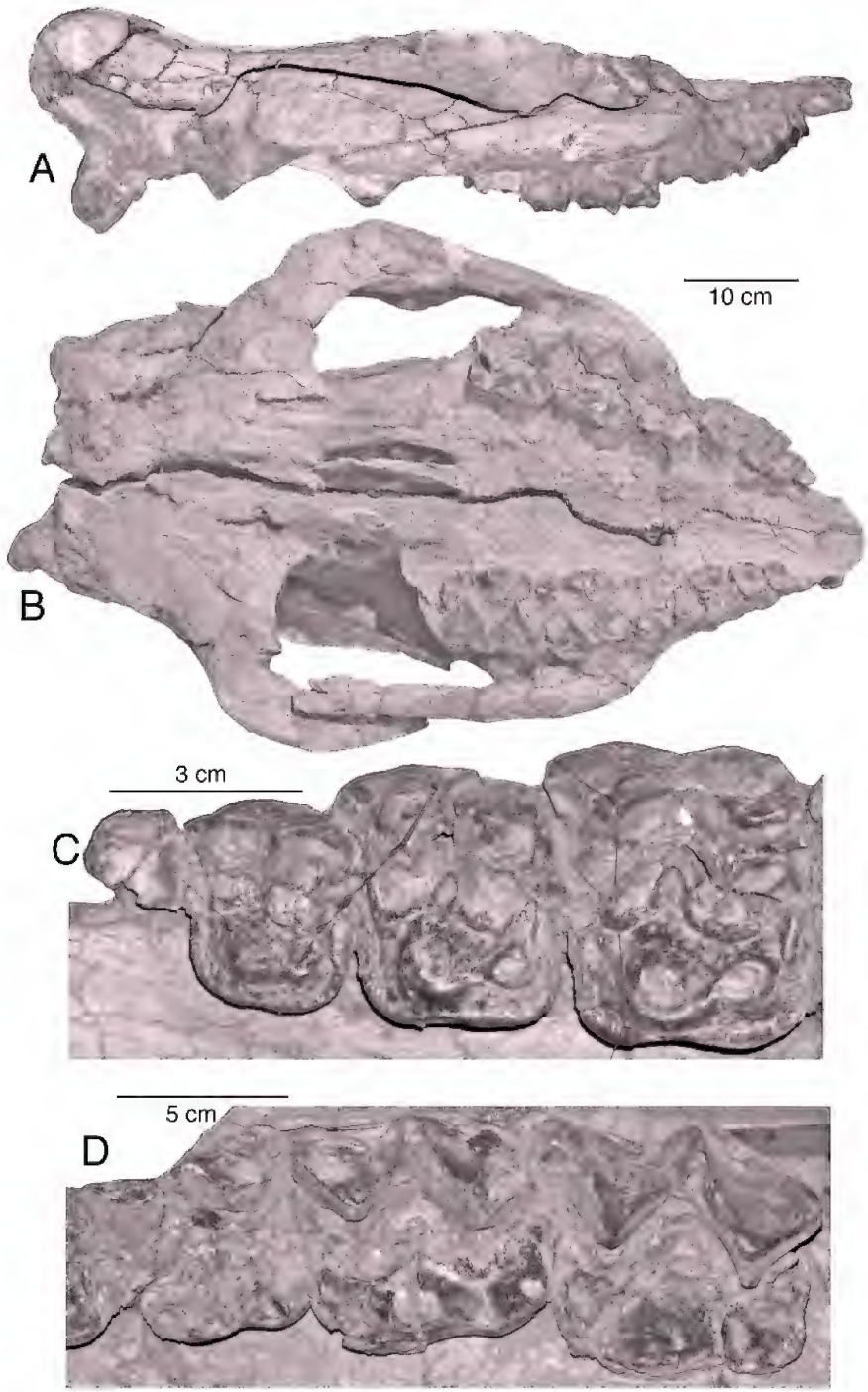

Fig. 183. Holotype skull of *Epimanteoceras amplus* (PIN 3109-41). **(A)** Right view, **(B)** ventral view, **(C)** left P1–P4, **(D)** left M1–M3.

eral root of M1. The rostrum is relatively long and shallow with a small ridge on its dorsal surface similar to *Embolotherium andrewsi* (e.g., AMNH 26009; see fig. 118a). It narrows considerably anterior to the cheek teeth. The entire dorsal surface of the skull appears to have been concave (saddle-shaped), and although it does not seem to have been as deeply concave as that of *Embolotherium* this relates in part to the dorsoventral taphonomic flattening. The parasagittal ridges remain widely separated throughout their length, but they do not greatly overhang the sides of the skull as in *E. andrewsi*. From a lateral view, the zygomatic arches are weakly curved. From the ventral view, the jugal process of the zygomatic arch extends posterolaterally (although the left side is distorted), giving the zygomatics a laterally bowed appearance. The degree to which the zygomatics are laterally bowed most closely resembles *Protembolotherium efremovi*. They are not extremely bowed out as in *E. grangeri*, nor are they parallel as in *E. andrewsi*. The zygomatics of PIN 3109-41 lack the conspicuous lateral bulges that are seen in all specimens of *Embolotherium* and *Protembolotherium*. From a lateral view, the posterior end of the skull most closely resembles *P. efremovi*, with a robust but relatively short and moderately swept-back occiput. The occiput is not nearly as deep as those of *Embolotherium*, and not nearly as massive as that of *E. andrewsi*.

The anterior margin of the posterior nares is positioned near the posterior margin of M3; this position is similar to *Protembolotherium efremovi* and more anterior than that of *Embolotherium*. Other characteristics of the ventral surface of PIN 3109-41 are indistinguishable from *Protembolotherium* and *Embolotherium*. The anterior and lateral sides of the posterior narial opening are rimmed by a wide U-shaped emargination. The ridge demarcating this emargination is faint, but it can be seen when examining the actual specimen. This emargination is widest on the anterior margin and tapers along the lateral margins. The opening of the posterior nares is rather short and does not extend up onto the sphenoid. The basicranium itself is rather narrow; the total width of the basicranium at the position of the mastoid processes does not exceed the distance across the right and left M3s. The configuration of the basicranial foramina is typical. The mastoid process is shorter than the postglenoid process and it curves anteroventrally, forming a tube-shaped external auditory pseudomeatus. The external auditory pseudomeatus extends into the basicranium in a strongly posteromedial direction.

Upper Dentition: The incisors and canines are not preserved, although their alveoli are preserved, indicating an unreduced dental formula: 3-1-4-3. The incisor and canine alveoli indicate that these elements were rather small, but by no means reduced to a completely vestigial state. The alveolar border of the rostrum arches anterior to the canines. There is a distinct postcanine diastema.

Close-ups of the cheek teeth can be seen in fig. 183c–d. The P1 is heavily worn, but its broad shape is consistent with those that have relatively advanced crown morphology. The P2–P4 are nearly rectangular and they have thick, beaded lingual cingula and dual lingual cusps. The hypocone is consistently smaller than the protocone and connected to the protocone by a small lingual crest. The premolars are essentially indistinguishable from those of *Protembolotherium efremovi* and *Embolotherium andrewsi* but the lingual cusps of *E. grangeri* tend to be more completely separated. The upper molars show typical brontotheriine apomorphies including tall and lingually angled ectolophs, very weak labial ribs, thin lingual ectoloph enamel, and wedge-shaped lingual sides of the paracone and metacone in the least worn molars. Deep central molar fossae can still be seen on M2 and M3, though it is worn off on M1. A small anterolingual cingular cusp can still be seen on M3, but it is damaged. The M3 hypocone is a large as those of the other molars. Labial molar cingula are very weak and lingual molar cingula are mostly absent or have been worn off.

Mandible and Lower Dentition: I could not find the holotype mandible of PIN 3109-41, although Yanovskaya (1980) provided a photo of it (reproduced here in fig. 184). The mandible has a fairly broad symphysis with a strongly arched incisor row that compares well with *Embolotherium*

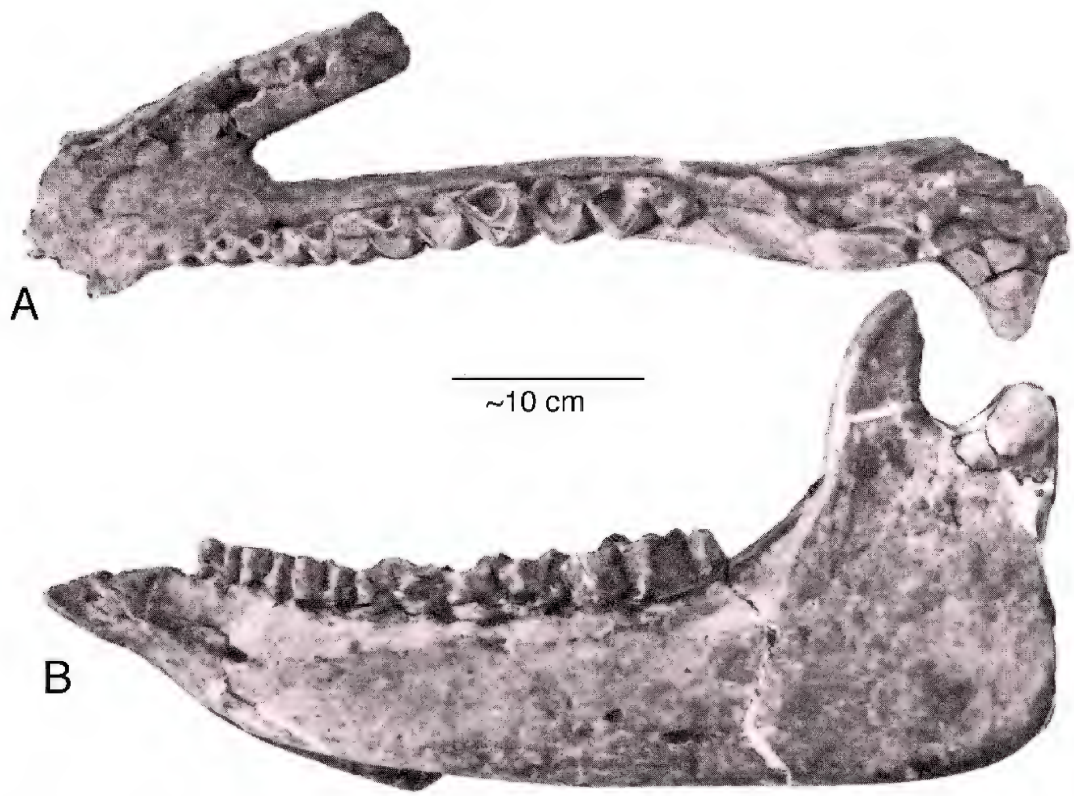

Fig. 184. Holotype mandible of *Epimanteoceras amplus* (PIN 3109-41). **(A)** Dorsal view, **(B)** left view. From Yanovskaya (1980: plate 2).

andrewsi. The symphysis of *E. grangeri* is longer and more slender. The horizontal ramus of PIN 3109-41 does not seem to deepen posteriorly as strongly as *E. andrewsi*. The postcanine diastema is also somewhat longer. The premolars also compare well with *Embolotherium*, including the broad and nearly molariform p2 talonid, in addition to the strongly molariform p3 with a distinct metaconid. The thin lingual enamel of the lower molars and the elongate m3 are typical brontotheriine characters. In *Embolotherium* the trigonids and talonids form deep valleys rather than the broad shallow basins that are typical of most other brontotheres. The photograph of PIN 3109-41 suggests similar deep molar valleys.

Remarks

Yanovskaya (1976) erected *Epimanteoceras amplus* on a nearly complete skull and associated partial mandible from Ergilin Dzo, Mongolia (PIN 3109-41). I was able to relocate the skull but not the mandible. Yanovskaya (1980) later incorrectly synonomized this species with *Protitan robustus* Granger and Gregory (1943). She also erroneously transferred *Protitan robustus* to the genus *Epimanteoceras*. At any rate, PIN 3109-41 clearly differs from all the species that Granger and Gregory (1943) originally assigned to *Protitan* and *Epimanteoceras*. PIN 3109-41 has a shorter, broader symphysis, and significantly more molarized lower premolars than the holotype mandible of *Protitan robustus* (AMH 20104: fig. 69). Furthermore, PIN 3109-41 differs substantially from *E. formosus* and *P. grangeri* (the senior synonym of *P. robustus*) due to its widened parasagittal ridges, reduced rostrum, smallish incisors, more posteriorly positioned posterior nares, shortened posterior narial canal, narrow basicranium, tubular and

strongly posteromedially angled external auditory pseudomeati, advanced P1, advanced P2–P4 with dual lingual cusps, central molar fossae, anterolingual cingular cusp, and a prominent M3 hypocone.

PIN 3109-41 belongs to a more advanced brontothere similar to *Embolotherium* and *Protembolotherium*, as suggested by the posteriorly positioned posterior nares, short posterior narial canal, steeply angled external auditory pseudomeatus, narrow basicranium, and widely separated parasagittal ridges. Nonetheless, PIN 3109-41 can be assigned to none of the species of these genera. The reduced rostrum most closely resembles *Embolotherium andrewsi*; although the shorter occiput, more anterior position of the posterior nares, and less prominent parasagittal ridges are more similar to *Protembolotherium efremovi*. Unlike *Protembolotherium* and *Embolotherium*, PIN 3109-41 lacks lateral swellings on the zygomatic arches.

Nasamplus progressus, another late Eocene brontothere, from the "Ulan Gochu" faunal zone (sensu Radinsky, 1964) of Inner Mongolia, is closely related to *Embolotherium* and *Protembolotherium*, and is a possible synonym of *Epimanteoceras amplus*. Presently, *Nasamplus progressus* is known only from a cranial fragment (AMNH 26014: fig. 112) including the frontal, nasal, and part of the maxilla; therefore, only a very limited comparison is possible. The diagnostic features of *Nasamplus progressus* are found in the nasal and frontal elements, portions of the skull that are missing in PIN 3109-41. Therefore, *Epimanteoceras amplus* is a nomen dubium, but if it is found to be synonymous with *Nasamplus progressus*, this fossil material will provide valuable character data for an otherwise poorly known species.

Arctotitan honghoensis Wang, 1978

HOLOTYPE: IVPP V3201, a skull fragment consisting of the premaxillomaxillary rostrum with right I1–P2 and left I1–I2, P1–P3.

TYPE LOCALITY: Yinpocun locality, near Xian (loc. 65009), Shaanxi Province, Lantian District, Hongho Formation.

AGE: Middle Eocene (Russell and Zhai, 1987).

DETERMINATION: Nomen dubium. This species could be a synonym of *Gnathotitan berkeyi*.

DESCRIPTION

IVPP V3201 is the anterior portion of a premaxillomaxillary rostrum of an extremely large brontothere (fig. 185). The dorsolateral surface of the rostrum is intact from its anterior edge to a point about above the P1, indicating that the lateral nasal incision extended to a point posterior to the P1. The rostrum itself is very broad and shallow. The premaxillomaxillary sutures are clearly visible on both sides of the specimen. The nasal processes of the premaxillae diverge posterolaterally from the midline symphysis and extend posteriorly to a point above the P1s.

For the most part, the teeth are only moderately worn. The incisors form a moderately arched row and compare well with most hornless brontothere species in their subcaniniform shape. Though moderately worn, each incisor has a short lingual heel and a poorly defined labial cingulum. The incisor crowns progress in size laterally; the I1 is the smallest and the I3 is the largest incisor. There is a sizeable diastema between the median incisors and a rather long postcanine diastema.

The morphology of the P1 crown is obscured by wear, although it appears to have been relatively complex. The labial side of the P1 crown forms a curved ectoloph. The anterior portion of the P1 ectoloph contains a large paracone. A distinct metacone could have been present on P1, and there is certainly room for a metacone to have been present on the posterior portion of the ectoloph. The lingual side of the crown contains a broad, obliquely shaped heel. Any distinct cusps (protocone) or crest that might have been present on this lingual heel have been obliterated by wear.

The crown of P2 is rhomboidal with parallel anterior and posterior margins that form oblique angles with the lingual and labial sides. The P3 is nearly rectangular. The parastyles of P2 and P3 are slightly angled labially; otherwise, the ectolophs of these premolars are straight. Labial ribs curve in a posterodorsal direction across the labial face

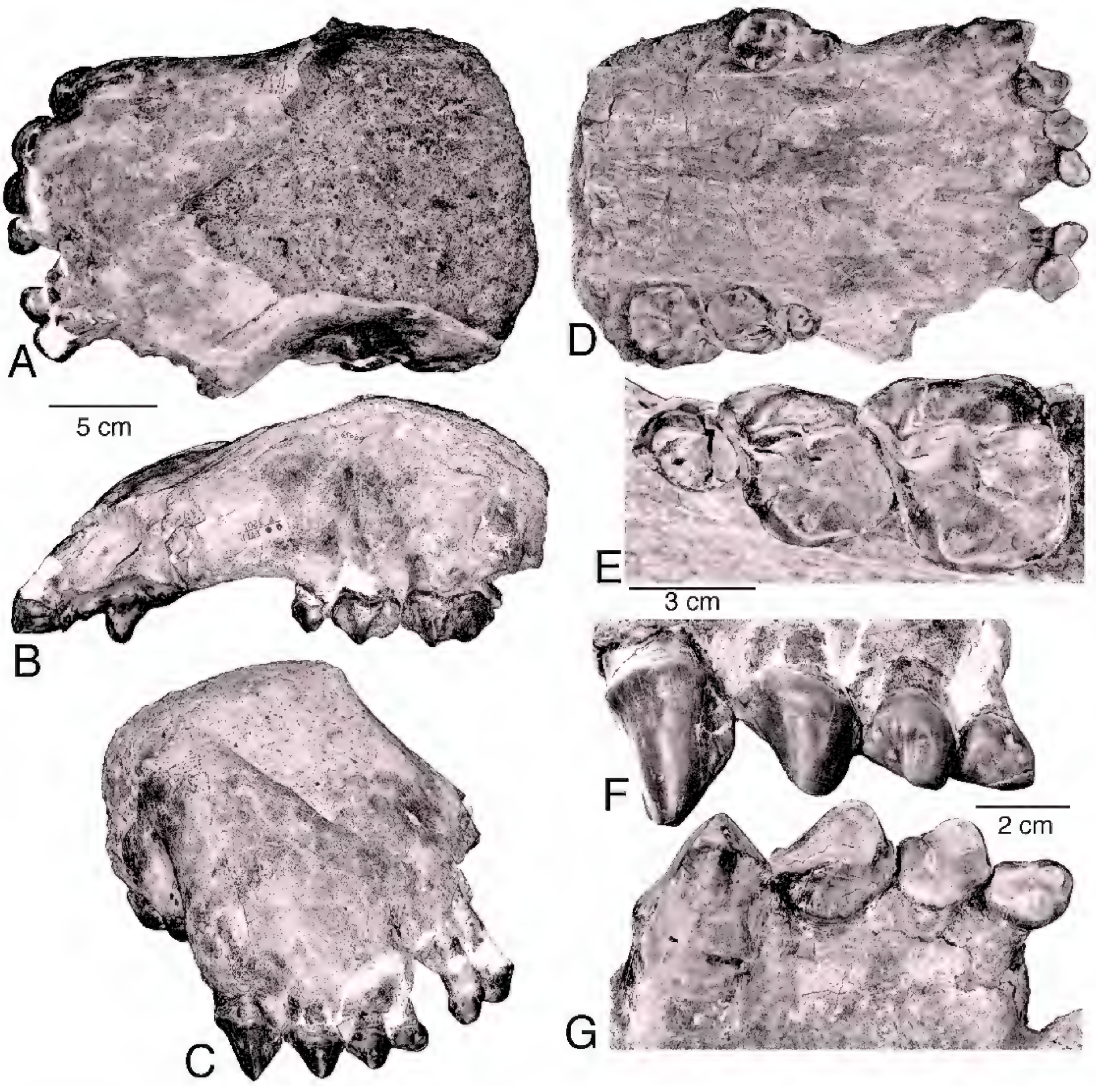

Fig. 185. The holotype specimen of *Arctotitan honghoensis* IVPP V3201. **(A)** Dorsal view of rostrum, **(B)** left view, **(C)** oblique view, **(D)** ventral view, **(E)** left P1–P3, **(F)** labial view of right incisors and canine, **(G)** lingual view of incisors and canine.

of the paracone on each tooth. The lingual paracone rib of the P3 is somewhat narrower than that of P2. Labial metacone ribs are not seen on these teeth.

There are heavily worn protocones on both P2 and P3. On each tooth the protocone is positioned on the anterior portion of the broad lingual heel. There is certainly room for a hypocone to have been present on P2, but if it was present it has been erased by wear. On P3 the hypocone is represented by a small circular exposure of dentin on the posterolingual corner of the crown that is well separated from the protocone. On both of these premolars, there is an indistinct preprotocrista. There is no evidence of a lingual crest on either the P2 or P3 of IVPP V3201, although wear may have erased it. The P2 and P3 have distinctly continuous anterior and posterior cingula. The labial and lingual cingula are relatively weak and discontinuous; however, the labial cingulum below the metacone of P3 is relatively strong.

REMARKS

Arctotitan honghoensis Wang 1978 is based on the rostral fragment (IVPP V3201) of an enormous brontothere. This specimen is one of just three fossil mammal specimens (all perissodactyls) from the Hongho Formation (Wang, 1978; Russell and Zhai, 1987). The remaining specimens, identified as cf. *Deperetella* and *Breviodon*, suggest a middle Eocene age (Russell and Zhai, 1987).

Wang (1978) and Russell and Zhai (1987) note that *Arctotitan honghoensis* is larger than any early or middle Eocene brontothere, and that it compares in size only with late Eocene brontotheres. However, at least one middle Eocene (Irdinmanhan) species, *Gnathotitan berkeyi*, is of a similar size. IVPP V3201 differs from other very large brontotheres, such as *Embolotherium* and *Protembolotherium* by its plesiomorphic incisor morphology and poorly developed premolar hypocones. *Aktautitan hippopotamopus* has large incisors like IVPP V3201, although I1 is substantially more spherical. Moreover, the premolars of *Aktautitan* have slightly narrower lingual heels that completely lack hypocones, the rostrum seems deeper and the postcanine diastema is much shorter (Mihlbachler et al., 2004a). The broad and shallow rostrum, the relatively long postcanine diastema, and the low relief of the lingual features of the premolars of IVPP V3201 closely resemble *Rhinotitan*. *Rhinotitan kaiseni* retains large subcaniniform incisors, like IVPP V3201. However, the P1 of *Rhinotitan kaiseni* is narrower and simpler. Moreover, *Rhinotitan kaiseni* is the smaller species of *Rhinotitan*, and none of the known specimens approaches IVPP V3201 in size. On the other hand, the larger specimens of *Rhinotitan andrewsi* approach IVPP V3201 in size, and P1 is equally as advanced. However, the incisors of *Rhinotitan andrewsi* are distinctly more globular in shape. Therefore, IVPP V3201 is consistent with neither species of *Rhinotitan*.

Gnathotitan berkeyi is essentially the same size as IVPP V3201; premolar measurements differ by no more than a few millimeters. The upper incisors of *G. berkeyi* are unknown, although the lower incisors of that species are large and subcaniniform, and are thus consistent with the upper incisors of IVPP V3201. Some of the apparent differences between *G. berkeyi* and IVPP V3201 can be attributed to taphonomic deformation or they are traits found to have intraspecific polymorphic tendencies. For instance, the narrow symphyseal region of the *G. berkeyi* mandible (AMNH 20106) is inconsistent with the broad rostrum of IVPP V3201; however, that mandible is transversely crushed. The limited sets of upper premolars of *G. berkeyi* either lack hypocones (AMNH 141231), or have poorly developed hypocones that are not well separated from the protocones (AMNH 20121). IVPP V3201 seems to have better developed hypocones that are well separated from the premolars. However, premolar hypocone development is highly variable in many brontothere species, and the taxonomic significance of this difference is dubious. Finally, the lingual heel of the P1 of IVPP V3201 is wider, broader, and more fully developed than the P1 of any specimen of *G. berkeyi*; however some species, such as *Protitanotherium emarginatum* show notable variation in the P1. Because IVPP V3201 does not offer conclusive evidence for a unique species, *Arctotitan honghoensis* is a nomen dubium, but it is possibly synonymous with *Gnathotitan berkeyi*.

Pakotitanops latidentatus West, 1980

HOLOTYPE: H-GSP 1050, a maxillary fragment with left M2 and roots of M3.

TYPE LOCALITY: H-GSP locality 146, Kuldana Formation, Ganda Kas area, Pakistan.

AGE: Middle Eocene.

DETERMINATION: Problematic taxon; the species is probably valid, but the holotype is insufficient for a thorough description or adequate diagnosis.

REMARKS

West (1980) described *Pakotitanops latidentatus* from a heavily worn M2 (H-GSP 1050) (fig. 186). Thewissen et al. (2001) described several more highly fragmentary specimens, all from the Kuldana Formation of the Ganda Kas area. Many of the diagnostic features of this specimen, as listed

by West (1980), such as the weakly developed ectoloph and the wide length/width ratio have to do with the fact that the holotype is severely worn, and its proportions have been significantly altered by wear. The tooth is too worn to make precise measurements. However, it is much larger than "*Eotitanops*?" *dayi* and *Mulkrajanops moghliensis*; it seems similar in size to many North American Bridgerian and Uintan hornless brontotheres such as *Palaeosyops*, *Telmatherium*, and *Dolichorhinus*. The M2 of *Pakotitanops latidentatus* has a paraconule similar in size to that of *Palaeosyops* and *Mesatirhinus*, but this structure is much larger than the occasional paraconules seen on the molars of *Dolichorhinus* and *Telmatherium*. H-GSP 1050 exhibits a distinct central molar fossa, a character not seen in *Palaeosyops* or *Mesatirhinus*. Among similarly sized brontotheres, only *Dolichorhinus* has central molar fossae but also retains vestigial paraconules. The combination of a central molar fossa and a *Mesatirhinus*-sized paraconule seems unique. The holotype of *Pakotitanops latidentatus* seems to represent a valid species, although the present material is insufficient to differentiate it from *Dolichorhinus* (a species where the paraconule is intraspecifically polymorphic).

Fig. 186. Holotype left M2 of *Pakotitanops latidentatus* (H-GSP 1050). Scale bar = 1 cm. Photo from West, 1980.

Mulkrajanops moghliensis Kumar and Sahni, 1985

HOLOTYPE: VPL/K 563, a skull containing partial dentition of both sides.

TYPE LOCALITY: Maroon Shales, Upper Subathu Formation exposed West of Moghla on the Metka-Moghla road, Rajauri District, Pakistan.

AGE: Middle Eocene.

DETERMINATION: Problematic taxon; this species is probably valid, though it might not be a brontotheriid. A reanalysis of this species is needed.

REMARKS

Kumar and Sahni (1985) named *Mulkrajanops moghliensis* from a partial skull (VPL/K 563) of a species similar size to *Eotitanops* (fig. 187). No other specimens are referred to this species. I was unable to directly examine the holotype; therefore, I refer to the figures and description of Kumar and Sahni (1985) but point out the following interesting details that seem to differentiate it from other brontotheres of similar size. P1 is advanced in that it has a large paracone and metacone. There is no P1–P2 diastema. The remaining premolars are unusually elongate, and P2 bears a large paraconule. M1 has a large lophoid paraconule similar to that of *Eotitanops*. M3 is the only complete molar; it is squarish in outline, although it lacks a hypocone. Unlike other brontotheres, the upper molars do not appear to have had well-developed mesostyles. *Mulkrajanops moghliensis* further differs from North American *Eotitanops* in the absence of a long P1–P2 diastema and the more complex morphology of the P1. It differs from North American *Eotitanops* and "*Eotitanops*?" *dayi* in the more squarish M3 and possibly in the more elongated cheek teeth. Additionally, it can be distinguished from other small species such as *Microtitan* by the relatively steep angle and shorter height of the molar ectoloph and the presence of a large M1 paraconule. *Mulkrajanops moghliensis* is possibly a valid species of an unusual brontothere-like animal. However, judging from

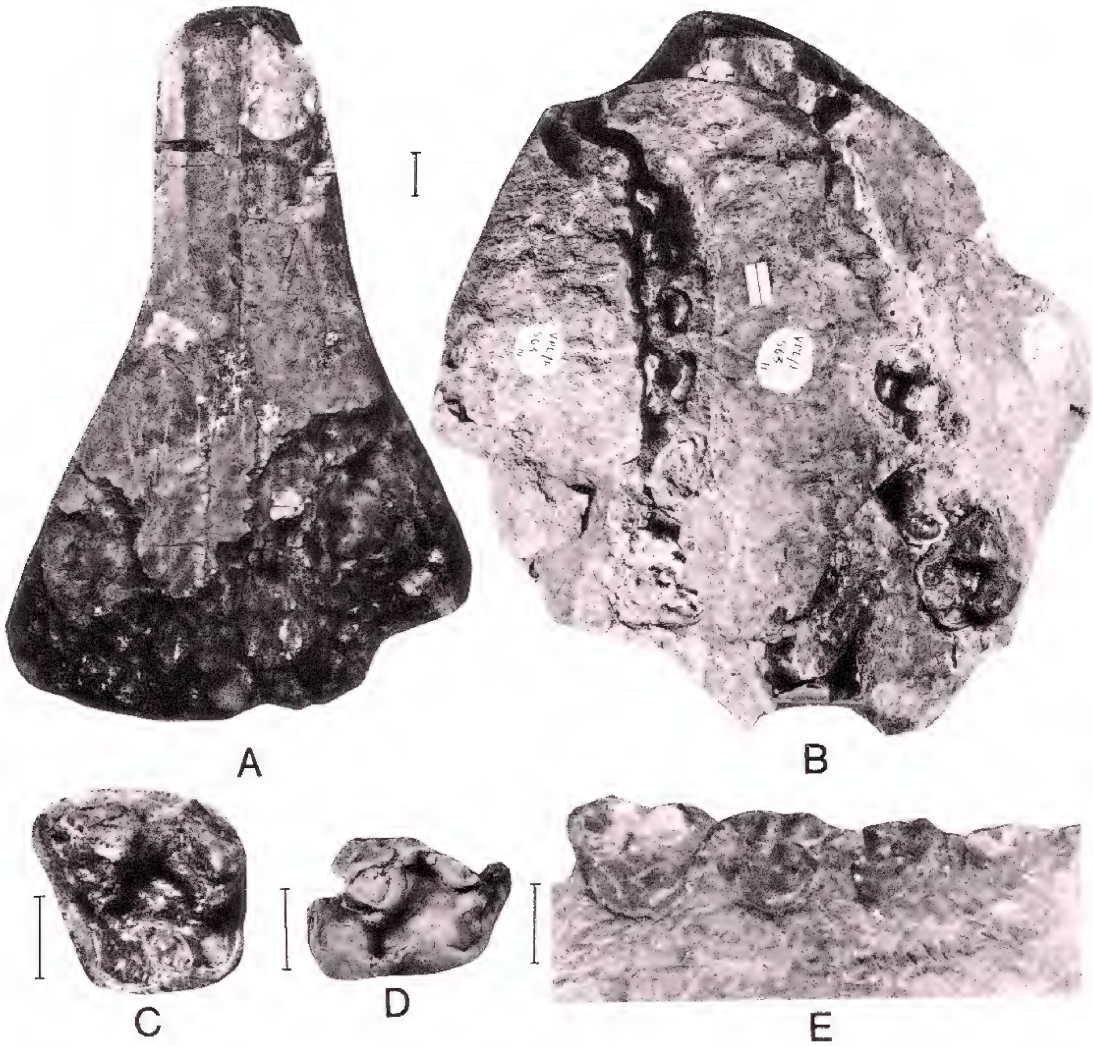

Fig. 187. The holotype of *Mulkrajanops moghliensis* (VPL/K 563). **(A)** Dorsal view, **(B)** ventral view, **(C)** left M3, **(D)** right M1, **(E)** right P1–P4. (Scale bars = 1 cm). Modified from Kumar and Sahni (1985).

the figures provided by Kumar and Sahni (1985), its identification as a brontothere is questionable; although many aspects of its dentition, such as the isolated lingual molar cusps, are certainly consistent with a brontotheriid, the absence of a well-developed molar mesostyle is different from other brontotheres and their probable sisters, *Lambdotherium* and *Danjiangia*, all of which have conspicuous labially expanded molar mesostyles. The published figures of *Mulkrajanops* are not of sufficient quality to collect reliable character data; therefore, further analysis of the actual specimen is needed.

"*Microtitan*?" *elongatus* Qi, 1987

HOLOTYPE: IVPP V5767, a right P3–M3 (M1 and M2 largely broken; M3 preserves only mesostyle and metacone).

TYPE LOCALITY: Daatein Obo, lower beds (Arshanto) of the Irdin Manha Formation, Inner Mongolia.

AGE: Middle Eocene (Irdinmanhan land mammal "age").

DETERMINATION: Nomen dubium: holotype lacks diagnostic features.

REMARKS

The holotype of "*Microtitan*?" *elongatus* (IVPP V5767), consisting of a partial series of upper cheek teeth is similar to *M. mongoliensis*, but slightly larger. It was described by Qi (1987) as having well-developed mesostyles on P3 and P4, characteristics that are not seen in *M. mongoliensis*. The original specimen was not available; Qi's figure of the type (Qi, 1987: fig. 44) shows only a small P4 mesostyle, but it is much less developed than typical molar mesostyles. A P3 mesostyle is not evident. Considering that premolar mesostyles occasionally occur in many brontothere species, there is not enough evidence for a distinct species; *elongatus* potentially fits within a species concept of *M. mongoliensis*, but the material lacks diagnostic characters of *Microtitan*. There is evidence for multiple *Microtitan*-sized brontotheres from the middle Eocene of Asia. For instance, Qi and Beard (1996) referred other brontothere material to *Microtitan* sp., but that material, described further below, actually represents a small *Metarhinus*-like brontothere. *Metarhinus fluviatilis*, a brontothere from North America, was similar in size to the *elongatus* specimen. Given the lack of diagnostic features in the holotype of "*Microtitan*?" *elongatus*, this species is a nomen dubium.

Protitan major Huang and Zheng, 2004

HOLOTYPE: IVPP V13802, a maxillary fragment with right P5–M3.

TYPE LOCALITY: Nearby Lumeiyi Village, Lunan County, Yunnan Province; lower part of middle Eocene Lumeiyi Formation.

AGE: Middle Eocene (Sharamurunian land mammal "age"?).

DETERMINATION: Nomen dubium: holotype lacks diagnostic features, but it may be synonymous with *Metarhinus*.

REMARKS

Protitan major Huang and Zheng (2004) is a nomen dubium that was based on a maxilla fragment with P4–M3 (IVPP V13802). The fossil lacks sufficient character data to justify a new species. Moreover, the assignment of the specimen to the genus *Protitan* is erroneous. As Huang and Zheng (2004) note, the specimen is too large for any other known species of *Protitan*. More importantly, the molars of IVPP V13802 clearly display derived features not seen in species originally referred to *Protitan* by Granger and Gregory (1943), including a prominent anterolingual cingular cusp and a distinct central molar fossa. These same traits are seen in many advanced brontothere species. The holotype specimen has a molar-row length (220.5 mm) that is within the acceptable size range of many brontotheres that possess a set of molar characters identical to those of IVPP V13802, including anterolingual cingular cusps and central molar fossae. The P4 of the holotype, and the referred P2 (IVPP V13803) limit the taxonomic identity of IVPP V13802 considerably. These premolars lack hypocones, thus eliminating *Dianotitan* (from the same geologic formation), *Parabrontops*, *Pachytitan*, *Eubrontotherium*, and other similarly sized taxa that have well-developed hypocones on their premolars. Other taxa, including *Metatitan*, *Aktautitan*, and *Gnathotitan*, on the other hand, show more unstable lingual premolar morphologies, with more poorly developed premolar hypocones that are variably present and absent. Considering the intraspecific variability in premolar morphology, IVPP V13802 is consistent with any of these taxa. The proportions of the molars and the high relief on the lingual features of the P4 are particularly reminiscent of *Metatitan*. Therefore, *Protitan major* is a nomen dubium, and its holotype IVPP V13802 possibly belongs to a species of *Metatitan*.

cf. *Palaeosyops* sp. (*Palaeosyops* sp. sensu Gabounia, 1977)

AGE: Middle Eocene (Russell and Zhai, 1987).

REFERRED SPECIMEN: **(From Aksyr River, Lower Obayla Subsvita in the Zaysan Basin, central Kazakstan)** a right M1 or M2 (no number provided by Gabounia, 1977).

DETERMINATION: this tooth represents a small, unnamed *Palaeosyops*-like species, but

there is not a sufficient amount of character data to sufficiently describe or diagnose it.

REMARKS

The upper molar identified as *Palaeosyops* sp. by Gabounia (1977) from the Zaysan Basin of Kazakstan indicates a relatively primitive *Palaeosyops*- or *Eotitanops*-like brontothere (fig. 188). The tooth lacks derived brontotheriine characters and is more similar to *Palaeosyops* and *Eotitanops*; it has a short ectoloph, prominent labial ribs, rounded lingual margins of the paracone and metacone, a thickened parastyle cingular shelf, and a distinct paraconule. The ectoloph is wide, more than half as wide as the entire crown. In this respect, the tooth more closely resembles *Palaeosyops*; *Eotitanops* has slightly narrower ectoloph. However, this tooth is much smaller than any North American *Palaeosyops*. It also has very crenulated enamel, similar to *Bunobrontops savagei*. This specimen seems to represent an Asian species of *Palaeosyops*-like brontothere. Other *Palaeosyops*-like materials known from southeast Asia are described further below.

cf. *Metarhinus* sp. (*Microtitan* sp. sensu Qi and Beard, 1996)

AGE: Middle Eocene (Irdinmanhan land mammal "age").

REFERRED SPECIMENS: **(From IVPP locality 93006D, a fissure-filling located in the Shanghuang Limestone Quarry, near the village of Shanghuang, Liyang County, southern Jiangsu Province, China.)** IVPP V11017, a partial upper right M1 or M2, IVPP V11016, a left m1 or m2.

DETERMINATION: This material represents an additional species of Asian brontothere, possibly a species of *Metarhinus*. However, any species named from this material would be dubious; it cannot be differentiated from North American species of *Metarhinus*.

REMARKS

Qi and Beard (1996) referred a couple of small brontothere dental elements to *Microtitan* sp. The only complete element, the lower molar (m1 or m2) has a length of 26.1 mm and a width of 14.7 mm and is the right size for *Microtitan*. However, in other details, this material does not compare well with *M. mongoliensis*, the only valid species of *Microtitan*. The lower molar (IVPP V11016) has a less prominent hypoconulid in comparison to the neotype of *M. mongoliensis* (fig. 189a). The partial upper molar (IVPP V11017) exhibits a well-developed central molar fossa and a small anterolingual cingular cusp (fig. 189b); these are derived dental features not seen in *M. mongoliensis*. *Pygmaetitan panxianensis*, another small Asian brontotheriid, approaches these specimens in size; however, the lower molar of *Pygmaetitan* is higher crowned with much deeper trigonid and talonid basins. Among the remaining brontotheres with similarly advanced upper molars, only *Metarhinus* approaches the size range of these specimens. Although the material is consistent with *Metarhinus* it lacks specific characteristics that are diagnostic of *Metarhinus*. Therefore, the taxonomic identity of the material is dubious, although it can be differentiated from all other known Asian species and therefore represents an additional species on that continent.

Fig. 188. Upper molar from the Zaysan Basin of Kazakstan identified as cf. *Palaeosyops* sp. Actual size from Gabounia, 1977.

cf. *Palaeosyops* sp. (*Bunobrontops* sp. sensu Holroyd and Ciochon, 2000)

AGE: Middle Eocene.

REFERRED SPECIMEN: **(From "1 mi. N. Koniwa", Pondaung Formation, Myanmar)** two right m3 fragments, AMNH 32523a and AMNH 32523b.

DETERMINATION: Problematic taxon; this represents a *Palaeosyops*-like species, but the material lacks a sufficient amount of character data to justify a new species, nor

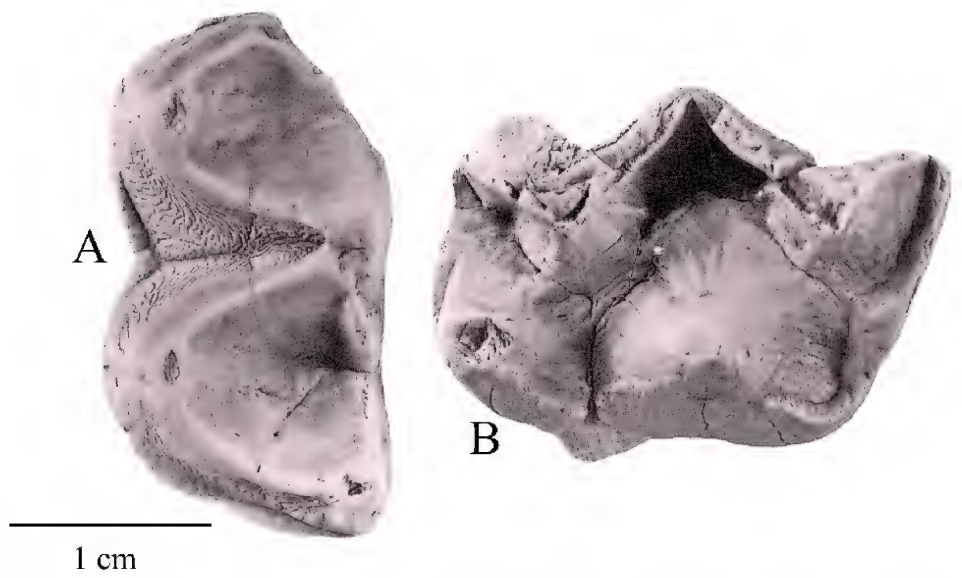

Fig. 189. Teeth referred to *Microtitan* sp. by Qi and Beard [1996] but probably representing a new brontotheres species of another genus. **(A)** Left m1 or m2 (IVPP V11016), **(B)** right M1 or M2 (IVPP V11017). Modified from Qi and Beard (1996).

can it be assigned to any particular genus or species.

Remarks

Holroyd and Ciochon (2000) referred two right m3 fragments, AMNH 32523a and AMNH 32523b, from "1 mi. N. Koniwa", to *Bunobrontops* sp. (fig. 190). The specimens are roughly 20 percent smaller than the material referred to *Bunobrontops savagei* by Holroyd and Ciochon (2000), but such minor size differences are of dubious taxonomic significance. The more complete of the two specimens, AMNH 32423b, a right m3, is less elongate than the m3 of *B. savagei* (UCMP 128414) and is more similar to *Palaeosyops* in its length/width ratio (~1.71). More importantly, it has developed a wear pattern that seems inconsistent with that of the upper molars of *Bunobrontops savagei*, but is consistent with more plesiomorphic brontotheres such as *Palaeosyops*. The peaks of the labial cusps have formed rounded pondlike exposures of dentin, bordered labially and lingually by very thick enamel. This is a wear pattern seen in the upper and lower dentition of basal brontotheres such as *Palaeosyops* and *Eotitanops*. *Bunobrontops savagei* upper molars seem to exhibit a more derived wear pattern seen in more advanced brontotheres where the upper and lower molars develop a strongly W-shaped wear facet along the ectoloph. A lower molar fragment referred to *Bunobrontops savagei* (UCMP 147048) exhibits the more derived lower molar wear pattern. However, AMNH 32523b exhibits the plesiomorphic wear pattern with rounded pondlike exposures of dentin. Therefore, these molars (AMNH 32523a and AMNH 32523b) seem to represent a species other than *Bunobrontops savagei*. The molar is similar in size and proportion to those of *Palaeosyops*, although the enamel is much thicker than that of *Palaeosyops* and the molar displays deep crenulations in the talonid and trigonid basins, similar to that of *Bunobrontops savagei*. Along with an upper molar of a small *Palaeosyops*-like species from Kazakstan reported by Gabounia (1977) (referred to above as cf. *Palaeosyops* sp.), this material represents one of the most primitive brontothere species in Asia.

Camp Margetts "taxon A"

Age: Middle Eocene (Irdinmanhan land mammal "age").

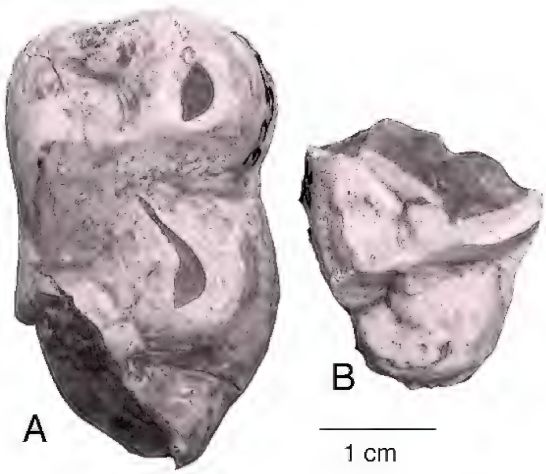

Fig. 190. Dental fragments from the Pondaung formation of Myanmar referred to *Bunobrontops* sp. by Holroyd and Ciochon, 2000, but referred to here as cf. *Palaeosyops* sp. **(A)** partial right m3 (AMNH 32423b), **(B)** posterior fragment of right m3 (AMNH 32423a).

REFERRED SPECIMENS: **(From the "Houldjin" Formation, Camp Margetts, Inner Mongolia)** AMNH 26408, a partial mandible with p2–m3; AMNH 26410, a partial mandible with right i1–i3?, p1–p4, and left i2?; AMNH 26415, a partial mandible with symphysis and left ramus with i2–m3; AMNH 26418, a juvenile mandible with right i3, p2–m2, m3 (erupting), left i3, p1–m2, and m3 (erupting); AMNH 26430, a partial left ramus with p3–m3; AMNH 26431, a right partial ramus with c–p1; AMNH 26432, a crushed left ramus with poorly preserved i3–m3.

DETERMINATION: This appears to be a new species, although it could represent *Protitan minor*.

DESCRIPTION

Seven mandibles from the Camp Margetts area of Inner Mongolia constitute a group that appears to represent an unrecognized species referred to as Camp Margetts "taxon A". None of these mandibles is complete. Among the specimens figured are AMNH 26415 (fig. 191a), AMNH 26410 (fig. 191b–f), and AMNH 26418 (fig. 191g). The most complete lateral view is of AMNH 26410. The inferior margin of the symphysis is slightly less than 45°. The symphysis of AMNH 26410 is not preserved, but the symphysis of AMNH 26415 extends to the talonid of p3. The incisors of AMNH 26415 are mostly broken, but the shape of the incisor row is intact in that specimen. There do not appear to be any diastemata between the incisors or between the incisors and canine of that specimen. The incisor row forms a moderate arch anterior to the canines. AMNH 26410 has a complete right incisor row. The right incisors of that specimen are large and relatively subcaniniform, with a mesiodistally elongated i3. Each has a lingual cingulid, but labial cingulids are absent. However, the incisor alveoli are not preserved in that specimen; the incisors are simply plastered onto the specimen and their arrangement is questionable. Nonetheless, the left i2 and i3 of AMNH 26410 are consistent with those of AMNH 26415. Finally, AMNH 26418 has an intact and unworn left i3 that is rooted inside an intact alveolus. The i3 crown of that specimen is distinctly more symmetrical than those of AMNH 26410 and AMNH 26415. There are no complete canines among any of these specimens, although the canine alveoli and/or canine fragments suggest canines of moderate size. The postcanine diastema is similar in length to p2.

The premolars are relatively slender and low crowned. The p1 is a narrow, single cusped tooth with a talonid heel. The p2 trigonid is distinctly longer than the talonid. The p3 trigonid is barely longer than the talonid. The p4 trigonid is a little shorter than the talonid. The p2 trigonid and talonid are of similar width, while the trigonids of p3 and p4 are slightly narrower than their talonids. The paralophid of p2 extends anteriorly from the protoconid. In AMNH 26410 the p2 paralophid is damaged, but in other specimens (e.g., AMNH 26418), the p2 paralophid arches in a slightly lingual direction and forms a small but distinct lingual trigonid notch. The protolophid of p2 is directed slightly lingually. The paralophids of p3 and p4 arch very strongly lingually and the protolophids of these premolars arch lingually a full 90°, thus forming molariform trigonid basins. Both the p3 and p4 have large, lingually positioned metaconids, but

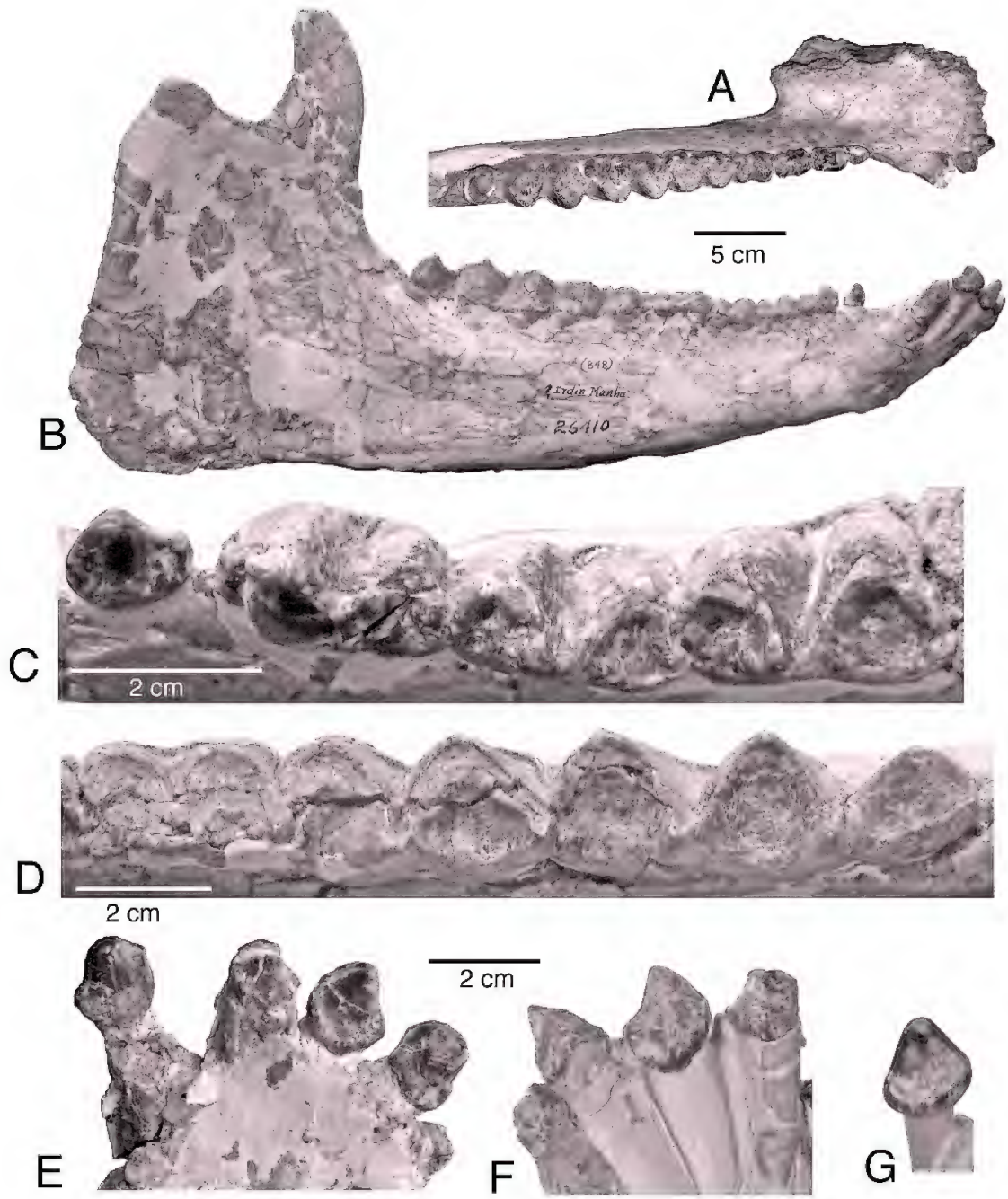

Fig. 191. Selected mandibles referred to Camp Margetts "mandible taxon A". **(A)** Dorsal view of AMNH 26415, **(B)** right view of AMNH 26410, **(C)** right premolars of AMNH 26410, **(D)** right molars of AMNH 26410, **(E)** lingual view of incisors of AMNH 26410, **(F)** labial view of incisors of AMNH 26410, **(G)** lingual view of i3 of AMNH 26418.

the p2 lacks a metaconid. Well-developed cristids obliqua and hypolophids can be seen on p2–p4. However, these structures are longer in more posterior premolars, thus forming broader and more nearly molariform talonid basins in p3 and p4. Lingual premolar cingulids are absent, while the labial premolar cingulids are weak.

The lower molars have relatively thin lingual enamel and shallow trigonid and talonid basins. The m3 of AMNH 26410 is among the most elongate for brontotheres with a length/width ratio of 2.95. However, the length/width ratios of other specimens (AMNH 26418, AMNH 26415, AMNH 26432, and AMNH 26413) are more moderate and range between 2.3 and 2.5. There are no lingual molar cingulids, but there are weak labial molar cingulids.

Remarks

Granger and Gregory (1943) referred three of the Camp Margetts "taxon A" specimens (AMNH 26410, AMNH 26415, AMNH 26418) to *Protitan minor*. However, these referrals were conjectural since none of the *P. minor* skulls is associated with a mandible or lower dentition. Another mandible (AMNH 26408) from the Camp Margetts area was referred to *Protitan grangeri* by Granger and Gregory (1943). In addition to these mandibles, other specimens (AMNH 26430, AMNH 26431, AMNH 26432) from Camp Margetts seem to represent a potentially unknown species of brontothere that can be characterized as having subcaniniform incisors and a relatively molariform p3 with a large molariform metaconid. The incisors are similar to "*Protitan*?" *cingulatus* although they appear to be more subcaniniform than those of *Protitan grangeri*. The relatively molariform p3 is altogether inconsistent with *Protitan grangeri*. The incisors and premolars lack the strong labial incisor and premolar cingulids seen in "*Protitan*?" *cingulatus* and the premolar crowns are not as tall. These specimens are similar to *Protitan minor* in size, but aspects of the lower dentition are not consistent with what one might predict for *Protitan minor*. The upper dentition of *Protitan minor* is undifferentiated from that of *P. grangeri*. Neither of these species has strongly molarized premolars; consequently, it is improbable that the p3 of *P. minor* would have possessed a large metaconid and strongly lingually arched paralophid and protolophid as seen in Camp Margetts "taxon A". For this reason, it seems improbable that Camp Margetts "taxon A" represents the mandibles of *P. minor*, although without associated skulls and mandibles this possibility cannot be discounted.

Camp Margetts "taxon B"

Age: Middle Eocene (Irdinmanhan land mammal "age").

Referred Specimen: **(From the "Houldjin" Formation, Camp Margetts, Inner Mongolia)** AMNH 26400, a partial mandible with right i1, i2, c, p2–m3, left i1, i2, i3 (partial), and p1–m1.

Determination: Probably a new species, but better material is needed to fully describe and diagnose it.

Description

The right ramus of AMNH 26400 is complete and its shape and proportions are reasonably intact (fig. 192). In comparison to other brontotheres, there is an unusually long gap between m3 and the ascending ramus. The inferior margin of the symphysis is angled less than 45°. From the dorsal view, the symphysis is relatively short and broad, and it extends to the talonid of p4.

The incisors project almost horizontally from the mandible and form a straight and narrow row between the incisors. Parts of all three incisors (i1–i3) are preserved on the left side, while i3 has been lost on the right side. Only the crowns of i1 and i2 are complete. Both are very small and are essentially vestigial with featureless, globular crowns. The i2 is slightly larger in diameter than the i1. Remnants of i3 on the left side suggest that the i3 was grossly similar in size to i1 and i2. The canines are of moderate size. There is no precanine diastema, but a short postcanine diastema can be seen on both sides.

The left p1 (present only on the left side) is very small with a single cusp and a small but wide talonid heel. The p1 is not preserved on the right side, but the remaining premolars of

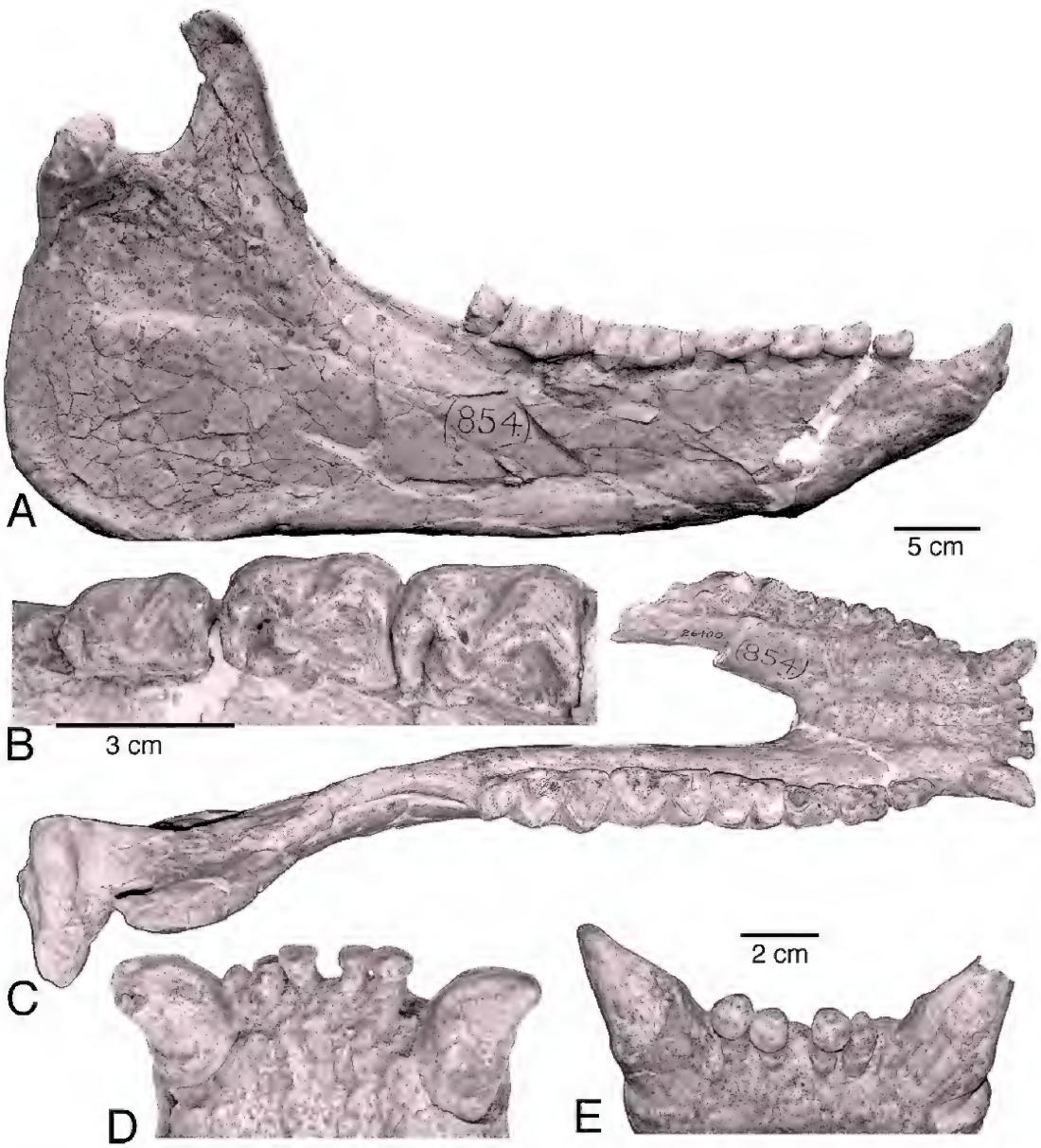

Fig. 192. Selected views of Camp Margetts "mandible taxon B" (AMNH 26400). **(A)** Right view, **(B)** right p2–p4, **(C)** dorsal view, **(D)** lingual view of incisors and canines, **(E)** labial view of incisors and canines.

that side are in better condition and are shown in close-up. The crowns of p2–p4 are relatively broad. The trigonid and talonid of p2 are of similar length and width. The trigonids of p3 and p4 are shorter and narrower than the talonids. The paralophid of p2 is very strongly arched lingually, and the protolophid is straight but angled lingually, thus creating a narrow but deep lingual trigonid notch. The paralophids and protolophids of the p3 and p4 are fully lingually arched, creating deep and broader lingual trigonid notches. A large lingually positioned metaconid can be seen only on p3 and p4. The labial notch of the p2 between the trigonid and talonid is broad and

shallow; it is not deep and narrow as the same notch in *Metatitan primus* or *M. relictus*. The talonids of the p2–p4 have long cristids obliqua and hypolophids with nearly molariform talonid basins. The molars are typical, with shallow talonid and trigonid basins and thin lingual enamel; however, m3 is atypically short in comparison to most brontotheres of similar size (e.g., *Metatitan*). The m3 length/width ratio (2.0) is more similar to more primitive species like *Palaeosyops* and *Bunobrontops*.

Remarks

The mandible, AMNH 26400, shows a combination of traits that strongly suggests yet another species of brontothere from the Camp Margetts area although, in my judgment, the material is too incomplete to properly diagnose or describe it. This mandible is grossly similar in size to those of *Metatitan*. The broad premolars, unreduced number of incisors, and posteriorly shifted mandibular symphysis are a *Metatitan*-like combination of traits. AMNH 26400 is most similar to *Metatitan khaitshinus*. Both have broad labial notches on p2, whereas the p2 labial notches of *M. primus* and *M. relictus* are deep and narrow. The incisors of AMNH 26400 seem smaller and more globular than those of *M. khaitshinus*, but this could relate to extensive incisor wear in AMNH 26400. Nonetheless, there are more substantial differences. For instance, AMNMH 26400 has a short postcanine diastema, while postcanine diastemata are lacking in all three species of *Metatitan*. Perhaps more compellingly, the m3 of AMNH 26400 is very short, with a long gap between the m3 and the ascending ramus. The short m3 and associated gap is unlike *Metatitan* and other brontotheres of similar size.

Hyotitan thomsoni is another large brontothere from the Camp Margetts area with small incisors and a short m3. However, *Hyotitan* is substantially larger than AMNH 26400, the symphysis is more elongate and it does not extend as far posteriorly, and the postcanine diastema is much longer, and the hypoconulid of m3 is much narrower. Moreover, the gap between the m3 and the ascending ramus is very narrow in *Hyotitan thomsoni*.

Camp Margetts "taxon C"

Referred Specimen: **(From Camp Margetts, ?"Houldjin" Formation, Inner Mongolia)** AMNH 26425, a crushed right ramus with canine and p1 alveoli, crushed root remnants of p2 and p3, and incompletely preserved p4–m3.

Age: Middle Eocene (Irdinmanhan land mammal "age").

Determination: This is a new species, but better material is needed to fully describe and diagnose it.

Description

This single mandible (AMNH 26425) indicates an individual roughly similar in size to *Protitan* and *Epimanteoceras* (fig. 193). The ramus is flattened, but from a lateral view, the proportions of the ramus seem more or less intact. The symphysis is incomplete, but it extended at least to the anterior margin of the p2. The incisors, canine, and p1 are not preserved. However, parts of the canine alveolus are present and the p1 alveolus is intact. The p2 is represented only by root fragments. A small portion of the posterior end of the p3 crown is preserved. The p4 and molars are mostly complete. The postcanine diastema is at least 3.5 cm in length; however, the exact margin of the canine alveolus is not preserved. Additionally, there is a diastema nearly 2 cm long between the p1 alveolus and fragmented p2 roots. The dorsal surface of the ramus between the p1 alveolus and p2 is relatively undamaged and clearly forms a distinct p1–p2 diastema.

The remaining dental elements are not particularly informative. The p4 trigonid is incomplete, but a large molariform metaconid can be identified. The molars have shallow trigonid and talonid basins and the m3, though incomplete, is elongate.

Remarks

Not many brontotheres have a long p1–p2 diastema. A short-long p1–p2 diastema can be found in the primitive brontotheres *Eotitanops* and *Palaeosyops*, but these taxa can clearly be ruled out due to their smaller

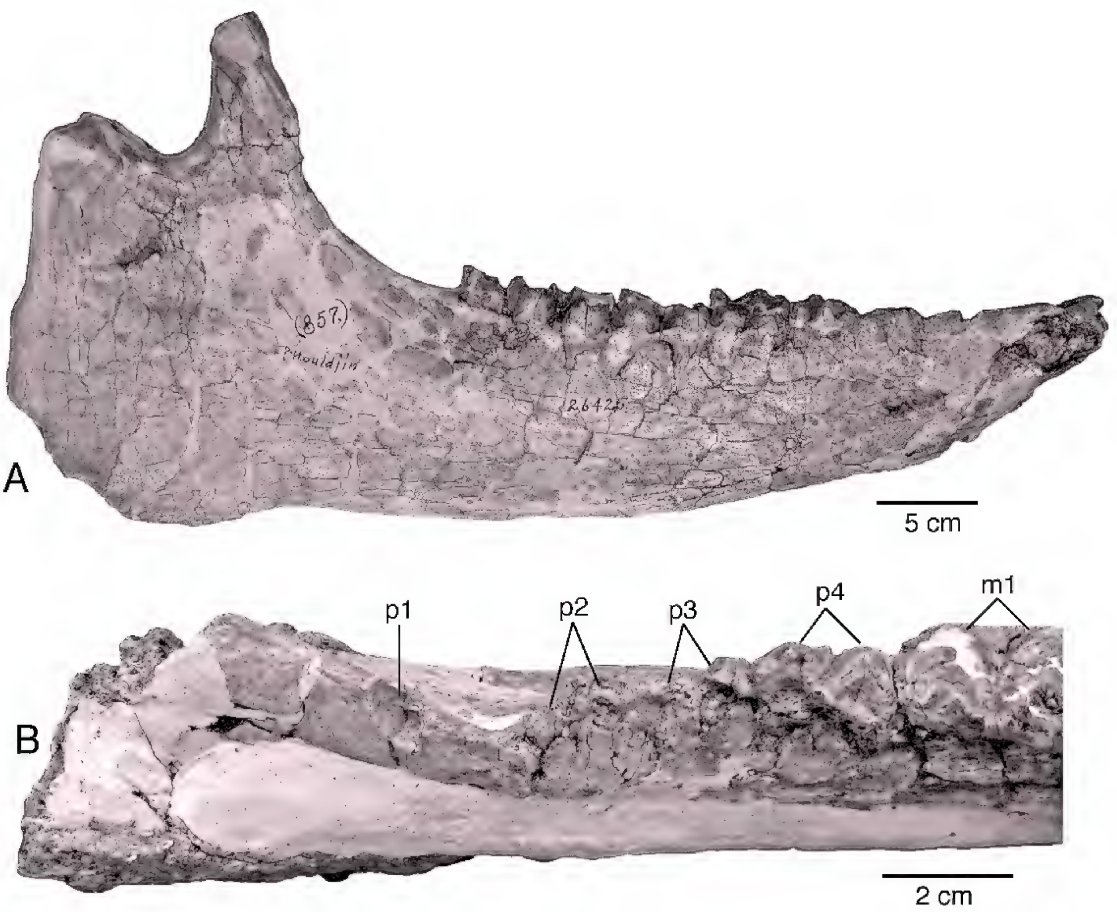

Fig. 193. Selected views of Camp Margetts "mandible taxon C" (AMNH 26425). **(A)** Lateral view, **(B)** dorsal view, showing p1–p2 diastema.

size and shorter m3 proportions. *Desmatotitan tukhumensis*, *Mesatirhinus megarhinus*, *Metatelmatherium ultimum*, and occasionally *Telmatherium validus* exhibit a very short p1–p2 diastema. In *Dolichorhinus hyognathus* the p1–p2 diastema is variable and ranges from 7–18 mm. The p1–p2 diastema of AMNH 26425 (17 mm) falls in the upper range of diastema length of *Dolichorhinus hyognathus*. However, AMNH 26425 (m1–m3 length = 175 mm) falls well above the size range of *Dolichorhinus* (tooth-row length = 115 mm–141 mm). This specimen is possibly a close Asian relative of *D. hyognathus*.

PHYLOGENETIC CHARACTERS

Described and included in the following phylogenetic analysis are 87 cranial, dental, and mandibular characters. The sources for the characters are based mostly on direct observations of fossil specimens or casts. For the most part, I found the preexisting descriptions of brontotheres, the vast majority of which are in the older literature (e.g., Earle, 1892; Osborn, 1929a; Granger and Gregory, 1943), to be unsuitable for compiling phylogenetic character data. Earlier researchers tended to place emphasis on certain characters (premolar cusps) or their proportions (e.g., tooth length/width proportions) that were perceived as phylogenetically important, often describing these characters to a meticulous degree (especially in terms of perceived evolutionary direction rather than describing the morphologically static specimen), but tended to ignore or only make brief mention of other phylogenetically informa-

tive characters. Moreover, earlier authors did not always carefully consider taphonomic distortion and ontogenetic effects, such as dental wear. For instance, the relative proportions of the cheek teeth have often been used to diagnose species and postulate phylogenetic relationships; however, much of the apparent variation in length/width proportions of brontothere teeth relates to dental wear. Additionally, many of the illustrations published in older monographs of important holotypes and other specimens are often misleading. Frequently, specimens are incorrectly depicted as complete, undamaged, undistorted, and in some cases with cracks misrepresented as sutures. Therefore, characters described or figured in the literature were not used unless they were verified on actual specimens, or in a few cases, on casts and photographs.

Throughout the processes of character discovery and character-data collection, the influences of ontogeny (particularly dental wear) and taphonomic distortion were considered to the extent that is was possible by examining fossil specimens with the naked eye. For the most part, characters whose variable states seemed related to taphonomy or ontogeny rather than phylogeny were not used. The majority of the skulls and mandibles used in this analysis are distorted, and although many times the distortion is obvious, other specimens show very subtle (and often plastic) deformation that is often easy to overlook. Subtle, plastic deformation is particularly troublesome for species known from very few specimens. Brontotheres vary most conspicuously in the shapes of their skulls; consequently, many of the characters must relate to aspects of skull shape. It is entirely possible that at least a small amount of character data has been incorrectly coded due to subtle distortion, particularly for characters relating to differences in skull shape. Further discoveries or different methods of analysis (e.g., quantitative morphometrics) may lead to the modification of some of the character data in the future.

A limited number of the characters used here are similar to those used by Mader (1989; 1998), although in many cases these characters were defined somewhat differently and/or have been further subdivided into more character states. Selection criteria for the inclusion of characters are a nonautapomorphic distribution and amenability to description as states that differentiate taxa. For some potential characters, I found it difficult or impossible to define character states due to excessive intraspecific polymorphism. For instance, there are several potential characters among the lingual structures of the upper premolars such as the hypocone lingual crest and cingulum; however, these structures were found to have intraspecific polymorphic tendencies. For characters that showed polymorphic tendencies, I defined the characters and their character states in such a way that the definitions were sufficiently broad to encompass the morphological variation seen within species but narrow enough to delimit differences between taxa. Some highly polymorphic characters were impossible to divide into character states because all or most of the observed variability appeared to be intraspecific rather than interspecific. For instance, canine size is so variable among many of the species that all of the potential states (e.g., small canine, large canine, intermediate sized canine) were found to be intraspecifically polymorphic. It was therefore impossible to define character states of canine size in a way that was sufficiently broad to encompass the observed intraspecific variability, but that also clearly defined differences between taxa.

Conspicuous variability was also found with horn size, although it is not possible to divide this variability into a multitude of discrete character states. Species known from large samples tend to consist of a mixture of robust specimens with large horns, and more gracile specimens with smaller horns. Lucas and Schoch (1989b) and Mihlbachler et al. (2004b) point out that much of the seemingly continuous variation in horn size and general cranial robustness is consistent with sexual dimorphism. Whether brontotheres are sexually dimorphic is open to question, but in any case, it was mostly impossible to define character states of horn size that were sufficiently broadly defined to encompasses intraspecific variation and at the same time sufficiently narrowly defined to delimit clear morphological boundaries between taxa.

Throughout the following descriptions of characters and their states, I use the terms "horned" brontotheres (those species with conspicuous frontonasal protuberances that have been assigned states 3–4 for character 3) and "hornless" brontotheres (those without conspicuous frontonasal protuberances, assigned states 0–2 for character 3). These terms are not meant to denote clades (although horned brontotheres do appear to form a clade), but for many characters they provide a convenient way to describe the distribution of character states since roughly half of brontotheres are hornless and the other half are horned. The outgroup referred to in the following character descriptions includes *Hyracotherium* sensu lato (specifically, *Xenicohippus osborni* of Froehlich, 2002), *Pachynolophus*, *Danjiangia*, and *Lambdotherium*.

Cranial Characters

Character 1: *Postorbital cranium: (0) not elongate, (1) elongate.*

In *Hyracotherium*, *Pachynolophus*, and *Lambdotherium* the portion of the skull anterior to the orbit is nearly equal in length to the part of the skull posterior to the orbit (state 0). In true brontotheres, the postorbital cranium is longer than the preorbital portion of the skull (state 1). In an earlier analysis, Mader (1989, 1998) regarded *Eotitanops* as having an elongate face and short postorbital cranium. However, this interpretation was based on a partial skull (AMNH 14887) that is heavily reconstructed with plaster. A complete skull of *Eotitanops* (UCMP 132049) indicates that it shared the condition seen in other brontotheres where the postorbital cranium is longer than preorbital portion of the skull.

Character 2: *Overall skull proportions: (0) not elongate, length/width ratio* $\leq$ *2.0, (1) elongate, length/width* $>$ *2.0.*

There is considerable variation in the general length/width proportions of the skulls of brontotheres. Previously, length/width cranial indexes were used for interpreting brontothere phylogeny (Osborn, 1929a; Granger and Gregory, 1943). However, changes in length/width proportions are affected by a variety of separate characters, such as lateral expansion of the zygomatic arches, widening of the occiput, and/or the reduction of the premaxillae. Each of these derived conditions is treated as a different character below.

Character 2 refers to changes in head proportions that are unrelated to specializations in any particular region of the skull. The length/width ratios of most brontothere outgroup skulls range from 1.2–2.0 (state 0). However, there are two brontotheres, *Dolichorhinus hyognathus* and *Sphenocoelus uintensis*, whose skulls are conspicuously elongate with length/width ratios exceeding 2.0, and ranging as high as 2.8 (state 1). Neither of these species has unusual derived specializations in any specific region of their skulls. Rather their hyperdolichocephalic proportions are a reflection of the overall elongate shape of their heads.

Character 3: *Bony protuberance (horn): (0) absent, (1) small swelling primarily on nasal bone, (2) inconspicuous frontonasal swelling, (3) conspicuous paired frontonasal horns, (4) frontonasal horns extremely long.*

The earliest brontotheres, mostly from the Wasatchian, Bridgerian, and Uintan land mammal ages of North America, lack distinct hornlike protuberances altogether (state 0). Some species, such as *Telmatherium validus* are often interpreted as having small horns, but the actual specimens reveal no such structures. *Dolichorhinus* is the only brontothere known to have a small swelling that is primarily on the nasal bone (state 1). In other brontotheres, the swelling occurs on both the nasal and frontal bone. In *Epimanteoceras*, there is a small frontonasal swelling, but it is rather inconspicuous in comparison to horned brontotheres (state 2). Most other horned brontotheres (e.g., *Protitan*, *Diplacodon*) have more conspicuous frontonasal swellings (state 3). Horn size appears to vary intraspecifically about as much as it does interspecifically. Horn size variation in brontothere species follows a pattern that is consistent with mammalian sexual dimorphism, whereby sexually dimorphic structures (e.g., horns, tusks) tend to be far more variable than other metric variables (e.g., tooth-row length) (Mihlbachler et al., 2004b). For example, *Diplacodon elatus* skulls vary only slightly in overall size, although the

horns vary in size from virtually absent to large and conspicuous. Finally, two species, *Megacerops kuwagatarhinus* and *Megacerops coloradensis*, have horn lengths that greatly exceed those of all other species, despite the conspicuous intraspecific variability in horn length (state 4).

Character 4: *Frontonasal horns: (0) widely spaced, (1) narrowly spaced, (2) fused into a single transverse crest.*

This character is inapplicable to taxa that lack nasal or frontonasal protuberances. The paired horns are most commonly spaced widely apart transversely (e.g., *Protitan*) (state 0). In other words, there is a significant gap between the horns. In all three species of *Metatitan* and in *Aktautitan hippopotamopus* the horns are positioned more closely together (state 1). In *Nasamplus*, *Protembolotherium*, and *Embolotherium*, the frontonasal protuberances are completely fused into a single transverse crest at the peak of the large ramlike frontonasal process (state 2).

Character 5: *Frontal bone: (0) does not overlap the nasal bone or intrude into the nasal bone, (1) overlaps the nasal bone or intrudes into the nasal bone.*

In the outgroup and among some hornless brontotheres, the frontal does not overlap, or intrude into, the nasal bone (state 0). In some hornless brontotheres (e.g., *Telmatherium validus*), a pair of anteriorly projecting triangular processes of the frontal bone either overlaps the nasal bone or appears to intrude into its posterior side (state 0). In this condition, the overlapping or intruding triangular frontal process appears to split the nasal bone at the surface of the skull, thus forming a posterolaterally arched process of the nasal bone that stretches between the maxilla and frontal bone, thus maintaining a contact of the nasal and lacrimal. The presence of the overlapping frontal processes has long been recognized in *Telmatherium* (Osborn, 1929a; Mader, 1989, 1998). However, this condition is found to be far more widespread among hornless brontotheres and is now observed in *Sthenodectes incisivum*, *Metarhinus fluviatilis*, *Metatelmatherium ultimum*, *Qufutitan zhoui*, and *Wickia brevirhinus*. Horned brontotheres for which facial sutures are visible share the same frontonasal configuration; the horn is actually formed by the nasal bone and the overlapping triangular projection of the frontal bone. This character was could not be scored for several species due to a lack of discernable facial sutures in the available specimens.

Character 6: *Position of posterior margin of nasal incision: (0) anterior to the premolars, (1) between the anterior margin of P1 and the anterior margin of P2, (2) between the anterior margin of P2 and the posterior margin of P3, (3) between the anterior margin of P4 and the posterolateral root of M1, (4) positioned at the posterior margin of M1 or more posterior.*

Within brontothere species, there is typically a minor amount of fluctuation in the exact position of the posterior border of the nasal incision with respect to the teeth. Some of this minor intraspecific variation may relate to subtle taphonomic distortion. The character states, as they are here defined, fully encompass the intraspecific fluctuation observed for this character. The exact positions of the posterior margin of the nasal incisions of *Microtitan mongoliensis* and *Gnathotitan berkeyi* are uncertain although the available fossil material is sufficient to rule out states zero and one for both species. However, the available fossil material of both species is consistent with states two, three, and four. Therefore, these species were assigned all three of these states.

Character 7: *Nasal process: (0) originates from an unelevated position, (1) semielevated, (2) fully elevated, (3) sometimes present in elevated position, but very reduced, (4) lost or absorbed by the frontonasal process.*

In most brontotheres, the nasal process projects from the skull at a point that is about as high as the upper margin of the orbit (state 0), although several brontotheres have nasal processes that are elevated to varying degrees, resulting in a dorsoventrally deepened nasal cavity. For instance, in *Rhinotitan* and *Diplacodon*, the nasal process is semielevated (state 1). In these taxa, the nasal process originates from a point much higher than the orbit. A further derived condition is seen in *Aktautitan*, *Metatitan*, and *Nasamplus* (state 2). In these taxa, a large frontonasal process extends anterodorsally from the top of the skull and the horizontal nasal process is elevated to the peak of this

frontonasal process. The nasal process of *Protembolotherium* is reduced and sometimes absent, but when present it is extremely elevated at the peak of the tall ram (frontonasal process) (state 3). Finally, in *Embolotherium*, the free end of the nasal process, which originally would have been elevated to the peak of the frontonasal ram, as seen in *Protembolotherium*, has been completely lost or absorbed (Mihlbachler et al., 2004a) (state 4).

Character 8: *Nasal process: (0) narrow, (1) broad.*

All hornless brontotheres have narrow nasal processes. In this condition, the premaxillomaxillary rostrum is typically wider than the nasal process and, therefore, the nasal process does not completely obscure the premaxillomaxillary rostrum from a dorsal view of the skull (state 0). Horned brontotheres (e.g., *Protitan grangeri*) typically have a broader nasal process. In this state, the nasal process is typically as wide or wider than the rostrum, so that it entirely obscures the rostrum from a dorsal view of the skull (state 1).

Character 9: *Distal edge of nasal: (0) thin, (1) thickened.*

In *Hyracotherium*, *Pachynolophus*, *Danjiangia*, and *Lambdotherium*, the distal margin of the nasal process is relatively thin (state 0). This condition characterizes hornless brontotheres, and some horned brontotheres as well (e.g., *Protitan grangeri*). In the majority of horned brontotheres, the distal margin of the nasal process is substantially thickened (e.g., *Protitanotherium emarginatum*) (state 1).

Character 10: *Lateral walls of the nasal process: (0) thin, shallow lateral walls, (1) thin, deep lateral walls, (2) thickened lateral walls, (3) thickened lateral walls with upturned lateral edges.*

In *Hyracotherium*, *Pachynolophus*, and *Danjiangia*, the lateral walls of the nasal process are relatively shallow and thin (state 0). This condition also characterizes *Metarhinus fluviatilis* and *Metarhinus abbotti*. In other hornless brontotheres and in some horned brontotheres (e.g., *Metatitan primus*), the lateral walls of the nasal process are deeper but are still relatively thin (state 1). In other horned brontotheres (e.g., *Protitan grangeri*), the lateral walls of the nasal process are thickened and shallow (state 2). In this condition, the lateral walls are deepest proximally and shallower distally. *Diplacodon* possesses a further derived state where the lateral margins of the premaxillary processes are thickened and upturned slightly (state 3). *Lambdotherium* was assigned states 0 and 1 because the available fossil material was sufficient to rule out other states but not to distinguish between these two conditions. This character is inapplicable to *Protembolotherium* and *Embolotherium* due to the reduction and eventual loss of a free nasal process.

Character 11: *Lateral walls of nasal process: (0) not inrolled, (1) inrolled.*

In the outgroup and among most brontotheres the lateral walls of the nasal process are nearly vertical or very weakly angled medially at the proximal end of the nasal process (state 0). However, in *Rhinotitan andrewsi* and *Pachytitan ajax*, the lateral walls at the proximal end of the nasal process are strongly angled ventromedially and constrict the portion of the nasal cavity between the lateral walls (state 1). In some specimens of *Rhinotitan andrewsi*, the lateral nasal walls nearly make contact at the midline of the skull (Wang, 1982). This character could not be applied to *Protembolotherium* and *Embolotherium* due to the reduction and eventual loss of the free nasal process.

Character 12: *Frontonasal process (ram): (0) straight, (1) posterodorsally curved.*

From a lateral view, the horns of nearly all horned brontotheres are perched upon a short bony pillar that rises from above the orbits at an anterodorsal angle that is typically about 45° or less. The highly modified rams of *Protembolotherium* and *Embolotherium* are structurally equivalent to the frontonasal process, but with the horns fused together at the distal peak. The ram of *Embolotherium grangeri* retains the straight, roughly 45° orientation seen in other horned brontotheres. Therefore *E. grangeri* retains state 0. In *E. andrewsi* and *Protembolotherium efremovi*, however, the frontonasal process is steeper and it curves in a posterodorsal direction so that the peak of the frontonasal process is either nearly vertical or fully vertical (state 1).

Character 13: *Position of anterior rim of orbit: (0) above M2 (1) above M1, (2) anterior to M1.*

This character describes the relative position of the orbits with respect to the molars. Most brontotheres differ little from the outgroup, with the anterior rim of the orbit above M2 (state 0) or M1 (state 1). However, some brontotheres (e.g., *Notiotitanops* and *Megacerops*) have more anteriorly shifted orbits where the anterior orbital rim is anterior to M1 (state 2).

Character 14: *Orbits: (0) not laterally protruding, (1) moderately laterally protruding, (2) more extremely laterally protruding.*

The appearance of laterally protruding orbits is manifested by a recessed surface of bone between the nasal incision and the anterior border of the orbit that forms a narrow wall of bone just in front of the orbits that faces partly anteriorly, rather than completely laterally as in other brontotheres. This condition gives the appearance of laterally protruding orbits, and is most extreme in *Metarhinus fluviatilis* and *Metarhinus abbotti* (state 2), while more moderate in *Sthenodectes incisivum* and *Fossendorhinus diploconus* (state 1). Other brontotheres lack laterally protruding orbits (state 0).

Character 15: *Infraorbital jugal process: (0) absent, (1) small, (2) large.*

Mesatirhinus, *Sphenocoelus*, and *Dolichorhinus* have a prominent process on the ventral surface of the jugal just under the orbit (state 2). Among these taxa, the infraorbital jugal process is large and often projects in a nearly lateral direction. *Metarhinus fluviatilis and Metarhinus abbotti* have similar infraorbital processes, but they are smaller and not as laterally oriented (state 1). Other brontotheres lack an infraorbital jugal process (state 0).

Character 16: *Premaxillomaxillary rostrum: (0) deepens proximally, (1) does not deepen proximally.*

Normally, the premaxillomaxillary rostrum is roughly triangular from a lateral view. In other words, the dorsolateral margin of the rostrum is sloped posterodorsally; consequently the rostrum is deep proximally and shallow distally (state 0). However, *Fossendorhinus diploconus*, *Metarhinus fluviatilis*, *Metarhinus abbotti*, and *Dolichorhinus hyognathus* have a rostrum that is shallower overall. In these taxa, the dorsal surface of the rostrum is more or less horizontal, and the rostrum does not deepen posteriorly. Rather the depth of the rostrum is nearly constant throughout its length (state 1).

Character 17: *Premaxillomaxillary rostral cavity: (0) open dorsally and continuous with the nasal cavity, (1) sealed dorsally by a bony cover, separated from the nasal cavity.*

Normally, the ventral and lateral sides of the premaxillomaxillary rostrum encapsulate a cavity that is open dorsally and forms a continuous space with the nasal cavity (state 0). Three brontotheres, *Dolichorhinus*, *Metarhinus fluviatilis*, and *Metarhinus abbotti*, share a unique and highly derived condition whereby the rostrum is enclosed dorsally by a bony covering (state 1). This dorsal covering completely seals off the rostral cavity and separates it from the nasal cavity. The dorsal bony covering emerges from the medial walls of the maxillaries, is sutured to the inner edges of the nasal processes of the premaxillae, and extends posteriorly into the skull. The bony cover is possibly derived from the ventral maxilloturbinate crest.

Character 18: *Premaxilla: (0) thin, contacts nasals, (1) robust, does not contact nasals, highly constricted symphysis, (2) robust, does not contact nasals, longer symphysis.*

This character is similar to one used by Holbrook (1999, 2001) for analyses of tapiromorph phylogeny. Primitively, the premaxilla is a small, thin bone with a short premaxillary symphysis, and a tall ascending process that contacts the nasals (state 0). This state persists in *Eotitanops*. In all other brontotheres the premaxilla is a much thicker element and contact with the nasal is lost entirely. Among those taxa with robust premaxillae, there is variation in the length of the symphysis. In *Palaeosyops*, the premaxillary symphysis is still very short, despite the robust state of the premaxilla (state 1). In contrast, the premaxillary symphyses of other brontotheres with robust premaxillae tend to be longer (state 2).

Character 19: *Premaxillary symphysis: (0) angled with flat or convex anterodorsal surface, (1) vertical with concave anterior surface.*

In the majority of brontotheres, the premaxillary symphysis is angled with a convex anterodorsal surface (state 0). In *Qufutitan* and *Embolotherium*, however, the premaxillary symphysis is decidedly more vertical with a somewhat concave anterior surface (state 1).

Character 20: *Dorsal surface of skull: (0) nearly flat above the orbits, strongly convex over the postorbital cranial region, (1) slightly concave above orbits and nearly flat over the postorbital cranial region, (2) entire dorsal surface of the skull is concave, or saddle-shaped.*

In the outgroup and among some hornless brontotheres, the dorsal surface of the skull above the orbits is nearly flat from a lateral view, while the dorsal surface of the postorbital cranial region is convex (state 0). Other brontotheres, such as *Telmatherium validus* and *Epimanteoceras formosus*, show an intermediate condition in which the midcranial dorsal surface is convex, while the dorsal surface over the posterior portion of the skull is slightly convex or nearly flat (state 1). Most horned brontotheres have completely saddle-shaped crania (e.g., *Protitan grangeri*), where the dorsal surface of the cranium is completely concave from the horns to the nuchal crest (state 2); however, the *Telmatherium*-like intermediate condition (state 1) seems to have been secondarily derived in *Metatitan* and *Rhinotitan kaiseni*. *Rhinotitan andrewsi* was coded with states 1 and 2, due to ambiguity in the interpretation of the existing specimens.

Character 21: *Dorsal cranial dome: (0) absent, (1) small, variably present, (2) present.*

Duchesneodus uintensis has a large dome on the dorsal surface of the skull between the parasagittal ridges (state 2). The size of this dome varies, but it is always present. *Metatitan primus* has a dorsal dome similar to that of *Duchesneodus*. Numerous specimens of *Megacerops coloradensis* have smaller domes, but they are sometimes absent (state 1). Other brontotheres lack this cranial dome (state 0).

Character 22: *Postorbital width of skull (0) constricted, (1) not constricted.*

The crania of *Hyracotherium*, *Pachynolophus*, and *Lambdotherium* are strongly transversely constricted behind the orbit (state 0). All true brontotheres lack a strong postorbital constriction (state 1). This trait is unknown for *Danjiangia*.

Character 23: *Sagittal crest: (0) true sagittal crest, (1) parasagittal ridges closely converge, but do not actually make contact, (2) parasagittal ridges remain separate, but the dorsal surface of the skull is strongly constricted, (3) dorsal surface of skull is moderately constricted, (4) dorsal surface of skull is minimally constricted by parasagittal ridges, if at all.*

In the outgroup and among most of the hornless brontotheres (e.g., *Mesatirhinus*), the parasagittal ridges merge posteriorly into a sagittal crest (state 0). In others (*Telmatherium* and *Wickia*), the parasagittal ridges strongly converge medially, but they do not actually make contact. Instead, they remain separated by a narrow gap, and form a relatively thick sagittal crest (state 1). In *Dolichorhinus* and a number of horned brontotheres (e.g., *Protitan*), a true sagittal crest is absent. Instead, the parasagittal ridges remain separated, but they strongly constrict the dorsal surface of the cranium (state 2). Other brontotheres (e.g., *Eubrontotherium clarnoensis*) express another intermediate condition by which the parasagittal ridges only moderately constrict the dorsal surface of the cranium (state 3). Finally, *Rhinotitan*, *Metatitan*, *Protembolotherium*, and *Embolotherium* express the most extreme condition, by which the dorsal surface of the skull is comparatively wide and barely constricted, if at all, by the parasagittal ridges (state 4).

Character 24: *Zygomatic arch: (0) strongly curved, (1) weakly curved, (2) straight.*

From lateral views of the skulls of brontotheres, the curvature of the zygomatic arch varies. The zygomatic process of the jugal bone is always more or less horizontal and the degree of zygomatic curvature is mostly determined by the angle of the zygomatic process of the squamosal, which is either strongly sloped posterodorsally, weakly sloped posterodorsally, or it is roughly the same angle as the zygomatic process of the jugal. In *Hyracotherium*, *Pachynolophus*, *Lambdotherium*, and many hornless brontotheres (e.g., *Sphenocoelus*) the

zygomatic arch is weakly curved (state 1). Several of the most advanced horned brontotheres such as *Embolotherium grangeri* also have weakly curved zygomatic arches. A variety of hornless brontotheres have more strongly curved zygomatic arches, including *Eotitanops*, *Palaeosyops*, *Sthenodectes*, *Metarhinus, Metatelmatherium*, and others (state 0). Finally, many horned brontotheres, such as *Protitan*, *Rhinotitan*, and *Metatitan*, have essentially straight zygomatic arches (state 2).

Character 25: *Zygomatic arches: (0) nearly parallel, (1) posteriorly divergent, (2) strongly arched laterally.*

In *Hyracotherium* and *Pachynolophus*, the zygomatic arches are nearly parallel from dorsal or ventral views of their skulls (state 0). A similar condition is retained by a number of hornless brontotheres such as *Mesatirhinus*, *Dolichorhinus*, and *Sphenocoelus*. Discounting the large swelling in the center of the arch (see character 26), *Embolotherium andrewsi* has parallel zygomatic arches as well. In a number of hornless brontotheres (e.g., *Sthenodectes*) and all horned brontotheres except *E. andrewsi*, the jugal process of the zygomatic arch is strongly angled posterolaterally, resulting in posteriorly diverging zygomatics arches (state 1). Finally, three taxa, *Palaeosyops*, *Metatelmatherium*, and *Wickia*, depart from both of the above conditions and have zygomatic arches that are very strongly bowed laterally (state 3).

Character 26: *Lateral swellings of zygomatic arch: (0) absent, (1) present.*

A large bony swelling in the center of the zygomatic arch at the junction of the jugal and squamosal bones is common among many of the larger horned brontothere taxa, such as *Protitanops*, *Dianotitan*, *Duchesneodus*, *Megacerops*, *Embolotherium* and *Protembolotherium*. Such swellings are absent in other brontotheres and within the outgroup (state 0).

Character 27: *Postzygomatic process: (0) absent, (1) present.*

Species of *Metatitan* and *Protitan* have a distinct postzygomatic process on the squamosals (state 1). This process ascends from the superior surface of the posterior end of the zygomatic arch. It may have served as an enlarged attachment for the temporal branch of the frontoscutularis or the zygomaticoauricularis muscles that elevate and rotate the ear (Sisson and Grossman, 1953). Other brontotheres do not have a prominent postzygomatic process (state 0).

Character 28: *Position of anterior margin of posterior nares: (0) anterior to the protocone of the M3, (1) usually between the M3 protocones or somewhat behind the M3 protocones, (2) at the posterior margin of the M3 or behind the M3.*

In the majority of brontotheres, the anterior margin of the posterior nares is situated between the M2 and the M3 (states 0 and 1). *Dolichorhinus*, *Metatitan*, *Protembolotherium*, and *Embolotherium* have posterior nares that are positioned at the posterior margin of M3 or even farther behind M3 (state 2).

Character 29. *Emargination of posterior nares: (0) absent or very narrow, (1) present and of moderate width, (2) present and wide.*

In most brontotheres, the posterior nares are emarginated on the anterior and lateral sides by a horseshoe-shaped rim of bone. This rim is absent in some hornless brontotheres (e.g., *Mesatirhinus*) and horned taxa, *Diplacodon*, *Dianotitan*, *Duchesneodus*, and *Megacerops* (state 0). An emargination of moderate width is seen in some hornless brontotheres (e.g., *Telmatherium*) and most horned brontotheres (state 1). The emarginations of the posterior nares of *Metatitan*, *Protembolotherium*, and *Embolotherium* are considerably wider than those of other taxa (state 2).

Character 30: *Maxilloturbinates: (0) not exposed in choanae of posterior nares, (1) extend behind the anterior rim of the posterior nares.*

The maxilloturbinates typically do not extend posteriorly beyond the choanae of the posterior nares (state 0). However, in some brontotheres, the ventral maxilloturbinates appear to form thin pouches that extend beyond the posterior nares and into the elongated posterior narial passageway on the ventral surface of the skull (state 1). Riggs (1912) and Peterson (1924) noted this peculiar feature in *Dolichorhinus*, and Osborn (1929a) first identified these bony pouches as part of the ventral maxilloturbinate bones in a cross-sectioned *Dolichorhinus* skull

(AMNH 1851). The maxilloturbinates of *Dolichorhinus* extend far past the choanae and fill the anterior two thirds of the ventral narial canal, thus shifting the functional posterior nares to an extremely posterior position behind the pterygoid processes. I have found that several other brontotheres, including *Telmatherium validus*, *Metarhinus fluviatilis*, *Metarhinus abbotti*, and *Epimanteoceras formosus*, have posteriorly shifted maxilloturbinates that are exposed in the choanae of the posterior nares. It is difficult to evaluate this character for most taxa. The fragile turbinates, if preserved, are usually buried in sediment, or they were destroyed during preparation. Therefore, this character was treated as missing data for many species.

Character 31: *Ventral sphenoidal fossae: (0) absent, (1) present.*

In brontotheres the posterior nares form an elongate ventral narial canal on the ventral surface of the skull. Typically the ventral narial canal does not extend posterior to the foramen ovale (state 0). However, in several taxa, the sphenoid bone is highly modified with a pair of large pits in the body of the sphenoid that are continuous with the ventral narial canal, extending it past the foramen ovale. The basisphenoid forms a thin partition that joins with the elongate vomer to bisect the entire ventral narial canal. The large sphenoidal pits were first recognized in *Sphenocoelus uintensis* by Osborn (1895), in *Protitan* by Granger and Gregory (1943), in *Metatitan khaitshinus* by Yanovskaya, 1980, but they are also present in other species of *Metatitan* and *Diplacodon elatus*.

Character 32: *External auditory pseudomeatus: (0) mediolaterally angled, (1) posteromedially angled.*

In the outgroup and most true brontotheres the external auditory pseudomeatus formed by the postglenoid and the mastoid processes of the squamosal bone enters the skull in a mediolateral direction (state 0). However, in *Dolichorhinus hyognathus*, *Sphenocoelus uintensis*, *Protitan minor*, *Rhinotitan*, *Protembolotherium*, and *Embolotherium*, the auditory pseudomeatus enters the skull in a more oblique posteromedial direction (state 1).

Character 33: *Foramen ovale: (0) not confluent with foramen lacerum, (1) confluent.*

This character is similar to one used by Froehlich (2002) and describes the position of the foramen ovale with respect to the foramen lacerum. This character varies among the outgroup. *Pachynolophus* and *Lambdotherium* are the only taxa in this study in which the foramen ovale is known to be confluent with the foramen lacerum (state 1). The condition for *Danjiangia* is unknown. In *Hyracotherium* and all brontotheres, the foramen ovale is completely separate from the foramen lacerum (state 0).

Character 34: *External auditory pseudomeatus: (0) not constricted ventrally, (1) highly constricted ventrally.*

In the outgroup, most hornless brontotheres, and *Protitan*, the postglenoid process and the mastoid process form a broad and ventrally unconstricted auditory pseudomeatus. However, in *Palaeosyops* and horned brontotheres other than *Protitan*, the mastoid process angles anteroventrally toward the postglenoid process, often making contact with it, resulting in an external auditory pseudomeatus that is constricted ventrally and often tube-shaped (state 2).

Character 35: *Occipital condyles: (0) small (1) large.*

Most brontotheres have occipital condyles that are relatively small (normally proportioned) and are much narrower than the total width of the occiput (state 0). However, *Mesatirhinus*, *Sphenocoelus*, and *Dolichorhinus* have disproportionately large occipital condyles that are nearly as wide as the entire occiput (state 1).

Character 36: *Proportions of occiput: (0) dorsal portion narrower than ventral portion, (1) dorsal portion as wide or wider than ventral portion.*

Among the outgroup, hornless brontotheres, and *Protitan grangeri*, the dorsal portion of the occiput is narrower than the ventral portion of the occiput (state 0). Among the remaining horned brontotheres, the dorsal portion of the occiput is either equal in width to the ventral portion of the occiput, or it is somewhat wider (e.g., *Embolotherium andrewsi*) (state 1).

Character 37: *Posterior end of skull: (0) narrow, (1) widened.*

In comparison to the outgroup and other brontotheres, the posterior ends of the skulls of *Rhinotitan andrewsi* and *Metatitan* are disproportionately broadened. In these taxa, the width of the skull measured from the lateral sides of the left and right mastoid processes, is greater than the width measured from the lateral sides of the M3s (state 1). Ratios calculated from the width of the basicranium divided by the width across the M3s yield values between 1.2 and 1.7. For other brontotheres for which the same ratio can be calculated, the value is generally less than one or very near one (state 0). *Aktautitan hippopotamopus* may have had a widened occiput and basicranium similar to that of *Metatitan*, although the available material is too crushed to accurately judge this character for that species.

Character 38: *Basicranium: (0) normally proportioned, (1) shortened.*

In brontotheres with typically proportioned basicrania, the external auditory pseudomeatus enters the skull at a point that is significantly anterior to the foramen magnum (state 0). In species of *Metatitan*, the basicranium is anteroposteriorly compressed, so that the external auditory pseudomeatus enters the skull at the posteriormost end of the cranium near a point that is entirely lateral to the foramen magnum (state 1).

Character 39: *Nuchal crest: (0) thin, (1) thick.*

Although there is some degree of variability in the thickness of the nuchal crest of brontotheres, most species could be generally described as retaining a relatively thin nuchal crest (state 0) in comparison to *Dianotitan*, *Megacerops coloradensis*, *Protembolotherium*, and *Embolotherium andrewsi*, all of which are characterized by extremely thickened and rugose nuchal crests (state 1).

Character 40: *Occipital pillars: (0) weak, (1) massive.*

Two pillarlike columns of bone are visible on the surface of the occiputs of the taxa included in this analysis. These occipital pillars originate above the foramen magnum and extend dorsolaterally to the nuchal crest, thus forming a V-shaped configuration with a pit or shallow depression in the center of the occiput between these two occipital pillars. Typically, the occipital pillars are relatively weak and the central occipital depression is shallow (state 0). However, *Embolotherium andrewsi* and *Megacerops* have massive occipital pillars that form a very deep recession in the center of the occiput (state 1).

Character 41: *Tilt of occiput: (0) relatively vertical, (1) moderately to strongly tilted, (2) elevated.*

From lateral views, the occiputs of the majority of brontotheres and the outgroup are moderately to strongly tilted backward (angled posterodorsally) (state 1). However, both species of *Rhinotitan* and two of the three species of *Metatitan*, *M. primus* and *M. khaitshinus*, have occiputs that are substantially more vertical (state 0). On the other hand, the occiput of *Embolotherium* is distinctive in its strong backward tilt and elevated appearance that relates to the strong upturned shape of the posterior end of the cranium (state 2).

Upper Dental Characters

Character 42: *Pairs of upper incisors: (0) three, (1) two.*

In the outgroup and among most true brontotheres there are three pairs of upper incisors (state 0). *Eubrontotherium*, *Protitanops*, *Notiotitanops*, *Dianotitan*, *Duchesneodus*, and *Megacerops coloradensis* have only two pairs of upper incisors (state 1). Note that the number of lower incisors differs for these taxa and is treated as a separate character.

Character 43: *Upper and lower incisors: (0) very large, (1) large, (2) small, (3) very small.*

Although the upper and lower incisors are not always equal in number, the size of the upper and lower incisors correspond closely in all brontotheres whose upper and lower incisors are known; therefore this character (incisor size) is applicable to both upper and lower incisors. The outgroup and most hornless brontotheres (e.g., *Dolichorhinus*) retain relatively large incisors (state 1). Some advanced horned brontotheres, such as *Rhinotitan*, *Aktautitan*, and *Embolotherium gran-*

geri retain large incisors as well. Both *Sthenodectes* and *Pygmaetitan* have atypically enlarged incisors (state 0). On the other hand, numerous brontotheres have incisors that are reduced in size, including *Qufutitan*, *Protitanotherium*, *Diplacodon*, and others (state 2). Many of the more advanced horned brontotheres such as *Megacerops coloradensis*, *Parabrontops gobiensis*, and *Embolotherium andrewsi* (among others) have incisors that are so reduced in size that they appear to be vestigial (state 3). Three species, *Acrotitan ulanshirehensis*, *Pachytitan ajax*, and *Pollyosbornia altidens* were assigned multiple states due to partial ambiguity related to poor fossil preservation.

Character 44: *Upper incisors: (0) spatulate with flat or rounded apices, (1) all subcaniniform, (2) semiglobular-globular I1–I2 and subcaniniform I3, (3) all globular.*

The upper incisors are generally flat or spatulate in the outgroup (state 0). Many of the hornless brontotheres (e.g., *Dolichorhinus*) and some horned brontotheres (e.g., *Protitan grangeri*) have incisors that are subcaniniform with conical, pointed crowns and broad lingual cingula (state 1). *Aktautitan hippopotamopus* and *Rhinotitan andrewsi* have a globular or semiglobular I1 and I2, but the I3 is subcaniniform (state 2). The most derived condition, all globular incisors, is seen among several of the most derived brontotheres including *Megacerops coloradensis*, *Parabrontops*, and *Embolotherium* (state 3). The reduction of the incisors to a featureless, globular state does not necessarily co-occur with the reduction of incisor size. *Embolotherium grangeri*, for instance, retains large upper incisors, but they are essentially globular and featureless. *Pachytitan* and *Pygmaetitan* were assigned multiple states due to partial ambiguity relating to poor preservation.

Character 45: *Shape of incisor row: (0) arched, (1) straight.*

Among the outgroup and most brontotheres the incisors form a semicircular arch that extends anterior to the canines (state 0). This character applies to both upper and lower incisor rows, although typically the upper incisor row is somewhat more arched than the lower incisor row. In many of the more advanced horned species such as *Metatitan primus*, *M. relictus*, *Parabrontops gobiensis*, *Eubrontotherium clarnoensis*, *Megacerops coloradensis*, and others, the incisors form nearly a nearly straight row directly between the anterior margins of the canines (state 1).

Character 46: *Upper postcanine diastema: (0) present, (1) absent.*

There is not a precise correspondence between the presence or absence of a postcanine diastema in the maxilla and mandible, and they are therefore treated as separate characters. *Sthenodectes*, *Pygmaetitan*, *Metatitan*, *Embolotherium andrewsi*, *Dianotitan*, *Duchesneodus*, and *Megacerops* are examples of species in which the postcanine diastema has been lost or is reduced to an insignificant gap of no more than a few millimeters between the canine and P1. Other brontotheres and the outgroup have a significant postcanine diastema (state 0).

Character 47: *P1: (0) simple (1) complex.*

The outgroup and most hornless brontotheres retain a relatively simple P1 with a paracone and short posterior heel (state 0). However, most horned brontotheres, with the exception of *Protitan*, have a more complex P1 that includes a distinct paracone and metacone (state 1). Additionally, the P1s of most of these taxa have a small lingual heel with a protocone or a small lingual crest. When the P1 is heavily worn this character can be scored by the overall shape of the crown: in the simple state the crown is narrow and ovoid in outline; in the more complex state the P1 is much broader and usually nearly circular.

Character 48: *Diastema between P1 and P2: (0) absent, (1) present.*

Hyracotherium, *Pachynolophus*, and *Danjiangia* lack a significant gap between P1 and P2 (state 0). *Lambdotherium*, *Eotitanops*, and *Palaeosyops* have a short diastema between P1 and P2 (state 1). A similar diastema is occasionally seen in *Telmatherium validus*. A P1–P2 diastema is not seen in any other brontothere.

Character 49: *P2 metacone: (0) small swelling, (1) distinct cusp.*

This character varies within the outgroup as well as among brontotheres. *Pachynolophus*, *Lambdotherium*, *Danjiangia*, and *Eotitanops* lack a distinct P2 metacone, although

in relatively unworn teeth there is a small swelling posterior to the paracone of P2 that could be interpreted as a rudimentary metacone. In *Hyracotherium* and the remaining brontotheres, there is a well-developed metacone on P2 (state 1).

Character 50: *Labial upper premolar ribs: (0) paracone and metacone ribs large and equal, (1) paracone rib strong, metacone rib weak, (2) paracone rib narrow, metacone rib very weak, (3) all labial ribs very weak.*

Among the outgroup there are two large labial swellings, or ribs, on the ectolophs of the premolars. The paracone and metacone labial ribs are roughly equally sized, although the metacone rib tends to be somewhat smaller (state 0). There are strong paracone ribs on the premolars of *Eotitanops* and *Palaeosyops*, but the metacone rib is weak (state 1). Among the majority of other brontotheres, the labial paracone ribs are distinct but not as strong as those of *Palaeosyops*, and the metacone rib is weak or even absent (state 2). Finally, in some brontotheres (e.g., *Embolotherium*, *Eubrontotherium*, and *Microtitan*) the labial ribs of the paracone and metacone are either very weak or absent (state 3).

Character 51: *Preprotocristae and paraconules of P2, P3, and P4: (0) absent or very weakly developed on P2, strongly developed on P3 and P4 (1) weakly developed on P2, faint to absent on P3 and P4, (2) strongly developed on P2 and weakly developed on P3 and P4.*

There is a distinct morphocline in the relative prominence of preprotocristae (anterior crest connecting the protocone to the lingual base of the ectoloph) and paraconules on the premolars (P2–P4). In the outgroup the P2 crown lacks a distinct preprotocrista, but P3 and P4 have a distinct preprotocrista and/or a strong crescentic paraconules (state 0). In most brontotheres there is a very weak (essentially vestigial) paraconule or preprotocrista on P2, and in more posterior molars the preprotocrista becomes progressively less distinct and is often not even detectable on P3 and P4 (state 1). Finally, a limited number of more derived brontotheres such as *Diplacodon* and *Megacerops* tend to have a taller and more distinct preprotocrista on P2; the preprotocristae of the P3 and P4 are always discernable, but they tend to be weaker than that of P2 (state 2).

Character 52: *Upper premolar postprotocrista: (0) present on P3 and P4, (1) absent.*

In the outgroup a distinct postprotocrista can be seen connecting the protocone to the lingual base of the metacone on the P3 and P4 (state 0). In all true brontotheres, a postprotocrista connecting these cusps is absent (state 1).

Character 53: *Upper premolar lingual morphology: (0) lingual side of crown is narrow with cone-shaped protocone, (1) lingual side of crown is somewhat wider, protocone often associated with lingual crest, (2) small hypocones variably present and situated closely to protocone and connected by lingual crest, (3) well-developed hypocones always present and spaced more posteriorly from hypocone and variably connected by a lingual crest.*

In an earlier analysis of Asian brontothere phylogeny (Mihlbachler et al., 2004a), the hypocone of each premolar (P2–P4) was treated as a separate phylogenetic character. However, the high degree of intraspecific variability that characterizes the premolars of brontotheres complicates the use of premolar characters. The distinctness of the lingual crests, the size the hypocones, their degree of separation from the protocones, and often even the presence of hypocones, varies in many species. However, some phylogenetically informative character information can be retrieved. For instance, there are brontothere species (e.g., *Mesatirhinus*) that lack hypocones altogether. On the other hand, there are numerous brontotheres in which hypocones are always distinct on P3 and P4 (e.g., *Duchesneodus uintensis*). As an alternative to treating every aspect of premolar morphology as a separate character (whereby many taxa would be coded as polymorphic for many characters), I have opted for a simpler solution by which most of the lingual premolar variation seen in brontotheres is reduced to a single character whose states are defined in such a way that takes into account the seemingly random aspects of intraspecific variation.

In *Hyracotherium* and *Pachynolophus*, the lingual sides of the premolar crowns are rather narrow, giving the crown a strong

triangular appearance and the protocone is a simple, cone-shaped cusp (state 0). In *Danjiangia*, *Lambdotherium* and many true brontotheres (e.g., *Dolichorhinus*), the lingual sides of the premolars are wider; additionally, a lingual crest often extends posteriorly from the protocones (state 1). In this state, a premolar hypocone is either absent or is rudimentary and rare. In a more derived condition, small hypocones are variably present (e.g., *Epimanteoceras formosus*) (state 2). When present they are positioned closely to the protocone and connected to it by a connecting crest. Among taxa with this condition, I found no apparent pattern of hypocone distribution. In other words, within a single specimen, the hypocone can be present or absent among any of the premolars irrespective of the presence or absence of a hypocone on other premolars. Finally, in other taxa (e.g., *Duchesneodus uintensis*), a well-developed hypocone on P3 and P4 is always present and is positioned farther posteriorly from the protocones (state 3). In this state, the P2 sometimes has a distinct hypocone, and sometimes it absorbed by the lingual connecting crest.

Character 54: *Upper molar parastyle: (0) low, (1) high.*

This character is similar to one used by Froehlich (2002) in an analysis of early Eocene equids. In *Hyracotherium* and *Pachynolophus* the parastyle of the upper molar is relatively low; it is intermediate in height between the labial cingulum and the apex of the paracone (state 0). The parastyles of *Danjiangia*, *Lambdotherium*, and true brontotheres are taller and rival the paracone in total height (state 1).

Character 55: *Upper molar parastyle: (0) mainly anterior to paracone, (1) mainly labial to paracone.*

In *Hyracotherium* and *Pachynolophus*, the main mass of the upper molar parastyle is mostly anterior to the paracone (state. 0), while the parastyles of *Danjiangia*, *Lambdotherium*, and true brontotheres are shifted labially, so that the main mass of the parastyle is labial to a line that runs through the apices of the paracone and metacone (state 1).

Character 56: *Upper molar anterior cingulum (0) forms parastyle shelf, (1) does not form parastyle shelf.*

In the outgroup and the earliest brontotheres, *Eotitanops* and *Palaeosyops*, the anterior cingulum of the upper molars is relatively thick and forms a small cingular shelf at the apex of the parastyle (state 0). In other brontotheres, the labial portion of the anterior molar cingulum is much thinner and it passes around the anterolabial corner of the tooth at a level proximal to the peak of the parastyle; it does not form a small cingular shelf at the peak of the parastyle (state 1).

Character 57: *Upper molar metastyle: (0) straight, (1) angled labially.*

This character is similar to one used by Froehlich (2002). In *Hyracotherium* and *Pachynolophus*, the metastyles of the upper molars (M1–M2) are relatively straight (state 0). In *Danjiangia*, *Lambdotherium*, and true brontotheres the upper molar metastyle is strongly angled in a posterolabial direction.

Character 58: *Upper molar ectoloph: (0) brachydont, (1) hypsodont.*

This character refers to the height of the ectoloph. *Danjiangia*, *Lambdotherium*, *Eotitanops*, and *Palaeosyops* all have relatively low-crowned dentitions comparable to those of *Hyracotherium* and *Pachynolophus* (state 0). In this condition, the ectoloph is only marginally taller than the lingual cusps. A crown height ratio, defined as the height of the paracone (in an unworn specimen) divided by the anteroposterior length of M3 yields values between 0.5 and 0.6. In other brontotheres, the ectoloph is significantly taller and the crown height ratio always yields values higher than 0.7 (state 1).

This character can also be scored without calculating a ratio. The upper molar mesostyle is widest near the dentinoenamel junction. It gradually narrows toward its apex, and at the apex it forms a short transverse ridge of enamel. In brachydont brontotheres, such as *Palaeosyops*, the apical enamel ridge of the mesostyle is horizontal and forms a right angle with the labial side of the mesostyle (state 0). In more hypsodont brontotheres, the apical mesostyle ridge is longer and is rotated labially, forming an obtuse angle with the labial side of the mesostyle (state 1). The lateral rotation and lengthening of this mesostylar ridge is struc-

turally related to the increase in the total height of the ectoloph.

Several taxa are known only from heavily worn molars (e.g., *Notiotitanops mississippiensis*). It is therefore impossible to quantify total (unworn) crown height in these species, or to even evaluate the angle of the apical mesostyle ridge, which, in very worn teeth, is no longer present. However, it is obvious that when heavily worn molars (i.e., there is a very broad exposure of dentin on the occlusal surface of the ectoloph) have actual crown heights that are similar to those of brachydont brontotheres, the ectoloph was originally much taller and therefore should be coded as having the hypsodont condition (state 1).

Character 59: *Labial side of upper molar paracone and metacone: (0) erect, (1) lingually angled and concave, (2) lingually angled and convex.*

In the outgroup the paracone and metacone of the molars are erect (state 0). In these taxa, the labial margins of the paracone and metacone are nearly straight from the dentinoenamel junction to the cusp apex. In other brontotheres the labial sides of the paracone and metacone are angled strongly lingually. In *Palaeosyops* and *Eotitanops*, the labial sides of the paracone and metacone are strongly angled lingually at their base. However, the labial sides of the paracone and metacone are concave from the dentinoenamel junction to the apex. In other words, the labial sides of the paracone and metacone curve labially and the apices of these cusps remain erect (state 1). In all other brontotheres, the paracone and metacone are more strongly angled lingually. Moreover, the labial margins of the paracone and metacone are convex. In other words, the labial margins of these cusps are curved lingually and the cusp apices are not erect, but are angled in a notably lingual direction (state 2).

Character 60: *Molar ribs (0) strong, (1) weak.*

The paracone and metacone each have a labial vertical rib that extends from the proximal base of the ectoloph to the cusp apex. Corresponding lingual protoconid and hypoconid ribs can be seen in the talonid and trigonid occlusal basins of the lower molars. In *Hyracotherium* and *Pachynolophus*, the molar ribs are topographically the most distinct features on the labial side of the upper molar crowns and in the lingual basins of the lower molars (state 0). In *Danjiangia*, *Lambdotherium*, *Eotitanops*, *Palaeosyops*, and *Bunobrontops*, strong molar ribs are retained, even though the large and labially expanded parastyle and mesostyle (not present in the outgroup) tends to diminish their presence (The parastyle and mesostyle are treated as separate characters). In the lower molars of these taxa, the protoconid rib tends to be stronger than the hypoconid rib. All other brontotheres are more derived in having much weaker upper and lower molar ribs (state 1). In this condition, the labial ribs of the upper molars and the lingual ribs of the lower molars tend to be weak on the paracone/protoconid and are faint or absent on the metacone/metaconid, although they occasionally are not discernable on any of the molars.

Character 61: *Upper molar mesostyle: (0) absent, (1) present.*

Danjiangia, *Lambdotherium*, and all true brontotheres possess a large upper molar mesostyle that contributes to the distinctive W-shaped ectoloph (state 1). Mesostyles are not seen on the molars of in *Hyracotherium* and *Pachynolophus* (state 0).

Character 62: *Lingual margins of molar paracone and metacone: (0) rounded (1) wedged.*

Eotitanops, *Palaeosyops*, and *Bunobrontops* retain the condition seen in the outgroup in which the lingual sides of the paracone and metacone have a rounded cross section (state 0). After initial wear of the paracone and metacone, the rounded semicircular cross section of the cusp can be seen. Other brontotheres demonstrate another state where the lingual sides of the paracone and metacone form a more acute wedge shape near the apex (state 2). Consequently, in these taxa, the initial wear surfaces of the paracone and metacone form the lower edges of a more distinctly W-shaped wear facet. However, despite the derived wedge-shaped condition near the apex of the crown, the more rounded cross-sectional shape is retained near the base of the crown. Therefore, this character cannot be scored on heavily

worn molars. Most often this character can be scored on M3.

Character 63: *Thickness of the lingual enamel of the upper molar ectoloph: (0) equal in thickness to the labial ectoloph enamel, (1) thickened around the paracone and metacone, (2) moderately thinned between paracone and metacone, (3) completely thinner than labial ectoloph enamel.*

This character is coded by comparing the thickness of the lingual band of ectoloph enamel, which tends to vary greatly between taxa, with the thickness of the labial band of enamel of the ectoloph, which is less variable between taxa. In *Hyracotherium*, *Pachynolophus*, and *Danjiangia*, the lingual and labial enamel bands of the upper molar ectoloph are similar in thickness. Moreover, the thickness of the lingual ectoloph enamel is the same around the margins of the paracone and metacone as it is between these cusps. In *Lambdotherium* and true brontotheres, the thickness of the labial enamel does not vary, however the thickness of the lingual ectoloph enamel band varies within a single molar. In *Lambdotherium*, *Eotitanops*, and *Palaeosyops*, the enamel that defines the lingual sides of the paracone and metacone is much thicker than the labial enamel. However, the lingual intercusp enamel is similar in thickness to the labial intercusp enamel (state 1). In *Bunobrontops* and *Mesatirhinus*, the enamel defining the lingual margins of the paracone and metacone are not thickened. However, the lingual intercusp enamel is somewhat thinner than the labial ectoloph enamel (state 2). The most derived condition is seen in the remaining brontotheres in which all the lingual enamel of the ectoloph is thinner than the labial enamel (state 3). This condition is carried to extremes in some specimens of *Megacerops* where the lingual ectoloph enamel is paper-thin. The above patterns can be easily seen in moderately worn molars, where the wear facet of the ectoloph creates a cross-sectional view of the labial and lingual ectoloph enamel. It is possible to differentiate between states 0, 1, and 2: 3 in very worn molars. However, state 2 and 3 can only be differentiated in molars that are moderately worn because the lingual ectoloph enamel tends to thicken near the base of the ectoloph among all taxa with states 2 and 3.

Character 64: *Labiolingual width of upper molar ectoloph: (0) narrow, (1) intermediate, (2) wide.*

This character describes the labiolingual width of the ectoloph in relation to the total labiolingual width of the upper molar. This character can easily be coded with quantitative data and/or with discrete landmarks. The width of the ectoloph can be quantified by calculating a ratio defined as the distance from the labial side of the parastyle to the lingual side of the paracone (measured at the lingual base of the paracone, not from the apex, which tends to migrate lingually with wear in many brontotheres), divided by the distance from the labial side of the parastyle to the lingual side of the protocone. In the outgroup, the ectoloph width ratio always yields values less than 0.5 (state 0). *Eotitanops* exhibits an intermediate state in which paracone width ratio is always about 0.5 (state 1). In *Palaeosyops* and all other brontotheres, the paracone width ratio is always greater than 0.56 (state 2).

As an alternative to ratios, this character can be scored easily with discrete landmarks. In the outgroup, the paracone is posterior to a line running through the protocone and the labial margin of the parastyle (state 0). In *Eotitanops* the lingual base of the paracone is intersected by this line (state 1). Among other brontotheres the lingual base of the paracone is anterior to the same line (state 2). It should be emphasized that the lingual base of the paracone should be used as the landmark to code this character regardless of whether it is done quantitatively or discretely. The apex of the paracone should be avoided because it tends to migrate lingually with wear in many brontotheres.

Character 65: *Central molar fossa: (0) absent, (1) present.*

The upper molars of many brontotheres have a small central fossa that is positioned at the lingual base of the ectoloph directly between the paracone and metacone (state 1). The central molar fossa is a derived condition and it is absent in the outgroup and many of the more primitive hornless brontotheres (state 0).

Character 66: *Upper molar protoloph and paraconules: (0) large, (1) reduced, but functional, (2) very small, (3) pinhead-sized paraconule variably present (4) absent.*

The loss of the protoloph and paraconules in the upper molars of brontotheres seems to have occurred in a series of gradational stages. *Hyracotherium*, *Pachynolophus*, and *Danjiangia* molars have a large, functional, lophoid protoloph with a large paraconule embedded in it (state 0). *Lambdotherium* retains a distinct paraconule with a crescentic crest that is smaller; however the paraconule and protoloph of *Lambdotherium* are large enough for a regular wear facet (wearing away of the cusp apex to an extent that the underlying lake of dentin is exposed) to develop on the paraconule, suggesting that this structure retained an occlusal function (state 1). The protoloph-paraconule complex of *Eotitanops*, *Palaeosyops*, and *Mesatirhinus* is so reduced that it does not appear to have had a significant masticatory function. The structure is essentially vestigial in these taxa and the specific morphology is variable, usually with the paraconule appearing as a small swelling with a short crest, and sometimes simply as a small bump of enamel with no crest (state 2). In *Dolichorhinus*, *Telmatherium*, *Wickia*, and *Nanotitanops*, a pinhead-sized paraconule is seen among molars of that species, although they can be variably present and absent (state 3). Finally, all traces of a protoloph or paraconule appear to be lost in the remaining brontotheres (state 4).

Character 67: *M1–M2 metaloph: (0) well developed, (1) small but distinct, (2) vestigial metalophlike ridge, (3) absent.*

In *Hyracotherium*, *Pachynolophus*, and *Danjiangia*, the metaloph of the M1 and M2 is well developed (state 0). In *Lambdotherium* a small but distinct metaloph persists, but it is clearly reduced (state 1). In *Eotitanops*, *Palaeosyops*, *Bunobrontops*, and *Mesatirhinus* the metaloph is further reduced (state 2). In this state, an essentially vestigial remnant of the metaloph is visible as a small ridge of enamel running down the labial slope of the hypocone, toward the lingual base of the metacone. For the remaining brontotheres there is no trace of a metaloph or metalophlike ridge of enamel (state 3), with the exception of *Megacerops kuwagatarhinus*, whose M3 shows a small metaloph like ridge similar to those of the most primitive brontotheriids.

Character 68: *Upper molar anterolingual cingular cusp: (0) absent, (1) small, (2) large.*

Among the outgroup the lingual portion of the anterior upper molar cingulum is nearly flat (state 0). This condition is retained in some hornless brontotheres (e.g., *Dolichorhinus*) as well as some horned brontotheres (e.g., *Protitan*). In many horned brontotheres (e.g., *Eubrontotherium*) and some hornless brontotheres (e.g., *Metarhinus*) the anterior cingulum forms a small but distinct anterolingual cusp just anterior to the protocones (state 1). In worn molars the anterolingual cusp can often be worn flat, but the presence of the anterolingual cingular cusp can still be identified by a wear facet that has developed on the anterior cingulum. Finally, in *Protembolotherium* and *Embolotherium andrewsi*, the anterolingual cingular cusp tends to be quite large and more developed in comparison other brontotheres (state 2).

Character 69: *M3 hypocone: (0) present, (1) variably present and absent, (2) absent or very rare.*

The M3 hypocone shows intraspecific polymorphic tendencies among brontotheres. In some taxa, such as *Dolichorhinus*, it is variably present and absent (state 1). In other taxa, the hypocone is more consistently either present (state 0) or absent (state 2), although when present, it tends to vary conspicuously in size and shape, and can vary from being a small pinheaded structure (or multiple pinheaded structures) to a large functional cusp similar in size to the hypocones of M1 and M2. Therefore, it is difficult to define a phylogenetic character based on the M3 hypocone. Nonetheless, there does appear to be some potential phylogenetic signal in this character because there are species in which the M3 hypocone is invariably present (e.g., *Embolotherium*) and others other where the hypocone is always absent (e.g., *Rhinotitan*). In *Hyracotherium* and *Pachynolophus*, a large M3 hypocone is present. *Danjiangia* and *Lambdotherium* share this condition. In *Dolichorhinus* and *Metarhinus*, a M3 hypocone is commonly present, but sometimes

absent. Finally, numerous brontotheres show a condition in which the M3 hypocone is either completely lost, or it is rare and never well developed when present (e.g., *Eotitanops*). It is possible that species represented by one or a few specimens have been incorrectly coded as having either state 0 or state 2 when the condition was really variable (state 1).

Mandible and Lower Dental Characters

Character 70: *Shape of mandibular symphysis: (0) long and narrow, (1) short and robust.*

Danjiangia and *Lambdotherium* share with *Hyracotherium* and *Pachynolophus* an elongate and slender mandibular symphysis with a correspondingly long postcanine diastema (state 0). Although there is variation in the proportions of the mandibular symphyses of brontotheres, they are all are substantially shorter, broader, and more robust, and with a shorter postcanine diastema (state 1) in comparison to the outgroup.

Character 71: *Position of posterior margin of mandibular symphysis: (0) anterior to the premolars, (1) between the p2 talonid and p3 trigonid, (2) between the p3 talonid and p4 trigonid, (3) between the p4 talonid and m1 trigonid.*

There is limited amount of intraspecific fluctuation in the exact position of the posterior edge of the mandibular symphysis, but generally, each species ranges within the character states as they are defined here.

Character 72: *Number of lower incisors: (0) three pairs, (1) two pairs.*

The outgroup and most true brontotheres retain three pairs of lower incisors (state 0). Two brontothere species, *Acrotitan ulanshirehensis* and *Megacerops coloradensis* have only two pairs of lower incisors. It is quite possible that a number of other species, particularly *Protitanops curryi*, *Dianotitan lunanensis*, *Megacerops kuwagatarhinus*, and *Notiotitanops mississippiensis*, also have a reduced number of lower incisors; however, the lower dentitions of these species are not known.

Character 73: *Lower incisor morphology: (0) thin and spatulate, (1) i1–i2 semispatulate, i3 subcaniniform, (2) all incisors subcaniniform, (3) all incisors short and wedge-shaped or globular.*

The shapes of the lower incisors can be divided into at least four states. The outgroup taxa have relatively thin and spatulate incisors (state 0). Some brontotheres, including *Eotitanops*, *Palaeosyops*, *Mesatirhinus*, and numerous horned brontotheres (e.g., *Rhinotitan*) have thicker, semispatulate i1s and i2s; however, the i3 tends to be more subcaniniform (state 1). Yet other brontotheres, including both some hornless species (e.g., *Metarhinus*) and some horned species (e.g., *Aktautitan*) have more subcaniniform incisors with more conular and pointed crowns (state 2). Finally, many of the most derived brontotheres, such as *Duchesneodus* and *Eubrontotherium*, have very short incisors that are squarish or shaped like a thick wedge (state 3); these tend to take on an amorphous globular appearance after some amount of wear. In the analysis presented below, this character was not treated as a normal ordered character, because the states do not form a clear morphocline. Rather the morphological conditions represented by states zero, two, and three seem to be derived in separate directions from state one. For the analysis of ordered characters, a character tree was built in MacClade in which any transformation to state 1 or from state 1 was a single step. Any other character transformation must pass through state 1, costing two steps.

Character 74: *Relative lower incisor size: (0) i2 about the same size as i3, (1) i2 is larger than i3.*

Within the outgroup and among hornless brontotheres, the i2 is about the same size as i3 (state 0). Among horned brontotheres, except *Protitan grangeri*, the i2 is clearly the largest incisor, particularly in crown height and labiolingual width (state 1).

Character 75: *Diastema between p1 and p2: (0) absent, (1) variably present, (2) present.*

The mandibular p1–p2 diastema is not distributed across the taxa in the same way as the maxillary P1–P2 diastema and is therefore treated as a separate character. *Hyracotherium*, *Pachynolophus*, and most brontotheres lack p1–p2 diastemata (state 0). However, *Danjiangia*, *Eotitanops*, *Palaeosyops*, *Mesatirhinus*, and *Dolichorhinus* have

short p1–p2 diastemata (state 2). A p1–p2 diastema is variably present in *Telmatherium validus* (state 1). This character is inapplicable to *Lambdotherium*, due to the absence of the p1.

Character 76: *Mandibular postcanine (c–p1) diastema: (0) present, (1) absent.*

The mandibular postcanine diastema is not distributed across the taxa in the same way as the maxillary postcanine diastema and is treated as a separate character. The outgroup taxa and the vast majority of true brontotheres have a distinct postcanine diastema of variable length (state 0). *Sthenodectes*, *Metatitan*, *Brachydiastematherium*, *Embolotherium andrewsi*, and *Megacerops* lack postcanine diastemata altogether or have only an exceedingly short gap between the canine and p1 (state 1).

Character 77: *p1 orientation: (0) vertical, (1) rooted into the jaw at an oblique angle.*

Typically, p1 inserts in the jaw at a nearly vertical angle (state 0). However, *Danjiangia*, *Desmatotitan*, and *Acrotitan* have a p1 that inserts into the jaw obliquely in a posteroventral direction (state 1). When p1 is not preserved, this character can be determined by examining the angle of the p1 alveolus. This character is inapplicable to *Lambdotherium* due to the absence of p1.

Character 78: *Length of p2 trigonid: (0) much longer than talonid, (1) slightly longer than talonid.*

Typically, the trigonid of p2 is twice as long or nearly twice as long as the talonid (state 0). On the other hand, the p2 talonid of some horned brontotheres (e.g., *Metatitan*) is enlarged and the trigonid is only slightly longer than the talonid (state 1). The trigonid length is defined as the portion of the tooth between the anterior margin of the tooth and the junction of the protolophid and the cristid obliqua. The talonid is defined as the portion between the posterior margin of the tooth and the junction of the protolophid and the cristid obliqua. Note that when a p2 cristid obliqua is absent, as in *Lambdotherium*, the protolophid extends almost to the posterior end of the tooth, and the trigonid is obviously much longer than the talonid despite the lack of equivalent landmark.

Character 79: *Cristid obliqua of p2: (0) absent, (1) present.*

Hyracotherium, *Pachynolophus*, *Danjiangia*, and *Lambdotherium* lack cristids obliqua on their p2s (state 0). All true brontotheres have a distinct p2 cristid obliqua (state 1).

Character 80: *Labial notch of p2: (0) broad, (1) narrow, deep.*

A labial notch is formed between the trigonid and the talonid of the lower premolars (p2–p4) of brontotheres. In most brontotheres, the labial notch of p2 is relatively broad (state 0). However, in *Metatitan relictus* and *Metatitan primus* the labial notch of p2 is very deep, narrow, and angled anterolingually (state 1). The narrow labial notch is largely due to a lobelike extension of the protoconid that extends posterolabially from the protoconid and is parallel with the cristid obliqua, thus forming a narrow, obliquely angled notch.

Character 81: *Metaconid of p2: (0) absent, (1) variably present and absent.*

A metaconid does not occur on the p2 of any outgroup taxon or brontothere (state 0) with the exceptions of *Metatitan relictus*, *Embolotherium grangeri*, and *Embolotherium andrewsi* (state 1). The lingually angled protolophid of the p2 of *Metatitan primus* suggests that a metacone could have been present on the p2 of this species as well. However, the p2 of the only available specimen of *M. primus* is too damaged to confirm the presence of a metaconid. Therefore, this character was treated as missing data for *M. primus*.

Character 82: *Metaconid of p3: (0) absent, (1) variable, (2) present.*

The outgroup taxa show difference states. *Hyracotherium* and *Danjiangia* each lack a p3 metaconid (state 0), while *Pachynolophus* has a distinct p3 metaconid (state 2). Metaconids of the p3 are absent in a variety of hornless (e.g., *Dolichorhinus*) and horned brontotheres (*Eubrontotherium*) (state 0). Metaconids on p3 are also variably present and absent among a variety of taxa including *Lambdotherium*, *Metarhinus*, and *Rhinotitan* (state 1). Finally, most horned brontotheres possess a large, lingually positioned p3 metaconid (state 2).

Character 83: *Lower molar cristid obliqua: (0) low, (1) high.*

This character is similar to one used by Froehlich (2002). In *Hyracotherium* and *Pachynolophus*, the cristid obliqua of the lower molar contacts the posterior wall of

the trigonid at a low point near the base of the protolophid (state 0). In the derived condition shared by *Danjiangia*, *Lambdotherium*, and true brontotheres, the cristid obliqua contacts the posterior wall of the trigonid at a high position, nearly at the top of the protolophid (state 1).

Character 84: *Molar metaconid: (0) single, (1) twinned.*

This character is similar to one used by Froehlich (2002). In *Pachynolophus*, *Danjiangia*, and *Lambdotherium*, the metaconid of the lower molars is doubled (state 1). *Hyracotherium* and all true brontotheres have only a single metaconid (state 0).

Character 85: *Lower molar occlusal basins: (0) shallow, (1) deep.*

The trigonid and talonid basins of the lower molars of brontotheres are generally shallow (state 0). However, *Embolotherium* and *Pygmaetitan* are exceptions. In these taxa, the talonid and trigonid basins of the molars form deep, V-shaped valleys (state 1).

Character 86: *Lower m3: (0) short, (1) long.*

In the outgroup, and among a few true brontotheres, including *Eotitanops*, *Palaeosyops*, *Bunobrontops*, and *Hyotitan*, m3 is relatively short; the length of the crown is no more than twice the width of the tooth (measured at the trigonid) (state 0). However, in all other brontotheres the m3s are more elongate; the length of the crown is more than twice the width (state 1).

Character 87: *Hypoconulid of m3: (0) connected labially, (1) middle, (2) lingually.*

This character varies within the outgroup. In *Hyracotherium*, the m3 hypoconulid is connected to the entoconid on the labial side of the tooth (state 0). In *Pachynolophus* and *Lambdotherium*, the hypoconulid is connected to the hypolophid nearer to the middle of the tooth (state 1). In *Danjiangia* and true brontotheres, the m3 hypoconulid is connected to the entoconid on the lingual side of the tooth (state 2).

PHYLOGENETIC ANALYSIS OF BRONTOTHERIIDAE

Ingroup Taxa

The present study focuses on developing a cladistically derived phylogenetic hypothesis for species traditionally included within the Brontotheriidae. The monophyly of the Brontotheriidae is assumed in this study. The analysis does not attempt to test the phylogenetic position of the Brontotheriidae within the order Perissodactyla, although it is hoped that this work will ultimately facilitate further investigation of this problem. Included in the analysis are 51 taxa, consisting of 4 outgroup taxa plus 47 brontotheriids. Most (42) of the intaxa are those determined to be valid in the above species revision. Taxa that were determined to be nomina dubia or problematic were excluded. Five additional brontotheres were included in the analysis: (1) *Eotitanops*, (2) *Palaeosyops* (both included at the genus level), (3) an unnamed species recently described by Eberle (2006) and referred to cf. *Eotitanops* sp., and the late Eocene species (4) *Megacerops coloradensis* (sensu Mihlbachler et al., 2004b) and (5) *Megacerops kuwagatarhinus*. Those taxa not discussed in the above species revision are discussed briefly below.

Eotitanops Osborn (1907) is a small hornless brontothere from the late Wasatchian and Early Bridgerian of North America (Mader, 1998). It is the earliest and one of the smallest brontotheres and is typically regarded as the most primitive or basal member of this family (Osborn, 1929a; Mader, 1989, 1998). Although many species of *Eotitanops* have been named (summarized by Osborn, 1929a), Gunnell and Yarborough (2000) recognized only two species, *E. borealis* (Cope, 1880), and *E. minimus* Osborn (1919). *E. minimus* is diminutive and known only from a small number of fragmentary specimens consisting primarily of teeth. *Eotitanops borealis*, on the other hand, is known from much better material including a partial skull (AMNH 14487), a skull and mandible (UCMP 132049), and many other partial sets of upper and lower dentitions. In scoring character data for *Eotitanops*, I examined material from the AMNH, YPM, UCM, and UCMP collections.

Palaeosyops Leidy (1870a) is another Bridgerian hornless brontothere that is considered one of the more primitive members of the family, slightly more derived than *Eotitanops* (Osborn, 1929a; Mader, 1989, 1998). It is larger than *Eotitanops* but with similar

dentition. *Palaeosyops* is known from abundant material including complete skeletons and many skulls and mandibles. *Palaeosyops* was divided into three genera and many species by Osborn (1929a). However, recent revisions have considered *Palaeosyops* to consist of three (Mader, 1998) or five (Gunnell and Yarbrough, 2000) species, all belonging to the same genus. Mader (1998) did not provide diagnoses or descriptions for the three *Palaeosyops* species of his classification. Gunnell and Yarborough (2000) recognized five *Palaeosyops* species based on dental morphology, *P. paludosus* Leidy (1870a), *P. laticeps* Marsh (1872), *P. robustus* Marsh (1872), *P. fontinalis* (Cope, 1873a), and *P. laevidens* (Cope, 1873a). The characters used by Gunnell and Yarbrough (2000) to diagnose different species of *Palaeosyops* are dental variations (e.g., variability in degree of development of the M3 hypocone, or minor overall size differences) that I found to be unreliable as species indicators for other brontotheres because of their intraspecific polymorphic tendencies. I have examined many of the specimens listed in the species hypodigms (lists of referred specimens) of Gunnell and Yarbrough (2000) and I can find no clear-cut morphological discontinuities between the species of *Palaeosyops* as delimited by Gunnell and Yarbrough (2000); their species concepts for *Palaeosyops* are not necessarily wrong, depending on what theoretical species concept was applied (stratigraphic, biological, phylogenetic etc.). Unfortunately, an explicit statement of species concept does not generally accompany taxonomic works. However, the species of *Palaeosyops* as delimited by Gunnell and Yarbrough (2000) are not valid under the phylogenetic species concept adopted in this paper. In my experience the many *Palaeosyops* specimens from the Blacks Fork member (Bridger B, middle Bridgerian) and the Twin Buttes member (Bridger C–D, late Bridgerian) (see Robinson et al., 2004) cannot clearly be subdivided into phylogenetic species. There appears to be substantial overlap between specimens in these two subunits of the Bridger Formation. However, there does appear to be a (possibly anagenic) trend in increasing size and general robusticity throughout the Bridgerian. Ultimately, it will be desirable to apply a consistent species concept to all taxa. If a phylogenetic species concept similar to the one adopted in this paper is to be applied to all brontotheres, the species-level taxonomy of *Palaeosyops* is in need of revision. For the present analysis, *Palaeosyops* is included at the genus level. However, for the present analysis the character data for *Palaeosyops* was derived primarily from the AMNH, USNM, and YPM collections, generally from specimens from the Blacks Fork member (Bridger B) of the Bridger Formation (primarily *Palaeosyops paludosus* and *Palaeosyops laevidens* sensu Gunnell and Yarbrough, 2000).

Megacerops sensu Mihlbachler et al. (2004b) refers to Chadronian (late Eocene) brontotheres that have been previously assigned to the following genera: *Menodus* Pomel (1849), *Titanotherium* Leidy (1852), *Megacerops* Leidy (1870b), *Brontotherium* Marsh (1873), *Symborodon* Cope (1873b), *Brontops* Marsh (1887), *Menops* Marsh (1887), *Titanops* Marsh (1887), *Allops* Marsh (1887), *Teleodus* Marsh (1890), *Diploclonus* Marsh (1890), and *Ateleodon* Schlaikjer (1935). Early paleontologists Leidy, Cope, Marsh, Osborn, and others named many species of brontotheres based on fossils recovered from the classic White River deposits (primarily from the Chadron Formation) (reviewed by Osborn, 1929a). Finally, Osborn considered valid an overwhelming number of Chadronian species (N = 37), which he divided among seven genera, *Allops*, *Brontops*, *Brontotherium*, *Diploconus*, *Megacerops*, *Menodus*, and *Teleodus*. Osborn is widely considered to have been an oversplitter and his taxonomy was and is widely rejected, even by his peers (e.g., Scott, 1941); nonetheless, new Chadronian brontothere species have continued to be named (Russell, 1934, Schlaikjer, 1935; Stovall, 1948; Mader and Alexander, 1995). Although Chadronian brontothere taxonomy remains a widely recognized problem in vertebrate paleontology (Prothero, 1994; Alroy, 2003), no one has attempted to formally revise the species-level taxonomy, although various opinions have been expressed. Clark et al. (1967) considered classic Chadronian brontotheres to be a single species referable to *Menodus giganteus*. Mader (1989, 1998) divided Chadronian

brontotheres among three "monophyletic" genera, *Menops*, *Brontops*, and *Megacerops*. Mader's suggestion is questionable, however, because no species level revision was undertaken and no phylogenetic analysis was performed to establish the monophyly of these three genera. Presently Chadronian brontotheres are known from thousands of specimens, including complete skeletons and hundreds of complete skulls. Discounting taphonomic and ontogenetic effects, they vary most conspicuously in size, zygomatic thickness, and in the size and shape of the frontonasal horns. In particular, many specimens have enormous frontonasal horns. These characters are found to be intraspecifically variable in other brontothere species as well (e.g., *Duchesneodus uintensis*). The shape variation seen among the skulls of Chadronian brontotheres obviously does not constitute 37 species. Mihlbachler et al. (2004b) and Mihlbachler (2004) quantified the morphometric variation in skulls of Chadronian brontotheres and found it to be consistent with a pattern of variation found in sexually dimorphic species, in which probable secondary sex traits (horn size, zygomatic thickness) are extremely variable, but other variables (tooth-row length) are dramatically less variable. It was concluded that these brontotheres represent no more than a few sexually dimorphic species, and they should all be referred to a single genus, *Megacerops*, which includes at least two diagnosable species, *M. coloradens*is Leidy (1870b) and *M. kuwagatarhinus* Mader and Alexander (1995). The remaining species are nomina dubia or synonyms of these two species (see Janis et al., in press). *Megacerops coloradensis* lacks bifurcating horns and is represented by the vast majority of specimens, whereas *M. kuwagatarhinus* has bifurcating horns and is relatively rare. A more comprehensive survey of the morphology of *Megacerops* may indicate more species, but for the present study, the character data for *Megacerops coloradensis* sensu Mihlbachler et al. (2004b) is primarily derived from many skulls and mandibles in the AMNH, FMNH, CMNH, and YPM collections. Data on *Megacerops kuwagatarhinus* is derived from the three known skulls (F:AM 126800, DMNH 40416, SMNH P2317.1).

Outgroup Taxa

Four perissodactyl taxa were chosen as the outgroup for this analysis, including an early North American equid *Hyracotherium*, an early European perissodactyl *Pachynolophus*, the North American perissodactyl *Lambdotherium*, and a Chinese *Lambdotherium*-like species *Danjiangia pingi*. *Hyracotherium* is used here in its traditional sense (e.g., MacFadden, 1998), although analyses by Hooker (1994) and Froehlich (2002) suggest that *Hyracotherium* (sensu lato) is a paraphyletic group with some members that do not actually belong in the family Equidae. Froehlich (2002) divided the traditional *Hyracotherium* into numerous genera. The specimens used in this analysis to code *Hyracotherium* are the skull and mandible, USNM 336125, as well as numerous AMNH specimens from the Castillo Pocket locality (identified by Froehlich as the equid, *Xenicohippus osborni*).

Some recent phylogenetic analyses of perissodactyl interrelationships nest *Lambdotherium* and the brontotheriid, *Palaeosyops*, within palaeotheriids (Froehlich, 1999). For this reason, *Pachynolophus* was chosen as an outgroup taxon for this analysis. *Pachynolophus* is a basal perissodactyl that has been allied with Equidae and Palaeotheriidae, although a recent analysis suggests a close relationship with palaeotheriids (Holbrook, 2006). Craniodental data for *Pachynolophus* are primarily from figures of *Pachynolophus livinierensis* in Savage et al. (1965) and casts of dental material in the AMNH.

Historically, *Lambdotherium* has either been considered the basalmost member of the Brontotheriidae, or the sister taxon of that family (Osborn, 1929a; Mader 1989, 1998), a distinction that is cladistically irrelevant. In an analysis of basal perissodactyl phylogeny that included *Lambdotherium* and the brontothere, *Palaeosyops*, Froehlich (1999) found these taxa to be sisters. However, an analysis of perissodactyl phylogeny by Lucas and Holbrook (2004) that included *Lambdotherium* and the brontotheriid *Eotitanops* did not find these taxa to be sisters. Because of the present ambiguity of the relationship between *Lambdotherium* and

other brontotheres, *Brontotheriidae* is defined here as including all members that have been traditionally included in this family, except *Lambdotherium*. Data from *Lambdotherium* are primarily from a skull (USNM 19761), a jaw and palate (LACM/CIT 1743), and numerous dental and partial cranial specimens in the CMNH and AMNH collections.

Finally, the fourth outgroup taxon, *Danjiangia pingi* Wang (1995) from the early Eocene of Hubei, China, was initially described as a primitive chalicothere. Later, Beard (1998), recognizing the similarity of *Danjiangia* to *Lambdotherium*, interpreted *Danjiangia* as a sister taxon of the Brontotheriidae. In an analysis of a limited number of early perissodactyl taxa, Hooker and Dashzeveg (2003) found *Lambdotherium* and *Danjiangia* to be sisters, although their analysis did not include true brontotheriids. However, based on Beard's (1998) assessment and Hooker and Dashzeveg's (2003) results, its position with respect to *Lambdotherium* and true brontotheriids is of obvious interest. Data from *Danjiangia pingi* were taken directly from the only known specimen, IVPP V10842, a partial skull and mandible.

Data

Data for 227 states distributed among 87 characters were compiled in MacClade (Maddison and Maddison, 1992) (table 13). For most of the taxa, the data are complete or nearly complete (70%–100%), although eleven taxa have greater than 50% missing entries. Missing entries mostly result from the fragmentary and poorly preserved condition of fossils. For instance, *Desmatotitan tukhumensis*, *Acrotitan ulanshirehensis*, *Brachydiastematherium transylvanicum*, and *Pollyosbornia altidens* are each known from one mandible. *Bunobrontops savagei* and *Nanotitanops shanghuangensis* are known only from a few isolated dental elements. *Pachytitan ajax* is known from a poorly preserved cranial fragment. In some instances character states were unobservable for other reasons, such as the complete fusion of bones. Another cause of missing entries is the inapplicability of character states to certain taxa. PAUP does not differentiate between these kinds of missing data, and all have been coded as "?".

In some instances, there was ambiguity of character states due to partial fossil preservation. In these instances the taxon was coded with whatever states could not be ruled out. PAUP was then set to treat polymorphisms (instances where multiple states of one character were assigned to a taxon) as ambiguities.

Methods of Phylogenetic Analysis

Phylogenetic analysis using parsimony, PAUP* version 4.0b10 (Swofford, 2001), was used to locate most parsimonious cladograms using the heuristic search algorithm, with the rooting option used to impose a monophyletic ingroup and a paraphyletic outgroup. (The number of included taxa prohibited the use of more exact algorithms, such as brand and bound). All characters were equally weighted. Two basic types of searches were performed: one with ordered multistate characters and another with unordered multistate characters. In the searches where multistate characters were ordered, all but two of the characters (26 and 73) were ordered in the usual sense (i.e., 0–1–2–3...). Character 26 (angle of zygomatics arches) was treated as unordered at all times. A special character-state tree was constructed for character 73 (lower incisor morphology) in MacClade and used in the searches involving ordered character states. The character tree is explained above with the description of character 73. The heuristic searches yielded large numbers of most parsimonious trees (MPTs) and incompletely resolved strict consensus trees. To more thoroughly assess the underlying phylogenetic structure common to all of the most parsimonious trees, a reduced strict consensus was used to generate a series of summary trees (similar to those of Kearney, 2002) depicting both the phylogenetic positions of stable taxa and the multiple possible positions of the wildcard taxa.

Results of PAUP Searches

For each analysis, 20 replicate searches were performed (see Schuh, 2000), all pro-

TABLE 13
Phylogenetic character matrix of Brontotheriidae and outgroup taxa

	1 1234567890	1111111112 1234567890	2222222223 1234567890	3333333334 1234567890	4444444445 1234567890	5555555556 1234567890	6666666667 1234567890	7777777778 1234567890	8888888 1234567
Hyracotherium	000?000001	0?10000000	0001000000	0000000000	1010000010	0000000000	0000000000	0000000000	0000000
Pachynolophus	000?0000?0	0?00000000	0001000100	001000000?	1010000000	0000000000	0000000000	0000000000	0201001
Danjiangia	?00?000000	0?1000?000 1	???????00?	??????0???	?010000000	0001101000	1000000000	1000201000	0211001
Lambdotherium	000?010000 1	??10000000	0001?0010?	0010000000	1010000100	0011101000	1010011000	1000?0?000	0111001
Eotitanops	100?010001	0?00000000	0100?00?0?	0000000000	101?000101	1111101010	1011022021	101?200010	0010002
cf. *Eotitanops*	??????????	??????????	??????????	??????????	????????11	1111101010	1011022021	??????????	??100?2
Palaeosyops	100?020001	0?00000100	0100200000	0001000000	1011000111	1111101010	1012022021	1010200010	0010002
Bunobrontops savagei	??????????	??????????	??????????	??????????	??????????	???1111020	1022022022	??????????	??10002
Mesatirhinus junius	100?030001	0?00200200	0101000000	0000100000	1011000012	1111111121	1122022021	1010200010	0010012
Desmatotitan tukhum.	??????????	??????????	??????????	??????????	??1?0?????	?????????1	?????????1	1010201010	0010012
Acrotitan ulanshireh.	??????????	??????????	??????????	??????????	??1?0????? 2	?????????1	??3???????1	11??201???	?2??????
Dolichorhinus hyog.	1110030001	0?00211200	0121000201	0100100000	1011000012	1111111121	1132133011	1020200010	0010012
Sphenocoelus uinten.	110?030001	0?00200200	0101000000	1100100000	1011000012	1111111121	1132143021	1010000010	0010012
Microtitan mongol.	?????2???? 3 4	??0??00???	??????????	??????????	?????00013	1111111121	1132043001	1???0?0010	0010012
Fossendorhinus diplo.	100??30???	0?11?10201	010000000?	0000000000	101?00?012	1121111121	113214300?	??20??????	0??????
Metarhinus fluviatilis	100?140000	0?12111200	0100100001	0000000000	1011000012	1111111121	1132143111	1020000010	0110012
Metarhinus abbotti	100??40000	0?12111200	0100100001	0000000000	1011000012	1111111121	1132143101	1020000010	?110012
Sthenodectes incisivum	100?1100?1	0?11000201	0100100001	0000000000	1001010012	1111111121	1132143121	1020010010	0010012
Telmatherium validus	100?120001	0?10000201	0110100011	0000000000	1011000112	1111111121	1132033021	1020100010	0010012
Wickia brevirhinus	100?110001	0?10000201	0110200001	0000000000	1011000012	1111111121	1132033121	10??000010	0010012
Metatelmatherium ulti.	100?110001	0?10000200	0100200001	0000000000	1011000012	1111111121	1132043121	1020100010	0010012
Qufutitan zhoui	??0?100001 1 2	0?10000210 1	???????01?	??????????	?023001012	1121111121	1132043022	??????????	???????
Epimanteoceras formosus	1020120001	0?10000201	0120100111	0000000000	1011001012	1121111121	1132143022	??????????	???????
Protitan grangeri	1030120102	0000000202	012210111?	1000000000	1011000012	1111111121	1132143021	2010000010	0010012
Protitan minor	1030130001	0010000202	0122101???	11000?0000	1011000012	1111111121	1132143022	??????????	???????
Protitanotherium emarg.	1030130112	0000000202	012210?11?	0001010000	1022001012	1111111121	1?32143021	2011000110	0010012
Rhinotitan kaiseni	1030121101	0010000201	014210011?	0101010000	0011001012	1121111121	1132143021	2011000110	0110012
Rhinotitan andrewsi	1030131102	1010000201 2	014210011?	0101011000	0012001012	1121111121	1132143021	2011000110	0110012
Nanotitanops shang.	??????????	??????????	??????????	??????????	??????1?12	1121111121	1132133022	??????????	??100??
Pollyosbornia altidens	??????????	??????????	??????????	??????????	??1?0????? 2	?????????1	?????????1	20??0?0010	0210012
Pygmaetitan panxianen.	??????????	??????????	??????????	??????????	??01011012 2 3	1121111121	1132142101	?010??0???	??10112
Gnathotitan berkeyi	?????2???? 3 4	??00000???	??????????	??????????	?01?001012	1121111121	1132143101	2021000010	0210012

TABLE 13
(Continued)

	1 1234567890	1111111112 1234567890	2222222223 1234567890	3333333334 1234567890	4444444445 1234567890	5555555556 1234567890	6666666667 1234567890	7777777778 1234567890	8888888 1234567
Aktautitan hippopot.	1031132101	0010000202	013210011?	???1????00	1012001012	1111111121	1132143101	2021000110	0210012
Brachydiast. transylv.	??????????	??????????	??????????	??????????	???2?0?????	??????????	?????????1	3?11010110	02100??
Metatitan primus	1031132101	0000000201	2142101122?	?0?1?11100	0?3?111012	1121111121	1132143121	3031010111	?210012
Metatitan relictus	1031142101	0000000201	0142101122?	1001011100	1032111012	1121111121	1132143121	3031010111	1210012
Metatitan khaitshinus	1031142101	0000000201	0142101112?	1001011100	002?011012	1121111121	1132143121	3011010110	0210012
Nasamplus progressus	??32132l?1	0010?0????	?1????????	??????????	?????????3	1131111121	11321?3???	??????????	???????
Protembolotherium efr.	1032?3301?	?110000202	0141111022?	0101010010	1???00?013	1131111121	1132143207	??????????	???????
Embolotherium andrewsi	1032134???	?110000212	0141010222?	0101010011	2033011013	1131111121	1132143201	301?010110	1210112
Embolotherium grangeri	1032?44???	?010000212	0141111022?	0101010000	2013001013	1131111121	1132143201	3011000110	1210112
Pachytitan ajax	??30?30112 1	1????0020?	??????????	??????????	?01100?01? 22	1131111121	1132143???	??????????	???????
Diplacodon elatus	1030?31113	0010000202	0122100107	1001010000	1022001012	2131111121	1132143121	2011000110	02?0012
Parabrontops gobiensis	1030130112	0010000202	013210011?	000?0?0000	?033101013	1131111121	1132143107	??????????	???????
Eubrontotherium clarn.	1030130112	0010000202	0131100017	0001010000	1133101013	2131111121	1132143111	3031000110	0010012
Protitanops curryi	1030?30112	0010000202	013211011?	0001010000	1133101013	2131111121	1132143121	??????????	??10012
Notiotitanops mississi.	10????2l??	0?20000207	0??11??11?	00010?00??	1133101013	2131111121	1132143101	3?????????	?210012
Dianotitan lunanensis	1030?30112	0010000202	0131110007	0001010010	?133111013	2131111121	1132143107	??????0???	???????
Duchesneodus uintensis	1030130112	0010000202	2131110007	0001010000	1133111013	2131111121	1132143101	3031000110	0210012
Megacerops coloradensis	1040120112	0020000202	1131110100	0001010011	1133111013	2131111121	1132143101	3131010110	0210012
Megacerops kuwakata.	1040?20112	0020000202	0141110007	?0?1010001	1????1?0??	2131111121	1132142107	??????????	???????

ducing the same results. The searches with ordered data yielded 3967 most parsimonious trees (MPTs) with a relatively well-resolved strict consensus (fig. 194). The search using unordered data resulted in 603,705 MPTs and a less resolved strict consensus (fig. 196). The MPTs based on ordered characters have the following parameters: tree length (TL) = 309; consistency index (CI) = 0.453; homoplasy index (HI) = 0.547; and retention index (RI) = 0.814. The MPTs based on unordered characters have the following parameters: TL = 319; CI = 0.439; HI = 0.561; and RI = 0.803.

Consensus Trees and Wildcards

The analysis of brontothere phylogeny is aimed at reconstructing the phylogeny of the entire family; therefore, all valid taxa were included regardless of the amount of missing data. In general, paleontological data are plagued with fragmentary taxa that tend to act as wildcards (sensu Nixon and Wheeler, 1992), thus increasing the number of MPTs. Inevitably, any attempt to reconstruct complete phylogenies, including all known extinct members of a clade (e.g., Grande and Bemis, 1998), will include highly fragmentary taxa, inevitably resulting in poorly resolved strict consensus trees. Neither analysis performed here yielded a completely resolved strict consensus.

The strict component consensus (SCC) (figs. 194, 196) is the most common and widely accepted consensus method, but it is incapable of depicting all the phylogenetic information common to all the MPTs, and wildcards tend to render the SCC relatively uninformative. The SCC includes only those components (or parts of trees) that are replicated in all MPTs while other components are collapsed to polytomies (Wilkinson, 1994). Many have argued that the SCC is too strict (e.g., Swofford, 1991) because it is insensitive to all the strictly supported relationships that are common to all the primary trees (Wilkinson, 1994, and references therein). More specifically, all primary trees may share a common set of cladistic information (i.e., a common set of *n*-taxon statements) that the SCC is incapable of graphically depicting because one or more wildcard taxa, whose positions are highly unstable, can collapse a component of the tree into a polytomy, even though there are strictly supported relationships between other taxa within that component.

Prior approaches to deal with the problem of missing data include alternative consensus techniques and a priori removal of fragmentary taxa (see Kearney, 2002 and Kearney and Clark, 2003, for summaries). A priori exclusion of fragmentary taxa is not the best solution to the problem of poor SCC resolution. A priori removal of fragmentary taxa denies us the opportunity of learning at least something about their phylogenetic positions, however unresolved they may be. Moreover, there is not necessarily a correspondence between erratic wildcard behavior and missing data entries (Kearney, 2002 and Kearney and Clark, 2003). The analysis of brontotheres clearly bears this out. For instance, *Bunobrontops savagei* consists of only a few teeth, but its position is completely resolved. Moreover, those taxa that possess a unique combination of character states may affect the apparent relationships of other taxa in the analysis (Wilkinson, 1995a, 2003) and/or they may nest within a well-resolved position in the cladogram despite their fragmentary nature. Wildcard behavior can either result from character conflict (homoplasy) or from ambiguities related to missing data, or from both (Kearney, 2002). Therefore, complete taxa may also act as wildcards because of homoplasy. It is not possible to determine a priori how a taxon will influence the analysis regardless of its degree of completeness. Therefore, rather than deleting taxa a priori, alternative consensus methods should be used to pull a greater degree of phylogenetic resolution out of the analysis.

As noted above the amount of phylogenetic resolution retained by the strict component consensus diminishes as the number of MPTs increases. Other common consensus methods such as majority rule or Adams consensus are problematic because they contradict some or all of the MPTs. The strict reduced consensus (SRC) method, on the other hand, depicts only relationships that are common to all of the MPTs, but unlike the SCC, this method is capable of graphically depicting all the common phylo-

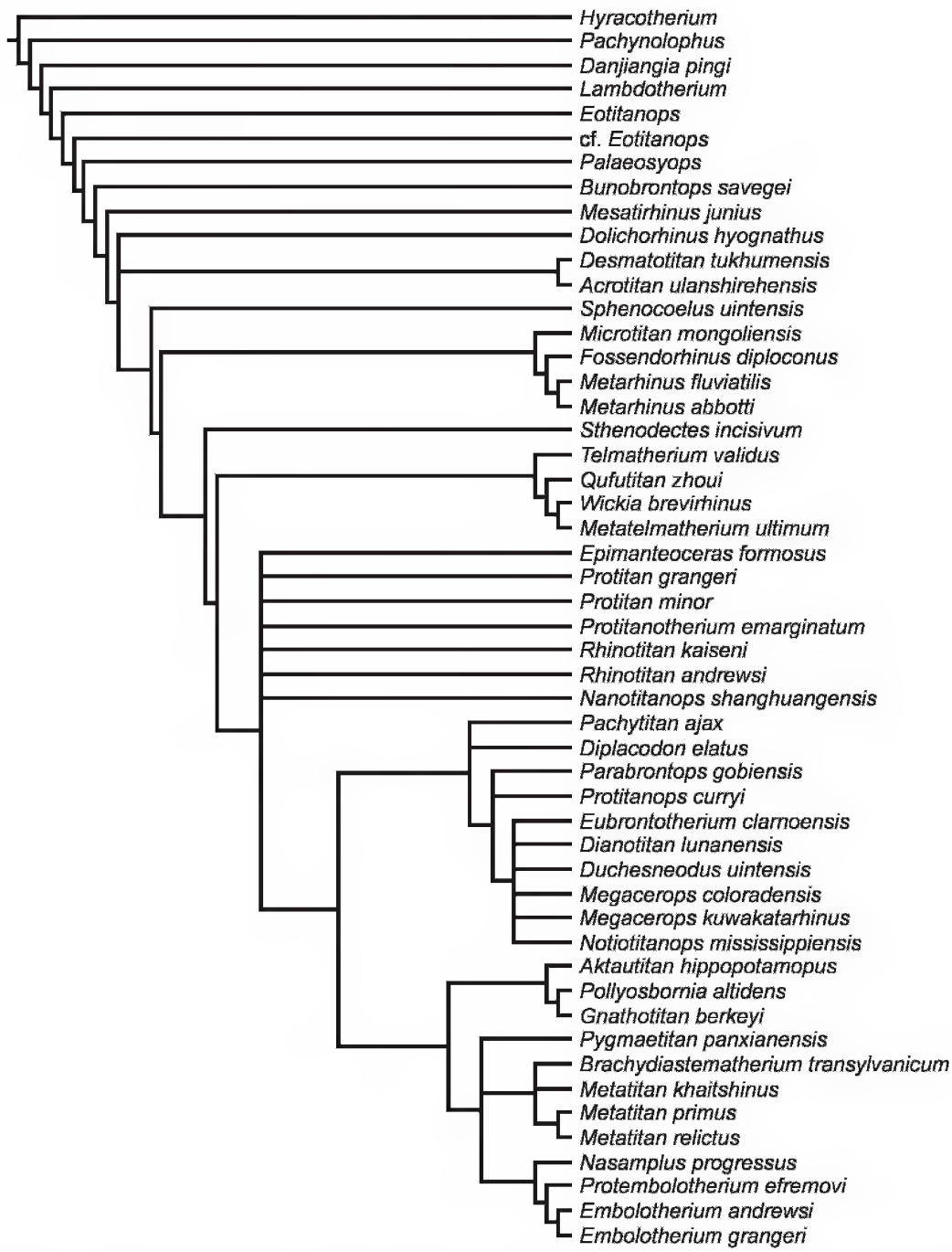

Fig. 194. Strict component consensus of heuristic search performed with ordered multistate characters.

genetic relationships (Wilkinson, 1994, 2003). The SRC is an a posteriori taxon-pruning method that identifies and removes various combinations of wildcards from the primary trees. The SRC consists of a profile of consensus trees with different combinations of taxon omissions. The number of trees in the SRC profile varies with the analysis; it includes as many trees as needed to depict all the phylogenetic relationships common to all

the MPTs. The SRC profile can be large; however, derivative trees can be constructed by fusing trees within the profile to produce a tree that includes only those taxa that are common to all the trees being fused, and that includes all the relationships among these taxa that are represented in any of the trees being fused (Wilkinson, 1995b, 2003). Wilkinson (1995b) suggested that derivative trees could be reconstructed by hand. This is true, although one can also assemble derivative SRC trees by using PAUP to prune (a posteriori) all taxa from the primary trees already pruned by SRC and then computing a strict consensus. Furthermore, summary trees can be constructed from derivative SRC trees by mapping the omitted wildcards back onto the tree.

In fig. 195 (ordered character analysis) and figs. 197–198 (unordered character analysis), I have depicted a combination of summary trees, derived from the SRCs of the analyses of both ordered and unordered characters. RadCon (Thorley and Page, 2000) software was used to generate SRC profiles and to identify wildcard taxa (Wilkinson, 1994, 1995b, 2003). RadCon can handle an upper limit of 10,000 primary trees. The summary tree of the 3967 MPTs resulting from the analysis of ordered character data is seen in fig. 195; two taxa were flagged as wildcards and the resulting summary tree is a derivative of two SRC trees fused into one, with the two wildcards (*Nanotitanops* and *Notiotitanops*) mapped back onto it.

The excessive number of MPTs (603,705) resulting from the unordered analysis prohibited the direct production of an SRC. To arrive at the summary trees in figs. 197 and 198, it was necessary to perform SRC in two sequential steps. First, SRC was performed in RadCon with 10,000 trees extracted from the PAUP tree file of 603,705 trees. The SRC of these 10,000 trees flagged numerous fragmentary wildcard taxa. Using PAUP, the most erratic and fragmentary of these were then omitted from the full set of 603,705 trees, and the redundant trees were discarded, resulting in 977 unique trees. The strict consensus of these 977 trees is seen in fig. 197, with wildcards mapped back onto it. This tree is equivalent to a derivative tree with the same taxon omissions had SRC been performed on the entire set of 603,705 trees. A second SRC was performed in RadCon with the remaining 977 unique trees. The resulting summary tree (fig. 198) is equivalent to a derivative of the SRC on the full set of 603,705 trees with all of the wildcards removed (all taxa listed as omitted from figs. 197 and 198). These two summary trees depict all the phylogenetic information common to all the MPTs, except for any common relationships relating to the wildcards that have been omitted.

Fragmentary taxa with more than 50% missing entries were found to behave in three fundamental ways. (1) Some always nested in an unambiguous position (e.g., *Bunobrontops savagei*). (2) Others (e.g., *Nanotitanops shanghuangensis*) were unstable in the analyses of both ordered and unordered character data. (3) Other fragmentary taxa were stable or erratic, depending on the use of ordered or unordered character data (e.g., *Pollyosbornia altidens*). In the analysis of unordered characters, numerous complete taxa exhibited wildcard behaviors (e.g., *Diplacodon elatus*), indicating instances where homoplasy, rather than missing data, obscure relationships.

BRONTOTHERE PHYLOGENY AND CLASSIFICATION

The trees resulting from the unordered and ordered character searches have roughly similar topologies, although there are conspicuous differences. It is pointless to discuss the topologies of these trees in terms of support or lack of support for higher brontothere taxa (e.g., subfamilies) without providing a historical review of brontothere higher taxonomy and phylogenetics, because many of the names for higher brontothere taxa have fallen out of widespread use, and, for the most part, were not even originally intended to imply monophyly and, thus, are not necessarily suitable for cladistic testing.

History

The earliest attempt to graphically outline brontothere phylogeny was made by Earle (1892) who proposed a straight-line ancestor-descendant hypothesis of a *Lambdotherium-Palaeosyops-Telmatherium-Dolichorhinus* lin-

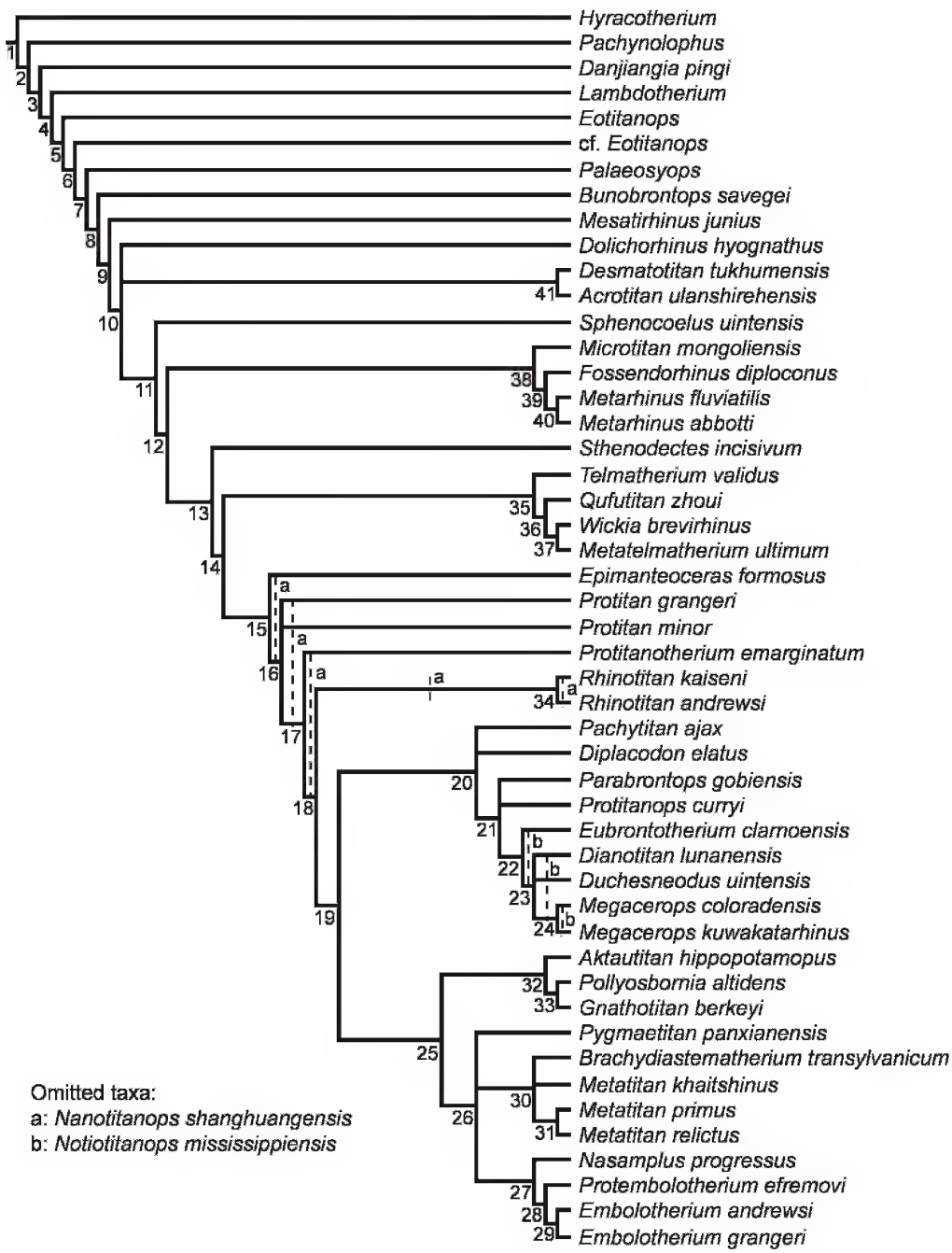

Fig. 195. Summary tree of the analysis of ordered characters, depicting the primary strict reduced consensus and the possible positions of pruned wildcards as represented by lettered dotted lines. Those branches intersected by dotted lines show the variable phylogenetic positions of the wildcard taxa among the most parsimonious trees. Node numbers correspond to table 14.

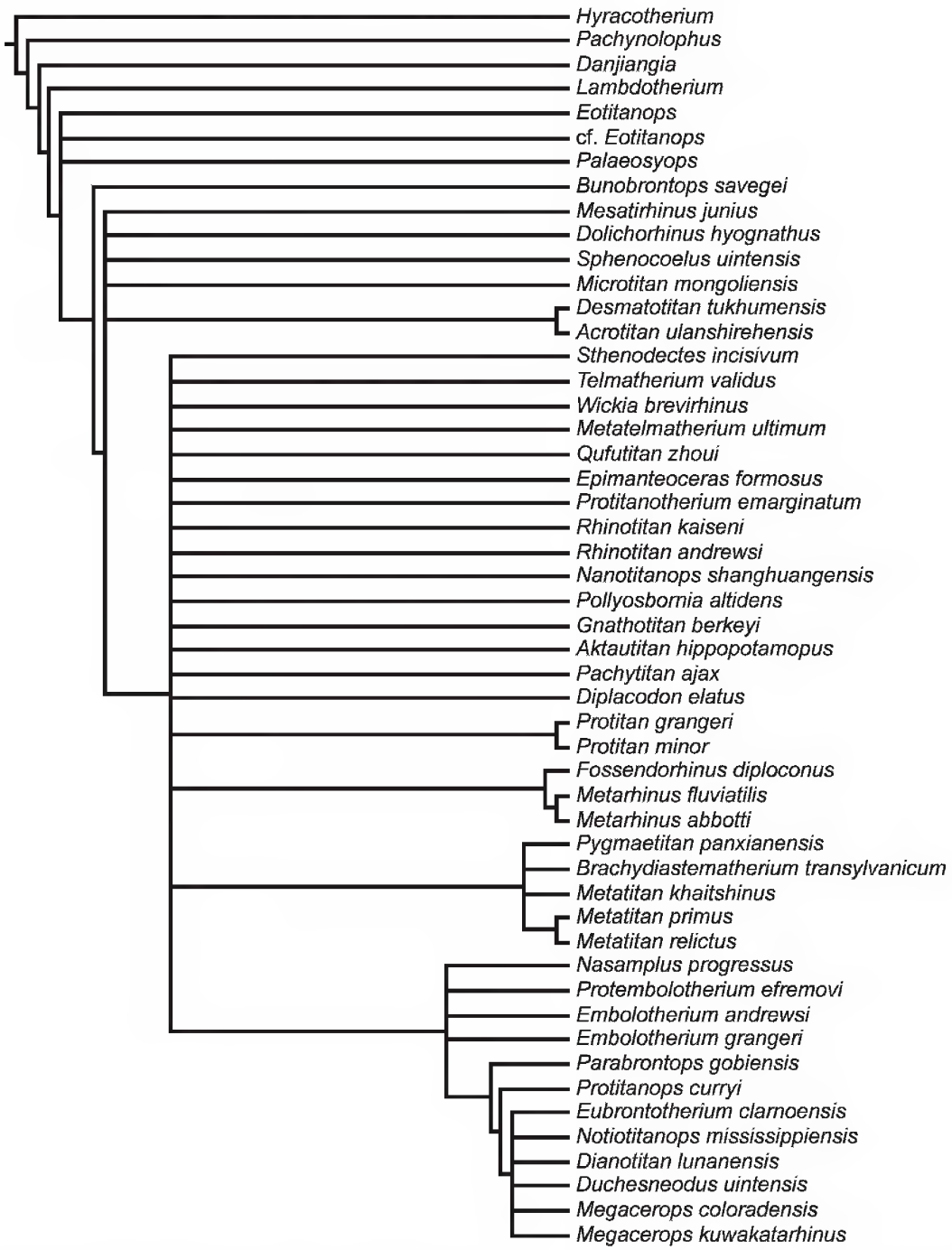

Fig. 196. Strict component consensus of heuristic search performed with unordered multistate characters.

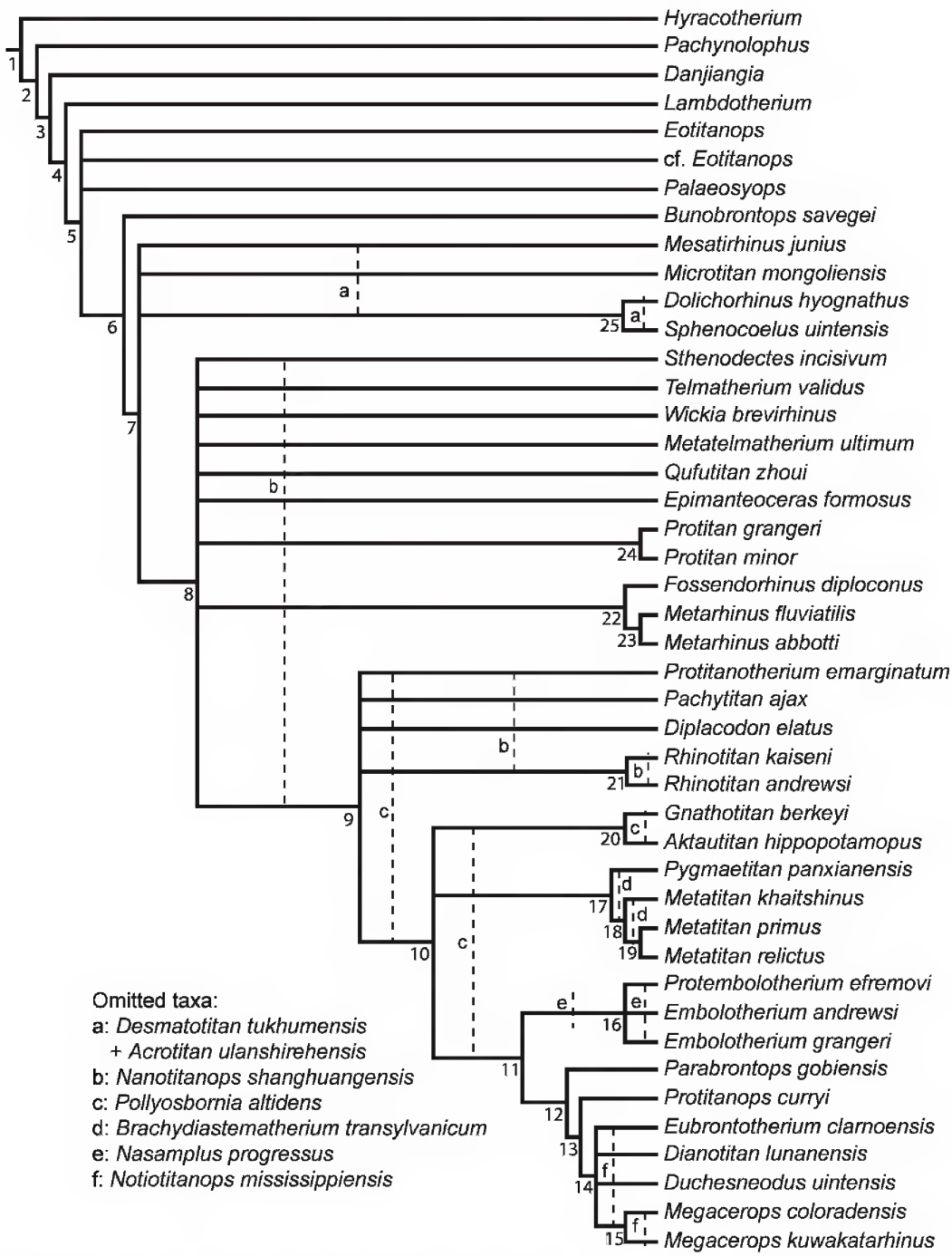

Fig. 197. Summary tree of the analysis of unordered characters, depicting a strict reduced consensus where only the unstable fragmentary wildcards have been removed. Those branches intersected by dotted lines show the variable phylogenetic positions of the wildcard taxa among the most parsimonious trees. Node numbers correspond to table 15.

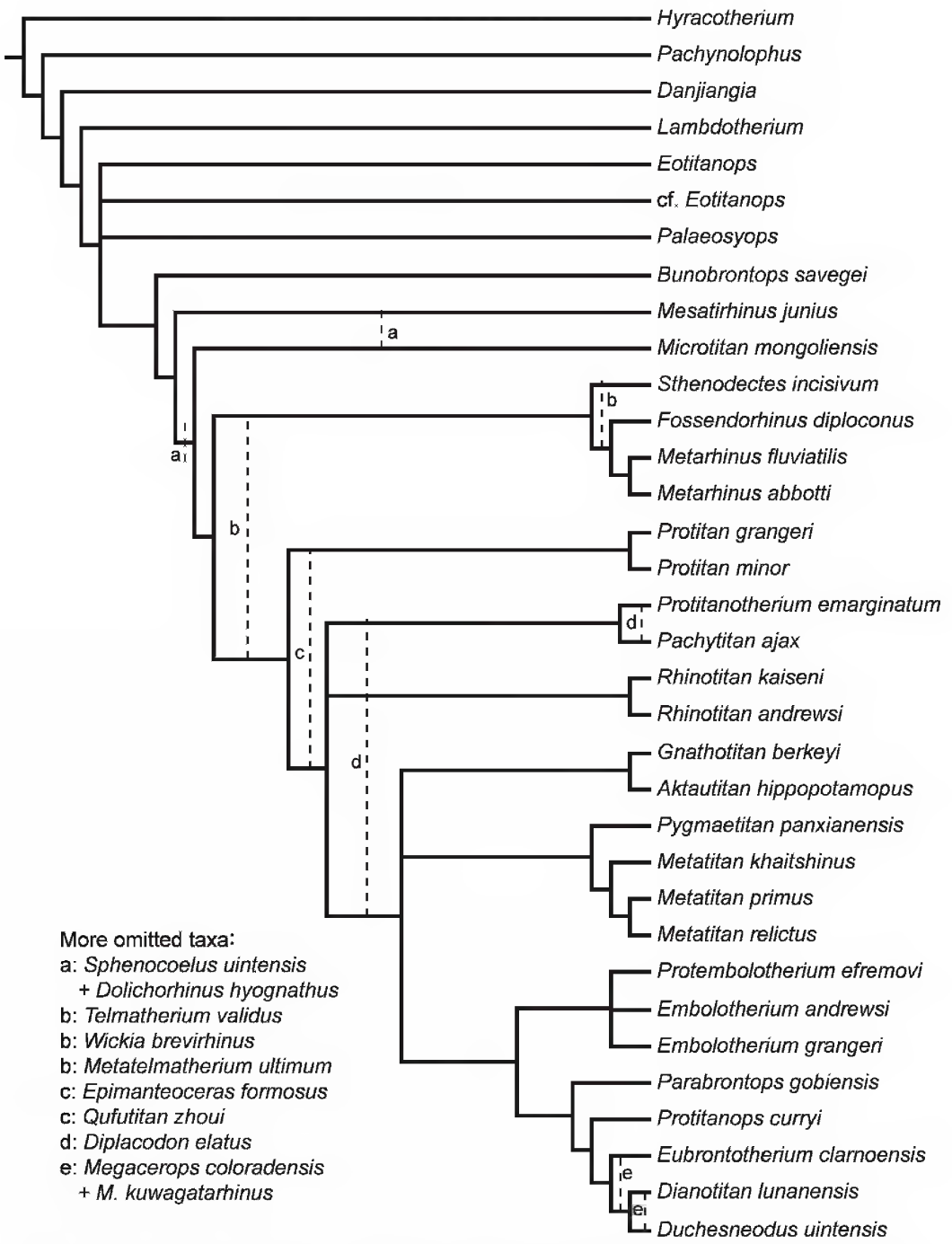

Fig. 198. Summary tree of the analysis of unordered characters showing the remainder of phylogenetic relationships common to all of the MPTs as revealed by a further series of taxon deletions, including the deletion of nonfragmentary wildcards. In this tree, all wildcards have been omitted, including those listed in figure 197, as well as those listed above.

TABLE 14
Uniquivocal character state transformations as they occur in fig. 195 (analysis of ordered character data)

Node 2→Node 3: (54: 0→1) (55: 0→1) (57: 0→1) (61: 0→1) (71: 0→1) (75 0→2) (83: 0→1)
Node 3→Node 4: (6: 0→1) (48: 0→1) (53: 0→1) (63: 0→1) (66: 0→1) (67: 0→1) (82: 2→1)
Node 4→Node 5: (Brontotheriidae) (1: 0→1) (13: 1→0) (22: 0→1) (50: 0→1) (51: 0→1) (52: 0→1) (59: 0→1) (64: 0→1) (66: 1→2) (67: 1→2) (69: 0→2) (70: 0→1) (73: 0→1) (79: 0→1) (82: 1→0) (84: 1→0) (87: 1→2)
Node 5→Node 6: (49: 0→1)
Node 6→Node 7: (64: 1→2)
Node 7→Node 8: (Brontotheriinae) (56: 0→1) (59: 1→2) (63: 1→2)
Node 8→Node 9: (58: 0→1) (60: 0→1) (62: 0→1) (86: 0→1)
Node 9→Node 10: (63: 2→3)
Node 10→Node 41: (77: 0→1)
Node 11→Node 12: (5: 0→1) (35: 1→0)
Node 12→Node 38: (69: 2→0)
Node 38→Node 39: (16: 0→1)
Node 39→Node 40: (6: 3→4) (14: 0→2) (17: 0→1) (68: 0→1)
Node 12→Node 13: (6: 3→2) (15: 1→0)
Node 13→Node 14: (23: 0→1) (29: 0→1)
Node 14→Node 35: (65: 1→0)
Node 35→Node 36: (6: 2→1)
Node 36→Node 37: (68: 0→1)
Node 14→Node 15: (3: 0→2) (23: 1→2) (28: 0→1)
Node 15→Node 16: (3: 2→3) (20: 1→2) (24: 0→2)
Node 16→Node 17: (34: 0→1) (36: 0→1) (44: 1→2) (74: 0→1) (78: 0→1)
Node 17→Node 18: (7: 0→1) (23: 2→3) (53: 1→2) (82: 0→1)
Node 18→Node 34: (23: 3→4) (32: 0→1) (41: 1→0)
Node 18→Node 19: (68: 0→1) (82: 1→2)
Node 19→Node 25: (4: 0→1) (7: 1→2)
Node 25→Node 32: (73: 1→2)
Node 32→Node 33: (78: 1→0)
Node 25→Node 26: (23: 3→4) (29: 1→2) (71: 2→3)
Node 71→Node 67: (85: 0→1)
Node 26→Node 27: (53: 2→3)
Node 27→Node 28: (7: 2→3)
Node 28→Node 29: (7: 3→4) (19: 0→1) (41: 1→2)
Node 26→Node 30: (6: 3→4) (13: 1→0) (20: 2→1) (27: 0→1) (31: 0→1) (37: 0→1) (38: 0→1) (43: 1→2)
Node 30→Node 30: 43: 2→3) (45: 0→1) (73: 1→3) (80: 0→1)
Node 19→Node 20: (9: 0→1) (53: 2→3)
Node 20→Node 21: (7: 1→0) (43: 2→3) (44: 2→3) (45: 0→1) (50: 2→3)
Node 78→Node 76: (24: 2→1)
Node 21→Node 22: (28: 1→0)
Node 22→Node 23: (26: 0→1) (29: (1→0) (46: 0→1)
Node 23→Node 24: (3: 3→4) (6: 3→2) (13: 1→2) (40: 0→1) (76 0→1)

eage, with some side branches, such as *Mesatirhinus*, independently stemming off of *Palaeosyops*. *Eotitanops* was regarded as possibly having a separate origin and independently giving rise to another independent lineage of *Palaeosyops*. Later Earle (1895) revised his hypothesis to have parallel lineages, *Mesatirhinus-Dolichorhinus* and *Palaeosyops-Telmatherium*.

Earle's early hypotheses about brontothere phylogeny foreshadowed Osborn's (1914, 1929a) extremely orthogenetic interpretation, where many lineages were envisioned as evolving in parallel with similar taxa having independent origins. Osborn's (1929a) methods were wedded to his orthogenetic philosophy and his resulting classification is clearly incompatible with evolutionary theory or modern methods of taxonomy and phylogeny reconstruction. By 1914 Osborn was essentially preoccupied with discovering the "appearance" of rudimentary structures (rec-

TABLE 15
Uniquivocal character state transformations as they occur fig. 197 (analysis of unordered character data)

Node 2→Node3: (54: 0→1) (55: 0→1) (57: 0→1) (61: 0→1) (71: 0→1) (75: 0→2) (83: 0→1)
Node 3→Node 4: (6: 0→1) (53: 0→1) (63: 0→1)
Node 4→Node 5: (Brontotheriidae) (1: 0→1) (13: 1→0) (22: 0→1) (51: 0→1) (52: 0→1) (64: 0→2) (66: 0→2) (67: 0→2) (69: 0→2) (70: 0→1) (73: 0→1) (79: 0→1) (84: 1→0) (87: 1→2)
Node 5→Node 6: (Brontotheriinae) (56: 0→1) (59: 0→2) (63: 1→2)
Node 6→Node 7: (58: 0→1) (60: 0→1) (62: 0→1) (86: 0→1)
Node 8→Node 22: (16: 0→1) (69: 2→0)
Node 22→Node 23: (6: 1→4) (14: 1→2) (17: 0→1) (20: 1→0)
Node 8→Node 24: (27: 0→1) (31: 0→1) (47: 1→0) (53: 2→1)
Node 8→Node 9: (82: 0→2) (78: 0→1)
Node 9→Node 10: (7: 0→2) (68: 0→1) (69: 2→0)
Node 10→Node 17: (46: 0→1)
Node 17→Node 18: (69: 0→2)
Node 18→Node 19: (28: 1→2) (45: 0→1) (73: 1→3) (80: 0→1)
Node 11→Node 16: (4: 0→2)
Node 11→Node 12: (7: 2→0) (10: 1→2) (23: 4→3) (45: 0→1)
Node 12→Node 13: (42: 0→1) (51: 1→2)
Node 13→Node 14: (24: 2→1) (28: 1→0)
Node 14→Node 15: (3: 3→4) (6: 3→2) (13: 1→2) (40: 0→1)
Node 10→Node 20: (73: 1→2)
Node 7→Node 25: (2: 0→1) (32: 0→1) (65: 0→1)

tigradations) and tracing the evolution of character proportions (allometrons) through perceived phylogenetic sequences. Osborn (1914) began developing a phylogenetic hypothesis for North American brontotheres based on the following characters: limb proportions, skull proportions (brachycephaly versus dolichocephaly), the development of horns, the molarization of the premolars, and the number of incisors, which he carried though to his monographic treatment of the Brontotheriidae (Osborn, 1929a). Osborn (1914, 1929a) divided the Brontotheriidae into eleven subfamilies, based on these characters, some of them defined by evolutionary rates rather than explicit character states. For instance, one of the subfamilies, Diplacodontinae was partly characterized by accelerated molarization of the premolars (Osborn, 1914). Osborn's 11 subfamilies are more or less arbitrary divisions of his graphic phylogenetic hypothesis of North American brontotheres (fig. 199).

The 12 subfamilies used by Osborn (1929a) to classify North American (and the sole European) brontotheres include Lambdotheriinae Hay (1901) (includes *Lambdotherium*), Eotitanopinae Osborn (1914) (includes *Eotitanops*), Palaeosyopinae Steinmann and Döderlein (1890) (includes *Palaeosyops*), Telmatheriinae Osborn (1914) (includes *Telmatherium* [in part], *Metatelmatherium*, *Sthenodectes*), Manteoceratinae Osborn (1914) (includes *Telmatherium* [in part], *Protitanotherium*, *Brachydiastematherium*), Dolichorhininae Osborn (1929a) (includes *Mesatirhinus*, *Dolichorhinus*, *Metarhinus* [in part]), Rhadinorhininae Osborn (1929a) (includes *Metarhinus* [in part]). Diplacodontinae Osborn (1914) (includes *Diplacodon*), Brontopinae Osborn (1914) (includes *Megacerops* sensu Mihlbachler et al., 2004b [in part]), Menodontinae Osborn (1914), (includes *Megacerops* sensu Mihlbachler et al., 2004b [in part]), Megaceropinae Osborn (1914) (includes *Megacerops* sensu Mihlbachler et al., 2004b [in part]), and Brontotheriinae Steinmann and Döderlein (1890) (includes *Megacerops* sensu Mihlbachler et al., 2004b [in part]). The genera listed above in parentheses represent taxa included in these subfamilies by Osborn (1929a), but with terminology reflected by the present revision. After correcting for Osborn's oversplit species- and genus-level taxonomy, most of Osborn's (1929a) subfamilies turn out to be monogeneric (and in many cases, monospecific). Moreover, several of these subfamilies

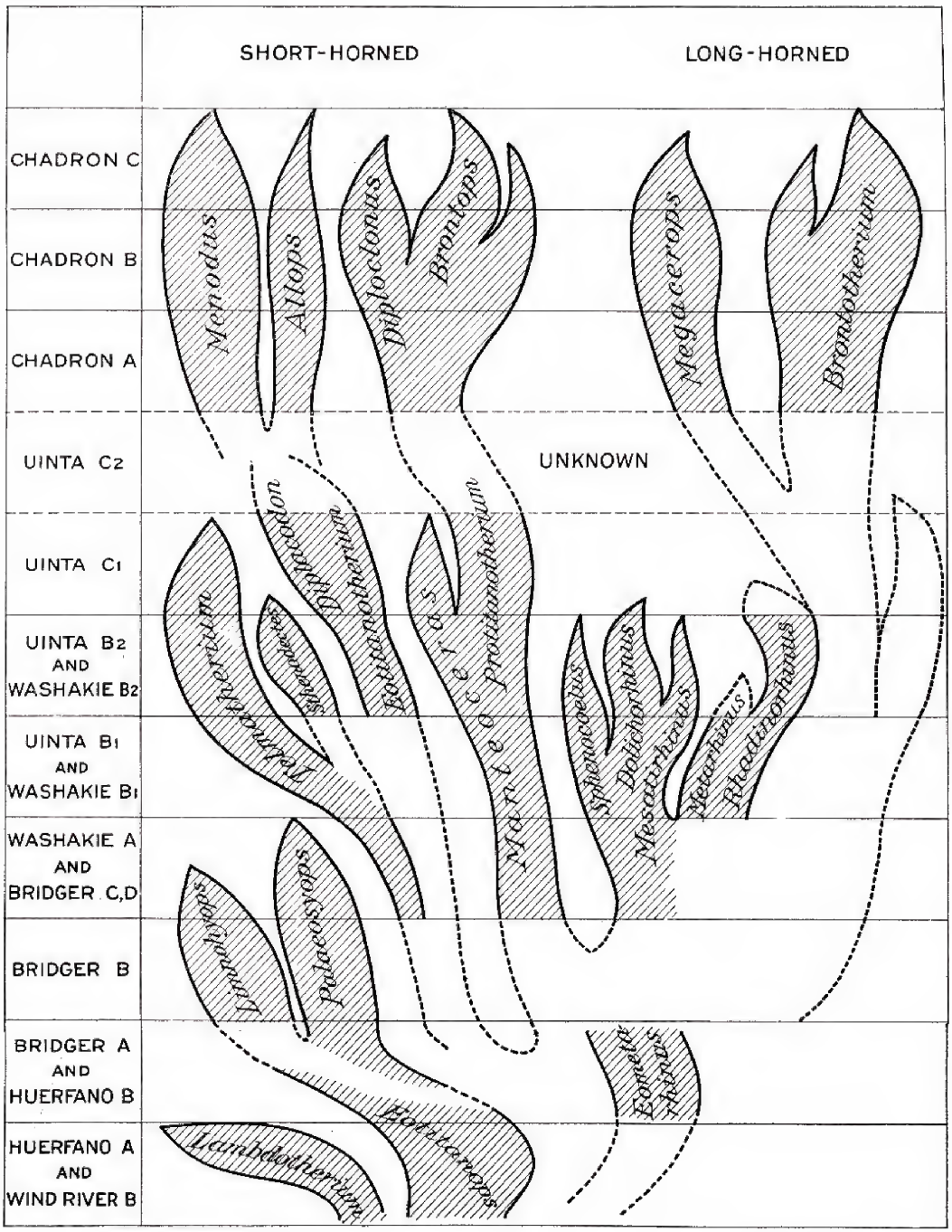

Fig. 199. Osborn's (1929a) "polyphyletic" phylogeny of North American Brontotheriidae. The key to taxonomic synonyms in this phylogeny are as follows: *Limnohyops*, *Eometarhinus* (= *Palaeosyops*); *Manteoceras* (= *Telmatherium*); *Rhadinorhinus* (= *Metarhinus*); *Eotitanotherium* (= *Diplacodon*); *Menodus*, *Allops*, *Diploconus*, *Brontops*, *Brontotherium* (= *Megacerops* sensu Mihlbachler et al., 2004b).

obviously do not represent monophyletic groups because they share taxa. For instance, Telmatheriinae and Manteocerotinae both contain *Telmatherium validus*. Additionally, Rhadinorhininae and Dolichorhininae both contain *Metarhinus*. Four of Osborn's (1929a) subfamilies, Brontopinae, Menodontinae, Megaceropinae, and Brontotheriinae are depicted as descending independently from members of other families. However, the taxa that were assigned to these four subfamilies may actually belong to a single species, *Megacerops coloradensis* (sensu Mihlbachler et al., 2004b).

In the past, Asian brontotheres were classified separately. Osborn (1929b) placed *Embolotherium* in its own subfamily, Embolotheriinae. Granger and Gregory (1943) were the first to propose an explicit hypothesis of Asian brontothere phylogeny (fig. 200). They erected two new additional subfamilies for Asian brontotheres, including Metatelmatheriinae (*Metatelmatherium*, *Desmatotitan*, *Hyotitan*) and Epimanteocerotinae (*Epimanteoceras*, *Protitan*, *Microtitan*, *Gnathotitan*, *Rhinotitan*, *Pachytitan*, *Parabrontops*, *Metatitan*). Metatelmatheriinae shares the monotypic genus, *Metatelmatherium*, with Osborn's (1929a) Telmatheriinae and is obviously invalid. Moreover, Granger and Gregory (1943) rendered Epimanteocerotinae paraphyletic by nesting the subfamily Embolotheriinae within it.

Rather than resolving the problem of brontothere taxonomy, subsequent attempts to revise the classification of brontothere higher taxa have only compounded it by arbitrarily combining subfamilies without explicit justifications, but essentially maintaining Osborn's (1929a) orthogenetic classification consisting mostly of nonmonophyletic groups. In his classic work on the classification of mammals, Simpson's (1945) classification is directly descended from Osborn's although he reduced the number of North American subfamilies from 11 to seven by arbitrarily combining Eotitanopinae with Palaeosyopinae, Rhadinorhininae with Dolichorhininae, Manteocerotinae with Brontopinae, Diplacodontinae with Menodontinae, and Megaceropinae with Brontotheriinae. Regarding Asian brontotheres, Simpson (1945) combined Metatelmatheriinae with Telmatheriinae, combined Epimanteocerotinae with Brontopinae (+ Manteocerotinae), and continued to accept Embolotheriinae. Simpson's classification is more or less inherited in the more recent mammal classification of McKenna and Bell (1997).

More recent suggestions regarding brontothere classification (Schoch and Lucas, 1985; Mader, 1989) were not adopted by McKenna and Bell (1997). In an abstract, Schoch and Lucas (1985) grouped brontotheres into two informal groups, the "paleobrontotheres" and the "eubrontotheres". The term paleobrontotheres was meant to represent "typical brontotheres from the middle Eocene from *Palaeosyops* to *Diplacodon*". "Paleobrontotheres" was not defined by apomorphies and it clearly represents a paraphyletic assemblage. "Eubrontotheres", on the other hand, were distinguished by rounded, spherical incisors, relatively molarized premolars, hypocone on upper third premolar, and distinct to well-developed horns.

Mader (1989) attempted to revise the genus level phylogeny of North American brontotheres and he provided a cladistic hypotheses of North American brontothere phylogeny, although it was limited in its taxonomic scope. Mader (1989) rejected the majority of brontothere subfamilies on grounds that they are monogeneric and recognized only two subfamilies, the Telmatheriinae (including *Telmatherium* and all North American horned brontotheres) and Dolichorhininae (including *Dolichorhinus*, *Mesatirhinus*, and *Rhadinorhinus* [= *Metarhinus*]). The Diplacodontinae (including all North American horned brontotheres) was recognized as a subset of Telmatheriinae and the "eubrontotheres" of Schoch and Lucas (1985) were recognized as a subset of Diplacodontinae. Mader (1989) also suggested that Metatelmatheriinae (including *Metatelmatherium* and *Sthenodectes*) could be valid although he omitted this taxon from his phylogenetic analysis. In a later revision, Mader (1998) reversed his decision to reject monogeneric subfamilies, and resurrected Palaeosyopinae and Eotitanopinae.

Mihlbachler et al. (2004a) developed the first cladistic hypothesis of Asian horned brontotheres, Epimanteocerotinae and Embolotheriinae of Granger and Gregory

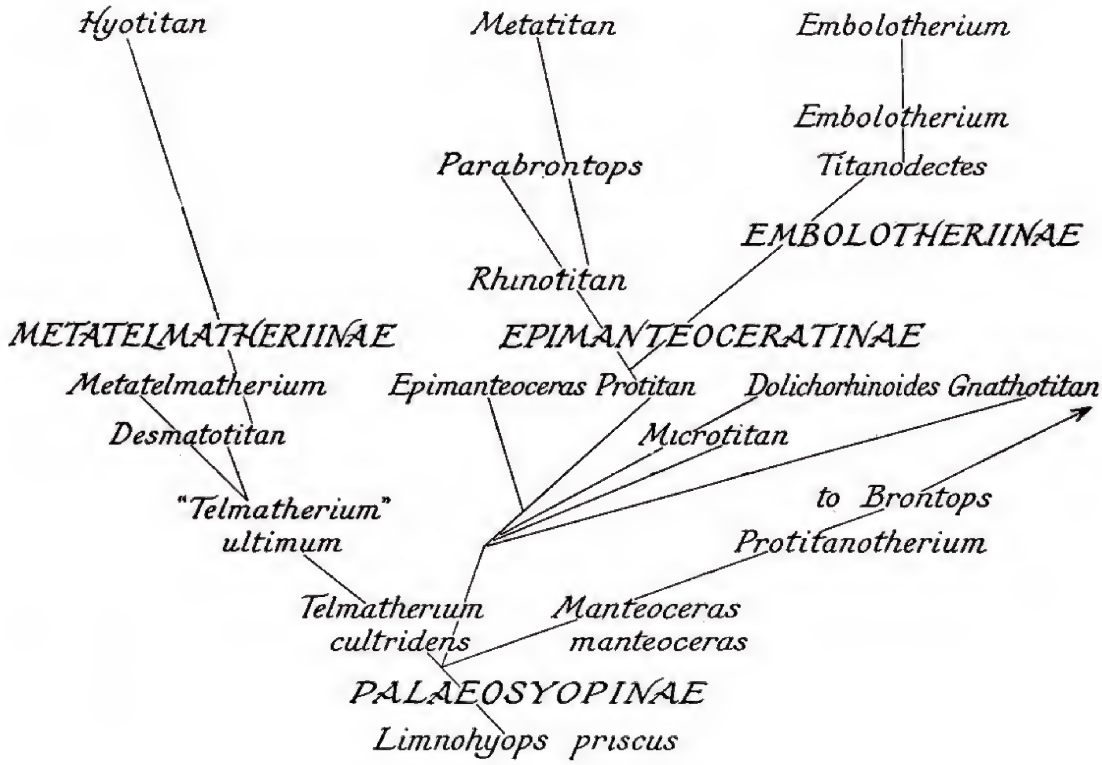

Fig. 200. Granger's and Gregory's (1943) hypothesis of Asian brontothere phylogeny. The key to taxonomic synonyms are as follows: *Limnohyops* (= *Palaeosyops*); *Manteoceras manteoceras*, *Telmatherium cultridens* (= *Telmatherium validus*); *Brontops* (= *Megacerops* sensu Mihlbachler et al., 2004b); "*Telmatherium*" *ultimum* (= *Metatelmatherium ultimum*), *Dolichorhinoides* (= *Epimanteoceras*); *Titanodectes* (= *Embolotherium grangeri*).

(1943). Epimanteocerotinae sensu Granger and Gregory (1943), consisting of *Epimanteoceras*, *Protitan*, *Pachytitan*, *Gnathotitan*, *Rhinotitan*, *Metatitan* and *Parabrontops*, was found to be paraphyletic with members of the Embolotheriinae, *Embolotherium* and its synonym, *Titanodectes*, nesting within it. Mihlbachler et al. (2004a) were cautious about accepting an Asian brontothere clade consisting of Epimanteocerotinae plus Embolotheriinae. At the time, no analysis of Asian and North American species had ever been undertaken, but they suggested that Asian and North American brontotheres were interrelated, and that neither continental assemblage formed a true clade. Based on the results of that study, the subfamily Embolotheriinae, originally used only for *Embolotherium* and its synonym, *Titanodectes*, was expanded to include *Aktautitan*, *Brachydiastematherium*, and *Metatitan*.

Brontothere Higher Taxa

In this paper, the delimitation and diagnosis of species was performed prior to the phylogenetic analysis and with the exceptions of two taxa that were included in the analysis at the genus level (*Eotitanops* and *Palaeosyops*), higher taxa were evaluated a posteriori; therefore, all higher taxa are discussed in this section as results of that phylogenetic analysis. The section discusses polytypic brontothere genera and higher taxa, and their support (or lack thereof) provided by the phylogenetic analysis. Monotypic genera are not discussed here; naturally, the phylogenetic analysis does not test for the monophyly of monotypic genera, nor would their diagnoses be any different than their species.

Most higher brontothere taxa as defined and used by earlier taxonomists were not

defined on the criterion of monophyly and they are not directly testable in the cladistic sense. On the other hand, brontothere clades discussed and redefined by Mader (1989, 1998) and Mihlbachler et al. (2004a) are testable in the cladistic sense; some of these are rejected by the present analysis while others require redefinition (due to improved character data and greater taxon sampling). Because many of the clades of brontotheres to which subfamily names have been previously applied actually nest within each other, new rankings have been applied where necessary and it has been necessary to radically revise how some higher names are used (see ICZN article 6.1). This unavoidable reranking of names could lead to confusion; therefore, in the ensuing discussion the use of subfamily names in quotes refers to older usages. Subfamily names and other higher taxa used outside of quotes refer to the revised classification introduced in this paper.

BRONTOTHERIIDAE: Marsh's (1873) original use of the name "brontothere" (i.e., Brontotheriidae Marsh, *Brontotherium* Marsh) was aimed at horned taxa that were known at the time (*Brontotherium*, *Titanotherium* [both = *Megacerops coloradensis* sensu Mihlbachler et al., 2004b]). Hornless brontotheres were originally placed into a separate family, Limnohyidae Marsh (1875). However, Limnohyidae has long since become obsolete and the family name Brontotheriidae was expanded to encompass the hornless members. *Lambdotherium* is historically considered to be the basal member of the Brontotheriidae or its sister taxon and part of the superfamily Brontotheriioidea (Earle, 1892; Osborn, 1929a; Hooker, 1989; Prothero and Schoch, 1989). Mader (1989; 1998) excluded *Lambdotherium* from the Brontotheriidae. An unpublished master's thesis (Wallace, 1980) considered *Lambdotherium* not to be a brontothere, but a palaeotheriid. Recent cladistic analyses do not provide a clear answer as to the position of *Lambdotherium* with respect to Brontotheriidae. Froehlich (1999) found *Lambdotherium* and a brontothere (*Palaeosyops*) to be sister taxa within the Palaeotheriidae. On the other hand, Lucas and Holbrook (2004) found *Lambdotherium* to be part of a clade that included palaeotheriids, but the brontothere *Eotitanops* was outside that clade. The phylogenetic position of *Lambdotherium* remains unresolved, and this study does not address the question. Therefore, I follow Mader (1989, 1998) in excluding *Lambdotherium* from the Brontotheriidae.

Mader (1989, 1998) defined brontotheriids as having a bunoselenodont molar with a W-shaped ectoloph, isolated lingual cusps, and possibly with a shortened face and elongate postorbital cranium. The W-shaped ectoloph is not strictly a brontothere character; it is shared with *Lambdotherium*, *Danjiangia*, and a variety of other perissodactyls. The isolated lingual cusps and shortened face, on the other hand, distinguish true brontotheriids from *Lambdotherium*.

Unequivocal apomorphies that support Brontotheriidae (node 5 in fig. 195) include an elongate postorbital cranium; orbit above M2; postorbital constriction of the skull lacking; upper premolar paracone and metacone ribs equally sized; preprotocristae and paraconules weakly developed on P2 but faint to absent on P3 and P4; upper premolar postprotocrista absent; labial side of upper molar paracone and metacone lingually angled and concave; labiolingual width of upper molar ectoloph half the total width of the tooth; upper molar protoloph and paraconules very small; M1–M2 metaloph vestigial; M3 hypocone absent or rare; mandibular symphysis short and robust; i1–i2 semispatulate but i3 subcaniniform; cristid obliqua of p2 present; p3 metaconid absent; single molar metaconid; and hypoconulid of m3 connected to the entoconid on the lingual side of the tooth.

EOTITANOPINAE: Eotitanopinae is presently a phylogenetically uninformative subfamily that is synonymous with the only North American genus *Eotitanops*. The new but unnamed taxon described by Eberle (2006) and referred to "cf. *Eotitanops*" is not a member of Eotitanopinae due the presence of a metacone on the P2, a derived trait lacking in *Eotitanops* but present in all other brontotheres. The problematic Asian species, "*Eotitanops*?" *dayi*, is probably not a member of Eotitanopinae.

PALAEOSYOPINAE: Palaeosyopinae is presently a phylogenetically uninformative subfamily that is synonymous with *Palaeosyops*.

In addition to North American *Palaeosyops*, Palaeosyopinae might include cf. *Palaeosyops* (*Palaeosyops* sp. sensu Gabounia, 1977) from Kazakstan and cf. *Palaeosyops* (*Bunobrontops* sp. sensu Holroyd and Ciochon, 2000) from the Pondaung Formation of Myanmar.

BRONTOTHERIINAE: Mader (1989, 1998) recognized an unnamed monophyletic clade of brontotheres that excluded *Eotitanops* and *Palaeosyops* but contained all other North American brontotheres. This clade was supported by "shear more emphasized on the ectoloph of the upper premolars" (Mader, 1989: 482). The same clade was recovered here, although, naturally, it contains Asian brontotheres as well as North American brontotheres. A name has never been applied to the clade, although it is one of the most robustly supported subclades of the Brontotheriidae. There is a clear distinction between the low-crowned, and nearly bunodont molar morphology of *Palaeosyops* and *Eotitanops* with those of other brontotheres in which the ectoloph is taller with functional emphasis placed on shearing on the labial enamel of the ectoloph. With the exceptions of the evolution of horns and radical changes in body size, this dental transformation is the most conspicuous aspect of brontothere evolution and involves seven molar apomorphies: (1) loss of the thick parastyle cingular shelf, (2) an increase in the height of the ectoloph, (3) a strongly lingually angled ectoloph, (4) the reduction of the labial upper molar ribs and lingual lower molar ribs, (5) more wedge-shaped lingual margins of the paracone and metacone, (6) thinned lingual ectoloph enamel, and (7) the elongation of the lower m3. These distinctions result in notably different wear patterns as well. *Eotitanops* (including cf. *Eotitanops* sensu Eberle, 2006) and *Palaeosyops* molars wear in a vertical direction, leaving large, rounded exposures of enamel at the apices of the paracone and metacone. On the other hand, the ectolophs of the molars of other brontotheres wear in a labial direction, producing a single, strongly W-shaped wear facet that runs along the lingual side of the ectoloph.

To recognize the well-supported clade consisting of brontotheres with derived molar morphology, the subfamily name Brontotheriinae should be applied (see ICZN article 6.1). Brontotheriinae as defined here is much broader than previous applications of this subfamily name. Previously "Brontotheriinae" was used in reference to a smaller subset (Mader, 1998), which has now been re-ranked to subtribe status, Brontotheriina (see below). Most other previously coined brontothere subfamilies are actually subsets of the Brontotheriinae and have been given new ranks below.

Establishing a precise definition of Brontotheriinae is complicated by the recent discovery of *Bunobrontops savagei* (Holroyd and Ciochon, 2000). Though very fragmentary, *B. savagei* is the only brontothere that exhibits only some of the seven molar apomorphies that otherwise characterized Brontotheriinae. It is essentially a "missing link" between dentally primitive and dentally derived brontotheres. However, I include it with the Brontotheriinae. Defined this way, Brontotheriinae (node 8 in fig. 195) is supported by the following unequivocally optimized apomorphies: loss of a cingular parastylar shelf, lingually angled ectoloph, and moderately thinned enamel on the lingual side of the ectoloph between the paracone and metacone.

DOLICHORHININI: The subfamily "Dolichorhininae" sensu Mader (1989; 1998), consisting of *Mesatirhinus*, *Metarhinus* sensu Mader (includes *Fossendorhinus*), and *Sphenocoelus* sensu Mader (includes *Dolichorhinus*), must be reranked to tribe Dolichorhinini because it contains a subset of the Brontotheriinae. This higher taxon was based on the infraorbital jugal process and "gracile" canines found in these taxa. The infraorbital jugal process was used as a character in this analysis. On the other hand, canine size was not used because of difficulty partitioning canine size into character states because of conspicuous intraspecific variability. The results do not support a monophyletic Dolichorhinini. *Fossendorhinus* and *Metarhinus* actually belong to the tribe Brontotheriini, whereas *Dolichorhinus*, *Mesatirhinus*, and *Sphenocoelus* form a paraphyletic series outside the Brontotheriini clade.

BRONTOTHERIINI: This tribal name refers to all brontotheres that possess a pair of triangular processes of frontal bone that

overlaps onto or intrudes into the nasal bone. *Telmatherium* is classically considered to be the ancestor or sister taxon of some or all of the horned brontotheres because it possesses a pair of triangular frontal processes that overlap the nasal bone, thus foreshadowing the evolution of the frontonasal horn (Osborn, 1929a; Granger and Gregory, 1943). Logically, based on the presumed phylogenetic importance of *Telmatherium* as the sister of horned brontotheres, Mader (1989) redefined "Telmatheriinae" to include *Telmatherium* and all North American brontotheres with conspicuous frontonasal horns. Mader's analyses excluded Asian brontotheres, although all Asian brontotheres with the same derived frontonasal configuration, previously included in the paraphyletic subfamily "Epimanteocerotinae" as well as "Embolotheriinae", would naturally be members of the same clade. This clade was defined by Mader (1989) as having a frontonasal-like horn swelling and a "? reduced sagittal crest". Later, Mader (1998) abandoned "Telmatheriinae" and used the name "Brontotheriinae" to refer to the same clade. "Brontotheriinae" sensu Mader (1998) was defined as having a "triangular projection of frontal overlapping nasal" and "cranial vertex relatively wide". The "triangular projection of frontal overlapping nasal" turns out to be more widespread than was recognized by Mader (1998) or Osborn (1929a) and it can be seen on the skulls of several taxa that Mader excluded from the "Brontotheriinae", including *Metarhinus fluviatilis*, *Sthenodectes incisivum*, and *Metatelmatherium ultimum*.

Both analyses of ordered and unordered character data support a monophyletic clade of brontotheres that possess the paired triangular frontal processes overlapping the nasal bone. This clade (node 12 of fig. 195) includes *Fossendorhinus*, *Metarhinus*, *Sthenodectes*, *Telmatherium*, *Wickia*, *Metatelmatherium*, *Qufutitan*, *Epimanteoceras*, plus all brontotheres with conspicuous frontonasal horns. The analysis of ordered character data includes *Microtitan* in the Brontotheriini, while its membership is uncertain according to the analysis of unordered data. Unequivocally optimized apomorphies supporting Brontotheriini include: frontal bone overlapping onto or intruding into the nasal bone, and reduced occipital condyles.

RHADINORHININA: "Rhadinorhininae", as used by Osborn (1929a), is a phylogenetically uninformative monotypic subfamily including only *Metarhinus* (= *Rhadinorhinus*) *abbotti*. This name was not adopted by Mader (1989, 1998). If used, the name must be reranked to subtribe Rhadinorhinina. This subtribe can be broadened to include *Fossendorhinus diploconus*, *Metarhinus fluviatilis*, and *Metarhinus abbotti*. These three species form a small clade supported by both analyses of ordered and unordered character data (node 39 of fig. 195). The single unequivocal apomorphy supporting Rhadinorhinina is a premaxillomaxillary rostrum that does not deepen ventrally. The same apomorphy is found in *Dolichorhinus hyognathus*, but based on the cladistic results it represents a convergence.

TELMATHERIINA: The subfamily "Telmatheriinae" was employed by Osborn (1929a) to refer to what is now recognized as *Telmatherium* (in part) and *Metatelmatherium*. "Metatelmatheriinae" of Granger and Gregory (1943) is synonymous with Osborn's "Telmatheriinae". Mader (1989) expanded the use of "Telmatheriinae" to include only Telmatherium and North American horned brontotheres, but later abandoned the use of "Telmatheriinae", replacing it with "Brontotheriinae". I reject Mader's concepts of "Telmatheriinae" and "Brontotheriinae" (see discussions of Brontotheriini and Brontotheriina); however, Osborn's original concept of "Telmatheriinae" may have validity. The analysis of ordered character data yields a clade similar to Osborn's original concept of "Telmatheriinae", although it must be reranked to subtribe Telmatheriina (node 35 of fig. 195); it includes *Telmatherium*, *Metatelmatherium*, and the more recently named taxa, *Wickia* and *Qufutitan*. The only unequivocal apomorphy supporting that clade is a character reversal, the loss of central molar fossae. These taxa lack stable phylogenetic positions in the analysis of unordered character data and the clade is not supported by that analysis.

BRONTOTHERIINA: This subtribe includes only brontotheres that possess conspicuous frontonasal protuberances. It excludes *Tel-*

matherium and other hornless species that were previously hypothesized to be sister taxa or ancestors of horned brontotheres. Classically, *Telmatherium* (or its synonym, *Manteoceras*), is identified as the sister taxon or ancestor of some or all of the horned brontotheres because its frontonasal configuration appears to foreshadow the evolution of the frontonasal horn. Based on this classic notion, *Telmatherium* was grouped with North American horned brontotheres into the "Brontotheriinae" by Mader (1998). However, any clade including *Telmatherium* plus horned brontotheres is problematic for two reasons: (1) other hornless brontotheres have a similar frontonasal configuration, and (2) a sister relationship of *Telmatherium* and horned brontotheres is not supported by phylogenetic evidence. Hornless and horned brontotheres expressing this specialized frontonasal configuration are now grouped into the tribe Brontotheriini. I restrict the subtribe Brontotheriina to those species with conspicuous frontonasal horns (node 16 on fig. 195). Brontotheriina includes the horned North American forms and the horned Asian forms. Unequivocal apomorphies supporting Brontotheriina include conspicuous paired frontonasal horns, saddle-shaped skull, and straight zygomatic arches. Based on the analysis of unordered data, the phylogenetic positions of *Epimanteoceras* and *Qufutitan* with respect to this clade are still uncertain (see summary tree in fig. 198); they could be sisters of Brontotheriina, or nest within it. If either *Qufutitan* or *Epimanteoceras* are found to nest within the Brontotheriina, this clade will have to be rejected or redefined to accommodate these taxa.

BRONTOTHERIITA: Four different subfamily names, "Brontopinae", "Menodontinae", "Megaceropinae", and "Brontotheriinae", have been applied to brontotheres of the late Eocene Chadron Formation of North America. However, all these subfamilies are synonymous with the genus *Megacerops*. Schoch and Lucas (1985) informally coined the term "eubrontotheres", for a somewhat broader group that included *Megacerops* and other brontotheres with "rounded, spherical incisors, relatively molarized premolars, hypocone on upper third premolar, and distinct to well-developed horns". Mader (1989; 1998) continued the informal use of "eubrontotheres" for a clade that includes *Duchesneodus uintensis* and other taxa (*Brontops*, *Megacerops*, *Menops*) that are considered equivalent to *Megacerops* sensu Mihlbachler et al. (2004b). However, the traits named by Schoch and Lucas (1985) do not appear on a single node in any of the trees produced by the phylogenetic analysis. Schoch and Lucas (1985) intended to apply the name "eubrontotheres" to North American horned brontotheres excluding *Protitanotherium* and *Diplacodon*. Among those characters mentioned by Schoch and Lucas (1985) the most useful character that differentiates other North American horned species from *Protitanotherium* and *Diplacodon* is the rounded, spherical (globular) upper incisors. Indeed, the trees derived from both analyses of ordered and unordered data yield a monophyletic clade of brontotheres with rounded, spherical upper incisors, consisting of *Parabrontops*, *Eubrontotherium*, *Protitanops*, *Dianotitan*, *Notiotitanops*, *Duchesneodus*, and *Megacerops*. In recognizing this clade (node 21 of fig. 195), the infratribal term Brontotheriita should be applied to "eubrontotheres" (see ICZN article 6.1). Unequivocal apomorphies that support Brontotheriita include an unelevated nasal process; very small upper and lower incisors; globular upper incisors, a straight incisor row, and very weak labial premolar ribs. Based on the analysis of ordered data, *Diplacodon* and *Pachytitan* are sisters of the Brontotheriita; however, the unordered analysis places *Protembolotherium* and *Embolotherium* as sisters of Brontotheriita.

EMBOLOTHERIITA: Osborn (1929b) erected the subfamily "Embolotheriinae" for a single genus, *Embolotherium*. However, Mihlbachler et al. (2004a) broadened the "Embolotheriinae" to include *Aktautitan*, *Metatitan*, *Brachydiastematherium*, *Nasamplus* (= "*Metatitan*" *progressus*), *Embolotherium*, and *Protembolotherium*. "Embolotheriinae" sensu Mihlbachler et al. (2004a) was suggested by several structural details of the skull, including a singular frontonasal process with frontonasal protuberances and nasal process elevated to its peak. "Embolotheriinae" as defined by Mihlbachler et al. (2004a) was recovered in the analysis of ordered data. For

the time being, I reassign this clade to infratribal rank (node 25 of fig. 195), Embolotheriita, and retain a definition similar to that of Mihlbachler et al. (2004a). Unequivocal apomorphies include transversely narrowly spaced and fused frontonasal protuberances, elevated frontonasal process, and thin, deep lateral walls of the nasal process.

In the analysis presented here, additional species were found to nest within Embolotheriita, including *Gnathotitan berkeyi*, *Pollyosbornia altidens*, and *Pygmaetitan panxianensis*; however, these species are highly fragmentary and the actual apomorphies used to define the Embolotheriita clade are not known for these species. The analysis of unordered data did not recover "Embolotheriinae" sensu Mihlbachler et al. (2004a). Rather, that analysis produced a clade more in line with Osborn's original concept of "Embolotheriinae" including only *Embolotherium* and *Protembolotherium*.

Metarhinus: In this paper two species were placed in the genus *Metarhinus* Osborn (1908), *M. fluviatilis* and *M. abbotti*. Phylogenetic analysis supports *Metarhinus* as presently defined (node 40 in fig. 195) Unequivocal apomorphies are: posterior margin of nasal incision positioned at the posterior margin of M1 or more posterior, orbits protruding prominently laterally, premaxillomaxillary rostral cavity sealed dorsally by a bony cover, and large upper molar anterolingual cingular cusp.

Protitan: Granger and Gregory (1943) initially assigned five species to this genus, although only two of them were found to represent valid diagnosable species. *P. grangeri* and *P. minor* are basal members of the subtribe Brontotheriina. Unfortunately, both species of *Protitan* contribute to a polytomy at the base of the Brontotheriina clade. Thus, the status of this genus is ambiguous.

Rhinotitan: Granger and Gregory (1943) initially assigned three species to this genus, and two of them, *R. kaiseni* and *R. andrewsi*, were found to represent valid diagnosable species. Phylogenetic analysis supports *Rhinotitan* (node 34 in fig. 195) with the following apomorphies: dorsal surface of skull minimally constricted by parasagittal ridges, external auditory pseudomeatus posteromedially angled, and relatively vertical occiput.

Metatitan: In the current revision three species were assigned to *Metatitan*. Two of these species, *M. primus* and *M. relictus*, were originally assigned to *Metatitan* by Granger and Gregory (1943). The third species, *M. khaitshinus*, was mistakenly assigned to *Protitan* by Yanovskaya (1980). The status of the genus *Metatitan*, as presently defined, is ambiguous because its members form a polytomy with *Brachydiastematherium transylvanicum*. Nonetheless, the *Brachydiastematherium-Metatitan* clade (node 30 in fig. 195) is supported by numerous apomorphies including, posterior margin of nasal incision positioned at the posterior margin of M1 or more posterior, anterior rim of orbit positioned above M2, dorsal surface of skull nearly flat above the orbits and convex over the cranial region (i.e., the saddle-shaped skull shape seen in other horned brontotheres is lost), postzygomatic process and ventral sphenoidal fossae present, posterior end of skull extremely widened, shortened basicranium, and small upper and lower incisors. *Brachydiastematherium transylvanicum* is a highly fragmentary taxon, known only from a partial mandible, while *Metatitan* itself is characterized by numerous cranial specializations. *Brachydiastematherium* could either be the sister of *Metatitan*, or it may in fact nest within *Metatitan*; however, better material is simply needed to determine which is the case.

Embolotherium: Embolotherium Osborn (1929b) includes two valid diagnosable species, *E. andrewsi* and *E. grangeri*. This genus is one of the most derived and easily identified brontothere genera. However, the enlarged and conspicuous frontonasal ram of *Embolotherium* is not an apomorphy of this genus; this condition is shared with *Protembolotherium*. *Embolotherium* is supported by the analysis of ordered character data. Unequivocal apomorphies of *Embolotherium* (node 29 in fig. 195) include: nasal process lost or absorbed by the frontonasal process, premaxillary symphysis vertical with a concave anterior surface, elevated occiput. The interrelationships of *Embolotherium* and

Protembolotherium are unresolved in the analysis of unordered character data.

MEGACEROPS: Despite the fact that late Eocene brontotheres of North America were previously split into numerous species, genera, and subfamilies, there are only two diagnosable species that are now assigned to a single genus, *M. coloradensis* and *M. kuwagatarhinus* (Mihlbachler et al., 2004b). The strict reduced consensus in fig. 195 portrays *Megacerops* as a monophyletic genus (node 24) with the following apomorphies: frontonasal horns extremely long (at least in some individuals), posterior margin of nasal incision between the anterior margin of P2 and the posterior margin of P3, orbits anterior to M1, massive occipital pillars, and absence of a mandibular postcanine diastema. However, the status of this genus is uncertain due to the unstable phylogenetic position of *Notiotitanops mississippiensis* in analyses of both ordered and unordered character data. Among the most parsimonious arrangements demonstrating the multiple possible phylogenetic positions on *Notiotitanops mississippiensis*, this species nests within *Megacerops* in some of the trees.

A REVISED CLASSIFICATION OF THE BRONTOTHERIIDAE

A revised classification of the Brontotheriidae follows, including only those taxa considered valid currently. The brontothere classification differs considerably from previous schemes (Osborn, 1929a; Simpson, 1945; McKenna and Bell, 1997). I have organized the classification based on phylogenetically informative clades discussed above that were recovered by the analysis of ordered character data.

Family Brontotheriidae Marsh, 1873
- *Eotitanops* Osborn, 1907
  - *E. borealis* (Cope, 1880) (sensu Gunnell and Yarbrough, 2000)
  - *E. minimus* Osborn, 1919 (sensu Gunnell and Yarbrough, 2000)
- *Palaeosyops* Leidy, 1870a
  - *P. paludosus* Leidy, 1870a (sensu Gunnell and Yarbrough, 2000)
  - *P. laticeps* Marsh, 1872 (sensu Gunnell and Yarbrough, 2000)
  - *P. robustus* Marsh, 1872 (sensu Gunnell and Yarbrough, 2000)
  - *P. fontinalis* (Cope, 1873a) (sensu Gunnell and Yarbrough, 2000)
  - *P. laevidens* (Cope, 1873a) (sensu Gunnell and Yarbrough, 2000)

Subfamily Brontotheriinae Marsh, 1873
- *Bunobrontops* Holroyd and Ciochon, 2000
  - *B. savagei* Holroyd and Ciochon, 2000
- *Mesatirhinus* Osborn, 1908
  - *M. junius* (Leidy, 1872)
- *Dolichorhinus* Hatcher, 1895
  - *D. hyognathus* (Osborn, 1889)
- *Sphenocoelus* Osborn, 1895
  - *S. uintensis* Osborn, 1895
- *Desmatotitan* Granger and Gregory, 1943
  - *D. tukhumensis* Granger and Gregory, 1943
- *Acrotitan* Ye, 1983 (incertae sedis)
  - *A. ulanshirehensis* Ye, 1983

Tribe Brontotheriini Marsh, 1873
- *Microtitan* Granger and Gregory, 1943
  - *M. mongoliensis* (Osborn, 1925)
- *Sthenodectes* Gregory, 1912
  - *S. incisivum* (Douglass, 1909)
- *Epimanteoceras* Granger and Gregory, 1943
  - *E. formosus* Granger and Gregory, 1943
- *Nanotitanops* Qi and Beard, 1998 (incertae sedis)
  - *N. shanghuangensis* (Qi and Beard, 1996)

Subtribe Rhadinorhinina (Osborn, 1929a)
- *Fossendorhinus* Mihlbachler, this paper
  - *F. diploconus* (Osborn, 1895)
- *Metarhinus* Osborn, 1908
  - *M. fluviatilis* Osborn, 1908a
  - *M. abbotti* (Riggs, 1912)

Subtribe Telmatheriina (Osborn, 1914)
- *Telmatherium* Marsh, 1872
  - *T. validus* Marsh, 1872
- *Metatelmatherium* Granger and Gregory, 1938
  - *M. ultimum* (Osborn, 1908a)
- *Wickia* Mihlbachler, this paper
  - *W. brevirhinus* Mihlbachler, this paper
- *Qufutitan* Wang, 1997
  - *Q. zhoui* Wang, 1997 (incertae sedis)

Subtribe Brontotheriina Marsh, 1873
- *Protitan* Granger and Gregory, 1943
  - *P. grangeri* (Osborn, 1925)
  - *P. minor* Granger and Gregory, 1943
- *Protitanotherium* Hatcher, 1895
  - *P. emarginatum* Hatcher, 1895

Rhinotitan Granger and Gregory, 1943
R. andrewsi (Osborn, 1925)
R. kaiseni (Osborn, 1925)
Diplacodon Marsh, 1875
D. elatus Marsh, 1875
Pachytitan Granger and Gregory, 1943
P. ajax Granger and Gregory, 1943
Infratribe Embolotheriita Osborn, 1929b
Pollyosbornia, this paper
P. altidens (Osborn, 1908)
Gnathotitan Granger and Gregory, 1943
G. berkeyi (Osborn, 1925)
Aktautitan Mihlbachler et al., 2004a
A. hippopotamopus Mihlbachler et al., 2004a
Pygmaetitan Miao, 1982
P. panxianensis Miao, 1982
Brachydiastematherium Böckh and Maty, 1876 (incertae sedis)
B. transylvanicum Böckh and Maty, 1876
Metatitan Granger and Gregory, 1943
M. primus Granger and Gregory, 1943
M. relictus Granger and Gregory, 1943
M. khaitshinus (Yanovskaya, 1980)
Nasamplus Mihlbachler, this paper
N. progressus (Granger and Gregory, 1943)
Protembolotherium Yanovskaya, 1954
P. efremovi Yanovskaya, 1954
Embolotherium Osborn, 1929b
E. andrewsi Osborn, 1929b
E. grangeri Osborn, 1929b
Infratribe Brontotheriita Marsh, 1875
Parabrontops Granger and Gregory, 1943)
P. gobiensis (Osborn, 1925)
Eubrontotherium Mihlbachler, 2007
E. clarnoensis Mihlbachler, 2007
Protitanops Stock, 1936
P. curryi Stock, 1936
Notiotitanops Gazin and Sullivan, 1942
N. mississippiensis Gazin and Sullivan, 1942
Dianotitan Chow et al., 1974
D. lunanensis (Chow and Hu, 1959)
Duchesneodus Lucas and Schoch, 1982
D. uintensis (Peterson, 1931)
Megacerops Leidy, 1870b
M. coloradensis Leidy, 1870b (sensu Mihlbachler et al., 2004b)
M. kuwagatarhinus Mader and Alexander, 1995

BRONTOTHERE ORIGINS AND CLADISTIC BIOGEOGRAPHY

The fossil mammal records of North America, Europe, and Asia reveal an intricate history of faunal interchanges, resulting in a complex web of phylogenetic relationships among the faunas of these continents. Biogeographic hypotheses are implicit in any phylogeny; however, most prior attempts to reconstruct patterns of Cenozoic mammalian intercontinental dispersals, attempts to relate them to tectonic and global climate trends, and to explain such dispersal patterns using biogeographic theories, such as MacArthur-Wilson island biogeography (MacArthur and Wilson, 1967), are not tied to explicit hypotheses of phylogeny. Rather, immigrants, and thus dispersal events, are usually inferred on a local basis by origination events,i.e., first appearances (Stucky, 1990, 1992; Webb, 1969, 1977, 1989; Webb and Opdyke, 1995; Woodburne and Swisher, 1995). However, at least two processes result in localized originations of taxa. These include immigration as well as endemic speciation. Differentiating immigrants from those taxa arising from endemic speciation is not possible without considering phylogeny. Few have bothered to explain how immigrants were differentiated from localized speciation, and those who have are not explicit. For instance, Webb and Opdyke (1995) explained how they identified North American immigrant genera; "Immigrants (first appearances) were recognized on the basis of two criteria: (1) the absence of that genus or closely related genera in prior North American records and (2) the presence of related forms (sister group) earlier in another continental fauna." (Webb and Opdyke, 1995: 188). Plainly, their criteria for identifying immigrants are based on inferences of phylogeny, but without the rigor of explicit reference to a cladogram. Stucky (1992) has recognized that results of such studies need to be reevaluated in a cladistic context.

Optimizing geographic location (e.g., continent) a posteriori on a cladogram identifies the minimum number of dispersal events implicit in any phylogenetic hypothesis. Beard (1998) examined the geographic origins of major mammalian higher taxa (e.g., orders) by mapping geographic location (continent) on the cladograms of numerous placental mammal clades. Beard (1998) proposed the "East of Eden" model that views "North America as a biogeographical cul-de-sac that received repeated innoculations [sic] of more...taxa from Asia." (Beard, 1998: 25). Thus, Asia is postulated as the primary source for North American mammalian diversity. However, Beard's focus on the geographic origins of higher taxa is not entirely satisfactory as an analysis of North American–Asia dispersal trends, because the emphasis on nodes representing the origins of higher taxa, as opposed to all nodes on a cladogram, results in arbitrary emphasis on certain nodes, while ignoring other nodes where immigration events might also be indicated. Ultimately, all of the nodes on a cladogram represent speciation events that, as historical events, are not fundamentally different from other speciation events regardless of whether they are arbitrarily associated with higher taxonomic names.

A nonarbitrary approach for examining the frequency, timing, and polarity of intercontinental dispersal events would be to reconstruct geographic histories on species-comprehensive cladograms in which all known members (or as many as can possibly be sampled) of a clade are included. This approach utilizes all of the available evidence and is the only way to guarantee the discovery of all the dispersal events implied by the known members of a clade. Here, I compare the history of dispersals implied by brontothere phylogeny to previous ideas about brontothere dispersal, and to more generalized ideas about the history of North America–Asia biotic interchanges.

The trees resulting from both analyses of ordered and unordered data imply numerous intercontinental dispersals. The 3967 trees produced by the ordered character data imply 12 dispersals within the Brontotheriidae. An example of one of these trees is seen in fig. 201, with continental location optimized onto it as a character, showing 12 dispersals within the Brontotheriidae. (An additional dispersal of uncertain polarity also occurs at the base of the tree relating to *Lambdotherium* and *Danjiangia*.) The 603,705 MPTs resulting from the analysis of unordered data imply 9–12 dispersal events within the Brontotheriidae. Figure 202 is one tree from the unordered character search showing the minimum number of nine dispersals allowed by that analysis. To be clear, the cladograms are generated purely from morphological characters with the geographic character mapped on a posteriori. *Brachydiastematherium transylvanicum*, the sole brontothere taxon from eastern Europe included in the analysis, is coded as Asian because the locality from which it comes was biogeographically part of Asia and not Europe.

Brontothere Origins

Geographic location is optimized on all the cladograms in such a way that indicates a North American origin for Brontotheriidae. The primitive North American brontothere genera, *Eotitanops* and *Palaeosyops*, have previously been interpreted as immigrants from Asia (Stucky, 1992; Woodburne and Swisher, 1995; Beard, 1998); however, there is little evidence that these early brontotheres or their ancestors resided in Asia. A few fossils from Asia have been tentatively identified as primitive brontotheres similar to *Eotitanops* and *Palaeosyops*. Cladistically, *Eotitanops* is the most primitive brontothere. Presently there are no indisputable *Eotitanops* fossils known from Asia. "*Eotitanops*?" *dayi* Dehm and Oettingen-Spielberg (1958) is not clearly a member of *Eotitanops*; the known specimens are far too incomplete to determine their taxonomic identity or evaluate their phylogenetic position. A small *Eotitanops*-like brontothere from Japan has been preliminarily reported by Miyata and Tomida (2003); this material may ultimately have a strong bearing on brontothere origins. *Palaeosyops*-like fossils have been reported from Asia, but they are based on very fragmentary specimens (Gabounia, 1977; Xu et al., 1979). An upper premolar (P4) identified as *Palaeosyops* sp. by Xu et al. (1979) is an indeterminate specimen that could belong to one of several relatively small brontotheres; however, the thin enamel of that specimen suggests something more derived than *Palaeosyops*. On the other hand,

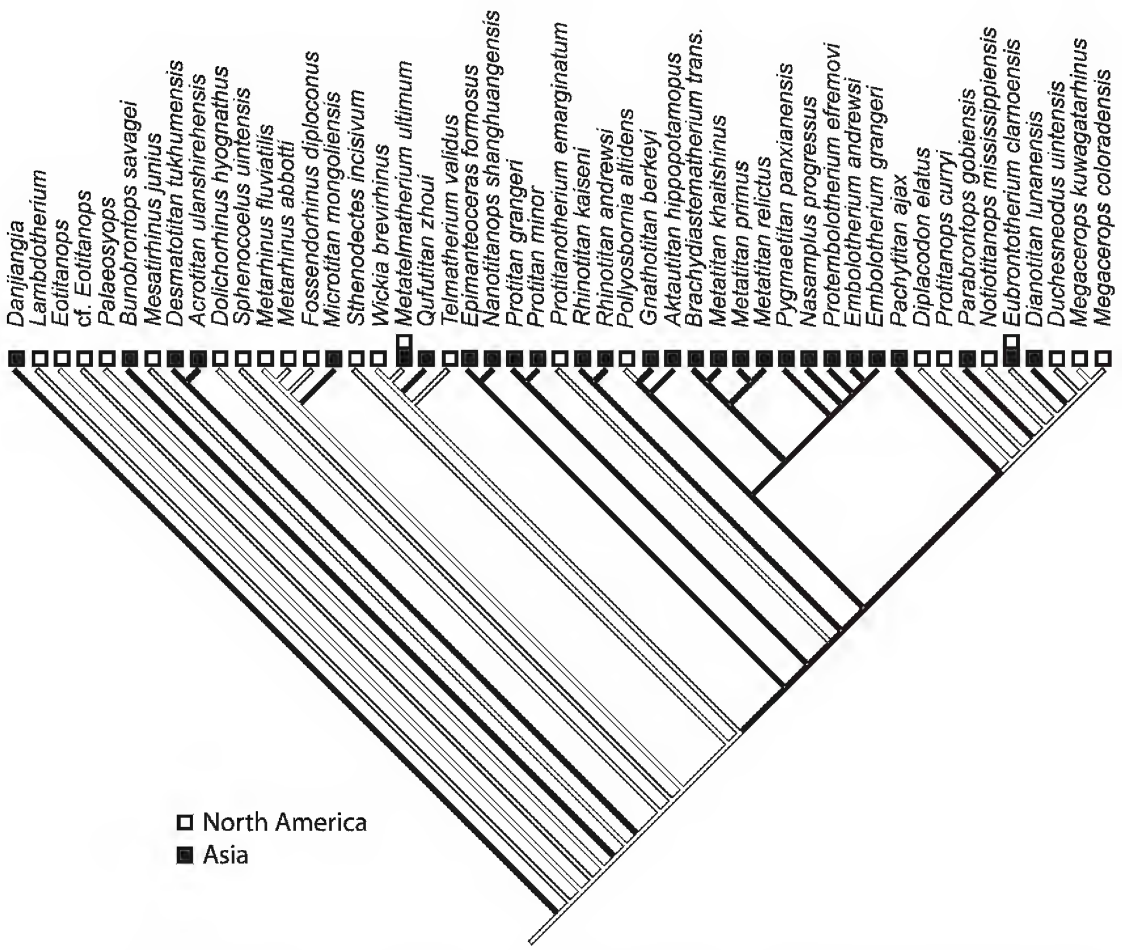

Fig. 201. One of 3967 trees produced from the analysis of ordered character data with a geographic character mapped onto it a posteriori showing 12 possible dispersal events within the Brontotheriidae occurring between North American and Asia.

the upper molar specimen identified as *Palaeosyops* sp. by Gabounia (1977) from the Zaysan Basin of Kazakstan most certainly indicates a *Palaeosyops*-like brontothere in Asia. Based on its wide ectoloph but otherwise plesiomorphic condition, it would fit onto the cladograms in the same position as *Palaeosyops*. Based on this specimen, if *Palaeosyops* were recoded as "polymorphic" for geographic location (i.e., having occurred on both continents), the geographic character would be optimized the same way on the cladograms, still suggesting a North American origin for Brontotheriidae, and subsequent dispersal of *Palaeosyops* into Asia.

To determine the origin of the Brontotheriidae, it is necessary to look outside the family to its sister taxa. If the North American genus, *Lambdotherium* is the sister taxon of the Brontotheriidae, as it is historically presumed to be, then it is likely that the Brontotheriidae originated in North America. In contrast, Beard (1998) suggested that "the ancestry of the Bridgerian brontotheres [*Eotitanops* and *Palaeosyops*] must be sought outside of North America, where only the autapomorphous *Lambdotherium* is known from earlier rock" (Beard, 1998: 27). Regarding the autapomorphous condition of *Lambdotherium*, autapomorphies are phylogenetically uninformative and, thus, cannot influence cladistically derived hypotheses of biogeography. Currently the best hypothesis is a North American origin for brontotheres.

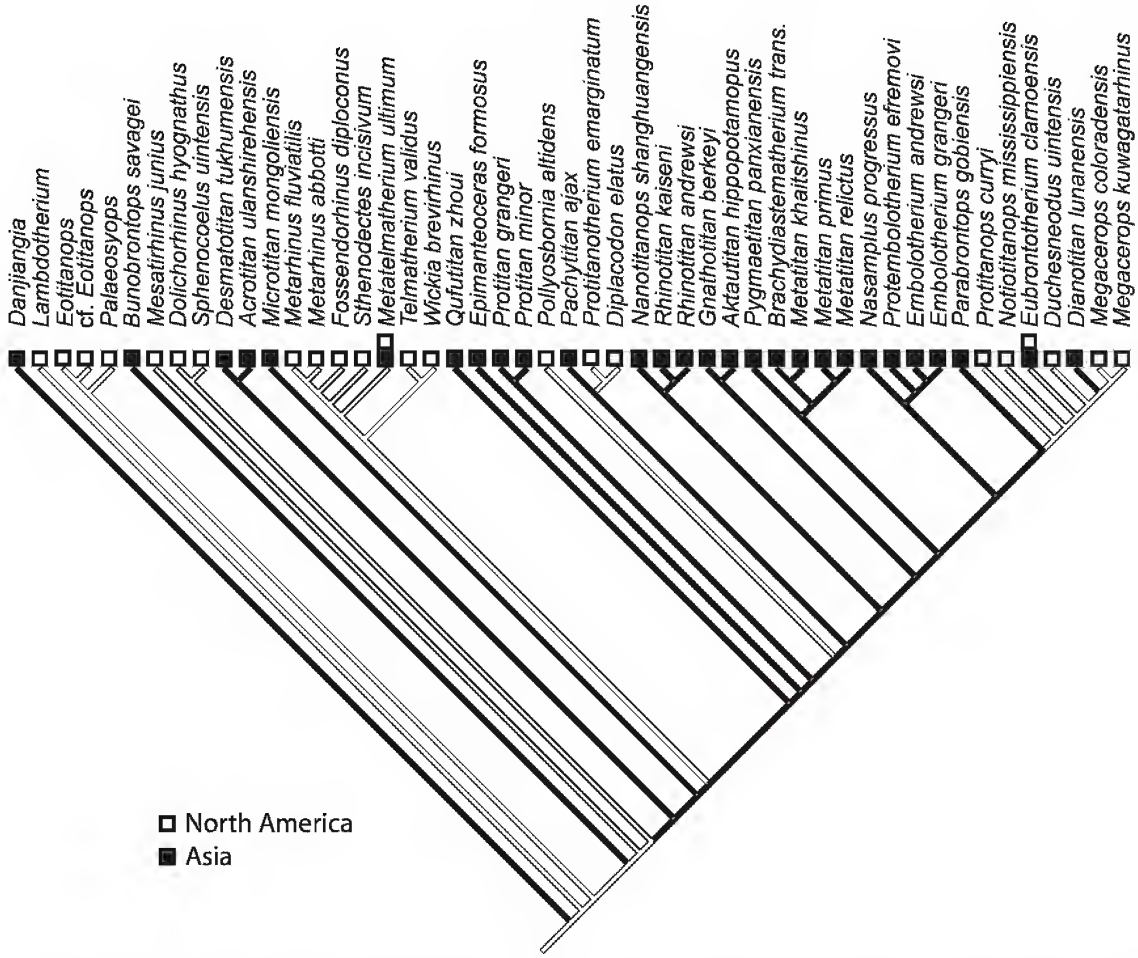

Fig. 202. One of 603,705 trees produced from the analysis of unordered character data, with a geographic character mapped onto it a posteriori, showing nine intercontinental dispersal events within the Brontotheriidae, the minimum allowed by this analysis.

Recent discoveries of *Lambdotherium*-like mammals in Asia demand reconsideration of a possible Asian origin for brontotheres. *Danjiangia pingi* Wang (1995), from late early Eocene Yuhuangding Formation of Liguanqiao Basin of China was considered the primitive sister of *Lambdotherium* by Beard (1998) and a more plausible stem taxon for the Brontotheriidae (this is in contrast to the original assessment of Wang [1995], who suggested that it is an early Chalicothere). However, these statements by Beard (1998) are contradictory. If *Danjiangia* is the closest relative of brontotheres, and *Lambdotherium* and *Danjiangia* are sisters, as Beard suggests, then *Lambdotherium* must also be the sister of brontotheres. Meng et al. (1998) described dental fragments of an unnamed *Lambdotherium*-like mammal from the late Paleocene Bayan Ulan fauna of China that add additional uncertainly to the geographic origin of the Brontotheriidae. The present cladistic analysis places *Lambdotherium* as the sister of the Brontotheriidae, with *Danjiangia* one step removed. A more comprehensive analysis, utilizing more outgroup taxa is needed to determine the phylogenetic position of Brontotheriidae within Perissodactyla and, simultaneously, to develop the best hypothesis for the geography of its origin.

Cladistically Implied Intercontinental Dispersals

The recovered phylogenies imply numerous intercontinental dispersal events. Moreover, the frequency of implied dispersals is greater than had been previously surmised for this family. All trees resulting from the analysis of ordered data imply 10 dispersals occurring on internal branches within the Brontotheriidae, while all trees resulting from the analysis of unordered data imply between 7–10 dispersals occurring on internal branches. Two additional "autapomorphic" dispersals occur on distal branches; *Metatelmatherium ultimum* and *Eubrontotherium clarnoensis* are found in both North America and Asia. Therefore, the total number of dispersals implicit in all of the cladistic results ranges from 9–12. Problematic taxa not included in the phylogenetic analysis, particularly cf. *Palaeosyops* (*Palaeosyops* sp. of Gabounia, 1977), *Eotitanops*? *dayi*, *Pakotitanops latidentatus*, and *Mulkrajanops moghliensis*, may indicate additional dispersal events.

In the example tree in fig. 201, nine of these events imply dispersal from North America to Asia, while only three imply dispersal in the opposite direction. Other MPTs resulting from the same analysis show conflicting dispersal patterns within the Brontotheriita. These discrepancies relate to the wildcard behavior of *Notiotitanops*. Ultimately, the polarities of any of the three possible dispersal events occurring within the Brontotheriita are uncertain. Despite these few discrepancies, the analysis of ordered data shows a dispersal pattern that indicates predominantly dispersal to Asia from North America. In contrast to the East of Eden model of Beard (1998), no tree shows a predominance of dispersal from Asia to North America.

The minimum age of a dispersal event is constrained by the age of the taxon (either a terminal taxon or a clade) that results from the dispersal event. In other words, the dispersal could have occurred any time before the appearance of the immigrant and its descendants but not after. Most brontothere dispersal events occurred no later than the middle Eocene. The following interpretation is based on the tree in fig. 201. The appearance of *Bunobrontops* in Asia results from a dispersal from North America by the middle Eocene. Another dispersal from North American into Asia occurring by the Irdinmanhan land mammal age involves the appearance of *Desmatotitan* and *Acrotitan* in Asia. The dispersal events involving the appearances of *Microtitan*, *Qufutitan*, *Metatelmatherium*, and *Epimanteoceras* also occurred before or during the Irdinmanhan land mammal age. The existence of *Metatelmatherium ultimum* in the Irdinmanhan of Asia and in the Late Uintan of North America strongly pinpoints the Irdinmanhan and late Uintan as the time of dispersal.

Horned brontotheres (Brontotheriina) appear to have originated in Asia, with *Protitan* as the most basal member. Subsequent dispersal of members of the Brontotheriina back into North America involved Uintan taxa *Protitanotherium emarginatum*, *Pollyosbornia altidens*, and *Diplacodon elatus*. Fig. 201 depicts three subsequent back-dispersals to Asia involving members of the Brontotheriita, *Parabrontops*, *Dianotitan*, and *Eubrontotherium*. The timing of the dispersal of *Eubrontotherium clarnoensis*, either from Asia to North America or vice versa is difficult to evaluate. In Asia it is known from late Eocene Ulangochuian deposits, but its age in North America is controversial, with opinions ranging from Uintan to Chadronian. Likewise, the age of *Dianotitan* is poorly constrained, but possibly suggests a middle Eocene dispersal before or during the Irdinmanhan or Sharamurunian land mammal ages. Finally, the late Eocene appearance of *Parabrontops* in Asia indicates dispersal before or during the Ulangochuian; this is the latest possible dispersal event implied by this tree. As noted above, the dispersal pattern and polarity within the Brontotheriita varies in other trees depending on the position of the wildcard, *Notiotitanops*, and the timing of these events are poorly constrained in comparison to those dispersal events that lie in more resolved parts of the consensus trees resulting from the analysis of ordered character data.

The number, polarity, and nodal positions of the dispersal events implied by the analysis of unordered data are more difficult to evaluate due to the excessive number of MPTs and large number of erratic wildcard taxa. The example shown in fig. 202 implies

five dispersal events from North America to Asia, with an additional four occurring in the opposite direction. Other trees resulting from this analysis show differing dispersal patterns and the predominant direction of dispersal is indeterminate from the analysis of unordered character data.

CONCLUSION

Three general conclusions regarding brontothere biogeography are apparent in the phylogenetic results. (1) Contrary to the earlier statements of an Asian origin, a North American origin seems likely, but this is contingent upon *Lambdotherium* being the sister-taxon of the Brontotheriidae. A more comprehensive analysis with a more extensive outgroup needs to be performed. Brontotheres have yet to be sufficiently incorporated into analyses of perissodactyl phylogeny.

(2) Several successive intercontinental brontothere dispersals occurred in the middle Eocene, roughly corresponding to the Uintan and Irdinmanhan land mammal ages. The dispersal patterns implied by the phylogenetic results differ markedly from previous ideas about brontothere dispersal. Granger and Gregory (1943) viewed the Asian brontotheres largely as a separate radiation from North American horned brontotheres, both of them having arisen from a North American *Telmatherium* ancestry. In general, paleontologists have oversimplified brontothere paleobiogeography. For instance, Stucky (1992), Webb and Opdyke (1995), and Woodburne and Swisher (1995) identified the arrival of *Duchesneodus* in North America as the sole immigration event for brontotheres. The number of brontothere dispersals is greater than previously thought; however, the timing of the majority of brontothere-dispersal events, in the Irdinmanhan and late Uintan land mammal ages (late middle Eocene), is consistent with Woodburne's and Swisher's (1995) finding that this time period, with the Wasatchian (early Eocene), represent the two most significant periods of Asian–North American faunal interchanges of the Tertiary.

(3) The dispersal patterns implied by the cladograms do not support the East of Eden model of Beard (1998) by which the majority of dispersal events are thought to have gone from Asia into North America. The East of Eden model follows classic island biogeography theory whereby immigrant taxa are more likely to hail from a larger land mass (Asia) and disperse to the smaller land mass (North America) (Beard, 1998). Dispersal in the opposite direction, from North America into Asia, is more strongly supported by the analysis of ordered character data, thus calling into question the validity of island biogeography theory in explaining continent-scale diversity dynamics. The predominant dispersal polarity is inconclusive according to the analysis of unordered data; nevertheless, the results offer no positive support for the East of Eden model. It is possible that brontotheres went the opposite direction with respect to the dispersal-polarity tendencies of other clades, or that the middle and late Eocene interchanges were predominantly reversed in comparison to other times such as the early Eocene, when dispersal trends appear to have been predominantly consistent with the East of Eden model (Beard, 1998). Presently there are no clear answers for the inconsistency of brontothere dispersal trends with the East of Eden model. Dispersal trends in other mammalian clades need to be rigorously examined in a cladistic context before intercontinental overland dispersal patterns and their effect on biodiversity can be precisely understood.

ACKNOWLEDGEMENTS

I remain in awe of how the former curators and staff of the American Museum and other natural history institutions built such wonderful and scientifically important collections out of nothing more than scraps of old bones that mostly lay scattered across the unpopulated badlands of the world. For the past several years I have had the pleasure of discovering many wonders in these collections. I wish to thank Malcolm McKenna, Jin Meng, and Mark Norell for welcoming me into the venerable Columbia/American Museum vertebrate paleontology program to study brontotheres, my favorite extinct creatures since the third grade. The staff, students, and volunteers at the Division of Paleontology at the American Museum were all enormously helpful during my years

there: (in no particular order) Jeanne Kelly, Robert Evander, Denny Dively, Chris Norris, Chris Collins, Carl Mehling, Jim Clausen, Michael Ellison, Rick Edwards, Tom Rothwell, Robert Asher, Julia Clarke, Sunny Hwang, Diego Pol, Jonathan Geisler, Yaoming Hu, Xu Xing, Benjamin Burger, Bolortsetseg Minjin, Susan Bell, Ivy Rutzky, Alejandra Lora, Lorraine Meeker. I also wish to thank Robert Emry, Robert Purdy (NMNH), Lyndon Murray, Daniel Brinkman, Marilyn Fox (YPM), Chris Beard, Alan Tabrum, Mary Dawson (CMNH), John Flynn, William Simpson, William Turnbull (FMNH), Jaelyn Eberle (UCM), Logan Ivy, Richard Stucky (DMNH), Patricia Holroyd, Robert Feranec (UCMP), Lyndon Murray, Dennis Ruez (TMM), Xiaoming Wang, Sam Macleod (LACM), Alexandre Agadjanian, (PIN), Li Qian, Wang Yuanqing, Deng Tao (IVPP), Dou Wenxiu (VM), and Takenori Sasaki (UMUT) for access and help with specimens in their respective institutions and/or hospitality. Hiromichi Hirano (Waseda University) helped me track down *Protitanotherium koreanicum* specimens. Collaborative research with Nikos Solounias, Spencer Lucas, and Robert Emry was of tremendous value in the development and undertaking of this project. Others who provided valuable information and advice are Paul Olsen, Florent Rivals, Bryn Mader, Luke Holbrook, Mark Siddall, Don Prothero, Jeremy Hooker, Demberelyin Dashzeveg, and Joel Cracraft. Mariko Mihlbachler aided in the production of the figures. Spencer Lucas provided the photo of *Epimanteoceras praecursor*. Finally, this work could not have been completed without funding from Columbia University, the American Museum of Natural History, the Evolving Earth Foundation, the Geological Society of America, the Paleontological Society, and the New York College of Osteopathic Medicine.

REFERENCES

Alroy, J. 2003. Taxonomic inflation and body mass distributions in North American fossil mammals. Journal of Mammalogy 84: 431–443.

Antoine, P.-O. 2002. Phylogenie et evolution des Elasmotheriina (Mammalia, Rhinocerotidae). Memoires du Museum National d'Histoire Naturelle 188: 1–359.

Beard, K.C. 1998. East of Eden: Asia as an important center of taxonomic origination in mammalian evolution. *In* K.C. Beard and M.R. Dawson (editors), Dawn of the age of mammals in Asia. Bulletin of the Carnegie Museum of Natural History 34: 5–39.

Berger, J. 1983. Ecology and catastrophic mortality in wild horses: implications for interpreting fossil assemblages. Science 220: 1403–1404.

Berger, J., S. Dulamtseren, S. Cain, D. Enkkhbileg, P. Lichtman, Z. Namshir, G. Wingard, and R. Reading. 2001. Back-casting sociality in extinct species: new perspectives using mass death assemblages and sex ratios. Proceedings of the Royal Society of London B: Biological Sciences 268: 131–139.

Bjork, P.R. 1967. Latest Eocene vertebrates from northwestern South Dakota. Journal of Paleontology 41: 227–236.

Böckh, J. 1876. *Brachydiastematherium transylvanicum* Böckh et Maty, ein Neues Pachydermen-Genusaus den eocänen Schichten Siebenburgens. Mitteilungen aus dem Jahrbuche der Königlichen Ungarischen Geologischen Anstalt 4: 121–150.

Bonillas, Y. 1936. The dentition of *Lambdotherium*. Journal of Mammalogy 17: 139–142.

Butler, P.M. 1952. The milk molars of Perissodactyla, with remarks on molar occlusion. Proceedings of the Zoological Society of London 121: 777–817.

Cerdeño, E. 1995. Cladistic analysis of the family Rhinocerotidae (Perissodactyla). American Museum Novitates 3143: 1–25.

Chow, M., and C.C. Hu. 1959. A new species of *Parabrontops* from the Oligocene of Lunan, Yunnan. Acta Palaeontologica Sinica 7: 85–88.

Chow, M., Y.-P. Chang, and S.-Y. Ting. 1974. Some early Tertiary Perissodactyla from Lunan Basin, east Yunnan. Vertebrata Palasiatica 12: 262–273.

Clark, J., J.R. Beerbower, and K.K. Kietzke. 1967. Oligocene sedimentation, stratigraphy, paleoecology and paleoclimatology on the Big Badlands of South Dakota. Fieldiana 5: 1–158.

Colbert, E.H. 1938. Fossil mammals from Burma in the American Museum of Natural History. Bulletin of the American Museum of Natural History 74: 255–436.

Cook, H.J. 1926. New Eocene titanotheres from Moffat County, Colorado. Proceedings of the Colorado Museum of Natural History 7: 12–18.

Combs, M.C. 1998. Chalicotheriodea. *In* C.M. Janis, K.M. Scott, and L.L. Jacobs (editors), Evolution of Tertiary mammals of North

America: Vol. I: Terrestrial carnivores, ungulates, and ungulate-like mammals: 560–568. Cambridge: Cambridge University Press.

Cope, E.D. 1872. Second notice of extinct vertebrates from Bitter Creek, Wyoming. Proceedings of the American Philosophical Society 12: 487–488.

Cope, E.D. 1873a. On the new Perissodactylo [sic] from the Bridger Eocene. Paleontological Bulletin 11: 1–2.

Cope, E.D. 1873b. Second notice of extinct vertebrata from the Tertiary of the plains. Palaeontological Bulletin 15: 1–6.

Cope, E.D. 1880. The bad lands of the Wind River and their fauna. American Naturalist 14: 745–748.

Cope, E.D. 1881. The systematic arrangement of the order Perissodactyla. Proceedings of the American Philosophical Society 19: 377–403.

Cope, E.D. 1884. The Vertebrata of the Tertiary Formations of the West. Book 1. *In* F.V. Hayden (editor), Report of the United States Geological Survey of the Territories: 1–1009. Washington, DC.

Cope, E.D. 1887. The Perissodactyla. American Naturalist 21: 1060–1076.

Cracraft, J. 1989. Speciation and its ontology: the empirical consequences of alternative species concepts for understanding patterns and processes of differentiation. *In* D. Otte and J.A. Endler (editors), Speciation and its consequences: 28–59. Sunderland, MA: Sinauer.

Dashzeveg, D. 1975. New representatives of the genus *Embolotherium* from the Oligocene of Mongolia. Paleontologicheskii Zhurnal 3: 150–152.

Davis, J.I., and K.C. Nixon. 1992. Populations, genetic variation, and the delimitation of phylogenetic species. Systematic Biology 41: 421–435.

Dehm, R., and T.Z. Oettingen-Spielberg. 1958. Die mitteleocanen Saugertiers von ganda Kas bei Basal in Nordwest Pakistan. Bayerische Akademie der Wissenschaften New Series 91: 1–54.

Dong, M., and L. Ai. 2001. The lower part of Tunggur formation and the age of its underlying stratum. *In* T. Deng and Y. Wang (editors), Proceedings of the Eighth Annual Meeting of the Chinese Society of Vertebrate Paleontology: 83–90. Beijing: China Ocean Press.

Douglass, E. 1909. Preliminary descriptions of some new titanotheres from the Uinta deposits. Annals of the Carnegie Museum 6: 304–313.

Earle, C. 1891. *Palaeosyops* and allied genera. Proceedings of the Academy of Natural Sciences of Philadelphia 43: 106–117.

Earle, C. 1892. A memoir upon the genus *Palaeosyops* Leidy, and its allies. Journal of the Academy of Natural Sciences of Philadelphia 9: 267–387.

Earle, C. 1895. On the supposed case of parallelism in the genus *Palaeosyops*. American Naturalist 29: 622–626.

Eberle, J.J. 2006. Early Eocene Brontotheriidae (Perissodactyla) from the Eureka Sound group, Ellesmere Island, Canadian High Arctic—implications for brontothere origins and high-latitude dispersal. Journal of Vertebrate Paleontology 26: 381–386.

Eberle, J.J., and J.E. Storer. 1999. Northernmost record of brontotheres, Axel Heiberg Island, Canada—implications for age of the Buchanan Lake formation and brontothere paleobiology. Journal of Paleontology 73: 979–983.

Emry, R.J., and S.G. Lucas. 2002. Brontothere (Mammalia, Perissodactyla) footprints from the Eocene of the Ily Basin, Kazakstan. Journal of Vertebrate Paleontology 22(suppl.): 51A.

Emry, R.J., and S.G. Lucas. 2003. New ceratomorphs (Mammalia, Perissodactyla) footprints from the Eocene of the Ily Basin, Kazakstan. Journal of Vertebrate Paleontology 23(suppl.): 44A.

Emry, R.J., S.G. Lucas, and B.U. Bayshashov. 1997. Brontothere bone bed in the Eocene of eastern Kazakstan. Journal of Vertebrate Paleontology 17(suppl.): 44A.

Emry, R.J., S.G. Lucas, L. Tyutkova, and B. Wang. 1998. The Ergilian–Shandgolian (Eocene-Oligocene) transition in the Zaysan Basin, Kazakstan. *In* K.C. Beard and M.R. Dawson (editors), Dawn of the age of mammals in Asia. Bulletin of the Carnegie Museum of Natural History 34: 298–312.

Emry, R.J., L.S. Russell, and P.R. Bjork. 1987. The Chadronian, Orellan, and Whitneyan North American land mammal ages. *In* M.O. Woodburne (editor), Cenozoic mammals of North America: geochronology and biostratigraphy: 118–152. Berkeley: University of California Press.

Flower, W.H. 1876. On the relation of extinct to existing Mammalia with special reference to the derivative hypothesis. Nature 13: 307–308, 327–328, 350–352, 387–388, 409–410, 449–450, 487–488, 513–514.

Froehlich, D.J. 1999. Phylogenetic systematics of basal perissodactyls. Journal of Vertebrate Paleontology 19: 140–159.

Froehlich, D.J. 2002. Quo vadis *Eohippus*? The systematics and taxonomy of the early Eocene equids (Perissodactyla). Zoological Journal of the Linnaean Society 134: 141–256.

Gabounia, L. 1977. Contribution a la connaissance des mammiféres paléogènes du bassin de

Zaissan (Kazakhstan Central). Geobios Special Mémoire 1: 29–37.

Gazin, C.L., and J.M. Sullivan. 1942. A new titanothere from the Eocene of Mississippi with notes on the correlation between the marine Eocene of the Gulf coastal plain and continental Eocene of the Rocky Mountain region. Smithsonian Miscellaneous Collections 101 13: 1–13.

Grande, L., and W.E. Bemis. 1998. A comprehensive phylogenetic study of Amiid fishes (Amiidae) based on comparative skeletal anatomy: an empirical search for interconnected patterns of natural history. Journal of Vertebrate Paleontology 18(Suppl.): 1–690.

Granger, W., and W.K. Gregory. 1938. A new titanothere genus from the upper Eocene of Mongolia and North America. Bulletin of the American Museum of Natural History 74: 435–436.

Granger, W., and W.K. Gregory. 1943. A revision of the Mongolian titanotheres. Bulletin of the American Museum of Natural History 80: 349–389.

Granger, W.D. 1909. Faunal horizons of the Washakie formation of southern Wyoming. Bulletin of the American Museum of Natural History 26: 13–23.

Gregory, W.K. 1912. Note on the upper Eocene titanotheroid *Telmatherium* (?) *incisivum* Douglass from the Uinta Basin. Science 35: 545.

Gregory, W.K., and H.J. Cook. 1928. New material for the study of evolution: a series of primitive rhinoceros skulls (*Trigonias*) from the lower Oligocene of Colorado. Proceedings of the Colorado Museum of Natural History 8: 1–32.

Gunnell, G.F., and V.L. Yarborough. 2000. Brontotheriidae (Perissodactyla) from the late early Eocene (Bridgerian), Wasatch and Bridger formations, southern Green River Basins, southwestern Wyoming. Journal of Vertebrate Paleontology 20: 349–368.

Hanson, C.B. 1989. *Teletaceras radinskyi*, a new primitive rhinocerotid from the late Eocene Clarno formation of Oregon. *In* D.R. Prothero and R.M. Schoch (editors), The evolution of Perissodactyls: 379–421. New York: Oxford University Press.

Hanson, C.B. 1996. Stratigraphy and vertebrate faunas of the Bridgerian-Duchesnean Clarno Formation, north-central Oregon. *In* D.R. Prothero and R.J. Emry (editors), The terrestrial Eocene-Oligocene transition in North America: 206–239. Cambridge: Cambridge University Press.

Hatcher, J.B. 1895. On a new species of *Diplacodon*, with a discussion of the relations of that genus to *Telmatotherium*. American Naturalist 29: 1084–1090.

Hay, O.P. 1901. Bibliography and catalogue of the fossil vertebrates of North America. Washington, DC: Government Printing Office.

Holbrook, L.T. 1999. The phylogeny and classification of tapiromorph Perissodactyls (Mammalia). Cladistics 15: 331–350.

Holbrook, L.T. 2001. Comparative osteology of early Tertiary tapiromorphs (Mammalia, Perissodactyla). Zoological Journal of the Linnaean Society 132: 1–54.

Holbrook, L.T. 2006. Cranial and postcranial perspectives on the affinities of *Pachynolophus* (Mammalia, Perissodactyla). Journal of Vertebrate Paleontology 26(suppl.): 77A.

Holroyd, P.A., and R.L. Ciochon. 2000. *Bunobrontops savagei*: a new genus and species of brontotheriid perissodactyl from the Eocene Pondaung fauna of Myanmar. Journal of Vertebrate Paleontology 20: 408–410.

Hooker, J.J. 1984. A primitive ceratomorph (Perissodactyla, Mammalia) from the early Tertiary of Europe. Zoological Journal of the Linnaean Society 82: 229–244.

Hooker, J.J. 1989. Character polarities in early perissodactyls and their significance for *Hyracotherium* and infraordinal relationships. *In* D.R. Prothero and R.M. Schoch (editors), The evolution of Perissodactyls: 79–101. New York: Oxford University Press.

Hooker, J.J. 1994. The beginning of the equoid radiation. Zoological Journal of the Linnaean Society 112: 29–63.

Hooker, J.J., and D. Dashzeveg. 2003. Evidence for direct mammalian faunal interchange between Europe and Asia near the Paleocene-Eocene boundary. *In* S.L. Wing, P.D. Gingerich, B. Schmitz, and E. Thomas (editors), Causes and consequences of globally warm climates in the early Paleogene. Special Paper of the Geological Society of America 369: 479–500.

Hu, C. 1961. The occurrence of *Parabrontops* in Hami, Sinkiang. Vertebrata Palasiatica 3: 41–42.

Huang, X., and J. Zheng. 2004. Brontotheres (Perissodactyla, Mammalia) from the middle Eocene of Lunan, Yunnan. Vertebrata Palasiatica 42: 334–339.

Janis, C., R.C. Hulbert, and M.C. Mihlbachler. In press. Addendum: Update to Vol. I. *In* C. Janis and G. Gunnell (editors), Evolution of Tertiary mammals of North America: Vol. II. Cambridge: Cambridge University Press.

Janis, C.M. 2000. Patterns in the evolution of herbivory in large terrestrial mammals: the Paleogene of North America. *In* H.D. Sues (editor), Evolution of herbivory in terrestrial vertebrates: 168–222. Cambridge: Cambridge University Press.

Janis, C.M., M.W. Colbert, M.C. Coombs, W.D. Lambert, B.J. MacFadden, B.J. Mader, D.R. Prothero, R.M. Schoch, J. Shoshani, and W.P. Wall. 1998. Perissodactyla and Proboscidea. *In* C.M. Janis, K.M. Scott, and L.L. Jacobs (editors), Evolution of Tertiary mammals of North America: Vol. I: Terrestrial carnivores, ungulates, and ungulate-like mammals: 511–524. Cambridge: Cambridge University Press.

Jarman, P. 1983. Mating system and sexual dimorphism in large, terrestrial, mammalian herbivores. Biological Reviews of the Cambridge Philosophical Society 58: 485–520.

Kearney, M. 2002. Fragmentary taxa, missing data, and ambiguity: mistaken assumptions and conclusions. Systematic Biology 51: 368–381.

Kearney, M., and J.M. Clark. 2003. Problems due to missing data in phylogenetic analyses including fossils: a critical review. Journal of Vertebrate Paleontology 23: 263–274.

Kelly, T.S. 1990. Biostratigraphy of Uintan and Duchesnean land mammal assemblages from the middle member of the Sespe formation, Simi Valley, California. Natural History Museum of Los Angeles County Contributions in Science 419: 1–42.

Krishtalka, L., R.M. West, C.C. Black, M.R. Dawson, J.J. Flynn, W.D. Turnbull, R.K. Stucky, M.C. McKenna, T.M. Brown, and J.A. Lilligraven. 1987. Eocene (Wasatchian through Duchesnean) biochronology of North America. *In* M.O. Woodburn (editor), Cenozoic mammals of North America: geochronology and biostratigraphy. Berkeley: University of California Press.

Kumar, K., and A. Sahni. 1985. Eocene mammals from the upper Subathu group, Kashmir Himalaya, India. Journal of Vertebrate Paleontology 5: 153–168.

Lambe, L.M. 1908. Part 4: The vertebrata of the Oligocene of the Cypress Hills, Saskatchewan. Contributions to Canadian Paleontology 3: 1–64.

Lane, H.H. 1932. Variation in *Palaeosyops*. University of Kansas Science Bulletin 20: 319–326.

Leidy, J. 1852. Description of the remains of extinct Mammalia and Chelonia, from Nebraska territory, collected during the Geological Survey under the direction of Dr. D.D. Owen. *In* D.D. Owen (editor), Report of a geological survey of Wisconsin, Iowa, and Minnesota and incidentally of a portion of Nebraska Territory: 534–572. Philadelphia: Lippincott, Grambo.

Leidy, J. 1870a. (Descriptions of *Palaeosyops paludosus*, *Microsus cuspidatus*, and *Notharctus tenebrosus*). Proceedings of the Academy of Natural Sciences of Philadelphia 22: 113–114.

Leidy, J. 1870b. (Description of a new genus and species, *Megacerops coloradensis*). Proceedings of the Academy of Natural Sciences of Philadelphia 22: 1–2.

Leidy, J. 1872. Remarks on fossils from Wyoming. Proceedings of the Academy of Natural Sciences of Philadelphia 23: 228–229.

Leidy, J. 1873. Contributions to the extinct vertebrate fauna of the western territories. *In* F.V. Hayden (editor), Report of the United States Geological Survey of the Territories 1: 14–358. Washington, DC: Department of the Interior.

Loison, A., J.-M. Gaillard, C. Pelabon, and N.G. Yoccuz. 1999. What factors shape sexual size dimorphism in ungulates? Evolutionary Ecology Research 1: 611–633.

Lucas, S.G. 1982. Vertebrate paleontology, stratigraphy, and biostratigraphy of Eocene Galisteo formation, north-central New Mexico. New Mexico Bureau of Mines and Mineral Resources Circular 186: 1–34.

Lucas, S.G. 1983a. *Protitanotherium* (Mammalia, Perissodactyla) from the Eocene Baca formation, west-central New Mexico. New Mexico Journal of Sciences 23: 39–47.

Lucas, S.G. 1983b. The Baca formation and the Eocene-Oligocene boundary in New Mexico. New Mexico Geological Society Guidebook for Field Conference 3: 187–192.

Lucas, S.G. 1992. Redefinition of the Duchesnean land mammal "age", late Eocene of western North America. *In* D.R. Prothero and W.A. Berggren (editors), Eocene-Oligocene climatic and biotic evolution: 88–105. Princeton, NJ: Princeton University Press.

Lucas, S.G. 2004. O.C. Marsh and the Eocene Brontothere *Teleodus*: a paleontological hoax. *In* S.G. Lucas, K.E. Zeigler, and P.E. Kondrashov (editors), Paleogene mammals. New Mexico Museum of Natural History and Science Bulletin 26: 119–127.

Lucas, S.G., and R.J. Emry. 2001. *Sharamynodon* (Mammalia: Perissodactyla) from the Eocene of the Ily Basin, Kazakstan and the antiquity of Asian amynodonts. Proceedings of the Biological Society of Washington 114: 527–525.

Lucas, S.G., S.G. Foss, and M.C. Mihlbachler. 2004. *Archaenodon* (Mammalia, Artiodactyla) from the Eocene Clarno formation, Oregon, and the age of the Hancock Quarry Local fauna. *In* S.G. Lucas, K.E. Zeigler, and P.E. Kondrashov (editors), Paleogene mammals. New Mexico Museum of Natural History and Science Bulletin 26: 89–95.

Lucas, S.G., and L.T. Holbrook. 2004. The skull of the Eocene perissodactyl *Lambdotherium* and its phylogenetic significance. *In* S.G. Lucas, K.E. Zeigler, and P.E. Kondrashov (editors), Paleogene mammals. New Mexico Museum of Natural History and Science Bulletin 26: 81–87.

Lucas, S.G., and P.E. Kondrashov. 2004. Early Eocene (Bumbanian) Perissodactyls from Mongolia and their biochronological significance. *In* S.G. Lucas, K.E. Zeigler, and P.E. Kondrashov (editors), Paleogene mammals. New Mexico Museum of Natural History and Science Bulletin 26: 215–220.

Lucas, S.G., and R.M. Schoch. 1982. *Duchesneodus*, a new name for some titanotheres (Perissodactyla, Brontotheriidae) from the late Eocene of western North America. Journal of Paleontology 56: 1018–1023.

Lucas, S.G., and R.M. Schoch. 1989a. European brontotheres. *In* D.R. Prothero and R.M. Schoch (editors), The evolution of Perissodactyls: 485–489. New York: Oxford University Press.

Lucas, S.G., and R.M. Schoch. 1989b. Taxonomy of *Duchesneodus* (Brontotheriidae) from the late Eocene of North America. *In* D.R. Prothero and R.M. Schoch (editors), The evolution of Perissodactyls: 490–503. New York: Oxford University Press.

MacArthur, R.H., and E.O. Wilson. 1967. The theory of island biogeography. Princeton, NJ: Princeton University Press.

MacFadden, B.J. 1992. Fossil horses. New York: Cambridge University Press.

MacFadden, B.J. 1998. Equidae. *In* C.M. Janis, K.M. Scott, and L.L. Jacobs (editors), Evolution of Tertiary mammals of North America: Vol. I: Terrestrial carnivores, ungulates, and ungulate-like mammals: 537–559. Cambridge: Cambridge University Press.

Maddison, W.P., and D.R. Maddison. 1992. MacClade: analysis of phylogeny and character evolution. Sunderland, MA: Sinauer.

Mader, B.J. 1989. The Brontotheriidae: a systematic revision and preliminary phylogeny of North American genera. *In* D.R. Prothero and R.M. Schoch (editors), The evolution of Perissodactyls: 458–484. New York: Oxford University Press.

Mader, B.J. 1998. Brontotheriidae. *In* C.M. Janis, K.M. Scott, and L.L. Jacobs (editors), Evolution of Tertiary mammals of North America: Vol. I: Terrestrial carnivores, ungulates, and ungulate-like Mammals: 525–536. Cambridge: Cambridge University Press.

Mader, B.J. 2000. *Pseudodiplacodon*, a new generic name for *Diplacodon progressum* Peterson (Mammalia, Perissodactyla, Brontotheriidae). Journal of Vertebrate Paleontology 20: 164–166.

Mader, B.J., and J.P. Alexander. 1995. *Megacerops kuwagatarhinus* n. sp., an unusual brontothere (Mammalia, Perissodactyla) with distally forked horns. Journal of Paleontology 69: 581–587.

Marsh, O.C. 1872. Preliminary description of new Tertiary mammals. American Journal of Science and Arts 4: 1–35.

Marsh, O.C. 1873. Notice of new Tertiary mammals. American Journal of Science and Arts 5: 1–9.

Marsh, O.C. 1874. Structure and affinities of the Brontotheriidae. American Journal of Science and Arts 7: 1–8.

Marsh, O.C. 1875. Notice of new Tertiary mammals. IV. American Journal of Science and Arts 9: 239–250.

Marsh, O.C. 1876. Principal characters of the Brontotheriidae. American Journal of Science and Arts 11: 335–340.

Marsh, O.C. 1880. List of genera established by Professor O.C. Marsh, 1862–1879. New Haven, CT.

Marsh, O.C. 1887. Notice of new fossil mammals. American Journal of Science 34: 1–9.

Marsh, O.C. 1889. Restoration of *Brontops robustus* from the Miocene of America. American Journal of Science 37: 163–165.

Marsh, O.C. 1890. Notice of new Tertiary mammals. American Journal of Science 39: 523–525.

Matthew, W.D. 1899. A provisional classification of the fresh-water Tertiary of the west. Bulletin of the American Museum of Natural History 22: 19–75.

Matthew, W.D. 1931. Critical observations on the phylogeny of the rhinoceroses. University of California Publications in Geological Sciences 20: 1–9.

McCarroll, S.M., J.J. Flynn, and W.D. Turnbull. 1996a. The mammalian faunas of the Washakie formation, Eocene age, of Southern Wyoming. Part III. Perissodactyls. Fieldiana 33: 1–38.

McCarroll, S.M., J.J. Flynn, and W.D. Turnbull. 1996b. Biostratigraphy and magnetostratigraphy of the Bridgerian-Uintan Washakie formation, Washakie Basin, Wyoming. *In* D.R. Prothero and R.J. Emry (editors), The Terrestrial Eocene-Oligocene transition in North America: 25–39. Cambridge: Cambridge University Press.

McKenna, M.C., and S.K. Bell. 1997. Classification of mammals above the species level. New York: Columbia University Press.

Meng, J., R. Zhai, and A.R. Wyss. 1998. The late Paleocene Bayan Ulan fauna of Inner Mongolia, China. *In* K.C. Beard and M.R. Dawson (editors), Dawn of the age of mammals in Asia.

Bulletin of the Carnegie Museum of Natural History 34: 148–185.

Miao, D. 1982. Early Tertiary fossil mammals from the Shinao basin, Panxian County, Guizhou Province. Acta Palaeontologica Sinica 21: 527–536.

Mihlbachler, M.C. 2003a. A preliminary cladistic phylogeny of the Eocene Brontotheriidae (Mammalia, Perissodactyla). Journal of Vertebrate Paleontology 23(suppl.): 78A.

Mihlbachler, M.C. 2003b. Demography of late Miocene rhinoceroses (*Teleoceras proterum* and *Aphelops malacorhinus*) from Florida: linking mortality and sociality in fossil assemblages. Paleobiology 29: 412–428.

Mihlbachler, M.C. 2004. Taxonomic diversity or sexual dimorphism? Towards a rational taxonomy of North American late Eocene Brontotheriidae. Journal of Vertebrate Paleontology 24(Suppl.): 94A.

Mihlbachler, M.C. 2005. Linking sexual dimorphism and sociality in rhinoceroses: insights from *Teleoceras proterum* and *Aphelops malacorhinus* from the late Miocene of Florida. Bulletin of the Florida Museum of Natural History 45: 495–520.

Mihlbachler, M.C. 2007. *Eubrontotherium clarnoensis*, a new genus and species of brontothere (Brontotheriidae, Perissodactyla) from the Hancock Quarry, Clarno Formation, Wheeler County, Oregon. Paleobios 27: 19–39.

Mihlbachler, M.C., C.A. Hemmings, and S.D. Webb. 2002. Morphological chronoclines among late Pleistocene muskrats (*Ondatra zibethicus*: Muridae, Rodentia) from northern Florida. Quaternary Research 58: 289–295.

Mihlbachler, M.C., S.G. Lucas, and R. Emry. 2004a. A new brontothere (Brontotheriidae, Perissodactyla, Mammalia) from the Eocene of the Ily Basin of Kazakstan and a phylogeny of Asian "horned" brontotheres. American Museum Novitates 3439: 1–43.

Mihlbachler, M.C., S.G. Lucas, and R.J. Emry. 2004b. The holotype specimen of *Menodus giganteus*, and the "insoluble" problem of Chadronian brontothere taxonomy. *In* S.G. Lucas, K.E. Zeigler, and P.E. Kondrashov (editors), Paleogene mammals. New Mexico Museum of Natural History and Science Bulletin 26: 129–135.

Mihlbachler, M.C., and N. Solounias. 2002. Body size, dental microwear and brontothere diets through the Eocene. Journal of Vertebrate Paleontology 22(Suppl.): 88A.

Mihlbachler, M.C., and N. Solounias. 2004. Anatomy and evolution of the bizarre "battering ram" of the brontothere, *Embolotherium* (Mammalia, Perissodactyla). Journal of Morphology 260: 313.

Miyata, K., and Y. Tomida. 2003. First discovery of brontotheres from the Eocene of Japan. Journal of Vertebrate Paleontology 23(suppl.): 79A.

Nelson, M.E., J.H. Madsen, and W.L. Stokes. 1980. A titanothere from the Green River formation, central Utah: *Teleodus uintensis* (Perissodactyla: Brontotheriidae). University of Wyoming Contributions to Geology 18: 127–134.

Nikolov, V.I., and K. Heissig. 1985. Fossile Saugertiere aus dem Obereozan und Unteroligozan Bulgariens und Bedeuntung fur die Palaeogeographie. Mitteilungen der Bayerischen Staatssammlung für Paläontologie und Historische Geologie 25: 61–79.

Nixon, K.C., and K.C. Wheeler. 1990. An amplification of the phylogenetic species concept. Cladistics 6: 211–223.

Nixon, K.C., and Q.D. Wheeler. 1992. Extinction and the origin of species. *In* M. Novacek and Q.D. Wheeler (editors), Extinction and phylogeny: 119–143. New York: Columbia University Press.

Osborn, H.F. 1889. The Mammalia of the Uinta formation. Part III. The Perissodactyla. Transactions of the American Philosophical Society 16: 505–530.

Osborn, H.F. 1895. Fossil mammals of the Uinta Basin. Expedition of 1894. Bulletin of the American Museum of Natural History 7: 71–105.

Osborn, H.F. 1896. The cranial evolution of *Titanotherium*. Bulletin of the American Museum of Natural History 8: 157–197.

Osborn, H.F. 1897. Phylogeny of the early Eocene titanotheres: redefinition of the Ceneutheria and Meseutheria: origin of the multituberculate teeth among Gomphodonts. Science 6: 107.

Osborn, H.F. 1902a. The four phyla of Oligocene titanotheres. Bulletin of the American Museum of Natural History 16: 91–109.

Osborn, H.F. 1902b. The law of adaptive radiation. American Naturalist 36: 353–363.

Osborn, H.F. 1902c. Dolichocephaly and brachycephaly in the lower mammals. Bulletin of the American Museum of Natural History 16: 77–89.

Osborn, H.F. 1907. Tertiary mammal horizons of North America. Bulletin of the American Museum of Natural History 23: 237–253.

Osborn, H.F. 1908a. New or little known titanotheres from the Eocene and Oligocene. Bulletin of the American Museum of Natural History 24: 599–617.

Osborn, H.F. 1908b. The four inseparable factors of evolution: theory of their distinct and combined action in the transformation of the titanotheres, an extinct family of hoofed animals in the order Perissodactyla. Science 27: 148–150.

Osborn, H.F. 1911. Biological conclusions drawn from the study of the titanotheres. Science 33: 825–828.

Osborn, H.F. 1913. Lower Eocene titanotheres. Genera *Lambdotherium*, *Eotitanops*. Bulletin of the American Museum of Natural History 21: 407–415.

Osborn, H.F. 1914. Recent results in the phylogeny of the titanotheres. Geological Society of America Bulletin 25: 403–405.

Osborn, H.F. 1916. Two new Oligocene titanotheres. Bulletin of the American Museum of Natural History 35: 721–723.

Osborn, H.F. 1919. New titanotheres of the Huerfano. Bulletin of the American Museum of Natural History 41: 557–569.

Osborn, H.F. 1923. Titanotheres and lophiodonts in Mongolia. American Museum Novitates 91: 1–5.

Osborn, H.F. 1925. Upper Eocene and lower Oligocene titanotheres of Mongolia. American Museum Novitates 202: 1–12.

Osborn, H.F. 1929a. Titanotheres of ancient Wyoming, Dakota, and Nebraska. United States Geological Survey Monographs 55: 1–894.

Osborn, H.F. 1929b. *Embolotherium*, gen. nov., of the Ulan Gochu, Mongolia. American Museum Novitates 353: 1–20.

Osborn, H.F. 1930. Fifty-Two years of research, observation, and publication, 1877–1929. New York: Charles Scribner's Sons.

Osborn, H.F. 1931. New conceptions of species and genera, and of classification, discovered in the evolution of the titanotheres. Journal of Mammalogy 12: 1–12.

Osborn, H.F. 1934. Aristogenesis, the creative principle on the origin of species. Science 79: 41–45.

Osborn, H.F., W.B. Scott, and F. Spier. 1878. Palaeontological report of the Princeton Scientific Expedition of 1877. Contributions from the Museum of Geology and Archaeology of Princeton College 1: 1–106.

Osborn, H.F., and J.L. Wortman. 1895. Perissodactyls of the lower Miocene White River beds. Bulletin of the American Museum of Natural History 7: 343–375.

Peterson, O.A. 1914a. A small titanothere from the lower Uinta beds. Annals of the Carnegie Museum 9: 53–57.

Peterson, O.A. 1914b. A new titanothere from the Uinta Eocene. Annals of the Carnegie Museum 9: 29–52.

Peterson, O.A. 1914c. Correction of generic name. Annals of the Carnegie Museum 9: 220.

Peterson, O.A. 1924. Osteology of *Dolichorhinus longiceps* Douglass, with a review of the species of *Dolichorhinus* in the order of their publication. Memoirs of the Carnegie Museum 9: 405–472.

Peterson, O.A. 1931. New species of the genus *Teleodus* from the Upper Uinta of northeastern Utah. Annals of the Carnegie Museum 20: 307–312.

Peterson, O.A. 1934. New titanotheres from the Uinta Eocene in Utah. Annals of the Carnegie Museum 22: 351–361.

Pilgrim, G.E. 1925. The Perissodactyla of the Eocene of Burma. Paleontologia Indica 8: 1–28.

Pilgrim, G.E., and G.de P. Cotter. 1916. Some newly discovered Eocene mammals from Burma. Records of the Geological Survey of India 47: 42–77.

Pomel, A. 1849. Description d'un os maxillaire fossile de *Palaeotherium* par Hiram Prout. American Journal of Science by Silliman's [sic] and J. Dana, 2e série, vol. 3, no. 8, p. 248. Bibliothéque Universelle de Geneve Archives Des Sciences Physiques et Naturelles 10: 73–75.

Prothero, D.R. 1994. The Eocene-Oligocene transition: paradise lost. New York: Columbia University Press.

Prothero, D.R. 1996. Magnetic stratigraphy and biostratigraphy of the middle Eocene Uinta formation, Uinta Basin, Utah. *In* D.R. Prothero and R.J. Emry (editors), The Terrestrial Eocene-Oligocene transition in North America: 3–24. Cambridge: Cambridge University Press.

Prothero, D.R. 2005. The evolution of North American rhinoceroses. Cambridge: Cambridge University Press.

Prothero, D.R., and R.M. Schoch. 1989. Classification of the Perissodactyla. *In* D.R. Prothero and R.M. Schoch (editors), The evolution of Perissodactyls: 530–537. New York: Oxford University Press.

Prothero, D.R., and R.M. Schoch. 2002. Horns, tusks, and flippers: the evolution of hoofed mammals. Baltimore, MD: Johns Hopkins University Press.

Qi, T. 1987. The middle Eocene Arshanto fauna (Mammalia) of inner Mongolia. Annals of the Carnegie Museum 56: 1–73.

Qi, T., and K.C. Beard. 1996. *Nanotitan shanghuangensis*, gen. et sp. nov.: the smallest known brontothere. Journal of Vertebrate Paleontology 16: 578–581.

Qi, T., and K.C. Beard. 1998. *Nanotitanops*, a new name for *Nanotitan* Qi and Beard, 1996 not *Nanotitan* Sharov, 1968. Journal of Vertebrate Paleontology 18: 812.

Qi, T., L. Wu, and Q. Chang. 1992. Discovery of *Protitan* (Perissodactyla, Brontotheriidae) from late Eocene Tukhum beds, Nei Mongol. Vertebrata Palasiatica 30: 162–167.

Radinsky, L.B. 1963. Origin and early evolution of North American Tapiroidea. Peabody Museum of Natural History Bulletin 17: 1–106.

Radinsky, L.B. 1964. Notes of the Eocene and Oligocene fossil localities in Inner Mongolia. American Museum Novitates 2180: 1–11.

Radinsky, L.B. 1967a. *Hyrachyus*, *Chasmotherium*, and the early evolution of helaletid tapiroids. American Museum Novitates 2313: 1–23.

Radinsky, L.B. 1967b. A review of the rhinocerotoid family Hyracodontidae (Perissodactyla). Bulletin of the American Museum of Natural History 136: 5–45.

Radinsky, L.B. 1969. The early evolution of Perissodactyla. Evolution 23: 308–328.

Riggs, E.S. 1912. New or little known titanotheres from the lower Uintah formations with notes on the stratigraphy and distribution of fossils. Field Museum of Natural History Publications Geological Series 4: 17–41.

Robinson, P., G.F. Gunnell, S.L. Walsh, W.C. Clyde, J.E. Storer, R.K. Stucky, D.J. Froehlich, I. Ferresquila-Villafranca, and M.C. McKenna. 2004. Wasatchian through Duchesnean biochronology. *In* M.O. Woodburne (editor), Late Cretaceous and Cenozoic mammals of North America: 106–155. New York: Columbia University Press.

Russell, D.E., and R. Zhai. 1987. The Paleogene of Asia: mammals and stratigraphy. Memoires du Museum National D'Histoire Naturelle Serie C, Sciences de la Terre 52: 1–488.

Russell, L.S. 1934. Revision of the lower Oligocene vertebrate fauna of the Cypress Hills, Saskatchewan. Transactions of the Royal Society of Canada 20: 49–67.

Russell, L.S. 1940. Titanotheres from the lower Oligocene Cypress Hills formation of Saskatchewan. Transactions of the Royal Society of Canada 34: 89–100.

Savage, D.E., D.E. Russell, and P. Louis. 1965. European Eocene Equidae. University of California Publications in Geological Sciences 56: 1–94.

Schlaikjer, E.M. 1935. Contributions to the stratigraphy and paleontology of the Goshen Hole area, Wyoming. Bulletin of the Museum of Comparative Zoology 76: 71–93.

Schoch, R.M., and S.G. Lucas. 1985. The Brontotheriidae, a group of Eocene and Oligocene Perissodactyls from North America, Asia and Eastern Europe: abstracts of papers and posters, Fourth International Theriological Congress abstract 0558.

Schuh, R.T. 2000. Biological Systematics. Ithaca, NY: Cornell University Press.

Scott, W.B. 1939. Some memories of a paleontologist. Princeton, NJ: Princeton University Press.

Scott, W.B. 1941. The mammalian fauna of the White River Oligocene. Part 5. Perissodactyla. Transactions of the American Philosophical Society 28: 747–980.

Scott, W.B. 1945. The mammalia of the Duchesne River Oligocene. Transactions of the American Philosophical Society 34: 209–253.

Scott, W.B., and H.F. Osborn. 1887. Preliminary account of the fossil mammals from the White River formation contained in the Museum of Comparative Zoology. Bulletin of the Museum of Comparative Zoology 13: 151–171.

Simpson, G.G. 1945. The principles of classification and a classification of mammals. Bulletin of the American Museum of Natural History 85: 1–350.

Simpson, G.G. 1951. Horses: the story of the horse family in the modern world and through sixty million years of history. New York: Oxford University Press.

Sisson, S., and J.D. Grossman. 1953. The anatomy of the domestic animals, 4th ed. Philadelphia: W.B. Saunders.

Sites, J.W., Jr., and J.C. Marshall. 2004. Operational criteria for delimiting species. Annual Review of Ecology, Evolution, and Systematics 35: 199–227.

Spamer, E.E., E. Daeschler, and L.G. Vostreys-Shapiro. 1995. A study of the fossil vertebrate types in the Academy of Natural Sciences of Philadelphia: taxonomic, systematic, and historical perspectives. Academy of Natural Sciences of Philadelphia Special Publication 16: 1–434.

Steinmann, G., and L. Döderlein. 1890. Elemente de Paläontologie. Leipzig.

Stock, C. 1935. Titanothere remains from the Sespe of California. Proceedings of the National Academy of Sciences 21: 456–462.

Stock, C. 1936a. Perissodactyls of the Sespe Eocene, California. Proceedings of the National Academy of Sciences 22: 260–265.

Stock, C. 1936b. Titanotheres from the Titus Canyon formation, California. Proceedings of the National Academy of Sciences 22: 656–661.

Stock, C. 1937. An Eocene titanothere from San Diego County, California, with remarks on the age of the Poway Conglomerate. Proceedings of the National Academy of Sciences 23: 48–53.

Stock, C. 1938. A titanothere from the type Sespe of California. Proceedings of the National Academy of Sciences 24: 507–512.

Stovall, J.W. 1948. Chadron vertebrate fossils from below the Rim Rock of Presidio County, Texas. American Journal of Science 246: 78–95.

Stucky, R.K. 1990. Evolution of land mammal diversity in North America during the Cenozoic. Current Mammalogy 2: 375–432.

Stucky, R.K. 1992. Mammalian faunas in North America of Bridgerian to early Arikareean "ages" (Eocene to Oligocene). *In* D.R. Prothero and W.A. Berggren (editors), Eocene-Oligocene climatic and biotic evolution: 464–493. Princeton, NJ: Princeton University Press.

Swofford, D.L. 1991. When are phylogeny estimates from molecular and morphological data incongruent. *In* M.M. Miyamoto and J. Cracraft (editors), Phylogenetic analyses of DNA sequences: 295–333. New York: Oxford University Press.

Swofford, D.L. 2001. PAUP* (phylogenetic analysis using parsimony [*and other methods] version 4. 0b10 [PPC]). Sunderland, MA: Sinauer.

Takai, F. 1939. Eocene mammals found from the Hosan coal-field, Tyosen. Journal of the Faculty of Science Imperial University of Tokyo 5: 199–217.

Thewisse, J.G.M., P.D. Gingerich, and D.E. Russell. 1987. Artiodactyla and Perissodactyla (Mammalia) from the Early-Middle Eocene Kuldana Formation of Kohat (Pakistan). Contributions from the Museum of Paleontology, Univeristy of Michigan 27: 247–274.

Thewissen, J.G.M., E.M. Williams, and S.T. Hussain. 2001. Eocene mammal faunas from northern Indo-Pakistan. Journal of Vertebrate Paleontology 21: 347–366.

Thorley, J.L., and R.D.M. Page. 2000. RadCon: phylogenetic tree comparison and consensus. Bioinformatics 16: 486–487.

Tsubamoto, T., N. Egi, M. Takai, N. Shigehara, A.K. Aung, T. Thein, A.N. Soe, and S.T. Tun. 2000. A preliminary report of the Eocene mammals of the Pondaung fauna, Myanmar. Asian Paleoprimatology 1: 29–101.

Turnbull, W.D., and D.M. Martill. 1988. Taphonomy and preservation of a monospecific titanothere assemblage from the Washakie formation (Late Eocene), southern Wyoming: an ecological accident in the fossil record. Palaeogeography Palaeoclimatology Palaeoecology 63: 91–108.

Voorhies, M.R. 1969. Taphonomy and population dynamics of an early Pliocene vertebrate fauna, Knox County, Nebraska. University of Wyoming Contributions to Geology Special Paper 1: 1–69.

Wallace, S.W. 1980. A revision of North American early Eocene Brontotheriidae (Mammalia, Perissodactyla) Master's thesis, University of Colorado, Boulder.

Wang, B. 1978. Perissodactyla from the late Eocene of Lantian, Shensi. Professional Papers of Stratigraphy and Palaeontology 7: 118–121.

Wang, B. 1982. Osteology and phylogenetic relationships of *Rhinotitan mongoliensis*. Academia Sinica Institute of Vertebrate Paleontology and Paleoanthropology Memoirs 16: 1–75.

Wang, B. 2000. A skull of *Embolotherium* (Perissodactyla, Mammalia) from Erden Obo, Nei Mongol, China. Vertebrata Palasiatica 38: 237–240.

Wang, Y. 1995. A new primitive Chalicothere (Perissodactyla, Mammalia) from the early Eocene of Hubei, China. Vertebrata Palasiatica 33: 138–159.

Wang, Y., and J. Wang. 1997. A new brontothere from late middle Eocene of Qufu, Shandong. Vertebrata Palasiatica 35: 68–77.

Wang, Y., J. Guo, and J. Wang. 1999. A review of Chinese brontotheres. *In* Y. Wang and T. Deng (editors), Proceedings of the Seventh Annual Meeting of the Chinese Society of Vertebrate Paleontology: 139–145. Beijing: China Ocean Press.

Webb, S.D. 1969. Extinction-origination equilibria in late Cenozoic land mammals of North America. Evolution 23: 688–702.

Webb, S.D. 1977. A history of savanna vertebrates in the new world. Part I. North America. Annual Review of Ecology and Systematics 8: 355–380.

Webb, S.D. 1989. The fourth dimension in North American terrestrial mammal communities. Special Publication of the Museum of Texas Tech University 28: 181–203.

Webb, S.D., N.D. Opdyke. 1995. Global climatic influence on Cenozoic land mammal faunas. *In* Board on Earth Sciences and Resources (editor), Effects of past global change on life: 184–208. Washington: National Academy Press.

West, R.M. 1980. Middle Eocene large mammal assemblage with Tethyan affinities, Ganda Kas region, Pakistan. Journal of Paleontology 54: 508–533.

West, R.M., and M.R. Dawson. 1975. Eocene fossil mammals from the Sand Wash Basin, northwestern Moffat County, Colorado. Annals of the Carnegie Museum 45: 231–253.

Wheeler, Q.D., and N.I. Platnick. 2000. The phylogenetic species concept (*sensu* Wheeler and Platnick). *In* Q.D. Wheeler and R. Meier (editors), Species concepts in phylogenetic

theory: a debate: 55–69. New York: Columbia University Press.

White, T. 2003. Early hominids—diversity or distortion? Science 299: 1994–1997.

Wilkinson, M. 1994. Common cladistic information and its consensus representation: reduced Adams and reduced cladistic consensus trees and profiles. Systematic Biology 43: 343–368.

Wilkinson, M. 1995a. Coping with abundant missing entries in phylogenetic inference using parsimony. Systematic Biology 44: 501–514.

Wilkinson, M. 1995b. More on reduced consensus methods. Systematic Biology 44: 435–439.

Wilkinson, M. 2001. TAXEQ3: software and documentation. London: Department of Zoology: Natural History Museum.

Wilkinson, M. 2003. Missing entries and multiple trees: instability, relationships, and support in parsimony analysis. Journal of Vertebrate Paleontology 23: 311–323.

Wilson, J.A. 1977. Early Tertiary vertebrate faunas Big Bend area Trans-Pecos Texas: Brontotheriidae. Pearce-Sellards Series 25: 1–17.

Wood, H.E. 1937. Perissodactyl suborders. Journal of Mammalogy 18: 106.

Wood, H.E. 1938. Causal factors in shortening tooth series with age. Journal of Dental Research 17: 1–13.

Woodburne, M.O., and C.C., III Swisher. 1995. Land mammal high-resolution geochronology, intercontinental overland dispersals, sea level, climate, and vicariance. *In* W.A. Berggren, D.V. Kent, and M.-P. Aubry (editors), Geochronology, time scales, and global stratigraphic correlation. SEPM (Society of Economic Paleontologists and Mineralogists) Special Publication 54: 335–364.

Xu, Y.-X., and C.-S. Chiu. 1962. Early Tertiary mammalian fossils from Lunan, Yunnan. Vertebrata Palasiatica 6: 313–332.

Xu, Y., D. Yan, S. Zhou, Y. Zhong. 1979. Subdivision of the Red Beds of Li-Guan-Qiao Basin with description of fossil mammals therefrom [sic]. *In* Institute of Vertebrate Paleontology and Paleoanthropology and Nanking Institute of Geology and Paleontology (editors), Mesozoic and Cenozoic Red Beds of South China: 416–432. Beijing: Science Press.

Yanovskaya, N.M. 1953. First discovery of a brontothere in Russia. Doklady Akademiya Nauk SSSR 93: 147–149.

Yanovskaya, N.M. 1954. A new genus of Embolotheriinae from the Paleogene in Mongolia. Akademiya Nauk SSSR 55: 4–43.

Yanovskaya, N.M. 1957. First discovery of *Rhinotitan*, family Brontotheriidae in the USSR. Vertebrata Palasiatica 1: 187–192.

Yanovskaya, N.M. 1976. *Epimanteoceras amplus* sp. nov. (Mammalia, Perissodactyla, Brontotheriidae) from Mongolia. Trudy Sovmestnaya Sovestko-Mongoliskaia Paleontologicheskaia Ekspeditsiia 5: 38–46.

Yanovskaya, N.M. 1980. Brontoterii Mongolii (The Brontotheres of Mongolia). Trudy Sovmestnaya Sovestko-Mongoliskaia Paleontologicheskaia Ekspeditsiia 12: 1–220.

Ye, J. 1983. Mammalian fauna from the late Eocene of Ulan Shireh area, Inner Mongolia. Vertebrata Palasiatica 21: 109–118.

Zheng, J., Y. Tang, R. Zhai, S. Ding, and X. Huang. 1978. Early Tertiary strata of Lunan basin, Yunnan. Professional Papers of Stratigraphy and Paleontology 7: 22–29.

APPENDIX 1
Craniodental measurements for Brontotheriidae
(See Methods for measurement definitions. Units are in millimeters.)

	I1L	I1W	I2L	I2W	I3L	I3W	CL	P1L	P1W	P2L	P2W
Arctotitan honghoensis											
IVPP V3201	18.5	18.2	22.7	22.4	29	26.5	30.5	22.3	17.2	32.9	31.8
Dianotitan lunanensis											
VM 547			9.99	11.8				12	13.5	23.5	27.2
Diplacodon elatus											
AMNH 21887								15.3	13.5	22.0	23.6
CMNH 10200								18.2	12.4	22.4	26.2
CMNH 11828							14.4	14.4	12.0	20.8	23.5
CMNH 11879								16.0	13.6		
CMNH 11881							22.3	16.2	11.0	22.2	25.5
CMNH 11895					11.0	11.0				23.9	25.3
CMNH 2858	8.8	9.3	10.7	10.4	13.8	8.1	21.3			22.7	25.1
CMNH 2859	9.4	10.2	10.3	11.1	13.2	12.3	17.2	17.6	12.2	23.1	25.2
FMNH P14632					14.2	14.1	22.6	15.5	14.2	23.7	27.3
FMNH P14633	9.6	11.5	10.1	11.3	13.8	12.5	21.4	14.6	13.0	23.9	25.6
FMNH P14799								16.8	12.5	23.7	23.3
FMNH P15446	9.8	9.8	8.7	9.2	11.9	10.7	21.9	13.7	11.0	23.5	25.9
YPM 11180										20.8	
cf. *Diplacodon sp.*											
AMNH 117163					15.8	16.5	32.6			26.2	29
Dolichorhinus hyognathus											
AMNH 13164	15.2	12.3	16.0	13.3	17.8	14.0	16.0	18.2	11.1	23.5	19.3
AMNH 1837							16.2			18.7	16.7
AMNH 1843								17.5	11.0	20.0	18.8
AMNH 1850							24.3	16.8	9.7	21.4	19.7
AMNH 1851			17.4	14.0	19.2	15.3	17.4	16.4	10.7	22.4	18.8
AMNH 1852								16.2	11.2		15.7
CMNH 11071								17.1		19.5	
CMNH 11080							25.3	16.9	10.3	23.1	18.7
CMNH 11081							18.5			21.8	20.2
CMNH 2347										19.4	21.0
CMNH 9413			14.2	11.4	17.4			16.7		18.7	17.1
FMNH P12167	14.7	11.4	16.2	13.7			24.6	17.9	9.8	22.3	20.6
FMNH P12168							17.7	17.1		20.8	19.0
FMNH P12175							17.7	18.3	9.9	22.5	20.5

APPENDIX 1
(Continued)

	I1L	I1W	I2L	I2W	I3L	I3W	CL	P1L	P1W	P2L	P2W
FMNH P12193								14.6	8.8	18.8	18.7
FMNH P12205	11.6	8.9	12.1	7.8	15.4	12.2	18.7	16.1	8.4	16.8	16.3
FMNH P12215	11.5	12.7	12.7	10.8	14.5	12.7	19.2	14.7	8.7	16.4	16.3
FMNH PM3870					16.7	13.3	19.7	17.1	9.7	21.5	20.0
FMNH PM3873								19.7	10.2	24.5	19.3
LACM 128402										16.9	16.7
UCMP 31845							15.9	15.4	8.8	17.3	15.6
UCMP 31846			13.4	11.0	16.5		18.0				
USNM 6703								19.0	11.5	21.9	21.2
USNM uncataloged	11.0	11.2	13.5	10.4	13.1	13.0	19.1	17.1	9.7	21.1	19.5
Duchesneodus uintensis											
CMNH 11754	7.8	7.7	8.3	8.5			21.3	15.8	14.1	21.2	26.0
CMNH 11757			9.9	10.6			21.5	16.3	12.7	23.8	27.3
CMNH 11758								12.7	12.7	22.3	23.1
CMNH 11759	6.6	7.8	7.7	7.9			15.6	14.5	13.6	19.6	23.8
CMNH 11760								16.7	16.0		
CMNH 11766							20.6			20.2	26.2
CMNH 11767	7.3	8.3	6.7	8.2				16.1	12.7	21.5	24.5
CMNH 11815	6.1	6.4	7.3	6.7			16.1				
CMNH 11816										20.0	27.2
CMNH 9958			7.5	8.4			16.3	17.5	14.3	23.5	26.7
CMNH 9960								14.9	15.0	21.4	24.8
F:AM 108521										20.1	29.0
FMNH PM136	6.7	6.9					13.2	14.0	13.2	19.8	27.0
FMNH PM22410			12.2	13.8			23.6	19.6	17.2	28.4	32.2
FMNH PM396	9.7	12.0	10.5	12.4							
FMNH PM522			7.9	8.7			22.7				
LACM 128401			6.9	8.1			20.5				
Embolotherium andrewsi											
AMNH 26000								1.5	9.0		
AMNH 26003					12.2	13.1		18.1	16.8	32.8	32.1
AMNH 26009	9.2	10.1	8.4	9.1	8.2	8.3		20.6	12.8	25.5	28.7
AMNH 26010					9.5	9.1	10.7	17.1	14.5	27.5	31.7
IVPP V11959										27.2	31.8
Embolotherium grangeri											
AMNH 26002	16.8	13.8	14.2	12.6	14.3	15.1		15.4	12.0	25.2	28.6

APPENDIX 1
(Continued)

	I1L	I1W	I2L	I2W	I3L	I3W	CL	P1L	P1W	P2L	P2W
AMNH 26004										26.4	33.1
AMNH 26040			18.6		16.0			18.1	12.1		
Epimanteoceras amplus											
PIN 3109-41								17.9	13.8	28.5	33.2
Epimanteoceras formosus											
AMNH 21607									10.5	28.1	27.2
AMNH 21613	13.4	14.3	14.5	13.3	18.8	16.9	32.7	16.7	10.7	26.2	28.8
Eubrontotherium clarnoensis											
UCMP 126100			9.9	11.6			20.8	19.9	17.3	24.1	26.4
UCMP 126101										28.5	28.0
UCMP 126143										23.9	27.2
UCMP 126145							23.3				
UCMP 126160										24.5	27.8
PIN 3109-39	10.8	13.1	11.8	11.3			28.4			25.8	29.5
PIN 3109-90	9.38	12.7	10.4	10.4			25.3	20.9	13.4	25.7	24.9
Gnathotitan berkeyi											
AMNH 141231							36.4	22.2	15.0	35.4	39.0
AMNH 20121								23.3	13.3	34.4	36.2
Mesatirhinus junius											
AMNH 12184										16.9	17.2
AMNH 12202							15.5	13.6	8.2	16.6	15.6
AMNH 12206							15.8	15.6	8.3	15.5	15.6
AMNH 12686					13.1	12.1					
AMNH 1509								14.7	8.7	17.2	16.4
AMNH 1513							16.8	14.2	8.8	18.6	17.1
AMNH 1514	9.8	8.3	10.9	9.2	11.6	10.2	20.5	13.3	8.1	16.6	13.8
AMNH 1523								12.9	7.5	17.6	12.9
AMNH 1571			11.2	10.4	12.9	11.5	18.2	15.3	8.2	17.2	17.0
DMNH 8103							18.7			16.0	18.3
FMNH PM36045							17.4			16.5	15.2
FMNH PM54864								15.4	8.5	17.7	15.3
USNM 26116										16.7	12.0
USNM 26123										18.7	15.0
USNM 26136							18.1	11.5	6.3	15.0	14.0
YPM 11070										14.7	16.2

APPENDIX 1
(Continued)

	I1L	I1W	I2L	I2W	I3L	I3W	CL	P1L	P1W	P2L	P2W
YPM 11148								10.1	8.4	17.1	18.2
YPM 16420										16.1	17.6
YPM 16423										18.1	17.1
YPM PU10242										18.0	16.9
YPM PU25021										16.7	15.9
Metarhinus abbotti											
CMNH 2866								13.0	9.7	16.0	18.3
CMNH 3510					14.0	13.4		14.7	11.4	18.6	20.6
FMNH P12179	12.7	13.2	14.6	14.4	16.3	14.9		13.4	9.3	18.2	19.8
Metarhinus fluviatilis											
FMNH P12173							15.6			14.5	16.8
FMNH P12186							17.9	15.0	8.4	16.0	15.9
FMNH P12187							16.0	13.5	7.8	17.6	18.2
FMNH P12201								13.8	10.1		
FMNH PM1733							15.1	13.3	8.0	18.1	17.9
FMNH PM3935								13.4	7.6	16.5	16.9
FMNH PM44655										15.8	16.3
UCM 44939										16.3	17.6
UCMP 81278							18.2			18.1	18.6
YPM 13125							18.9	14.4	8.3	16.1	16.7
Metarhinus sp.											
AMNH 13166										16.5	16.2
AMNH 1500	10.2	9.4	10.9	9.0	11.9	9.3	19.4			14.6	15.4
AMNH 1946							14.8			16.1	18.6
CMNH 16736							16.2	13.8	10.1		
CMNH 3098							17.3	12.2	9.4	15.0	18.6
CMNH 9409								15.7	9.4	15.1	17.4
FMNH P12169					15.3	12.4		14.0	8.4	18.4	17.3
FMNH P12183					15.5	13.3	17.8			16.4	
FMNH PM1517										19.2	18.1
FMNH PM1730										15.8	17.0
FMNH PM1732								13.9	10.8	17.0	19.2
FMNH PM28345										15.1	1.8
FMNH PM28348			13.1	13.6			16.6	13.9	9.3	16.6	18.6
FMNH PM30388										15.6	18.1
FMNH PM30432										17.6	17.5

APPENDIX 1
(Continued)

	I1L	I1W	I2L	I2W	I3L	I3W	CL	P1L	P1W	P2L	P2W
FMNH PM35932								13.7	8.1	16.5	16.6
FMNH PM36054								12.5	9.1	14.2	18.0
LACM/CIT 2037							20.4	12.1	7.6	18.1	17.9
Metatelmatherium ultimum											
AMNH 2004	14.6	15.4	12.8	15.6	24.4	20.4	24.3	19.8	11.4	24.4	23.0
AMNH 2029	13.6	15.2	14.6	15.8	19.6	18.4		16.9	10.8	20.3	22.5
AMNH 2060			15.2	16.0	19.3	18.2	24.7	19.1	12.3	19.7	19.7
AMNH 26411			17.3	17.0	19.1	18.1	32.4	20.8	12.4	24.0	26.4
CMNH 2354										24.4	24.6
CMNH 2388	15.4	18.3	17.2	18.5	20.5	21.8	29.0	22.4	11.7	26.3	20.8
UCMP 81447							17.6	16.8	11.9	16.4	17.9
Metatitan primus											
AMNH 26101							28.6	17.1	14.8	32.6	30.8
Metatitan relictus											
AMNH 26391			7.7	8.0	13.6	13.1	25.0	13.0	6.7	24.1	33.5
AMNH 26397	7.8	8.2	7.1	9.1	11.8	14.6					
AMNH 26398	7.9	8.8	8.3	9.6	13.2	15.9	27.0	16.7	12.9	28.4	37.1
AMNH 26399					12.1	15.9	28.3	16.5	19.1	26.7	33.6
AMNH 26406					14.0	13.6		14.0	15.1	27.6	30.0
Metatitan khaitshinus											
PIN 3745-12							23	12.2	13	25.6	31.6
PIN 3745-1								17.3	14.2	26.9	27.6
PIN 3745-11							25.9			31.7	34.2
PIN 3745-3							22.2	18	16.3	28.9	32.1
PIN 3745-4								15.8	12.1	24	28.3
Microtitan mongoliensis											
AMNH 21611							15.9	10.6	5.4	14.0	16.1
Notiotitanops mississippiensis			8.4	10.5							
USNM 16646							24.2	16.4	12.9	21.5	23.9
Pachytitan ajax											
AMNH 21612					14.9	12.9				31.7	32.6
Parabrontops gobiensis											
AMNH 20354								16.5		27.5	33.4
AMNH 26020	9.4	10.6	11.0	10.6			20.6	17.7		24.5	24.9
Protembolotherium efremovi											
PIN 473-311											29.4

APPENDIX 1
(Continued)

	I1L	I1W	I2L	I2W	I3L	I3W	CL	P1L	P1W	P2L	P2W
Protitan grangeri											
AMNH 20103	12.2	13.4	14.1	15.4	17.7	17.2	21.5	16.5	12.6	22.3	25.4
AMNH 20108								14.1	1.1	22.6	22.8
AMNH 20113							20.5	16.4	11.1	25.5	24.3
AMNH 20114			12.6	12.4	14.7	14.6	19.8	18.0	12.5	26.1	25.4
AMNH 20125								18.0	11.9	28.9	27.9
AMNH 26104	13.4	16.1	17.7	17.3	23.6	19.9	30.4	17.3	10.7	26.4	28.0
Protitan minor											
AMNH 26416	12.3	12.3	14.8	15.2	19.7	16.4		16.8	10.4	23.8	23.5
AMNH 26417					22.3	20.6		17.1		22.9	22.7
Protitanops curryi											
LACM/CIT 1854	6.4	8.1	7.6	8.9			23.2	18.4		26.1	28.9
cf. *Protitanops curryi*											
LACM/CIT 2143	9.3	10.0	10.8	11.5			18.7			19.0	25.3
Protitanotherium emarginatum											
YPM PU11242	10.7	11.4	12.9	14.2	16.8	17.4	28.4				
TMM 41723-3							28.4	18.9	14.4	22.7	24.5
TMM 41723-6								17.2	13.2	22.4	25.4
TMM 41747-106					16.3	17.0	26.6	19.7	14.1	26.3	28.4
Protitanotherium koreanicum											
UMUT CV 6029							31.2				
UMUT CV 6035										24.4	24.4
Pygmaetitan panxianensis											
IVPP V6521					16	14.6		5.64	6.57		
IVPP V6523										12.5	13.3
IVPP V6526-1								9.84	4.85		
Qufutitan zhoui											
IVPP V8067			11.2	11.5	12.6	12.7	39.5	16.4	16.7	30.6	32.9
Rhinotitan andrewsi											
AMNH 20254	8.8	11.4	13.8	9.8	16.0	14.9		21.1	18.5	30.6	28.7
AMNH 20261					13.3	12.2	17.8	18.1	15.4	25.4	26.5
AMNH 20263			16.3	16.4	20.5	17.0	32.9	20.3	18.0	29.4	30.2
AMNH 20271			16.4	13.2	21.1	15.8	32.2	20.0	15.7	30.5	30.1
IVPP V3254-1	16.7	16.4	18.8	19.8	22.1	22.1				30.5	31.2
IVPP V3254-2	13.2	14.0	17.1	16.8	18.8	15.7		18.5	19.4	29.5	29.5
IVPP V3254-1	16.7	16.4	18.8	19.8	22.1	22.1				30.5	31.2

APPENDIX 1
(Continued)

	I1L	I1W	I2L	I2W	I3L	I3W	CL	P1L	P1W	P2L	P2W
IVPP V3254-2	13.2	14	17.1	16.8	18.8	15.7		18.5	19.4	29.5	29.5
PIN 2198-3								18.1	14.9	32.2	28.8
PIN 2198-5			16.1	15.5	17.5	15.7	31.5	18	18.2	28.3	26
PIN 7130-3										27.6	28.6
Rhinotitan kaiseni											
AMNH 20252	11.4	11.9	14.8	12.3	16.7	15.4	18.5				
AMNH 20257	13.7	14.0	13.1	15.9	17.9	17.8	17.1	16.5	11.2	27.6	27.1
FMNH P14048	15.6	14.5	16.6	14.9	18.2	16.5	20.7	17.3	17.1	26.1	26.0
Rhinotitan sp.											
AMNH 20256								19.8	15.4	30.6	28.1
AMNH 20270								19.8	17.1		
AMNH 20280								20.7	17.1	32.0	38.8
AMNH 21598								22.2	17.5	30.9	30.1
Sphenocoelus uintensis											
DMNH 2830			15.1	15.2	18.5	15.8	25.0	17.2	10.5	20.5	20.7
DMNH 29411							22.1	17.3	9.8	20.2	20.7
DMNH 479								16.0		20.0	
DMNH 484							21.5			21.4	20.1
DMNH 507							20.4	15.8	9.7	20.7	19.8
DMNH 509										18.3	19.5
DMNH 517	11.4	11.5	14.5	13.3	13.4	14.5				20.8	20.6
DMNH 541								17.4	11.4	22.5	24.6
cf. *Sphenocoelus uintensis*											
UCMP 81402								19.6	11.3	24.5	20.0
UCMP 81412										22.4	20.1
UCMP 81438										19.3	20.9
Sthenodectes incisivum											
CMNH 11437							25.1	15.7	11.5	20.7	24.5
CMNH 2398	20.8	21.4	26.6	24.5	27.7	23.0	31.1			25.3	22.5
FMNH P12165	19.8	19.4	21.2	21.8	22.6	21.7	27.0	16.4	12.1	20.9	24.3
Telmatherium validus											
AMNH 105429										19.4	20.2
AMNH 12678			14.7	13.4	13.7		22.8	18.3	9.4	21.7	19.5
AMNH 12683	10.9	10.5	12.7	11.3	17.1	13.1	24.6	14.5	8.9	19.3	16.6
AMNH 13165							27.0	14.4	8.5	21.0	
AMNH 1511							26.9	17.1	10.2	23.4	18.5

APPENDIX 1
(Continued)

	I1L	I1W	I2L	I2W	I3L	I3W	CL	P1L	P1W	P2L	P2W
AMNH 1532							31.3			24.2	18.4
AMNH 1570										21.9	21.8
AMNH 1587								17.2			
AMNH 2353								16.8	10.0	21.7	17.3
AMNH 2354							26.0	15.8	10.2	18.0	17.1
UCM 73736								16.0	13.9	18.5	21.7
USNM 13456	11.3	11.3			16.9	13.5	29.1	23.8	18.2	20.6	18.5
USNM 26119							22.5			19.7	17.9
USNM 26140								12.7	8.6		
USNM 26162										20.4	18.7
USNM 6700					12.4	10.3	31.0	16.1	9.8	21.2	18.5
YPM 16729										20.9	18.0
YPM 47288										23.3	23.4
YPM PU10027			13.2	12.6	17.4	15.3		15.6	8.7	21.4	18.8
YPM PU25022								18.6	11.1	24.2	
Wickia brevirhinus											
CMNH 11380										22.0	21.5
CMNH 11382	15.8	14.6	16.6	16.2	16.2	15.8	27.1	17.9	11.7	21.3	20.2
UCMP 81300	14.2	14.0	15.6	15.4	18.1	16.9	30.4	19.4	12.4	20.9	23.7

	P3L	P3W	P4L	P4W	M1L	M1W	M2L	M2W	M3L	M3W
Arctotitan honghoensis										
IVPP V3201	38.3	40								
Bunobrontops savegei										
NMMP-KU 0312									45.0	42.7
NMMP-KU 0313									38.3	40.9
NMMP-KU 0319							38.2	39.7		
UCMP 128391							40.7	43.1		
UCMP 128416							41.3	42.9		
UCMP 147045									45.2	44.5
Dianotitan lunanensis										
VM 547	31.3	35.5	33.1	42.6	43.3	51.9	60.1	61.7	68.3	63.5
VM 573			32.9	41			57.3	63.2	66.8	64.3
Diplacodon elatus										
AMNH 21887	25.0	29.6	27.3	36.6	40.0	41.6	42.2	51.6	64.2	53.4

APPENDIX 1
(Continued)

	P3L	P3W	P4L	P4W	M1L	M1W	M2L	M2W	M3L	M3W
CMNH 10200	28.8	31.1	35.4	36.8	42.4	44.1	64.3	55.0	71.4	61.4
CMNH 11819					44.3	46.8	49.8	52.8	69.1	60.9
CMNH 11828	24.8	27.8	29.2	35.1	39.7	43.1	59.6	51.6	67.1	59.8
CMNH 11879			29.6				56.1		63.7	
CMNH 11881	23.6	31.4	27.8	38.1	37.3	43.5	49.4		63.8	56.3
CMNH 11895	28.1	30.6	34.5	36.8	45.9	44.7	62.7	54.9	63.3	
CMNH 2858	29.7		30.3	37.4						
CMNH 2859	28.2	30.4	34.1	37.8	37.2	47.5	52.2	54.0	69.5	61.9
FMNH P14632	31.4	34.7	33.8	42.0	42.9	44.7	61.6	58.3	68.8	59.1
FMNH P14633	27.0	28.8	32.0	32.1	40.3	39.3	59.6	49.6	66.2	52.9
FMNH P14799	26.9	28.6	30.6	36.0	40.3	43.5	54.7	53.9	67.3	56.8
FMNH P15446	25.1	31.0	31.1	39.2	40.4	48.5	60.4	58.9	74.0	63.3
YPM 11180	25.1	30.0	32.4	36.1	44.5	43.9	63.7	56.1	71.9	59.4
cf. Diplacodon sp.										
AMNH 117163	30	35.8					57.4	56.6	58	57.4
Dolichorhinus hyognathus										
AMNH 13164	24.7	24.4	26.8	30.0	39.2	35.9	49.1	43.7	48.9	44.8
AMNH 1837	19.4	20.4	20.0	21.1	34.4		44.1	39.4	47.4	40.1
AMNH 1843			20.6	22.9					56.9	
AMNH 1845			25.3	32.1	39.8	35.7	52.1	43.7	54.3	43.3
AMNH 1850	21.4	23.8	22.3	26.4	39.3	32.8	45.2	37.8	45.2	37.8
AMNH 1851	24.0	24.3	26.7	30.1	38.0	38.3	44.9	45.1	54.2	47.8
AMNH 1852	21.6	21.7	25.3	29.5	37.3	35.6	48.4	42.6	47.9	43.4
CMNH 11071			23.7		31.3		37.4		50.6	
CMNH 11080	23.4	22.8	26.6	26.0	38.8	36.5		43.1		43.3
CMNH 11081	26.6	23.0	24.1	27.6	32.6	33.4	38.6	39.5	51.1	43.2
CMNH 11091										42.0
CMNH 2340	22.7	21.2	23.7	26.6	31.8	36.1	44.3	43.4	49.2	44.2
CMNH 2347	22.5	25.2	24.8	29.5						
CMNH 2865							44.3	47.0	47.8	46.3
CMNH 3096									43.6	37.3
CMNH 3117							43.3	37.0	45.3	38.1
CMNH 9413	21.8	23.5	22.7		32.0	32.4	43.3	39.0	45.8	38.3
FMNH P12167	23.0	22.7	27.3	29.3	41.4	38.7	50.9	46.4	57.3	47.8
FMNH P12168	21.8	23.2	23.0	25.9			40.8	39.5	41.8	38.3
FMNH P12175	23.7	26.0	25.8	30.4	42.0	39.0	51.0	45.9	50.7	44.7

APPENDIX 1
(Continued)

	P3L	P3W	P4L	P4W	M1L	M1W	M2L	M2W	M3L	M3W
FMNH P12182	25.3	24.8	26.8	29.7	34.4	35.2	48.6	42.6	52.4	44.8
FMNH P12193	20.6	23.5	21.2	27.8	32.5	32.9	40.1	39.9	47.6	43.2
FMNH P12200	24.5	21.3	23.1	27.7	37.9	31.1	46.7	40.6	50.6	39.8
FMNH P12205	17.8	19.6	19.6	26.0	29.9		35.0		42.7	
FMNH P12215	17.4	20.2	20.3	25.8	28.3	32.8	34.2	36.1	43.5	38.6
FMNH PM3870	22.4	23.8	24.7	29.8	36.2	32.8	41.8	39.8	45.3	41.2
FMNH PM3873	26.9	25.3	27.9	31.2	40.1		49.8	44.1	56.1	47.4
LACM 128402	19.4	21.3	20.4	26.2	29.5	31.6	37.5	35.4		
UCMP 31845	18.5	20.0	18.3	23.8	25.5	31.6	39.0	35.4	41.1	34.0
USNM 6703	23.7	24.0	23.2	29.0					53.0	
USNM uncataloged	20.6	22.5	22.6	27.0						
Duchesneodus uintensis										
AMNH 32604			32.4	38.4	46.0	49.4	61.9	60.6	69.0	64.1
CMNH 11754	28.8	30.7	33.4	40.2	47.9	43.7	61.8	56.4	69.2	64.2
CMNH 11757	27.2	31.2	34.9	39.8	49.1	44.3	66.7	56.1	70.4	
CMNH 11758	26.6	26.6			45.5	37.6				
CMNH 11759	24.2	31.0	29.5	36.4	34.3	39.8	51.2	51.0	57.5	52.5
CMNH 11760					46.6	42.5				
CMNH 11766	26.5	33.4	31.8	42.1	46.8	52.3	66.6	58.6	70.0	66.4
CMNH 11767	25.3	28.8	29.0	36.6	43.3	45.0	61.4	54.5	71.2	65.1
CMNH 11815									51.2	51.1
CMNH 11816	24.1	30.4	32.2	37.2			52.3	52.4	73.5	63.2
CMNH 9958	24.9	31.6								
CMNH 9960	25.2	30.5	33.2	35.2	49.3	42.0				
F:AM 108521	25.7	37.2	31.0	46.2	46.6		60.4	64.3	73.1	70.8
FMNH PM136	25.2	33.8	34.0	42.6	47.8	50.4	65.1	62.4	71.0	66.3
FMNH PM22410	34.9	39.4	44.7	47.8	54.0	53.7	71.7	65.6		
FMNH PM522	20.6	29.6		38.8			54.4	54.1	65.9	62.1
LACM 128401	24.8	31.5	29.4	38.2	37.3	42.7	54.7	50.9	68.4	61.8
Embolotherium andrewsi										
AMNH 21604							75.7		106.8	
AMNH 22114	40.5	42.7	44.7	52.0						
AMNH 26000				50.0	43.0	56.0			85.0	80.0
AMNH 26003	41.8	45.6	42.4	55.4	54.6	70.6	88.8	86.7	108.4	101.2
AMNH 26009	31.0	41.0	42.2	51.6	53.7	67.7	71.4	80.0	93.0	81.0
AMNH 26010	36.5	38.3	39.0	50.6	58.2	59.7	85.5	83.8	95.8	90.7

APPENDIX 1
(Continued)

	P3L	P3W	P4L	P4W	M1L	M1W	M2L	M2W	M3L	M3W
IVPP V11959	34.8	45.9	47.3	55.7			89.6	86.0	115.0	107.7
Embolotherium grangeri										
AMNH 21610							92.2			
AMNH 26002	32.4	39.3	37.7	44.6	59.3	61.3	85.8	75.3	96.8	82.4
AMNH 26004	34.8	43.4	41.7	52.5	63.2	61.5	89.3	77.9	104.8	84.9
AMNH 26040					70.6	59.8				
PIN 3110-52					46.7		63.2		81.5	
Epimanteoceras amplus										
PIN 3109-41	39.1	42.3	41.6	46.9	60.5	53.8	74.1	65.7	86.8	72.4
Epimanteoceras formosus										
AMNH 21607	30.7	33.3	32.8	39.2	51.9	37.8	65.9	48.9	69.8	52.8
AMNH 21613	26.6	32.8	28.6	36.5	38.6	44.1	54.0	53.0	70.4	52.0
Eubrontotherium clarnoensis										
UCMP 126100	27.8	32.7	41.4	43.9	54.8	56.5	71.0	62.4	76.1	66.8
UCMP 126101	28.3	36.4	40.0	48.1	59.4	58.5	77.5	74.7	86.4	80.4
UCMP 126143	27.7	31.7	37.7	41.4	54.6	53.4				
UCMP 126149			33.7	40.6						
UCMP 126150			37.9	42.6						
UCMP 126153							67.8	65.4		
UCMP 126154							62.0			
UCMP 126155								67.0		
UCMP 126157									70.6	73.4
UCMP 126158									73.2	
UCMP 126159									80.1	74.9
PIN 3109-39	30.7	37.4	31.5			58.6	61.4	73.1	81.4	69.9
PIN 3109-90	33.2	31.9	34.4	37.9	55.2	51.6	68.8	62.7	64.9	57.4
Fossendorhinus diploconus										
AMNH 1863	20.7	21.9	21.6	26.0	32.9	29.0	41.9	36.1	45.0	39.1
Gnathotitan berkeyi										
AMNH 141231	37.8	44.2	41.2	47.0	64.9	54.6	86.6	69.4	111.8	72.6
AMNH 20121	37.1	40.2	39.7	43.2	61.9	49.0	82.1	67.8	90.5	60.6
Mesatirhinus junius										
AMNH 12184	19.1	23.0	20.7	26.6	27.5	27.1			39.1	40.1
AMNH 12191								33.9	37.6	33.6
AMNH 12202	17.5	20.3	18.3	23.1	27.7	24.3	35.2	30.8	36.1	32.0
AMNH 12206	14.7	19.1	17.6	24.1						

APPENDIX 1
(Continued)

	P3L	P3W	P4L	P4W	M1L	M1W	M2L	M2W	M3L	M3W
AMNH 12686					22.6	23.7			31.6	29.1
AMNH 1509	18.7	20.6	20.0	25.9	26.8	26.0	37.8	32.5	36.1	32.8
AMNH 1513	19.8	20.8	19.7	25.0	28.4	27.3	34.0	32.9		
AMNH 1514	17.7	18.0	18.2	24.0	23.9		32.9	31.5	36.9	32.6
AMNH 1523	16.8	19.6	18.4	19.2	26.0			29.7	35.3	32.6
AMNH 1571	19.7	23.2	21.5	24.0	28.9	27.4	38.2	34.3	39.3	34.4
AMNH 1651a					24.0	25.5	36.0	33.2	42.2	
BMNH.M10471			18.0	23.0	26.0	27.0				
DMNH 29950							37.0	36.2	39.8	35.9
DMNH 8103	19.3	22.7	23.0	26.5	31.9	31.8	41.0	37.1	41.2	38.2
FMNH PM1676			21.0	24.3	29.2	28.5	38.7	34.8	43.5	36.1
FMNH PM36045	16.0	18.7	17.3	23.3					37.6	33.9
FMNH PM39945			24.3				34.7		39.0	
FMNH PM54864	19.3	20.1	21.4	25.4		30.1	39.0	32.2		
USNM 26116	16.2	18.4	18.7	23.8	25.5		32.2		38.8	
USNM 26123	17.4	20.1	18.3	23.3			33.0		38.3	
USNM 26136	14.9	18.4	18.0	20.3	23.3		31.0		34.7	
YPM 11070	15.8	18.9	16.1	21.8			30.1	31.3	35.9	33.0
YPM 11148	19.0	20.5	20.1	24.5					37.6	33.4
YPM 11149									32.8	30.6
YPM 16420	15.9	21.1			28.1	28.0	37.9		37.7	33.9
YPM 16423	19.0	20.3	18.6	25.7	29.2		37.3	34.8	38.3	33.3
YPM 16722			19.7	23.6	26.3	25.8	31.8	31.3	35.4	31.8
YPM PU10242	19.6	20.6	22.8	24.6	30.4	28.2	31.7	29.0		
YPM PU25021	16.3	18.7	18.3	23.3	23.7	28.2	32.6	34.8	38.4	34.9
Metarhinus abbotti										
CMNH 2866	21.3	23.2	23.9	2.8	24.1		36.1			
CMNH 3510	19.3	24.3	21.6	27.9	31.0	36.6	34.7	43.2	38.0	41.1
FMNH P12179	19.9	22.6	20.9	26.6	30.5	19.6	38.1	38.8	38.8	36.1
Metarhinus fluviatilis										
FMNH P12173	16.8	21.9	21.0	26.0					39.0	36.6
FMNH P12186	17.4	19.9	17.9	24.6			36.4	32.8	37.4	35.6
FMNH P12187	19.5	22.4	21.0	25.9	31.3	28.6	39.1	34.6	37.6	34.1
FMNH P12201					34.4	34.6	41.4	36.2		
FMNH PM1733	19.9	22.2	21.4	25.4	24.9	30.2	36.9	37.1	42.8	37.7
FMNH PM3935	17.3	20.6	20.0	24.8	26.0	26.8	36.6	32.9	39.0	34.7

APPENDIX 1
(Continued)

	P3L	P3W	P4L	P4W	M1L	M1W	M2L	M2W	M3L	M3W
FMNH PM44655	17.8	21.1	22.0	26.1			36.6	35.6	39.0	36.6
UCM 44939			20.0		28.8	29.2	39.6	36.1	43.5	36.1
UCMP 81278	19.6	22.8	21.3	25.8	29.2	31.2	36.8	36.1	40.0	37.5
YPM 13125	18.0	21.4	20.3	24.8					35.9	39.1
Metarhinus sp.										
AMNH 13166			21.0	26.1				37.7	42.5	36.7
AMNH 1500	14.8	19.7	18.6	23.9				34.4	38.0	37.1
AMNH 1864	17.3	20.9	20.9	24.5	30.6	30.7		37.7		
AMNH 1946	16.9	21.1	17.9	23.9	27.8	28.8	35.5	34.6	35.7	34.7
CMNH 16736	19.2	23.8	21.0	26.6		31.9	34.6	35.3	39.5	36.0
CMNH 3098	18.2	21.2	21.2	25.8	27.2	31.6	33.8	37.6	40.3	36.3
CMNH 9409	20.5	24.6	21.0	26.1	32.5	31.8	39.9	36.3	42.5	36.8
FMNH P12169	20.1	21.8	24.5	25.4	28.3	32.0	39.0	41.2	39.5	39.9
FMNH P12174					32.7	31.1				
FMNH P12183	17.6		17.6		24.7				39.2	
FMNH P12194							34.8	34.0	35.7	34.5
FMNH PM1517	20.0	22.3	21.6							
FMNH PM1519	15.3		16.6		23.3	36.1	35.4	35.7	39.0	36.0
FMNH PM1680			18.8		25.5					
FMNH PM1730	16.3	21.5	19.0	25.3	29.0	31.7				
FMNH PM1731	16.8	19.4		22.8				34.3	43.1	37.9
FMNH PM1732	18.9	22.1	21.6				38.9	37.3		38.5
FMNH PM28345	18.4	21.9	20.9	26.2	26.1	30.5	37.5	36.0	43.4	39.2
FMNH PM28348	18.8	21.4	21.2	26.2	32.1	32.2	39.7	37.1	39.5	34.9
FMNH PM30388	21.8						36.9	38.9		
FMNH PM30432	19.2	21.6	21.9	25.9	26.1	30.0	36.6	36.2	43.0	36.8
FMNH PM35932	18.3	20.4	21.5	26.2	29.9	28.7	40.5	34.0	41.6	33.6
FMNH PM36053			17.7	25.0						
FMNH PM36054	17.3	22.8	20.3	27.5		32.0			44.2	39.7
LACM/CIT 2037	21.6	22.3	23.4	25.4	29.2	30.0	37.6	34.9	43.7	40.1
UCMP 81285	19.1	21.8	21.5	21.5	31.8	31.7				
UCMP 95744					37.7	36.2	40.6	38.6		
UCMP 95809	19.3	22.0	21.9	25.5						
UCMP 95831							39.8	36.4		
"Metatelmatherium?" browni										
AMNH 20008									57.9	55

APPENDIX 1
(Continued)

	P3L	P3W	P4L	P4W	M1L	M1W	M2L	M2W	M3L	M3W
Metatelmatherium ultimum										
AMNH 2004	27.2	28.9	30.5	36.0	44.6	41.9	54.8	48.7	52.3	50.8
AMNH 2029	20.9	22.1	22.7	29.3						
AMNH 2033									42.0	43.9
AMNH 2060	22.6	28.5	28.1	35.1	40.0	43.0	51.7	53.9	56.8	54.8
AMNH 26411	22.8	30.1	29.9	34.3	43.7	43.3	51.1	53.4	51.4	57.4
CMNH 2354	28.3	30.6	30.6	36.2						
CMNH 2388	27.0	31.3	31.6	35.8			58.1	56.5	58.6	58.8
UCMP 81447	19.9	23.7	20.5	27.5					44.0	40.5
Metatitan primus										
AMNH 26101	37.8	39.2	37.8	45.3	55.0	51.8	74.1	60.9	85.9	67.3
Metatitan relictus										
AMNH 26391	28.7	37.7	35.4	42.9	51.7	52.2	63.3	58.9	83.9	63.4
AMNH 26395							72.3	66.1	78.9	75.0
AMNH 26396			38.5	43.7	57.4	54.5	70.2	68.8	77.6	69.1
AMNH 26397			30.9		51.0		76.1	65.1	83.9	71.0
AMNH 26398	35.0	49.9	39.1	54.0	53.3	63.1	78.1	69.5	88.8	71.2
AMNH 26399	33.8	41.0	41.4	47.1			69.6		83.0	68.0
AMNH 26406	32.1	35.0	36.3	43.9	56.1	49.1	77.9	59.7		
Metatitan khaitshinus										
PIN 3745-12	34.6	36.7	36.2	43.4	49.7	49.9	72.7	61.1	79.1	60.4
PIN 3745-1	30.3	35.2	33.1	42.6	51.1	47.1	65.7	55.6	73.8	60
PIN 3745-11	37	38	41	48.6	65.3	56.3	78.1	64.7	78.1	64.7
PIN 3745-3	38	38.6			58	55.2	86.9	63.4	90.2	66.8
PIN 3745-4	30.3	32.2	35.8	39.8	45.4	43.8		53.7		
Microtitan mongoliensis										
AMNH 21611	17.1	16.5	18.9	20.1	28.5	24.3	37.1	30.7	38.5	32.0
Nasamplus progressus										
AMNH 26014			48.0	60.5						
Notiotitanops mississippiensis										
USNM 16646	25.6	29.6	30.8	37.1	43.3	41.0	53.6	51.3	56.6	55.0
Pachytitan ajax										
AMNH 21612	35.2	41.7	40.6	48.3	53.1	57.0	77.2	65.4		
Parabrontops gobiensis										
AMNH 20354	30.4	39.9					67.6	65.5	83.0	72.7
AMNH 26020	28.1	33.2	35.1	42.0	45.3	44.5	63.1	54.0	71.3	60.1

APPENDIX 1
(Continued)

	P3L	P3W	P4L	P4W	M1L	M1W	M2L	M2W	M3L	M3W
Protembolotherium efremovi										
PIN 473-311	28	36	38.5	46.1	46.2	50	69.4	68.3	79	69
Protitan grangeri										
AMNH 20103	24.6	29.3	29.2	34.8	40.8	41.3	67.9		74.9	61.4
AMNH 20108	22.3	27.7	26.5	34.0	38.1		59.3	48.3	76.2	
AMNH 20113	27.8	31.1	28.8	34.9						
AMNH 20114	26.4	30.4	29.5	35.5	46.6	39.9	67.0	53.9	78.5	61.5
AMNH 20120					44.6	43.8	69.5	57.7	64.2	56.8
AMNH 20123	28.0	32.1	31.1	37.2	47.2	41.9	61.0	55.4		
AMNH 20125	31.6	35.9								
AMNH 26104	29.1	30.5	32.7	35.7	50.8	44.1	74.7	56.6	74.3	62.5
Protitan minor										
AMNH 26416	28.6	28.2	30.7	33.0	45.6	43.2	62.5	53.0	66.7	56.8
AMNH 26417	27.3	31.7	26.9	39.3	40.7	47.1	62.0	59.2	68.5	57.3
Protitanops curryi										
LACM/CIT 1854	28.7	37.7	32.3	45.5	48.9	50.3	64.9	64.2	75.5	69.0
cf. *Protitanops curryi*										
LACM/CIT 2007	37.0	45.9	49.1	55.7		66.4	82.5	68.6		
LACM/CIT 2143	24.9	35.9	30.9	40.6	42.1	45.3	54.8	54.7	66.9	65.3
Protitanotherium emarginatum										
TMM 41723-3	26.6	32.0	30.2	36.7	42.9	43.4	59.1	53.1	64.7	55.7
TMM 41723-6	28.1	30.5	30.3	36.7	44.7	40.8	58.0	49.6	62.8	54.4
TMM 41747-106	32.1	34.2		38.5	53.1	48.5	70.8	56.8	77.3	63.9
Protitanotherium koreanicum										
UMUT CV 6028			32.4	38	44.4	46.6	64.3	59		65.2
Pygmaetitan panxianensis										
IVPP V6521	12.4	16.5	13.9	20.3	19.2	22.2	28.6	29	30.3	31.2
IVPP V6522			17.1		23.4	25.5	28.9	28.2	32.3	29.9
Qufutitan zhoui										
IVPP V8067	34.2	40.9	38.3	48.4	52	52.6	73	64.6		65
Rhinotitan andrewsi										
AMNH 20254	34.2	35.5	41.2	43.3	55.2	46.3	71.2	61.2	79.2	74.2
AMNH 20261	31.6	33.4	37.3	39.6	51.1	49.2	64.3	62.0	70.1	64.1
AMNH 20263	35.1	35.9	40.7	45.0	57.6	54.8	73.5	64.4	83.2	69.0
AMNH 20271	35.9	37.8	40.7	44.9	54.9	50.4	76.8	64.4	84.9	74.5
IVPP V3254-1	33.3	36.3	38.8	49.6	53.6	50.8	69.5	64.5	87.4	74.4

APPENDIX 1
(Continued)

	P3L	P3W	P4L	P4W	M1L	M1W	M2L	M2W	M3L	M3W
IVPP V3254-2	37.1	35.4	44.2	44.3	57.2	61.0	67.1	61.3	82.2	72.0
IVPP V3254-1	33.3	36.3	38.8	49.6	53.6	50.8	69.5	64.5	87.4	74.4
IVPP V3254-2	37.1	35.4	44.2	44.3	52.2	51	67.1	61.3	82.2	72
PIN 2198-3	34.6	33			59.2	49.5	77.5	60.5		
PIN 2198-5	32.8	33.9	35.9	38.1	55.1	49.4	64.8	57.5	72	63
PIN 7130-3	34	35	39.5	42.1	51.1	51	67.7	62.5	83.2	69.4
Rhinotitan kaiseni										
AMNH 20252	25.3	33.6	29.6	40.5			57.9	61.2	68.0	68.1
AMNH 20257	32.9	33.9	35.2	43.4	52.9	52.0	52.9	59.0	71.4	67.0
FMNH P14048	30.0	32.3	34.7	39.6	48.3	43.5	62.9	56.5	72.8	59.7
Rhinotitan sp.										
AMNH 20256	35.2	39.0	40.4	45.4	58.2	47.0	73.4	65.6		64.2
AMNH 20270			39.3	46.2	62.7	54.0	75.8	66.0		
AMNH 20280		34.9			60.1	54.3				
AMNH 21598	33.5	36.3			62.5	55.3	82.1	63.6		
Sphenocoelus uintensis										
DMNH 2830	20.6	24.2	24.1	29.3	33.6	38.1	42.7	46.2	54.6	45.0
DMNH 29411	22.7	25.4	26.0	29.8	36.5	34.9	47.1	45.4	50.5	44.7
DMNH 479	19.0		23.0		33.0		42.0			
DMNH 484	22.5	23.5	24.9	27.1	35.4	32.3	45.6	40.1		
DMNH 507	21.6	24.8	24.7	28.2	32.5	34.6	48.5	43.8	50.5	40.5
DMNH 509	17.7	22.6	22.0							
DMNH 517	21.8	25.3	26.7	30.9	36.3	36.6				
DMNH 541	23.1	28.8	27.9		37.1	39.9	47.5	46.5	56.1	47.0
UCMP 81301			25.2	28.6	37.9	37.3	49.2	40.6	49.5	40.1
cf. *Sphenocoelus uintensis*										
DMNH 506							42.9	42.4	53.1	44.5
UCMP 81369								40.9		
UCMP 81402	24.0	26.1	28.1	30.5						
UCMP 81414	21.9	25.0								
UCMP 81422									46.2	43.8
UCMP 81438	19.0	25.2								
Sthenodectes incisivum										
CMNH 11437	26.4	31.1	25.0	34.9	36.0	44.0	48.0	52.1	51.4	51.2
CMNH 2398	25.4	31.1	28.9	38.1	45.6	48.8	55.9	42.6	53.4	47.7
CMNH 9928	29.0	35.0	30.2	34.4						

APPENDIX 1
(Continued)

	P3L	P3W	P4L	P4W	M1L	M1W	M2L	M2W	M3L	M3W
FMNH P12165	24.8	30.3	25.4	36.6	41.6	46.6	56.0	53.4	49.0	50.3
Telmatherium validus										
AMNH 105429	21.3	25.0	26.4	29.7	35.4	37.4	50.7	47.4	50.8	
AMNH 12194				28.1	29.5	32.1	43.0	41.9	45.3	42.3
AMNH 12204									36.5	
AMNH 12214									46.0	42.9
AMNH 12678	23.5	25.7	23.4	31.2			38.3	41.5	47.1	45.8
AMNH 12683	19.4	22.0	22.2	26.1	30.2		41.0	39.7	42.9	42.1
AMNH 13165	22.4	25.9	25.7	31.3	38.0		47.0		51.5	
AMNH 1511	23.9	24.8	23.8	28.1	29.0		40.9	40.4	45.7	42.6
AMNH 1532	21.8	25.1	25.1	29.0	35.5	36.1	46.8	44.5	50.2	46.7
AMNH 1570	20.0	26.3	22.8	29.7	33.0	36.1	46.1	43.4	47.4	46.0
AMNH 1587	23.1					34.6	42.0	43.3	58.4	45.4
AMNH 2353	21.0	17.3	23.5	29.5	31.1		43.7		44.1	
AMNH 2354	19.6	22.6	19.7	25.3	28.6	31.4	38.5	38.6	44.8	41.1
UCM 73736	20.8								46.2	46.7
USNM 13456	22.2	25.6	24.9	30.2	33.4		45.7		46.2	
USNM 26113					38.1	38.2	44.2	44.9		
USNM 26114					36.2		45.4			
USNM 26119	22.2	23.8	21.7	28.7	30.7	29.2	41.2	39.6	44.6	42.8
USNM 26140	19.8	24.1	21.0	21.7	29.7		43.7		48.0	
USNM 26162	21.3	25.6	24.2	29.3	31.9		44.2		48.7	
USNM 6700	21.2	24.5	25.5	25.6	32.5		43.7		46.3	
YPM 16415					34.5	36.5	41.0	40.9		
YPM 16729	20.4	21.7	21.8	28.5	32.4	32.4	42.0	40.0	44.5	43.4
YPM 47288	23.5	27.4	26.1	32.2	37.2	26.8	46.3	45.5	47.3	46.3
YPM PU10027	21.9	22.9	23.9	26.9	34.1	31.4	44.3	39.6	44.8	42.2
YPM PU25022	24.1	27.0	23.0	31.3	32.8	38.1	47.7	47.5	55.7	50.4
Wickia brevirhinus										
CMNH 11380	22.9	25.9	24.3	32.0			43.6	46.2	53.8	49.9
CMNH 11382	23.7	29.7	27.4	33.4	31.8	39.1	41.9	47.1	47.6	48.2
UCMP 81300	23.6	27.6	28.6	34.2	38.5	41.4	50.6	49.2	51.3	51.6

APPENDIX 1
(Continued)

	P2–P4	M1–M3	P2–M3	VL	MVL	SW
Dianotitan lunanensis						
VM 547	78.6	158.56	236.7	540	498	453
Diplacodon elatus						
AMNH 21887	73.7	149	222	550	488	340
CMNH 10200	82.5	170	245	570		
CMNH 11819		170				
CMNH 11828	75.7	157	230			
CMNH 11879				550		
CMNH 11881	74.5	140	215	585	500	340
CMNH 11895	81.1	160	240			
CMNH 2859	80.7	149	230			
FMNH P14632	79.7	170	240	580	510	395
FMNH P14633	76.8	152	229	607	528	353
FMNH P14799	78.7	157	233	570	520	380
FMNH P15446	83.7	160	245			
YPM 11180	76.1	172	240			
cf. *Diplacodon sp.*						
AMNH 117163				720		460
Dolichorhinus hyognathus						
AMNH 13164	65.2	128	194	540	460	256
AMNH 1837	56.0	121	171	465		
AMNH 1845		140				213
AMNH 1850	63.7	128	189	560	478	205
AMNH 1851	67.9	130	195	555	470	247
AMNH 1852	63.6	126	193			232
CMNH 11071	62.2	119	180	540	450	
CMNH 11080	63.6	134	200	550	447	
CMNH 11081	63.0	113	180	540	450	235
CMNH 11091		119				
CMNH 2340		119				
CMNH 2347	63.2	123	184			265
CMNH 2865		121				
CMNH 3096		95	152	460		
CMNH 9413	61.8	117	179	570	475	
FMNH P12167	68.5	134	201	585	495	284

APPENDIX 1
(Continued)

	P2–P4	M1–M3	P2–M3	VL	MVL	SW
FMNH P12168	61.6	103	168			134
FMNH P12175	69.1	131	200	550	450	250
FMNH P12182		126				
FMNH P12193	57.3	115	170			
FMNH P12200		121				210
FMNH P12205	53.0	104	154	520	450	225
FMNH P12215	53.1	106	158	520	440	235
FMNH PM3870	64.6	116	180	530	470	263
FMNH PM3873	71.6	135	200	582	500	258
LACM 128402	54.6		163	480	405	
UCMP 31845	55.6	108	162	440	383	
USNM 6703		124	195	570		200
USNM uncataloged	64.6					
Duchesneodus uintensis						
AMNH 32604		174		610	515	
CMNH 11754	82.0	179	268	530	510	355
CMNH 11757	81.3	190	260	550		
CMNH 11759	78.1	142	220	520	495	290
CMNH 11766	75.6	175	79			
CMNH 11767	76.8	160	240	545	530	415
CMNH 11815				470		390
CMNH 11816	76.6	155	185	550		
CMNH 9960	77.7					
F:AM 108521	77.2	173	252		535	
FMNH PM136	77.7	171	242	510	495	440
FMNH PM22410	115.6					
FMNH PM396	85.6	161	240	580		420
FMNH PM522				470		
LACM 128401	75.0	162	190	578	527	
Embolotherium andrewsi						
AMNH 21604						640
AMNH 26000		12		780		500
AMNH 26001						660
AMNH 26003	108.9	244	350	830	760	564
AMNH 26009	101.9	217	310	730		513
AMNH 26010	96.8	235	317	700	650	513

APPENDIX 1
(Continued)

	P2–P4	M1–M3	P2–M3	VL	MVL	SW
IVPP V11959	106.5	247	350	920	820	
PIN 2200-1				720		
Embolotherium grangeri						
AMNH 26002	92.0	205	295	755	650	589
AMNH 26004	107.3	230	333	830	720	640
PIN 3110-52		185.14				
Epimanteoceras amplus						
PIN 3109-41	101	216.24	315	720	663	453
Epimanteoceras formosus						
AMNH 21607	92.8	187	268			
AMNH 21613	77.9	158	236	690	588	395
Eubrontoherium clarnoensis						
UCMP 126100	89.6	190	275	645	580	410
UCMP 126101	89.2	187	274		600	
UCMP 126143	89.5					
PIN 3109-39	88.1	186.46	264	655	600	
PIN 3109-90	89.2	178.36	263.9	660	610	
Fossendorhinus diploconus						
AMNH 1863	55.7	111	160	450		195
Gnathotitan berkeyi						
AMNH 141231	113.3	245	350			
AMNH 20121	105.0	218	320			
Mesatirhinus junius						
AMNH 12184	54.6	95	148			
AMNH 12202	48.9	90	135		318	217
AMNH 12206	50.5		135			
AMNH 1509	54.4	96	146	395	350	195
AMNH 1513		88	134			
AMNH 1514	46.9	86	131			
AMNH 1523	51.7	87	137			
AMNH 1571	52.9	97	145			
AMNH 1651a		100				
BMNH.M10471		90	141			
DMNH 29950		95				
DMNH 8103	58.4	105	160			
FMNH PM1676		104				250

APPENDIX 1
(Continued)

	P2–P4	M1–M3	P2–M3	VL	MVL	SW
FMNH PM36045	48.8	90	135	430	364	223
FMNH PM54864	57.8					
USNM 26116	50.5	90	136	410		230
USNM 26136	47.7	82	128	372		196
YPM 11070	45.2	84	125			
YPM 11148	53.3	89	127		294	215
YPM 16420		97				
YPM 16423	53.1	95	146			
YPM 16722		90				
YPM PU10008	45.7	83	128			
YPM PU10242	56.7					
YPM PU25021	50.8	93	139			
Metarhinus abbotti						
CMNH 2866	56.5	101	159	426	360	222
CMNH 3510	55.9	102	151			
FMNH P12179	55.9	104	157	410	360	225
Metarhinus fluviatilis						
FMNH P12173	51.8	92	145	404	347	192
FMNH P12186	49.9	94	143	395	337	200
FMNH P12187	54.4	99	148	375	332	235
FMNH P12201				360	290	178
FMNH PM1733	54.6	99	154			
FMNH PM3935	50.9	97	146			
FMNH PM44655	52.9					230
UCM 44939	52.4	103	150	408	350	210
UCMP 81278	54.2	98	148			
YPM 13125	51.9	89	138	405	350	275
Metarhinus sp.						
AMNH 13166			163	395	347	240
AMNH 1500	47.8	87	134	350	290	207
AMNH 1946	48.3	87	134			
CMNH 16736	53.5	96				
CMNH 3098	51.4	99	148	413	345	247
CMNH 9409	55.5	104	162	400		
FMNH P12169	60.1	102	167	440	387	285
FMNH P12183	52.0	94	144	400		

APPENDIX 1
(Continued)

	P2–P4	M1–M3	P2–M3	VL	MVL	SW
FMNH P12194						245
FMNH PM1517	59.0					
FMNH PM1519		93				
FMNH PM1730	50.3					
FMNH PM1731						225
FMNH PM1732	55.0	104	160			
FMNH PM28345	51.9	105	152			
FMNH PM28348	53.9	102	152			
FMNH PM30388	51.3		151			
FMNH PM30432	57.6	100	158	420		250
FMNH PM35932	53.6	108	163	370		
FMNH PM36054	50.0	102				
LACM/CIT 2037	55.6	104	158			
Metatelmatherium ultimum						
AMNH 2004	75.5	138	210			
AMNH 2029	67.4		214	562		
AMNH 2060	70.6	130	202	500	400	300
AMNH 26411	71.0	133	210	570	468	325
CMNH 2339				570		
CMNH 2388	82.4	145	228			
UCMP 81447	56.3	111	169	475	390	255
YPM 14158			165			
Metatitan primus						
AMNH 26101	94.3	200	290			
Metatitan relictus						
AMNH 26391	82.1	180	270	635	594	465
AMNH 26395		198				
AMNH 26396	98.9	180	270	620		500
AMNH 26397		195		635	595	470
AMNH 26398	101.3	210	305	760	710	528
AMNH 26399	93.6	195	275	720	670	
AMNH 26406	99.6					
Metatitan khaitshinus						
PIN 3745-12	91.8	190.9	274.8		595	520
PIN 3745-1	86.2	174.67	100.7	600	565	440
PIN 3745-11	104	208.08	299.3	615	570	390

APPENDIX 1
(Continued)

	P2–P4	M1–M3	P2–M3	VL	MVL	SW
PIN 3745-3	102	210.45	303.4	620	612	447
PIN 3745-4	84.6					420
Microtitan mongoliensis						
AMNH 21611	48.3	96	139			
Notiotitanops mississippiensis						
USNM 16646	76.4	145		570		426
Pachytitan ajax						
AMNH 21612	104.4	210				
Parabrontops gobiensis						
AMNH 20354		220		600		
AMNH 26020	92.5	173	265			440
Protembolotherium efremovi						
PIN 3109-40					660	
PIN 473-311	88.4	192.83	274.9	715	665	530
Protitan grangeri						
AMNH 20103	80.6	169	240	711	600	447
AMNH 20113	83.2					
AMNH 20114	80.0	168	250			
AMNH 20120		162				
AMNH 26104	79.9	188	265	711	610	424
Protitan minor						
AMNH 26416	74.2	170	233	559	478	300
AMNH 26417	73.7	150	225			
Protitanops curryi						
LACM/CIT 1854	83.8	182	267	688	632	490
cf. *Protitanops curryi*						
LACM/CIT 2143	74.4	149	231			
Protitanotherium emarginatum						
TMM 41723-3	62.6	156	214	560		389
TMM 41723-6	72.6	146	217	650	560	395
TMM 41723-106	89.0	180	260	650	580	455
Pygmaetitan panxianensis						
IVPP V6521	36.4	75.61	107.2			
IVPP V6522		78.73				
Qufutitan zhoui						
IVPP V8067	102					

APPENDIX 1
(Continued)

	P2–P4	M1–M3	P2–M3	VL	MVL	SW
Rhinotitan andrewsi						
AMNH 20254	97.7	183	274	711	617	424
AMNH 20261	91.2	188	260	673	610	
AMNH 20263	98.9	188	280			
AMNH 20271	99.4	200	288	770	660	439
IVPP V3254-1	103.2	201	310			
IVPP V3254-2		203	330	790	665	
IVPP V3254-1	103	200.84	310			
IVPP V3254-2		202.72	330	790	665	
PIN 2198-5	99.4	174.25	280.9	710	614	
PIN 7130-3	95	200.97	297.3		647	
Rhinotitan kaiseni						
AMNH 20252	77.6	162	238	660	560	310
AMNH 20257	91.3	180	265	690	594	328
FMNH P14048	87.1	170	250	680	570	340
Rhinotitan sp.						
AMNH 20256	97.5	195	293			
AMNH 20270	96.9					
Sphenocoelus uintensis						
AMNH 1501						250
DMNH 2830	63.4	129	190	527	461	230
DMNH 29411	63.7	122	188		398	
DMNH 479		116		524		231
DMNH 484	67.8					
DMNH 507	64.0	119	185			
DMNH 517	65.1					
DMNH 541	75.3	135	206	565	208	230
UCMP 81301		128				
cf. *Sphenocoelus uintensis*						
UCMP 81402	65.6					
Sthenodectes incisivum						
CMNH 11437	66.8	127	190			
CMNH 2398	72.2	141	207	478	388	300
FMNH P12165	69.3	132	198	440	380	290
Telmatherium validus						
AMNH 12194		114				

APPENDIX 1
(Continued)

	P2–P4	M1–M3	P2–M3	VL	MVL	SW
AMNH 12678	65.9	105	174	495	409	235
AMNH 12683	59.9	105	162			
AMNH 13165	67.4	127	192			
AMNH 1511	66.1	110		460	387	290
AMNH 1532	67.9	124	195			
AMNH 1569	57.4	106	163	470	390	315
AMNH 1570	62.8	114	176			
AMNH 1587	67.4	115				
AMNH 2353	60.1	109	166			
AMNH 2354	56.4	104	156			
USNM 13456	65.3	115	184			
USNM 26119	62.0	113	172			
USNM 26140		111		480		
USNM 26162	67.8		185			
USNM 6700	64.2	120	197	515		342
YPM 16729	59.5	111	170			
YPM 47288	69.6	127	200			
YPM PU10027	83.4	111	170			
YPM PU25022	71.4	127	200			
Wickia brevirhinus						
CMNH 11380	69.4	123	198	520	440	360
CMNH 11382	68.9	119	187			
UCMP 81300	72.4	132	200	510	415	

	i1L	i1W	i2L	i2W	i3L	i3W	cL	p1L
Brachydiastematherium trans.								
AMNH 108188 c							33.6	20.5
Camp Margetts "taxon A"								
AMNH 26410	14.1	13.0	16.0	14.9	16.5	14.1		12.8
AMNH 26415			14.4	13.2	15.1	13.4	23.2	13.6
AMNH 26418					15.6	12.8		12.7
AMNH 26431							27.9	19.4
AMNH 26432							26.0	
Camp Margetts "taxon B"								
AMNH 26400	9.3	10.6	9.8	11.1			26.0	14.0

APPENDIX 1
(Continued)

	i1L	i1W	i2L	i2W	i3L	i3W	cL	p1L
Desmatotitan tukhumensis								
AMNH 21606	15.8	13.7	16.3	14.7	17.2	12.9	26.8	
Diplacodon elatus								
CMNH 11876					13.0	14.7		9.9
CMNH 11877							17.9	13.3
CMNH 11879	12.0	13.2	14.0		13.4		18.2	
CMNH 11967			113.4	14.8	13.5	12.4	23.6	12.0
CMNH 2859					12.4	12.2	15.8	14.7
FMNH P14634	10.3	11.5	11.6	13.4	12.3	12.3	20.3	12.6
FMNH P14640			12.4	13.7			25.0	11.5
Dolichorhinus hyognathus								
AMNH 13164	15.5	11.6	17.4	12.1	17.2	12.2	18.3	15.4
AMNH 1854			17.0	13.3	17.5	12.3	21.5	
AMNH 1856	16.2	11.6	18.0	12.5	16.3	12.2	19.3	15.9
AMNH 1857							17.3	14.8
AMNH 1858								13.0
CMNH 11071							20.2	15.0
FMNH P12200					14.6	11.6	19.1	
USNM 6702							22.6	16.5
YPU PU 10273	13.2	13.6	15.6	13.1	16.0	12.8	22.8	
Duchesneodus uintensis								
CMNH 11761			7.9	9.4	5.7	7.6	13.2	
CMNH 11809					8.8	11.4	18.0	
FMNH PM401	7.7	11.1	11.8	16.0	7.9	10.9		
Embolotherium andrewsi								
AMNH 26009	14.3	14.4	10.2	10.9		9.6	14.0	15.0
IVPP V11959			16.8	15.0	15.4	14.1	12.7	
Embolotherium grangeri								
AMNH 21600	17.6	17.6	17.1	14.7	14.2	14.9	15.0	
AMNH 26005	21.4	22.5	27.7	23.4	23.1	21.3	22.0	18.2
AMNH 26018			18.0	19.9			16.6	
AMNH 26040	22.4	16.7		16.4	19.9			15.5
AMNH 26132	15.7	17.9	18.8	23.0	17.4	17.7	20.5	
Eubrontotherium clarnoensis								
UCMP 126101							34.1	
UCMP 126102	8.0	12.3	11.2	15.0	8.5	10.4	33.2	15.9

APPENDIX 1
(Continued)

	i1L	i1W	i2L	i2W	i3L	i3W	cL	p1L
PIN 3109-91	7.9	10.1	10.4	12.9	9.2	10.2	22.3	13.8
Gnathotitan berkeyi								
AMNH 20106			18.3	10.9			21.2	18.4
AMNH 20107	21.1	16.2	21.1	17.7	21.3	15.6	29.0	18.1
AMNH 20115					24.2	20.9		18.9
Hyotitan thomsoni								
AMNH 26401	11.6	13.4	11.7	12.2	11.6	13.0	40.3	16.3
Mesatirhinus junius								
AMNH 13178							13.6	
AMNH 1520							15.1	10.3
AMNH 1551							16.4	
AMNH 1567							18.3	
AMNH 1575			10.7	10.3	10.9	8.7	14.4	
USNM 26116							17.7	
USNM 26148	10.5	10.5	11.2	10.4			15.3	
USNM 26151								
USNM 363884	12.0	8.7	11.4	9.0	10.7	10.8		
YPM 16732							16.7	
Metarhinus sp.								
AMNH 13179							19.8	11.5
AMNH 1859					12.9	11.7	15.3	13.8
AMNH 1946							16.4	9.9
AMNH 2059	9.8	10.5	11.3	11.3	11.5	10.7	14.9	9.4
CMNH 11924	10.3	11.0	12.6	11.4	12.7	9.9	19.3	10.9
CMNH 3133			11.2	13.1			22.1	11.6
CMNH 3142	10.5		11.6	11.4	11.6	10.8	12.4	7.6
CMNH 3371								12.6
CMNH 3842	9.7	10.1	11.9	11.2	12.4	10.6	16.8	11.6
DMNH 543								15.1
DMNH 544					11.3	9.8	15.7	12.0
DMNH 550	11.7	10.7						
FMNH P12178			14.4	13.2				12.9
FMNH P12183							18.4	
FMNH P12195					14.7	13.0	20.4	
FMNH PM1511							21.5	14.6
FMNH PM1715							20.7	13.0

APPENDIX 1
(Continued)

	i1L	i1W	i2L	i2W	i3L	i3W	cL	p1L
FMNH PM28001			12.6	12.2	12.7	10.8	19.4	10.5
FMNH PM28002			12.6	12.0	13.9	10.6	19.2	12.1
FMNH PM28004								11.8
FMNH PM28006							19.5	
FMNH PM28014								11.7
FMNH PM28342								12.4
FMNH PM28342								12.4
FMNH PM30422								12.1
FMNH PM30434								12.8
FMNH PM30435			12.8	12.3	13.5	10.4		11.4
FMNH PM35996			11.6	11.6	10.8	10.9		
UCMP 81273							16.0	11.8
YPM 16834	9.1	8.6	9.5	9.2	9.3	7.7	13.9	
Metatelmatherium ultimum								
AMNH 26411	11.8	13.3	13.2	15.3	14.6	13.0	26.4	16.8
Metatitan primus								
AMNH 26101	9.7	9.9	11.1	13.9	10.7	11.2	29.3	
AMNH 26102							27.0	
Metatitan relictus								
AMNH 26391	9.4	11.0	11.1	11.0	10.8	10.6	23.2	
AMNH 26402	9.1	10.3	11.0	11.6	10.4	10.0	26.0	12.6
AMNH 26404	9.4	10.8	10.3	11.5	11.8	9.5		
AMNH 26405							24.9	
AMNH 26427					11.0	12.8	27.4	13.1
Metatitan khaitshinus								
PIN 3745-31	10.5	12.6	10.5	12.9	13.4	13.3	25.0	
cf. *Parabrontops gobiensis*								
AMNH 26019							20.0	14.0
AMNH 26021								11.8
AMNH 26131	9.8	12.9	12.4	9.4	8.9	11.5	32.1	13.3
Pollyosbornia altidens								
AMNH 2025							33.6	19.0
Protitan grangeri								
AMNH 20103	14.4	14.3	15.9	15.6	18.3	14.5	20.0	13.8
AMNH 20104	17.1	16.7	19.6	17.9	21.2	16.0	28.3	14.0
AMNH 20109							17.9	13.2

APPENDIX 1
(Continued)

	i1L	i1W	i2L	i2W	i3L	i3W	cL	p1L
AMNH 20112			13.6	12.6		13.5	22.0	
AMNH 26421					18.1	17.1		13.7
cf. *Protitan minor*								
AMNH 26419	15.5	12.3	15.2	14.6	14.8	11.9	20.5	12.7
"Protitan?" cingulatus								
AMNH 20110	13.9	14.8	14.8	15.2	14.9	13.2	21.5	13.0
AMNH 26403								11.2
AMNH 26412								11.8
Protitanotherium emarginatum								
AMNH 2501							32.2	
YPM 11146	14.1	14.5	15.1	17.5	14.9	14.5	30.2	19.1
YPM PU11242	12.0	14.1	14.6	18.2	13.5	13.2	31.8	16.6
Protitanotherium koreanicum								
UMUT CV29047					13.9	12.6		
Pygmaetitan panxianensis								
IVPP V6523	11.2	10.8	11.7	11.3	14.7	10.4		
Rhinotitan andrewsi								
IVPP V3245-1	18.1	19.4	21.0	26.7	19.4	17.4	33.2	
Rhinotitan kaiseni								
AMNH 20252	9.3	15.2	16.2	20.5	16.6	15.5	18.8	12.8
FMNH P14048	15.6	17.7	18.0	20.8	19.1	17.3	21.9	16.6
Rhinotitan sp.								
AMNH 20256	16.6	18.1	20.0	20.8				15.1
AMNH 20262	15.3	13.5	18.1	18.7	20.0	22.5		8.1
AMNH 20269	14.7	17.3	18.0	22.6			38.0	18.1
AMNH 20272					18.4	20.0	28.7	
AMNH 21603	16.3	17.3	19.8	22.8	18.5	17.1		15.8
AMNH 21605		9.7			16.7			
Sphenocoelus uintensis								
DMNH 14219	13.7	13.1	14.0	12.8	14.1	11.3	18.8	12.9
DMNH 2830		12.9	14.9	13.8	17.4	13.8	22.0	12.9
UCMP 81443	16.7	14.2	16.2	13.8	15.8		19.5	13.9
cf. *Sphenocoelus uintensis*								
DMNH 504								14.0
DMNH 505							20.9	
UCMP 81440	15.4	12.7						

APPENDIX 1
(Continued)

	i1L	i1W	i2L	i2W	i3L	i3W	cL	p1L
UCMP 81462					19.3	16.0		
Sthenodectes incisivum								
CMNH 11437	14.9	18.4	17.8	22.8	10.4	20.5	24.6	17.2
FMNH P12166	10.9	13.5	12.9	17.6	16.8		18.2	16.0
YPM 16883	17.1	13.4	16.5	13.6	17.9	13.0	20.2	14.7
Pollyosbornia altidens								
AMNH 2025							33.6	19.0
Telmatherium validus								
AMNH 12193							25.1	
AMNH 12204							23.0	
AMNH 13176								14.1
AMNH 1560					14.5	10.8	18.3	12.7
AMNH 1566							22.0	12.3
FMNH PM2328	12.4	13.3	14.1	13.7	13.7	14.2	24.3	15.0
FMNH PM55576	10.6	11.8	14.2	13.7	14.9	12.3	21.0	14.1
UCM 69355	12.9	12.1	13.1	11.6	14.0	13.5		12.0
USNM 12836							25.4	
USNM 26121			13.6	12.7	14.2	10.7	25.2	12.7
USNM 26302			10.1	11.1	13.3	11.3	23.3	11.7
YPM PU16103							26.6	14.3
Wicki brevirhinus								
CMNH 11382		13.4	14.7	15.8	13.3	13.8	24.2	15.5

	p1W	p2L	p2W	p3L	p3W	p4L	p4W	m1L
Acrotitan ulanshirehensis								
IVPP V6686				22.5	15.3	22.3	17.5	
Brachydiastematherium trans.								
AMNH 108188 (cast of type)	15.5	28.0	21.5	32.1	26.5	39.5	31.5	53.4
Camp Margetts "taxon A"								
AMNH 26408		23.3	13.9	26.8	21.4	30.1	20.6	41.0
AMNH 26410	8.7	23.1	13.9	24.7	15.2	26.8	19.1	36.6
AMNH 26415	8.5	20.2	13.0	20.9	15.6	24.9	18.2	40.3
AMNH 26418	8.1	22.6	12.2	24.7	14.5	28.0	16.8	40.7
AMNH 26430								41.9
AMNH 26431	8.6	23.5	15.5	22.2	20.3	30.2	21.3	

APPENDIX 1
(Continued)

	p1W	p2L	p2W	p3L	p3W	p4L	p4W	m1L
AMNH 26432	8.7					26.8	18.9	35.1
Camp Margetts "taxon B"								
AMNH 26400	9.9	26.4	17.7	30.2	22.7	31.7	25.1	44.8
Camp Margetts "taxon C"								
AMNH 26425						29.1	41.7	26.3
Desmatotitan tukhumensis								
AMNH 21606		25.2		25.6	17.8	25.3	19.6	35.3
Diplacodon elatus								
CMNH 11876	9.6	24.0	15.3	24.9	17.9	28.8	22.3	41.3
CMNH 11877	9.0	23.1	14.7	27.7	17.5	31.6	21.5	44.3
CMNH 11879				25.0		28.3		
CMNH 11967	8.9	22.9	14.2	24.1	17.6	28.6	21.5	42.3
CMNH 2859	9.2	22.7	13.7	23.4	17.8	29.3	17.5	37.3
FMNH P14634	8.9	18.9	13.4	21.2	14.5	27.7	19.1	35.1
FMNH P14638		23.4	14.1	22.8	16.6	28.2	20.3	36.2
FMNH P14640	11.5	23.1	15.3	25.6	17.7	28.4	19.8	35.3
Dolichorhinus hyognathus								
AMNH 13164	9.4	22.6	12.4	23.6	15.6	25.7	17.9	35.5
AMNH 1836		20.2		20.6	13.6	22.6	16.7	34.3
AMNH 1840		21.7	11.8	20.6	14.1	21.8	16.8	31.2
AMNH 1854		23.5	11.8	24.2	15.4	24.9	17.9	34.3
AMNH 1856	12.8	24.0	12.4	22.7	15.6	24.6	17.9	36.6
AMNH 1857	8.6	22.4	11.7	20.8	14.3	23.4	16.8	28.2
AMNH 1858	7.7							18.4
CMNH 11071		18.6				22.1		32.0
CMNH 11092		21.9	12.8	20.3	14.2	23.0	17.8	32.4
FMNH PM12167		22.2		24.4		26.8		34.6
FMNH PM12200		22.7	10.5	22.3	12.9	25.0	16.4	31.6
USNM 6702	12.3	24.3		24.9	14.2	26.7	18.6	34.8
YPU PU 10273		24.3	12.0					
Duchesneodus uintensis								
CMNH 11761		20.5	12.9	21.1	16.7	24.7	19.8	32.2
CMNH 11809		21.2	15.1	23.8	20.4	30.7	23.1	33.2
FMNH PM163	12.1	18.7	12.9	25.0	18.9	32.9	25.1	38.6
FMNH PM401								52.2
Embolotherium andrewsi								

APPENDIX 1
(Continued)

	p1W	p2L	p2W	p3L	p3W	p4L	p4W	m1L
AMNH 26006		31.6	18.0	38.0	23.4	42.6	31.4	61.9
AMNH 26007		30.5	18.3	35.8	25.9	42.3	33.1	55.1
AMNH 26008		32.6	19.8	38.3	27.4	46.1	35.6	71.7
AMNH 26009	11.1	28.8	18.7	27.5	24.1	38.1	31.9	51.0
AMNH 26011				34.8	25.3	43.0	29.9	
IVPP V11959		33.2	21.9	45.3	29.3	48.6	32.7	60.3
Embolotherium grangeri								
AMNH 21600		24.3	16.5	31.2	23.9	36.2	29.7	49.5
AMNH 26005	11.7	33.0	21.9	36.0	28.9	40.9	35.5	55.5
AMNH 26018						40.8	30.4	51.2
AMNH 26040	8.9							53.2
AMNH 26132		26.6	20.3	31.2	26.7	37.7	27.9	46.5
Eubrontotherium clarnoensis								
UCMP 126101				26.0	17.6	28.7	21.1	
UCMP 126102	11.0	24.5	15.0	30.5	18.8	35.4	25.1	50.6
UCMP 126161		27.3	16.3	27.7	19.1	34.9	25.9	46.5
UCMP 126162				28.1	17.8	33.3	23.4	50.2
PIN 3109-91	10.1	23.6	13.9	27.9	17.6	34.2	24.5	44.9
Gnathotitan berkeyi								
AMNH 20106	11.0	29.7	17.2	32.9	20.6	34.6	24.2	52.8
AMNH 20107	12.2	33.2	18.8	35.3	24.1	40.4	26.5	55.0
MNH 20115	13.0							
Hyotitan thomsoni								
AMNH 26401	11.8	29.6	20.6	34.7	24.9	38.9	29.4	49.8
Mesatirhinus junius								
AMNH 12191		19.3		18.8	11.6	19.3	13.3	24.9
AMNH 12199				17.8	10.6	18.2	12.6	22.3
AMNH 13178		18.5	10.5			19.5	13.8	25.5
AMNH 1512		18.0	9.4	18.7	10.7	19.5	12.4	25.8
AMNH 1520	6.5	17.9	9.1	17.4	10.2	16.8	12.6	23.3
AMNH 1551		18.1	8.7	16.5	10.4	17.9	12.1	22.9
AMNH 1567		18.7	9.4	17.5	11.6	18.8	14.2	24.7
AMNH 1575		16.2	10.7	15.8		17.6		21.5
AMNH 1577		19.1	9.2	17.1	10.0	17.9	13.7	23.8
ANSP 319						16.9	11.8	
DMNH 9687				17.9		18.4	13.9	26.2

APPENDIX 1
(Continued)

	p1W	p2L	p2W	p3L	p3W	p4L	p4W	m1L
FMNH PM36045		18.1	9.4	16.7	11.2	18.2	14.4	23.9
FMNH PM39945						19.3		
USNM 26111		20.1	10.7	19.2	11.9	21.0	13.2	
USNM 26116		19.1		16.3	10.9	18.8	14.7	22.6
USNM 26148		19.4				17.5	12.3	19.4
USNM 26151				16.1	9.5	17.5	12.2	25.4
USNM 363884								27.7
YPM 16421						16.0	11.6	21.1
YPM 16725				17.8	11.7	18.7	13.4	25.8
YPM 16732		17.9	8.6	16.5	10.9	18.8	13.2	24.1
YPM PU10184				17.5	12.4	19.4	13.9	26.2
YPM PU25021				17.4	10.5	19.5	13.7	
Metarhinus fluviatilis								
YPM 13125		18.7	12.4	21.5				
Metarhinus sp.								
AMNH 13179	8.4	17.0	11.5	16.2	14.2	20.5	17.0	24.4
AMNH 1859	9.0	19.8	10.6	20.7	13.8	23.1	16.5	29.5
AMNH 1865				14.5	10.9	16.8	11.8	25.3
AMNH 1946	6.5	15.5	10.2	16.9	12.9	19.2	14.5	
AMNH 2059	6.6	16.1	10.8	17.2	12.2	19.1	14.1	25.9
CMNH 11924	6.7	14.7	10.0	16.5	11.1	19.0	13.4	25.6
CMNH 3125				15.2	12.1	17.1	12.2	24.0
CMNH 3133	7.9	19.8	12.1	17.5	14.2	20.0	15.9	26.2
CMNH 3142	6.6	14.1	10.1	15.5	11.8	17.7	13.1	23.1
CMNH 3371	9.0	18.0	11.8	18.1	14.6	21.3	15.9	28.5
CMNH 3842	8.4	17.6	10.8	17.0	13.9	20.7	16.1	24.6
DMNH 543	8.5	15.9		18.2		18.9		25.9
DMNH 544	7.7	18.9	11.1	19.2	14.0	18.2	15.6	28.0
DMNH 550		17.9	12.2	20.4	14.1	22.1	16.0	28.7
FMNH P12178	9.1	17.6	12.0	18.9	14.7	20.8	16.8	25.4
FMNH P12178		18.5	10.1	18.9	13.7	21.6	16.1	27.7
MNH P12183		18.7		18.7		18.5		25.5
FMNH P12190						19.5	16.4	25.9
FMNH P12195		18.7	11.9	18.0	14.4	21.5	15.4	26.5
FMNH PM1511	11.3	21.3	13.6	22.5	16.7	25.9	16.4	29.9
FMNH PM1675								27.1

APPENDIX 1
(Continued)

	p1W	p2L	p2W	p3L	p3W	p4L	p4W	m1L
FMNH PM1715	7.6	21.2	12.6	19.6	14.5	22.3	27.0	
FMNH PM1734		18.4	11.0	18.3	13.4	20.2	15.5	26.8
FMNH PM28001	8.0	17.7	11.6	19.5	14.1	20.8	14.3	28.7
FMNH PM28002	8.7	17.5	11.5	17.6	15.6	20.0	17.0	28.9
FMNH PM28003		16.7	9.8	18.3	13.9	18.3	16.2	27.9
FMNH PM28004	7.8	18.2	12.1	18.3	14.4	21.6	17.7	28.0
FMNH PM28006		19.2	11.7	17.8	14.5	22.1	17.1	24.4
FMNH PM28014	7.6							
FMNH PM28342	8.4	18.3	11.0	17.7	14.2	19.3	15.9	29.0
FMNH PM28343		18.8	11.2	19.5	14.7	22.4	16.2	28.7
FMNH PM28344		18.3	11.2	19.4	14.3	19.6	17.7	
FMNH PM28359		17.8	11.0	16.6	13.3	22.1	16.8	
FMNH PM30422	8.3	18.5	13.4	19.1	16.6	24.6	20.3	27.3
FMNH PM30434	7.7							
FMNH PM30435	8.3	15.2	10.7	16.7		18.6	15.7	29.1
FMNH PM35933		17.6	12.4	17.7	15.1	20.1	17.7	24.6
FMNH PM35970		17.4	10.1	17.1	13.4	21.6	16.3	25.3
FMNH PM35996		16.9	11.0	16.7	13.9	18.5	15.6	23.7
FMNH PM39947				17.9		18.8	12.8	27.0
UCMP 113182				15.6		18.4	12.6	23.7
UCMP 113189		18.3	10.0					
UCMP 113201								28.4
UCMP 81273	8.2	19.0	10.6	21.1	15.0	21.7	18.0	28.6
UCMP 95780								25.0
UCMP 95841		18.3	9.7	11.3				
YPM 16834		16.4	8.2	14.3	8.8	17.1	11.9	26.7
YPM PU11284						21.0	13.9	26.5
"Metatelmatherium?" browni								
AMNH 20016						26.3	17.3	33.2
AMNH 20022								36.9
Metatelmatherium parvum								
AMNH 20168				21.5	14.1	22.7	16.6	
Metatelmatherium ultimum								
AMNH 2033		21.7	14.0	23.7	16.2	27.1	19.6	38.4
AMNH 2060						28.0	21.9	39.4
AMNH 26411	11.1	25.0	14.7	24.8	18.5	28.2	20.7	38.1

APPENDIX 1
(Continued)

	p1W	p2L	p2W	p3L	p3W	p4L	p4W	m1L
Metatitan primus								
AMNH 26101		26.4	18.8	30.7	25.0	35.3	29.3	49.3
AMNH 26102								48.8
Metatitan relictus								
AMNH 26391				29.0	21.4	33.6	24.2	43.9
AMNH 26402	9.6	25.8	16.5	28.5	20.8	33.5	25.0	46.8
MNH 26404		29.9	16.7	31.2	23.5	40.9	26.8	
MNH 26405					20.9	34.0		42.0
AMNH 26407		26.3	19.2	28.2	24.6	32.9	29.1	37.7
AMNH 26420				30.5	27.0	40.1	31.2	53.2
AMNH 26427	10.5	23.4	17.6					51.2
AMNH 26429								51.1
Metatitan khaitshinus								
PIN 3745-31		28.6	20.2	32.1	26.2	38.4	25.0	53.1
Microtitan mongoliensis								
AMNH 22099		16.0	7.6	16.2	9.1	17.9	10.6	25.2
AMNH 20167						18.4	10.8	24.2
Notiotitanops mississipp.								
USNM 16646				26.1	18.7	28.6	23.0	37.9
cf. *Parabrontops gobiensis*								
AMNH 26019	10.6	25.0	14.9	27.1	18.5	32.5	22.0	44.6
AMNH 26021	9.4	25.9	15.4	28.9	21.5	32.2	25.5	46.3
AMNH 26131	10.0	27.8	17.4	31.3	22.0	32.5	24.2	52.4
Pollyosbornia altidens								
AMNH 2025	12.5	27.9	15.0	29.0	18.2	31.2	23.6	49.2
Protitan grangeri								
AMNH 19179		27.6	16.7	29.1	20.7			57.7
AMNH 20103	8.9	25.0	13.4	27.0	14.5	28.4	20.0	40.4
AMNH 20104	9.7	27.8	14.4	29.1	18.0	33.0	22.9	45.7
AMNH 20109	7.8	26.0	11.8	26.8	13.8	29.0	18.6	39.8
AMNH 20111								41.2
AMNH 20112		27.3	18.1	31.8	21.6	34.5	23.6	48.9
AMNH 20119						30.9	22.7	40.7
AMNH 20126				27.0	16.8	27.6	19.9	40.5
AMNH 26421	8.9	23.2	14.4	24.0	16.9	27.2	21.8	41.5
cf. *Protitan minor*								

APPENDIX 1
(Continued)

	p1W	p2L	p2W	p3L	p3W	p4L	p4W	m1L
AMNH 26419		22.9	13.7	22.8	16.2	31.1	20.0	
"Protitan?" cingulatus								
AMNH 20110	10.6	28.4	17.9	33.4	21.6	34.4	24.7	49.5
AMNH 26403	9.6	25.4	17.4		18.6	30.8	23.8	40.2
AMNH 26412	9.8	24.2	17.1	24.4	20.6	29.6	26.0	37.5
Protitanops curryi								
CIT 1854								44.6
Protitanotherium emarginatum								
AMNH 2501		27.8	16.3	27.7	20.6	33.9	22.3	54.4
YPM 11146	10.7	27.2	16.1	28.2	19.8	36.4	21.9	
YPM PU11242	10.2	27.5	16.8	26.7	18.5	33.7	23.6	47.4
Protitanotherium koreanicum								
MUT CV6047								57.6
Rhinotitan andrewsi								
PIN 2198-2		30.2	18.3	32.3	22.3	36.5	27.0	51.3
IVPP V3254-1		31.2	21.0	31.4	26.4	36.7	30.2	49.7
Rhinotitan kaiseni								
AMNH 20252	9.5	26.6	17.3	27.9	21.2	30.2	26.3	39.6
FMNH P14048	12.2	26.1	16.4	29.0	19.6	31.9	23.5	46.9
Rhinotitan sp.								
AMNH 18653		27.9	16.6	31.2	21.9	30.9	25.2	48.2
AMNH 20251			18.7	31.8	24.1	38.2	27.8	51.4
AMNH 20256	10.0	30.3	16.9	32.7	22.2	36.5	25.1	52.7
AMNH 20262	12.4	29.6	19.0	32.2	22.4	37.1	25.8	52.5
AMNH 20269	11.6							
AMNH 20272		27.4	16.2	29.9	21.4	34.0	27.1	47.1
AMNH 20273		31.8	17.7	31.3	22.4	36.7	25.4	48.7
Rhinotitan orientalis								
PIN 858-84				29.1	20.9			
Rhinotitan quadridens								
IVPP V2651		28.0	15.3	34.8	26.0	34.8	26.8	51.8
Sphenocoelus uintensis								
AMNH 21603	2.0	29.2	18.5	31.2	21.9	34.0	25.0	49.4
AMNH 21605		23.4			19.9	37.6	27.5	50.1
DMNH 14219	9.3	21.8	12.2	20.5	14.4	24.3	16.4	32.0
DMNH 2830	8.1	22.3	13.1	21.6	13.9	23.0	17.3	32.3

APPENDIX 1
(Continued)

	p1W	p2L	p2W	p3L	p3W	p4L	p4W	m1L
DMNH 542		21.0	13.9	23.0	17.7	26.2	20.8	
UCMP 81281		22.8	12.4	23.3	14.3	25.1	16.7	32.2
UCMP 81443	8.5	23.0	12.2	22.9	14.5	26.0	17.3	30.8
cf. *Sphenocoelus uintensis*								
DMNH 2584		23.6	12.2	23.7	16.9	25.0	18.9	32.0
DMNH 504		24.0		23.0		26.0		29.0
DMNH 505						27.0	16.8	
DMNH 556						25.4	18.8	32.3
UCMP 81294				23.0	17.1	24.7	19.3	35.6
UCMP 81299				23.2	15.0	21.5	19.9	36.1
UCMP 81366						23.1	17.5	30.9
UCMP 81370				23.0	14.8	25.2	17.1	
UCMP 81413		22.5	11.2					
UCMP 81416				23.2				
UCMP 81440		23.6	12.1	23.5	14.9	25.8	17.9	
UCMP 81448				22.5	15.3	23.8	19.3	30.7
UCMP 81451			12.0	21.0	14.7	23.4	17.2	30.5
Sthenodectes incisivum								
CMNH 11437	10.7	22.1	14.9	23.5	18.3	25.0	22.7	33.9
FMNH P12166	10.4	22.7	14.7	22.0	17.6	25.1	21.2	31.8
YPM 16883	9.5	23.6	13.3	23.6	16.9	25.9	19.8	36.8
Telmatherium validus								
AMNH 12193						24.2	14.1	31.3
AMNH 12204				20.2	13.8	23.0	15.7	29.5
AMNH 12210						21.5		26.5
AMNH 12681				22.1	14.5	23.3	15.4	31.2
AMNH 12687		22.8		21.9	14.7	22.3	17.0	30.5
AMNH 13176	8.3	23.4	11.9	20.0	14.3	21.0		29.2
AMNH 1532		18.1		19.0	12.3	25.3	18.1	32.8
AMNH 1545						24.7	18.7	
AMNH 1560	7.4	22.8	10.8	21.0	13.4	24.7	15.0	30.2
AMNH 1563						22.3	15.9	30.4
AMNH 1566	9.1	20.9	9.7	19.6	13.1	19.4	14.5	30.2
AMNH 2353		26.7	10.9	20.8	13.9	21.9	16.1	29.7
AMNH 2356		21.5						30.1
FMNH PM2328	10.1	23.5	13.8	22.5	16.1	24.3	18.1	31.5

APPENDIX 1
(Continued)

	p1W	p2L	p2W	p3L	p3W	p4L	p4W	m1L
FMNH PM55576	10.6	23.7	11.8	23.3	14.9	24.0	17.5	31.6
UCM 69355	8.5	21.7	12.0	22.3	10.6			31.8
UCMP 31344				23.1	14.5		17.2	33.0
USNM 12836				23.3	14.7	23.8	16.0	31.6
USNM 13455				20.4	14.6	21.0	16.7	30.2
USNM 26121	9.8	24.2	12.0	23.9	14.9	23.8	17.0	31.6
USNM 26162		24.1		22.6	15.0	24.2		30.2
USNM 26302	7.1	22.1		20.3	12.8	21.6	15.4	28.2
YPM PU10027			11.9	20.8	13.5	23.4	15.6	29.6
YPM PU10361								30.4
YPM PU16103	10.3		12.0	20.2	14.2	21.0	16.2	30.7
Wicki brevirhinus								
CMNH 11382	10.3	24.3	13.2	23.2	15.8	25.0	19.2	32.1

	m1W	m2L	m2W	m3L	m3W	p2–p4	m1–m3	p2–m3
Acrotitan unlanshirehensis								
IVPP V6686						65.6		
Brachydiastematherium trans.								
AMNH 108188 c	31.6					96.7		
Bunobrontops savegei								
UCMP 128414				58.0	28.5			
Camp Margetts "taxon A"								
AMNH 26408	26.4	56.5	31.4	87.0	30.3	80.1	182	266
AMNH 26410	26.4	49.8	27.5	79.0	26.7	75.6	168	241
AMNH 26415	25.7	48.2	28.6	74.6		66.0	161	224
AMNH 26418	22.5	50.0	26.8	74.0	33.7	73.3	160	231
AMNH 26430	24.3	59.4	28.3	95.1	29.8		190	
AMNH 26431						75.9		
AMNH 26432		51.5	32.6	78.0	32.8	75.7	163	236
Camp Margetts "taxon B"								
AMNH 26400	32.1	58.9	37.0	78.9	36.2	88.0	185	273
Camp Margetts "taxon C"								
AMNH 26425	26.3	54.5		84.1			175	
Desmatotitan tukhumensis								
AMNH 21606	23.6	48.0	29.3	61.9	28.6	75.2	145	221

APPENDIX 1
(Continued)

	m1W	m2L	m2W	m3L	m3W	p2–p4	m1–m3	p2–m3
Diplacodon elatus								
CMNH 11876	25.3	54.0	32.5	75.5	30.8	78.9	168	243
CMNH 11877	25.7	54.3	29.4	76.2	29.0	81.6	172	252
CMNH 11879		47.4		71.1	30.1	66.3	155	220
CMNH 11967	24.9	52.1	29.4	75.9	29.0	76.8	170	245
CMNH 2859	26.0	49.3	29.3	78.2	28.0	79.6	160	240
FMNH P14634	24.6	49.3	30.9	72.9	27.6	67.5	122	223
FMNH P14638	26.4	50.0		70.0		76.2	160	227
FMNH P14640	23.3	48.4	27.9	76.5	28.6	77.3	164	244
Dolichorhinus hyognathus								
AMNH 13164	23.1	43.2	26.5			72.6	140	215
AMNH 1836	22.0	40.4	24.6	58.1	23.1	63.3	132	195
AMNH 1840	20.9	37.4	23.5	56.4	23.0	64.3	125	189
AMNH 1854	23.1					70.7		
AMNH 1856	21.7	42.7	25.3	61.7	24.4	67.9	140	210
AMNH 1857	20.5	40.7		62.9		67.6	128	198
AMNH 1858	17.9	38.3	21.8					
CMNH 11071		39.5		58.7		65.2	127	195
CMNH 11091				60.0	26.5			
CMNH 11092	22.6	36.0	27.6	62.4	25.3	66.2	135	197
CMNH 2865		39.0	26.7	59.1	24.3			
FMNH P12167	22.7	46.2	26.5	63.8	25.8	71.7	141	213
FMNH P12200	21.2	37.2	23.5	55.6	23.8	68.4	123	
USNM 6702	23.0	45.2	28.3			74.0		
YPU PU 10273				62.6	25.2	77.3	139	217
Duchesneodus uintensis								
CMNH 11761	22.9	44.8	28.8	64.1	29.4	67.2	131	210
CMNH 11809	25.4	46.8	32.2	78.8	33.9	76.5	165	230
CMNH 11821				76.5	32.7			
FMNH PM136							185	
FMNH PM163						74.9		250
MNH PM401							200	300
Embolotherium andrewsi								
AMNH 26006	41.8	81.2	43.9	130.0	46.6	113.0	274	381
AMNH 26007	40.6	78.5	46.1	111.0	45.0	106.0	250	346
AMNH 26008	45.3	86.9	47.9	134.1	47.5	115.2	300	416

APPENDIX 1
(Continued)

	m1W	m2L	m2W	m3L	m3W	p2–p4	m1–m3	p2–m3
AMNH 26009	38.7	75.0	45.1	108.3	39.6	102.1	240	332
AMNH 26011		83.2	45.7	112.1	44.6		244	
IVPP V11959	40.2	84.3	49.8	140.4	48.3	123.4	288	
PIN 2200-2				126.4	52.4			
Embolotherium grangeri								
AMNH 21600	36.2	72.7		105.3	41.8	90.1	233	323
AMNH 26005	39.8	79.9	52.2	122.9	51.9	103.0	265	365
AMNH 26018	34.8	70.8	40.3	112.6	40.0		225	
AMNH 26040	32.5	74.2	37.7					
AMNH 26132	33.4					97.3		
Eubrontotherium clarnoensis								
UCMP 126102	32.3	61.9	37.7	91.7	38.8	92.6	206	300
UCMP 126161		62.0				88.5		
UCMP 126162	29.8							
UCMP 126165				87.6	36.4			
PIN 3109-91	28.6	59.1	33.2	83.8	32.6	85.3	183	273
Gnathotitan berkeyi								
AMNH 20106	31.4	71.5	36.9	109.8	37.4	99.2	245	337
AMNH 20107	31.3					112.9		
Hyotitan thomsoni								
AMNH 26401	35.2	63.0	39.7	84.8	36.6	101.2	195	296
Mesatirhinus junius								
AMNH 12191	17.6	30.9	20.3	45.0	18.9	55.0	99	153
AMNH 12199	15.7	27.9	18.6	43.6	18.0		95	
AMNH 12686				36.8	14.7			
AMNH 13178	15.9	28.4		45.2	18.7	53.4	98	151
AMNH 1512	15.6	31.1	18.2	46.3	18.1	59.1	105	162
AMNH 1520	15.4	29.1	18.7	43.8	17.4	52.5	95	146
AMNH 1551	15.2	27.3	18.4			52.3		
AMNH 1567	16.5	29.0	19.8		13.2	53.4	100	152
AMNH 1575		29.5	19.4		19.0	50.5	97	148
AMNH 1577	16.3	28.9	19.1	43.8	18.0	53.6	95	149
AMNH 1627				45.6	18.9			
ANSP 10348					15.0			
DMNH 9687	16.7	31.1	19.3	43.2	18.3		95	
FMNH PM36045	16.9	28.5	20.1	46.0	18.3	52.6		151

APPENDIX 1
(Continued)

	m1W	m2L	m2W	m3L	m3W	p2–p4	m1–m3	p2–m3
USNM 26111	15.2	29.4	20.2	45.6		59.9	100	
USNM 26116	15.4	28.8	18.1	43.8		51.6	94	145
USNM 26148	15.0	24.8	16.6	46.3		59.1	102	158
USNM 26151	25.0	30.8	18.2	40.1			96	149
USNM 363884	15.7	29.1	14.9					
YPM 16421	13.4	25.6	15.6		14.6		85	
YPM 16725	16.0	30.8	19.1	44.6	17.3		100	
YPM 16732	15.7	30.8	19.0	45.8	17.6	52.9	100	152
YPM 16743		30.8	17.4	45.8	16.2			
YPM PU10118				48.9	20.3		104	
YPM PU10184	16.9	30.6	19.7	48.6	18.6		104	
YPM PU25021		32.5	21.4	46.9	18.6	50.1	102	152
Metarhinus fluviatilis								
YPM 13125				51.9		58.9	109	166
Metarhinus sp.								
AMNH 13179	19.5	33.0	23.1	48.5	20.2	55.4	108	163
AMNH 1859	21.1	37.0	21.1	51.5	23.7	64.5	119	184
AMNH 1865	14.6	30.1	17.0	40.6	16.8		93	
AMNH 1946		30.9	18.2	43.8	18.8	50.5	102	152
AMNH 2059	16.8	31.3	18.4	42.3	17.6	50.8	98	147
CMNH 11924	16.5	32.4	18.2		17.2	50.2		
CMNH 3125	15.4	31.8	17.5	41.4	17.7		94	
CMNH 3133	18.7	33.7	22.3	51.0	22.0	56.0	111	164
CMNH 3142	15.2	30.0	18.0	41.8	16.7	46.0	93	140
CMNH 3371	18.5	38.4				55.9		
CMNH 3842	18.1	34.0	21.1	49.4	22.5	52.5	103	155
DMNH 543		30.7		46.8	21.8	51.7	98	147
DMNH 544	19.9	33.3	21.5	48.0	20.0	54.3	108	161
DMNH 550	18.5	37.4				61.7		
FMNH P12178	18.4	32.5	22.7	48.9	21.1	55.5	106	160
FMNH P12178	18.0	36.1	21.2	49.4	20.7	56.6	111	165
FMNH P12183		30.8		45.0		56.7	101	145
FMNH P12190	17.7	32.1	20.8	44.6	19.7		100	
FMNH P12195	18.2	36.8	21.5	49.3	19.9	58.9	110	170
FMNH PM1456				57.7	25.6			
FMNH PM1511	25.1	40.0	27.5	59.5	26.4	67.8	129	196

APPENDIX 1
(Continued)

	m1W	m2L	m2W	m3L	m3W	p2–p4	m1–m3	p2–m3
FMNH PM1675	15.7							
FMNH PM1715				53.5	22.3	63.1	107	171
FMNH PM1734	18.0	33.4	21.0	47.6	19.4	57.1	107	161
FMNH PM28001	19.9	36.2	23.7	49.7	20.9	57.3	116	175
FMNH PM28002	20.4	35.5	23.2	52.1	21.3	53.5	114	165
FMNH PM28003	19.9	35.1	21.6	51.4	21.3	52.5	113	165
FMNH PM28004	18.5			46.1	21.3	56.8	105	162
FMNH PM28006	19.9	33.7	23.9	49.9	21.2	55.9	107	162
FMNH PM28342	20.5	33.4	24.0	47.9	20.5	55.5	109	162
FMNH PM28343	18.3	35.2	21.4	46.5	20.5	59.2	107	165
FMNH PM28359						55.9		
FMNH PM30422	21.1	36.5	24.3	58.9	24.5	61.1	122	176
FMNH PM30435	18.4	34.9	20.3	48.5	19.2	51.2	109	157
FMNH PM35933	18.3	33.2	21.6	49.9	21.3	55.8	107	161
FMNH PM35970	18.9	32.6	21.5	46.8	20.6	56.1	105	157
FMNH PM35996	18.9	31.8	22.6		21.2	51.4	106	155
FMNH PM39947		37.2	18.7	45.3	18.3	57.9	110	170
UCMP 113182	15.6	30.3	18.7	40.2	16.1			
UCMP 113201	17.0							
UCMP 113203				48.4	19.2			
UCMP 81273	20.1	35.3	23.9	49.2	22.0	60.8	112	161
UCMP 95780	18.0	32.8	20.4	49.3	19.1			
UCMP 95813				49.1	18.6			
YPM 16834	17.0					48.1		
YPM PU11284		34.1		52.0			110	
"Metatelmatherium?" browni								
AMNH 20016	17.9		18.3	21.4				
AMNH 20022	19.8							
Metatelmatherium ultimum								
AMNH 2029				64.9				
AMNH 2033	25.2	46.8	28.4	61.6	26.9	74.0	148	225
AMNH 2060	27.8	49.1	31.3	67.3	29.5		154	
AMNH 26411	25.1	48.6	30.0	71.4	29.1	77.5	157	240
Metatitan primus								
AMNH 26101	31.3	64.6	35.5	97.3	37.9	90.4	207	297
AMNH 26102	35.8	64.8	36.8	94.2	35.3	91.2	208	294

APPENDIX 1
(Continued)

	m1W	m2L	m2W	m3L	m3W	p2–p4	m1–m3	p2–m3
Metatitan relictus								
AMNH 26391	31.3	63.6	35.1	93.8	35.9		197	
AMNH 26402	32.5	67.0	36.8	97.1	38.5	86.9	211	298
AMNH 26404								
AMNH 26405	29.5	61.7	33.9	96.0			198	
AMNH 26407	31.6	58.9	34.5	91.6	33.4		185	269
AMNH 26420	38.3	67.0	42.1	102.0			230	
AMNH 26427		62.9	34.7	102.1	39.7		213	
AMNH 26429	32.9	67.7	37.9	101.7	37.1		220	
Metatitan khaitshinus								
PIN 3745-31	30.8	69.1	34.8	95.3	34.5	95.4	216	310
Microtitan mongoliensis								
AMNH 22099	14.0	32.6	16.1	49.0	16.7	49.8	104	155
AMNH 20167	13.6							
Notiotitanops mississipp.								
USNM 16646	26.1	46.5	30.4	68.8	30.5		158	
cf. *Parabrontops gobiensis*								
AMNH 26019	28.8	53.4	32.9	79.0	32.4	84.5	180	263
AMNH 26021	29.8	59.9	35.8	90.1		85.8	202	284
AMNH 26131	32.1	69.8	35.6	97.4	36.1	89.3	210	300
Pollyosbornia altidens								
AMNH 2025	32.1	59.6	33.4	90.4		95.6	197	290
Protitan grangeri								
AMNH 19179	32.2							
AMNH 20103	25.9	52.8	32.3	83.3	33.4	80.7	177	257
AMNH 20104	27.5	60.8	33.7	95.6	35.2	89.0	204	294
AMNH 20109	23.1	53.8	28.1	84.4	27.4	82.7	175	258
AMNH 20111		60.1	29.5	84.6			185	
AMNH 20112	27.6	62.0	38.1		30.3	94.7	200	294
AMNH 20119	26.3	61.5	34.7					
AMNH 20126	25.1	56.4	31.8					
AMNH 26421	30.5	53.8	33.8	81.8		75.9	168	238
cf. *Protitan minor*								
AMNH 26419		55.9	29.7	75.0			173	242
"Protitan?" cingulatus								
AMNH 20110	30.4	60.4	33.8	89.7	32.0	93.9	194	286

APPENDIX 1
(Continued)

	m1W	m2L	m2W	m3L	m3W	p2–p4	m1–m3	p2–m3
AMNH 26403	29.6	61.6	34.6	86.4	32.4	77.2	190	269
AMNH 26412	28.2	51.5	33.0	79.2	30.6	79.4	164	241
Protitanops curryi								
CIT 1854		56.7		88.8	37.9	68.4	190	252
Protitanotherium emarginatum								
AMNH 2501	30.6	66.6	36.4	96.3	37.8	90.6	215	303
YPM 11146						92.2		
YPM PU11242	28.1	60.0				84.3		286
Protitanotherium koreanicum								
UMUT CV6047	31.0							
Pygmaetitan panxianensis								
IVPP V6523	12.8	28.7	13.9					
IVPP V6524			13.2	34.7	12.8			
Rhinotitan andrewsi								
PIN 2198-2	33.2	62.1	37.0	91.7	35.7	97.3	198	293
IVPP V3254-1	29.9	64.6	35.9	95.0	38.5	100.2	212	307
Rhinotitan kaiseni								
AMNH 20252	32.0	55.3	35.8	83.7	19.7	88.5	182	270
FMNH P14048	27.0	57.7	32.4	88.0	31.8	90.1	185	275
Rhinotitan sp.								
AMNH 18653	30.0	62.2	35.0	92.1	23.0	93.5	200	294
AMNH 20251	31.3	62.5	36.2	99.6	34.8	97.0	205	302
AMNH 20256		66.0	35.4			101.0	210	
AMNH 20262	30.4	63.8	34.4	95.0		99.9	209	
AMNH 20272	31.6	60.6	33.5	91.6	36.0	89.6	200	290
AMNH 20273	27.9	57.1	32.6	83.0	32.1	99.4	188	287
AMNH 21603	28.5	67.2	34.3	94.0		99.9	212	306
AMNH 21605	32.5	60.0	36.6	94.9	38.3	92.0	205	267
Rhinotitan quadridens								
IVPP V2651	23.4							
Sphenocoelus uintensis								
DMNH 14219	21.3	38.7	24.3	60.4		66.5	128	194
DMNH 2830	22.6	42.4	27.0	61.7	24.8	69.0	134	204
DMNH 542		44.1	30.9			72.5		
UCMP 81281	20.6					68.4		
UCMP 81443	20.6	41.6	25.4		25.2	68.0	139	205

APPENDIX 1
(Continued)

	m1W	m2L	m2W	m3L	m3W	p2–p4	m1–m3	p2–m3
cf. *Sphenocoelus uintensis*								
DMNH 2584		41.7		62.4	25.1	70.9	135	207
DMNH 504		37.0		58.0			126	
DMNH 505	21.2	40.0	25.8	61.3	24.1			
DMNH 556	22.3	42.8	28.3					
UCMP 81294	22.5	42.8	27.2	65.6	23.9		142	
UCMP 81299	20.5	44.0	24.5	61.7	22.9		142	
UCMP 81366	20.1							
UCMP 81440				63.4	23.3	70.3		
UCMP 81448	22.8	38.7	28.9	62.7				
UCMP 81451	20.1	41.6	24.5		23.3			
Sthenodectes incisivum								
CMNH 11437	26.4	44.1	29.7	58.9	26.4	68.0	134	200
FMNH P12166	24.6	42.2	28.5	59.0	24.8	70.7	134	198
YPM 16883	25.3	45.6	28.1	62.4	25.7	70.6	144	215
Telmatherium validus								
AMNH 12193	19.0	38.0	23.1	56.7				186
AMNH 12204	19.7	36.5	23.5					
AMNH 12210		36.7		52.9			115	
AMNH 12681	19.9	40.3	23.2	53.0	23.1		125	
AMNH 12687		35.7	23.7	52.2		66.6	121	190
AMNH 13176	18.9	38.2	22.5	55.2		63.7	118	180
AMNH 1532	21.9	40.2	24.6					
AMNH 1545		44.4	29.1	60.6	26.7			
AMNH 1560	18.0	38.0	21.4	49.5	20.6	67.7		
AMNH 1563	20.7	37.8	23.7	53.2	23.3		120	
AMNH 1566	19.6	34.2	21.8	49.6	21.4	59.0	110	170
AMNH 2353	19.7	36.0	23.2	54.0	21.4	68.5	118	185
AMNH 2356	18.0	38.1	21.4					
FMNH PM2328	21.2	41.4	25.4	59.9	24.8	70.7	130	200
FMNH PM55576	20.4	40.2	25.1			71.6		
UCM 69355	18.2	36.1	20.4					
UCMP 31344	19.4	40.4	24.3	57.7	23.2		126	
USNM 12836	20.1	38.9	23.8	55.4			123	
USNM 13455	19.7	32.0	29.1	55.2			120	
USNM 26121	20.8	42.0	24.9	57.2		73.8	125	197

APPENDIX 1
(Continued)

	m1W	m2L	m2W	m3L	m3W	p2–p4	m1–m3	p2–m3
USNM 26162		36.3		58.4				
USNM 26302	18.8	37.2	23.2	54.3		62.9	120	185
YPM PU10027	18.8	38.6	22.2	53.7	21.2			
YPM PU10361	17.8	38.5	20.8	56.3	20.6		125	
YPM PU16103	21.8	39.7	26.1	59.5	24.1		132	199
Wicki brevirhinus								
CMNH 11382	22.7	39.9	25.4	58.7	25.2	72.2	129	197